PIERS 2012 Moscow

Progress In Electromagnetics Research Symposium

Abstracts

August 19–23, 2012
Moscow, RUSSIA

www.emacademy.org
www.piers.org

PIERS 2012 Moscow Abstracts

Published by

The Electromagnetics Academy
777 Concord Avenue, Suite 207
Cambridge, MA 02138

www.emacademy.org
www.piers.org

ISSN: 1559-9450
ISBN: 978-1-934142-21-9

Progress In Electromagnetics Research Symposium

August 19–23, 2012

Moscow, RUSSIA

PIERS 2012 MOSCOW ORGANIZATION

PIERS Founding Chair

J. A. Kong, MIT, USA

PIERS Chair

L. Tsang, University of Washington, USA

PIERS 2012 Moscow General Chair

A. B. Samokhin,

Moscow Technical University of Radio Engineering, Electronics and Automatics, Moscow, RUSSIA

PIERS 2012 Moscow General Vice Chairs

Y. V. Shestopalov, Karlstad University, SWEDEN

K. Kobayashi, Chuo University, JAPAN

PIERS 2012 Moscow International Advisory Committee

Y. M. Antar	A. Buyukaksoy	D.-C. Chang	W. C. Chew
H. T. Chuah	A. S. Dmitriev	N. Engheta	V. Freilikher
Y. V. Gulyaev	L. Gurel	T. M. Habashy	M. Hallikainen
W. J. R. Hoefer	M. Idemen	A. S. Ilinski	A. Ishimaru
E. O. Kamenetskii	A. A. Kirilenko	A. Komiyama	A. N. Lagarkov
K. J. Langenberg	L.-W. Li	I. V. Lindell	K. M. Luk
D. S. Lukin	P. N. Melezhik	Y. Miyazaki	Z. T. Nazarchuk
S. A. Nikitov	P. Pampaloni	P. H. Pathak	A. Priou
J. W. Ra	Y. Rahmat-Samii	M. Raugi	H. W. Schürmann
A. H. Serbest	L. Shafai	A. S. Sigov	P. D. Smith
A. Stolin	M. Tateiba	A. V. Tikhonravov	E. E. Tyrtyshnikov
P. Y. Ufimtsev	P. L. E. Uslenghi	P. M. van den Berg	J. Vrba
J. Wu	R.-B. Wu	T. Yamasaki	K. Yasumoto
V. A. Zernov	W.-X. Zhang	A. Zhukov	S. Zouhdi

PIERS 2012 Moscow Technical Program Committee

A. Altintas	Y. Ando	S. Barmada	W.-M. Boerner
D. Caratelli	D. Censor	V. V. Chebyshev	H. S. Chen
K.-S. Chen	Y. K. Cho	H. T. Ewe	G. N. Georgiev
F. Gunes	S. L. He	A. Hirata	K. Iwatsuki
Q. Jiang	R. Kastner	S.-Y. Kim	V. F. Kravchenko
Y. A. Kravtsov	A. S. Kryukovsky	V. E. Kunitsyn	D. B. Kuryliak
G. A. Kyriacou	K. S. Lukin	M. A. Lyalinov	G. Manara
F. Molinet	P. Nepa	M. Nishimoto	Y. Okuno
A. V. Osipov	K. Ouchi	Y. K. Podlipenko	B. Polat
L. X. Ran	A. K. Sarychev	T. Sengor	V. Serov
X.-Q. Sheng	H. Shirai	B. Shishkov	A. Sihvola
Y. G. Smirnov	R. Talhi	O. A. Tretyakov	S. Tretyakov
A. A. Vertiy	B.-I. Wu	G. Q. Xie	V. V. Yakovlev
N. P. Yashina			

PIERS 2012 Moscow Organizing Committee

A. I. Bogdanov
Q. Jiang
A. I. Morozov
Y. V. Shestopalov (Vice Chair)
V. V. Cherdincev
K. Kobayashi (Vice Chair)
D. V. Rastyagaev
I. V. Skljar
I. E. Fedotov
B. A. Lagovsky
A. S. Samokhin (Chair)
B.-I. Wu
P. A. Gabusu
O. V. Mikheev
A. S. Samokhina

PIERS 2012 MOSCOW SESSION ORGANIZERS

Y. N. Barabanenkov
N.-K. Chen
V. D. Freilikher
M. N. Georgieva-Grosse
S. Iezekiel
V. F. Kravchenko
A. N. Lagarkov
G. S. Makeeva
J. Ojeda-Castañeda
K.-C. Peng
A. K. Sarychev
Y. V. Shestopalov
Y. G. Smirnov
S. A. Tretyakov
G. Q. Xie
A. P. Zhukov
M. E. Belkin
L. El Amraoui-Ouni
T. Fukusako
E. Gescheidtová
E. M. Karchevskiy
A. V. Kudrin
J. H. Li
E. D. Mishina
Y. Okuno
B. Polat
C. K. Seow
J.-C. Shi
R. Talhi
N. K. Uzunoglu
V. V. Yakovlev
D. Censor
N. S. Erokhin
F. Gao
G. Z. Guo
K. Y. Kim
V. E. Kunitsyn
M. E. Likhachev
F. Molinet
G. M. Pacheco
R. Przesmycki
V. N. Serkin
A. B. Shvartsburg
S. Y. Tan
J. Vrba
T. Yamasaki
D.-C. Chang
A. A. Ezhov
G. N. Georgiev
X. F. Han
K. Kobayashi
G. A. Kyriacou
N. M. Makarov
L. Nowosielski
L. V. Panina
A. B. Samokhin
V. Serov
A. S. Sigov
J. Tong
C.-J. Wu
T.-J. Yang

PIERS 2012 MOSCOW SPONSORS

- ☐ Moscow State Institute of Radio Engineering, Electronics and Automation
- ☐ Russian New University
- ☐ NVK "VIST"
- ☐ Russian Foundation for Basic Research
- ☐ The Swedish Institute
- ☐ Russian Academy of Sciences
- ☐ The Electromagnetics Academy at Zhejiang University
- ☐ The Electromagnetics Academy

PIERS 2012 MOSCOW EXHIBITOR

- ☐ Centurion System Inc. — USA

PIERS 2012 SESSIONS

Session 1A1
Fiber, Optics and Photonics, Laser

Spectrum-sliced Split-step Fourier Method for Precise Simulation of Supercontinuum Generation in Dispersion-Engineered Photonic Crystal Fibers

Di Yang[1, 2], **Ming Tang**[1, 2], **Songnian Fu**[1, 2], **and P. Shum**[1, 2]

[1]National Engineering Laboratory for Next Generation Internet Access System (NGIA)
Huazhong University of Science and Technology (HUST), Wuhan 430074, China
[2]Wuhan National Laboratory for Optoelectronics (WNLO), Wuhan 430074, China

Abstract— Supercontinuum (SC) generation in the nonlinear optical fiber is an attractive solution to produce significantly broadened intense spectrum (several hundreds of nm or even more) using laser pulse with moderate peak power. Traditionally, split-step Fourier (SSF) method and its variations have been developed and utilized to simulate complicated nonlinear dynamics associated with the continuum process successfully. Nonlinearity and dispersion are two key players in the formation of SC and the numerical operation about them determines the validity and accuracy of SSF algorithm. While the nonlinearity shows less wavelength dependence, the dispersion map of the nonlinear optical fiber exhibits strong spectrum related features. Since the dispersion property is essential to control the ultra-short pulse evolution along the fiber length, photonic crystal fibers (PCFs) are employed to tailor the dispersion profile precisely in favor of the applied pump wavelength. Due to the air-hole cladding structure surrounding the central silica core, PCF has the flexibility to create non-traditional dispersion map (parabolic profile for instance) to optimize the spectral and temporal properties of SC pulses. However, the dispersion engineering of PCF raises difficulties of numerical simulations because only the dispersion coefficient at the central frequency of the injected pump pulse is used to present dispersion value of the entire spectrum window in normal SSF algorithm. Since the simulation covers an extremely broad bandwidth and generally a broadband optical pulse is used as the seeding pump, SSF simulation using single point dispersion value fails to produce accurate results even considering higher order dispersion coefficients.

In this paper, we propose a modified SSF algorithm to accurately simulate SC process in optical fibers with arbitrary dispersion profiles. We formulate the dispersion curve into multiple sections at different wavelengths and put them into the generalized nonlinear Schrödinger equation (GNLSE). The reconstructed GNLSE system takes into account dispersion properties at different wavelength separately and the section number of the sliced dispersion curve is decided by the sampling points set in the entire time-window we observe in the simulation and therefore no additional computational efforts are needed for the modified GNLSE simulation.

Two types of dispersion profiles in PCF are considered for numerical simulation. One is the conventional dispersion curve with one zero dispersion wavelength (ZDW), namely type I; another is a parabolic dispersion curve with two ZDWs, namely type II. We conduct intensive numerical experiments to investigate our proposed algorithm and compare results with the conventional SSF method. The results show that the accuracy of SC simulation with the spectrum-sliced SSF method can be improved especially for type II dispersion curve. This method is effective to foresee wideband pulse propagation along the nonlinear fiber with complex dispersion map while the conventional SSF method always overestimate the spectrum broadening and predict the pulse shape improperly. We will demonstrate the simulation results and analysis comprehensively in our presentation.

A Novel Wide-angle Beam Propagation Algorithm

Dusan Z. Djurdjevic
Faculty of Technical Sciences, University of Pristina
Kneza Milosa 7, Kosovska Mitrovica 38220, Serbia

Abstract— The beam propagation method (BPM) is certainly one of the most popular simulation techniques employed in design of waveguide-based photonics structures. The basic assumptions and advantages of the BPM, paraxial and SVEA approximations, at the same time limit the field simulations to paraxial beams along primary longitudinal direction of the propagation and weakly-guiding waveguide structures. In last two decades, starting from [1], several wide-angle (WA) schemes have been proposed to remove (or relax) these limitations, see for example [2–4].

In this work a novel WA-BPM approach is proposed, leading to the multi-step operator algorithm where the Padé approximant schemes are not used. It is shown that the scalar one-way wave equation under the SVEA can be formally solved in terms of higher-order field derivatives. By using this formal solution the z-directed multi-step operator method is enabled, where every single step "behaves" like the Padé (1, 1) scheme. The z-directed multi-step algorithm is then easily designed with usual finite-difference (FD) discretization (FD-BPM) and simple computer coding. The proposed algorithm enables the proper treatment of both guiding and evanescent modes. By choosing appropriate value of the dumping parameter involved in the solution, an unconditionally stable algorithm is obtained where the longitudinal propagation BPM step Δz is fairly relaxed, compared with the transverse FD mesh size (e.g., Δx). Although the solution for two-dimensional (2D) scalar cases is derived only, the approach presented is easily and directly extendable to 2D and 3D semi-vectorial (polarized), and by the inclusion of the improved FD formulas, for 3D full-vectorial cases. A new WA-BPM algorithm will be presented for the analysis of 2D and 3D tilted rectangular dielectric waveguides and compared with the published results.

ACKNOWLEDGMENT

This work is based on research conducted within the Project (Project code: TR32052) funded by the Ministry of Science and Technological Development of the Republic of Serbia.

REFERENCES

1. Hadley, G. R., "Wide-angle beam propagation using Padé approximant operators," *Opt. Lett.*, Vol. 17, 1426–1428, 1992.
2. Sharma, A. and A. Agrawal, "New method for nonparaxial beam propagation," *J. Opt. Soc. Am. A*, Vol. 21, 1082–1087, 2004.
3. Hadley, G. R., "Slanted-wall beam propagation," *J. Lightw. Technol.*, Vol. 25, No. 9, 2367–2375, 2007.
4. Sujecki, S., "Generalized rectangular finite difference beam propagation method," *Appl. Opt.*, Vol. 47, No. 23, 4280–4286, 2008.

Influence of Geometric Parameters on the SOI Racetrack Resonator Properties

P. Matavulj[1] **and T. Keča**[2]

[1]Faculty of Electrical Engineering, University of Belgrade, Serbia
[2]ICT College of Vocational Studies, Belgrade, Serbia

Abstract— In this paper, we investigate the influence of SIO racetrack resonator's geometric parameters on its transfer function. The silicone rib racetrack resonators have several geometric parameters with significant influence on propagation of light. Investigated geometric parameters could be separated in two groups (Fig. 1). First is ring-shape parameters, coupling length (L_c) and ring circumference (ρ). Those parameters are usually a few hundreds micrometers long. Second is smaller cross-section parameters: waveguide width (w), oxide layer thickness (t) and slope angle (α). Influence of ring-shape parameters has already been studied [1]. We also analyze the way cross-section parameters affect propagation of light.

To investigate geometric parameters influence, transfer function (output-input light intensity ratio) is calculated for both input modes TE and TM [2–4]. Wavelength of used light is around 1.55 µm. In transfer function, two or more resonant minima can be seen for all geometric parameters of our interest. Therefore, Free Spectral Range (FSR) and first resonant wavelength on calculated curves are fitted for each geometric parameter.

FSR shows reciprocal dependencies on both ring-shape parameters. These relations are slightly weaker for coupling length compared to ring circumference. In case of cross-section geometric parameters, FSR does not depend on layer thickness and slope angle. Considering waveguide width, FSR shows no dependence for one input mode and very weak one for the other.

Unlike the FSR, first resonant wavelength strongly depends on all studied geometric parameters. Ring-shape parameters dependencies have periodic property, due to the transfer function itself and its FSR. In other words, the increase of one resonant wavelength towards upper values causes the subsequent resonant wavelength to be the first. Spatial periods of these periodic functions are small, especially for ring circumference dependency. In one spatial period both dependencies are linear. In case of cross-section parameters, first resonant wavelength changes very rapidly. Considering their size is few micrometers, establishing the exact functions dependencies is feasible.

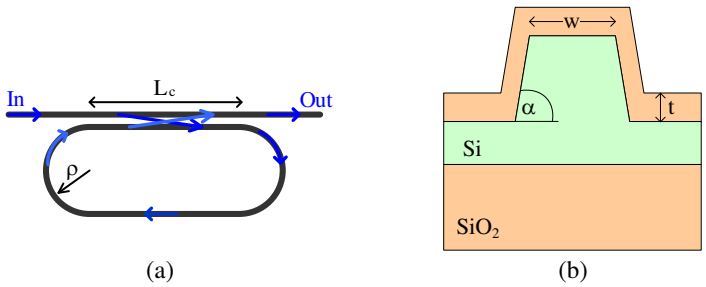

Figure 1: Ring resonator's geometric parameters. (a) Ring-shape and (b) cross-section.

REFERENCES

1. Keča, T., P. Matavulj, W. Headley, and G. Mashanovich, "FSR adjustment of silicone rib racetrack resonator," *III International School and Conference on Photonics*, Belgrade, Serbia, 2011.
2. Cusmai, G., F. Morichetti, P. Rosotti, R. Costa, and A. Melloni, *Opt. Quant. El.*, Vol. 37, 343–258, 2005.
3. Morichetti, F., A. Melloni, and M. Martinelli, *J. Lightwave Technol*, Vol. 24, 573–585, 2006.
4. Milošević, M., P. Matavulj, B. Timotijević, G. Reed, and G. Mashanovich, *J. Lightwave Technol.*, Vol. 26, 1840–1846, 2008.

Formation Mechanism and Applications of Laser Induced Elemental Distribution in Glasses

K. Miura[1], **M. Shimizu**[1], **M. Sakakura**[2], **T. Kurita**[1], **Y. Shimotsuma**[1], **and K. Hirao**[1]

[1]Department of Material Chemistry, Kyoto University, Nishikyo-ku, Kyoto 615-8510, Japan
[2]International Innovation Center, Kyoto University, Nishikyo-ku, Kyoto 615-8510, Japan

Abstract— We investigated the irradiation effects of a femtosecond laser pulse inside the glass using the transient lens method with a sub-picosecond time resolution. By irradiating a single pulse of 1.0 μJ, It was cleared that the temperature at the center of the laser beam reaches 3000°C or more within 1 ps, and then the temperature decreases from ∼ 3000°C to ∼ 300°C within 10 μs. This result suggests that the heat accumulation becomes critical when the repetition rate of the irradiation is higher than 100 kHz. When a lot of laser pulses are focused at high repetition rate (more than several hundred kHz), the released heat is accumulated around the photoexcited region and the surrounding glass is modified due to high temperature increase. Under such a condition, it was confirmed that the elemental distribution of a ring shaped pattern can be formed in a glass. Figure 1 shows an elemental distribution around the focal point after laser irradiation, as analyzed by EPMA. The relative concentration of Si and O ions increase and those of K, Na, Ca, and Zn decrease at the focal point. We also confirmed that various shapes of element distribution can be produced by the adjusting of temperature distribution Figure 2 shows various shaped-element distributions in a glass by making multiple irradiated points with a LCOS-SLM. The spatial distribution of glass components is very important for controlling the property of glass, because the composition of glasses affects its chemical, mechanical and optical properties.

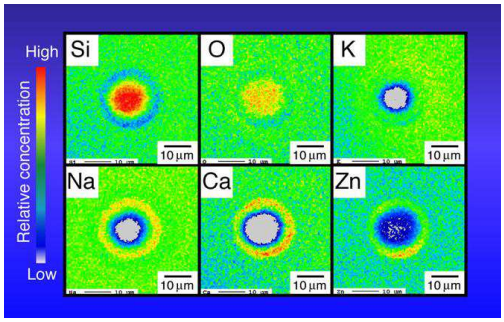

Figure 1: Profile of the elemental concentration around the focal point in a silicate glass after laser irradiation.

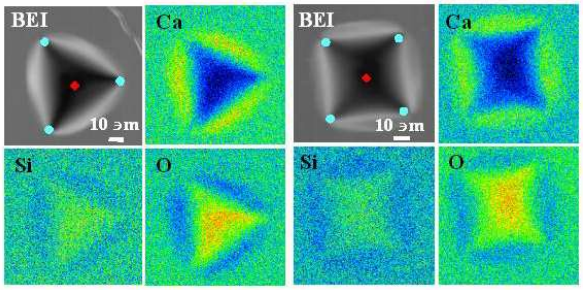

Figure 2: Element distributions in CaO-SiO_2 glass after simultaneous fs laser irradiations at multiple positions. Red and blue points depict the photoexcited points.

Effect of Gap Shape on the Spectral Response and Field Enhancement of Dimer-based Biosensor

Sameh Kessentini and Dominique Barchiesi
Project Group for Automatic Mesh Generation and Advanced Methods
Gamma 3 Project (UTT-INRIA), University of Technology of Troyes, France

Abstract— Metallic nanoparticles have interesting optical properties resulting in several physical processes such as resonanace with incident electromagnetic field at a given wavelength yielding a strongly enhanced field. The field enhancement can be exploited in vibrational spectroscopy. For instance, Raman signal enhancement factor can reach several orders of magnitude [1, 2] which enables the observation of a very low amount of molecules or even the single-molecule sensitivity [3, 4].

The sensitivity of the metallic nanoparticles strongly depends on the geometrical features. Then, the objective of this study is to depict the impact of some geometrical features on the optical properties of a specific biosensor in this visible range to ensure important signal enhancement. The considered biosensor, dimer antenna (Figure 1(a)), consists of a coupled array of dimers that exhibits great potential as reported in many previous studies. For instance, Fischer and Martin [5] compared the dimer bowtie to the dimer antenna (with straight gap) and found that the dimers-antenna produces a stronger field enhancement than the dimer bowtie for all investigated dimer geometries (different shapes and dimensions). For this, in this study, we focus on the dimer antenna, however with an additional geometrical parameter which is the gap shape that has never been studied previously.

The effect of gap shape on the optical properties of dimers-based biosensor is investigated in this study. The discrete dipole approximation (DDA) [6] is used to model the biosensor with different shapes of the gap separating the dimers. The considered shapes are straight, slanted and tie gap (triangular edges in the gap) as well as the circular tips (Figure 1). Assuming constant total length, width and height of the dimers, the effect of the gap shape on both the near field and the far field are depicted. The results show important effect on the far field quantities such as important shifts of the extinction peak wavelength exceeding 100 nm. It follows that the gap shape can be used to tune the plasmon resonance of the biosensor (almost same same level of extinction peak amplitude). Furthermore, the preliminary results show that the near field enhancement may present a doubled resonance.

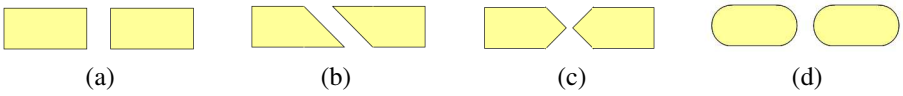

Figure 1: Upper view of dimers with (a) straight gap, (b) slanted gap, (c) tie gap and (d) cylindrical tips.

REFERENCES

1. Kottmann, J. P. and O. J. F. Martin, "Plasmon resonant coupling in metallic nanowires," *Optics Express*, Vol. 8, 655–663, 2001.
2. Zou, S. and G. C. Schatz, "Silver nanoparticle array structures that produce giant enhancements in electromagnetic fields," *Chem. Phys. Lett.*, Vol. 403, 62–67, 2005.
3. Nie, S. and S. R. Emory, "Probing single molecules and single nanoparticles by surface-enhanced raman scattering," *Science*, Vol. 275, No. 5303, 1102–1106, 1997.
4. Kneipp, K., Y. Wang, H. L. T. Perelman, I. Itzkan, R. R. Dasari, and M. S. Feld, "Single molecule detection using surface-enhanced raman scattering," *Phys. Rev. Lett.*, Vol. 78, 1667–1670, 1997.
5. Fischer, H. and O. J. F. Martin, "Engineering the optical response of plasmonic nanoantennas," *Optics Express*, Vol. 16, No. 12, 9144–9154, 2008.
6. Draine, B. T. and P. J. Flatau, "Discrete-dipole approximation for periodic targets: Theory and tests," *J. Opt. Soc. Am. A*, Vol. 25, 2693–2703, 2008.

Periodically Gated Two-dimensional Electron System: Tunable Planar Plasmonic Crystal at Terahertz Frequencies

V. V. Popov[1, 2]

[1]Kotelnikov Institute of Radio Engineering and Electronics
Russian Academy of Sciences, Saratov 410019, Russia
[2]Saratov State University, Saratov 410012, Russia

Abstract— The frequencies of the plasma oscillations (plasmons) in two-dimensional electron systems (2DES) fall within terahertz (THz) range while the plasmon wavelength is typically of a submicron scale [1]. Therefore, the plasmon excitation in 2DES is a good candidate for probing mesascopic electronic processes in 2DES and for creating THz plasmonic nanodevices. In this paper, we discuss the plasmon mode spectrum in a planar one-dimensional plasmonic crystal formed by a periodically gated 2DES (Fig. 1). Plasmon mode spectrum in such a structure can be electrically tuned by varying the gate voltage. We describe the transformation and interaction of different types of the plasmon modes that depend on both geometry of the grating gate and the spatial modulation of the electron density in 2DES. We also show that the plasmon modes in the planar plasmonic crystal can be strongly coupled to THz radiation.

Collective as well as localized plasmon modes can be excited in the planar plasmonic crystal formed by a periodically gated 2DES [1, 2]. Interaction between the plasmon modes localized in the gated and ungated regions of the 2DES can take place due to their resonant coupling. The conditions of strong interaction between the collective and localized plasmon modes are discussed. Terahertz radiation can be strongly coupled to the planar plasmonic crystal due to synchronizing the plasmon oscillations in different unit cells of the planar plasmonic crystal and its large lateral aperture [1, 3]. These properties of the planar plasmonic crystals make them very promising as tunable modulators and concentrators of the near field at THz frequencies.

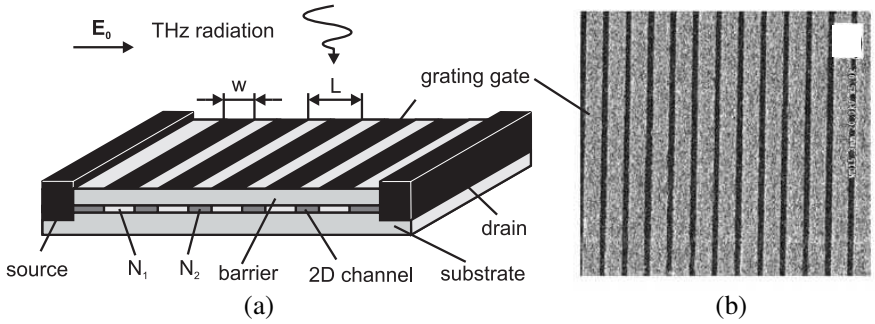

Figure 1: (a) Schematic of the grating-gated 2DES. Terahertz radiation with polarization of the electric field across the gate fingers is incident from the top. (b) Scanning electron microscopy image of the grating-gate fragment. The period of the grating gate is 1.5 μm with the width of the slits between the grating-gate fingers of 0.35 μm (after Ref. [3]).

REFERENCES

1. Popov, V. V., "Plasmon excitation and plasmonic detection of terahertz radiation in the grating-gate field-effect-transistor structures," *J. Infrared Millim. Terahertz Waves*, Vol. 32, No. 10, 1178–1191, 2011.
2. Nogajewski, K., J. Lusakowski, W. Knap, V. V. Popov, F. Teppe, S. L. Rumyantsev, and M. S. Shur, "Localized and collective magneto-plasmon excitations in AlGaN/GaN-based grating-gate terahertz modulators," *Appl. Phys. Lett.*, Vol. 99, No. 21, 213501/3, 2011.
3. Muravjov, A. V., D. B. Veksler, V. V. Popov, O. V. Polischuk, N. Pala, X. Hu, R. Gaska, H. Saxena, R. E. Peale, and M. S. Shur, "Temperature dependence of plasmonic terahertz absorption in grating-gate gallium-nitride transistor structures," *Appl. Phys. Lett.*, Vol. 96, No. 4, 042105/3, 2010.

Rare Earth Doping into Wide Bandgap Semiconductors for Photonic Applications

Abdul Majid
Physics Department, University of Gujrat, Pakistan

Abstract— Compound semiconductors after doping with Rare earth (RE) elements played vital role due to their potential applications in photonic devices. Partially filled 4f shell shielded by completely filled outer orbitals, provide intra 4f shell transitions to produce sharp optical emissions from IR to UV. In this study, energy levels induced by RE doping have been discussed. A variety of experimental techniques were used to study significant shift in absorption edge of GaN after Ce doping. In addition to this, Density Function Theory based computational results are also given to show the effects of RE doping into GaN. Doping of Ce induced formation of impurity band merged with bottom of conduction band whereas doping of Sm into GaN produced formation of two impurity bands, one merged with bottom of CB and other with top of VB. Similar results were obtained for Tm doped ZnO in which impurity band was observed merged with bottom of CB. Formation of such impurity band related to REs and their merging with principal bands points to band gap narrowing in the materials.

Session 1A2
Active Metamaterials

Artificial Neural Network Model for MNG-Metamaterial Spiral Resonator

R. Pandeeswari[1], **S. Raghavan**[1], **Amrit Krishnan**[2], **and Priyank Jain**[2]

[1]Electronics and Communication Department, National Institute of Technology, Trichy, India
[2]National Institute of Technology, Trichy, India

Abstract— In this paper, an Artificial Neural Network model for Spiral Resonators with miniaturized resonant inclusions is presented which approximates the design using four different training algorithms. The design model used to train the neural network is suitable to be employed in the practical realization of magnetic metamaterials, such as μ-negative (MNG) materials and artificial magnetodielectrics. The paper compares the performance and the capability of the four algorithms. The algorithms are Levenberg-Marquardt (LM), Scaled Conjugate Gradient (SCG), BFGS quasi-Newton backpropagation algorithms and Radial Basis Approximation. The approximation involves the determination of three parameters which are side length, strip width and dielectric spacing of the resonators for a given resonant frequency. The equivalent circuit model considered is accurate and takes care of the main physical aspects related to the interaction of the electromagnetic field with the Spiral Ring Resonator. The use of these algorithms in the paper encourages their subsequent feasibility in the field of metamaterials research. The field of metamaterials research involves models that keep changing due to the nascent nature of the field and thus any computational tool needs to be adaptive. In the paper, a model representing the Equivalent Circuit of Spiral Ring Resonator which has been updated over time has been studied and the neural network retrained to accommodate the change. The performance of the adapted neural network was re-analysed and was compared with the previous results. The results highlight the exceptional capability of neural networks in solving approximation and curve fitting problems and the ease with which we obtain the solution without tedious calculations.

Guiding Behavior of a Periodic Subwavelength Metallic Domino Array

Y. H. Kao[1], **D. J. Hou**[2], **T. J. Yang**[3], **and J. J. Wu**[2]

[1]Department of Communication Engineering, Chung Hua University, Hsinchu 30012, Taiwan, R.O.C.
[2]Department of Electrical Engineering, Chung Hua University, Hsinchu 30012, Taiwan, R.O.C.
[3]College of Engineering, Chung Hua University, Hsinchu 30012, Taiwan, R.O.C.

Abstract— Based on the mechanism of spoof surface plasmon polaritions (spoof SPPs), we present a kind of microwave waveguide, which is realized by periodic subwavelength metallic Domino array. The electromagnetic field is locally confined and penetration depth is enhanced. So that it is suitable for using as a waveguide. The transmission bandwidth of spoof SPPs is controllable by the geometric parameters of the periodic structure. The structure is shown in Fig. 1(a). The pass band is investigated by 3-D software. The calculated results are shown in Fig. 1(b) under different pitch d. Simulation and experimental results of the spoof SPPs agree well with each other. The abrupt cutoff behavior at high end is obvious and can be hopefully utilized in filter applications.

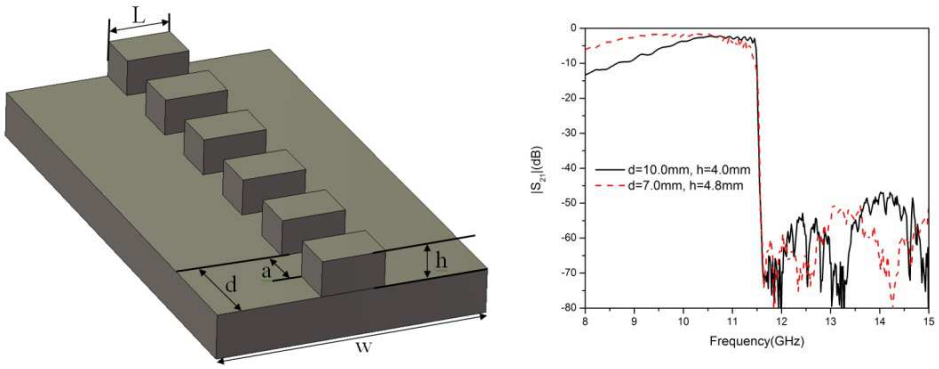

(a) (b)

Figure 1: (a) Subwavelength periodic Domino strucuture supporting spoof surface plasmon polaritons. (b) S parameters measurement for the spoof SPPs waveguide, the spacing $a = 0.5d$, the width $L = 5\,\text{mm}$. The solid black line represents the case $d = 10\,\text{mm}$, $h = 4\,\text{mm}$, and the dashed red line represents the case $d = 7.0\,\text{mm}$, $h = 4.8\,\text{mmm}$.

General Method for Modeling Nonlinear Waves in Layered Structures of Different Physical Nature Including Bi-anisotropic and Active Metamaterials

Yu. G. Rapoport
Physics Facuty, Taras Shevchenko National University of Kyiv, Kyiv, Ukraine

Abstract— New perspectives are connected with application of active and bi-anisotropic metamaterials, based on "artificial molecules", with negative refraction. In the present paper, the general method is presented, for modeling active media, where electromagnetic waves are amplifies or their losses are compensated. The method is an extension to the active media of the method [1]. This method is suitable for waves in the nonlinear layered structures including gyrotropic, nonlinear dielectric and (nonlinear and active) bi-anisotropic metamaterial layers based on "artificial molecules". The present method unifies the "microscopic" and "macroscopic" approaches. Modeling covers the individual properties of "artificial molecules", then nonlinear homogenization, and finally, determination of the (macroscopic) coefficients of the nonlinear envelope equations for the slowly varying amplitude of the narrow wave packet. It is known, for example, that amplification of the electromagnetic waves in the active "negative phase" media based on the split ring resonators with active inclusions is possible, while real parts of the dielectric permittivity and magnetic permeability are negative [2]. Moreover, active inclusion can be placed on the surface of nonlinear metamaterial layer, instead of embedding inside such a layer. Using the present method, the amplification of backward nonlinear electromagnetic waves in such media can be described in general form [3]. In addition, surface nonlinearities in layered active bi-anisotropic media are included in very natural form, basing on "transverse energy flow" and "work of nonlinear effective surface sources". Another example of active media considered in the present paper, is nonlinear parametric coupling of 2D pulses of magnetostatic waves in ferrite films [4]. It is shown that coefficient of parametric coupling can be derived, using present method, in very simple and convenient way, as well as all nonlinear coefficients [1]. Nonlinear effects of electromagnetic wave propagation in active media are investigated now. In particular, a possibility of strongly nonlinear multi-bullet (spatial-temporal soliton) structure formation (in particular four bullets) is shown, while in [5], formation of only two-bullet structures under parametric coupling was considered.

Note that the generality of the developed method is proven by it's successful application also to modeling giant second harmonics generation of nonlinear surface plasmons under temporal resonance [6], parametric amplification of electromagnetic pulses in bi-anisotropic media [7] and superheterodyne (three-wave) amplification of electromagnetic waves in layered "semiconductor-metamaterial" structures in IR range [8]. These issues are not considered here and will be published elsewhere. Nevertheless, the general method for active layered media including both surface and volume nonlinearities, reported here, can be useful for modeling nonlinear wave propagation and a lot of nonlinear devices, based in nonlinear media of different physical nature, including bi-anisotropic metamaterials.

REFERENCES

1. Rapoport, Y. G., C. E. Zaspel, V. V. Grimalsky, and S. Mondragon, *Proceedings of the 2004 14th Intern. Crimean Conf. "Microwave and Telecommunication Technology" (CriMiCo'2004)*, 361–363, IEEE Catalog No. 04EX843, Sevastopol, Crimea, Ukraine, Sept. 13–17, 2004.
2. Boardman, A. D., V. V. Grymalsky, Y. S. Kivshar, S. V. Koshevaya, M. Lapine, N. M. Litchinitser, V. N. Malnev, M. Noginov, Y. G. Rapoport, and V. M. Shalaev, *Laser & Photonics Reviews*, Vol. 5, 287–307, 2011.
3. Rapoport, Y. G., A. D. Boardman, V. I. Kanevskiy, V. N. Malnev, N. King, and L. Velasco, *16th Int. Crimean Conference "Microwave & Telecommunication Technology" (CriMiCo'2006)*, IEEE Catalog Number: 06EX1376, Sept. 11–15, Sevastopol, Crimea, Ukraine, 2006.
4. Grimalsky, V., Y. Rapoport, C. Zaspel, and A. N. Slavin, *Abstracts of the 8th European Magnetic Material and Applications Conference*, We-OB01, 38, Kiev, Ukraine, Jun. 2000.
5. Serga, A. A., B. Hillebrand, S. O. Demokrito, A. N. Slavin, P. Wierbzbicki, V. Vasyuchka, O. Dzyapko, and A. Chumak, *Phys. Rev. Lett.*, Vol. 94, 167202, 2005.
6. Grimalsky, V. V. and Y. G. Rapoport, *Plasma Phys. Reports*, Vol. 24, No. 11, 980–982, 1998.

7. Boardman, A. D., R. Mitchell-Thomas, and Y. G. Rapoport, *Proceedings of "3rd International Congress on Advanced Electromagnetic Materials in Microwaves and Optics: Metamaterials-2009"*, 495–497, London, UK, Aug. 30–Sept. 4, 2009.
8. Boardman, A. D., R. Mitchell-Tomas, and Y. G. Rapoport, *Proceedings of "3rd International Congress on Advanced Electromagnetic Materials in Microwaves and Optics: Metamaterials-2009"*, 417–419, London, UK, Aug. 30–Sept. 4, 2009.

Wave Processes and New Effects in Hyperbolic and Chiral Nonlinear and Active Metamaterials

A. D. Boardman[1], **V. V. Grimalsky**[2], **Yu. G. Rapoport**[3], **and N. A. Kalinich**[3]

[1]Salford University, Salford, United Kingdom
[2]CIICAp, Autonomous University of State Morelos, Cuernavaca, Mor., Mexico
[3]Physics Facuty, Taras Shevchenko National University of Kyiv, Kyiv, Ukraine

Abstract— Composed and active media that possess unusual electromagnetic and acoustic properties are of great interest now. When combining the thin layers of the metal (semimetal or doped semiconductor) with a negative permittivity and dielectric ones with a positive permittivity, it is possible to obtain the (anisotropic) hyperbolic medium [1] with effective (averaged) permittivities, which are positive for tangential components of electric fields and negative for normal ones. In previous paper, we developed the new method for modeling the nonlinear field concentrator based on layered inhomogeneous isotropic dielectric medium [2]. A layered cylindrical media in concentrator [2] includes external linear graded dielectric with permittivity increasing toward the center and linearly homogeneous internal dielectric cylinder with focusing and saturating Kerr nonlinearity. Consequent linear and nonlinear focusing of incident beam(s) causes the new nonlinear effect: "nonlinear focusing switching". When an amplitude of incident beam(s) exceeds some "threshold" value, very strong focusing occurs and "hot spot" is formed, while a position of focusing "jumps" from some point inside a nonlinear region to interface between nonlinear and linear media (internal and external cylinders, respectively).

It is shown in the present paper, that cylindrical and spherical hyperbolic media are also effective concentrators of energy, while the electromagnetic wave rays propagate inside the media perpendicularly to the interfaces of the layers. The values of the electric fields near the center of the structure can reach high values, and nonlinearity can manifest there.

In the present paper, the combined method [2] is extended to hyperbolic field concentrator, where electromagnetic beam propagates within the cylindrical hyperbolic medium. TM wave with the components E_r, E_θ, H_z is investigated. The saturating nonlinearity of the layers with the negative permittivity has been considered as: $\varepsilon_{1NL} = \varepsilon_1 + \alpha_1|\vec{E}|^2/(1+\alpha_2|\vec{E}|^2)$, $\mathrm{Re}(\varepsilon_1) < 0$. Here $\alpha_{1,2}$ are complex coefficients. The thicknesses of the layers are much smaller that the wavelength in vacuum.

The electromagnetic beams are incident onto the surface of the outer cylinder and propagate to the axis of the cylinder. The internal cylinder is made from the hyperbolic medium too but it is assumed as nonlinear. It seems impossible (not accurate enough) to use the averaged permittivities in the case of nonlinear media whereas in the linear media they are acceptable. The complex geometrical optics is considered within the outer cylinder, and the effective permittivities $\varepsilon_{t,n}$ are used there. The rays that reach the surface of the inner cylinder are considered as the incident waves in the derived boundary conditions. Each ray corresponds to the Gaussian wave beam. Within the internal cylinder, the full-wave approach is used for the magnetic field $H \equiv H_z$. The nonlinear wave equation for H has been solved by the expansion on the azimuthal harmonics with iterations due to nonlinearity. The nonlinearity leads to the essential redistribution of the electromagnetic energy within the internal cylinder. Moreover, when the intensities of the incident electromagnetic beams reach some threshold, the switching into the highly nonlinear regime occurs. This can be explained by the accumulation of the electromagnetic energy at the interfaces between nonlinear (with negative permittivity) and linear layers. Effects of active media (with linear/nonlinear losses/gain) on field concentration are under investigation.

Nonlinear pulses are considered in nonlinear active bi-anisotropic media and a possibility of quasisoliton amplification under a condition of parametric coupling of counterpropagating pulses is shown.

REFERENCES

1. Smolyaninov, I. I. and E. E. Narimanov, *PRL*, Vol. 105, 067402, 2010.
2. Boardman, A. D., V. V. Grimalsky, and Yu. G. Rapoport, *TaCona, AIP Conf. Proc.*, Vol. 398, 120–122, 2011.

Hydrodynamical Approach to Linear and Nonlinear Laser Excitation of the Collective Electron Motion in Metal Nanoparticles with General Shape

S. V. Fomichev[1, 2] **and A. B. Bratkovsky**[3]

[1]NRC "Kurchatov Institute", Kurchatov Place, Moscow 123182, Russia
[2]Moscow Institute of Physics and Technology, Dolgoprudny, Moscow Region 141700, Russia
[3]Hewlett Packard Labs, Palo Alto, California 94304, USA

Abstract— Collective electron excitations in metal nanoparticles (plasmons) play an important role in physics, materials science, biology, nanoelectronics and numerous applications. They can be excited by the laser light in the linear regime with respect to the laser intensity, but also in a nonlinear regime resulting, in particular, in resonance-enhanced harmonic generation. Here, we present unified hydrodynamical approach to study both linear and nonlinear forced electron dynamics in metal nanoparticles with general shape under linearly polarized laser radiation. It generally involves the nanoparticles with diffuse surface due to its importance for the nonlinear plasmon excitation. This approach is the generalization of the hydrodynamical model used before to study both the plasmon excitations in the linear regime and the second- and the third-harmonic generation resonance-enhanced by nonlinear plasmon excitation in thin metal films and spherical nanoparticles with diffuse surface. We discuss prior results of this model, and then applications to nanoparticles with more compex shapes.

Plasmonic Devices for Enhanced Raman Sensors and Other Applications

A. M. Bratkovsky[1, 2]

[1]Hewlett-Packard Laboratories, 1501 Page Mill Road, Palo Alto, California 94304, USA
[2]P. L. Kapitza Institute for Physical Problems RAS, Moscow

Abstract— Strong light confinement at a nanoscale is desirable for future optical interconnects in sensors, as well as high performance computing systems. It would also open up new possibilities for integrated sensors with much enhanced detection level. The refraction index contrast provided by group IV and III-V materials becomes insufficient for that, and one has to use metals to facilitate much larger contrast. Here, we shall describe plasmon excitations and local field enhancement by recently developed nanoparticles, like Ag octopods [1]. Star-shape geometry provides very interesting functionality of interest to surface enhanced Raman sensors. We shall describe configurable assemblies of nanoparticles supported by 'nanofingers' that provide exceptional enhancement of Raman scattering in excess of eleven orders of magnitude [2].

REFERENCES

1. Naumov, I., Z. Li, and A. Bratkovsky, *Appl. Phys. Lett.*, Vol. 96, 033105, 2010.
2. Hu, M., et al., *Nano Lett.*, Vol. 11, 2538, 2011.

A Compact Split Ring Resonator Loaded Antenna

R. Pandeeswari[1], **Singaravelu Raghavan**[1], **and Keloth Ramesh**[2]

[1]Electronics and Communication Department, National Institute of Technology, Trichy, India
[2]National Institute of Technology, Trichy, India

Abstract— In recent years, there has been a growing interest for the use of metamaterials in the antenna design. Antenna researchers tried to use the metamaterial properties to the maximum extend. It has been proved that metamaterials are a good candidate for the enhancement of antenna performance over the past years. The metamaterial property is particularly used for miniaturization of antenna.

In this paper, a compact Split ring resonator loaded antenna is presented. The proposed structure is designed on an FR4 substrate with dielectric constant 2.4 with thickness 1.6 mm, and consists of rectangular patch and circular SRR. The antenna resonates at 15.5 GHz without SRR. After loading by SRR resonant frequency is reduced to 10.35 GHz. The reduction in resonant frequency is 33.22%. The distance between the patch and the SRR is very important in determining the resonant frequency. Coaxial feeding is used for the excitation of antenna. Simulation tool, based on the method of moments (MOM)-Zeland IE3d version 12.0 has been used to analyze and optimize the antenna. The fundamental parameters of the antenna such as return loss, VSWR, gain, directivity are obtained and all meets the acceptable antenna standard.

Radiation of Chiral Molecule near Chiral Nanostructure

V. V. Klimov[1], **D. V. Guzatov**[2], **and I. V. Zabkov**[3]

[1]Lebedev Physical Institute, 53, Leninskij Prospekt, Moscow 119991, Russia
[2]YankaKupala State University of Grodno, 22 Ozheshko Str., Grodno 230023, Belarus
[3]Moscow Institute of Physics and Technology
9, Institutskij Pereulok, Dolgoprudnj, Moscow Region 141701, Russia

Abstract— Chirality is geometrical property of 3 dimensional bodiesdo not coincide with its mirror image. Chirality is very important in biology and pharmaceuticals, because many complex organic compounds have chiral properties. That's the reason for different influence of various isomers to human body. For example, enantiomers of the same substance can have different tastes, smells and effects. The chiral media in physics are under attention mostly because of current possibility of creation metamaterials on the basis of chiral objects.

In this work, we have investigateddecay rate of optically active molecule near cluster consisting of two optically active (chiral) spheres. All analytical results were obtained for arbitrary size of spheres, distance between them and materials. For describing the electric and magnetic fields in the chiral spherical particles, we use the constitutive equations in the Drude-Born-Fedorov form: $\vec{D} = \varepsilon(\vec{E} + \chi\, rot\, \vec{E})$; $\vec{B} = \mu(\vec{H} + \chi\, rot\, \vec{H})$, where $\vec{D}$, $\vec{E}$ and $\vec{B}$, $\vec{H}$ — are the inductions and the strengths of the electric and magnetic fields respectively, ε, μ — are permittivity and permeability, χ is the dimensional chirality parameter. As a model of an optically active molecule we assume that its radiation is of both electric ($\mathbf{d}_0$) and magnetic ($\mathbf{m}_0$) dipole nature. Relative decay rate of excited molecule can be obtained as the ratio of the radiation power of the molecule near cluster and the radiation power of a molecule in free space. For numerical calculations we use RF module of Comsol 4.2a.

The geometry of a problem is shown in Fig. 1(a). Effective radiative decay rate of a chiral molecule places near two chiral spheres is shown in Fig. 1(b). The difference between "left": $\mathbf{m}_0 = -0.1\mathbf{d}_0$ and "right": $\mathbf{m}_0 = +0.1\mathbf{d}_0$ molecules can be clearly seen and it can be increased significantly for double negative material and negative material.

As the results the analytic expression for decay rate of radiation of optical active molecule near two chiral spheres was obtained. The numerical modeling of such system was performed and good agreement with analytical results was found. It is shown that decay rate of "left" and "right" enantiomer molecules situated near cluster of two chiral nanoparticles can differ significantly (by 2 or 3 orders of magnitude) which allow using such system for detection and separation left and right enantiomer molecules.

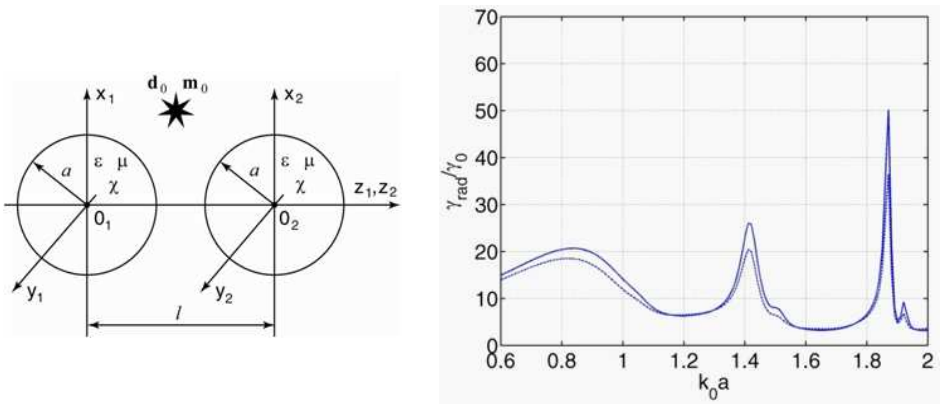

(a) (b)

Figure 1: (a) Geometry of the structure under investigation. (b) Relative decay rate of a chiral molecule placed near first sphere ($z \to a$) as a function of $k_0 a$ with fixed distance $l/2a = 1.1$ between spheres. Optical properties of spheres are following: $\varepsilon = 6$; $\mu = 1$; $\chi = 0.1$. The solid line corresponds to the "right" molecule, and the dashed line corresponds to the "left" molecule.

Luminescence in Plasmonic Antennas and Nanolasing

A. Bogdanov[1], **I. Fedorov**[2], **A. N. Lagarkov**[3], **G. Tartakovsky**[4], **and A. K. Sarychev**[3]

[1]Hitachi Global Storage Technologies, San Jose Research Center
3403 Yerba Buena Road, San Jose, CA 95135, USA
[2]Moscow Institute of Physics and Technology, 9 Institutskii per.
Dolgoprudny, Moscow Region 141700, Russia
[3]Institute for Theoretical and Applied Electrodynamics, Russian Academy of Sciences
13 Izhorskaya St., Moscow 125412, Russia
[4]Innovative Optical Solutions, 5235 Fiore Terrace Unit, San Diego, CA 92122, USA

Abstract— In recent years, the surface plasmonic excitations in the nanoantennas and in the ordered array of metal nanoparticles have attracted significant attention of researchers studying the plasmonic metamaterials due to their numerous potential applications in modern optics. In our paper we consider nanoantennas and set of ordered metal particles shaped as horseshoes arranged inside the layer of actively pumped dielectric medium. Size of the considered nanoantennas is much less than the wavelength of the light. On this scale the laser pumping can be treated as a random external force because of the process of photon absorption by the active medium is intrinsically incoherent. Thus, the response of the plasmonic nanoantennas immersed in the active medium is caused by the action of the random electromagnetic field and should be treated at the microscopic level. We have shown that this response is different from the usual plasmon resonances in metal particles. The main result of this paper is the prediction of the evolution of the luminescence spectrum in response to the changes in shape of the nanoantennas and level of the inversion. The predicted luminescence spectrum manifests some minima and maxima which correspond to the excitation of various SP resonances and is in a good agreement with our experiments. We have calculated the gain required to achieve the lasing threshold as a function of the antennae structure. Resonant frequencies of the nanoantennas and the field enhancement factor can be conveniently tuned by the variation of the size and shape of the plasmonic nanoantennas. The proposed nanolaser can have many applications, such as the core device for the transmission and processing of optical signals on a scale much smaller than the wavelength.

Spaser-effect for Loss Compensation in Metamaterials

A. P. Vinogradov[1], **E. S. Andrianov**[1], **A. A. Pukhov**[1], **A. V. Dorofeenko**[1], **and A. A. Lisyansky**[2]

[1]ITAE RAS, 13 Izhorskaya, Moscow 125412, Russia
[2]Department of Physics, Queens College
The City University of New York, Flushing, NY 11367, USA

Abstract— Numerous attractive applications of metamaterials are ordinarily killed by Joule losses. It may be possible to overcome this obstacle by introducing active media into the metamaterial matrix [1–3]. This leads to the formation of a system of spasers inside a metamaterial.

Above the pumping threshold the spaser is an autonomic system with frequency and amplitude depending only on spaser's parameters [4, 5]. Even though it is possible to force the spaser to operate at the frequency of an external field, the amplitude of the spaser oscillations depends weakly on the external field [6, 7].

We show that a spaser operating below threshold can be used for loss compensation in metamaterials. Such a spaser is no longer autonomic. It is always synchronized with the external electromagnetic wave and its amplitude of oscillations depends nonlinearly on the field's amplitude. Even though the external wave adds to Joule losses, it is still possible to achieve complete loss compensation over a wide pumping range.

REFERENCES

1. Ramakrishna, S. A. and J. B. Pendry, *Phys. Rev. B*, Vol. 67, 201101, 2003.
2. Popov, A. K. and V. M. Shalaev, *Opt. Lett.*, Vol. 31, 2169, 2006.
3. Sarychev, A. K. and G. Tartakovsky, *Phys. Rev. B*, Vol. 75, 085436, 2007.
4. Bergman, D. J. and M. I. Stockman, *Phys. Rev. Lett.*, Vol. 90, 027402, 2003.
5. Protsenko, I. E., *Phys. Rev. A*, Vol. 71, 063812, 2005.
6. Vinogradov, A. P., et al., *Opt. Express*, Vol. 19, 24849, 2011.
7. Vinogradov, A. P., et al., *Opt. Lett.*, Vol. 36, 4302, 2011.

Dynamical Metamorphoses in Arrays of Nonlinear Plasmonic Nanoparticles

Roman E. Noskov[1], **Pavel A. Belov**[1], **and Yuri S. Kivshar**[1, 2]

[1]National Research University of Information Technologies
Mechanics and Optics (ITMO), St. Petersburg 197101, Russia
[2]Nonlinear Physics Centre, Research School of Physics and Engineering
Australian National University, Canberra ACT 0200, Australia

Abstract— Nonlinearity-induced instabilities are observed in many different branches of physics, and they provide probably the most dramatic manifestation of strongly nonlinear effects that can occur in nature. Modulational instability (MI) in optics manifests itself in a decay of broad optical beams into optical filaments (or pulse trains) [1], and such effects are well documented in both theory and experiment. It is expected that the study of subwavelength nonlinear systems such as metallic nanowires or nanoparticle arrays may bring many new features to the physics of MI and the scenarios of its development; however, such effects have attracted researcher's attention only recently.

Over the past decade, surface plasmons were suggested as the mean to overcome the diffraction limit in optical systems. In particular, by using plasmons excited in a chain of resonantly coupled metallic nanoparticles, one can spatially confine and manipulate optical energy over distances much smaller than the wavelength. In addition, strong geometric confinement can boost efficiency of nonlinear optical effects, including the existence of subwavelength solitons [2, 3].

In this work, we introduce and study a novel class of nonlinear effects in arrays of subwavelength metallic nanoparticles with a nonlinear response. More specifically, we focus on two fundamental nonlinear phenomena: (i) modulational instability and (ii) bistability. In particular, we demonstrate that a bistable nonlinear response of each nanoparticle in the array can lead to the formation of a novel type of nonlinear localized modes — plasmonic kinks, which describe switching waves connecting two different states of polarization of metallic nanoparticles [4]. Such plasmonic kinks are characterized by a subwavelength extent and a tunable velocity. Moreover, two slowly moving kinks of the opposite polarity are able to create a stable bound state which can be regarded as a deeply subwavelength dissipative plasmon soliton.

We also show that modulational instability in such nanostructures can lead to generation of long-lived standing and moving nonlinear localized modes in the forms of oscillons [5] and solitons. We reveal that a wide variety of scenarios of MI development allows mode transformation from one type to another, changing movement direction and a velocity of drifting oscillons and solitons as well as formation of stable domain walls connecting not only different stationary states but also the states with different types of nonlinear dynamics (e.g., chaotic-like and regular).

ACKNOWLEDGMENT

The authors acknowledge a support from the Australian Research Council and a megagrant of the Ministry of Education and Science of Russian Federation, as well as fruitful discussions with A. A. Zharov.

REFERENCES

1. Bespalov, V. I. and V. I. Talanov, "Filamentary structure of light beams in nonlinear liquids," *JETP Lett.*, Vol. 3, 307, 1966.
2. Liu, Y., G. Bartal, D. A. Genov, and X. Zhang, "Subwavelength discrete solitons in nonlinear metamaterials," *Phys. Rev. Lett.*, Vol. 99, 153901, 2007.
3. Ye, F., D. Mihalache, B. Hu, and N. C. Panoiu, "Subwavelength plasmonic lattice solitons in arrays of metallic nanowires," *Phys. Rev. Lett.*, Vol. 104, 106802, 2010.
4. Noskov, R. E., P. A. Belov, and Y. S. Kivshar, "Subwavelength plasmonic kinks in arrays of metallic nanoparticles," *Opt. Express*, Vol. 20, 2733, 2012.
5. Noskov, R. E., P. A. Belov, and Y. S. Kivshar, "Subwavelength modulational instability and plasmon oscillons in nanoparticle arrays," *Phys. Rev. Lett.*, Vol. 108, 093901, 2012.

Session 1A3
Theory and Methods of Digital Signal and Image Processing 1

WA-systems of Functions in Reconstruction and Visualization of 2D and 3D Images

V. F. Kravchrnko[1], **D. V. Churikov**[1], **V. I. Ponomaryov**[2], **and H. M. Perez-Meana**[2]

[1]Kotel'nikov Institute of Radio Engineering and Electronics
Russian Academy of Sciences, Moscow, Russia
[2]National Polytechnic Institute of Mexico, Mexico-city, Mexico

Abstract— This invited report presents short review of novel class of functions*: Atomic Functions* (AF) and following from them novel families of wavelets: *Wavelet Atomic Function* (WAF). Second part of this paper exposes several examples of successful applications of WAF in different problems explained below. **3D Video Visualization Employing Wavelet Multilevel Decomposition**: Novel approach based on WAF has been efficiently employed in 3D video sequence visualization. The procedure consists of multilevel decomposition and 3D visualization applying color anaglyphs synthesis. Simulations on synthetic images and video sequences, also on real-life video sequences have confirmed sufficiently better proposal performance in depth and spatial perception in comparison with existing methods. **Super-resolution applying classic wavelets and WAF:** Novel method in high-resolution uses WAF in the reconstruction of colour and greyscale video sequences of different types. The approach is theoretically justified by analysis based on key wavelet properties (*cosine projection*, *Reisz values*, etc.). Statistical simulation results have shown that method based on WAFs performs better at improving resolution than do existing frameworks. Implementations on DSP have demonstrated the possibility of real-time processing in super-resolution. **Mammography features classification in wavelet transform space:** The principal mammography (MG) signs of breast cancer are clustered in the micro calcifications (MCs) and masses. Novel method for masses and MCs classification in the MG employs Wavelet Transform (WT) based on classical and WAF, decomposing MG for reducing data volume in the classification stage that is performed via multilayer artificial neural network (ANN) type classifier. The experimental results have shown sufficiently good performance of proposal on real data, showing better rate of recognition for *benign*, *malign* and *normal* MGs. Daubechies wavelets and WAF have been adapted in mentioned network in classification of MG principal features: MCs, speculated and circumscribed masses, presenting sufficiently better classification results than existed methods can do.

Other examples of sufficiently effective AF and WAF employment are exposed in this lecture, among them: *pulse compression in radars, medical image compression*, and *image segmentation.*

REFERENCES

1. Kravchenko, V. F., *Lectures on the Theory of Atomic Functions and Their Some Applications*, Radiotechnika, Moscow, 2003.
2. Kravchenko, V. F. and V. L. Rvachev, *Boolean Algebra, Atomic Functions and Wavelets in Physical Applications*, Fizmatlit, Moscow, 2006.
3. Kravchenko, V. F., H. M. Perez-Meana, and V. I. Ponomaryov, *Adaptive Digital Processing of Multidimensional Signals with Applications*, Fizmatlit Edit., Moscow, 2009, (http://www.posgrados.esimecu.ipn.mx/docs/Kravchenko_Perez_Ponomaryov_Book.pdf).

Nonparametric Estimations of Probability Density Functions Based on the Family of Atomic Functions $ch_{a,n}(x)$ in Problems of Digital Signal Processing

V. F. Kravchrnko[1], **Ya. Yu. Konovalov**[2], **and D. V. Churikov**[1]

[1]Kotel'nikov Institute of Radio Engineering and Electronics
Russian Academy of Sciences, Moscow, Russia
[2]Bauman Moscow State Technical University, Moscow, Russia

Abstract— Atomic functions (AF) [1–6] have found wide application at the decision of applied problems of physics and technics. The most known and studied AF is function $up(x)$. Its natural generalization is family of AF $h_a(x)$. The convolutions of these functions $\Xi_n(x) = \underbrace{h_{n+1} * \ldots * h_{n+1}}_{n}$ and $cup(x) = up(x) * up(x)$ which also are AFs have practical importance. In the report the family of AFs $ch_{a,n}(x) = \underbrace{h_a * \ldots * h_a}_{n}$ which is generalization of listed families of functions is considered. Using of new family of AFs $ch_{a,n}(x)$ as weight functions (WF) offers the following advantages:

- Allows to investigate properties of known AFs $up(x)$, $h_a(x)$, $cup(x)$, and $\Xi_n(x)$ from uniform positions.
- Presence of two parameters allows applying the AFs $ch_{a,n}(x)$ more flexibly for a wide range of problems of digital signal processing (DSP) and the mathematical physics, choosing for each of them the most suitable functions from this family.
- As the AFs $ch_{a,n}(x)$ are generalization of known AFs then their application is possible in any problems to which decision the AFs $up(x)$, $h_a(x)$, $cup(x)$, and $\Xi_n(x)$ are applied.

Rigorous definition of family of AF $ch_{a,n}(x)$ and also the proof of their existence is made. Methods of their calculation are offered. On basis of the new WFs the nonparametric estimations of probability density function and its derivatives are considered. The technique offered in the report is illustrated on concrete physical models.

REFERENCES

1. Kravchenko, V. F., "Lectures on the theory of atomic functions and their some applications," *Radiotechnika*, Moscow, 2003.
2. Kravchenko, V. F., "New synthesized windows," *Dokl. Akad. Nauk*, Vol. 382, No. 2, 190–198, 2002.
3. Kravchenko, V. F., V. L. Rvachev, and V. A. Rvachev, "Mathematical methods for signal processing based on atomic functions," *Journal of Communications Technology and Electronics*, Vol. 40, No. 12, 118–137, 1995.
4. Kravchenko, V. F., V. I. Pustovoit, and D. V. Churikov, "Atomic Functions and the probability density function estimations," *Doklady Physics*, Vol. 56, No. 9, 74–478, 2011.
5. Kravchenko, V. F. and D. V. Churikov, "Atomic functions in nonparametric estimations of probability density functions and their derivatives," *Proceedings. Int. Conference "DAYS on DIFFRACTION"*, 103–105, St. Petersburg, Russia, 30 May–3 June 2011.
6. Konovalov, Y. Y., "Iterative algorithms for numerical solution of differential equations with linearly transformed argument," *Electromagnetic Waves and Electronic Systems*, Vol. 16, No. 9, 49–57, 2011.

Statistical Synthesis of Optimal and Quasi-optimal Chopper Radiometers

Victor F. Kravchenko[1], **Valery K. Volosyuk**[2], **and Vladimir V. Pavlikov**[2]

[1]Kotel'nikov Institute of Radio Engineering and Electronics
Russian Academy of Sciences, Moscow, Russia
[2]N. Ye. Zhukovsky National Aerospace University ("Kharkov Aviation Institute")
Kharkov, Ukraine

Abstract— It is known that for antenna parameter measurement in remote sensing, radio astronomy, medicine problems it is using the radiometric devices. The most using devices in science and engineering sectors are chopper radiometers videlicet, classical chopper radiometer, null balancing and their modifications. These radiometers are designed on base of engineering experience. This is can't show refinements of optimal radiometric signal processing and their potential characteristics. At the same time essential experience of use of the theory of statistical decisions and estimations of parameters for the decision of various problems of a radar-location, remote sounding etc are now stored. In the present the practical interest causes the decision of statistical synthesis of modulation radiometers problems with partially definition structure, creation of the block diagrams corresponding to optimum and quasioptimum algorithms of processing, and also their research potential accuracy and fluctuation sensibility. All it makes an important and actual direction of researches. In active location by choosing of a sounding signal the parameters and characteristics of system are changed [1]. In a passive location stochastic signals are subject to processing. This is limiting control of radiometers characteristic. Therefore at synthesis of optimum devices and systems in a passive radar-location it is expediently to set of partially structures of entrance radio meter circuits. Such structure usually follows from generalization of practical experience. So it is known that modulation of a useful signal reduces influence of instability of entrance chains of radio meters. Therefore radio meters of modulation type are widely applied at carrying out of practical researches. Accordingly search of optimum structure of such radio meter assumes statement of a problem of synthesis with the partial task of the entrance path including the modulator. For a correctness of synthesized algorithms it is necessary to include in partially set structure the peak-frequency characteristic of entrance chains [2]. Besides, it is frequent for maintenance of calibration in the course of measurements in structure include a basic source with known parameters. Connect such source through the operating switch (modulator) during time moments when the receiver input on a useful signal of the aerial is locked. The aim of this report is statistical synthesis of optimal and quasi-optimal chopper radiometers, analysis of their potential accuracy and fluctuating sensitivity. It is shown that the optimum algorithm of estimation object brightness temperature is not effect on instability of input frequency radiometer characteristic. The modeling in the environment of SystemVue completely confirms the received theoretical results and conclusions.

REFERENCES

1. Volosyuk, V. K. and V. F. Kravchenko, *Statistical Theory of Radio Technical Systems of Remote Sensing and Radar*, Fizmatlit, Moscow, 2008.
2. Volosyuk, V. K. and V. V. Pavlikov, "Statistical synthesis of one-antenna chopper radiometric receivers," *Applied Radio Electronics: Sci. Mag.*, Vol. 10, No. 3, 285–294, 2011.

Maximum Permissible Values of Biometric Code Bits Correlation

V. Bezyaev[1], **I. Serikov**[1], **A. Kruchinin**[1], **N. Ivanushchak**[1], **and M. Sekretov**[2]

[1]Public Corporation "Research and Production Enterprise 'Rubin'", Russia
[2]Public Corporation "Penza Research Electrical Engineering Institute", Russia

Abstract— The article considers a problem of modeling long output codes of the neural network "biometrics-code" transformer.

The work shows that it is complicated to investigate statistical features of the 256-bit "Foe" code with its entropy of around 60 bits by common techniques.

In order to simplify the problem under investigation the authors suggest a conversion into Hamming distances dimension between "Friend" and "Foe" codes. The conversion from investigating statistics of normal codes emergence to investigating statistics of distribution of Hamming distances emergence probabilities theoretically allows to decrease problem's complexity from exponential to nearly linear complexity. The cause of such cardinal simplification of the problem is the fact that the Hamming distances distribution for long biometric codes is well-described by the normal law of values distribution.

The researchers have built a nomogram of the Hamming distance distribution for 256-bit codes and various correlation values between biometric code bits. The nomogram shows that provided low values of code bits correlation coefficient the distribution of Hamming distance values is close to the normal distribution law. However, as the controlled parameter — r increases, the normal law of distribution gradually transforms into the uniform law of values distribution. As the code bits correlation changes from 0.0 to 0.35, the hypothesis of normality of the Hamming code distribution remains operable.

The authors emphasize that, according to the nomogram, for the codes of any length with bits correlation of 0.5 the Hamming distance distribution remains uniform. This means that $r = 0.5$ is the maximum permissible point. In case the code bits correlation is higher, the neural network "biometrics-code" transformer is absolutely unable to protect user's biometrics data, marked during the instruction in its artificial neuronet parameters.

When the code bits correlation decreases, the "biometrics-code" transformer exponentially recovers its protective capability. If the biometric code bits correlation tends to 0.0, the level of biometric data security is comparable to the cryptographic algorithm security level.

On the Issue of Modeling Long Biometric Codes with Dependent Bit States

V. Bezyaev[1], **I. Serikov**[1], **A. Ivanov**[2], **I. Urnev**[3], **A. Kruchinin**[1], **and N. Ivanushchak**[1]

[1]Public Corporation "Research and Production Enterprise 'Rubin'", Russia
[2]Public Corporation "Penza Research Electrical Engineering Institute", Russia
[3]Penza State University, Russia

Abstract— The article considers a problem of modeling long output codes for the neural network transformer of analogue (continuous) biometric data into the output digital code. Modeling of independent code strings is not a complicated problem. For example, in order to model a single 256-bit it is sufficient to execute a 256-fold reference to the software or hardware random-number generator. After that, one may find a matrix of biometric code bits correlations and build a proper matrix of transformation for it. It is technically feasible to calculate the correlation matrix and the corresponding matrix transformation for codes of 2–16 bits length. However, this method works out only for the codes of short length. Beyond this limit the problem becomes incorrect.

Thereby, it is necessary to synthesize the matrix binding independent data by means of another non-classical algorithm. The new concept of binding independent pseudorandom data is based on the necessity to synthesize a certain data-binding matrix which would save only statistics of correlations. If the precise transformation is impossible to create, the transformation providing the required dual correlation coefficient distribution is real.

As a result of statistical investigation the authors have built a nomogram of connection between the controlled modeling parameters and the mathematical expectation of the module of pair correlation coefficients with the length of parameters' vector $n = 2, 4, 8, 16, 32, 64, 128$. Nomogram results show that the increase of problem's dimensionality causes the values of dual correlation coefficients $r(a)$ to tend closer and closer to the coordinate axes. In general, evaluation of $r(a)$ function is quite a simple problem not requiring any considerable computing resources. The controlled parameter "a" is conveniently located in the range from 0.0 to 1.0, as well as the module of dual correlation coefficients.

Thus, one may obtain the distribution of biometric data (biometric codes) generator with the possibility to control the mathematical expectation and the root-mean-square deviation of distribution of dual correlation coefficients of biometric data and biometric codes.

Statistical Description of Output States of the Neural Network "Biometrics-code" Transformers

A. Ivanov[1], **B. Akhmetov**[2], **V. Funtikov**[1],
A. Malygin[3], **and I. Urnev**[3]

[1]Public Corporation "Penza Research Electrical Engineering Institute", Russia
[2]Institute of Information and Telecommunication Technologies, Republic of Kazakhstan
[3]Penza State University, Russia

Abstract— The article considers a problem of statistical description of the neural network "biometrics- code" transformer. It is shown that the classic binominal law of distribution is applicable only for ideal "biometrics-code" transformers. According to the standard ГОСТР 52633.0-2006 stipulating general requirements for output codes, the ideal "biometrics-code" transformers should provide absolute dual independence of output code bits.

For real "biometrics-code" transformers it is necessary to modify the binary law of distribution to take into consideration the misbalance of probabilities of biometric code bits' states and the correlation of the bits. Any misbalance of "0" and "1" states emergence probability will inevitably result in quality decrease of "biometrics-code" transformers (decrease in output codes entropy).

The article also considers registration of existing correlations between biometric code bits. During statistical analysis the authors have imitated the operation of a "biometrics-code" transformer with 256 outputs. The identical value of dual coefficients of correlation between output code bits has been taken as the only controlled parameter — "r". The article adduces the distribution of Hamming distance values' emergence probabilities with different values of the controlled parameter $r = 0.05, 0.10, \ldots, 0.48$.

Another peculiarity of real "biometrics-code" transformer is that the values of dual coefficients of correlation between code bits have a symmetric distribution relative to the point $r = 0.0$. The article gives an example of correlation coefficients distribution in the 256-bit "biometrics-code" transformer. The most probable value of correlation coefficients is zero; all the obtained values of correlation coefficients remain in the range ± 0.5. Simple averaging of correlation coefficients is inadmissible. According to the experience, the best approach to obtain a good match of imitation results with reality is to use mathematical expectation of modules of dual correlation coefficients as the controlled parameter — r.

In case of averaged parameters application the dimensionality of statistical description of output code states may significantly decrease. If the key length is $n = 256$, the statistical description in the Hamming distances dimension is displayed in the form of corresponding tables with convertible parameters r (pitch 0.01, interval from 0.00 to 0.99) and P ("0") (pitch 0.01, interval from 0.01 to 0.5).

Evaluation of Multidimensional Entropy on Short Strings of Biometric Codes with Dependent Bits

V. Funtikov[1], **B. Akhmetov**[2], **A. Ivanov**[1], **and I. Urnev**[3]

[1]Public Corporation "Penza Research Electrical Engineering Institute", Russia
[2]Institute of Information and Telecommunication Technologies, Republic of Kazakhstan
[3]Penza State University, Russia

Abstract— This study demonstrates resonant frequencies of several shorting pin loaded circular antennas, which are dual-frequency antennas. Dual-frequency operation is formed by using a shorting pin, which is connected between ground and the radiated part of the antenna. There are various studies, which are used to produce dual-frequency operation, and among those methods, a shorting pin is used to form dual frequency circular patch antennas since there are rare studies on this issue and size reduction is possible by inserting a pin to an antenna. This study is done to expand the studies in the literature about a shorting pin loaded circular patch antennas. The parameters that affect the resonant frequencies of the antenna are also evaluated. The thickness, permittivity and shorting pin positions are varied and the resonant frequencies are examined according to the change of these parameters. Frequency ratios are determined for each variation and the results are compared.

Antennas are the crucial element of wireless systems and patch antennas are one of the most important elements in today's communication systems. Microstrip patch antennas, which are resonant antennas, are popular due to their low weight, low profile and cheap for printed circuit construction [1–7]. Efficient design of an antenna can increase the overall performance of the communication systems. Since the efficient design of a patch antenna is crucial, calculating design parameters such as resonant frequency and input impedance is getting more and more important [1–3]. Dual frequency operations are also popular in wireless communications and there are several methods to form a dual frequency such as slot, slit and shorting pin loading [2]. In designing the dual frequency antenna, an important parameter is to achieve higher frequency ratios with lower sizes. The frequency ratio is determined as the ratio of the upper frequency to the lower frequency in literature [3]. Inserting a shorting pin is mostly preferred because it significantly reduces the size of the antenna [3]. In this study, a dual frequency antenna is presented and a shorting pin is used to form a dual circular patch antenna. Inserting a shorting pin to a circular patch is preferred because the studies in literature show that shorting pin loaded circular antennas have larger frequency ratios when compared to the rectangular ones [4]. Frequency ratio characteristics examined and the ratios are determined for different permittivity, thickness and shorting pin positions. The upper and lower frequencies are examined for different permittivity values.

The variation of frequencies with respect to a ratio of shorting pin position to the radius of the circle is demonstrated for a substrate thickness 0.16 cm. A decrease is observed in the lower frequency with an increase in the position ratio. An increment is also observed in the upper frequency with an increment in the ratio of the positions. The frequency ratios (r) are also demonstrated according to the permittivity and shorting pin positions. Maximum frequency ratio is observed with an antenna which has a permittivity value $\varepsilon_r = 2.2$ at a position ratio $d_S/d = 0.9$. Minimum frequency ratio is observed with an antenna which has a permittivity value $\varepsilon_r = 4.4$ at a position ratio $d_S/d = 0.1$. All these data prove that the permittivity of the substrate changes the upper and the lower frequencies but the effect of the permittivity value to the frequency ratio is not significant. Besides, the ratio of the radius and the shorting pin position from the centre of the circle (d_S/d) increase the frequency ratio. The antennas with different permittivity values which have a radius = 2.186 cm and a substrate thickness $h = 0.16$ achieve a frequency ratio approximately 3.5 at a ratio 0.9 while it was about 2.2 at a ratio was 0.1. The effect of the thickness to the frequency ratio is also examined for an antenna with a radius 2.186 cm which has a permittivity value of $\varepsilon_r = 4.4$. Varying the thickness changes the frequency ratio and the lowest thickness value, which is 1 mm, achieved the maximum frequency ratio. The studies in the literature demonstrate a null voltage point according to the ratios of the positions in equilateral patches [3]. The null voltage point is determined at a ratio around 0.33. A null voltage point is observed at a distance ratio around 0.3. Thickness parameter has a negligible effect at that point and the frequency ratio remains around 2.45 for each thickness value.

Table 1: Comparison with simulated results of the proposed antennas with ones proposed in [6] and frequency ratio.

Antenna	d (cm)	d_s (cm)	h (cm)	ε_r	F_{lower} (MHz)	F_{upper} (MHz)	F_{lower} error (%)	F_{upper} error (%)	r
A [6]	2.186	2.1	0.16	4.4	568	2176	–	–	3.83
B	2.186	2.1	0.16	4.4	596.9	2190	5.09	0.64	3.66
C	2.186	2.12	0.03	2.08	834.5	3185.6	–	–	3.82

Reducing the size of the antenna is important for the designers. An antenna (C) with a frequency ratio 3.82 is proposed with a side length 2.186 cm and permittivity value $\varepsilon_r = 2.08$ which has a lower thickness when compared to the one in the literature [6]. However, the antenna C is capable of achieving the same frequency ratio. The antenna proposed in the literature (A) is compared with the antenna (B) and error calculated for both upper and lower frequency. The error obtained is 5.09% for the lower frequency and 0.64% for the upper frequency. Several antennas are proposed for achieving high frequency ratios for dual frequency operations. The frequency ratios are demonstrated for different radius, thickness and position ratios. It is concluded that increasing the distance ratio of the shorting pin to the radius significantly increases the frequency ratio in shorting pin loaded circular patch antennas. It is also obtained that an antenna with lower size and thickness higher frequency ratios are achievable. It is also seen that thickness parameter has a negligible effect on frequency ratio at a critical point where the ratio d_S/d is around 0.3. An antenna is also proposed with smaller size, but achieves the same frequency ratio.

REFERENCES

1. Aydın, E. and S. Can, "Modified resonant frequency computation for tunable equilateral triangular microstrip patch," *IEICE Electronics Express*, Vol. 7, No. 7, 500–505, 2010.
2. Can, S., "Computation of resonant frequency of dual band triangular patch antenna," Master's Thesis in Electrical & Electronics Engineering, Atılım University, Turkey, Jul. 2011.
3. Aydın, E. and S. Can, "Operating frequency calculation of a shorting pin-loaded ETMA," *Microwave and Optical Technology Letters*, Vol. 54, No. 6, 1432–1435, Jun. 2012.
4. Kumar, P. and G. Sing, "Microstrip antennas loaded with shorting post," *Engineering*, Vol. 1, No. 1, 41–45, Jun. 2009.
5. Kumar, P. and G. Sing, "Theoretical computation of input impedance of gap-coupled circular microstrip patch antennas loaded with shorting post," *Journal of Computational Electronics*, Vol. 10, No. 1–2, 195–200, Jun. 2011.
6. Tang, C. L., H. T. Chen, and K. L. Wong, "Small circular microstrip antenna with dual frequency operation," *Electronic Letters*, Vol. 33, No. 13, 1112–1113, Jun. 1997.
7. Gurel, Ç. S., E. Aydın, and E. Yazgan, "Computation and optimization of resonant frequency and input impedance of a coax-fed circular patch microstrip antenna," *Microwave and Optical Technology Letters*, Vol. 49, No. 9, 2263–2267, Sep. 2007.

Information-telecommunication System with Multibiometric Protection of User's Personal Data

Vladimir Volchikhin[1], **Alexander Ivanov**[2], **Ivan Urnev**[1], **and Alexander Malygin**[1]

[1]Penza State University, 40 Krasnaya Str., Penza 440026, Russia
[2]Penza Research Electrical Engineering Institute, 9 Sovetskaya Str., Penza 440000, Russia

Abstract— The development of digital information technologies has faced a problem of access and protection of information resources from unauthorized access.

Penza State University (PSU) together with "Rubin" plc. and "Penza Research Electrical Engineering Institute" plc. is on the final stage of development and preproduction of telecommunication equipment, as well as development of network, applied and special software to build a digital communication network with personal access, maintaining high-level protection of personal data on the basis of biometric methods.

The system provides transformation of personal biometric data into the access code and safe storage in a neural network container in accordance with the standard ГОСТ Р 526333.0-2006.

The authors have used the following image processing methods as personal biometric parameters:

- processing of papillary finger print;
- processing of handwritten password;
- processing of 3D face image.

Research and technical solutions offered in the given project are based on the concept of a neural network biometric depersonalized container, which can be created by instructing a neuronet. It is a person with his/her fingers, handwriting and face who is the access key into the information-telecommunication system. He/she doesn't have to wright down and memorize a pin-code or any other key information vulnerable to external threats and attacks.

The developed means of highly reliable multibiometric authentication have to provide the personal authentication index on the level 10^{-12} in accordance with the standard ГОСТ Р 52633.0 ÷ 52633.5. American Bio IP systems of standards provide this index on the level 10^{-5}.

At the present time PSU in cooperation with its contractors is completing the development of construction and technological documents on component elements of the information-telecommunication system, intended to be applied by corporative structures (schools, universities, organizations, business), as well as by government bodies.

Testing samples of components and software have already passed the preliminary testing and are ready for operation testing.

Optimum Algorithm of Formation of Radar-tracking Images in CW SAR

A. A. Prilutskiy, **A. N. Detkov**, **and D. A. Nitsak**
JSC Distant Radiocommunication Scientific Research Institute
d.12/11, 1-ya vul. Buhvostova, Moscow 107258, Russia

Abstract— The report is devoted the decision of an actual problem of synthesis of optimum system of processing of trajectory signals for CW-SAR. The offered model of a radar-tracking relief allows to synthesize optimum algorithm of formation of the radar-tracking image in the SAR and to receive an estimation of function of a radar-tracking relief by criterion of a minimum of an average square of an error. Conditions at which application of the Bayes's approach for formation of optimum algorithms of processing of trajectory signals of the onboard SAR is possible are scrupulously analyzed.

As a whole the offered algorithm of a recurrent estimation represents a variant of linear Kalman filter adapted for processing of signals of the SAR. One of advantages of this way is that unlike all others the algorithm of processing of signals is recurrent, the estimation of a radar-tracking relief begins with the beginning of sounding with a delay for the period of accumulation of signals, by the end of an interval of synthesizing with a delay for the period of accumulation of signals process of formation of the radar-tracking image comes to an end.

Results of modeling confirm efficiency of the offered optimum algorithm of processing of trajectory signals. The algorithm allows receiving high resolution on an azimuth, realizing super resolution principles (resolutions of higher, than on an exit of the marched filter). The synthesized kvazioptimal filter is a basis for the subsequent operations of the automated or automatic autofocusing of radar-tracking images.

Wavelet-based Human Synthetic Movement Recognition in Sterile Zone Scenario

Ioannis Kypraios
Department of Engineering & Informatics, ICTM, London, E1 1EG, UK

Abstract— In the last decade, there has been a growing research into video content analytics algorithms for smart cameras or for server-based environments. Video content analytics algorithms have been applied for detecting and classifying different events in real-time applications and scenarios. Recently, UK's Home Office has developed several video datasets for being used as benchmarks in evaluating the performance of state-of-the art algorithms. In this paper, we focus on sterile zone scenario for detecting the presence of persons in a restricted area. We have categorised monitored human object movement into basic, synthetic, and complex synthetic, in order to be recognised by our developed algorithm. We define basic movement to consist of 'walking' or 'crawling', synthetic movement to consist of a linear combination of basic movements, and complex synthetic movement to consist of a non-linear function of basic movements. Previously, we have conducted extensive research work on wavelet-based filters. It was proven that wavelets can be used for extracting illumination invariance scene features. In particular, here, we use Non-Linear Difference of Gaussians-based wavelet filter for selecting illumination invariant features and, then, combine them efficiently into the background reference frame. Non-Linear Difference of Gaussians-based wavelet filter forms a type of band-pass filter with lower and upper cutoff frequencies set by the two Gaussian kernels. Our algorithm exploits a robust tracking mask for separating multiple object categories, as those are defined by the given scenario, and, then, recognising the different human movements in the monitored area. We have applied it on Home Office's video datasets. The recorded results have shown the algorithm to successfully recognise the different object events.

Session 1A4
Patch Antenna and Array

Design and Manufacturing of a Dual-band, Dual-polarized and Dual Fed Perforated Array Patch Antenna Pair

T. D. Sudikila and T. E. Gilles
Department of Communication, Information, Systems and Signals
Royal Military Academy, Brussels, Belgium

Abstract— For spaceborne SAR applications, the weight of the large array antennas required is an important factor in the design phase. Moreover, optimum use of a satellite often dictates that several bands are used simultaneously. Finally, polarimetric measurements also require dual polarization. Patch antennas are easy to operate simultaneously in perpendicular linear polarizations, though care must be taken to ensure sufficient cross polarization isolation. An interesting solution to reduce the overall weight of two dual polarized arrays of patch antennas is to embed the high frequency array in the low frequency one. Again, this complex design requires that special attention be paid to the colocation and crossings of the feeding networks, as well as to the interactions between the two superimposed arrays. We present in this study the simulation and measurements performances of an optimized C band array embedded in a L band patch antenna, both vertically and horizontally polarized.

Dual-frequency, Two Shorting Pin-loaded Equilateral Triangular Patch Antennas

Sultan Can, **K. Yavuz Kapusuz**, **and Elif Aydın**
Department of Electrical & Electronics Engineering, Atilim University, Ankara, Turkey

Abstract— This study presents resonant frequencies of several antennas, which are dual-frequency antennas. The proposed dual antennas have two shorting pins to form dual frequency. Among several methods, two shorting pins are used to form dual frequency equilateral triangular antennas since there are rare studies on this issue and higher frequency ratios (r) are achievable. This study is done to expand the studies in the literature about two shorting pin loaded equilateral triangular patch antennas. The parameters that affect the resonant frequencies of the antenna are also evaluated. The thickness, side length and shorting pin positions are varied and the resonant frequencies are examined according to the change of these parameters. Frequency ratios are determined for each variation and the results are compared. Three antennas with different side length are determined as seen in Table 1. The antennas A, B and C have side length of 45, 60, and 100, respectively. FR4 is used as a substrate, which has a permittivity value of 4.4 in all three antennas. The proposed antenna in [11] with side length 45 mm has an upper frequency of 2150 MHz and lower frequency of 1470 MHz. For the antennas proposed in [11] the upper and lower frequencies are compared and the average error for lower frequency is 8.01% and the average error for upper frequency is 5%. The proposed antenna in this study with a side length 100 mm has an upper frequency 2106.7 MHz and a lower frequency of 493.3 MHz.

The frequency ratio of upper and lower resonant frequencies; obtained from the previous studies in literature was in between 1.51 and 1.61. As mentioned before frequency ratio is a critical parameter for various applications. So achieving higher frequency ratio is an advantage in dual-frequency antenna designs. On this purpose, an antenna with side length 100 mm is achieved with a frequency ratio 4.27, which is a satisfactory result for achieving high frequency ratios. The effects of the shorting pin position and thickness are also examined and the results are presented. The thickness is varied in between 1 mm to 10 mm and the variation of the frequency ratio according to the thickness is examined. With the lower thickness, the higher frequency ratios are obtained for every distance value. The frequency ratio for a thickness of 1 mm is in between 1.35 and 1.76 while it is in between 1.72 and 2.03 for a thickness value of 10 mm. The position difference is another parameter that affects the frequency ratio. The increment in the distance d causes an increment in the frequency ratio. Frequency ratio of an antenna with a side length 100 mm is examined for different thickness and distance (d) values. The frequency ratio is 3.9 when the thickness is 1 mm and 4.45 for a thickness value 10 mm. The frequency ratio is reached to 5.78 for a thickness 10 mm at a distance value $d = 6.86$ while this ratio was 4.45 at a distance $d = 5.5$. The maximum frequency ratio is 4.59 for 1 mm thickness at a distance $d = 6.86$. Several antennas are proposed to analyze two shorting pin-loaded equilateral antennas. Resonant frequencies of these antennas are examined for various antenna parameters such as side length, thickness of the substrate and shorting pin positions. It is concluded that the thickness parameter has an effect on both upper and lower frequency of the antenna. The frequency ratio

Table 1: Comparison of the simulated results of the proposed antennas with the ones proposed in [11] and frequency ratios.

Antenna	S(mm)	p_{s1}(mm)	p_{s2}–p_{s1}(mm)	f_{lower} [11] (MHz)	f_{upper} [11] (MHz)
A	45	10	3.7	1470	2150
B	60	13	4	1020	1600
C	100	15	0.3	-	-
Antenna	r [11]	$f_{lowersim}$	$f_{lowersim}$	$r_{proposed}$	
A	1.46	1352.2	2042.5	1.51	
B	1.56	974.9	1576.9	1.61	
C	-	493.3	2106.7	4.27	

r increases if the thickness increases. A relation between the distance d and the frequency ratio is also observed. An increment in distance d causes an increment in frequency ratios. The side length is also varied in between 45 mm to 100 mm. It is observed that if the side length increases the frequency ratio increases. In this study, the importance of higher frequency and the accurate calculation of resonant frequency underlined. The various results of resonant frequencies of dual frequency two shorting pin-loaded antenna are proposed which is a background for computation of resonant frequencies in an accurate way by using curve fitting. Also higher frequency ratio values are obtained with the proposed antennas, which varies in between 3.99 and 5.78 for different thickness and for different pin position. Validation of side length effect is also done by this study.

REFERENCES

1. Aydın, E. and S. Can, "Modified resonant frequency computation for tunable equilateral triangular microstrip patch," *IEICE Electronics Express*, Vol. 7, No. 7, 500–505, 2010.
2. Can, S., "Computation of resonant frequency of dual band triangular patch antenna," Master's Thesis in Electrical & Electronics Engineering, Atılım University, Turkey, Jul. 2011.
3. Pant, R., P. Kala, R. C. Saraswat, and S. S. Pattnaik, "Analysis of dual frequency equilateral triangular microstrip patch antenna with shorting pin," *Microwave and Optical Technology Letters*, Vol. 3, No. 2, 63-68, 2008.
4. Wong, K. L. and S. C. Pan, "Compact triangular microstrip antenna," *Electron Lett.*, Vol. 33, No. 6, 433–434, Mar. 1997.
5. Aydın, E., "Computation of a tunable-slot loaded equilateral triangular microstrip antenna," *Journal of Electromagnetic Waves and Applications*, Vol. 23, No. 14–15, 2001–2009, 2009.
6. Pan, S. C. and K. L. Wong, "Design of dual-frequency microstrip antennas with a shorting pin loading," *Antennas and Propagation Society International Symposium*, Vol. 1, 312–315, 1998.
7. Wong, K. L. and S. C. Pan, "Compact triangular microstrip antenna," *Electronics Letters,* Vol. 33, No. 6, 433–434, 1997.
8. Aydın, E. and S. Can, "Operating frequency calculation of a shorting pin-loaded ETMA," *Microwave and Optical Technology Letters*, accepted.
9. Liu, Q. and W. C. Chew, "Curve-fitting formulas for fast determination of accurate resonant frequency of circular microstrip patches," *IEE Proceedings*, Vol. 135, No. 5, Pt. H, Oct. 1988.
10. Wong, K. L., S. T. Fang, and J. H. Lu, "Dual frequency equilateral triangular microstrip antenna with a slit," *Microwave Optical Technol. Lett.*, Vol. 19, No. 5, 348–350, Dec. 1998.
11. Row, J.-S. and K.-W. Lin, "Low-profile design of dual frequency and dual polarized triangular microstrip antennas," *Electron Lett.*, Vol. 40, No. 3, 156–157, Feb. 5, 2004.

Design of Monopole Antenna Using Coupling Characteristic of Spiral Parasitic Patch

Kwangyeol Yoon, Seungwoo Lee, and Nam Kim
Chungbuk National University, Korea

Abstract— This paper presents the monopole antenna with a parasitic patch coupling characteristics. The proposed antenna structure consists of a rectangular shape patch, a spiral-shaped parasitic patch, and two L-shaped resonator. At using the rectangular patch only, return loss characteristic is shown at $3.50 \sim 6.17\,\mathrm{GHz}$ band. By adding the spiral parasitic patch in the ground plane coupled to the rectangular patch, resonance frequency properties at 2 GHz, 3.5 GHz, 5 GHz, and 6.1 GHz bands are obtained. To achieve the frequency notched characteristics at 4.5 GHz band, two short-circuited quarter wavelength L-shaped resonator connected to the ground plane is inserted beside the feed-line. The proposed antenna dimension is $60 * 40 * 1\,\mathrm{mm}^3$, and is designed on the FR-4 substrate having a relative dielectric constant of 4.4. The designed antenna shows that the resonant frequency is $1.75 \sim 2.55\,\mathrm{GHz}$, $3.18 \sim 3.88\,\mathrm{GHz}$, and $4.82 \sim 6.30\,\mathrm{GHz}$ below the return loss of $-10\,\mathrm{dB}$, also radiation pattern has omni-directional characteristics.

Design of the Dual-band Planner Monopole Antenna for Coupled Rectangular-loop Structure and T-shape Rectangular Patch

J. D. Jang, S. W. Lee, and N. Kim
Chungbuk National University, South Korea

Abstract— In this paper, a broadband planar monopole antenna for mobile communication services is designed. The Proposed antenna is composed of a small loop structure with a T-shaped patch and two rectangular patches for the wide bandwidth characteristics. Two rectangular patches are affected to the current flow, therefore the resonant bandwidth is increased. The frequency characteristics are modified and optimized by varying the size of each parameter of the antenna.

Whole antenna dimension including the ground plane is $40 \times 60 \times 1\,\mathrm{mm}^3$. The impedance bandwidth below a VSWR of 2 is 858 $\sim$ 988 MHz and 1,496 MHz $\sim$ 3,955 MHz. The designed antenna is satisfied with the impedance bandwidth in GSM900 (880 $\sim$ 960 MHz, DCS1900 (1850 $\sim$ 1990 MHz), US-PCS (1850 $\sim$ 1990 MHz), WCDMA1900 (1850 $\sim$ 1930 MHz), ISM band (2400 $\sim$ 2500 MHz), WLAN (2400 $\sim$ 2483 MHz), m-WIMAX (2300 $\sim$ 2400 MHz, 2500 MHz $\sim$ 2690 MHz), and LTE next-generation (3.5 GHz and 3.8 GHz). Moreover, the radiation patterns are omni-directional shapes, which are appropriated for the mobile handset. Therefore, this antenna can be applicable to the small size multi-band mobile devices.

Design and Relative Permittivity Determination of an EBG-based Wearable Antenna

N. R. Rishani, **M. Al-Husseini**, **A. El-Hajj**, **and K. Y. Kabalan**
ECE Department, American University of Beirut, Beirut 1107 2020, Lebanon

Abstract— A simple technique to determine the permittivity of a textile material is presented in this paper. This is used for wearable antennas, whose substrate is some type of textile and finding its permittivity is usually a challenge. Furthermore, the stacking of several layers, of the same material to get the required thickness, alters the whole structure permittivity. A patch antenna that resonates at 1.575 GHz was designed on a Cordura fabric dielectric material, assuming a permittivity (ε_r) of 1.9, and copper tape as the conductive material. An Electromagnetic Band Gap (EBG) structures layer is incorporated between the patch and the ground plane, as in Figure 1(a). The EBG layer minimizes backward radiation when transmitting and keeps the antenna performance steady while operating in the body vicinity. For this ε_r value of Cordura, the patch dimensions are 66 mm × 69 mm and those of the full ground plane are 106 mm × 108 mm. The embedded EBG layer has 5 × 5 patches where each is 18.5 mm × 19 mm. A prototype of the designed antenna was fabricated, and its reflection coefficient was measured. Figure 1(b) shows a shift in the resonant frequency from 1.575 GHz to 1.74 GHz, and this implies a lower substrate permittivity. The same design was simulated for several values of ε_r and the attained results show that the antenna resonates at 1.74 GHz for a permittivity of 1.5, as in Figure 1(b). Considering $\varepsilon_r = 1.5$, the patch was redesigned and 1.575 GHz resonance was obtained for a patch size of 66 mm × 69 mm. The re-designed antenna was fabricated, and measured. As illustrated in Figure 1(c), high correlation between simulated and measured reflection coefficient plots was obtained. As a result, the permittivity of the used textile material was concluded to be 1.5.

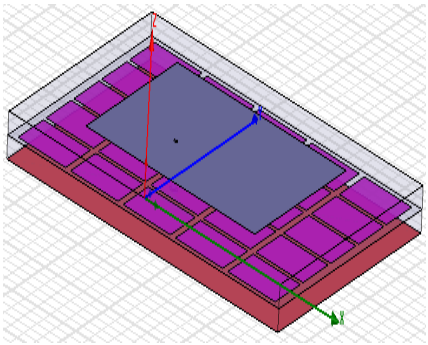

(a)

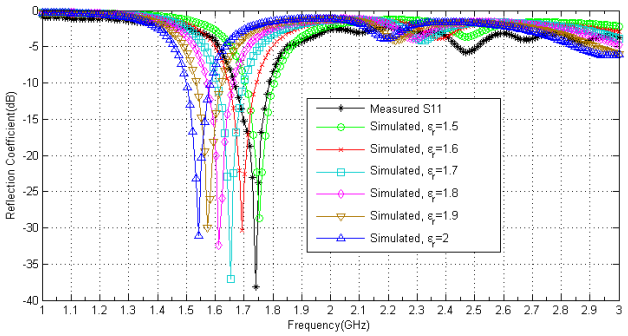

(b)

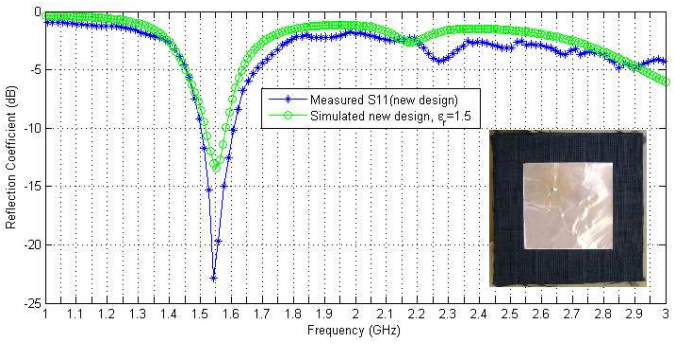

(c)

Figure 1: (a) 3D configuration of the proposed antenna showing patch, EBG layer and ground plane. (b) Simulated and measured reflection coefficients for several ε_r values. (c) Re-fabricated prototype with its simulated and measured reflection coefficient.

Antenna Array for IEEE 802.11/a/b MIMO Application

Dau-Chyrh Chang, **Yi-Jhen Li**, **and Chao-Hsiang Liao**
Communication Research Center, Oriental Institute of Technology
No. 58, Sec. 2, Sichuan Rd., Banqiao Dist., New Taipei City 220, Taiwan, R.O.C.

Abstract— In this paper, antenna array for WiFi IEEE 802.11a/b with frequency at 2.4 GHz ∼ 2.5 GHz and 5.2 GHz ∼ 5.8 GHz is implemented. The results from both simulation and measurement are compared. Figure 1 the geometry of the antenna array simulated by GEMS. Top patch arrays is dual polarizations with frequency at 5.5 GHz. The bottom patch array is dual polarizations with frequency at 2.4 GHz. The 5.5 GHz array is located on the top of 2.4 GHz array. The hardware implementation for 2.4 GHz and 5.5 GHz is shown in Figure 2. The return loss, power pattern, efficiency for two orthogonal polarizations at 2.4 GHz and 5.5 GHz will be discussed in full paper.

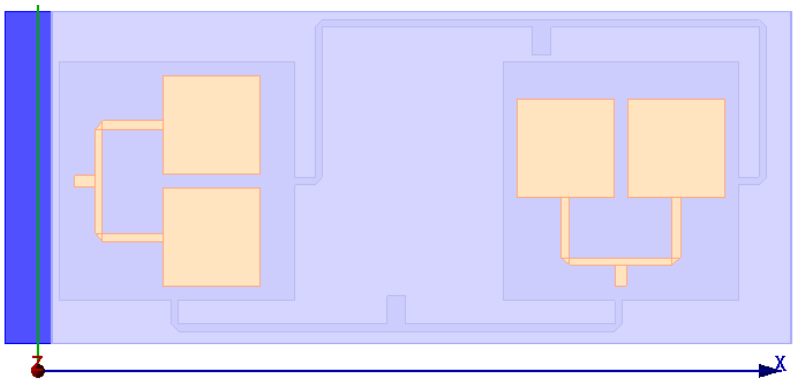

Figure 1: The simulation model.

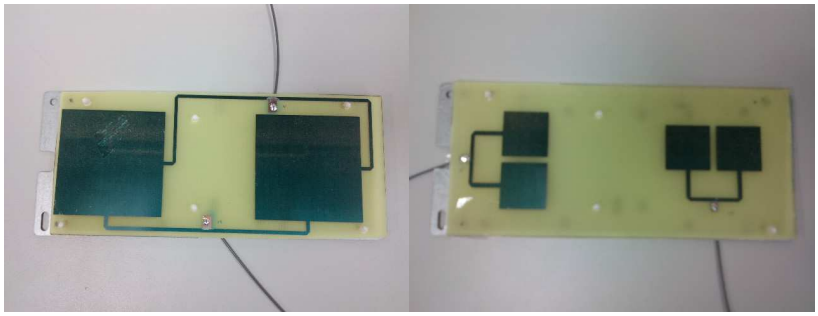

Figure 2: Hardware implementation for 2.4 GHz and 5.5 GHz.

Analysis of a Dual Frequency Circular Patch Antenna

Sultan Can, K. Yavuz Kapusuz, and Elif Aydın
Department of Electrical and Electronics Engineering, Atılım University, Ankara, Turkey

Abstract— This study demonstrates resonant frequencies of several shorting pin loaded circular antennas, which are dual-frequency antennas. Dual-frequency operation is formed by using a shorting pin, which is connected between ground and the radiated part of the antenna. There are various studies, which are used to produce dual-frequency operation, and among those methods, a shorting pin is used to form dual frequency circular patch antennas since there are rare studies on this issue and size reduction is possible by inserting a pin to an antenna. This study is done to expand the studies in the literature about a shorting pin loaded circular patch antennas. The parameters that affect the resonant frequencies of the antenna are also evaluated. The thickness, permittivity and shorting pin positions are varied and the resonant frequencies are examined according to the change of these parameters. Frequency ratios are determined for each variation and the results are compared.

Antennas are the crucial element of wireless systems and patch antennas are one of the most important elements in today's communication systems. Microstrip patch antennas, which are resonant antennas, are popular due to their low weight, low profile and cheap for printed circuit construction [1–7]. Efficient design of an antenna can increase the overall performance of the communication systems. Since the efficient design of a patch antenna is crucial, calculating design parameters such as resonant frequency and input impedance is getting more and more important [1–3]. Dual frequency operations are also popular in wireless communications and there are several methods to form a dual frequency such as slot, slit and shorting pin loading [2]. In designing the dual frequency antenna, an important parameter is to achieve higher frequency ratios with lower sizes. The frequency ratio is determined as the ratio of the upper frequency to the lower frequency in literature [3]. Inserting a shorting pin is mostly preferred because it significantly reduces the size of the antenna [3]. In this study, a dual frequency antenna is presented and a shorting pin is used to form a dual circular patch antenna. Inserting a shorting pin to a circular patch is preferred because the studies in literature show that shorting pin loaded circular antennas have larger frequency ratios when compared to the rectangular ones [4]. Frequency ratio characteristics examined and the ratios are determined for different permittivity, thickness and shorting pin positions. The upper and lower frequencies are examined for different permittivity values.

The variation of frequencies with respect to a ratio of shorting pin position to the radius of the circle is demonstrated for a substrate thickness 0.16 cm. A decrease is observed in the lower frequency with an increase in the position ratio. An increment is also observed in the upper frequency with an increment in the ratio of the positions. The frequency ratios (r) are also demonstrated according to the permittivity and shorting pin positions. Maximum frequency ratio is observed with an antenna which has a permittivity value $\varepsilon_r = 2.2$ at a position ratio $d_S/d = 0.9$. Minimum frequency ratio is observed with an antenna which has a permittivity value $\varepsilon_r = 4.4$ at a position ratio $d_S/d = 0.1$. All these data prove that the permittivity of the substrate changes the upper and the lower frequencies but the effect of the permittivity value to the frequency ratio is not significant. Besides, the ratio of the radius and the shorting pin position from the centre of the circle (d_S/d) increase the frequency ratio. The antennas with different permittivity values which have a radius = 2.186 cm and a substrate thickness $h = 0.16$ achieve a frequency ratio approximately 3.5 at a ratio 0.9 while it was about 2.2 at a ratio was 0.1. The effect of the thickness to the frequency ratio is also examined for an antenna with a radius 2.186 cm which has a permittivity value of $\varepsilon_r = 4.4$. Varying the thickness changes the frequency ratio and the lowest thickness value, which is 1 mm, achieved the maximum frequency ratio. The studies in the literature demonstrate a null voltage point according to the ratios of the positions in equilateral patches [3]. The null voltage point is determined at a ratio around 0.33. A null voltage point is observed at a distance ratio around 0.3. Thickness parameter has a negligible effect at that point and the frequency ratio remains around 2.45 for each thickness value.

Reducing the size of the antenna is important for the designers. An antenna (C) with a frequency ratio 3.82 is proposed with a side length 2.186 cm and permittivity value $\varepsilon_r = 2.08$ which has a lower thickness when compared to the one in the literature [6]. However, the antenna C is capable of achieving the same frequency ratio. The antenna proposed in the literature (A) is compared with the antenna (B) and error calculated for both upper and lower frequency. The error obtained

Table 1: Comparison with simulated results of the proposed antennas with ones proposed in [6] and frequency ratio.

Antenna	d (cm)	d_s (cm)	h (cm)	ε_r	F_{lower} (MHz)	F_{upper} (MHz)	F_{lower} error (%)	F_{upper} error (%)	r
A [6]	2.186	2.1	0.16	4.4	568	2176	–	–	3.83
B	2.186	2.1	0.16	4.4	596.9	2190	5.09	0.64	3.66
C	2.186	2.12	0.03	2.08	834.5	3185.6	–	–	3.82

is 5.09% for the lower frequency and 0.64% for the upper frequency. Several antennas are proposed for achieving high frequency ratios for dual frequency operations. The frequency ratios are demonstrated for different radius, thickness and position ratios. It is concluded that increasing the distance ratio of the shorting pin to the radius significantly increases the frequency ratio in shorting pin loaded circular patch antennas. It is also obtained that an antenna with lower size and thickness higher frequency ratios are achievable. It is also seen that thickness parameter has a negligible effect on frequency ratio at a critical point where the ratio d_S/d is around 0.3. An antenna is also proposed with smaller size, but achieves the same frequency ratio.

REFERENCES

1. Aydın, E. and S. Can, "Modified resonant frequency computation for tunable equilateral triangular microstrip patch," *IEICE Electronics Express*, Vol. 7, No. 7, 500–505, 2010.
2. Can, S., "Computation of resonant frequency of dual band triangular patch antenna," Master's Thesis in Electrical & Electronics Engineering, Atılım University, Turkey, Jul. 2011.
3. Aydın, E. and S. Can, "Operating frequency calculation of a shorting pin-loaded ETMA," *Microwave and Optical Technology Letters*, Vol. 54, No. 6, 1432–1435, Jun. 2012.
4. Kumar, P. and G. Sing, "Microstrip antennas loaded with shorting post," *Engineering*, Vol. 1, No. 1, 41–45, Jun. 2009.
5. Kumar, P. and G. Sing, "Theoretical computation of input impedance of gap-coupled circular microstrip patch antennas loaded with shorting post," *Journal of Computational Electronics*, Vol. 10, No. 1–2, 195–200, Jun. 2011.
6. Tang, C. L., H. T. Chen, and K. L. Wong, "Small circular microstrip antenna with dual frequency operation," *Electronic Letters*, Vol. 33, No. 13, 1112–1113, Jun. 1997.
7. Gurel, Ç. S., E. Aydın, and E. Yazgan, "Computation and optimization of resonant frequency and input impedance of a coax-fed circular patch microstrip antenna," *Microwave and Optical Technology Letters*, Vol. 49, No. 9, 2263–2267, Sep. 2007.

Design and Simulation of E-shaped Compact Microstrip Antenna for WLAN Applications

Mahmoud Abdipour[1], **Gholamreza Moradi**[2], **and Reza Sarraf Shirazi**[2]

[1]Azad Branch, Islamic Azad University, Arak, Iran
[2]Amirkabir University of Technology, Tehran, Iran

Abstract— In this paper, an E-shaped compact microstrip antenna for high speed Wireless Local Area Networks (WLANs) applications is presented. We use only a single patch for our proposed antenna. In the simulation result impedance bandwidth (VSWR < 1.3) is obtained. During this design on the top, conductor Substrate manufactured from RT_DURIOD_5880 with dielectric constant 2.21 and height of 20 mil on other hand backed manufactured from conductor ground plane. Tiny circuit size, high gain and low return loss are advantages of this study than other similar works.

A Compact Ultra Wideband EBG Antenna with Band Notched Characteristics

S. Raghavan, Ch. Anandkumar, A. Subbarao, M. Ramaraj, and R. Pandeeswari
National Institute of Technology, Tiruchirappalli-620015, India

Abstract— Ultra wideband communication systems have received great attraction in wireless world. It is popularly used technology in radar and remote sensing. Ultra wideband technology provides promising solutions for future communication systems due to excellent immunity to multi path interference, large bandwidth and high speed data rate. A bandwidth from 3.1 GHz to 10.6 GHz is allocated for UWB systems by Federal Communication Commission. UWB antenna is a key component in UWB systems. In this paper, a novel compact Ultra wideband antenna is presented. The antenna is constructed with low cost FR4 substrate with relative permittivity = 4.4 and thickness $h = 0.8$ mm. The antenna has a size of 30 mm × 34 mm. The antenna has hexagonal tuning stub which is fed by microstrip line. The antenna has band width of 3.1 GHz to 10.7 GHz which covers entire band width specified by Federal Communication Commission. Since WLAN band (5.15–5.85 GHz), occupies a portion of UWB band, there is electromagnetic interference between them. An electromagnetic band gap (EBG) cell is introduced near the feeding part of structure to avoid interference from WLAN band from 5.1 GHz to 5.85 GHz. The effects of width, height of EBG cell on antenna are studied. The antenna has Omni directional radiation pattern in operating bandwidth and it has good radiation efficiency. The gain and radiation pattern of antenna have been investigated and found to be stable. The group delay variation of antenna is less than 1 ns in operating bandwidth which represent linear phase response. The antenna can be easily integrated with radio frequency circuit for low cost.

Session 1A5
Novel Mathematical Methods in Electromagnetics 1

Ab initio Method for Calculating the Electric Multipole Moments of Diatomic Molecules at Small Internuclear Separations

E. V. Koryukina
Tomsk State University, Lenin Avenue 36, Tomsk 634050, Russia

Abstract— In this work, multipole moments characterizing electric properties of diatomic molecules are studied theoretically. These moments are induced by the electric field existing within a molecule. Electric multipole moments are necessary for estimating the polarity of chemical bonds and the asymmetry of charge distribution within a molecule, as well as for investigating intermolecular interactions. In addition, the calculated values of the moments allow us to predict the response of molecules to external electric fields.

Within the adiabatic approximation, the multipole moments of diatomic molecules are functions of the internuclear separation R. The available *ab initio* methods (in particular, MOLPRO, GAUSSIAN, and GAMESS code packages) allow us to perform high-precision calculations of the diatomic-molecule multipole functions in the vicinity of equilibrium internuclear separation and at large R, but, in principle, make it impossible to compute these functions at $R \to 0$. At small internuclear separations, the multipole moment functions are calculated by semi-empirical methods, whose adequacy is to be verified in every case.

In the present work, an *ab initio* method for calculating the electric multipole moment functions of diatomic molecules at small internuclear separations is proposed. In the framework of this method, based on the united-atom model, the calculations are performed within first-order perturbation theory using the formalism of irreducible tensor operators. The approach is implemented in a special two-block software package. In first block written in Maple, the formulas are derived for calculating multipole moment functions in an analytical form. In second block written in FORTRAN, numerical computations are performed by means of the derived formulas with the Hartree-Fock basis functions of united atoms computed using the Froese-Fischer code [1]. Our earlier calculations of the dipole moment functions of diatomic molecules enabled us to reveal a number of interesting regularities in the behavior of these functions [2]. The obtained results have stimulated derivation of general formulas and investigation into higher-order multipole moment functions of diatomic molecules within the framework of the proposed approach.

A comparison of the dipole and quadrupole moment functions obtained in this work with semi-empirical functions calculated by other authors shows that the suggested approach allows us to unambiguously determine the behavior of the foregoing functions at $R \to 0$. For a number of molecules, (in particular, for the NO and CO molecules), there were found qualitative differences in the behavior of the multipole functions computed in this work and those obtained by semi-empirical methods. The calculations have shown a possibility of repeated change in the sign of the dipole moment functions with an increase in R, which permits to clarify the problem of changing the polarity of chemical bonds in diatomic molecules. In conclusion, it should be noted that the proposed method in combination with other *ab initio* and semi-empirical methods allows us to construct multipole moment functions of any diatomic molecules physically correct over the entire internuclear separation range.

REFERENCES

1. Froese Fischer, C., *Comput. Phys. Commun.*, Vol. 64, 369–398, 1991.
2. Buldakov, M. A., E. V. Koryukina, V. N. Cherepanov, and Y. N. Kalugina, *Phys. Rev. A*, Vol. 78, 032516, 2008.

Space Curve Type Distributions with Applications in Electromagnetic Theory

B. Polat
Electrical and Electronics Engineering Department
Trakya University, Edirne, TR-22030, Turkey

Abstract— The theory of generalized functions was first introduced by Sobolev (cf. [1]) in early 20th century and later developed extensively by mid 20th century as documented in the reference works by many great mathematicians led by the pioneers Schwartz [2], Gel'fand and Shilov [3]. The requirement for generalized functions in a field theory can be realized immediately in an attempt to express analytically the volume density function of a source quantity concentrated in a non-volumetric domain. Since the point form field equations in mathematical physics are always given through density functions in space and time, such equations would otherwise not permit algebraic operations in non-volumetric domains.

In this work, we introduce the basic theory of space curve type distributions and electromagnetic sources concentrated on a space curve in a Schwartz-Sobolev space setting. To the best of our knowledge, in literature the distributional analysis of curve type singularities suitable for our purposes is available only for the derivatives of plane curves, whose theory is very similar to that of surface singularities, as summarized in [4, Secs. 5.8, 11.14, 11.15, 12.11, Ex. 3]. The contribution of the present work to analysis can be outlined as

i) an extension of the singularity domain from plane to space curves involving the differential geometric parameters introduced in Serret-Frenet equations;
ii) derivation and employment of
   – three line operators acting on a regular singular function;
   – distributional derivatives of first order space curve type singularities.

Then these tools are employed in the distributional investigation of electromagnetic field behavior in presence of first and second order ("free" and "polarized") arbitrary and impulse radiating space curve type sources. The full paper will appear in [5].

REFERENCES

1. Demidenko, G. V. and V. L. Vaskevich, *Selected Works of S.L. Sobolev*, 1st Edition, Vol. I, Springer, 2006.
2. Schwartz, L., *Theorie des Distributions*, 2nd Edition, Vol. 1, Hermann, Paris, 1957; Vol. 2, Hermann, Paris, 1959.
3. Gel'fand, I. M. and G. E. Shilov, *Generalized Functions*, Vol. 1–5, Academic Press, NY, 1977.
4. Kanwal, R. P., *Generalized Functions: Theory and Technique*, 3rd Edition, Birkhauser Boston, 2004.
5. Polat, B., "Space curve type distributions and sources," *IEEE Antennas and Propagation Magazine*, Vol. 54, No. 3, 2012.

Eigenanalysis of Arbitrarily Shaped 2-D and 3-D Closed and Open-Radiating Structures: A Review

G. A. Kyriacou[1], P. C. Allilomes[1], C. S. Lavranos[1], C. L. Zekios[1], S. J. Lavdas[1], and A. V. Kudrin[2]

[1]Microwaves Lab., Department of Electrical and Computer Engineering
Democritus University of Thrace, Xanthi, Greece
[2]Department of Radiophysics, University of Nizhny Novrogod, Russia

Abstract— A review of our research effort on the eigenanalysis of open-radiating and closed, straight as well as curved, structures is presented herein. The elaborated geometries are arbitrary shaped and loaded in general with inhomogeneous and/or anisotropic media. Our previous work was focused on two dimensional (2-D) waveguiding structures and particularly on open-radiating waveguides including leaky wave phenomena, as well as curved geometries in the transverse and possibly curved along the propagation direction. Regarding our previous work, a hybrid Finite Element in conjunction with a cylindrical harmonics expansion is established for the analysis of open waveguides. The transparency of the fictitious circular contour truncating the finite element mesh is ensured by enforcing the field continuity conditions according to a vector Dirichlet-to-Neumann mapping [1]. The eigenanalysis of curved waveguides is confronted by a Finite Difference frequency domain method in orthogonal curvilinear coordinates [2]. The latter eliminates the usually encountered stair case effects by making the grid conformal to the material boundaries. Additionally it supports multi-coordinate systems and inhomogeneous grids enabling fine mesh around current carrying conductors and coarse mesh in the area of low field variations. These features offer high accuracy with minimum computer resources.

Aiming at the eigenanalysis of electrically large structures like the reverberation chambers or focused microwave cavities our previous Finite Element Method is extended accordingly [3]. For this purpose the perturbations inside the cavity are enclosed within a canonically shaped fictitious surface and the interior field is described using a vector FEM. Outside these perturbations, within the large canonical cavity, the electromagnetic field is represented through an analytical eigenfunctions expansion. The field continuity across the fictitious surface is exactly enforced according to the DtN formalism to yield an appropriate eigenvalue problem. This is in turn solved for the resonant frequencies and the related quality factors. Within this effort we are currently working toward extending this methodology for the eigenanalysis of open-cavities including various types of cavity backed antennas.

The design of a variety of periodic structures like filters, frequency selective surfaces and traveling wave antennas can be served very efficiently though the knowledge of the associated modes propagation constants and characteristic impedances. Motivated by these requirements, our previous FDFD eigenanalysis methods are now appropriately extended to account for the periodicity by simulating a single unit cell [4]. However, this approach is currently limited to an ω-formulation where the dispersion curves are evaluated by scanning the propagation constant (β) range of values. But this is possible when β is real and only for certain simple geometries. For arbitrary geometries and anisotropic material loadings (especially regarding leaky and frozen wave modes), β is complex and its range is unknown. For this purpose we put an effort in formulating a β-eigenproblem, which is possible by incorporating the Floquet expansion within the FDFD formulation.

Finally, our current work aims at the development of a novel tool for the electromagnetic simula- tion and design of digitally controlled and multifunctional multiple input-multiple output (MIMO) antennas integrated on the device's chassis and/or package utilizing Characteristic Mode theory. During the presentation the basic principles of the above described eigenanalysis methodologies will be presented, along with a series of numerical results as well as validations in comparison to results published by other researchers.

ACKNOWLEDGMENT

This work was financially supported by the Greek Ministry of Education, Lifelong Learning and Religious Affairs through the research project THALIS Design Techniques for Digitally Controlled RF-Microwave Structures Appropriate for Software Defined-Cognitive Radio (RF-EIGEN-SDR).

REFERENCES

1. Allilomes, P. C. and G. A. Kyriacou, "Nonlinear finite-element leaky-waveguide solver," *IEEE Transactions on Microwave Theory and Techniques*, Vol. 55, 1496–1510, July 2007.
2. Lavranos, C. S. and G. A. Kyriacou, "Eigenvalue analysis of curved waveguiding structures employing an orthogonal curvilinear frequency domain finite difference method," *IEEE Transactions on Microwave Theory and Techniques*, Vol. 57, No. 3, 594–611, March 2009.
3. Zekios, C. L., P. C. Allilomes, and G. A. Kyriacou, "Eigenfunction expansion for the analysis of closed cavities," *2010 Loughborough Antennas and Propagation Conference*, 537–540, UK, November 2010.
4. Lavdas, S., C. S. Lavranos, and G. A. Kyriacou, "Periodic structures eigenanalysis incorporating the floquet field expansion," *Proc. of the ICEAA IEEE ARWC Conference*, Turin, Italy, September 2011.

Energetic Wave Processes Concomitant Propagation of the Time-Domain Modal Waves

Oleg A. Tretyakov and Mehmet Kaya
Department of Electronics Engineering, GebzeInstitute of Technology, Gebze 41400, Kocaeli, Turkey

Abstract— The waveguide is bounded by a surface with the properties of the perfect electric conductor. Its volume is filled with a lossy medium parametrized by a constant conductivity. The time-domain waveguide problem is formulated and solved analytically in a Hilbert space of the real-valued functions. A complete set of the waveguide modes is obtained. Every field component is a product of two factors, one of which is a vector element of the modal basis and the other one is a scalar modal amplitude. The elements of the modal basis depend on the transverse waveguide coordinates, only. Successful normalization of them provides the basis element with required physical dimensions (volt per meter) and (ampere per meter) for the electric and magnetic field quantities, respectively. The modal amplitudes are dimensionless scalar functions of axial waveguide coordinate, z, and time, t. Modal amplitude of the longitudinal field component is governed by the Klein-Gordon equation (KGE). The amplitudes of transverse field components are expressible via z- and t-derivatives of the KGE solutions. The KGE is capable to provide with a wide set of exact explicit solutions for the modal amplitudes dependent on (z, t) variables. In turn, these solutions enable us to find out explicitly the energetic field characteristics as some functions of (z, t) variables. In particular, the following quantities were calculated and analyzed: the power flow density, $P_z(z, t)$, averaged over the waveguide cross section, the energy density, $W(z, t)$, averaged over the waveguide cross section, and an electromagnetic energy converted into a heat energy. A continuity equation for the energetic quantities was derived in which z- and t-derivatives participate. Instant velocity of transportation of the modal field energy is obtained as a function of (z, t) variables. Minimal and maximal values of the velocity are calculated. The maximal velocity never exceeds the light speed. Dynamic phenomena pertinent to transportation of energy are analyzed especially. A specific wave energetic process is discovered which accompanies of the modal wave propagation.

A Novel Time Reversal Imaging of Cylindrical Objects

Toshifumi Moriyama and Takashi Takenaka
Graduate School of Engineering, Nagasaki University
1-14 Bunkyo-machi, Nagasaki 852-8521, Japan

Abstract— Inverse scattering problems have been attracting many researchers because of their theoretical interests and practical importance. They have a lot of potential applications in various fields such as medical imaging, geophysical exploration, nondestructive material testing and subsurface prospecting. Many inversion approaches have been proposed to identify objects of interest from scattered field data measured on a surface enclosing the objects. So far the time-reversal (TR) techniques are applied mainly to detect and identify point-like or extended targets. There are few papers that deal with reconstructing material parameter distributions of unknown objects with TR techniques.

In this paper, we consider a time-reversal approach for determining electrical parameter distributions of cylindrical objects. Let objects of interest be illuminated by a TM wave pulse generated by a line current source $\mathbf{j}$ flowing in the z-direction. Transient total fields are measured on the measurement curve $\partial\Omega$ during a time interval $[0, T]$. The waveform of the total field are reversed in time and sent back into the region Ω enclosed by $\partial\Omega$. Under the same scenario within the region Ω as the forward propagating problem, i.e., the existence of the unknown objects, the back-propagating time-reversed field refocuses perfectly at the original source point and cancels out the time-reversed field generated by the original source $\mathbf{j}$ outside the boundary $\partial\Omega$ so that no fields there. Replacing the original objects with different ones in the region Ω, however, does not give null field outside $\partial\Omega$. From this, in order to estimate electric parameters $\varepsilon_r(\mathbf{r})$, $\mu_r(\mathbf{r})$, and $\sigma(\mathbf{r})$ of the unknown objects, we introduce the following functional:

$$F(\mathbf{p}) = \int_0^T \int_{\bar{\Omega}} |\mathbf{u}(\mathbf{p}; \mathbf{r}, t)|^2 d\mathbf{r}dt$$

where $\mathbf{p}(\mathbf{r})$ is a vector function consisting of electric parameters and $\bar{\Omega}$ is the complementary region of Ω. The minimizer $\breve{\mathbf{p}}$ of the functional gives the optimal estimate for the unknown objects. In order to assess the effectiveness of the approach, numerical simulations are carried out using a genetic algorithm. The results will be shown in the presentation.

Guaranteed Estimates of Functionals from Solutions and Right-hand Sides of Maxwell Equations under Uncertainties

Yury Podlipenko[1] **and Yury Shestopalov**[2]

[1]Kiev National University, Kiev, Ukraine
[2]Karlstad University, Karlstad, Sweden

Abstract— In the analysis of complex processes of electromagnetic wave scattering described by Maxwell equations, an important problem is the optimal reconstruction (estimation) of parameters of the equations, like values of some functionals on their solutions or right-hand sides, from observations which depend on the same solutions. Let D be a domain bounded by a perfect conductor and occupied by a dissipative dielectric with unknown electric and magnetic current densities $\mathbf{J}$ and $\mathbf{M}$ belonging to a certain bounded set of vector-functions square integrable in D. The considered problem of estimation consists in the following: estimate linear continuous functionals from $\mathbf{E}$, $\mathbf{J}$, and $\mathbf{M}$ by observations of electric field $\mathbf{E}$ under the assumption that observations are liner transformations of $\mathbf{E}$ perturbed by additive random noises with unknown second moments and belonging to a certain given set in the corresponding Hilbert space. This leads to the necessity of introducing minimax statement of the estimation problem when optimal estimates of linear functionals from $\mathbf{E}$, $\mathbf{J}$, and $\mathbf{M}$ are defined as linear, with respect to observations, estimates for which the maximum of the mean square error of estimation taken over the above-mentioned sets attains minimal value. Such estimates are called minimax mean square or guaranteed estimates. We develop constructive methods for finding these estimates and estimation errors which are expressed in terms of solutions to special variational equations and prove that Galerkin approximations of the obtained variational equations converge to their exact solutions.

It should be noted that beyond purely theoretical interest, the mentioned estimation problems may have various interesting applications, e.g., for automatized measurement data processing systems and interpretation of electromagnetic observations.

A CIP-BS Implementation for Inhomogeneous Media

Yoshiaki Ando and Yusuke Takahashi
The University of Electro-Communications
1-5-1 Chofugaoka, Chofu, Tokyo 182-8585, Japan

Abstract— The constrained interpolation profile (CIP) method is the numerical method using field values and their spatial derivatives. Recently, another CIP method, which is called as CIP-basis set (CIP-BS) method, is developed to solve general hyperbolic equations in the time domain. In this paper, we consider the CIP-BS implementation for arbitrarily inhomogeneous media.

The basis function set can be defined as

$$\mathbf{E}(\mathbf{r},t) = \sum_{i,j,k}^{N_x,N_y,N_s} \sum_{l=0}^{L} \sum_{m=1}^{3} E_m^N(i,j,k,t)\Phi_{i,j,k}^l(\mathbf{r})\hat{\mathbf{x}}_m, \tag{1}$$

where N_x, N_y, and N_z are the number of cells in x, y, and z-direction, respectively, and $E_m(i,j,k,t)$ is a time-dependent constant, $\phi_{i,j,k}(\mathbf{r})$ is a three-dimensional CIP-BS function, and $\hat{\mathbf{x}}_m$ is the unit vector. l is the compound index and represents the derivatives in x, y, and z-direction.

The CIP-BS functions set is defined as

$$\Phi_{i,j,k}^l(\mathbf{r}) = \phi_i^{l_1}(x)\phi_j^{l_2}(y)\phi_k^{l_3}(z), \tag{2}$$

and

$$\frac{d^{l_a}}{dx^{l_a}}\phi_i^{l_b}(x_i) = \begin{cases} 1, & \text{for } l_a = l_b \\ 0, & \text{for } l_a \neq l_b \end{cases}, \quad \frac{d^{l_a}}{dx^{l_a}}\phi_i^{l_b}(x_{i\pm1}) = 0. \tag{3}$$

The update equations can be derived by applying the Galerkin method to the curl equations. In the Galerkin method, we can take into account inhomogeneity by using the permittivity and the permeability as spatial functions. Various time schemes can be chosen in CIP-BS method, for example, the leap-frog, the full implicit, and the Crank- Nicolson schemes.

The precision is much better than typical finite difference methods. The phase errors are much smaller than the FDTD method when a material with high permittity is considered.

A Nonlinear Layered Structure and the Eigen Oscillations of the Linearised Problems near the Frequencies of Scattering and Generation

L. Angermann[1], V. V. Yatsyk[2], and M. V. Yatsyk[3]

[1]Institute of Mathematics, TU Clausthal, Clausthal-Zellerfeld, Germany
[2]Usikov Institute of Radiophysics and Electronics NASU, Kharkov, Ukraine
[3]Kharkov National University of Radio Electronics, Kharkov, Ukraine

Abstract— Nonlinear dielectrics with controllable permittivity are the subject of intense studies and begin to find broad applications in device technology and electronics. We develop a model of resonance scattering and generation of waves on an isotropic nonmagnetic nonlinear layered dielectric structure excited by a packet of plane waves in the resonance frequency range in a self-consistent formulation [1–3]. Here, both the radio [4] and optical [5] frequency ranges are of interest. Our mathematical model reduces to a system of nonlinear boundary-value problems of Sturm-Liouville type or, equivalently, to a system of nonlinear Fredholm integral equations. Here, for the first time, the solution to nonlinear boundary-value problems is obtained rigorously in a self-consistent formulation and without using approximations of the given field, slowly varying amplitudes etc. [4, 5]. The analytical continuation to the complex frequency region allows us to turn to the analysis of spectral problems and to reveal various resonance phenomena related to the nonlinearity of the structure, see [2]. We present and discuss results of calculations of the scattered field taking into account the third harmonic generated by nonlinear layer.

The results indicate a possibility of designing a frequency multiplier and nonlinear dielectrics with controllable permittivity. The transformation of the frequency and angular spectra, the rapid control of amplitude and phase of the waves form the basis of a broad class of technical systems [6].

ACKNOWLEDGMENT

This work was partially supported by the Visby Program of the Swedish Institute.

REFERENCES

1. Shestopalov, Y. V. and V. V. Yatsyk, "Diffraction of electromagnetic waves by a layer filled with a Kerr-type nonlinear medium," *J. of Nonlinear Mathem. Physics*, Vol. 17, No. 3, 311–335, 2010.
2. Angermann, L. and V. V. Yatsyk, "Generation and resonance scattering of waves on cubically polarisable layered structures," *Numerical Simulations — Applications, Examples and Theory*, L. Angermann, Ed., 175–212, InTech, Rijeka/Vienna, Croatia/Austria, 2011.
3. Angermann, L. and V. V. Yatsyk, "Resonance properties of scattering and generation of waves on cubically polarisable dielectric layers," *Electromagnetic Waves*, V. Zhurbenko, Ed., 299–340, InTech, Rijeka/Vienna, Croatia/Austria, 2011,
4. Chernogor, L. F., *Nonlinear Radio Physics*, V. N. Karazin, KSU, Kharkov, 2004.
5. Miloslavsky, B. K., *Nonlinear Optics*, V. N. Karazin, KSU, Kharkov, 2008.
6. Shen, Y. R., *The Principles of Nonlinear Optics*, John Wiley & Sons, Inc., NY, 1984.

Introducing Clifford Analysis as the Natural Tool for Electromagnetic Research

G. R. Franssens
Belgian Institute for Space Aeronomy, Belgium

Abstract— The aim of this talk is to introduce Clifford algebra and the thereupon based Clifford analysis as the natural mathematical tools to formulate and solve electromagnetic problems. The Clifford approach to electromagnetism is a rather new and powerful method, which allows to make new progress in both the understanding and computation of electromagnetic fields.

The underlying idea is that we should use that mathematical framework which is best adapted to the structure of the universe that we live in; in our case this is, in the absence of gravity, a pseudo-Euclidean space (Minkowski space) or when gravity is present, a pseudo-Riemannian space. An important part of such spaces is their quadratic inner product structure (called the metric by physicists), which profoundly shapes the form of the laws of physics. Further, the laws of physics appear to essentially express geometrical relationships between quantities, which themselves have geometrical content. By combining these two observations we naturally arrive at what are now called Clifford algebras, and by Clifford himself were called geometrical algebras.

Any (real) linear space V that is equipped with an inner product of signature (p, q) has a Clifford algebra $Cl_{p,q}$ associated to it. The signature denotes the number of plus signs p and the number of minus signs q in the canonical quadratic form of the inner product. This associated Clifford algebra is the natural (hypercomplex) number system in which we can express all possible geometrical operations on the oriented subspaces (vectors, oriented plane segments, etc.) of V. Familiar examples of Clifford algebras are the complex algebra $Cl_{0,1}$, the quaternion algebra $Cl_{0,2}$, the Pauli algebra $Cl_{3,0}$ and most importantly the time-space (or Majorana) algebra $Cl_{1,3}$. In terms of $Cl_{1,3}$, the Maxwell-Heaviside equations can be formulated as a single simple equation of the form $\partial F = -S$, (1).

Clifford Analysis (CA) can be regarded as a higher-dimensional function theory which generalizes the 2-dimensional theory of complex holomorphic functions. In CA, the algebra of complex numbers is replaced with a Clifford algebra $Cl_{p,q}$ and the classical complex Cauchy-Riemann (CR) equation is replaced with a $Cl_{p,q}$-valued equation, having physical relevance. CA is the proper mathematical setting for studying generalized physics (encoded in a chosen CR equation) in universes with an arbitrary number p of time dimensions and an arbitrary number q of space dimensions. The particular case, $p = 1$ and $q = 3$, has direct relevance for the physics in our own universe, and thus provides us with a function theory over Minkowski space in which the functions represent electromagnetic or quantum fields.

Armed with this mathematical machinery we can study electromagnetism to a depth that can not be reached with the very limited and totally inappropriate classical vector calculus. Of all the mathematical formulations of electromagnetism produced so far, is CA the only framework which is capable of actually solving Eq. (1) in a totally new and rigorous way. To illustrate the superiority of this new approach, I will discuss the following subset of new results:

(i) Any electromagnetic field, in a region without sources, is holomorphic. Holomorphy can be interpreted as being intrinsically holographic. In physical terms, this means that any such field can be reconstructed inside a region from its values on the boundary of the region. Any field (static, evanescent, transient, etc.)!
(ii) Our curent model for electromagnetism (irrespective of its formulation) has no solution in general! It requires that integrability conditions are fulfilled, which turn out to be exactly local conservation of electric and magnetic monopole charge density.
(ii) The general solution to the electromagnetic radiation problem with given compact smooth sources in vacuum can be solved directly in time-space, without making the detour of invoking potentials and without the need of a Green's dyadic. It only requires a fundamental solution (i.e., a Green's distribution) of the wave equation. The particular solution of the electromagnetic radiation problem is already known as Jefimenko's equations, but the more general CA derivation reveals that a second, new and less singular, form exists, which is far more practical to use than Jefimenko's form. Furthermore, the CA derivation continues to hold in the presence of an arbitrary gravity field (i.e., in a curved background vacuum).

(iv) A radiation boundary condition can be formulated, by using a Cauchy kernel with appropriate causality. A Cauchy kernel is a vector-valued derivative of a fundamental solution of the wave equation. A practical application for such a condition is e.g., the construction of a perfectly reflection less grid boundary (without having to introduce locally a dissipating medium), useful for simulating wave propagation in time-space over an arbitrarily truncated discretization mesh.

(v) Although it is not yet definitely proved, CA strongly suggests that the problem of electromagnetic scattering by arbitrarily shaped (homogeneous and isotropic) dielectric bodies (i.e., a generalization of Mie's problem) might be solvable analytically in time-space.

REFERENCES

1. Brackx, F., R. Delanghe, and F. Sommen, *Clifford Analysis*, Pitman, London, 1982.
2. Doran, C. and A. Lasenby, *Geometric Algebra for Physicists*, Cambridge Univ. Press, Cambridge, 2003.
3. Franssens, G. R., "Introduction to Clifford analysis," *Proceedings of the IKM 2009*, K. Grlebeck and C. Knke, eds., Weimar, Germany, Jul. 7–9, 2009, Available online at: http://euklid.bauing.uni-weimar.de/ikm2009/paper.php.
4. Franssens, G. R., "A physical interpretation of Clifford analysis," *Proceedings of the 18th ICFIDCAA*, Macau, China SAR, Aug. 13–17, 2010.
5. Franssens, G. R., "Clifford analysis solution of the electromagnetic boundary value problem in a gravitational background vacuum," *Advances in Applied Clifford Algebras*, Vol. 20, 587–616, 2010.
6. Franssens, G. R., "Fundamental theorems for Clifford algebra-valued distributions in Elliptic Clifford analysis," *Advances in Applied Clifford Algebras*, Vol. 21, No. 4, 697–705, 2011.
7. Hestenes, D., *Space-Time Algebra*, Gordon and Breach, New York, 1966.

Generation of Large-scale EM Simulation Scenarios from Mechanical CAD Models

Piotr Lukasik[1], **Andrzej Wieckowski**[1], **Malgorzata Celuch**[2], **and Bartlomiej Salski**[2]

[1]QWED Sp. Z O.O., Ul. Krzywickiego 12, Lok. 1, Warsaw 02-078, Poland
[2]Institute of Radioelectronics, Warsaw University of Technology
Ul. Nowowiejska 15/19, Warsaw 00-665, Poland

Abstract— With the continuous development of electromagnetic (EM) simulation software, and everincreasing power of computer hardware, researchers and engineers feel encouraged to analyse EM scenarios that become larger and geometrically more complicated. When EM software was practically entering the simulation market in 1990s, a coax-to-waveguide transition was a representative example of what could then be modelled. Considering relative structural simplicity of such examples, EM solvers tended to come with their own geometry editors, dedicated to the needs and incorporating the specific knowledge of EM solvers.

Later, throughout 2000s, in response to the ever-increasing expectations of microwave designers, several academic centres and also commercial companies invested vast efforts to replace simple "editors" by more advanced CAD-based "modellers" serving as an alternative EM GUI. Despite a notable success of several such solutions [1, 2], three disadvantages can be depicted and have, in fact, been found problematic in several EU-funded research projects such as [3, 4]:

- a substantial amount of work previously funded in "mechanical" projects was being repeated from scratch,
- automatic conversion between various CAD formats, though theoretically declared, was never working as expected
- some extra work of adding EM ports, ensuring EM mesh consistency, defining specific EM postprocessing, etc., were extra tasks often incompatible with the overall CAD format.

Our recent solution has been to base our geometry definition on the Autodesk® Inventor® software — a software package well-known in the the microwave society and especially popular at SMEs.

Our presentation will address the above-mentioned difficulties in detail and describe our novel methods of obviating them. In particular, it will show how the new algorithms implemented within the QuickWave software environment [5] allow for effectively solving several EM scenarios of direct interest for the on-going EU projects [3, 4], automatically and consistently converting their geometry from their pre-validated mechanical counterparts.

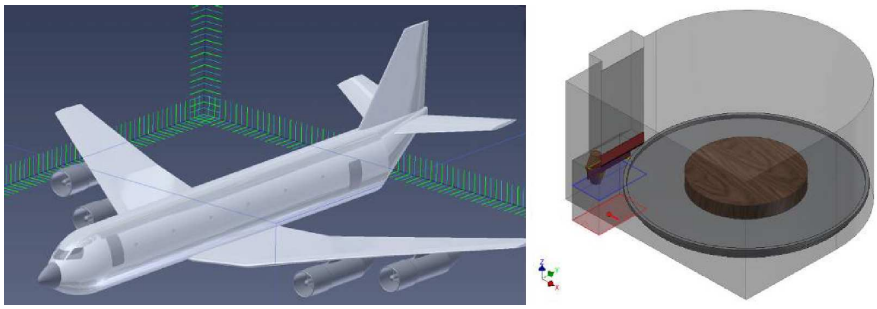

(a) (b)

Figure 1: Examples of large-scale mechanical models automatically converted from Autodesk Inventor® to FDTD simulation scenarios with QW-AddIn: (a) an aircraft [3], (b) a domestic microwave oven with its feeding system [4] (details omitted in the figure for clarity).

REFERENCES

1. http://www.cobham.com/about-cobham/aerospace-and-security/about-us/antenna-systems/aurora/products/concerto/modeler.aspx.
2. www.cst.com.
3. http://www.hirf-se.eu/hirf.
4. http://www.heecs.eu/.
5. http://www.qwed.eu/v2012ais.html.
6. http://usa.autodesk.com/autodesk-inventor/.

Session 1A6a
Nonlinear Electromagnetic Problems

Numerical Technique to Calculate Propagation Constants for the Problem of Polarized Wave Propagation in a Layer with Nonlinear Permittivity

D. V. Valovik and E. V. Zarembo
Penza State University, 40 Krasnaya Street, Penza 440026, Russia

Abstract— During many years problems of TE and TM waves propagation through nonlinear layers are intensively investigated. Such problems attract more and more attention due to their importance in different areas such as nonlinear optics, plasma physics, microelectronics etc..

We consider a plane layered waveguide structure. The layer is located between two half-spaces with constant permittivities. The permittivity inside the layer is an arbitrary function of the electric field intensity. We consider propagation of polarized (TE or TM) electromagnetic waves in such a structure. The physical problem for surface waves is reduced to (nonlinear) boundary eigenvalue problem for nonlinear ordinary differential equations. Usually, in such problems, the main goal is to obtain a dispersion equation (DE) for propagation constants (eigenvalues). In spite of the fact that for such a structure formed by a layer with constant permittivity it is easy to find exact DEs it is a serious problem to obtain exact DEs for a layer with nonlinear permittivity. For many physically interesting nonlinear permittivities it is far beyond our abilities to obtain and analyze exact DEs. So it is necessary to develop numerical methods to solve such nonlinear boundary eigenvalue problems. We suggest a numerical approach to calculate propagation constants (eigenvalues) for (nonlinear) layered waveguide structures based on numerical solution of a Cauchy problem in the layer. By means of transmission conditions on the layer boundaries we can define initial data for this Cauchy problem. When this Cauchy problem is solved we construct a function that depends on the spectral parameter. The zeros of this function which can be effectively calculated are the sought-for propagation constants (eigenvalues). Numerical results are presented for TE and TM waves and for different permittivities. The comparison with known results for Kerr nonlinearity is drawn.

Electromagnetic TE Wave Propagation in Nonlinear Layered Waveguide Structures. Computational Approach to Determine Propagation Constants

D. V. Valovik
Penza State University, 40 Krasnaya Street, Penza 440026, Russia

Abstract— During many years problems of TE and TM waves propagation through nonlinear layers are intensively investigated. Such problems attract more and more attention due to their importance in different areas such as nonlinear optics, plasma physics, microelectronics etc..

We consider a plane multilayered waveguide structure. The layers are located between two half-spaces with constant permittivities. The permittivities inside the layers can be constants or nonlinear (depending on the electric field intensity). This structure can be treated as a 1D (nonlinear) photonic crystal. We consider propagation of polarized electromagnetic waves in such a structure. The physical problem is reduced to (nonlinear) boundary eigenvalue problem in a multiply-connected domain. Usually, in such problems, the main goal is to obtain a dispersion equation (DE) for propagation constants (eigenvalues). In spite of the fact that for such structures formed by layers with constant permittivities it is possible to find exact DEs it is getting tiresome to find it for several layers. It is even harder (if at all possible) to obtain exact DEs for layers with nonlinear permittivities. For many physically interesting nonlinear permittivities it is far beyond our abilities to obtain and analyze exact DEs. We suggest a numerical approach to calculate propagation constants (eigenvalues) for (nonlinear) layered waveguide structures based on numerical solution of a Cauchy problem in each layer. By means of transmission conditions on the layer boundaries we can define initial data for each Cauchy problem. When all Cauchy problems are solved we construct a function that depends on the spectral parameter. The zeros of this function which can be effectively calculated are the sought-for propagation constants (eigenvalues). In the most general case we are forced to work with $(N + 1)$-dimensional grid where N refers to N layers and one dimension to the propagation constant.

Electromagnetic Wave Diffraction on the Conducting Thin Screen Placed on the Isotropic and Anisotropic Media Interface

A. F. Bourganov, E. M. Karchevskiy, and N. B. Pleshchinskii
Kazan Federal University, Russia

Abstract— Let the conducting thin screen be placed on the media interface. The upper medium is isotropic and the lower medium is anisotropic. The two-dimensional diffraction problems of the electromagnetic wave on the screen are reduced to integral equation.

First of all, the waves reflected into the upper semi-space and transmitted into the lower semi-space are found by the over-determined boundary value problem method. The main idea of the over-determined problem method is the following: the auxiliary boundary value problems are considered in the partial domains of the structure being under consideration. These problems contain more conditions on the boundary than it is necessary to select the unique solution. The connections between boundary functions (necessary and sufficient conditions for solvability of the over-determined problems) are to be considered together with the conjugation fields conditions in the auxiliary problem.

The different cases are presented when the conditions for solvability of the over-determined problems can be found in the analytical form. It is essentially that in these cases the equation for the Fourier transform of the potential functions of the electromagnetic field has the solution of the simple form.

The field perturbation by the screen is determined by the same over-determined boundary value problem method. The diffraction problem in the case of TE-polarization is equivalent to the integral equation with logarithmic singularity in the kernel, and in the case of TM-polarization it can be reduced to hyper singular integral equation. The Galerkin method with set of basic functions being the Chebyshev polynomials of the first or second kind is usually used for approximate solving integral equations in both cases.

Parallel Algorithm of Solving the Electromagnetic Wave Diffraction Problem on the Spherical Screen

E. M. Karchevskiy and N. B. Pleshchinskii
Kazan Federal University, Russia

Abstract— The electromagnetic wave diffraction problem on a thin conducting screen can be formulated as a boundary value problem for the Maxwell set of equations with respect to complex-valued amplitudes of field components (by harmonic dependence on time). In the case of screen being a part of spherical surface it is necessary to construct solutions of the Maxwell set inside and outside of sphere satisfying the boundary conditions and the conjunction conditions.

Any solution in the spherical coordinate system can be represented as a sum of solutions of magnetic and electric types. All components of every individual summand can be represented by potential functions. These functions have the form of the series of radial and spherical function products.

Let the coefficients of expansion into a series of the exterior field be given. It is necessary to find the coefficients of expansion of the field interior sphere and exterior sphere (in view of condition at the infinity).

The field conjunction conditions on a sphere represent by themselves the pair summatorial equation relative to unknown coefficients. This equation can be reduced to a regular infinite set of linear algebraic equations by integral-summatorial identities method. Coefficients of this set contain the integrals over screen of the products of spherical functions.

For all stages of numerical algorithm of solving the problem the parallel calculating processes are possible.

At first, if field traces of outside source at the sphere are decomposed onto magnetic and electric parts then magnetic and electric parts of the unknown field can be found independently. Secondly, if coefficients of field conjunction conditions at the sphere do not depend on longitude coordinate then calculations also can be fulfilled independently for every number of the series coefficients. Thirdly, if by reduction of infinite set the finite set of linear equations of large dimension is obtained, then it can be solved by one of parallel algorithm. But the most effect can be obtained just at the stage of calculating of the integrals over screen.

Integral Equation Methods in Optical Waveguide Theory

A. S. Il'inskii[1] **and E. M. Karchevskiy**[2]

[1]Lomonosov Moscow State University, Russia
[2]Kazan Federal University, Russia

Abstract— Optical waveguides are regular dielectric rods having various cross sectional shapes where generally the permittivity may vary in the waveguide's cross section. The permittivity of the surrounding medium may be a step-index function of coordinates. The eigenvalue problems for natural modes (surface, leaky, and complex eigenmodes) of inhomogeneous optical waveguides and for step-index optical waveguides with the smooth boundary of the cross-section are formulated as problems for the set of time-harmonic Maxwell equations with partial radiation conditions at infinity in the cross-sectional plane.

The original problems are reduced with the aid of the integral equation method (using appropriate Green functions) to nonlinear spectral problems with Fredholm integral operators. Theorems on the spectrum localization are proved. It is shown that the sets of all eigenvalues of the original problems may consist of isolated points on the Reimann surface and each eigenvalue depends continuously on the frequency and permittivity and can appear or disappear only at the boundary of the Reimann surface.

The original problems for surface waves are reduced to linear eigenvalue problems for integral operators with real-valued symmetric polar kernels. The existence, localization, and dependence on parameters of the spectrum are investigated.

Collocation and Galerkin methods for numerical calculations of the natural modes are proposed, the convergence of the methods is proved, and some results of numerical experiments are discussed.

TM Wave Propagation in a Cylindrical Waveguide with Kerr Nonlinearity

Yu. G. Smirnov
Penza State University, 40 Krasnaya Street, Penza 440026, Russia

Abstract— We consider three-dimensional space filled by isotropic medium with constant permittivity. In this medium a circle cylindrical waveguide is placed. The waveguide is filled by anisotropic nonmagnetic nonlinear medium with Kerr nonlinearity. We consider TM- electromagnetic waves propagating along the waveguide axis, that is eigenmodes of the structure.

It is necessary to find eigenvalues of the problem that correspond to surface waves propagating along waveguide axis, i.e., the eigenvalues corresponding to the eigenmodes of the structure. We seek the real values of spectral parameter.

The results about the properties of the boundary value problem solutions are proved under certain sufficient conditions for the problem's parameters. Especially the proposition about eigenvalues (solutions of dispersion equation existence for the nonlinear boundary eigenvalue problem are proved. The small parameter method is used for proving. In this problem the nonlinearity coefficient is the small parameter. This is the natural approach, as it is known, that Kerr law (which we use in this work) holds in this case.

The problem is reduced to the nonlinear eigenvalue problem for system of integral equations. The iteration method to calculate approximate eigenvalues of the boundary problem is formulated. Also the existence and convergence (the approximate solution to the exact one) theorems are proved.

Numerical results are presented. Comparison numerical results for nonlinear structure with well-known linear case is also obtained. Convergence of the approximate solutions is analyzed. New effects for TM- wave propagation in a cylindrical waveguide with Kerr nonlinearity are presented. Dependence of eigenvalues with respect to the parameters of the problem is demonstrated.

Session 1A6b
Scattering, Diffraction, and Inverse Scattering

On Rayleigh and Mie Theory

Jerald W. Caruthers
University of Southern Mississippi, 1020 Balch Blvd, Stennis Space Center, MS 39529, USA

Abstract— Scattering described today as "Rayleigh Scattering" represents a phenomenon that is far short of what Rayleigh actually contributed to the topic in both optics and acoustics. This limited view seems to lie in a few papers in which he truncates series solutions for practical computations, thus leading to scattering of the form $(ka)^4$ for ka much greater than unity, where k is the wavenumber and a is the radius of the sphere, and for a few selected limitations on the index of refraction. These approximations led optical scientists to equating "Rayleigh scattering" to little more than the reason the sky is blue. In 1908 Gustav Mie developed a theory for plane-wave scattering from a sphere to which the names "Mie theory" and "Mie scattering" have been indelibly attached to many applications in optics. It is virtually unknown, especially in electromagnetics, that Rayleigh actually developed the full theory of plane-wave scattering from a sphere in 1872 [1] and, as we follow herein, in 1878 [2], including original contributions in the concurrent development of mathematics of Bessel functions, Legendre functions, and spherical harmonics. Although Rayleigh did not solve the fully electromagnetic problem (i.e., two coupled partial differential equations with differing boundary conditions), his acoustic-field solutions are equivalent to those of the electric-field part. The original motivation for this approach, as presented at the 162nd meeting of the Acoustical Society of America in 2011 [3], was to establish a means of treating weak acoustic scattering from non-resonating bubbles in water based on their contribution as a distribution of realistic absorbing spheres by combining Rayleigh and Mie theories versus the standard approach for such work involving the highly attenuative propagation and strong resonant scattering from bubbles. A version of the standard approach to acoustic scattering in a bubbly medium was presented at PIERS 2000 [4]. Here the objective is limited to presenting a brief historical context for the work of Mie, and including, in addition to Rayleigh's work, the works of Clebsch (1861), Lorenz (1890), and Debye (1909), and others.

ACKNOWLEDGMENT

This work was supported by the U.S. Office of Naval Research, Code 322.

REFERENCES

1. Rayleigh, B. J. W. S., *Proc. London Math. Soc.*, Vol. 4, 253–283, 1872.
2. Rayleigh, B. J. W. S. and R. B. Lindsay, *The Theory of Sound*, Primarily Section §334, Vol. 2, Macmillan, 1878.
3. Caruthers, J. W., "On Rayleigh and Mie scattering," *Proceedings of Meetings on Acoustics*, Vol. 14, 070001-13, 2011.
4. Goodman, R. R. and J. W. Caruthers, "On the propagation and scattering from random bubble clouds in the sea," *Progress In Electromagnetics Research Symposium*, Cambridge, MA, 2000.

Paradoxes in Laser Heating of Nanoparticles

M. I. Tribelsky[1, 2], **B. S. Luk'yanchuk**[3], **A. E. Miroshnichenko**[4], **Yu. S. Kivshar**[4], **and A. R. Khokhlov**[1, 5]

[1]Faculty of Physics, M. V. Lomonosov Moscow State University, Moscow 119991, Russia
[2]Moscow State Institute of Radioengineering, Electronics and Automation (Technical University) Moscow 119454, Russia
[3]Agency for Science, Technology and Research, Data Storage Institute, Singapore 117608, Singapore
[4]Nonlinear Physics Centre, Research School of Physics and Engineering Australian National University, Canberra ACT 0200, Auatralia
[5]A. N. Nesmeyanov Institute of Organoelement Compounds RAS, Moscow 119991, Russia

Abstract— Light absorption by a spatially uniform non-magnetic spherical nanopartile in the vicinity of surface plasmon (polariton) resonances is studied in detail based on the exact Mie solution. It is shown that, in sharp contrast to the common belief, a weakly dissipating particle absorbs much more energy than a particle with strong losses. The absorption may have very unusual properties and cannot be described by the Rayleigh approximation, no matter how small the particle is. A simple universal formula for the resonant absorption lineshape as a function of the particle size and its complex dielectric permittivity is obtained. The obtained results are applied to the problem of laser heating of nanoparticles. The optimization of the input of the laser pulse energy into a particle is performed at fixed fluence with respect to the particle size, wavelength and duration of the laser pulse. We introduce a new quantity, *an effective absorption coefficient* of a particle, which allows to compare quantitatively the light absorption by nanoparticles with the absorption of a bulk material. We describe the range of parameters where *giant absorption enhancement* can be observed, and give practical examples for metals whose optical properties vary from weak (potassium) to strong (platinum) dissipation. We also point out that even larger absorption can be achieved for core-shell nanoparticles. Effects of heat transfer from the particle to a host medium are inspected too. The results obtained may be employed in biology, medicine, storage and processing of information and in other nanotechnologies. Our main publications devoted to the subject are as follows [1, 2].

ACKNOWLEDGMENT

The work is partly supported by the Russian Foundation for Basic Research, Grant 12-02-00391-a.

REFERENCES

1. Tribelsky, M. I., "Anomalous light absorption by small particles," *Europhys. Lett.*, Vol. 94, 14004, 2011.
2. Tribelsky, M. I., A. E. Miroshnichenko, Y. S. Kivshar, B. S. Lukyanchuk, and A. R. Khokhlov, "Laser pulse heating of spherical metal particles," *Phys. Rev. X*, Vol. 1, 021024, 2011.

Millimetre-wave Sea Clutter at Low Depression Angles

Helmut Essen[1], **Andreas Danklmayer**[2], **and Gregor Biegel**[2]

[1]Maxonic GmbH, Wachtberg, Germany
[2]Fraunhofer Institute for High Frequency Physics and Radar Techniques, Wachtberg, Germany

Abstract— The reflectivity of the sea surface is of high importance for the prediction of ship-borne radar performance. Such radars typically operate under shallow depression angles. Available clutter data, however, very often have been gathered from the air or even from space and consequently are representative for steep depression angles. A specific lack of data exists for millimetre wave bands, which are very well suited for close-in applications as for the detection and tracking of small boats carrying illegal refugees or in the struggle against piracy. To improve detection algorithms for small maritime targets, a quantitative analysis based upon a thorough knowledge of the sea scattering mechanism is necessary and experimental investigations have to be done. The lack of millimetre wave sea clutter data is primarily due to the fact, that the atmospheric absorption is relatively high in comparison to the classical radar bands and that due to this reason millimetre waves for possible sensor applications have been neglected. With the advance of close-in applications this attitude against these radar bands has changed, especially as millimetre-waves offer extremely good multipath propagation properties and often are able to cover a considerable range even over the horizon with the help of duct phenomena and even the attenuation properties under many weather conditions in a maritime environment are much better than those for t IR sensors, which are currently in use.

To help to close this lack of knowledge, sea clutter measurements at millimetre-wave bands have been conducted at several occasions under Atlantic Ocean conditions at different places in Europe, like Brittany and the German Bight of the North Sea.

The paper discusses the measurement instruments and the geometry and gives typical results. Wave front patterns are analysed and compared with clutter models. A statistical evaluation is done base upon dependencies on Wave direction and sea state.

Millimetre-wave Propagation in Atlantic and Tropical Environment

Helmut Essen[1], **Andreas Danklmayer**[2], **Gregor Biegel**[2], **Stefan Sieger**[2], **and Sebastian Hantscher**[2]

[1]Maxonic GmbH, Wachtberg, Germany
[2]Fraunhofer Institute for High Frequency Physics and Radar Techniques, Wachtberg, Germany

Abstract— For maritime applications at short to medium range electro-optical sensors are competing with radars. Among these applications are ship-traffic control in coastal regions, maritime border surveillance, protection against terrorist attacks and naval applications. Sensors with a stable and predictable performance under any environmental conditions are demanded. The performance of radar sensors operating within the marine boundary layer is influenced by the actual atmospheric conditions, the sea surface and the geometry between radar and reflection point. To assess the propagation within defined layers, experiments were performed using a radar operating against reference reflectors carried on naval vessels, which moved on outbound and inbound courses. Based on measurements of atmospheric properties and sea surface parameters, refractivity profiles were calculated and using the parabolic equation model TERPEM, propagation factors were determined.

Under multinational research programs propagation measurements were performed in the Mediterranean and under Baltic Sea conditions. Ships equipped with corner reflectors serving as point targets at defined height above sea performed outbound and inbound runs, while the atmosphere and sea surface was probed to be able to determine the relevant refractive index. The Experimental data have been compared with results from modeling, mainly giving a good prediction of the experimental data. In the framework of a cooperative program between Singapore and Germany radar measurements were carried out in the tropical area of Singapore Strait. Those data have undergone the same evaluation procedures using the relevant environmental information. It turned out that the tropical atmospheric conditions were considerably different to those of moderate climate areas, and modeling exhibited considerable shortcomings.

The paper discusses the measurement instruments and the geometry and gives typical results for experiment and simulation.

Recent Activities in the Area of mmW-signals Propagation Research with Respect to the Maritime Boundary Layer

A. Danklmayer[1], **H. Essen**[1], **G. Biegel**[1], **J. Förster**[2], **M. Behn**[2], **Y. Hurtaud,**[3], **L. Castanet**[4], **and V. Fabbro**[4]

[1]Fraunhofer-FHR, Germany
[2]Technical Center for Ships and Naval Weapons, Germany
[3]DGA/MI, BP 54519, France
[4]Departement Electromagnetique et Radar, ONERA, France

Abstract— Electromagnetic wave propagation of microwaves and millimeter-waves in the troposphere above the sea surface continues to be a topic of current research. Depending on the atmospheric conditions like air temperature, humidity, air pressure as well as the sea state, the signal characteristics and the measurement geometries, the propagation mechanisms can vary to a large degree. Especially for point to point transmission, small target detection from land- or ship based radar systems and for tactical decision aids the knowledge of the propagation conditions is indispensible.

Within a technical arrangement between France and Germany two measurement campaigns using a variety of radars in a wide spectra of frequencies (C-band, X-band, Ka-band up to W-band) are performed in May and Sepember 2012. The radar measurements will take place during two dedicated campaigns at two different sites, on one hand at the island Sylt in the Baltic Sea in Germany in order to cover Atlantic weather conditions, and on the other hand near Toulon (France) to cover the mediterranean conditions. Beside the radar measurements a sophisticated approach is foreseen in order to characterize the meteorological and sea state conditions. For each campaign specific research vessels and a number of sensors are available allowing for measurements along specific in- and outbound runs.

The overall goal of the study is to derive the refractivity based on clutter measurements by taking resource to the refractivity from clutter (RFC) technique developed previously. Recent activities in the area of mmW-signal propagation research in the maritime boundary layer will be reported and latest results from 2012 are shown.

Session 1A7
Extended/Unconventional Electromagnetic Theory, EHD(Electro-hydrodynamics)/EMHD(Electro-magneto-hydrodynamics), and Electro-biology 1

X-ray Image Processing in Studying Jawbone Tissues

J. Mikulka and M. Kabrda
Department of Theoretical and Experimental Electrical Engineering
Brno University of Technology, Kolejní 4, Brno 612 00, Czech Republic

Abstract— Image processing in biomedical applications is strongly developing issue. Many methods and approaches for image preprocessing, segmentation and visualization were described. This paper describes X-ray image processing. The aim of processing is to segment regions of jawbone cysts and evaluate their local descriptors. It is necessary to choose suitable segmentation method because of adverse parameters of regions. The regions of the cysts are of low contrast and the pixel intensity distribution is not homogenous. The semiautomatic live-wire method was chosen. This approach to image segmentation is faster and more accurate than manual segmentation. It is very good compromise between simple manual edge tracing and automatic methods such as thresholding, watershed segmentation or other methods whose results must be post-processed. The second step of processing is to evaluate local descriptors of segmented regions which correspond to cysts. Several parameters were chosen to describe these regions — region area, mean gray value of intensities, modal gray value of intensities, standard deviation of intensities, minimal and maximal gray value of intensities, integrated intensity, median of intensities and shape descriptors of region (perimeter, circularity, aspect ratio, roundness and solidity). Values of these parameters will be used in following development of semiautomatic processing method with regard to current assessment of cysts by doctors.

Sensors and Experimental Model Verification on HV Transformers Measurement

P. Drexler, P. Fiala, M. Friedl, P. Marcon, M. Steinbauer, Z. Szabo, and M. Hadinec
Department of Theoretical and Experimental Electrical Engineering,
Brno University of Technology, Kolejni 2906/4, Brno 612 00, Czech Republic

Abstract— One of the problematic phenomena in the field of high-voltage technology, is the occurrence of partial discharge. Several other effects have combined with this notion over time [1]. In consequence of these effects there emerge short electromagnetic pulses with a defined and measurable spectre in the characteristic frequency band [2]. The group of end products attributable to the emergence of interfering signals involves, for example, displacement current in a dielectric, pulse current on the interface between dielectrics, or the dielectric/metal interface owing to high electric field intensity and structure of the dielectric.

In HV and VHV transformers the dielectric is mineral or synthetic oil. Due to the increase in partial discharge activity in transformer oil free atoms of carbon, hydrogen and oxygen develop from hydrocarbons, and there also generates a certain percentage of water and other organic compounds. All of these elements decrease the quality of the dielectric. In addition to that, rapid increase in pulse activity may cause the formation of a hazardous explosive compound of oxygen and hydrogen. Then, this situation may result in explosion and damage to the device.

In order to prevent the transformer failure the observation of pulse activity is necessary. The occurrence of discharge with substantial charge transport level can be localized in critical areas of the transformers. Having a possibility to localize the increased discharge activity in some of the critical areas allows us to undertake precautions in order to avoid the critical transformer failure. The discharge activity localization can be determined on the basis of processing of signals from suitable installed sensors. The evaluation of the discharge location utilizes the model of wave propagation inside the transformer, which has been presented in early work [3].

For the experimental verification of localization method a model setup has been built, Fig. 1. The model setup is equipped with antenna sensors, RF amplifiers and data acquisition unit. The model setup is described in the paper as a following step of the research. The result of the measurement which has been performed up to the present are presented also.

ACKNOWLEDGMENT

The research described in the paper was financially supported by grant of Czech ministry of industry and trade No. FR-TI1/001, GACR 102/09/0314 and project of the BUT Grant Agency FEKT-S-10-13.

REFERENCES

1. Fiala, P., "Transformer partial discharge modeling, minimal breakdown value set in a critical parts of transformer design," *Research Report*, Laboratory of Modeling and Optimization Field in Electromagnetic Systems, FEI VUT and ABB EJF a.s. Brno No. 2/99, Brno, Czech Republic, Mar. 18, 1999.
2. Sarathi, R., A. J. Reid, and M. D. Judd, "Partial discharge study in transformer oil due to particle movement under DC voltage using the UHF technique," *Electric Power Systems Research*, Vol. 78, 1819–1825, Elsevier, 2008.
3. Fiala, P., T. Jirk, P. Drexler, and T. Jirku, "Detection of partial discharge inside of HV transformer, modeling, sensors and measurement," *PIERS Proceedings*, 1013–1016, Cambridge, USA, Jul. 5–8, 2010.

Quantum Hydrodynamics of Charge Carriers in Graphene

P. A. Andreev
Department of General Physics, Physics Faculty, Moscow State University, Russian Federation

Abstract— Graphene is the carbon monolayer. This material has a lot of interesting properties and is in a centre of many present day researches. In literature graphene is considered as independent system *and* as a part of semiconductor geterostructures and field effect transistor. Thus, especially the graphene conductivity properties and properties of graphene carriers have been studied. One of the unusual and important properties of graphene carriers is the carrier dispersion. The energy of free nonrelativistic electron is proportional to the square of the momentum then the dispersion law is quadratic. Novoselov et al. shown that graphene carriers has linear dispersion law and they are massless. This result is analogous to the free ultrarelativistic electrons and massless particles. In quantum case the massless Dirac's equation gives the linear dispersion law. Thereby, the massless Dirac's equation was suggested for description of grapnene carrier dynamics. Instead of speed of light in Dirac's equation the Fermi velocity graphene electron were used.

Properties of single carrier quasi-particle in graphene is a fundamental properties which give us understanding of microscopic carrier dynamics, but for understanding of a graphene role in semiconductor structures we need to study collective dynamics of graphene carriers. For this purpose in literature many-particle massless Dirac's equation including the Coulomb interaction between carriers is used. Feynman's diagram method has been used in many papers for studying collective properties of graphene carriers.

In this paper we present a new method of studying of graphene carriers collective properties. This method is called many-particle quantum hydrodynamics (QHD). One is based on many-particle massless Dirac's equation. QHD method allows us to derive equation which described dynamic of particles in physical space (for graphene it is a two dimensional space) instead of 2N dimensional configuration space where the wave's spinor is defined.

We derive QHD equations for the graphene carriers and use these equations for the calculation of dispersion properties of collective excitations in graphene. We suppose that graphene situated in external uniform magnetic field directed at different angles to the grapheme plane. As the results we present dispersion dependencies for collective excitations in grapheme and make comparison with the results of other authors which they found by other methods.

Microscopic Classic Hydrodynamic and Methods of Averaging

L. S. Kuzmenkov[1] and P. A. Andreev[2]

[1]Department of Theoretical Physics, Physics Faculty, Moscow State University, Russian Federation
[2]Department of General Physics, Physics Faculty, Moscow State University, Russian Federation

Abstract— In classic mechanics there are at least two general methods for hydrodynamic equation derivation. The first one is the consideration of macroscopic parallelogram in a medium and calculation for number of particles, momentum or energy passing through the planes. It is the way of macroscopic hydrodynamics. The second method of the hydrodynamic equations derivation includes the physical kinetics and offers the microscopic method starting from Liouville equation. Using of the physical kinetics as intermediate step leads to additional unnecessary limitation. This method includes derivation of the kinetic equation chain which also called BBGKY chain. The hydrodynamic equation arises as moments of the frequency function.

We present a new method for derivation of the hydrodynamic equation directly from classic motion equations. The first and most important step is the definition of the particles density in vicinity of the point of the physical space. This definition contains generalized function (Dirac's delta function) and represents analytical representation of a notion of the physically infinitesimal volume. The Newton law of motion is used for motion description of each particle in vicinity of point of physical space. Particle density is the first collective variable in our description. Next step is the derivation of equation of temporal evolution for the particle density. In the result new physical quantities are appeared and we can derive evolution equations for these quantities. During derivation a chain of equations is arisen, this chain is an analog of the BBGKY chain, but other framework lies behind.

This method is developed as for the neutral as for the charged particles, but in our presentation we consider charged particles only and we consider non-relativistic limit. However, this method can be used for derivation of equations for relativistic hydrodynamic and kinetic as well. We demonstrate this method, as it has written, for simplest case. One of the interesting consequences is that electric dipole field, electric quadrupole field and etc are arise in equations of collective motion *and* in Maxwell equation as sources of electric field.

Building NMR/NQR Spectrometer

R. Kubásek and M. Alkhaddour
Department of Theoretical and Experimental Electrical Engineering
Brno University of Technology, Kolejni 4, Brno 612 00, Czech Republic

Abstract— Article deals with the topics of NMR or NQR spectrometer design. There will be described two basic approach of that design. Problem of excitation circuits and its matching and tuning will be solved. Free induction decay signal handing in RF and, or, in IF domain will be described. The basic experiment is made at spectrometer with varied B_0 field. In our case the resonating frequency is about 10 MHz. The NQR experiment will be made wit use of material consist of chlorine or nitrogen base. The own design with today non-expensive RF and IF pars respect to required SNR for small signal of FID signal is made. The basis principle can be seen at Fig. 1. The possibility of excitation and receiver circuit tuning with in frequency range will be discussed.

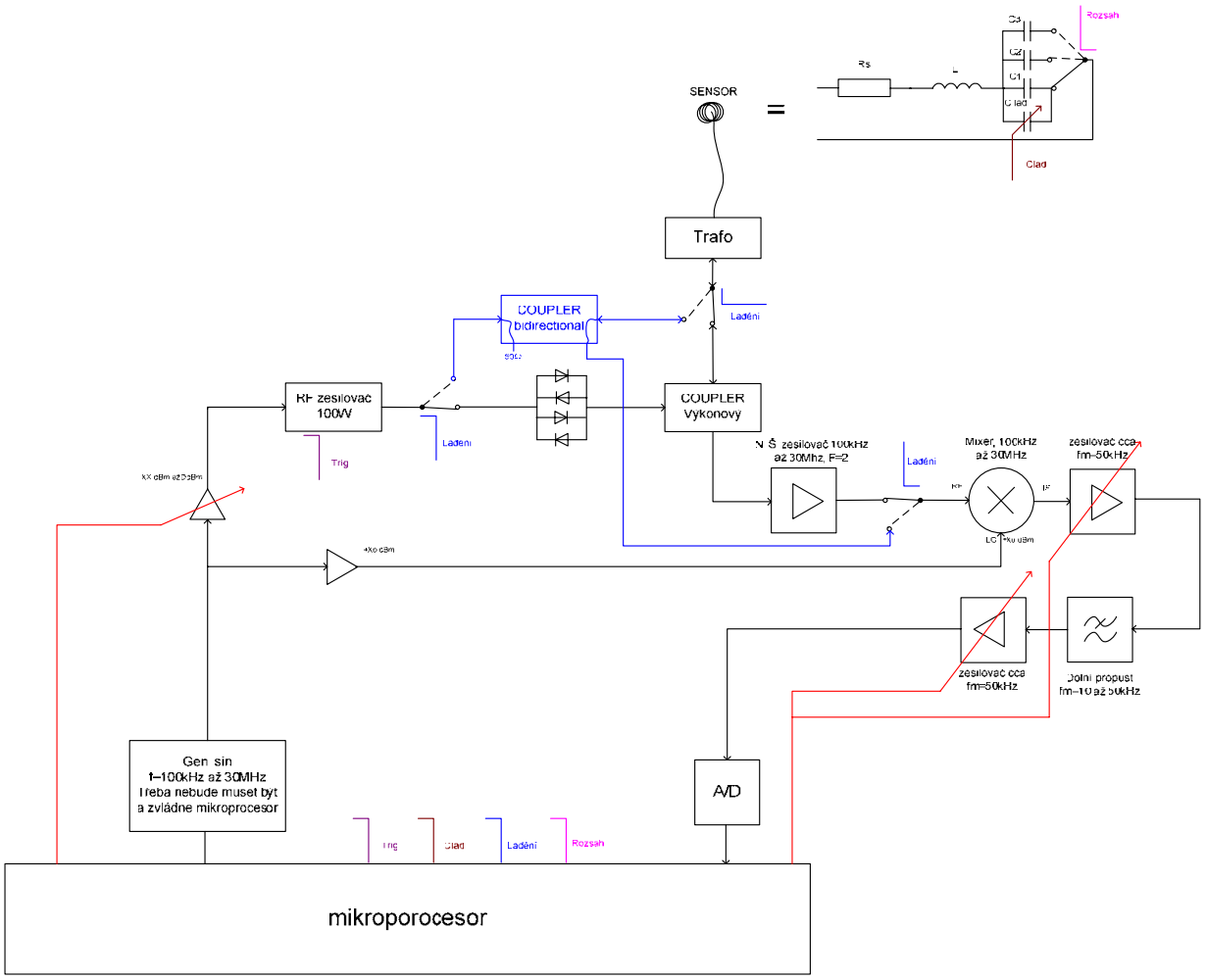

Figure 1: The principle diagram of NMR/NQR spectrometer.

Magnetic Flux Density Reconstruction Method

M. Hadinec
Department of Theoretical and Experimental Electrical Engineering
Brno University of Technology, Czech Republic

Abstract— This article deals with the measurement of magnetic flux density around copper specimens, which are created using printed circuit board technology. The current that flows in the specimen creates magnetic field. Such magnetic fields can be mapped using magnetic resonance tomography or by Hall probes. The magnetic flux density is measured in several planes around specimens, using Halls probes. The proper mapping of magnetic flux density around these specific specimens is important for electric impedance tomography and other further numerical purposes.

The method for reconstruction of magnetic flux density inside the measured volume will be presented and analyzed. The reconstruction method is based on Legendre polynomials approximation, using Least Mean Squares solver programmed in Matlab. This reconstruction method could be usable for acceleration of the mapping process, which is lengthy and can lead to many errors while measuring many points and many planes around the specimen. Using proper approximation coefficients, it is possible to compute individual approximated maps of magnetic flux density, so there is no need of fine mapping and meshing inside desired volume. These coefficients can be obtained from values measured on the edge of desired volume, using Laplaces's equation solution.The measured and approximated maps of magnetic flux density are compared and differences analyzed.

The theoretical model of magnetic flux density around measured specimen is made in COMSOL, magnetic flux density maps are simulated in several distances and axis above the specimen. The differences between measurement and simulation results are discussed.

REFERENCES

1. Dědek, L. and J. Dědková, *Elektromagnetismus*, Vol. 2, 232, Vutium, Brno, 2000, ISBN 80-214-1548-7.
2. Bergan, P. G., K.-J. Bathe, and W. Wunderlich., *Finite Element Methods for Nonlinear Problems: Proceedings of the Europe-US Symposium, the Norwegian Institute of Technology, Trondheim, Norway, August*, Springer-Verlag, New York, c1986, 817s, 1985, ISBN 03-871-6226-7.

Self-consistent Electrodynamics

Konstantin Meyl
Faculty of Computer and Electrical Engineering, Furtwangen University, Germany

Abstract— Even though one usually calculates capacitor losses with a complex epsilon it still offends the principle of a constant speed of light. Maxwell's term $c^2 = 1/\varepsilon \cdot \mu$ suggests a physically inexplicable complex speed. By such an offence against basic principles every physicist is asked to search and to repair the mistake in the textbooks.

The contribution clearly explains how vortex losses occur instead of using the postulated and fictive imaginary part of the material constant epsilon. The theory better explains the function of a microwave oven, the welding of PVC foils or how capacitor losses occur. The responsible potential vortices can be derived without postulate them from the established laws of physics. Vortex losses can even be proven experimentally and are clearly shown.

The potential vortex is substituted for the vector potential A, which has controlled electrodynamics as "impurity factors" ever since its introduction. A unified theory of all interactions and physical phenomena is missing without potential vortices. This theory justifies the efforts and the rationale for rebuilding electrodynamics and in so doing effectively removes contradictions of the vector potential and loss theory.

Consequences are discussed such as the discovery of magnetic monopoles by the German Helmholtz Center, the extended Poynting vector, and many more effects involved with the new approach of the potential vortex, that is replacing the vector potential in the dielectric.

REFERENCES

1. Meyl, K., *Self-consistent Electrodynamics, The Unified Theory Is Evolving, If the Potential Vortex Is Replacing the Vector Potential in the Dielectric.*, INDEL Publ., Villingen, 2010.

Low-level Measurement of Electric Field Intensity

P. Fiala, M. Friedl, and J. Mikulka
Department of Theoretical and Experimental Electrical Engineering
Brno University of Technology, Kolejni 2906/4, Brno 612 00, Czech Republic

Abstract— This article deals about the measurement of the electric field intensity in biological structures area. It is quantity which can be measured remotely, without touching the plant and which is a fact of exceptional importance for in-terrain applications. Yet the decisive aspect consists in the possibility of deciphering the information (about a living object) that may be carried by the electric field. Therefore, the most vital problem is to find out whether the electric field will be utilizable for contactless diagnostics. The principle of the method will consist in electric charge measurement on the electrodes of a capacitive sensor, showing the elimination of interferences and leakage currents. Theoretical analysis will be performed for setting the measurement method sensitivity with respect to anticipated magnitudes of the electric field during the day in different instantaneous weather conditions. The method of measurement using one test tree within the stand will be analyzed, with the group of other related steps comprising modification proposals for the sensor and measurement methodology, a comparison with the theoretical model, and a direct comparison with the data evaluated by other laboratory or experimental techniques.

ACKNOWLEDGMENT

The research described in the paper was financially supported by grant of Czech ministry of industry and trade no. FR-TI1/001, GACR 102/09/0314 and project of the BUT Grant Agency FEKT-S-11-5/1012.

REFERENCES

1. Meleschenko, S. N., "Nature of changes in electrical properties of plant tissue with change in the external conditions," *Biofyzika*, Vol. 10, No. 3, 507–513, 1965.
2. Aubrecht, L., Z. Stanek, and J. Koller, "Systematic study of the characteristics of the point to-plane corona on natural objects," *Proceedings of the International Congress on Plasma Physics 25th EPS Conference on Controlled Fusion and Plasma Physics*, 2431–2433, Prague, ECA 22C, 1998.
3. Aubrecht, L., J. Koller, and Z. Staněk, "Onset voltages of atmospheric corona discharges on coniferous trees," *Journal of Atmospheric and Solar Terrestrial Physics*, Vol. 83, 1901–1906, 2001.
4. Steinbauer, M., P. Fiala, K. Bartušek, and Z. Szabó, "Experiments with accuracy of air ion field measurement," *PIERS Proceedings*, 1062–1066, Hangzhou, China, Mar. 24–28, 2008.
5. Vojtek, T., M. Steinbauer, P. Fiala, and K. Bartušek, "Gerdien condenser measuring and numerical modeling of air ion fields," *Applied Electronics*, 225, 2006.

Utilization of Digital Potentiometers in ARC Filter Re-tuning

Z. Szabó and J. Sedláček
Department of Theoretical and Experimental Electrical Engineering
Brno University of Technology, Czech Republic

Abstract— In spite of the current dominance of digital technology, analog filters have retained their importance for applications such as data preprocessing in electronic systems. Within the field, various methods of connecting universal and easily retunable ARC filters are used to provide the best attainable form of the parameters required for signal processing circuits; the group of these parameters includes, for example, the separation of effective signals from noise. The aim of this work is to explore and verify different utilization possibilities related to modern digital potentiometers that could enable us to realize a comparatively simple connection of the tunable block of an active filter. Such a filter is applicable within a broad frequency range and can be used universally in the circuits of analog data preprocessing systems. Even though these circuits were originally designed for application in acoustic devices, they appear to be a promising solution for the realization of tuning of universal retunable filters. At present, the circuits are also commonly available in the form of integrated circuits and produced in manifold versions, which facilitates the performance of simultaneous tuning of multiple elements; this type of tuning is often necessary for us to carry out successful tuning of universal filters. General application of the circuits in universal tunable filters could produce substantial simplification of the process of realizing the final connection of filters.

ACKNOWLEDGMENT

The research described in the paper was financially supported by grant of Czech ministry of industry and trade No. FR-TI1/368, project of the BUT Grant Agency FEKT-S-11-5/1012 and projekt CZ.1.07.2.3.00.20.0175, Elektro-vyzkumník.

REFERENCES

1. Szabó, Z., "Příspěvek k optimální syntéze filtračních obvodů," 118 s, Vysoké učení technické v Brně, Fakulta elektrotechniky a komunikačích technologií, Vedoucí dizertační práce doc. Ing. Jiří Sedláček, CSc, Brno, 2012.

Image Reconstruction by EIT Utilizing Magnetic Field

T. Kříž and J. Dědková
Department of Theoretical and Experimental Electrical Engineering
Brno University of Technology, Kolejní 4, Brno 612 00, Czech Republic

Abstract— A possibility of the electric conductivity calculation from a magnetic field obtained outside the measured specimen is described in this paper. Electrical impedance tomography (EIT) principle is exploited for the conductivity calculation inside a specimen. The standard EIT is using voltage measurement on potential electrodes which are placed on the surface of the specimen whilst the direct current source is connected to a measured object. The EIT algorithm for a conductivity reconstruction is an inverse and an ill-posed problem. The solution of this problem is described as a minimization of a suitable objective function $\Psi(\sigma)$ which is dependent on a conductivity σ. The least squares method is very often used for a minimization of the objective function. This method converges very fast. The regularization methods are used for better stability of the solution. The Tikhonov regularization method can be used. The regularization term is added to the objective function if the Tikhonov regularization method is used. This term makes the solution stable. The square of the norm of measured voltages and calculated voltages by finite element method is involved in the standard EIT objective function.

The current inside a specimen produces also a magnetic field. Biot-Savart's law can be used for a calculation of a magnetic flux density outside the specimen. Triangle elements were used to build a numerical model. The elements have centers with coordinates $[x_j,\, y_j,\, z_j]$ and calculated points have coordinates $[x_i,\, y_i,\, z_i]$. Biot-Savart's law can be written in the form

$$\mathbf{B}_i \approx \frac{\mu_0}{4\pi} \sum_{j=1}^{NE} \frac{\mathbf{K}_j \times \mathbf{R}_{ij}}{\|\mathbf{R}_{ij}\|^3} \Delta S_j. \tag{1}$$

The current density is calculated on each element by means of superposition of the outside magnetic field values. We suppose that the current density is constant on elements. The created objective function for the minimization by the least squares method for a conductivity image reconstruction is

$$\Psi(\sigma) = \frac{1}{2} \sum \|\mathbf{J}_{\mathrm{M}} - \mathbf{J}_{\mathrm{FEM}}(\sigma)\|^2 + \alpha \|\mathbf{R}\sigma\|^2. \tag{2}$$

The conductivity reconstruction result, the accuracy and the reconstruction time is presented in the article.

The Influence of Magnetic Field on the Dew Point of Tissue Culture

M. Pokludová and E. Hutová
Department of Theoretical and Experimental Electrical Engineering
Brno University of Technology, Kolejni 4, Brno 61200, Czech Republic

Abstract— The temperature of plants is a necessary factor for the physiological processes and is the result of the actual heat balance of vegetation. If the temperature of the plant falls below the temperature of the dew point (air), it begins to condense dew. The dew point is the temperature to which moist air must be cooled at constant barometric pressure, so the water vapor condensed from it. From the known temperature and relative humidity, dew point can be calculated using the Magnus formula. If the plant is inserted into the translucent plastic box, then there is no air circulation inside the bowl affected by external environment. This article deals with the early stages of pine embryos grown in Petri's dishes, when the temperature change, condensation is evident. Effect of magnetic field on tissue culture is shifting the dew point temperature and under normal temperature there is no condensation. The aim of this project is to determine how much is shifted the dew point of tissue cultures grown in Petri's dishes between the permanent magnets embedded on a defined magnetic field gradient. To determine the change in dew point temperature, the samples were divided into two groups. The first group was placed between the permanent magnets and the second group (control) was placed outside the scope of magnets. The measurement was carried out in a Peltier device, where the ambient temperature gradually decreased to low levels and then increased to determine the dew point of the dish. The device was placed in a room where constant terms are provided to eliminate errors caused by the external environment.

Session 1P1a
Modelling of Electromagnetic Structures: Application to Electrical Machines

Analysis of Rotor Winding Self-inductance of Synchronous Machines Under Air-gap Asymmetries

Homayoun Meshgin Kelk, Hourieh Mirmoeini Kerahroudi, and Aboulghasem Hashemi
Department of Electrical Engineering, Tafresh University, Tafresh, Iran

Abstract— Using a two dimensional finite element method rotor winding inductance of a salient rotor pole synchronous machine is calculated under air-gap asymmetry. It will be shown that mixed air gap eccentricity can be detected by measuring and analysis of self-inductance of the rotor winding. Experimental results verify our results obtained from simulations.

Introduction and Results: Analysis of electrical machines under healthy and faulty conditions can be made by an appropriate calculation of inductance values. In a real machine there are some percentages of inherent static and dynamic air gap asymmetries even in new machine, simultaneously. It is called mixed air-gap eccentricity. Mixed air-gap eccentricity leads to variation of inductance coefficients of the machine so that it is possible to detect the existence of air gap asymmetries.

The most precise method for the calculation of inductance coefficient of a machine is finite element method (FEM) which is reported in literatures [1]. However, one of the well-known methods to calculate machine inductances is the winding function method. This method has been used for the analysis of induction and synchronous machines in different conditions [2]. On the other hand, magnetic equivalent circuit method can be used to analyze the various types of electric machines [3].

We have presented our results obtained through a transient solver of a finite element package. It is very important to note that modeling of air-gap asymmetries is the most important part to obtain acceptable results in simulation.

To calculate the rotor winding self-inductance, we adjusted the rotor position and applied a sinusoidal voltage only to the rotor winding. Then the current flowing in the rotor winding is measured and the rotor self-inductance is calculated. By adjusting the rotor position, variation of rotor winding self-inductance is obtained both in simulation and experiment.

Figure 1 shows the variation of rotor winding self-inductance under symmetric and asymmetric (5% dynamic and 50% static asymmetries, respectively) air-gap conditions and their spatial harmonic distributions. Dc component is removed. It is seen the magnitude of lowest sub-harmonic increases as the level of mixed air-gap eccentricity increases. Fig. 2 shows the results obtained from experiment (inherent dynamic asymmetry and 60% static asymmetry). It is clear

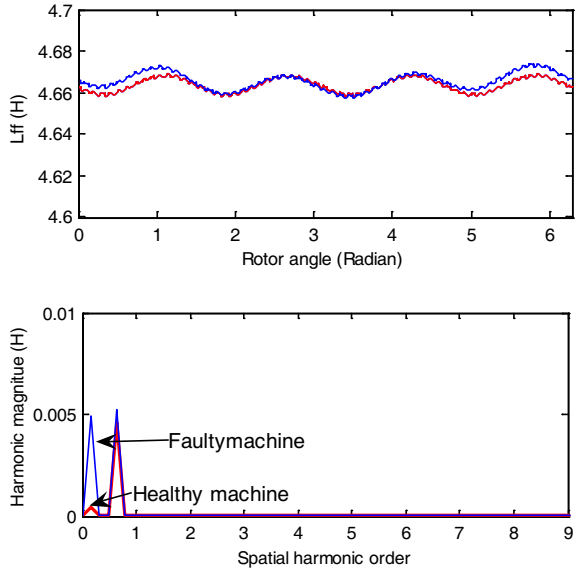

Figure 1: Rotor winding self-inductances and their spatial harmonics.

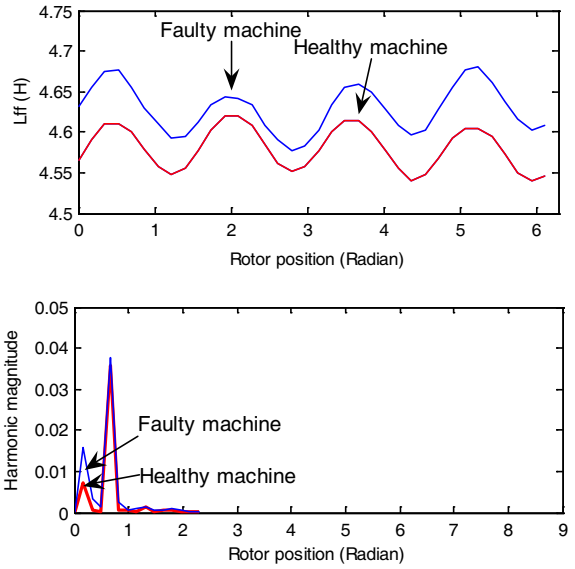

Figure 2: Rotor winding self-inductances and their spatial harmonics.

that the magnitude of lowest sub-harmonic increases as the level of mixed air-gap eccentricity increases. Dc component is not shown here. Details will be presented in full paper. It is clear that experimental results confirm the results obtained from simulations.

REFERENCES

1. Babaei. M., J. Faiz, et al., "A detailed analytical model of a salient-pole synchronous generator under dynamic eccentiricity fault," *IEEE Trans. Magnet.*, Vol. 47, No. 4, 764–771, 2011.
2. Akbari, H., et al., "A novel technique for the computation of inductance coefficients of salinet pole synchronous machine under different eccentricity conditions," *Electric Power Components and Systems*, No. 39, 1507–1522, 2011.
3. Meshgin Kelk, H., et al., "A comprehensive method for the calculation of inductance coefficients of cage induction machines," *IEEE Trans. on EC*, Vol. 18, No. 2, 187–193, 2003.

Optimal Design Approaches for Linear Tubular Actuators

I. Amdouni[1], **L. El Amraoui**[1], **F. Gillon**[2, 3], **M. Benrejeb**[1], **and P. Brochet**[2, 3]

[1]Unité de Recherche LARA Automatique, Ecole Nationale d'Ingénieurs de Tunis
BP. 37, le Belvédère 1002, Tunis
[2]Univ. Lille Nord de France, F-59000 Lille, France
[3]EC-Lille, L2EP, BP48 F-59650 Villeneuve d'Ascq, France

Abstract— An optimal design approach is developed for an incremental linear actuator. First, parameterized design model is built. Second the optimization problem is formulated. Finally, in order to solve the optimization problem, two different algorithms are developed.

Introduction: The design of electrical systems is a very complex task which needs experts from various fields of competence. Such difficulties resolution has been the subject of many studies using stochastic and deterministic optimization methods [1, 2]. This paper reports on the optimal design of an incremental linear actuator. At first, one parameterized FE model of the actuator is built. Then, the design parameters of the linear actuator are performed using parallel hybrid Genetic Algorithm (GA) optimization method and parallel hybrid Simulated Annealing (SA) method. In order to solve the optimization problem, two different algorithms are developed.

Modeling of an Incremental Linear Actuator: The electromagnetic structure, on which the optimal design approach is tested, is a linear tubular switched reluctance actuator. It presents four statoric phases and a toothed plunger. Non-magnetic separations are set between the statoric phases so that only one statoric phase can be aligned with plunger teeth when it is supplied.

A parameterized FE model is developed for the studied actuator under Opera2D® software environment. This model is based on an integral formulation of partial differential equations describing the actuator static behavior to determine a specific solution under or vector form.

Actuator Performance Optimization: The aim of this section is to increase the thrust force level developed by an incremental actuator by changing its design parameters. In this direction, a finite element model is developed for the actuator. This model allows determining changes of the force developed by the actuator according to dimension variations.

The objective function of the considered optimization problem is then defined as being the static force f developed by the actuator. Considering rr, the stator and rotor tooth height, zr, the tooth inclination and lb, the stator slot width, as optimization problem parameters. The goal of the optimization procedure is to maximize the starting static force, f developed by the actuator, by varying rr, zr and lb under the following constraints: constant heat, constant bulck, constant radius and thickness of the air gap.

The optimization problem is expressed as follow:

$$\begin{cases} 2.0000\,\text{mm} \leq rr \leq 3.5000\,\text{mm} \\ 0.0508\,\text{mm} \leq zr \leq 1.5700\,\text{mm} \\ 1.5000\,\text{mm} \leq lb \leq 3.0000\,\text{mm} \\ f_{\max} = \max(f(rr, zr, lb)) \end{cases} \tag{1}$$

In order to solve the optimization problem, two different methods are developed for the actuator static performance optimization. The first one is based on parallel hybrid GA optimization

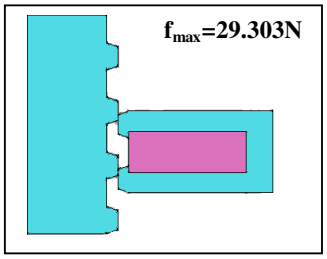

Figure 1: Initial structure of the studied actuator.

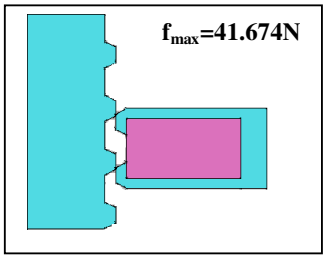

Figure 2: Optimal design structure of the studied actuator_hybrid_SA.

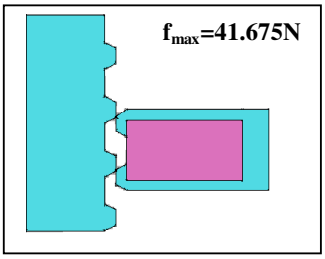

Figure 3: Optimal design structure of the studied actuator_hybrid_GA.

method and the second one is based on parallel hybrid SA method. Hooke and Jeeves method is used as hybrid solver with these two methods. Figure 1 shows the initial structure of the optimization process. The optimization of the actuator design parameters shows that the maximum force obtained from the parallel hybrid SA applied to a finite element model of the actuator, is quite the same as that obtained from the parallel hybrid GA applied to the same model.

In addition, achieving the global optimum by hybrid SA method much depends on the initial parameters, Figure 2. If they are well chosen, it improves the optimum and consumes less computing time compared to the hybrid GA optimization method, Figure 3.

Conclusion: Through this paper an optimal design approach is developed for incremental linear actuators. First, a parameterized FE model is developed for the studied actuator. Second, the optimization problem is formulated. The study focuses on the maximization of the static force developed by the actuator. Finally, the optimization problem is solved using two developed hybrid methods; parallel hybrid GA optimization method and parallel hybrid SA method. These two methods use Hooke and Jeeves method as hybrid solver. The obtained optimization results show that the hybrid GA optimization method consumes more computing time than the hybrid SA method. Indeed, GA optimization method and SA method are based on randomness, which allows exploring more robust optimization field. In both cases, parallelization leads to a significant reduction of computing time which is halved when using two-core machine.

REFERENCES

1. Xue, X. D., K. W. E. Cheng, T. W. Ng, and N. C. Cheung, "Multi-objective optimization design of in-wheel switched reluctance motors in electric vehicles," *IEEE Transactions on Industrial Electronics*, Vol. 57, No. 9, September 2010.
2. Brisset, S., "Approaches and tools for optimal design of electrical machines," *Empowerment to Supervise Research*, April 2008.

Analysis of Contactless Power Transfer Systems for Maglev

S. Hasanzadeh and S. Vaez-Zadeh

A Center of Excellence on Applied Electromagnetic Systems and Advanced Motion Systems Research Laboratory, School of Electrical and Computer Engineering, University of Tehran, Tehran, Iran

Abstract— Maglev systems with linear synchronous motors are practical now. They require primary windings distributed along the track resulting in substantial increase in the construction and maintenance cost. Placing windings on the mover plus a proper contactless power transfer (CPT) system considerably reduces the cost. A suitable structure for CPT system should be designed to satisfy the best performance and meet the requirement of the system. The simplicity of implementation taking into account the practical limitations are essential in selecting the CPT structure.

In the contactless operation, the power transfer apparatus is very similar to a transformer, except for a small air gap along the main flux path that links the two coils. The primary coil is located

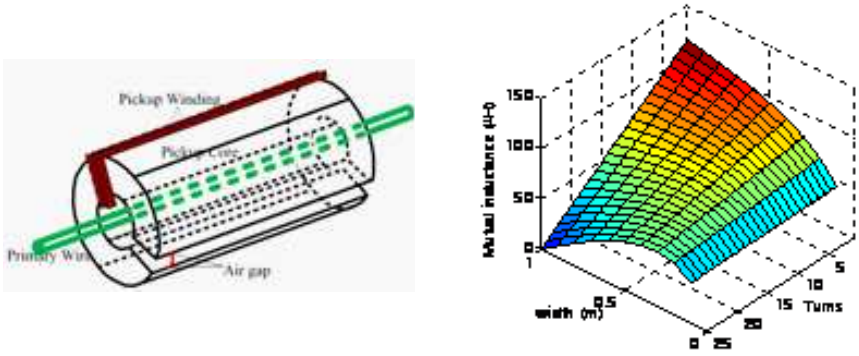

Figure 1: A schematic view of the Coaxial CPT system, Mutual inductance vs. width and turn numbers.

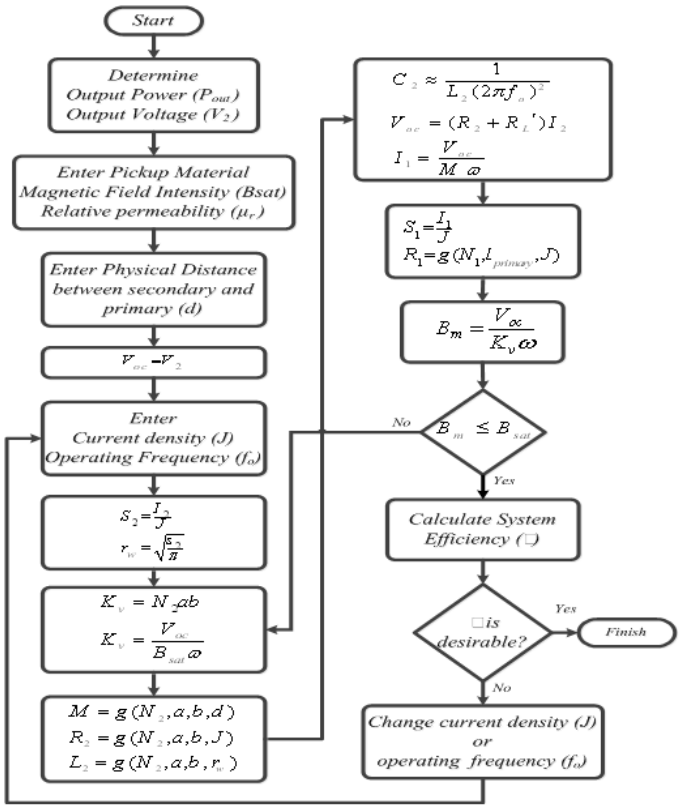

Figure 2: The flowchart of system analysis.

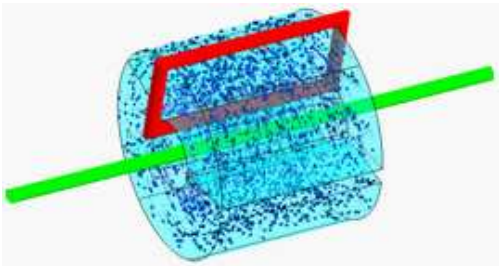

Figure 3: Magnetic flux vector by 3D FEM simulation.

on the stationary base unit while the secondary coil is located on the vehicle. The latter coil effectively receives the power of primary through the air gap and delivers it to the vehicle. The power can be used immediately by the traction motor or can be stored for later use.

Coaxial CPT systems including strait primary wires passing through the center of a cylindrical secondary core with an air gap have already been recognized [1]. Their design and applications has gained attention recently [2]. Needless to say that a solid system design must be established based on a systematic modeling and analysis. The literature lacks such an analysis.

In this work, a coaxial CPT system as in Fig. 1 is chosen for maglev applications with some considerations such as providing high linkage flux and having low volume. A mathematical model is derived for the system including the compensating capacitors.

Using the model, a procedure is given for a thorough system analysis including the calculation of power transfer efficiency. The system parameters can also be obtained based on the system physical specifications as presented in Fig. 1. The system current density and operating frequency are adjusted iteratively to provide a desirable output power and efficiency. A flowchart of the procedure is given in Fig. 2. Analytical results are verified by 3D FEM simulations to confirm the modeling and the analysis procedure as presented in Fig. 3. The proposed analysis can be used as a tool for further studies including system design and optimization.

REFERENCES

1. Klontz, K., D. Divan, and D. Novotny, "An actively cooled 120-kW coaxial winding transformer for fast charging electric vehicles," *IEEE Transactions on Industry Applications*, Vol. 31, No. 6, 1257–1263, 1995.
2. Lastowiecki, J. and P. Staszewski, "Sliding transformer with long magnetic circuit for contactless electrical energy delivery to mobile receivers," *IEEE Transactions on Industrial Electronics*, Vol. 53, No. 6, 1943–1948, 2006.

Optimum Design of an Active Magnetic Bearing System

Arman Ramazan-Nejad, **Homayoun Meshgin Kelk**, **and Mahsa Rahmati**
Tafresh University, Tafresh, Iran

Abstract— Active magnetic bearings (AMBs) are used in electrical machines to levitate the rotor in a contact-less form. Without physical contact between bearing and rotary part, friction is removed, lubrication is not needed, and precise position control is feasible. Therefore applications of AMBs are going to increase in modern industries.

Introduction: This paper is focused on the design of stator winding of AMBs to achieve an optimal solution. In conventional AMBs cross-section area of stator windings have rectangular shape as shown in Fig. 1. There is empty or unused area between adjacent stator legs. These unused areas could be utilized if stator windings with rectangular cross sections are substituted by a trapezoidal one as shown in Fig. 2. This design leads to AMB with smaller diameter. Fig. 3 shows how the cross section of each stator winding could be varied provided that the area of each stator winding is not changed. Various design lead to different performance of AMB. Stator winding inductance and levitating forces varies due to the variation of stator winding cross section and bearing legs height. We have analyzed different bearing designs through a magneto-static solver of a 2 dimensional Finite element package. Analytical Hierarchy Process (AHP) is used to find an optimal bearing design.

Application of Analytical Hierarchy Process to Acheive an Optimum AMB System: Optimization is carried out using an Analytic Hierarchy Process (AHP). One of the major strengths of AHP is the use of pair-wise comparison to derive accurate ratio scale priorities. AHP is one of the more widely applied multi-attribute decision making methods. In this method the final decision is based on the evaluation of a number of alternatives in terms of a number of criteria. The main decision criteria which describe the AMB performance are: levitating force,

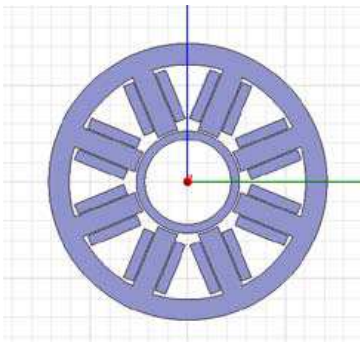

Figure 1: Active magnetic bearing.

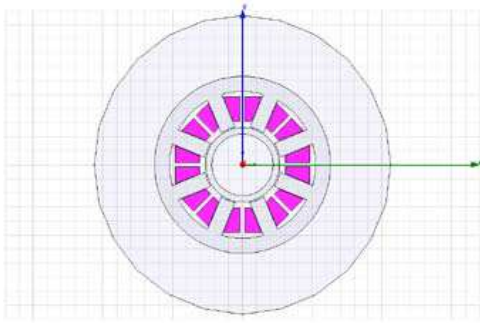

Figure 2: New design of active magnetic be.

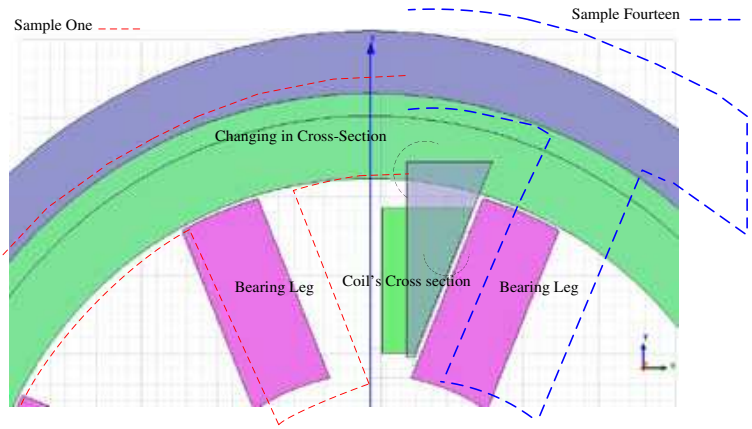

Figure 3: Change in winding cross-section area.

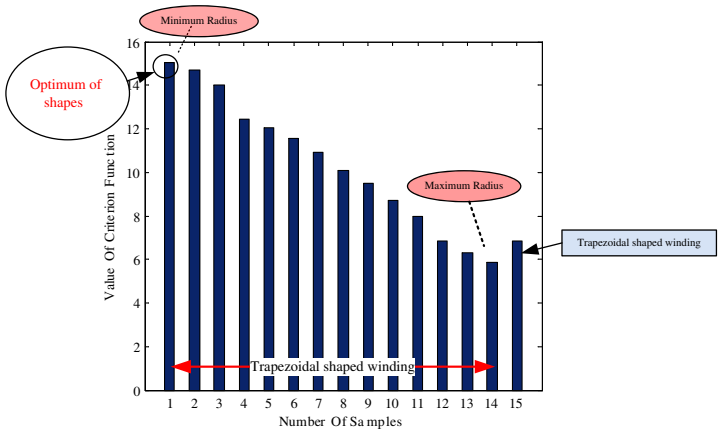

$$\text{Trapezoidal shaped winding}\left\{ m_w = \begin{bmatrix} 2.249 \\ 2.316 \\ 2.348 \\ 2.379 \\ 2.413 \\ 2.446 \\ 2.476 \\ 2.509 \\ 2.544 \\ 2.575 \\ 2.612 \\ 2.639 \\ 2.674 \\ 2.706 \end{bmatrix}, \quad m_L = \begin{bmatrix} 23.36 & 23.36 & 22.599 & 22.63 \\ 23.42 & 23.42 & 22.69 & 22.699 \\ 23.49 & 23.49 & 22.73 & 22.73 \\ 23.5 & 23.51 & 22.71 & 22.72 \\ 23.57 & 23.57 & 22.76 & 22.78 \\ 23.6 & 23.6 & 22.8 & 22.82 \\ 23.69 & 23.69 & 22.9 & 22.9 \\ 23.69 & 23.69 & 23.91 & 23.91 \\ 23.74 & 23.74 & 22.93 & 22.89 \\ 23.81 & 23.8 & 22.95 & 22.98 \\ 23.86 & 23.86 & 22.99 & 22.99 \\ 23.94 & 23.94 & 23 & 23 \\ 24 & 24 & 23.1 & 23.1 \\ 24.1 & 24.1 & 23.2 & 23.2 \end{bmatrix}, \quad m_f = \begin{bmatrix} 838.0723 \\ 838.026 \\ 836.3609 \\ 830.265 \\ 829.853 \\ 828.484 \\ 827.116 \\ 824 \\ 822.5 \\ 820.2 \\ 818.29 \\ 814.54 \\ 813.43 \\ 812.82 \end{bmatrix}, \quad m_s = \begin{bmatrix} -1.518 \\ -1.488 \\ -1.466 \\ -1.428 \\ -1.434 \\ -1.418 \\ -1.399 \\ -1.38 \\ -1.378 \\ -1.359 \\ -1.3471 \\ -1.3279 \\ -1.3196 \\ -1.3174 \end{bmatrix} \times 10^{-5}$$

$$\text{Rectangular shape}\left\{ m_w = [2.737], m_L = [23.48, 23.49, 22.49, 22.46], m_f = [811.79], m_s = \left[-4.54 \times 10^{-3}\right] \right.$$

Figure 4: Variation of criterion function for all samples in design space.

inductance of coils, stray fluxes, and weight of stator. Our design space includes fifteen solutions. 7TCriterion Function is given as the following

$$Criterion\ Function = \sum_{i=1}^{15} [(m_i \times m_f) - (m_i \times m_w) - (m_i \times m_L) - (m_i \times m_S)] \qquad (1)$$

where m_i = *Sample coefficient*, m_f = *force coefficient*, m_L = *Inductanc coefficient*, m_w = *Weight coefficient*, m_S = *stray flux coefficient*.

Figure 4, depicts the values of criterion function for all fifteen samples. Optimum design is shown on this figure.

Conclusion: Optimal design of a radial active magnetic bearing is presented. Stator winding with trapezoidal cross section leads to AMB design with smaller diameter and good performances. Optimum design is carried out using an Analytical Hierarchy Process (AHP). Overall performance of the optimized designed will be presented in full paper.

Dynamic Modeling of Tubular PM Linear Synchronous Actuator Using Multimodal Interpolation of 3D Finite Element Results

I. Ben Salem[1] and L. El Amraoui[2]

[1]LARA Automatique Research Laboratory, Ecole Nationale d'Ingénieurs de Tunis, Tunisia
[2]Ecole Supérieure d'Informatique et de Technologie Tunis, Tunisia

Abstract— Permanent magnet linear synchronous motors (PMLSM) are carried out to be mostly used in wide range of power systems, thanks to their high massive force. However, its definition can be ambiguous when very saturated devices are to be studied. This magnetic phenomenon introduces considerable nonlinearities into static, as well as, dynamic behaviours of the actuator [1]. It can cause fails to the control system and constraints the drive system to stop. So, an interpolation method of modelling can be used to evaluate the nonlinear parameters in order to perform the dynamic modelling of the actuator.

In this paper, the dynamic modelling of a three phase Tubular Permanent Magnet Linear Synchronous actuator is elaborated using multimodal interpolation of 3D finite element results. To achieve this, a two dimensional axi-symmetric finite element model is built for each phase [2]. The magnetic phenomena are taken into account in the static and dynamic characterization of this actuator. The force and inductance characteristics are then calculated, according to plunger position and supply current densities.

When the actuator is supplied by high current densities, in order to maximize the force, the iron is magnetically saturated and the central phase characteristics are attenuated. In fact, to reduce the importance of these magnetic nonlinearity effects on the dynamic behaviour of the actuator, the multimodal interpolated functions of force and inductances are elaborate using FE results. These functions are performed with linear interpolation-extrapolation functions. The obtained characteristics of force and inductances are stored then on 3D response surfaces and they are introduced into the dynamic simulation process delivering as final output the mechanical plunger speed.

The simulation results present two cases of study: when the FE results are mathematically interpolated (case 1) and when they are stored on 3D MATLAB functions (case 2). Figures 1, 2, 3 and 4 present the plunger speeds and the electromagnetic forces generated by the actuator in the two cases for a loaded force equal to 500 N. In the first case, the fluctuations are observed only in the transient state. They are important but they can be controlled using the current

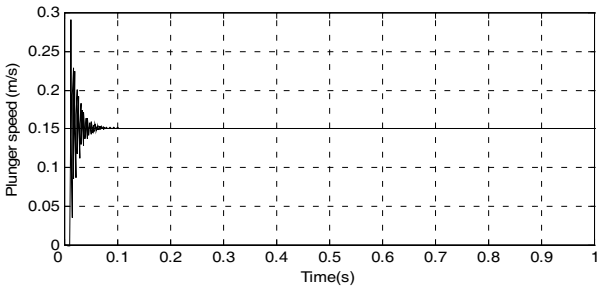

Figure 1: Plunger speed characteristic, case 1.

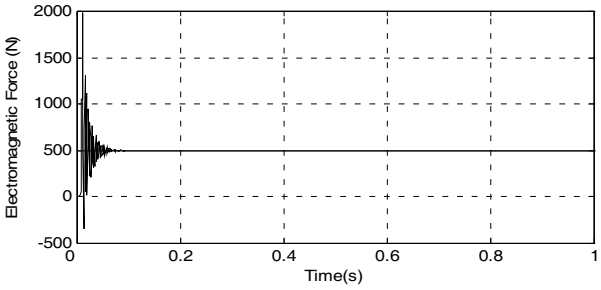

Figure 2: Electromagnetic force, case 1.

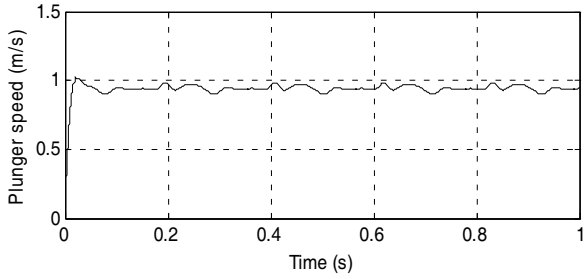

Figure 3: Plunger speed characteristic, case 2.

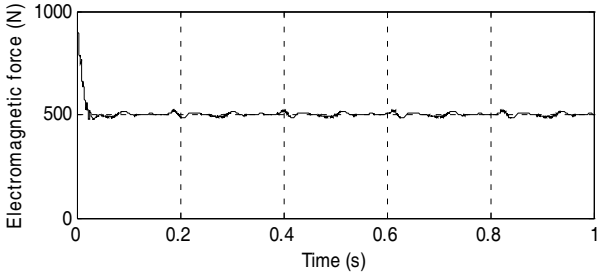

Figure 4: Electromagnetic force, case 2.

control loops. In the second case, the fluctuations observed in the steady state are few but the final value of the plunger speed is greater than the plunger speed observed in Figure 1.

REFERENCES

1. Palinder, H., J. G. Slootweg, J. C. Compter, and M. J. Hoeijmarkers, "Modeling a linear PM motor including magnetic saturation," *Power Electronics, Machines and Drives*, Conference Publication No. 497, IEE 2002, Apr. 16–18, 2002.
2. Ben Salem, I., L. El Amraoui Ouni, M. Benrejeb, F. Gillon, and P. Brochet, "Flux linkage approach used for phase inductance computation of a three phase tubular linear PM synchronous actuator," *International Review of Electrical Engineering IREE*, Vol. 4, Oct. 2011.

Branch-and-bound Technics in the Problems of Optimal Design of Induction Machines

D. Samarkanov[1], **F. Gillon**[1], **P. Brochet**[1], **and D. Laloy**[2]

[1]Ecole Centrale de Lille, France
[2]Jeumont Electric, France

Abstract— In the article we show usage of different modifications of branch and bound (BB) algorithm [1] for the inverse problem of induction machine design. More specifically, the task consisted in finding the domain of optimal configurations of induction machine (IM) taking into consideration technical specification. Two objective functions were chosen: efficiency of IM and its total costs of production. Considered problem had 20 constraints which must be satisfied for all optimal configurations.

As a numerical model for calculating efficiency and all other parameters of IM we used conventional approach using equivalent circuit [2]. For computing the total costs of production (TC) we employed the method of surrogate modelling using kriging approach [3].

Optimization problem has 8 variables where all of them are geometrical parameters of IM. For each the feasible domain is finite, therefore gradient-free methods can only be applied for finding the set of global solutions. In the work, we used different branching strategies during the search procedure inside BB algorithm. Also we showed the application of interval version of BB algorithm [4] for the same optimization problem. More formally, following approaches were tested for considered problem [1]:

1. Depth-first search;
2. A^* search;
3. Hybridizing entropic branching (EB);
4. Interval branch-and-bound (IBBA) [4].

The algorithm for resolving this bi-objective optimization problem is presented in the following way:

1. Taking into consideration specification sheet, calculate efficiency and all other constraints parameters of the problem;
2. Verify that the error between results obtained in previous step and the one used the fine model is less than some critical threshold. The finite element model was employed for the validation and Euclidean norm is used for calculating the discrepancy;
3. If at least for one configuration from cross-validation (CV) set the error is larger than the threshold, then use space-mapping technique [5] until for entire CV set the discrepancy will be less than the threshold;
4. Construct the model of total costs of production using kriging approach;
5. Transform the bi-objective optimization problem to mono-objective one using the weighting method;
6. Resolve the problem using one of the four algorithms listed above.

In the paper we reveal the results of using all of the algorithms, compare them and discuss the difficulties of its implementation in the industrial conditions.

REFERENCES

1. Gilpin, A. and T. Sandholm, "Information-theoretic approaches to branching in search," *Discrete Optimization*, Vol. 8, No. 2, 147–159, 2011.
2. Boldea, I. and S. Nasar, *The Induction Machine Handbook*, CRC Press, 2010.
3. Vazquez, E. and J. Bect, "Convergence properties of the expected improvement algorithm with fixed mean and covariance functions," *Journal of Statistical Planning and Inference*, Vol. 140, No. 11, 3088–3095, 2010.
4. Fontchastagner, J., Y. Lefevre, and F. Messine, "Some co-axial magnetic couplings designed using an analytical model and an exact global optimization code," *IEEE Transactions on Magnetics*, Vol. 45, No. 3, 1458–1461, March 2009.
5. Bandler, J., Q. Cheng, S. Dakroury, A. Mohamed, M. Bakr, K. Madsen, and J. Sondergaard, "Space mapping: The state of the art," *IEEE Transactions on Microwave Theory and Techniques*, Vol. 52, No. 1, 337–361, January 2004.

Session 1P2a
Microwave Processing of Materials Recent Advances in Modeling and Experimentation

Advanced Computer Modeling for Microwave Power Engineering — State of the Art

Malgorzata Celuch[1] and Vadim V. Yakovlev[2]

[1]Institute of Radioelectronics, Warsaw University of Technology, Warsaw, Poland
[2]Department of Mathematical Sciences, Worcester Polytechnic Institute, Worcester, MA, USA

Abstract— An introductory talk to the session gives a review of the current status of modeling activities in microwave power engineering. The review analyzes the related materials recently presented at three major forums held in summer 2012: the IEEE MTT-S International Microwave Symposium, Montreal, Canada, June 17–22, 2012, 46th IMPI International Microwave Power Symposium, Las Vegas, NV, June 20–22, 2012, and the 2nd Global Congress on Microwave Energy Applications, Long Beach, CA, July 23–27, 2012. The talk also presents the major topics of the upcoming book [1] displaying the contemporary level of development of mathematical and computer models and illustrating their use in a number of applications. The talk is concluded by generalizing comments aiming to form a general background and outline a context for the materials of the papers presented in the session.

REFERENCES

1. Celuch, M. C. and V. V. Yakovlev, *Microwave Power Engineering with Advanced Computer Modeling*, CRC Press, 2012, to be published.

A New Modeling Technique for Processes of Hybrid Heating by Microwaves and Thermal Radiation

Pawel Kopyt[1] **and Vadim V. Yakovlev**[2]

[1]Institute of Radioelectronics, Warsaw University of Technology, Warsaw, Poland
[2]Department of Mathematical Sciences, Worcester Polytechnic Institute, Worcester, MA, USA

Abstract— The imperative need for alternative sources of energy and efficient energy use has recently initiated an array of insightful studies in microwave (MW) power engineering. MW heating is known for its ability to improve the efficiency and quality of a variety of applied thermal processes; however, the intrinsic non-uniformity of MW-induced temperature fields remains the factor essentially limiting the range and productivity of the related industrial technologies. Among different approaches addressing this issue, there is a hybrid technique combining MW heating with conventional thermal processing when latter and former are responsible for treatment of the exterior and interior of the product, respectively. While this technique has demonstrated a strong potential for certain industrial applications, corresponding applicators have always been developed on the basis of expensive and inefficient cut-and-try experimentation. This is explained by the fact that the known attempts to model the phenomena of heating by microwave and thermal radiation have had so far very limited capabilities in terms of both electromagnetic and computational fluid dynamics analyses.

This paper reports on the development of an original modeling technique capable of accurate and adequate simulation of processes in specialized hybrid systems. Incorporation of radiative boundary conditions is proposed for multiphysics (electromagnetic and thermal) modeling. The algorithm is implemented by making the models of radiation in *ANSYS Fluent* available for the electromagnetic models in *QuickWave-3D*. The technique was presented for the first time in [1] as a part of the development of the hybrid technology for high temperature processing of limestone. Here we report new results in modeling of the process of hybrid heating of a variety of limestone samples in Ceralink's MAT^{TM} kiln. Time-temperature histories of the heating process are simulated along with the temperature fields. Hybrid heating is shown to be much more efficient in terms of heating rate and temperature uniformity. The developed modeling technique demonstrates its capabilities to clarify such important (but inaccessible for experimental determination) characteristics of the process as evolution of temperature field inside all the materials in the kiln that absorb microwave energy. Comparison of the heating regimes gives us an insight into the operation of the hybrid system and thus should be beneficial in the computational analysis and computer-aided design of these systems.

REFERENCES

1. Allan, S. M., M. L. Fall, E. M. Kiley, P. Kopyt, H. S. Shulman, and V. V. Yakovlev, "Modeling of hybrid (heat radiation and microwave) high temperature processing of limestone," *IEEE MTT-S Intern. Microwave Symp. Dig.*, Montreal, Canada, June 2012 (to be published).

Microwave Processing of Nanoporous Carbons with Tailored Properties

Ana Arenillas and J. Ángel Menéndez
Instituto Nacional del Carbón, CSIC, Apartado 73, Oviedo 33080, Spain

Abstract— Carbon gels are porous materials that are prepared by drying and carbonizing organic gels. Under suitable synthesis conditions, the textural and chemical properties of these gels can be adjusted and tailored to fit specific requirements for many applications, e.g., as adsorbents, molecular sieves for gas separation, catalyst supports, energy storage, electrocatalysts, etc. An additional advantage of these materials is that they can be obtained in different forms as monoliths, specific shapes, powder, spheres, films, etc. without the need of binders or sophisticated processes. However, in order to produce materials with a particular shape, it is necessary to control the gelation stage (i.e., the time in which the solution loses fluidity). Moreover, the main barrier to the widespread use of carbon gels is the long time required for their synthesis following the conventional methods making their fabrication expensive and low competitive. Based on microwave heating, a novel one-step fast synthesis method for producing organic xerogels is presented in this work. In addition this method allows the precise determination of the gelation point just by recording the variations of the energy consumed by the microwave device during the synthesis of the organic gel[1]. Consequently, it is believed that this new method of synthesis of carbon gel could make these materials more competitive in terms of costs while ensuring a good control of their textural and chemical properties.

Figure 1: Microwave processing of carbon xerogels permits to design the properties along the final shape of these carbon materials.

REFERENCES

1. Juárez-Pérez, E. J., E. G. Calvo, A. Arenillas, J. A. Menéndez, *Carbon*, Vol. 48, 3305, 2010.

Modeling-based Technique for 3-D Microwave Imaging of Dielectric Samples in Closed Systems

Alexander V. Brovko[1], **Ethan K. Murthy**[2], **and Vadim V. Yakovlev**[3]

[1]Faculty of Applied Information Technologies, Saratov State Technical University, Saratov, Russia
[2]Applied Mathematics, Inc., Gales Ferry, CT, USA
[3]Department of Mathematical Sciences, Worcester Polytechnic Institute, Worcester, MA, USA

Abstract— Microwave (MW) imaging as a technique of non-destructive evaluation and testing has recently become of a particular interest for various applications involving MW processing of materials. Main potential uses of MW imaging technology in this field include testing and monitoring of the internal structure of the samples prior to and in the course of MW processing. Non-uniformity of the materials comprising the samples to be processed/sintered by microwaves may lead to unpredictable results as distribution of the electromagnetic field and efficiency of absorption of microwave energy depend on internal permittivity profiles. Nonuniformity may be caused by density variations formed at the stage of pre-processing of the samples by pressing, extrusion, rolling, and expansion. Reconstructed permittivity profiles may therefore provide information crucial for controllable and efficient operation of systems of MW thermal processing.

In this paper, we present a new microwave imaging technique for reconstruction of 3-D permittivity profiles of a dielectric sample in a closed cavity. We consider a specific scenario in which the sample is located inside a six-port waveguide turnstile junction. The profiles are determined from measurement of parameters of the full S-matrix of the system. The reconstruction is performed with a neural network technique backed by full-wave finite-difference time-domain (FDTD) analysis. The spatial distributions of the dielectric constant are approximated by either a quadratic polynomial function, or a set of Gaussian functions, whose coefficients are determined with a neural network trained with the results of FDTD analysis. The approach presented here follows the principles described in [1], however, in this paper, we generalize them for the cases of arbitrary 3-D profiles and, to improve the accuracy of reconstruction, we apply the technique of optimal design. Operational capabilities of the technique are illustrated through a series of computational experiments for a rectangular sample with different distributions of complex permittivity. The results demonstrate reasonable agreement between the reconstructed and actual profiles. We then analyze the accuracy of reconstruction obtained with quadratic polynomials and Gaussian approximating functions and finally discuss ways of improving the quality of 3-D microwave imaging in closed systems.

REFERENCES

1. Brovko, A. V., E. K. Murphy, and V. V. Yakovlev, "Waveguide microwave imaging: Neural network reconstruction of functional 2-D permittivity profiles," *IEEE Trans. Microwave Theory Tech.*, Vol. 57, No. 2, 406–414, 2009.

Inexpensive Microwave Q-Meter for Precise Dielectric Measurements with Split-post Dielectric Resonators

Przemysław Korpas[1], **Wojciech Wojtasiak**[1], **Jerzy Krupka**[2], **Łukasz Usydus**[3], **Małgorzata Celuch**[4], **and Bartlomiej Salski**[1]

[1]Institute of Radioelectronics, Warsaw University of Technology
ul. Nowowiejska 15/19, Warsaw 00-665, Poland
[2]Institute of Microelectronics and Optoelectronics, Warsaw University of Technology
ul. Nowowiejska 15/19, Warsaw 00-665, Poland
[3]Central Office of Measures, ul. Elektoralna 2, Warszawa 00-139, Poland
[4]QWED Sp. z o.o., ul. Krzywickiego 12 lok. 1, Warsaw 02-078, Poland

Abstract— Split post dielectric resonators (SPDRs) that were developed about 15 years ago [1] are now commonly used for the measurements of the complex permittivity of printed wiring board and low temperature co-fired ceramic materials [2], ferroelectric films [3], and conductive materials [4]. The principle of the measurement method used is based on the $TE_{01\delta}$ mode's Q-factor and resonant frequency change between two states: unloaded (without a sample) and loaded (with a sample inserted into the resonator). Those parameters can easily be extracted using Automatic Network Analyzer and recalculated into the complex permittivity of the sample. Whereas a Network Analyzer is a very common equipment for microwave laboratories, there is still a large group of potential users (chemists, material scientists, etc.) who do not need such a rich featured and expensive device every day. Only recently, we have developed an inexpensive computer controlled microwave oscillator system that enables quick and automatic measurements of the complex permittivity with a dedicated resonator [5]. It is dedicated for those users, who need accuracy offered by SPDRs but cannot afford to buy Automatic Network Analyzer.

Our set-up has been based on the handy Microwave Q-Meter device and a control software running on any modern PC computer. The Split-Post Dielectric Resonator is connected between a PLL-stabilized Voltage Controlled Oscillator and monolithic power detector as a pass-band filter (Figure 1). The transmission characteristic is gathered point by point on consecutive frequencies, exciting the resonator with a signal of a known level. A multipoint resonance curve fitting procedure has been implemented for accurate Q-factor extraction. On the detector side, a great simplification has been achieved using a single-chip logarithmic power detector in place of a complex super-heterodyne receiver with narrow IF filters. Due to higher order modes in SPDR, this approach needs a proper filtering-out of the oscillator's harmonics.

The Microwave Q-Meter is connected to a standard PC-computer with USB cable and is controlled by a dedicated Windows-based application. Its graphical user interface allows visualizing the resonance curve, in a similar way as it is done by Network Analyzers. The whole procedure has been greatly simplified and takes only few seconds to get results for a new sample inserted into the resonator.

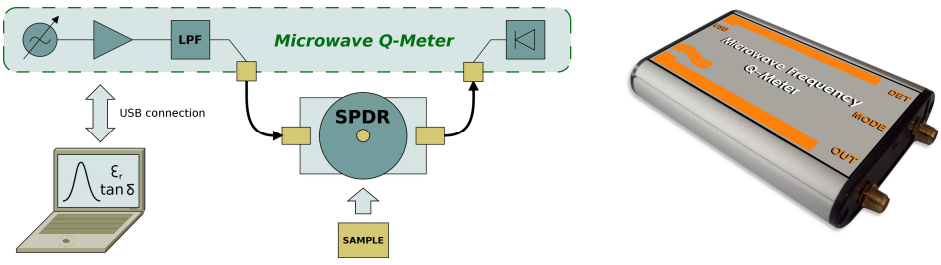

Figure 1: Block diagram of our measurement set-up and the Microwave Q-Meter.

REFERENCES

1. Krupka, J., R. G. Geyer, J. Baker-Jarvis, and J. Ceremuga, "Measurements of the complex permittivity of microwave circuit board substrates using split dielectric resonator and reentrant cavity techniques," *DMMA'96 Conference*, 21–24, Bath, UK, Sep. 23–26, 1996.

2. Krupka, J., A. P. Gregory, O. C. Rochard, R. N. Clarke, B. Riddle, and J. Baker-Jarvis, "Uncertainty of complex permittivity measurements by split-post dielectric resonator technique," *Journal of the European Ceramic Society*, Vol. 21, 2673–2676, 2001.
3. Krupka, J., W.-T. Huang, and M.-J. Tung, "Complex permittivity measurements of thin ferroelectric films employing split post dielectric resonator," *Ferroelectrics*, Vol. 335, No. 1, 89–94, 2006.
4. Krupka, J., D. Nguyen, and J. Mazierska, "Microwave and RF methods of contact less mapping of the sheet resistance and the complex permittivity of conductive materials and semiconductors," *Measurements Science and Technology*, Vol. 22, 085703-1–6, 2011.
5. Korpas, P., W. Wojtasiak, J. Krupka, and W. Gwarek, "Inexpensive approach to dielectric measurements," *MIKON 2012, 19th International Conference on Microwaves, Radar and Wireless Communications*, 154–157, Warsaw, Poland, May 21–23, 2012.

A Wide-band Microwave Absorber Based on a Cellular Slab

Marzena Olszewska[1], **Wojciech Gwarek**[1], **Malgorzata Celuch**[2], **and Bartlomiej Salski**[2]

[1]QWED Sp. z o.o., ul. Krzywickiego 12 lok.1, Warsaw 02-078, Poland
[2]Institute of Radioelectronics, Warsaw University of Technology
ul. Nowowiejska 15/19, Warsaw 00-665, Poland

Abstract— With an increasing proliferation of high-power microwave transmitters on the one hand, and sensitive microwave diagnostic equipment on the other hand, effective separation between the two domains has become a necessity. In many cases, a small scattering footprint is simultaneously required. Moreover, a need for low-cost solutions often arises, as one may wish, for example, to shield full hulls (of yachts, aircrafts, etc.) or all walls (of laboratories, clinics, etc.) against their external high-intensity radiated fields environment.

Classical designs are based on a Salisbury screen concept (Fig. 1(a)). A wave incident with a positive kz propagation coefficient component first impinges onto a resistive layer (magenta), passes through a bulk dielectric spacer (green), and finally reflects from a perfect conductive plate (yellow). Dissipation of microwave energy occurs in the resistive layer. The design is low-cost, but bulky and narrow-band, as the dielectric spacer must have a quarter-wavelength thickness and low permittivity [1, 2].

In a recent work [2], we have proposed a modification wherein the homogeneous resistive layer is replaced by a patterned foil layer. We have optimised the pattern so that it simultaneously increases the operating frequency band and decreases the dimensions. We have reached an octave absolute bandwidth of the reflection coefficient below -20 dB, maintaining the thickness below quarter-wavelength. However, in that preliminary work, the spacer has been fixed as air, which is not technologically feasible.

In this contribution, we explore a novel concept of depositing the patterned metal foil on an inhomogeneous cellular structure (Fig. 1(b)). Cellular materials, and especially chiral or auxetic ones, have been long explored for their mechanical virtues [3, 4]. We have previously proven their effective permittivity to be low and of minor dispersion [5, 6].

Our new screens combining cellular spacers with patterned foils exhibit noteworthy advantages from a multiphysics perspective:

1. **Electromagnetic**: effective absorption of microwave power over a competitively wide band of frequency and incidence angles. This has been proven by periodic 3D FDTD modelling and modelling results for various cellular geometries will be presented at the Symposium.

2. **Mechanical**: enhanced compressive strength and shear stiffness.

3. **Structural**: light weight and small thickness. Also, adjusting dimensions so as to obtain auxetic behaviour, leads to a sinclastic curvature feature. This allows manufacturing domed shields, conforming to non-flat shapes of vessels or housing.

4. **Thermal**: Due to a high volumetric fraction of air and low thermal conductivity, cellular spacers are subject to low temperature rise. Forced ventillation can be additionally applied. Low thermal deformation coefficients result and thereby, designs made at a room temperature remain reliable under high incident microwave power conditions.

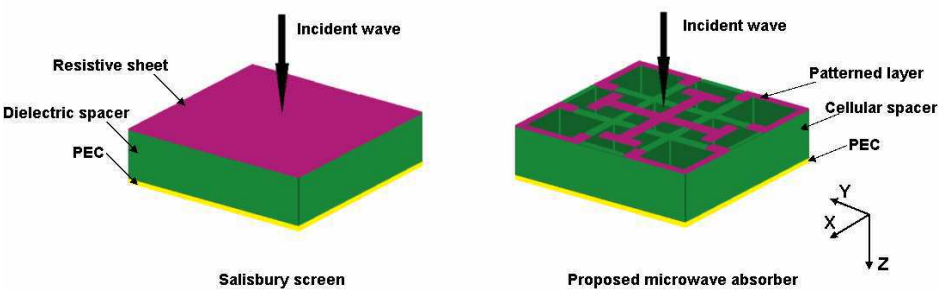

Figure 1: Model of the considered microwave absorber with periodic boundary conditions along the X and Y directions.

ACKNOWLEDGMENT

Part of this work was funded by the Polish National Centre for Research and Development under ERA-NET-MNT/14/2009 contract.

REFERENCES

1. Chambers, B., "Optimum design of a Salisbury screen radar absorber," *Electronics Letters*, Vol. 30, No. 16, 1353–1354, August 1994.
2. Olszewska, M. and W. Gwarek, "A novel wide-band microwave absorber with a decreased thickness," *19th Intl. Conference on Microwaves, Radar and Wireless Communications MIKON-2012*, Warsaw, Poland, May 2012, accepted for publication.
3. David, B. V., I. Nica, and A. Salceanu, "Electromagnetic absorbers based on chiral honeycomb slab," *International Symposium on Electromagnetic Compatibility — EMC Europe 2009*, 1–4, June 2009.
4. Scarpa, F., G. Burriesci, F. C. Smith, and B. Chambers, "Mechanical and electromagnetic behaviour of auxetic honeycomb structures," *The Aeronautical Journal*, Vol. 107, 175–183, 2003.
5. Kopyt, P., R. Damian, M. Celuch, and R. Ciobanu, "Dielectric properties of chiral honeycombs — Modelling and experiment," *Composites Science and Technology*, Vol. 70, No. 7, 1080–1088, July 2010.
6. Lira, C., F. Scarpa, M. Olszewska, and M. Celuch, "The SILICOMB cellular structure: Mechanical and dielectric properties," *Phys. Status Solidi B*, Vol. 246, No. 9, 2055–2062, August 2009.

Geometrical Model of a Resonance as One of the Basic Means of Strengthening of Signals

B. A. Shiyanov, **A. I. Shiyanov**, **and A. V. Krutov**
International Institute of Computer the Technologies, Russia

Abstract— Between fluctuations, in particular, electromagnetic, and properties of curves alongside with known electromechanical analogy [1] the close connection shown in geometric-oscillatory of analogy of compelled fluctuations (AVK) is revealed.

In this analogies the role of the oscillitory value x carries out distance h (basic function) from poles up to its projection on the tangent of the simulating curve (the locus of these by projection also gives the curve, called the podera this curve, the size h is polar radius for its points); thus the role of compelling force plays radius of curvature simulating curve in function of the angle of rotation of the tangent, which performs the role of the time.

Geometrical model (geometrical generator) physical phenomenon of a resonance is the cycloidal curve — bending of straight linees. To the resounding value corresponds a polar radius of the points of the podere of envelope relative to the origin of coordinates.

With the help of kinematic-geometrical model on the basis of analogies the connection of tasks of nonlinear dynamics, theory of chaos with the phenomenon of a resonance is revealed, which is logical to consider as process of transition of system of one condition in qualitatively other. The universal law and appropriate sizes (for example $\alpha = 0.4224$), having the certain geometrical sense, which appear in particular in display of Feygenbaum as universal constant, describing in nonlinear dynamics transition to chaos [2].

The expression allowing to pass from the parametrized resonance curve to the usual diagram of resonant fluctuations is received. It can serve also as key to an establishment of the formulas of transition from the cartesian coordinates to polar with algebraic polar radius.

Example. The equations similar to the differential equations flat curve in basic function, describe also movement of the charged particle in the crossed electrical and magnetic fields. The decision in a projection to a plane turns out as a trajectory of a particle as cycloidal curve (curve of Landau) [1]. It is interesting, that polar radius of podere cycloidal by a curve, including and curve of Landau, varies under the same law, as amplitude in a resonance.

The method proposed and the revealed possibility of the geometric interpretation of the solution, made it possible to reveal the new properties in the phenomenon of resonance, which result from its geometric model, which can be used for the solution of the technical problem of strengthening the signals. with the development of resonators and other dynamic systems in different regions.

During the supplying to the entrance of the sinusoidal oscillitory value $2c(E_{\text{y}}/H)\sin\omega t$ on an output(exit) is received ??? size $h = (cE_{\text{y}}/H)(\sin\omega t - \varphi\cos\omega t)$ at the output we obtain the resounding value.

In our view, questions examined here have the important scientific, methodological and educational methods value [3–5].

If the interesting observed geometric properties are revealed in the simulating curves, then by the force of analogy we can establish interesting properties, also, in physics of the corresponding processes. In this sense the represented approach is similar to the mathematical expression of phase transitions, in particular, in the ferromagnetic materials (Curie point) and in the model of Van der Waals of imperfect gas, in which to point of inflection with the horizontal tangent corresponds the isotherm with the critical temperature of phase transition "Gaz-Liquid".

Van der Waals model is examined as the model of the theory of catastrophes [6]. The phenomenon of resonance is not less than the foundations for examining in the same quality (catastrophic resonance).

This geometric approach can be used also in the theory of pattern recognition and its applications, for studying the physical and physiological special features of sight, etc.

REFERENCES

1. Landau, D. L. and E. M. Lifschitz, *The Mechanics. Electrodynamics*, 272, Nauka, 1969.
2. Schuster, G., *The Determined Chaos: Introduction*, 250, Mir, 1988.

3. Mukonin, A. K. and A. I. Shiyanov, *Frequency Drives with Current Control: The Monography*, 143, VSTU, Voronezh, 2006.
4. Krutov, A. V., *Some Applied Tasks: Geometrical-kinematic Models*, 252, PFUR, 2001.
5. Shiyanov, A. I. and V. I. Pisarev, *Certification of Conditions and Character of Work of the User of the Computer: Training. The Benefit*, 209, International institute of computer the Technologies, VSTU, Voronezh, 2006.
6. Malinetskiy, G. G., *Chaos. Structures. Computational Experiment: Introduction into Nonlinear Dynamics*, 256, Editorial URSS, 2000.

Session 1P3a
Theory and Methods of Digital Signal and Image Processing 2

New Constructions of Kravchenko-Poisson Wavelets and Their Applications for Digital Signal Processing

M. S. Sautbekova and S. S. Sautbekov
Eurasian National University Named after L.N. Gumilyov, Kazakhstan

Abstract— In practice can be useful the finite distributions which are under construction on the basis of Atomic Functions up(x). According to results and the ideas presented in works [1–4], recent paper is dedicated to the application of Kravchenko-Poisson distribution in digital signal processing.

This work consists of two parts. In the first part the theory of building of the Kravchenko-Poisson distributions [1] is represented:

$$p(x) = \begin{cases} \frac{1}{c}\mathrm{up}\left(\frac{x}{b}\right)\exp\left(-\frac{x}{a}\right), & \text{if} \quad x \geq 0, \\ 0, & \text{if} \quad x < 0. \end{cases} \tag{1}$$

Here c is chosen such that in (1)

$$\int_{\mathbb{R}} p(x)dx = 1.$$

With the help of this relation the new family of Kravchenko-Poisson wavelets are discussed. The next physical quantities are considered: wavelet spectra, energy density of the wavelet-skeletons, the scalograms. Analysis of signal distortion was determined in the presence of noise and digitization. The relations for the optimal transformation parameters were obtained. The wavelets of the second generation were obtained on the base of Kravchenko-Rvachev structures, etc..

The second part is devoted to the computer simulation by the formula (1).

REFERENCES

1. Kravchenko, V. F., O. V. Kravchenko, and A. R. Safin, "Atomic functions in probability theory and stochastic processes," *Uspekhi Sovremennoi Radioelektroniki*, No. 5, 23–38, 2009 (in Russian).
2. Kravchenko, V. F., *Lectures on the Theory of Atomic Functions and Their Some Applications*, Radiotekhnika, Moscow, 2003 (in Russian).
3. Kravchenko, V. F. and V. L. Rvachev, *Algebra of Logic, Atomic Functions and Wavelets in Physical Applications*, Fizmatlit, Moscow, 2006 (in Russian).
4. Kravchenko, V. F., O. S. Labunko, A. M. Lerer, and G. P. Sinyavsky, *Computing Methods in the Modern Radio Physics*, Fizmatlit, Moscow, 2009 (in Russian).

Application of WA-functions of Distribution of Kravchenko-Rvachev for Digital Signal Processing

M. S. Sautbekova and S. S. Sautbekov
Eurasian National University Named after L. N. Gumilyov, Kazakhstan

Abstract— The recent report is dedicated to the application of Kravchenko-Rvachev [1–3] distribution of digital processing problems of new signal constructions.

This work consists of two parts. In the first part the theory of building of the Kravchenko-Gauss, Kravchenko-Rayleigh distributions [1] is represented:

$$p(x) = \frac{1}{\sqrt{2\pi}c}\exp\left(-\frac{x^2}{2a^2}\right)\mathrm{up}\left(\frac{x}{b}\right), \qquad a,b,c\in\mathbb{R}. \tag{1}$$

$$p(x) = \begin{cases} \frac{x}{c}\mathrm{up}\left(\frac{x}{b}\right)\exp\left(-\frac{x^2}{2a^2}\right), & \text{if} \quad x\geq 0, \\ 0, & \text{if} \quad x<0. \end{cases} \tag{2}$$

Here c is chosen such that in (1), (2)

$$\int\limits_{\mathbb{R}} p(x)dx = 1.$$

With the help of these relations the new families of Kravchenko-Gauss and Kravchenko-Rayleigh wavelets are discussed. The next physical quantities are considered: wavelet spectra, energy density of the wavelet-skeletons, the scalograms. Analysis of signal distortion was determined in the presence of noise and digitization. The relations for the optimal transformation parameters were obtained. The wavelets of the second generation were obtained on the base of Kravchenko-Rvachev structures, etc..

The second part is devoted to the computer simulation by the formulas (1) and (2).

REFERENCES

1. Kravchenko, V. F., O. V. Kravchenko, and A. R. Safin, "Atomic functions in probability theory and stochastic processes," *Uspekhi Sovremennoi Radioelektroniki*, No. 5, 23–38, 2009, in Russian.
2. Kravchenko, V. F., *Lectures on the Theory of Atomic Functions and Their Some Applications*, Radiotekhnika, Moscow, 2003, in Russian.
3. Kravchenko, V. F. and V. L. Rvachev, *Algebra of Logic, Atomic Functions and Wavelets in Physical Applications*, Fizmatlit, Moscow, 2006, in Russian.

Embedded Object Detection by Using Planar Antenna Measurement System

O. Kurnaz, S. Helhel, and S. Ozen
Department of Electrical and Electronics Engineering, Akdeniz University, Turkey

Abstract— Detection of objects embedded in or behind a medium is of great importance regarding especially security and medical applications. In this study, planar near-field antenna measurement system implementing a two dimensional scanning process and being combined with a network analyzer has been used as a controlled radar setup to detect a metallic object embedded in a non-metallic medium at X-band. Bistatic wave scattering conditions have been formed in the experimental setup. A standard gain horn antenna operating at X-band frequencies is used as transmitter and rectangular shaped and open ended waveguide having a measurement frequency range between 8.2 GHz and 12 GHz is used as measuring probe. A metal ribbon having 1 cm × 5 cm dimensions has been buried in a dielectric cylinder having a diameter of 5 cm and height of 11 cm. By placing the transmitter-receiver system and the target 1 meter away from each other, electromagnetic scattering pattern of the target has been obtained by using S_{21} parameter, where square of $|S_{21}|$ gives the ratio of received power to the transmitted power. Not only scattering pattern of the cylinder containing metal ribbon but also the pattern of cylinder without metal ribbon has been obtained and background subtraction method including image processing techniques has been applied in order to approximate the scattering effect resulting from the metal itself by eliminating other effects. It has been observed that the scattered electric field intensity decreases as frequency increases; field intensity at 7.8 GHz is almost two times the intensity at 9 GHz, which leads to the conclusion that the accuracy of detection process would be low at very high frequencies. Different from the studies where generally ground penetrating radar is used, embedded object detection has been realized by using a planar near-field antenna measurement system as a bistatic radar setup and image processing techniques have been applied to the obtained measured data.

Electromagnetic Object Recognition for Dielectric Coated Conductors Based on WD-PCA Type Fused Feature Extraction

G. Turhan-Sayan[1] **and E. Ergin**[1,2]

[1]Department of Electrical-Electronics Engineering
Middle East Technical University (METU), Ankara, Turkey
[2]Turkish Aerospace Industries, Inc. (TAI), Ankara, Turkey

Abstract— This paper presents the design of an electromagnetic object classifier based on a feature extraction approach, called WD-PCA technique, to recognize dielectric coated conducting objects using their band-limited scattered signals at only a few different reference combinations of aspect and/or polarization.

Electromagnetic object recognition is a highly complicated problem because of the aspect and polarization dependent nature of scattered data. In resonance region, however, the late-time scattered signals implicitly possess the aspect-polarization independent features, the complex natural resonance (CNR) frequencies, for the object of concern. Based on the Singularity Expansion Method (SEM), when an object is approximately modeled as a linear time-invariant system, CNR frequencies can be computed as the poles of system function in complex frequency domain. A complete set of system poles can describe a finite-size object uniquely in an aspect and polarization independent manner. Methods suggested for the extraction of CNR frequencies directly from electromagnetic scattered signals are known to be very sensitive to noise. Therefore, alternative indirect methods are needed for the extraction of natural resonance related object features while paying special attention to aspect/polarization invariance and robustness with respect to noise. One of such indirect electromagnetic target/object recognition techniques is the WD-PCA method that is based on the use of Wigner Distribution (WD), a quadratic time-frequency transformation used here for CNR-related feature extraction, and the Principal Component Analysis (PCA), a well known signal processing tool used here for feature fusion. In WDPCA method, each object of the target library is represented in the classifier database by a single aspect/polarization invariant feature vector.

The WD-PCA method has been successfully applied to perfectly conducting or lossless dielectric targets so far. In this paper, it will be applied to a more complicated target library composed of dielectric coated conducting spheres which may have varying conducting sphere diameters or coating thicknesses and different permittivity values in the coating layer. Although the former applications of the WD-PCA method have been focused mostly in defense-related applications, this method is considered to be useful also in medical applications to recognize/monitor tumors or metallic man-made pieces embedded in human tissue for treatment purposes.

Cross Validation Technique Selection of Features Extraction Methods for UWB Radar Target Classification

M. Khodjet-Kesba[1, 2], **K. El Khamlichi Drissi**[1, 2], **C. Faure**[1, 2], **and C. Pasquier**[1, 2]

[1]Clermont Université, Université Blaise Pascal, BP 10448
Clermont Ferrand F-63000, France
[2]CNRS, UMR 6602, Institut Pascal, Aubière F-63177, France

Abstract— In the last fifteen years, the interest in Ultra Wideband systems has grown rapidly. One of several applications of the UWB is automatic radar identification in intelligent vehicles.

A convenient method for features extraction is important to distinguish different targets. In our work a comparison of Discrete Wavelet Transform (DWT) [1] and Matrix Pencil Method (MPM) [2] will be carried out by applying the methods to the late time part of the backscattered signal. This part of signal arises from resonance phenomena of the target and can be used for identification. The late time response depends theoretically, on the target geometry only and its associated physical properties. Thus it is independent of the aspect and polarization of the excitation source.

Two databases are built, one containing the features extracted by DWT, and the other containing the features extracted by MPM. The accuracy of the classification between three different classifiers: Naive Bayes, K-NN and SVM [3] is calculated.

In order to minimize the bias associated with the random sampling of the training and testing data samples while comparing the predictive accuracy of classification methods, stratified 10-fold cross validation is used. Using the proposed method, the entire dataset is divided into 10 mutually exclusive subsets (or folds) with approximately the same class distribution as the original dataset (stratified). Each fold is used once for testing and the nine remaining folds are used to train the models, leading to 10 independent performance estimates. Ten cross validation estimates are then averaged to provide the classifier accuracy.

The results indicate that the classification of MPM features is the most accurate extraction method, and SVM classifier provides the best results compared to the other classifiers.

REFERENCES

1. Addison, P. S., *The Illustrated Wavelet Transform Handbook*, Institute of Physics, Naiper University, Edinburgh, UK, 2002.
2. Sarkar, T. K. and O. Pereira, "Using the matrix pencil method to estimate the parameters of a sum of complex exponentials," *IEEE Ant. and Prop. Mag.*, Vol. 37, No. 1, 48–55, 1995.
3. Khodjet-Kesba, M., K. Chahine, K. El Khamlichi Drissi, and K. Kerroum, "Comparison of ultra-wideband radar target classification methods based on complex natural resonances," *PIERS Proceedings*, 318–321, Kuala Lumpur, Malaysia, Mar. 27–30, 2012.

Session 1P4a
Small Size Antenna

A New Small and Low-cost Wideband PIFA with Corrugations Based on Digital Dividend

C. D. Nikolopoulos, K. D. Stravoskoufis, and C. N. Capsalis
Division of Information Transmission Systems and Material Technology
School of Electrical and Computer Engineering
National Technical University of Athens, Greece

Abstract— Nowdays more than ever the modern society has become dependent on radio spectrum and the demand for new wireless communications services in the so-called area of Digital Dividend make the necessity present to form a wideband antenna based on this area (698–862 America & Asia, 790–862 Europe). WC-07 made positive steps towards making spectrum available for future LTE deployments. In particular, WRC-07 began the process of migrating broadcast spectrum in the 698–862 MHz band to mobile applications. For that reason a lot of effort is carried out to optimize a structure in the central frequency of 790 MHz. Exploiting corrugations scheme we optimize the new antenna, suitable to operate from channel 52 to 69 (corresponding frequencies 698–862 MHz). The present mobile terminal antenna is expected to show increased bandwidth (200 MHz) as well as low-loss impedance matching (VSWR = 1.05). The proposed structure consists of a conductive top lying over a finite sized ground plane which is interconnected through a wire (feeding wire), and one other element as shorting strip, in a configuration design to cover all the digital dividend area.

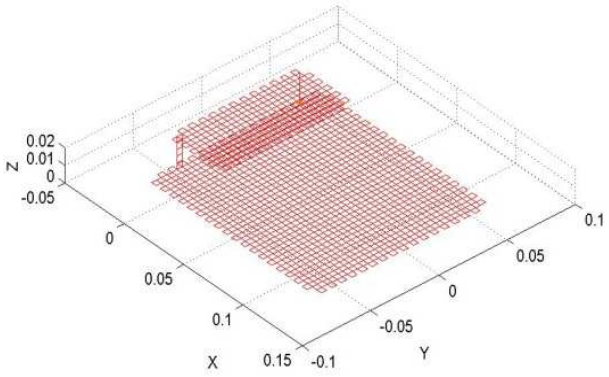

Figure 1: Implementation and analysis of the Corrugated PIFA using wire segments and the SNEC platform.

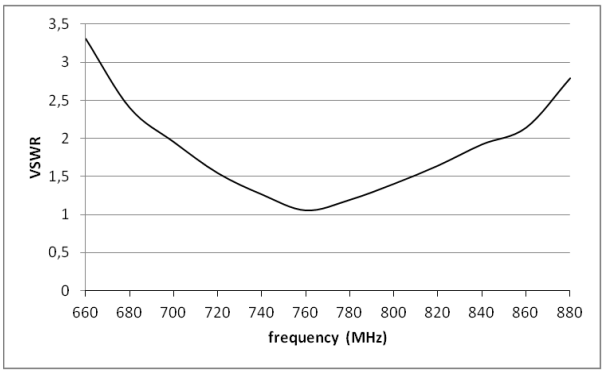

Figure 2: VSWR of optimized corrugated PIFA at 790 MHz.

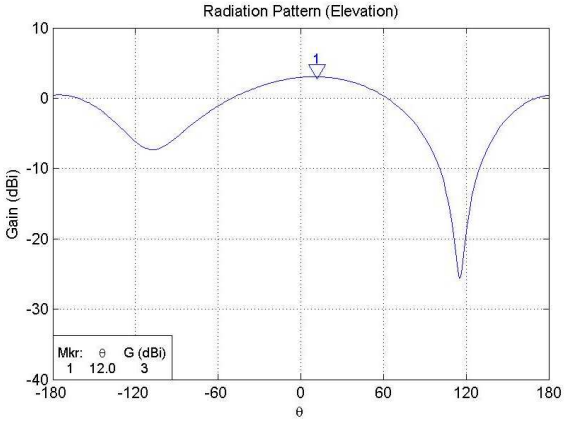

Figure 3: Radiation pattern of the optimized Corrugated PIFA at 790 MHz.

Table 1: Genetic algorithm parameters range and results. (wavelength equal to $\lambda_o = 0.379\,\mathrm{m}$ corresponding to an operating freq. of 790 MHz).

Element	Range of Variation	Step	Results
Length of top plate (UpLen)	$0.015\lambda_o$–$0.01\lambda_o$	$0.01\lambda_o$	$0.05\lambda_o$
Width of top plate (UpWid)	$0.015\lambda_o$–$0.01\lambda_o$	$0.01\lambda_o$	$0.12\lambda_o$
Length of ground plate	UpLen + ($0.15\lambda_o$–$0.01\lambda_o$)	$0.01\lambda_o$	UpLen + $0.13\lambda_o$
Width of ground plate	UpWid + ($0.015\lambda_o$–$0.01\lambda_o$)	$0.01\lambda_o$	UpWid + $0.4\lambda_o$
Height of wires/shorting strips	$0.06\lambda_o$–$0.01\lambda_o$	$0.01\lambda_o$	$0.05\lambda_o$
Width of shorting strips	$0.015\lambda_o$–$0.01\lambda_o$	$0.01\lambda_o$	$0.01\lambda_o$

A custom Genetic Algorithm is used in order to optimize the antenna parameters regarding resonation frequency and radiation pattern orientation angle. The optimized antenna exhibits satisfactory directivity for mobile terminal applications of 3 dBi over an operational bandwidth of 180 MHz, corresponding to a percentage of 25.6%. Simulation results and parameters range are exposed below followed by the according radiation pattern and variation of the simulated VSWR.

Accurate Measurement of Power Transfer to an RFID Tag with On-chip Antenna

Philipp K. Gentner[1], **Günter Hofer**[2], **Arpad L. Scholtz**[1], **and Christoph F. Mecklenbräuker**[1]

[1]Institute of Telecommunications, Vienna University of Technology
Gusshausstrasse 25/389, Vienna 1040, Austria
[2]Infineon Technologies Austria AG, Contactless and RF Exploration
Babenberger Strasse 10, Graz 8020, Austria

Abstract— Dramatically decreasing the size of an RFID tag is possible by using on-chip antennas, so-called OCAs [1, 2]. For the applications in mind, such as identifying goods in the food supply chain or in medical supply, the systems on chip need to be externally powered. This is challenging due to the small aperture available and because the antenna typically resides on a lossy substrate such as silicon.

Accurate measurement of the power inductively transferred to the tag is impossible using bond wires or probes, because both would introduce severe distortions of the electromagnetic field. Questionable results concerning the voltage induced into the on-chip antenna would be such obtained.

We present a novel method to accurately measure the voltage induced into an on-chip antenna and demonstrate its application in the UHF band at 850 MHz. To verify the proposed method we have designed and manufactured a system on chip. This chip consists of a loop antenna (similar design as reported in [1] and [2]), a rectifier, and a voltage controlled oscillator [3]. The latter modulates the energy backscattered by the chip with a frequency proportional to the voltage delivered by the rectifier. Hence, by measuring the modulation frequency the exact value of the voltage induced into the chip's antenna can be revealed.

In the full paper, comprehensive measurements of the inductive coupling between an elaborate reader station and an RFID tag with on-chip antenna will be shown. The silicon is moved in planes above an excitation coil, and the modulation frequency of the signal backscattered is measured. With the relation between the voltage induced into the chip's antenna and the backscattered signal's modulation frequency being calibrated, the energy received by the chip as a function of its position in space is mapped.

ACKNOWLEDGMENT

This work was performed as part of the project 'Smart Data Grain' which is embedded into the program 'Forschung, Innovation, Technologie-Informationstechnologie' (FIT-IT) of the 'Bundesministerium für Verkehr, Innovation und Technologie' (BMVIT). This program is funded by the 'Österreichische Forschungsförderungsgesellschaft' (FFG). This work is partly supported by the Christian Doppler Laboratory for Wireless Technologies for Sustainable Mobility.

REFERENCES

1. Xi, J., N. Yan, W. Che, X. Wang, H. Jian, and H. Min, "On-chip antenna design for UHF RFID," *Electronics Letters*, Vol. 45, No. 1, 14–16, 2009.
2. Guo, L., A. Popov, H. Li, Y. Wang, V. Bliznetsov, G. Lo, N. Balasubramanian, and D. Kwong, "A small OCA on a $1 \times 0.5\,\mathrm{mm}^2$ 2.45 GHz RFID tag-design and integration based on a CMOS-compatible manufacturing technology," *IEEE Electron Device Letters*, Vol. 27, No. 2, 96–98, 2006.
3. Klapf, C., A. Missoni, W. Pribyl, G. Holweg, and G. Hofer, "Analyses and design of low power clock generators for RFID TAGs," *Proc. Ph.D. Research in Microelectronics and Electronics PRIME 2008*, 181–184, 2008.

A Reduced-size Antipodal Vivaldi Antenna with a Reconfigurable Band Notch

L. Safatly, **M. Al-Husseini**, **A. El-Hajj**, **and K. Y. Kabalan**
ECE Department, American University of Beirut, Beirut 1107 2020, Lebanon

Abstract— The design of a reduced-size antipodal Vivaldi antenna with a reconfigurable band notch is presented in this paper. The antenna could be mainly used for UWB applications since it covers a very wide frequency band. Also, it is suitable for Cognitive Radio (CR) systems because it is capable to sense the spectrum to determine the bands used by primary users, and to communicate pulses that ensure interference avoidance to primary users. For that, a reconfigurable band stop filter, based on three nested complementary split-ring resonators (CSRRs), is integrated on the ground plane. The antenna is illustrated in Figure 1(a). It is printed on a $60 \times 35 \times 1.6\,\text{mm}^3$ FR4-epoxy substrate with $\varepsilon_r = 4.4$. The dimensions of the different parts are optimized for an impedance bandwidth covering frequencies starting from 1.5 GHz as depicted in Figure 1(b). The incorporated band stop filter is equipped with three electronic switches S_1, S_2 and S_3. When a switch is activated, the functioning of a larger CSRR is launched, and thus a notch at a lower frequency occurs. The CSRR sizes are optimized so that the notch occurs at 3.5 GHz, 5.2 GHz or 7.3 GHz. The proposed antenna is designed and simulated using Ansoft HFSS. A prototype is fabricated, and the reflection coefficient is measured for the possible operation scenarios. As illustrated in Figures 1(c) and 1(d), adequate analogy is shown between the simulated and measured results. For Case 1, in which all switches are ON, a UWB response is obtained. The results for Cases 2, 3 and 4, where the switches are sequentially activated, reveal a single notch in the 3.5 GHz, 5.2 GHz or 7.3 GHz band, respectively.

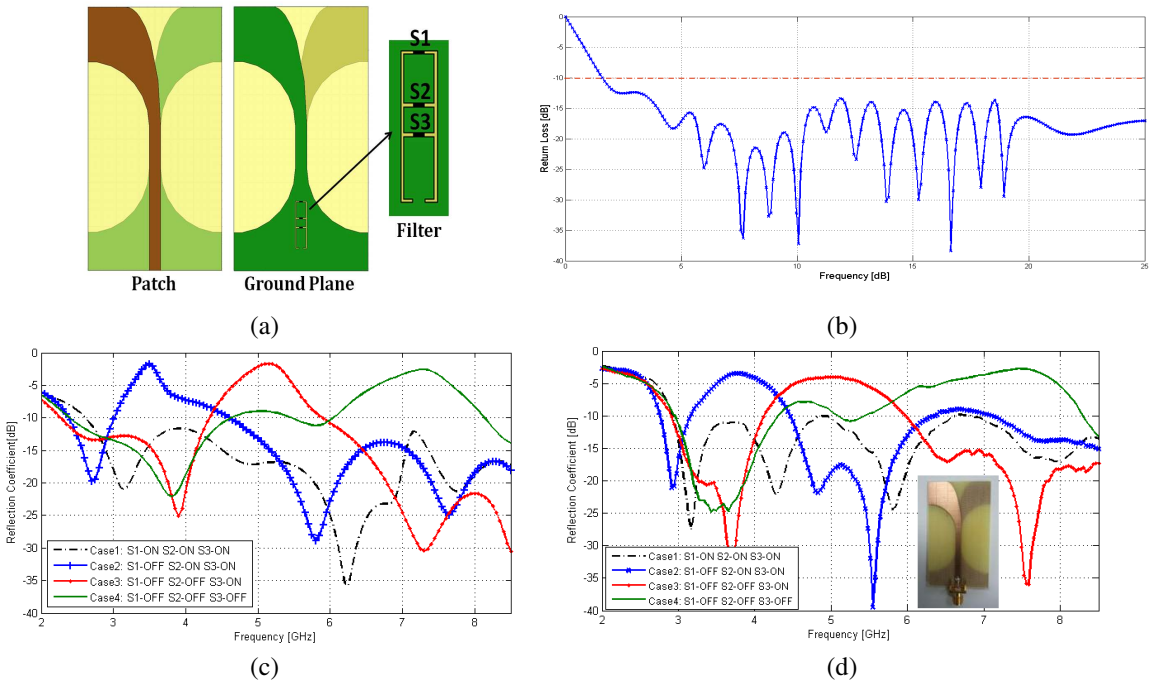

Figure 1: (a) Configuration of the proposed antenna, (b) reflection Coefficient of the antenna without the filter, (c) computed reflection coefficient for the different switching cases of the antenna and (d) fabricated prototype with its measured reflection coefficient for the different switching cases of the antenna.

Effect of Small Size Antenna inside Complex PCB

Dau-Chyrh Chang[1], **Cheng-Wei Chen**[2], **Hsiao-Bin Liang**[2], **Chi-Hsiung Wang**[2], **and Tsan-Hung Wu**[2]

[1]Oriental Institute of Technology, Taiwan
[2]Climax Technology Co., Ltd, Taiwan

Abstract— In general, there are many communication antennas inside GSM PCB (Print Circuit Board) for various applications. The radiation of smaller size of antenna will not only radiate to the outside system, but also radiate inside the system. This effect will cause the serious EMI problem. In this paper, on board modified PIFA is used to reduce the EMI effect due to complex PCB environment. The EM simulation tool, GEMS [1], is used to design and analyze the performance of antenna and 3D EM environment in this work. The measured results of TRP/TIS (total radiation power/total isotropic sensitivity) for GSM module of the PCB for wireless home security system verifies the improvement of this proposed on board modified PIFA.

An Evaluation of Capacitive Feed Methods for Electrically Small and Low-profile Meander Line Antennas

T. Fukusako, Y. Saito, and H. Maema
Computer Science and Electrical Engineering
Graduate School of Science and Technology, Kumamoto University, Japan

Abstract— Electrically small and low-profile antennas (ESLA) have been widely studied in recent years. An antenna which is close to a back conductor can reduce the electrical effects from the backing material when installed on IC chips, human body or any metallic or lossy material. However, typical electrically and low-profile antennas have low radiation efficiency resulting in a difficulty of impedance matching to 50 Ω.

For designing an ESLA, a capacitive feed (C-feed) technique has been proposed by the authors' group previously. Using the C-feed structure, the imaginary part of the input impedance of the antenna can be easily controlled by varying the size of the feed plate which is installed in between the radiating element and ground plane. Furthermore, a modified quarter-wavelength capacitive-feed meander line antenna (QCFMA) has been proposed for gain improvement satisfying $ka = 0.435 < 0.5$, k: wave number, a: radius of a sphere surrounding the antenna.

In this paper, the QCFMA is compared with the same dimension of meander line antenna with an inverted-F antenna structure (IFMA) in order to evaluate the performance of C-feed structure. As a result, QCFMA shows better radiation characteristics than IFMA. Furthermore, performances of some modified C-feed structures are discussed.

Broadband Circularly Polarized Moxon Based Antennae for RFID and GPS

Haojiong Liu[1], **Oksana Manzhura**[1], **İbrahim Tekin**[2], **and Edip Niver**[1]

[1]Electrical Engineering, New Jersey Institute of Technology, Newark, NJ, USA
[2]Electronics Engineering, Sabancı University, İstanbul, Turkey

Abstract— Novel circularly polarized (CP) antenna configurations were proposed based on Moxon antenna (bent dipole element over a ground plane) for broadband VHF SATCOM applications. A sequence of topologies starting from a single vertical element to two vertical elements of the Moxon arms, then widened strip arm elements were investigated to understand the effects on increase of the bandwidth. The logic in this evolution was to obtain highest possible gain based on Fano-Chu limits, which suggests that more metalization in the radiating configuration that fill the volume would yield higher gain for electrically small antenna. Extending the width of the strip of the equivalent dipole elements lead to a wider bandwidth and improved cross-polarization ratio. Further, widening the strips lead to further improvement in the performance leading to confirmation of Fano-Chu limits [4–7] for electrically small antenna with maximum radiating elements in a given volume. Furthermore, splitting the tapered bow tie elements increased the volume filled with radiating elements leading to improved overall performance. Ultimately bends at the tip of the tapered sections parallel to the ground plane helped to improve overall performance in terms of bandwidth and gain pushing to optimized performance in terms of the Fano-Chu limits. In overall, the antenna suggested here produced lower height, higher gain, wider bandwidth and better cross-polarization and lower back lobe radiation compared to SATCOM antenna such as an eggbeater currently used in practice. Circular polarization is obtained by two Moxon based cross elements that are fed through a hybrid quadrature coupler.

Here, the concept is extended to cover RFID (850–1050 MHz) and GPS (centered at 1227 and 1575 MHz) bands leading to new applications at a significant cost reductions and much improved performance. Prototype antennas were built based on HFSS simulations yielded better than −25 dB return loss. During simulations attention was paid to identify the effects of individual antenna parameters on the overall effect on the bandwidth. Simulated results predict higher than industrial counterpart antenna gain and gain measurements are currently in progress.

Bended Rectangular Slotted Waveguide Antenna

Dana Baz Radwan[1], **Ali Harmouch**[2], **and Mustapha Ziade**[2]

[1]American University of Science & Technology, Beirut, Lebanon
[2]Faculty of Engineering, Lebanese University, Lebanon

Abstract— Rectangular slotted waveguide antennas have been widely used in many areas of telecommunications from plane antennas to wireless internet applications due to their high directivity, compactness and feasibility. One of the major drawbacks of such antennas is that the Sidelobe level is significant since the slots are placed on a finite conducting plate which consequently leads to a decrease in the overall directivity of such radiators. A bended slotted rectangular waveguide antenna is presented in this paper which provides narrower beamwidth in addition to a significant decrease in the Sidelobe level. FEKO Simulations and experimental results done to the bended slotted waveguide antenna have obviously shown a significant improvement in the directional characteristics for about 4 dB without any increase in the antenna's dimensions.

Session 1P5a
Novel Mathematical Methods in Electromagnetics 2

Leaky Wave Radiation for Body-centric Wireless Communications

Xenofon M. Mitsalas[1], **Alexander V. Kudrin**[2], **and George A. Kyriacou**[1]

[1]Microwaves Laboratory, Department of Electrical & Computer Engineering
Democritus University of Thrace, Xanthi, Greece
[2]Department of Radiophysics, University of Nizhny Novrogod, Russia

Abstract— In recent years, body-centric wireless communications have become an active area of research because of their various applications such as e-healthcare and personal communications. For example, Ito and Haga [1] have studied with the aid of finite difference time domain method the frequency dependent bioelectromagnetic models of body-centric wireless communication channels in the range of HF to UHF (3 MHz–3 GHz). Extensive numerical studies have been performed by an impressive number of researchers aiming at the characterization of the human body as an electromagnetic signal channel. Even though such analysis could be highly accurate, especially when realistic human body models are employed, however they are just snapshots (samples) of a very extended physical phenomenon. Theoretical analysis is thus inevitable to understand physical mechanism and to reveal their hidden characteristics. A step toward this direction was indeed tried by Prof. Hall group [2] with a simplified analysis aiming at characterizing the important role of surface and creeping waves on body communication channels. In this paper an analytical study of the electromagnetic waves propagation along the human body is attempted in order to understand the specific characteristics of the possible excited waves. For this purpose the human body is considered as an infinitely extended open radiating cylinder filled with a highly lossy dielectric fluid media $\epsilon_r \approx 80$, $\sigma = 1.2\,\mathrm{S/m}$ and diameter = 40 cm. Both surface and leaky waves are supported by such a cylindrical structure which is extensively studied in the past, especially by Kim [3], but only for a low loss and non-dispersive dielectric media. It was suspected and indeed verified herein that very high losses of the human electrolytes may completely change the excited waves characteristics. Besides losses the human tissues (electrolytes) present a very high frequency dispersion by means of a complicated variation of both dielectric constant (ϵ_r) and conductivity (σ) versus frequency.

The Debye model given in [1] is employed herein for the characterization of the whole human body. Actually the debye equation is adopted with different parameters for the frequency ranges (3–30, 30–300, 300–3000 MHz) as given in [1]. Explicitly, based on Kim's [3] approach the characteristic equation for both surface and leaky modes is extracted and numerically solved. A special technique proposed by the group of Berral, Mesa & Medina [4] is adopted in order to circumvent the numerical difficulties introduced by the involved branch cut singularity. In turn dispersion curves are obtained for both leaky and surface wave modes for three different cases of an infinite dielectric cylinder with 40 cm diameter (modeling the human body): (i) low losses dielectric cylinder $\epsilon_r \approx 80$, $\tan\delta = 0.01$, (ii) lossy dielectric column $\epsilon_r \approx 80$, $\sigma = 1.2\,\mathrm{S/m}$ and (iii) a dielectric fluid column described by the Debye model. These curves are compared in order reveal the underlined physical phenomena in the 3 MHz to 3 GHz range. Additionally, for selected surface and leaky wave modes which constitute candidates for practical operation of communication channels the electric and magnetic field eigenfunctions are calculated and plotted on a cross-section of the structure. Particular attention in devoted to leaky modes, since these are well established to behave as non-uniform (attenuated) waves along a specific direction in the unbounded space outside the cylinder. This is actually the direction along which the leaky waves excited along lossless dielectric cylinders present their maximum radiation (beam maximum). It is along this direction that the leaky modes eigenfuction is plotted for 2 the region outside the cylinder. The next essential step of this research is to identify proper excitation techniques of the desired modes. Ultimately this analysis will be utilized as a guide to repeat the study on realistic human models with the aid of numerical techniques.

REFERENCES

1. Ito, K. and N. Haga, "Basic characteristics of wearable antennas for body-centric wireless communications," *Loughborough Antennas & Propagation Conference*, Nov. 8–9, 2010.
2. Akhoondzadeh-Asl, L., Y. Nechayev, and P. S. Hall, "Surface and creeping waves excitation by body — Worn antennas," *Loughborough Antennas & Propagation Conference*, 48–51, Nov. 8–9, 2010.
3. Kim, K. Y., "Guided and leaky modes for circular open electromagnetic waveguides: Dielectric, plasma and metamaterial column," Ph.D. Thesis, Dec. 2004.

4. Berral, R. R., F. Mesa, and F. Medina, "Appropriate formulation of the characteristic equation for open non-reciprocal layered waveguides with afferent upper and lower half-spaces," *IEEE Trans. on Microwave Th. & Tech.*, Vol. 53, 1613–1623, May 2005.

Full Wave Maxwell's Equations Solver EMWSolver3D

A. P. Smirnov and A. N. Semenov
Lomonosov Moscow State University, Moscow, Russia

Abstract— In this work we are introducing 3-dimensional FDTD solver EMWSolver3D. Based on Maxwell equations approximation in integral form on Yee lattice, it provides numerical solution in time domain. EMWSolver3D supports multi-core single processors machines and provides hybrid MPI/OpenMP support for IBM BlueGene/P series. Large-scale electromagnetic and optical problems with size of the order of 400 wavelengths in every dimension for a problem with arbitrary complex geometry structure can be solved. The parallel implementation on MSU BlueGene/P supercomputer, based on asynchronous operations, provides good scalability factor for large problems. Solver supports Dirichlet and periodic boundary conditions on any boundary interface. Uniaxial perfect matched layer conditions also implemented in solver, so wide range of problems in unbounded region can be solved. Effective layer parameters obtained for a particular class of unbounded problems. Comparison of solutions for infinite layers and half-spaces of materials with different permittivity and permeability is shown. Numerical solution of point hard source problem verified with Hankel function analytical solution. For dispersive materials problems EMWSolver3D uses Drude model and can be used in modeling of metamaterials with specific parameters. The illustration of electric field component of plane wave impinging on left-handed material half-space with $\varepsilon = \mu = -1$ are shown. Numerical solution of metamaterial perfect lens problem with point source is provided.

FDTD Numerical Simulation of Waveguide with Non-uniform Dielectric Media

A. P. Smirnov[1], **A. N. Semenov**[1], **and Y. V. Shestopalov**[1, 2]

[1]Lomonosov Moscow State University, Moscow, Russia
[2]Karlstad University, Karlstad, Sweden

Abstract— We consider scattering in the time domain of electromagnetic waves from inhomogeneous dielectric inclusions in a 3D waveguide of rectangular cross section. All electromagnetic field components are calculated and transport of energy in the guide is investigated using Finite Difference Time Domain (FDTD) method in different frequency ranges. An efficient 3D FDTD *EMWSolver3D* solver for the nonstationary Maxwell equation system is used. The model computations are performed for the H_{10}-mode scattering from parallelepiped-shaped dielectric inclusions. Attenuation and propagation factors are calculated for the transmitted modes and field distribution are visualized. The present method can be used for a wide class of waveguide problems that meet substantial difficulties as far as numerical solution by conventional FDTD methods is concerned due to complex geometries or computational requirements. The solver employs algorithms of parallel computations and is implemented on supercomputers of last generation for solving large-scale problems with characteristic matrix dimensions achieving 10^{12}.

Fast Analysis of Multiscale Geometries with RWG Moment Method Accelerated via Barnes-Hut Algorithm for Helmholtz Kernel

K. Butt and V. Okhmatovski
Department of ECE, University of Manitoba, Winnipeg, MB R3T5V, Canada

Abstract— Boundary element electromagnetic analysis of multiscale models with Method of Moments (MoM) presents various challenges. Among those are the low-frequency break down of the electric field integral equation (EFIE), growth of the MoM impedance matrix condition number due to geometric oversampling, loss of efficiency in the fast algorithms for solution of matrix equations, and various others. In this work we demonstrate how electromagnetic analysis can be done efficiently for multiscale structures reaching one wavelength in size and nearly independently on the disparity of involved geometrical scales. To maintain $O(N \log N)$ computational complexity, N being the number of unknowns in MoM discretization of EFIE, we accelerate the RWG MoM solution of EFIE with the Barnes-Hut (BH) algorithm [1]. The latter was originated in astrophysics and utilized for simulation of star dynamics in galaxies. As such it is particularly suited for rapid solution of multiscale problems. The BH algorithm was initially proposed for $O(N \log N)$ solution of static N-body problems with Laplace kernel. We subsequently extended it to handle solution of electrically small N-body problem with Helmholtz kernel [2]. In the proposed method the latter is utilized for acceleration of Rao-Wilton-Glisson (RWG) MoM solution of EFIE. To eliminate the low-frequency instability of the EFIE and overcome its breakdown due to multiscale oversampling the MoM discretization is performed using loop-tree basis functions. The proposed simulation framework allows for handling multiscale MoM solutions featuring several million degrees of freedom N on conventional workstations. The method has been found to be particularly useful for the analysis of chip and package level interconnect layouts.

REFERENCES

1. Barnes, J. and P. Hut, *Nature*, Vol. 324, Dec. 1986.
2. Aronsson, J., et al., *IEEE AWPL*, Vol. 8, 425–428, 2009.

New Mathematical Model and Measurement Scheme of Electrical Tomography and Its Fast Resolution by General Ray Method

Alexandre Grebennikov
Facultad de Ciencias Físico Matemáticas, Benemérita Universidad Autónoma de Puebla
Av. San Claudio y Río verde, Ciudad Universitaria, CP 72570, Puebla, Pue., México

Abstract— Computer Tomography consists in the image reconstruction of an interior of a body using the measurements on its surface of characteristics of some external field. Very often this reconstruction can be posed mathematically as a coefficient inverse problem for a differential equation describing the distribution of the field in considered region. Coefficients are functions of the space variables and characterize properties of a media. Well known are X-rays, ultrasonic, radioisotopes, infrared and electrical impedance tomography. For example, X-rays tomography leads to the linear mathematical model and for its resolving can be used corresponding linear fast algorithms, but the know methods for the electrical impedance tomography imaging are non-linear, that leads to algorithms which require a large time of calculations on computer.

We propose here another approach for the mathematical modelling and the measurement scheme for the external data. We explain it for the plane case and describe adaptation for space case. We construct the mathematical model on the basis of General Ray Principle, proposed by the author for distribution of different, in particular electromagnetic, fields. Proposed model leads to the classic Radon transformation that appears as specific element in new General Ray Method, constructed and realized by the author as a simple linear fast numerical algorithm. This approach and algorithms are justified with the numerical experiments on the simulated model examples in MATLAB system.

Session 1P6a
Nano Scale Electromagnetics, MEMS 2

Effect on Transmissivity of Interaction between Subwavelength Slits

Huai-Yu Wang[1], **Fei-Fei Wei**[2], **and Yun-Song Zhou**[2]

[1]Department of Physics, Tsinghua University, China
[2]Department of Physics, Capital Normal University, China

Abstract— When light goes through a subwavelength multi-slit structure, there is inevitably interaction between slits that greatly influence the transmissivity of the structure. We have studied the effect of the interaction.

Our model structure is, in xz plane, that an ideal metal film extends infinitely along the x direction, with a thickness w in the z direction. There are N identical slits, each with width a, are arranged with equal spaced b along the x direction. The transmissivity with various structural parameters is calculated. When the light wavelength λ is fixed while the a varies, the transmissivity shows only one peak. Transmissivity oscillates with the spacing b, and the oscillation period is just λ. The maximum values of the peaks and minimum values of the valleys of the curve are denoted by $T_{\max}$ and $T_{\min}$, respectively, and they can be fitted by expressions $T_{\max} = T_{\max 0}e^{-b/\alpha_1} + c_1$ and $T_{\min} = T_{\min 0}e^{-b/\alpha_2} + c_2$. The parameters depend on structural parameters and λ. Especially, $T_{\max 0}$ increase and $T_{\min 0}$ decreases with N. $T_{\min 0}$ can even touch zero. As the slit number N increases, transmissivity varies in three manners depending on b value: oscillatorily increase, attenuate or basically unchanged.

The interaction between slits is reflected by the distribution of the magnetic fields of the light, or electric current, on the metal surface between adjacent two slits. The waveform can be well expressed by the formula

$$j = j_{10}e^{-(x+x_0)/a_1}\cos(q_1(x+x_0)+\varphi_1) + j_{20}e^{(x+x_0)/a_2}\cos(q_2(x+x_0)-\varphi_2),$$

where x_0 merely depends on the choice of the origin. The formula shows that the current is the superposition of two components, each starting at one slit corner and oscillatorily decaying toward the center between the slits. In the case that the two slits are arranged symmetrically, all the parameters in the two terms are the same. It is this cosine waveform of the current between slits that causes the transmissivity oscillation with the variation of spacing b. Of cause, when b becomes large, the transmissivity behavior of the multi-slit structure degrades to that of a single structure.

It is well-known that a single subwavelength slit is of extraordinary optical transmission. The interaction in a multi-slit structure can cause constructive or destructive interference, which may be of potential application in nano optical devices.

ACKNOWLEDGMENT

This work is supported by the National Nature Science Foundation of China (Grant No. 11074145) and (Grant No. 10874124).

Magnetodielectric Effect from the Onset of Ferrimagnetic Transition in $CoCr_2O_4$

Sen Yang and Xiaoping Song
MOE Key Laboratory for Nonequilibrium Synthesis and Modulation of Condensed Matter
Xi'an Jiaotong University, Xi'an 710049, China

Abstract— Multiferroics in $CoCr_2O_4$ is generally regarded to emerge from the onset of non-collinear spiral magnetic order ($T_s \approx 28\,\mathrm{K}$) due to the inverse Dzyaloshinskii-Moriya interaction, far below the temperature of collinear ferrimagnetic transition ($T_c \approx 96\,\mathrm{K}$). So far, the possibility of multiferroics appearing in collinear magnetic order has been rarely explored. In this letter, we report a magnetodielectric effect emerging from the onset of collinear ferrimagnetic transition T_c in $CoCr_2O_4$. Based on the postulation of non-centric crystal symmetry and Landau theory, we deduce that such a magnetodielectric effect was attributed to the coexistence of electric and magnetic order by the magnetoelectric coupling below T_c. Our results suggest that a magnetic insulator may be a natural multiferroics.

An Approach of Chain of Ellipsoid-rings to Magnetic Nanotubes

Sen Yang, **Xiaoping Song**, **Zhanbo Sun**, **Zhimao Yang**, **and Bingjun Ding**
MOE Key Laboratory for Nonequilibrium Synthesis and Modulation of Condensed Matter
Xi'an Jiaotong University, Xi'an 710049, China

Abstract— Numerical calculation of magnetic properties is a very effective way to understand the whole magnetic behavior of nanotubes. Currently, the most studies of calculation of magnetic properties of nanotubes are mainly grounded on the Stoner-Wohlfarth (S-W) model, starting from an elongated prolate ellipsoid with single-domain. But, it is hard to imagine how such an ellipsoid is arranged in the hollow tubular structure and hence the realization of predicted magnetic properties has been hindered by the experimental difficulties. Here, an alternative model of chain of ellipsoid-rings is proposed to calculate the magnetic properties of nanotubes, where the chain of rings with ellipsoid particles is assumed to compose nanotube. Based on this new model, we calculate the magnetic properties of nanotube and further discuss the influence of tubular geometric parameters on the magnetic properties. All the results are well consistent with the experimental data of Ni nanotube and moreover are available for the Ni nanowire. Consequently, our model provides an easy and general approach to both magnetic nanotubes and magnetic nanowires.

Silver Nanoparticles Assembly under an External Magnetic Field

Zhimao Yang, **Yunxia Zhang**, **Zhanbo Sun**, **Bingjun Ding**, **and Xiaoping Song**
MOE Key Laboratory for Nonequilibrium Synthesis and Modulation of Condensed Matter
Xi'an Jiaotong University, Xi'an 710049, China

Abstract— Shape control of silver crystals has received considerable attention due to their numerous applications including surface plasmonics, surface-enhanced Raman scattering (SERS), as well as chemical and biological sensing. Noticeably, the external magnetic field plays a significant role in the assembly of silver nanoparticles based on the previous references on morphology of silver crystals. Herein, we will reveal the silver nanostructures organized by silver nanoparticles through a replacement reaction assisted by an external magnetic field. In our study, we have explored the influences of the parameters (including applied magnetic field, reactant, growth time and concentration of $AgNO_3$ solution) on the growth of the silver nanostructures. The applied magnetic field played a critical role in the shape control of silver nanostructures. The present study might contribute to exploring the influences of external magnetic field on the shape control, growth mechanism and corresponding properties of the noble metal, and we expect that this external magnetic field mediated assembly approach would be used to design much more architectures with novel external morphologies and internal structures as well as potential applications.

Nanoring or Nano-elliptic-ring Shaped Magnetic Tunneling Junctions and Their Typical Applications in STT-MRAM Design

Xiu Feng Han
Institute of Physics, Chinese Academy of Sciences, Beijing 100190, China

Abstract— A series of nanoring (NR) or nano-elliptic-ring (NER)-shaped magnetic tunnel junctions (MTJs) with the diameter of 100 nm, or the major axis of around 120 nm and minor axis of around 60 nm, and ring width of around 25 nm was fabricated successfully. Magnetic field and current-driven magnetization switching were observed in such NR- or NER-MTJs with key stack layers of both spin-valve-type antiferromagnetic (AFM)/ferromagnetic (FM)/insulator (I)/ferromagnetic (FM) and sandwich-type hard-FM/I/soft-FM structures. For example, the sandwich-type NER-MTJ stack layer consists of Ta(5 nm)/Ru(30)/Ta(5)/ Co(2)CoFeB(1)/Al(0.7)-O/CoFeB(2.5)/Ta(5)/Ru(6). When the electric current density exceeds a critical value of the order of 7.8×10^6 A/cm^2 (critical driven current is 0.40 mA), the magnetization of the free (soft-FM) and reference (hard-FM) layer nano-elliptic-rings can be switched back and forth between parallel and antiparallel onion states. Tunneling magneto-resistance (TMR) ratio between 10% and 40% with different thickness of thin Al-O barrier were measured at room temperature as we apply a magnetic field or a pulsed current. The experiments and micromagnetic analysis show that the spin transfer torque (STT) plays a main switching role in the magnetization reversal and the pulse-current-induced elliptic magnetic field play an assisted-switching role in such NER-MTJs. Compared with the NR-shaped MTJ and Nanoring MRAM [1–3], the NER-MTJ has a relative symmetric current driven critical behavior, which is due to the shape anisotropy of elliptic-ring architecture. The NER-MTJ also show the comparative lower switching field or critical current value (or density) and can be as the memery bit cells. Therefore, the manipulation of anisotropy in NER-shaped MTJs open a new way to develop more reliable and easier operational NER-MRAM devices.

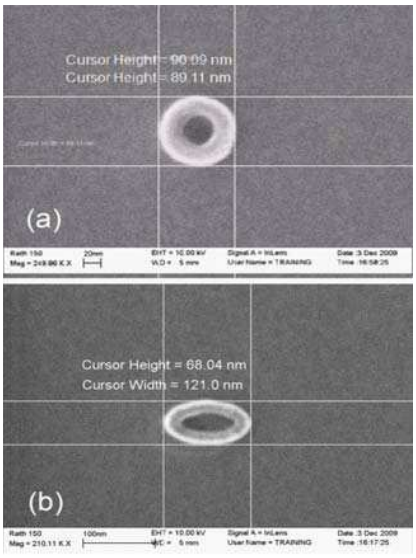

Figure 1: The SEM images of a single patterned NR-MTJ and NER-MTJ. The images are taken from the array. Fig. 1(a) is a typical NR-MTJ with outer diameter of about 90 nm, and ring width of 30 nm; Fig. 1(b) is a typical NER-MTJs with major outer diameter of about 120 nm, and the minor outer diameter of about 70 nm. The ring width is designed at 30 nm.

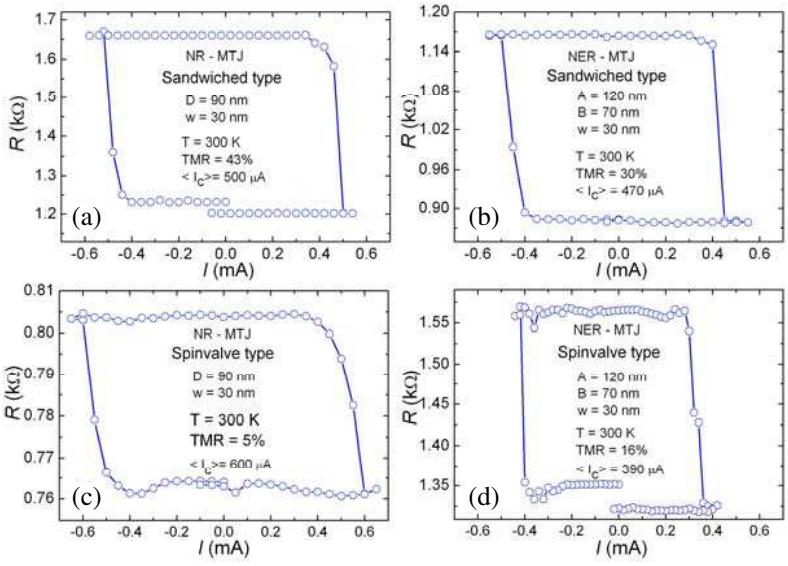

Figure 2: Tunneling resistance (R) as a function of pulsed current (I) at room temperature (Current switching loop). Fig. 2(a) is a typical R-I loop of a Sandwiched-Type NR-MTJ. The outer diameter of NR-MTJ is designed at $D = 90$ nm and $W = 30$ nm. Fig. 2(b) shows a typical R-I loop of a Sandwiched-Type NER-MTJ with a major outer diameter of $A = 120$ nm, minor outer diameter of $B = 70$ nm, and the ring width of $W = 30$ nm. Figs. 2(c) and (d) are typical R-I loops of Spin-Valve-Type NR-MTJ and NER-MTJ under the same designed values as described in (a) and (b), respectively.

REFERENCES

1. Han, X. F., Z. C. Wen, and H. X. Wei, "Nanoring MTJ and its application in MRAM demo devices with spin-polarized current switching," *J. Appl. Phys.*, Vol. 103, 07E933, 2008.
2. Wei, H. X., X. F. Han, S. Zhang, et al., "Effects of the current on the nanoscale ring-shaped magnetic tunnel junctions," *Phys. Rev. B*, Vol. 77, 134432, 2008.
3. Han, X. F., Z. C. Wen, et al., "Nano-elliptic-ring shaped MTJ and its application in MRAM design with spin-polarized current switching," *IEEE Trans. Magn.*, Vol. 47, 2957, 2011.

Possible Ferromagnetism in Li, Na and K-doped AlN: A First-principles Study

Ruilin Han and Yu Yan
Department of Physics, Jilin University, China

Abstract— AlN is one of the promising host semiconductors in the field of spintronics, and it has been reported that nonmagnetic Si, Sc and Cu doped AlN are ferromagnetic above room temperature. Therefore, it is desirable to investigate effect of nonmagnetic alkali dopants on the magnetic properties of alkali doped AlN materials. We investigate the magnetic properties of Li, Na and K doped AlN by using first-principles calculations within the generalized gradient approximation. The calculations show that the substitutional doping by an alkali atom X (X = Li, Na and K) introduce some holes in localized $2p$ orbitals of the N atoms and the introduced holes are confined to the minority-spin states at the top of the valence band. The magnetic moment induced by a doping atom X is 2.0 μB and the moment mainly comes from the $2p$ orbitals of the N atoms, among which the moment of the four first neighboring N atoms around the doping atom are the biggest. The magnetic coupling between magnetic moments induced by two doping atoms X is found to be FM even if the distance between two doping atoms is large. The calculated DOS and the spin density distribution show that the p-p interaction between the $2p$ states of the N atom is responsible for the longrange FM coupling between the magnetic moments induced by doping. Our results indicate that Li, Na and K doped AlN are likely to be p-type half-metallic FM semiconductor.

Session 1P7a
Extended/Unconventional Electromagnetic Theory, EHD(Electro-hydrodynamics)/EMHD(Electro-magneto-hydrodynamics), and Electro-biology 2

Noise Influence of Magnetic Field to Conductivity Image Reconstruction

T. Kříž
Department of Theoretical and Experimental Electrical Engineering
Brno University of Technology, Kolejní 4, Brno 612 00, Czech Republic

Abstract— The paper presents a conductivity calculation from values of the magnetic flux density measured outside the specimen. There is described the analysis of the noise influence that is presented in the measured values of a magnetic field. A conductivity calculation is based on the electrical impedance tomography (EIT) algorithm. The standard EIT exploited measured voltage values on electrodes placed at specimen boundaries to a conductivity calculation. The direct current source or the low frequency current source is connected to a specimen. A conductivity calculation is based on a minimizing of a suitable objective function. The least squares method is very often used for a minimization of an objective function. The Tikhonov regularization method is used in order to ensure the stability of an algorithm. The stability and the accuracy are dependent on an accuracy of measured voltage values.

Values of a magnetic flux density were calculated outside a specimen by Biot-Savart's law. The noise with different levels or an offset is added to a calculated magnetic field data.

Results of the described reconstruction based on a magnetic field evaluation with an added noise or offset will be compared with results obtained without the noise in the article. The analysis of a stability will be presented also together with a solution time and an accuracy of calculated conductivity values.

Electric and Magnetic Components of Waves on the Interface

R. Kadlec, **E. Kroutilová**, **and P. Fiala**
Department of Theoretical and Experimental Electrical Engineering
Brno University of Technology, Kolejní 2906/4, Brno 612 00, Czech Republic

Abstract— The paper presents an analytic solution of propagation, reflection and refraction of broadband electromagnetic signals on field of multilayer optical materials in Matlab program, which is suitable for specific purposes of detail analysis of a general issue.

Generally, the inhomogeneities and regions with different parameters appear even in the cleanest materials. During the electromagnetic wave passage through a material there occur an amplitude decrease and the wave phase shift, owing to the material characteristics such as conductivity, permittivity, or permeability. If a wave impinges on an inhomogeneity, a change of its propagation there occurs. This change materializes in two forms, namely the reflection and refraction. In addition to this process, polarization and interference may appear in the waves. The paper includes a theoretical analysis and references to the generated algorithms, which are verified using numerical models. Numerical models are applied to facilitate the calculation process, and a wide range of programs like ANSYS, Comsol.

The paper deals with the problem of complex angle of refraction in the losing medium. Methods describe in this paper are suitable for the analysis of beam refraction to the other side from the perpendicular line during the passage through the interface. This phenomenon is occur in metamaterials.

ACKNOWLEDGMENT

The research described in the paper was financially supported by the research program of Ministry of Industry and Trade of the CR (Diagnostics of Superfast Objects for Safety Testing, FR-TI1/368), Czech Science Foundation (102/09/0314), project of the BUT Grant Agency FEKT-S-11-5/1012 and project Operational Programme Education for Competitiveness CZ.1.07.2.3.00.20.0175.

REFERENCES

1. Dedek, L. and J. Dedková, *Elektromagnetismus*, 2, 232, VITIUM, Brno, 2000, ISBN 80-214-1548-7.
2. Nešpor, D., *Electromagnetic Wave Propagation Study in Heterogeneous Structures*, 20, Supervisor Doc. Ing. Pavel Fiala, Ph.D., 2009.
3. Orfanidis, S., *Electromagnetic Waves and Antennas*, 1031, 2008, Available from WWW: www.ece.rutgers.edu/∼orfanidi/ewa.

Measurement of Electric Potential on Biological Objects

Z. Szabó, E. Kroutilová, and M. Janiček
Department of Theoretical and Experimental Electrical Engineering
Brno University of Technology, Kolejni 2906/4, Brno 612 00, Czech Republic

Abstract— The measurement of electric potential in plants falls within the class of interdisciplinary subjects often referred to as electrophysiology of plants. At present, the measurement of electrical processes in humans and animals constitutes a comparatively well-established activity with multiple practical applications; in this context, electrical signals in plants have been measured for approximately two hundred years. These signals embody the result of plants' incessant need to obtain information related to their environment. Changes within the environment induce various types of biological reaction; furthermore, plants synchronize their normal biological functions according to the response of the environment. Thus, they react to any variation in conditions such as the intensity of lighting, water availability, osmotic pressure, temperature, and respond to aspects including mechanical stimulation, injury, chemical compounds like herbicides and salts, or even the action of other organisms. Plants regulate not only stressful situations, but also the process of photosynthesis. In order to facilitate quick response to the stimuli mentioned, they have developed a mechanism similar to the neural system of animals. This mechanism is located inside phloem, and even though its structure does not possess the complexity of the system found in animals, it enables long-distance signal transmission via a channel of relatively low impedance [2]. The aim of this work is to report on the author's attempt at measuring these electrical signals on plants.

ACKNOWLEDGMENT

The research described in the paper was financially supported by grant of Czech ministry of industry and trade No. FR-TI1/368, project of the BUT Grant Agency FEKT-S-11-5/1012 and projekt CZ.1.07.2.3.00.20.0175, Elektro-vyzkumník.

REFERENCES

1. Avies, E., "Electric signals in plants: Facts and hypotheses," *Plant Electrophysiology Theory and Methods*, A. G. Volkov, Ed., Springer Berlin Heidelberg, New York, 2006.
2. Fromm, J., "Long-distance electrical signaling and physiological functions in higher plants," *Plant Electrophysiology Theory and Methods*, A. G. Volkov, Ed., Springer Berlin Heidelberg, New York, 2006.

Mixed Signal Processing for Cable Diagnostics

M. Hadinec
Department of Theoretical and Experimental Electrical Engineering
Brno University of Technology, Kolejní 2906/4, Brno 612 00, Czech Republic

Abstract— The analysis of failures on cable is very actual theme. Aging of cables is important problem for manufactures of cars, planes and power distribution systems. This topic is highly desired in many industry branches, where aging of cable insulation is serious problem, especially in point of view of reliability. It is also common problem in telephone cables, where it is important to locate water failures or just to find topology of network. There are many reflectometry methods for locating of open or short circuits at the end of wire, but it is very complicated to detect small anomalies caused by water or other aging of wire isolation. This article describes principles of present frequency domain reflectometry (FDR) methods and time domain reflectometry (TDR) methods, which are compared, advantages or disadvantages are discussed. Experimental part of the article deals with locating of cable failures using TDR techniques, which are compared to the PSpice simulations. Simulations in PSpice are based on model using RLCG parameters. The small anomalies are then implemented into the measured cable and studied with FDR method. The experiment is based on mixed signal reflectometry method, where measured DC voltage is extracted from the sum of incident and reflected sine waves. The advantage of this method is low demands for measuring circuit hardware, but it has quite high demands for post-processing of results. The measuring is automated by HP VEE software, obtained values are processed with FFT in Matlab. The detection of anomalies and accuracy of MSR method is discussed.

REFERENCES

1. Furse, C., C. C. You, R. Dangol, M. Nielsen, G. Mabey, and R. Woodward, "Frequency-domain reflectometry for on-board testing of aging aircraft wiring," *IEEE Transactions on Electromagnetic Compatibility*, Vol. 45, No. 2, 306–315, May 2003.
2. Shi, Q., U. Troeltzsch, and O. Kanoun, "Detection and localization of cable faults by time and frequency domain measurements," *2010 7th International Multi-conference on Systems Signals and Devices (SSD)*, 1–6, Jun. 27–30, 2010.

Session 1P8a
The Electrodynamics of Inhomogeneous Media and Gradient Metamaterials 1

Negative Refraction, Light Pressure and Attraction, Equation $E = mc^2$, and Wave-particle Dualism

V. G. Veselago
A. M. Prokhorov Institute of General Physics, Moscow, Russia

Abstract— The process of mass transfer from the emitter to the receiver is considered for different connection between energy and momentum. Shown, in particular, that in the case when the energy is transferred by radiation, this relationship has the form $E = mv_{ph}v_{gr}$, where v_{ph}-phase velocity, and v_{gr}-group velocity.

From this equation immediately shows that in media with negative refraction radiation transfers the mass not from the transmitter to receiver, but rather from the receiver to the transmitter.

In addition, from the above conclusion follows, that the mass transferred from the transmitter to the receiver is determined not only by transferred energy, but also by transferred linear momentum, which may be associated with energy in different ways. Thus, the well-known relation $E = mc^2$ is a special case of relation $E = mv_{ph}v_{gr.}$

It is shown that the relation $E = mc^2$ corresponds to the transfer of energy from the transmitter to the receiver in the form of a moving material particle, and the relation $E = mv_{ph}v_{gr}$ corresponds to the transfer of energy in the form of electromagnetic waves. The first case can be described by the Abraham tensor, and the second case — with the help of the Minkowski tensor.

Light Scattering from Nanostructured Media

Gerard Berginc
Thales Optronique, France

Abstract— In this paper, we present some considerations concerning the field of nanophotonics. The light scattering from random surface structures, controlled random surface structures is discussed. The consequences of the nanostructure of thin films on their optical properties are also described. This last problem is described by random volume and surface scattering. Useful phenomena in the optical range can be produced by random media with randomly rough surfaces. Designing these disordered slabs with rough surfaces can produce new optical components, which can transmit or scatter optical field with specified angular, spatial or spectral properties.

New formulations have been developed for a three-dimensional disordered medium with randomly rough interfaces [1–4]. This structure can describe a device based on metallic nano-particles embedded in insulators or dielectric media. We present a theory of transport based on the Bethe-Salpeter equation. For a three-dimensional system composed of a random medium bounded by two randomly rough surfaces, the Bethe-Salpeter equation is constructed in order that the medium and the boundaries are treated on the same footing. With this unified Bethe-Salpeter equation, a general expression is obtained, whatever the choice of the scattering operators used at the boundaries. The calculation of the intensities scattered by the considered structure for the ladder and most-crossed contributions is given by a Green tensor. Diagrammatic expansions are very useful for investigation of mesoscopic effects. These calculations were performed with the Mueller matrices taking into account the different polarization components.

For 3-dimensional slabs with nanoscale roughness and nano-particles, the enhanced backscattering is produced by different mechanisms, the wave scattering by the same boundary, the wave coupling by the two boundaries or the wave scattering by the nano-particles. The different simulation computation can give some experimental conditions and specifications to realize highly integrated optical devices that use metallic or metallo-dielectric nanoscale structures.

REFERENCES

1. Soubret, A. and G. Berginc, "Electromagnetic wave scattering from a random layer with rough interfaces. II: Diffusive intensity," arXiv:physics/0312136, 2003.
2. Berginc, G. and C. Bourrely, "Electromagnetic wave scattering from a random layer with rough interfaces. I: Multiple scattering theory," *Progress In Electromagnetics Research Symposium Abstracts*, Cambridge, USA, Jul. 2–6, 2008.
3. Berginc, G. and C. Bourrely, "Electromagnetic wave scattering from a random layer with rough interfaces. II: Numerical experiments," *Progress In Electromagnetics Research Symposium Abstracts*, Cambridge, USA, Jul. 2–6, 2008.
4. Berginc, G. and C. Bourrely, "Light scattering from 3-D nanoscale disordered media," *PIERS Online*, Vol. 6, No. 8, 730–734, 2010.

Bose Einstein Condensation (BEC) of Photons in the Infrared (IR)

F. T. Arecchi[1, 2]

[1]Università di Firenze, Italy
[2]INO-CNR.-Largo E. Fermi-6, Firenze 50125, Italy

Abstract— BEC is a thermal equilibrium phenomenon whereby bosons at different energies collapse into the lowest energy state, provided the DeBroglie thermal length λ_T, that scales with the inverse square root of m (mass of bosons) and T (temperature) be larger than the particle separation.

It has been implemented in dilute gases of alkali atoms at sub-micro Kelvin temperatures so that [1]

$$\lambda_T = 0.1\,\mu\text{m}.$$

A photon BEC in the visible has been recently realized [2] with the following recipe:

i)- a micro cavity fed by an excited dye is filled with photons in many transverse modes k_i satellites of a single longitudinal mode k_0; this requires a *FSR* (free spectral range) larger than the dye linewidth; indeed the cavity length is 1.58 µm;
ii)- a scattering mechanism at room temperature T_{room} (provided by the same dye molecules) induces a mode-mode transfer with probablities p_i that scale as the occupation numbers n_i, thus favouring the lowest energy mode k_0

$$p_0/p_i = n_0/n_i > 1$$

iii)- the *FSR* is not only wider than the dye width, so that a single longitudinal mode is excited, but also wider than the thermal spread (in frequency units, $6 \times 10^{12}\,\text{s}^{-1}$) so that no other longitudinal modes can be thermally reached; as a result, the mode frequency acts as a cut-off in the ω-k dispersion relation, yielding a photon mass 10^{-5} the electronic mass; it results

$$\lambda_T = 1.6\,\mu\text{m}.$$

We have implemented a photon BEC at $\lambda = 10\,\mu$m as follows:

i)- a large Fresnel number ($F = 10$) CO_2 laser ($FSR = 200\,\text{MHz} > linewidth = 7\,\text{MHz}$) provides about $F^2 \approx 100$ transverse modes within a single longitudinal mode);
ii)- a room temperature scatterer would have a frequency spread $\gg FSR$; we rather replace it with an AOD (acousto-optical deflector) with a bandwidth 680 kHz $\ll FSR$, so that a single longitudinal mode plays a role;
iii)- scaling photon mass and temperature, we have

$$\lambda_T = 10^4\,\mu\text{m} = 1\,\text{cm}.$$

In order to have an average photon separation less than λ_T, we adequately focuse the beam at the AOD location, thus observing BEC.

REFERENCES

1. For this discovery, Eric Cornell, Carl Wieman, and Wolfgang Ketterle shared the 2001 Nobel prize in physics.
2. Klaers, J., J. Schmitt, F. Vewinger, and M. Weitz, *Nature*, Vol. 468, 545–548, 2010.

Technological Aspects of Obtaining Gradient Optical Metamaterial

O. D. Volpian[1], **A. I. Kuzmichev**[2], **and Yu. A. Obod**[3]

[1]Federal State Unitary Enterprise "M. F. Stelmakh Research Institute — Polyus"
Vvedensky Str. 3, Moscow 117342, Russian Federation
[2]Electron Device Department, National Technical University "Kiev Polytechnical Institute"
Pobedy Pr. 37, KPI-2230, Kiev 03056, Ukraine
[3]Scientific-Manufacturing Enterprise "Fotron-Auto Ltd."
Novodanilovskaya Naberezhnaya 8, Moscow 117105, Russian Federation

Abstract— Optical thin film coatings are the important element of photonic apparatus and need sophisticated approaches for their producing. Traditionally, an optical coating design is based on multilayer systems of alternating high n_h and low n_l refraction indexes and presents an interference system of a kind. Certain functional possibilities are given by another type of interference systems based on gradient coatings (e.g., rugate filters), where the refraction index $n(z)$ is gradually, sometimes sinuously, varied across the coating thickness. Note, the thickness of layers in the interference systems is order of wavelength λ. On the contrary, there is an interest in optical gradient coatings, as a new metamaterial or metacoating, with total thickness of $n(z)$ variation less than λ. Such coatings are factually a nanogradient metamaterial. The technology of obtaining the nanogradient optical coatings is not developed yet. Thus, we present the deposition process and characteristics of such nanogradient metamaterials based on thin dielectric layer(s) for future use in laser technique.

For obtaining the variable $n(z)$, dielectric compounds (oxides, nitrides, oxynitrides, fluorides, sulfides, etc.) may be deposited or co-deposited in PVD or CVD processes in reactive gas medium. We consider the best approach is use of the reactive pulse magnetron sputtering (RPMS) because this method, providing energy activation of the condensation process, ensures obtaining dense condensate with low surface roughness and light scattering loss. Besides, this kind of magnetron sputtering meets the case of target arc prevention processes in reactive gas medium, deposition process stability, coating thickness uniformity, stability of deposited coatings against light radiation, environment and mechanics factors. That is RPMS may ensure optical coatings of high quality. Earlier, this method was used for obtaining interference gradient multilayer systems.

A multicathode/target magnetron system with computer control and monitoring *in situ* has been developed, manufactured and employed for obtaining 1D-3D gradient multi-wave antireflection coatings. Variation of $n(z)$ was received by parametric regulation of the combined deposition of different sputtered target materials (e.g., Si and Ti) in reactive gas mixture (Ar + O_2). Reflection spectra of the nanogradient metamaterials were measured and numerically calculated with use of specially adopted PC software. The practical reflection spectra of the manufactured nanogradient coatings were close to the calculated ones. The advantage of these coatings is that their physical thickness is less than the thickness of multilayer interference coatings with similar spectral characteristics. Testing the coatings showed they were stable against light laser radiation, environment and mechanics factors due to low optical loss, small thickness and high dense of the deposited material.

Obtained results demonstrate that the precisely controlled RPMS method of dielectric material deposition is a very perspective one for manufacturing high quality gradient and nanogradient metamaterials for use in optics and photonics.

Transillumination of Gradient Barriers for Modulated Electromagnetic Wave in the Inhomogeneous Plasmas. The Exact Solution

N. S. Erokhin[1], **E. S. Merkulov**[2], **and M. V. Poverenyi**[2]

[1]Space Research Institute of RAS, Moscow, Russia
[2]I.A. Bunin Elets State University, Elets, Russia

Abstract— It is considered the exact solutions of linear Helmholtz equation descibing the effective transillumination of plasma gradient wave barriers for the incident electromagnetic wave. It is shownt that the inhomogeneous plasma layer may includes both the wide enough wave opaque structures and sublayers with strong wave amplitude splashes. Moreover under the suitable choice of incoming parameters the dielectric permettivity in plasma layers may has also small variations in the contrast to large modulations of wave amplitude. It is shown that plasma layer may contains the arbitrary number of sublayers with different parameters for each one including the sublayer thickness, the characteristics of effective dielectric function variations. The effective transillumination of inhomogeneous plasma structures for incident electromagnetic waves is very important for such applications as dense plasma heating by the powerful electromagnetic radiation, the understanding of the mechanisms for escape of radiation from sources in a high density astrophysical plasma, to prepare the efficient of antireflecting and absorbing coatings in radiophysics and so on. In the reflectionless wave passage problem, it is of large interest to seek an optimum spatial profile of the dielectric function that allows a minimum coefficient of reflection and/or an efficient transmission of electromagnetic signals from antennas with a high density plasma layer on their surface. It should be noted that the exactly solvable models considered must demonstrate fundamentally new features of the wave dynamics and propagation in inhomogeneous media and can also demonstrate various interesting practical applications when the medium parameters are varying significantly. The results obtained may be applied both to the magnetoactive plasmas and chiral one.

Formation of the Bidomain Structure in Lithium Niobate Single Crystals

A. S. Bykov, **R. N. Zhukov**, **D. A. Kiselev**, **M. D. Malinkovich**, **and Yu. N. Parkhomenko**
National University of Science and Technology "MISiS"
Leninskiy pr. 4, Moscow 119049, Russian Federation

Abstract— Possibility control the topology and location of the domain boundaries opens perspectives for fabrication of wide spectra the different devices based on a transformation of electrical energy into mechanical deformation because the active piezoelectric element creates as a bimorph structure with volume modulated piezoelectric coefficients. In particular plates of the optical lithium niobate single crystals with formed bidomain structure can be used to light flux control.

Bidomain single crystal elements in compare with piezoelectric ceramics have such advantages as the lack of hysteresis, creep, fatigue and high Curie temperature.

In present work two methods of oxygen-octahedral piezoelecrics direct poling on lithium niobate single crystals as an example were developed. First is based on applying of non-uniform electric field at Curie temperature, second on a gradient of the light annealing.

In the first case the crystal after cooling from Curie temperature with poling potential application represents structure that consist of two equal-volume domains but with opposite polarization directions, i.e., bidomain structure forms. The system of the electrode form that, inside of the sample vectors intensity of an electric field have been directed opposite, and the plane the zero potential passed approximately in the middle of the sample on thickness.

Formation bidomain structures in $LiNbO_3$ single crystals based by pulse heating on creation in a plate gradient of temperature, which, in turn creates the gradient of diffusion causing moving of atom of lithium in neighbouring oxygen octahedron.

The distribution of temperature on thickness sample calculated in conditions uniform and asymmetric light streams, optimum parameters of formation bidomain structures are determine. The parameters of the interdomain boundaries investigate by scanning probe microscopy techniques.

Session 1P9
Poster Session 1

Measurers' Exposure to Extremely Low Frequency Magnetic Fields at 400 kV Substations

L. Korpinen[1], **H. Kuisti**[2], **H. Tarao**[1, 3], **and R. Pääkkönen**[4]

[1]Environmental Health, Tampere University of Technology, Finland
[2]Fingrid Oyj, Helsinki, Finland
[3]Department of Electrical and Computer Engineering
Kagawa National College of Technology, Japan
[4]Finnish Institute of Occupational Health, Tampere, Finland

Abstract— In earlier studies we have presented a range of measurement results, drawn from the occupational exposure to extremely low frequency (ELF) electric fields at 400 kV substations and under 400 kV power lines. Occupational magnetic field (MF) exposure has been only briefly studied at 400 kV substations. The aim of this work was to present a measurers' personal MF exposure at 400 kV substations. Measurements were obtained using small, portable Radians Innova ML-1 (accuracy ±10%) MF loggers (at the wrist). Measuring ranges were 0.01–100 μT (Meter1) and 0.1–1000 μT (Meter2), with a measurement interval of 10 seconds. Measurements were taken over 16 working days, of which 15 had two measurers and the remaining day only one. The maximum values obtained varied from 6.2 μT to 481 μT (average 2.0 μT to 67.9 μT). At five substations, the Meter1 (measuring range 0.01–100 μT) could not measured, because the values exceeded the maximum value of the meter used. In those substations, Meter2 measured the follow maximum values: (1) substation2; max 481 μT, (2) substation3; max 357 μT, (3) substation5; max 299 μT, (4) substation7; max 290 μT and (5) substation8; max 300 μT. During those days when the magnetic flux densities were measured around reactors, the measured values were higher than at other times of exposure. On these occasions, the largest MF exposure averaged close to 70 μT. In conclusion, whilst the average magnetic field exposure was between 10 μT–50 μT, both the maximum and average values do not exceed the proposed EC directive (2011/0152) MF exposure levels.

The Possible Exposure of Children to Extremely Low Frequency Magnetic Fields in the Home

F. Gobba[1], **R. Pääkkönen**[2], **H. Tarao**[3, 4], **and L. Korpinen**[3]

[1]Department of Public Health Sciences, University of Modena and Reggio Emilia, Italy
[2]Finnish Institute of Occupational Health, Tampere, Finland
[3]Environmental Health, Tampere University of Technology, Finland
[4]Department of Electrical and Computer Engineering
Kagawa National College of Technology, Japan

Abstract— Extremely low frequency electric fields are considered as suspected carcinogens (Group 2B IARC), based on consistent epidemiological data on childhood leukemia, although the biological evidence is considered weak. An increase in risk was observed at exposure levels exceeding 0.4 microT. This paper aims to analyze common exposure situations to children in the home, to determine possibly relevant sources. Part of the data presented here derives from measurements performed in projects in Finland and Italy. Additionally, we measured exposure from some new devices (e.g., laptops etc). In the home, the important sources of children's exposure are electrical systems and devices. In a detached house, exposure was measured at 0.1 μT. In apartments, the max exposure was usually > 0.4 μT (8 apartments), but in those located above the indoor distribution point, the average (max) exposure reached 6.5 μT. In the kitchen, the MF levels measured 0.3–0.5 μT and 2.5–4.2 μT respectively in front of the oven and microwave oven. All data was derived from spot measurements obtained using instantaneous RMS meters. In Italy, the median TWA exposure measured using personal meters in 513 homes was 0.03 μT, and levels were below 0.4 μT in 97% of the homes sampled. These levels are most likely representative of the exposures of children living in the same house. In the final paper we will present more measurement data from childrens exposure situations, e.g., exposure to devices.

Electrical Impedance of Plasma Filled Waveguides in the MHz Range

D. Melazzi[1], **D. Curreli**[2], **M. Manente**[1], **and D. Pavarin**[1]

[1]CISAS "G. Colombo" Centro Interdipartimentale Studi Attività Spaziali
University of Padova, Italy
[2]Deptartment of Nuclear, Plasma and Radiological Engineering
University of Illinois Urbana Champaign, USA

Abstract— The Maxwell wave Equations have been numerically solved for the case of a cylindrical plasma-filled waveguide with perfectly conductive walls. The calculations have been done using the SPIREs code, which solves the electromagnetic propagation in frequency domain along the radius of the waveguide by means of a mixed spatial-spectral method (1D-space along radius, spectral domain along azimuthal and axial directions). The waveguide contains a column of plasma, magnetized along the axis of the cylinder, and an antenna, comprised in the gap between the plasma and the conducting wall. The antenna forces an oscillating current at radio-frequency in the Megahertz range. The electromagnetic response of the plasma is described by the Stix dielectric tensor plus the Fried-Conte Z dispersion function for finite-temperature Maxwellian effects. From the numerical solutions of the fields, the electrical impedance of the waveguides has been derived, and showed for a wide range of plasma parameters and waveguide radial sizes. The plasma density ranges from 10^{17} to 10^{21} particles/m^3, the magnetic field is below $B < 0.1$ Tesla, the frequencies are 13.56 and 27.12 (MHz), and the plasma cylinders have radius < 5 cm. The electrical resistance per unit length of the plasma is reported for each case. For a given geometry, the trends allow to find the maximum load conditions, corresponding to the maximum power coupling between the antenna and the plasma load. The results are relevant for many applications, ranging from the electrical design of the plasma-wave coupling in actual plasma devices, to the optimization of the RF plasma sources commonly used in industry. The method can also be proficiently applied to the design of high efficiency plasma sources used on board of spacecrafts for RF plasma thrusters.

Equilibrium Conditions of Radiofrequency-heated Plasma Cylinders

D. Curreli[1], **D. Melazzi**[2], **M. Manente**[2], **and D. Pavarin**[2]

[1]Department of Nuclear, Plasma and Radiological Engineering
University of Illinois Urbana Champaign, USA
[2]CISAS "G. Colombo" Centro Interdipartimentale Studi Attività Spaziali
University of Padova, Italy

Abstract— The equilibrium conditions of radiofrequency heated plasma cylinders have been calculated by solving the two coupled problems of the electromagnetic power deposition and the macroscopic transport of charged and neutral species. The two Maxwell wave equations have been finite-differenced along the radius of the cylinder (SPIREs code), providing the input source terms for the transport problem. The continuity and momentum equations of a single-ionized cold plasma, together with energy conservation, have been solved along the same radial direction (EQM code). An iterative procedure has been used between the two problems in order to evaluate the profiles at equilibrium. The method allows the prediction of the profiles of plasma density, electron temperature and neutral density in RF heated plasma cylinders. Calculations have been done for typical conditions encountered in low-pressure helicon discharges, where the plasma is magnetized with an external field directed along the axis of the cylinder. The plasma density profiles are peaked at the center, even if most of the RF deposition occurs at the edge of the discharge. The increase of plasma density with the RF power has been calculated for a direct comparison with Langmuir probe measurements in helicon experiments. The electron temperature remains constant with the increasing power, but increases at the edge of the cylinder where the RF wave is strongly dumped via the Trivelpiece-Gould mode. Neutrals are depleted at the center of the discharge, where the plasma density reaches its maximum.

The Labyrinth Structure in the Synthesis of Fractal Antennas

A. A. Potapov and V. I. Grachev
Kotel'nikov Institute of Radio Engineering and Electronics, Russian Academy of Sciences, Russia

Abstract— Theory and practice of application of fractal and of the scaling properties of the genetic and self-affine synthesis of antennas allows you to control the radiation pattern (RP) today modern arrays [1, 2]. Random fractal arrays are synthesized by introducing equidistant sub lattices in random lattices, which allows you to vary the energy of the side lobes RP. Compactness of the distribution of frequency bands is best realized in the tree fractal antennas. Fractal graphs reflect the rich spectral structure with many resonant frequencies and coordinated over the entire frequency range. In the design of large and very large tree-like fractal arrays are often self-intersections occur vibrators, imposing certain RP and the emergence of virtual RP and false zeros, which in general have a negative effect on the performance of fractal radiating structures. Labyrinth fractals are a tree, pathways which can be described by way matrices [3]. On the basis of the theorems proved in [3], the authors of this report proposed to use the features of the labyrinth fractal structures obtained by iterative procedures in the synthesis of multi-element fractal arrays. Research of a more general problems, such as the subdiffusion and superdiffusion in disordered media [1, 4, 5], may also use developed in this report approaches.

REFERENCES

1. Potapov, A. A., *Fractals in Radio Physics and Radar: Topology of Sample*, 2nd Issue Ed. and Correct, 848, University Library, 2005.
2. Potapov, A. A. and V. A. Chernykh, *Fractional Calculation of A. V. Letnikov in the Fractal Physics*, 688, LAMBERT Academic Publishing, Saarbrücken, 2012.
3. Cristea, L. L. and B. Steinsky, "Curves of infinite length in 4×4-labyrinth fractals," *Geom. Dedicata*, Vol. 141, 1–17, 2009.
4. Metzler, R. and J. Klafter, "The random Walk's guide to anomalous diffusion: A fractional dynamics approach," *Phys. Rep.*, Vol. 339, 1–77, 2000.
5. Potapov, A. A. and V. I. Grachev, "Fractal labyrinths," *RENSIT*, Vol. 3, No. 2, 90, 2011.

LogicView: An Open Source Software for 3D Visualization of Models and Fields in Electromagnetics

A. O. Rodrigues[1], **J. J. Viana**[2], **and J. A. Ramirez**[1]

[1]Universidade Federal de Minas Gerais, Belo Horizonte, Minas Gerais, Brazil
[2]Independent Consultant, Logic Style, Belo Horizonte, Minas Gerais, Brazil

Abstract— The visualization of the results in three dimensional (3D) electromagnetic problems, which may involve the distribution of vector field quantities, is not well exploited and still poses some challenges. Existing softwares for the visualization of scientific data are either expensive or offers only a small set of features. We present LogicView, an open source software available under a public domain license which offers several tools and useful features for the visualization of scientific data, physical model and fields, in particular in electromagnetics. LogicView was developed in Java, allowing its use in multiple plataforms (Windows, Unix or Mac). It allows 3D visualization of any set of data presented in a matrix of values. It can, therefore, be used to visualize physical models, such as human head models, and field quantities, such as electromagnetic field distributions, the specific absorption rate (SAR) distribution and temperature distribution hot spots. The paper describes the software architecture and the computing platform. It explains in a step by step example how LogicView reads any set of values. It also presents usages of LogicView through 3D visualization of two open source models of the human body: the Zubal phantoms and the John3Doe phantom, and the visualization of electromagnetic fields generated by mobile telephones in the human head. It also shows the tools available in the software such as the zoom, rotate, plane cut, materials and snapshot used for physical models, and the colour scale and value used to visualize fields.

Nonautonomous Spatiotemporal Localized Structures

Chao-Qing Dai[1, 2] **and Jie-Fang Zhang**[2, 3]

[1]School of Sciences, Zhejiang Agriculture and Forestry University, Lin'an, Zhejiang 311300, China
[2]School of Physical Science and Technology, Soochow University, Suzhou, Jiangsu 215006, China
[3]Zhejiang University of Media and Communications, Hangzhou 310018, China

Abstract— We develop a systematic way to find the similarity transformation and investigate nonautonomous optical similariton dynamics for $(n+1)$-dimensional nonlinear Schrödinger equation in the inhomogeneous optical fibers. A condition between the parameters of the mediums, which hints a exact balance between the dispersion/diffraction, nonlinearity and the gain/loss, has been obtained. Under this condition, self-similar bright and dark solitons with and without background waves, and rogue waves (rogons) are analytically constructed. Their novel propagation dynamics in the dispersion-decreasing fibers can be investigated. The major conclusions are as follows:

- We can trap the velocity of each similariton to control the interaction between two- similaritons by proper dispersion management. Moreover, the spectral parameters η_k and ξ_k control separating or interacting evolutional behavior of similaritons with the suitable initial separation.
- The similaritons interaction on the background waves can be control by choosing appropriately form parameters θ and λ.
- One can dominate the travelling velocity of the dark similariton across the cnoidal wave by choosing suitable form parameters p, w and modulus m.
- The snake propagation traces and the interaction of optical nonautonomous rogons are exhibited by choosing some free functions of distance. These solutions modify the known solutions related to the optical rogons.

The results obtained in this paper may have potential values for all-optical data-processing schemes and the design of pulse compressors and amplifiers. Our results also indicate that a new higher dimensional similariton control technique might be developed. Of course, due to the lack of experimental and designed basis related to these theoretical results, we could not give further details about the real physical application. We hope that our results will be very useful to initiate the experimental verification.

REFERENCES

1. Dai, C. Q., X. G. Wang, and J. F. Zhang, "Nonautonomous spatiotemporal localized structures in the inhomogeneous optical fibers: Interaction and control," *Annals of Physics*, Vol. 326, 645–656, 2011.
2. Dai, C. Q., Y. Y. Wang, and J. F. Zhang, "Analytical spatiotemporal localizations for the generalized (3+1)-dimensional nonlinear Schrödinger equation," *Optical Letters*, Vol. 35, 1437–1439, 2010.

A Method to Model a Spindle System with an Electromagnetic Actuator

Jong Hyun Kim, **Gyu Ha Kim**, **and Sun-Kyu Lee**
School of Mechatronics, Gwangju Institute of Science and Technology
Oryong-dong, Buk-gu, Gwangju 500-712, Republic of Korea

Abstract— The goal of this research is to model a spindle system with an electromagnetic actuator. This model will be applied to a spindle run-out control. The spindle system is consisted of ball bearing units and four electromagnetic actuators. The electromagnetic actuator is used to compensate the run-out error of the spindle in this system. A bondgraph modeling method is used to model the spindle system including the electromagnetic forces. The dynamic mechanical model of the spindle system is represented and the dynamic equations are specified based on the model. In bearing units, bidirectional bearing compliance expresses the fact that a certain load on a spindle does not only induce compliance in the load direction but also induce relatively small compliance in the orthogonal direction due to the bearing structure. The electromagnetic forces are acted at the end of the shaft and considered as the external load on the shaft. The bondgraph model of the spindle system considered all the relations between electrical systems and mechanical systems. Therefore it respected that it is easy to model the spindle system using the bondgraph modeling method and apply the model to the spindle control.

Changes of Specific Heat of Water Arising from a Magnetic-field

Xiao-Feng Pang and Bo Tang
Institute of Life Science and Technology
University of Electronic Science and Technology of China, Chengdu, Sichuan 610054, China

Abstract— We measured the specific heat of magnetized water using the heat capacity measured instruments with a calorimeter made by China. In the experiment the dc power device, electronic balance, delicate electronic-watch, temperature sensor and two digital multimeters are used, where the dc power device provides a steady dc current and voltage to heat the magnetized mater in the calorimeter, the sizes of the dc current and voltage are measured by the digital multimeter, the weight of magnetized water is determined by the electronic balance, the temperature sensor is inserted into the magnetized water in the calorimeter to measure its temperaturethe delicate electronic-watch is used to record the times heating the magnetized water. The magnetized waters are extracted from the beater with 800 mL purified water exposed in the statically magnetic-field of 4400 G about magnetizing time of 30 minutes. The purified water we use here is prepared using the Simplicity 185 Water System (Millipore) made by USA. We measured properties of purified water and the elementary elements contained in it using the instruments including the mass and color spectrometers at 25°C. Its pH value is 7.1–7.2, electric resistivity is about 1 MΩ·cm, absorption ratio of light (254 nm, 1 cm light path) is ≤ 0.01; Ca, Si, Na, K, nitrate, oxide (or O) and soluble silicon (i.e., SiO_2) involved in the purified water are 0.01 mg/L, 0.005 mg/L, 0.007 mg/L, 0.002 mg/L, 1 mg/L, ≤ 0.08 mg/L and ≤ 0.02 mg/L, respectively.

In the experiment, we first inject 502 g magnetized water and insert the temperature sensor into the calorimeter to determine the initial temperature T_1 of the magnetized water. When the electric power is switched on the electric electrodes of the calorimeter, we used immediately the delicate electronic-watch to record the time heating the magnetized water in the calorimeter, while the digital multimeter is also used to measure the sizes of the electric current I and voltage V as well as the sensor is used to inspect the changes of temperature of magnetized water.

After certain heated times, such as $t = 356.4$ seconds (S), which is early set, we switch off the electric power, meanwhile we record immediately the final temperature of heated magnetized water, T_2. Using the above data recorded in this experiment and according to the following formula: $(MC + z)(T_2 - T_1) = 0.24\,\mathrm{IVt}$, we can find the specific heat of the magnetized water, C, which is obtained from $C = (1/M)[0.24\,\mathrm{IVt}/(T_2 - T_1) - z]$, where M is the mass of heated magnetized water, z is a parameter related to the feature of the calorimeter, we here can determine $z = 254.87\,\mathrm{J/°C} = 60.88\,\mathrm{Cal/°C}$. In this experiment, we repeat many times to measure each datum and result up to they are all same for acquiring an accurate and credible result. In the meanwhile, we measured also the specific heat of purified water using the above method in this case. The results of measurement of magnetized and purified water are obtained simultaneously from the above equations. The former is obtained from flowing water of 472 g which flows over a cylinder magnet with the diameter of 1.5 cm about 10 minutes in the speed of 1 cm/s, where the strength of magnetic-field of the cylinder magnet at center is 4400 G. The latter is obtained from static water of 502 g exposed in a magnetic-field of 4400 G about 30 minutes.

We conclude from Table 1 that the specific heat of magnetized water is small than that of pure water, but the specific heat of statically magnetized water is larger than that of dynamically magnetized water. This is a new and interesting result. Owing to the feature magnetized water has a wide application in industry and daily life.

Variations of Surface Tension Force of Water Resulting from Magnetic-field

Xiao-Feng Pang and Bo Deng
Institute of Life Science and Technology
University of Electronic Science and Technology of China, Chengdu, Sichuan 610054, China

Abstract— We measure also the variation of surface tension force or the soaking degree of magnetized water on a planar surface of material. This effect is signed in the size of angle of contact of water on a planar surface of materials (Joshi and Kamat, 1965). In this experiment, we measure the angle of contact of magnetized and pure water on a planar surface of copper, graphite, muscovite and silica gel of PDMS183 in the region of 0°–180° and in the condition of humidity of 27° by using OCA40 and OCA20 Micro optical-vision instrument with the accuracy of ±0.3° made by Germany, respectively, where the magnetized water is taken from a beaker of 250 ml of pure water at 25°C, which is exposed in the magnetic-field of 4400 G for 30 minutes. In this measurement, the water injected is about 3 μL, the speed of water injected is about 0.5 μL/s. As are known, the muscovite is hydrophilic, but copper, graphite and silica gel of PDMS183 have different hydrophobicities. We measure first the sizes of angle of contact of magnetized and pure water at five different positions on the planar surface of these materials, respectively, finally find the average value of five different values for the angle of contact of magnetized and pure water, respectively. The experimental results of the copper, graphite, muscovite and silica gel of PDMS183 are obtained, respectively. From the four figures we see that the angles of contact of magnetized and pure water on the muscovite are almost zero, the difference between them is extremely small. Therefore, the soaking degree of pure and magnetized water to the muscovite are very large. However, for the copper, the angles of contact of magnetized and pure water are about 146.8° and 147.2°, respectively; for the graphite, they are about 91.2° and 92.6°, respectively; for the silica gel of PDMS183, they are about 97.9° and 101.03°, respectively. Therefore the angles of contact of magnetized water on the surfaces of hydrophobic materials are decreased relative to that of pure water, the extenuation quantities of the angles of contact are about 0.4°, 1.4° and 3.13° for the copper, graphite and silica gel of PDM S183, respectively, i.e., for the silica gel of PDMS183, the extenuation of the angles of contact of magnetized water is extremely evident. This means that the soaking degree of magnetized water to the hydrophobic materials increases relative to that of pure water, thus its hydrophobicity decreases. This shows that the magnetic-field changes the hydrophobicity of water. This is a quite useful and valuable result, which has well foreground of application in industry, agriculture and medicine. Obviously, the extenuation of angles of contact of magnetized water is due to the increases of polarized effect and the changes of distribution of molecules in water under action of the magnetic-field. Thus we conclude the surface tension force of magnetized water does decrease relative to that of pure water.

On the Maxwell Stress Tensor and Electromagnetic Wave Momentum in Continuous Medium

A. V. Kondratov and M. V. Gorkunov
A. V. Shubnikov Institute of Crystallography, Russian Academy of Sciences, Moscow 119333, Russia

Abstract— The momentum of electromagnetic (EM) wave in continuous medium has been intensively discussed since more than a century, and the debates on the issue are still ongoing (see e.g., [1–3]). Eventually, alternative expressions for the EM-wave momentum in addition to the classical Abraham and Minkowski forms [4] appear in the literature, and the modern view is best expressed by the statement: "*the preferred form is therefore effectively a matter of personal choice*" [2]. In our work we show that although there is indeed a substantial degree of freedom in defining the light momentum and spatial distribution of light pressure, there exists a unique possibility of very natural and self-consistent description of the related elementary physical phenomena.

We demonstrate that starting from the well established form of the EM-stress tensor in continuous medium:

$$T_{ij} = \frac{1}{4\pi}\left[E_i D_j + H_i B_j - \frac{\delta_{ij}}{2}\left(\mathbf{E}\cdot\mathbf{D} + \mathbf{H}\cdot\mathbf{B}\right)\right]$$

and calculating the forces acting on the medium as $F_i = \partial T_{ij}/\partial x_j$ one can successfully describe the momentum balance both in conventional (ε, $\mu > 0$) and left-handed (ε, $\mu < 0$) medium during such processes as:

- reflection/transmission by a semi-infinite medium or slab
- weak EM-wave absorption inside isotropic medium
- nonlinear second-harmonic generation

We show that the chosen approach effectively assigns the momentum $\hbar\mathbf{k}$ to each quant $\hbar\omega$ of the EM energy.

We also discuss disadvantages of alternative approaches and, in particular, show that postulating the macroscopic Lorentz force as $\mathbf{F}_L = \rho\mathbf{E} + [\mathbf{j}\times\mathbf{B}]/c$ [2, 5] leads to questionable consequences, such as momentum exchange in presence of non-interacting EM-waves, virtual light pressure during nonlinear frequency conversion, etc..

ACKNOWLEDGMENT

The work has been supported by the Program of BPS RAS "Physics of new materials and structures".

REFERENCES

1. Barnett, S. M., *Phys. Rev. Lett.*, Vol. 104, 070401, 2010.
2. Pfeifer, R. N. C., T. A. Nieminen, N. R. Heckenberg, and H. Rubinsztein-Dunlop, *Rev. of Mod. Phys.*, Vol. 79, 1197, 2007.
3. Barnett, S. M. and R. Loudon, *Phil. Trans. Royal Soc. A Math. Phys. and Eng. Sc.*, Vol. 368, 927, 2010.
4. Ginzburg, V. L., *Sov. Phys. Usp.*, Vol. 16, 434, 1973.
5. Gordon, J. P., *Phys. Rev. A*, Vol. 8, 14, 1973.

A Direct Experimental Inspection of Displacement Currents

Zi-Hua Weng[1], **Jing-Yan He**[1], **Jin-Pan Zhu**[1], **and Ying Weng**[2]

[1]School of Physics and Mechanical & Electrical Engineering
Xiamen University, Xiamen 361005, China
[2]College of Chemistry & Chemical Engineering, Xiamen University, Xiamen 361005, China

Abstract— J. C. Maxwell was first to mix two methods, the quaternion and the vector terminology, to describe the electromagnetic features. The quaternion is divided into the scalar part and the vectorial part. And the latter was evolved into the conventional 3-dimensional vector. Up to the present, the electromagnetic theory described by the vector is quite successful, and it seems to hint at that it may be feasible to accept the quaternion and the octonion to represent the electromagnetic features. Unfortunately it is not successful to adopt the quaternion directly to depict electromagnetic features.

The octonion is decomposed into the quaternion and the S-quaternion. The S-quaternion can be used to describe the electromagnetic equations, and that the equations are capable of transforming into the Maxwell's equations in the 3-dimensional vector space equivalently. The electromagnetic equations described with the S-quaternion are the same as Maxwell's equations in the classical electromagnetic theory, except for the orientation of the displacement current.

H. R. Hertz discovered firstly the electromagnetic waves, thereby confirmed indirectly the conceptual validity of the displacement currents. Subsequently other scholars repeated and modified the Hertz's experiment, but none of them verified directly the orientation of displacement currents. Along with the recent development of measurement technologies, the scholars originate to scrutinize directly the accuracy of displacement currents.

During the recent years, some scholars are making an attempt at verifying directly the amplitude of magnetic effects induced by the displacement current. They brought forward one experimental proposal of the parallel-plate capacitor. On the basis of some scholars' studying, the paper brings forward and fulfills one experimental proposal with the phase measurement method. The experiment is capable of inspecting directly the orientation of displacement currents, by means of measuring the amplitude and the phase value of the induced electromotive force which produced from the magnetic effect of displacement currents.

ACKNOWLEDGMENT

The authors are grateful for the financial support from the National Natural Science Foundation of China under grant number 60677039.

Static Magnetic Fields Increase Endotoxin Tolerance of Microglia Cells

Che-Tong Lin[1], **Po-Chieh Yang**[2], **Hsin-Yua Tsai**[1], **Kuo-Ning Ho**[1], **Yuh-Yuan Shiau**[3, 4], **Wei Fang Lee**[5], **and Haw-Ming Huang**[2]

[1]School of Dentistry, Taipei Medical University, Taipei, Taiwan
[2]Graduate Institute of Biomedical Materials and Tissue Engineering
Taipei Medical University, Taipei, Taiwan
[3]School of Dentistry, National Taiwan University, Taipei, Taiwan
[4]School of Dentistry, China Medical University, Taichung, Taiwan
[5]School of Dental Technology, Taipei Medical University, Taipei, Taiwan

Abstract— To prevent brain-damage and neurodegeneration caused by inflammation, down-expression of the lipopolysaccharide (LPS)-induced inflammatory cytokines was reported to be a new aspect. To obtain this goal, increase of endotoxin tolerance was reported to be an anti-infection treatment. However, the dosage and action site of low-dose LPS injection in brain tissue are hard to control. The aim of this study was to test the hypothesis whether static magnetic field (SMF) can be a stimulation source for inducing endotoxin tolerance of mocroglia cells in brain tissue. In this study, the effects of SMF exposure on growth rate and cytokines expression of LPS-challenged BV-2 microglia cells were monitored. Our results showed that SMF pre-exposure significantly increased IL-6 expression of BV-2 cell ($p < 0.05$) and resulted in a significant reduction ($p < 0.05$) of cytotoxicity in LPS treated cells. According to these results, it is reasonable to suggest that SMF has potential to be an alternative simulation source for inducing endotoxin tolerance in brain tissue.

Influence of Static Magnetic Fields on Cytotoxicity of Natural Killer Cells

Yung-Kai Huang[1], **Yi-Tsai Su**[2], **Sheng-Wei Feng**[3], **Ya-Hui Chan**[3], **Kan-Shin Fan**[4], **Horng-Mo Lee**[5] **and Haw-Ming Huang**[2]

[1]School of Oral Hygiene, Taipei Medical University, Taipei, Taiwan
[2]Graduate Institute of Biomedical Materials and Tissue Engineering
Taipei Medical University, Taipei, Taiwan
[3]School of Dentistry, Taipei Medical University, Taipei, Taiwan
[4]Dental Department, En-Chu-Kong Hospital, Taipei, Taiwan
[5]The Graduate Institute of Pharmaceutical Science and Technology
Central Taiwan University of Science and Technology, Taiwan

Abstract— Natural killer (NK) lymphocytes are population representing the 10–20% of PBMC. Since the cells can lyse MHC class I — negative tumor and virus-infected cells, they play important role in the innate immunity. NK cells express surface receptors that can be classified as inhibitory and activatory. The mechanism of the cytotoxicity of NK cells is via activating a set of triggering receptors. It has been reported that, static magnetic fields (SMF) has strong effects on the cell viability and can alternate the rigidity of cellular membrane which may result in the conformation change of cross membrane receptors. Accordingly this study aimed to test the possible biological effects of NK cells exposed to a SMF. In this study, NK-92M1 cell line were used as tested subject. The cells were cultured with a 0.8 T SMF. Then the proliferation rate, ultra morphology, membrane fluidity and cytotoxicity of the SMF-exposed NK cells were evaluated. Our results indicated that 0.8 T SMF exposure has positive effects on the proliferation rate of the NK-92M1cell. In addition, the cytotoxicity of the SMF-exposed NK cells was significantly higher ($p < 0.05$) than the sham-exposed cells at effector to target (E : T) ratio of 10 : 1 and 1 : 1. These results demonstrated that SMF has positive effects on the cytotoxicity of the natural killer (NK) lymphocytes.

The Influence of Static Magnetic Field on Growth of Dental Pulp Stem Cells

Haw-Ming Huang[1], **Sheng-Yang Lee**[2], **Shu-Hui Yang**[3], **Chien-Wu Yeh**[4], **Shu-Li Lin**[4], **Chii Jeng**[5], **and Kuo-Ning Ho**[2]

[1]Graduate Institute of Biomedical Materials and Engineering
Taipei Medical University, Taipei, Taiwan
[2]School of Dentistry, Taipei Medical University, Taipei, Taiwan
[3]Graduate Institute of Biomedical Materials and Tissue Engineering
Taipei Medical University, Taipei, Taiwan
[4]Dental Department, Cathay General Hospital, Taipei Taiwan
[5]Graduate Institute of Nursing, Taipei Medical University, Taipei, Taiwan

Abstract— Several studies have indicated that postnatal stem cells are present in bone marrow, neural tissue, skin, retina, and dental pulp. Among these cells, dental pulp stem cells (DPSC) exhibit capacities for differentiation into various cells and development into diverse tissue. These self-renewal capabilities also make DPSCs become an effective material for regenerative medicine. Since human dental pulp stem cells have been reported to be useful material for tissue engineering, How to increase the proliferation and/or differentiation of DPSCs in vitro become an issue future regenerative medicine. In this study, DPSCs were isolated from human teeth and then exposed to a 0.4 T static magnetic field (SMF). The growth curves, morphology, stem cell specific markers, and the multi-lineage differentiation of DPSCs exposed to SMF were evaluated and compared to the sham-exposed controls. Our results show that dental pulp stem cells exposed to 0.4-T SMF exhibited a significant increase in fluorescence anisotropy at 4 hrs, then significant increase in the viability and proliferation rates at 72 hrs. However there were no visible differences between the two groups of DPSCs in morphology, expression of stem-cell markers, or multi-lineage differentiation. The results suggest that SMF affect proliferation rate of dental pulp stem cells without reducing the capability of multi-lineage differentiation.

Static Magnetic Field Exposure Has Positive Effects on Mechanical and Histological Properties of Cryopreserved Human Dental Pulp

Sheng-Yang Lee[1], **Yen-Chuang Lin**[1], **Shu-Li Lin**[2], **Chii Jeng**[3], **and Haw-Ming Huang**[4]

[1]School of Dentistry, Taipei Medical University, Taipei, Taiwan
[2]Dental Department, Cathay General Hospital, Taipei Taiwan
[3]Graduate Institute of Nursing, Taipei Medical University, Taipei, Taiwan
[4]Graduate Institute of Biomedical Materials and Tissue Engineering
Taipei Medical University, Taipei, Taiwan

Abstract— The aim of this study was to investigate whether storage of extracted teeth in static magnetic field (SMF)-coupled program freezer for 24 hours has a positive effect on the cell density and mechanical properties of thawed pulp tissue extracted from intact teeth. For the methodology, the tested teeth were divided into two experimental groups: teeth that had been frozen in a magnetic program freezer (PF, $n = 5$) and in a traditional freezer at $-20°$C (TF, $n = 5$). The tested teeth were then stored at $-150°$C for 7 days. After thawing, the extracted pulp was subjected to histological examination and mechanical testing. Our results showed that freezing with static magnetic field had significant positive effects on the histological and mechanical properties of pulp tissue extracted from cryopreserved intact teeth. The elastic modulus of pulp from teeth that had been frozen at $-20°$C with SMF exposure was significantly higher ($p < 0.05$) in samples that had been stored for 24 hour without SMF exposure. This study demonstrated that exposure to SMF for 24 hours during freezing storage in a program freezer has positive affect on extracted pulp cell density or the elastic modulus of pulp tissue.

Remote Diagnostics of Inhomogeneities with Enhanced Resolution

M. V. Tinin and S. I. Knizhin
Irkutsk State University, Gagarin blvd. 20, Irkutsk 664003, Russia

Abstract— Measurements of linear integrals (i.e., integrals of inhomogeneous medium parameters along the straight line) play an important role in studying inhomogeneous media by wave techniques. In computed tomography of ionospheric plasma, in particular, phase advance along the path from the source to the observer is measured. In the geometrical optics (GO) approximation, this phase shift at high frequencies is equal to the linear integral of electron density of ionospheric plasma. The use of the GO approximation in diagnosing inhomogeneous media is impeded by the diffraction limit of the resolution and by the multipathing which takes place when signal propagates in inhomogeneous medium. These problems can be solved by the spatial signal processing which has been proposed earlier and which is based on the inverse double weighted Fourier transform (DWFT). This optimum spatial signal processing for inhomogeneous medium is often hindered by the necessity to perform the double Fourier transform in the receiving and radiating planes. The paper deals with the DWFT modification that allows us to enhance spatial resolution when diagnosing inhomogeneous media with the use of the signal processing in a single plane. For this purpose, we consider the problem of wave propagation in inhomogeneous medium when inhomogeneities are in the layer at relatively large distances from the source and observer. In this case, the uniform asymptotic approximation which has previously been obtained with DWFT, with change of variables in the integral representation of the field, and with the method of stationary phase, reduces to a single weighted Fourier transform. The approximation obtained and the back propagation technique are shown to be in good agreement. When the thickness of the layer tends to zero, the expression obtained is reduced to the phase screen approximation. Conditions of validity of the phasescreen model and criteria for choosing location of this screen are determined. Also presented here are the results of numerical modeling of the proposed approach when diagnosing inhomogeneous medium with enhanced spatial resolution.

Analysis of the Forbidden Regions for Multilayer Planar Waveguide with LHM

Yaw-Dong Wu[1], **Ming-Shiung Cheng**[1], **Shih-Yuan Chen**[2], **and Tien-Tsorng Shih**[1]

[1]Department of Electronic Engineering
National Kaohsiung University of Applied Sciences, Kaohsiung, Taiwan, R.O.C.
[2]Department of Electric Engineering
National Sun Yat-Sen University, Kaohsiung, Taiwan, R.O.C.

Abstract— In recent years, the planar waveguides with Left-Handed Medium (LHM) have been widely studied and proposed. A feature of the LHM has both the permittivity ε and permeability μ less than zero. There always exist two forbidden regions for guided modes in the three-layer planar waveguide with LHM guiding layer. Most of the multilayer planar waveguides with the LHM films were supposed to have an enough width of the interaction layer and the same forbidden region as the three-layer planar waveguide with LHM film to discuss optical modes. The forbidden region was not reported previously to the multilayer planar waveguide with the narrow interaction layer. In this study, the modal theory and the boundary condition were used to analyze the forbidden region of the five-layer planar waveguide with LHM film in the narrow interaction layer. The numerical results show that the forbidden regions are separated and differ from the three-layer planar waveguide with LHM film. The variation of the forbidden region depends on the narrow width of the interaction layer and the ratio value of the permeability of the guiding layer and the interaction layer. We also show a phenomenon that the forbidden region and the dispersion cure of the effective refraction in five-layer planar waveguide with LHM film are almost similar to that of the three-layer planar waveguide with LHM film when the width of the interaction layer is wide enough. The simulation results would be very useful for designing waveguide devices with the LHM films.

On the Geometric Representations of Electromagnetism

S. L. Vesely[1] and A. A. Vesely[2]

[1]I.T.B. — C.N.R., Italy
[2]Via L. Anelli 13, Milano, Italy

Abstract— Nowadays receivers allow to process more elaborated electromagnetic signals than data points taken one at a time, and to visualize frequencies well beyond the visible range. Well-defined graphical accounts can be considered measurements, and to ask how classic electromagnetism explains them is the same as wondering how to visualize the collected signals. A coherent geometric model can provide the rationale whereby a graphical presentation can be said to be well defined. The concept of geometry used to be bound to the "external world" more tightly than that, in the 19th century. In order to interpret his findings on electricity and magnetism, M. Faraday attributed to those phenomena the ability to exert forces as well as to propagate. Force and motion were understood in the framework of mechanics. Three dimensional geometrical representations of classical mechanics were difficult because the positions of mass points and the forces acting on them cannot be easily depicted in the same figure, unless one resorts to virtual displacements. Therefore, those representations were split into a geometry of forces, one of motions, and a relationship between them. Two significant approaches toward pure geometries can be traced back to (i) A. Möbius who extended plane graphical statics to space, and (ii) H. Grassmann who introduced vector spaces. Although Maxwell's theory was developed at a time when geometry aimed at suiting mechanics, both developments (i) and (ii) are formally independent of it, and lend themselves to interpretations and applications of electromagnetism not related with forces and displacements. F. Klein, in the spirit of the Erlangen program and in the scope of Einstein's relativity, showed that Maxwell's equations in vacuum can be interpreted geometrically as transformations of a projective space of lines onto itself; the linear complex of lines that is invariant under those transformations was named a *null-system* by Möbius. On the other hand, Heaviside's formulation as well as more recent physical theories utilized the n-dimension analytical mechanics of Lagrange and Hamilton, developed after Grassmann's linear algebra, the geometric traits of which were formalized by Hilbert.

A different aspect of electromagnetism, born to be visual, arises from its relationship with optics. Graphical constructions of light fronts propagation stem from Huygens' principle, and were adapted to the transverse wave model by Fresnel. This introduces (iii) the envelops of spherical waves associated with wave fronts as further way of drawing. (iii) is not rooted in statics, thence neither the invariant forms nor the relationship between forces and motions are the same as those found in (i) and (ii). The energy associated with propagation was investigated by Poynting, Kirchhoff and others. The approach developed by Hamilton and Hadamard does not separate time domain from frequency domain, while the Fourier transform between t and ω, dualizes the corresponding spaces. In Einstein's special relativity the form-invariance of electromagnetic laws relies on representations of static origin (i), while the invariance of c agrees with (iii). Trying to conciliate the geometric foundations of space-time, F. Klein encouraged E. Noether to investigate the relationship between the equations of motion and the action integral, and F. Bessel-Hagen to apply her results to the invariance under conformal inversion. The latter transformation is at the core of both the Huygens principle and the Smith chart construction. The analysis developed by F. Bolinder [1] shows how linear networks transfer functions can be represented by conformal mappings in general.

In most cases, the geometry upon which received signals can be interpreted does not seem to be justifiable based on "external world" properties, but rather belongs to how incoming radiation is actually detected. In particular, the conformal inversion that Klein tried to interpret in a relativistic sense can interpret space-temporal transmissions as registered by electronic devices. These considerations may inspire geometric models expedient to electromagnetism, alternative to analyses based on wave propagation or Fermat's principle.

REFERENCES

1. Bolinder, E. F., "Microwave theory," *RLE QPR*, Vol. 44, No. XXI, 149–154, 1957.

A Radar-based Technique for Anomaly Detection in Biomedical Diagnostic Applications

S. Caorsi and M. Stasolla
Department of Electronics, University of Pavia, Pavia, Italy

Abstract— High false-negative/positive rates, employment of ionizing radiation, uncomfortable breast compression represent some of the major limitations of conventional X-ray mammography [1]. Although it remains the most effective and well-established tool for breast cancer detection, there is a demanding need of technological improvements, and new screening non-invasive techniques are currently under investigation. Recent efforts have been focused on the development of probing equipments that operate within the frequency range of the microwaves, whose principal advantage is the significant contrast in the dielectric properties of normal and malignant breast tissue [2].

In this work, an inverse scattering approach based on artificial neural networks is presented, that exploits microwave imaging to reveal in a (semi-)automatic way possible dielectric anomalies and therefore assist radiologists with breast cancer screening.

The approach is stratified. First, the e.m. signals acquired by a multi-source illumination system, composed of an array of antennas in monostatic configuration, are pre-processed to determine the presence and position of dielectric contrasts. Then, if anomalies have been revealed, a suitable set of features extracted from the corresponding backscattered signals are fed into a Multi-Layer Perceptron [3], a feed forward artificial neural network capable of finding a regression model that relates the e.m. data to the desired output, i.e., the permittivity of the anomaly. Depending on the obtained values, it is possible to establish whether or not that anomaly can be ascribed to breast cancer.

The performance assessment of the method has been carried out within a large set of clinical scenarios, simulated by means of a FDTD software [4]. Numerical results have confirmed its potentialities, showing that the presence of dielectric anomalies can be provided with good accuracy.

REFERENCES

1. Nass, S. J., I. Craig Henderson, and J. C. Lashof, *Mammography and Beyond: Developing Technologies for the Early Detection of Breast Cancer*, The National Academies Press, 2001.
2. Bond, E., X. Li, S. Hagness, and B. Van Veen, "Microwave imaging via space-time beamforming for early detection of breast cancer," *IEEE Transactions on Antennas and Propagation*, Vol. 51, No. 8, 1690–1705, Aug. 2003.
3. Haykin, S., *Neural Networks: A Comprehensive Foundation*, 2nd Ed., Prentice Hall, Jul. 1998.
4. Giannopoulos, A., "Modelling ground penetrating radar by GprMax," *Construction Building Mater.*, Vol. 19, No. 10, 755–762, Dec. 2005.

Study on the Human Effect of a Wireless Power Transfer Device at Low Frequency

Ji-Yeon Mun[1], **Min-Gyeong Seo**[1], **Woo-Geun Kang**[2], **Hae-Young Jun**[3], **Yong-Ho Park**[3], **and Jeong-Ki Pack**[1]

[1]Department of Radio Science and Engineering
Chungnam National University, Daejeon, Korea
[2]Electromagnetic Environment Research Center, Korea
[3]DMC R&D Center, SAMSUNG Electronics, Korea

Abstract— In this paper, we analyzed the human effect of a wireless power transfer (WPT) device operating at 6.78 MHz. A commercial simulator, XFDTD Ver. 7.2 based on the finite discrete time domain (FDTD) method, was applied to the analysis of the specific absorption rate (SAR) and the induced electric field inside of the Korean human model and a flat phantoms. The human model used is a numerical phantom developed by Electronics and Telecommunications Research Institute (ETRI) and the size of the flat phantom modelis based on the human model's bust. The simulation results were compared with the ICNIRP 2010 Guideline. The SAR values averaged over 1-g and 10-g were maximum in the groin of the human model, and the maximum SAR values at 5 cm distance were 3.41×10^{-3} W/kg (1-g averaged SAR) and 1.92×10^{-3} W/kg (10-g averaged SAR) for 1 W input power. The maximum allowed input power compared to the SAR limit is about 470 W. The calculated value of the maximum induced electric field was 11.1 V/m at the same position, and it is far below the exposure limit of 915.3 V/m. So, the SAR value is the limiting factor of the human exposure of the WPT device. The results for the flat phantom were about a half of the human model. Since the nominal input power of the WPT device is below 10 W, it can be concluded that the exposure level of the device is well within the exposure limit of the ICNIRP 2010 guideline.

Design of Novel Artificial Magnetic Conductor as Reflector and Its SAR Analysis

S. Lee[1], **N. Kim**[1], **and S.-Y. Rhee**[2]

[1]Chungbuk National University, South Korea
[2]Chonnam National University, South Korea

Abstract— Novel artificial magnetic conductor is designed and measured as reflectors to reduce the specific absorption rate (SAR). We designed a transformed symmetrical mushroom-like surface without via holes in cells. Each slot in the structure plays a key role in modeling at the desired frequencies. The structure of the unit cell is focused on the wireless local network band (2.4 GHz). The antenna on the artificial magnetic conductor's reflector is working within a quarter-wavelength. For simulated and measured results, reflection coefficients show similar patterns between the artificial magnetic conductor's reflector close to the antenna and the perfect electric conductor's reflector separated a quarter-wavelength from the antenna. The designed reflector has broad bandwidth, small size, and is easy to fabricate because the proposed structure has no via holes. The human effect is analyzed with applying the designed reflector. The calculated peak SAR averaged over 1 g is only 0.002 W/kg, when the input power is 1 W. For analyzing more serious status, if the input power is injected 12.8 W, which shows the maximum reference level of 1.6 W/kg, the calculated peak SAR is only 0.0078 kg. In conclusion, the designed reflector should be blocked the electromagnetic waves to the human body.

A Broadband Active Integrated Microstrip Antenna Array Design in Millimeter Wave Frequency Band

Mohammad Mahdi Honari, **Abdolali Abdipour**, **and Gholamreza Moradi**
Microwave/Millimeter Wave and Wireless Communication Research Lab
Department of Electrical Engineering, Amirkabir University of Technology
Tehran 15914, Iran

Abstract— In this paper, a broadband active integrated antenna array in millimeter-wave frequency band is presented. For the direct integration, the output matching network is omitted so microstrip antenna array operates as an output matching network of the power amplifier and radiator. Optimum load impedance of the power amplifier is obtained by load-pull analysis and the antenna array is designed for the optimum load of power amplifier. The power amplifier and antenna array are designed to operate in wide bandwidth. The simulated results of the power amplifier confirm circuit operation. The analysis of power amplifier is done by ADS simulator. The output power of the amplifier is obtained almost 20 dBm for optimized load by load-pull analysis. In design of the antenna array, it is employed aperture-coupled antenna due to its wide bandwidth and isolation with the power amplifier by the ground. Here, a new antenna array is designed to operate as load of the amplifier. The structure of the antenna array consists of a 3-dB 180°-phase shifter, two 1-port's and two 2-port's aperture-coupled microstrip antennas. The antenna array works based on the back coupling to the microstrip line of 2-port aperture-coupled antenna. The simulations of antenna array are done with a frequency domain simulator (HFSS) and a time domain simulator (CST) to be sure about the results. The simulated input impedance, radiation pattern, side-lobe level, and cross-polarization are suitable within impedance bandwidth of the power amplifier of 25 to 31 GHz.

Three-dimensional Finite Element Modelling of Current Density in Maternal Transthoracic Defibrillation

A. Jeremic[1], **J. Pots**[2], **and E. Khosroshahli**[3]

[1]Department of Electrical and Computer Engineering, McMaster University, Hamilton, ON, Canada
[2]Department of Medicine, McMaster University Hospital, Hamilton, ON, Canada
[3]Department of Biomedical Engineering, McMaster University, Hamilton, ON, Canada

Abstract— Although resuscitation during pregnancy is relatively uncommon and rarely cause deaths they have a particularly large impact in terms of the mortality of the unborn child and long-term effects on families and society as whole. Although modeling of current density distribution and conductive anatomy of the human transthoracic defibrillation has been subject of certain research interest the attempts to model this phenomenon in pregnant women using 3D finite element have been nonexistent.

In this paper, we present simplified 3D finite element model of a pregnant female torso and calculate current density distribution in the uterus. In order to simplify the problem in this preliminary analysis we use cylindrical model consisting of following compartments: left and right lung, interstice, diaphragm, equivalent lower torso and skin/fat tissue (Figure 1). We assume that the uterus and intestine in the lower torso can be approximated using a homogeneous equivalent tissue with slightly larger conductivity. Note that in general a non-homogeneous model can be used in order to model the electromagnetic properties more accurately. However in this preliminary approach we believe that the above approximation is justified in order to confirm or disprove existence of significant current in the lower torso.

To model the defibrillation process we assume that biphasic defibrillator with cycle length of 10 milliseconds with anterior-posterior position of the electrodes. We evaluate the current density as a function of voltage difference in order to obtain maximum allowed voltage. Note that it is believed that exposing a fetus to a current of 25 mA for 0.3 s may be consider as lethal dose. The purpose of our study therefore is to evaluate maximum possible voltage for a given position of electrodes which can still be considered safe for a fetus. In addition we also consider anterior-anterior position as well as the effect of incorporating additional ground points in order to remove conductive pathways leading to lower uterus.

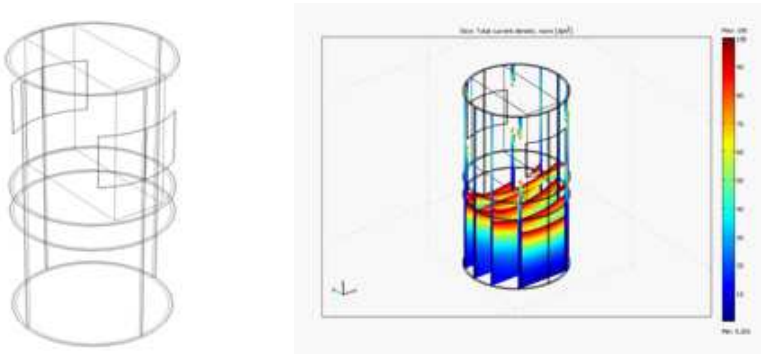

(a) (b)

Figure 1: (a) Geometry and (b) current density.

Evaluation of Tissue Properties in MR Images

J. Mikulka[1], **E. Gescheidtová**[1], **P. Marcoň**[1], **K. Bartušek**[2], **and A. Šprláková**[3]

[1]Department of Theoretical and Experimental Electrical Engineering
Brno University of Technology, Kolejni 4, Brno 612 00, Czech Republic
[2]Institute of Scientific Instruments of the ASCR, v.v.i
Královopolská 147, Brno 612 64, Czech Republic
[3]Radiological Clinic, The University Hospital Brno
Jihlavská 20, Brno 625 00, Czech Republic

Abstract— Image processing in biomedical applications is strongly developing issue. Many methods and approaches for image preprocessing, segmentation and visualization were described. This paper deals with image evaluation obtained by magnetic resonance tomography. Soft tissues can be observed in these images and their characteristics can be used to further processing and to diagnose diseases. Intensity distribution (mean, maximum, minimum, standard deviation and area) in regions of human head tissues are evaluated and compared for two healthy persons. The obtained values will be compared with the same parameters of unhealthy persons in studying jawbone diseases. The aim of this research is to find relations between tissue parameters which can be observed by often available magnetic resonance measuring sequences (T1/T2 weighted images, diffusion weighted images). The relations and similarity of some tissues and regions in mentioned images could help to increase yield of data obtained by magnetic resonance tomography and thus use of MR to pathological tissues and diseases recognition which must currently be diagnoses by other, often invasive, methods.

EM Exposure Chamber for Small Animals

Jaroslav Vorlíček, **Ladislav Oppl**, **and Jan Vrba**
Department of Electromagnetic Field, Czech Technical University, Czech Republic

Abstract— In connection with the rapid development of wireless communication devices we have witnessed a rapid increase of manmade sources of electromagnetic fields. The benefit of these technologies to society is undeniable; the influence of electromagnetic field to their users and other living organisms has not been satisfactorily evaluated yet.

In 1997, the World Health Organization (WHO) announced research project whose task was to obtain sufficient information for the final decision whether effects of short time exposure to electromagnetic fields infrequency range 0 Hz–300 GHz (heating of body tissue and nervous system) (Jelinek 2009) and other effects, such long-term, causing serious diseases such as cancer (Feychting 1993, Savitz 1988), Alzheimer's Parkinson's disease (Gabriel 1996). Studies dealing with this topic over the past 20 years says a lot, but still showed no harmful effects of electromagnetic fields. The theme of "electromagnetic fields and health", yet remains a big issue today.

In order to create in vivo EM exposure chamber for experiment on small animals we have designed and later created an exposure chamber of the type of cylindrical waveguide with the inner diameter of 120 mm and the total length of 1140 mm, wall of the waveguide is made of copper. Exposure chamber has two feeds for creating the circular polarization and it is designed to work on frequency of $f = 1800$ MHz, which is from the GSM frequencies. The feed are two simple monopole antennas which lies in the same cut plane but are shifted by 90°.

Specific absorption rate of EM field inside the waveguide is due to the waveguide perfectly homogenously distributed which is shown on the exposure of agar phantom of the mice. The results of the EM field exposure are evaluated by the infrared camera.

Why Gamma Photons Induce Cherenkov Effect

Antonio Puccini
Department of Neurophysiology, Order of Malta, Naples, Italy

Abstract— Pavel Alekseyevich Cherenkov was the first one to point out (1934) the effect coming from the impact of γ radiation with the high terrestrial atmosphere layers. Gamma photons (Ps) hit the molecules of the terrestrial atmosphere with such a strong impact to remove electrons with a speed bigger than the solar light in the same mean. Besides, these electrons, so much accelerated, emit ultraviolet (UV) Ps as well as visible Ps, with a violet colour and a brilliant blue: *Cherenkov Light* (CL). CL too travels with a speed higher than the visible light in high atmosphere.

As we know our atmosphere is constantly bombarded by electromagnetic radiations (EMRs). As for γ rays, X or UV radiation too hit atoms of the atmosphere molecules pushing away the electrons but in these circumstances the removed electron is not able to emit the CL, since the emitted Ps are not quicker than the common light in the atmosphere. Why is a γP able to accelerate the electron with a bigger speed than a XP or a less energetic P, that is with a lower frequency, can do? We think that the difference comes from the impact force with which the EMR hit the atmospheric molecules and their electrons. The force can be quantified by the value of the *momentum* (p) coming from the formula $p = h/\lambda$ where h is Planck'constant and λ is the wave length of the considered P.

Our calculations show that a visible P has a $p = 1.325 \cdot 10^{-22}\,[\mathrm{g \cdot cm/s}]$,whereas a XP with $\lambda = 10^{-9}\,[\mathrm{cm}]$ has a $p = 6.625 \cdot 10^{-18}\,[\mathrm{g \cdot cm/s}]$, and a γP with $\lambda = 10^{-12}\,[\mathrm{cm}]$ has a $p = 6.625 \cdot 10^{-15}\,[\mathrm{g \cdot cm/s}]$.

Since, as Fermi reminds us, the p of an EMR *quantum* is transferred entirely to the hit electron (we only detract the value of W_o indicating the energy necessary to extract the electron, about a few eV), we could explain why only electrons removed by γPs manage to acquire such a *kinetic energy* to be able to exceed the light speed, in the same mean, and emit a light, the CL, faster than the common light.

Anderson Transition May Be Induced by the Self Collapse of the Electron Wave Function

Antonio Puccini
Department of Neurophysiology, Order of Malta, Naples, Italy

Abstract— When in a crystalline solid, perfectly regular and good conductor, there are *impurities* we have that the solid undergoes a sudden change of state, that is a *transition* from conductor to insulating.In these circumstances the electrical current does not pass freely since electrons meet significant resistances (i.e., the *impurities*), as a consequence they tend to concentrate in a restricted area of the crystal. What happens is that the Wave Function (WF) of the electron previously extensive, *delocalised*, is now *localised*. We wonder how all these take place. What is the physical mechanism which makes the electron become localizable?

What we can clearly notice is that the behaviour of the electron is completely changed. At first it propagated as a wave, without resistances and dissipation of energy, just as a quantum object (QO), *delocalised* and propagating as a superimposition of quantum states. Whereas, when the electron meets, along its path, a certain number of *impurities* (represented by atoms different from those making the solid crystalline), the electron is *localised* as a corpuscle.

The drastic change of the QO behaviour (from undulating-like to corpuscular-like) normally happens when we try to observe it, when we carry out a measurement. Though in our case no measurement has taken place, the electron behaves as it had been measured. What happens is that electrons, or rather their WFs, reflecting on the *impurities* and other reflected electrons, concentrate in a restricted area of the crystal.

We believe that in these circumstances, as a consequence of the impact, a self collapse of the electron's WF takes place. In this way electron become localizable, behaving as particles rather than waves.

The Momentum of Luminous Photon Can Explain the Mystery of the Scission of the Water Molecule, Fundamental Event in the Clorophyllose Photosynthesis

Antonio Puccini
Department of Neurophysiology, Order of Malta, Naples, Italy

Abstract— The complex phenomenon of clorophyllose photosynthesis (CP) has been largely clarified in detail, covering both the Light or Photochemistry Phase (Light Reaction), and the Dark or Chemistry (Dark Reaction) Phase. As it is known, Light Reaction, which works only in the presence of light, occurs within the chloroplast where chlorophyllose Photo Systems, using a system of electronic transport which uses *conjugated double bindings* present in the chlorophyll porphyrin ring, allow the storage of the captured sunlight. It is also the light to make the breakdown of individual water molecules contained in the chloroplasts occur. What happens is that the chlorophyll behaves as a pump which removes electrons from a *provider* (the molecule of water), after the latter has been severed from the sunlight: Water photolysis (WP).

Yet, to date, the performance of the WP has not yet been clarified. In a rather simplistic and non-specific way, it is argued that it is the energy of light to induce the WP, but without going into details, without specifying the physical manners with which the phenomenon is performed. According to our calculations, the *momentum* (p) of common sunlight striking chloroplasts and water molecules contained therein is equal to $1.325{\cdot}10^{-22}$ [g·cm/s]. It is a truly remarkable impact strength, 100.000 times higher than the restmass of the electrons involved in the 2 *covalent bindings* between the oxygen atom and the 2 hydrogen atoms the water molecule is made of. Therefore, we think it is this *push effect* induced by luminous Ps to cause the WP, as well as being transmitted in full to the hit electrons, giving them a high kinetic energy, such as to make them take the porphyrin ring of chlorophylls, with its consequences (activation of the CP).

Multiparametric Data Collection and Data Processing of Animal Tissues in MRI Images

P. Marcon[1], **K. Bartusek**[2], **and M. Cap**[1]

[1]Department of Theoretical and Experimental Electrical Engineering,
Brno University of Technology, Kolejni 2906/4, Brno 612 00, Czech Republic
[2]Institute of Scientific Instruments, Academy of Sciences of the Czech Republic,
Kralovopolska 147, Brno 612 64, Czech Republic

Abstract— The research of pathology of bone and bone marrow is currently very interesting. The introduction for MRI revolutionized bone marrow imaging because this technique provides images with excellent soft tissue contrast. In adults the bone marrow is in general composed of fatty tissue, which appears hyperintense on T_1 and T_2 weighted images and occurs hypointense on MR-sequences with fat-saturation [4]. In case of trauma, tumor or infection infiltration, replacement and depletion of fatty bone marrow takes place resulting in intermediate to hypointense signals on T_1-weighted images and hyperintense signals on STIR (short-tau inversion recovery) and T_2 weighted images with fat-saturation. These changes obscure the distinct appearance of fatty bone marrow and serve as early indicators of pathology, which makes this imaging technique a very sensitive diagnostic tool.

To determine the properties of bone and bone marrow and their pathology, we have to know the properties of surrounding tissues. It is also important for the segmentation of individual tissues. The size and shape of tissues can often help to diagnose various pathologies. The quality o any image segmentation, however, is limited by the quality of the obtained images from MR tomography system. In magnetic resonance imaging (MRI), tissue contrast is based mostly on the T_1 and T_2 (T_2^*) relaxation times, proton spin density (PD) and susceptibility weighted imaging (SWI) and diffusion. Classification of tissues can be improved by optimizing the imaging protocol based on the underlying statistics of these parameters.

In this paper, we focused on multiparametric data collection of animals' tissues. As the source images was these weighted images chosen: PD, T_1, T_2, and SWI tissue parameters in terms of a multivariate. As a measured sample chicken wing was used. Several parameters (maximal value, minimal value, mean value and standard deviation) were evaluated in this sample in displayed tissues: skin, fat, muscle, bone and bone marrow. The obtained data could be used with advantage for multi-parametric analysis and for image segmentation.

The Method of Correction the B_1 Errors in Magnetization Transfer Ratio MTR

M. Alkhaddour and R. Kubasek
Department of Theoretical and Experimental Electrical Engineering
Brno University of Technology, Kolejni 4, Brno 612 00, Czech Republic

Abstract— The meaning of MRI is based on the consept of The magnetic sum vectors, Mz and Mxy, which realeted with resonant frequency RF, where the physics idea in MRI is influnced by the external magnetic field B_0 on the nuclear magnetic moment vector of proton in hydrogen, but the radiofrequency RF field B_1 errors is based on magnetization transfer ratio MTR measurements, and radio frequency RF nonuniformity, so it is important to correcte the B_1 errors in magnetization transfer ratio measurements, so this paper will discuse about the methods of correction at large volumetric radio frequency RF field, and this correction based on the double-angle method DAM.

Tow factors are realeted with B_1 field mapping techniquete, the first one is double angle method DAM, and the other one is the fast spin-echo FSE, where the value of magnetization transfer ratio depends on the amplitude of the magnetization transfer MT pulse.

The aim from this paper to explain the B_1 errors in the MTR and the method of correction of these errores, by using B_1 field mapping, to obtain a minimum histogram dispersion of MTR, where the RF causes MTR histograms to be wided, thus the non-uniformity of B_1 causes changes in the intensity of across MR images.

Influence of Material Properties on the Quality of NMR Images

R. Kubásek and M. Alkhaddour
Department of Theoretical and Experimental Electrical Engineering
Brno University of Technology, Kolejni 2906/4, Brno 612 00, Czech Republic

Abstract— The possibility of artifact in NMR image as distortion by conductive parts like implants was described well in many literatures. The possible distortion in images made by less significant aspect of materials like permittivity and permeability was described fewer. The possible artifact reveal due to own measured objects such as bones, organs or tissues wasn't defined or verified ever. The fact is that this contribution of artifact distortion in NMR images is probably very low. Question is how much. Answer can make out experiment which will be presented in this paper. The goal is to experimentally find out the contribution of material sample in B_1 homogeneity distortion. The numerical modeling simulation will be made for simplest attempts for many types of materials defined by material constants like permittivity, permeability and conductivity. Of course only if experiment and numerical simulation will match.

The Measured of Air Ions Mobility Spectrum

Z. Roubal and R. Kadlec
Department of Theoretical and Experimental Electrical Engineering
Brno University of Technology, Kolejní 2906/4, Brno 612 00, Czech Republic

Abstract— It was confirmed that concentration of light air ions has positive influence on the human health. For objective appraisal of the influence of synthetic sources of negative air ions the comparison with natural environment is necessary. The concentration of air ions and their mobility spectrum can be found out by aspiration condenser. When measure with the condenser, the spectrum mobility can be calculated from measured saturation characteristics. It will be discussed the most advantageous approximation of saturation characteristics from point of view of minimal numeric error. The saturation characteristic approximation will be made in Matlab. In the Faraday cage was measured saturation characteristic for different aspiration condenser. The measure for same ions source is compared. In the result was discussed influence construction and measure order to determine air ions mobility spectrum.

REFERENCES

1. Tammet, H. F., "The aspiration method for determination of atmosphericion spectra," *IPST*, Jerusalem, 1970.
2. Charry, J. M. and R. Kavet, *Air Ions: Physical and Biological Aspects*, CRC Press, Inc. Boca Raton, Florida, 1987.
3. Kondrashova, M. N., E. V. Grigigorreko, A. N. Tikhonov, T. V. Sirota, A. V. Temnov, I. G. Stavrovskaya, N. I. Kosyakova, N. V. Lange, and V. P. Tikonov, "The primary physic-ochemical mechanism for the beneficia biological/medical effects of negative air ions," *IEEE Trans. Plasma Scien.*, Vol. 28, No. 1, 230–237, 2000.
4. Vojtek, T., T. Skoupil, P. Fiala, and K. Bartusek, "Accuracy of air ion field measurement," *PIERS Online*, Vol. 2, No. 4, 412–415, 2006.
5. Steinbauer, M., P. Fiala, K. Bartušek, and Z. Szabó, *PIERS Proceedings*, 1062–1066, Hangzhou, China, March 24–28, 2008.
6. Roubal, Z. and M. Steinbauer, "Design of electrometric amplifier for aspiration condenser measurement," *PIERS Proceedings*, 1430–1434, Xi'an, China, March 22–26, 2010.

The Study of Cell Growth in Tissue Culture in the Magnetic Field

M. Pokludová and E. Hutová
Department of Theoretical and Experimental Electrical Engineering
Brno University of Technology, Kolejni 4, Brno 61200, Czech Republic

Abstract— Most materials have a property to create their own magnetic field when exposed to an external field. The human body is partly diamagnetic, which means that the effect of the external field can cause the body's own field. Long-term exposure of magnetic fields on blood and nervous system has positive effects, these effects are utilized in the treatment method called magneto therapy. Similar positive effects can be traced in the plant tissue culture. Samples of spruce embryos grown in the plastic Petri's dishes were placed between the permanent magnets (with defined magnetic field gradient) in a dark place with no effect of the external lighting at a constant temperature and humidity. Samples were periodically removed from the magnetic field and moved in isolated box throughout the outdoor environment into the room with NMR tomograph for imaging individual tissue cultures. The aim of this project is to confirm the hypothesis that the samples in a magnetic field of permanent magnets will grow faster than the control samples taken off the effect of magnets while keeping both in a constant temperature and humidity. After the fifteen days the last measurement was carried out and the results of all measurements were evaluated using the programs Marevisi and Matlab. Observed parameters of individual samples were processed into graphs. The graphs can confirm the hypothesis of faster growth in samples of the magnetic field of permanent magnets, although the transfer was not maintained at constant temperature which resulted in fogging of dishes. This had no significant effect on the growth of the samples.

Methodology of Thermal Properties Measurement

J. Hrozek[1], **M. Pokludova**[1], **D. Nespor**[1], **and K. Bartusek**[2]

[1]Deptartment of Theoretical and Experimental Electrical Engineering
Brno University of Technology, Kolejni 2906/4, Brno 612 00, Czech Republic
[2]Institute of Scientific Instruments, Academy of Sciences of the Czech Republic
Kralovopolska 147, Brno 612 64, Czech Republic

Abstract— This paper deals with a methodology of temperature dependencies measurement of thermal properties. Specific heat and thermal conductivity are two thermal properties contained here. Thermal properties of each matter are dependent on their own temperature and are various in whole temperature range. Temperature dependencies of many commercial materials are well known. But temperature dependencies of biological tissues are very bad to find. However knowledge of these parameters is very important for the thermal processes computer simulation. The methodology described here goes out of current methods deficiencies. Thermal conductivity of biological tissues is measured with the needle probe. This method has some deficiencies which are described in this paper. Specific heat is measured with Differential Scanning Calorimetry (DSC). The DSC is conventional method without serious deficiencies. Big disadvantage of current thermal properties measurement is in necessary using of both methods, i.e., two devices are used. Simultaneous measurement of thermal conductivity and specific heat is the main advantage of our methodology.

Measurement of Magnetic Flux Density by NMR Using Unsymmetrical Spin Echo

T. Kříž[1], **K. Bartušek**[1, 2], **and R. Kořínek**[1, 2]

[1]Department of Theoretical and Experimental Electrical Engineering
Brno University of Technology, Kolejní 4, Brno 612 00, Czech Republic
[2]Academy of Science of the Czech Republic, Institute of Scientific Instruments
Královopolská 147, Brno 612 64, Czech Republic

Abstract— Measurement of magnetic flux density **B** by nuclear magnetic resonance is described in this article. Unsymmetrical spin echo was used to a magnetic field measurement. Magnetic flux density was measured outside the conductive specimen. The cooper specimen was made on surface of Printed Circuit Board (PCB). Direct current source was connected to the measured specimen. The current is passing through specimen and induces magnetic field outside the specimen. Differential measuring was used to obtain magnetic flux density values. Four measurements were taken for each component of the magnetic field. Two measurements for each time shift of the spin echo value $+T_p$ and $-T_p$ were taken. One of the measurements was taken for a positive current direction and the second fort the negative current direction. Information about magnetic flux density is encoded in phase image if unsymmetrical spin echo is used. For calculation of magnetic flux density values is equation

$$\Delta B = \frac{\Delta\varphi}{\gamma T_p}. \tag{1}$$

Measured values of magnetic field by means of NMR were compared with the results of numerical simulation. The Biot-Savat's law was used for calculation of magnetic field outside the same specimen. Numerical model was built as a 2D model. Triangle elements were used for the discrete geometrical model. We suppose that current density is constant on each element and elements have centers $[x_j,\, y_j,\, z_j]$. For magnetic field calculation can be used the superposition principle. Thus, the magnetic field was calculated at point with coordinates $[x_i,\, y_i,\, z_i]$. Biot-Savart's law can by written as

$$\mathbf{B}_i \approx \frac{\mu_0}{4\pi} \sum_{j=1}^{NE} \frac{\mathbf{K}_j \times \mathbf{R}_{ij}}{\|R_{ij}\|^3} \Delta S_j. \tag{2}$$

Measured magnetic field values could be used as an input data for conductivity calculation based on electrical impedance tomography. Relative error was evaluated. Taking the error into account, the possibility of measured data exploitation for conductivity calculation will be discussed.

A Comparison of Characteristics in Parallel and Series Connections of Active Lossy FDNR Blocks

Z. Szabó and J. Sedláček
Department of Theoretical and Experimental Electrical Engineering
Brno University of Technology, Czech Republic

Abstract— At present, modern active elements together with the utilization of the synthesis method based on purposefully lossy RLC prototypes enable us to realize ARC filters (for the frequency range within units of Mhz) applying simple and economical selective building FDNR blocks that successfully work with one active element (OZ). This research report contains a complex analysis of attributes characterizing lossy active functional blocks; the authors show that the connection of active blocks with a series substitute model is significantly more advantageous than the commonly used parallel substitute scheme solution. A substantial benefit brought by this type of connection consists in the fact that, at higher frequencies, it does not exhibit the parasitic transmission zero which causes considerable problems in the case of parallel connections. Other related advantages of the described solution can be seen in its lower sensitivity to real parameters of the active elements, lower sensitivity to the variation of impedance level, and significantly higher (up to 20 dB) attainable circuit dynamics.

ACKNOWLEDGMENT

The research described in the paper was financially supported by grant of Czech ministry of industry and trade no. FR-TI1/368, project of the BUT Grant Agency FEKT-S-11-5/1012 and projekt CZ.1.07.2.3.00.20.0175, Elektro-výzkumník.

REFERENCES

1. Avies, E., "Electric signals in plants: Facts and hypotheses," *Plant Electrophysiology Theory and Methods*, Volkov, A. G., editor, Springer Berlin Heidelberg, New York, 2006.
2. Fromm, J., "Long-distance electrical signaling and physiological functions in higher plants," *Plant Electrophysiology Theory and Methods*, Volkov, A. G., editor, Springer Berlin Heidelberg, New York, 2006.

The Magnetizing Behavior Analysis of a Variable Inductor Based on the Orthogonal Magnetization

Zhengrong Jiang[1, 2], **Haichang Ding**[1, 2], **Zhengxi Li**[1, 2], **and Jianye Chen**[3]

[1]Beijing Variable Frequency Technologies Research Center, Beijing 100144, China
[2]College of Mechanical and Electrical Engineering
North China University of Technology, Beijing 100144, China
[3]Electronic Machine Department, Tsinghua University, Beijing 100084, China

Abstract— A novel variable inductor subject to a semi-rotating field has many advantages of application, such as its high reliability, robustness and potentially low cost. This paper presents the configuration of this inductor, the analysis method based on Garshelis and Fiegel formulation is applied to investigate the magnetization mechanism of the laminated steel core inductor. Experimental measurements are acquired and found in agreement with corresponding simulations.

Introduction: With the wide application of power electronics, a greater demand for high quality variable inductor is expected [1]. A convincing explanation which can describe the magnetization behavior of an no "flux coupling" inductor subject to a semi-rotating field has not yet been given. This paper compares the operating process between the conventional variable inductor and the novel inductor, and then deals with the relationship between the ac control flux and the dc bias current in the novel inductor. At last, its analytical aspects, numerical simulations and laboratory inductance measurements are given in the following sections [2].

Inductor Configuration and Magnetization Analysis:

A. Topology and Modulation Method: The novel inductor consists of two parts. One is the cylinder iron core in which the dc coil windings circle. The other is the main coil which windings along axis and links ac loop. It is clear that the two coils are orthogonal each other. The flux links the main coil but not the dc coil. Consequently, no voltage will be induced in dc winding. It can be said that there is no magnetic coupling between the two coils under the arrangement. The novel inductor with a semi-core subject to a semi-rotating field can reach the purpose. Fig. 1 is the schematic diagram of the inductor.

B. Theoretical Analysis: In fact, the coupling is a result of the irreversible motion of the domain walls which can be described by a complex permeability [3]. The dc current changes the *B-H* curve into a new one and the magnetic behavior of the core depends on the new characteristics. A semi-rotating field is created in the core due to the combination of the current flowing in the main inductor coil and an orthogonal coil dc bias current [4].

Simulation And Experiment Results: The presented analysis has been numerically implemented and computer simulation has been performed. The inductor cylinder core is made of non-oriented silicon steel sheets. The changes of *B-H* Curves under different DC current biases have been simulated. It is clear from the characteristic that varying the orthogonal dc bias current of the inductor can lead to a variation in its inductance value. In order to investigate the relationship between the orthogonal bias current and the harmonic content, a further experiment has been performed.

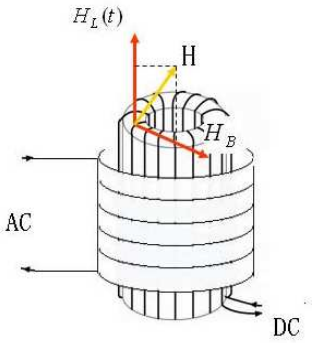

Figure 1: Diagram of the novel inductor.

Conclusion: The variable inductor based on orthogonal magnetization can change its inductance while maintaining a lower harmonic content. The magnetization mechanism can be described from the additional energy from the bias field to change the anisotropic contribution of the inductor core; hence, the effective permeability is varied. Proper bias current can be chosen to drive the core far below saturation in order to get the less distorting work waveform.

REFERENCES

1. Adly, A. A., "Controlling linearity and permeability of iron core inductors using field orientation techniques," *IEEE Transactions on Magnetics*, Vol. 37, No. 4, July 2001.
2. Misrikhanov, M. S. and A. O. Mirzzabdullaev, "Analysis of the reasons for accidents and of protective measures against induced voltage on alrial electrocal transmission lines," *Power Technology and Engineering*, Vol. 43, No. 1, 2009.
3. Stupakov, O., R. Wood, D. Jiles, et al., "Measurement of electrical steels with direct field determination," *IEEE Transaction on Magnetics*, Vol. 46, No. 2, February 2010.
4. Hauser, H., Y. Melikhov, and D. C. Jiles, "Examination of the equivalence of ferromagnetic hystersis models describing the dependence of magnetization on magnetic field and stress," *IEEE Transactions on Magnetics*, Vol. 45, No. 4, April 2009.

Nanoradar

N. S. Lapshina[1], **R. E. Noskov**[1], **and Y. S. Kivshar**[1,2]

[1]National Research University of Information Technologies, Mechanics and Optics (ITMO)
St. Petersburg 197101, Russia
[2]Nonlinear Physics Centre, Research School of Physics and Engineering
Australian National University, Canberra ACT 0200, Australia

Abstract— The study of optical nanoantennas became a subject of intensive research [1]. Nanoantennas hold a promise for the subwavelength manipulation and control of optical radiation for solar cells and sensing [2]. In a majority of applications, a crucial factor is a control over nanoantenna radiation pattern and its tunability. Spectral tunability and variable directionality have been proposed for bimetallic antennas [3], the Yagi-Uda architectures [4], high-permittivity dielectric nanoparticles [5], and nanoparticle chains [6]. In addition, several suggestions employed the concept of plasmonic nanoantennas with a nonlinear load where the spectral tunability is achieved by varying the pumping energy [7, 8].

In this work, we introduce a novel concept of *a nanoradar* or a nanoantenna with self-tunable directivity composed of two nonlinear subwavelength silver nanoparticles. More specifically, we consider modulation instability (MI) in this nanodimer and find that MI development allows dynamical exchange of energy between cluster eigenmodes resulting in a periodical rotation of the nanoantenna scattering pattern similar to classical radar systems. We carry out a detailed analysis of the impact of an external field on the rotation period of the scattering pattern, and find out that it can be tuned in a wide range from several tens to several hundreds femtoseconds. Our results open promising perspectives for using nanoradars in systems providing dynamical tracing of different nanotargets as well as ultrafast nanophotonic-plasmonic devices.

ACKNOWLEDGMENT

The authors acknowledge a support from the Australian Research Council and a megagrant of the Ministry of Education and Science of Russian Federation.

REFERENCES

1. Novotny, L. and N. van Hulst, "Antennas for light," *Nature Photon.*, Vol. 5, 83, 2011.
2. Giannini, V., A. I. Fernández-Domínguez, S. C. Heck, et al., "Plasmonic nanoantennas: Fundamentals and their use in controlling the radiative properties of nanoemitters," *Chem. Rev.*, Vol. 111, 3888, 2011.
3. Shegai, T., S. Chen, V. D. Miljković, et al., "A bimetallic nanoantenna for directional colour routing," *Nature Commun.*, Vol. 2, 481, 2011.
4. Dorfmuller, J., D. Dregely, M. Esslinger, et al., "Near-field dynamics of optical Yagi-Uda nanoantennas," *Nano Lett.*, Vol. 11, 2819, 2011.
5. Krasnok, A. E., A. E. Miroshnichenko, P. A. Belov, and Y. S. Kivshar, "Huygens optical elements and Yagi-Uda nanoantennas based on dielectric nanoparticles," *JETP Lett.*, Vol. 94, 593, 2011.
6. Chen, Y., P. Lodahl, and A. F. Koenderink, "Dynamically reconfigurable directionality of plasmon-based single photon sources," *Phys. Rev. B*, Vol. 82, 081402, 2010.
7. Chen, P.-Y. and A. Alù, "Optical nanoantenna arrays loaded with nonlinear materials," *Phys. Rev. B*, Vol. 82, 235405, 2010.
8. Novotny, L. and N. van Hulst, "Photoconductively loaded plasmonic nanoantenna as building block for ultracompact optical switches," *Nano Lett.*, Vol. 10, 1741, 2010.

Session 2A1
Advancements in Phase-space Representations

The Use of the Wigner Distribution Function for Defining the Concept of Quasi-point Source, and the Application of this Concept to the Restoration of Defocused Images

L. R. Berriel-Valdos[1], **J. F. Aguilar**[1], **I. J. Orlando-Guerrero**[2], **R. Ortiz-Sosa**[1], **S. Mejía-Romero**[1], **and J. E. A Landgrave**[3]

[1]Instituto Nacional de Astrofísica, Óptica y Electrónica, Pue., México
[2]Univ. de la Cañada (UNCA), Oax, México
[3]Centro de Investigaciones en Óptica, Gto., México

Abstract— We introduce the concept of quasi-point source (QPS) [1, 2] by means of the Wigner distribution function (WDF) [3], as applied to the detected image [4] of a small binary disc. A QPS is realized when the WDF of such image is always positive within the extended bandwidth of the optical system [5]. The system that we used to substantiate the use of this concept was a conventional microscope with Köhler illumination.

We made use of a QPS, as defined above, to obtain the defocused point spread function of a specific optical system. This function was employed next to construct the corresponding Wiener filter [6, 7], in order to restore defocused images of extended objects produced with this system.

REFERENCES

1. Weinstein, W., "Image of incoherent illuminated bright and opaque disks," *J. Opt. Soc. Am.*, Vol. 45, 1006–1007, 1955.
2. Singer, W., M. Totzek, and H. Gross, *Handbook of Optical Systems, Vol. 2: Physical Image Formation*, Herbert Gross Ed., Wiley-VCH, Weinheim, 2005.
3. Wigner, E., "On the quantum correction for thermodynamic equilibrium," *Physics Review*, Vol. 40, 749–759, 1932.
4. Ronchi, V., "Resolving power of calculated and detected images," *J. Opt. Soc. Am.*, Vol. 51, 458–460, 1960.
5. Mejía-Romero, S., L. R. Berriel-Valdos, J. F. Aguilar, I. J. Orlando, and J. E. A. Landgrave, "Discrete wigner distribution function applied on images of quasi-point source objects in coherent illumination," *Proc. SPIE*, Vol. 8011, 8011831 2011.
6. Wiener, N., *The Extrapolation, Interpolation, and Smoothing of Stationary Time Series*, Wiley, New York, 1949.
7. Ortiz-Sosa, R., L. R. Berriel-Valdos, J. F. Aguilar, J. Carranza-Gallardo, I. J. Orlando-Guerrero, and S. Mejía-Romero, "Optical-digital restoration of out-of-focus color images detected in microscopy," *Proc. SPIE*, Vol. 8011, 8011841, 2011.

Projections of Wigner Distribution for Optical Beam Characterization

Tatiana Alieva, **Alejandro Cámara**, **Jose A. Rodrigo**, **and María Luisa Calvo**
Facultad de Ciencias Físicas, Universidad Complutense de Madrid
Avda. Complutense, s/n, Madrid E-28040, Spain

Abstract— Optical beam characterization is a crucial task in many applications including microscopy, astronomy, metrology, communication, etc. The analysis of the spatial structure of quasi-monochromatic scalar paraxial beams is usually based on the measurements of the intensity distributions of the beam after its propagation through free space and quadratic phase elements. These images correspond to the projections of the Wigner distribution of the beam. A method to completely reconstruct the Wigner distribution of an arbitrary optical beam using its projections was proposed in Ref. [1]. We demonstrate that additional information about the beam, such as its degree of coherence or symmetry, can significantly reduce the number of the projections needed for beam description and simplify the setup for their acquisition. For example, only a few projections are needed for phase recovery, and therefore complete characterization, of a coherent beam [2, 3]. Other examples are completely or partially coherent beams described by mutual intensity separable in Cartesian coordinates or rotational symmetric, which can be reconstructed from a limited number of projections [4–6]. Moreover, coherent beams that are rotationally symmetric can be characterized by the Wigner distribution of any diagonal one-dimensional sample of the beam [5, 7]. We discuss appropriate optical setups for measurement of the required projections and the recovery methods of the Wigner distribution for every mentioned case.

REFERENCES

1. Raymer, M. G., M. Beck, and D. F. Mc Alister, *Phys. Rev. Lett.*, Vol. 72, 1137, 1994.
2. Alieva, T. and J. A. Rodrigo, "OSA Annual meeting," *Frontiers in Optics 2009*, STuD2.San Jose, USA, October 11–15, 2009.
3. Rodrigo, J. A., T. Alieva, A. Cámara, O. Martínez-Matos, P. Cheben, and M. L. Calvo, *Optics Express*, Vol. 19, 6064, 2011.
4. Cámara A., T. Alieva, J. A. Rodrigo, and M. L. Calvo, *JOSA A*, Vol. 29, 1301, 2009.
5. Agarwal, G. S. and R. Simon, *Opt. Lett.*, Vol. 25, 1379, 2000.
6. Alieva, T. and M. J. Bastiaans, *JOSA A*, Vol. 17, 2319, 2000.
7. Cámara A., T. Alieva, J. A. Rodrigo, and M. L. Calvo, *Opt. Lett.*, Vol. 36, 2441, 2011.

Experimental Reconstruction of the Wigner Distribution of Rotationally Symmetric Beams

Alejandro Cámara, Izan Castro, and Tatiana Alieva
Facultad de Ciencias Físicas, Universidad Complutense de Madrid
Avda. Complutense, s/n, Madrid E-28040, Spain

Abstract— The characterization of completely or partially coherent optical beams by means of the Wigner distribution (WD) is widely accepted approach frequently used for theoretical beam description. Experimental beam characterization is usually limited by the estimation of the WD second order moments since the reconstruction of the entire WD, which is a function of four variables, requires rather sophisticate optical systems. Most of the optical beams used in practice possess rotational symmetry that reduces the number of variables of the WD to three for the case of partially coherent beams and to two for the case of completely coherent ones. Theoretically it has been shown that the WD of the rotationally symmetric coherent beams can be obtained from the WD of one dimensional sample along the beam diagonal [1, 2]. While in this case the WD can be measured instantaneously, the method is not energetically efficient and may provide artifacts due to the experimental selection of the one-dimensional sample. The setup we propose to use for the reconstruction of the WD overcomes these limitations. The method of the reconstruction of the WD of rotationally symmetric beams from a limited number of its projections has been proposed in Ref. [3]. These projections can be obtained using the optical system performing the antisymmetrical fractional Fourier transform which was previously applied for the reconstruction of the WD of fields separable in Cartesian coordinates [4]. It consists of four cylindrical lenses, whose rotation allows changing the transformation parameter. The experimental reconstruction of the WD of a laser beam and of beams shaped by a circular aperture is demonstrated. The experimental results are in good agreement with numerical simulations.

REFERENCES

1. Agarwal, G. S. and R. Simon, *Opt. Lett.*, Vol. 25, 1379, 2000.
2. Dragoman, D., *Opt. Lett.*, Vol. 25, 281, 2000.
3. Alieva, T. and M. J. Bastiaans, *JOSA A*, Vol. 17, 2319, 2000.
4. Cámara, A., T. Alieva, J. Rodrigo, and M. L. Calvo, *JOSA A*, Vol. 2009.

Phase-space Measurement of Partially Coherent Beams Using Spatial Spectrograms

L. Waller, G. Situ, and J. W. Fleischer
Department of Electrical Engineering, Princeton University, USA

Abstract— Phase-space optics allows simultaneous visualization of both space (x) and spatial frequency (k) information. Coherent (laser) beams are fully described by a 2D complex function (e.g., amplitude and phase), whereas partially coherent beams inherently have more degrees-of-freedom and require a 4D description. Typical 4D functions describe coherence properties in terms of their coherent mode decomposition, their mutual coherence function, or any of the Cohen class of phase-space distributions (e.g., the Wigner distribution function or the Ambiguity function). These descriptions are particularly important for propagation, in which coherence properties determine the evolution of intensity. In phase space, linear propagation of both coherent and partially coherent beams amounts to a simple geometric shearing operation. In nonlinear propagation, however, the propagation transfer function is both shift-variant and object-dependent, and the dynamics depend on the entire 4D phase-space function. Thus, a full 4D measurement is necessary in order to predict beam evolution, or to numerically invert its effects. Despite this, previous studies in nonlinear optics have observed intensities in x-space or k-space only, i.e., projections along the axes of the $\{x, k\}$ space, with no measurements within its volume. Here, we present experimental methods for both measurement and control of phase-space distributions with partially coherent light, for both linear and nonlinear optics. For measurement, we record a spatial spectrogram (windowed Wigner distribution function) by using a Spatial Light Modulator (SLM) to scan an aperture across the transverse field of the beam. The method is simple, fast, and free of mechanical scanning errors and artifacts. For coherence control, we use a second SLM as a dynamically changing local diffuser with spatially varying statistics, allowing design and creation of arbitrary phase-space distributions. Measurement and control of such higher-dimensional beams will have applications in coherence holography encoding, illumination, and display.

Pseudo-random Sequences with Chirp Modulation

J. Ojeda-Castañeda[1], **P. Cerna-García**[1], **and A. Sauceda-Carvajal**[2]

[1]University of Guanajuato, Salamanca, Guanajuato 36885, México
[2]Research Center for Nanotechnologies, University of Veracruz, 94292, México

Abstract— We employ the ambiguity function for relating the use of chirping pseudo-random sequences with the methods used for extending the depth of field of an imaging device.

Introduction: Pseudo random sequences find a myriad of applications in digital signal processing and optics [1]. The autocorrelation of a given sequence approaches a Dirac's delta, while the cross-correlation between two sequences approaches a uniform, but noisy background.

Krile et al. has suggested exploiting the above property as follows. One can record multiple holograms, in the same plate, by using reference beams encoded with pseudo-random sequences [2]. In the same work, the authors indicate that the multiplexing technique has good discrimination capabilities, if one modulates the pseudo-random sequence with a chirp wavefront. Since chirp wavefronts can be thought of as introducing focus errors, here we relate chirping pseudo-random sequences with the masks used for extending the depth of field.

Cross-correlation of Chirp Sequences: If one denotes the complex amplitude distribution of chirp sequence as $u_m(x) := s_m(x)\exp(i\pi a x^2)$, then one obtains that the cross correlation of two chirp sequences, say $u_m(x)$ and $u_n(x)$, is proportional to the cross ambiguity function of $s_m(x)$ and $s_n(x)$.

Hence, first, we analyze the cross-ambiguity functions of several sequences, used in spread spectrum communications. Second, we suggest the use of certain pseudo-random encoded masks, for extending the depth of field of an imaging device.

REFERENCES

1. Harwit, M. and N. J. Sloane, *Hadamard Transform Optics*, Academic Press, New York, 1979.
2. Krile, T. F., M. O. Hagler, W. D. Redus, and J. F. Walkup, "Multiplexed Ambiguity function display using a single 1-D input," *Appl. Opt.*, Vol. 18, 52–56, 1979.

Diffraction of Chain-like Beams with Phase Singularity

D. Yu. Cherepko[1], **N. D. Kundikova**[1, 2], **and I. I. Popkov**[1, 2]

[1]Joint Nonlinear Optics Laboratory, South-Ural State University
76, Lenin Av., Chelyabinsk 454080, Russia
[2]Institute of Electrophysics, Ural Branch of the Russian Academy of Sciences
106, Amundsena Str., Ekaterinburg 620016, Russia

Abstract— The wide usage of light beams of various structures for both fundamental research and technical applications requires new information concerning properties of such beams.

Almost all special laser beams can be divided into three groups: beams with non-uniform distribution of intensity, beams with non-uniform phase structure and beams with non-uniform distribution of polarization.

The examples of beams with non-uniform distribution of transverse and longitudinal intensity are chain-like beams. We were successful to create light beams which have got both non-uniform distribution of transverse and longitudinal intensity and non-uniform phase structure (wave front dislocation), i.e., the chain-like beams with a phase singularity [1]. These beams are the result of Bessel beams diffraction from a zone plate with two open zones.

The presence of the phase singularity (wave frond dislocation) has been checked by means of an interference method: a spiral interference pattern has been observed as a result of the beam under investigation and Gauss beam interference. This method has allowed checking the sign of the wave front singularity and the topological charge.

It is possible to determine the sign of phase singularity by means of diffraction. Here we present the results of computer modeling and experimental results of chain-like beams with phase singularity diffraction from a slit placed at the different distances from zone plate position. The experiment and modeling have been performed for the different slit width.

It has been shown that the diffraction pattern depends on the slit position and the slit width. The experimental results can be used for the phase retrieval on the base of the algorithm similar to Gershberg-Saxton algorithm in which the intensity distributions in any beam sections are used [2].

REFERENCES

1. Cherepko, D., N. Kundikova, I. Popkov, and T. Alieva, "Chain-like beams with phase singularity," *SPIE Proceedings*, Vol. 8011, 116[5Y-1–5Y-7], 2011.
2. Doogin, A. V., N. D. Kundikova, and B. Y. Zel'dovich, "Phase retrieval from laser beam intensity profiles," *Optics Communication*, Vol. 91, 193–196, 1992.

Gaussian Filter with Tunable Half-width

Jorge Ojeda-Castañeda, **Emmanuel Yépez-Vidal**, **and Eloy García-Almanza**
University of Guanajuato, Salamanca, Guanajuato 36885, México

Abstract— We present a Gaussian absorption filter, with tunable half-width. Our device is useful for improving the modulation transfer functions, associated to filters that reduce the influence of focus errors. We show that phase-space representations provide suitably tools for describing this device.

Introduction: Alvarez and Lohmann have described a nonconventional method for setting lenses with tunable focal length [1, 2]. A similar method is useful for implementing phase filters with tunable depth of field [3]. Albeit, as other phase filters, their associated modulation transfer function (MTF) exhibit unwanted oscillations around a tendency line. Here, we discuss a method for generating a Gaussian filter, with tunable half-width. The proposed filter reduces, in a tunable fashion, the unwanted oscillations of the MTF.

Phase-space Description: For implementing a phase-space representation of a 1-D optical signal, $u(x)$, it is convenient to generate an intermediate 2-D signal, $p(x, y) = u(x + y/2)u^*(x - y/2)$, here denoted as the product space [4]. We show that this intermediate representation is well-suited for describing the optical features of the tunable, Gaussian filter.

Furthermore, the 2-D Fourier transform of the product space is the product spectrum, $P(\mu, \nu)$, which is useful for discussing the behavior of the MTF with focus error. We exploit the advantages of the ambiguity function for illustrating our mathematical models and numerical simulations.

REFERENCES

1. Alvarez, L. W., U.S. Patent 3,305,294, Dec. 3, 1964.
2. Lohmann, A. W., Italian Patent 727,848, Jun. 19, 1964.
3. Ojeda-Castaneda, J., J. E. A. Landgrave, and C. M. Gómez-Sarabia, *Appl. Opt.*, Vol. 47, No. 22, E99–E105, 2008.
4. Testorf, M., M. B. Hennelly, and J. Ojeda-Castaneda, *Phase-space Optics Fundamentals and Applications*, McGraw-Hill Professional, 2010.

Optical Similarity Using Orthonormal Expansions

J. Ojeda-Castañeda[1], **C. M. Gómez-Sarabia**[1], **and C. Frausto**[2]

[1]University of Guanajuato, Salamanca, Guanajuato 36885, México
[2]Centro de Investigaciones en Optica, Aguascalientes, México

Abstract— We define a *similarity coefficient* as a cross-correlation between two members of a complete, orthonormal set of functions. Next, we apply the *similarity coefficient* for evaluating a *similarity function*, which quantifies the semblance between two optical signals. Finally, we describe the impact of wave aberrations by measuring the similarity between the input and the output of an imaging device.

Introduction: For several optical problems as pattern recognition, analyzing modes in optical fibers, holography with encoded beams, and optical coherence tomography, it is convenient to have measurement of similarity between two optical signals [1–3].

Cross-correlation of Chirp Sequences: Here our aim is threefold. First, we use a cross correlation for defining a *similarity coefficient* between two members of a complete set of orthonormal functions. Second, we show that this coefficient is useful for defining a *similarity function*, which quantifies the semblance between two optical signals, which can be expanded as a linear combination of the same set of orthonormal functions. Third, for image formation, we show that one can describe the influence of wave aberrations, by evaluating the similarity between the input and the output. If the input is periodic, then the *similarity function* takes a simple mathematical expression.

REFERENCES

1. Feit, M. D. and J. A. Fleck, "Computation of mode properties in optical fiber waveguides by a propagating beam method," *Appl. Opt.*, Vol. 19, 1155–1164, 1980.
2. Lohmann, A. W. and J. Ojeda-Castaneda, "Fresnel similarity," *Opt. Comm.*, Vol. 249, 397–405, 2005.
3. Ojeda-Castaneda, J. and C. M. Gomez-Sarabia, "Temporal similarity for optical short pulses," *Photonics Letters of Poland*, Vol. 2, 165–167, 2010.

Conservation of Angular Momentum and Nonconservative Optical Forces in Scattering

Sergey Sukhov, David Haefner, and Aristide Dogariu
CREOL & FPCE, The College of Optics and Photonics
University of Central Florida, Orlando, FL 32816, USA

Abstract— Optical waves carry spin and angular momenta. We show that the spin angular momentum of the incident wave is distributed between spin and orbital momentum of the wave scattered from a spherically symmetric scattering potential resulting in a spiral power flow. This spiral flow can have effect on a dynamics of optically bound particles. The existence of torques due to optical interaction in the multi-particle system is demonstrated and applications to nano-rotator machines are discussed.

Conservation laws are ubiquitous in all physical disciplines. In optics, the conservation of energy, and conservation of linear and angular momentum are of particular interest. The angular momentum of a propagating electromagnetic field is [1]:

$$j_z(x,y,z) = \frac{c\varepsilon_0}{i2\omega}\mathbf{E}^*\left(\widehat{\mathbf{r}}\times\nabla\right)\mathbf{E}|_z + \frac{c\varepsilon_0}{i2\omega}\mathbf{E}^*\times\mathbf{E}|_z\,,$$

where the first term represents the orbital angular momentum and the second term accounts for the spin angular momentum. The presence of orbital and spin momentum in optical field is determined by the distribution of phase and polarization.

Polarization related phenomena in both single and multiple scattering can be attributed to processes in which angular momentum is exchanged between the electromagnetic wave and the scattering medium [2, 3]. We will show how the spin angular momentum carried by the incident wave is distributed between the spin and orbital momentum of the wave scattered from a spherically symmetric scattering potential. Solving the corresponding Mie problem, we will demonstrate that there are directions where the angular momentum can completely transform into orbital momentum. The transformation of spin momentum into orbital results in the spiral flow of energy in the near-field zone around the scattering particle. A number of peculiarities including resonant effects and directional shifts with regards to the flow of energy (spin-Hall effect of light) in scattering of circularly polarized light from nano- and microspheres will be discussed and experimental results will be presented.

Understanding the physical implications of conservation laws at subwavelength scales leads to optimized approaches for near-field coupling between nano-sized structures. The electromagnetic interaction between bound spheres, for example, leads to interplay between the conservative and non-conservative torques. A consequence of this is that the spheres can be subjected to both orbital torques about the mutual center of mass as well as spin around the individual centers. We found that this complex mechanism is determined by the polarization of the incident field [4]. The mere existence of these nonconservative torques is a significant result, demonstrating that optical interaction with angular momentum can lead to rotations of lossless dielectric objects.

REFERENCES

1. Allen, L., S. M. Barnett, and M. J. Padgett, *Optical Angular Momentum*, IOP Publishing, Bristol, 2003.
2. Schwartz, C. and A. Dogariu, "Conservation of angular momentum of light in single scattering," *Optics Express*, Vol. 14, 8425–8433, 2006.
3. Schwartz, C. and A. Dogariu, "Backscattered polarization patterns determined by conservation of angular momentum," *JOSA A*, Vol. 25, 431–436, 2008.
4. Haefner, D., S. Sukhov, and A. Dogariu, "Conservative and nonconservative torques in optical binding," *Phys. Rev. Lett.*, Vol. 103, 173602, 2009.

Session 2A2
Microwave Photonics Techniques, Technology & Applications

Integration of Radio-over-fiber with WDM Passive Optical Networks

Stavros Iezekiel, **George Ellinas**, **and Andreas Perentos**
Department of Electrical and Computer Engineering
University of Cyprus, Nicosia 1678, Cyprus

Abstract— This paper examines the technological requirements and assesses the performance analysis and feasibility for implementing several novel architectures that integrate both WDM-PON and mm-wave radio-over-fiber networks, for the delivery of bandwidth-intensive integrated voice, data, and video services at distances beyond 20 km in the subscriber access network. We propose a test-bed that will enhance the access network's capabilities to ensure that real-time voice and IP video services can be delivered over a single platform with the same quality of service and ease of management as ATM or SONET. The inclusion of radio-over-fiber technology will provide a wireless interface that can extend the transmission distance compared to coaxial cable, and can offer secure communications, low power consumption, as well as simplified antenna configurations.

ACKNOWLEDGMENT

The authors thank the Cyprus Research Promotion Foundation for providing financial support under the program ΑΝΑΒΑΘΜΙΣΗ/ΠΑΓΙΟ/0308/30.

Compact Metamaterial-based Bias Tee Design for 1.55 μm Waveguide-photodiode Based 71–76 GHz Wireless Transmitter

Merih Palandöken[1], **Vitaly Rymanov**[2], **Andreas Stöhr**[2], **and Tolga Tekin**[1]

[1]Technische Universität Berlin, Gustav-Meyer-Allee 25, Berlin 13355, Germany
[2]Universität Duisburg-Essen, Lotharstr. 55, Duisburg 47057, Germany

Abstract— The progressive growth in communication technologies has been brought about by optical and wireless communications technologies. These two technologies have started to merge to create a new interdisciplinary area called Microwave and Millimeter-Wave Photonics (MWP). MWP technology aims at achieving advancement and improved functions in telecommunications systems that cannot be achieved by the individual technologies, but can be achieved mainly through the combination of radio-wave technology and photonic technology. Therefore, MWP is nowadays an important technology for various commercially available high data-rate applications in millimeter-wave and even THz frequency ranges. One photonic component in miniaturized MWP systems is the photodiode. It is necessary in order to generate high power millimeter waves in broad frequency band. However, for the optimum operation of photodiodes in wireless communication networks, in addition to the design parameters, DC biasing of photodiodes has to be correspondingly achieved with a sufficiently good RF isolation.

In this paper, a compact meta-material-based Bias-Tee design is proposed in order for 1.55 μm waveguide photodetectors to be integrated in E-band wireless transmitter module. The photodiode is isolated from DC bias line with an RF signal suppression level better than 28 dB between 71–76 GHz by two slotted Split-Ring Resonators (SRR) in the signal line. The insertion loss is better 0.3 dB with the maximum return loss of 20 dB in the whole operation band. Due to the sub-wavelength resonance feature of SRRs, the bias tee can be correspondingly miniaturized in length and width. The RF performance of proposed bias tee is compared with that of conventional $\lambda/4$ bias tee. The effects of geometrical parameters on the transmission and isolation are additionally investigated in order to verify the design approach and determine the critical design parameters.

On-chip Frequency Discriminator for Microwave Photonics Signal Processing

D. Marpaung and C. G. H. Roeloffzen
Telecommunication Engineering Group, University of Twente
Enschede, The Netherlands

Abstract— Microwave photonics (MWP) techniques for the generation, distribution and processing of radio frequency (RF) signals have enjoyed a surge of interest in the last few years. The workhorse behind these MWP functionalities is a high performance MWP link. Such a link needs to fulfill several criteria namely high link gain, low noise figure and high spurious-free dynamic range (SFDR). High SFDR dictates high linearity and low noise in the links. In a conventional intensity modulated direct detection (IMDD) link the SFDR is mainly limited by the laser relative intensity noise (RIN) and the third order intermodulation distortion (IMD) either from the directly modulated laser or the electro-optic modulator. To break way from these limitations, one might look towards alternative modulation schemes where phase or frequency modulations are used. A type of MWP link that gains significant interest recently is the phase (or frequency)-modulated direct detection link. In such a link, a phase modulated signal is converted to intensity modulation (PM-IM conversion) using an optical frequency discriminator, thereby allowing a simple direct detection scheme instead of the complicated coherent detection. The interest in such a scheme stems from two reasons; first, a phase modulator can provide high linearity and its operation does not require biasing. The second reason is that there is an additional degree of freedom in tailoring the characteristic of the optical filter discriminator to enhance the link performance, i.e., for noise and distortion suppressions.

In this work the we report a high performance phase modulation direct detection microwave photonic link employing a photonic chip as a frequency discriminator. The photonic chip consists of five optical ring resonators (ORRs) which are fully programmable using thermo-optical tuning. In this discriminator a drop-port response of an ORR is cascaded with a through response of another ORR to yield a linear phase modulation (PM) to intensity modulation (IM) conversion. The balanced photonic link employing the PM-IM conversion exhibits high second-order and third-order input intercept points (IIP2 and IIP3) of +46 dBm and +36 dBm, respectively, which are simultaneously achieved at one bias point.

Using the same photonic chip frequency discriminator, we extend the concept of PM-IM conversion to demonstrate the generation of impulse radio ultrawideband (UWB) pulses. We show that the discriminator chip in combination with a phase modulator forms a temporal differentiator. By means of tailoring the discriminator response using either the individual or the cascade of drop and through responses of the ORRs, first-order or second-order temporal differentiations are obtained. Using this principle, the generation of UWB monocycle, doublet and modified doublet pulses are demonstrated. The use of this CMOS-compatible discriminator is promising for the realization of a compact and low cost UWB transmitter.

Toward an Eigenanalysis Study of Arbitrarily Shaped Photonic Ring Resonators

P. C. Allilomes[1], **C. L. Zekios**[1], **S. Iezekiel**[2], **and G. A. Kyriacou**[1]

[1]Microwaves Lab., Department of Electrical and Computer Engineering
Democritus University of Thrace, Xanthi, Greece
[2]Department of Electrical and Computer Engineering, University of Cyprus, Cyprus

Abstract— Open dielectric resonators in general are one of the most widely used basic components of a photonic system. For example whispering gallery mode resonators (WGRs) play a key role in a number of passive (e.g., Filters) and active (e.g., Modulators, spiral microlasers) photonic devices [1]. Besides its widespread utilization, the lack of robust simulation technique able to cope with this open type of resonator with excessively high quality factors has led the designers to confine themselves to simple geometries where classical analytical techniques like the separation of variables can be applied. Accurate numerical simulation of arbitrarily shaped dielectric resonators might produce a set of design rules and give a change to shapes other than spheres, cylinders and torroides to be utilized as WGRs in photonics. However, it is a very challenging task. For the time being, utilization of classical numerical techniques like Finite Difference in Time Domain (FDTD) has been proven inaccurate even on simple shaped WGM [2]. Moreover, more accurate Boundary Integral Equation (BIE) formulations are contaminated with false eigenvalues (spurious modes) and, in general, are not combined with robust non-linear eigenvalue solvers able to calculate efficiently a chosen spectrum of eigenvalues [4]. Indeed the nonlinearities appear first of all due to the open radiating boundaries, e.g., [3] of the cavity and in general due to nonlinear material properties [5], as well as through the Floquet terms when periodic structures are considered.

Relatively recent advances on nonlinear eigenanalysis algorithms have shown that it is numerically feasible to attack a nonlinear eigenvalue problem of large dimensions [6]. Combining these nonlinear eigenvalue solvers with robust numerical technique like the Finite Element (FEM) and the BIE could lead to efficient eigensolvers capable to handleWGM and in general open dielectric cavities. Indeed, herein the performance and behavior of nonlinear eigenanalysis algorithms on formulation based on the Finite Element Method (FEM) is investigated. In the proposed algorithm technique like the tree-co tree splitting [7] and formulations based on the Discontinuous Galerking method [8] for the suppression of non-physical solution, the enhancement of the numerical stability and efficiency, is incorporated. Moreover an accurate (global) mesh truncation techniques is incorporated and refined for the case of eigenvalue problem. In the nonlinear case deflation of the eigenvectors is not possible as in the linear case, thus approximate linear formulations (corresponding to closed geometries) able to reveal the spectrum of the resonator and serve as an initial starting point of the nonlinear algorithm are also considered, e.g., [3].

ACKNOWLEDGMENT

This work was financially supported by the Greek Ministry of Education, Lifelong Learning and Religious Affairs through the research project THALIS Design Techniques for Digitally Controlled RF-Microwave Structures Appropriate for Software Defined — Cognitive Radio (RF-EIGEN-SDR).

REFERENCES

1. Yao, J., "Microwave photonics," *Journal of Lightwave Technology*, Vol. 27, No. 3, 314–335, Feb. 2009.
2. Boriskin, A. V., S. V. Boriskina, A. Rolland, R. Sauleau, and A. I. Nosich, "Test of the FDTD accuracy in the analysis of the scattering resonances associated with high-Q whispering-gallery modes of a circular cylinder," *Opt. Soc. Am. A*, Vol. 25, No. 5, 1169–1173, 2008.
3. Allilomes, P. C. and G. A. Kyriacou, "A nonlinear finite-element leaky-waveguide solver," *IEEE Transactions on Microwave Theory and Techniques*, Vol. 55, 1496–1510, Jul. 2007.
4. Smotrova, E., V. O. Byelobrov, T. M. Benson, J. Ctyroky, R. Saulean, and A. I. Nosich, "Optical theorem helps understanding thresholds of lasing in microcavities with active regions," *IEEE Journal Quantum Electronics*, Vol. 47, No. 1, 20–30, Jan. 2011.
5. Vernooy, D. W., V. S. Ilchenko, H. Mabuchi, E. W. Streed, and H. J. Kimble, "High-Q measurements of fused-silica microspheres in the near infrared," *Opt. Lett.*, Vol. 23, 247–249, 1998.

6. Voss, H., "An Arnoldi method for nonlinear eigenvalue problem," *BIT Numerical Mathematics*, Vol. 44, No. 2, 384–401, 2004.
7. Venkatarayalu, N. V. and J. Lee, "Removal of spurious DC modes in edge element solutions for modelling three-dimensional resonators," *IEEE Transactions on Microwave Theory and Techniques*, Vol. 54, No. 7, Jul. 2006.
8. Perugia, I., D. Schotzau, and P. Monk, "Stabilized interior penalty methods for the time-harmonic Maxwell equations," *Computer Methods in Applied Mechanics and Engineering*, Vol. 191, Nos. 41–42, 4675–4697, Sept. 2002.

Ultra-wideband Radio Frequency Beamforming Using Microwave BFNs

F. E. Fakoukakis[1], **T. N. Kaifas**[2], **and G. A. Kyriacou**[1]

[1]Department of Electrical and Computer Engineering
Democritus University of Thrace, Xanthi 67100, Greece
[2]Department of Physics, Aristotle University of Thessaloniki, Thessaloniki 54124, Greece

Abstract— Radio frequency systems have been used in a large variety of applications, such as communications, military, aviation and atmospheric (ionospheric) research. Throughout the years, the need for wideband operation has become more intense, since systems' requirements demand broadband operation in multiple octaves. Many radio frequency systems use phased arrays (or multibeam antennas) for transmit/receive operation, exploiting beamforming and directional beam-steering. This necessity became inevitable with the current trend towards Software Defined Radio (SDR) and its ultimate form the Cognitive Radio (CR). Their concepts ask for digitally (software) controllable and multifunctional radio frequency front-ends. Regarding the antenna this demand is translated to ultra-wideband structures able to precisely control their beam direction and radiation pattern shaping, but should be miniaturized to yield compact structures conformably integrated over the device package (e.g., mobile unit). Thus, a wideband phased array must be integrated in the system. However, nontrivial difficulties arise when trying to design a wideband array, since the operation frequency band of the components is always limited. Despite that, quite enough wideband systems have been operated, presenting an operational frequency range of a few octaves.

In the present research effort, a new technique of ultra-wideband radio frequency beamforming fulfilling SDR or CR specifications will be presented, based on the recently introduced microwave photonics techniques. In microwave photonics systems, a microwave signal is translated to optical or THz regime, where it undergoes the required processing. That is, the microwave signal modulates an optical one and is processed, e.g., splitted into multiple channels each one delayed appropriately, while it is then demodulated usually by simple PIN diodes. The use of an optical signal as a carrier allows for the use of ultra-wideband microwave signals, which occupy a very small fraction (percent) of bandwidth at these high optical frequencies, thus operational bandwidth extends to many GHz. That means that an ultra-wideband microwave signal can be used, without the need for wideband techniques. Regarding microwave phased arrays, the microwave signal modulates an optical carrier which is in turn split into a number of channels equal to the number of the antenna elements. The optical signal in each channel undergoes the desired phase shift, which is the same independently of the microwave frequency, within a multiple GHz band, thus introducing the precious "true time delay" (TTD). The signal of each channel is then demodulated by a simple PIN diode, amplified accordingly and fed to the corresponding antenna element. A similar approach is followed in the receiver phased array.

According to the above method, we study and present a corresponding technique for ultra-wideband radio frequency systems using a microwave signal as a carrier. The aim of the research is to develop such techniques for ultra-wideband radio frequency systems in general and not just for modulation. More explicitly, small fractional bandwidth (e.g., 10%) of a microwave signal with a center frequency of several GHz presents an operational bandwidth of multiple hundreds of MHz. The bandwidth of the modulating radio frequency signal is just a small fraction of the microwave signal operational bandwidth. Thus, using the microwave signal as a carrier offers multiple octaves of radio frequency operation, leading to an ultra-wideband system.

The general design idea of the technique will be introduced. Both transmit and receive arrays are elaborated following a procedure similar to the microwave photonics approaches. For the transmit function the RF signal modulates a microwave carrier which is in turn split into multiple channels which undergo the desired phase shift by a Butler matrix beamforming network. Crystal detectors (Schottky diodes) are introduced at the network outputs to downconvert the signal to RF. These are cascaded by RF amplifiers and fed to each antenna element. In the receive architecture, the output of each antenna element is upconverted to the same microwave frequency, amplified by a low noise amplifier and applied to the corresponding (output) ports of a Butler matrix. This network provides the appropriate beamforming to yield the desired combined signal at one of its input ports. A downconversion follows to re-establish the synthesized RF signal. The possibility of exploiting the same Butler matrix in both transmit and receive functions will be also examined,

utilizing digitally controllable microwave PIN diode switches. The challenge of the required ultra-wideband antenna elements is more general and is elaborated by a lot of researchers.

Moreover, the design of microwave beamforming networks based on the Butler matrix will be presented. The microwave BFNs are designed without the use of wideband techniques. However, some techniques offering advantages to antenna array systems will be presented, such as sidelobe level reduction and increased beam-steering accuracy. Finally, possibilities of extending the technique to millimeter waves will be studied.

Wideband 1.55 μm Waveguide Photodiodes Employing Planar Resonant Circuits for E-band (60–90 GHz) Operation

Vitaly Rymanov[1], **Sascha Lutzmann**[2], **Merih Palandöken**[2], **Tolga Tekin**[2], **and Andreas Stöhr**[1]

[1]Universität Duisburg-Essen, Lotharstraße 55, Duisburg 47057, Germany
[2]Technische Universität Berlin, Gustav-Meyer-Allee 25, Berlin 13355, Germany

Abstract— The recently regulated 10 GHz bandwidth (71–76 GHz and 81–86 GHz) within the E-band (60–90 GHz) is of particular interest for fixed wireless systems. Since radio-over-fiber (RoF) techniques have opened up the possibility to transmit up to 100 Gb/s in such a wide bandwidth, it is one of the most interesting technologies for ultra-broadband wireless link.

In this work, we will present E-band waveguide photodiodes (PDs) with high external quantum efficiency, which are required for such ultra-broadband RoF links. In detail, we demonstrate advanced partially p-doped, partially non-intentionally doped (PDPN) absorbing 1.55 μm waveguide PDs implemented in a mushroom-type layer structure primarily approaching 71–76 GHz operation within the E-band. Furthermore, a passive optical waveguide (POW) is monolithically integrated in the layer structure and is used for efficient optical coupling. As a result, an extremely flat frequency response with a deviation of less than ±1 dB in the complete E-band is experimentally achieved. Moreover, an output radio frequency (RF) power level exceeding 0 dBm at a photocurrent in the order of ∼ 15 mA is obtained, e.g., at a frequency of 72 GHz. Since no 1 dB compression point is adumbrated, maximum safely working photocurrent levels of ∼ 20 mA are expected for cooled operation. For superlative devices, a DC responsivity of up to 0.5 A/W was actually found even without additional anti-reflection (AR) coating.

For hybrid integration in a wireless E-band transmitter module, the PDs comprise a grounded coplanar waveguide (GCPW) output circuitry employing linearly tapered feeds. Thus, a matched GCPW circuitry with a 50 Ω output impedance is realized. To ensure a return loss exceeding 20 dB for the 70 GHz band operation, additional LC resonant GCPW circuits were studied and modeled using the method of moments (MoM). Applying the designed GCPW circuitries to the devices, the resulting return loss was optimized about 10–20 dB in the frequency range of 70–90 GHz.

Analysis and Design of Ferroelectric Phase Shifters Appropriate for Printed Phased Arrays

A. S. Paraskevopoulos, **C. I. Kolitsidas**, **F. E. Fakoukakis**, **and G. A. Kyriacou**
Microwaves Laboratoty, Department of Electrical and Computer Engineering
Democritus University of Thrace, Xanthi 67100, Greece

Abstract— The trend in mobile communications is clearly moving toward increasing number of communication standards and services which occupy increasingly wide frequency ranges. At the same time the physical dimensions of handheld user devices are shrinking. In order to meet these rapidly increasing demands, the need for directional antennas with different functionalities arises. Such antennas could be implemented in mobile devices or base stations and work together with analogue phase shifters in order to electronically control their performance without changing the geometrical characteristics of the antenna. Many applications of ferroelectric phased array antennas are encountered in smart base station antennas for WLAN and cellular communications, in traffic control and collision-avoidance radars, wireless sensor networks, environmental monitoring and RFID tags. The so called smart antenna applications serving the Space Division Multiple Access (SDMA) is considered herein.

The analogue phase shifter structure that will be used in the present work is based on a multilayer transmission line uniformly loaded with a ferroelectric $BaSrTiO_3$ layer (film) exhibiting its exotic properties at room temperature. By applying a suitable DC electric field between the metallic parts (e.g., strip conductors) of the transmission line, the value of dielectric constant of the ferroelectric layer is controlled and a desired phase shift can be provided. Three different transmission line structures (microstrip, coplanar strips CPS and coplanar waveguide CPW) are investigated and signed in order to choose which provides the better tunability. The advantage of ferroelectric phase shifters is found in fast speed of tuning and lower cost in comparison with semiconductor and ferrite devices, as well as, convenient integration in microelectronic circuits [1–4]. Explicitly, the main advantage of ferroelectric devices is the ability of electronic control through a DC-voltage (just as in a transistor device), instead of the DC magnetic field control required by ferrite devices.

At the next level the phase shifters will feed a microstrip patch antenna array providing different phase shift in each radiating element and, therefore, producing an electronically steerable radiated beam. For this incorporation a CPS/CPW-to-microstrip transition for microstrip antenna feeding may be needed in order to accomplish low insertion and return loss of the network.

A four element phased array antenna based on ferroelectric material is designed with the objective of achieving large phase shifts and a corresponding wide beam steering. Simple rectangular patch antennas are currently considered, but more wideband elements will be tried next as soon as a wideband operation of the ferroelectric phase shifters becomes possible. The simulated results will be extracted using Ansoft HFSS and Agilent ADS.

REFERENCES

1. Gevorgian, S., *Ferroelectrics in Microwave Devices, Circuits and Systems*, 1st Edtion, Springer-Verlag London Limited, 2009.
2. Miranda, F. A., G. Subramanyam, F. W. van Keuls, R. R. Romanofsky, J. D. Warner, and C. H. Mueller, "Design and development of ferroelectric tunable microwave components for Ku- and K-Band satellite communication systems," *IEEE Trans. on Microwave Theory and Tech.*, Vol. 48, No. 7, Jul. 2000.
3. Kirchoefer, S. W., J. M. Pond, H. S. Newman, W.-J. Kim, and J. S. Horwitz, "Ferroelectric-ferrite tunable phase shifters," *2000 IEEE MTT-S International Microwave Symposium Digest*, Jun. 2002.
4. De Flaviis, F., O. M. Stafsudd, and N. G. Alexopoulos, "Planar microwave integrated phase shifter design with high purity ferroelectric materials," *IEEE Trans. Microwave Theory Tech.*, Vol. 45, 963–969, 1997.

Magnetostatic Oscillations for Near-field Microwave Sensing

R. Joffe, E. O. Kamenetskii, and R. Shavit
Microwave Magnetic Laboratory, Department of Electrical and Computer Engineering
Ben Gurion University of the Negev, Beer Sheva, Israel

Abstract— A coupled state of an electromagnetic field with an electric or magnetic dipole-carrying excitation is well known as a polariton. This is a resonant state which appears due to the mixing of a photon with an excitation of a material. In optics, the resonant interaction between plasmon (or electrostatic) oscillations of metal nanoparticles results in strong subwavelength localization of electromagnetic energy. This fundamental effect found important applications for optical near-field sensing. Localized surface plasmon resonance spectroscopy of metallic nanoparticles is a powerful technique for chemical and biological optical sensing [1]. For biomedical diagnostics and pathogen detection, special plasmonic chiral structures are used. These structures may create left- and right-handed optical superchiral fields that effectively interact with large biomolecules, in particular, and chiral materials in general [2]. Can one use the main ideas and results of the optical subwavelength photonics to create microwave photonic structures with subwavelength confinement? Since resonance frequencies of electrostatic (plasmon) oscillations in small particles are very far from microwave frequencies, an answer to this question should be negative. Nevertheless, there exists another type of particles which show strong resonant interactions in microwaves. There are small ferrite particles with magnetostatic (MS) (or MS-magnon) oscillations. Recent studies of interactions between electromagnetic fields and small ferrite-disk particles with MS-magnon oscillations showed strong subwavelength localization of electromagnetic energy in microwaves [3, 4]. This allows realization of near-field sensors for direct microwave characterization of microscopic material structure with application to biology and nanotechnology. Special chiral near-field structures can give an answer to the problem of biomedical diagnostics and pathogen detection of non-thermal microwave effects. In Ref. [5], such microwave near-field structures and their interaction with dielectric materials and chiral objects were demonstrated.

REFERENCES

1. Willets, K. A. and R. P. van Duyne, "Localized surface plasmon resonance spectroscopy and sensing," *Annual Rev. Phys. Chem.*, Vol. 58, 267, 2007.
2. Hendry, E., et al., "Ultrasensitive detection and characterization of biomolecules using superchiral fields," *Nature Nanotechnol*, Vol. 5, 783, 2010.
3. Kamenetskii, E. O., M. Sigalov, and R. Shavit, "Manipulating microwaves with magnetic-dipolar-mode vortices," *Phys. Rev. A*, Vol. 81, 053823, 2010.
4. Kamenetskii, E. O., R. Joffe, and R. Shavit, "Coupled states of electromagnetic fields with magnetic-dipolar-mode vortices: MDM-vortex polaritons," *Phys. Rev. A*, Vol. 84, 023836, 2011.
5. Kamenetskii, E. O., R. Joffe, and R. Shavit, "Microwave near-field helicity and its role in the matter-field interaction," *Phys. Rev. E*, 2011, arXiv:1111.4361.

Session 2A3
Inverse Problems

General Ray Method for Solution of Direct and Inverse Problems of Electromagnetism

Alexandre Grebennikov
Facultad de Ciencias Físico Matemáticas, Benemérita Universidad Autónoma de Puebla
Av. San Claudio y Río Verde, Ciudad Universitaria, CP 72570, Puebla, Pue., México

Abstract— Some actual theoretical and applied problems of electromagnetism can be posed mathematically as direct boundary value problems or inverse coefficient problems for elliptic partial differential equations. There are two main approaches for solving boundary value problems for partial differential equations in analytical form: Fourier decomposition and the Green function method. The numerical algorithms are based on the Finite Differences method, Finite Elements (Finite Volume) method and the Boundary Integral Equation method. All methods and algorithms constructed on the bases of these approaches have some difficulties in realization for the complex geometrical form of the domain. The Green function method is the explicit one, but for arbitrary coefficients of equations it is difficult to construct the Green function even for the simple geometry of domain. Numerical approaches lead to solving systems of linear algebraic equations that require a lot of computer time and memory. Hence, the development of new fast algorithms for solution of the problems under investigation is very actual.

We consider here a new approach for the solution of direct and inverse problems on the base of the General Ray Principle (*GRP*), proposed by the author for the stationary waves field. *GRP* leads to explicit analytical formulas (*GR*-method) for the Dirichlet boundary value problem in an arbitrary convex domain that was constructed by author as fast algorithms with regularization by spline approximation method.

Here we extend the proposed approach to more general type of equations and simple connected star domains for direct boundary problems. We describe also explicit formulas of the *GR*-method for the solution of the coefficient inverse problems for the Laplace type equations. New variants of *GR*-method are realized by fast algorithms and MATLAB software, whose quality is justified by numerical experiments.

Inverse Problems to Determine Constant Permittivity and Coefficient of Nonlinearity in the Problem of TE Wave Propagation in a Layer with Kerr Nonlinearity

D. V. Valovik
Penza State University, 40 Krasnaya Street, Penza 440026, Russia

Abstract— We consider a plane one-layer waveguide structure. The layer is located between two half-spaces with constant permittivities. The permittivity inside the layer is described by Kerr law: $\varepsilon = \varepsilon_2 + \alpha|\mathbf{E}|^2$, where ε_2 is a constant part of permittivity ε and α is a coefficient of nonlinearity, and $\mathbf{E} = (E_x, E_y, E_z)^T$ is the electric field. We suppose that ε_2 and α are unknown constants. The problem is to find these unknown constants. We have incident (I), reflected (R), and transmitted (T) waves. Coefficient I is supposed to be prescribed and R, T are supposed to be measured. We suggest to cut the whole problem into two simpler pieces. To be precise, we suggest to consider (I) a linear layer in order to find ε_2 and then consider (II) a nonlinear layer with known ε_2 in order to find unknown α. For (I) problem we obtain a linear differential equation with boundary conditions. Its solution is easily found and using the boundary conditions we obtain a transcendental equations with respect to ε_2. For (II) problem we obtain nonlinear differential equation with boundary conditions. This equation can be integrated in Weierstrass elliptic functions. Then we obtain a system of algebraic and transcendental equations with respect to α. Equations with respect to ε_2 and α can be studied both analytically and numerically.

Reconstruction of Complex Permittivity of a Nonhomogeneous Body of Arbitrary Shape in a Rectangular Waveguide

Yury G. Smirnov, **Mikhail Yu. Medvedik**, **and Elena E. Grishina**
Penza State University, 40 Krasnaya Street, Penza 440026, Russia

Abstract— We develop a method of solution to the inverse problem of reconstructing the media parameters (complex permittivity) of a body of arbitrary shape in a waveguide. The analysis is based on the use of a volume singular integral equation and its reduction to an equation which can be solved, using iterations, both numerically and analytically. This enables us to determine, for a given single mode rectangular waveguide, the complex permittivity from the measurements of reflection coefficient on different frequencies. The approach also yields the proof of uniqueness of reconstruction of complex permittivity in a rectangular waveguide from the reflection characteristics. The results of test computations performed for the inclusion in the form of a parallelepiped justify the proposed approach.

Using a volume singular integral equation technique elaborated earlier for (forward) diffraction problems in waveguides, we have developed a method aimed at reconstruction of complex permittivity of arbitrarily-shaped body inside a waveguide of rectangular cross-section from the complex reflection coefficient. The approach can be implemented for a cylindrical or rectangular sample and generalized for a waveguide of arbitrary cross-section. The latter implies that the methods presented in this work can be used with data obtained from a variety of laboratory equipment and in a wide range of practical applications.

Numerical results for reconstruction of complex permittivity of arbitrarily-shaped bodies are presented. The comparison of numerical results with measurements of permittivity for well-known materials are also presented. Numerical results are obtained on Supercomputer "Chebyshev" in Scientific Research Center at Moscow State University.

Permittivity Reconstruction of Layered Dielectrics in a Rectangular Waveguide from the Reflection and Transmission Coefficients at Different Frequencies

Yury G. Smirnov and Ekaterina D. Derevyanchuk
Penza State University, Penza, Russia

Abstract— Determination of electromagnetic parameters of dielectric bodies of complicated structure is an urgent problem. However, as a rule, these parameters cannot be directly measured (because of composite character of the material and small size of samples), which leads to the necessity of applying methods of mathematical modeling and numerical solution of the corresponding forward and inverse electromagnetic problems. It is especially important to develop the solution techniques when the inverse problem for bodies of complicated shape is considered in the resonance frequency range. In this paper we develop a method of solution to the inverse problem of reconstructing (complex) permittivity of layered dielectrics in the form of diaphragms in a waveguide of rectangular cross section from the transmission and reflection coefficients measured at different frequencies. The method enables in particular obtaining solutions in a closed form in the case of one-sectional diaphragm. In the case of an n-sectional diaphragm we solve the inverse problem using numerical solution of a nonlinear equation system of n complex variables.

In the case of thin diaphragms we present approximate formulas for complex permittivity of the layers. The comparison analytical results with numerical calculations of reconstructing (complex) permittivity of layered dielectrics are also presented.

Solvability and uniqueness of the system are studied and convergence of the method is discussed. Numerical results of calculating (complex) permittivity of the layers are presented. The case of metamaterials is also considered. The results of solution to the inverse problem can be applied in nanotechnology, optics, and design of microwave devices.

Analysis of Electromagnetic Wave Propagation through a Layer with Graded-index Distribution of Refraction Index

N. B. Pleshchinskii and D. N. Tumakov
Kazan Federal University, Russia

Abstract— Let the plane electromagnetic harmonic wave fall on a layer of some thickness with the known refraction index from a homogenous isotropic medium. It is necessary to find the diffracted field, more precisely, the reflected wave, the transited wave and the field in the layer.

The diffraction problem is reduced to an ordinary differential equation with necessary boundary condition. These conditions are formed by elimination of two semi-infinite domains from the wave guide structure. The case when refraction index (wave number) of a layer monotonically increases and then monotonically decreases is considered here.

The diffraction problem on the layer for some profiles is solved analytically, for other profiles it is researched numerically. The approximate algorithm for the field calculation is proposed and tested. Numerical experiments are carried out. The situations are selected when the maximum of wave energy is reflected or is transited.

The diffraction problem on the layer for some profiles is solved analytically, for other profiles it is researched numerically. The approximate algorithm for the field calculation is proposed and tested. Numerical experiments are carried out. The situations are selected when the maximum of wave energy is reflected or is transited.

Cases of the linear, parabolic, sinusoidal, exponential and logarithmic refractive index profiles of the layer are investigated. The characteristic likeness and specificities of influence of each profile on wave propagation through the graded-index layer are presented.

In the case of elastic waves the problem of wave propagation through non-homogeneous layer can be considered by analogous method but this case is more complicated for the calculus.

Reconstruction of Heterogeneity Parameters by Reflected Field in the Wave Guided Structure

I. L. Aleksandrova, S. V. Baranov, and N. B. Pleshchinskii
Kazan Federal University, Russia

Abstract— We will show that the coefficients of the reflection matrix describing heterogeneities in the plane waveguide with metallic walls can be calculated in the case of limited number of characteristics of the reflected field. To get the additional information it is proposed to use a thin conducting scanning screen placed in front of the investigated heterogeneity.

The transmission problem is an auxiliary problem for scanning screen method. This problem consists of the following. It is necessary to find the electromagnetic field on one side of the heterogeneity if the field is known on another side. The infinite set of linear algebraic equations for the coefficients of the field expansion in terms of eigen waves can be constructed on the basis of set of equations for the diffraction problem. This set of equations is regular, its solution can be obtained by reduction method. The numerical experiments show that the solution of the transmission problem can be found with admissible accuracy but there exist some restrictions on the parameters of wave guided structure.

The properties of the periodical grating of the conducting thin bands used as a scanning screen were investigated by analogous method.

To solve the heterogeneity reconstruction problem the artificial neural network method was used. The model of the multilayer perceptron with one hidden layer consisting of forty neurons was developed. The error of the network response was minimized by Levenberg-Marquardt method. The training set was constructed on the base of numerical solutions of the different variants of diffraction problems. The trained neural network was tested on the set of examples that were not included in the training sample.

Wave Diffraction Problems on Periodical Sets of Heterogeneities in the Stratified Media

I. L. Aleksandrova, E. A. Osipov, N. B. Pleshchinskii, and P. A. Rogozhin
Kazan Federal University, Russia

Abstract— The universal approach to solving the diffraction problems on the periodical set of heterogeneities in the stratified media is proposed. The infinite periodic grating consisting of thin conducting bands embedded into a dielectric plate is considered as an example.

The boundary value problem for the quasi-periodic potential functions is equivalent to the dual summatorial functional equation for the Floquet coefficients. At first, it is advisable to solve the auxiliary diffraction problem for the stratified medium in the case when the heterogeneities are moved off. The heterogeneities generate the field perturbation; it is a solution of a similar dual equation. Secondly, we need to define new unknown variables in such way that the dual equation should have the similar form. To get this result we propose to use the boundary value conditions on the heterogeneities. Then the other conditions on the media interface can be transformed to standard form.

The dual equation is equivalent to regular infinite set of linear algebraic equations for the coefficients of decomposition of the electromagnetic field by Floquet harmonics. By this set of equations the algorithms are constructed for numerical solving the diffraction problem.

In the case of elastic waves the wave diffraction problems on the periodical sets of heterogeneities can be reduced to vector dual summatorial functional equations. Therefore the infinite sets of linear algebraic equations for these problems are complicated.

The electromagnetic wave diffraction problems on the periodical knife grating and on the periodical grating of the heavy bars were investigated by analogous scheme.

Session 2A4
Near to Mid-range Wireless Power Transfer Technology: Principles and Applications 1

Uniform Magnetic Field Resonator for Proximity Wireless Charging System

Young-Ho Ryu, Jae-Hyun Park, Ki Young Kim, Eunseok Park, Keum-Su Song, Chi-Hyung Ahn, Yun-Kwon Park, and Sangwook Kwon
Future IT Research Center, Samsung Advanced Institute of Technology, Yongin 446-712, Korea

Abstract— Recently, wireless power transfer (WPT) technology using magnetic resonance coupling has been actively studied due to its potential applicability of the convenient wireless charging for various electronic/electrical devices. Especially, proximity wireless charging system of pad type for recharging mobile devices is one of very attractive WPT applications and relevant commercial products are expected soon to be available in near future. In the proximity WPT system, the source resonator with uniform magnetic fields needs to be considered because the non-uniform magnetic field distribution of the conventional resonators in the proximate near-field region can cause the variation of the input impedance according to the different positions of the target resonator on the source resonator. To solve this problem, many studies have been suggested in the WPT research areas. In this work, a resonator with uniform magnetic field distribution adopting the field guiding concept has been proposed for proximity wireless charging system. Principle of enhancing/cancelling magnetic field in the resonator has been analyzed by circuit theory and simulation. To confirm the field uniformity, the power transfer efficiency is obtained with simulations and measurements at various positions of target resonator. The proposed concept of the magnetic field uniformity can be suitably applied to the proximity wireless charging system of pad type featuring of high efficiency and equal power distribution to multi-targets.

Magnetic Resonance Wireless Power Transfer over Mid-range with Non-coaxially Aligned Resonators

Ki Young Kim, Young-Ho Ryu, Eunseok Park, Keum-Su Song,
Chi-Hyung Ahn, Jae-Hyun Park, Yun-Kwon Park, and Sangwook Kwon
Future IT Research Center, Samsung Advanced Institute of Technology, Yongin 446-712, Korea

Abstract— Wireless power transfer technology using magnetic resonance coupling has received much attention due to its potentials toward convenient noncontact electric energy supplying manners for various modern electric devices from low-power biomedical implants to high-power electric vehicles. Much effort of analyzing fundamental theory of magnetic resonance coupling as well as realization and standardization issues in industry has been recently made. Since it utilizes non-radiative magnetic near-field, usually the powering distance limitation exists, i.e., the magnetic near-field intensity rapidly decreases on the order of $1/R^3$, where the R is the distance. In order to extend the distance range of wireless powering, a concept of relay resonator placing between source and device resonators has been introduced. Before going through the wireless power link with relay resonator, analysis of misalignment effects between source and device resonators of mid-range wireless power transmission is presented. Some interesting phenomena of the nullification of the power transfer have been experimentally discovered with theoretical prediction, which can be explained by the sign transitions of the mutual inductances. Then, power transfer efficiency of the wireless power link with a relay resonator is investigated, i.e., the cases of various misalignment conditions of relay resonator. Both angular and lateral misalignment cases without the relay resonator have been found to be closely associated with the results of the cases when the relay resonator presents, i.e., the relay resonator is in angular or lateral misalignments with the source and device resonators, while the source and device resonators are face-to-face aligned. Measurement results are also shown with theoretical predictions, both of which are in quite good agreements.

Composite Right-/Left-handed Resonator for Wireless Power Transfer

Jae-Hyun Park, Young-Ho Ryu, Ki Young Kim, Eunseok Park, Keum-Su Song, Chi-Hyung Ahn, Yun-Kwon Park, and Sangwook Kwon
Future IT Research Center, Samsung Advanced Institute of Technology, Yongin 446-712, Korea

Abstract— A resonator using a composite right-/left-handed (CRLH) transmission line is presented for wireless power transfer (WPT) using magnetic resonance coupling. The CRLH resonator has many resonant modes including zeroth order mode and multiple positive/negative modes, which are produced from extraordinary phenomena of metamaterials. An analysis of the resonant modes and a design of the 2-cell CRLH resonator have been performed by theory based on a dispersion diagram. In order to find out suitable resonant mode for efficient WPT among various modes of the CRLH resonator, full-wave simulations of the magnetic field distribution of a 2-cell CRLH resonator have been performed for the zeroth, first positive, and first negative modes. To confirm the characteristics of the WPT system using the resonance modes of the CRLH resonator, experimental measurements were also performed, showing good agreements with the simulation results. Detailed dimensions, quality factors, and WPT efficiencies will be discussed in the presentation.

Automated Adaptive Frequency and Power-level Tracking System for Near- to Mid-range Wireless Power Transfer via Magnetic Resonance Coupling

Nam Yoon Kim, Ki Young Kim, Jinsung Choi, Changwook Yoon,
Dong-Zo Kim, Young-Ho Ryu, Yun-Kwon Park, and Sangwook Kwon
Future IT Research Center, Samsung Advanced Institute of Technology, Yongin 446-712, Korea

Abstract— Due to extensive industrial application areas, wireless power transfer (WPT) technologies over near- to mid-range distances via magnetic resonance coupling have recently received much attention. However, when considering the practical circumstances of a mid-range WPT under the condition of a transfer distance range variation, a significant technical issue has been addressed; the changes in the resonant coupling frequency and input impedance of the wireless power link seen at the transmitter side lead to a degradation of the power transfer efficiency (PTE) and consecutive instability of the entire WPT system. Previous solutions to this problem have mainly focused on frequency and/or impedance tracking techniques based on checking the reflection level at the transmitter to find the optimum coupling frequency with the minimum reflection. Yet, even when the power is transferring at the optimum resonant coupling frequency, there is still a need to regulate the required received power-level, i.e., the optimum amount of power for charging batteries or directly supplying electric/electronic devices. This is because the PTE of a wireless power link can also change with a variation in the transfer distance, which can be an important issue when applying WPT technology to electronic/electric devices with specific power ratings. Accordingly, this work presents an adaptive frequency and power-level tracking system for an efficient and stable WPT based on direct monitoring of the PTE and received power-level via wireless communication. The proposed system is advantageous over other conventional adaptive tracking schemes, since it facilitates link efficiency based on setting reasonable criteria in an adaptive tracking algorithm. In addition, the effectiveness of the proposed automatic adaptive frequency and power-level tracking system was successfully demonstrated using a normal digital LED TV. Thus, it is anticipated that the proposed adaptive tracking solution will be useful for any near- to mid-range WPT application.

Mid-range Wireless Power Transmission System Using Real-time Complex Impedance Control

K. Takei
Hitachi Research Laboratory, Hitachi, Ltd., Japan

Abstract— The magnetic resonant method that uses only magnetic fields are expected to achieve a high-efficient power transmission in mid-range. When the distance between these devices is so large that a part of the transmitting magnetic field is dispersed, the other method that uses both electric and magnetic fields is expected to achieve higher efficiency of the power transmission than that of the magnetic resonant method. The equivalent circuit of a pair of the transmitting receiving antenna is expressed by the 2-port circuit, of which mutual impedance has both imaginary and real parts. Precise calculation of the power transmission efficiency using this 2-port circuit and the power generating and loading circuits with the complex impedances indicates that very high efficiency can be obtained using the special values both of the imaginary and real parts of these complex impedances. Because this value of the real part is very small and limited in a narrow range, the transmitting energy must be stored in a rechargeable battery to activate practical equipments and the real time control of this value is necessary to stabilize power transmission against changes of propagation environments. This report proposes the power transmission system which controls the imaginary and real parts of the impedances in the circuits using the reflection power from the antennas and the modulated signal on the transmitting reactive power, respectively. The numerical and experimental designs of the proposed system show the stable power transmission of which efficiency is up to several tens percents.

Development of Wireless Power Transmission System with Automatic Impedance Matching System for a Toy Helicopter

Jun Ishida[1], **Masayoshi Koizumi**[2], **and Kimiya Komurasaki**[2]

[1]Department of Aeronautics and Astronautics, The University of Tokyo, Tokyo, Japan
[2]Department of Advanced Energy, The University of Tokyo, Chiba, Japan

Abstract— Wireless power transmission with strongly coupled magnetic resonance for an electric powered toy helicopter was challenged. Considering the applications of wireless power transmission to mobile electric devices, evaluation from the viewpoint of receiving system's weight and size is essential. Moreover, to obtain and keep high transmission efficiency while transmission distance is changing, impedance matching is very important. Through this demonstration, these two points are mainly discussed. A light-weight and compact receiver resonator and automatic impedance matching system are developed.

The system consists of an excitation coil, a transmitter resonator, a receiver resonator, a pickup coil and a rectifier circuit. The transmitter resonator is a spiral coil made of a copper wire and the receiver resonator is a single loop antenna using a copper foil for weight saving. Its Q factor was greater than 200 and the weight was 3.8 g.

Impedance on the transmitting side was matched to keep high transmission efficiency and not on the receiving side to reduce the weight of receiver. For impedance matching, the coupled coefficient was automatically tuned between the excitation coil and the transmitter resonator by controlling their relative altitude, using feedback of the reflected wave from the system. Applying this one-side matching system, transmission efficiency was improved by about 10% at short distance compared with the case without automatic impedance matching. Furthermore, the measurement transmission efficiency showed good agreement with the theoretical predictions. A helicopter with a receiver resonator, a pickup coil and a rectifier circuit of 32 g weight was lifted up.

Wireless Power System for Implantable Heart Pumps Based on Energy Injection Control

H. Y. Leung[1], **D. M. Budgett**[1], **D. McCormick**[1], **and A. P. Hu**[2]

[1]Auckland Bioengineering Institute, University of Auckland
Auckland 1142, New Zealand
[2]Department of Electrical and Computer Engineering
University of Auckland, Auckland 1142, New Zealand

Abstract— Inductive power transfer (IPT) for powering high power implantable devices, such as total artificial hearts and heart assist devices, greatly reduces the risk of infection by eliminating the driveline cable which otherwise needs to puncture the skin to provide power. The operating conditions are demanding in terms of the power level, a wide range of coupling variations, restrictions on heat generated and resultant temperature rise in the surrounding tissue. This paper presents a wireless power transfer system which satisfies the requirements for powering a high power implant. The system consists of a half-bridge energy injection circuit which is fully soft-switched. No extra switching or power components are required to regulate the power flow. This is achieved by injecting energy into the tank when required, and allowing the resonant tank to free oscillate when power is sufficient. Feedback from the implanted device is provided via a radio link completing the feedback control loop. The external and internal power transfer coils are air-cored and have a maximum diameter of 75 mm and thickness of 7 mm including the biocompatible encapsulation, making a light and compact transcutaneous energy transfer (TET) system. The presented system is capable of delivering over 15 W to the implanted load over a wide range of coupling variation (k = 0.15 to 0.3) which corresponds to 20 mm to 10 mm coil separation. The system has achieved an end to end power efficiency of 78.7% to 82.2%.

Design of Power Receiver IC for Wireless Resonant Power Transfer

Dong-Zo Kim[1], **Ki Young Kim**[1], **Nam-Yoon Kim**[1], **Keum-Su Song**[1], **Changwook Yoon**[1], **Chi-Hyoung Ahn**[1], **Young-Jin Moon**[2], **Hosoo Park**[1], **Yun-Kwon Park**[1], **and Sangwook Kwon**[1]

[1]Future IT Research Center, Samsung Advanced Institute of Technology, Yongin 446-712, Korea
[2]Department of Electronic Engineering, Hanyang University, Seoul 133-791, Korea

Abstract— The resonant magnetic coupling can significantly enhance the efficiency and transfer distance range of a wireless power transmission (WPT) system and the potential applications of the WPT are currently ranging from mobile charging platform to wireless electric vehicle charging. In this presentation, the high efficient power receiver for system integration of WPT is reported. The proposed receiver IC is composed of full bridge rectifier and DC-DC converter. Since the Schottky diode has lower turn-on voltage drop and fast reverse recovery time, compared with the PN junction diode, our full bridge rectifier has been implemented with four Schottky diodes. The DC-DC buck converter employs the conventional voltage-mode control scheme with type-III frequency compensation for fast transient response. The proposed receiver IC has been fabricated with the 0.35 µm 2P4M BCDMOS technology. The entire die dimension of the designed chip is 5.0 mm × 5.0 mm. The dimension of the full bridge rectifier and the DC-DC converter is identically 2.5 mm × 5.0 mm. The measured efficiencies of the rectifier and the DC-DC converter are ∼ 87% and ∼ 92%, respectively. The fabricated receiver IC is connected to the battery charger of a mobile phone that is equipped with receiving resonator for picking up the magnetic near-field from the source resonator. The overall power efficiency of the wireless power receiver is measured as high as 80% when the resonant coupling frequency is 13.56 MHz at the output power of 2.8 W. The maximum efficiency has been observed at 2.5–2.8 W because the impedance of the receiving resonator is matched to a load impedance (∼ 10 Ω). We have experimentally verified wireless charging performance of the proposed power receiver IC.

Analysis of Power/Ground Resonance Frequency in Printed Circuit Board inside Strong Magnetic Field for Wireless Power Transmission (WPT) System

Changwook Yoon, Nam Yoon Kim, Ki Young Kim, Jinsung Choi,
Dong-Zo Kim, Young-Ho Ryu, Yun-Kwon Park, and Sangwook Kwon
Future IT Research Center, Samsung Advanced Institute of Technology, Yongin 446-712, Korea

Abstract— Wireless power transmission (WPT) system has been very popular to charge high-capacity battery without wires in electrical vehicle (EV). WPT system based on magnetic resonance generates very strong magnetic-field to transfer the energy from a transmitter system (TX) to a receiver system (RX) when both two resonators have same resonant frequency. Although various technologies to guide and shield magnetic-field have been introduced in these days, it is impossible to prevent a leakage of magnetic-field out of enclosure. Therefore, the leakage of magnetic-field inevitably affects other electrical devices inside or nearby electrical vehicle. Even if all individual electrical devices operate well before being equipped, the magnetic-field from WPT system increases an electrical noise inside brings printed circuit board (PCB) and finally brings system malfunctions.

One of main variations caused by magnetic-field is a shift of resonance frequency at power/ground plane to supply electrical power to electrical components in PCB. Worst of all, if an operating frequency meets a shifted resonance frequency, generated noise increases degrades final bit-error rate (BER), signal to noise ratio (SNR) and electromagnetic interference (EMI). Therefore, it is very important to analyze a change of resonance frequency in power/ground plane inside magnetic-field. This paper provides a point up/down of resonance frequencies depending on field strength and direction and analyzes a relation between resonance frequency and magnetic-field.

Wireless Power Transfer in the Condition of Foreign Object Existence

Chi-Hyung Ahn, Young-Ho Ryu, Ki Young Kim, Eunseok Park,
Keum-Su Song, Jae-Hyun Park, Yun-Kwon Park, and Sangwook Kwon
Future IT Research Center, Samsung Advanced Institute of Technology, Yongin 446-712, Korea

Abstract— Wireless power transfer (WPT) based on magnetic resonance has been actively studied not only for its fundamental theory to extend WPT distance, but also for its potentials to apply the technology into numerous consumer electronics products since MIT research team made it to experimentally couple magnetic fields between two resonators in non-radiative near field region. So far, WPT researches in the change of WPT environment are mainly focused on the changes of transfer distance and angular rotation of one resonator. Several techniques such as frequency and impedance tracking have been introduced to compensate the efficiency distortion caused by changed WPT system parameters. However, WPT system performance might be changed more dramatically when foreign objects such as electric/magnetic conductors are located close to resonators. In this presentation, parameter variations of the WPT system in the condition of foreign objects existence are introduced.

Session 2A5
Advanced Mathematical and Computational Methods in Electromagnetic Theory and Their Applications

Plane Wave Diffraction by a Strip with Sinusoidal Corrugation

T. Eizawa[1], **T. Matsuyama**[2], **and K. Kobayashi**[3]

[1]NEC Engineering, Ltd., Japan
[2]Tokai Rika Co., Ltd., Japan
[3]Chuo University, Japan

Abstract— The analysis of the scattering by gratings and periodic structures is important in electromagnetic theory and optics. Various analytical and numerical methods have been developed thus far, and the diffraction phenomena have been investigated for a number of periodic structures [1, 2]. However, the analysis in most of the past works is restricted to periodic structures of infinite extent and plane boundaries. Therefore, it is important to investigate scattering problems involving periodic structures without these restrictions. In this paper, we shall consider a strip with sinusoidal corrugation as an example of periodic structures of finite extent and non-plane boundaries, and analyze the plane wave diffraction for both E and H polarizations using the Wiener-Hopf technique together with the perturbation method. The analysis presented in this paper provides an important extension of the results obtained in our previous paper [3].

The geometry of the problem is shown in Figure 1, where ϕ^i is the incident field of E or H polarization. The surface of the strip is assumed to be infinitely thin, perfectly conducting, and uniform in the y-direction, and it is defined by $x = h\sin mz$ for $|z| \leq a$ where m and h are some positive constants. Assuming that the corrugation amplitude of the strip is small compared with the wavelength, the original problem is replaced by the problem of diffraction by a flat strip with an impedance-type boundary condition. We also expand the scattered field using a perturbation series, and separate the diffraction problem under consideration into the zero- and the first-order boundary value problems. Introducing the Fourier transform for the scattered field and applying boundary conditions in the transform domain, the problem is formulated in terms of the zero- and first-order Wiener-Hopf equations. The Wiener-Hopf equations are then solved via the factorization and decomposition leading to the exact solution. However, the solution is formal in the sense that infinite, branch-cut integrals with unknown integrands are contained. We shall further employ a rigorous asymptotics to derive an explicit, high-frequency solution that is valid for the strip width large compared with the wavelength. Taking the Fourier inverse of the solution in the transform domain and applying the saddle point method, the scattered field in the real space are evaluated asymptotically. Illustrative numerical examples on the scattered far field are presented, and the effect of sinusoidal corrugation is investigated in detail.

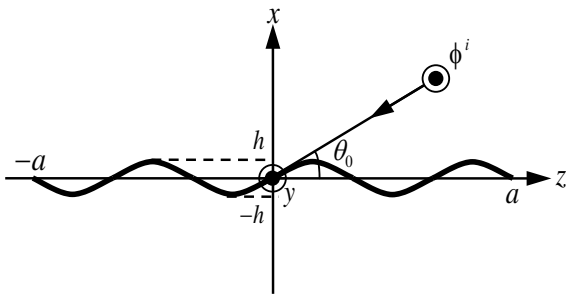

Figure 1: Geometry of the problem.

REFERENCES

1. Shestopalov, V. P., L. N. Litvinenko, S. A. Masalov, and V. G. Sologub, *Diffraction of Waves by Gratings*, Kharkov University Press, Kharkov, 1973 (in Russian).
2. Petit, R., Ed., *Electromagnetic Theory of Gratings*, Springer-Verlag, Berlin, 1980.
3. Kobayashi, K. and T. Eizawa, "Plane wave diffraction by a finite sinusoidal grating," *IEICE Trans.*, Vol. E74, No. 9, 2815–2826, 1991.

Theory of the $\hat{L}_2(\hat{c},\hat{\rho},\hat{n})$ Numbers and Its Application to the Slow Wave Propagation in the Coaxial Ferrite Waveguide

Georgi Nikolov Georgiev[1] **and Mariana Nikolova Georgieva-Grosse**[2]

[1]Faculty of Mathematics and Informatics
University of Veliko Tirnovo "St. St. Cyril and Methodius"
BG-5000 Veliko Tirnovo, Bulgaria
[2]Consulting and Researcher in Physics and Computer Sciences
Meterstrasse 4, Gerlingen D-70839, Germany

Abstract— $L(c,\rho,n)$ and $\hat{L}(\hat{c},\hat{\rho},\hat{n})$ numbers [1, 2] are called the common limits of certain infinite sequences of positive real numbers with terms, proportional to the positive purely imaginary, resp. real zeros of definite functions, constructed by means of four complex, resp. real confluent hypergeometric ones [3] of specially chosen parameters. They came into being in connection with the analysis of normal TE_{0n} and slow $T\hat{E}_{0\hat{n}}$ modes in the coaxial ferrite waveguides with azimuthal magnetization [1, 2]. To distinguish the quantities and functions, connected with the second type of waves, all of which are real, it is accepted above the characters, standing for them, to put hats "ˆ" [1]. Quite recently it has been suggested instead of the notation $L(c,\rho,n)$ to use $L_2(c,\rho,n)$ or the simpler one — L_2 [4]. This allowed to omit in the relevant symbol the parameters on which the numbers depend. In a similar manner, the akin to them $L(c,n)$ ones have been designated as $L_1(c,n)$ or L_1 [4].

In this study the theorem for existence and for the basic properties of the $\hat{L}_2(\hat{c},\hat{\rho},\hat{n})$ ($\hat{L}_2$ or $\hat{L}(\hat{c},\hat{\rho},\hat{n})$) numbers (which could be regarded as a general definition of the latter), is formulated and proved numerically, assuming $\hat{c}$, $\hat{\rho}$ — real, $0<\hat{\rho}<1$ and $\hat{n}$ — restricted positive integer. It is composed of three lemmas. Lemma 1 (Lemma for existence) determines the quantities for any finite $\hat{c}>0$ or $\hat{c}<0$, except for $\hat{c}\neq\hat{l}$, $\hat{l}=0,-1,-2,\ldots$, $0<\hat{\rho}<1$ and $\hat{n}=1,2,\ldots,\hat{t}$. For the purpose, the new real function $\hat{F}_2(\hat{a},\hat{c};\hat{x},\hat{\rho})=\hat{\Phi}(\hat{a},\hat{c};\hat{x})\hat{\Psi}(\hat{a},\hat{c};\hat{\rho}\hat{x})-\hat{\Phi}(\hat{a},\hat{c};\hat{\rho}\hat{x})\hat{\Psi}(\hat{a},\hat{c};\rho\hat{x})$ is advanced in which $\hat{\Phi}(\hat{a},\hat{c};\hat{x})$ and $\hat{\Psi}(\hat{a},\hat{c};\hat{x})$ are the Kummer and Tricomi CHFs, resp. [3], $\hat{a}$, $\hat{c}$, $\hat{x}$ and $\hat{\rho}$ — real, $\hat{a}<0$, $\hat{a}\neq-\hat{m}$, $\hat{m}=1,2,3,\ldots$, $\hat{a}=\hat{c}/2+\hat{k}_-$, $\hat{k}_-$ — real, $\hat{k}_-<0$, $\hat{c}>0$ or $\hat{c}<0$, $\hat{c}\neq\hat{l}$, (in both cases $\hat{a}<\hat{c}$), $\hat{x}>0$, $\hat{\rho}>0$, $0<\hat{\rho}<1$. The positive real zeros $\hat{\chi}^{(\hat{c})}_{\hat{k}_-,\hat{n}}(\hat{\rho})$ of $\hat{F}_2$ in $\hat{x}$ coincide with the roots of characteristic equation of a coaxial ferrite waveguide that sustains slow $T\hat{E}_{0\hat{n}}$ modes [1]. Their number $\hat{n}=1,2,\ldots,\hat{t}$ is a bounded positive integer. Its maximum value $\hat{t}$ is specified by the parameters of the function mentioned. It is proved numerically that if $\hat{k}_-\to-\infty$, the products of $\hat{\chi}^{(\hat{c})}_{\hat{k}_-,\hat{n}}(\hat{\rho})$ by the moduli of $\hat{a}$ and $\hat{k}$ tend to the same finite positive real limit, named $\hat{L}_2(\hat{c},\hat{\rho},\hat{n})$ number. Lemma 2 (Lemma for continuation of the definition at $\hat{c}=\hat{l}$) pays special attention to the case in that the second parameter of the confluent functions is a negative integer or zero. Using numerical means and a limiting process, it extends the definition of the numbers considered for $\hat{c}=\hat{l}$ for which the $\hat{\Phi}(\hat{a},\hat{c};\hat{x})$ has no sense [3]. Lemma 3 (Lemma for the properties) reveals the symmetry of quantities under study with respect to the point $\hat{c}=1$.

It is shown that the $\hat{L}_2$ numbers for $\hat{c}=3$ determine special envelope curves in the phase diagrams of the aforesaid structures at which the characteristics for negative magnetization end [1]. These envelopes serve as a border of the area of propagation of the one of the two possible $T\hat{E}_{0\hat{n}}$ mode — the $T\hat{E}^{(1)}_{0\hat{n}}$ wave from the side of lower frequencies [1].

REFERENCES

1. Georgiev, G. N. and M. N. Georgieva-Grosse, "A property of the $L(c,\rho,n)$ numbers and its application to waveguide propagation," *Proc. XXIX URSI General Assembly*, Chicago, IL, USA, August 7–16, 2008, article ID BK.6(120), 4 pages, in CDROM.
2. Georgiev, G. N. and M. N. Georgieva-Grosse, "Theorem for the $L(c,\rho,n)$ numbers," *PIERS Proceedings*, 1478–1482, Moscow, Russia, August 18–21, 2009.
3. Tricomi, F. G., *Funzioni Ipergeometriche Confluenti*, Edizioni Cremonese, Rome, Italy, 1954.
4. Georgiev, G. N. and M. N. Georgieva-Grosse, "Theory of the L numbers: Definition, computational modeling, properties and application," *Proc. Thirteenth Int. Conf. Electromagn. Adv. Applicat. ICEAA'11*, 544–547, Turin, Italy, September 12–16, 2011, in CDROM, (Invited Paper

in the Special Session "Future challenges in mathematical and computational electromagnetics and its applications" organized by G. N. Georgiev and M. N. Georgieva-Grosse).

Guided Modes of an Open Circular Magnetized Plasma Waveguide in the Resonant and Nonresonant Frequency Ranges

G. A. Markov, **M. G. Shkokov**, **and N. M. Shmeleva**
University of Nizhny Novgorod, Russia

Abstract— Study of open plasma waveguides in an external dc magnetic field is of great importance for many applications including guiding structures in laboratory and ionospheric plasmas, as well as solid-state plasma devices. Although guided waves in such systems were discussed in many publications (see, e.g., [1, 2] and references therein), most works on the subject either deal with analyzing the dispersion properties and field structures of modes of such waveguides in rather limited spectral intervals not containing resonant frequencies or consider only the neighborhoods of these frequencies under some simplifying assumptions. It is the purpose of the present work to study in a systematic manner the characteristics of modes guided by an open circular magnetized plasma waveguide in wide frequency intervals covering both the resonant and nonresonant frequency ranges of a magnetoplasma [2]. Note that by resonant ranges of a cold collisionless magnetoplasma, we understand the frequency intervals in which the refractive-index surface of one of the normal waves extends to infinity at a certain angle between the wave vector and the external dc magnetic field. In nonresonant ranges, on the contrary, the refractive-index surfaces have no such unbounded branches.

We consider axisymmetric and nonsymmetric guided modes of an open plasma waveguide in the form of a circular column placed in free space and aligned with the external magnetic field. It is assumed that the medium inside the column is a two-component cold plasma described by the general dielectric tensor. Using the formulation developed for open magnetized plasma waveguides in [1, 2], we calculate numerically the dispersion characteristics and field structures of the guided modes in a wide frequency band containing the Alfvén and whistler ranges and all basic resonant frequencies of a two-component magnetoplasma. Types of modes and their regions of existence have been determined. The emphasis has been placed on the behavior of the mode dispersion characteristics near the boundaries between these regions, as well as in the vicinity of the resonant frequencies. It is shown that to correctly describe the behavior of modes in these cases, minor collisional losses in the plasma should be taken into account. In addition, the dependences of the propagation constants of nonsymmetric modes on their azimuthal indices have been analyzed in detail. The results obtained are useful in interpreting the data of experiments on wideband excitation and propagation of electromagnetic waves in open magnetized plasma waveguides.

ACKNOWLEDGMENT

This work was supported by the RFBR (project No. 12–02–00904-a), the Government of the Russian Federation (contract No. 11.G34.31.0048), the Russian Federal Program "Scientific and Education Personnel of the Innovative Russia" (contract Nos. P313 and 02.740.11.0565), and the Dynasty Foundation.

REFERENCES

1. Kondratenko, A. N., *Plasma Waveguides*, Atomizdat, Moscow, 1976 (in Russian)
2. Kondratev, I. G., A. V. Kudrin, and T. M. Zaboronkova, *Electrodynamics of Density Ducts in Magnetized Plasmas*, Gordon and Breach, Amsterdam, 1999.

Green's Function for Paraxial Equation

Alexander G. Nerukh[1], **D. A. Zolotariov**[1], **D. A. Nerukh**[2], **and Georgi N. Georgiev**[3]

[1]Kharkov National University of Radio Electronics, 14 Lenin Ave., Kharkov 61166, Ukraine
[2]Non-linearity and Complexity Research Group, Aston University, Birmingham B4 7ET, UK
[3]Faculty of Mathematics and Informatics, University of Veliko Tirnovo "St. St. Cyril and Methodius" BG-5000 Veliko Tirnovo, Bulgaria

Abstract— The theory and experimental applications of optical Airy beams are in active development recently. The Airy beams are characterised by very special properties: they are non-diffractive and propagate along parabolic trajectories. Among the striking applications of the optical Airy beams are optical micro-manipulation implemented as the transport of small particles along the parabolic trajectory, Airy-Bessel linear light bullets, electron acceleration by the Airy beams, plasmonic energy routing. The detailed analysis of the mathematical aspects as well as physical interpretation of the electromagnetic Airy beams was done by considering the wave as a function of spatial coordinates only, related by the parabolic dependence between the transverse and the longitudinal coordinates. Their time dependence is assumed to be harmonic. Only a few papers consider a more general temporal dependence where such a relationship exists between the temporal and the spatial variables. This relationship is derived mostly by applying the Fourier transform to the expressions obtained for the harmonic time dependence or by a Fourier synthesis using the specific modulated spectrum near some central frequency. Spatial-temporal Airy pulses in the form of contour integrals is analysed near the caustic and the numerical solution of the nonlinear paraxial equation in time domain shows soliton shedding from the Airy pulse in Kerr medium.

In this paper the explicitly time dependent solutions of the electromagnetic problem in the form of time-spatial pulses are derived in paraxial approximation through the Green's function for the paraxial equation. It is shown that a Gaussian and an Airy pulse can be obtained by applying the Green's function to a proper source current. We emphasize that the processes in time domain are directional, which leads to unexpected conclusions especially for the paraxial approximation.

A Simple Analytical Method for Describing Important Optical Beams Truncated by Finite Apertures

Michel Zamboni-Rached[1,*] , **Erasmo Recami**[2], **and Massimo Balma**[3]

[1]FEEC, Universidade Estadual de Campinas, Campinas, SP, Brazil
[2]Facoltà di Ingegneria, Università Statale di Bergamo, Bergamo, Italy
[3]SELEX Galileo, San Maurizio, Caselle, Torino, Italy

Abstract— In this work, we present a simple analytical method [1], based on appropriate superpositions of Bessel-Gauss beams [2], which in the Fresnel regime is able to describe the 3D evolution of important waves as Bessel beams, plane waves, gaussian beams, Bessel-Gauss beams, when truncated by finite apertures. At variance with the previous Wen and Breazele's approach [3], which uses a computational method of numerical optimization to obtain gaussian beam superpositions describing truncated beams, and even at variance with Ding and Zhang's approach [4], which is an improved version of Ref. [3], our method does not need any numerical optimizations, nor the numerical solution of any coupled equation systems. One of the byproducts of our mathematical method [1] is that one can get in few seconds, or minutes, high-precision results which normally require quite long times of numerical simulation. The method works in Electromagnetism (Optics, Microwaves, ...), as well as in Acoustics. Below we show a few results obtained through our approach when applied for describing a Bessel beam and a gaussian beam, in the optical regime, both truncated by finite circular apertures. Figures 1 and 2 present the 3D evolutions of the intensities of the truncated Bessel and gaussian beams respectively.

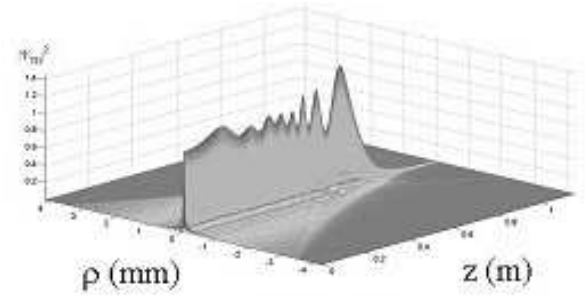

Figure 1.

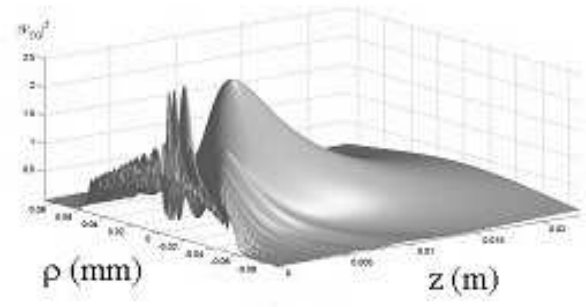

Figure 2.

REFERENCES

1. Zamboni-Rached, M., E. Recami, and M. Balma, "A simple and effective method for the analytic description of important optical beams, when truncated by finite apertures," 2012, arXiv:1203.2604 [phys.gen-ph].
2. Gori, F. and G. Guattari, "Bessel-Gauss beams," *Optics Communications*, Vol. 64, 491–495, 1987.
3. Wen, J. J. and M. A. Breazele, "A diffraction beam field expressed as the superposition of Gaussian beams," *J. Acoust. Soc. Am.*, Vol. 83, 1752–1756, 1988.
4. Ding, D. and Y. Zhang, "Notes on the Gaussian beam expansion," *J. Acoust. Soc. Am.*, Vol. 116, 1401–1405, 2004.

*Corresponding author: Michel Zamboni Rached (mzamboni@dmo.fee.unicamp.br).

A Novel Interactive Approach for Modal Analysis of Nonlinear Waveguides Based on a Fully Hybrid Vectorial Finite Element Method

K. Z. Nóbrega[1] and A. M. F. Frasson[2]

[1]Departamento de Eletro-Eletrônica, Instituto Federal do Maranhão, São Luis, Ma, Brazil
[2]Departamento de Engenharia Elétrica, Universidade Federal do Espírito Santo, Vitória, Es, Brazil

Abstract— An interactive method for solving full anisotropic nonlinear wave guiding problems is presented. To do this, a vectorial finite element scheme using edge/nodal basis element with curved triangle is discussed. Actually, there are two methods commonly used to find the stationary solutions of nonlinear structures. The first one has already been realized using a vectorial formulation but that procedure only computes stable modes, which means that for those situations where bistability effects are present, the solution does not converge and such effects can not be properly discussed. Contrary to the former, the second one has the main characteristic of always reaching convergence, being very useful to describe bistable behaviour and nonlinear switching characteristics, but it has been implemented considering only scalar electromagnetic field modelling. Here, we will describe and present results of a new approach in which its main characteristics are the presence of all electric field components with no need of any adjust parameters, and the possibility to deal with a full nonlinear permittivity tensor.

Kummer Function Method for Analysis of the Azimuthally Magnetized Circular Ferrite Waveguides

Mariana Nikolova Georgieva-Grosse[1] and Georgi Nikolov Georgiev[2]

[1]Consulting and Researcher in Physics and Computer Sciences
Meterstrasse 4, D-70839 Gerlingen, Germany
[2]Faculty of Mathematics and Informatics, University of Veliko Tirnovo "St. St. Cyril and Methodius"
BG-5000 Veliko Tirnovo, Bulgaria

Abstract— The propagation problems of normal TE_{0n} or slow $\widehat{TE}_{0\hat{n}}$ modes in the circular waveguides, containing a co-axially positioned azimuthally magnetized ferrite cylinder (completely or partially filling the geometry) or toroid are one of the challenges of the modern computational electromagnetics [1–8]. Though formulated years ago [9–12], due to their complexity, still they are not solved in sufficient depth. Different approaches have been suggested, aiming at clarifying the phenomena of anisotropic medium-microwave field interaction, based on: *i*) the Bolle-Heller functions [9], *ii*) the transverse network representation [10], *iii*) the perturbation techniques [11], *iv*) the variational calculus [12], *v*) the confluent hypergeometric functions [1–7], *vi*) the Coulomb wave functions [8].

This work presents the main features of the Kummer confluent hypergeometric function method, applicable to configurations in which the cross-section of the anisotropic load is single-connected and involves the structure axis [2, 5, 7]. The cases of normal TE_{0n} and slow $\widehat{TE}_{0\hat{n}}$ wave transmission are considered. It is shown that the relevant wave equation is a form of the Kummer confluent hypergeometric equation [13]. Correspondingly, the field components of the normal modes are expressed in terms of complex and of the slow ones — by real Kummer functions $\Phi(a, c; x)$ and $\hat{\Phi}(\hat{a}, \hat{c}; \hat{x})$, resp. It is accepted for the first (second) of them and for its parameters to use symbols without (with) hats "$\widehat{\ }$". The analysis shows that it holds: $a = c/2 - jk$ — complex, $c = 1$ or $c = 3$ (positive integers) and $x = jz$ — purely imaginary, k, z — real, $-\infty < k < +\infty$, $z > 0$ and $\hat{a}$ — real, $\hat{a} = \hat{c}/2 + \hat{k}$, $\hat{c} = 1$ or $\hat{c} = 3$ (positive integers), $\hat{k}$, $\hat{x}$ — real, $-\infty < \hat{k} < -\hat{c}/2$, $\hat{k} < 0$, $(\hat{a} < 0)$, $\hat{x} > 0$. [The characters without (with) hats stand for both complex and real (only real) quantities. Accordingly, $\Phi(a, c; x)$ $(\hat{\Phi}(\hat{a}, \hat{c}; \hat{x}))$ is complex (real).] A numerical study of the function in question is performed in the complex and real field. An evaluation of the first several zeros of $\Phi(a, c; x)$ $(\hat{\Phi}(\hat{a}, \hat{c}; \hat{x}))$ for $c = 1$ and $c = 3$ ($\hat{c} = 1$ and $\hat{c} = 3$) is also made and the outcomes are given in tabular and graphical form. It is shown that the complex (real) function has an infinite (finite) number n $(\hat{n})$ of zeros. Accordingly, $n = 1, 2, 3, \ldots$, irrespective of the particular values of a and c. $\hat{\Phi}(\hat{a}, \hat{c}; \hat{x})$, however, possesses zeros exclusively, if $\hat{a} < 0$ (if $-\infty < \hat{k} < -\hat{c}/2$, provided $\hat{c} > 0$, and if $-\infty < \hat{k} < \hat{c}/2$, on condition that $\hat{c} < 0$, i.e., in both cases $\hat{k} < 0$). On the understanding that $\hat{c} > 0$ their number $\hat{n}$ depends on $\hat{a}$ only $(\hat{n} = 1, 2, \ldots, \hat{p},\ \hat{p} = abs[\hat{a}])$, while stipulating that $\hat{c} < 0$ and $\hat{a} < \hat{c} < 0$, then it is specified by both parameters of the function $(\hat{n} = 1, 2, \ldots, \hat{s},\ \hat{s} = \hat{p} - \hat{q},\ \hat{p} = abs[\hat{a}],\ \hat{q} = abs[\hat{c}],\ \hat{q} = 1, 2, \ldots, \hat{p} - 1)$, ($[\hat{a}]$ denotes the largest integer less or equal to $\hat{a}$).

The application of results of the investigation in the theory of circular waveguide, entirely filled with azimuthally magnetized ferrite [2, 7], is demonstrated. The most important points of it are: *i*) An infinite (finite) number of normal TE_{0n} (slow $\widehat{TE}_{0\hat{n}}$) modes may be sustained in the structure, equal to the number of roots of the concurring characteristic equations (of the zeros of pertinent wave functions n and $\hat{n}$, resp., in case $c = 3$ and $\hat{c} = 3$). Obviously, in this instance $\hat{n} = 1, 2, \ldots, \hat{p}$, since $\hat{c} > 0$; *ii*) The normal (slow) waves are observed both for positive and negative (exclusively for negative) magnetization of the ferrite filling; *iii*) There are two regions of propagation of the slow waves for different values of the off-diagonal element of ferrite permeability tensor element $\hat{\alpha}$ [2] (two slow waves $\widehat{TE}^{(1)}_{0\hat{n}}$ and $\widehat{TE}^{(2)}_{0\hat{n}}$ might exist for $-1 < \hat{\alpha}^{(1)} < 0$ and $-\infty < \hat{\alpha}^{(2)} < -(2\hat{n} + 1)$; *iv*) The zone of transmission of the normal waves, observed for $-1 < \alpha < 1$ in case of negative (positive) magnetization is bilaterally restricted (is limited from below and unbounded from the side of higher frequencies); *v*) The area of propagation of the slow $\widehat{TE}^{(1)}_{0\hat{n}}$ wave, conforming to $-1 < \hat{\alpha}^{(1)} < 0$, is bounded from the side of lower frequencies; *vi*) The upper limit of the domain in which the normal TE_{0n} mode may get excited coincides with the lower one of the area of existence of the slow $\widehat{TE}^{(1)}_{0\hat{n}}$ mode, when $n = \hat{n}$.

REFERENCES

1. Georgiev, G. N. and M. N. Georgieva-Grosse, "Effect of the dielectric filling on the phase behaviour of the circular waveguide with azimuthally magnetized ferrite toroid and dielectric cylinder," *Proc. Asia-Pacific Microwave Conf. APMC-2009*, article ID WE4B-4, 870–873, in CDROM, Singapore, Dec. 7–10, 2009.
2. Georgiev, G. N. and M. N. Georgieva-Grosse, "Theorem for the identity of the $L(c,n)$ and $\hat{L}(\hat{c},\hat{n})$ numbers and its application in the theory of waveguides," *PIERS Proceedings*, 357–361, Marrakesh, Morocco, Mar. 20–23, 2011.
3. Georgieva-Grosse, M. N. and G. N. Georgiev, "Transmission properties of the circular waveguide, containing an azimuthally magnetized ferrite toroid and a dielectric cylinder," *Proc. 5th Europ. Conf. Antennas Propagat. EuCAP 2011*, 1870–1874, Rome, Italy, Apr. 11–15, 2011.
4. Georgiev, G. N. and M. N. Georgieva-Grosse, "On the confluent hypergeometric functions and their application: Basic elements of the Tricomi theory. Case of waveguide propagation," *Telecomm. and Radioeng.*, Vol. 71, No. 3, 209–216, 2012.
5. Georgiev, G. N. and M. N. Georgieva-Grosse, "Propagation in the circular waveguide, containing an azimuthally magnetized ferrite cylinder and a dielectric toroid," *Proc. 6th Europ. Conf. Antennas Propagat. EuCAP 2012*, article ID P-75, 5 pages, Prague, Czech Republic, Mar. 26–30, 2012.
6. Georgiev, G. N. and M. N. Georgieva-Grosse, "Theory of the $\hat{L}_2(\hat{c},\hat{\rho},\hat{n})$ numbers and its application to the slow wave propagation in the coaxial ferrite waveguide," *Progress In Electromagnetics Research Symposium*, Moscow, Russia, Aug. 19–23, 2012, (in the Special Session: "Advanced mathematical and computational methods in the electromagnetic theory and their applications", organized by M. N. Georgieva-Grosse and G. N. Georgiev), in print.
7. Georgiev, G. N. and M. N. Georgieva-Grosse, "Advanced computational methods for analysis of the circular waveguide completely filled with azimuthally magnetized ferrite: Review of recent results," *Proc. Fourteenth Int. Conf. Electromagn. Adv. Applicat. ICEAA'12 Offshore*, 62–65, Cape Town, South Africa, Sept. 2–7, 2012, in CDROM, (Invited Paper in the Special Session: "Modern problems of mathematical and computational electromagnetics and their advanced applications", organized by M. N. Georgieva-Grosse and G. N. Georgiev).
8. Georgiev, G. N. and M. N. Georgieva-Grosse, "Circular waveguide, completely filled with azimuthally magnetized ferrite," *Wave Propagation*, Academy Publish, Cheyenne, Wyoming, U.S.A., 2012, in print.
9. Bolle, D. M. and G. S. Heller, "Theoretical considerations on the use of circularly symmetric *TE* modes for digital ferrite phase shifters," *IEEE Trans. Microwave Theory Tech.*, Vol. 13, No. 4, 421–426, July 1965; Correction, *IEEE Trans. Microwave Theory Tech.*, Vol. 34, No. 4, 427, Apr. 1986.
10. Clarricoats, P. J. B. and A. D. Olver, "Propagation in anisotropic radially stratified circular waveguides," *Electron. Lett.*, Vol. 2, No. 1, 37–38, Jan. 1966.
11. Eaves, R. E. and D. M. Bolle, "Perturbation theoretic calculations of differential phase shifts in ferrite-loaded circularly cylindrical waveguides in the TE_{01} mode," *Electron. Lett.*, Vol. 2, No. 7, 275–277, Jul. 1966.
12. Lindell, I. V., "Variational methods for nonstandard eigenvalue problems in waveguide and resonator analysis," *IEEE Trans. Microwave Theory Tech.*, Vol. 30, No. 8, 1194–1204, Aug. 1982.
13. Tricomi, F. G., *Funzioni Ipergeometriche Confluenti*, Edizioni Cremonese, Rome, Italy, 1954.

The Electrodynamics of the Induction Motor

Shayak Bhattacharjee
Department of Physics, Indian Institute of Technology Kanpur, Uttar Pradesh 208016, India

Abstract— In this paper we present a new technique for analysing a three-phase induction motor. The technique consists of writing Maxwell's equations for the motor and solving them by an iterative procedure.

Three-phase induction motors are a topic of considerable contemporary interest on account of their versatility and high performance. They are used extensively in industry, railways and more recently in consumer appliances. The standard analytic technique for these motors is the equivalent circuit method [1] where the motor is modelled as a transformer. The parameters in this circuit, i.e., the stator and rotor resistances and inductances, are difficult to determine [2], especially for a cage rotor. A derivation of the cage resistance and inductance may be found in the literature. It uses classical electromagnetism but assumes the rotor to be composed of bars of infinitesimal cross-section thereby approximating the angular current distribution as a set of delta functions. More accurate values of the rotor resistance and inductance are found by experiment — indeed, blocked rotor, no load and similar tests are the primary means of determining the equivalent circuit parameters.

Recently, a calculation [3] has been shown which bypasses circuit theory entirely. That paper uses a crude motor model which we improve significantly in this work. We start by writing Maxwell's equations for the motor in plane polar co-ordinates as the fields are reasonably uniform along its axis. A direct solution is not feasible since we do not know the constitutive equations between electric field and current. We propose an iterative solution starting with the Fourier angular decomposition of the stator and rotor currents. We assume the stator and rotor to be continuous conducting cylindrical shells. Using $J = \sigma E$ with real σ, we find the stator current arising from the applied stator voltage and the magnetic field [4] corresponding to this current. We then calculate the currents induced by this field in the rotor and stator. The key observation is that the moment the induced currents are computed, the expression for the original magnetic field, which was based solely on the applied stator current, becomes inadequate. A correctional term arises from the induced currents. Likewise the corrected field is responsible for inducing currents of its own, and these have to be taken into account. Thus the incorporation of successive correctional terms leads to series developments for the fields and currents; summation of these series yields compact closed form expressions, which we detail below.

Let the rotor have a radius of r, let its conductor have a conductivity σ and a thickness τ, and its core have an effective permeability μ_{eff} near the surface. Let the stator excitation frequency be Ω, the rotor rotation frequency be ω, and the slip frequency $\varepsilon = \Omega - \omega$. The first Fourier harmonic of the net stator current has the form $K_s \sin(\theta - \Omega t)\hat{z}$. We then obtain: the time constant of the rotor circuit is $\tilde{L} = \frac{1}{2}\mu_{\mathit{eff}} r\sigma\tau$, the net rotor current is $K_r = \frac{K_s \tilde{L}\varepsilon}{1+\tilde{L}^2\varepsilon^2}\left(\cos(\theta-\Omega t) - \tilde{L}\varepsilon\sin(\theta-\Omega t)\right)\hat{z}$, the net radial magnetic field at the rotor surface is $B_r = \frac{\mu_{\mathit{eff}}}{2}\frac{K_s}{1+\tilde{L}^2\varepsilon^2}\left(\cos(\theta-\Omega t) - \tilde{L}\varepsilon\sin(\theta-\Omega t)\right)\hat{\rho}$, and the torque output of the motor is $\Gamma = \frac{\pi}{2}\mu_{\mathit{eff}} K_s^2 r^2 h \frac{\tilde{L}\varepsilon}{1+\tilde{L}^2\varepsilon^2}$.

As can be seen, the predictions of our model are in good agreement with those of the standard models.

Our formulae will be useful in predicting the performance of motors on the basis of their geometry. Very few assumptions, and that too very reasonable ones, have been made in our derivation. The formulae will be especially convenient in designing matched motor/drive applications where a priori knowledge of the motor performance can lead to conceptualization of the entire design before beginning with implementation.

REFERENCES

1. Del Toro, V., *Electrical Engineering Fundamentals*, Prentice Hall, New Jersey, USA, 1972.
2. Chapman, S. J., *Electric Machinery Fundamentals,* 4th Edition, Mc Graw Hill, New York, USA, 2005.
3. Bhattacharjee, S., "Analysis of a three-phase induction motor directly from Maxwell's equations," *Am. J. Phys.*, Vol. 80, No. 1, 43–46, 2012.

4. Griffiths, D. J., *Introduction to Electrodynamics,* 3rd Edition, Pearson Education, Saddle River, New Jersey, USA, 2008.

Scattering of Electromagnetic Waves by Many Thin Cylinders and Creation of Medium with Desired Refraction Coefficient

Mykhaylo I. Andriychuk
Institute for Applied Problems in Mechanics and Mathematics, NASU
Naukova St., 3B, Lviv 79060, Ukraine

Abstract— Electromagnetic wave scattering by many parallel infinite cylinders is studied asymptotically as $a \to 0$, where a is radius of cylinders. It is assumed that centers of cylinders x_m are distributed so that $\mathrm{N}(\Delta) = \ln \frac{1}{a} \int\limits_{\Delta} N(x)dx[1 + o(1)]$, where $\mathrm{N}(\Delta)$ is the number of points $x_m = (x_{m1}, x_{m2})$ in an arbitrary open subset of the plane xOy, the axes of cylinders are parallel to z-axis. The function $N(x) \geq 0$ is given continuous function. An equation for the self-consistent (limiting) field is derived as $a \to 0$. The cylinders are assumed perfectly conducting. Formula for the effective refraction coefficient of the resulting medium is derived.

In spite of fact that there is a large literature related to EM wave scattering by the array of parallel cylinders, the proposed approach has sufficient novelty because of the following points:

- the cylinders are of small radius a, and value of $ka \ll 1$, where k is wave number of media outside of cylinders;
- the solution to the wave scattering problem is considered at $a \to 0$ when the number $M = M(a)$ of cylinders tends to infinity at a suitable rate, distance d between cylinders is much greater than a;
- the proposed approach is a basis for a method for changing the refraction coefficient $n^2(x)$ of resulting medium.

The paper will be organized as follows.

Firstly, we obtain a linear algebraic system (LAS) for finding some numbers that define the solution to some auxiliary problem. We demonstrate here also an integral equation for the effective (self-consistent) field in the medium with $M(a) \to \infty$ cylinders as $a \to 0$. These results are applied to the problem of changing the refraction coefficient of an initial material by embedding many thin perfectly conducting cylinders into it.

Secondly, the numerical results approving the applicability of the proposed asymptotic approach to solve the respective scattering problems are presented. The relative error of obtained LAS is investigated; the optimal parameters of domain D that provide the minimal error for the asymptotic solution are determined. One shown numerically that the refraction coefficient of the resulting media depends on the ratio of parameters M, a, and d in the considerably extent.

The algorithms for computational modeling the wave scattering by many small particles were developed in [1]. The results, presented there, demonstrated the applicability of the asymptotic approach for the correct description of the scattered fields in the presence of the big number of small bodies and possibility to create the media with desired refraction coefficient.

The following numerical experiments are important from the practical point of view:

- to determine the values of geometrical parameters of media (namely M, a, and d) that provide the solution to LAS corresponding to the limiting equation with the desired exactness (e.g., $10^{-3} - 10^{-4}$);
- to investigate the convergence of the LAS obtained by the collocation method and determine the optimal parameters of Dwhich provide such convergence;
- to compare the solution to two LAS and to find the range of parameters that provide more close solutions;
- to determine the values of problem's parameters, which yield obtaining the desired refraction coefficient.

A series of numerical results testifies the ability to use the asymptotical approach to solve the EM wave scattering problem in the media with many embedded cylinders of small radius as well as to create the media with desired refraction coefficient. In particular, a media with negative refraction coefficient can be created.

REFERENCES

1. Andriychuk, M. I. and A. G. Ramm, "Scattering by many small particles and creating materials with a desired refraction coefficient," *Int. Journ. of Comp. Sci. and Math.*, Vol. 3, Nos. 1–2, 102–121, 2010.

Session 2A6
Medical Electromagnetics, Biological Effects, MRI

Protective Effect of 900 MHz Radiofrequency Fields on DNA Damage Induced by γ-radiation in Mice

Yi Cao, Bingcheng Jiang, Jihua Nie, Zhen Zhou, Jie Zhang, and Jian Tong
School of Public Health, Soochow University, Suzhou, Jiangsu 215123, China

Abstract— Protective effect of 900 MHz radiofrequency fields in animal and human cells exposed to ionizing radiation is well documented in scientific literature. We have examined whether 900 MHz radiofrequency fields could protect mice from DNA damage induced γ-radiation. Mice were pre-exposed to 900 MHz RF at 120 $\mu W/cm^2$ power density for 4 hours/day for 1, 3, 5, 7 and 14 days and then subjected to an acute dose of 3 Gy γ-radiation. The primary DNA damage in the form of alkali labile base damage and single strand breaks in the DNA of peripheral blood leukocytes was determined using the alkaline comet assay. The results indicated that the extent of damage in mice which were pre-exposed to RF for 1 day and then subjected to γ-radiation was similar and not significantly different from those exposed to γ-radiation alone. However, mice which were pre-exposed to RF for 3, 5, 7 and 14 days showed progressively decreased damage and was significantly different from those exposed to γ-radiation alone. Thus, the data indicated that RF pre-exposure is capable of inducing adaptive response (AR) to decrease DNA damages induced by γ-radiation, and suggested that the pre-exposure for more than 4 hours for 1 day is necessary to elicit such AR.

Nonlinear Mapping of Electromagnetic Properties to Breast Tissues Using T1-Weighted 3-D MRI Data

A. H. Tunçay and İ. Akduman
Electronics & Communications Department, Istanbul Technical University, Istanbul, Turkey

Abstract— In the last decade, microwave imaging of breasts emerged as an important multidisciplinary research subject concerning bioelectromagnetics and signal processing. There are nearly hundreds of publications on the subject, which in turn stimulated the development of realistic breast phantoms for electromagnetic simulations. The increased interest in breast phantoms resulted in development realistic 3-D breast phantoms extracted from T1-weighted 3-D MRI data [1]. However development of numerical 3-D breast phantoms are still open to improvements in many areas such as effective filtering of MRI data, tissue classification, phantom shape and electromagnetic properties mapping.

In this context, we present an effective and automated method for numerical breast phantom development to be used in microwave breast imaging research. We used T1-weighted 3-D MRI data of anonymous patients' with normal breast tissue (not malignant or abnormal) to get the heterogeneity of the structure. Our work involves the processing of each MRI slice separately than integrate the process results to get efficient results. First we estimate and removed biased field appears on each slice by using the improved and adapted version of the method proposed in [2]. We estimate the bias field exists in each MRI slice by fitting a surface using thin plate spline method and then we filter this corruptive signal from the corresponding images represented by MRI data. After filtering of all slices, we classify the pixel values belong to adipose and glandular tissues in each slice and divide them into seven intervals by using a nonlinear segmentation method based on both histogram and other structural parameters. Seven MRI pixel intensity intervals in each slice are combined together and are related to electromagnetic properties of relative permittivity (ε_r) and conductivity (σ_r) by a smoothing spline function. Electromagnetic properties of the breast tissue are taken from [3] and expanded to desired frequency using Debye parameters. We nonlinearly mapped every pixels intensity value to the appropriate electromagnetic properties. Later, we linearly interpolate the resultant slices of ε_r and σ_r to form a proper breast shape. The resultant numerical phantoms are very satisfying, and the method allows transforming any axial T1 weighted 3-D MRI breast data into conductivity and permittivity distributions.

REFERENCES

1. Zastrow, E., S. K. Davis, M. Lazebnik, F. Kelcz, B. D. Van Veen, and S. Hagness, "Development of anatomically realistic numerical breast phantoms with accurate dielectric properties for modeling microwave interactions with the human breast," *IEEE Trans. on Biomedical Engineering*, Vol. 55, No. 12, 2792–2799, 2008.
2. Jørgensen, F. S., "Segmentation of male abdominal fat using MRI," 11–35, Master's Thesis, Technical University of Denmark, Kongens Lyngby, Denmark, 2006.
3. Converse, M., E. J. Bond, D. V. Barry Veen, and S. C. Hagness, "A Computational study of ultra-wideband versus narrowband microwave hyperthermia for breast cancer treatment," *IEEE Trans. on Microwave Theory and Techniques*, Vol. 54, No. 5, 2169–2180, 2006.

Robust Differential Multifrequency Microwave Biomedical Imaging

L. Jofre, S. Capdevila, M. Guardiola, and G. Roqueta
Universitat Politechnica de Catalunya, Barcelona, Spain

Abstract— Microwave imaging has been a promising technique for biomedical diagnostics for more than 20 years and now is moving towards clinical systems. Recent results on breast cancer and brain stroke detection are confronted the first clinical trials, but to go deeper two main aspects need to be improved: a) robust sensitive algorithms, and b) non-bulky acquisition equipment. This paper proposes a new technique to improve the algorithm reconstruction quality. We propose a new frequency differential linearized (FDL) technique based on the use of the extra information available with the emerging multifrequency measuring techniques. Existing algorithms either are a) quite noise-sensitive quantitative iterative monofrequency (QIM) algorithms [1] or qualitative location UWB algorithms [2].

The proposed technique consists on combining the simplicity and robustness of the linear reconstruction Born-based techniques with the accuracy of the QIM. Based on the wide frequency range measurement availability a frequency stepped reconstruction process is performed. Starting at the lowest frequency where the low object electrical size-contrast may be linearly treated a first image is obtained in both space and spectrum domains. Using a differential approach the next and subsequent frequency space-spectral information are added until completing the whole space-spectrum domains. The technique has been successfully applied to breast models. A comparative study, in terms of accuracy and sensitivity, with existing QIM and UWB techniques will be presented and the different accuracies discussed.

As a preliminary result, Fig. 1 presents the results of the reconstruction of a simple breast model consisting of a small layer of skin, a breast tissue, and a centered tumor like tissue. Table 1 summarizes the permittivity values considered, as well as the retrieved values.

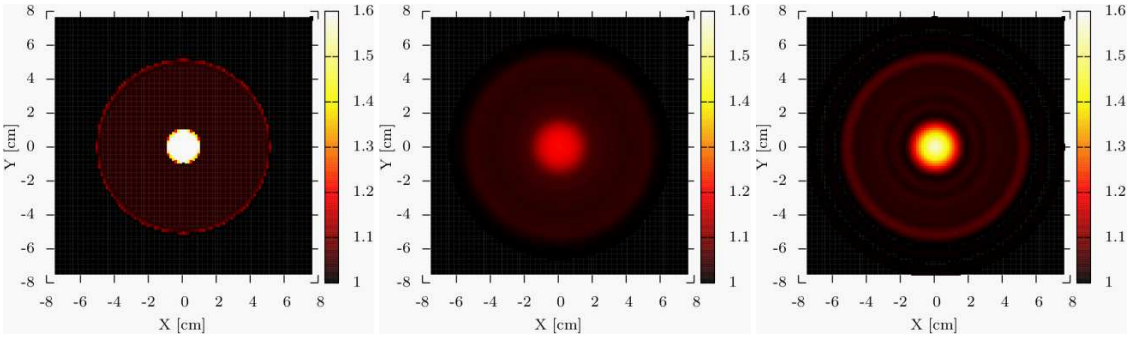

(a) Scenario (b) UWB Coherent (c) Differential Multifrequency

Figure 1: Comparison between (b) a UWB-based algorithm and (c) the proposed multifrequency differential algorithm.

Table 1: Real part of the permittivity retrieved for each algorithm. In the scenario the matching medium (outer permittivity) has a $\varepsilon_r = 33$.

	Scenario	UWB	Differential
Skin	37	34.2	35
Breast	34	39.8	34
Tumor	54	34	51

REFERENCES

1. Bolomey, J. C. and L. Jofre, "Three decades of active microwave imaging achievements, difficulties and future challenges," *IEEE-ICWITS*, 2010.
2. Guardiola, M., L. Jofre, et al., "3D UWB magnitud-combined tomographic imaging for biomedical application," *Radioengineering*, Vol. 20, No. 2, 2011.

Millimeter-wave Dosimetry for bioEM and BAN Applications

Maxim Zhadobov[1], **Nacer Chahat**[1], **Stanislav Alekseev**[2], **and Ronan Sauleau**[1]

[1]Institut d'Électronique et de Télécommunications de Rennes (IETR)
UMR CNRS 6164, Université de Rennes 1, Rennes, France
[2]Institute of Cell Biophysics, Puschino, Russia

Abstract— Recent advances in millimeter-wave technologies have triggered an exponential interest to wireless applications at millimeter waves. Antennas and devices operating in this band have a reduced size compared to their counterparts in the lower part of the microwave spectrum. Furthermore, very high data rates (5 Gb/s, or even beyond) can be reached for short- or long-range communications. The 16 dB/km peak of oxygen-induced absorption around 60 GHz makes this frequency range extremely attractive for secured local communications, particularly in indoor environments, guaranteeing low interference with other wireless services and devices, as well as between adjacent network cells. At the same time, because of the strong atmospheric attenuation, human body has never been exposed to 57–64 GHz radiations in the natural environmental conditions.

60-GHz broadband short-range communications for Wireless Personal Area Networks (WPAN) have been promoted by the Wireless HD Interest Group and WiGig alliance. The current target market applications are mainly restricted to indoor wireless high-definition multimedia devices. Integrated 60-GHz front-ends are expected to be commercialized by 2014 on lap tops. Moreover, recent progress in miniaturization and low-cost devices has triggered research activities aiming at developing future millimeter-wave body area networks (BAN). In such systems, the antennas might be placed directly on the body inducing localized exposures of the superficial body layers. Recently, several research groups have focused on the characterization of the body channel, development of on-body antennas, and integration with already existing devices.

In this context, it is fundamental to analyze millimeter wave/human body interactions from electromagnetic (EM) and thermodynamic viewpoints, as well as the potential biological consequences and their power thresholds. This presentation will make an overview of the state-of-the-art and of the most recent results in dosimetric evaluation of millimeter-wave interactions with the human body. First, we will summarize existing, emerging, and future applications at millimeter waves involving or not interactions with the human body. Second, we will consider the peculiarities of the millimeter waves compared to the lower part of the microwave spectrum from the point of view of interaction with the human body and living systems. Third, different methodological approaches and dosimetric tools (first broadband millimeter-wave phantoms, IR thermometry for multi-physics analysis, etc.) that can be used to quantify the incident power density and SAR at these frequencies will be presented through several representative examples (near-field dosimetry for exposure of human cells *in vitro*, exposure of a human body model by a wearable millimeter-wave antenna). Finally, the most significant dosimetric results for an incident on the human body millimeter wave will be presented and discussed.

ACKNOWLEDGMENT

This work was supported by "Agence Nationale de la Recherche" (ANR), France under Grants ANR-09-RPDOC-003-01 (Bio-CEM project), and by a joint grant of French National Center for Scientific Research (CNRS) and Russian Academy of Sciences (grant No. EDC25185).

Effects of 1800 MHz Microwave on Circadian Rhythm of Testicular Spermatogenic Function in Male Rats

Fenju Qin[1, 2], **Yi Cao**[1], **Jianxiang Li**[1], **Meiju Geng**[3], **and Jian Tong**[1]

[1]School of Radiation Medicine and Public Health
Soochow University, Suzhou 215021, China
[2]School of Chemistry and Biological Engineering
Suzhou University of Science and Technology, Suzhou 215009, China
[3]Experimental Center of Medical College
Soochow University, Suzhou 215021, China

Abstract— Radiofrequency microwave has been shown to interfere with testicular spermatogenic function in animal models, but it remains obscure if the interference may result in alteration of circadian rhythm of the testicular function. To understand this possibility, Male Sprague Dawley rats maintained in 12 hours dark-light cycles were exposed to 1800 MHz Microwave (MW) at 208 $\mu w/cm^2$ power density (SAR: 0.5762 W/kg) at different zeitgeber (ZT) periods of the day, i.e., 0 (ZT0), 4 (ZT4), 8 (ZT8), 12 (ZT12), 16 (ZT16) and 20 (ZT20) hours, 2 hours a day for 32 days. From each rat, the concentrations of plasma testosterone at zeitgeber (ZT2, 6, 10, 14, 18 and 22) were determined. At the same zeitgeber time after the MW exposure, the rats were executed and daily sperm productions (DSP) were determined. The results revealed a circadian rhythm in the synthesis of testosterone with the peak time at ZT 2 in the control rats. DSP didn't show circadian rhythms, but the peak time of was at ZT 23 hour. After exposure to MW, the rhythm of testosterone concentration was disturbed with a distinct effect at ZT 0. Histopathological observation showed more obvious damage to the seminiferous tubules than leydig cells. The results provide with new evidence of chronotoxicity of MW on testicular spermatogenic function in male rats.

Study of Mechanism of Biological Effect of Magnetic-field

Xiao-Feng Pang[1, 2]

[1]Institute of Life Science and Technology
University of Electronic Science and Technology of China
Chengdu, Sichuan 610054, China
[2]International Center for Materials Physics
Chinese Academy of Sciences, Shenyang 110015, China

Abstract— A new mechanism of biological effect of magnetic-field is proposed and established based on the changes of molecular structure and properties of water, which exists widely and abundantly in life body, under influence of magnetic-field, which results in variations of structure and property of biomacromolecules, cell and bio-tissues through the actions of hydrophobicity, hydrophilia and hydration of ions. In order to verify experimentally the correctness of this mechanism we study the distribution of water and its biological functions in life systems, provide the experimental evidences of magnetization of water in a magnetic-field and inspect the really biological effects of magnetized water, respectively. These investigations show that water has important biological functions in life systems, it can interacts with magnetic-field to change its properties and structure of molecules, thus can be magnetized in a magnetic-field, magnetized water has certain magnetism and induces obviously biological effects. In study of biological effect we can conclude the results. Magnetized water restrained the proliferation of SMMC-7221 cells, changed the properties of infrared spectrum and molecular structure of the liver tissue, increases the spleen index, number of leukocyte, index of engulfing of the macrophage and pushed speed of carbon powder, and enhances the activity of SOD in the mice with low immunity, thus the immunity function of the mice is lifted through drinking magnetized water, and decreases numbers of cholesterol, high tangent viscosity of flowing of blood and weight of rats with high blood fat, thus its blood fat index is depressed by magnetized water. Therefore, magnetized water has a obvious biological function. From these investigated results we can finally conclude and affirm that the water in life system is a target of action of magnetic-field, the magnetized water can change the conformation and structure of biomacromolecules, such as proteins and DNA, and of features of bio-tissues and cells, thus a series of biological effect of animals occur under influences of magnetized water. These changes are enough to verify the correctness of the above mechanism of biological effect of magnetic-field.

ACKNOWLEDGMENT

The authors would like to acknowledge the National "973" project of China for financial support (grate No: 212011CB503701)

Wireless Power Transfer Systems: RF Standard Compliance Issues

Andrew W. Wood, **Yohan Jayasinghe**, **and Vitas Anderson**
Bioelectromagnetics Laboratory, BPsyC (H99)
Swinburne University of Technology Hawthorn, Vic 3122, Australia

Abstract— Wireless power transfer (WPT), using magnetically coupled resonators, offers a convenient way of delivering power to electronic equipment without the need for wall sockets and trailing leads. A number of prototypes have been constructed, with reported efficiencies of up to 70% [1]. However, the high values of the electric (E) and magnetic (H) fields in the region between the transmitter and receiver coils, indicate that compliance with international standards for RF exposure could be an issue in practical applications. For example, at 10 MHz, the E and H field ICNIRP limits are 27.4 V/m and 72.9 mA/m respectively (for the general public). Even at 1 W input power, the fields are likely to be well in excess of this. However, the more appropriate metric for to demonstrate compliance is the Specific Absorption Rate (SAR) averaged over 10 g of tissue. This can be estimated by the use of modelling software in relation to a representative human phantom.

In the present study, we have constructed a WPT system similar to that of [1]. We have measured E and H fields around and between the Tx and Rx coils and can confirm that (for 1 W) both fields exceed the ICNIRP limits in most of this region, by a factor of up to 18. We also estimated likely SAR values by constructing an ellipsoidal model of the torso and head using the software FEKO (EMSS, Stellenbosch, South Africa), a Method of Moments (MoM) Maxwell's equations solver. The E and H values predicted by the FEKO model for the WPT system were similar to those measured. For SAR value estimation, the body composition was considered homogeneous, with ε_r and σ values corresponding to 7–10 MHz (133 and 0.41 S/m respectively). High SAR values were obtained within the ellipsoidal phantom when placed near either the Rx or the Tx coil. Between the two coils the SAR values were more modest, for example 0.2 W/kg for an input power of 300 W (which would be appropriate for powering a typical laptop) and Tx-Rx separation of 100 cm. At this input power the SAR limit of 2 W/kg was exceeded for phantom positions close to the Tx coil, but were marginally below for the Rx coil. Assuming that the coils can be enclosed in a physical barrier to prevent close approach to the coils, we can assume that WPT systems will comply with the ICNIRP basic restrictions for practical situations, even though the reference levels are exceeded by a large margin. Homogeneous phantoms are usually assumed to be more conservative than non-homogeneous phantoms, but the effect of including organ-specific electrical parameters will be discussed.

REFERENCES

1. Sample, et al., *IEEE Trans. Indust. Electron.*, Vol. 58, 544–554, 2011.

Effects of 900 MHz Microwave Radiation on Haematopoietic Injueries Induced by Γ-rays

Jian-Xiang Li, Yi Cao, Qian Xu, Zong-Da Jin, Jun Zhang, Min-Xia Lu, Ji-Hua Nie, and Jian Tong
School of Public Health, Medical College, Soochow University, Suzhou, China

Abstract— Exposure of humans simultaneously to microwave and γ-ray is a commonly phenomenon. Previous data showed that low dose microwave radiation increased the survival rate of mice irradiated with 8 Gy γ-ray. However, the mechanisms remain unclear. Present aim is to study the protective effects of microwave pre-exposure on haematopoietic system parameters adversely altered by γ-ray irradiation in mice. Ninety-six male Kunming mice weighing approximately 20 g were randomly divided into 4 groups, including control (C), microwave (M, 120 μW/cm^2), γ-ray (I, 5 Gy ^{60}Co γ-ray), and combined (M + I, microwave + γ-ray). Group C mice were not exposed to γ-ray or microwave radiation. Group M and Group M + I were exposed initially to 900 MHz microwave radiation, 1 hr/day for 14 days. On day 15, Group I and Group M + I were subsequently exposure to 5 Gy ^{60}Co γ-ray irradiation. The pathological changes were quantitatively analyzed at 3, 6, 9 or 12 days after γ-ray exposure. To functionally evaluate microwave-stimulated and -mobilized hematopoietic progenitor cells (HPCs), colony-forming unit-granulocyte macrophage (CFU-GM) of bone marrow was assayed, and the serum levels of GM-CSF, IL-3 were measured with ELISA kits. Our results indicated that pre-exposure to low dose microwaves reduced the damage produced by γ-ray radiation as evidenced by less severe pathological alterations in bone marrow and spleen. The protective effects of microwaves were related to stimulation of hematopoietic growth factors, proliferation of granulocyte-macrophage cells in bone marrow, and inhibition of the γ-ray induced suppression of hematopoietic stem cells/hematopoietic progenitor cells. Data indicate that prior exposure to microwaves is benificial in providing protection against the effects of γ-ray on the haematopoietic system.

Session 2A7
Electromagnetic Modeling, Inversion and Applications

The Stripline Structure with Multilayer Dielectrics by FDTD

Ellen Yoshie Sudo Lutif[1, 2], **Alberto José de Faro Orlando**[1], **and Antonio Carlos da Cunha Migliano**[1, 2]

[1]Aerospace Technological Institute (ITA), CTA, Brazil
[2]Advanced Study Institute (IEAv), CTA, Brazil

Abstract— The past few years have seen tremendous progress in solid state devices used for microwave applications. Many different materials are used to construct microwave components such as transmission lines, filters, capacitors, inductors, and many others. To properly design these microwave components, it is important to know the characteristics of the materials used in fabricating the circuit are very important as any anomalies result in degradation of electrical performance. Characterization of materials at microwave frequencies generally requires finding the properties, which described both conductor and dielectric materials. Conductor materials are described by their conductivity; dielectric materials may be described by their complex permittivity. Full-wave analysis of stripline planar structure with vertical interconnects in multilayer dielectric media is presented. The use of FDTD method for the description of the electromagnetic behavior of the cell discontinuities in the analysis of the S-parameters, input and output impedance and potency at the feeding ports, permits in the 0 GHz–20 GHz frequency band the achievement of a good precision for the results on materials with low electromagnetic characteristics ($\varepsilon_r \leq 10$). The results show that changes in the permittivity could lead to significant changes in the overall performance of the designed circuit.

New Extensive Fermat Principle For Discontinuous Ray In GL Cloak

Jianhua Li[1, 2], **Ganquan Xie**[1, 2], **Lee Xie**[1], **and Feng Xie**[1]

[1]GL Geophysical Laboratory, USA
[2]Hunan Super Computational Science Center, Hunan University, China

Abstract— In this paper, we proposal a new extensive Fermat principle for discontinuous ray in the GL cloak. In our GL cloak, the refractive index $N(r)$ is going to infinite when the radius r is going to inner boundary R_1. the right hand of Eikonal equation is going to infinite, when the radius r is going to inner boundary R_1, the ray died or ray born. The FEM and conventional numerical method can not be used for simulation of the EM full wave propagation in the GL cloak medium. Our GL EM Modeling and inversion are powerful tool for GL EM cloak. The copyright and patents and all rights of the idea and method and software are reserved by authors in GL Geophysical Laboratory.

Simultaneous Joint Inversion of Refraction Tomography and Magnetic Data

M. De Stefano
WesternGeco GeoSolutions, Integrated EM Center of Excellence, Milan, Italy

Abstract— I describe initial results of on-going research on a magnetic inversion algorithm exploiting a novel positivity constraint and a nonlinear conjugate gradients (NLCG) algorithm for the optimization. The inversion unknown is the magnetization amplitude and not the susceptibility directly. The positivity constraint is a double-limiting quasi-linear function that allows performing a constrained optimization with an unconstrained minimization algorithm. I propose also an effective way to integrate magnetic data with refraction tomography data through simultaneous joint inversion (SJI) using a cross-gradients relation. The approach to SJI that I present minimizes, in the least-squares sense, a joint objective function that is the weighted sum of the so-called "single-domain" objective functions and the objective function of a "structural link", which relates unknowns belonging to two different model domains. The structural link is imposed through the requirement to minimize the local cross product of model gradients. This corresponds to requiring parallel gradients in the same spatial positions: because gradients are always perpendicular to shape boundaries, minimizing the cross-gradients link imposes the same shapes at the same spatial positions. Furthermore, the cross-gradients relation, and, in general, any link relation, is evaluated at specific spatial positions without requiring the velocity and the magnetization domains to be sampled on the same grid or model mesh. The benefits of using SJI with respect to separate, single-domain inversions are demonstrated through a synthetic example. As for the case of simultaneous joint inversion of seismic and gravity or seismic and magnetotelluric (MT) data, a seismic-magnetic SJI is effective for complex imaging problems, such as regions with volcanic intrusions or faults. SJI is, in general, able to compensate for poor-quality seismic illumination using another measurement. In this paper, I also discuss possible improvements to the current implementation of the algorithm: for instance, the current magnetic inversion algorithm does not yet take into account remanent magnetization. This limits at the moment its applicability to regions where remanent magnetization is very small or absent.

Data-driving Algorithms for 3D Reconstruction from Ladar Data

Gerard Berginc[1], **Ion Berechet**[2], **and Stefan Berechet**[2]

[1]Thales Optronique S.A., 2 Avenue Gay Lussac, Elancourt Cedex 78995, France
[2]SISPIA SARL, 18 Allée Henri Dunant, Vincennes 94300, France

Abstract— There is a considerable interest in the development of new optical imaging systems that are able to give three-dimensional images. In this paper, we present some considerations concerning the field of three-dimensional laser images where significant technological advances have encouraged research over the past decade. Potential applications range across medical imaging, surveillance and robotic vision. Identifying targets or objects concealed by foliage or camouflage is a critical requirement for operations in public safety, law enforcement and defense.

Synthetic images of three-dimensional objects are based on extraction of laser backscattered signals. The principle of 3D laser radar is based on the use of movable light sources and detectors to collect information on laser scattering, and to reconstruct the 3D object. 3D reconstruction algorithm is a major component in these optical systems for identification of camouflaged objects. But 3D reconstruction must take into account sparse collected data, i.e., concealed objects and reconstruction algorithms must solve a complex multi-parameter inverse problem. Therefore the inverse problem of recovering the surface three-dimensional shape function from intensity data is more challenging. The robustness of identification of three-dimensional reconstructed images is directly related to the inversion algorithms used in the process of identification. Artifacts from the reconstruction algorithms degrade the quality of identification and the object recognition. A notable limitation of numerous methods is that inversion algorithms produce sparse, blurred and noisy three-dimensional images. Therefore, the strategy of inversion must be optimized.

The objective of our paper is to present a new data-driving algorithmic approach for the generation of 3D surface data from sparse 3D point clouds corresponding to the reconstruction algorithm. The role of this type of algorithmic data-driving process is to complete the missing parts of the 3D image at satisfactory levels for reliable identification of concealed objects. In this paper, we present examples of reconstruction and completion of three-dimensional images. The data used in this paper come from experiments or simulations that will be described. The simulations are based on the calculation of the electromagnetic interactions with the different interfaces of the scene of interest. We analyze the different parameters of the identification process such as resolution, scenario of camouflage and we compare the different techniques of completion.

The Generalized n-th Order Maxwell's Equations

F. B. M. Belgacem[1] and R. Silambarasan[2]

[1]Department of Mathematics, Faculty of Basic Education, PAAET, Shaamyia, Kuwait
[2]M. S. Software Engineering, School of Information Technology
V.I.T. University, Vellore, Tamilnadu, India

Abstract— We intend to expand the transversal electromagnetic planar (TEMP) waves travelling in lossy conducting (conductivity $\sigma > 0$) media governed by Maxwell's equations to the n-th order (time t and z-axis). Therefore the existing Maxwell's equations

$$\begin{cases} \dfrac{\partial \mathbf{E}_x(z,t)}{\partial z} + \mu \dfrac{\partial \mathbf{H}_y(z,t)}{\partial t} = 0 \\ \dfrac{\partial \mathbf{H}_y(z,t)}{\partial z} + \epsilon \dfrac{\partial \mathbf{E}_x(z,t)}{\partial t} + \sigma \mathbf{E}_x(z,t) = 0 \end{cases} \tag{1}$$

are expanded as, provided the constants such as permittivity ϵ, permeability μ and conductivity σ are all unchanged (we explained in our major paper)

$$\begin{cases} \dfrac{\partial^n \mathbf{E}_x(z,t)}{\partial z^n} + \mu \dfrac{\partial^n \mathbf{H}_y(z,t)}{\partial t^n} = 0 \\ \dfrac{\partial^n \mathbf{H}_y(z,t)}{\partial z^n} + \epsilon \dfrac{\partial^n \mathbf{E}_x(z,t)}{\partial t^n} + \sigma \mathbf{E}_x(z,t) = 0 \end{cases} \tag{2}$$

Hence the n-th order Maxwell's equations requires the $2n$ initial and n boundary conditions. We then apply the new integral Natural transform

$$\mathbb{N}^+[f(t)] = R^+(s,u) \quad = \quad \int_0^\infty e^{-st} f(ut)dt \ ; \ \mathrm{Re}(s) \in (0,\infty) \ , \ u \in (-\tau_1, \tau_2) \tag{3}$$

with the function $f(t)$ being defined in the set $A = \{f(t) | \exists M, \ \tau_1, \ \tau_2 > 0, \ |f(t)| < Me^{\frac{|t|}{\tau_j}}, \text{ if } t \in (-1)^j \times [0,\infty)\}$. We then explained the derivation of electric $\mathbf{E}_x(z,t)$ and magnetic field $\mathbf{H}_y(z,t)$ solution of the n-th order Maxwell's Eq. (2) under the prescribed initial and boundary conditions. In particular for the electric field $\mathbf{E}_x(z,t)$ we assume the following initial and boundary conditions respectively.

$$\left\{ \lim_{t \to 0} \frac{\partial^i \mathbf{E}_x(z,t)}{\partial t^i} \right\}_{i=0}^{2n-1} = f_0^i(z) \tag{4}$$

$$\lim_{z \to 0} \mathbf{E}_x(z,t) = \begin{cases} \sum_{i=1}^n f_i(t) & \text{if} \quad t \geq 0 \\ 0 & \text{if} \quad t < 0 \end{cases} \tag{5}$$

As an example we described the 2-*nd* order equation by taking $n \equiv 2$ in Eqs. (2), (4) and (5).

REFERENCES

1. Belgacem, F. B. M. and R. Silambarasan, "Theory of the natural transform," *Mathematics is Engg. Sci. and Aerospace (MESA) Journal*, Vol. 3, No. 1, 99–124, 2012.
2. El-Shandwily, M. E., "Solutions of Maxwell's equations for general non-periodic waves in lossy media," *IEEE Transactions Electromagn. Compact.*, Vol. 30. No. 4, 577–582, Nov. 1988.
3. Hussain, M. G. M. and F. B. M. Belgacem, "Transient solutions of Maxwell's equations based on Sumudu transform," *Progress In Electromagnetics Research*, Vol. 74, 273–289, 2007.
4. Silambarasan, R. and F. B. M. Belgacem, "Applications of the natural transform to Maxwell's equations," *PIERS Proceedings*, 899–902, Suzhou, China, Sep. 12–16, 2011.
5. Stratton, J. A., *Electromagnetic Theory*, McGraw Hill Book Company, New York, 1941.

Optimization of the Near-field Optical Force Patterning for Micromanipulation

Víctor Ruiz-Cortés[1] and Demetrio Macías[2]

[1]Departemento de Óptica, División de Física Aplicada
Centro de Investigación Científica y de Educación Superior de Ensenada (CICESE), Russia
[2]Laboratoire de Nanotechnologie et d'Instrumentation Optique
Université de Technologie de Troyes, France

Abstract— We present a study for patterning the optical near-field force by total internal reflection illumination of a rough surface. The surface scattering problem is used together with evolutionary strategies [1]. The input data consists of the force profile exerted upon a micrometer-sized spherical dielectric particle by a near-field optical distribution, and the objective is to reconstruct the surface profile function that produced the data. To simplify the problem, the random surface is assumed to be one-dimensional. The method of calculation is based on the integral equation formalism [2]. The scattering geometry we studied is depicted in Fig. 1(a).

The rough surface inverse scattering problem is approached with a combination of evolutionary strategies. We represented the one-dimensional random surface profile as a spline curve, this allow us to treat more general surfaces and also more general optimization strategies. In Fig. 1(b), we presented the numerical calculation of the near-field distribution scattered by a spherical particle from a rough surface, the circles shown the control points to be represented by a spline curve. Once electromagnetic fields have been calculated, the time-averaged force on the surface particle can be calculated by using the Maxwell's stress tensor.

The optimization of the our cost functional is searched using two versions of the evolutionary strategies; the non-elitist strategy, and the elitist strategy and can be estimated through the discrete difference between the proposed near-field optical force profile and the one obtained by solving the direct scattering problem.

We find that, for the conditions and parameters employed, the surface profile that produces the near-field optical force proposed can be retrieved with high degree of confidence. Some aspects of the convergence and the lack of uniqueness of the solution are also discussed. This concept can offer a convenient way to elaborate extended optical trap landscapes for manipulation of micrometer-sized particles.

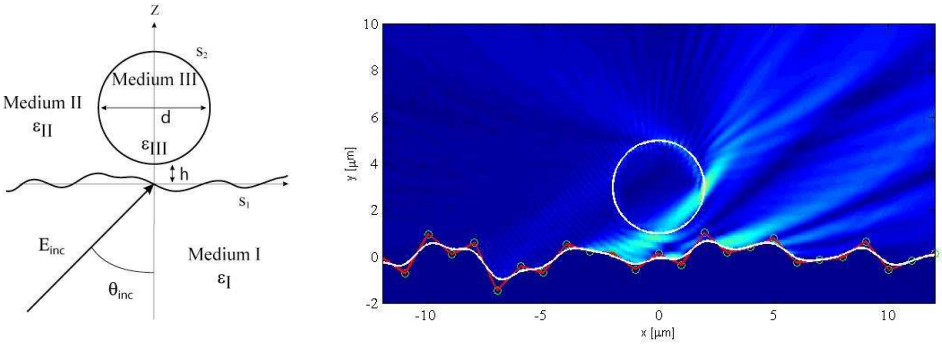

(a) (b)

Figure 1: (a) Schematic diagram of geometry of the scattering problem considered, (b) near-field distribution of a 5 m diameter spherical particle and a rough surface.

REFERENCES

1. Macías, D., G. Olague, and E. R. Méndez, "Hybrid evolution strategy-dowhill simplex algorithm for inverse light scatterimg problems," *Proceedings of the Applications of Evolutionary Computing on EvoWorkshops, 2003: EvoCOP, EvoIASP, EvoSTIM/EvoPLAN*, 399–409, 2003.
2. Maradudin, A. A., T. Michel, A. R. McGurn, and E. R. Méndez, "Enhance backscattering of light from a radom grating," *Ann. Phys.*, Vol. 203, 255, 1990.

Sumudu Characterization of the Maxwell Eigenvalue Problem

Ahmad Alkandari[1], **Jamal Madouh**[1], **and Fethi Bin Muhammad Belgacem**[2]

[1]Department of Electrical Engineering Technology
College of Technological Studies, PAAET, Shuwaikh, Kuwait
[2]Department of Mathematics, Faculty of Basic Education, PAAET, Shaamyia, Kuwait

Abstract— In this paper, we investigate the distinction ensued by adding an eigenvalue Magnetically related forcing term, $\lambda m(z,t)H$, on the ynamics of a planar, transverse electromagnetic (TEMP) wave propagating in the direction z in lossy media with constant permittivity ϵ, permeability μ, and conductivity $\sigma > 0$. In the presence of the magnetic eigenvalue forcing term, the TEMP is then best described by the Modified Maxwell's equations, or Maxwell Eigenvalue Problem,

$$\begin{cases} (i) \ \ \nabla \times \mathbf{E} = -\mu \frac{\partial \mathbf{H}}{\partial t} + \lambda m(z,t)\mathbf{H} \\ (ii) \ \ \nabla \times \mathbf{H} = \epsilon \frac{\partial \mathbf{E}}{\partial t} + \sigma \mathbf{E}. \end{cases} \tag{1}$$

When the source term, $m(z,t) = 0$, various forms of solutions for the electric and magnetic fields have been determined by various authors, using various techniques. Recently, many aspects of Maxwell TEMP Connoted problem were resolved by using the Sumudu transform technique (See for instance, Belgacem, Husein-Belgacem, Rathinavel-Belgacem).

The Sumudu transform technique is not only robust due to its various desirable attributes such as scale and units preserving properties, elaborated upon in the body of the paper, but also it turns out to be user friendly so to speak. In this instance, we use the Sumudu to variationally charecterize the principal eigenvalue of Maxwell's eigenproblem as was done for the Indefinite Ecological problem by Belgacem and Belgacem-Cosner.

The function, $G(u)$, being *the Sumudu of* $f(t)$, is obtained by integartion against the kernel, e^{-t}, as follows,

$$G(u) = \mathbb{S}[f(t)] = \int_{-\infty}^{\infty} f(ut)\, e^{-t} dt, \ u \in (-\tau_1, \tau_2). \tag{2}$$

As an operator, The domain of the Sumudu extends over the set of functions,

$$A = \left\{ f(t) \,/\, \exists\, M, \tau_1, \tau_2 > 0, \ |f(t)| < M e^{\frac{|t|}{\tau_j}}, \text{ if } \ t \in (-1)^j \times [0,\infty) \right\}. \tag{3}$$

For instance, we have, $\mathbb{S}[t^\alpha] = \Gamma(\alpha+1)\, u^\alpha$, $\mathbb{S}[t^n] = n! u^n$, & $\mathbb{S}[\exp(at)] = 1/(1-au)$, for $a \in (-1/a, 1/a)$.

The sumudu operator exhibits very direct convolution, properties, namely, when $M(u)$, and $N(u)$, are the respective sumudi for the functions, $f(t)$ and $g(t)$, with convolution, $(f * g)(t)$, then, the Sumudu of the convolution of the functions, $f(t)$, and $g(t)$, is given by, $S[(f*g)(t)] = uM(u)N(u)$. *In particular, the Sumudu of the anti-derivative,* $(f*1)$, *of the function,* $f(t)$, *is given by,* $uM(u)$. *The Sumudu of the* n'*th derivative,* $f^{(n)}(t)$, *of* $f(t)$, is, $G_n(u) = \frac{G(u)}{u^n} - \sum_{k=0}^{n-1} \frac{f^{(k)}(0)}{u^{n-k}}$.

For, $n = 1$, & 2, we have, $G_1(u) = \mathbb{S}(f'(t)) = \frac{G(u)-f(0)}{u}$, &, $G_2(u) = \mathbb{S}(f''(t)) = \frac{G(u)-f(0)}{u^2} - \frac{f'(0)}{u}$.

Setting, $a = 1/\sqrt{\mu\epsilon}$, $b = \sigma/2\epsilon$, some of the main results obtained via the Sumudu method are,

Theorem 1 [Husein-Belgacem]: *For* $m(z,t) = 0$, *the transient electric field,* $E(z,t)$, *in the TEMP problem as described in (1), is given by,*

$$E(z,t) = e^{-\frac{b}{a}z} f(t - z/a) - a \int_{z/a}^{\infty} f(t-\tau) e^{-b\lambda} \frac{\partial}{\partial z} J_0\left(\frac{b}{a}\sqrt{z^2 - (a\tau)^2}\right) e^{-t/u} d\tau.$$

Theorem 2 [Rathinavel-Belgacem]: *For* $m(z,t) = 0$, *the transient magnetic field,* $H(z,t)$, *in the TEMP problem as described in (1), is given by,*

$$H(z,t) = e^{-\frac{b}{a}z} h(t - z/a) - a \int_{z/a}^{\infty} h(t-\tau) e^{-b\lambda} \frac{\partial}{\partial z} J_0\left(\frac{b}{a}\sqrt{z^2 + (a\tau)^2}\right) e^{-t/u} d\tau.$$

In this work, we extend theorems 1 & 2 to cases where the source term is acting positively (a positive source) and uniformly, $m(x,t) = m > 0$, and distinguish them from cases where the sourcing term, $m = f(x,t) > 0$, is positive but varying in space and/or time. We give a meaning a nomenclature to the various cases and variationally characterize the eingenvalue in each case.

GL Electromagnetic Modeling Scenery Method in the Industrial Design

Jianhua Li[1, 2], **Ganquan Xie**[1, 2], **Qing Xie**[2], **Lee Xie**[1], **and Feng Xie**[1]

[1]GL Geophysical Laboratory, USA
[2]Hunan Super Computational Science Center, Hunan University, China

Abstract— Using the GL electromagnetic modeling simulation, we propose a novel electromagnetic scene plot method in the industrial design. GL method consistent combines the analytical and numerical methods. In the GL method, no big matrix solving to cost massive storage and computational time. No artificial boundary condition and absorption boundary condition needed to truncate the infinite domain to finite domain. The GL EM method is full parallel computational method and available for all frequency, in particular, high frequency. The above advantages of the GL method are over other conventional numerical method and analytical method. Multiple frequencies EM wave laminate the industrial structures to produce novel and beautiful scenery.

Comparison of Microwave Path Lengths between Temperate and Tropical Region Based on Effects of Rain

U. Kesavan[1, 2], **A. R. Tharek**[1], **and Md. Rafiqul Islam**[3]

[1]Wireless Communication Centre, Electrical Engineering Faculty
Technology University of Malaysia, Malaysia
[2]Electrical Engineering Department, Sultan Haji Ahmad Shah Polytechnic, Pahang, Malaysia
[3]Faculty of Engineering, International Islamic Malaysia University, Malaysia

Abstract— Rain is a major source of attenuation for microwave propagation above 7 GHz. The problem of rain attenuation prediction has been studied along the years. In spite of the effort developed in different parts of the world, there are yet some points to be clarified. This problem is quite difficult to be solved, mainly due to the complexity of rain structure. This clearly suggests that reduction factor is the major yardstick for comparing rain attenuation prediction models. However, important parameter need to consider in the path reduction factor is the maximum effective path length for a particular link at specific operating frequency. This paper presents the summary of allowable path length for designing terrestrial microwave link at particular operating frequency at temperate and tropical region. The objective of this paper, to establish the maximum path length or hop length for terrestrial link on line of sight point to point communication at 99.99% of availability. Various frequency band such as 7 GHz, 15 GHz, 23 GHz, 26 GHz and 38 GHz been investigated using the ITU-R path reduction model. From the studies conducted, there are significant differences in path length between temperate region and tropical region. The differences are 22 km, 10 km, 5 km, 4 km and 3 km in the path length for operating frequency 7 GHz, 15 GHz, 23 GHz, 26 GHz & 38 GHz. This paper will provide useful information for microwave engineers and researchers in making valuable decision on path length for any terrestrial links point to point communication operating in a temperate and tropical region in future.

Estimation of Rain Attenuation at C, Ka, Ku and V Bands for Satellite Links in South Africa

S. J. Malinga and P. A. Owolawi
Department of Electrical Engineering
Mangosuthu University of Technology, Umlazi, KwaZulu-Natal, South Africa

Abstract— Despite the fact that over 20 fibre optic cable networks have been rolled out in Africa, satellite infrastructures continue to fulfil an important role in providing communication access to rural, remote and inland areas across the globe. The fast growth in telecommunications, increased demand for bandwidth, congestion in lower frequency bands and miniaturization of communication equipment have forced the designers to employ higher frequency bands such as the C (4 to 8 GHz), Ka (26.5 to 40 GHz), Ku (12–18 GHz) and V (40–75 GHz) bands. Rain is the most deleterious to signal propagation in these bands. The contribution of rain attenuation to the quality of signal in these bands, especially in the tropical and subtropical bands in which South Africa is located, need to be studied. The aims of this paper is to estimate the magnitude of rain attenuation using the ITU-R model, carry out link performance analysis; then propose that fade margin be applied for all provinces in South Africa.

Session 2A8
The Electrodynamics of Inhomogeneous Media and Gradient Metamaterials 2

Pulsed EM Propulsion of Unconventional Flying Objects

A. Meessen
Institute of Physics, Catholic University of Louvain, 1348, Louvain-la-Neuve, Belgium

Abstract— Specific properties of Unconventional Flying Objects of unknown origin were widely documentated in the past, but they seemed to be too mysterious for scientific studies. Indeed, the *propulsion system* of these objects is radically different from those that are familiar to us, since they have neither wings, nor propellers or jet engines. However, we can deduce from observed facts and known physical laws that they ionize the surrounding air and exert forces on the resulting charged particles by means of adequate EM fields. Lift and propulsion result then from the reaction force, but this requires *very intense magnetic fields, oscillating at low frequencies.* Having shown that they can be produced, when the surface of the object is superconducting, we explain here *why these fields are needed and how they act.* This model is confirmed by observations of interactions with water. Observational evidence concerning these fields will follow.

Tunneling of EM Waves in Metamaterials: Gradient Dielectric Nanofilms Vs Plasmonics

A. B. Shvartsburg
Laser Research Center "Pole"
Joint Institute for High Temperatures Russian Academy of Sciences, Moscow, Russia

Abstract— Giant artificial dispersion, both normal and abnormal, of nanogradient photonic barriers, formed by transparent dielectric films with continuous spatial distributions of refractive index across the film, is considered. Controlled non-Fresnel reflectance and transmittance spectra, stipulated by the profound influence of gradient and curvature of refractive index distribution, are examined. Formation of cut-off frequency of transparent barrier, governed by the technologically managed spatial profile of refractive index, is shown to provide the resonant tunneling of EM wave through barrier. Unlike the traditional tunneling through media with negative dielectric susceptibility ε, the new trends in energy and information transfer, arising due to reflectionless tunneling through the barrier with $\varepsilon > 0$, but grad $\varepsilon < 0$, are shown. Ultrafast reshaping of tunneling femtosecond pulse, accompanied by formation of superluminal precursors on the pulse front edge, while the center of gravity of reshaped pulse stays subluminal, is visualized. Applications of these tunneling effects to design of new generation of miniaturized filters, large angle polarizers, frequency-selective interfaces, highly dispersive photonic crystals, broadband subwavelength coatings and reflectors are considered. Scaling of these effects, based on new exact analytical solutions of Maxwell equations, to microwave range is illustrated. Merits of these plasma-like media with artificial characteristic frequency, similar to plasma frequency, are compared with the related plasmonics-based devices.

Quantum Blooming: The Possibility of Passing through the Classically Inaccessible Area without Attenuation

A. S. Kaklyugin
Atmospheric Plasma Instant Technology Corp., Hangenbieten 67980, France

Abstract— Tunneling of a quantum particle through the barrier is known to result in exponential decrease of the amplitude of the penetrated wave and to appearance of the reflected wave. At the same time, the examples of sub-barrier quantum particle penetration without attenuation, e.g., the Bloch functions in the crystal, are known too.

The problem of the quantum barrier blooming by supplementing additional barriers in the form of a local perturbation is formulated. This problem is solved analytically for the simplest case of one-dimensional rectangular potential barrier. The antireflection perturbation in the situation discussed is presented by two singular potential wells. It is proved for specific range of barrier (small barrier) that the effect of blooming takes place for any values of wave number of incident waves and the limitations for barriers out of the range are obtained: in such a case quantum blooming is available only under certain wave number restriction. The blooming possibility for the classically passable barriers as well as blooming providing the penetration over the potential well without scattering, are discussed.

The estimations of amplitude of transmitted wave, when it's wave number or the shape of blooming perturbation are distinguished slightly from the conditions of reflection less tunneling, are performed. This allows us to determine how a plane wave passing through the slightly detuned blooming barrier will behave. So it gives an opportunity to see, how to change the wave packet shape when passing the blooming barrier. It turns out that if the main component of the wave packet propagates without attenuation then the spectral width of the wave packet, traversing the barrier increases and the spatial spreading increases as well.

The analogy of quantum blooming with similar effects in electrodynamics and penetration through the gradient barriers is discussed. The most significant qualitative difference in quantum case is an inability to form the barrier providing total reflection without transmission.

The possibility of blooming generalization for the barriers of arbitrary shape discusses as well. The conditions when singular blooming wells are replaced by regular potential perturbations are considered.

Growth and Investigation of $LiNbO_3$ Thin Films at Nanoscale by Scanning Force Microscopy

D. A. Kiselev, **R. N. Zhukov**, **A. S. Bykov**, **M. D. Malinkovich**, **and Y. N. Parkhomenko**
National University of Science and Technology "MISiS"
Leninskiy pr. 4, Moscow 119049, Russian Federation

Abstract— Thin films of Lithium Niobate (LN) posses a number of advantages over bulk material including the possibilities of producing step index profiles, selectively introducing dopants, and the fabrication of multilayer structures. In addition there are certain applications where only thin films can be used as, for example, when a large refractive index difference between the film and the substrate is necessary. The prospect of producing high quality (oriented and possessing low optical loss) thin films of $LiNbO_3$ on silicon substrates is particularly attractive because the silicon provides a rigid and flat substrate ideal for large area processing of devices by lithographic techniques and it allows for the integration of lithium niobate electro-optic and silicon integrated circuit technology.

In this work, an Atomic Force Microscope (AFM) is used to image the topography and ferroelectric domains in lithium niobate thin films. LN films with a 100 nm thickness were sputtered (radio-frequency (RF) sputtering) onto commercial (100) Si substrates with SiO_2 layer. Such as-deposited films exhibit a granular morphology, without any predominant crystallographic orientation. A typical X-ray diffraction pattern is illustrated that $LiNbO_3$ films deposited through a continuous one-step process are polycrystalline. The surface of the sample shows small grains which diameter ranges from 70 nm to 150 nm and roughness is less than 13 nm. Using the electric field from a biased conducting AFM tip, we show that possible to form and subsequently to visualize ferroelectric domains. We present quantitative study of 180° domain wall motion in LN films, which can be treated as a nearly ideal single-domain environment. The domains were dynamically written by applying voltage pulse magnitude and duration and examined by the piezoresponse force microscope technique. It was shown that the sidewise domain kinetics reveals an activation mechanism of the wall motion in LN films. Also, we report surface charge retention and enhanced ferroelectric polarization effect on ferroelectric thin films by Kelvin probe force microscope.

CRDL Spectrometer for Carbon Dioxide, Nitrogen Oxides, and Methane Monitoring at Technological Medium and Atmosphere Based on Multiwave Optical Resonators with Gradient Mirrors

Oleg D. Volpian[1], **Georgiy A. Ermakov**[1], **Elena A. Voronina**[1], **Alexander G. Marunkov**[2], **and Yuri A. Obod**[2]

[1] "M.F. Stelmakh Research & Development Institute-Polyus"
Federal State Unitary Enterprise, Moscow, Russian Federation
[2]Scientific-Manufacturing Enterprise "Fotron-Auto Ltd."
Moscow, Russian Federation

Abstract— Control the precision analytical processes involving gas component and investigation of climate active gases in the atmosphere requires devices for defining extremely small quantities of gas determination "in situ", i.e., in real time conditions and without probe preparation. In many cases the traces gases determination take place at the unfavorable conditions of high temperature, high or low pressure, and with presence of significant amounts of other interfering gases and compounds. The devices necessary for the cases pointed based on direct, noninvasive and nondestructive method of different gases concentrations with high speed, selectivity and adaptability. At the present work the possibility of such devices is investigated in respect to carbon dioxide, nitrogen oxides, and methane gases. All of them are the climatic active gases playing a vital role at the processes defining the greenhouse effect and global warming.

As it have been shown by some investigations performed in the number of publications, one of the most effective method of carbon dioxide traces measurements in gas mixtures is the CRDLS method (Cavity Ring Down Laser Spectroscopy). The method is based on time decay measurements of laser radiation inside the high-finesse cavity which contains the gas mixture investigated. CRDLS method has two significant advantages. First, the absorption value of the medium directly depends only from the radiation time of attenuation and it does not depend from the intensity fluctuations of the source of light energy. Second, the usage of high-finesse cavity increases the absorption length of the medium examined tremendously — up to several tens kilometers with one meter or lower cavity lengths. These two circumstances combined with very narrow spectral line width of CW laser sources provide the CRDLS method with very high sensitivity (up to $10^{-9}\,\mathrm{cm}^{-1}$ absorption detectability) and spectral selectivity simultaneously at the relatively simple and not expensive experimental equipment.

Experimental investigations of CRDLS method for trace carbon dioxide, nitrogen oxides, and methane gases determination have been performed in our laboratory. The determination of above mentioned gases took place in gas containers at different temperatures and pressures. It has been demonstrated that the CRDLS method allows performing determination of carbon dioxide and methane molecules without standard etalon calibration with sensitivity not less than 10 ppmv and 5ppmv respectively. For the device utilizing that method the way of off-axis excitation of high-finesse resonator was developed which gives the opportunity to simplify the construction, increase reliability and keep the sensitivity of determination. At the first time for CRDLS method it has been developed theoretically and experimentally the usage of multiwave optical resonators based on gradient optical elements. This elements gave an opportunity to improve considerably the working parameters of sensing cavity. Including the extremely high reflected multilayer dielectric mirrors technology and production ($R > 0.9999$) has been developed.

Computational Design for Gradient Optical Films

Oleg D. Volpian[1], **Yuri A. Obod**[2], **and Sergey V. Shkatula**[2]

[1] "M.F. Stelmakh Research Institute-Polus", Federal State Unitary Enterprise, Moscow, Russian Federation
[2] Scientific-Manufacturing Enterprise "Fotron-Auto Ltd.", Moscow, Russian Federation

Abstract— Optical thin film coatings are the important element of photonic apparatus and need sophisticated approaches for their producing. Traditionally, an optical coating design is based on multilayer systems of alternating high n_h and low n_l refraction indexes and presents an interference system of a kind. Certain functional possibilities are given by another type of interference systems based on gradient coatings (e.g., rugate filters), where the refraction index $n(z)$ is gradually, sometimes sinuously, varied across the coating thickness [1, 2].

We have developed a set of programs allowing to calculate the spectral properties of planar thin-film interference structures with continuously varying refractive index across the film thickness (1Dz gradient structure) and synthesize these structures for a given spectral properties. For the maximum approximation of the calculated structures to the real coatings scattering at the boundaries of layers caused by their roughness are included in their computer design, along with absorption and dispersion of the materials. The practice of making high-precision optical and laser coatings shows that even low roughness of the coating layer boundaries has a significant influence on their optical properties and its consideration in the design of coatings has become necessary. We have developed a laser stand for the measurement of small volume and surface scattering of gradient optical coatings and formed the experimental database of input parameters for the design of optical interference coatings on the basis of a physical model that takes into account a small scattering caused by surface roughness.

A heuristic algorithm of global search for an extremum of the objective function has been developed to design the optimal structure of the thin-film interference gradient [3]. A distinctive feature of the algorithm is efficient use of the parameters exchange operator, which implements the recombination of solution-candidates. On the basis of created software new gradient optical coating designs have been constructed providing better spectral characteristics and performance compared with traditional multilayer structures. Examples include narrow-band filter (Fig. 1) reflecting the narrow part of the spectrum with width of 1 nm at a wavelength of 633 nm and transmits all the incident radiation with other wavelengths within the transparency of the materials used, and the polarizer (Fig. 2) separating the s-and p-polarization with high contrast over a wide range of wavelengths ($\Delta\lambda \geq 100$ nm) and angles of incidence ($\Delta\alpha = \pm 3°$). Computer simulation shows that 1Dz gradient structures of polarizing and filtering interference coatings have significant advantages over the spectral characteristics. It is practically impossible to achieve these characteristics of interference polarizers and filters for coatings with a step structure made

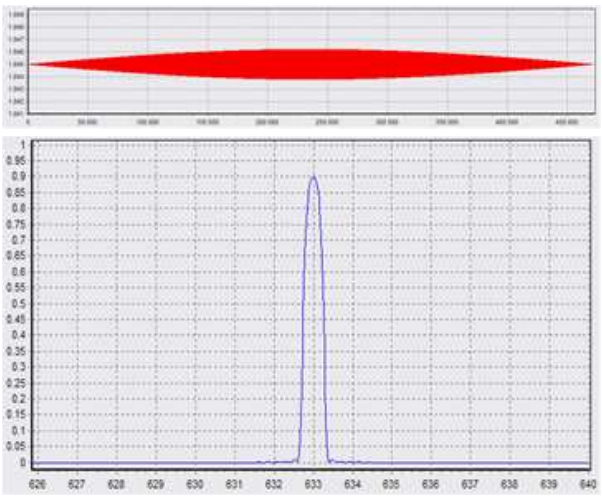

Figure 1: Structure and reflection spectra of narrow-band gradient filter.

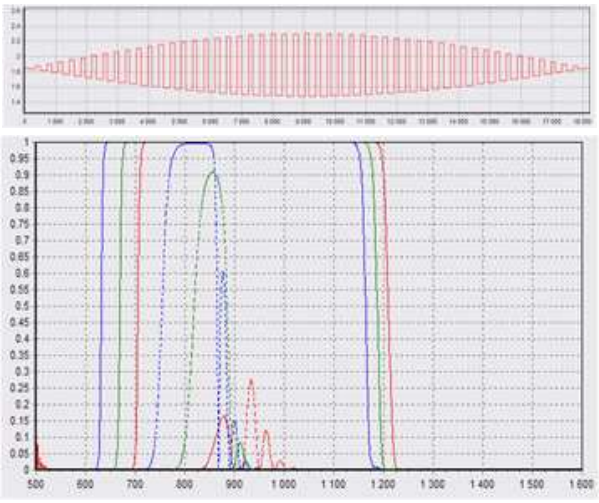

Figure 2: The structure and the reflection spectra of 1Dz gradient polarizer. Red corresponds to the $\alpha = 41°$, green $\alpha = 45°$, blue $\alpha = 48°$.

of available materials. The authors and colleagues developed the technology and automated equipment for construction of 1Dz gradient coatings by dual magnetron sputtering [1, 4, 5].

We carry out researches on software package that allows calculating spectral characteristics of 3Dx, y, z gradient planar metal-dielectric structures with gradients of permittivity and permeability, that significantly enhance the ability of the design of planar thin-film metamaterial films with predetermined properties in the optical region.

REFERENCES

1. Volpian, O. D., A. I. Kuzmichev, Y. A. Obod, and P. P. Yakovlev, "The experience of optical coatings coverage by magnetron method. The problem the gradient coating obtaining," *III International Scientific-Technical Conference*, Vacuum Technology, Materials and Technology, Moscow, 2008.
2. Volpian, O. D., A. I. Kuzmichev, Y. A. Obod, and P. P. Yakovlev, "Optical nanogradient metacoating production by reactive magnetron sputtering," *15th Int. Conf. "High Technology Industry in Russia — Materials and Devices of Functional Electronics and Microphotonics" and the 22-th Int. Symp. "Thin Films in Electronics"*, 447–450, Moscow, 2009.
3. Shkatula, S. V., Y. A. Obod, and O. D. Volpian, "Engineering design methods of nanogradient optical coatings," in the press.
4. Volpian, O. D. and A. I. Kuzmichev, "Magnetron deposition of optical coatings by magnetron power high frequency AC voltage," *Applied Physics*, Vol. 3, 34–51, 2008.
5. Volpian, O. D. and A. I. Kuzmichev, "Pulsed magnetron sputtering application for creation of optical metacoatings with the longitudinal refractive index nanogradient," *Electronics and Communication (Kiev)*, Vol. 2, No. 55, 28–33, 2010.

Surface Induced Refractive Index Variations in Inhomogeneous Slabs

Sergey Sukhov, **Veerachart Kajorndejnukul**, **David Haefner**, **and Aristide Dogariu**
CREOL & FPCE, the College of Optics and Photonics
University of Central Florida, Orlando, FL 32816, USA

Abstract— In the continuous pursuit for materials with unique or exotic properties (antireflection coatings, ideal absorbers, nano-focusing lenses, optical cloaks, etc.), there is a significant interest in characterizing the optical properties of structures and inhomogeneous materials. Often the unusual properties of materials are determined by optical birefringence or gradual change of refractive index. We demonstrate that in arbitrary, inhomogeneous media there are intrinsic surface induced anisotropies and gradual variations of refractive index that should be taken into account. The strength of the anisotropy and the thickness of transition surface layer can be finely tuned to provide means for manipulating the optical properties of nanoscale devices.

Several mechanisms can be singled out that contribute to the surface induced anisotropies in randomly inhomogeneous media having macroscopically isotropic properties. One mechanism relates to the change in local fields near the surface. The local field at the position of some inclusion is determined by surrounding inclusions. The surrounding changes near the surface result in a change of the local dielectric properties. In particular, due to the loss of symmetry, the permittivity (and therefore the effective refractive index) becomes a tensor. Tensorial dielectric properties of the surface region of uniformly inhomogeneous slabs should lead to different values for the effective refractive index corresponding to s- and p-polarized incident waves.

Another mechanism for the surface-induced anisotropy can be simply explained by the interaction between the inclusions and their own images with respect to the surface. This interaction changes the polarizability of inclusions located near the surface and, consequently, modifies the effective properties of the medium. We demonstrate that this effect is significant for metal-dielectric composites.

A proof of concept demonstration of surface induced changes in effective refractive index was demonstrated using numerical methods (finite element software Comsol Multiphysics). Spherical inclusions with dimensions much smaller than the wavelength were distributed inside the volume of a thin slab. The slab was illuminated with a polarized plane wave. The calculations provide the distribution of electric field inside the slab as well as the amplitudes and phases of the reflected and transmitted waves. Averaging over a large number of realizations of the inhomogeneous medium is then done to evaluate the averaged optical properties of the slab.

Knowing all the parameters of the slab (thickness, composition) and the field distribution we can reconstruct the effective refractive indices for s- and p-polarized incident waves. The effective refractive indices differ; the magnitude of this induced birefringence depends on the slab's dimensions, composition, and structural morphology.

Evidence of Very Strong Low Frequency Magnetic Fields

A. Meessen
Institute of Physics, Catholic University of Louvain, 1348, Louvain-la-Neuve, Belgium

Abstract— We showed *why* the propulsion of unconventional flying objects of unknown origin could result from very intense low-frequency magnetic fields and pulsed ionization. We also showed *how* these fields could be produced, if the surface of these objects were superconducting. Here, we present *evidence* of the existence of these fields. It results from traces left on the ground by the induced current, from rotating compass needles, from direct magnetometer recordings and from highly remarkable Faraday effects. Pulsed ionization was revealed by optical refraction, perturbations of the radio navigation system of aircraft, detection of pulsed microwaves and so-called EM effects. This subject calls for scientific scrutiny.

Production of EM Surface Waves by Superconducting Spheres: A New Type of Harmonic Oscillators

A. Meessen
Institute of Physics, Catholic University of Louvain, Louvain-la-Neuve 1348, Belgium

Abstract— It is shown that a superconducting sphere or spherical shell can produce EM surface waves that are stationary at *any* low frequency. This applies in particular to *magnetic dipole oscillations*, generated by a current density **J** that oscilllates around a given axis on the surface of the sphere. In the quasistatic approximation, it creates a synchronously oscillating magnetic field **B**, while the resulting electric field **E** provides feedback to sustain the current. This yields a new type of oscillators, where the magnetic energy is not completely transformed into electric energy as in classical LC circuits. EM energy is conserved, however, by means of energy fluxes. The purpose of this theory is to account for *evidence of very intense magnetic dipole fields*, produced by unconventional flying objects of unknown origin. These observations would make sense and suggest that superconductivity is possible at normal atmospheric temperatures. We also examine the propagation of plasma waves along superconducting surfaces and consider possible pairing mechanisms.

Session 2A9
Poster Session 2

Miniaturized Multi-band Microstrip Antenna Design for Implantable Device Communication

S. Suganthi[1], **D. Kumar**[2], **and S. Raghavan**[3]

[1]Shri Angalamman College of Engineering and Technology, Trichy, India
[2]Periyar Maniammai University, Thanjavur, India
[3]National Institute of Technology, Trichy, India

Abstract— This paper proposes a novel design of a miniaturized microstrip antenna for communication with body implanted antenna. One of the main areas of research in wireless technology is miniature antenna design for microwave communication. The feasibility of implementation of implantable devices in the human body are being studied by many researchers and found increasing with the recent improvements in both engineering and medical technologies. An implantable antenna is a device that is capable of being implanted inside the human body for various sensing applications such as monitoring blood pressure, heart beat, tissues characteristics, treating cancerous cells etc.. This antenna should have the minimum return loss (< -10 dB) for maximum antenna performance. Therefore, the design and simulation of miniaturized microstrip antenna for body implantable antenna communication was carried out using HFSS 3D EM simulation software. This miniature antenna is printed on a FR4 substrate using copper. The near filed pattern and the return loss characteristics are appreciably good. This antenna is found to resonate well in multiple bands in the frequency range from 1 to 10 GHz. The multiple resonances enable applications in GSM, GPS (1.9 GHz), Bluetooth and RFID (2.45 GHz), ISM (902–928 MHz, 2.4–2.483 GHz & 5.725–5.875 GHz) Wi-Fi (lower 2.4–2.48 GHz & higher 5.7–5.98 GHz).

An Ultra-wideband Dielectric Resonator Antenna with Reconfigurable Band Rejection

M. Y. Abou Shahine, **M. Al-Husseini**, **K. Y. Kabalan**, **and A. El-Hajj**
ECE Department, American University of Beirut, Beirut 1107 2020, Lebanon

Abstract— The design of a UWB dielectric resonator antenna with reconfigurable band rejection is presented in this paper. The induced band notch helps to limit interference to a narrowband service operated inside the 3.1–10.6 GHz UWB frequency range. The proposed antenna is designed on a Rogers RO3203 substrate of thickness $h = 1.6$ mm. It is based on a cylindrical dielectric resonator (DR) with a radius of 4 mm and a height of 3 mm. The DR, which is made of TCI Ceramic-K12 material with relative permittivity of 12, is excited by a bevel-shaped patch fed by a microstrip line over a partial ground plane. A rectangular split-ring slot is etched on the patch, as shown in Fig. 1. This slot is responsible for the created notch, whose frequency depends on the dimensions of the slot, as well as on the DR dielectric constant and its position. Notch reconfigurability is attained by rotating the DR to change its position with respect to the patch and the slot. This is achieved by connecting the DR, at point A, to a DC stepper motor placed below the substrate. The stepper motor can be controlled using an FPGA. The idea of rotating parts of an antenna was used in [1]. Fig. 1 shows the DR in position 0. Figs. 2(a) and 2(b) show the DR rotated clockwise by 90 and 180 degrees, respectively.

The antenna is designed and simulated using Ansoft HFSS. The reflection coefficient plots for different rotation angles are shown in Fig. 3, clearly revealing notch reconfigurability over the lower part of the UWB range, where many narrowband systems transmit.

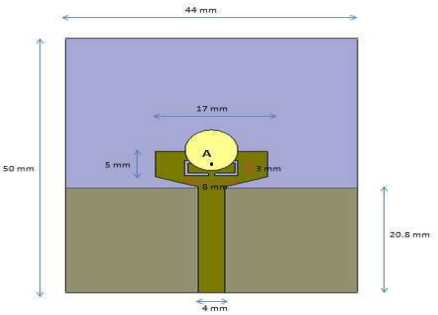

Figure 1: Antenna configuration.

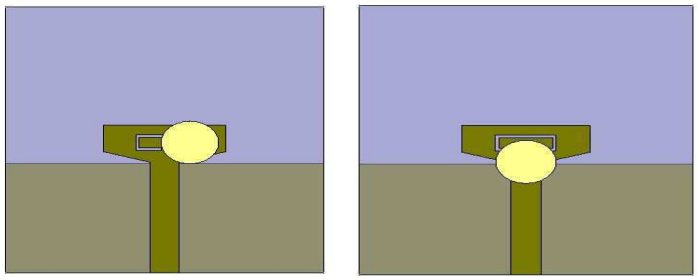

Figure 2: DR rotated by (a) 90°, and (b) 180°.

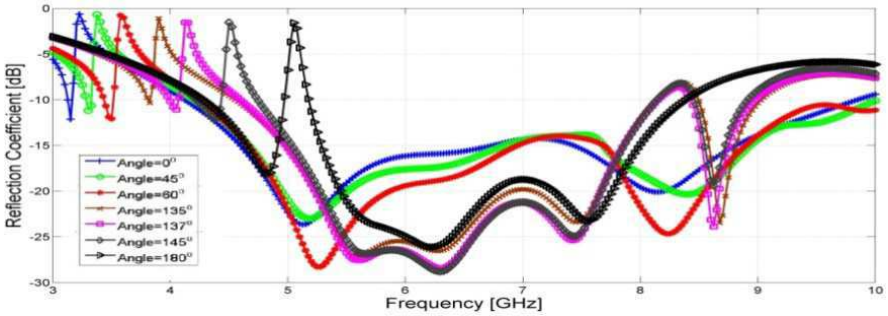

Figure 3: Reflection coefficient of the antenna for different rotation of the DR.

REFERENCES

1. Tawk, Y. and C. G. Christodoulou, "A new reconfigurable antenna design for cognitive radio," *IEEE Antennas and Wireless Propagation Letters*, Vol. 8, 1378–1381, December 2009.

Symmetrical Slot Loaded Dual Band Elliptical Microstrip Patch Antenna

Abdullah Al Noman Ovi[1], **Nandita Saha**[2], **Shuvashis Dey**[2], **and Nuzat Naury Alam**[2]

[1]Department of Electrical and Electronic Engineering
Bangladesh University of Engineering and Technology, Dhaka, Bangladesh
[2]Department of Electrical and Electronic Engineering
American International University of Bangladesh, Dhaka, Bangladesh

Abstract— In this paper, a concept of mode modification to obtain dual band performance in elliptical microstrip patch antenna has been proposed. Previously, mode modification in rectangular microstrip patch antenna was performed by using symmetrical rectangular slots closed to radiating edges [1]. Symmetrical slots were introduced in rectangular microstrip patch antenna to lower the resonant frequency of TM_{030} mode to act like TM_{010} mode and thus dual band antennas were successfully modeled. But implementing this concept in elliptical microstrip patch antenna is a novel idea. In this paper the effect of symmetrical slot in an elliptical microstrip patch antenna is analyzed both theoretically and mathematically. The original TM_{010} mode and the modified TM_{030} mode constitute the dual band and two modes of operations show almost similar radiating properties, with high directivity and gain. The dual band results and their radiation performances are observed using 'CST Microwave Studio' based realistic simulations. The potential application of symmetrical slots in elliptical microstrip patch antenna to obtain dual band may help the researchers to obtain dual band antennas for elliptical patches. It also leads the way to design multiband antennas using appropriate metamaterials (ENG or MNG) and using the idea of additional modified modes [2, 3] in elliptical patches also. In short, realistic numerical simulations are presented in this paper, considering losses and the presence of the antenna feed, showing how a practical realization is foreseeable.

Results:

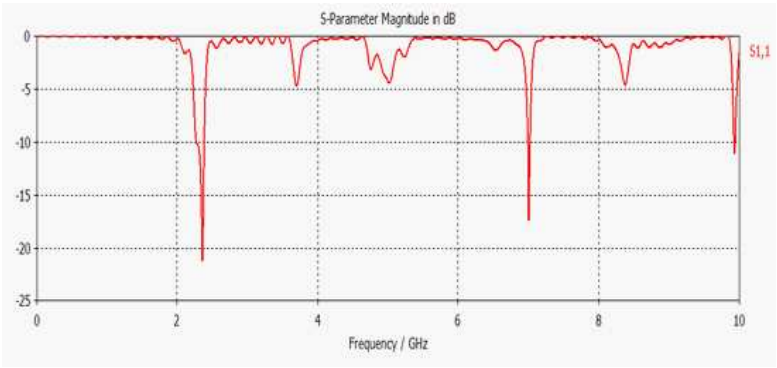

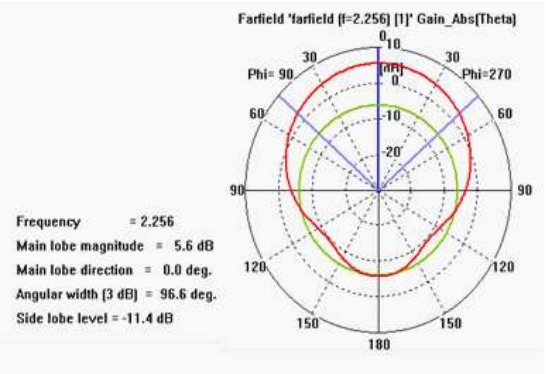

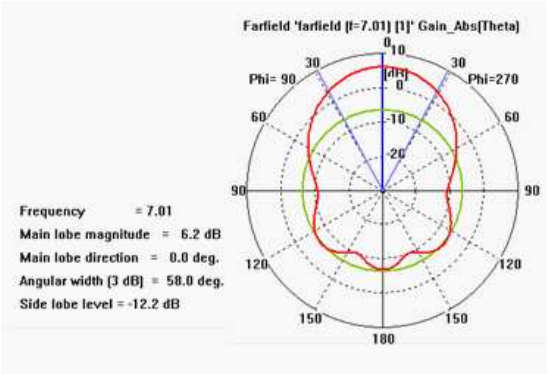

REFERENCES

1. Maci, S., G. B. Gentili, P. Piazzesi, and C. Salvador, "Dual-band slot-loaded patch antenna," *IEE Proc. — Microw. Antennas Propag.*, Vol. 142, No. 3, June 1995.

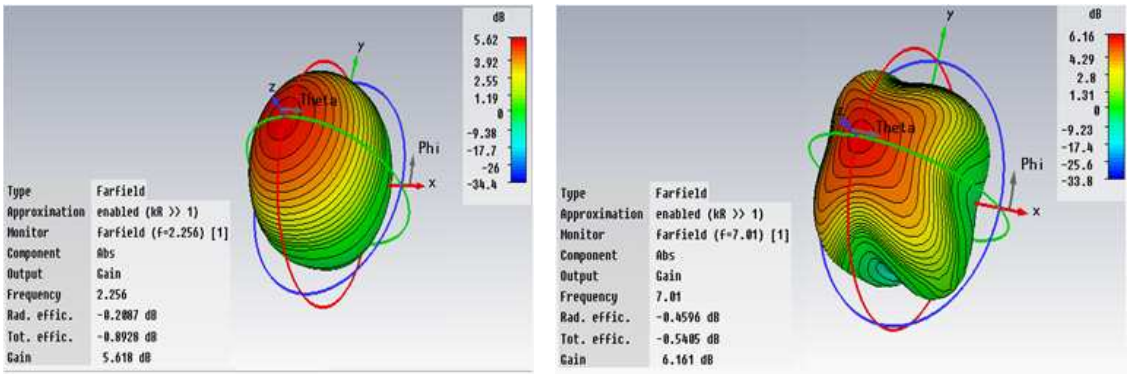

2. Chowdhury, M. R. C., M. R. A. Zuboraj, A. A. N. Ovi, and M. A. Matin, "Novel design of triple band rectangular patch antenna loaded with metamaterial," *Progress In Electromagnetics Research Letters*, Vol. 21, 99–107, 2011.
3. Mahdy, M. R. C., M. R. A. Zuboraj, A. A. N. Ovi, and M. A. Matin, "An idea of additional modified modes in rectangular patch antennas loaded with metamaterial," *IEEE Antennas and Wireless Propagation Letters*, Vol. 10, 869–872, August 2011.

Symmetrical Slot Loading in Elliptical Microstrip Patch Antennas Partially Filled with Mue Negative Metamaterials

Abdullah Al Noman Ovi[1], **Nandita Saha**[2], **Shuvashis Dey**[2], **and Nuzat Naury Alam**[2]

[1]Department of Electrical and Electronic Engineering
Bangladesh University of Engineering and Technology, Dhaka, Bangladesh
[2]Department of Electrical and Electronic Engineering
American International University of Bangladesh, Dhaka, Bangladesh

Abstract— In this paper, an idea of radiation pattern modification using symmetrical slots in an elliptical microstrip patch antenna partially loaded with mue-negative (MNG) metamaterial has been proposed. Previously, size reduction of conventional elliptical microstrip patch antenna has been reported in [1, 2] by using MNG metamaterial. But the idea of using symmetrical slots to modify higher modes in such metamaterial loaded elliptical patch antennas is different and a novel concept. Using this idea novel design of slot loaded elliptical microstrip patch antenna partially loaded with MNG metamaterial has been introduced successfully. In this paper, slot loaded elliptical patch antenna partially loaded with mue-negative metamaterial is theoretically and numerically analyzed. Actually, this mode modification has been done by MNG metamaterial & newly introduced symmetrical arc shaped slots with the help of proposed better radiation conditions [3], relevant theory of dispersive metamaterial and 'CST MICROWAVE STUDIO' based realistic simulated results. The potential application of this novel idea is the way to design multiband antennas using appropriate metamaterials (ENG or MNG) and using the idea of additional modified modes [3, 4] in elliptical patches also. In short, full wave realistic numerical simulations; considering finite ground plane, material dispersion, influence of metamaterial losses and the realistic antenna feed, prove that the elliptical geometry represents great potentials for a variety of electrically small low-profile antenna applications and a practical realization is foreseeable.

REFERENCES

1. Chen, P. Y. and A. Alù, "Dual-mode miniaturized elliptical patch antenna with μ-negative metamaterials," *IEEE Antennas and Wireless Propagation Letters*, Vol. 9, 2010.
2. Chen, P. Y. and A. Alu, "Sub-wavelength elliptical patch antenna loaded with μ-negative metamaterials," AP0911-1144.R1.
3. Mahdy, M. R. C., M. R. A. Zuboraj, A. A. N. Ovi, and M. A. Matin, "Novel design of triple band rectangular patch antenna loaded with metamaterial," *Progress In Electromagnetics Research Letters*, Vol. 21, 99–107, 2011.
4. Mahdy, M. R. C., M. R. A. Zuboraj, A. A. N. Ovi, and M. A. Matin, "An idea of additional modified modes in rectangular patch antennas loaded with metamaterial," *IEEE Antennas and Wireless Propagation Letters*, Vol. 10, 869–872, August 2011.

Compact Wideband Strip Monopole Antenna for Wireless USB Application

Yung-Lun Chen, Wen-Chung Liu, and Chao-Ming Wu
Department of Aeronautical Engineering, National Formosa University
Yunlin 632, Taiwan, R.O.C.

Abstract— Presently, there is much interest in developing wideband antennas with a compact size for use in wireless communication devices, in particular, for the universal serial bus (USB) dongle. Usually, such kind of antenna is demanded at a compact size, a simple structure, and a potential function on wide or multiband operation for being easily integrated with the USB circuit and sufficiently covering the possible operating bands. In this work, we propose a simple antenna design with not only wideband operation but also compactness in size suitable for wireless USB application. The antenna printed on part of a PCB was etched by slots to thus form two symmetrical folded strips and is fed by a strip line (Fig. 1(a)). By optimally selecting the geometry parameters of the antenna, dual-resonance with a much wider impedance matching can be achieved. The resulted overall size of the antenna is only $10 \times 10 \times 1.6\,\text{mm}^3$. We have constructed and tested the prototypes of the obtained design, and the experimental results explore good wideband operation with -10 dB impedance bandwidths of 1.9 GHz, ranging from 2.9 to 4.8 GHz (Fig. 1(b)). Agreement between the measurement and simulation is good. Also, good antenna performances such as radiation patterns and antenna gains over the operating bands have been examined. Additionally, details of effects of the embedded slots on the antenna performance and the physical implementation for the optimized configuration are all presented and discussed.

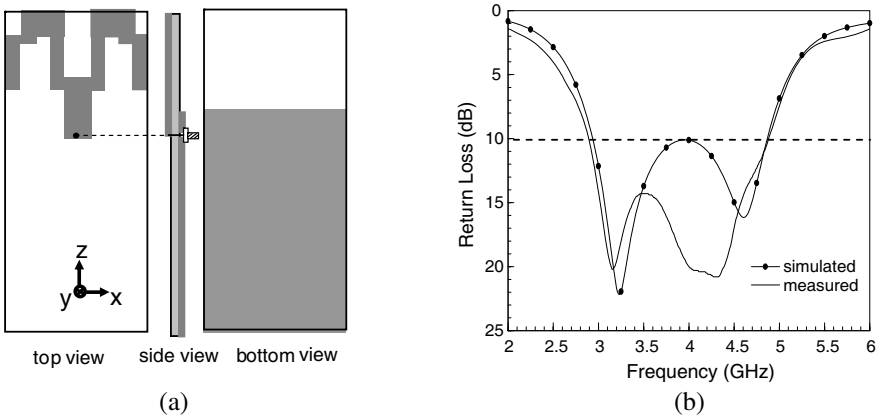

Figure 1: (a) Configuration of the proposed wideband dual-strip monopole antenna for wireless USB application; (b) measured and simulated return losses versus frequency of the proposed design.

ACKNOWLEDGMENT

This work was supported by the National Science Council of the Republic of China under Grant NSC 100-2221-E-150-046.

Research on Capacity Performance of TD-LTE System with Different Antenna Schemes

Jiangbo Dong, Yuan Fang, Nan Li, Wei Liu, Hao Sun, Yunbo Han, and YanLei Chen
China Mobile Design Institute, Beijing, China

Abstract— There are several different transmission modes in TD-LTE system. For transmission mode 7/8, 8-path smart antenna is necessary to implement beamforming, and for transmission mode 2/3, 2-path antenna can also work well. Considering the engineering factors, such as antenna size, antenna weight, the 8-path antenna is more difficult to build than 2-path antenna during the real network deployment; while the cell edge data rate performance maybe worse than the latter. Therefore, performance comparison between 2-path and 8-path antennas is an important problem.

This paper addresses the planning of TD-LTE cellular radio networks for data services, enabling the evaluation of the network capacity performance, such as cell edge user data rate with different antenna scenarios. The modeling schemes of TD-LTE key techniques are proposed and developed to finish the research. Such schemes are also embedded in ANPOP® radio network planning tool.

Considering the practical application scenarios, the 2-path and 8-path antennas are both dual-polarized, and the antenna gain and antenna pattern used in the simulation are the same with which used in the real networks. The performance comparison between 2-path and 8-path antenna schemes are respectively evaluated with and without the static ICIC (Inter Cell Interference Cancellation) function in the dense urban area, which has 340 base stations.

The simulation results show that, when the ICIC function is off, cell edge user data rate with 8-path antenna is 32.4% higher than that with 2-path antenna; and this is also met with the field test results. When the ICIC function is on, the gain is down to 28.8%. It shows that ICIC can also enhance the ability of cell edge interference cancellation in the 2-path case. So we can draw an conclusion from the simulation results that 8-path antenna is a better choice for TD-LTE system, when the real construction condition is unlimited. This research is very important for construction of the large scale TD-LTE network.

A Reconfigurable Antenna Based on an Ultrawideband to Narrowband Transformation

M. Al-Husseini, **A. Ramadan**, **A. El-Hajj**, **and K. Y. Kabalan**
ECE Department, American University of Beirut, Beirut 1107 2020, Lebanon

Abstract— This paper presents a narrowband frequency reconfigurable antenna obtained by modifying a simple ultrawideband (UWB) design. The UWB version is based on a microstrip-line-fed patch having round corners, for smoother current flow. The ground plane is partial and rectangular in shape. The used substrate is a Rogers RO3203 board with $\varepsilon_r = 3.02$ and a height of 1.52 mm.

The narrowband (NB) antenna is obtained by making the following changes to the UWB design: 1) A rectangular split-ring slot is incorporated in the ground plane below the feed line, and 2) a gap is made in the feed line. The ground slot acts as a single-ring complementary split-ring resonator (CSRR). CSRRs are used for the synthesis of negative-permittivity media. They are known to create band notches around their resonance frequency. The feed gap acts as a capacitor, which transforms the band rejection behavior caused by the ground slot to a band pass one. The resulting relative narrowband operation depends on the dimensions of the CSRR, and the width of the feed gap. The position of the split in the ground slot also affects the resonance frequency. Frequency reconfigurability is obtained by mounting switches at several locations across the ring slot, and activating the switches, one at a time, to act like a split.

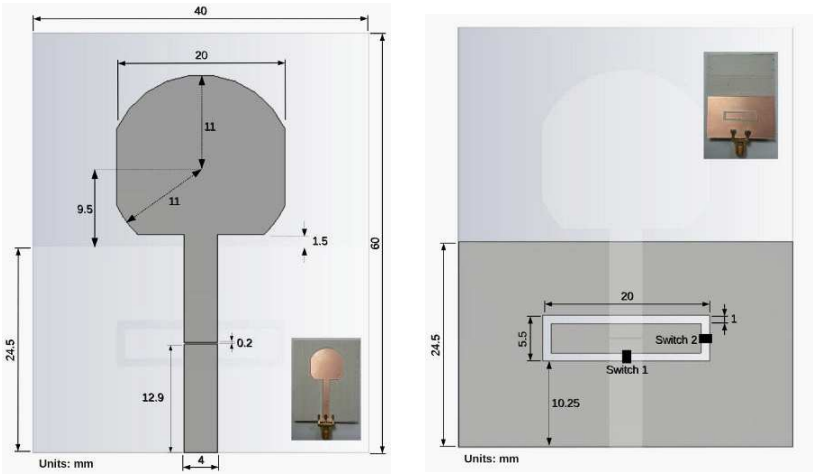

(a) (b)

Figure 1: NB antenna configuration and prototype photo. (a) Top view, (b) bottom view.

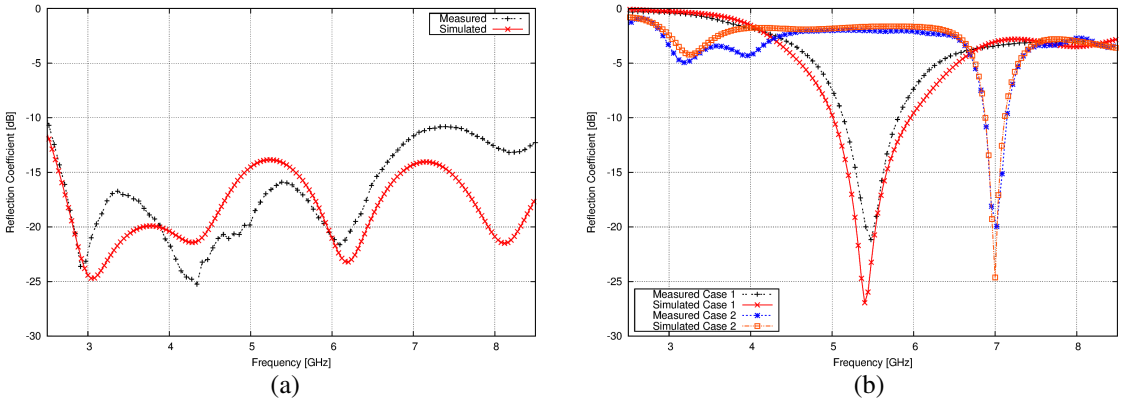

(a) (b)

Figure 2: Measured and simulated S_{11}. (a) UWB antenna, (b) NB antenna.

The NB antenna is shown in Fig. 1. The UWB antenna has the same structure, without the feed gap and the ground slot. Two electronic switches are used, as depicted. In Case 1, Switch 1 is ON and Switch 2 is OFF. Opposite switching is used for Case 2. Having the switches in the ground plane makes it easier to bias them with little effect on the antenna characteristics. The antenna is designed using Ansoft HFSS. Prototypes of the UWB and NB versions are fabricated and tested. The operation of the UWB antenna is shown through the measured and simulated S_{11} plots of Fig. 2(a). The narrowband behavior and frequency reconfigurability of the NB antenna are revealed by the S_{11} plots in Fig. 2(b), which are done for the two adopted switching cases. For these two cases, corresponding to these switch positions, narrowband resonances are obtained at 5.5 GHz, and at 7 GHz.

Urban Environment Path Loss Modelling by Support Vector Regression Machines on GPU: The Case Study of the City of Reggio Calabria

G. Angiulli[1], **S. Calcagno**[2], **D. De Carlo**[1], **and A. Sgró**[1]

[1]DIMET, University of Mediterranea
via Graziella n.1, Reggio Calabria 89100, Italy
[2]MECMAT, University of Mediterranea
via Graziella n.1, Reggio Calabria 89100, Italy

Abstract— It is well known as the prediction of radio wave path loss in urban environment plays a key role in order to correctly plan wireless systems and mobile communication networks [1]. Basically, the theoretical models of this phenomenon available in literature can be grouped as empirical and deterministic models. Both categories have advantages and limitations. The empirical models are computationally fast but often they lack of the necessary accuracy. Deterministic models provide accurate predictions but involving an high computational effort as well as the necessity of detailed information about the coverage area [1]. In the last years, path loss models based on the soft computing approach have emerged as a valid alternative to empirical and determinisi models [2]. Furthermore, the rapid growth of the use of graphics processing unit (GPU) in the field of the numerical computing have enabled software implementations of high performance machine learning algorithms [3]. In this context, we have developed a soft computing approach to model the radio wave path loss in the urban environment of the city of Reggio Calabria based on the use of Support Vectore Regression Machines on GPU. Computational results on the performances of the proposed SVRM-GPGPU model compared with COST Hata, Ray Tracing, and Neural Network models will be shown at the conference.

REFERENCES

1. Iskander, M. F. and Z. Yun, "Propagation prediction models for wireless communication systems," *IEEE Trans. on Microwave Theory and Techniques*, Vol. 50, No. 3, 662–673, 2002.
2. Alotaibi, F. D., A. Abdennour, and A. A. Ali, "A robust prediction model using ANFIS based on recent TETRA outdoor RF measurements conducted in Riyadh city Saudi Arabia," *Int. J. Electron. Commun.*, Vol. 62, No. 9, 674–682, 2008.
3. Catanzaro, B. C., N. Sundaram, and K. Keutzer, "Fast support vector machine training and classification on graphics processors," *Proceedings of ACM International Conference on Machine Learning (ICML)*, 104–111, 2008.

Multi-band Dual Polarized Indoor Antenna for Diversity and MIMO Applications

Feng Gao[1], **Peng Gao**[1], **Tong Wu**[2], **and Runhong Shan**[3]

[1]China Mobile Group Design Institute, Beijing 100080, China
[2]China National Institute of Metrology, China
[3]Copyright Protection Center of China, China

Abstract— This paper proposes a novel dual polarized omni-directional indoor antenna, which can be used as multi-input multi-output (MIMO) antenna in LTE system. The vertical dipole covers from $0.8 \sim 3$ GHz and the horizontal dipole covers GSM1800, TD-SCDMA, wireless local area network (WLAN) and long term evolution (LTE) systems. This indoor antenna has been experimented in MIMO systems for the WLAN system and LTE-TDD scale testing network separately. Based on the experiment, the cumulative distribution function (CDF) curve of Timing offset between uplink and downlink radio frames, reference signal received power (RSRP), signal to noise ratio (SNR) and throughput of downlink and uplink are studied, compared with single-input single-output (SISO) system.

Applicability of DCA in HAPS-based Systems in 5850–7075 MHz Band

Mastaneh Mokayef[1], **Walid A. Hassan**[1], **Yassir A. Ahmad**[2], **and Tharek Abd. Rahman**[1]

[1]Wireless Communication Center, University of Technology Malaysia (UTM), Malaysia
[2]Department of Communications Engineering, University of Diyala, Iraq

Abstract— High Altitude Platform System (HAPS) which will provide a worldwide connectivity in wireless networks, operates in 5850–7075 MHz spectrum endorsing the safety of primary services such as terrestrial systems (TS). The suppleness and innate characteristics of HAPS made it a trustable system that can adapt itself to operate as a secondary system in this allotment. To efficiently develop the restricted resources of the radio spectrum, the spectrum has to be divided into sub-channels to be reused. This paper offers status of feasibility study on the Dynamic Channel Assignment (DCA) in mentioned band. As opposed to other mitigation techniques, DCA is likely to evade either causing or accepting interference from/to TS by seeking for a part of spectrum that is out of action so far; hence, sensing carriers transmitted from TS is the most critical issue in this technique. A computer simulation is dispensed to assess the effect of utilizing HAPS as a secondary activated system with respect to TS operation, is presented in this paper. The performance of DCA scheme to mitigate the interference caused by HAPS is also evaluated in this paper. Additionally, the possibility of assigning DCA and the ability of sensing signal of victim by HAPS gateway (HAPSGS) with separation distance of up to 6 km is proved. In order to enhance the DCA performance, the sensing threshold level is diminished from 1 dB to 0.3 dB. Accordingly, the feasibility of DCA improved up to 7 km far from the Urban Edge of Coverage (EOC) area of HAPS.

Utilizing ATPC Scheme to Facilitate Sharing between HAPS and Terrestrial in 5.7 GHz Band

Mastaneh Mokayef[1], **Walid A. Hassan**[1], **Yassir A. Ahmad**[2], **and Tharek Abd. Rahman**[1]

[1]Wireless Communication Center, University of Technology Malaysia (UTM), Malaysia
[2]Department of Communications Engineering, University of Diyala, Iraq

Abstract— The development of sharing spectrum between High Altitude Platform System (HAPS) and Terrestrial System (TS) is the center of attention of our study. This paper focuses on Automatic Transmitting Power Control (ATPC) as an interference mitigation scheme competent of employing to HAPS and TS operating at 5.7 GHz band. Since ATPC reduces the transmission power from HAPS airship (HAPSAS) or HAPS gate station (HAPSGS), it can be used as a fundamental mitigation technique. Although customarily, ATPC techniques have been utilized to conflict rain attenuation by increasing or decreasing the transmission power, we utilized it to mitigate the co-channel interference (CCI) from HAPS to TS where both systems operate in the spectrum bellow 11 GHz band with negligible rain attenuation. Hence, deep discussion on the interference analysis procedure and interference mitigation possessions from both HAPSAS and HAPSGS is done. Our paper presents the performance of an ATPC in a single HAPS-based system subject to TS. The performance of the system is evaluated based on the Interference to Noise Ratio (INR) level. Accordingly, results show that the adjusted power between −46.1 and −13.67 dBW/MHz is required for HAPS to bring a better coexistence with TS at 5.7 GHz band; and on the other hand, potential of ATPC to ease the coexistence and sharing between HAPS and TS is also illustrated. Finally, the computer model depicted the smooth progress of ATPC mitigation performance.

Enhancement of Coexistence between HAPS and Terrestrial System in 5.8 GHz Band

Mastaneh Mokayef[1], **Walid A. Hassan**[1], **Yassir A. Ahmad**[2], **and Tharek Abd. Rahman**[1]

[1]Wireless Communication Center, University of Technology Malaysia (UTM), Malaysia
[2]Department of Communications Engineering, University of Diyala, Iraq

Abstract— The frequency band 5.850–7.075 GHz is allocated utterly for terrestrial radio communications. The High Altitude Platform System (HAPS) operates in this allotment certifying the protection of existing services. The expected sharing scenario in the mentioned band is between the HAPS system and the Terrestrial System (TS). Both systems operate in the adjacent channel frequency band; and thus, interference between these systems is a critical issue, which requires comprehensive spectrum sharing study. This paper investigates the performance of uplink (UL) and down link (DL) communications of both systems. The study analyzes the interference caused to TS by HAPS as a function of distance from the Nadir Point (NP) to the HAPS Gateway Station (HAPSGS). It is assumed that HAPS system operates at an adjacent channel to the TS system. The coexistence performance is evaluated based on the Interference to Noise Ratio (INR) of the victim link. In order to avoid adjacent channel interference, the simulation results show that the separation distance should be 10 km from HAPS airship (HAPSAS), and 22 km from HAPSGS. Therefore in order to mitigate the interference, the required isolations for TS to coexist with the HAPSAS and HAPSGS should be 5.6 dB and 45.14 dB respectively.

Proficiency Testing of Radiated Emission Testing Laboratory in China

Tong Wu[1], **Qingfei Shen**[1], **Bin Lin**[2], **and Hongyan Yin**[3]

[1]China National Institute of Metrology, China
[2]Shenzhen Academy of Metrology and Quality Inspection, China
[3]Beijing Entry-Exit Inspection and Quarantine Bureau, China

Abstract— This paper reports the results of a radiated emission proficiency testing round with the major electromagnetic compatibility (EMC) laboratories in China. Nineteen Radiated emission sites are compared using a comb generator in the frequency range of 30 to 1000 MHz. The guidelines of international standards such as ISO/IEC Guide 43-1 was followed, while the scope of the tests focused on EMC compliance of information technology devices, based on CISPR 22. Statistical metrics such as Z-score and normalized error have been adopted to assess global and individual performances of the participant laboratories. As the result of this program, to find the laboratory which had an isolated data from the group and analysis influence factors of difference of the test results.

On Performance Analysis of SLNR-based Multistream Transceiver in Multiuser MIMO Downlink Channels

R. K. Mai, F. Y. Qian, Y. S. Zhu, and H. Li
Peking University, China

Abstract— Directed transmission offered by smart antennas has made it possible to implement spatial multiplexing (SM) in multiple-input-multiple-output (MIMO) wireless communications. On the level of digital signal processing, appropriate design of transceivers becomes an enabling technology to harness such a capability to dramatically increase data rates while still achieving decent error performance. In the case of multiuser MIMO downlink channels, special attention should be paid to handle system performance degradation caused by interchannel interferences (ICI) among users. Traditionally, the focus of a wide variety of designs is on optimization of received signal-to-interference-noise ratio (SINR) per user, which is directly relevant to the channel capacity and bit error rate (BER). Recently, the so-called signal-to-leakage-plus-noise ratio (SLNR) has been proposed as the ratio of one user's received signal power to the interference posed by its transmission to the other users. This can be interpreted as SINR from the perspective of the transmitter. Although SLNR is not exactly the same as SINR, a remarkable benefit of such a definition lies in its decoupling of all users' precoders which would otherwise depend on each other in the conventional SINR. In this paper, a closed-form optimal precoder is derived based on the generalized Rayleigh quotient theorem to the optimization of SLNR. In light of the disparity, the capacity of multiple receive antennas to cooperate is utilized for compensation. Geometric mean decomposition (GMD) is employed to decompose the effective channels, followed by successive interference cancellation to create equivalently parallel subchannels. Each subchannel is endowed with an equal channel gain, which translates to improvement in one user's overall BER since the BER is dominated by the weakest subchannel at moderate to high signal-to-noise ratios (SNR). Numerical results verify the superiority of the proposed scheme to the original one with matched filters in terms of error performance and outage probability.

Comparison of Matrix Synthesis Method and Heuristic Techniques for Waveguide-fed Slot Antenna Array on Circular Cylinder

Mikhail Manuilov
Southern Federal University, Russia

Abstract— Recently, the phased antenna arrays with the multi-beam radiation patterns are the subject of growing interest, because they are the promising candidates for many communications and radar applications.

In this paper, the comparison of multi-beam radiation pattern synthesis methods based on ring harmonics concept are discussed for the case of waveguide-fed axial slot arrays on circular cylinder. Two heuristic methods for single-lobe pattern shaping and the matrix synthesis method are proposed. The first heuristic method is based on exception of some selected ring harmonics from the process of radiation pattern shaping. In the second heuristic technique the radiation pattern shaping is implemented by means of the harmonic weights introduction.

The proposed matrix synthesis technique allows independent controlling the direction, amplitude and phase of each individual main beam of the multi-lobe pattern. The vector of currents on the slots is calculated to maximize the functional that is the physical analogue of directivity in the case of multi-lobe pattern. In accordance with the suggested approach the functional is represented as the Hermitian forms ratio that includes the information about specified orientations, amplitudes and phases of the all main beams of radiation pattern. The optimal vector of current amplitudes on the slots is evaluated analytically using the matrix theory formalism. The suggested matrix synthesis technique combined with 3D electromagnetic model of cylindrical array provides the ability to control the local as well as the total side-lobe level.

The very fast and accurate electromagnetic analysis technique of the cylindrical array is employed. The problem is reduced to the system of integral equations for unknown magnetic currents on the apertures of slots. Free space Green's function is represented in the form of infinite spectrum of cylindrical waves propagating in radial direction. The fields in waveguides are written as the superposition of incident and reflected modes. By implementation of the Galerkin method the basis functions are chosen, which take into account the field asymptotic at the edges of radiating slots.

The synthesis results for multi-element cylindrical arrays with single-beam and multi-beam radiation patterns are considered. It was shown that by implementation of proposed matrix synthesis method the substitution of the ring harmonic radiation patterns instead of array element radiation patterns provides the absolutely equal final results. The synthesis techniques based on ring harmonics concept may be appropriate in the case of array excitation by means of Butler matrices.

Design of Novel Monopole Antenna Using Dual Rectangular Ring Patches and L-slots

Y. J. Shin, S. W. Lee, and N. Kim
Chungbuk National University, South Korea

Abstract— A dual square-ring shaped monopole antenna for DCS, US-PCS, UMTS, Wibro, WLAN and Mobile WiMAX operation is presented. The antenna is composed of two square-ring shaped antenna and two different size of slots on the ground plane. By using coupling between the inner and the outer square-ring patches, the optimized matching characteristic is obtained. At using the square-ring shaped patches only, two impedance bandwidths, which are occurred at 1.44 GHz–2.72 GHz and 3.19–3.84 GHz are obtained. By adding the two L-slots on the ground plane, two impedance bandwidths, which are operated at 5.14 GHz–5.35 GHz and 5.56–5.89 GHz are additionally obtained. Finally, the proposed square-ring shaped monopole antenna can realize quad impedance bandwidths of 1270 MHz (1.46–2.73 GHz), 740 MHz (3.14–3.88 GHz), 210 MHz (5.14–5.35 GHz) and 330 MHz (5.56–5.89 GHz), which can be applicable to DCS bands ($1.710 \sim 1.880$ GHz), US-PCS bands ($1,850 \sim 1,990$ MHz), UMTS bands ($1,920 \sim 2,170$ MHz), Wibro bands ($2,300 \sim 2,380$ MHz), WLAN bands ($2,400 \sim 2,480$ MHz, $5,150 \sim 5,350$ MHz, $5,725 \sim 5,825$ MHz) and Mobile WiMAX bands ($2,500 \sim 2600$ MHz, $3,400 \sim 3,600$ MHz) services.

A Multiband Antenna Based on Mushroom Composite Right/Left-handed Transmission Line Structure

X. Li, Q.-Y. Feng, and Q.-Y. Xiang
School of Information Science and Technology
Southwest Jiaotong University, Chengdu, Sichuan 610031, China

Abstract— In this paper, a novel multiband planar antenna based on 2-D mushroom-like composite right/left-handed transmission line (CRLH-TL) structure is proposed. The metal patch of the mushroom cell is connected to the ground plane through via and planar inductor. It shows that the proposed structure gives an efficient approach to achieve multiband response and miniaturization. The operation frequency of the multiband antenna is dependent on the mushroom structure size and the equivalent parameters of the CRLH-TL, including capacitance and inductance. The proposed antenna is built with a total volume of 21 mm ∗ 26 mm ∗ 1 mm, and four resonant bands have been gotten. The radiation patterns are similar with the omnidirectional characteristics and the maximum gains are 1.27 dBi, 2.23 dBi, 2.86 dBi, and 5.2 dBi at 2.62 GHz, 3.91 GHz, 6.52 GHz, and 8.05 GHz, respectively. The results show that the presented structure has reasonable radiation characteristics of efficiency, bandwidth, and size that it will be suitable for multiband wireless application.

New Multiple Loop Antenna Design for 13.56 MHz RFID Reader

Cheol Yong Yang, **Seong Ha Lee**, **and Woon Geun Yang**
Department of Electronics, University of Incheon, Incheon 406-772, South Korea

Abstract— In this paper, a new multiple loop antenna structure for 13.56 MHz RFID (Radio Frequency IDentification) reader was proposed. As the size of the loop antenna for 13.56 MHz RFID reader is enlarged, the magnetic field at the central area of the loop antenna is weakened. To compensate this, serial feed multiple loop antenna, parallel feed multiple loop antenna and serial-parallel feed multiple loop antenna were proposed.

From previous our design, the simulation results on the magnetic field strength averaged for transponder size in the central area showed about 0.15 A/m, 0.32 A/m, 0.84 A/m and 0.95 A/m in the cases of the single loop antenna and serial feed multiple loop antenna and parallel feed multiple loop antenna and serial-parallel feed multiple loop antenna. In addition, as to the induced voltage for the center area of the antenna, the single loop antenna showed 0.84 V and serial feed multiple loop antenna was 2.84 V and parallel feed multiple loop antenna was 4.24 V and serial-parallel feed multiple loop antenna was 7.01 V. That is, we obtained a better magnetic field strength performance and induced voltage performance which will result longer interrogation distance

In this paper, we propose a new antenna structure. It consists of outer loop and inner parallel loops. Outer loop looks like primary coil of the transformer and one inner loop operates just like secondary coil of the transformer. In fact, inner loops operate accepter and donor antennas of the repeater. HFSS (High Frequency Structure Simulator) based on the FEM (Finite Element Method) from Ansoft was used for the simulations of the proposed antenna. The outer most loop diameter of the proposed example design was 150 mm and number of turns was 2.

The performance of the proposed antenna was compared with the those of single loop antenna, serial feed multiple loop antenna, parallel feed multiple loop antenna, and serial-parallel feed multiple loop antenna in the view points of the transponder sized average magnetic field intensity and the induced voltages especially at the central area of each antennas.

High Isolation MIMO Antenna Design by Using Ground Slits for Mobile Handset

Seong Ha Lee, **Cheol Yong Yang**, **and Woon Geun Yang**
Department of Electronics, University of Incheon, Incheon 406-772, South Korea

Abstract— In this paper, we designed and implemented the MIMO(Multiple-Input Multiple-Output) antenna with high isolation by using ground slits for the mobile handset that could be used for multiple services. The proposed system incorporates multiple slits between two antennas in the ground plane, which operate just like a band-stop filter, suppressing mutual coupling between the antennas and resulting in improved isolation.

The commercial program SEMCAD X by SPEAG based on the FDTD (Finite Differential Time Domain) was used to obtain suitable values of parameters and analyze the behavior of the proposed antenna. Simulation results on S11 values less than $-6\,\mathrm{dB}$ (VSWR < 3) were obtained for LTE (Long Term Evolution) 700/2300/2500, Wibro ($2,300 \sim 2,390\,\mathrm{MHz}$), Bluetooth ($2,400 \sim 2,483\,\mathrm{MHz}$), and US-WiMAX (US-World interoperability for Microwave Access: $2,400 \sim 2,590\,\mathrm{MHz}$) frequency bands.

The MIMO antenna was designed with two monopole antennas and each monopole antenna has a folded structure in order to reduce the size of the antenna. The proposed each monopole antenna is composed of two branches. On the right side, there is a long branch which is the major radiation element for the proposed antenna at low band. On the left side, there is a short branch which plays a major role for high frequency band. And a long branch has a rectangular slit. The rectangular slit has influences on whole impedance matching. The each monopole antenna size of example design is $50\,\mathrm{mm}\,(W) \times 20\,\mathrm{mm}\,(L) \times 5\,\mathrm{mm}\,(H)$. For the design studied here, the antenna is fabricated on an inexpensive FR4 substrate with the dielectric constant of 4.4 and the substrate thickness of 1.60 mm. Ground size is $60\,\mathrm{mm}\,(W) \times 100\,\mathrm{mm}\,(L)$. Measured results of the fabricated antenna are validated for using at the LTE 700/2300/2500, Wibro, Bluetooth, US-WiMAX bands.

Phase Retrieval Algorithm Combining Iterative and Optimization Technique for Near Field Antenna Measurements

A. Kusiek, W. Marynowski, and M. Mazur
Gdansk University of Technology, Poland

Abstract— Measurements of the antenna characteristics in the far zone are performed in an anechoic chambers or at specialized measurement polygons. The main limitation in such measurements is the electric size of the antenna which determines the Fraunhofer distance. In addition, measurements are usually performed only for two orthogonal planes and there is no information about antenna radiation in other directions. Nowadays, the near field antenna measurement technique become more popular [1–3] which overcomes the above limitations. This approach involves measuring the amplitude of radiated field in two planes in front of antenna. Next, by applying iterative or optimization algorithms, the field distribution in the aperture of antenna is found from which the far field antenna radiation pattern can be simply determined.

The main stage of antenna near field measurement approach is exact determination of field distribution in aperture of antenna under test based on measured field amplitudes. One of the most basic technique is an iterative algorithm [1]. This approach is based on propagation of initially guessed field distribution using plane wave spectrum technique between measurement planes and aperture of antenna and updating the amplitudes of the propagated field distribution with the measured ones. As a result of iterative process the approximated solution is obtained, which in many cases may not be accurate enough. Another group of algorithms are optimization procedures which are based on the determination of the global minimum of the properly defined functional. Due to the existence of local minima these algorithms may not converge to the correct solution. Thus, in the case of these approaches, in the literature one can find techniques of setting proper conditions to increase the area of global minimum occurrence [2].

In this paper we propose the phase retrieval algorithm combining iterative method [1] with the global minimum optimization techniques, e.g., Simulated Annealing (SA) or Particle Swarm Optimization (PSO) [4]. In our approach at first the iterative technique is applied to determine a rough solution to the problem. Next, the obtained solution is utilized as a starting point in PSO or SA to determine the exact field distribution in aperture of antenna. Due to the fact that in the optimization procedure the starting point is assumed to be an approximate solution of the problem, the number of iterations required to determine the exact solution is significantly reduced. The proposed algorithm was used to investigate numerically different types of slot and aperture antenna arrays. The obtained far field characteristics were compared with the results of commercial software calculations and a good agreement was observed. Based on the obtained results, it was observed that the proposed algorithm yields a significantly higher accuracy than the iterative process and requires less time than optimization technique with random initial point.

ACKNOWLEDGMENT

This work was supported by the Polish Ministry of Science and Higher Education and carried out within the framework of The National Center for Research and Development under agreement LIDER/21/94/L-2/10/NCBiR/2011.

REFERENCES

1. Anderson, A. P. and S. Sali, "New possibilities for phaseless microwave diagnostics, Part 1: Error reduction techniques," *IEE Proc. of Microwaves, Antennas and Propagation*, Vol. 132, No. 5, 291–298, Aug. 1985.
2. Isernia, T., G. Leone, and R. Pierri, "Radiation pattern evaluation from near-field intensities on planes," *IEEE Transactions on Antennas and Propagation*, Vol. 44, No. 5, 701, May 1996.
3. Yaccarino, R. G. and Y. Rahmat-Samii, "Phaseless bi-polar planar near-field measurements and diagnostics of array antennas," *IEEE Transactions on Antennas and Propagation*, Vol. 47, No. 3, 574–583, Mar. 1999.
4. Robinson, J. and Y. Rahmat-Samii, "Particle swarm optimization in electromagnetics," *IEEE Transactions on Antennas and Propagation*, Vol. 52, No. 2, 397–407, Feb. 2004.

Cylindrical Coil with Uniform Magnetic Field Distribution for Planar Wireless Charging System

Wang-Sang Lee, **Won-Seok Lee**, **Kyoung-Sub Oh**, **and Jong-Won Yu**
Department of Electrical Engineering, Korea Advanced Institute of Science and Technology (KAIST)
291 Daehak-ro, Yuseong-gu, Daejeon 305-701, Republic of Korea

Abstract— Although wireless power transfer technology has been widespread in the various fields, the practical use is limited due to the variable transfer efficiencies with regard to the charging distances and position, regulations for the human exposure effects, and EMI/EMC problems. On the other hand, according to the tremendous demands for the mobile devices such as smartphones, PDAs, and E-readers, the wireless charging markets show signs of prosperity. However, a wireless charging system has different charging efficiency with regard to receiving coil position. In other words, when the transmitting and receiving coils are positioned to correspond, the wireless charging system has the best charging efficiency. In this paper, in order to achieve the uniform magnetic field distribution for planar wireless charging system, a cylindrical transmitting coil with a three-dimensional shape with circular ends of equal size is presented. Compared to the conventional coil structure having a two-dimensional shape fabricated on PCB, the proposed coil improves the uniform magnetic field distribution over the charging surface regardless of receiving coil position. The uniform characteristic of magnetic field distribution in the proposed coil is verified by theoretical analysis and electromagnetic simulation. Additionally, by implementing the proposed transmitting coil, the maximum improved charging efficiency of 22% as the various position of the receiving coil is obtained in comparison to the conventional transmitting coil.

Frequency Selective Absorber Surface at the 2.4 GHz Unlicensed ISM Band

Mesut Kartal[1] and Bora Döken[2]

[1]Department of Electronics and Communications Engineering
Istanbul Technical University, Turkey
[2]Vocational School, Istanbul Technical University, Turkey

Abstract— This work is proposed to design frequency selective absorber surface (FSAS) at the unlicensed 2.4 GHz ISM (Industrial, scientific and medical) band. An attenuation of 10 dB on the transmission (S_{21}) parameter and reflection parameter (S_{11}) is desired for this frequency band. Attenuation of 10 dB on the transmission (S_{21}) parameter is for shielding for interference mitigation and network security within the buildings. Attenuation of 10 dB on the transmission (S_{11}) parameter is to reduce mutual interference reduce additional multipath and resultant fading. FSAS is attached onto the existing common construction material to transform the standard material into an absorb/transmit frequency selective wall.

Periodic structures have filter characteristics depending upon their geometries when interacting with electromagnetic waves. FSAS which is introduced consists of three layers (consist of periodic structures); upper layer with resistive periodic geometries (to achieve an attenuation of 10 dB on the reflection (S_{11}) parameter), inner layer with capacitive and resistive periodic geometries (to achieve an attenuation of 10 dB on the reflection (S_{11}) parameter) and bottom layer with conducting periodic geometries (to achieve an attenuation of 10 dB on the transmission (S_{21}) parameter). To fill the space between these layers "Expanded Polystyrene Foam" (EPS) is chosen. These foams are light weight, good thermal insulators and are often used as building insulation materials. Another advantage of these foams is its relative dielectric constant value is almost 1.04 (does not attenuate the signal which passes through it).

For classical FSS designs, 2.4 GHz ISM band is a relatively low frequency band and has a narrower bandwidth. Therefore, to achieve a narrower band frequency response "Four Legged Loaded" periodic element geometry is used which has the advantages of simple in structure, easy fabrication, polarization insensitivity and adjustable frequency bandwidth. HFSS software is used for simulation and optimization purposes. The obtained results show that the desired frequency response is achieved.

Design and Simulation of Different Types of Meander Line Antennas with Improved Efficiency

A. Jahanbakhshi[1], **Gh. Moradi**[2], **and R. Sarraf Shirazi**[2]

[1]Amirkabir University of Technology, Iran
[2]Electrical Department, Amirkabir University of Technology, Iran

Abstract— The advent of new technology in communication systems and widespread use of this technology, leads engineers to design cheaper and simpler communication equipments. One of the most usage aspect of communication field is WLAN[1] and RFID[2] systems. Antenna is an inseparable part of these systems. Meander line antenna is the most usage of antenna that use in design of these applications. Classic meander line antenna has low efficiency in some aspects, such as antenna bandwidth and operation in only one resonance frequency (single band). In this paper various kind of these antennas have been proposed, to get better characteristics and efficiency such as log periodic meander line antenna, meander line antenna with different length of vertical segment and symmetrical meander line antenna.

[1]Wireless Local Area Network
[2]Radio Frequency Identification

Miniaturized MIMO Antenna with Improved Radiation Pattern

Se-Hwan Choi, **Jin-Sup Kim**, **and Jae-Young Lee**
Korea Electronics Technology Institute, Republic of Korea

Abstract— In recent years, multiple input multiple output (MIMO) antenna is widely used to increase the data rate of next generation communication system because the rayleigh fading effect in channel can be reduced by that MIMO antenna provides the space diversity. Space diversity technique can get rid of fading dips that can be occurred while mobile handsets are moving. In order to develop effective MIMO antenna, single antenna must have higher mean effective gain (MEG) and multiple antenna must meet the requirements such as isolation, correlation and diversity gain. But it is difficult that antennas satisfy these specifications because recent wireless communication systems requires small-size and multi-mode.

In this paper, MIMO antenna using two dipole is proposed in the 850 MHz band. For the orthogonal polarization, two dipole are located vertically and fabricated on the both side of FR-4 substrate. Reflector and additional stub structure are made of metal plate and used to increase the directivity of dipole. This stub structure acts on the antenna miniaturization, back-lobe reduction and bandwidth enhancement.

Antennas are simulated by Ansys HFSS and analyzed by Agilent E5071c network analyzer. The size of FR-4 substrate is about 85 mm $*$ 85 mm and the gap between substrate and reflector is about 25 mm. The single antenna has the bandwidth of 70 MHz, the gain of 3.5 dBi and backlobe of -0.54 dBi. MIMO antenna has the isolation of -25 dB and MEG of -4.3 dB. This antenna can be used for commercial small base transceiver station by reason of that this antenna satisfied the requirements of wireless communication system.

Design of Dual Frequency Notched Semicircular Slot Antenna with Semicircular Tuning Stub

Anwer S. Abd El-Hameed[1], **Haythem H. Abdullah**[2], **Deena A. Salem**[1], **and Esmat A. F. Abdallah**[1]

[1]Microstrip Department, Electronic Research Institute, Egypt
[2]Microwave Department, Electronic Research Institute, Egypt

Abstract— The release of the unlicensed UWB technology for commercial communications by the Federal Communication Commission (FCC) increased the interest in UWB communication systems [1], in which the antennas received the greatest portion. The planar structures attracted most of this attention for its intrinsic advantages over other types, such as simple structure, small size, low profile, small emission power, low cost for short range access and remote sensing application, easiness of fabrication and conformity and most important of which is that they lend themselves to miniaturization [2, 3]. Among the popular planar structures is the CPW fed planar slot antennas, which have increased attention mainly for the ease of integration of MMIC. However, coexistence of UWB systems with the narrow band wireless systems such as WLAN IEEE802.11a and HIPERLAN/2 WLAN operating in the 5–6 GHz has been a concern due to the inherently ultra-wide operating frequency range of the UWB systems. Besides the WLAN, in some European and Asian countries, for WiMAX service from 3.3 to 3.6 GHz, for which UWB antennas uses filters to prohibit operation in these bands. Recently, designs of UWB antennas with band-notch characteristics have also been reported [4, 5].

In this paper a novel compact UWB antenna design constituting a semicircular slot excited by an extended semicircular patch fed by a 50 ohm CPW is presented. The antenna was printed on FR4 substrate of relative permittivity of 4.65 with dimensions ($28 \times 30\,\text{mm}^2$). The operational bandwidth of this antenna extends from 2.3 GHz to 12.5 GHz. Two frequency notches were implemented to ensure coexistence with the narrow band applications WLAN and WiMAX. These notches are obtained by using L-slit in the ground plane and C-slot in the tuning patch. The parameters of the structure, C-slot and L-slit were optimized using EM simulator "CST Microwave studio", to obtain the required UWB range of frequencies and frequency notch characteristics.

The proposed antenna was fabricated using photolithographic technique. Measured and simulated results were compared and very good agreement was observed. Return loss and radiation patterns of the proposed antenna were measured using compact multi probe antenna test station, STARLAB-18 and VNA Agilent PNA E8363B. The antenna showed stable gain and near omnidirectional patterns. Thus, the proposed antenna can be a good candidate for various UWB applications.

REFERENCES

1. Federal Communications Commission, "First report and order," Revision of Part 15 of the Commission's Rules Regarding Ultra-Wideband Transmission Systems, Feb. 2002.
2. Eesuola, A., Y. Chen, and G. Y. Tian, "Novel ultra-wideband directional antennas for microwave breast cancer detection," *IEEE International Symposium on Antennas and Propagation*, 90–93, Aug. 2011.
3. Tayeb, D. A., H. M. Adnane, D. Azzeddine, and N. Mourad, "Design of UWB triangular slot antenna," *IEEE International Symposium on Antennas and Propagation (APSURSI)*, 1456–1458, Jul. 2011.
4. Nikolaou, S., M. Davidovi, and M. Nikoli, "Triple Notch UWB antenna controlled by three types of resonators," *IEEE International Symposium on Antennas and Propagation*, 1478–1481, Aug. 2011.
5. Ijiguchi, S., H. Kanaya, D. Kanemoto, K. Yoshida, R. K. Pokharel, K. Yoshitomi, A. Ishikawa, S. Fukagawa, and A. Tahira, "Development of one-sided directional printed slot antenna for high-band UWB systems," *IEEE International Symposium on Antennas and Propagation (APSURSI)*, 1474–1477, Jul. 2011.

Gradient of Radio Refractivity in Troposphere

M. Zilinskas[1, 2], **M. Tamosiunaite**[2], **M. Tamosiuniene**[3], **E. Valma**[2], **and S. Tamosiunas**[2, 4]

[1]Department of Radio Communication
Communications Regulatory Authority of the Republic of Lithuania, Lithuania
[2]Faculty of Physics, Vilnius University, Lithuania
[3]Semiconductor Physics Institute, Center for Physical Sciences and Technology, Lithuania
[4]Institute of Applied Research, Vilnius University, Lithuania

Abstract— The atmospheric radio refractive index, n, is defined as the ratio of the velocities of a propagating radio wave in free space and in a specified medium. The knowledge of n is always required when making measurements in air. The changes of the value n are very small in space and time. However, even such small changes can be significant for curvature of electromagnetic wave trajectory. Therefore, the dimensionless parameter of radio refractivity, N, is used with the aim to make those changes more notable. N is the number of parts that n exceeds unit, multiplied by million. N depends on atmospheric temperature, pressure and humidity.

The Lithuanian climate is humid and variable. A temperate climate similar to Lithuanian climate predominates in most of Europe. The dependence of radio refractivity on the height above the Earth's surface has been analyzed. The method proposed by International Telecommunication Union has been used. The gradient of radio refractivity has been analyzed over Kaunas, the city of Lithuania. We chose this location considering our previous studies, which showed that the yearly variation of N is highest in Kaunas, in comparison with other localities of Lithuania. The local meteorological data, measured near the ground and at the different heights above the Earth's surface, have been used in calculation of radio refractivity. It was concluded, that the super-refraction of radio waves and ducting phenomenon could occur at the end of April in Kaunas.

Reconfigurable Slot Element of Reflectarray

Andrey A. Prilutskiy, **Sergey V. Bogdanov**,
Marat A. Zheksenov, **and Sergey N. Potapov**
JSC "Research-and-production complex Scientific-Research Institute of Long Distance Radiocommunication", Moscow, Russia

Abstract— Now the great attention is given to scanning reflective array. Reflectarray unites in themselves advantages of ordinary microstrip antennas and mirror antennas. The basic advantages reflective array over the first is absence of the difficult beam forming circuits and expensive active modules. In comparison with mirror antennas reflective array have smaller overall dimensions, can be conformal with a surface on which they are located, have wide sector of corners of scanning.

In work results of electrodynamics modeling by a method of final elements and an experimental research in the waveguide simulator of characteristics reconfigurable a slot element of a reflective antenna array are considered. Change of a phase of the reflected wave from a slotelement is regulated by change of length of slot. It is shown that for smooth change of a phase it is expedient to use in one period of the array doubled or triplesslots. Comparison of the measured and computing values of a reflection phase from aarray element has good coincidence.

Compact Integrated Broadband Circularly Polarized Diversity Antenna for Wireless Communications

Dong-Jin Lee, Wang-Sang Lee, Kyoung-Sub Oh, and Jong-Won Yu
Department of Electrical Engineering
Korea Advanced Institute of Science and Technology (KAIST)
291 Daehak-ro, Yuseong-gu, Daejeon 305-701, Korea

Abstract— Antenna diversity is a well-known technique to enhance the performance of wireless communication systems and quality of services by increasing channel capacity. To overcome the physical limitation of diversity antenna due to strong mutual coupling between adjacent antennas, this is still very much a work in progress. The purpose of this paper is to design compact integrated broadband circularly polarized diversity antenna that has 13 feed ports with more than 15 dB isolation between them. Several methods were used for that purpose. More specifically, printed quadrifilar spiral antenna which has good axial ratio characteristics against size of ground plane was selected and optimum simulation for structure of diversity antenna was conducted. It was found that antenna has an impedance bandwidth of 700 MHz ranging from 2.2 GHz to 2.9 GHz ($S_{11} < 10$ dB) and 13 ports antenna is integrated in half wavelength volume ($0.5\lambda * 0.5\lambda * 0.5\lambda$).

Radiation and Mutual Coupling between Apertures on a Conducting Cylinder

R. Lech, A. Kusiek, and J. Mazur
Gdansk University of Technology, Poland

Abstract— Conformal antennas are becoming popular due to their many advantages and possibilities of applications they offer. The advantages of using antennas with a curved surface arise not only from the possibility of integrating them with the object on which they are mounted on but also from the increase, relatively to planar antennas, of their visible angular range. The circular antenna arrays, or arrays of radiators located on the surface of a cylinder may be the examples of such antenna that provide omni-directional radiation patterns in azimuth plane or provide, in this plane, the possibility of beam control. Such antennas can be used, e.g., in base stations for mobile communications systems. In the analysis of conformal antennas one encounters the electromagnetic problem which consists in finding the electromagnetic field resulting from radiation sources placed on curved surfaces. It is a boundary problem, where the fields in the area outside antenna surface and the fields or current distribution on the radiating elements have to be matched. Determination of radiation characteristics is reduced to finding the electromagnetic field in the antenna far zone. For this case, the simplified relations are often used. Determination of the mutual-couplings between the radiators requires finding the fields in the antenna near zone and is therefore more difficult issue, because no simplifications can be utilized. The inclusion of mutual-coupling effect is of great importance in pattern synthesis problems [1, 2], where if the mutual-coupling is neglected, poor results are obtained especially in the shaped beam region.

The method of the analysis of radiating apertures mounted on a conducting circular cylinder is discussed in the paper. The problem of calculating radiation pattern and mutual coupling between apertures is considered. The approach is based on a modal solution and utilizes the technique to transform the three-dimensional problem into a spectrum of two-dimensional solutions. This method works efficiently for electrically small structures, while with the increase of the structure dimensions the convergence problems may occur. The purpose of the analysis is to determine the scattering matrix defining the self- and mutual-coupling between radiating apertures. In order to improve the accuracy the existence of higher order modes of the fields in the radiating apertures is assumed. The investigation starts by defining the fields for the analyzed problem in areas inside the cylinder (waveguides) and outside the structure. In order to determine the scattering matrix describing relation between the coefficients of incident and reflected waves in the waveguides, proper continuity conditions for tangential components of electric and magnetic fields on the surface between the regions have to be imposed. In the case of the electric field components φ and z are continuous over the entire surface of the antenna, while the magnetic field components φ and z are continuous only in the areas of individual apertures. Due to the fact that the characters of the electric and magnetic fields in the area outside are unknown, in order to solve the problem under consideration, the continuity conditions of tangential components of the electric field are written in the transform domain. It is possible to determine the relationship between the transform of the electric field in the waveguide and transform of the magnetic field in the outer area. Calculating the inverse transform of the fields and enforcing the continuity conditions for the individual tangential components of magnetic field the desired scattering matrix can be calculated.

ACKNOWLEDGMENT

This work was supported from sources of National Science Center under grant decision No. DEC-2011/01/D/ST7/06639.

REFERENCES

1. Josefsson, L. and P. Persson, "Conformal array synthesis including mutual-coupling," *Electroinic Letters*, Vol. 35, No. 8, 625–627, Apr. 1999.
2. Xu, Z., H. Li, Q.-Z. Liu, and J.-Y. Li, "Pattern synthesis of conformal antenna array by the hybrid genetic algorithm," *Progress In Electromagnetics Research*, Vol. 79, 75–90, 2008.

UWB Antennas Fed with Coplanar Three-strip Line

W. Marynowski, **R. Lech**, **and J. Mazur**
Gdansk University of Technology, Poland

Abstract— Microstrip and coplanar ultra wideband (UWB) antennas are very attractive to short pulse technology and have been proposed for wireless communication systems to transmit coded signals. Their integrated and simple structures with small dimensions and light weight are suitable for easy integration with system components of phased and active antenna arrays. Several structures of antennas have been proposed for widening their operation frequency range [1–7]. Commonly known technique is to use various shapes of slot antenna configurations implemented in coplanar waveguides (CPW) technology [1–5] to fulfill this requirement. In literature on can find simple circular, elliptical or rectangular monopoles fed by coplanar or microstrip lines with several gigahertz bandwidth. In order to achieve cutoff capability or bandstop properties at the required frequencies the meandered or U-shaped slots etched in microstrip monopoles are applied in UWB structures.

Recently, the coplanar antenna with circular patch surrounded by a ground plane reduced to circular ring was investigated [5]. It was found, that the effect of external edge of the ground ring significantly affects the antenna bandwidth at low frequencies.

The paper presents the design of a compact UWB antennas composed of two different shapes of coplanar strips which enclose slot aperture. The band-notch capability of an additional slot etched in one of the strips is verified. The antennas are fed with three coplanar strip-lines of $50\,\Omega$ and are designed using ADS Momentum Software. The fabricated prototypes are tested using vector network analyzer and in anechoic chamber. The obtained measured results well agree with the simulated ones. The proposed UWB structures ensure the reflection losses better than $-12\,\mathrm{dB}$ in the frequency range from 3 to 13 GHz. In the case of antenna with the band rejection the reflection losses are $-1\,\mathrm{dB}$ at the desired frequency $f = 5.41\,\mathrm{GHz}$.

ACKNOWLEDGMENT

This work was supported from sources of National Science Center under grant decision No. DEC-2011/01/D/ST7/06639.

REFERENCES

1. Denidni, T. A. and M. A. Habib, "Broadband printed CPW-fed circular slot antenna," *Electronics Letters*, Vol. 42, No. 3, 135–136, Feb. 2, 2006.
2. Angelopoulos, E. S., et al., "Circular and elliptical CPW-fed slot and microstrip-fed antennas for ultrawideband applications," *IEEE Antennas and Wireless Propagation Letters*, Vol. 5, No. 1, 294–297, Dec. 2006.
3. Liu, Y. F., K. L. Lau, Q. Xue, and C. H. Chan, "Experimental studies of printed wide-slot antenna for wide-band applications," *IEEE Antennas and Wireless Propagation Letters*, Vol. 3, No. 1, 273–275, 2004.
4. Kanj, H. and M. Popovic, "A novel ultra-compact broadband antenna for microwave breast tumor detection," *Progress In Electromagnetics Research*, Vol. 86, 169–198, 2008.
5. Marynowski, W. and J. Mazur, "Design of UWB coplanar antenna with reduced ground plane," *Journal of Electromagnetic Waves and Applications*, Vol. 23, No. 13, 1707–1713, 2009.
6. Bialkowski, M. E. and A. M. Abbosh, "Design of UWB planar antenna with improved cut-off at the out-of-band frequencies, *IEEE Antennas and Wireless Propagation Letters*, Vol. 7, 408–410, 2008.
7. Su, S.-W., K.-L. Wong, and F.-S. Chang, "Compact printed ultra-wideband slot antenna with a band-notched operation," *Microwave and Optical Technology Letters*, Vol. 45, No. 2, 128–130, Apr. 20, 2005.

A Simple Miniaturized Triple-band Antenna for WLAN/WiMAX Applications

H. M. El Misilmani, **M. Al-Husseini**, **K. Y. Kabalan**, **and A. El-Hajj**
ECE Department, American University of Beirut, Beirut 1107 2020, Lebanon

Abstract— The design of a simple small-size multi-band antenna for wireless local area network (WLAN) and worldwide interoperability for microwave access (WiMAX) application is presented in this paper. The antenna covers the 2.4–2.5, 3–4, and 5.4–5.9 GHz bands, making it suitable for WLAN operating in the 2.4 GHz and 5.8 GHz bands, and WiMAX networks operating in the 2.5 GHz, 3.5 GHz and 5.5 GHz bands. The proposed printed-type antenna is based on a 1.6 mm-thick FR4 epoxy substrate with dimensions 25 mm × 38 mm. It has a rectangular split-ring slot enclosed inside a rectangular patch. Initially, the antenna covers the 3–4 GHz band. The inclusion of the split-ring slot leads to additional coverage of the 2.4–2.5 GHz band. The third band (5.4–5.9 GHz) is obtained by etching a U-shaped slot in the partial ground plane. The dimensions of the patch, the ground, and the two slots are optimized to obtain these desired functional frequency ranges.

The antenna is designed and simulated using Ansoft HFSS. A prototype is fabricated and experimentally tested. The detailed configuration and photo of the prototype are shown in Fig. 1. The computed and measured reflection coefficient plots are given in Fig. 2, where good analogy is revealed. Due to its geometry as a printed monopole, and the partial ground plane, the antenna possesses omnidirectional radiation patterns over its three coverage bands.

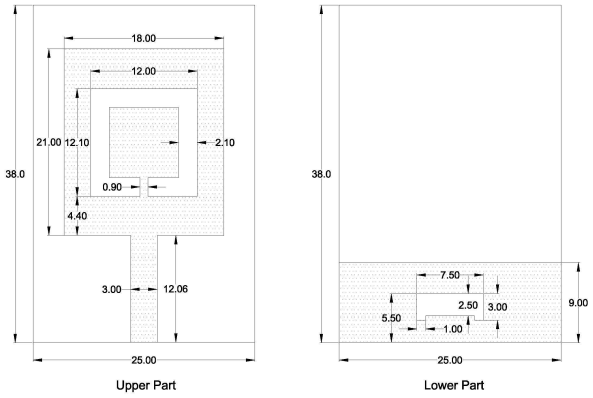

Figure 1: Antenna configuration and photo of prototype.

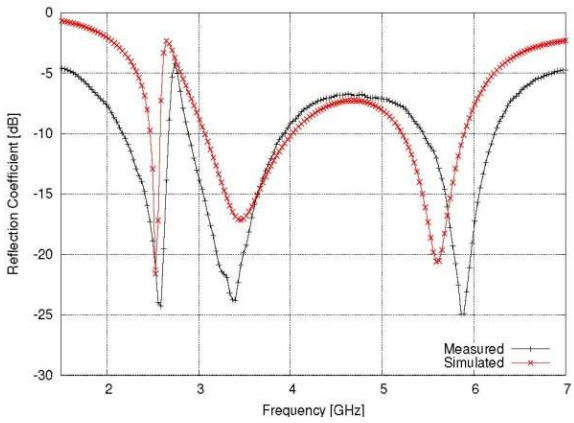

Figure 2: Simulated and measured reflection coefficient.

An Ultra-wideband Printed Monopole Antenna with a Fractal Based Reduced Ground Plane

Jawad K. Ali, **Ali J. Salim**, **Ali I. Hammoodi**, **and Hussam Alsaedi**
Microwave Research Group, Department of Electrical Engineering
University of Technology, Baghdad, Iraq

Abstract— Recently, the ultra-wideband (UWB) systems have attracted much attention because of its advantages including high speed data, small size, low cost, and low complexity. Consequently, the UWB antenna has received an increased attention due to its impedance bandwidth, simple structure and omni-directional radiation pattern. In this paper, the effects of the ground plane of a printed monopole UWB antenna, fed with a 50 Ω microstrip line, have been investigated. A Koch fractal based ground plane structure has been proposed as a means to enhance the UWB antenna performance. Different ground plane structures and feeding methods have been applied to a notched band monopole antenna structure that is a nearly square with embedded E-shaped slot. The proposed antenna has been supposed to be etched using a substrate with relative permittivity of 4.6 and thickness of 1.6 mm. Modeling and performance evaluation of the presented antenna designs have been carried out using a method of moments based EM simulator, IE3D. Simulation results have shown that the antenna with Koch based ground plane and asymmetrical feed offers larger fractional bandwidth of about 124%. By this increment in the antenna bandwidth, it is expected that by suitable dimension scaling of the enhanced bandwidth UWB antenna, many communication services below 3.1 GHz could be integrated with the UWB systems.

A Printed Fractal Based Slot Antenna for Multi-band Wireless Communication Applications

Jawad K. Ali, **Mahmood T. Yassen**, **Mohammed R. Hussan**, **and Ali J. Salim**
Microwave Research Group, Department of Electrical Engineering
University of Technology, Baghdad, Iraq

Abstract— Different slot structures have been widely used in numerous designs to produce antennas with enhanced bandwidths. In this paper, a printed slot antenna has been introduced as a candidate for use in the multi-band wireless communication applications. The antenna slot structure has a rectangular shape with its width, from the side of feed, has been modified in the form of Koch fractal curve of the second iteration. The antenna has been fed with 50 Ohm microstrip transmission line etched on the reverse side of the substrate. Modeling and performance evaluation of the proposed antenna design have been carried out using a method of moments based EM simulator, IE3D. Simulation results show that the resulting antenna exhibits a multi-resonant behavior making it suitable for a wide variety of multi-band wireless communication applications. The first resonant band, centered at 2.58 GHz, extends from 2.40 to 2.89 GHz. This band covers the 2.4 GHz WLAN band (frequency range 2.4–2.483 GHz) and the 2.5 GHz mobile WiMAX operating band (frequency range 2.5–2.7 GHz). The second resonant band, centered at 4.03 GHz, extends from 3.40 to 4.50 GHz. This band covers the 3.5 GHz mobile WiMAX operating band (frequency range 3.4–3.6 GHz). While the third resonant band centered at 5.74 GHz, extends from 5.42 to 6.18 GHz. This band covers the U-NII mid-band (frequency range 5.47–5.725 GHz) and U-NII high-band (frequency range 5.725–5.875 GHz). Parametric study has been carried out to explore the effects of varying the antenna feed line length on its performance.

C-band 360° Digitally-controlled Analog Phase Shifter with Low Amplitude Modulation Value

Michael D. Parnes[1], **Anton I. Zadorozhny**[1, 2], **and Orest G. Vendik**[2]

[1]Resonance Ltd., Russia
[2]Saint Petersburg State Electrotechnical University, Russia

Abstract— Described here is an analog microstrip phase shifter with required moderate insertion loss level, low cost, and low phase error. The phase shifter is based on varactor diodes and operates in C-band, providing a phase shift of 0–360°. To realize a low value of amplitude modulation for different phase states, a two-stage impedance transformation scheme was proposed. This ap-proach is practicable by using low Q-factor diodes. The phase shifter contains two similar reflec-tion phase shifters connected to the coupled and direct ports of a hybrid coupler. Each of the re-flection phase shifters includes two tunable resonant circuits and two quarter-wavelength mi-crostrip transformers to transform the input reflection phase shifter impedance compare to 50 ohm transmission line impedance to increase reflection coefficient. The operating frequency range of the phase shifter is bounded by the operating frequency range of the coupler, and equals 8% in C frequency band. The phase shifter module contains a digital control block for reducing the phase error to a minimum determined by the measurement equipment and DAC precision. After phase shift vs. voltage characteristic is measured, it is stored in the digital control block memory cell. Thus, the input control signal is digital (frequency and phase shift digital code). The voltage on varactors is generated by DAC according to the input control signal and memorized data. The described phase shifter was designed for phase array antenna application and has been serially produced. The low phase error and continuous phase shift allows forming the phase array antenna radiation pattern with zeros in noise directions, and enables precision steering.

Wide Band Switched Beam Circular Patch Antenna

W. M. A. Abdulkawi, A. F. A. Sheta, and M. A. S. Alkanhal
Department of Electrical Engineering, King Saud University
P. O. Box 800, Riyadh 11421, Kingdom of Saudi Arabia

Abstract— The paper presents a new wideband switched beam patch antenna for the recent wireless applications. The proposed antenna is designed to cover the band from 1.23 GHz to 1.96 GHz with $S_{11} < -10$ dB. The presented antenna has the ability to switch the beam into two different directions at the same resonant frequency. Tow artificial switches (PIN diodes) are used in this antenna to make reconfigurability. The design has been achieved on Duroid substrate with a dielectric constant 2.2, thickness 1.57 mm, and loss tangent 0.0009. The proposed antenna consists of ground plane of dimension $60 \times 170\,\text{mm}^2$ and two circular patches with radius $R = 30$ mm. The two radiating circular patches are placed on the top layer and fed with a microstrip lines as shown in Fig. 1. Bothe patches are fed by a coaxial probe in the center of the microstrip feed line. The two PIN diodes (S_1 and S_2) are used to connect or disconnect the two circular patches. For this antenna the beam switch into two different directions depending on the states of the two switches, explained as ON-OFF state and OFF-ON state. In ON-OFF state the antenna has a maximum beam direction of $\theta_{\max} = 215°$ at $\phi = 80°$. In OFF-ON state the maximum beam direction switched to $\theta_{\max} = 145°$ at $\phi = 80°$. Fig. 2 shows the 3D of the radiation patterns in the two states. The peak gains of the proposed antenna are 2.81 dBi and 2.86 dBi for case ON-OFF and case OFF-ON, respectively. The characteristics of the proposed antenna have been investigated using IE3D simulator. Experimental verification is underway.

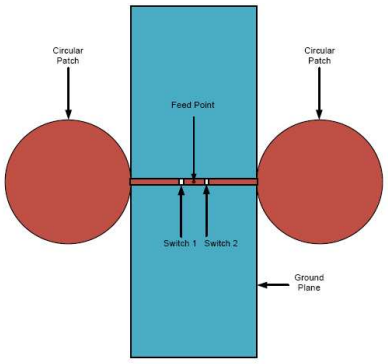

Figure 1: The proposed circular patch antenna.

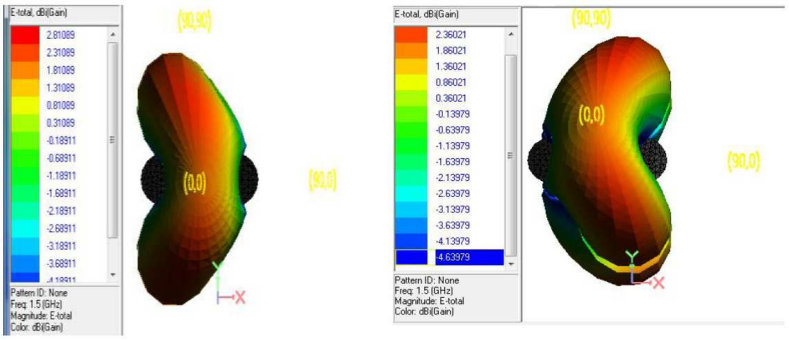

Figure 2: 3D radiation pattern for ON-OFF and OFF-ON states respectively.

ACKNOWLEDGMENT

This work is supported by the National Plan for Science and Technology Program, Kingdom of Saudi Arabia, Research Grant: 08- ADV210-2.

Propagation Model for Pine Tree Forest Environment at GSM 900/GSM1800/CDMA 2100

Selcuk Helhel, **Murat Bitirgan**, **Osman Kurnaz**, **Y. Emre Yoruk**, **and Sami Celik**
Engineering Faculty, Electrical and Engineering, Akdeniz University, Antalya, Turkey

Abstract— This study presents how to obtain an empiric propagation model in forest area by using both open area measuremensts as a reference and model field area measurements. Plane earth path loss propagation model was selected as a starting point, and certain field measurements were by then. An obstruction loss factor L was added to plane earth path loss equation of $P_r/P_t = G_t G_r h_r^2 h_t^2/d^4 L$ where P_r, P_t, G_t, $G_r d$, λ and L are received power, transmitting power, transmitting antenna gain, receiving antenna gain, distance, wavelength and obstruction loss factor, respectively. Tens of field measurements were carried out for obtaining denominator factor L, and generated model was applied to different forest area for model checking. It has been observed that our model predicts better progation model than Cost 235, Weissberger and ITU-R model for a certain conditions. Generated model has mean relative error of 3.92% for GSM900, 1.667% for GSM1800 and 1.04% for CDMA2100 systems. Maximum standart daviation of 2.64 has been observed at GSM900.

Enhanced Security Technology Using Concealed Electromagnetic Contact Barcode for e-ID

Won-Seok Lee, Dong-Jin Lee, Kyoung-Sub Oh, and Jong-Won Yu
Department of Electrical Engineering
Korea Advanced Institute of Science and Technology (KAIST)
291 Daehak-ro, Yuseong-gu, Daejeon 305-701, Korea

Abstract— This study aims at the enhanced security technology with concealed electromagnetic contact bar-code type chipless tag for e-ID and e-passport using 13.56 MHz HF RFID (Radio Frequency Identification). In these days, RFID technology used in identification, such as e-ID and e-passport, can store large amounts of personal information; whereas it has some problems that unauthorized access of unauthorized users are exposed. To solve this problem, we add new security codes of X-band (8–12 GHz) which can detect by contacting with proposed reader system. These security codes consist of barcode type chipless tag and are added under the coil of tag antenna.

In this paper, we verified the possibility of inserting new chipless tag by measuring the electromagnetic field and S_{21} between reader antenna and tag antenna with the presence of conductive material under the coil of tag antenna. We also proposed new barcode type chipless tags which can be inserted under the tag antenna. The validity of the proposed method applicable on HF RFID was verified by comparison of simulation results with 3-D EM simulation tools and measurement results.

A Compact Size Monopole Antenna for WLAN

Ho-Jun Lee[1], **Jung-Ho Park**[2], **and Young-Jun Kim**[3]

[1]Korea Electronics Technology Institute, Korea
[2]Samkwang Co., Ltd, Korea
[3]Microtech Co., Ltd, Korea

Abstract— In this paper, we proposed a novel design of short-range wireless communications antenna for mobile handsets. The proposed antenna configuration is shown in Figure 1. Antennas in this paper are simulated by using the Ansoft simulation software high-frequency structure simulator (HFSS). A prototype of this antenna was fabricated on FR4 substrate with thickness $h = 1.6\,\text{mm}$ and dielectric constant $\varepsilon_r = 4.4$. The measurements of electrical characteristics such as radiation patterns, VSWR, and return loss of the implemented antenna were conducted in an anechoic chamber equipped with a HP 8510C network analyzer and far field measurement system. Figure 2 shows return loss (S_{11}) characteristics. The measured impedance bandwidth of the antenna is from 2.385 to 2.5 GHz for VSWR < 2. Figure 3 shows a photograph of the fabricated antenna. We manufactured the antenna based on the results of optimized simulation results and measured characteristics of the suggested antenna in the anechoic chamber. Details of the proposed antenna designs are described, and typical experimental results are presented and discussed.

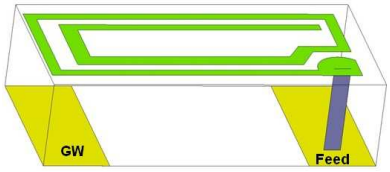

Figure 1: Proposed antenna.

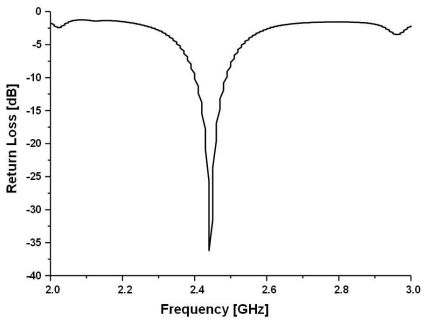

Figure 2: Measured return loss.

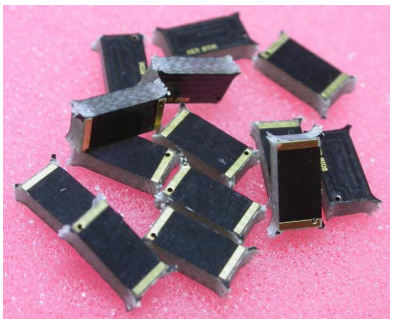

Figure 3: Photograph of the fabricated antenna.

REFERENCES

1. Stutzman, W. L. and G. A. Thiele, *Antenna Theory and Design*, 2nd Edition, Hohn Wiley & Sons, New York, 1998.

In-mold Antenna Using Mobile Phone Case

Ho-Jun Lee[1], **Jung-Ho Park**[2], **and Young-Jun Kim**[3]

[1]Korea Electronics Technology Institute, Korea
[2]Samkwang Co., Ltd, Korea
[3]Microtech Co., Ltd, Korea

Abstract— In this paper, we proposed a novel design of in-mold antenna integrated into the case of a mobile phone. Antennas in this paper are simulated by using CST Microwave Studio 2011. The proposed antennas are fabricated on a 0.1 mm thick metal substrate. The measurements of electrical characteristics such as radiation patterns, VSWR, and return loss of the implemented antenna were conducted in an anechoic chamber equipped with a HP 8510C network analyzer and far field measurement system. Figure 1 shows VSWR characteristics. The measured gains and radiation efficiency of the antennas are about 2.285 dBi and 64.424% at 2.4 GHz. Figure 2 shows a photograph of the fabricated antenna. We manufactured the antenna based on the results of optimized simulation results and measured characteristics of the suggested antenna in the anechoic chamber. Details of the proposed antenna designs are described, and typical experimental results are presented and discussed.

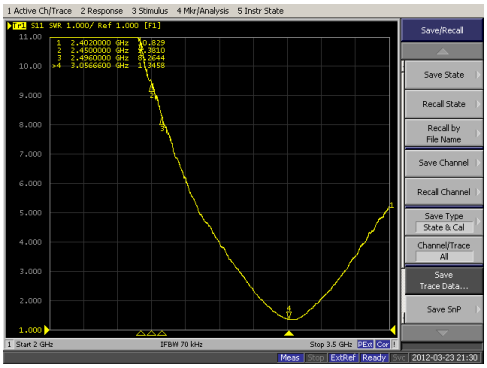

Figure 1: Measured VSWR.

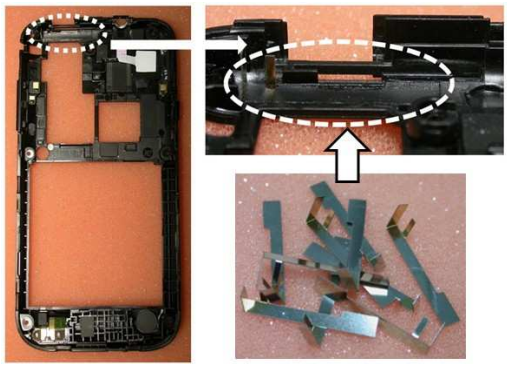

Figure 2: Photograph of the fabricated antenna.

REFERENCES

1. Stutzman, W. L. and G. A. Thiele, *Antenna Theory and Design*, 2nd Edition, Hohn Wiley & Sons, New York, 1998.
2. Harrington, R. F., "Effect of antenna size on gain, bandwidth and efficiency," *J. Res. Nat. Bur. Stand.*, Vol. 64, 1–12, Jan.–Feb. 1960.
3. Wong, K. L., Y. C. Lin, and B. Chen, "Internal patch antenna with a thin air-layer substrate for GSM/DCS operation in a PDA phone," *IEEE Trans. Antennas Propagat.*, Vol. 55, 1165–1172, Apr. 2007.

An Overview of Microwave Imaging towards for Breast Cancer Diagnosis

S. Raghavan and M. Ramaraj
Department of Electronics and Communication Engineering
National Institute of Technology (NIT), Tiruchirappalli-620015, India

Abstract—

Background: Breast cancer is the most common type of cancer in women worldwide. Digital Mammography is considered the "gold standard" in the evaluation of the breast from an imaging perspective. Apart from mammography, ultrasound examination, magnetic resonance imaging and microwave imaging techniques are being offered as adjuncts to the preoperative workup. However, there is still controversy over the most appropriate use of these new modalities. Based on the literature, this review concentrates mainly on the evaluation of microwave techniques in the screening and diagnosis of breast cancer and in the medical field. It reviews the current applications and future potential of microwave imaging methods.

Methods: This report gives an overview of the old and new modalities used in the field of breast imaging based on relevant literatures. A narrative literature review of all the relevant papers known to the authors was conducted. Additional references were found through bibliography reviews of relevant articles. It was clear that though various new techniques and methods have emerged, none have substituted mammography. Last two decades, medical imaging applications on microwaves has been developed. The emerging ultra wide band microwave (UWB) imaging gives better result with the advantages of non-ionizing, comfortable, sensitive to tumors and specific to malignancies. In microwave imaging techniques recently developed in hybrid microwave induced acoustic imaging, Ultra wide band radar based imaging and microwave tomography are also being offered.

Results & Conclusion: From the literature it is clear that modern radiology's impact on diagnosis, endorsement and patient's record and Mammography is the only screening test proven in breast imaging. Hybrid methods use microwave to selectively heat tumors and ultrasound transducers to detect pressure waves generated by the expansion of heated tissues. Microwave holography is a near field imaging method with transmitting and receiving antenna. This is experimentally with phantom tissues only but not yet used at clinical trials.

Microwave tomography also plays an important role in diagnosing breast cancer and monitoring treatment response. As imaging techniques improve, the role of imaging will continue to evolve with the goal remaining a decrease in breast cancer mortality. Progress in the design and development of UWB breast imaging system will definitely help to promote other systems and applications based on the radar imaging methods. The design of ultra wide band antenna and image reconstruction algorithm is the important challenges in microwave imaging modalities. But, Microwave based imaging modalities will be the best in tomorrow's clinical practice and these techniques enhance the radiologist's ability to detect cancer and assess disease extent, which is crucial in treatment development and performance.

Elliptical Split Ring Resonator: Mathematical Analysis, HFSS Modeling and Genetic Algorithm Optimization

M. Ramaraj, S. Raghavan, Sumanta Bose, and Swadhyaya Kumar
National Institute of Technology, Trichirappalli 620 015, India

Abstract— Negative Index Metamaterials (NIMs) are artificial structures having negative refractive index owing to their negative electrical permittivity ε and negative magnetic permeability μ simultaneously in certain range of frequencies. The elementary building blocks of NIMs are Split Ring Resonators (SRRs) and the variations in the properties of the NIMs arise due the varying geometry, size and material of the SRRs.

This paper proposes a novel quasi-static equivalent circuit model and mathematical analysis to characterize an Elliptical Split Ring Resonator (ESRR) depending on its geometry, configuration and electric field distribution. Numerical analysis using infinite series expansion and Ramanajun's formula led to the analytical calculation of the inductance and capacitance of the equivalent circuit determining the resonant frequencies of the ESRR.

Electromagnetic simulation in the microwave regime using Ansoft's High Frequency Structure Simulator (HFSS) was used to model the ESRR and plots its S-parameters. Verification of the proposed model showed good agreement between equivalent circuit analysis and simulation results. The simulated return loss, S_{11}, and transmission coefficient, S_{12}, led to the computation of the refractive index of the ESRR as a function of frequency. The dips and zero-crossings in the plot of the refractive index clearly indicated the presence of NIM property in ESRR.

The ESRR physical parameters were subsequently optimised using MATLAB based genetic algorithm (GA) implementation for minimizing the error in resonant frequency to obtain best performance. Graphical plots of appreciably converged parameters resulted in the performance optimization, which is essential from fabrication point of view specially because the ESRR can be easily incorporated with microstrip antennas to get highly directional beam patterns because of its NRIM properties.

Novel Microstrip-fed UWB Antenna with CSRR Slot for Signal Rejection in 5–6 GHz Band

S. Raghavan, **A. Subbarao**, **and M. Ramaraj**
National Institute of Technology, Tiruchirappalli 620015, India

Abstract— Ultra Wideband technology (UWB) has become popular due to high speed data rate, low power spectral density and robustness to multipath fading. Federal Communication Commission (FCC) has assigned bandwidth of 3.1–10.6 GHz is allocated for UWB systems. Since UWB antenna is important device in UWB systems, the design of UWB antenna became challenging task for engineers. One major issue in UWB is the design of compact size and wide band antenna. The planar antennas are better for UWB applications due to small size and stable radiation pattern.

In this paper, a novel compact microstrip-fed planar antenna is presented for UWB applications. The antenna is printed on low cost FR4 substrate with relative permittivity $\varepsilon_r = 4.4$ and thickness of 1 mm. The antenna has a compact a size of 24 mm × 30 mm. The antenna is fed by microstrip line since it offers low profile, wide bandwidth and ease of integration with circuits. The antenna is excited by pentagonal shaped patch. It provides band width ranging from 2.8 GHz to 10.8 GHz. A circular complementary split ring resonator (CSRR) is etched on radiating patch to avoid interference from WLAN band (5.1–6 GHz). Details of antenna are presented with parametric study. The ultra wide bandwidth is obtained by varying the width and height of pentagonal patch. The antenna has Omni directional radiation pattern in H-plane and dumb bell shaped pattern in E-plane. It has good radiation efficiency throughout operating band. The various parameters return loss, radiation pattern satisfy standard specifications.

The antenna is analyzed in frequency domain using method of moments based IE3D electromagnetic solver. The antenna has consistent gain except in the notched WLAN band. The gain falls to −8 dB in notched WLAN band, which is desired. In UWB wireless communication system, the digital information signals are transformed into impulse or non sinusoidal signals with very short pulse below nanoseconds. Since time domain group delay represents negative rate of change of phase with respect to frequency, it is important parameter for UWB antenna. The group delay of proposed antenna is less than 1 nano-second throughout the operating bandwidth except in notched band, which indicates linear phase response. The antenna is useful for microwave and millimetre applications because it offers low profile, ease of integration with circuits and ultra wide bandwidth.

Session 2P1
Nonlinear Guided Wave Phenomena and Optical Solitons

Optical Vortex Beams in Nematic Liquid Crystals

Yana V. Izdebskaya[1], **Anton S. Desyatnikov**[1], **Johannes Rebling**[2], **G. Assanto**[3], **and Yuri S. Kivshar**[1]

[1]Nonlinear Physics Centre, Research School of Physics and Engineering
The Australian National University, Canberra ACT 0200, Australia
[2]University of Applied Sciences, Zwickau 08056, Germany
[3]NooEL-Nonlinear Optics and OptoElectronics Lab
University of Rome "Roma Tre", Rome 00146, Italy

Abstract— A light beam which carries a phase singularity is an optical vortex. Such singular beams can be experimentally generated in various linear and nonlinear media. The unique features of vortex beams can be exploited in several applications, including optical data transfer. Here we report on the generation of self-trapped laser beams carrying optical vortices in nematic liquid crystals. We observe experimentally and describe theoretically the astigmatic transformation of vortex beams into spiraling dipole azimuthons. We report on the nonlinearity-induced topological charge-flipping of the central phase dislocation in the form of splitting of the on-axis phase singularity into three vortex lines, analogous to pitchfork bifurcations. We argue that these transformations are due to self-induced astigmatic deformations of the vortex beam, not relying on the external anisotropy stemming from the boundaries of the nematic liquid crystal cell.

When two or more mutually incoherent beams interact via cross-phase modulation, composite or vector solitons can be formed. We report on the first experimental observation of composite vortex beams in nematics with a strong dependence on their total vorticity, i.e., whether the two components carry equal or opposite topological charges. We demonstrate that incoherently coupled vortex beams, with identical charges and explicit vorticity, undergo astigmatic transformations and split into two filaments, creating a dipole vector soliton at higher powers similar to the scalar counterpart. In contrast, a vector soliton formed by two counter-rotating vortex beams with hidden vorticity and zero orbital angular momentum remain remarkably stable, preserving its ring-shaped total intensity profile.

Long Range Filament as Soliton

L. M. Kovachev
Institute of Electronics, Bulgarian Academy of Sciences, Bulgaria

Abstract— The femtosecond region is remarkable with the possibility for quick transformation of narrow band pulses to large band ones in nonlinear regime. From other hand, following the tradition from the nano- and picosecond optics, basic theoretical studies continue to investigate the processes with femtosecond (fs) pulses by using paraxial spatio-temporal envelope equation and Kerr type nonlinearity. To cover the new effects in fs region as conical emission, coherent THz and GHz radiation, filamentation and long range wave guiding, more of the authors start to add to this paraxial nonlinear equation terms, corresponding to additional processes as plasma generation, higher order Kerr terms, optical rectification and others. It is easy to show that plasma generation and the influence of higher order Kerr terms are negligible in respect to nonlinearity of third order for pulses with intensities of order of $I \sim 10^{12}\,\mathrm{W/cm^2}$. This is typical intensity for observing the above new processes in air. From other hand optical rectification request an additional power wave on second harmonics, which is not observed in the experiments also. That why we start to look for theory and equations governed simultaneously evolution of narrow band and large band pulses in air. As a first step in linear regime we introduce new linear amplitude equations allow to solve numerically and analytically the problem with propagation of pulses with super-broad spectrum. Different regimes of diffraction are analyzed. In the process of investigation we found also that in fs region the nonlinearity of third order is not Kerr type only, proportional to the intensity. This allows a mechanism of THz and GHz generation, bases of carrier to envelope phase and group-phase velocity difference. For pulses with power a little above the critical for self-focusing, we investigate two basic cases: pulses with initially narrow-band spectrum and pulses with broad-band ones. The numerical simulation of evolution of narrow-band pulses (typical 100 fs pulses), gives conical emission and a spectral enlargement to the short wavelengths. Our study of broad-band pulses leads to the conclusion that their propagation is governed by nonlinear wave equation. An exact soliton solution of the corresponding equation is obtained. The soliton appears as a balance between parabolic divergent type wave diffraction and parabolic convergent type of nonlinear self-focusing. Numerically, we demonstrate a relative stability of the soliton with respect to the THz and GHz oscillations.

Soliton-plasma Interactions I: Experiment

J. C. Travers[1], **P. Hölzer**[1], **K. F. Mak**[1], **F. Tani**[1], **F. Vinzent**[2], **W. Chang**[1], **N. Y. Joly**[1, 2], **M. F. Saleh**[1], **F. Biancalana**[1], **and P. St. J. Russell**[1, 2]

[1]Max Planck Institute for the Science of Light, Gnther-Scharowsky-Str. 1, Erlangen 91058, Germany
[2]Department of Physics, University of Erlangen-Nuremberg, Germany

Abstract— We report the demonstration of optical soliton-driven ionization effects in gas filled photonic crystal fibers — allowing the rich dynamics of nonlinear fiber optics to be complemented by high-field plasma-generating processes [1]. We show how the fast changing free-electron density, induced by photoionization, along with long recombination times, acts back on the solitons leading to a blue-shift, comparable but opposite in sign to the Raman self-frequency shift [1, 2].

The system uses kagom-lattice hollow-core photonic crystal fiber filled with noble gas, which offers broad-band transmission at low loss ($\sim 1\,\mathrm{dB/m}$) together with tight mode confinement and low anomalous dispersion (a few $\mathrm{fs}^2/\mathrm{cm}$) that can be balanced against the weak normal dispersion of the gas at pressure of a few atmospheres [3–5]. This means, for example, that the zero dispersion wavelength can be tuned from the UV to the IR simply by varying the gas pressure. By tuning the zero dispersion wavelength deep into the UV (to 380 nm, far from the pump wavelength at 800 nm) and using noble gases, an ideal anomalously dispersive system can be created for studying soliton propagation without conventional perturbations such as Raman scattering and higher order dispersion.

When 65 fs pulses of few μJ energies, corresponding to high order solitons, are launched into the fiber they undergo soliton-effect self-compression to intensities of over $10^{14}\,\mathrm{W/cm}^2$, well into the ionization regime. Spectral measurements show the emission of several blue-shifting side-bands [1], which we have identified as localized blue-shifting solitons by means of XFROG measurements.

REFERENCES

1. Hölzer, P., W. Chang, J. C. Travers, A. Nazarkin, J. Nold, N. Y. Joly, M. F. Saleh, F. Biancalana, and P. S. J. Russell, "Femtosecond nonlinear fiber optics in the ionization regime," *Phys. Rev. Lett.*, Vol. 107, 203901, 2011.
2. Saleh, M. F., W. Chang, P. Hölzer, A. Nazarkin, J. C. Travers, N. Y. Joly, P. S. J. Russell, and F. Biancalana, "Theory of photoionization-induced blueshift of ultrashort solitons in gas-filled hollow-core photonic crystal fibers," *Phys. Rev. Lett.*, Vol. 107, 203902, 2011.
3. Travers, J. C., W. Chang, J. Nold, N. Y. Joly, and P. S. J. Russell, "Ultrafast nonlinear optics in gas-filled hollow-core photonic crystal fibers [invited]," *J. Opt. Soc. Am. B*, Vol. 28, A11CA26, 2011.
4. Joly, N. Y., J. Nold, W. Chang, P. Hölzer, A. Nazarkin, G. K. L. Wong, F. Biancalana, and P. S. J. Russell, "Bright spatially coherent wavelength-tunable deep-UV laser source using an ar-filled photonic crystal fiber," *Phys. Rev. Lett.*, Vol. 106, 203901, 2011.
5. Nold, J., P. Hölzer, N. Y. Joly, G. K. L. Wong, A. Nazarkin, A. Podlipensky, M. Scharrer, and P. S. J. Russell, "Pressure-controlled phase matching to third harmonic in Ar-filled hollow-core photonic crystal fiber," *Opt. Lett.*, Vol. 35, 2922–924, 2010.

Soliton-plasma Interactions II: Theory and Simulation

W. Chang[1], **J. C. Travers**[1], **M. F. Saleh**[1], **F. Biancalana**[1], **P. Hölzer**[1], **K. F. Mak**[1], **F. Tani**[1], **F. Vinzent**[2], **N. Y. Joly**[1, 2], **and P. St. J. Russell**[1, 2]

[1]Max Planck Institute for the Science of Light, Gnther-Scharowsky-Str. 1, Erlangen 91058, Germany
[2]Department of Physics, University of Erlangen-Nuremberg, Germany

Abstract— We describe detailed numerical and theoretical analyses of the interaction between intense solitons and a self-induced partial-plasma in a gas-filled kagom-style photonic crystal fiber [1]. Three techniques are used to study the soliton dynamics: (i) the numerical solution of a unidirectional, one-dimensional field-equation [2], which closely reproduces the experimental measurements; (ii) the analysis of the soliton eigenvalues obtained from the direct scattering transform (DST) of the NLSE [3, 4], which enables deep insight into the trajectories of individual solitons; (iii) analytical solutions of a new theoretical model which describes the interaction between solitons and plasma [5].

All three approaches confirm the experimental observation of a soliton self-frequency blue shift caused by ionization of the gas and provide further insight and suggestions for future work.

REFERENCES

1. Hölzer, P., W. Chang, J. C. Travers, A. Nazarkin, J. Nold, N. Y. Joly, M. F. Saleh, F. Biancalana, and P. S. J. Russell, "Femtosecond nonlinear fiber optics in the ionization regime," *Phys. Rev. Lett.*, Vol. 107, 203901, 2011.
2. Chang, W., A. Nazarkin, J. C. Travers, J. Nold, P. Hölzer, N. Y. Joly, and P. S. J. Russell, "Influence of ionization on ultrafast gas-based nonlinear fiber optics," *Opt. Express*, Vol. 19, 21018–21027, 2011.
3. Zakharov, V. E. and A. B. Shabat, "Exact theory of two-dimensional self-focusing and one-dimensional self-modulation of waves in nonlinear media," *Soviet Journal of Experimental and Theoretical Physics*, Vol. 34, 62, 1972.
4. Boffetta, G. and A. Osborne, "Computation of the direct scattering transform for the nonlinear Schroedinger equation," *Journal of Computational Physics*, Vol. 102, 252–264, 1992.
5. Saleh, M. F., W. Chang, P. Hölzer, A. Nazarkin, J. C. Travers, N. Y. Joly, P. S. J. Russell, and F. Biancalana, "Theory of photoionization-induced blueshift of ultrashort solitons in gas-filled hollow-core photonic crystal fibers," *Phys. Rev. Lett.*, Vol. 107, 203902, 2011.

Third Harmonic Generation in Positive-negative Refractive Media

E. I. Ostroukhova and A. I. Maimistov
Moscow Engineering Physics Institute, National Nuclear Research University
Kashirskoe Sh. 31, Moscow 115409, Russia

Abstract— The third harmonic generation in a medium with the negative refractive index at the fundamental frequency and the positive refractive index at the harmonic frequency is investigated theoretically. The effects of self-interaction are taken into account. The solution of the system of equations, describing the parametric interaction of continues waves, is obtained analytically. Behavior of this solution is analyzed in dependence of the phase mismatch — the difference between values of harmonic's wave vector and a triple wave vector of the pump wave. The existence of critical phase mismatch in certain range of nonlinear third-order susceptibilities is shown. When value of the phase mismatch is less than critical one, a conversion of the pump wave to third harmonic is monotonous. Otherwise, the conversion is periodic. The nonzero critical phase mismatch doesn't exist in case of the conventional materials with positive refractive index. A solution of the system of equations describing the parametric interaction of continues waves is analyzed. The propagation of interacting waves under condition of grate phase mismatch is considered.

A Class of Localized Solutions of the Linear and Nonlinear Wave Equations

L. M. Kovachev[1], **D. A. Georgieva**[2], **and K. L. Kovachev**[1]

[1]Institute of Electronics, Bulgarian Academy of Sciences, Bulgaria
[2]Faculty of Applied Mathematics and Computer Sciences, Technical University of Sofia, Bulgaria

Abstract— There is one main problem in the diffraction theory namely whether it is possible to build such 3D + 1 diffraction (and dispersion) model that corresponds to the following experimental results: a) at one diffraction length the spot of any spectrally limited laser pulse satisfies the Fresnel diffraction. b) at several diffraction lengths one-two cycle optical pulses diffract semi-spherically. To solve this problem we investigate new linear Diffraction-Dispersion Equation (DDE) governing the propagation of pulses up to second order of dispersion is [1]:

$$2ik_0\left[\frac{\partial A}{\partial z}+\frac{1}{v}\frac{\partial A}{\partial t}\right]=\Delta A-\left(\frac{1+\beta}{v^2}\right)\frac{\partial^2 A}{\partial t^2}, \tag{1}$$

where $\beta = k''k_0v^2$ is a number counting the influence of the second order of dispersion. In air $\beta \propto 0$ and Eq. (1) can be reduced to following Diffraction Equation (DE):

$$2ik_0\left[\frac{\partial V}{\partial z}+\frac{1}{v}\frac{\partial V}{\partial t}\right]=\Delta V-\frac{1}{v^2}\frac{\partial^2 V}{\partial t^2}. \tag{2}$$

We solve DDE (1) and DE (2), applying spatial Fourier transformation to the components of the amplitude functions A and V. The fundamental solutions of the Fourier images $\hat{A}$, and $\hat{V}$ in (k_x, k_y, k_z) space are:

$$\hat{A} = \hat{A}(k_x,k_y,k_z,0)\exp\left\{i\frac{v}{1+\beta}\left(k_0\pm\sqrt{k_0^2+(\beta+1)\left(k_x^2+k_y^2+k_z^2-2k_0k_z\right)}\right)t\right\} \tag{3}$$

$$\hat{V} = \hat{V}(k_x,k_y,k_z,0)\exp\left\{iv\left(k_0\pm\sqrt{k_x^2+k_y^2+(k_z-k_0)^2}\right)t\right\} \tag{4}$$

In air $\beta \cong 2.1\times10^{-5}\approx 0$, DDE (1) is equal to DE (2), and on hundred diffraction lengths appear only diffraction problems. We solve analytically the convolution problem (4) for initial Gaussian light bullet of kind of $V(x,y,z,t=0)=\exp\left[-\left(x^2+y^2+z^2\right)/2r_0^2\right]$ and obtain exact analytical solution [1]. The numerical solutions of the DDE (1) and the DE (2), as well as the analytical solution of DE (2), satisfy exactly the conditions a) and b) obtained in the experiments with fs and attosecond pulses. One systematic study on different kinds of exact solutions and methods for solving wave equation:

$$\Delta E-\frac{1}{v^2}\frac{\partial^2 E}{\partial t^2}=0, \tag{5}$$

was performed recently in [2]. Here and also in [1] we suggest one new method: In the beginning, we separate the main phase $E = V\exp\left[i\left(k_0z-\omega_0t\right)\right]$ to reduce the wave equation to 3D + 1 parabolic type one (Eq. (2)). Thus, one initial value problem can be solved and exact (or numerical) solutions of the corresponding amplitude Eq. (2) can be obtained. The solution of Eq. (2) (or numerical one), multiplied with the main phase, gives an exact (or numerical) solution of the wave Eq. (5). Using this method a large number of new exact solutions of the wave equation are presented. In nonlinear regime the equation for large band optical pulses is transformed to [3]:

$$\Delta B-\frac{1}{v_{gr}^2}\frac{\partial^2 B}{\partial t^2}+\gamma B^3=0. \tag{6}$$

Finite energy solutions of Eq. (5) and of one system of nonlinear wave equations are also presented.

REFERENCES

1. Kovachev, L. M. and K. Kovachev, "Diffraction of femtosecond pulses: Nonparaxial regime," *Journal of Opt. Soc. Am. A*, Vol. 25, 2232–2243, 2008; Erratum, Vol. 25, 3097–3098, 2008.
2. Kiselev, A. P., "Localized light waves: Paraxial and exact solutions of the wave equation," *Optics and Spectroscopy*, Vol. 102, 603–622, 2007.
3. Kovachev, L. M., "New mechanism for THz oscillation of the nonlinear refractive index in air: Particle-like solutions," *Journal of Modern Optics*, Vol. 56, 1797–1803, 2009.

Stable Vortex Modes and Spatial Solitons in $(2+1)$-dimensional Nonlinear Schrödinger Equation with the Spatially Modulated Nonlinearities

Jie-Fang Zhang[1, 3], **Chao-Qing Dai**[2, 3], **and Lei Wu**[4]

[1]Zhejiang University of Media and Communications, Hangzhou 310018, China
[2]School of Sciences, Zhejiang Agriculture and Forestry University, Lin'an, Zhejiang 311300, China
[3]School of Physical Science and Technology, Soochow University, Suzhou, Jiangsu 215006, China
[4]Department of Mechanical & Aerospace Engineering, University of Strathclyde, Glasgow, United Kingdom

Abstract— We investigate the exact solitons in the framework of the $(2+1)$-dimensional nonlinear Schrödinger equation with spatially modulated nonlinearities and harmonic potential. The existence condition for these exact solutions requires that the minimum energy eigenvalue of the corresponding linear Schrödinger equation with the harmonic potential is the cuto value of the chemical potential λ. In the case of two-body interaction, the number of vortex-soliton (VS) modes is determined by the discrete energy spectrum of a related linear Schrödinger equation. The VS families in the system with the attractive and repulsive nonlinearity are mutually complementary. Stable VSs with vorticity $S \geq 2$ and those corresponding to higher-order radial states are reported, in the case of the attraction and repulsion, respectively. In the case of two-body and three-body interactions, the competition between two-body and three-body interactions influences the energy of the localized state. For the attractive two-body and three-body interactions, the larger matter wave order number n, the larger the energy of the corresponding localized state. The linear stability analysis and direct simulations with initial white noise demonstrate that for the same state (fixed n), the increasing number of atoms can add the stability. A quasi-stable soliton with the ground state is also found for the repulsive two-body and three-body interactions. These results suggest a scenario for the creation of stable vortex solitons and spatial solitons in BEC and optics.

REFERENCES

1. Wu, L., L. Li, J. F. Zhang, D. Mihalache, B. A. Malomed, and W. M. Liu, "Exact solutions of the Gross-Pitaevskii equation for stable vortex modes in two-dimensional Bose-Einstein condensates," *Phys. Rev. A*, Vol. 81, 061805(R), 2010.
2. Dai, C. Q., D. S. Wang, L. L. Wang, J. F. Zhang, and W. M. Liu, "Quasi-two-dimensional Bose-Einstein condensates with spatially modulated cubic-quintic nonlinearities," *Annals of Physics*, Vol. 326, 2356–2368, 2011.

Controllable Rogue Waves

Chao-Qing Dai[1, 2], **Jie-Fang Zhang**[1, 3], **and Shi-Qun Zhu**[1]

[1]School of Physical Science and Technology, Soochow University, Suzhou, Jiangsu 215006, China
[2]School of Sciences, Zhejiang Agriculture and Forestry University, Lin'an, Zhejiang 311300, China
[3]Zhejiang University of Media and Communications, Hangzhou 310018, China

Abstract— Self-similar rogue wave solutions are analytically obtained for the nonautonomous non- linear Schrödinger system. The controllable behaviors of one-rogue wave, two-rogue wave and rogue wave triplets in two typical soliton management systems are discussed. Our results demonstrate that the propagation behaviors of rogue waves, including postpone, sustainment, recurrence and annihilation, can be manipulated by choosing the relation between the maximum value of the effective propagation distance Z_m and the parameter Z_0. The rogue waves can also be longitudinally controlled by modulating the parameter Z_0. Moreover,the excitation time of controllable rogue waves is decided by the parameter T_0. In the exponential dispersion decreasing fiber, if Z_m is slightly bigger than Z_0, the excitations of rogue waves are postponed. If $Z_m = Z_0$, the full excitations of rogue waves can maintain a rather long distance with self-similar propagating behaviors. If $Z_m < Z_0$, the thresholds of exciting all rogue waves are never reached and the excitations of them are restrained or even eliminated. In the periodic distributed system, if $Z_m > Z_0$, rogue waves recur periodically. When $Z_m < Z_0$, the threshold of exciting rogue waves are also never reached and the excitations of them are restrained or even eliminated. These results here help us comprehend rogue waves more thoroughly, that is, besides their arbitrariness, rogue waves can be manipulated as discussed by the similar method in this paper. This manipulation is also meaningful for rogue waves in Bose-Einstein condensations, plasmas and financial system.

REFERENCES

1. Dai, C. Q., Y. Y. Wang, Q. Tian, and J. F. Zhang, "The management and containment of self-similar rogue waves in the inhomogeneous nonlinear Schrödinger equation," *Annals of Physics*, Vol. 327, 512–521, 2012.
2. Dai, C. Q., Q. Tian, and S. Q. Zhu, "Controllable behaviours of rogue wave triplets in the nonautonomous nonlinear and dispersive system," *J. Phys. B: At. Mol. Opt. Phys.*, Online at stacks.iop.org/JPhysB/45/000000.

Parametric Resonance for Nonautonomous Solitons

C. Hernandez-Tenorio[1] and R. Peña[2]

[1]Instituto Tecnológico de Toluca, Metepec, Edo., México C.P. 52140, México
[2]Benemerita Universidad Autónoma de Puebla, 502, Puebla C.P. 72001, México

Abstract— The dynamics of nonlinear solitary waves is studied in the framework of the nonautonomous nonlinear Schrödinger equation (NLSE) model with varying nonlinearity, dispersion, gain or absorption and varying in time harmonic oscillator potential. The model allows one to analyze on the general basis a variety of nonlinear phenomena appearing both in Bose-Einstein condensate (BEC), condensed matter physics and in nonlinear optics and biophysics. It is shown that in the framework of the autonomous NLSE exact solutions for a quantum-mechanical particle in a harmonic potential and for the NLSE solitons in a parabolic profile trap are completely identical. The exact analytical solutions for the NLSE solitons in time varying parabolic potential are obtained by using the Miura transformation of the soliton theory. These novel solutions open up the possibility to control the dynamics of the NLSE solitons in the trap. The appearance of a parametric resonance for a soliton in the time varying trapping potential is also predicted. We have obtained the exact analytical solutions for nonautonomous solitons. These novel solutions open up the possibility to control the dynamics of the NLSE solitons in the confining potential. The appearance of a parametric resonance for nonautonomous solitons in the time varying trapping potentials is also investigated. To verify this conclusion, we performed numerical calculations in the framework of the nonautonomous NLSE model with varying in time harmonic potential for a broad range of variations of the initial parameters.

Solitonic Analogs of the de Broglie Wavelength and the Ramsauer-townsend Effect

V. N. Serkin[1] and T. L. Belyaeva[2]

[1]Benemerita Universidad Autónoma de Puebla, A.P. 502, Puebla C.P. 72001, México
[2]Universidad Autónoma del Estado de México, Toluca C.P. 50000, México

Abstract— Historically, the Ramsauer-Townsend effect can be considered as the "predecessor" of the famous de Broglie hypothesis of wave-particle duality. In 1921, Ramsauer, Bailey and Townsend discovered that for slow-moving electrons, the probability of collision between electrons and atoms of noble gases displays a minimum value at a certain kinetic energy. In quantum mechanical interpretation, this effect corresponds to the condition, at which (in the plane-wave representation of a particle) the whole numbers of its de Broglie half-wavelength are equal to the size of a finite potential well. In a similar manner, the solitonic Ramsauer-Townsend effect can be observed for low-energy solitons when the potential width equals an integral number of solitonic half-wavelengths inside the well.

In our report, we show that one further peculiarity of the wave-particle duality (that is yet hidden from us) can be exhibited for solitons: on the one hand, as the self-localized wave object, the soliton, by virtue of the Galilean symmetry, is characterized by its own solitonic analog of the de Broglie wavelength, and on the other hand, as the extended particle-like object, the soliton, because of the nonlinearity, becomes a bound state in its own self-induced trapping potential and, as a consequence, acquires a negative self-interaction ("binding") energy. We point the way to discover novel phenomena linking different fields of physics: we demonstrate that the solitonic analog of the Ramsauer-Taunsend effect can be discovered for solitons. We show that a reflection of low-kinetic-energy soliton from an attractive potential is a result of the wave nature of solitons. Essentially no energy is lost in this case. The "hidden" role of the soliton self-interaction energy in the wave-particle duality of scattered solitons comes into particular prominence by comparing various scattering scenarios for solitons with higher form factors. There exists the critical strength of the soliton self-interaction energy, above which all low-kinetic-energy solitons are transmitted and never reflected. In other words, the fact that the soliton with high self-interaction ("binding") energy resembles a classical particle has become clear. This soliton behavior has transparent physical explanation.

We show the possibility of controllable generation of high-energy de Broglie video-solitons through their emission ("shooting out") from arbitrary N-soliton superpositions. We propose experimentally accessible strategies which can find different applications, in particular, in the developing basically novel all-optical soliton logic and switching devices, in soliton lasers design, for soliton supercontinuum generation and formation of matter wave solitons in Bose-Einstein condensates (BECs).

It should be emphasized in conclusion that mathematical equivalence between the NLSE and the Gross-Pitaevskii equations opens the possibility to study optical and matter-wave solitons in parallel and due to the evident complexity of experiments with matter wave solitons, offers remarkable possibilities in studies of the BEC physics by performing experiments in photonics.

Session 2P2
Progress in Metamaterials Research

Composites of Dielectric Cylinders and Spheres with Electric and Magnetic First Mie Resonances: A Study of Their Trasmittivity as Metamaterials

Manuel Nieto-Vesperinas
Instituto de Ciencia de Materiales de Madrid, CSIC, Madrid, Spain

Abstract— We report numerical calculations of propagation of microwaves and mid-infrared light in composites of high refractive index dielectric rods at frequencies at which their first electric and magnetic Mie resonances are excited. In spite that these "metaatoms" have recently been exhaustively investigated as an alternative to model metamaterials with little absorption, to this date no test exists of their behavior as an effective continuous medium.

We show that the negative refraction, previously observed in ordered arrays of these particles, is due to diffraction. This result sorts out a remaining question. We also prove that an effective medium theory of these composites yields constitutive parameters that do not reproduce the observations; in addition, their transmittance depends on the sample shape. This is further confirmed by disordering the arrays. Then high losses take place due to the extinction by scattering in these resonant particles.

Performance Enhancement of Patch Antenna by Fishnet Metamaterial

Anand Kumar and Dinesh Kumar Vishwakarma
PDPM Indian Institute of Information Technology, Design and Manufacturing, Jabalpur, India

Abstract— In this paper, a novel fishnet metamaterial structure has been designed and investigated using CST Microwave Studio and this structure is used as a cover for a patch antenna having patch dimension 1.57 mm $*$ 1.10 mm resonating at frequency 93 GHz, to enhance its performance. Metamaterials are artificial materials engineered to have properties that may not be found in nature and recently they are widely being used to improve the performance of antenna [1, 2]. In this paper the gain of antenna is improved close to its theoretical maximum value $D_{\max} = 4\pi A/\lambda^2$. Effective medium theory and standard parameter retrieval methods [3] were used to retrieve real part of effective permittivity $\mathrm{Re}(\varepsilon_{eff}) = -2.2$ and real part of effective permeability $\mathrm{Re}(\mu_{eff}) = -2$ at the operating frequency of metamaterial.

Radiation characteristics of E-field and H-field of conventional and combined structure were investigated which show the congregation effect of metamaterial cover. It converts the spherical pattern of patch antenna into flat pattern and improves its directionality. The improvement in directionality is 5.2° from 72.2° in x-z plane and to 6.5° from 71.1° in y-z plane. In addition, its gain is improved to 19.5 dB from 8.52 dB. The reason of this improvement is interpreted and the variation of gain as a function of separation between patch and metamaterial cover is given in the text. To the best of our knowledge, this is the first metamaterial patch antenna with fishnet structure. Fishnet structure is very easy to fabricate and overall structure has very small size and light weight which can easily used in the application where high gain and very high directionality is required.

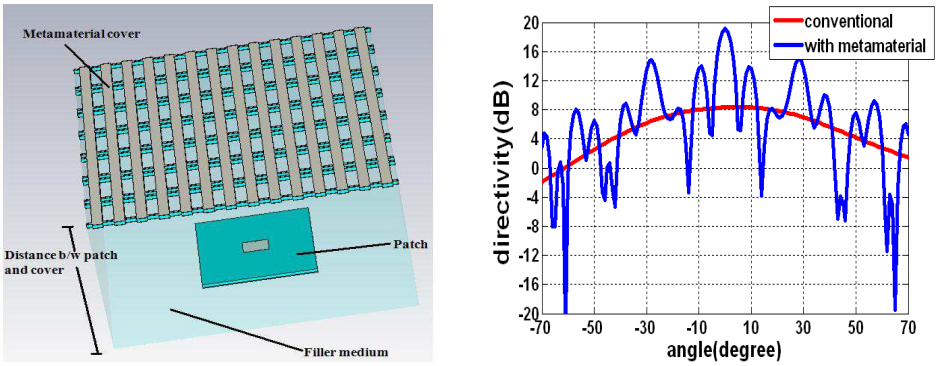

(a) (b)

Figure 1: (a) Metamaterial patch antenna. (b) Cartesian plot of directivity with and without metamaterial.

REFERENCES

1. Hu, J., C.-S. Yan, and Q.-C. Lin, "A new patch antenna with metmaterial cover," *Journal of Zhejiang University Science A*, Vol. 7, No. 1, 2006.
2. Weng, Z.-B., N.-B. Wang, and Y.-C. Jiao, "Study on high gain patch antenna with metamaterial cover," *7th International Symposium on Antennas, Propagation & EM Theory*, 1–2, 2006.
3. Szabó, Z., G.-H. Park, R. Hedge, and E.-P. Li, "A unique extraction of metamaterial parameters based on Kramers-Kronig relationship," *IEEE Transactions on Microwave Theory and Techniques*, 2646–2653, Oct. 2010.

Design and Fabrication of THz Index-gradient Metamaterials

L. K. Jian[1], **J. F. Wu**[2], **H. O. Moser**[3], **A. Banas**[1], **S. M. P. Kalaiselvi**[1], **S. P. Heussler**[1], **M. B. H. Breese**[1, 2], **H. S. Chen**[4, 5], **and X. X. Cheng**[4, 5]

[1]Singapore Synchrotron Light Source (SSLS), National University of Singapore (NUS)
5 Research Link, Singapore 117603, Singapore
[2]Department of Physics, National University of Singapore (NUS)
2 Science Drive 3, Singapore
[3]Karlsruhe Institute of Technology (KIT), Network of Excellent Retired Scientists (NES)
and Institute of Microstructure Technology (IMT), Postfach 3640, Karlsruhe 76021, Germany
[4]The Electromagnetics Academy at Zhejiang University, Zhejiang University, Hangzhou 310058, China
[5]Research Laboratory of Electronics, Massachusetts Institute of Technology
Cambridge, Massachusetts 02139, USA

Abstract— Present-day metamaterials are usually fabricated by including dielectrics as a structural material, either as a substrate or a matrix, which might substantially restrict their usefulness and applicability due to the electric, mechanical, and thermal properties of substrates or matrices as well as their sensitivity to humidity and radiation degradation. In our previous work [1, 2], metamaterial bi-layer chips which consisted of S-shape string-like microstructures held by a frame without any substrate or matrix, were fabricated and studied by means of simulation and experiment; and the meta-foils which are positioned up-right to facilitate magnetic field coupling to the structure under normal incidence and self-supporting (free-standing and matrix-free), locally stiff, but globally flexible.

In this presentation, we describe the design and fabrication of a novel THz index-gradient metamaterials. These index-gradient metamaterials have a spatially varying refractive index such as to enable optical functions due to the index gradient (gradient optics). In such a way, a parallel slab with an appropriate index distribution may work as a prism or a lens, and stacked aligned gradient slabs would allow building optical systems.

REFERENCES

1. Moser, H. O., J. A. Kong, L. K. Jian, H. S. Chen, G. Liu, M. Bahou, S. M. P. Kalaiselvi, S. M. Maniam, X. X. Cheng, B. I. Wu, P. D. Gu, A. Chen, and S. P. Heussler, S. bin Mahmood, and L. Wen, "Free-standing THz electromagnetic metamaterials," *Opt. Express*, Vol. 16, No. 18, 13773–13780, 2008.
2. Moser, H. O., L. K. Jian, H. S. Chen, M. Bahou, S. M. P. Kalaiselvi, S. Virasawmy, S. M. Maniam, X. X. Cheng, S. P. Heussler, S. bin Mahmood, and B.-I. Wu, "All-metal self-supported THz metamaterial — The meta-foil," *Opt. Express*, Vol. 17, No. 26, 23914–23919, 2009.

Double Dirac Cones in Metamaterials

Kazuaki Sakoda
Photonic Materials Unit, National Institute for Materials Science
1-1 Namiki, Tsukuba 305-0044, Japan

Abstract— As is well known, periodic materials like photonic crystals can realize peculiar optical properties such as inhibition of spontaneous emission, enhancement of stimulated emission and nonlinear optical processes, and low-threshold lasing [1]. In addition to these properties, metamaterials have another degree of freedom, that is, electromagnetic resonant states localized in unit structures, which bring about larger flexibility to photonic band engineering. Especially, realization of linear dispersion relations in the Brillouin zone center was proven by transmission line theory [2]. I recently reformulated the same problem based on tight-binding approximation and group theory, and clarified that the linear dispersion appears as a result of mixture of resonant states with particular symmetry combinations [3, 4]. In addition, I proved the presence of isotropic linear dispersions, or Dirac cones, with an auxiliary quadratic dispersion in the zone center of two- and three-dimensional metamaterials [5], which is a counterpart of Dirac cones in photonic crystals [6].

In this presentation, I will give another method to realize Dirac cones without an auxiliary quadratic dispersion, which is attained by accidental degeneracy of doubly degenerate E_1 and E_2 modes of triangular-lattice metamaterials (Fig. 1) [7]. The secular equation of Bloch eigen functions reduces to diagonalization of a 4 by 4 matrix of the following form:

$$B = \begin{pmatrix} B_{11} & B_{12} & B_{13} & B_{14} \\ B_{12}^* & B_{22} & B_{23} & -B_{13} \\ B_{13}^* & B_{23}^* & B_{33} & B_{34} \\ B_{14}^* & -B_{13}^* & B_{34}^* & B_{44} \end{pmatrix}.$$

$$B_{11} = \frac{\omega_1^2}{c^2} + 2M_{12}\cos k_x + 4M_{14}\cos\frac{k_x a}{2}\cos\frac{\sqrt{3}k_y a}{2},$$

$$B_{22} = \frac{\omega_1^2}{c^2} + 2M_{13}\cos k_x + 4M_{15}\cos\frac{k_x a}{2}\cos\frac{\sqrt{3}k_y a}{2},$$

$$B_{12} = -4M_{16}\sin\frac{k_x a}{2}\sin\frac{\sqrt{3}k_y a}{2},$$

$$B_{13} = 4iM_3\cos\frac{k_x a}{2}\sin\frac{\sqrt{3}k_y a}{2}, \quad \text{etc.}$$

when $\{M_n\}$ are electromagnetic transfer integrals. The dispersion relations are given by

$$\omega_k \approx \omega_\Gamma \pm \frac{\sqrt{3}|M_3|ac^2k}{\omega_\Gamma} - \frac{3Ma^2c^2k^2}{16\omega_\Gamma} \quad \text{(double roots)}.$$

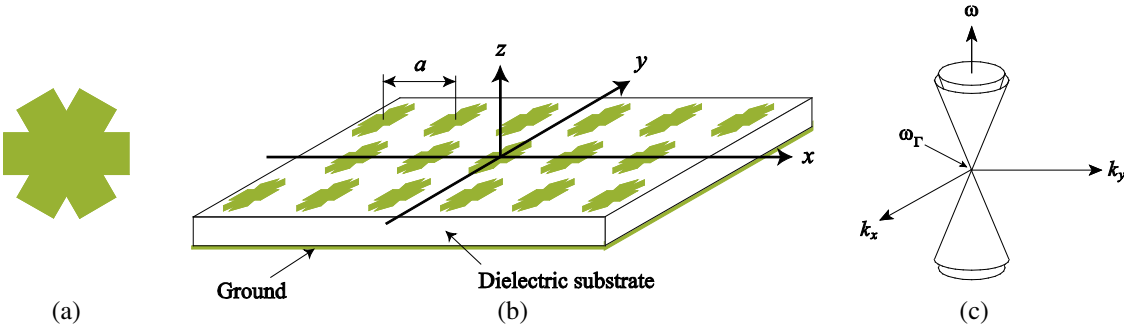

Figure 1: (a) Metallic unit structure with the C_{6v} (regular hexagon) symmetry. (b) Triangular array of the unit metallic structures on a uniform dielectric-slab waveguide with a back electrode. (c) Double Dirac cone realized by accidental degeneracy of E_1 and E_2 modes. The origin of the frequency is shifted to the degenerate frequency ω_Γ. Although the two cones are illustrated as slightly separated from each other to emphasize the presence of two cones, their actual shapes are identical.

where ω_Γ denotes the degenerate frequency. So, in the vicinity of the Brillouin zone center, the four solutions consist of two pairs of isotropic and linear dispersion relations, that is, double Dirac cones as shown in Fig. 1(c). To the best of the author's knowledge, this is the first proof of double Dirac cones in metamaterials.

REFERENCES

1. Sakoda, K., *Optical Properties of Photonic Crystals*, 2nd Edition, Springer Verlag, Berlin, 2004.
2. Caloz, C. and T. Itoh, *Electromagnetic Metamaterials — Transmission Line Theory and Microwave Applications*, Wiley, Hoboken, 2006.
3. Sakoda, K. and H.-F. Zhou, *Opt. Express*, Vol. 18, 27371, 2010.
4. Sakoda, K. and H.-F. Zhou, *Opt. Express*, Vol. 19, 13899, 2011.
5. Sakoda, K., *Opt. Express*, Vol. 20, 3898, 2012.
6. Huang, X., Y. Lai, Z. H. Hang, H. Zheng, and C. T. Chan, *Nature Mater.*, Vol. 10, 582, 2011.
7. Sakoda, K., submitted to *Opt. Express*.

A Improved Structure for Substrate Integrated Waveguide Composite Right/Left-handed Cell

Qingshan Yang, Xiangkun Zhang, and Yunhua Zhang
Key Laboratory of Microwave Remote Sensing
Chinese Academy of Sciences, Beijing 100190, China

Abstract— Composite right/left-handed (CRLH) transmission line (TL) metamaterials are defined as artificial electromagnetic structures that exhibits some special properties. Many CRLH TL structures based on microstrip and substrate integrated waveguide (SIW) have been proposed. Generally in the left-handness components, series capacitor and shunt inductor, are realized through interdigital structures and stub strips, respectively. The right-handness components are always come from the parasitic reactances and leads to a wide fast wave region of the cell dispersion.

In this work, we propose a novel SIW CRLH cell structure with a transverse slot included (see Fig. 1) and present simulation on its dispersion characteristic. It is shown that the transverse slot will act as a series inductor when its length is smaller than the resonant length. It is similar to a transverse slot on the broad face of a traditional rectangular waveguide. The analytic, simulated and experimental results show that the fast wave region of the balanced CRLH cell dispersion can be greatly compressed by introducing such a slot inductance. The larger the inductance, the narrower the fast wave region can be achieved (see Fig. 2). The newly proposed CRLH cell structure will be applied to a leaky wave antenna (LWA) for achieving large beam scanning range within a narrower frequency bandwidth, compared with other CRLH LWA structures proposed before.

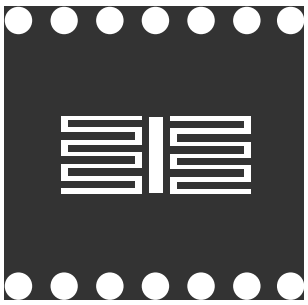

Figure 1: Proposed novel SIW CRLH cell with transverse slot.

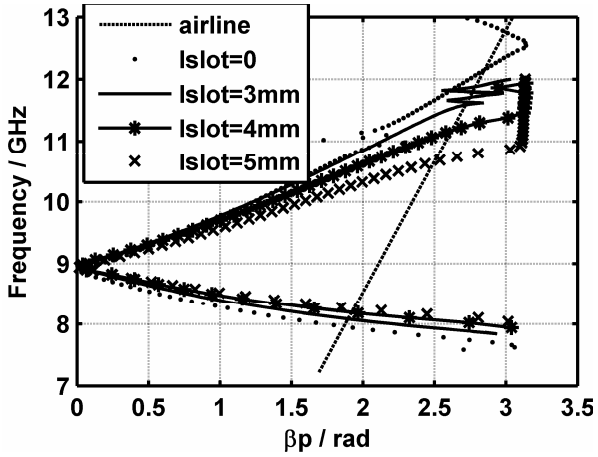

Figure 2: Dispersion curves of cells in this work with different slot lengths.

A Shunt-capacitance-aided Composite Right/Left-handed Leaky Wave Antenna with Large Scanning-range/Bandwidth Ratio

Qingshan Yang, Xiangkun Zhang, and Yunhua Zhang
Key Laboratory of Microwave Remote Sensing
Chinese Academy of Sciences, Beijing 100190, China

Abstract— Metamaterial leaky wave antenna (LWA) based on composite right/left-handed (CRLH) transmission line have been studied intensively for its outstanding advantage of continuous wide beam scanning range from backfire to endfire [1], which can be used in modern radar system for electric scanning application. Many researches on substrate integrated waveguide (SIW) structure CRLH transmission lines with the application in LWA have been reported [2, 3]. However, the required frequency scanning bandwidths of the before proposed CRLH SIW LWAs are usually as large as 40% fractional bandwidth in order to achieve certain beam scanning range of $[-60°, +60°]$ [2, 3].

In this work, we propose an improved SIW CRLH cell (see Fig. 1) for achieving large scanning-range/bandwidth ratio in application to LWA. We will demonstrate that this novel CRLH cell has a narrower fast wave region compared with other CRLH cells [2, 3], and this is resulted from the introduced extra right-handed capacitor (see the two longitude slots in Fig. 1). We compare the dispersion curves of this novel cell and that proposed in [2] (see Fig. 2). It is shown that both of them are balanced at 10 GHz, and the fast wave region of this novel cell is much narrower than that of the cell of [2].

The X-band LWA composed of 15 cells was designed and manufactured with two taper lines matched to 50 Ω at two ends (see Fig. 3). We will present both simulated and measured radiation patterns to show the achieved large scanning-range/bandwidth ratio with the mainlobe direction changes continuously from −57° to 68° within a fractional bandwidth of 27% (from 9.3 GHz to 12 GHz).

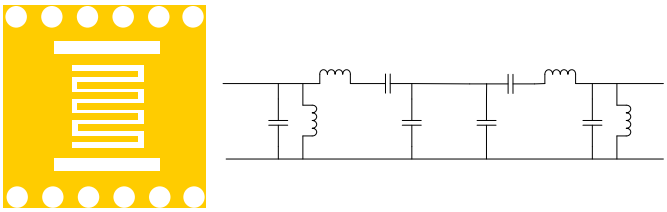

Figure 1: Proposed shunt-capacitance-aided CRLH cell and its equivalent circuit.

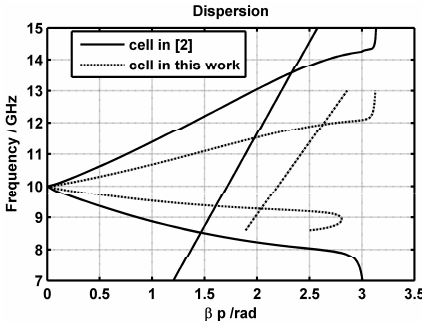

Figure 2: Dispersion of CRLH, real line: cell in [2]; dashed line: cell in this work.

Figure 3: Prototype of shunt-capacitance-aided SIW CRLH LWA.

REFERENCES

1. Lei, L., C. Caloz, and T. Itoh, *Electronics Letters*, Vol. 38, 1414, 2002.
2. Yuandan, D. and T. Itoh, *IEEE Transactions on Antennas and Propagation*, Vol. 59, 767, 2011.
3. Jin, C., A. Alphones, and L. C. Ong, *Electronics Letters*, Vol. 46, 1584, 2010.

Electromagnetic Scattering from Electrically Large Simply Shaped Bodies Coated with Metamaterial Absorbers

A. V. Osipov, A. E. Culhaoglu, E. Kemptner, and S. Thurner
German Aerospace Center (DLR), Microwaves and Radar Institute, Germany

Abstract— Metmaterial (MTM) technologies enable fabrication of thin and effective MTM absorbers [1, 2]. Such absorbers can be used as coatings to reduce radar visibility of various vehicles. A coating with the surface impedance equal to the wave impedance of the free space has a number of remarkable properties, including minimized specular reflection, low level of edge diffraction and backscattering vanishing in the optical limit (for compact convex bodies only) [3]. MTM absorbers are typically designed to reduce specular reflection from a flat and infinite metallic ground plane. In reality, however, absorbing coatings are applied to curved surfaces, implying the need of suppressing further scattering mechanisms (edge diffraction, creeping and surface waves). This paper is an overview of our recent theoretical and experimental results on electromagnetic scattering from canonically shaped electrically large scatterers with MTM coatings. Figs. 1 and 2 illustrate one of these results [4]. A simple MTM absorber with the reflection coefficient having a 10 dB minimum at the frequency $f_{res} \approx 37$ GHz has been designed and fabricated (Fig. 1). Application of this absorber to the three vertical faces of an aluminum cube with the 5 cm edge length has lowered the monostatic RCS at 0° and 90° (broadside illumination of the coated faces) by 9 and 14 dB, respectively (Fig. 2). The greater reduction at 90° is due to the lower level of edge diffraction. At 180° (broadside illumination of the uncoated face) RCS values for the coated and uncoated cube are almost equal. The level of RCS between 0° and 90° demonstrates effectiveness of the coating in the region dominated by the edge diffraction.

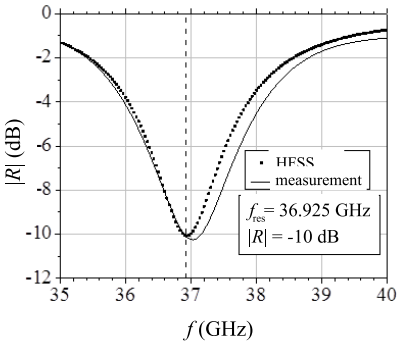

Figure 1: Measured and simulated frequency dependent reflection coefficient of a MTM absorber (array of sub-wavelength capacitively loaded copper strips printed on top of a grounded 0.1 mm thin layer of FR4).

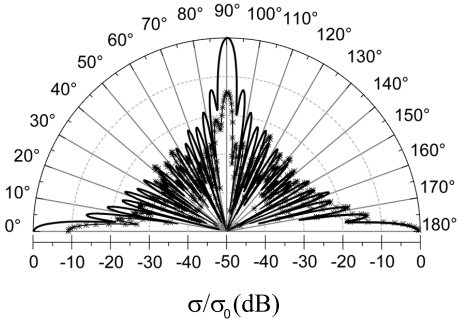

Figure 2: Measured RCS of the metal cube, uncoated (solid line) and coated with the absorber (solid line with star-shape markers) as a function of illumination angle in the horizontal plane and for horizontal polarization at f_{res}. Normalization to RCS of the uncoated cube at broadside illumination.

REFERENCES

1. Engheta, N., "Thin absorbing screens using metamaterial surfaces," *Digest of the IEEE Antennas and Propagation Society International Symposium*, Vol. 2, 392–395, San Antonio, Texas, Jun. 16–21, 2002.
2. Luukkonen, O., F. Costa, C. R. Simovski, A. Monorchio, and S. A. Tretyakov, "A thin electromagnetic absorber for wide incidence angles and both polarizations," *IEEE Trans. Antennas Propag.*, Vol. 57, No. 10, 3119–3125, 2009.
3. Osipov, A. V., "Electromagnetic scattering from objects with unit surface impedance," *Proceedings of ICEAA'12*, Cape Town, South Africa, Sep. 2–7, 2012, to Appear.
4. Culhaoglu, A. E., A. V. Osipov, and P. Russer, "Mono- and bistatic scattering reduction by a metamaterial low reflection coating," *IEEE Trans. Antennas Propag.*, submitted.

The Problem of Dielectric Metamaterial Homogenization for Electromagnetic Cloaking

Elena Semouchkina
Michigan Technological University, USA

Abstract— Metamaterials are usually analyzed by using the effective medium approach, which assumes that waves "do not see" sub-wavelength metamaterial particles and propagate in metamaterials as in uniform media. Such approach implies excitation of all particles in the medium at a single resonance frequency and identical orientation of the excited magnetic/electric dipoles, so that no resonance splitting phenomena caused by coupling between resonators are considered. Simulations performed for the plane wave incidence on a metamaterial unit cell with periodic boundary conditions in two orthogonal directions normal to the wave vector do not reveal resonance splitting and are typically used for predicting metamaterial properties. However, these simulations can only describe an infinite 2D array of unit cells, while 3D arrays formed by stacking 2D arrays in the direction of wave propagation, and, moreover, 3D arrays finite in three dimensions, demonstrate strong splitting of the resonances in typical metamaterial structures.

Here we present the results of investigation of homogenization and splitting phenomena in cloak metamaterials formed by concentric arrays of dielectric resonators. Concentric design is used in transmission cloaks to provide radial dispersion of the effective material parameters required for concealing object in accordance with the transformation optics relations. The prescribed dispersion could be achieved by contolling the difference in resonance responses from various concentric layers of resonators, while each concentric metamaterial layer should be homogenized. Satisfaction of these demands presents a serious challenge for the cloak designs utilizing identical dielectric resonators in all layers, when radial dispersion of the effective parameters should be provided by variable air fractions employed in the cloak medium. Here we demonstrate a possibility to achieve homogenization of elementary responses in metamaterial layers composed of significantly coupled resonators at frequencies corresponding to the so-called "superluminal" values of the relative effective parameters (between 0 and 1). The performance of a microwave cloak designed by using homogenized dielectric arrays is demonstrated.

Scattering Properties of Optimal Bi-anisotropic Particles

J. Vehmas, Y. Ra'di, A. Karilainen, and S. Tretyakov
Department of Radio Science and Engineering, Aalto University, Finland

Abstract— In this presentation we will discuss scattering from electrically small bi-anisotropic (BAI) particles. Our interest will be concentrated on particles with the *optimal* parameters, which ensure strongest interaction with the incident fields. In particular, we will analyze conditions for zero back-and forward scattering from general bi-anisotropic particles. All possible classes of bi-anisotropy (chirality, omega coupling, Tellegen, and artificial "velocity") are considered and compared.

Finite objects with zero backscattering are known from the literature, a classical example being an object with equal relative material parameters, $\mu_r = \epsilon_r$, and $\pi/2$ rotational symmetry when observed from the incident direction [1, 2]. Recently, it has been shown that in addition to the $\pi/2$ rotational symmetry, self-dual nature of the object is sufficient for zero backscattering [3]. For example, a DB sphere was studied in [4], and a D'B' sphere and cubein[3].

Here we study scattered fields from electrically small bi-anisotropic scatterers illuminated by an incident plane wave. The particle response can be described in terms of its polarizabilities defined as

$$\mathbf{p} = \bar{\bar{\alpha}}_{\mathrm{ee}} \cdot \mathbf{E}_{\mathrm{inc}} + \bar{\bar{\alpha}}_{\mathrm{em}} \cdot \mathbf{H}_{\mathrm{inc}} \quad (1)$$

$$\mathbf{m} = \bar{\bar{\alpha}}_{\mathrm{me}} \cdot \mathbf{E}_{\mathrm{inc}} + \bar{\bar{\alpha}}_{\mathrm{mm}} \cdot \mathbf{H}_{\mathrm{inc}} \quad (2)$$

where $\mathbf{p}$ and $\mathbf{m}$ are the induced electric and magnetic dipole moments, respectively, $\mathbf{E}_{\mathrm{inc}}$, $\mathbf{H}_{\mathrm{inc}}$ are the incident fields, and $\bar{\bar{\alpha}}$ are the polarizabilities [5].

Zero radiation or scattering in a certain direction defined by the unit vector $\mathbf{u}_r$ can be studied by demanding $\mathbf{F}_{\mathrm{sca}} = \mathbf{u}_r \times \mathbf{p} + \mathbf{m}/\eta_0 = 0$ (η_0 is the free-space wave impedance). For a plane-wave illumination along the direction of $\mathbf{u}$ we can nd the conditions on the polarizabilities which ensure zero scattering along an arbitrary direction in space. For zero backscattering we set $\mathbf{u}_r = -\mathbf{u}$ and get

$$-\mathbf{u} \times \bar{\bar{\alpha}}_{\mathrm{ee}} - \mathbf{u} \times \frac{1}{\eta_0} \bar{\bar{\alpha}}_{\mathrm{em}} \times \mathbf{u} + \frac{1}{\eta_0} \bar{\bar{\alpha}}_{\mathrm{me}} + \frac{1}{\eta_0^2} \bar{\bar{\alpha}}_{\mathrm{mm}} \times \mathbf{u} = 0. \quad (3)$$

For zero forward scattering we let $\mathbf{u}_r = \mathbf{u}$ and get the condition in form of

$$\mathbf{u} \times \bar{\bar{\alpha}}_{\mathrm{ee}} + \mathbf{u} \times \frac{1}{\eta_0} \bar{\bar{\alpha}}_{\mathrm{em}} \times \mathbf{u} + \frac{1}{\eta_0} \bar{\bar{\alpha}}_{\mathrm{me}} + \frac{1}{\eta_0^2} \bar{\bar{\alpha}}_{\mathrm{mm}} \times \mathbf{u} = 0. \quad (4)$$

In the presentation we will discuss the implications of these conditions for all fundamental classes of bi-anisotropic particles (chiral, omega, Tellegen, and "moving"). The results show that zero backscattering can be achieved with uniaxial magneto-dielectric, chiral and moving particles as long as the condition $\alpha_{ee} = \frac{1}{\eta_0^2} \alpha_{mm}$ is satisfied. Zero forward scattering, on the other hand, can only be achieved with a Tellegen particle, also fulling the same condition on co-polarizabilities. The results are useful in the design of scatterers (and their arrays) with desired electromagnetic response and in understanding limitations on achievable electromagnetic properties.

REFERENCES

1. Wagner, R. J. and P. J. Lynch, "Theorem on electromagnetic backscatter," *Phys. Rev.*, Vol. 131, No. 1, 21–23, 1963.
2. Weston, V., "Theory of absorbers in scattering," *IEEE Trans. Antennas Propag.*, Vol. 11, No. 5, 578–584, Sep. 1963.
3. Lindell, I. V., A. Sihvola, P. Ylä-Oijala, and H. Wallén, "Zero backscattering from self-dual objects of nite size," *IEEE Trans. Antennas Propag.*, Vol. 57, No. 9, 2725–2731, Sep. 2009.
4. Sihvola, A., H. Wallén, P. Ylä-Oijala, M. Taskinen, H. Kettunen, and I. V. Lindell, "Scattering by DB spheres," *IEEE Antennas Wireless Propag. Lett.*, Vol. 8, 542–545, 2009.
5. Serdyukov, A., I. Semchenko, S. Tretyakov, and A. Sihvola, *Electromagnetics of Bi-anisotropic Materias, Theory and Applications*, Gordon and Breach, Amsterdam, The Netherlands, 2001.

Graphene Metramaterials: Electron Density Waves and Carbone Nanotube-graphene-dielectric (CNTGD) Electrodynamic Characteristics

Yu. G. Rapoport[1], **V. V. Grimalsky**[2], **I. S. Nefedov**[3], **and N. A. Kalinich**[1]

[1]Physics Facuty, Taras Shevchenko National University of Kyiv, Kyiv, Ukraine
[2]Autonomous University of Morelos (UAEM), Cuernavaca, Mexico
[3]Department of Radio Science and Engineering, Aalto University, Aalto, Finland

Abstract— The concept of metatronics proposed recently [1] is merging with graphene metamaterials. In the context of this concept, at most electromagnetic (plasmonic) aspects of graphene metamaterials had been considered. We propose "three-level" approach to graphene metamaterials including "metamateruial treatment" of electron density waves in graphene (known example of which are graphene electron "perfect lenses" [2]), electron wave control upon electromagnetic characteristics (such as conductivity etc.) and, finally, electromagnetic/plasmonic effects (with proper periodical structures, electronically controllable waveguides and resonators etc.).

The first problem is to determine the characteristics of the electron wave transport in graphene layer, where the electric or magnetic field, the coefficient characterizing exchange or spin-orbit interaction, or magnetization, or these coefficients altogether could have proper inhomogeneity/periodicity. We use single-particle Hamiltonian and 4-component wave function $\vec{\psi} = (\psi_{A\uparrow}, \psi_{A\downarrow}, \psi_{B\uparrow}, \psi_{B\downarrow})^T$ where index "T" means transposition, "A", "B" correspond to one of two non-equivalent graphene sublattices ("pseudospin"), and arrows "↑" and "↓" correspond to "spin up" and "down". Extrinsic (or Rashba), intrinsic spin-orbit coupling, and an effects of magnetization (of an inhomogeneous or periodical ferromagnetic structure), and of scalar electrostatic potential describing (inhomogeneous/periodical) bias electric field are accounted for. Stationary Dirac-Weyl equations yields the new 2-component system of equations. If electron wave propagates in x direction and coefficients in (3) depend only on x, 2D wave packet is modeled numerically, using Fourier transform in transverse (y) direction. It is shown that for the system, finite in x direction (with length L_x), the boundary conditions at $x = 0$ and $x = L_x$ are reduced to the linear combination of vector wave function and it's x-derivative. Then, the new system of equations for pseudospin functions with the general 2D dependence of coefficients is derived. Method of numerical solution of such a system is under development now.

The next problem is modelling guiding electromagnetic waves in the layered structure "carbon nanotubes (CNT)-graphene-dielectric (CNTGD)", and investigation of controllable slowing down and energy flow propagation in THz range. The method of modeling guiding waves in the system CNTGD includes the effective medium model of CNT array [3], surface conductivity model of graphene [4] and transfer matrix method. The modeling shows high effectiveness of control over transfer characteristics of 2D electron wave characteristics and velocity of guided electromagnetic waves in CNTGD structure. In particular, for different quasiperiodical "magnetic barriers" (function $F_A(x)$), dependence on structure period of pseudospin transmission function $\sim |\psi_{A\downarrow}(x = L_x)|^2$ can be of "resonant" (for oscillating $F_A = F_A(x)$ with constant sign) or "switching" type (for oscillating $F_A = F_A(x)$ with alternating sign). An effective control of electromagnetic wave characteristics in CNTGD structures is provided by an external bias electric field which tunes the chemical potential in graphene layer. Distributions of the longitudinal and the transversal components of the local Poynting vector and energy velocity over the waveguide cross-section are calculated. For the considered structure, the group velocity v_g changes sign at the frequency $f \sim 16.6\,\mathrm{THz}$, while $c/v_{ph} \sim 4.32$ (v_{ph} and c are phase velocity and speed of light, respectively).

The following conclusions can be formulated. Transmission of 2D electron beam through the system with quasiperiodic structure (in particular, "magnetic barrier") and electromagnetic guiding wave characteristics in CNTGD structure are modeled. Depending of the type of quasiperiodical "magnetic barrier", pseudospin transmission function dependence on structure period can be of "resonant" or "switching" type. Conditions for very interesting regime, with large slowing down of waves, even $v_g = 0$ (and, at the same time, with increased energy concentration and decreased total energy flow) are found in CNTGD structure. High controllability of transmission electron wave function and electromagnetic characteristics can be useful for sensors, modulators and nonlinear effects in graphene, such as a very effective harmonic generation etc.

REFERENCES

1. Engheta, N., *Physics World*, 32–34, Sep. 2010.
2. Cheianov, V. M., V. Falko, and B. L. Altshuler, *Science*, Vol. 315, 1252–1255, Mar. 2007.
3. Nefedov, I. S. and S. A. Tretyakov, *Phys. Rev. B*, Vol. 84, 113410, 2011.
4. Hanson, G. W., *J. of Appl. Phys.*, Vol. 103, 064302, 2008.

Epsilon Near Zero Based Phenomena in Polaritonic Metamaterials: Total Transmission, Total Reflection and Subwavelength Propagation

Alexey A. Basharin[1], **Maria Kafesaki**[1, 2], **Eleftherios N. Economou**[1, 3], **and Costas M. Soukoulis**[1, 4]

[1]Institute of Electronic Structure and Laser (IESL)
Foundation for Research and Technology Hellas (FORTH), P. O. Box 1385, Heraklion, Crete 71110, Greece
[2]Department of Materials Science and Technology, University of Crete, Heraklion 71003, Greece
[3]Department of Physics, University of Crete, Heraklion 71003, Greece
[4]Ames Laboratory-USDOE, Department of Physics and Astronomy
Iowa State University, Ames, Iowa 50011, USA

Abstract— Metamaterials are composites characterized by unusual phenomena and properties not encountered in natural materials. In particular there are metamaterials with both negative electrical permittivity and magnetic permeability, and thus negative refractive index, there are giant permittivity metamaterials, permittivity near zero metamaterials, etc..

The aim of this work is to explain the underlying physics of total transmission and total reflection in epsilon near zero (ENZ) structures with embedded subwavelength dielectric scatterers.

We also establish that the reason of these phenomena has a resonance character and is the appearance of unusual natural modes in subwavelength dielectric defects and which are Mie- resonances. Also, we show, that these modes can be used as basis to build lenses with subwavelength resolution in such kind of systems. Finally, we apply our results in realistic systems made of polaritonic materials, namely LiF cylinders embedded in KCl matrix, demonstrating subwavelength lensing in the THz regime.

A Near/Far-field RFID Reader Metamaterial-inspired Loop Antenna with Reconfigurable Radiation Pattern and Flat Near *H*-field Distribution

V. Sanz, J. A. Martínez, A. Belenguer, J. Cascon, and A. L. Borja
Departamento de Ingeniería Eléctrica, Electrónica, Automática y Comunicaciones
Universidad de Castilla-La Mancha, Escuela Politcnica de Cuenca, Campus Universitario
Cuenca 16071, Spain.

Abstract— Radio frequency identification (RFID) is a rapidly growing technology for a variety of applications such as contactless payment, metro tickets or security. Commonly, far-field or inductively coupled near-field operation is used to interact between reader and tag [1–4]. Far-field communication is used for long read range covering areas and near-field reading is preferred for objects surrounded by metals and liquids in their vicinity. However, at UHF band the electrical size of these antennas become comparable to the operating wavelength and it cannot produce an uniform magnetic field. As a result, these antennas produce a weak and non-uniform field distribution at the center of the loop. Besides, to the best of the author knowledge, there is not deep research related to RFID antennas designs that allows multidirectional o reconfigurable far-field reading areas and near- and far-field operations at the same frequency simultaneously.

In this regard, we present different novel loop antennas incorporating a ladder network with lefthanded loading that has an isotropic covering area and improved magnetic near-field distributions. Fig. 1(a) shows the configuration of the loop antennas. The antenna is loaded by a left-handed ladder network composed of 4 unit cells where the unit cell consist of lumped capacitors in the series arm, and lumped inductors in the shunt arm.

The antenna has zero phase constant at 868 MHz, giving thus an omnidirectional pattern in the plane of the loop. The left-handed loop reader antenna offers improved performances as reconfigurable or optimized responses can easily be achieved. Also, the proposed loop antenna has demonstrated the capability of producing strong magnetic field with relatively uniform distributions in the near-field region of the antenna. This sort of study sheds light onto the potential uses of metamaterials, since conventional and emerging technologies have been compared directly. Several possible applications for these metamaterial based antennas can be foreseen in technologies such as RFID, automotive electronics, TV, and radio reception.

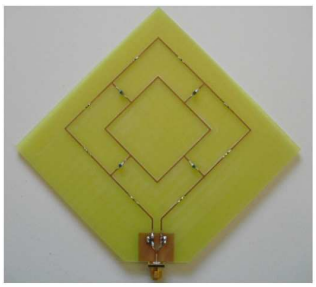

Figure 1: Fabricated prototypes of the loop antennas with left-handed loading.

REFERENCES

1. Chen, Z. N., C. K. Goh, and X. Qing, "Loop antenna for UHF near-field RFID reader," *European Conference on Antennas and Propagation*, April 12–16, 2010.
2. Ong, Y. S., X. Qing, C. K. Goh, and Z. N. Chen, "A segmented loop antenna for UHF near-field RFID," *Antennas and Propagation Society International Symposium*, July 11–17, 2010.
3. Qing, X., C. K. Goh, and Z. N. Chen, "A broadband UHF near-field RFID antenna," *IEEE Transactions on Antennas and Propagation*, Vol. 58, 3829–3838, 2010.
4. Shrestha, B., A. Elsherbeni, and L. Ukkonen, "UHF RFID reader antenna for near-field and far-field operations," *IEEE Antennas and Wireless Propagation Letters*, Vol. 10, 1274–1277, 2011.

Session 2P3
Remote Sensing of Earth Critical Parameters

A Multiple Scattering Model of Bicontinuous Medium for Radar Remote Sensing of Snow at X-band and Ku-band

Wenmo Chang[1], **Leung Tsang**[1], **Xiaolan Xu**[2], **Simon Yueh**[2], **and Kung Hau Ding**[3]

[1]Department of Electrical Engineering, University of Washington, Seattle, WA 98195-2500, USA
[2]Jet Propulsion Laboratory, California Institute of Technology, Pasadena, CA 91109, USA
[3]Sensor Directorate, Air Force Research Laboratory, Wright-Patterson AFB, OH 45433, USA

Abstract— Two models have been used to study microwave scattering by terrestrial snow: densely packed particles, and bicontinuous medium. For the case of densely packed particles, the Quasi-Crystalline Approximation (QCA) and the Foldy-Lax equations are used to study their scattering. For the case of bicontinuous media, the snow's porous structures are generated according to a continuous representation of ice-air interfaces. A large number of the stochastic sinusoidal waves are used to construct the interfaces. Various snow structures are demonstrated by adjusting the probability density function of the wave amplitude. We use the DDA/FFT to calculate the extinction coefficients, the absorption coefficients and the phase matrix. The extinction coefficients calculated for the bicontinuous media have a variety of frequency dependence ranging from as low as 1.5 to 4 for power law's index. Such varieties of frequency dependence of extinction have been observed in snow extinction measurements. The phase matrix calculated in the bicontinuous model agrees with analytical QCA method in co-polarization. However, bicontinuous model shows significant large cross-polarization, which is zero in QCA method. Then the results of phase matrix and extinctions are combined in the Dense Media Radiative Transfer theory (DMRT). The full multiple scattering solution is calculated through the quadrature approach. The surface scattering from the snow-ground interface is included by searching the look-up table. The look-up table is generated through performing large scale 3D simulations of numerical solutions of Maxwell equations of scattering by random rough surfaces. The volume and surface models are applied to study the snow scattering characteristics at X-band and Ku-band which are the two frequencies proposed in the Cold Regions Hydrology High-resolution Observatory (CoReH2O) mission by ESA and Snow and Cold Land Process (SCLP) mission by NASA. The results are compared with the POLSCAT's Ku-band airborne data and TerraSAR-X's X-band satellite data in Alaska region. We compared the multiple scattering solutions with the single scattering solutions. For large snow depths exceeding 1 meter, the optical thickness can be moderate at Ku-band and the multiple scattering effect becomes necessary.

Airborne Microwave Radiometer Measurements of Snow on Lake Ice

Martti Hallikainen[1], **Matti Vaaja**[1], **Annakaisa von Lerber**[1], **Juha Kainulainen**[1], **Jaakko Seppänen**[1], **and Juha Lemmetyinen**[2]

[1]Department of Radio Science and Engineering, School of Electrical Engineering
Aalto University, P. O. Box 13000, Aalto 00076, Finland
[2]Finnish Meteorological Institute, Finland

Abstract— Microwave radiometry has proved to be the best remote sensing tool for retrieval of dry snow characteristics, especially the snow water equivalent, from space. Regional algorithms have been developed and validated for this purpose. Accuracy of retrieved snow water equivalent is decreased, e.g., by the existence of several land cover types within a radiometer pixel (mixed pixel problem). The two main problems related to land use categories in microwave radiometry of snow are vegetation (forest) and water areas (lakes). On top of lake ice, snow depth, density and grain size may be substantially different from those on land and, additionally, the emission behavior of ice is different from that of frozen/thawed soil.

We have carried out radiometer measurements over lake ice in 2004, 2007, 2011 and 2012 using several frequencies. Our airborne microwave radiometer system HUTRAD operates at 6.8, 10.7, 18.7, 23.8, and 36.5 GHz, providing data for both vertical and horizontal polarization at an incidence angle of 50 degrees off nadir. The HUTRAD system is accommodated on our research aircraft Skyvan and looks to the rear along the flight track; the rear cargo door is removed before taking off for data collection.

The lakes over which radiometer measurements have been carried out are located in southern Finland. Lake Bodom is 5 km long and 1.4 km wide. The adjacent Lake Matalajärvi is separated from Lake Bodom by a narrow isthmus and is shallow and somewhat smaller. Measurements cover also land areas before (forested) and after (farmland) the start/end of the lake flight line, allowing comparison of results for snow-covered lake ice with those for snow-covered terrain including forested and open areas.

Four experiments were conducted in 2011 and two in 2012. The conditions covered dry snow/ice, occasional water on top of ice, moist snow surface, and the melting season. In situ data were collected simultaneously with airborne data acquisition. Results from these experiments are discussed in the presentation.

Electrical Characteristics Dependence of Monstera Leaf on Moisture Content

O. Kurnaz, Y. E. Yoruk, and S. Helhel
Department of Electrical and Electronics Engineering, Akdeniz University, Turkey

Abstract— Understanding the reflecting, absorbing, transmitting and scattering coefficients of vegetation canopies play an important role in success of some environmental, military or commercial applications such as agricultural planning, remote sensing and radio-link optimization. In this study, transmittance and reflection dependence of monstera leaf on moisture content has been investigated at frequencies between 7 GHz and 9 GHz. A piece of a monstera leaf having 6 cm length, 4 cm width and 770 µm thickness has been put within a thin metal box. One side of the box has been connected to an open-ended rectangular waveguide which is used as measuring probe and other side has been connected to the source signal. A network analyzer is used as both signal source and measuring device. Transmittance is measured by using S_{21} parameter and reflection is measured by using S_{11} parameter. Measurements have been carried out with 20 MHz intervals through eight days. At the end of eight-day period, the leaf has lost 65.93% of its total weight. It has been observed that transmittance increases as moisture content decreases and the transmittance at the end is almost two times that at the beginning. On the other hand, reflection does not show a monotonic increase or decrease and the change in reflection is very small, that is, reflection change is below 5% from beginning to the end. It is deducted from the result that most of the electrical power is absorbed within the moisture content of the leaf when the leaf is not dry. Also, it is found that maximum transmittance has occurred at 8 GHz and maximum reflection has occurred at 7.6 GHz where both coefficients show a fluctuating behavior between 7 GHz and 9 GHz.

Passive Microwave Remote Sensing Using Omega-tau Model with Rough Surface Boundary Conditions from NMM3D

L. Tsang[1], **I. Koh**[2], **T. Liao**[1], **and Shaowu Huang**[1]

[1]Department of Electrical Engineering, University of Washington
Seattle, WA 98195-2500, USA
[2]Inha University, South Korea

Abstract— In passive microwave remote sensing of the earth, the omega-tau model has been used for many years. The model has been the basis for retrieval algorithms for the AMSR, SMOS and SMAP missions. The omega-tau model is based on the zeroth order solution of the radiative transfer equation. For the roughness effects, the omega-tau model is based on the Kirchoff approximation of the coherent wave which gives a factor of $\exp(-h)$ where h is $4k^2s^2\cos^2\theta$, k is the wavenumber, s is the physical rms height and θ is the incident angle. However, the expression in terms of height is not useful as the incoherent waves are ignored. Thus in the omega tau model, the expression of $\exp(-h)$ is till retained but h becomes an empirical parameter. This makes the model an empirical model rather than a physical model. The NASA SMAP mission is to be launched in October 2014. In the mission, both active and passive remote sensing sensors will be used. In active remote sensing, a physical roughness model based on NMM3D (Numerical solutions of Maxwell equations) will be used. Thus it is useful to use the same roughness model for both active and passive.

In this paper, we derive expression of the brightness temperatures of vegetation canopy based on the omega-tau model, but with the traditional rough surface boundary condition $\exp(-h)$ of empirical h replaced by Numerical Simulations of 3D Maxwell equations (NMM3D). Using Numerical solutions of Maxwell equations, we calculate the bistatic scattering of random rough surfaces. The bistatic scattering are further decomposed into coherent waves which is specular scattering and bistatic scattering of incoherent waves. The bistatic incoherent waves are further decomposed into co-polarization and cross polarization. The model of Maxwell equations are based on physical parameters of rms heights, correlation lengths and correlation functions. Numerical results are illustrated for a variety of roughness conditions. The contributions of each component of coherent wave and incoherent waves are illustrated. Comparisons are made with the $\exp(-h)$ model and the Kirchoff approximation. For the vegetation and surface interactions, we examine the effects of bistatic scattering of the incoherent waves. The angular distributions of the incoherent waves are illustrated. Comparisons are made with experimental measurements.

Microwave Vegetation Index from SMOS

Jiancheng Shi
State Key Laboratory of Remote Sensing Science
Institute of Remote Sensing Applications and Beijing Normal University, Beijing, China

Abstract— Monitoring global vegetation can be of importance in understanding land surface processes and their interactions with the atmosphere, biogeochemical cycle, and primary productivity. The commonly used vegetation indices derived from the visible-near infrared sensors are mainly dependent on the green leaf material of the vegetation cover and often limited by the effects of atmosphere, background soil conditions, and saturation at high levels of vegetation. In our previous study [1], we developed the microwave vegetation indices (MVIs) with the dual-frequency technique under the Advanced Microwave Scanning Radiometer (AMSR-E) sensor configuration on the Aqua satellite. The MVIs derived in this study are less affected by soil surface emission signals, and depend mainly on vegetation properties such as vegetation fractional coverage, biomass, water content, temperature, the characteristics of the scatterer size, and the geometry of the vegetation canopy. It demonstrated that the microwave derived vegetation indices can provide complementary vegetation information (both the leafy and woody parts of the vegetation) by optical sensors. This method provides a new opportunity to establish a long-term global dataset for monitoring vegetation cover using all-weather passive microwave instruments. In this study, we will explore and demonstrate a new technique for deriving Microwave Vegetation Indices (MVIs) using the passive microwave radiometer SMOS data. It provides the global microwave brightness temperature observations at L-band (1.4 GHz) with dual polarizations (V, H) and a range of viewing angles [2].

REFERENCES

1. Shi, J., T. Jackson, J. Tao, J. Du, R. Bindlish, L. Lu, and K. S. Chen, "Global microwave vegetation indices from satellite passive microwave sensors," *Remote Sensing Environment*, Vol. 112, No. 12, 4285–4300, Dec. 2008, doi:10.1016/j.rse.2008.7.015.
2. Kerr, Y. H., P. Waldteufel, J.-P. Wigneron, S. Delwart, F. Cabot, J. Boutin, M.-J. Escorihuela, J. Font, N. Reul, C. Gruhier, S. E. Juglea, M. R. Drinkwater, A. Hahne, M. Martín-Neira, and S. Mecklenburg, "The SMOS mission: New tool for monitoring key elements of the global water cycle," *Proceedings of the IEEE*, Vol. 98, No. 5, May 2010.

Resolution Control for SAR Tomography with Optimized Track Distribution

A. Capozzoli, C. Curcio, and A. Liseno
Dipartimento di Ingegneria Biomedica, Elettronica e delle Telecomunicazioni
Università di Napoli Federico II, via Claudio 21, Napoli I 80125, Italy

Abstract— SAR tomography [1, 2] allows accessing 3D information on the investigated scenario by constructing a synthetic aperture transverse to the flight direction by exploiting several passes of the same sensor over the same scene or using sensors constellations working simultaneously.

Indeed, the amount of information that can be acquired in the height direction is limited by the difficulties and costs of realizing many passes of the same sensor on the same scene, including the effects of temporal decorrelation, or alternatively of implementing constellations of several sensors.

Operating with "few" acquisitions requires defining the measurement constellation maximizing the collected information, given some knowledge on the scene of interest. This problem, which arises to be crucial in defining the actual potentialities of SAR tomography, has been generally overlooked until very recently [3–6]. In particular, in [3, 4], it has been shown how, by properly exploiting the available a priori information through an appropriate representation of the problem unknowns and by a suitable optimization of the measurement constellation, the number of required acquisitions can be reduced.

The purpose of this paper is to extend the technique in [3, 4] so that the number and the (generally irregular) positions of the tracks to be flown can be flexibly linked both to the a priori information on the investigated scenario, and to the information one is actually interested to extract about the scene at hand. This includes the possibility to handling the number and positions of the tracks as a function of desired degree of resolution/multiresolution [7].

To this end, the reflectivity distribution of the scene is represented by prolate spheroidal wave functions, properly filtered to a desired resolution limit [7], and the measurement constellation is designed in terms of track number and positions, by a singular value optimization procedure [8]. A numerical analysis shows the potentialities of the technique.

REFERENCES

1. Reigber, A. and A. Moreira, "First demonstration of airborne SAR tomography using multibaseline L-band data," *IEEE Trans. Geosci. Remore Sens.*, Vol. 38, No. 5, 2142–2152, Sep. 2000.
2. Fornaro, G., F. Serafino, and F. Soldovieri, "Three-dimensional focusing with multipass SAR data," *IEEE Trans. Geosci. Remote Sens.*, Vol. 41, No. 3, 507–517, Mar. 2003.
3. Nannini, M., R. Scheiber, and A. Moreira, "Estimation of the minimum number of tracks for SAR tomography," *IEEE Trans. Geosci. Remote Sens.*, Vol. 47, No. 2, 531–543, Feb. 2009.
4. Severino, V., M. Nannini, A. Reigber, R. Scheiber, A. Capozzoli, G. D'Elia, A. Liseno, and P. Vinetti, "An approach to SAR tomography with limited number of tracks," *Proc. of the IEEE Int. Symp. on Geosci. Remote Sens.*, IV-216–IV-219, Cape Town, South Africa, Jul. 12–17, 2009.
5. Capozzoli, A., G. D'Elia, A. Liseno, P. Vinetti, M. Nannini, A. Reigber, R. Scheiber, and V. Severino, "SAR tomography with optimized constellation and its application to forested scenes," *Atti Della Fondazione G. Ronchi*, Vol. LXV, No. 3, 367–375, May–Jun. 2010.
6. Budillon, A., A. Evangelista, and G. Schirinzi, "Three-dimensional SAR focusing from multipass signals using compressive sampling," *IEEE Trans. Geosci. Remote Sens.*, Vol. 49, No. 1, 488–499, Jan. 2011.
7. Capozzoli, A., C. Curcio, and A. Liseno, "Controlling the far-field resolution in near-field antenna characterization," *Proc. of the Antenna Measur. Tech. Ass.*, 1–6, Englewood, CO, Oct. 16–21, 2011.
8. Capozzoli, A., C. Curcio, A. Liseno, and P. Vinetti, "Field sampling and field reconstruction: A new perspective," *Radio Sci.*, Vol. 45, RS6004, 31, 2010, doi:10.1029/2009RS004298.

A Simple Parameterization for Sensible and Latent Heat Fluxes during Unstable Daytime

Jing Lu[1, 2, 3], **Zhao-Liang Li**[1, 3], **Hua Wu**[1], **Bohui Tang**[1], **and Jelila Labed**[3]

[1]State Key Laboratory of Resources and Environmental Information System
Institute of Geographic Sciences and Natural Resources Research, Chinese Academy of Sciences
Beijing 100101, China
[2]Graduate University of Chinese Academy of Sciences, Beijing 100049, China
[3]LSIIT, UdS, CNRS, Bld Sebastien Brant, BP10413, Illkirch 67412, France

Abstract— This study firstly develops a simple parameterization for sensible and latent heat fluxes under unstable conditions. The parameterization consists of some unknown variables considered as constants during the daytime and some known functions related to surface temperature and air temperature. The sensible heat flux (H) is expressed as a quadratic function of the difference between surface temperature and air temperature, and the latent heat flux (LE) is parameterized as a function of the saturated water vapor pressure at surface temperature as well as the difference between surface temperature and air temperature. The accuracy of the parameterization for H and LE is evaluated by the measurements from Yucheng station, north of China. For H, the coefficient of determination (R^2) is 0.925, the root mean square error (RMSE) is 27.8 W/m^2, and the bias (BIAS) is -14.2 W/m^2, and for LE, the R^2, RMSE, and BIAS are 0.946, 24.7 W/m^2, and 0.5 W/m^2, respectively. With the assumption that surface available energy is known, the minimization technique is used to inverse heat fluxes. The H is underestimated by 30.7 W/m^2, and the corresponding LE is overestimated by 30.4 W/m^2. The RMSEs of H and LE are 54.1 and 56.6 W/m^2, and R^2 are 0.775 and 0.806, respectively. The method can estimate H and LE at any time during unstable daytime without the need to calculate the resistance. The remotely sensed data from the geostationary meteorological satellite can be utilized adequately by the method in the future.

Estimating Land Surface Variables from Satellite Observations: Chinese GLASS Products

Shunlin Liang[1, 2], **Y. Bai**[2], **J. Cheng**[2], **X. Cheng**[2], **Q. Liu**[2], **S. Liu**[2], **H. Ren**[2], **Y. H. Qu**[2], **Y. Qu**[2], **Z. Xiao**[2], **W. Yuan**[2], **X. Zhang**[2], **and X. Zhao**[2]

[1]Department of Geography, University of Maryland, USA
[2]Beijing Normal University, China

Abstract— To support the global environmental change studies and development of new generation of earth system models, China launched the 863 key project entitled "generation and application of global products of essential land variables". The key component of this project is to develop the Global LAnd Surface Satellite (GLASS) system for generating five land surface products: Leaf Area Index, Albedo, Emissivity, Downwelling Shortwave Radiation and Photosynthetically Active Radiation. The first three GLASS products span from 1985–2010 with 1 km and 5 km spatial resolutions and 8-day temporal resolution, and the last two GLASS products from 2008–2010 with 3-hour temporal resolution and 5 km spatial resolution. This presentation will provide an overview of this project, algorithms, characteristics and preliminary validation results of these five GLASS products.

Global Carbon Cycle Research Using Surface Remote Sensing and Atmospheric CO_2 Data

Jing M. Chen[1, 2]

[1]Department of Geography and Program in Planning, University of Toronto
Room 5047, 100 St. George St., Toronto, ON M5S 3G3, Canada
[2]International Institute of Earth System Science
Nanjing University, Hankou 22, Nanjing, Jiangsu 210093, China

Abstract— Terrestrial ecosystems are an important part of the global climate system and are profoundly influenced by human activities. Although the global carbon budget is closed in recent publications, mechanisms controlling the terrestrial carbon source and sink distribution are one of the most uncertain factors in projecting climate change in the near future. The focus of my research teams in Canada and China is on studying the terrestrial carbon source and sink distribution and its controlling mechanisms using both surface remote sensing and atmospheric CO_2 data. Surface remote sensing data provide vegetation type, structure, and disturbance information, and in combination with climate and soil data, this information is used for mapping the carbon source and sink distribution using an ecosystem model. The model is also used to attribute the distribution to disturbance (fire, insect and harvest) and non-disturbance (climate, CO_2, nitrogen deposition) factors. Hourly terrestrial carbon fluxes calculated by the model and data for other fluxes (fossil fuel emission, biomass burning, ocean flux) provide inputs to atmospheric transport models to simulate the spatiotemporal dynamics of the atmospheric CO_2 concentration. The modeled CO_2 concentration is sampled at over 200 GlobalView stations distributed globally, and the monthly or weakly differences between modeled and observed CO_2 concentrations at the GlobalView stations are used to optimize the carbon flux estimated by the ecosystem model through atmospheric inversion and data assimilation. Nested global inversion systems with foci on North America and Asia and a Global Carbon Assimilation System are developed for regional and global carbon cycle studies. Results from these systems will be introduced and discussed during in my presentation.

Estimated Radar Systems Attenuation at Millimetre Wave Using Backscattering Amplitude in Durban

P. A. Owolawi
Department of Electrical Engineering
Mangosuthu University of Technology, KwaZulu-Natal, South Africa

Abstract— Weather radar systems often operate at frequencies about 3 GHz, the exploitation of millimeter wave band is the interest of this paper. The use of shorter wavelength such as millimeter wave band has advantages like increase in radar beam precision, record reflected signal with lower rain rate effect, ability to use retrieving profile technique, reduction in radar equipment size and dimension such as antenna, transmitter and receiver modules.

One of the shortfalls of this frequency range is the impairment due to rain. The properties of raindrop size with relation to rain rate are presented. The properties such as radar reflectivity factor, liquid water content, optical extinction and median water volume are added to the component of this work. Power law relations are developed between rain rate and its properties for proper understanding of drop size characteristics.

The work presented here will develop raindrop size distribution model and backward scattering amplitudes are modeled for the estimation of backscattering rain attenuation. This type of attenuation is used to estimate signal loss in the reflected signal. The coefficients of the backscattering attenuation are determined and used to calculate radar cross section, estimate maximum range, signal to noise ratio at different rain rates and frequencies.

The obtained results may be of great interest to radar systems designer in the region.

Session 2P4
Near to Mid-range Wireless Power Transfer Technology: Principles and Applications 2

Wireless Power Transmission by Scalar Waves

Konstantin Meyl
Faculty of Computer and Electrical Engineering, Furtwangen University, Germany

Abstract— Current RFID technology explains how the transfer of energy takes place on a chip card by means of longitudinal wave components in close range of the transmitting antenna. It is scalar waves which spread towards the electrical or the magnetic field pointer. That provides the better explanation.

Using the wave equation proposed by Maxwell's field equations these wave components were set to zero. Why were only the postulated model computations provided after which the range is limited to the sixth part of the wavelength.

This text proposes instead the rationale for scalar wave components in the wave equation of Laplace. Physical conditions for the development of scalar wave transponders become operable well beyond the close range. Scalar wave information and energy is transferred with the same carrier wave and not carried over two separated ways as with RFID systems. Bi-directional signal transmission with energy transfer in both directions is achieved when there is a resonant coupling between transmitter and receiver.

The first far range transponders developed on the basis of the extended field equations are already functional as prototypes, *according to the US-Patent No. 787,412 of Nikola Tesla: Art of transmitting electrical energy through the natural medium, New York 1905.*

New areas of application with increased requirements are for example:

- In telemetry plants rotary sensors are to be supplied with energy (in the car, e.g., to control tire-pressure).
- Also with heat meters the energy should come from a central unit and be spreadly wireless in the whole house to the heating cost meters without the use of batteries (replacing active RFIDs).
- In airports contents of freight containers are to be seized, without having been opened or the forwarding trade wants to examine closed truck charges by transponder technology (security checks).
- In the robot and handling technique the wirings are to be replaced by a wireless technology due to wear-out problem.

Study of Transmission Performance on Strong Coupling Wireless Power Transfer System in Free Position

X. L. Huang, W. Wang, L. L. Tan, J. M. Zhao, and Y. L. Zhou
School of Electrical Engineering, Southeast University, Nanjing 210096, China

Abstract— With power frequency fixed, the output power and transmission efficiency maximum points of wireless power transmission system do not appear simultaneously under Series-Parallel (SP) resonance model. However, output power and transmission efficiency have key relationships with the impedance matching of system. With the change of spatial free position of two coils, the mutual inductance between two coils will change, which have a further influence on impedance matching of system. Therefore, an optimization scheme has been proposed which is based on pursuit of the maximum transmission efficiency or output power. That is to say, in different free position, power ascension or efficiency improving can be achieved through the appropriate regulation of axial distance, radial distance or offset angle.

It shows relationships between power, efficiency and axial distance, radial distance or offset angle in Figure 1 and Figure 2, which is achieved by theoretical simulation, and simulation parameters: two identical spiral copper laps $r = 10\,\text{cm}$, $N = 31$. Results show that the change of the axial distance, radial distance or offset angle has an apparent effect on the output power and transmission efficiency of system, which suggests that by changing the axial distance, radial distance or offset angle we can realize the adjustment of the power and efficiency of the system. So, the feasibility of the above conclusions theoretically has been proved. From the experimental results of Figure 3 and Figure 4, it is known that when the axial distance $d = 5\,\text{cm}$ and radial offset distance increases from 0 to 5 cm, output power increases 6 W. Offset angle ranges from 0° to 10°, the transmission efficiency decreases 3% and when the angle continues increasing to 30°, the efficiency has a sudden 4% increment. The feasibility of the above theories has been proved by experiment.

Meanwhile, another comparative experiment is designed to verify the impact of the surrounding environment upon the performance of the system. Two iron panels have been added to both sides of the 10 cm symmetry of the system in the case of fixed power frequency. It is found

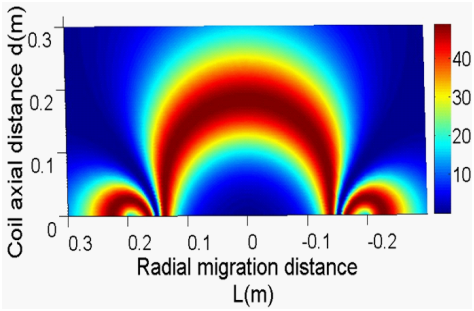

Figure 1: P with L and d, simulation.

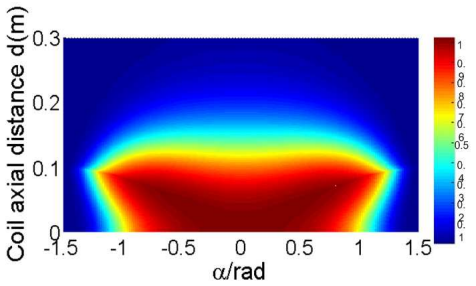

Figure 2: η with α and d, simulation.

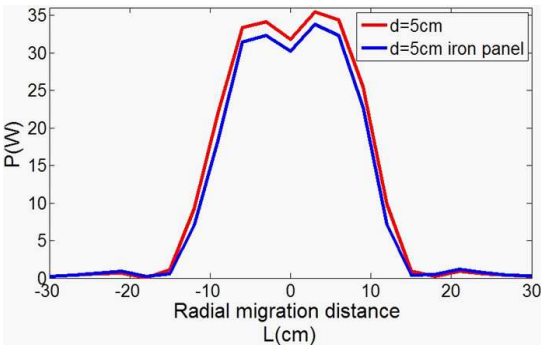

Figure 3: $d = 5\,\text{cm}$, P with L, experiment.

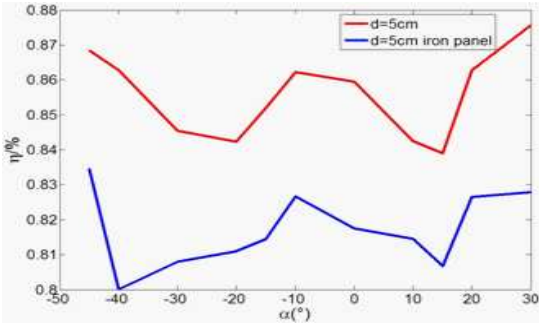

Figure 4: $d = 5\,\text{cm}$, η with α, experiment.

that transmission performance (transmission efficiency and output power) of system has declined (blue wire in Figures 3, 4), but the trend is the same as it with no obstacles. To sum up, this paper puts forward a way of adjustment to achieve the maximum output power and transmission efficiency of the system through changing axial distance, radial distance or offset angle between two coils. It will have a good significance for the design and control of practical applications.

Investigation of Characteristics of the Current for the Maximum Power Transfer in Wireless Power Transmission

X. L. Huang, Q. J. Ji, L. L. Tan, W. Wang, and H. Qiang
School of Electrical Engineering, Southeast University, Nanjing 210096, China

Abstract— The electromagnetic field distribution between the two coils of wireless power transmission (WPT) is investigated by the way of numerical calculation. Meanwhile the relationship between the current phase difference of the two coils (transmitting Tx coil and receiving Rx coil) and the transferred power is revealed and discussed.

In the WPT system, the energy is transferred with the aid of a coupling electromagnetic field between the two coils. The main working principles of WPT that are mostly referred and discussed are the electromagnetic induction and the magnetic resonance coupled mode theory. In this paper, the electromagnetic field distribution is obtained by the numerical calculation of finite element method. For the special coils, the electromagnetic field distribution is determined by the amplitude and phases of the current in two coils, labeled as $\dot{I}_1 = A\angle 0$, $\dot{I}_2 = B\angle\varphi$ (φ is the phase angle difference). With the numerical calculation of the Maxwell equation, the distribution of the Poynting vector between the Tx coil and Rx coil is obtained (Fig. 1). It can be seen that the power is transferred from one coil to another. Integrating the Poynting vector in the surface that in the middle of the two coils (as seen in the Fig. 1), the power (P_t) transferred from Tx coil to Rx could be obtained. Setting the current amplitudes of A and B, and adjusting the φ, we could find that the peak of P_t occurs when the $\varphi = \frac{\pi}{2}$ (Fig. 2). The relation of P_t and other factors, such as the frequency of work, current amplitudes, are also discussed. The conclusions proposed in this paper are deduced based on the theory of electromagnetic field, so it is universal to be benefit to understand the working principle of WPT and carry out the further researches.

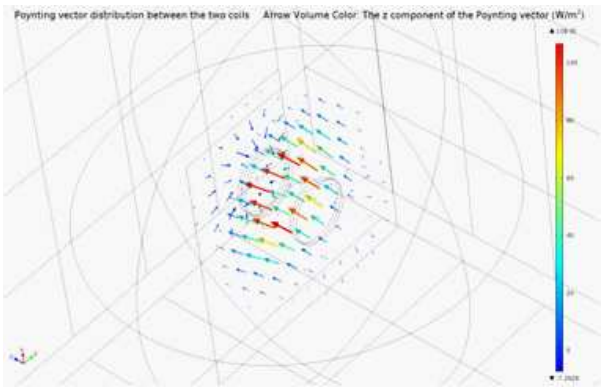

Figure 1: The Poynting vector distribution between the two coils.

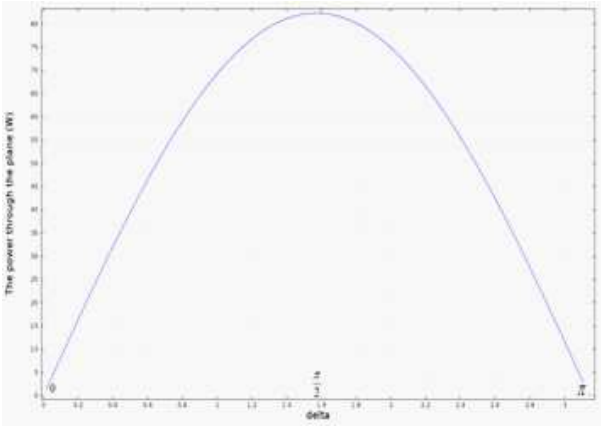

Figure 2: The P_t change with the φ.

The Coil Misalignment Model of Inductively Coupled Wireless Power Transfer System: Mutual Inductance Analysis and Transfer Efficiency Optimization

X. L. Huang[1], **H. Qiang**[1, 2], **and L. L. Tan**[1]

[1]School of Electrical Engineering, Southeast University, Nanjing 210096, China
[2]School of Information Science and Engineering, Changzhou University, Changzhou 213164, China

Abstract— A novel means of optimizing transfer efficiency of the inductively coupled wireless power transfer (ICWPT) system is presented for the first time by looking for the partial optimal solution of mutual inductance of coil misalignment.

Inductive coupling is one major technology of wireless power transfer, which transfers power from a primary transmitter (Tx) coil to a secondary receiver (Rx) coil with the aid of an alternating magnetic field. Many researches have deduced the expression of the transfer efficiency and results show that the high transfer efficiency is associated with the great mutual inductance. To the general knowledge, the Tx and Rx coils would be ideally coaxially orientated so that maximum coupling such as the maximum mutual inductance and the optimal transfer efficiency results. Meanwhile the mutual inductance is correlated with the parameters of coils and the separate distance, lateral distance and tilt angle between the two coils. In the applications envisaged, such as electric vehicles and biomedical implants, generally the receiving coil is laterally and angularly misaligned from the transmitting coil. The numerical solution of the mutual inductance between the two coils is derived and simulation result shows that there is a partial optimal solution in the ranges of lateral and angular misalignments with the special system parameters, as shown in Fig. 1. Then a novel means is presented for the first time to design the coil to be removable and rotatable for optimizing transfer efficiency by looking for the maximum mutual inductance in a special rangs. Finally the experimental results show it is accordant with the theory analysis and the proposed means is efficient and greatly improves the transfer efficiency. If the transfer distance is 15 cm and there is no lateral misalignment, the transfer efficiency can be improved about from 38.6% to 60.5% by turning the transmitting coil to vary the tilt angle from 0 to $\pi/4$, as shown in Fig. 2. This introduced technique can be widely applied to wireless power transfer system to optimize the transfer efficiency.

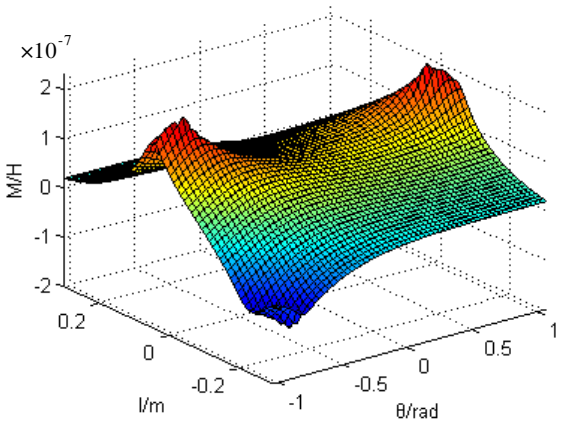

Figure 1: Mutual inductance M of coil misalignment with lateral distance l and tilt angle θ.

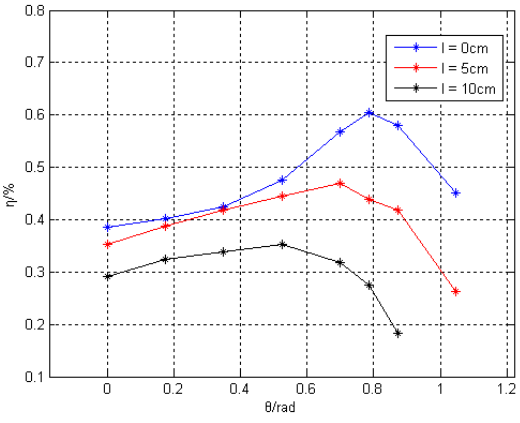

Figure 2: The measured transfer efficiency, where the Tx coil is removable and rotatable while the Rx coil is fixed.

Resonant Frequency Splitting Analysis and Optimation of Wireless Power Transfer System

X. L. Huang, L. L. Tan, W. Wang, Y. L. Zhou, and H. Qiang
School of Electrical Engineering, Southeast University, Nanjing 210096, China

Abstract— Studies reveal that while at long-distance transmission, the wireless power transfer system has only one stable resonant frequency and under this frequency the transmitting and receiving coils circuits in their self-resonance respectively, meanwhile, the system achieves efficient performance. But, at close transfer distance, the system resonant frequency will give rise to three resonant frequencies which increase the power transfer instability. Because of the system has more than one resonant frequency which means resonant frequency splitting occurs, it is difficult to determine an ideal frequency controlling points. So it is necessary to solve the resonant frequency splitting problem to improve the system stability and control ability at whole transfer distance.

In order to achieve system resonance, varieties of capacitor compensated modes can be used in transmitting and receiving circuits. In this paper the bilateral capacitor parallel-compensated topology (PP) is studied, and the system load equivalent model is established to analyze the variation characteristics of the system input impedance. Then the threshold conditions of the transfer distance and load are given while the system resonant frequency splitting occurs. In conclusion, an optimization control method is proposed to ensure the system a single stable resonant frequency and effective work in resonant status.

Based on the above analysis, it can be found that at close distance, a single stable resonant frequency of the transfer system for an easy control can be achieved through the following two methods: (1) with resonant frequency ω_0 and load R_L fixed, adjusting α to achieve the system's operation on ω_0, which $\omega = \beta\omega_0$, which α for capacitance ratio $\alpha = C_1/C_2$, C_1, C_2 are the capacitor compensated of system coils. This method has less requirements on power source frequency output and only needs change in small range. However, a too large α will cause a large gap between the system's transmitting and receiving circuits self-resonant frequency, which is not conducive to the effective power transfer; (2) with α fixed, and adjusting R_L to achieve only one resonant frequency at the whole distance under the context of $d < d_c$, where, d_c denoted as a threshold distance which makes the system has only one resonant frequency.

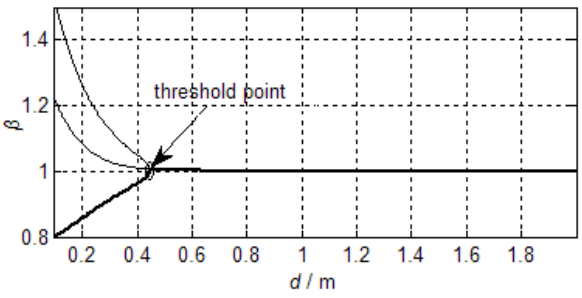

Figure 1: Frequency splitting, which $\omega = \beta\omega_0$.

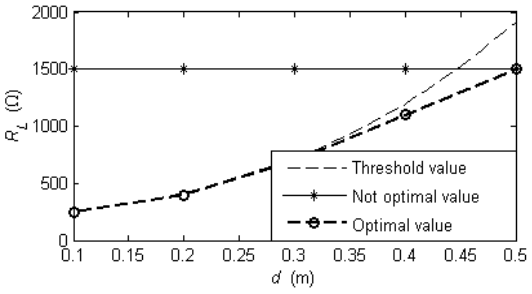

Figure 2: The curve of R_L varied with d.

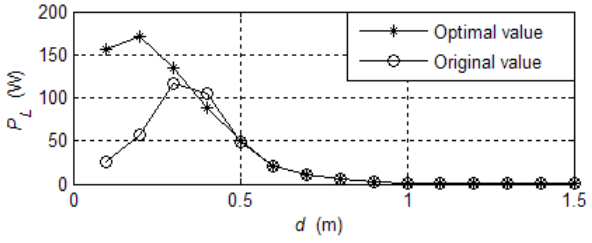

Figure 3: Load received power varied with d.

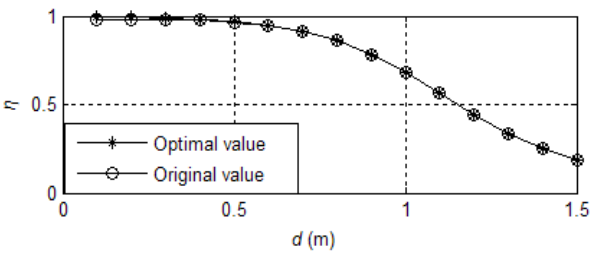

Figure 4: Transfer efficiency varied with d.

Equivalence of Inductive Coupling and Strongly Coupled Magnetic Resonance in Wireless Power Transfer

D. S. Ricketts and A. Hillenius
Carnegie Mellon University, Pittsburgh, USA

Abstract— Recent demonstrations of mid-range wireless power transfer using *strongly coupled magnetic resonance* [1] has created a resurgence in research activity in wireless power delivery using magnetoquasistatic fields. Inductively coupled wireless power transfer has been extensively studied and used over the past 100 years, in particular the last 50 years in biomedical and charging applications [2]. Works using coupled magnetic resonance have purported that the coupled resonance produces increased efficiency over non-resonant approaches [1, 3], e.g., inductive coupling. Several modeling papers have shown that the coupled magnetic resonance can be modeled by a simple mutual inductance and RLC network using standard network theory [4]. In particular, they show that the use of resonance can be interpreted simply as an optimal impedance matching of load and source, just as is done routinely in inductively coupled wireless power transfer. These works are very useful for modeling and calculations; however, they do not show explicitly or experimentally that that the maximum possible power transfer is dictated by coil geometry and separation only, and that optimum power transfer can be achieved with an optimally impedance matched inductively coupled 2-coil system or with a strongly coupled magnetic resonance 4-coil system. In this work we present experimental results of a non-resonant source coil (no resonating capacitor) impedance matched with a discrete T-matching network and a strongly coupled magnetic resonant source coil system tuned for optimal efficiency. We show that the maximum power transfer is the same for both systems and that the maximum power is determined by the geometry of the coils, i.e., inductors, only. We also show experimentally that the use of an external impedance matching network or a 2-coil strongly coupled magnetic resonant system is simply a different implementation of the same physical principles.

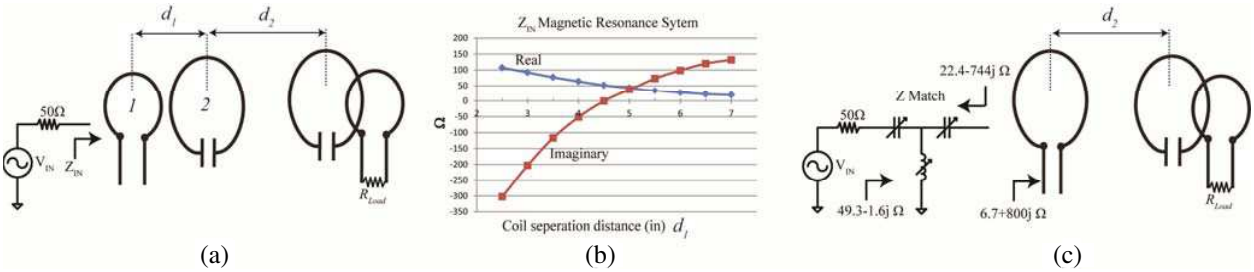

Figure 1: (a) Strongly coupled magnetic resonance. d_1 is adjusted for maximum power transfer d_2 is fixed at 10 in. (25.4 cm). (b) Input impedance of part (a) as a function of d_1. (c) Same loop as in (a) but without a resonance capacitor. Impedance match is achieved with discrete T-match circuit. Measured impedances shown. Both loops have identical loads and generate approximately the same output power (30 mW in this example).

REFERENCES

1. Kurs, A., et al., "Wireless power transfer via strongly coupled magnetic resonances," *Science*, Vol. 317, 83–86, July 2007.
2. Donaldson, N. de N. and T. A. Perkins, "Analysis of resonant coupled coils in the design of radio frequency transcutaneous links," *Med. & Biol. Eng. & Comput.*, Vol. 21, 612–627, 1983.
3. Ho, S. L., et al., "A comparative study between novel witricity and traditional inductive magnetic coupling in wirless charging," *IEEE Tran. on Mag.*, Vol. 47, 1522–25, May 2011.
4. Dionigi, M. and M. Mongiardo, "CAD of wireless resonant energy links (WREL) realized by coils," *IEEE Int. Microw. Symp.*, 1760–1763, 2010.

A Comparison of Analytical Models for Resonant Inductive Coupling Wireless Power Transfer

E. Bou[1], **E. Alarcon**[1], **and J. Gutierrez**[2]

[1]Electronic Engineering Department, Technical University of Catalonia UPC BarcelonaTech, Spain
[2]Applied Physics Department, Technical University of Catalonia UPC BarcelonaTech, Spain

Abstract— Recent research in wireless power transfer (WPT) using resonant inductive coupling has demonstrated very high efficiencies (above 40%) at large distances compared to the antenna dimensions, which has exponentially increased the number of potential applications of WPT. Since resonant inductive coupling is a very multidisciplinary field, different approaches have been proposed to predict the behaviour of these systems from physical theory of resonators, reflected load theory and the circuit point of view. However, the relation between these methods is still obscure. In this article, we compare the results of these models to find the efficiency of a Resonant Inductive Coupling WPT system under Steady-State conditions and to analyze the relation between the optimal load values obtained from this perspectives and the ones obtained using impedance matching techniques.

Optimization of Wireless Power Transfer with Intermediate Resonant Coil for Interfacing with the Central Nervous System

Lingyao Chen and Massood Tabib-Azar
University of Utah, 50 S. Central Campus Dr., Rm. 3280 MEB Salt Lake City, UT 84112-9206, USA

Abstract— Sensing and stimulating neurons using wireless telemetry systems are extensively used for prosthetics and mapping the circuitry of the brain [1]. In these systems, the preferred method for power and signal transmissions is to use an open-transformer configuration (Fig. 1) also known as magnetic dipole or inductive coupling [2]. Here we show that a third resonant coil can be used in-between the transmitting and receiving coils (Fig. 2) to enhance the telemetry efficiency by X5 in the inductive coupling scheme. Inductors and capacitors in all three coil circuits had the same value of 1 μH and 100 nF, respectively, yielding the same resonant frequency for the transmitter (TX), intermediate (IM) and receiving coils (RX). Furthermore, the RX coil's radius was fixed at 0.6 mm. Fig. 3 shows the output voltage as a function of TX coil's location for different radii of TX coils (all much larger than RX coil's) with no IM coil present. It can be seen that for each distance Z_{RT}, there is an optimized TX coil radius to achieve maximum V_{out}. Closer the distance Z_{RT}, smaller the radius of TX coil for optimum transmission. As with magnetic dipole theory, when $R_{\mathrm{TX}} \gg R_{\mathrm{RX}}$, $V_{\mathrm{out}} = N_{\mathrm{RX}} \frac{\mu_0 N_{\mathrm{TX}} R_{\mathrm{TX}}^2 \pi R_{\mathrm{RX}}^2 di}{2(R_{\mathrm{TX}}^2 + Z_{\mathrm{RT}}^2)^{3/2} dt}$. The behavior of V_{out} as a function of Z_{RT} follows the $1/Z_{\mathrm{RT}}^3$ law when $Z_{\mathrm{RT}} \gg R_{\mathrm{TX}}$, as expected.

Figure 4 shows V_{out} vs. IM coil's location for different IM radii, while TX and RX coils' distance (Z_{RT}) were fixed at 70 mm and TX and RX radii were 44.5 mm and 0.6 mm, respectively. When there was no IM coil, the transmitted V_{out} was 10.8 mVpp; when the IM coil was introduced, V_{out} increased by a factor of 2 to 5 for different IM coil radii and location. For different IM coil location (Z_{RM}), there was an optimized IM coil radius to maximize V_{out}. Closer the IM coil to

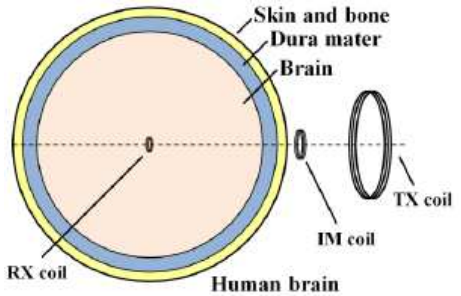

Figure 1: Schematic of coils transmitting and receiving inside/outside human brain with intermediate coil as power booster.

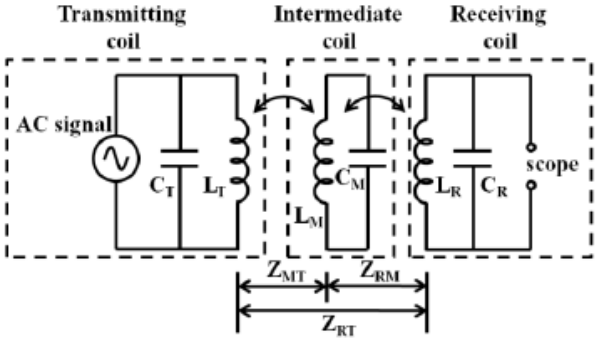

Figure 2: Circuit diagram of three transmitting, receiving and intermediate coils.

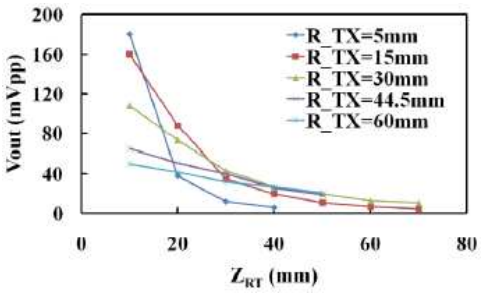

Figure 3: Output voltage vs. transmitting coil location (Z_{RT}) for two coils transmission with different transmitting coil radius. R_{RX} was fixed at 0.6 mm.

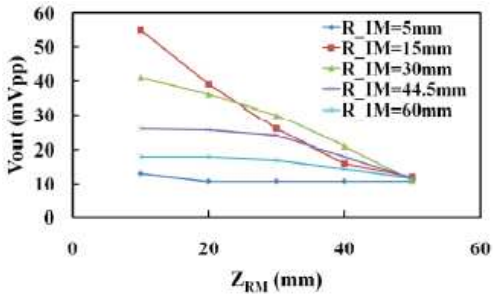

Figure 4: Output voltage vs. intermediate coil location (Z_{RM}) for three coils transmission with different intermediate coil radius. $Z_{\mathrm{RT}} = Z_{\mathrm{RM}} + Z_{\mathrm{MT}}$, and was fixed at 70 mm.

the RX coil, smaller was its radius for optimized V_{out}, but the value was always between the radii of TX and RX coils. This can be explained noting that V_{out} is maximized when magnetic fluxes (ϕ's) are equal: $\phi_{\mathrm{RT}} = \frac{\mu_0 I R_{\mathrm{RX}}^2 N_{\mathrm{RX}} \pi R_{\mathrm{TX}}^2}{2(R_{\mathrm{TX}}^2+Z_{\mathrm{RT}}^2)^{3/2}} = \phi_{\mathrm{RM}} = \frac{\mu_0 I R_{\mathrm{RX}}^2 N_{\mathrm{RX}} \pi R_{\mathrm{IM}}^2}{2(R_{\mathrm{IM}}^2+Z_{\mathrm{RM}}^2)^{3/2}}$.

REFERENCES

1. Murari, K., et al., "Wireless multichannel integrated potentiostat for distributed neurotransmitter sensing," *Engineering in Medicine and Biology Society*, 7329–7332, 2005.
2. Lenaerts, B. and R. Puers, *Omnidirectional Inductive Powering for Biomedical Implants*, Springer, 2009.

Undesired Emission from Spiral Resonators for Coupled Resonant Wireless Power Transfer

H. Hirayama, K. Komatsu, N. Kikuma, and K. Sakakibara
Department of Computer Science and Engineering
Nagoya Institute of Technology, Japan

Abstract—

Introduction: Wireless power transfer (WPT) technology is expected to realize ubiquitous power system. Since the WPT system handles power of kW order, it is necessary to assess undesired emission. Various kinds of resonators, such as helical coil or meander lines are possible for the WPT antenna. Spiral resonator has an advantage of low-profile structure. In this report, we discuss undesired emission from a spiral resonator.

Consideration Model: Spiral antenna model in which transmitting(TX) and receiving(RX) antennas are set in the same direction is shown in Fig. 1(a). It was reported that arrangement of TX and RX antenna in opposite direction increases coupling coefficient [2]. Fig. 2(b) shows the reverse arranged model. A power source and load were connected to the port 1 and 2, respectively. The source and load impedance were 50 ohm.

Results: S_{21} characteristics with respect to the transfer distance was calculated by method of moment (MoM). Although the self resonant frequency of the spiral antenna itself is 36.7 MHz, low-frequency and high-frequency resonances were caused because of a coupling [3]. S_{21} at the high-frequency mode is used in the Fig. 2. Transfer distance was extended by 19% by arranging antenna in reverse direction.

Far-field radiation power can be calculated through a gain as an antenna, where both TX and RX spirals are considered as a TX antenna. Calculation result is shown in Fig. 3. Far-field radiation was decreased by 4.5 dB in high-frequency mode resonant.

Conclusions: We show that transfer distance was extended by 19% and far-field radiation decreased by 4.5 dB by arranging spiral resonator in opposite direction.

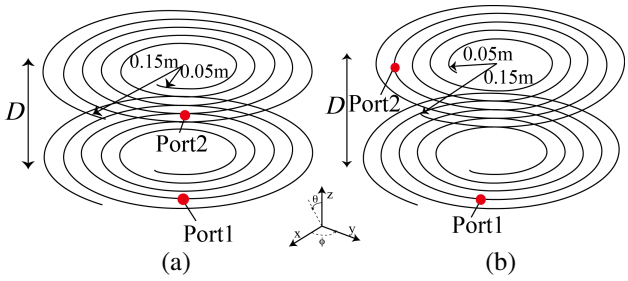

Figure 1: Consideration model.

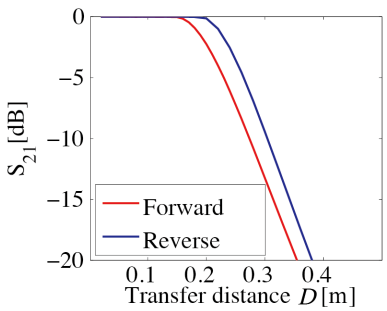

Figure 2: Distance characteristics of S_{21}.

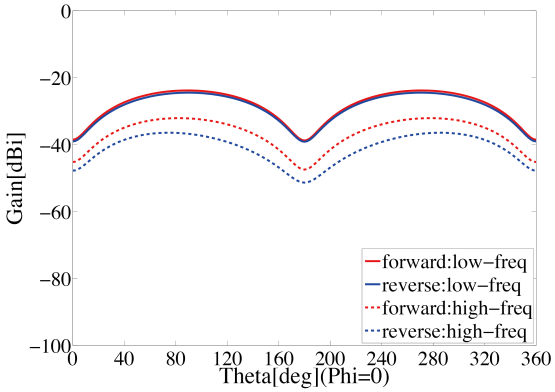

Figure 3: Gain as a TX antenna.

REFERENCES

1. Kurs, A., A. Karalis, et al., "Wireless power transfer via strongly coupled magnetic resonances," *Science Magazine*, Vol. 317, No. 5834, 83–86, 2007.
2. Awai, I., *Nikkei Electronics*, 11–14, 100–108, Nov. 2011.
3. Hirayama, H., et al., "A consideration of electromagnetic-resonant coupling mode in wireless power transmission," *IEICE ELEX*, Vol. 6, No. 19, 1421–1425, Oct. 2009.

Magnetostrictive Resonators for Wireless Energy Transfer

Alexander Chernokalov[1], **Mikhail Makurin**[1], **Nikolay Olyunin**[1], **Vladimir Arkhipenkov**[1], **Ki Young Kim**[2], **and Keum-Su Song**[2]

[1]Samsung Moscow Research Center, Russia
[2]Future IT Research Center, Samsung Advanced Institute of Technology, Yongin 446-712, Korea

Abstract— Magnetostrictive resonators are proposed to be used for wireless energy transfer in the sub-MHz range.

The operation in the sub-MHz frequency range is preferable for wireless energy transfer in the presence of lossy media: biological tissue, water, soil, conductive objects, and other. Low operating frequency allows reducing the losses in such media. One more issue in biological applications of wireless energy transfer is the EM field exposure level. The maximum permissible exposure levels for sub-MHz and MHz frequencies are less restrictive than for higher frequencies.

Most of the resonators used for wireless energy transfer via magnetic field are coil-based. At the same time there exists a problem of designing a compact coil-based resonator with high Q-factor for sub-MHz frequency range. There are few ideas of non coil-based resonator design suitable for low frequencies [1, 2]. The idea closest to the proposed one is described in [2], where a magnetoelectric resonating device is used for energy transmission comprising of piezoelectric and magnetostrictive layers. There exist two problems with this approach: first the Q-factor of the resonator is reduced because of composite structure of the device, and second this device is difficult to match to a variable load.

Instead of using a composite structure we propose to use a solid-state resonator composed of magnetostrictive material. The resonator is assumed to be biased by an external permanent magnet. The advantage of this approach is the intrinsically high Q-factor of the resonator ($\sim 10^3$).

The mechanical energy of the resonator is converted to electric energy using a coil wound around the resonator, which plays a role of energy transducer. The coil is connected to a load. Optimal load resistance depends on the number of turns in the coil. Therefore we can match the device to a wide range of load resistances by changing the number of turns in the coil.

REFERENCES

1. Cook, N. P., S. Dominiak, L. Sieber, and H. Widmer, "Transmitters and receivers for wireless energy transfer," US Patent App., 12/211, 706, September 16, 2008.
2. Liu, Y., J. Simon, R. C. O'handley, and J. Huang, "Wireless transfer of information using magneto-electric devices," US Patent App., 12/505, 151, July 17, 2009.

Resonant Structure Based on Bulk Acoustic Resonator (Metacapacitor)

Pavel Turalchuk[1], **Orest Vendik**[1], **Irina Vendik**[1], **Dmitry Kholodnyak**[1], **Ki Young Kim**[2], **and Keum-Su Song**[2]

[1]St. Petersburg Electrotechnical University, St. Petersburg 197376, Russia
[2]Future IT Research Center, Samsung Advanced Institute of Technology, Yongin 446-712, Korea

Abstract— The resonant structure based on Bulk Acoustic Resonator (BAR) is a planar multilayer structure, comprising the conducting loop and the BAR structure. The BAR (metacapacitor) structure consists of a thin layer of the piezoelectric ceramics terminated in thin metal upper and lower electrodes. The metacapacitor structure is mounted on silicon substrates. In this case, the silicon is used as a dielectric substrate. On the both sides of the metacapacitor structure, the dielectric substrates are etched in the center in order to provide almost free acoustic boundary conditions. In this case, the metacapacitor structure provides a high-Q shear-wave bulk acoustic resonance excited between two electrodes. At the operating frequency the equivalent input impedance of the metacapacitor exhibits a capacitive reactance, which corresponds to the capacitor with a high value of capacitance. The high value of the capacitance of the metacapacitor in combination with a small inductance of the loop provides a resonant response of the advanced resonant structure at the desired frequency in the MHz frequency range. Conducting loop formed as a round strip is located on the upper dielectric layer of the metacapacitor. The loop edges are connected to the metacapacitor electrodes by means of metallized "via" interconnections. The designed miniature resonator exhibits a high value of capacitance and a high Q-factor.

Adaptive Impedance Matching for Magnetically Coupled Resonators

Benjamin H. Waters[1], **Alanson P. Sample**[1, 2], **and Joshua R. Smith**[1, 2]

[1]Department of Electrical Engineering, University of Washington, USA
[2]Departments of Computer Science Engineering, University of Washington, USA

Abstract— Wireless power technology using magnetically coupled resonators (MCRs) is becoming more prevalent in common applications including electric vehicle charging, consumer electronics, and implantable biomedical devices [1, 2]. These applications require a practical end-to-end wireless power system that can achieve high efficiency for a volume of space and operate within the bandwidth limitations defined by wireless communication standards and regulations in various countries.

To maximize efficiency at a single operating frequency for a volume of space (corresponding to a full range of coupling coefficients), the constant source impedance of a power amplifier must be matched to the variable impedance of the MCRs which changes as a function of the coupling coefficient between the transmit (TX) and receive (RX) resonators. Previous work has demonstrated wideband frequency tracking techniques that automatically tunes the operating frequency to maximize wireless power transfer efficiency [2]. However, frequency-tuning may violates the regulated frequency bandwidths where commercial wireless power systems can operate.

A framework has been developed to accurately model any adaptive impedance matching (AIM) network in a high Q MCR wireless power system. AIM networks are critical blocks for these systems because maximum efficiency can be achieved for a full volume of space at a single operating frequency. First, a vector network analyzer (VNA) is used to extract S-parameters from a set of MCRs. After the admittance Y matrices for any AIM network has been defined, these S and Y matrices are converted into $ABCD$ transmission matrices. A single $ABCD$ matrix for the entire system can be defined by multiplying the cascaded $ABCD$ matrices [3]. This system $ABCD$ matrix is then converted back to an S matrix using complex termination impedances to match a source impedance (typically $50\,\Omega$) to a defined load impedance [4]. Finally, a constrained non-linear optimization algorithm in Matlab extracts the circuit component values in each AIM network that maximize S_{21} for any range of coupling coefficients.

To verify the algorithm, a low-pass π-match network has been implemented as the AIM network with the MCRs shown in Figure 1(a). Figure 1(b) shows the smith chart of S_{11} and Figure 1(c) shows $|S_{21}|^2$ (efficiency) for two scenarios where 1) the MCRs are terminated in $50\,\Omega$ source and load impedances and 2) AIM networks are placed at both the TX and RX sides. The plot in Figure 1(c) also compares the efficiency at a single frequency to that of wideband frequency tuning. Since nearly all parasitics have been accounted for, these efficiencies are achievable at a single frequency for a full range of coupling coefficients between any TX and RX resonator. Therefore this tool can be used to design and accurately model a practical end-to-end wireless power system using any AIM network with any set of MCRs.

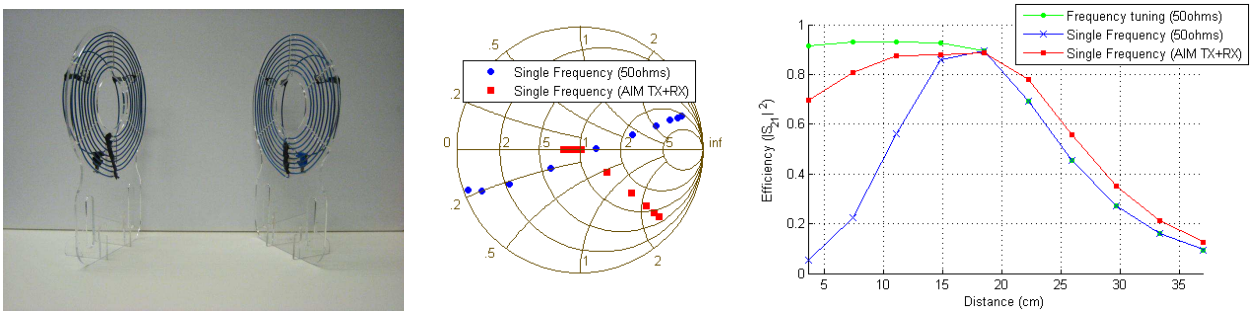

(a) (b) (c)

Figure 1: (a) Image of the TX and RX magnetically coupled resonators used for wireless power transfer. (b) Smith chart showing S_{11} for the actual set of MCRs terminated in 1) $50\,\Omega$ source and load impedances (blue circles) and 2) simulated TX and RX AIM π-match networks (red squares). (c) Plot comparing $|S_{21}|^2$ for the actual set of MCRs using 1) frequency tuning (green circles), 2) $50\,\Omega$ termination impedances (blue x's) and 3) TX and RX AIM π-match networks (red squares).

REFERENCES

1. Waters, B. H., A. P. Sample, P. Bonde, and J. R. Smith, "Powering a ventricular assist device (VAD) with the free-range resonant electrical energy delivery (FREE-D) system," *Proceedings of the IEEE*, Vol. 100, No. 1, 138–149, Jan. 2012.
2. Sample, A. P., D. Meyer, and J. R. Smith, "Analysis, experimental results, and range adaptation of magnetically coupled resonators for wireless power transfer," *IEEE Transactions on Industrial Electronics*, Vol. 58, No. 2, 544–554, Feb. 2011.
3. Pozar, F. M., *Microwave Engineering*, Wiley, New York, 2004.
4. Frickey, D. A., "Conversions between S, Z, Y, h, $ABCD$, and T parameters which are valid for complex source and load impedances," *IEEE Transactions on Microwave Theory and Techniques*, Vol. 42, No. 2, 205–211, Feb. 1994.

Session 2P5
Computational Electromagnetics

Fractal Labyrinths: Physics and Fractional Operators

A. A. Potapov and V. I. Grachev
Kotel'nikov Institute of Radio Engineering and Electronics, Russian Academy of Sciences, Russia

Abstract— In recent years, intensively developing methods for the synthesis of fractal artificial composites and metamaterials, such as, for example, fractal antennas subminiature, fractal structure in photon and magnon crystals, fractal modeling of impedance and fractional operators, percolation synthesis, fractal labyrinths, Cantor blocks, etc. Fractal labyrinths are quite common in nature and technology. These should include: transport and communication networks, systems of collection and distribution of resources and information, river systems, the system of blood circulation, lightning discharges, etc. The description of such systems does not fit into the traditional framework of differential equations of integer order. More precisely these processes and objects quantitatively describes by the operators of fractional integro-differentiation $D^{\alpha}[f(t)]$, where $-1 < \alpha < 1$ [1]. In this paper we define the fractal labyrinth. Physically, the operators of fractional integration play a role unique "filters" that emit only those components that are localized on the fractal (fractional) sets the process under investigation. The presence in the equations of fractional derivative taken interpreted as a reflection of the special properties of the process/system — memory, or nonMarkovian (hereditarity). The integro-differential nature of the Riemann-Liouville fractional operator ${}_0D_t^{1-\alpha}$ with the integral kernel $M(t) \propto t^{\alpha-1}$ ensures the non-Markovian nature of the subdiffusive process, defined by the fractional diffusion equation. A generalized diffusion equation of fractional order model is constructed using a continuous time random walk, in this case the probability density function of the jump length determined by the distribution of Levy. It should be noted that recently in the scientific world are intensively discussed fractal objects and processes that are negative and complex fractional powers. The extension of random walk theory to incorporate generalised statistics which no longer follow the central limit theorem, and hereditarity effects violating the Markovian nature of early days random walks, has created a rich tool to describe features of complex systems. The purpose of this paper — to draw attention to exotic fractal labyrinths and the theory of fractional calculus. Moreover, these questions are interesting and new research directions.

REFERENCES

1. Potapov, A. A., *Fractaly v Radiofizike i Radiolokatsii. [Fractals in Radiophysics and Radiolocation]*, 664, Logos Publ., Moscow, 2002.
2. Potapov, A. A., *Fractaly v Radiofizike i Radiolokatsii: Topologiya Vyborki. [Fractals in Radiophysics and Radiolocation: Topology of Sample]*, 848, Universitetskaya Kniga Publ., Moscow, 2005.

Analysis of Double Negative Meta-material Asymmetric Planar Slab Waveguide by Transmission Equivalent T-circuit Model

Sanjeev Kumar Raghuwanshi, **Santosh Kumar**, **and Radha Raman Pandey**
Department of Electronics Engineering
Indian School of Mines, Dhanbad, Jharkhand 826004, India

Abstract— The symmetric/asymmetric planar slab waveguide is simplest waveguide structure to be analyzed. These waveguides are used in optical communication systems. The transmission line (TL) method has great application to analyze waveguide structure having arbitrary refractive index profile. There is large number of current research papers on application of TL method of waveguide analysis [1–3]. The asymmetric waveguide is somewhat tough to analyze due to their asymmetric mode field profile. However the asymmetric waveguide have found certain advantage over the symmetric waveguide structure due to their easiness [4, 5]. In this paper, we have derived the exact Eigen value equation by using the transmission line (TL) method for the case of Double Negative Meta-material (DNG) asymmetric planar slab waveguide. The Usual properties of Meta material waveguide structures may have impact on WDM optical communication systems. The derived results have been exactly matched with the existing results found into the literatures. The unusual behaviour of double negative meta-material is predicted. Dispersion study (b-v graph), mode field profile and power confinement factor are also being discussed at the end. Finally we compare the guidance conditions obtained by TL method with Graphical method. The derivation presented into this paper is useful to the beginners who want to gain inside into TL method. One can easily extended these results to simulate multilayer DNG waveguide structure.

REFERENCES

1. Qian, X. and A. C. Boucouvalas, "Synthesis of symmetric and asymmetric planar optical waveguides," *IET Optoelectron.*, Vol. 1, No. 4, 185–190, 2007.
2. Mahmoud, S. F. and A. J. Viitanen, "Surface wave character on a slab of metamaterial with negative permittivity and permeability," *Progress In Electromagnetic Research*, Vol. 51, 127–137, 2005.
3. Baccarelli, P., P. Burghignoli, G. Lovat, and S. Paulotto, "Surface-wave suppression in a double-negative metamaterial grounded slab," *IEEE Antennas and Wireless Propagation Letters*, Vol. 2, 260–272, 2003.
4. Raghuwanshi, S. K., V. Kumar, and R. R. Pandey, "Derivation of eigen value equation by using equivalent transmission line method for the case of symmetric/asymmetric planar slab waveguide structure," *Journal of International Academy of Physical Sciences*, Vol. 15, No. 1, 1–14, 2011.
5. Wang, Z. J. and J. Dong, "Analysis of guided modes in asymmetric left-handed slab waveguides," *Progress In Electromagnetic Research*, Vol. 62, 203–215, 2006.

Reduction of the Staircasing Error in Finite Methods by Using Transformation Media

Mustafa Kuzuoglu[1] and Ozlem Ozgun[2]

[1]Department of Electrical and Electronics Engineering
Middle East Technical University, Ankara, Turkey
[2]Department of Electrical and Electronics Engineering
TED University, Ankara, Turkey

Abstract— The concept of a 'transformation medium' refers to an artificial medium whose constitutive parameters (i.e., the permittivity, permeability and conductivity) are obtained by means of coordinate transformations. Maxwell's equations preserve their form in the modified coordinate system, but the original material parameters are replaced by anisotropic and spatially-varying constitutive parameters to account for the resulting change in the field behavior after the coordinate transformation. This technique was employed in the literature to design several optical and electromagnetic structures, such as the 'invisibility cloak', reshapes, lenses, concentrators, miniaturized waveguides, etc.. However, most applications of this technique suffer from a lack of physical experiments, and hence, they are indeed living in 'virtual reality'. This is because the material specifications are challenging as a result of the spatially varying material parameters. The main objective of this paper is to utilize speciallydesigned transformation media (called *software metamaterials*, in order to distinguish them from the metamaterials constructed and used in the physical world), for enhancing the ability of numerical modeling methods in computational electromagnetics. Most of the numerical techniques (such as finite difference time or frequency methods, finite element method employing rectangular elements) are based on a Cartesian coordinate grid or mesh. However, curved geometries that do not conform to a Cartesian grid can only be modeled by using a staircased approximation of the curved surface. This approximation yields errors due to the inaccurate modeling of the geometry. The proposed method in this paper constructs transformation media within the computational domain adapted to the Cartesian grid, and obtains the material parameters by mapping the staircase-approximated boundary of the geometry to its original boundary. In other words, an equivalent model that mimics the original problem is created, through the use of transformation media. Hence, this approach reduces the approximation errors without the need for changing simple Cartesian grids. Several numerical results are demonstrated in the context of electromagnetic scattering problems.

A Thin Wire Method of Moments Scheme Employing King's Green Functions and Sinusoidal Basis Functions

Ö. Zor[1] and B. Polat[2]

[1]Electronics Engineering Department, Uludag University, Bursa, Turkey
[2]Electrical and Electronics Engineering Department, Trakya University, Edirne, Turkey

Abstract— In [1], we investigated electromagnetic scattering from metallic thin wire structures located over planar and spherical lossy dielectric half-spaces by applying the Green functions of R. W. P. King valid for arbitrary range under "high contrast approximation" (HCA) in a Method of Moments scheme employing pulse basis functions. In the present work we extend this methodology for more realistic sinusoidal basis functions, thereby generating the same results and programming capacity with the famous open software NEC-2 [2]. For a verification of the developed codes the current distributions obtained under plane wave illumination on the arms of a cross shaped thin wire structure are compared to the same results obtained by the commercial software SNEC^{TM} [3] as well as the same results computed in [1] using pulse basis functions over planar sea surface in HF band. As expected, the results for the amplitude and phase variations in case of sinusoidal basis functions matched perfectly to the same results derived by SNEC^{TM} with relative error limited by 0.5%, which we attribute to easily improvable round off errors. The numerical implementations put it very clearly that an electromagnetic simulation software that incorporates the Green functions of King may not only provide an alternative to the similar role of the extensive numerical/asymptotic libraries of NEC-2 whenever HCA applies, but also provides a capability to evolve by proper substitutions of Green functions to take into account various terrain features in any scenario. This is especially important since the physical (antenna) measurements around critical distances over earth have been reported to diverge seriously from those calculated by NEC-3 and NEC-4 while they follow the analytical results derived by King smoothly (see [4, Sec. 1] and the references cited therein). The research is planned to pursue along the following areas of investigation:

i. Providing a time domain analysis ability to investigate the scattering of actual radar wave forms from mesh structures above sea surface;
ii. Extending the impedance matrix for dielectric coated mesh structures for stealth applications;
iii. Incorporating Green functions of layered and complex media available in literature for arbitrary range;
iv. Investigation of most efficient NEC2 pre-processors, modeling guidelines, programming platforms and algorithms to minimize the computational time for integration and linear algebraic operations at the stage of developing a commercial product.

REFERENCES

1. Zor, Ö. and B. Polat, "An implementation of King's Green functions in thin wire scattering problems," *ACES Journal*, Vol. 26, No. 12, 1024–1038, 2011.
2. Burke, G. J. and A. J. Poggio, *Numerical Electromagnetics Code (NEC) — Method of Moments*, Lawrence Livermore Laboratory, Jan. 1981.
3. *SuperNec*, Poynting Software (Pty) Ltd., South Africa. http://www.supernec.com/.
4. King, R. W. P., "Electromagnetic ground wave field of vertical antennas for communication at 1 to 30 MHz," *IEEE Trans. Electromag. Compatibility*, Vol. 40, No. 4, 337–342, 1998.

A Monte-Carlo MPSTD Analysis of Electromagnetic Scattering of Objects Buried below a Random Rough Surface

Yueyang Dai, Wei Liu, and Xiao-Bang Xu
Holcombe Department of Electrical and Computer Engineering
Clemson University, Clemson, SC 29634-0915, USA

Abstract— Analysis of electromagnetic scattering of buried objects is a subject of practical interest due to its wide applications in subsurface investigations. To make the structure of the problem closer to reality, we need to consider the roughness of the earth surface as well as the layered structure, because they both contribute to the scattering signature and hence affect the detection of buried objects.

In this paper, we present a Monte-Carlo multidomain psuedospectral time-domain (MPSTD) numerical technique developed for the analysis of electromagnetic scattering of a two-dimensional (2-D) object buried below a random rough surface. The random rough surface is taken to be of finite length first. Then, the numerical technique is extended for the analysis of scattering of a periodic random rough surface of infinite length. The MPSTD method [1] is employed to solve the Maxwell's equations in time domain. And the Monte-Carlo method is used to obtain a statistic average of the solution involving a random rough surface. As the random rough surface becomes of infinite length, a periodic boundary condition is enforced. Using the numerical technique developed, sample numerical results are obtained, presented, and validated.

REFERENCES

1. Liu, Q. and G. Zhao, "Advances in PSTD techniques," *Computational Electromagnetics, The Finite-Difference Time-Domain Method*, A. Taflove and S. C. Hagness, Eds., 3rd Edition, Chapter 17, Artech House, 2005.

Fast Algorithms for Numerical Solution of Volume Singular Integral Equations of Electromagnetics

A. B. Samokhin
Moscow State Technical University of Radio Engineering, Electronics and Automatics
Moscow, Russia

Abstract— The method of volume singular integral equations (VSIEs) is one of the most advanced and efficient techniques for numerical solution of diffraction problems. By using the collocation or Galerkin methods and taking into account that the kernel of integral equations depend only on the difference of arguments we reduce VSIE to a system of linear algebraic equations (SLAE) with the matrix having special symmetry properties. Due to huge dimensions of SLAE we use iteration methods such as the generalized method of simple iteration, generalized Chebyshev iteration, and generalized minimal residual algorithm. Matrix-vector multiplication is the most laborious operation when iteration techniques are applied. Using discrete fast Fourier transform techniques we construct a fast algorithm for the multiplication of the SLAE matrix and the vector. We obtain estimations for parameters T (number of arithmetic operations necessary for obtaining the sought-for solution with the required accuracy) and M (memory volume required for implementation of the algorithm) that govern the efficiency of a numerical algorithm.

A Novel Multi-physics and Circuit Co-simulation Algorithm for the Electro-thermal Analysis of Semiconductors and Circuits

J. Q. Chen and X. Chen
College of Electronics and Information Engineering
Sichuan University, Chengdu 610064, China

Abstract— A novel co-simulation algorithm that combines the multi-physics simulation with the circuit simulation for the electro-thermal analysis of circuits with semiconductor devices is proposed. It utilizes a physical model based multi-physics simulation to analyze the semiconductor devices in a circuit, and incorporates the multi-physics simulation into an equivalent-model based circuit simulation to simulate the circuit. As a sample, the proposed algorithm is employed for analyzing the electronic and thermal characteristics of a limiter circuit consisting of commercial PIN diodes with model number mot_bal99lt1. The feasibility and accuracy of the proposed algorithm are certified through comparison with measurements. Besides high-fidelity solutions, the proposed algorithm provides physical mechanisms for better understanding of the behavior of the PIN diode.

Analysis of Light-emitting Diode with Patterned Contact by Conformal Mapping Technique

Ju. Kholopova[1], **A. Konishi**[2], **R. Yamase**[2], **A. Kovalchuk**[1], **E. Polushkin**[1], **V. Zemlyakov**[3], **S. Shapoval**[1], **and I. Khmyrova**[2]

[1]IMT, RAS, Chernogolovka 142432, Russia
[2]University of Aizu, Aizu-Wakamatsu, Fukushima 965-8580, Japan
[3]R&D Corporation "Istok", Fryazino 141190, Russia

Abstract— Tremendous efforts are focussed on the improvement of light extraction efficiency in the semiconductor light-emitting diodes (LEDs) limited by several factors. The main portion of generated light is trapped in the LED structure due to total internal reflection. Besides this fundamental limitation in the LEDs with the light extraction via top surface the opaque top contact also deteriorates the situation as practically all the light generated beneath it cannot be extracted. Different approaches have been implemented to cope with this problem, for example, fabrication of the current spreading layer, patterning of sapphire substrate [1] or top semiconductor contact layer [2]. However, the achievement of ultimate extraction efficiency in LEDs is still a challenging task. Recently, drastic enhancement of the light extraction efficiency has been reported in the InGaN/GaN-based LED with the patterned p-contact [3].

In this paper we develop an analytical model for the LED with a p-contact patterned as an array of narrow strips. Electric field created by the applied forward bias voltage reduces the heterojunction barriers which, in turn, allows a current to be injected into the active region. Due to electric field fringing [4] current injection may occur not only beneath the contact strips but in the uncovered regions as well. If the separation between the strips is not very large the electric fields created by the adjacent strips can overlap each other. To calculate spatial distribution of the electric field in two-strip configuration we apply conformal mapping technique and obtain expressions in parametric form. Spatial distributions of electric field, injection current and intensity of generated light are calculated at different parameters.

It is demonstrated that the effect of the contact patterning is twofold: (1) at properly chosen strip separation and bias voltage light can be generated even in the parts of the active region not covered by the contact strips; and (2) light can be extracted via the openings between the strips.

REFERENCES

1. Wang, H. C., Y. K. Su, C. L. Lin, et al., *IEEE Phot. Technol. Lett.*, Vol. 14, 1491, 2002.
2. Yamada, M., T. Mitani, Y. Narukawa, et al., *Jpn. J. Appl. Phys.*, Vol. 41, L1431, 2002.
3. Shapoval, S., M. Barabanenkov, V. Sirotkin, et al., *Proc. of WOCSDICE 2007*, Venice, Italy, May 20–23, 2007.
4. Khmyrova, I., R. Yamase, M. Fukuda, and N. Watanabe, *J. Appl. Phys.*, Vol. 108, 074511, 2010.

Propagation Study of Y-branch Having Inbuilt Optical Splitters and Combiner Using Beam Propagation Method

S. K. Raghuwanshi, S. Kumar, V. Kumar, and D. Chack
Department of Electronics Engineering, Indian School of Mines
Dhanbad, Jharkhand 826004, India

Abstract— The Beam propagation method (BPM) is one of the most power techniques to investigate axially varying waveguides. The single mode optical Y-junction as shown in Fig. 1, consisting of single mode channel waveguide is a fundamental component for dividing/combining guided light. Much theoretical work has been done upon the junction problems [1, 2]. Beam splitter/Combiner sections are a basic element of many optical fiber communication systems often providing a Y-junction by which signals separate sources can be combined or the received power divided between two channels. We present here theoretical results on channel waveguide in the form of Y-junction inbuilt splitter and combiner. We establish the fundamental concepts of guided wave for branching and combining waveguide suffer from power loss due to different branching angle as shown in Fig. 1. Beam propagation methods are used to obtain guided wave characteristics include power loss due to different branching angle. The input field is applied to the branching waveguide and combined after propagating through some distance. The output field is compared with respect to input field for the case two branching angles. It is expected to high power loss due to wide branching angle. All simulations are done using Opti-BPM software. Beam propagation study and exact power loss is estimated.

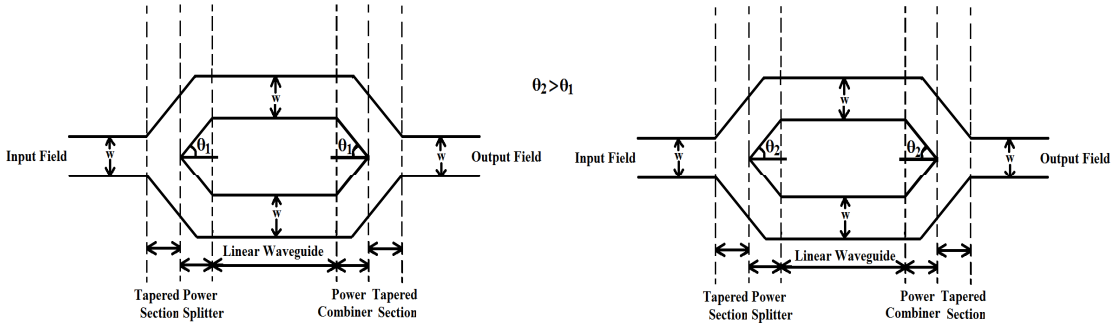

Figure 1: Y-branch inbuilt optical beam splitters and combiner.

REFERENCES

1. Tsutsumi, K., Y. Imada, H. Hirai, and Y. Yuba, "Analysis of single mode optical Y-junctions by the bounded step and bend approximation," *J. Lightwave Technol.*, Vol. 6, 590–600, Apr. 1988.
2. Kawano, K. and T. Kitoh, *Introduction to Optical Waveguide Analysis*, John Wiley & Sons, 2001.

An Efficient Hybrid KA-MoM for Backscattering RCS from Combined Objects by Adaptively Truncating the Size of the Rough Surface

X. Y. Zhang, Z. Li, and Z. W. Liu
School of Information Engineering, East China Jiaotong University, 330013, China

Abstract— The scattering from objects above a rough surface is a typical problem in the study of electromagnetic scattering characteristics of objects and their environments, which is important for target identification and radar design. However, since the multi-interactions between objects and rough surfaces are complicated, analysis of this problem is difficult. Since the unknowns for calculating the coupling fields are relative to the size of the objects and the rough surface, the computation of the multi-interactions from a rough surface to an object or from an object to a rough surface, is very time consuming. How to truncate the size of the rough surface is the key of solving this problem.

In this paper, a highly efficient hybrid method of the Kirchhoff approach (KA) and the method of moment (MoM) is proposed for calculating the monostatic radar cross section(RCS) of conducting objects above a rough surface. Similar with the conventional hybrid KA-MoM, the KA is used to calculate the scattering by the rough surface and the MoM is applied to calculate the scattering by the objects. Additionally, considering the engineering application, we have found that the hybrid KA-MoM could be further speed up by sacrificing the numerical accuracy. The main difference between the proposed method and the conventional KA-MoM algorithm is the size of the rough surface have been truncated when calculate the interactions between the objects and the rough surface, for depending on the scattering characteristics of the rough surface with various roughness. The adaptive selection method is used to define the truncated size of the rough surface. By executing the truncation, the memory and the computation time is significantly reduced.

Adaptive Compressed Sampling Method for Fast Comuatation of Monostatic Scattering

Zhiwei Liu[1], **Yueyuan Zhang**[2], **and Xiaoyan Zhang**[1]

[1]School of Information Engineering, East China Jiaotong Unviersity, 330013, China
[2]International School, East China Jiaotong University, 330013, China

Abstract— As well known, multi-level fast multi-pole algorithm (MLFMA) is able to result in an accuracy and efficient solution of integral equation. The use of MLFMA reduces the memory requirement to $O(N \log N)$ and the computational complexity of per-iteration to $O(N \log N)$. However, it is still time-consuming for calculation of monostatic RCS since it requires repeated solution of integral equation at each incident angle. Many interpolation methods are proposed to circumvent this difficulty recently. Accordingly, it is noteworthy that selection of sampling points is crucial for interpolation and extrapolation methods. Obviously, nonuniform sampling shows more flexible and efficient than uniform sampling. As a result, optimally select those angles that would be most informative will reduce the number of repeated solutions when one must consider for monostatic scattering computations or measurements.

An adaptive compressed sampling method is proposed to reduce the time requirement for computation of monostatic scattering. This method combines the adaptive sampling technique and low-rank compression technique. The angular samples which would be most informative can be selected optimally by use of the cubic-spline based adaptive sampling method. Different with our previous work, adaptive sampling is applied to choose the key excitation vectors instead of induced current vectors. Reduction number of multiple excitation vectors can lead to less computation time significantly. Moreover, with low-rank property, the excitation vectors at these selected angles could be further compressed by singular value decomposition (SVD), resulting in a more efficient adaptive sampling method. The SVD can be replaced by adaptive cross algorithm (ACA) to further reduce the computational complexity. The monostatic RCS of several PEC geometries is applied to verify the accuracy and efficiency of the proposed method. Numerical results demonstrate that this method is efficient for monostatic RCS calculation with high accuracy.

Calculating the Physical Optics Integral on the Realistic Object by an Efficient Numerical Steepest Path Method

Yu Mao Wu[1], **Li Jun Jiang**[1], **and Weng Cho Chew**[1, 2]

[1]Department of Electrical and Electronic Engineering
The University of Hong Kong, Pokfulam Road, Hong Kong, China
[2]Department of Electrical and Computer Engineering
University of Illinois, Urbana-Champaign, USA

Abstract— When the electrical size of the considered realistic object is on the order of hundreds or thousands of the working wavelength λ, that is, the essential frequencies k of the wave field are high enough, the physical optics (PO) approximation has been accepted as an efficient approach for analyzing the electromagnetic scattering and radiation problems, which was suggested by Macdonald early in 1912. However, the PO integrand is becoming more oscillatory as the electrical size of the object becomes larger compared with the incident wavelength λ. Therefore, the computational cost by a direct numerical integration scheme for the PO integral is extremely high.

In this work, we use the numerical steepest descent path (numerical SDP) technique to calculate the highly oscillatory PO integral with quadratic phase and amplitude variations on each triangular patch of the realistic objects. Physically, the stationary phase point contributions are carefully studied by the numerical SDP method and complex variables analysis using the contour deformation, which agrees very well with the leading terms of the traditional asymptotic expansion approach. The resonance points and vertex points contributions from the PO integral are also extracted. Cancellation of the internal resonance and vertex points contributions are mathematically proved when we assemble triangle meshes together. Numerical results for this type of highly oscillatory PO integral on the realistic objects are given to verify the proposed numerical SDP theory. Compared with the approximate asymptotic expansion approach, the numerical SDP method has significantly improved accuracy for evaluating the PO integral. Moreover, the computation effort is frequency independent.

Modeling of the Cell Membrane Response to Ultra Short and High Voltage Electric Pulses

J. A. Ramirez[1], **J. F. C. Vale**[1], **and D. A. Lowther**[2]

[1]Departamento de Engenharia Eletrica, Universidade Federal de Minas Gerais, Belo Horizonte, Brazil
[2]Department of Electrical and Computer Engineering, McGill University, Montreal, Canada

Abstract— This paper discusses the dynamics aspects of pore formation in the cell membrane submitted to ultra short (micro seconds to nano seconds) and high voltage (kV) electric pulses. The transient transmembrane potential (TMP) is calculated using an analytical approximation, which is subsequently coupled to the Smoluchowski equation to assess the pore generation, growth and size evolution in the cell membrane. The Smoluchowski equation is solved using the finite difference time domain method. Alternatively, the finite element method is also considered for the TMP calculation in which a nonlinear conductivity in the cell membrane is taken into account. Both formulations are employed to single shell spherical cells. The results indicate that the nonlinearity of the conductivity of the cell membrane play an importante role in the dynamics of the electroporation process.

Design of a Wideband RF Front End Based on Multilayer Technology

Christos I. Kolitsidas, Christos S. Lavranos, and George A. Kyriacou
Microwaves Laboratory, Department of Electrical and Computer Engineering
Democritus University of Thrace, Xanthi 67100, Greece

Abstract— A tremendous growth in the deployment of wireless technologies and devices has been observed over the last decade, as a result a significant amount of networks employing a wireless interface. A modern trend of wireless technology is the support of all commercially available radios in one device, which can be realized using techniques such as Software Defined Radio (SDR) or IEEE 802.15. The critical point for the development of these technologies is the RF interface, since the device should be able to operate in all possible commercial frequency bands. Hence, the development of a compact wideband RF front end for modern radio applications is crucial. Easy integration, cost effectiveness, low power consumption and reciprocal operation are the most important characteristics that this front end should meet.

Moreover, modern wireless applications employ Space Division Multiple Access (SDMA) technique aiming to achieve maximum capacity of the network and low interference. The most effective way to achieve SDMA in the network is by employing a beamforming network at both ends of the link. A significant increase of the channel capacity could be achieved by the parallel processing of all radiating beams re-using the frequency-time and code slot. Continuous beam steering and especially adaptive beams provide full implementation of SDMA, but it suffers from increased complexity often asking the re-development of systems from scratch. Alternative, switched beam steering enables the basic SDMA requirements, but it is quite simple and reciprocal and can be realized at the RF-stage. A classical topology of a switched beam beamforming network (BFN) is the Butler Matrix, [1]. The operation and functionality of SDMA systems based on the Butler matrix have already been studied in our previous work, [2–4]. Within this previous effort BFNs are designed in microstip printed technology for a specific narrow frequency band and the BFN could be tolerated only at the base station site. In contrary, a BFN providing SDMA to the mobile unit should be relatively small in order to fit in the device chassis or integrated over its package.

This study elaborates on the development on a wideband RF front end for SDR applications extending our previous work with new technologies providing switched beam capabilities in the SDR hardware interface. Our ultimate task is to reduce the BFN size and integrate the circuit on the mobile units' package. The proposed system is based on the combination of the Butler matrix with a linear phased array printed in a single three dimensional circuit using multilayer slot coupled technology. This technology allows the realization of compact devices using System in Package (SiP) approach. Conventional realization of the Butler matrix employs 90° hybrids, phase shifters and microstrip crossovers. In order to meet the bandwidth requirements of the system classical 90° hybrids are replaced by slot coupled couplers and all microstrip crossovers are avoided adopting multilayer technology. For the phase shifters also aperture coupling is exploited. Combing these features the result is a compact wideband Butler matrix. For the antenna type a number of wideband printed elements are examined among the vivaldi and the biconical, in order to meet the bandwidth and the small size requirements. The antenna array will be implemented along with the BFN board in the same geometry. The whole effort is focused in covering the range 3.1 GHz to 10.6 GHz.

The RF stages are designed using the CST Microwave Studio and Ansoft HFSS. Simulated results for each stage and the whole architecture, along with the layouts and the experimental results for some stages will be presented at the symposium.

REFERENCES

1. Butler, J. and R. Lowe, "Beam forming matrix simplifies design of electrically scanned antennas," *Electronic Design*, Apr. 1961.
2. Fakoukakis, F. E., S. G. Diamantis, A. P. Orfanides, and G. A. Kyriacou, "Development of an adaptive and a switched beam smart antenna system for wireless comunications," *Journal of Electromagnetic Waves and Applications*, Vol. 20, No. 3, 399–408, 2006.
3. Kolitsidas, C. I., F. E. Fakoukakis, D. G. Drogoudis, C. S. Lavranos, and G. A. Kyriacou, "Development of a full 360° azimuth coverage direction of arrival measurement unit," *Mediteranian Microwave Symposium*, 35–39, Syria, Oct. 2008.

4. Kolitsidas, C. I., F. E. Fakoukakis, D. G. Drogoudis, M. Chrysomallis, and G. A. Kyriacou, "Angular localization of interfering sources using a butler matrix driven circular array," *EMC Europe Workshop*, 215–218, Greece, Jun. 2009.

The Casimir Force for Arbitrary Three-dimensional Objects with Low Frequency Methods

P. R. Atkins[1], **W. C. Chew**[1], **Q. I. Dai**[2], **and W. E. I. Sha**[2]

[1]University of Illinois, Urbana, IL, USA
[2]University of Hong Kong, Pok Fu Lam, Hong Kong, China

Abstract— There has been much progress in recent years in the simulation of Casimir forces between various objects. Current methods have allowed traditional computational electromagnetic solvers to be used to find the Casimir forces in arbitrary three dimensional objects using finite-difference, finite element method, and the method of moments. The underlying theory to these approaches often relies upon knowledge and manipulation of advanced quantum field theory or quantum statistical physics. We present a means of deriving the Casimir force using the method of moments via the argument principle that presents a simplified derivation and greater freedom in the representation of the moment matrix. Using this derivation, we can adapt various computational electromagnetic techniques to improve the performance and robustness of the Casimir calculations. This includes addressing low-frequency breakdown via methods like the Augmented-Electric Field Integral Equation and expanding the range of materials supported using dielectric methods like the PMCHWT.

Session 2P6
Medical Electromagnetics, RF Biological Effect

Impact of Realistic Human Body Interaction in Indoor Wireless System Evaluation

Erik Aguirre[1], **Javier Arpon**[1], **Leire Azpilicueta**[1], **Silvia de Miguel**[2], **Victoria Ramos**[2], **and Francisco Falcone**[1]

[1]Electrical Engineering Department, Universidad Pública de Navarra, Spain
[2]Health Institute Carlos III, Telemedicine and e-Health Research Unit, Spain

Abstract— The use of wireless systems has experienced great growth in the last decade, mainly due to the adoption of communication systems that are of use in a broad range of applications. In the case of a conventional household, several wireless systems can be operating simultaneously, such as WLAN in different versions, personal area networks such as Bluetooth or ZigBee, or distribution in wireless fashion of DVB-T signals, among others. Also, Ambient Assisted Living scenarios make intensive use of wireless sensors in order to perform monitoring and control tasks, adding new elements of use within the wireless spectrum(mainly based on 802.15 standard as well as GSM/UMTS backup). The complexity of indoor scenarios due to strong multipath propagation as well as interaction with material elements poses a challenge in the determination of effects of EM signals as well as on the integrity of such communication signals. In this work, an additional element of complexity has been analyzed, by means of the inclusion of a realistic human body model in indoor scenarios. The model takes into account, by means of dispersive tissue models, the overall effect of human body in the prediction of wireless system operation within the framework of a 3D ray launching simulation scenario. In this way, by carefully adjusting the simulation scenario, both interactions with diverse material of the human body model and propagation analysis along the whole scenario can be calculated (Figure 1). These results can aid in dosimetric estimation as well as on the overall impact of human body presence in the operation of wireless systems within indoor scenarios.

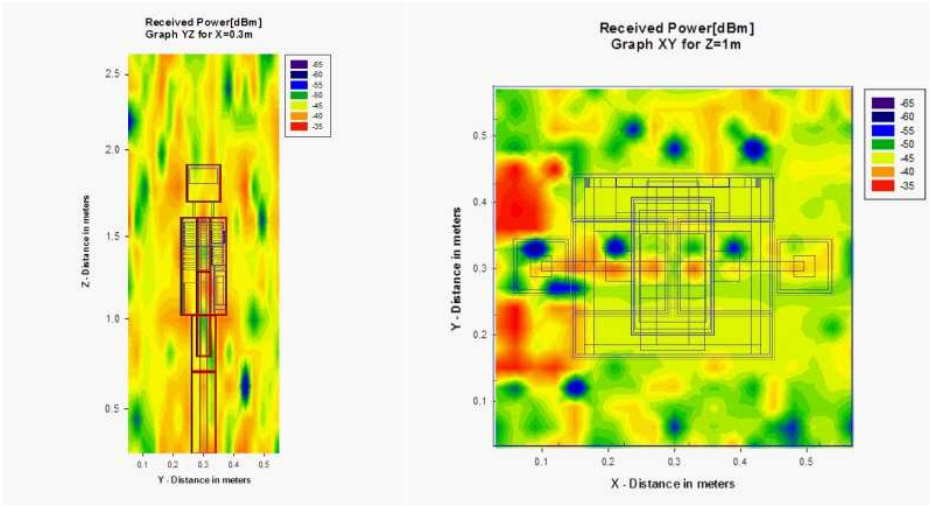

Figure 1: Estimation of received power level an indoor scenario. The human body model has been introduced in the scenario in order to take into account the overall effect.

Radio Frequency Identification Devices (RFID) in Prevention of Medication Errors: A Review

M. D. Marcos[1], **S. de Miguel**[2], **and V. Ramos**[2]

[1]Agency Laín Entralgo for Education and Health Research, Regional Ministry of Health, Madrid, Spain
[2]Health Institute Carlos III, Telemedicine and e-Health Research Unit, Madrid, Spain

Abstract— Medication errors in hospitals have been the focus of several studies since in 2000 the USA Medicine Institute reported on their quantity and severe side effects. For some years now the RFID technology has been considered a very promising option to solve that healthcare problem. Consequently, this work aims to expose the technological advances produced from 2001 to 2011 and which factors might explain both the RFID penetration rate in hospitals and RFID successes on preventing medical errors.

Likewise other scenarios are shown which may also benefit as hospitals from RFID technology in order to preserve the Patient's five Rights in administering medications — 1. Right patient, 2. Right time and frequency of administration, 3. Right dose, 4. Right route of administration and finally, 5. Right drug.

One of these technological options are low-cost information gathering and dissemination devices, such as sensors and RFID tags that facilitate fast-paced interactions among the objects themselves as well as the objects and persons in any place and at any time.

This overview on the current literature provides physicists, patients and healthcare providers with information about effectiveness and security of RFID in healthcare centers.

Manual searches have also been carried out on conference proceedings and other engineering journals not included in PubMed, as IEEExplore, to identify relevant articles published between 2001 and 2011.

On the whole, the evaluation of the methodological quality of studies has been a very difficult task because of the heterogeneity of the papers included in the review. This is due to the fact that there is a lack of published papers in the first two years considered, as is showed in Figure 1. Most of the papers included only partially cover the subject matter. The research performed for this document clearly demonstrates the high number of publications during the recent years on this subject. However, despite the large number of studies found, there is a lack of publications evaluating effectiveness of RFID and most of the studies only cover technological issues. Regarding the effectiveness of RFID and radiofrequency identification systems in patient's safety and medication errors prevention, the scarcity of studies is evident and it can be observed in Figure 2.

Since most reviewed articles are technological papers, this research will continue with the evaluation of other data base like Pubmed, Embase + Medline, Health Systems Evidence, etc., in order to identify additional relevant studies.

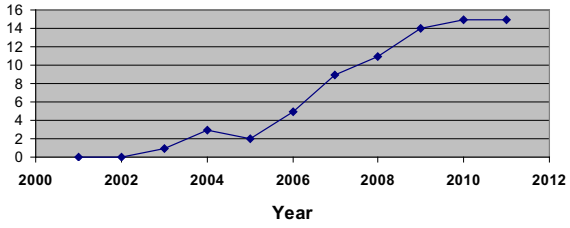

Figure 1: Number of papers.

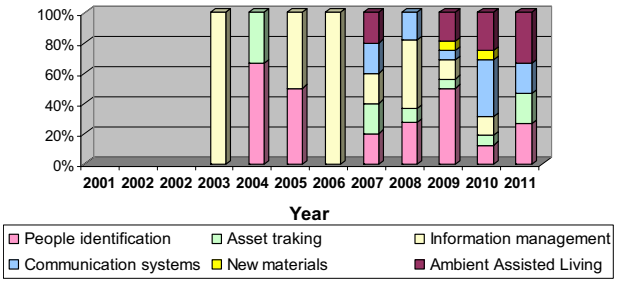

Figure 2: Application areas in terms of RFID functionality.

Assesment on Electromagnetic Spectrum within Large Enclosed Vehicles

Javier Arpon[1], **Erik Aguirre**[1], **Leire Azpilicueta**[1],
Silvia de Miguel[2], **Victoria Ramos**[2], **and Francisco Falcone**[1]

[1]EE. Department, Universidad Pública de Navarra, Spain
[2]Telemedicine and e-Health Research Unit, Health Institute Carlos III, Spain

Abstract— Wireless communication systems are being adopted in a wide range of sectors, ranging from domestic households, to administrative as well as industrial environments, with a broad and transverse application scope. One of the areas in which recently there has been expectation in the use of wireless systems is for on board communication systems in vessels, mainly in aircraft. The use of wireless systems, such as WLAN (including millimeter wave bands, such as 60 GHz spectrum), personal area networks based on Bluetooth or even the installation of on board GSM/UMTS base stations in order to provide mobile services can increase user experience and competitiveness of air carriers, while in some cases reduces overall weight (by reducing the amount of installed cable) has been explored and tested. Due to the characteristics of the enclosed environment within the airplane (i.e., strong multipath propagation and reflection due to high reflective materials within the airplane structure), careful analysis of the behavior of wireless systems and the use of EM spectrum is of importance in order to analyze overall performance of the systems under analysis (in terms of coverage/capacity analysis) as well as to foresee dosimetric implications of the use of such systems. Simulations of the inner cabin of real airplane scenario have been performed by means of in house 3D ray launching code in order to estimate power spectrum (an example of received power levels for a WiFi hotspot within the main cabin is shown in Figure 1) as well as time domain characteristics of the wireless channel within the airplane.

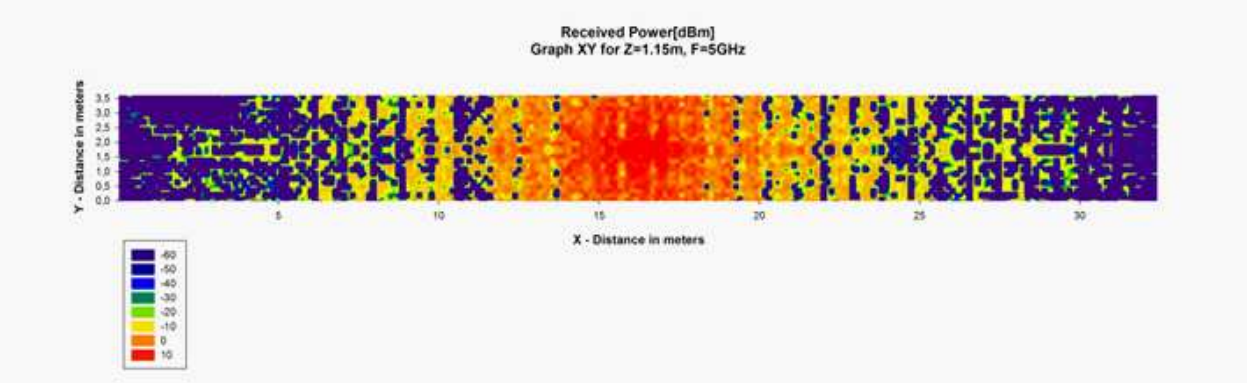

Figure 1: Estimation of received power level (WiFi hotspot at 5.8 GHz) for the main cabin of a conventional passenger plane.

Analysis of Electromagnetic Compatibility of Wireless Ambient Assisted Living Devices

S. de Miguel[1], **J. García**[1], **D. Rubio**[2], **O. Suarez**[2], **and V. Ramos**[1]

[1]Health Institute Carlos III, Telemedicine and e-Health Research Unit, Madrid, Spain
[2]General Direction of Telecommunications and Information Technologies
Electromagnetic Compatibility Services, Madrid, Spain

Abstract— The increasing average age and the consequent rise of chronic diseases will result in a dramatic growth of the need for assistance and healthcare within the years to come.

In the last years, the number of remote alarm systems has increased in residential environments. These systems provide a great variety of emerging applications such as tracking and mobile telecare and welfare, with the possibility of the inclusion of other types of conventional alarms (gas, smoke, flood, etc ...).

Environments equipped with such sensitive and responsive devices are referred to as being Ambient Assisted Living (AAL).

The main objective of domiciliary telealarm buttons is to communicate emergency situations due to domestic accidents or health emergencies. The special implication of these devices with welfare and safety requirements involves a special interest in its operating conditions.

The telealarm buttons are wireless communication devices and its working frequency is from 869.20 to 869.25 MHz, in accordance with European standards (2011/829/EU: Commission Implementing Decision of 8 December 2011 amending Decision 2006/771/EC on harmonisation of the radio spectrum for use by short-range devices). These systems operate in near field conditions and can affect the working of implantable and wearable electrical devices. As well as in far-field conditions it is necessary to assure the electromagnetic (EM) compatibility with the equipments and networks operating in the home environment.

In this work, the EM conditions have been analyzed and the radiation patterns of several models of telealarm buttons have been obtained. Given the increasing use of domiciliary telealarm devices, and the non-existence of previous studies of the working conditions and the emission levels, this paper analyzes two aspects that have to be considered to assure a proper, reliable and safe usage of these systems. The first is the compatibility with other communication networks and implanted electric devices. The second is the compliance with exposure levels threshold, to quantify and analyze the risk of exposure caused by the use of these devices.

Centurion System for Pulsed Electromagnetic Field Therapy

Wayne Kraushar[1] **and Marko Markov**[2]

[1]Centurion Systems, Mississauga, Ontario, Canada
[2]Research International, Williamsville, New York, USA

Abstract— Pulsed electromagnetic field therapy (PEMFT) became broadly applied worldwide in the recent decades. Most of the systems available elsewhere represent mattresses with incorporated 1–3 coils, connected to the generating unit. One of the most serious disadvantages of such units is the fact that the magnetic field generated by the coils decreases when assessed away from the coil. In other words, different body parts would receive different, in most cases, unpredictable magnetic field.

Just the opposite is the situation with ELEC system of generation and application of the stimulating field, developed in the 1970s in Germany. The same principle design is applied for the Centurion units. It utilizes cylindrical coils with 51 cm diameter and 23 cm height. The coil is capable of delivering desired homogeneous magnetic field through the entire cylindrical volume. Depending on the specific problem to be treated the magnetic field could vary from 1 to 60 Hz with magnetic flux density of 1 to 100 Gauss. The coil has absolutely round shape achieved by the special material and technology of production. The large diameter of the coil allows treating any body targets when the coil "wrapped" this part of the body. The Centurion magnetotherapy units are manufactured by Centurion Medical Corporation of Calgary, Canada.

The Centurion system for PEMFT has been successfully used for treatment of various health problems. This paper presents the application of Centurion units for treatment of join pain. Specific targets have been chronic pain and carpal tunnel syndrome pain. These two problems are in between the problems with largest distribution. While carpal tunnel syndrome is considered to be developed as result of professional conditions, the join pain occurs without specific reasons and basically include large portion of population, especially increasing with aging.

Patients with chronic join pain and carpal tunnel syndrome have been selected based upon the list of specific problems and after the medical diagnosis each individual received a protocol for treatment (at professional office or at home).

The benefit of PEMFT was compared to the progress of healing when conventional physical therapy methods have been in use. The severity of pain before, during and after the therapy was assessed by using Visual Analog Scale (VAS).

Depending on the type of the join problem, as well as on the severity of the problem, the benefit of therapy was achieved within 15–20 days with a successful rate up to 75%. It should be known that for different joins the benefit varies, but always is higher than at application of conventional therapy. The statistical analysis of the data is in progress and the results for specific applications will be presented at BEMS meeting.

A Thorough Analysis of SAR Evaluation in Human Head Models

A. O. Rodrigues and J. A. Ramirez
Universidade Federal de Minas Gerais, Belo Horizonte, Minas Gerais, Brazil

Abstract— This paper presents a thorough evaluation of the specific absorption rate (SAR) in the human head due to mobile telephones operating at 900 MHz, 1.8 GHz, 2.1 GHz and 2.4 GHz. The evaluation is performed using two complimentary approaches: direct measurements and computational simulations. The SAR measurements were performed using a DASY 4 system and two models of the human head: a flat phantom, and an homogeneous head model (SAM phantom). The numerical simulations were implemented using the finite-difference time-domain (FDTD) method for two models of the human head: an homogeneous and an heterogeneous head model, the latter is composed of 17 different materials and has a precision that complies with the IEEE Std1528. All SAR measurements are in agreement with the IEEE Std1528. Numerical simulations for the homogeneous head model resulted in differences in the SAR_{1g} of 2.6% for 900 MHz, 8.5% for 1.8 GHz, 11.8% for 2.1 GHz and 12.5% for 2.4 GHz in comparison with the IEEE Std1528, values that are in agreement with the literature. The simulations of a commercial mobile telephone operating with power of 23.44 mW (13.7 dBm) at 2.1 GHz, and at 2.4 GHz, in the heterogeneous head model, resulted in SAR_{1g} of 0.92 W/kg and of 0.85 W/kg, and SAR_{10g} of 0.30 W/kg and of 0.29 W/kg, respectively, values which are in accordance with the IEEE C95.1 safety regulation that prescribe a maximum of 1.6 W/kg. The use of homogeneous models in the numerical simulations yield more conservative results, on the other hand the use of heterogeneous models give more insight in terms of the SAR distribution within the human head.

Influence of Gold Nanodiscs on Light Absorption in Thin-film Amorphous Silicon Solar Cell

V. V. Klimov[1] **and I. V. Zabkov**[1, 2]

[1]Lebedev Physical Institute, 53, Leninskij Prospekt, Moscow 119991, Russia
[2]Moscow Institute of Physics and Technology
9, Institutskij Pereulok, Dolgoprudnj, Moscow Region 141701, Russia

Abstract— Nowadays the most important objective of photovoltaic is to reduce the price for solar energy compared to the price of other energy sources. Solar cells produced from amorphous (a-Si) or nanocrystalline silicon (ns-Si) have a good potential in this direction. However such solar cells suffer from low effectiveness because of low thickness of light absorbing layers and weak absorption of long wavelength photons. Recently much attention was paid to use noble metal nanoparticles to increase absorption of the light in Si. Here we will present results of our investigation of gold nanodiscs influence on light absorption in thin amorphous silicon film.

We have investigated absorption of light in 100 nm amorphous silicon film with gold nanodiscs on its surface. The geometry of a problem is shown in Fig. 1(a). Nanodiscs are characterized by their fixed diameter $D = 160\,\text{nm}$ and variable height h_{Au} and are arranged in a square lattice with period $T = 300\,\text{nm}$. Calculations with different height of antireflection coating (ITO) instead of Au nanodiscs have been performed as well. In our simulation it is assumed that bottom surface of Si is a perfect electric conductor. The wavelengths range is from 300 nm to 900 nm. We defined efficiency of our system as: $\{\int_{300\,\text{nm}}^{900\,\text{nm}} K(\lambda)A(\lambda)/(h\nu)\,d\lambda\}/\{\int_{300\,\text{nm}}^{1600\,\text{nm}} A(\lambda)/(h\nu)\,d\lambda\}$ where $K(\lambda)$ — normalized absorption coefficient, $A(\lambda)$ — AM 1.5 solar spectrum. We defined absorption enhancement as ratio of efficiency for current height of Au or ITO to the efficiency of aSi without covering.

Our results are shown in Fig. 1(b), where the absorption enhancement in aSi is shown as a function of h_{Au} for cylinder covering aSi and h_{ITO} for ITO covering aSi. The modeling (FEM) and analytical (Bruggeman) results are similar for small height of cylinders, i.e., small concentrations of gold. It can be seen that gold nanodiscs lead to the absorption weakening. On the other hand using ITO film without nanoparticles give the enhancement. Other periods T have been studied as well and in all cases gold nanodiscs do not lead to the enhancement of solar cell efficiency.

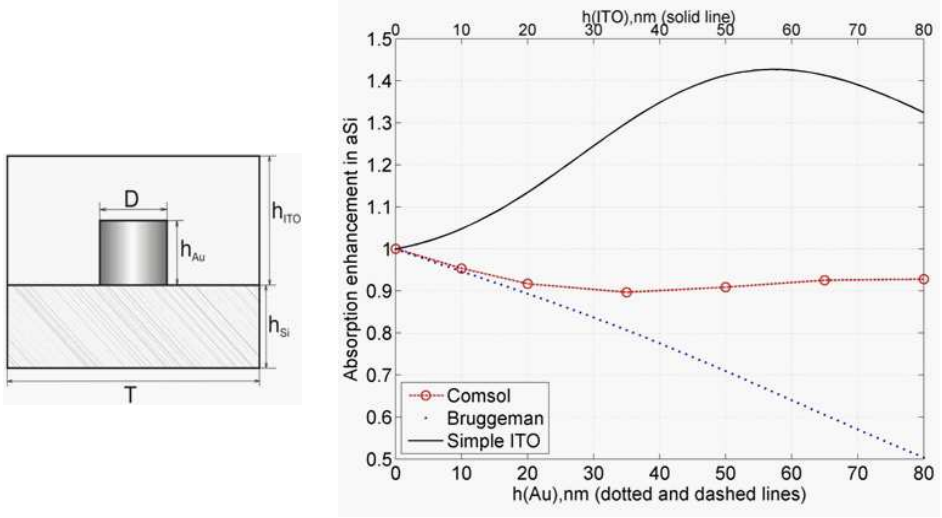

(a) (b)

Figure 1: (a) Geometry of the structure under investigation. (b) Absorption enhancement in a thin-film silicon ($h_{aSi} = 100\,\text{nm}$) as a function of h_{Au} (red, blue) and h_{ITO} (black). Dashed line corresponds to the results of FEM calculations in Comsol. Dotted line corresponds to an analytical calculation using Bruggeman formula. Solid line corresponds to an analytical calculation of ITO covering aSi for different height of ITO.

An *in vitro* Study of Apoptosis in Pancreatic Cancer Cells by High-intensity Nanosecond Pulses

N. Pausawasdi[1], **V. Sirivatanauksorn**[2], **C. Srisawat**[2], **and P. Kirawanich**[3]

[1]Department of Internal Medicine, Faculty of Medicine Siriraj Hospital
Mahidol University, Bangkoknoi, Bangkok 10700, Thailand
[2]Department of Biochemistry, Faculty of Medicine Siriraj Hospital
Mahidol University, Bangkoknoi, Bangkok 10700, Thailand
[3]Electrical Engineering Department, Mahidol University
Salaya, Nakhon Pathom 73170, Thailand

Abstract— In recent years, nanosecond second pulsed electric field (nsPEF) is emerging as a new application for cellular apoptosis induction. It has been employed to serve as an alternative tool for activation of apoptosis in a variety of cancer cell lines. Pancreatic cancer is known for treatment resistance owing to its ability to develop anti-apoptotic mechanisms. In this study, we reported the unique apoptotic responses of human pancreatic cancer cells (Panc-I) induced by nsPEF systems. *In vitro* experiments were carried out using laboratory-assembled apparatus, serving the cells with 10-ns and 500-ns high-intensity pulses. Our data suggested that the apoptotic effects of nsPEF on Panc-I cells are pulse characteristics dependent. In addition, both long pulse duration (500 ns) and increase incubation period (24 h) post treatment are required to initiate the apoptosis demonstrated by a maximal increase in activation of caspase-3, -7 activity of 52% ($p < 0.05$) at 24 h after nsPEF treatment. The slow progression rate of apoptosis induced by nsPEF appears to be a unique property of Panc-I cells when compared to other mammalian cells. The apoptotic responses of pancreatic cancer cells to pulsed electric fields are complex and unique partly due to the crosstalk between extrinsic and intrinsic pathways occurring in this particular cell type. nsPEF-induced apoptosis in Panc-I cells may involve multiple mechanisms but at least in part due to intrinsic pathway and activation of caspase signaling. In addition to a need for observing the cell apoptotic responses by other types of pulses, further studies to define the sites of action in the complex apoptotic pathways are suggested.

Session 2P7
Transport and Localization in Periodic and Disordered Media

Generation of a Localized Wave in a Waveguide System with an Imperfection Core

Akira Komiyama
Osaka Electro-Communication University, Hatsu-cho, Neyagawa-shi 572-8530, Japan

Abstract— Wave functions for electrons in a disordered atomic system are localized and are concentrated into a narrow region of space [1]. It has been known that all states are localized in one and two-dimensional disordered systems [2]. Consequently no diffusion of electrons at all takes place.

In a disordered waveguide system composed of randomly different cores in size mode waves are also localized and are concentrated into a narrow region of several cores [3]. When one of cores is illuminated at the input end of the waveguide system a number of localized modes are excited and their modes propagate through the system. The average amplitude of light has been analytically derived by the perturbation method [4]. The derivation is based on the exact solution for a waveguide system with a single imperfection core. In the waveguide system not only the localized wave but also the direct and scattered waves propagate. The direct wave is light propagating in an ordered waveguide system composed of identical cores and the scattered and localized waves are caused by an imperfection core. Since in a disordered waveguide system all modes are localized it is expected that the direct wave is completely canceled by the scattered wave.

In this paper, we deal with the localization and the scattering of light by a single imperfection core in a waveguide system. The coupled mode equation is analytically solved and it is shown that the mode wave localized at the imperfection core is excited by the direct wave and the scattering takes place there. The asymptotic expansions of the amplitudes of the direct and scattered waves show that the direct wave is partially canceled by the scattered wave and a shadow takes place [5]. The total power of light in the cross section of a waveguide system analytically derived shows that the generation of the localized wave is balanced by the cancellation of the direct wave by the scattered wave [6].

REFERENCES

1. Anderson, P. W., "Absence of diffusion in certain random lattice," *Phys. Rev.*, Vol. 109, 1492–1505, 1958.
2. Abraham, E., P. W. Anderson, D. C. Licciardello, and T. V. Ramakrishnam, "Scaling theory of localization: Absence of quantum diffusion in two dimensions," *Phys. Rev. Lett.*, Vol. 42, 673–676, 1979.
3. Komiyama, A., "Localization of mode waves in a disordered multi-waveguide system," *Opt. Commun.*, Vol. 151, 25–30, 1998.
4. Komiyama, A., "Propagation of light in a disordered waveguide system: Average amplitude," *IEICE Trans. Electron.*, Vol. E93-C, No. 1, 46–51, 2010.
5. Komiyama, A., "Scattering of light by a single imperfection core in a waveguide system," *IEICE Trans. Electron.*, Vol. E94-C, No. 1, 59–62, 2011.
6. Komiyama, A., "Conservation of energy in a waveguide system with an imperfection core," *IEICE Trans. Electron.*, Vol. E95-C, No. 1, 97–100, 2012.

Single Channel Transport in Disordered Systems

Abe Peña[1], **Adrian Girschik**[2], **Florian Libisch**[2], **Stefan Rotter**[2], **and Andrey Chabanov**[1]

[1]Department of Physics and Astronomy, University of Texas at San Antonio
San Antonio, Texas 78249, USA
[2]Institute for Theoretical Physics, Vienna University of Technology, A-1040 Vienna, Austria

Abstract— Electronic transport in conductors or light or sound in samples in which randomly scattered waves diffuse may be characterized by the transmittance T, which is equal to the number of effective open channels N_{eff} with transmission coefficients close to unity [1–3]. Beyond the localization length ξ, at which $N_{eff} = 1$, T is dominated by a single channel of largest transmission [4], which falls exponentially with the system length L due to Anderson localization [5, 6].

In this work, static and dynamic aspects of the crossover to single channel transport in disordered multichannel systems are studied by means of microwave measurements of quasi-1D random waveguides and numerical simulations of planar disordered systems. We show that the degree of fluctuations in transmitted intensity relative to conductance fluctuations exhibits a universal scaling behavior in the crossover to the single channel regime. The single channel regime is achieved at the system length $L \sim 4\xi$. We find that in the single channel regime the disordered system can be treated as a 1D random system coupled diffusely through all transverse channels to the surrounding medium and that the conductance probability density is in agreement with that of 1D localized system.

We also observe single-channel pulsed transmission in localized and diffusive samples. When the pulse bandwidth Δ is less than the average mode width δ, in an ensemble of random samples with $L > \xi$, single channel transport is observed for all time delays following a pulse excitation. When $\Delta > \delta$, single channel transport is achieved at longer times, when only a single long-lived mode contributes. Single channel transport is also observed in pulsed transmission in samples with $L < \xi$ at long times, reflecting the impact of long-lived modes in nominally diffusive samples.

Finally, we show that the localized eigenmodes of the disordered multichannel system, including rare-occurred, short-lived 'necklace' states [7], occupy distinct transmission eigenchannels of the system.

REFERENCES

1. Landauer, R., *IBM J. Res. Dev. Philos. Mag.*, Vol. 21, 863, 1970.
2. Buttiker, M., Y. Imry, R. Landauer, and S. Pinhas, *Phys. Rev. B*, Vol. 31, 6207, 1985.
3. Imry, Y., *Europhys. Lett.*, Vol. 1, 249, 1986.
4. Dorokhov, O. N., *Pis'ma Zh. Eksp. Teor. Fiz.*, Vol. 36, 259, 1982.
5. Anderson, P. W., *Phys. Rev.*, Vol. 109, 1492, 1958.
6. Anderson, P. W., D. J. Thouless, E. Abrahams, and D. S. Fisher, *Phys. Rev. B*, Vol. 22, 3519, 1980.
7. Pendry, J. B., *J. Phys. C*, Vol. 22, 733, 1987.

Surface Disordered Waveguide: How to Separate Distinct Mechanisms of Scattering in Different Frequency Bands

N. M. Makarov[1] and M. Rendón[2]

[1]Instituto de Ciencias, Universidad Autónoma de Puebla
Priv. 17 Norte No. 3417, Col. San Miguel Hueyotlipan, Puebla 72050, México
[2]Facultad de Ciencias de la Electrónica, Universidad Autónoma de Puebla
Av. San Claudio y 18 Sur, Col. San Manuel, Puebla 72570, México

Abstract— In waveguides with surface disorder, the propagating wave is attenuated due to multiple scattering from the surface roughness [1]. Recently, it has been shown that surface scattering in waveguides is governed by two basic mechanisms: the well known amplitude mechanism and the new square-gradient mechanism [2, 3]. As a consequence, each mechanism of scattering gives rise to the corresponding term in the expression for the inverse attenuation length of propagating waveguide mode. The term associated with the amplitude scattering depends on the variance of the disorder σ^2, whereas the term associated with the square-gradient scattering is due to the squared variance σ^4. Besides this dependence on σ, it is very important to consider that the terms differently depend on the correlation properties of surface disorder. Indeed, while the inverse amplitude-scattering length is conventionally proportional to the power spectrum (Fourier transform) of the roughness-height correlator, the inverse square-gradient scattering length contains the Fourier transform of the correlator of the squared roughness-gradient. In the case of Gaussian correlations in the rough surface, both mechanisms, competing with each other, contribute to the wave attenuation (see details in Refs. [2, 3]).

When the scattering mechanisms compete, their individual effects cannot be directly discriminated in actual measurements of waveguide transport. One of the scenarios for proper experimental observation of the mechanisms is when each of them works within its own separate interval of wave frequency. In this contribution, we suggest how to realize such a situation. Specifically, we construct a rough surface that possesses roughness-height power spectrum of the rectangular form, with nonzero value only within prescribed range of wave number. The profile of the surface exhibits long-range correlations and is described by two correlation parameters. Then, we give the conditions under which the amplitude and square-gradient mechanisms operate in different, nonoverlapping, frequency bands, and therefore, do not compete with each other [4]. After the application of our recipe to isolate the mechanisms, it is expected that the waveguide with this specific rough-surface profile has three different frequency bands in which its transmittance decreases: in the first and third bands the wave attenuation is due to the square-gradient scattering, whereas in the second one the scattering is driven by the amplitude surface scattering. Between these reflection bands, there are the frequency bands of complete transparency.

REFERENCES

1. Bass, F. G. and I. M. Fuks, *Wave Scattering from Statistically Rough Surfaces*, Pergamon, New York, 1979.
2. Izrailev, F. M., N. M. Makarov, and M. Rendón, "Gradient and amplitude scattering in surface-corrugated waveguides," *Phys. Rev. B*, Vol. 72, No. 4, 041403(R), 2005.
3. Izrailev, F. M., N. M. Makarov, and M. Rendón, "Manifestation of the roughness-square-gradient scattering in surface-corrugated waveguides," *Phys. Rev. B*, Vol. 73, No. 15, 155421, 2006.
4. Rendón, M., F. M. Izrailev, and N. M. Makarov, "Discrimination between two mechanisms of surface scattering in a single-mode waveguide," *Phys. Rev. E*, Vol. 84, No. 5, 051131, 2011.

Non-conventional Anderson Localization in Array of Matched and Balanced Bilayers

N. M. Makarov, E. J. Torres-Herrera, and F. M. Izrailev
Benemérita Universidad Autónoma de Puebla, Puebla, Pue., México

Abstract— We resolve the problem of Anderson localization emerging in one-dimensional periodic-on-average systems that represent an infinite array of two alternating a and b layers with equal impedances ($Z_a = Z_b$) and optical widths ($n_a d_a = |n_b| d_b$) in the absence of disorder. Two possible kinds of the systems are compared: the *homogeneous stack* with both basic slabs being made from right-handed (RH) optic materials (refractive indices are positive, $n_{a,b} > 0$), and *mixed stack* when a-slabs contain RH-material ($n_a > 0$), while b-layers are of left-handed (LH) material ($n_b < 0$). The uncorrelated weak disorder with zero average and variance $\sigma^2 \ll 1$, is incorporated via dielectric permittivities only. The localization length L_{loc}, which is the key parameter of the Anderson localization, is derived via the Lyapunov exponent within the Hamiltonian map method [1].

Homogeneous Stack: In such a structure the unperturbed wave-phase shift over a unit (a, b) cell is non-zero that gives rise to the uniform phase distribution. Therefore, the inverse localization length gets the conventional form,

$$d/L_{loc} = \sigma^2 \sin^2 \varphi, \quad \varphi = \omega n_a d_a / c, \quad d = d_a + d_b. \tag{1}$$

This expression provides the standard frequency dependence of the localization length. In particular, $L_{loc}^{-1} \propto \omega^2$ when $\omega \to 0$.

Mixed Stack: Without disorder, in periodic structure with $n_a d_a = -n_b d_b$ the phase shift φ of the wave gained in the RH a-layer is canceled by the subsequent shift $-\varphi$ in the next LH b-layer. Therefore, the total phase shift vanishes after passing every unit (a, b) cell, that, together with perfect impedance matching of slabs, results in a kind of quite interesting "non-visible" system. To great surprise, the numerical data [2, 3] obtained for this RH-LH model with weak fluctuations in refractive indices, have demonstrated enormously fast divergence of the localization length L_{loc} for $\omega \to 0$. We analytically show that this unusual effect is originated from the nonuniform phase distribution and cannot be described within the standard second-order perturbation theory. With a new approach allowing us to go to the fourth order in disorder, we derive the expression for L_{loc} valid for any frequency ω and small variance $\sigma^2 \ll 1$,

$$\frac{d}{L_{loc}} = \alpha \sigma^4 \frac{[(2\varphi^2 - \sin^2 \varphi) \cos \varphi - \varphi \sin \varphi]^2}{\varphi^2 - \sin^2 \varphi}. \tag{2}$$

The constant factor $\alpha = 1/5$ for the flat disorder-distribution. In the limit $\omega \to 0$ one gets a quite specific dependence, $L_{loc}^{-1} \propto \sigma^4 \omega^8$, providing an increase in the localization length by six orders of magnitude in the wavelength as compared with that for homogeneous structures. Our further study demonstrates that the crossover from quadratic to octal frequency dependence is governed by the ratio between detuning of optical widths and disorder variance. Therefore, with an additional weak disorder in the layer widths d_a and/or d_b the standard dependence $L_{loc}^{-1} \propto \sigma^2 \omega^2$ quickly recovers. Our numerical data manifest excellent agreement with the analytical results.

ACKNOWLEDGMENT

This work was partially supported by SEP-CONACYT (grant CB-2011-01-166382), México.

REFERENCES

1. Izrailev, F. M., A. A. Krokhin, and N. M. Makarov, "Anomalous localization in low-dimensional systems with correlated disorder," *Phys. Rep.*, Vol. 512, No. 3, 125–254, 2012.
2. Asatryan, A. A., L. C. Botten, M. A. Byrne, V. D. Freilikher, S. A. Gredeskul, I. V. Shadrivov, R. C. McPhedran, and Yu. S. Kivshar, "Suppression of anderson localization in disordered metamaterials," *Phys. Rev. Lett.*, Vol. 99, No. 19, 193902(4), 2007.
3. Asatryan, A. A., S. A. Gredeskul, L. C. Botten, M. A. Byrne, V. D. Freilikher, I. V. Shadrivov, R. C. McPhedran, and Yu. S. Kivshar, "Anderson localization of classical waves in weakly scattering metamaterials," *Phys. Rev. B*, Vol. 81, No. 7, 075124(17), 2010.
4. Torres-Herrera, E. J., F. M. Izrailev, and N. M. Makarov, "Non-conventional Anderson localization in bilayered structures," *Euro. Phys. Lett.*, Vol. 98, 2012, in press.

Anisotropic Voigt Effect and Other Magneto-optical Phenomena in Metamaterials with Periodic Microstructures

Y. M. Strelniker[1], **D. J. Bergman**[2], **A. O. Voznesenskaya**[3], **and A. P. Vinogradov**[4]

[1]Bar-Ilan University, IL-52900 Ramat-Gan, Israel
[2]Tel Aviv University, IL-69978 Tel Aviv, Israel
[3]National Research University of Information Technologies, Mechanics and Optics
St. Petersburg 197101, Russia
[4]Institute for Theoretical and Applied Electromagnetics, Moscow 125412, Russia

Abstract— It is known that the Faraday and other magneto-optical (MO) effects can be significantly enhanced in the presence of an electromagnetic (EM) resonance. One such resonance, which is currently under intensive study, is the surface plasma resonance. It is widely believed that this or similar resonances are responsible for the Extraordinary Light Transmission (ELT) through a metal film, perforated by a periodic array of sub-wavelength holes, as well for other new phenomena recently found in photonic crystals with band gaps. Application of a static magnetic field $\mathbf{B}_0$ to such systems induces strong optical and transport anisotropy and leads to the appearance of additional off-diagonal tensor components in the effective permittivity tensor and changes the frequency of the surface plasma resonance. Therefore, the application of a static magnetic field to a conducting system with dielectric islands or to a dielectric system with metallic islands, as well the introduction of gyrotropic inclusions into a photonic crystal, should lead to the appearance of strong magneto-optical effects and to possibilities for the manipulation of light propagation [1–3].

Application of a static magnetic field $\mathbf{B}_0$ to a metamaterial [1–3] can also lead to magneto-induced anisotropy and to the appearance of additional off-diagonal terms in the electric permittivity and magnetic permeability tensors. Therefore, the magneto-optical effects in metamaterial crystals need to be calculated using appropriate general expressions, where simplistic assumptions regarding the form of those tensors are avoided.

In the case where $\mathbf{B}_0$ has an arbitrary direction with respect to the lattice axes of the microstructure all components of the permittivity tensor can be nonzero. When both the external magnetic field $\mathbf{B}_0$ and the EM electric field $\mathbf{E}$ are rotated in the film plane, the angular profiles of all the permittivity tensor components are quite complicated. As a result of this, the general expressions for Faraday rotation and Voigt effect are also quite complicated in this case. It is found (using general expressions) that the Voigt effect and other magneto-optical phenomena strongly depend on the direction of the applied static magnetic field, as well as that of the time dependent electromagnetic field, with respect to the lattice axes of the periodic microstructure. That is, it is possible, in principle, to observe a magneto-induced angular anisotropy of the Voigt effect in periodic metamaterials. The angular anisotropy of other MO phenomena can be considered in a similar fashion.

REFERENCES

1. Bergman, D. J. and Y. M. Strelniker, "Anisotropic ac electrical permittivity of a periodic metal-dielectric composite film in a strong magnetic field," *Phys. Rev. Lett.*, Vol. 80, 857–860, 1998.
2. Strelniker, Y. M. and D. J. Bergman, "Optical transmission through metal films with a subwavelength hole array in the presence of a magnetic field," *Phys. Rev. B*, Vol. 59, R12763–R12766, 1999.
3. Strelniker, Y. M. and D. J. Bergman, "Transmittance and transparency of subwavelength-perforated conducting films in the presence of a magnetic field," *Phys. Rev. B*, Vol. 77, 205113-1–205113-5, 2008.

Controlling the Movement of Plasmonic Nanoparticles with Fast Electron Beams

A. Reyes-Coronado[1,5], **P. E. Batson**[2], **R. G. Barrera**[3], **A. Rivacoba**[4,5,6], **A. Howie**[7], **P. M. Echenique**[4,5,6], **and J. Aizpurua**[5,6]

[1]Instituto de Física, Benemérita Universidad Autónoma de Puebla, Mexico
[2]Institute for Advanced Materials, Devices, and Nanotechnology, Rutgers University, USA
[3]Instituto de Física, Universidad Nacional Autónoma de México, Mexico
[4]University of the Basque Country UPV/EHU, Spain
[5]Donostia International Physics Center DIPC, Spain
[6]Centro de Física de Materiales CSIC-UPV/EHU, Spain
[7]Cavendish Laboratory, Cambridge, United Kingdom

Abstract— The possibility of moving plasmonic nanoparticles in a controllable way with fast electron beams, like those typically used in electron microscopy, is now open. We have recently published results, both theoretically and experimentally [1, 2], showing that it is possible to induce movement on a small metallic nanoparticle (1-2 nanometers in radius), shifting it towards the electron beam or away of it. In our calculations of the momentum transfer from the electron to plasmonic nanoparticles we consider full relativistic effects. The attractive interaction between a plasmonic nanoparticle and a fast electron beam, occurring at large enough impact parameters, is what intuitively will be expected from the interaction of the electron and the positive induced charge in the closest region of the nanoparticle to the electron trajectory (excitation of dipolar plasmon mode mainly). However, it is well known that for small enough impact parameters, the dipolar plasmon mode of the nanoparticle is not the most strongly excited mode, so that the higher-energy multipolar modes play a predominant role [3, 4]. Under this circumstance, we have shown that the interaction between the electron and the nanoparticle turns out to be repulsive, that is, the electron beam expels the nanoparticle away. Thus, by controlling the impact parameter of the electron beam to the nanoparticles, it is possible for example to induce coalescence between pair of particles, as has been observed and studied experimentally [5], or avoid that two nanoparticles approach each other. The repulsive behavior at small impact parameters is predicted by theoretical calculations from classical electrodynamics, however other processes might be present in the experiment such as secondary electron emission and surface charging. Although the repulsive behavior between a swift electron and a silver nanoparticle was theoretically found by Garca de Abajo and studied in detail [6], no fully satisfactory theoretical explanation has been given. We propose, as a suitable explanation based on classical electrodynamics, that the repulsion effect is due to the recoil of the particle produced by the momentum carried on the electromagnetic field radiated away by the particle. In this sense, when the electron beam is traveling far from the nanoparticle, the distribution of the induced charges within the particle (mainly dipolar) will produce a symmetric spatial radiation pattern, with no net momentum. On the other hand, for close electron trajectories, the electron excites higher multipolar plasmon modes producing a constructive interference and resulting in a confined induced charge within the nanoparticle, giving to the radiation (and electromagnetic momentum) a specific direction. Even though the theoretical calculations predict attraction and repulsion effects with transition metals, a simpler analysis has been done with Drude-like metals, where the electromagnetic properties of the excitations are determined by the plasma frequency and the damping.

REFERENCES

1. Reyes-Coronado, A., R. G. Barrera, P. E. Batson, P. M. Echenique, A. Rivacoba, and J. Aizpurua, *Phys. Rev. B*, Vol. 82, 235429, 2010.
2. Batson, P. E., A. Reyes-Coronado, R. G. Barrera, A. Rivacoba, P. M. Echenique, and J. Aizpurua, *Nano Lett.*, Vol. 11, 3388–3393, 2011.
3. Ferrel, T. L. and P. M. Echenique, *Phys. Rev. Lett.*, Vol. 55, 1526–1529, 1985.
4. García de Abajo, F. J. and A. Howie, *Phys. Rev. Lett.*, Vol. 80, 5180–5183, 1998.
5. Batson, P. E., *Microsc. Microanal.*, Vol. 14, 89–97, 2008.
6. García de Abajo, F. J., *Phys. Rev. B,* Vol. 70, 115422, 2004.

Reflection of Electromagnetic Waves at a Half-space Filled with a Turbid Colloid: An Effective-medium Approach

E. Gutiérrez-Reyes[1], **A. García-Valenzuela**[2], **and R. G. Barrera**[1]

[1]Instituto de Física, Universidad Nacional Autónoma de México, México
[2]Centro de Ciencias Aplicadas y Desarrollo Tecnológico
Universidad Nacional Autónoma de México, México

Abstract— I has been found [1] that when scattering is important it is possible to describe the electromagnetic response of a bulk system composed of independent scatterers using an effective-medium approach. This is done in terms of the generalized effective conductivity tensor $\bar{\bar{\sigma}}_{eff}(\vec{k},\omega)$ which relates the total average current density with the average electric field, and it turns out to be spatially dispersive, that is, it depends not only on the frequency ω but also on the wavevector $\vec{k}$. Here, when we extend the concept of $\bar{\bar{\sigma}}_{eff}$ to a system with a planar interface it becomes spatially dispersive as $\bar{\bar{\sigma}}_{eff}(\vec{k},\vec{k}';\omega)$, which can be interpreted as the Fourier $\vec{k}$ component of the current density induced by a plane wave with wave-vector $\vec{k}'$. Then we calculate it for a system of identical spheres randomly located in a half space in vacuum, using a novel method based on an extension of the Mie scattering problem. Then we proceed to the calculation of the reflected electromagnetic field for an plane wave incident into the this system with a definite wavevector and frequency. We do this using a method based on an integral-equation method that we solve using as an *Ansatz* a plane wave with an effective wave-vector, amplitude and polarization. These effective parameters are determined using consistency relations which then are calculated within an approximation that we call: the light-cone approximation, and that turns out to be an extension of the multiple-scattering approach [2]. We end up with relatively simple formulas for the reflection amplitudes, and then we perform numerical calculations to compare and to discuss the merits of our approach and our results as compared to others. Finally, we include the presence of a matrix material in the half space by replacing in the formalism the free-space propagator by the half-space Green's function dyadic, in order to be able to compare our results with actual experimental data.

REFERENCES

1. Barrera, R. G., A. Reyes-Coronado, and A. García-Valenzuela, *Physical Review B*, Vol. 75, No. 184202, 1–19, 2007.
2. Tsang, L., J. A. Kong, and K.-H. Ding, *Scattering of Electromagnetic Waves: Theories ans Applications*, John Wiley & Sons, New York, 2000.

Enhanced Microwave Transmission and Magnetophotonic Response in One-Dimensional Magnetophotonic Crystals

K. Smith and A. A. Chabanov
Department of Physics and Astronomy, University of Texas at San Antonio
San Antonio, Texas 78249, USA

Abstract— Magnetic materials are of great importance to microwave engineering and photonics due to their nonreciprocal properties, such as Faraday and Kerr effects. They are utilized in various microwave and optical components, including isolators, circulators, phase shifters, modulators, etc. However, many magnetic materials exhibiting strong magnetophotonic responses have been ignored in applications due to their high losses in spectral ranges of interest.

In this work, we explored microwave absorption suppression and magnetophotonic properties of lossy magnetic thin films incorporated in a 1D photonic crystal. The implemented absorption suppression mechanism is due to a highly nonuniform electromagnetic field distribution inside the photonic crystal [1]: At a transmission resonance the nodes of the electric field coincide with antinodes of the magnetic field and vice versa. When a material with conductivity losses is placed at the node of electric field, absorption is greatly suppressed, whereas the magnetophotonic response remains the same or even enhanced.

Strongly enhanced microwave transmission and Faraday Effect in cobalt thin films incorporated in a periodic binary stack of dielectric layers have been studied by means of transfer-matrix calculations and microwave transmission measurements [2]. At a crystal defect resonance the microwave transmission was measured 10^3 the transmission through a stand-alone 275-nm thin cobalt layer. When magnetic field was applied, the ferromagnetic resonance (FMR) in the cobalt film was observed as a small dip in the transmission spectrum. The FMR frequency was found to increase linearly with magnetic field in agreement with Kittel's formula.

In conclusion, microwave transmission in cobalt thin films can be significantly enhanced by incorporating the film in 1D photonic crystal. Under resonance conditions of the magnetophotonic crystal, the electric field in the cobalt film is greatly diminished and thus its reflection and absorption are reduced. At the same time, the ac magnetic field is significantly increased, leading to enhanced nonreciprocal effects which may be controlled with magnetic field. Our study suggests that lossy magnetic materials incorporated in periodic photonic structures may have important applications in microwaves and photonics.

REFERENCES

1. Figotin, A. and I. Vitebskiy, *Phys. Rev. B*, Vol. 77, 104421, 2008.
2. Smith, K. and A. A. Chabanov, *Integrated Ferroelectrics*, Vol. 131, 61, 2011.

Damping Effects in the Metamaterial Response of Periodic Metallic Nanostructures

J. A. Reyes-Avendaño[1], **V. I. Mezhuyev**[2], **and F. Péerez-Rodríguez**[3]

[1]Escuela de Ingeniería y Ciencias Aplicadas, Tecnológico de Monterrey
Campus Puebla, Puebla, Pue. 72800, Mexico
[2]Berdyansk State Pedagogical University
Shmidta Str. 4, Berdyansk 71100, Ukraine
[3]Instituto de Física, Benemérita Universidad Autónoma de Puebla
Apdo. Post. J-48, Puebla, Pue. 72570, Mexico

Abstract— Metamaterials are characterized by extraordinary physical properties which could be totally different from those of the components because of their complicated structure. Thus, for example, metal-dielectric photonic crystals, having a negative index of refraction belong to such a class of materials. This unusual property has been achieved in double negative metamaterials with simultaneously-negative effective permittivity and permeability. Several forms for the metallic inclusion in the unit cell of such negative-index materials (NIM) has been proposed: split-ring resonators, dual-bar rods, fish-net structures, double crosses, etc.. In order to apply NIM in the optical range, it is necessary to fabricate periodic metal-dielectric nanostructures having a period of the order or smaller than the typical wavelength $\sim$ 390–750 nm. The effective bianisotropic response of 3D periodic metal-dielectric nanostructures can be investigated within the framework of the homogenization theory, recently developed in Ref. [1], which unlike other similar methods [2–4] based upon the Fourier formalism, can be applied even beyond the local regime. Indeed, previous homogenization theories [2–4] are valid in the regime of long wavelengths and neglect any nonlocal contribution to the effective permittivity tensor. However, a nanostructure composed of metallic and dielectric materials may have an effective magnetic response, as it is expected for a metamaterial, only if the spatial dispersion hiding magnetic effects is considered. The theory developed in [1] provides explicit expressions for all the tensors of the effective bianisotropic response of metal-dielectric photonic crystals. In such a theory the macroscopic magnetic field and electric displacement vector are redefined in such a way that nonmagnetic inclusions in metal-dielectric periodic arrays can give rise not only to magnetic effects, but also to chiral ones. Nevertheless, the calculation of the effective tensors of the bianisotropic response, namely the permittivity, the permeability and the crossed magneto-electric tensors, is complicated due to the inversion of very large matrices. To avoid these numerical difficulties, we have applied the form-factor division approach (FFDA) developed in [2], which leads to a substantial reduction of the computation effort. Specifically, we have studied the bianisotropic response of various 3D periodic metal-dielectric nanostructures exhibiting metamaterial behavior. Besides, the damping effects upon the frequency dependence of the effective permittivity, permeability and crossed magnetoelectric tensors are analyzed and discussed.

REFERENCES

1. Reyes-Avendaño, J. A., U. Algredo-Badillo, P. Halevi, and F. Pérez-Rodríguez, "From photonic crystals to metamaterials: The bianisotropic response," *New J. Phys.*, Vol. 13, 073041-1–33, 2011.
2. Cerdán-Ramírez, V., B. Zenteno-Mateo, M. P. Sampedro, M. A. Palomino-Ovando, B. Flores-Desirena, and F. Pérez-Rodríguez, "Anisotropy effects in homogenized magneto-dielectric photonic crystals," *J. Appl. Phys.*, Vol. 106, 103520-1–8, 2009.
3. Ortiz, G. P., B. E. Martínez-Zérega, B. S. Mendoza, and W. L. Mochán, "Effective optical response of metamaterials," *Phys. Rev. B*, Vol. 79, 245132-1–9, 2009.
4. Zenteno-Mateo, B., V. Cerdán-Ramírez, B. Flores-Desirena, M. P. Sampedro, E. Juárez-Ruiz, and F. Pérez-Rodríguez, "Effective permittivity tensor for a metal-dielectric superlattice," *Progress In Electromagnetics Research Letters*, Vol. 22, 165–174, 2011.

Scattering of Waves: Imperfect Coupling and Absorption or Amplification

R. A. Méndez-Sánchez[1], **A. M. Martínez-Argüello**[1, 2], **G. Báez**[3], **and M. Martínez-Mares**[2]

[1]Instituto de Ciencias Físicas, Universidad Nacional Autónoma de México
A. P. 48-3, Cuernavaca Mor. 62210, México
[2]Departamento de Física, Universidad Autónoma Metropolitana-Iztapalapa
A. P. 55-534, Distrito Federal 09340, Mexico
[3]Departamento de Ciencias Básicas, Universidad Autónoma Metropolitana-Azcapotzalco
A. P. 21-267, Distrito Federal 04000, Mexico

Abstract— A panorama on the scattering of waves of amplifying and absorbing systems, in wich imperfect coupling to the incoming and outgoing channels is also present, is given. The models of the parasitic channels and of the imaginary potential model, are discussed for amplification and absorption. The theoretical calculations for the non-unitary scattering matrix are also discussed from a perspective of the different theoretical frameworks. Several cases are discussed, from simple barriers in quantum mechanics, like delta potentials or potential barriers, to the complex scattering by chaotic and disordered systems in microwaves. The result for one and several channels is discussed in terms of the Poisson kernel squared. The theoretical predictions are supported by different numerical and experimental results. The Random Matrix Theory predictions seem to agree with the experimental and numerical results several orders of magnitude for both, the reflection coefficient and phase of the scattering matrix. For some simple systems with local absorption (amplification) and imperfect coupling the results are different than those with global absorption; it is given by the non-unitary Poisson kernel. In the one channel case, the movement of the non-unitary scattering matrix on the Argand plane is discussed for the reflection coefficient and the phase of the non-unitary scattering matrix in the case of a imaginary delta potential and for an imaginary constant potential with a real delta.

Session 2P8
Mobile Antennas, Printed Antennas, and Array Antennas

A Method for Reduction of the Negative Impact of the Instrument Leakage during Measurements of the Amplitude and Phase Characteristics of Array Elements on the Depth of the Nulls Synthesized in the Array Radiation Pattern

A. O. Manichev and B. V. Levkin
JSC "ALMAZ_ANTEY" MSDB", Russia

Abstract— In order to improve the noise immunity of a radio system, deep nulls may be placed in the radiation pattern of the system's phased array antenna (PAA) in the directions of the interfering sources. The null depths depend on the accuracy of realization of the synthesized amplitude-and-phase distribution (APD).

By now, a lot of factors (either systematic or random) causing APD distortions have been considered. However, the influence of the leakage of the instrument used for measuring the amplitude and phase characteristics of the PAA elements is studied insufficiently. At the same time, this factor can significantly limit the depth of synthesized nulls. In this report, we analyze this effect and propose a method for processing of the amplitude and phase characteristics of the PAA elements that enables one to reduce the adverse influence of the instrument leakage on the depth of the pattern nulls.

It can be shown that the instrument leakage results in the appearance of a systematic component of the background level of the PAA radiation pattern. This component is independent of the phase distribution over the PAA elements and limits the depth of synthesized nulls. The amplitude pattern of this component is similar to the radiation pattern of a virtual in-phase uniformly excited PAA with elements coinciding with the elements of the PAA under test. The amplitude of this component of the background level of the radiation pattern increases with the number of the PAA elements.

This background level not only degrades the noise immunity of the system but also complicates the process of testing the PAA ability to synthesize the pattern nulls. However, physical improvement of the instrument leakage is usually either impossible or inconvenient. In this report, a method for decreasing this negative effect is proposed. The method involves smoothing of the amplitude and phase characteristics of the PAA elements by means of linear regression.

The proposed method was tested on a real nonequispaced uniformly excited PAA. The array contains 384 elements with 6-bit phase shifters. Processing of the amplitude and phase characteristics with the use of this method resulted in a 10-fold decrease in the maximum level of the systematic background component caused by the instrument leakage.

Thus, the negative impact of the instrument leakage on the depth of the nulls synthesized in the radiation pattern of a PAA can easily be reduced with the use of the proposed method.

Design of Experiments and Data Processing for Diagnostics of Phased Array Antenna Elements with the Use of Reflected Signals

A. O. Manichev and V. A. Balagurovskii
JSC "ALMAZ_ANTEY" MSDB", Russia

Abstract— Detection of the element failures in a phased array antenna (PAA) is an important practical problem. There are a lot of diagnostic techniques using either low-frequency control loops or microwave testing equipment. The first group of these methods is unable to detect the change in the element amplitude (caused, for example, by the break of the feeding circuit). The methods of the other group overcome this drawback, but require either complicated PAA architecture or additional equipment. Therefore, a method for diagnostics PAA elements using "aperture reflections" [1] is a very attractive tool, since it uses microwave signals to test elements and does not require neither additional equipment nor changes in the PAA design.

This method is based on the fact that it is impossible to provide perfect matching between a radiator and free space in a limited frequency band. Thus, a portion of the signal fed to the PAA input is always reflected backward from the PAA aperture and arrives at the PAA output. It is possible to separate signals of individual PAA elements from the total reflected signal. In order to do this, a unique phase modulation sequence is applied to the phase shifter of each PAA element and the signal of this element is recovered from the sum output signal via a special mathematical processing. The failures of individual elements (modules, subarrays) are determined through the analysis of the values of the recovered signals of these elements.

However, in real PAAs, the total signal at the PAA output contains not only the useful reflected signal passing only through the tested element, but also "parasitic" signals induced by other PAA elements owing to the mutual coupling effects and modulated by their phase shifters in accordance with their own modulation sequences. These parasitic signals complicate recovery of individual signals and, hence, degrade the reliability of the diagnostic procedure.

This paper presents two methods for reduction of the influence of the mutual coupling effects on the characteristics of the diagnostics with the use of aperture reflections. The first method involves a kind of "spectral separation" of parasitic and useful signals via increasing the size of the Walsh-Hadamard matrix used for construction of the modulation sequences and renumbering of the PAA elements. The second method is based on the measurement of a set of "orthogonal" amplitude and phase distributions formed with the use of Walsh functions and corresponding mathematical processing of the measurement results.

The proposed methods were experimentally tested on a real L-band 64-element PAA. The experiments have shown high reliability of the proposed methods, especially when they are used together.

REFERENCES

1. Balagurovskii, V. A., A. O. Manichev, A. S. Kondratiev, and A. A. Zakharov, *Byull. Izobret.*, No. 6, RF Patent No. 2413345, 2011.

Accurate Recovering of the Amplitude and Phase Distribution of a Phased Array Antenna with Interacting Elements with the Help of the Switching Method

V. A. Balagurovskii, **A. S. Kondratiev**, **A. O. Manichev**, **and N. P. Polishchuk**
JSC "ALMAZ_ ANTEY" MSDB", Moscow, Russia

Abstract— Determination of the amplitude and phase distribution (APD) in the aperture of a phased array antenna (PAA) is an important part of the PAA design and diagnostics. The APD can be used to evaluate the radiation pattern of the PAA in arbitrary directions without movement of the PAA under test, find failures of its elements, estimate flatness of the radiation field of the auxiliary antenna used in the measurements, etc.

The switching method [1] is one of most convenient ways to measure the APD of a PAA, because it does not require any movements of the PAA under test relative to the auxiliary antenna. This method involves measurement of the PAA output signal for different phase distributions and recovery of the APD via special mathematical processing of the measured data.

Traditionally, the commutation method uses a simple PAA model to recover the APD. This model does not take into account mutual coupling between the PAA elements, which always present in real PAAs. Analysis shows that usage of this simple model leads to systematic errors in recovered APD.

This report presents the following method for the accurate recovery of the APD of a PAA with interacting elements:

1. The beam of the PAA under test is steered in the direction of the auxiliary antenna, which is characterized by angles θ_0, φ_0 in the spherical coordinate system used to describe the PAA pattern.

2. Currents I_k^{comm} of the PAA elements are measured using a version of the switching method described in [1]. Generally, these currents are not the actual (accurate) currents of the PAA elements.

3. To obtain accurate currents, each current I_m^{comm} of the mth element is replaced with the current $I_k^{comm} \cdot \exp(j2\xi_{m0})$, where k is the number of the element symmetric to mth element relatively the PAA center and ξ_{m0} is the geometrical phase shift for the direction θ_0, φ_0, which is specified by the formula

$$\xi_m(\theta, \varphi) = \frac{2\pi}{\lambda}(x_m \sin\theta\cos\varphi + y_m \sin\theta\sin\varphi + z_m \cos\theta).$$

Here, λ is the wavelength and (x_m, y_m, z_m) are the coordinates of the mth element in the Cartesian coordinate system of the PAA whose origin coincides with the aforementioned spherical coordinate system.

It is shown that the proposed method provides exact recovering of the APD in the case of linear phase distribution in a uniformly excited PAA of identical elements having central symmetry for any "strength" of the mutual coupling between the PAA elements. Mathematical simulation shows, that the method improves also the accuracy of the recovering procedure in the case of a tapered amplitude distribution.

REFERENCES

1. Bubnov, G. G., S. M. Nikulin, Y. N. Seryako, and S. A. Fursov, "Switching method for measurement of PAA characteristics," *Kommutatsionnyi Metod Izmereniya Kharakteristik FAR*, 120, Radio i svyaz', Moscow, 1988.

Synthesis Methods for Reactively Loaded Antenna Arrays

Alexander Sergeevich Kondratiev
JSC "ALMAZ_ANTEY" MSDB", Russia

Abstract— Reactively loaded antenna arrays are the arrays containing reactive loads at their ports, which are excited either by an external field or by one or several impressed sources connected to these ports. Such antennas are attractive candidates for cheap and flexibly controlled shaped-beam antenna structures. If the excitation sources are fixed, the antenna characteristics can be controlled by varying the loads [1].

However, reactive loads introduce nonlinearity into the synthesis problem, which complicates the solution of the corresponding pattern synthesis problem and, usually, requires application of iterative procedures. Such procedures are often found to be cumbersome and/or inefficient. Therefore, the development of efficient synthesis methods for such antennas is a topical problem.

Let us consider an amplitude pattern synthesis problem for a reactively loaded antenna array of arbitrary configuration. The problem is formulated as follows: it is required to synthesize the array amplitude pattern such that, for fixed excitation, gives the best rms approximation to the desired pattern by varying the reactive loads.

Two solution methods are described. In the first method, the amplitude pattern synthesis problem is based on solution of a complex synthesis problem and, in the second method, the synthesis problem is formulated directly for the desired amplitude pattern.

In the first case, the solution procedure contains three steps:

(i) Specify the desired amplitude pattern and form the complex pattern by assigning any phase to the amplitude pattern.
(ii) Synthesize the specified complex pattern, obtain optimum loads, and calculate the phase of the synthesized pattern.
(iii) Assign this (new) phase to the desired amplitude pattern, return to Step (ii) with new complex pattern and synthesize it starting from the initial point determined by the loads found at the previous step.

This procedure represents a monotonically converging iterative scheme, which was found to be very efficient in solving amplitude pattern synthesis problems [2]. The key point here is Step (ii), for which a specialized iterative algorithm based on sequential minimization of a rms objective function with respect to one selected load at each step is proposed. The calculations are similar to those used earlier for the phase-only synthesis of antenna arrays [3]. The algorithm was found to be rather fast due to analytical calculation of the objective function optimum at each iteration. It does not involve any restrictions on the specified amplitude pattern or the configuration of the antenna array.

In the second case, the synthesis problem is formulated for the squared amplitude (power) pattern, without such an artificial step as formation of the complex pattern from the desired amplitude pattern. This approach slightly complicates the objective function; however, it does nor require solution of a sequence of complex pattern synthesis problems. Here, an iterative algorithm based on sequential minimization of a rms objective function with respect to one load at each iteration is also used.

Both proposed synthesis methods are compared by the examples of the synthesis of arrays with pencil-beam, flat-topped, and cosecant patterns.

Similarities between phase-only synthesis problems and synthesis problems for reactively loaded antenna arrays are discussed.

REFERENCES

1. Harrington, R. F., "Reactively controlled directive arrays," *IEEE Trans. Antennas Propagat.*, Vol. 26, No. 3, 390–395, 1978.
2. Choni, Y. I., "Synthesis of an antenna according to a given amplitude radiation pattern," *Radio Engineering and Electronic Physics*, Vol. 16, No. 5, 770–778, 1971.
3. Kondrat'yev, A. S., "Method for phase synthesis of antenna arrays with additional requirements on the shape of the directivity pattern taken into account," *Soviet Journal on Communications Technology and Electronics*, Vol. 36, No. 6, 94–102, 1991.

A Novel Retrodirective Array by Removing Band Pass Filter

Shahrokh Jam and Mohsen Kalantari
Shiraz University of Technology, Shiraz, Iran

Abstract— Retrodirective Array (RDA) and Smart Antenna are two methods for achieving a device with beam forming property. RDAs have the characteristic of reflecting an incident wave toward the source direction without any prior information on the source location. Also, RDAs have shown much potential for use in many applications; automatic pointing and tracking systems, microwave tracking beacons, transponder, radar, RFID, solar power satellite (SPS) network and complex communication systems. Usually, a nonlinear component is used in heterodyne Retrodirective Array (RDA), for mixing RF and LO signals. The result of this mixing is the generation of harmonics of RF frequency (f_{RF}). In other side, a BPF couples the LO into the mixer at f_{LO} frequency, and is designed to isolate LO to mixer at f_{RF}. In this paper, BPF is replaced with configuration of two $\lambda/4$ length transmission lines. One of these transmission lines is located between LO and the mixer, and the second transmission line is used as an open stub and connected to the connection of the first transmission line and LO. This configuration of two transmission lines is called L-section. To implement this idea, we used three RDAs. With replacement of BPF with this configuration, no changes occur in diode voltage signal and power harmonics which incident to antenna port in this novel structure. With this change, a RDA is designed with less complexity and is fabricated smaller and lighter.

REFERENCES

1. Guo, Y. C., X. W. Shi, and L. Chen, "Retrodirective array technology," *Progress In Electromagnetics Research B*, Vol. 5, 153–167, 2008.
2. Van Atta, L. C., "Electromagnetic reflector," US Patent No. 2908002, 1959.
3. Pon, C. Y., "Retrodirective array using the heterodyne technique," *IEEE Transaction on Antennas and Propagation*, 176–180, March 1964.
4. Leong, K. M. K. H., R. Y. Miyamoto, and T. Itoh, "Moving forward in retrodirective antenna arrays," *IEEE Potentials*, Vol. 22, 16–21, 2003.
5. Pobanz, C. W. and T. Itoh, "A conformal retrodirective array for radar applications using a heterodyne phased scattering element," *IEEE MTT-S International Microwave Symposium Digest*, Vol. 2, 905–908, May 1995.
6. Diego, A. D., J. A. Garcia, and A. Mediavilla, "A retrodirective array using unbiased subharmonic resistive mixers," *IEEE MTT-S Digest*, 1249–1252, 2004.
7. Miyamoto, R. Y., Y. Qian, and T. Itoh, "Phase conjugator for active retrodirective array applications," *Electronic Letters*, Vol. 6, No. 1, 4–5, 2000.
8. Maas, S. A., *Nonlinear Microwave and RF Circuits*, 2nd Edition, Artech House Publishers, 2003.
9. Maas, S. A., *Microwave Mixer*, Artech House, 1986.

Design of Compact Dual-band Circularly Polarized Microstrip Antenna Based on Metamaterials

Ying Li, Qi Zhu, and Shanjia Xu
Department of EEIS, University of Science and Technology of China, China

Abstract— Metamaterials are artificial structures with specific electromagnetic properties, such as negative permittivity ε and negative permeability μ. Recently, metamaterials have been widely studied due to their great potential application in microwave and millimeter wave circuits and devices. Based on metamaterials, composite right/left-handed transmission line (CRLH-TL) and CRLH-TL based antenna are put forward, in which both positive and negative phase propagation constant β can be employed to realize multiple resonant frequencies and smaller physical size in a certain electrical length. Generally, dual orthogonal feeds are employed to realize circular polarization of CRLH antenna, because the feeding configuration is insensitive to the discontinuity in the metamaterial structures. However, an external hybrid coupler must be employed to generate the required 90° phase difference between the two feeds. In the design of dual-band circular polarization, the bandwidth requirement of hybrid coupler makes the antenna complex.

In this paper, a compact dual-band circularly polarized microstrip antenna composed of multi-layers is proposed based on metamaterial structures. A single feed and proper perturbation on the upper patch are introduced to realize circular polarization. Narrow slots on the lower patch and vias to the ground are introduced to realize the series capacitance and shunt inductance of metamaterial properties. Their locations are symmetric about the center of the lower patch to guarantee circular polarization of the antenna.

The prototype of the proposed antenna is designed and fabricated, as shown in Fig. 1. Simulated and measured results show that the return loss is less than −10 dB at both operating frequencies, namely 2.0686 GHz and 2.3875 GHz. The maximum antenna gain is 4.49 dBi and 4.81 dBi at respective operating frequency. At the broadside direction, the main polarization type is RHCP and the cross polarization is approximately −30 dB. The 3 dB axial ratio beamwith is more than 120° at both operating frequencies, which indicates that the proposed antenna has good performance on circular polarization. Compared to the conventional half-wavelength antenna operating at 2 GHz with the same substrate, a 46.2% patch area reduction can be obtained by the metamaterial-based antenna, and the radar cross section (RCS) depression is about 3 dB in average between $1 \sim 5$ GHz.

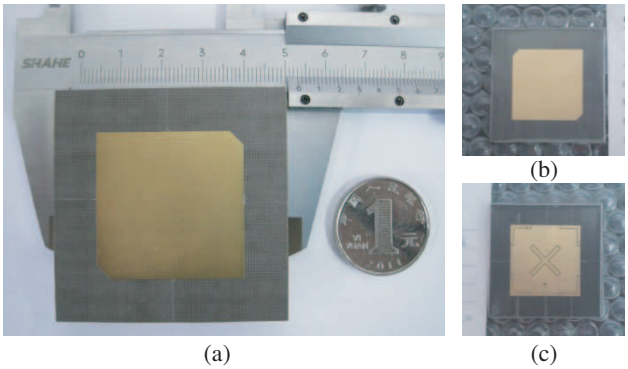

Figure 1: Photographs of the proposed antenna prototype. (a) Antenna dimensions, (b) upper patch, (c) lower patch.

Effect of Human Posture on Antenna Performance of Push-to-talk Transceiver in VHF and UHF Bands

Naoto Kogo and Tetsuomi Ikeda
Science & Technology Research Laboratories, NHK, Japan

Abstract— Push-to-talk (PTT) transceivers are used in the VHF (150–170 MHz) and UHF (440–460 MHz) bands for such organizations as the police, military, and television broadcasting corporations. PTT transceivers for broadcasting services are used for communication between staff for news gathering and television and radio program production. The transmitters for the PTT transceivers are mounted on the outside-broadcasting vans, helicopters, and handheld transceivers. Handheld transceivers are commonly called "walkie-talkies" and have been used for a long time; however, few studies have been reported on the effect of the human body on the radiation patterns and that of specific absorption rate (SAR) in the human body in the VHF and UHF bands.

The output power of handheld transceivers is usually 5 W. During operation, the transceiver is held in close proximity to the face. Hence, antenna performance is strongly affected by the electromagnetic couplings between the antenna and the human body and depends on various conditions such as human posture and operating frequencies. The amount of electromagnetic energy absorbed by the human head when handheld transceivers are used also needs to be evaluated to ensure safe use.

We investigated the effect of the human body on radiation patterns of the antenna for handheld transceivers with a numerical model of the human body. We propose a safe location of the antenna from the viewpoint of SAR. To evaluate the effect of human posture on antenna performance, we used free foam deformation (FFD) on the numerical model to change the posture of the model and calculated the antenna gain and radiation patterns when the antenna is in close proximity to the face. We also calculated the SAR in the human body exposed to electromagnetic waves from the antenna in the VHF and UHF bands.

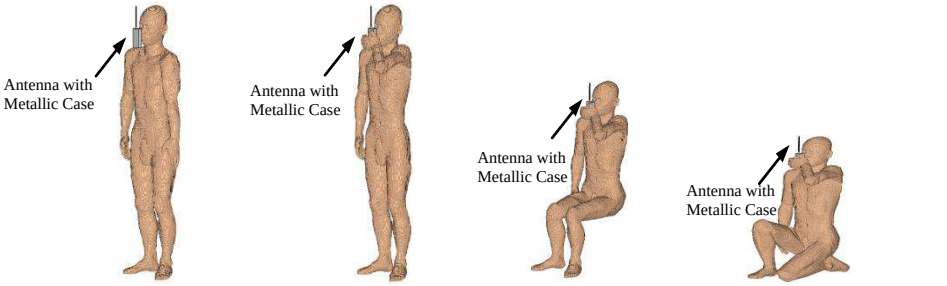

Figure 1: Human postures for calculations.

REFERENCES

1. TR-B21, "Operational guidelines for push-to-talk communication line for broadcasting service," ARIB Technical Report, Ver. 1.1, 2008.
2. Balzano, Q., O. Garay, and F. R. Steel, "Heating of biological tissue in the induction field of VHF portable radio transmitters," *IEEE Trans. on Vehicular Tech.*, Vol. 27, No. 2, 51–56, 1978.
3. Hill, C. and T. Kneisel, "Portable radio antenna performance in the 150, 450, 800 and 900 MHz bands outside and in-vehicle," *IEEE Trans. on Vehicular Tech.*, Vol. 40, No. 4, 750–756, 1991.
4. Koyanagi, Y., H. Kawai, K. Ogawa, H. Yoshimura, and K. Ito, "Estimation of the radiation and SAR characteristics of the NHA at 150 MHz by use of the cylindroid whole body phantom," *IEEE Antennas and Propagation Society Int. Symp.*, Vol. 3, 78–81, 2001.
5. Akimoto, S., S. Kikuchi, K. Saito, M. Takahashi, and K. Ito, "SAR evaluation in human body exposed to EM wave from NHA with metallic case," *IEICE Electronics Express*, Vol. 6, No. 8, 477–482, 2009.

A Novel Compact High-gain Dual-band Circularly Polarized Antenna for Base-station Application

H. Sarbandi Farahani and R. A. Sadeghzadeh
Khajeh Nasir Toosi University of Technology, Tehran, Iran

Abstract— In this paper, a new configuration for dual-band circularly polarized (CP) antenna is presented. The idea is to use two different helical antenna to obtain dual frequency band for return loss less than −10 in which the axial ratio is less than −3 dB about 90 degree around the main direction of the antenna. The proposed antenna is designed at the operating frequency ranges targeting in GSM-band and DCS-band applications. A novel coaxial-to-parallel plate transient technology is effectively used to feed the helical antenna. The proposed antenna has the advantages of compact, low weight and broadband axial ratio.

Introduction: Helical antenna has extensive use in communication and satellite systems duo to their attractive features of high directivity, Circular polarization, high power handling and etc.. In spite of all its advantages, helical antenna has some drawbacks. Its main shortcoming is limitation in both impedance and axial ratio bandwidth. Several methods have already been suggested for increasing bandwidth of helical antennas like using cavity-liked feeding and increasing or decreasing the radius ratio, while each of them has its own drawbacks and benefits such as complex feeding systems, bulky structures and difficult fabrication [1, 2]. By employing coaxial-to-parallel plate transient technology of the antenna and placing one resonant helix into another one, the proposed helical antenna can take the advantages of dual-band, circular polarized, broadband return loss and axial ratio, small size, low weight, simplicity of feeding system and fabrication.

Simulation Results: The proposed antenna is simulated with CST MWS. The results confirm the capability of our idea to use the proposed configuration in achieving broadband, directive and CP antennas. Fig. 1 and Table 1 show schematic view and parameters of the antenna. Fig. 2 depicts S_{11} of the proposed antenna. It can be seen in Fig. 3 that a significant axial ratio bandwidth enhancement is achieved.

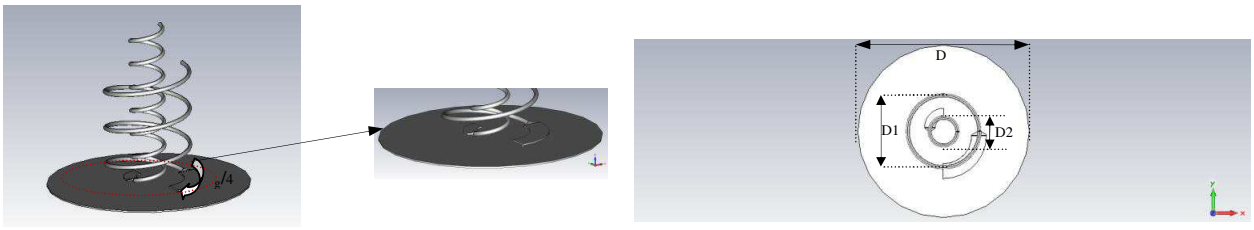

(a) (b)

Figure 1: Schematic view of the antenna: (a) perspective/proposed feeding system, (b) top view.

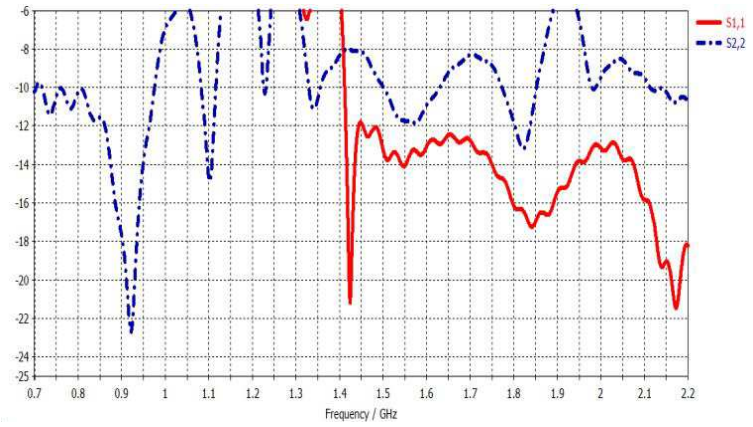

Figure 2: Antenna returns loss (solid: 1800 MHz/dashdotted: 900 MHz ports).

Table 1: Optimized dimensions.

Parameters	D	D_1	D_2
Value (mm)	300	120	46

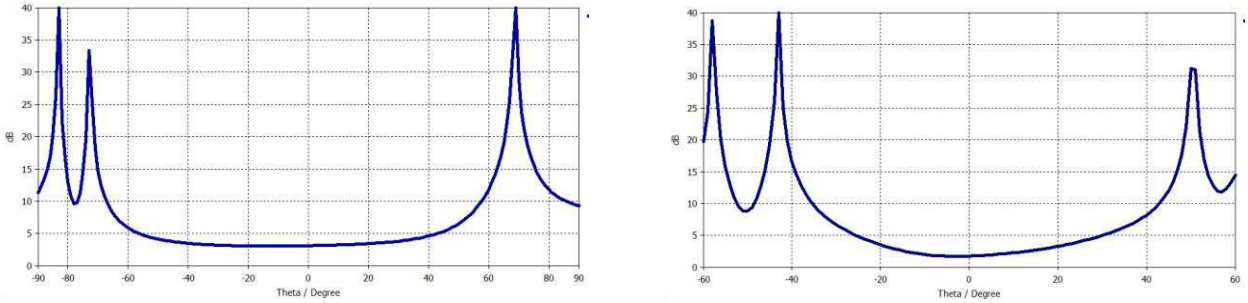

(a) (b)

Figure 3: Axial ratio of the antenna: (a) GSM-900 MHz, (b) DCS-1800 MHz.

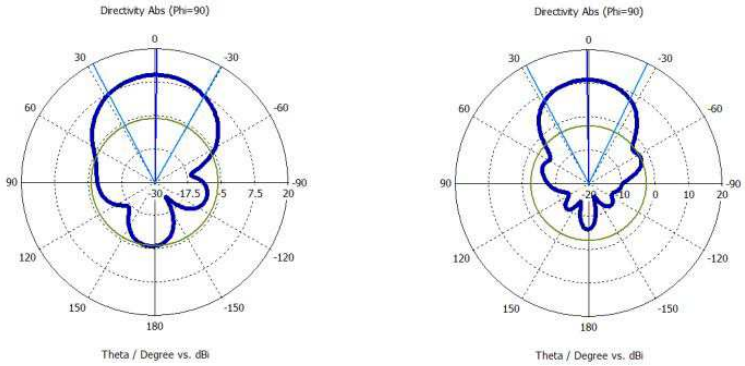

(a) (b)

Figure 4: Radiation pattern of the antenna: (a) GSM-900 MHz, (b) DCS-1800 MHz.

Conclusion: The results show that the bandwidth of $S_{11} \leq -10$ is 52.1% (in GSM) and 42.1% (in DCS). The radiation patterns of both the GSM and DCS bands are given in Fig. 4, showing the directivity of about 10 dBi in each band.

REFERENCES

1. Kraus, J. D., "A 50-ohm input impedance for helical beam antennas," *IEEE Trans. Antennas Propagat.*, Vol. 25, No. 6, 913, Nov. 1977.
2. Balanis, C. A., *Antenna Theory, Analysis and Design*, John Wiley & Sons, Inc., 2005.

Efficient Shape Optimization of Broadband Microstrip Antenna Design by Means of Genetic Algorithm and Finite Element Method

B. El Jaafari, M. A. González, J. García-Jiménez, and Juan Zapata
Universidad Politécnica de Madrid, Ciudad Universitaria s/n, Madrid 28040, Spain

Abstract— Nowadays, microwave engineers require powerful high-frequency system simulator tools that can predict efficiently the circuit device performance. Most of them are based on numerical techniques and many researchers have focused on the development of full-wave simulators. Nevertheless, current interests and advances in microwave technology demand increasingly complex microwave circuit designs which involve a continuous improvement of the techniques used by these system simulators. Actually, design strategies of microwave circuits are generally based on the application of global optimization techniques via numerical analysis methods. In this sense, the use of clever algorithms (not always available) reducing the number of electromagnetic analyses, or its computational cost, is required for an efficient optimization.

The finite element method is a very suitable technique for the analysis of microwave devices because of its versatility and robustness, regardless of complex structures be considered. However, the required CPU time frequently limits the effectiveness of this technique. Therefore, the way to proceed is to make some assumptions in the design strategy to achieve the required performance.

In this work, an efficient optimization procedure based on the Finite Element Method has been incorporated with a suitable genetic optimization algorithm for the design of arbitrarily-shaped microstrip antennas. A two dimensional design procedure is performed benefiting the advantages of a direct domain decomposition technique. For this purpose, the regions of the antenna which do not need to be modified during the CAD process are initially characterized only once from their corresponding matrix transfer function (Generalized Admittance Matrix, GAM) in a predesign step of the optimization procedure. In a second step (design process) the contour shape of the conducting surfaces of the microstrip antennas are iteratively modified in order to achieve a desired electromagnetic performance of radiating element. This step may be performed separately by using mixed conformal and non-conformal meshes. In this way, a new GAM of the radiating device which take into account each microstrip antenna shape is computed in each iteration. The optimization of the shape and feed point location of the microstrip antenna is performed via a genetic optimization algorithm in order to achieve a determined antenna operation around a desired resonance frequency.

Finally, in order to validate the proposed design procedure and to demonstrate its capability, a real design of a broadband microstrip antenna has been accomplished and the final design has been constructed and measured. A good agreement between the results of the theoretical design and measurement has been obtained.

A Method for Determination of the Coordinates of a Low-altitude Target

V. A. Balagurovskii, **A. S. Kondratiev**, **and N. P. Polishchuk**
JSC "ALMAZ_ ANTEY" MSDB", Moscow, Russia

Abstract— Operation of a modular phased array antenna (PAA) of a monopulse radar measuring the objects' angular coordinates under the conditions of multipath is analyzed for the case of tracking the objects located at small elevation angles above the underlying surface, which are traditionally referred to as low-altitude targets (LATs).

A method for measuring the LAT angular coordinates is proposed. The method is based on separation of the PAA aperture into four identical subapertures (partial channels of the radar meter) so that the phase centers of subapertures are located pairwise symmetrically in the horizontal and vertical planes and the entire aperture forms a rhombic structure. Four antennas corresponding to the subapertures of the radar antenna receive the sum of signals reflected from the LAT and from the underlying surface. Signals from the outputs of these antennas are used to form direction-finding characteristics (DFCs) in the azimuth and elevation planes as well as an additional DFC formed as the ratio of the difference of the sum signals from the outputs of the antenna pairs located in the horizontal and vertical planes to the sum output signal of all antennas.

It is assumed that the LAT is located in the far zone of the radar antenna at a distance not exceeding the line-of-sight distance and the underlying surface is assumed to be flat and smooth. Reflection from the underlying surface is assumed to be specular and originating from the point of the mirror reflection of the true LAT, which is located at the depth equal to the LAT height above the surface.

It is shown that, as the maximum of the sum pattern of the radar antenna is directed toward the region of the LAT projection onto the underlying surface, the additional DFC becomes independent of the characteristics of the underlying surface and can be used for determination of the LAT coordinates (theoretically, from the results of a single measurement of complex signals at the outputs of subapertures). In order to reduce the effect of random measurement errors, smoothing with the use of the sliding window technique is proposed.

An algorithm for determination of the LAT angular coordinates and height is described and the results of computer simulation of the operation of the radar meter in the presence random errors of the amplitude-phase distribution over the PAA elements, which distort the signal values at the subaperture outputs, are presented. The results were obtained for the following LAT trajectories: (i) motion at a specified fixed height, (ii) motion with a linear decrease in the LAT height, and (iii) motion along a cyclic (sine-shaped) trajectory with periodic descent and ascent.

Mobile Phone EMC Deterioration Due to Different Realistic Usage Patterns

S. I. Yahya Al-Mously
School of Computer Engineering, Koya University, Koya, Iraq

Abstract— Different realistic usage patterns during a call may extensively deteriorate the electromagnetic compatibility (EMC) of a mobile phone handset that includes holding the mobile phone handset next to head at different positions. This paper presents in details the effects of different realistic usage patterns on the EMC, that represented by the antenna total efficiency (η_{tot}) and the total isotropic sensitivity (**TIS**), of different mobile phone handsets, where a commercial FDTD-based EM solver is used to solve Maxwell's equations. Different semi-realistic mobile phone handset models operating in the GSM900, GSM1800, and UMTS/IMT-2000 bands are simulated to achieve the available commercial models, whereas, a heterogeneous MRI-based CAD model is used to simulate the mobile phone user's head.

The results achieved in this paper showed that certain realistic usage patterns during a call could dramatically affect the mobile phone antenna specifications, i.e., total efficiency, and total isotropic sensitivity, and consequently deteriorate its electromagnetic compatibility. This electromagnetic compatibility deterioration may, firstly; disables the mobile phone handset to function properly in its intended electromagnetic environment, and secondly; push the mobile phone handset to introduce excessive electromagnetic energy to keep a successful electromagnetic connection with the cellular base-station. The later may increase the specific absorption rate (SAR) in the user's head. Thus, the realistic usage pattern should be considered while the mobile phone designed and assembled by the manufacturer. The manufacturer may involve both the human head and handhold dielectric properties in advance while designing and attaching the antenna to PCB of the mobile phone handset and calculating the final electromagnetic specifications.

A Parametric Study and Design of the Balanced Antipodal Vivaldi Antenna (BAVA)

A. R. Bayat and R. Mirzakhani
International Imam Khomeini University (IKIU), Qazvin, Iran

Abstract— Now days the ultra wide band antenna (UWB) is widely used in different applications such as microwave imaging, wireless communications, ground penetrating radars, remote sensing and phased arrays. Since then the Vivaldi antenna is a suitable candidate for this applications. This antenna has 3 main categories: 1- co-planare Vivaldi antenna, 2- antipodal Vivaldi antenna and 3- balanced antipodal Vivaldi antenna (BAVA). the BAVA has very advantage rather than another type as well as better radiation characteristics and wider bandwith and better return loss characteristics. In this paper, a parametric study and design of the balanced antipodal Vivaldi antenna (BAVA) has been undertaken with the aim of using them as elements of wideband phased arrays. The study reported here was performed in the 0.5–20 GHz band by using commercial electromagnetic simulation software Ansoft HFSS. The BAVA is constructed using RT/duroid 6002 (Rogers Corporation.CT.USA) which has relative permittivity of 2.94. The simulation showed that the return loss is better than −10 dB within the band. This antenna is suitable for imaging radar or tissue scanning applications.

Session 2P9
Poster Session 3

Study of Performance Improvement on the Design of Compact SRR Embedded Microstrip Low Pass Filter

S. Suganthi[1], **S. Raghavan**[2], **and D. Kumar**[3]

[1]Shri Angalamman College of Engineering and Technology, Trichy, India
[2]National Institute of Technology, Trichy, India
[3]Periyar Maniammai University, Thanjavur, India

Abstract— This paper proposes a design of a Chebyshev type microstrip low pass filter (LPF) loaded with an array of split ring resonator (SRR) as an additional plane between ground and filter sections for superior performance. Metamaterials (MTM) are the artificial materials engineered to exhibit double negative (DNG) properties that are not found in nature. Such a material gains its properties from its structure rather than its chemical composition. Many researchers have introduced various MTM structures such as spiral resonator, split ring resonator, complementary slip ring resonators, omega, S structures etc., in recent years in that category. The advantage of MTM is its compact size with ability to provide improved performance. Firstly the conventional microstrip LPF was designed at 2 GHz. The novel SRR consisting of new V shaped structures was designed and verified separately for the existence of its μ negative and ε negative properties using a separate coding written in MATLAB for Nicolson-Ross-Wier (NRW) method. Finally the already designed LPF was loaded with the verified metamaterial structure and simulated. For the design and simulation, HFSS 3D simulation tool was used. On comparison it is observed that the SRR loaded low pass filter provides improved performance over the conventional type.

Optimized Design of Microstrip Low Pass Filter with ANN for Performance Improvement

S. Suganthi[1], **S. Raghavan**[2], **and D. Kumar**[3]

[1]Shri Angalamman College of Engineering and Technology, Trichy, India
[2]National Institute of Technology, Trichy, India
[3]Periyar Maniammai University, Thanjavur, India

Abstract— A compact artificial neural network (ANN) trained Chebyshev type microstrip low pass filter has been proposed in this paper. Micrstrip filters always find an important place in many microwave applications. They are most widely preferred for selecting or confining the microwave signals within specified spectral ranges. The challenges on the microwave filters with requirements such as improved performance, miniature size, lighter weight, and lower cost are ever increasing with the emerging applications of wireless communications. The microstrip type filters play vital role at microwave frequencies because of these features. The conventional and ANN trained filters were designed using HFSS simulation tool. The design and analysis of microstrip low pass filter at cut-off frequency of 2 GHz on a FR4 substrate was initially performed using HFSS and then the necessary filter design parameters were trained with an ANN optimization technique using MATLAB. The performance comparison of the conventional filter designed was executed with the ANN model. The best possible design dimensions of the filter could be obtained with the ANN and the reflection (S_{11}) and transmission (S_{21}) properties were obtained in a satisfactory level.

Millimeter-wave Rat-race Balun in a CMOS 65 nm Technology with Slow-wave Transmission Lines and Innovative Topology

F. Burdin, F. Podevin, B. Blampey, N. Corrao, E. Pistono, and P. Ferrari
IMEP-LAHC, University of Grenoble, France

Abstract— The objective of this paper is to show the design and characterization of a millimeter-wave balun in CMOS technology. Baluns are passive components widely spread in the microwave and millimeter-wave frequency ranges. In the context of millimeter-wave frequency bands, the design of circuits based on lumped components becomes more and more complex. Hence, the distributed rat-race coupler is an interesting candidate to be used as a balun. However, its main drawback still results from its large occupying area. Moreover, up to now, quality factors of conventional transmission lines (TLines), like microstrip or CoPlanar Waveguides (CPW), in CMOS technologies, were not acceptable enough to perform low loss integrated millimetre-wave rat-races. In this work an integrated rat-race coupler for balun applications at millimeter wave frequencies based on optimized high quality factor Slow-wave CoPlanar Waveguides (S-CPW) TLines [1, 2] is carried out in the 65-nm CMOS advanced digital technology from STMicroelectronics. Optimized criteria for a CPW phase-inverter and TLines' characteristic impedance [3] enable to minimize insertion loss and surface on the die. The various building blocks such as the S-CPW TLines, the microstrip TLines for the T junction, the CPW phase-inverter and the S-CPW/microstrip transition were designed thanks to a 3D full wave EM software coupled to a circuit simulator. Thanks to the use of the S-CPW TLines, the device occupies a small area of $0.085\,\mathrm{mm}^2$. From 51 GHz till a minimum of 67 GHz, the measured return loss is lower than $-15\,\mathrm{dB}$ at each port. The measured couplings are equal to $-4.2\,\mathrm{dB}$ and $-6.5\,\mathrm{dB}$, respectively, and are really flat over a wide bandwidth. After this first device realization, we have identified some solutions in order to improve the coupling in terms of better balance of the output magnitudes. Finally, in the bandwidth, the phase shift between the output ports is kept very flat, equal to $175.9^\circ \pm 0.4^\circ$, while the isolation between the output ports is better than $-26\,\mathrm{dB}$. In order to highlight the performances of the proposed design, comparisons with recently published works, focused on millimeter-wave rat-race baluns will be presented. Any discrepancy between ideal parameters and this work are truly explained and may be overcome in the future.

REFERENCES

1. Cheung, T. S. D. and J. R. Long, "Shielded passive devices for silicon-based monolithic microwave and millimeter-wave integrated circuits," *IEEE J. Solid-State Circuits*, Vol. 41, No. 5, 1183–1200, May 2006.
2. Franc, A.-L., D. Kaddour, H. Issa, E. Pistono, N. Corrao, J.-M. Fournier, and P. Ferrari, "Slow-wave high performance shielded CPW transmission lines: A lossy model," *IEEE European Microwave Conference*, 185–188, Sep. 2009.
3. Mandal, M. K. and S. Sanyal, "Reduced-length rat-race couplers," *IEEE T-MTT*, Vol. 12, 2593–2598, Dec. 2007.

Parametric Design of Stop Band Pass Filter Based on RF Metamaterials in LTCC Technology

M. Morata[1], I. Gil[2], and R. Fernández-Garcia[2]

[1]Escuela Universitaria Salesiana de Sarriá, Barcelona 08017, Spain
[2]Departament of Electronic Engineering, Universitat Politècnica de Catalunya, Terrassa 08222, Spain

Abstract— This work mainly focuses on the parametric design of RF Metamaterialsstop-band filters developed in Low Temperature Co-fired ceramic (LTCC) technology. The LTCC technology has become an alternative substrate for implementing RF passive components and circuits due to its high performance, reliability and low losses [1]. Therefore, the LTCC technology enables further miniaturization and developmentof compact structures using not only the standard xy planar circuit dimension but also the z-dimension [2]. The aim of this work is to design RF metamaterial filters based on stripline loaded with complementary split rings resonators (CSRRs) with LTCC technology. These implementations allow the design of negative effective permittivity transmission lines providing forbidden propagation frequency bands [3, 4]. Specifically, a parametric analysis of the influence of the xyz-location of the transmission line with regard to the CSRRs is carried out. A6-metal layerLTCC technologyA6Ferro ($\varepsilon_r = 5.96$) materialhas been usedwith metal thickness of 3.7 mil, the layers are interconnected by means of vias. As a reference, Fig. 1 shows the layout of one of the proposed devices.The designedstripline ispatterned on the LTCC layer number 3, whereas the CSRRs (depicted in negative) are etched on layers 2 and 4. In that case, the overall structure is connected to the access ports (layer 1) by means of vias. The CSRRsand the stripline dimensions correspond to $2000 \times 2000\,\mu m^2$ and $10580 \times 200\,\mu m^2$, respectively. Fig. 2 shows the electromagnetic simulation insertion losses of the filter depicted on Fig. 1. As can be observed, a rejection level about 40 dB is achieved at 17.8 GHz and the rest of the band remains matched. This paper presents an alternative procedure to design filters based on stripline RF metameterials in LTCC, as it has been demonstrated.

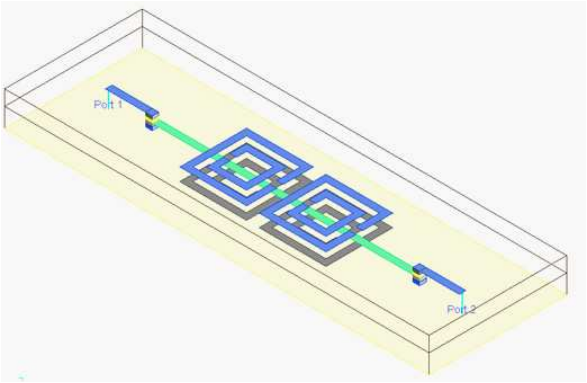

Figure 1: Proposed RF metamaterial stop band filter.

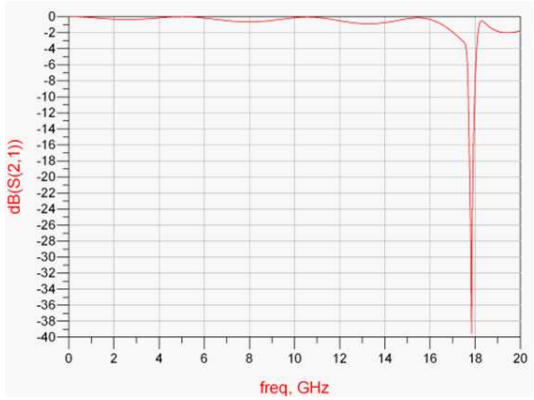

Figure 2: Filter electromagnetic simulated insertion losses.

ACKNOWLEDGMENT

This work has been supported by the Spain-MICINN under Project TEC2010-18550 and AGAUR 2009 SGR-1425.

REFERENCES

1. Li, Y., Y. Liu, H. Zhang, D. Lu, L. Bian, and Z. Yang, "The design and fabrication of rf band pass filter by LTCC technology," *International Conference on Electronic Packaging Technology & High Density, Packaging (ICEPT-HDP 2008)*, 1–4, August 2008.
2. Yang, T., M. Tamura, and T. Itoh, "Super compact low-temperature co-fired ceramic bandpass filters using the hybrid resonator," *IEEE Transaction on Microwave Theory and Techniques*, Vol. 58, No. 11, November 2010.

3. Falcone, F., T. Lopetegi, J. D. Baena, R. Marqués, F. Martín, and M. Sorolla, "Effective negative-ε stopbandmicrostrip linesbased on complementary split ring resonators," *IEEE Microwave Wireless Compon. Lett.*, Vol. 14, 280–282, June 2004.
4. Gil, I., M. Morata, R. Fernández, X. Rottenberg, and W. De Raedt, "Characterization and modelling of switchable stop-band filters based on RF-MEMS and complementary split ring resonators," *Microelectronic Engineering*, Vol. 13, August 2010.

Radiofrequency Interferece Filters Design Based on Complementary Split Rings Resonators

D. Pérez, I. Gil, and R. Fernández-García
Department of Electronic Engineering, Universitat Politècnica de Catalunya
Colom 1, Terrassa 08222, Spain

Abstract— Low frequency analog and digital electronic circuits are susceptible to radiofrequency interference (RFI). This disturbance is produced when the coupled RF signal is rectified by the non-linear behavior of the semiconductors used in the small signal analog input stages of the electronic system [1]. Operational Amplifiers (OpAmps) are found in a wide range of circuits, as input stages, in order to amplify and condition analog signals. These circuits present an AM demodulation effect produced by nonlinearity of internal transistors, generating parasitic signals in the low-frequency range and undesired offset voltage. In this paper, an alternative to the standard EMI filters is presented by combining the conventional printed circuit board layout with complementary split ring resonators (CSRRs), in order to reduce the output offset impact due to RFI. CSRRs are constitutive elements for the synthesis of metamaterials with negative effective permittivity which are mainly excited to the host line by means of electric coupling [2]. An operational amplifier circuit has been designed with a 4-stage CSRR filter, electromagnetically simulated and experimentally tested (Fig. 1(a)). In fact, two prototypes have been implemented, with and without CSRRs in order to compare the filter properties in standard FR4 substrate. The resonance frequency of the CSRRs has been designed in the vicinity of 2.4 GHz in order to prevent susceptibility in the ISM band. Electromagnetic and electrical equivalent model circuit simulations are also provided and compared with experimental results. Measurement data show an effective rejection of the undesired RF demodulation, and therefore a significant reduction concerning output offset voltage impact in terms of RFI amplitude (Fig. 1(b)), with no-extra cost

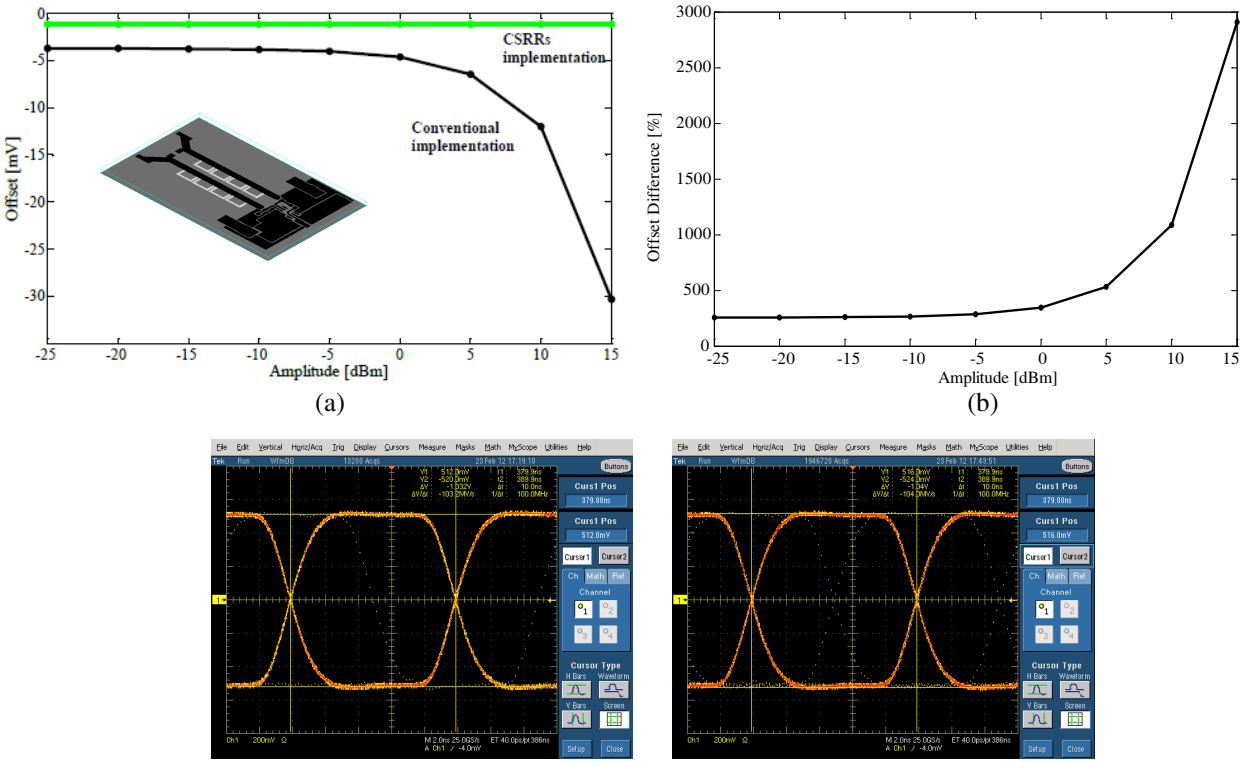

Figure 1: (a) Experimental prototype and offset impact vs RFI amplitude at 2.4 GHz. (b) Offset percentage variation of the conventional structure in comparison with the CSRR implementation at 2.4 GHz. (c) Experimental results of eye-diagram with CSRRs (left figure) and without CSRRs (right figure).

in terms of the device area or manufacturing process. Moreover, it is demonstrated that CSRRs do not affect the signal integrity out of the filter band since no significant impact is measured in the eye diagram concerning the comparison between both fabricated prototypes (Fig. 1(c)).

ACKNOWLEDGMENT

This work has been supported by the Spain-MINECO under Project TEC2010-18550 and AGAUR 2009 SGR 1425.

REFERENCES

1. Gago, J., J. Balcells, D. González, M. Lamich, J. Mon, and A. Santolaria, "EMI susceptibility model of signal conditioning circuits based on operational amplifiers," *IEEE Transactions on Electromagnetic Compatibility*, Vol. 49, 849–859, November 2007.
2. Baena, J. D., J. Bonache, F. Martín, R. Marqués, F. Falcone, T. Lopetegui, M. A. G. Laso, J. García-García, I. Gil, M. Flores Portillo, and M. Sorolla. "Equivalent-circuit models for split-ring resonators and complementary split-ring resonators coupled to planar transmission lines," *IEEE Transactions on Microwave Theory and Techniques*, Vol. 53, 1451–1461, April 2005.

Occupational Exposure to Extremely Low Frequency Electric Fields in Office Work

R. Pääkkönen[1], **H. Tarao**[2, 3], **F. Gobba**[4], **and L. Korpinen**[2]

[1]Finnish Institute of Occupational Health, Tampere, Finland
[2]Environmental Health, Tampere University of Technology, Finland
[3]Department of Electrical and Computer Engineering
Kagawa National College of Technology, Japan
[4]Department of Public Health Sciences, University of Modena and Reggio Emilia, Italy

Abstract— Previous studies have presented measurement results of exposure to extremely low frequency (ELF) magnetic fields in different work environments e.g., the office work environment. Electric fields (EF) have been studied at substations, where there are high voltages, but given less coverage in other locations. It is however important to monitor EF exposure at work places where voltages are low, in order to be able to gain some understanding of the disturbances or other minor effects resulting from EFs. The objective of this work was to investigate occupational exposure to ELF EF at office work. Measurements were taken using Holaday HI3604 (accuracy ±10%) and Wandel&Golterman EFA-3 (accuracy ±5%) meters. The background electric fields ($n = 4$) were 2–25 V/m. Different devices were sampled: (1) spot lamps 400 V/m and 1000 V/m (from surface) and 30 V/m (distance 50 cm), (2) coffee maker 10–20 V/m (from surface), (3) the transformers of a computer 100–200 V/m (from surface), (4) the alternator of a cellular phone 40–60 V/m, (5) UPS (uninterruptible power supply) 300 V/m (from surface) and 5 V/m (distance 1 m) and (6) a PC table speaker 250 V/m (from surface). The highest electric field measured was 1000 V/m. The measured values obtained are clearly below the action values of 10 000 V/m and do not exceed the newly proposed EC directive (2011/0152) for electric field exposure. However the amount of sampling was limited so it is important to conduct further measurements before strong conclusions can be drawn.

Analysis, Design and Implementation of a Useful Broadband Coaxial-to-microstrip Transition

Gholamreza Askari, Hoda Fadakar, and Hamid Mirmohammad-Sadeghi
Information and Communication Technology Institute
Isfahan University of Technology, Isfahan 84156, Iran

Abstract— A coaxial-to-microstrip transition is required in the most planner structures to extract accurate measurement results. The coaxial-to-microstrip transition must support only a single propagating mode over a broad frequency band for proper de-embedding of the transition from the measurement results [1]. Furthermore it is important to have simplex, low-cost and wideband coaxial-to-microstrip transition.There have been several studies on the end lunch microstrip to coaxial transition [2–5]. However in these transitions, the impedance is match only in the narrow frequency band [2]. In addition Eisenhart's transition that is discussed in [3], exhibits optimum performance but complicated structure, high cost and large size make it undesirable. Besides in [4, 5] only vertical mounted configuration of coaxial-to-microstrip transition are considered.

In this paper, two useful, simplex and broadband coaxial-to-microstrip transitions using CB-CPW, simple pre-transition, are designed and implemented. These transitions are designed by the use of conductor back coplanar waveguide (CB-CPW). The CPW and its various configurations such as CB-CPW have several attractive features in comparison with microstrip line. For example these lines have low wave propagation dispersion up to very high frequency [6]. There have been intensive studies on transition from CPW to other planner transmission lines [7–12]. In this work, CB-CPW, pre-transition section is used to improve the matching of electromagnetic field distribution at the transition. The design of signal and ground current paths through a transition are also critical and these paths must often be continuous and as near as possible to suppress radiation [2]. In these two transitions the effects of the field and impedance matching on the bandwidth are discussed. Moreover the influence of the fabrication and assembly error such as slightly gap, solder paste in connections at input and output, misalignment between microstrip and center of SMA connector, excitation of higher order modes of SMA in connections and uncertainty of measurement instruments are considered. The simulation results using CST and HFSS software indicate that the bandwidth is increased to maximum operating frequency of SMA connector. The experimental results are in good agreement with simulation results. Insertion loss less than 2.5 dB and return loss better than −10 dB are obtained from 2 to 18 GHz. The material used in the design is Rogers RT Duroid 6010 with $\varepsilon_r = 10.2$ and $\tan\delta = 0.0023$. The metal thickness is 0.035 mm and the substrate thickness is 0.635 mm. The SMA connector used in the design is 23_SMA-50-0-52/199_N from Huber-Suhner Company. This connector works at frequencies up to 18 GHz [13].

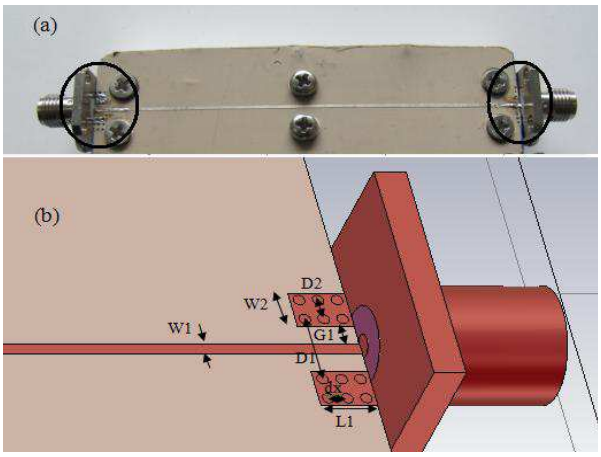

Figure 1: Second proposed transition (a) Photo of back to back configuration, (b) top view of simulation structure.

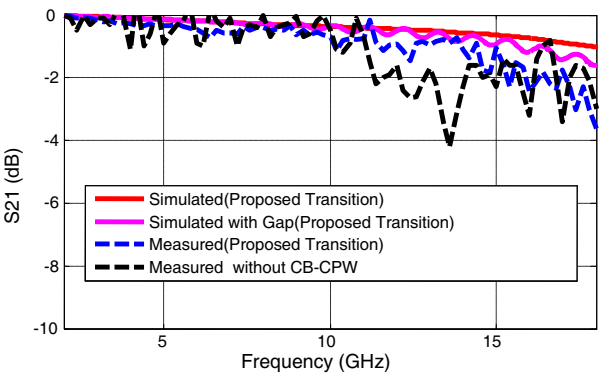

Figure 2: S-parameters of the second proposed transition and the transition without CB-CPW.

The structure of final proposed transition is shown in Fig. 1. In this transition center conductor of SMA is firmly cut from the butt to achieve impedance matching. This structure is very simplex and has good results compared with previous transition.

The simulation and measurement results verified that the fabricated back-to-back coaxial-to-microstrip transition can achieve a 3 dB bandwidth of 18 GHz and return loss better than −10 dB. Other transitions to improve bandwidth and reduce resonances in frequency response are under investigation and will be presented in future works.

REFERENCES

1. Zhou, Z. and K. L. Melde, "Development of a broadband coplanar waveguide-to-microstrip transition with vias," *IEEE Trans. Adv. Package.*, Vol. 31, No. 4, 861–872, Nov. 2008.
2. Holzman, E., *Essentials of RF and Microwave Grounding*, Artech House, Norwood, MA, 2006.
3. Gupta, K. C., R. Garg, I. Bahl, and P. Bhartia, *Microstrip Lines and Slotlines*, Artech House, Norwell, MA, 1996.
4. Agarwal, K. and R. Harlan, "Coax-to-Microstrip transition," US Patent 5552753, Sep. 1996.
5. Quan, C., S. W. Drost, M. Y. Hashimoto, and R. M. Jorgenson, "Microstrip to coax vertical launcher using fuzz button and solderless interconnects," US Patent 5886590, Mar. 1999.
6. Simons, R. N., *Coplanar Waveguide Circuits, Components, and Systems*, Wiley, New York, 2001.
7. Hung, C. F., A. S. Liu, C. H. Chien, C. L. Wang, and R. B. Wu, "Bandwidth enhancement on waveguide transition to conductor backed CPW with high dielectric constant substrate," *IEEE Microw. Wireless Components. Lett.*, Vol. 15, No. 2, 128–130, Feb. 2005.
8. Chiu, T. and Y. Shen, "A broadband transition between microstrip and coplanar stripline," *IEEE Microw. Wireless Components. Lett.*, Vol. 13, No. 2, 66–68, Feb. 2003.
9. Ma, K. P., Y. Qian, and T. Itoh, "Analysis and applications of a new CPW-Slotline transition," *IEEE Trans. Microw. Theory Tech.*, Vol. 47, No. 4, 426–432, Apr. 1999.
10. Nedil, M., T. A. Denidni, and A. Djaiz, "Ultra-wideband microstrip to CB-CPW transition applied to broadband filter," *IEEE Electronics Lett.*, Vol. 43, No. 8, Apr. 2007.
11. Mao, S. G., C. T. Hwang, R. B. Wu, and C. H. Chen, "Analysis of coplanar waveguide-to-coplanar stripline transitions," *IEEE Trans. Microw. Theory Tech.*, Vol. 48, No. 1, 23–29, Jan. 2000.
12. Kamei, T., Y. Utsumi, N. Q. Dinh, and N. Thanh, "Wide-Band coaxial-to-coplanar transition," *IEICE Trans. Electron.*, Vol. E90-C, No. 10, 2030–2036, Oct. 2007.
13. Data sheet [On line], Avalible: http://www.hubersuhner.co.th.

Radar Absorbing Structure with Periodic Pattern Surface for Wind Blade

J. Kim
Korea Institute of Materials Science, Composites Research Center, Korea

Abstract— Wind turbine blade is one of the largest composite structures in the world. For the 3 MW wind turbine system which is very popular grade in these days, the blade is over 10 ton in weight and over 40 m in length. Most of rotors of wind turbines have 3 blades and the size of rotor disks is larger than Airbus A380 wing span of 80 m. The rotating speed of the rotors of 3 MW wind turbines is about $15 \sim 16$ RPM. Even though the angular velocity seems to be not so high, the rotor tip speed is over 250 km/h which is equivalent to the take-off and/or landing speeds of a jumbo airplane. Recently, the radar interference is a hot issue for the construction of the wind farms due to the fact that traditional turbine blades cause interference to radar screens. This paper presents radar absorbing structure with periodic pattern surface for wind blades. The radar absorbing structure is composed of the periodic pattern surface and dielectric substrate grounded with PEC. The dielectric substrate is the glass fibre-reinforced polymer composite for wind blade structure. The surface conductivity of the pattern is controlled with the thickness of the pattern made with the electrical conductive ink. The periodic pattern is optimally designed for X-band band by using CST MICROWAVE STUDIO. The optimal dimensions and surface conductivity of the pattern are obtained for various optimization targets. The target includes the thickness variation of the composite substrate determined by the internal configuration of the wind blade structure.

Metastructure to Achieving of Voltage Tunable Magnetic Resonance in a Single Longitudinal Cut-wire

Galina Kraftmakher, **Valery Butylkin**, **and Yury Kazantsev**
Kotelnikov Institute of Radioengineering & Electronics RAS, Fryazino Branch, Russia

Abstract— In this presentation it is observed that varactor loaded nonmagnetic single split longitudinal cut-wire arranged in necessary planar metastructure can show a voltage tunable magnetic resonance response. Previously like metastructure has been investigated without varactor in waveguides and free space [1, 2]. It has been shown by experiment at microwaves that metastructure containing cut-wire grating and longitudinal cut-wire of resonant length can provide strong magnetic resonant response of a single nonmagnetic cut-wire in dependence on configuration and sizes t, s, l_p, l_m. Metastructure is oriented along the direction of wave propagation and cut-wires of grating are parallel to the electric field of a plane electromagnetic wave. It has been shown a practical way to the excitation of a magnetic resonance in nonmagnetic longitudinal line cut-wire which is arranged perpendicularly to the electric field of incident electromagnetic wave near a grating of cut-wires. It is suggested a concept of magnetic response based on antiparallel resonant currents excited by magnetic field of surface polaritons in many spatial *LC-circuits* created from cut-wire pairs of a grating and section of longitudinal cut-wire. Three separately observed resonant effects connected with grating, *LC-circuits* and with longitudinal cut-wire have been identified applying measurements in waveguides, cutoff waveguides and free space. The first resonance is due to parallel currents induction in grating's wires l_p, the second resonance effect is due to excitation of antiparallel currents in *LC-circuits* and the third resonance is due to contribute of total currents from *LC-circuits* along longitudinal cut-wire l_m. It is special interest to study a metastructure using varactor diodes. In [3] it has been demonstrated that the resonant frequency of split ring resonators (SRRs) can be tuned using varactor diodes. The resulting particle has been called a varactor-loaded split ring resonator (VLSRR). In this paper we use varactor diodes to tune resonance response related to cut-wires in metastructures. With varactor one can also match the resonance minima of transmission T to concrete resonant elements with certainty what is important for multi-resonance system.

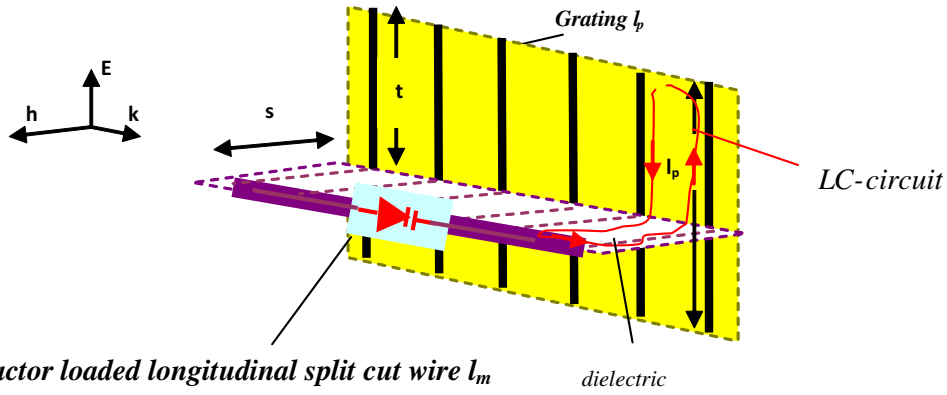

ACKNOWLEDGMENT

This study was supported by the RFBR, projects Nos. 10-08-00018 and 11-02-90403.

REFERENCES

1. Butylkin, V. S. and G. A. Kraftmakher, "Magnetic type resonance in nonmagnetic line wire excited by surface plasmons in microwave range," *Tech. Phys. Letters*, Vol. 37, No. 4, 399–312, 2011; *Proceedings of Metamaterials'2010*, 450–452, Karlsruhe, Germany, 2010.
2. Kraftmakher, G. and V. Butylkin, "Cut-wires grating — Single longitudinal wire planar metastructure to achieve microwave magnetic resonance in a single wire," *Proc. of AES'2012, Paris*, 2012.
3. Gil, I., J. Garcia-Garcia, J. Bonache, F. Martin, M. Sorolla, and R. Marques, "Varactor-loaded splt ring resonators for tunable notch filters at microwave frequencies," *Electronics Letters,* Vol. 40, No. 21, 2004.

Radar Coverage Predictions in Coastal Areas — Case Studies Issued from PREDEM Campaigns Analysis

J. Claverie[1] and Y. Hurtaud[2]

[1]CREC St-Cyr/LESTP & IETR, Guer CEDEX 56381, France
[2]DGA MI/CGN2/SDO, Rennes Armées 35998, France

Abstract— Two measurement campaigns, associated with the French PREDEM project, took place at the end of June 2005 and in February 2006 near the French Mediterranean coast. The experimental setup associated radar measurements (S band and C band) over 2 canonical targets (a surface one and an airborne one), meteorological and oceanographic buoys and radiosondes launching at 3 different locations along the propagation path. AROME, a Meteo-France mesoscale model, was also used in analyze mode to generate refractivity profiles, 2D fields of duct heights and PTU 3D raw data. In addition, the evaporation duct heights were computed with PIRAM, the French bulk model.

Our presentation will concern data collected during the summer and winter campaigns. During the winter campaign, the computed evaporation duct heights were less than 10 m. Above the evaporation duct the refractivity profiles were almost standard. Nevertheless, the low duct height has a non negligible effect on radar coverage. Direct radar measurements and predicted coverage from modeled or measured meteorological profiles are in very good agreement.

The data obtained during the 29th of June 2005 are also very interesting. The meteorological data give evidence of strong surface and elevated ducts all along the day. The computed evaporation duct heights were varying in the interval [5; 25 m]. The radiosondes data also illustrate the horizontal variability of the refractivity profiles. Taking into account all the available meteorological information, we will compare the predicted radar performances with the measured ones. A particular emphasis will be put on the interest of using mesoscale models for radar propagation purposes.

We will also present our latest results concerning the blending of refractivity profiles between the surface layer and the convective layer, the critical point still being the refractivity gradient continuity. As a matter of fact, non continuous refractivity gradients could generate artificial propagation effects.

A Full-band High Linearity CMOS T/R Switch for UWB Systems

Ro-Min Weng, **Yun-Chih Lu**, **and Huo-Ying Chang**
Department of Electrical Engineering, National Dong Hwa University, Hualien, Taiwan

Abstract— A transmitter/receiver (T/R) Switch in radio frequency front-end for 3.1∼10.6 GHz ultra-wideband Systems is presented. The design focuses on the techniques to increase both power handling capability and isolation using deep n-well and floating bulk technology. The proposed switch achieves P1dB of 9 dBm and IIP3 of 20 dBm in transmitting (TX) mode which represents higher linearity than other CMOS T/R switches. The proposed T/R switch provides the TX and receiving (RX) paths with different switching topologies. Different signal paths can minimize the power leakage into the RX/TX path during TX/RX mode selection so as to improve the linearity. The proposed T/R switch uses a 1.8 V digital control signal for TX/RX mode selection. The simulated insertion loss is less than 2.3 dB and return loss is less than −10 dB during 3.1∼10.6 GHz full-band operation.

A Novel Defecect Microstrip Structure (DMS) Coupled Line Band Pass Filter in C Band

S. R. Hosseini, **R. Sarraf Shirazi**, **and Gh. Moradi**
Wave Propagation & Microwave Measurement Research Lab., Department of Electrical Engineering
Amirkabir University of Technology, 424 Hafez Avenue, Tehran 15914, Iran

Abstract— Bandpass filters are one of most usable structures in microwave engineering. Band pass filters have found numerous applications in approximately all aspects of microwave engineering and communication technology.

Satellite communications are one of important and specific way for sending and receiving data. Ku frequency band contains frequency range from 12 GHz to 18 GHz which is suitable for satellite communications.

There are various techniques for microwave filters implementation.

Since Planar filter structures are shapeable, light, easily fabrication and etc. can be appropriate ones for satellite communications.

New bandpass filter which designed in this paper is defected microstrip structure (DMS) filter.

Novel coupled line band pass filter using defected microstrop structure (DMS) was designed which has nearly 10% relative bandwidth in KU frequency band. A circuit model based on coupled line concept was developed to validate full wave simulation behavior.

Optimized Rat-race Coupler with Different Shapes of Defected Ground Structure

M. Shirazi, R. Sarraf Shirazi, and Gh. R. Moradi
School of Electrical Engineering, Amirkabir University of Technology, Iran

Abstract— In this paper, a new type of rat-race ring coupler with different shapes of DGS is presented. Three shapes of defect on ground have been investigated and after optimization with Genetic Algorithm (GA) the best one is presented. Benefits and drawbacks of each type will be surveyed. Changing the shapes and dimensions of the defect on ground will lead to better performance of a rat-race coupler such as less return loss, smaller size or wider bandwidth than conventional rat-race coupler with DGS. All designs are validated by using the full-wave electromagnetic simulator. At first a circular DGS have been designed and investigated. After optimization we can see the advantages of this type to the conventional one. The next type is triangular DGS; the optimum case of this type is presented. Based on the triangular DGS results and distribution of electromagnetic current on the ground plane, a fractal DGS have been designed and simulated. After optimization with Genetic Algorithm the optimum shape and dimension of the defect on ground plane is proposed. Simulations are carried out using HFSS 13, a commercial electromagnetic simulator based on a finite element method.

New Wilkinson Power Dividers Using Dual and T-shaped Transmission Lines

Sung-Yen Juang, Li-Chi Dai, Yu-Ta Chen, Wen-Chian Lai, and Pu-Hua Deng
Department of Electrical Engineering, National University of Kaohsiung, Taiwan

Abstract— The conventional single uniform transmission line can be equivalent to the dual and the T-shaped transmission lines, which have been proposed in the previous works. This paper proposes two new compact Wilkinson power dividers. The first power divider uses dual and T-shaped transmission lines to replace the two quarter-wavelength ($\lambda/4$) transmission lines in the conventional equal-split Wilkinson power divider. The second divider utilizes new dual transmission line section, which is composed of one single uniform and one T-shaped transmission lines, to replace each $\lambda/4$ transmission line in the conventional equal-split Wilkinson power divider. The result of each proposed new Wilkinson power divider can demonstrate a compact size and similar frequency responses as the conventional Wilkinson power divider around the operating band.

Design of Bandpass Filter with Transmission Zeros Using Zeroth-order Resonator and U-shaped Resonator

X.-G. Huang, Q.-Y. Feng, Q.-Y. Xiang, and D.-H. Jia
School of Information Science and Technology
Southwest Jiaotong University, Chengdu, Sichuan 610031, China

Abstract— In this article, a novel bandpass filter using symmetrical composite right/left-handed transmission lines (CRLH TL) ZOR and U-shaped resonator with three transmission zeros (TZs) is proposed. The method starts from the dispersion diagram of CRLH TL and pure right handed (PRH) TL and is based on the opposite phase response between the zeroth-order resonance mode of CRLH TL and the positive first order resonance mode of PRH TL. By adding the signal of ZOR into the PRH TL resonator signal path, TZs can be obtained. However, it is hard to get two TZs by the method of combine ZOR with PRH TL resonator since the phase shift are not opposite at every frequency around resonance frequency for the reality two resonators. Then, two L-shaped coupling arms are introduced to improve the selectivity. To validate the proposed method, the bandpass filter (centre frequency 2.20 GHz) composed of symmetrical CRLH TL ZOR and U-shaped resonator (half-wavelength open-ended resonator) is presented, providing a pair of TZs at 2.07 (provided by U-shaped resonant circuit) and 2.25 GHz, thus featuring steep roll-off at both edges of the passband.

Substrate Integrated Waveguide (SIW) Filters and Its Application to Switchable Filters

Q.-Y. Xiang, Q.-Y. Feng, X.-G. Huang, and D.-H. Jia
School of Information Science and Technology
Southwest Jiaotong University, Chengdu, Sichuan 610031, China

Abstract— In this paper, novel substrated integrated waveguide (SIW) and half mode substrate integrated waveguide (HMSIW) structures for bandpass filter and switchable bandpass filter applications are proposed. The SIW resonators are realized by etching the electrical coupled complementary resonators on the surface of waveguide, and the resonances are generated below the characteristic waveguide cut-off frequency. Lumped equivalent circuit analysis models are developed. The half mode configuration of the proposed SIW bandpass filter is open structure, and this kind of HMSIW filter is easy to load with the control elements. By using a floating capacitor with mechanical switches loaded on the HMSIW resonators, a 1-bit HMSIW switchable bandpass filter is demonstrated. The simulated and measured results for the filter are provided. The prototype with compact core size of 16 mm × 12 mm was designed and fabricated so as to validate the new structure. The measured central frequency is 2.1 GHz and 2.6 GHz, the fractional bandwidth is 7.3% and 7.6%, and the insertion loss is 2.5 dB and 1.5 dB, at switch-on state and switch-off state, respectively.

Four-port Circulator Utilizing Longitudinally Magnetized Cylindrical Ferrite Coupled Line Junction

A. Kusiek, W. Marynowski, and J. Mazur
Gdansk University of Technology, Poland

Abstract— Recently, the longitudinally magnetized ferrite coupled strip- or slotlines are being developed and employed to realize integrated nonreciprocal devices [1–3]. Significant interest in these devices results from their advantages which are weak biasing magnetic field and wide operation bandwidth. The disadvantage are high insertion losses which disqualify the use of these devices in commercial applications. Hence, the recent research are focused on reduction of insertion losses in such devices.

The reduction of insertion losses and the length of ferrite section can be obtained in cylindrical coupled stripline junctions [4]. Due to the similar geometry to the circular waveguide with coaxially located ferrite rod such structure allows one to obtain close to optimal Faraday rotation effect [5]. Moreover, in such configuration stronger gyromagnetic coupling occurs which is a result of high magnetic field concentration in the ferrite medium. These make possible to design shorter ferrite junctions ensuring lower insertion losses and better performance, e.g., better isolation and wider operation bandwidth in comparison to planar ones [1–3].

In this paper, we apply the cylindrical ferrite coupled line junction (CFCL) to a realization of integrated four-port circulator. The proposed structure is realized as a cascade connection of planar four-port magic-T junction [6], cylindrical ferrite coupled line section and transformer from multilayered coupled slotlines to uncoupled microstrip lines. To design CFCL junction with $\pi/4$ Faraday rotation angle the hybrid technique combining finite-difference frequency-domain technique, method of moments and mode matching technique (FDFD/MoM/MM) is utilized. In this method at first the propagation coefficients and field distributions of two fundamental modes in dielectric and ferrite coupled lines composing CFCL junction are determined using FDFD/MoM. Then, by enforcing the continuity of tangential field components at the ferrite-dielectric interfaces of the junction and utilizing MM technique the scattering parameters of four-port CFCL junction are obtained.

Utilizing commercial software HFSS we validate results of FDFD/MoM/MM and design planar reciprocal circuits of the structure. The overall scattering parameters of the circulator are obtained by cascading the scattering parameters of the planar circuits and CFCL junction. The simulated results are verified experimentally.

ACKNOWLEDGMENT

This work was supported in part by Polish Ministry of Science and Higher Education from sources for science in the years 2012-2013 under Contract No. 0282/IP3/2011/71 and under COST Action IC0803, decision No. 618/N-COST/09/2010/0.

REFERENCES

1. Queck, C. K. and L. E. Davis, "Broad-band three-port and four-port stripline ferrite coupled line circulators," *IEEE Transactions on Microwave Theory and Techniques*, Vol. 52, No. 2, 625–632, Feb. 2004.
2. Cao, M. and R. Pietig, "Ferrite coupled-line circulator with reduced length," *IEEE Transactions on Microwave Theory and Techniques*, Vol. 53, No. 8, 2572–2579, Aug. 2005.
3. Marynowski, W. and J. Mazur, "Study of nonreciprocal devices using three-strip ferrite coupled line," *Progress In Electromagnetics Research*, Vol. 118, 487–504, 2011.
4. Kusiek, A., W. Marynowski, and J. Mazur, "Investigations of cylindrical ferrite coupled line junction using hybrid technique," *Progress In Electromagnetics Research*, Vol. 120, 143–164, 2011.
5. Mazur, J. and M. Mrozowski, "On the mode coupling in longitudinally magnetized waveguiding structures," *IEEE Transactions on Microwave Theory and Techniques*, Vol. 37, No. 1, 159–164, Jan. 1989.
6. Davidovitz, M., "A compact planar magic-T junction with aperture-coupled difference port," *IEEE Microwave and Guided Wave Letters*, Vol. 7, No. 8, 217–218, Aug. 1997.

A Wide-stopband Bandpass Filter Using Wide Gap CPW

Jin-Sup Kim and Se-Hwan Choi
Wireless Communication Research Center, Korea Electronics Technology Institute, R. O. Korea

Abstract— A compact bandpass filter using a very short capacitively-coupled resonator exhibits wide stopband characteristics. It is based on two $< \lambda/16$ short-circuited resonators built on a coplanar waveguide (CPW) having unusually wide gap. The filter's input/output ports are connected to the resonator through microstrip-to-CPW broadside-coupled transition structure. The proposed filter is simple and compact without employing any additional structural elements that are often used in conventional approaches. It is found that the stopband characteristic can be significantly extended only by properly setting the coupling capacitance of the broadside coupling structure, the length of the resonator, and the CPW gap. A second-order bandpass filter with the center frequency (f_o) of 2.45 GHz and the 3-dB bandwidth of 10.6% is fabricated on a liquid crystal polymer substrate, demonstrating dramatically extended stopband suppression of 30 dB up to $9.8f_o$.

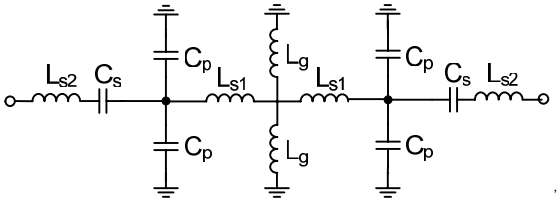

Figure 1: Equivalent circuit of the proposed bandpass filter ($L_{s1} = 1.369$ nH, $L_{s2} = 0.073$ nH, $L_g = 0.316$ nH, $C_s = 0.76$ pF, $C_p = 1.128$ pF).

Electromagnetic Properties of Natural and Synthetic Ilmenite Materials in Millimeter Waveband

Yu. I. Ryabkov[1], **A. B. Rinkevich**[2], **and D. V. Perov**[2]

[1]Institute of Chemistry Ural Branch of Russian Academy of Sciences, Syktyvkar, Russia
[2]Institute of Metal Physics Ural Branch of Russian Academy of Sciences, Ekaterinburg, Russia

Abstract— At present materials with chosen wave resistance are widely adopted in microwave technics. Such materials are necessary for electromagnetic shielding, matching of impedances in microwave circuits, for optical and infrared windows and for thermal chambers. For the task of electromagnetic shielding it is necessary at first to secure minimal reflection in the fixed frequency range. In the second place development of shielding enclosures is required for protection of devices from the action of outer electromagnetic interferences.

Investigation of physical properties of ilmenite compounds gives good impact to solve the tasks mentioned. The methods have been developed of synthesis of ilmenite compounds and their phases and optimization of the synthesis procedure is achieved.

Measurements of electromagnetic properties of ilmenites in the frequency range from 12 to 38 GHz have been carried out by using of non-resonant microwave methods. Electro-physical and other properties of ilmenites are measured which are valuable for interaction between microwave irradiation with medium. The share of absorbed power is calculated from the frequency dependences of transmission and reflection coefficients and besides, the complex dielectric permittivity was reconstructed. Compounds with low reflection coefficient in millimeter waveband were obtained.

Peculiarity of composition and structure are specified influencing the microwave and electrical properties and therefore on the methods of chemical synthesis of compounds and their phases with desired radio-physical properties.

Peculiarity of composition and structure are specified influencing the microwave and electrical properties and therefore on the methods of chemical synthesis of compounds and their phases with desired radio-physical properties.

ACKNOWLEDGMENT

This work was supported by the grant 12-M-23-2052 of the Ural Branch of the Russian Academy of Sciences.

High Power Autonomous Pulse-train UWB Source

V. E. Fortov, Yu. I. Isaenkov, V. M. Mikhailov, E. V. Nesterov, V. E. Ostashev, Yu. V. Semenov, and V. A. Stroganov
Joint Institute for High Temperatures of RAS (JIHT RAS), Russia

Abstract— Design and characteristics of powerful nanosecond UWB pulse oscillator intended for study of particular electromagnetic compatibility problems are given.

For excitation of the oscillator we use high voltage drive-pulse generator based on resonance transformer. Voltage output of the generator is approximately $U_G \approx 550\,\mathrm{kV}$. Power supply is a set of nickel metal hydride rechargeable batteries.

Double dipole-type antenna with length of dipole equal 0.35 m is triggered by high-pressure spark-gap switch. Oscillator as a whole is combined into monoblock of 50 liters in volume and 60 kg in weight approximately.

Single pulse of radiation is characterized by the following parameters: field range product (FRP) equals to 320 kV (with reflector 650 kV approx.), effective radiated power (ERP) is approximately 4 GW (12 GW). Short-time amplitude instability of generated pulse is less than 10%. For average pulse-repetition frequency equal 400 Hz the power of primary supply is 4 kW. Energy spectrum of radiation is spread mainly over two ranges: the first range is $0.1 \ldots 0.4\,\mathrm{GHz}$ and the second range is $0.7 \ldots 1.0\,\mathrm{GHz}$.

Tested oscillator demonstrated high performance reliability, stability of radiation parameters and good usability.

Modelization of the Coupling of Mini-resonators for Microwaves Photonics Applications

Patrice Salzenstein[1] and Taron Makaryan[2]

[1]Franche Comté Electronique Thermique Optique Sciences et Technologies (FEMTO-ST)
Centre National de la Recherche Scientifique (CNRS), Besançon, France
[2]Yerevan State University, Yerevan, Armenia

Abstract— Optoelectronic oscillators (OEO) are microwave generators based on optical energy storage instead of high finesse radio-frequency resonators [1]. In our case we investigate in mini-resonator based OEO to increase the compacity of oscillators and achieve stable delivered microwves signals. The resonator can be in MgF_2 [2], CaF2 or Fused silica [3]. Optical fiber coupled to a resonator consists in a mini disc with whispering gallery modes at its circumference. Resonator behaves as a sphere because energy is trapped in whispering-gallery-modes in the equatorial region. A critical point is the critical coupling in order to take part of the high quality factor of the resonator [4]. The coupling is a critical step. That's why it was necessary to develop simulations in order to help the better coupling of the resonator to the optical fiber taper. Semi analytical method allows transforming the problem to numerical solution of two simple algebraic equations for arbitrary values of parameters. It is especially easy to get the obvious graphical solution. The calculated profile presents a slightly good agreement with the experimental results [5]. Results of these modelization and comparison with experimental results are to be presented at the conference.

REFERENCES

1. Volyanskiy, K., P. Salzenstein, H. Tavernier, M. Pogurmirskiy, Y. K. Chembo, and L. Larger, "Compact optoelectronic microwave oscillators using ultra-high Q whispering gallery mode disk-resonators and phase modulation," *Optics Express*, Vol. 18, No. 21, 22358–22363, 2010.
2. Tavernier, H., P. Salzenstein, K. Volyanskiy, Y. K. Chembo, and L. Larger, "Magnesium fluoride whispering gallery mode disk-resonators for microwave photonics applications," *IEEE Photonics Technology Letters*, Vol. 22, No. 22, 1629–1631, 2010.
3. Salzenstein, P., K. Volyanskiy, H. Tavernier, E. Rubiola, and L. Larger, "Compact optoelectronic oscillators using WGM modes on fused silica and MgF mini-disks resonators," *Proc. of SPIE*, Vol. 7716, 77162C, 2010.
4. Salzenstein, P., M. Jelínek, Y. K. Chembo, M. Pogurmiskiy, H. Tavernier, K. Volyanskiy, K. P. Huy, M. Chauvet, L. Larger, and V. Kubecek, "Resonance measurements techniques of optical whispering gallery mode mini-disc resonators for microwave photonics applications," *Proc. of SPIE*, Vol. 8071, 807104, 2011.
5. Makarian, T., A. Melikyan, and H. Minassian, "Surface plasmon frequency spectrum in a system of two spherical dielectric coated metallic nanoparticules," *Acta Physica Polonica A*, Vol. 112, No. 5, 1025–1029, 2007.

Dependence of Avalanche Response Time on Photon Flux Incident on DDR Silicon IMPATT Devices

A. Acharyya and J. P. Banerjee
Institute of Radio Physics and Electronics
University of Calcutta, 92, APC Road, Kolkata 700009, India

Abstract— Effect of photo-irradiation on the avalanche response time [1] of Millimeter-wave Double Drift Region (DDR) Silicon IMPATT devices is investigated in this paper. A model to study the photo-irradiation effect on the DC and high-frequency properties of the mm-wave IMPATTs is developed by the authors based on which the simulation is carried out to calculate the avalanche response time of 94 GHz, 140 GHz, 220 GHz and 300 GHz DDR Silicon IMPATTs under two different optical illumination configurations (Top Mount (TM) and Flip Chip (FC)). It is interesting to observe that the DC and high-frequency parameters of the device are more sensitive to electron dominated photo current (TM structure) compared to the hole dominated photo current (FC structure) which was earlier demonstrated [2, 3] and explained in [4, 5]. Results show that the avalanche response time of the device decreases due to optical illumination on both TM and FC structures and percentage of decrease in avalanche response time in TM structure is higher compared to FC structure. For example 7.57% and 3.14% decrease in avalanche response time is observed in TM and FC structure of 94 GHz IMPATT respectively for the incident photon flux density of $10^{26}\,\mathrm{m}^{-2}\,\mathrm{sec}^{-1}$ at 1000 nm wavelength near band gap absorption of Silicon. Larger decrement of avalanche response time due to optical illumination in TM structure causes larger deviation of phase shift between RF voltage and terminal current of the device from 180° which is the ideal phase difference between current and voltage for maximum RF power output; this is the main cause of greater reduction in RF power output in TM structure compared to FC structure due to optical illumination.

REFERENCES

1. Acharyya, A., S. Banerjee, and J. P. Banerjee, "Calculation of avalanche response time for determining the high frequency performance limitations of IMPATT devices," *Journal of Electron Devices*, Vol. 12, 756–760, 2012.
2. Vyas, H. P., R. J. Gutmann, and J. M. Borrego, "Leakage current enhancement in IMPATT oscillator by photo-excitation," *Eletron. Lett.*, Vol. 13, 189–190, 1977.
3. Vyas, H. P., R. J. Gutmann, and J. M. Borrego, "Effect of hole versus electron photocurrent on microwave-optical interactions in impatt oscillators," *IEEE Transactions on Electron Devices*, Vol. 26, No. 3, 232–234, 1979.
4. Acharyya, A. and J. P. Banerjee, "A comparative study on the effect of optical illumination on $Si_{1-x}Ge_x$ and Si based DDR IMPATT diodes at W-band," *Iranian Journal of Electronics & Electrical Engineering*, Vol. 7, No. 3, 179–189, 2011.
5. Mukherjee, R. and J. P. Banerjee, "Effect of electron and hole dominant photocurrent on the millimeter-wave properties of indium phosphide impatt diode at 94 GHz," *Semiconductor Science and Technology*, Vol. 9, 1–4, 1994.

Compact Wide-band 90° Differential Phase Shifters

W. Marynowski, R. Lech, and J. Mazur
Gdansk University of Technology, Poland

Abstract— Differential phase shifters are four-port passive microwave devices providing, in the specified bandwidth, a constant phase difference between the signals at their output ports. Ideally, such devices should produce proper phase shift values, exhibit relatively small attenuation and operate effectively over a wide frequency band. They are used, for example, in wide-band phased array antennas and find application in various microwave equipments and measurement systems.

Here we presents a new configuration of a broadside coupled 90° phase shifter consisting of two elliptical or rectangular shaped microstrip patches that are coupled through a slot in a common ground plane [1, 2]. The patches are etched at the top and bottom layer and coupled through a slot. The shape of the slot is the same as microstrip patch and it is cut in the ground plane located at the mid of the structure. The phase shifter is a modification of Abbosh [3] phase shifter configuration and is designed as a four-port coupler in which its two coupled and transmitted ports are terminated by reactive loads. The other two ports are the input and output ports.

The proposed modification of the Abbosh phase shifter arrangement involving introduction of reactive loads allows to obtain larger phase shift values. A design procedure uses a simple scattering matrix model to explain the performance of the proposed phase shifter and to optimize the proposed configuration. The phase shifter frequency dependent return and insertion losses, frequency characteristics and frequency variation of the reactance load are calculated using this simple theoretical model. The configuration of the considered phase shifter was optimized and its characteristics were simulated using full-wave electromagnetic software ADS Momentum and validated by the measurement. Results of calculation and measurement show that the developed circuit provides a 90° differential phase shift with deviation less than ±4° across the 3 to 7 GHz frequency band.

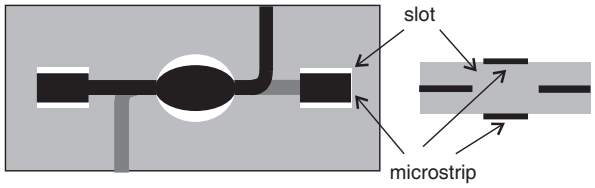

Figure 1: Configuration of the proposed 90° phase shifter — schematic representation.

ACKNOWLEDGMENT

This work was supported by the Polish Ministry of Science and Higher Education from sources for science in years 2012-2013 under Contract No. 0340/IP2/2011/71.

REFERENCES

1. Abbosh, A. M. and M. Bialkowski, "Design of compact directional couplers for UWB applications," *IEEE Trans. Microw. Theory Tech.*, Vol. 55, No. 10, 2262–2269, Oct. 2007.
2. Marynowski, W., A. Kusiek, A. Walesieniuk, and J. Mazur, "Investigation of broadband multilayered coupled line coupler," *14th Conference on Microwave Techniques, COMITE*, 1–4, Apr. 2008.
3. Abbosh, A. M., "Ultra-wideband phase shifters," *IEEE Trans. Microw. Theory Tech.*, Vol. 55, No. 9, 1935–1941, Sep. 2007.

Compact and Broadband Integrated Magic-T Configuration

W. Marynowski and J. Mazur
Gdansk University of Technology, Poland

Abstract— Integrated magic-T structures have been widely used at high frequencies as functional components of complex circuits and systems. They allow the in-phase and out-of-phase signal division between their output ports. They can be applied as power dividers and combiners or used for construction of balanced mixers, receivers, feeding structures of antenna arrays and bridges for measurement instruments. One can find many different arrangements of magic-T utilizing different integrated planar circuits such as branch-line, rat-race or directional couplers. In order to improve their performances double-sided and two-layers magic-T structures have been proposed in [1–5]. These configurations using coplanar or substrate integrated waveguide to slotline field conversion broaden their frequency range. They comprise of the out-of-phase and in-phase slot and microstrip dividers which are coupled by a suitably designed transition. The double-sided configurations are commonly composed of microstrip tee-junction and the slot resonator structure which are oppositely located on the common substrate and coupled through microstrip-slotline transitions. These structures are characterized by a wide, up to 50%, fractional bandwidth with a high isolation, better than 40 dB, between the sum and difference ports. However, there is a large radiation from the slotline, which causes high insertion loss in these networks.

Compact integrated magic-T configurations comprising of multilayer arrangements of microstrip tee-junction and microstrip patch coupled by slotline resonator are described. The slot is etched in the common ground plane and located along the symmetric microstrip line of the tee-junction and microstrip patch, which realize sum port and difference port of magic-T, respectively. The remaining ports of the structure are dividing ports of tee-junction. The patch consists of open-circuited microstrip line with shunt-connected open-circuited microstrip stub or radial resonator. The theoretical basis and design procedure of the proposed configurations are carried within the general integrated magic-T principles and their performance has been verified numerically using full wave commercial software. The results of simulation showed that the structure works in 40% fractional bandwidth with amplitude and phase imbalance less than 0.2 dB and 1°, respectively, and isolation between difference and sum ports below 30 dB. The simulations have also been verified by measurements of manufactured prototype.

ACKNOWLEDGMENT

This work was supported by the Polish Ministry of Science and Higher Education from sources for science in years 2012–2013: partially under Contract No. 0340/IP2/2011/71 and under funding for Statutory Activities for ETI Gdansk University of Technology.

REFERENCES

1. Davidovitz, M., "A compact planar magic-T junction with aperture-coupled difference port," *IEEE Microwave and Guided Wave Letters*, Vol. 7, No. 8, 217–218, August 1997.
2. Kim, J. P. and W. S. Park, "Novel configurations of planar multilayer magic-T using microstrip-slotline transitions," *IEEE Transactions on Microwave Theory and Techniques*, Vol. 50, No. 7, 1683–1688, July 2002.
3. Liu, M. and Z. Feng, "A novel hybrid planar SIW magic tee and monopulse antenna," *Microwave and Optical Technology Letters*, Vol. 52, No. 3, 686–689, March 2010.
4. Feng, W., W. Che, and K. Deng, "Compact planar magic-T using E-plane substrate integrated waveguide (SIW) power divider and slotline transition," *IEEE Microwave and Wireless Components Letters*, Vol. 20, No. 6, 331–333, June 2010.
5. Feng, W., Q. Xue, and W. Che, "Compact planar magic-T based on the double-sided parallel-strip line and the slotline coupling," *IEEE Transactions on Microwave Theory and Techniques*, Vol. 58, No. 11, 2915–2923, November 2010.

ARC Filters Parameters Comparison Regarding to Possible Use in MRI Applications

L. Fröhlich, M. Friedl, J. Sedláček, and E. Gescheidtová
Department of Theoretical and Experimental Electrical Engineering
Brno University of Technology, Kolejni 2906/4, Brno 612 00, Czech Republic

Abstract— ARC filters of higher order can be realized using several design variants. The most common variants of ARC filters use can be cascade block connection, non-cascade block connection or their combination. Individual variants of block connection can be divided into next sub-realizations. Thus, many different designs of ARC filters of higher order are created. We will be interested mainly in advantages and disadvantages and also defining possible areas of use for set of ARC filters.

For the choice of the suitable variant of use in NMR area, we will be interested mainly in filter parameters regarding to sensitivity concerning tolerance of values of used elements, spread of value of building elements, amount of OA (operation amplifier), spread of quality factors, dynamical spread and realization of types of filters etc.

The article will deal with the parameters for cascade circuit realization with the use of circuits Sallen — Key or GIC. For non-cascade circuit realization we will apply methods FLF (follow the leader feedback) and PRB (primary resonator block). And for the last combine method we will use Leap-Frog method. Individual parameters will be stated in a table for higher design of filter order of stated ARC filters LP, HP, BP and BR.

ACKNOWLEDGMENT

The research described in the paper was financially supported by grant of Czech ministry of industry and trade No. FR-TI1/001 and projects GACR 102/09/0314, GACR 102/11/0318, and FEKT-S-11-15.

REFERENCES

1. Sedlácek, J. and K. Hájek, *Kmitočtové Filtry*, 1. vydání, 535, BEN, technická literatura, Praha, 2002, ISBN 80-7300-023-7.
2. Dimopoulos, H. G. and A. G. Constantinidis, "Linear transformation active filters," *IEEE Trans. CAS*, Vol. 25, No. 10, 845–852, 1978.
3. Ghausi, M. S. and K. R. Laker, *Modern Filter Design*, Practice Hall, New Jersey, 1981.
4. Sedra, A. and K. Martin, "Design of signal-flow graph (SFG) active filters," *IEEE Trans., CAS*, Vol. 25, No. 4, 185–195, 1978.
5. DostáL, T., *Elektrické Filtry*, VUT FEI, Skriptum, Brno, 2001.

Analysis of Displacement Current in Coplanar and Microstrip Lines

W. Marynowski and P. Kowalczyk
Gdansk University of Technology, Poland

Abstract— According to increasing speed of digital electronic devices, the full-wave analysis of microstrip and coplanar structures becomes crucial in their designing process. For higher frequencies a standard printed circuit board must be treated as a system of unshielded coplanar/microstrip waveguides. Microstrip and coplanar lines have been analyzed and utilized for last five decades. However, the coplanar lines with a finite ground plane have been considered only in a few papers, mostly utilizing the quasistatic approximation [1].

In this paper multi-strip structures are analyzed in terms of the displacement current I_d. This current is related with the longitudinal component of the electric field in the cross section of the guide and its value depends on the geometry and substrate parameters, as well as operation frequency. Current I_d is required to balance outgoing and incoming longitudinal conducting currents. This effect results in ambiguous determination of structure parameters such as characteristic impedance. Even the reliable commercial software [2, 3] generates different results for very simple two-strip coplanar structure. Such lines are shown in Figs. 1(a) and (b) with the distribution of longitudinal component of the electric field for the symmetrical and asymmetrical guide, respectively. Due to a field asymmetry for structure (b) the displacement current cannot be neglected. As a result the characteristic impedance (depicted in Fig. 1(c)) is ambiguous. The described effect is significant especially at higher frequencies. For lower frequencies the value of the displacement current is small enough that can be neglected and the impedances obtained from different methods converge to one value, close to the one obtained from commonly utilized quasi static model.

The performed analysis shows that the value of displacement current is significant especially for asymmetrical structures (including microstrip lines) and its neglect may lead to improper results.

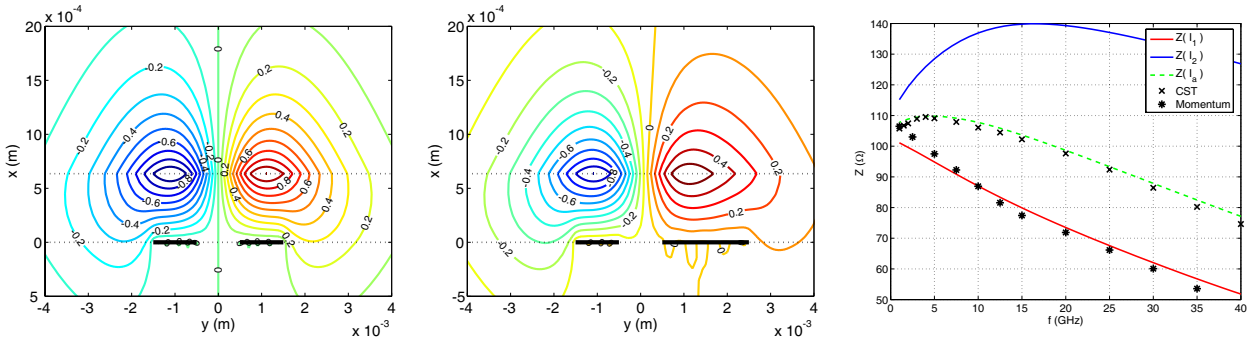

(a) (b) (c)

Figure 1: Two strip coplanar structure: (a) symmetrical, (b) asymmetrical, (c) characteristic impedance.

ACKNOWLEDGMENT

This work was supported by the Polish Ministry of Science and Higher Education from sources for science in years 2012-2013 under Contract No. 0340/IP2/2011/71.

REFERENCES

1. Görür, A. and C. Karpuz, "Effect of finite ground-plane widths on quasistatic parameters of asymmetrical coplanar waveguides," *IEE Proceedings — Microwaves, Antennas and Propagation*, Vol. 147, 343–347, 2000.
2. CST Micrwave Studio (CST MWS), https://www.cst.com.
3. Advanced Design System — Momentum, Agilent Technologies, http://www.agilent.com.

Accurate Calculation of Propagation Losses in Arbitrarily Shaped Waveguide Based Components Using Perturbation of Boundary Condition

S. Marini[1], **S. Bleda**[1], **M. Mattes**[2], **B. Gimeno**[3], **and V. E. Boria**[4]

[1]Department de Física, Ing. de Sistemas y Teoría de la Señal
Instituto de Física Aplicad a las Ciencias y Tecnologías
Universidad de Alicante, Spain
[2]Laboratory of Electromagnetics and Acoustics
Ecole Polytechnique Fédérale de Lausanne, Switzerland
[3]Departamento de Física Aplicada, Instituto de Ciencia de los materiales
Universidad de Valencia, Spain
[4]Departamento de Comunicaciones
Instituto de Telecomunicaciones y Aplicaciones Multimedia
Universidad Politécnica de Valencia, Spain

Abstract— The accurate consideration of propagation losses effects in arbitrarily shaped waveguide based structures is studied in this paper. For such purpose, a software tool based on the perturbation of the boundary conditions on the metallic walls of the waveguides combined with an Integral-Equation (IE) analysis technique is proposed [1–3]. In order to obtain the modal chart of waveguides with arbitrary cross-section, the Boundary Integral-Resonant Mode Expansion (BI-RME) method is also employed [4].

Following the proposed technique all the drawbacks of the classical power-loss method [1], such as the meaningless results at the cut-off frequency or the losses associated with the evanescent modes, are overcome and at each analysis frequency both attenuation α and phase constant β are computed taking positive real values ($e^{-\gamma z} = e^{-\alpha z} e^{-j\beta z}$). Furthermore, from Figure 1 it can be clearly noticed that, due to the finite conductivity of the metallic walls, the change in the phase constant results in a small deviation of the filter response with respect to the ideal case. This shift, which can be critical for narrow-band applications, cannot be considered either by the classical power-loss method.

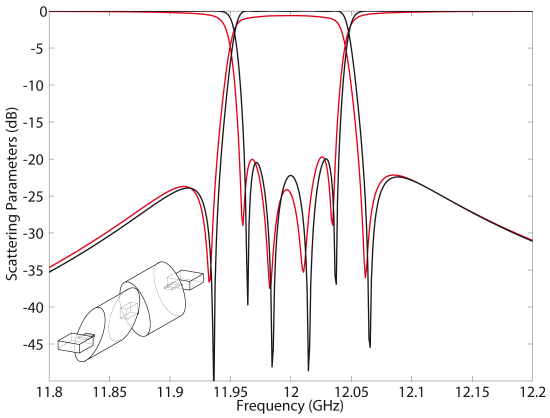

Figure 1: Scattering parameters of a four-pole dual-mode filter with elliptical waveguide resonators in standard WR-75 rectangular waveguides computed considering losses ($\sigma = 0.3 * 10^7$ S/m, red lines) and perfect conductor (black lines). The filter was originally proposed and designed in [5].

ACKNOWLEDGMENT

This work was supported by the Ministerio de Educación y Ciencia, Spanish Government, under Grant JC2009-0221 and the coordinated R & D project TEC2010-21520-C04, and by the University of Alicante under the project GRE10-22.

REFERENCES

1. Jackson, J. D., *Classical Electrodynamics*, Wiley, New York, 2001.
2. Marini, S., M. Mattes, B. Gimeno, and V. E. Boria, "Improved computation of propagation losses in waveguides structures using perturbation of boundary conditions," *IEEE Microwave and Wireless Comp. Letters*, Vol. 21, No. 11, 577–579, 2011.
3. Gerini, G., M. Guglielmi, and G. Lastoria, "Efficient integral equation formulations for admittance or impedance representation of planar waveguide junctions," *Proceeding of IEEE MTT-S Int. Dig.*, Vol. 3, 1747–1750, Jun. 1998.
4. Cogollos, S., S. Marini, V. E. Boria, P. Soto, A. Vidal, H. Esteban, J. V. Morro, and B. Gimeno, "Efficient modal analysis of arbitrarily shaped waveguides composed of linear, circular, and elliptical arcs using the BI-RME method," *IEEE Transactions on Microwave Theory and Tech.*, Vol. 51, No. 12, 2378–2390, 2003.
5. Accatino, L., G. Bertin, and M. Mongiardo, "Elliptical cavity resonators for dual-mode narrowband filters," *IEEE Transactions on Microwave Theory and Tech.*, Vol. 45, No. 12, 2393–2401, 1997.

Universal Filters for Processing of NMR Signals

L. Fröhlich, **J. Sedláček**, **M. Friedl**, **and R. Kadlec**
FEEC BUT, UTEE, Kolejní 2906/4, Brno 612 00, Czech Republic

Abstract— An analysis of the parameters and usage of universal filters in NMR area can be very interesting. In certain cases, there are situations when it is not possible to use standard filters, mainly because of requirements for tuning complete filter or using higher amount of transfer functions, which can be LP, HP, BP, BR but also LPN or HPN and AP. For this purpose, there can be used the universal filters which usually contain three and more OAs. One of these filter types are Akerberg-Mossberg or Kerwin-Huelsman-Newcomb circuits.

To be able to use their universality, it is necessary to realize suitable digital processing of their basic parameters of the set filter. These parameters are mainly resonant frequency, quality factor and transfer factor. For processing or tuning of filters it is possible to use digital potentiometers, digitally controlled switchers or other modern active blocks.

This article deals with the usage of these filters by control of their parameters with the help of microprocessor.

ACKNOWLEDGMENT

The research described in the paper was financially supported by grant of Czech ministry of industry and trade No. FR-TI1/001, GACR 102/09/0314 and project of the BUT Grant Agency FEKT-S-11-15.

REFERENCES

1. Sedláček, J. and K. Hájek, *Kmitoctové Filtry*, 1. vydání, Praha, BEN — technická literatura, 535 s, 2002, ISBN 80-7300-023-7.
2. Dostál, T., *Elektrické Filtry*, VUT FEI, Skriptum, Brno, 2001.
3. Ghausi, M. S. and K. R. Laker, *Modern Filter Design*, Practice Hall, New Jersey, 1981.
4. Chen, W. K., *The Circuits and Filters Handbook*, CRC Press, Florida, 2000.
5. Galiamichev, I. P., A. A. Lanne, V. Z. Lundin, and V. A. Petrakov, "The synthesis of active RC network," *Izdatel'stvo Sviaz'*, 296, Moscow, 1975 (in Russian),

Design of an Effective Architecture for the Envelope Tracking Power Amplifier for LTE Applications

S. H. Kam[1], **O. S. Kwon**[1], **and Y. H. Jeong**[1,2]

[1]Department of Electrical Engineering
Pohang University of Science and Technology, Pohang, Gyeongbuk 790-784, Republic of Korea
[2]Department of Creative IT Excellence Engineering
Pohang University of Science and Technology, Pohang, Gyeongbuk 790-784, Republic of Korea

Abstract— This paper reports an effective architecture for the envelope tracking (ET) transmitter using an emitter follower. To achieve the stable circuit and high efficiency, an emitter follower which can sub for the role of the tantalum capacitor is used at the drain network. For verification, the proposed ET power amplifier (PA) is implemented with a 25 W class-AB PA and tested using continuous wave (CW) and LTE signals at 2.6 GHz. From the measured results for the LTE signal, the drain efficiency of 38.3% is achieved at an output power of 34 dBm, which is a 10 dB back-off region. After the digital predistortion (DPD) linearization, the proposed ET PA also shows the significant linearity improvement.

We have proposed an effective architecture for the envelope tracking (ET) transmitter using an emitter follower as shown in Fig. 1. Fig. 2 and Fig. 3 show the measured results of class-AB PA using the LTE signal and measured power spectral densities (PSDs) before and after DPD, respectively. The results show that the proposed circuit has excellent efficiency and linearity performances.

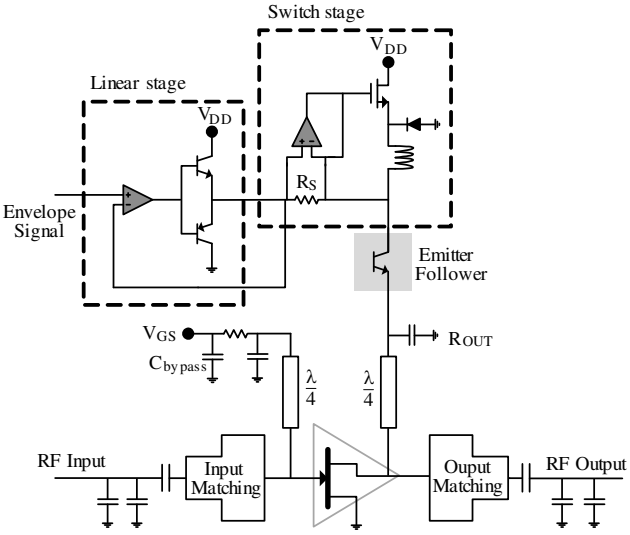

Figure 1: Schematic of the proposed ET PA using an emitter follower.

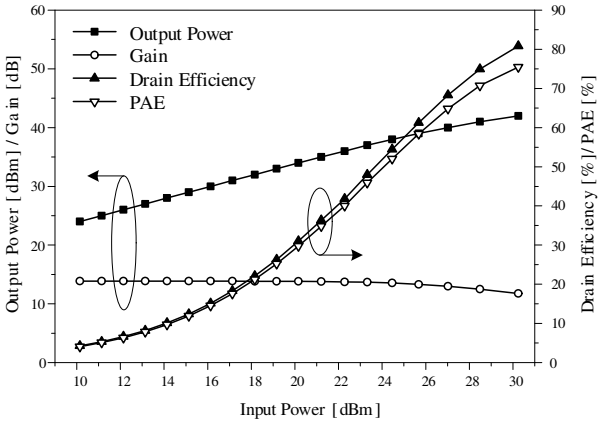

Figure 2: Measured results using LTE signal.

Figure 3: Measured PSDs before and after DPD.

A Dual Band (WLAN & WiMAX) Filter with Koch Fractal Shaped Using the Imperialist Competitive Algorithm

Shahrokh Jam and B. Hoda khabir
Shiraz University of Technology, Shiraz, Iran

Abstract— In this paper, a dual band microstrip filter with Koch fractal shaped coupled line for WLAN and WiMAX applications has been designed and proper dimensions have been achieved with Imperialist Competitive Algorithm (ICA). Using fractal shaped structures, is implemented to create dual banded trait also filter performances such as, BW, rejection between two bands, miniaturization are enhanced. Using the ICA provides a method for presenting this kind of filters with proper performance. The center frequency of first band of the proposed microstrip fractal shaped dual band filter is 2.515 GHz and second band is 3.4975 GHz. This filter has been designed for WLAN and WiMAX applications. Finally the designed filter has been fabricated (with Rogers R03210) and tested by 8510B network analyzer; there is a good agreement between HFSS simulation and experimental results. Comparing a dual band filter with the same performances introduce in [1] with the proposed one, shows that, this filter has better performances. Also, it has so improvements at BW, dimensions, fabrication technology, rejection between two bands in compare to that.

REFERENCES

1. Packiaraj, D., M. Ramesh, A. T. Kalghatgi, and K. J. Vinoy, "Dual band (WLAN & WiMAX) suppressed harmonic microstrip filter with perturbed ground," *Seventeenth National Conference on Communications*, NCC, Jan. 2011.
2. Atashpaz-Gargari, E. and C. Lucasm, "Imperialist competitive algorithm: An algorithm for optimization inspired by imperialistic competition," *IEEE Congress on Evolutionary Computation*, 4661–4667, Singapore, 2007.
3. Hsu, C.-Y., H.-R. Chuang, and C.-Y. Chen, "Compact microstrip UWB dual-band band-pass filter with tunable rejection band," *Journal of Electromagnetic Wave and Application*, Vol. 23, No. 5–6, 617–626, 2009.
4. Mohra, A. S., "Coupled microstrip line bandpass filter with harmonic suppression using right angle triangle grooves," *Microwave and Optical Technology Letters*, Vol. 51, 2313–2318, Oct. 2009.

UWB Wilkinson Power Divider Using Tapered Transmission Lines

Faroq Razzaz, **Majeed A. S. Alkanhal**, **and Abdel-Fattah Sheta**
Department of Electrical Engineering, King Saud University
P. O. Box 800, Riyadh 11421, Kingdom of Saudi Arabia

Abstract— A Wilkinson power divider with ultra-wide band (UWB) performance is proposed in this paper. The Wilkinson power divider is one of the most common components in microwave systems. Power dividers are commonly used in microwave circuits such as in balanced mixers, phase shifters, amplifiers and antenna array feed networks. The transmission lines whose characteristic impedances vary continuously are called tapered transmission line. Using of tapered transmission lines in microwave components results in reduction of the element length and therefore the overall component-size will be reduced. Using tapered transmission lines, also, results in wider band-widths. The proposed power divider is symmetric in configuration, and then, the even-odd analysis method can be used to analyze this power divider. This power divider has superior performance in the UWB band (3.1 GHz–10.6 GHz) and is smaller in size as compared to traditional power dividers. The designed power divider has been simulated using a full-wave electromagnetic simulator tool. The proposed UWB power divider is very simple to fabricate, designed without stubs, and has only one isolation resistor. The overall size of this power divider is $15.51 \times 15.47\,\mathrm{mm}^2$ on Roger RT5880 substrate with relative permittivity of 2.2 and thickness of 0.508 mm. The simulation results show good insertion loss which is approximately -3 dB, good return loss that is less than 11 dB for the input port over the entire UWB band and less than 16 dB for the other two ports. The power is divided equally between the output two ports and the isolation between the output ports is better than 11 dB. The group delay of the proposed UWB power divider is approximately flat and is less than 100 ps.

A 0.6 V Concurrent Dual-band Low Noise Amplifier for Portable Biomedical Receivers

Ro-Min Weng and Shan-Rong Chen
Department of Electrical Engineering, National Dong Hwa University, Hualien, Taiwan

Abstract— A 0.6 V concurrent dual-band low noise amplifier (DB-LNA) is presented with ultra low power for portable biomedical receivers performed in ZigBee and/or Bluetooth bands. The configuration is composed of a folded-cascode topology, a common-source input stage, and a common-gate output stage. Employed with forward body-biased techniques for MOSs of the first stage, the circuit can be operated under lower supply voltage while maintaining sufficient gain in dual-band operation. The proposed DB-LNA was simulated with TSMC 0.18 µm CMOS process. The power consumption is 4.76 mW at 0.6 V supply voltage. For 900 MHz, the input third-order intercept point (IIP3) is −24 dBm. The gain (S_{21}) is 14.7 dB. The input return loss (S_{11}) and output return loss (S_{22}) are −13.5 dB and −13.8 dB, respectively. The noise figure is 4.6 dB. For 2.45 GHz, the IIP3 is −16 dBm. S_{21} is 10.1 dB. S_{11} and S_{22} are −11.4 dB and −10 dB, respectively. The noise figure is 3.6 dB. The design specifications of the proposed DB-LNA are achieved and proved to be suitable for portable biomedical receivers.

Nonreciprocal Magnetoelectric Microwave Attenuator

D. V. Lavrentieva, **M. I. Bichurin**, **and A. S. Tatarenko**
Institute of Electronic and Information Systems, Novgorod State University
Veliky Novgorod 173003, Russia

Abstract— The combination of magnetic and electrical properties and properties caused by magnetoelectric (ME) interaction in composite layered materials offer great features for the design of new microwave devices. Microwave devices are designed on the basis of the various manifestations of the ME effect. Most strongly this effect is manifested in the form of microwave ME effect, which consists in a shift of the FMR resonance line under the control of the electric field. ME microwave attenuator is designed and researched. ME composite in this case acts as a resonator, which is a three-layer structure, based on a single-crystal yttrium iron garnet (YIG) on a substrate on a gadolinium gallium garnet (GGG) and a thin disk of magnesium niobate-lead titanate (PMN-PT).

The base of the attenuator is a microstrip transmission line on alumina substrate ($\varepsilon = 9.8$, thickness of 1 mm) and layered ferrit-piezoelectric resonator consisting of epitaxial single crystal (111) YIG films on GGG substrates and (001) PMN-PT with thicknesses 110 μm, 300 μm and 500 μm respectively. Diameter of ME resonator is about 4 mm. Metal electrodes (200 nm in thickness of gold and 30 nm in thickness of chromium) were deposited on PMN-PT for electrical contacts and the crystal was initially poled in $E = 2$ kV/cm. A thin layer (-0.02 mm) of an past epoxy, ethylcyanoacrylate, was used to bond YIG to PMN-PT. ME resonator is included as an absorbing inhomogeneity in a microstrip transmission line. Circular polarization of the magnetic field in volume of the ferrit-piezoelectric resonator results from using the microstrip stubs of $\lambda/8$ and $3\lambda/8$. The power absorption in ferromagnetic resonance occurs in a variable magnetic field with circular polarization and right direction of rotation relative to the direction of permanent magnetization. The variable magnetic field in the ME cavity has a circular polarization with different directions of rotations of the polarization for different directions of propagation. Therefore, the energy losses are small at resonance for direct direction of propagation and large for converse one.

A bias field corresponding to FMR is applied to the resonator. Electrical tuning is realized with the application of a control voltage to electrodes leading to a shift of FMR line.

We designed, fabricated and tested microwave attenuator in a standard thin film passive technology. Experemental results showed 38 dB attenuation at frecuency range 5–10 GHz with electric field $E = 0$–7 kV/cm. This technology can significantly reduce the cost of devices, and enhance speed of operation.

A Peano Fractal-based Dual-mode Microstrip Bandpass Filters for Wireless Communication Systems

Jawad K. Ali, **Hussam Alsaedi**, **Mohammed F. Hasan**, **and Hussain A. Hammas**
Microwave Research Group, Department of Electrical Engineering
University of Technology, Baghdad, Iraq

Abstract— Peano fractal geometries are characterized by their high space filling properties. In this paper, a new compact dual-mode microstrip filter design, based on this fractal geometry, is presented as a candidate for use in modern wireless communication systems. A bandpass filter with a quasi-elliptic response has been designed based on the 2nd iteration Peano fractal curve at 2.45 GHz using a substrate of a relative dielectric constant of 9.6 and thickness of 0.508 mm. The resulting filter structure based on the second iteration Peano geometry leads to compact size dual-mode resonator with a side length of about $0.1\lambda_g$. This represents better miniaturization level compared with the other microstrip bandpass filters with structures based on other space-filling geometries and designed at the same frequency using the same substrate material specifications. Simulation and theoretical performance of the resulting filter structures have been carried out using method of moments (MoM) based electromagnetic simulator IE3D, from Zeland Software Inc. The results also show that the proposed filter structure possesses good return loss and transmission responses besides the size reduction gained, making it suitable for use in a wide variety of wireless communication applications. Furthermore, the out-of-band response indicates that the proposed filter has less tendency to support higher harmonics.

Piezoelectric Multilayer Transformer

A. N. Soloviev, **M. I. Bichuri**, **and D. V. Kovalenko**
Novgorod State University, Russia

Abstract— The purpose of this report is to study model of wideband magnetoelectric transformer (WMET). WMET relates to the field of electronics, its new direction — magnetoelectric electronics. The WMET is part of a secondary source of power, replacing the conventional piezoelectric transformers. The main objectives of this work are the modeling of processes that are inherent in the WMET, measuring of WMET, construction and analysis of amplitude-frequency characteristics.

The magnetoelectric transformer is a combination of magnetostrictive and piezoelectric components. Piezoelectric component consists of two sections: the input section and the output one. The input section is responsible for converting the electrical signal into the mechanical vibrations. The output section converts the mechanical vibrations into an electrical signal at the same frequency. The magnetostrictive component converts the variable constituent of the magnetic field into the elastic vibrations. This component is located on the surface and inside the output section. The magnetostrictive component should have high magnetostriction, which gives an effective increase of the amplitude of mechanical vibrations in the output section WMET.

The transformer design is following. The input section is designed as of an even number layers. The output section performed in the form of the piezoelectric fibers. Piezo-fiber is a structure of an even number of piezoelectric elements. To increase the amplitude of mechanical vibrations the output electrodes are made of magnetostrictive material. Dielectric layer (fluoroplastic film) is placed between input and output sections.

The sample WMET-1 was simulated, it has a four-input section and the four-segmental piezofiber (output section), their sizes: the length of 10 mm, the width of 5 mm, the thickness of 1 mm. The study showed that the parameters of suggested transformer are 35% higher than the similar piezoelectric transformer. For sample 1 the following parameters were obtained: the resonant frequency is 102 kHz, the ratio of transformation at the resonant frequency is 100, the efficiency is 95%, the load resistance is 100 Mohm, the input capacitance is 10 nF. With the help of mathematical models were obtained The plot of the output power versus frequency and magnitude of the alternating magnetic field were obtained with the help of mathematical models.

The analysis of amplitude-frequency characteristic was observed that the investigated WMET should be used as a power transformer with a coefficient of 10 in the lower range of frequencies from 10 Hz to 20 kHz. This transformer can be used as a transformer element in the power supply units notebook, which significantly reduces ot its size.

EMC Pre-compliance Test of RFIC and RF Systems Using a Laboratory GTEM Chamber

H. X. Araujo and L. C. Kretly
University of Campinas, Brazil

Abstract— In this work, the EMC — Electromagnetic Compatibility of Integrated Circuits is deal with the use of techniques for low emission and susceptibility. In general, as the IC the major responsible of unintentional emissions and coupling, some specific pre-compliance setup tests were employed to analyze these detrimental effects to the system as a whole. A GTEM cell operating from 500 MHz–18 GHz was designed and built. Additional techniques were done to improve this chamber in terms of frequency range and cost effect. It is also shown others pre-compliance setup tests to evaluate the disturbance caused by an IC. Simulated and experimental results are compared to validate the proposed EMC setup.

Nowadays, the necessity to control the electromagnetic emissions and interference between circuits and electronic devices becomes a crucial point to assure its correct operation inside an electromagnetic environment [1]. Some approaches were designed to support the pre-compliance tests (EMC/EMI/EMS) setups, which are not designed to replace the well-known compliance equipments (anechoic chamber, stirring chamber, blue test chamber, etc.) but, it gives a previously information about the device behavior. All of them have consolidated standards and regulations.

Based on the advantages in terms of frequency range, cost effect, and its versatility to realize both EMI/EMS a GTEM to operate from 500 MHz–18 GHz was designed and built [2]. Basically, the GTEM cell has a internal conductor called septum to carry the radiation over the DUT — device under test, in case of immunity test, or couple the interferences from the DUT, EMI test. Similar to a rectangular coaxial transmission line with outer conductors closed and joined together, the GTEM cell has tapered ends acting as transitions to adapt it to standard 50 Ω

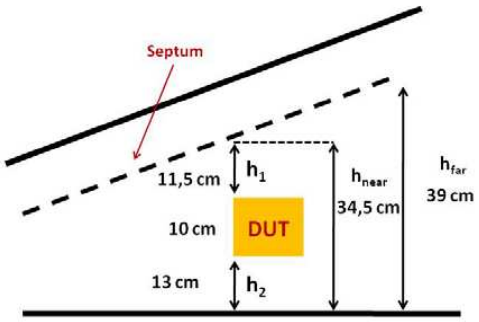

Figure 1: Internal details of the GTEM cell.

Figure 2: APEX preliminary test.

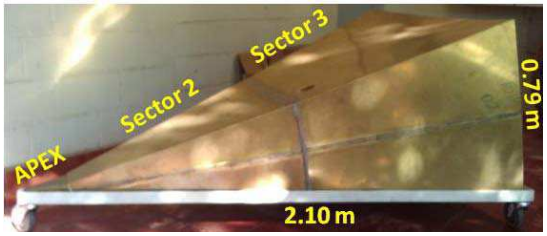

Figure 3: GTEM chamber.

Figure 4: GTEM chamber preliminary test.

coaxial connectors [3]. The central conductor of the cell provides electromagnetic propagation in TEM mode. Therefore, the electromagnetic field is uniform only within a certain region of the chamber, normally in its middle, where the DUT should be located.

EMC problems associated to ICs are basically classified as intra-chip or externally-coupled [4]. When a circuit is interfered by the noise from another circuit on the same chip, an intra-chip problem is related. On the other hand, when the noise from an IC interferes with circuits or devices off the chip, it is called externally-coupled. Particularly, both of them can be analyzed with a GTEM cell.

REFERENCES

1. Montrose, M. I. and E. M. Nakauchi, *Testing for EMC Compliance*, Wiley Interscience, New York, 2004.
2. Araujo, H. X. and L. C. Kretly, "An EM simulation and design a GTEM chamber for EMC pre-compliance tests on electronic board and ICs in 500 MHz–18 GHz range," *Momag 2010*, Vila Velha, Brazil, August 2010.
3. Konigstein, D. and D. Hansen, "A new family of TEM-cells with enlarged bandwidth and optimized working volume," *Proceedings of the 7th International Zurich Symposium on Electromagnetic Compatibility*, 127–130, Zurich, March 1987.
4. Dhia, S. B., M. Ramdani, and E. Sicard, *Electromagnetic Compatibility of Integrated Circuits: Techniques for Low Emission and Susceptibility*, Springer, New York, 2006.

Application of the Generalized Integrator in Parallel Hybrid Active Power Filter

Zhengrong Jiang[1, 2], **Haichang Ding**[1, 2], **Zhengxi Li**[1, 2], **and Ke Wang**[3]

[1]Beijing Variable Frequency Technologies Research Center, Beijing 100144, China
[2]College of Mechanical and Electrical Engineering
North China University of Technology, Beijing 100144, China
[3]Tsinghua University, Beijing 100084, China

Abstract— In order to suppress the harmonic circulation of the parallel hybrid active filter, the generalized integrator control method is proposed. Based on the advantages of the passive filter and the active power filter, the new control method can effectively depart the passive filter compensation harmonic component, active filter compensation component and fundamental component. The feasibility and effectiveness of the hybrid active filter system are verified by simulations and experiments.

Introduction: With the wide application of the power electronic devices in modern industry, the harmonic pollution in the grid is inevitable. The problems of the suppressing harmonic and improving the power factor attract more concerns. Along with the improvement of the power electronic control technology, the hybrid active power filter has become the new direction of development of the power filter [1]. This paper is mainly focused on the topology and the control of the inverter [2].

A new control method is proposed to reduce the capacity of the active power filter and avoid the circulation channel of the hybrid active filter.

Control Algorithms Based on the Composite Generalized Integrator:

A. The Working Principle of Generalized Integrator: As shown in Fig. 1, the generalized integrator is hoped to use for amplitude values of cycle but not for its frequency and phase Angle in terms of volume of cycle, the generalized integrator transfer function is obtained by the Laplace Alternation of the signal [3].

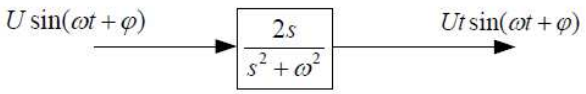

Figure 1: General integrator principle diagram.

In order to take advantage of the hybrid active filter, a generalized integrator control strategies are designed. Switching loss of power device can be further reduced and high efficiency can be reached.

B. The Generalized Integrator Control Algorithm for Harmonic Current Compensation: In order to avoid the harmonic circulation of the parallel hybrid filter, the total harmonic current is extracted through the PQ algorithm, and the 3rd, 5th harmonic currents are extracted by the generalized integrator, then inverter output currents reference signal is obtained through the total harmonic current minus 3rd, 5th harmonic currents, so as to avoid the harmonic circulation between active filter and passive filter.

Simulation and Experiment Results: The simulations are carried out by Matlab and Simulink, the results show that the hybrid active filter can suppress the harmonic current effectively. Several switching frequencies are simulated and compared.

The generalized integrator control algorithm is validated through the experiment. Experiment results demonstrated that the harmonic circulation is avoided and the active filter capacity is reduced.

Conclusion: A high performance generalized integrator is presented in this paper. The topology and the modulation method ensure the efficiency performance of the parallel hybrid active filter.

The functions of the proposed method are used to division the compensation currents task between the passive filter and the active power filter. In order to reach the new control performance,

the active filter reference currents doesn't include 3rd, 5th harmonic currents, and the passive filter compensates the fundamental reactive power and 3rd, 5th harmonic currents.

The effectiveness of the method has been confirmed through both the theory analysis and the experiment results, the harmonic circulation is avoided and active filter compensation capacity is reduced in this way.

REFERENCES

1. Wang, Z., J. Yang, and J. Liu, *Harmonic Control and Reactive Power Compensation*, 2nd Edition, Machinery Industry Press, Beijing, 2005.
2. Dixon, J. W., J. J. Garcia, and L. Moran, "Control system for three phase activepower filter which simultaneously compensates power factor and unbalanced loads," *IEEE Trans. on Industrial Electronics*, Vol. 42, No. 6, 636–641, 1995.
3. Herrera, R. S., P. Salmeron, S. P. Litran, and J. Prieto, "Different approaches assessment in active power filter compensation," *IEEE MELECON*, 1090–1093, 2006.

Problem of Generating of Periodic Structure in EHD Model of Charged Jet Flow

Oleg Kravchenko
Bauman Moscow State Technical University, Russia

Abstract— In present work a problem of generating periodic strucutre which has been introduced in [1] is considered.

An approach of transformation a nonlinear system of partial differential equations (PDEs) into one nonlinear Burgers type equation has been introduced by [1, 2]. In paper [3] this approach has been introduced independently in consideration the mechanism of lightning discharge. It has been noticed in [3] that the electrical breakdown is realized in between the regions with a virtually periodic structure. Apparently, this virtual periodical is observed for real lightning.

In this work aproblem of generating periodic strucutre in static case is considered and discontinuous solutions are presented governed by conservation low according to [4].

ACKNOWLEDGMENT

The author would like to thank Academician of Russian Academy of Sciense, Professor Vladislav Ivanovich Pustovoit and Professor Vladimir Georgievich Sapogin for their useful comments.

REFERENCES

1. Olsen, P., "Integrable version of Burgers equation in magnetohydrodynamics," *Phys. Rev. E*, Vol. 68, 016307, 2003.
2. Moreau, E. and O. Vallee, "Connection between the Burgers equation with an elastic forcing term and a stochastic process," *Phys. Rev. E*, Vol. 73, 016112, 2006.
3. Pustovoit, V. I., "Mechanism of lightning discharge," *Journal of Communications Technology and Electronics*, Vol. 51, No. 8, 937–943, 2006.
4. Sapogin, V. G., "On compensation of coulomb interaction of charges by beams self-consistent field (model of isotermal equilibrium with homogeneous temperature)," *Proceedings 1st IEEE International Conference on Circuits and Systems for Communications*, 408–411, St. Petersburg, Russia, 2002.

Discontinuous Solutions in EHD Model of Charged Jet Flow

Oleg Kravchenko
Bauman Moscow State Technical University, Russia

Abstract— In present work, a mathematical two-fluid EHD (Electro-hydrodynamics) model of charged jet ow is investigated. System of nonlinear partial differential equations (PDE) is transformed into Burgers equation with constant source. Afterwards a static case is considered and discontinuous solutions are presented.

It is well known that the uid equations are difficult to handle because of their nonlinearity and mathematical complexity as a result. So, there are at least two approaches to transform a system of nonlinear equations describing uid models into one model equation. One of them has been proposed by P. Olesen [1]. In this approach a $1+1$ dimensional magnetohydrodinamics problem with particular configuration for the velocity and the magnetic field. The other one consists to study the in uence of an electric field on a velocity field. This approach has been introduced by E. Moreau and O. Vallee [2] as a complementary approach facing Olesen's work [1]. The second approach has been introduced in [3] by V. I. Pustovoit independently.

In present work, a mathematical two- uid model of charged jet ow is investigated by means of the second approach. Hence, system of nonlinear PDEs is transformed into one nonlinear Burgers type equation with constant source. Afterwards a static case is considered and discontinuous solutions are presented governed by conservation low according to [4].

ACKNOWLEDGMENT

The author would like to thank Academician of Russian Academy of Sciense, Professor Vladislav Ivanovich Pustovoit and Professor Vladimir Georgievich Sapogin for their useful comments.

REFERENCES

1. Olsen, P., "Integrable version of Burgers equation in magnetohydrodynamics," *Phys. Rev. E*, Vol. 68, 016307, 2003.
2. Moreau, E. and O. Vallee, "Connection between the Burgers equation with an elastic forcing term and a stochastic process," *Phys. Rev. E*, Vol. 73, 016112, 2006.
3. Pustovoit, V. I., "Mechanism of lightning discharge," *Journal of Communications Technology and Electronics*, Vol. 51, No. 8, 937–943, 2006.
4. Sapogin, V. G., "On compensation of coulomb interaction of charges by beams self-consistent field (model of isotermal equilibrium with homogeneous temperature)," *Proceedings 1st IEEE International Conference on Circuits and Systems for Communications*, 408–411, St. Petersburg, Russia, 2002.

Bayesian Estimation of Tumours in Breasts Using Microwave Imaging

E. Khosrowshahli[1] and A. Jeremić[2]

[1]Department of Biomedical Engineering, McMaster University, Hamilton, ON, Canada
[2]Department of Electrical Engineering, McMaster University, Hamilton, ON, Canada

Abstract— According to Canadian Cancer Society, breast cancer is the most frequently diagnosed cancer in women with over 23,400 new cases expected in 2011 [1]. Our ability to potentially detect breast cancer in an early stage has potential of significantly decreasing mortality. Therefore, early detection is a very important issue in healthcare. Mammography has been used widely for screening women over 50 who are more vulnerable. However mammography suffers from some limitations such as false negative and positive results, using ionizing radiation and patient's discomfort. Microwave imaging has been introduced recently to overcome drawbacks of this method. It is based on electromagnetic properties difference between normal and malignant tissues in microwave frequencies. In breast microwave imaging the imaging system consists of an array of antennas which can serve both as transmitting and receiving antennas. Therefore it is possible to illuminate object of interest (breast) from multiple directions thus obtaining a full three dimensional scan whose resolution depends only on the number of antennas. This process is mathematically described by Maxwell's equations, which in this particular case can be reduced to the phasor form since microwave antennas operate in a single-frequency mode. One of the most difficult parts when detecting potential tumours in breasts is presence of modeling noise due to large amount of scattering, which severely deteriorates performance of estimation and detection algorithms.

In this paper, we propose a parametric 3D model of breast microwave propagation, i.e., signal measured on antennas with respect to tumours' and breast parameters including electromagnetic properties and geometry (our model includes multiple tumors with arbitrary shapes.) For illustration purposes, in this study tumor is considered as a sphere inside the breast with an arbitrary size and in arbitrary position. As an example of wave propagation in simulation, y-component of electric field is shown for the case of eccentric tumor. In this figure tumor is located between second and third plates, and scattering electric field is clearly seen around the tumor, and higher intensity of electric field immediately after the source is obvious.

In order to detect the presence of tumours we propose an error measure based between model predicted signal measurements in the absence of scattering (potential tumours) and actual measurements. Obviously false positives will be due to the fact that certain amount of scattering is present even in a healthy tissue. To this purpose we propose to model electromagnetic properties of the healthy and malignant tissue using two different sets of probability density functions.

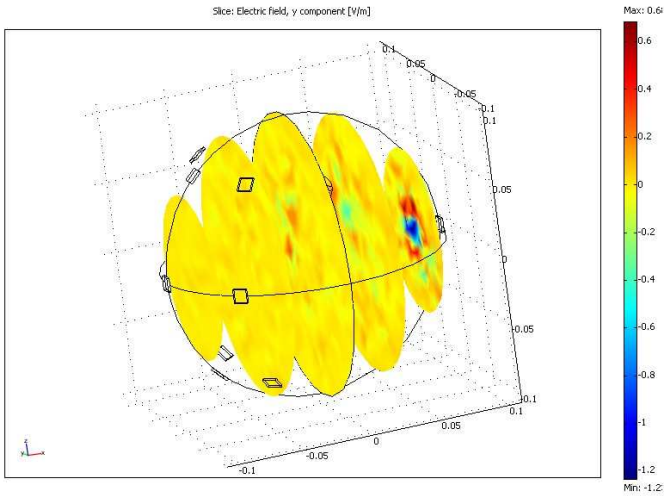

Figure 1: y-component of electric field for eccentric tumor.

Consequently detection and estimation of parameters in such models require Bayesian class of estimators and adequately defined likelihood-ratio detectors. In this paper we evaluate performance and computational complexity of the aforementioned estimators and detectors as a preliminary step in defining required antenna parameters with respect to noise levels.

In addition to technical issues one of the most important questions that needs to be answered is related to screening frequency of such technology that would make it acceptable from a clinical standpoint of view. To this purpose we derive sequential likelihood ratio tests in which current decision is made using previous decisions in an optimal way. We expect that these results will provide useful insight into how often groups with different risk levels should be screened using this technology.

Puzzles of the "Nonlinear" Ehrenfest Theorem for Solitons

T. L. Belyaeva[1], **C. A. Ramrez-Medina**[1], **and V. N. Serkin**[2]

[1]Universidad Autónoma del Estado de México, Toluca, C. P. 50000, México
[2]Benemerita Universidad Autónoma de Puebla, C. P. 502, Puebla 72001, México

Abstract— Quantum mechanical tunneling is one of the most fruitful concepts in modern physics. While the study of linear microscopic quantum tunneling has a very long history going back to the first days of quantum mechanics, the field of nonlinear (soliton-like) macroscopic quantum tunneling is relatively young and was born only after two discoveries — solitons and BEC.

Nonlinear wave excitations and solitons — self-localized robust and long-lived solitary waves that do not disperse and preserve their identity as they travel through a medium — are ubiquitous in Nature, they arise in many fundamental areas of physics and technology: from nonlinear optics and ultrafast photonics, condensed matter and plasma physics to elementary particle physics, cosmology and monster (rogue) waves in oceans and Bose-Einstein condensates. Owing to their remarkable features solitons might appear as the idealized structures for the description of extended "elementary" particles. Consequently, general questions naturally arise: To what extent the soliton can be regarded as a classical point-like particle which is governed by Newton's equations of motion? As to whether the wave-particle duality and intrinsic ("hidden") degrees of freedom can show up in the soliton tunneling through potential barriers and wells? Previously, it was demonstrated that so-called nonautonomous solitons in the exactly integrable nonautonomous and nonlinear systems can be adapted to both the external potentials and the dispersion and nonlinearity changes and generally move with varying amplitudes, speeds and spectra. We stress that in this Report, we consider the soliton dynamics in the frameworks of exclusively nonintegrable models with arbitrary localized external potentials.

Our main purpose is to present the conceptual consideration of the underlying physical principles involved into the soliton tunneling effect. We prove that scaling symmetry breaking in soliton scattering reveals the hidden role of the soliton self-interaction ("binding") energy and its dramatic impact on the wave-particle duality of solitons. Deep analogies between nonlinear Schrödinger solitons scattering on external potentials and the Gamow model for alpha particles tunneling are demonstrated. Based on these analogies, the hidden features of the nonlinear Ehrenfest theorem and the leading role of the soliton binding energy in the soliton tunneling through classically forbidden potential barriers are revealed. Simple physical criteria for classical Newtonian like and quantum mechanical like dynamics of the Schrödinger solitons in external potentials are obtained and confirmed by direct computer experiments. Main experimentally accessible strategies to reveal the hidden role of the soliton binding energy are presented. The results obtained can find different applications in the developing basically novel all-optical soliton logic and switching devices, in soliton lasers design, soliton supercontinuum generation and formation of matter wave solitons in Bose-Einstein condensates.

Dynamics of "Dancing" Gray and Dark Solitons in Time-dependent Harmonic Oscillator Potential

C. Hernandez-Tenorio[1], **T. L. Belyaeva**[2], **and V. N. Serkin**[3]

[1]Instituto Tecnológico de Toluca, Metepec, Edo. México C.P. 52140, México
[2]Universidad Autónoma del Estado de Mxico, Toluca C.P. 50000, México
[3]Benemerita Universidad Autnoma de Puebla, 502, Puebla C.P. 72001, México

Abstract— We study the dynamics of dark and gray solitons in the framework of the nonlinear Schrödinger equation (NLSE) model with the time-dependent harmonic oscillator potential. A comparative analysis of the solutions is performed both for a linear harmonic oscillator and the NLSE model with different signs of the self-action potential.

The exact analytical solutions and numerical experiments reveal many specific features of dark soliton dynamics corresponding to the different experimental conditions. We have found that stable dark-soliton configurations can be formed in the confinement potential independently on a positive or negative sign of nonlinearity, contrary to the sign-dependent dynamics of solitons in the absent of a harmonic potential.

It is shown that the main specific feature of the dynamics of dark NLSE solitons in a parabolic trap is the formation of solitons with dynamically changing form-factors producing the periodic variation in the modulation depth (the degree of "blackness") of dark solitons. In general, the period of dark soliton oscillations in trapping potential depends on the specific conditions of the experiment and does not coincide with the oscillation period of a linear quantum-mechanical oscillator. In the case of an immobile pedestal in the trap, the oscillation period of the black soliton considerably increases because of the periodic transformation of the black soliton to the gray one and vice versa. Surprisingly, that if the dark soliton is superimposed on the base pedestal oscillating in the trap and displaced from the trap center, the oscillation period of the dark soliton coincides with the period of oscillations of the linear harmonic oscillator, while the dynamics of the dark soliton is similar to that of a classical particle obeying the Newton mechanics laws.

The remarkable possibility of generation of the so-called "dancing" nonautonomous gray and dark solitons in time-dependent harmonic oscillator potential is also demonstrated. This nonlinear dynamics is compared with dynamics of bright nonautonomous solitons trapped in time-dependent harmonic oscillator potential.

Design of High Isolation Electronically Switchable Bandpass Filter

Shih-Fong Chao and Ming-Wei Shih
National Kaohsiung Marine University, Taiwan

Abstract— In this paper, a simple method to design a high isolation electronically switchable bandpass filter is proposed. The circuit integrates a microwave switch and a microwave bandpass filter into a single circuit component. The uniform impedance resonator is loaded with a pin diode to change its resonant frequencies under different bias voltages. By loading the pin diode at different positions of the constituted resonators, the resonant frequencies can be misaligned over the band of interest to achieve a wideband isolation in the isolated state. In the thru state, the circuit shows a bandpass response with a measured insertion loss of 3 dB at the center frequency of 1 GHz, and the 3 dB fractional bandwidth is 8%. In the isolated state, the measured isolation is 51 dB at the center frequency and is higher than 30 dB from dc to 5 GHz. The paper proposed a simple and effective method to realized an electronically switchable bandpass filter with high isolation, and the circuit successfully increases the level of integration of the RF front end.

Session 3A1
Fiber Lasers and Fiber Micro/Nano-Photonic Components

All-Fiber Cladding Pumped at 976 nm Er-doped Fiber Laser and Amplifier

Mikhail E. Likhachev[1], **Leonid V. Kotov**[1], **Mikhail M. Bubnov**[1], **Oleg I. Medvedkov**[1], **Denis S. Lipatov**[2], **Nikolaj N. Vechkanov**[2], **and Alexej N. Guryanov**[2]

[1]Fiber Optics Research Center of RAS, 38 Vavilov Street, Moscow 119333, Russia
[2]Institute of Chemistry of High Purity Substances of RAS
49 Tropinin Street, Nizhny Novgorod 603950, Russia

Abstract— We propose a new ytterbium-free erbium-doped fiber design that allows an implementation of highly efficient lasers and amplifier. The main factors limiting the efficiency of double clad erbium-doped systems are a small absorption cross section of Er^{3+} ions and an increase of unbleachable losses due to pair induced quenching even at medium erbium concentrations. The major goal of the fiber optimization was to decrease negative influence of such losses by decreasing fiber length owing to increase the cladding pump absorption at fixed erbium content. For this core-to-clad ratio should be increased. Fabrication of the large single mode core ($D \sim 22\,\mu m$) becomes possible owing to utilization of novel P_2O_5-Al_2O_3-SiO_2 (PAS) glass matrix as the host for Er^{3+} ions. According to our previous study, such matrix allows to rich higher efficiency at the same core refractive index than conventional Al_2O_3-SiO_2 one. Minimal first cladding diameter is mainly limited by its numerical aperture. Using of an extremely low refractive index Teflon coating (NA $\sim$ 0.6) allow us to decrease first cladding diameter down to 95 μm in all-fiber amplifier and down to 80 μm in laser scheme.

All-fiber cw laser and amplifier based on newly developed fiber were realized. The highest slope efficiency of 40% with respect to the absorbed pump power was obtained in the laser. The maximum output signal amounted to 7.5 W at 1570 nm and was limited by the available pump power. The amplifier operated in the spectral range from 1560 to 1600 nm with a maximum output power of 7.2 W (slope efficiency up to 31%). Achieved efficiencies are not less than ones in commonly used erbium-ytterbium co-doped lasers and amplifiers, but proposed schemes devoid of main drawbacks of erbium-ytterbium systems: unwanted lasing at 1: m.

Polarizing Very-large-mode-area Bragg fiber

M. E. Likhachev[1], **S. S. Aleshkina**[1], **A. D. Pryamikov**[1], **D. A. Gaponov**[1, 2], **A. N. Denisov**[1], **M. M. Bubnov**[1], **M. Yu. Salganskii**[3], **A. N. Guryanov**[3], **Yu. A. Uspenskii**[4], **and S. Février**[2]

[1]Fiber Optics Research Center of the Russian Academy of Sciences
38 Vavilov Street, Moscow 119333, Russia
[2]Xlim, UMR 6172 CNRS, University of Limoges, 123 Avenue A. Thomas, Limoges 87060, France
[3]Institute of High Purity Substances of Russian Academy of Sciences
49 Tropinin Street, Nizhny Novgorod 603950, Russia
[4]P. N. Lebedev Physical Institute of RAS, 53 Leninskii Prospekt, Moscow 119333, Russia

Abstract— Now numerous works are devoted to increasing the average and peak output power of fiber lasers and amplifiers which requires suppression of the nonlinear effects and, consequently, utilization of Large-mode-area (LMA) fibers. An additional requirement for most of high power fiber lasers and amplifiers is that the output beam should have linear polarization. For those reasons there are several types of fibers: polarization maintaining fiber, polarizing fiber and single-polarization fiber.

In this work, we propose a design of single mode polarizing LMA-Bragg fiber operating in a wide spectral range. Cross section of the Bragg fiber consists of a core with a refractive index lower to or equal to the pure silica outer cladding and a Bragg mirror composed of cylindrical layers with alternating high and low refractive index, located between the core and the outer cladding. Light is confined in the core owing to coherent Fresnel reflection from the Bragg mirror.

The major characteristic of Bragg fibers is that they are inherently multi-mode and high-order modes (HOMs) can be filtered out owing to their higher optical loss as compared to the fundamental mode. Introduction to the core of Bragg fiber two B-doped and two F-doped rods resulted from necessity of additional suppression HOMs in LMA-Bragg fibers. Suppression one of the polarization states of the fundamental mode was achieved owing to B-doped rods was significantly smaller than diameter of the Bragg fiber core. Thus the stress was distributed non-uniformly over the fiber cross-section and, consequently, the refractive index was not uniform too. Thus non-optimal conditions for propagation of fast polarization were created while slow polarization could propagate in the core with low loss.

Fabrication of the Bragg fiber preform was carried out by a new and simple method based on a combination of the MCVD-process and the rod-in-tube technique. Fiber was drawn with outer cladding diameter of 170 μm and core diameter of 80 μm. The mode field area was estimate to be as large as 870 μm^2. HOMs together with the fast polarization of the LP_{01} mode were efficiently removed after propagating of 1.7 m of a fiber bent to a radius of 70 cm. The Polarization Extinction Ratio better than 13 dB was obtained in the spectral range from 1 to 1.4 m (it is about 33%) at a bend radius of about 70 cm. To the best of our knowledge it is the widest polarizing spectral range reported for all-solid single-polarization fibers.

Tapered Fiber-optic LSPR Sensor with Metal Nanoparticle Layers

Hsing-Ying Lin[1], **Chen-Han Huang**[1], **Chia-Ling Cheng**[2], **Nan-Kuang Chen**[2], **and Hsiang-Chen Chui**[3, 4]

[1]Center for Nano Bio-detection, National Chung Cheng University, Chiayi 621, Taiwan
[2]Department of Electro-optical Engineering, National United University, Miaoli 360, Taiwan
[3]Department of Photonics, National Cheng Kung University, Tainan 701, Taiwan
[4]Advanced Optoelectronic Technology Center, National Cheng Kung University, Tainan 701, Taiwan

Abstract— This paper presents a fast, highly sensitive and low-cost localized surface plasmon resonance (LSPR) sensor by tapered optical fiber. The tapered optical fiber is achieved by tapering a standard telecommunication single-mode fiber (SMF-28) and fabricated using the hydrogen flame-brushing technique to achieve a uniform waist [1, 2]. Total elongation length of the tapered fiber is around 4.5 cm and uniform waist length is approximately 1 cm. The abrupt taper is a taper transition with a suddenly changed profile to break the adiabaticity of power so that higher-order cladding modes are generated. Therefore, the opportunity to make evanescent field generated in the fiber surface. The tapered area of fiber is used as the sensing region then the gold nanoparticles are deposited on the tapered sensing region and excited by the evanescent wave from the tapered optical fiber. When the incident photon frequency is resonant with the collective oscillation of the conduction electrons which is known as the LSPR and the results will produce a strong absorption band. The spectral characteristics of the LSPR band are highly dependent on the local refractive index of the surrounding medium near the nanoparticle surface [3, 4]. We systematically characterize the dependence of the transmission spectra of the optical fiber carrying nanoparticle on the refractive index of the surrounding medium. The ensemble response of the LSPR of Au nanoparticles to varying dielectric environments by measuring the intensity and spectrum of the light transmitted through the tapered optical fiber. With the increase of the refractive index, the transmission spectra of the red shift and intensity gradually decreased steadily. The result shows a linear fit (adjusted correlation coefficient, $R^2 = 0.9998$) to the plot of transmittance intensity at 540 nm as a function of RI (a sucrose solution increased in the range of 1.333–1.403). This wavelength is chosen in the plot because a maximum sensitivity is found at that wavelength and the ensemble index sensitivity is fund to be 5×10^{-5} RIU. Such sensor resolution is comparable to those of the fiber-optic PSPR sensor [5]. These results suggest the potential for high index sensitivities of tapered fiber-optic LSPR sensor which with the attractive sensing features to develop real-time, low-cost and ultrasensitive sensors.

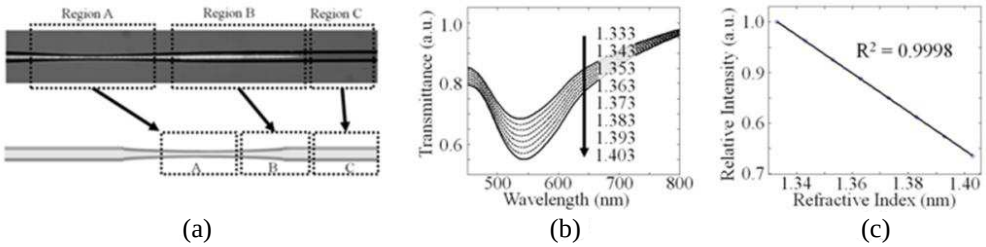

(a) (b) (c)

Figure 1: (a) Picture and schematic showing of the tapered fiber. Region A, B, and C were tapered sensing region, transition-stretching region and the general fiber region. (b) Transmission spectra measured when the optical fiber carrying Au nanoparticle is exposed to varying surrounding environments. (c) Relative transmittance intensity at 540 nm as a function of the refractive index.

REFERENCES

1. Hsu, K. C., N. K. Chen, S. Y. Chou, S. K. Liaw, Y. Lai, and S. Chi, "Bandpass filter with variable bandwidth based on a tapered fiber with external polymer cladding," *IEEE Photonics Technology Letters*, Vol. 21, No. 13, 935–937, 2009.
2. Hsu, K. C., S. Chi, and S. M. Tsend, "Title of the journal paper," *Journal Title Abbreviation*, Vol. 34, No. 10, 1064–1076, 1986.

3. Huang, C. H., H. Y. Lin, H. C. Chui, Y. C. Lan, and S. W. Chu, "The phase-response effect of size-dependent optical enhancement in a single nanoparticle," *Optics Express*, Vol. 16, No. 13, 9580–9586, 2009.
4. Lin, H. Y., C. H. Huang, C. H. Chang, Y. C. Lan, and H. C. Chui, "Direct near-field optical imaging of plasmonic resonances in metal nanoparticle pairs," *Optics Express*, Vol. 18, No. 1, 165–172, 2010.
5. Jorgenson, R. C. and S. S. Yee, "A fiber-optic chemical sensor based on surface plasmon resonance," *Sens. Actuators B*, Vol. 12, 213–220, 1993.

A Method of High Repetition Rate Femtosecond Optical Pulse Generation by Using Bi-stable Optical Micro-ring Resonators

Sanjeev Kumar Raghuwanshi, **Ajay Kumar**, **and Santosh Kumar**
Department of Electronics Engineering
Indian School of Mines, Dhanbad, Jharkhand 826004, India

Abstract— Generation of high repetition rate, short an optical pulse is an important topic of research at the present time. This is because in order to realize a high capacity optical communication system we need a combination of wavelength division multiplexing (WDM) and optical time division multiplexing (OTDM) techniques. A combination of WDM and OTDM can result in a high capacity optical communication system within existing limitations. At present the electro-optic modulators can be operated at a rate of 40 Gb/s. To utilize this modulation rate, we must generate optical pulses having a repetition rate much greater than 40 GHz. Thus, to realize a high speed OTDM system, we need a high repetition rate, and short optical pulses. Various methods of optical pulse generation exist in the literature [1–5]. Some of the methods of optical pulse generation are mode locking of semiconductor lasers, harmonically mode locked fiber laser, soliton-assisted time lens compression, short pulse generation by interferometers, and repetition rate multiplication of a low rate pulse source. In this paper our attempts are to generate optical pulses having very high repetition rates. We propose a novel scheme of high repetition rate, femtoseconds optical pulse generation by using bi-stable optical micro ring resonator where it is possible to achieve a repetition rate of more than few hundred GHz. The repetition rate of the pulse can be tuned over a wide range. Two examples have been considered in the paper and shown that the pulse width decreases substantially without getting distortion when pulse passed through into our proposed bi-stable micro ring resonator.

REFERENCES

1. Das, S. and T. Chattopadhyay, "A method of tunable high repetition rate picosecond optical pulse generation using injection locking of laser diodes," *Appl. Physics B*, Vol. 83, 549–551, 2006.
2. Azafia, J., R. Slavik, P. Kockaert, L. R. Chen, and S. LaRochelle, "Generation of ultra-high repetition rate optical pulse bursts by means of fiber Bragg gratings operating in transmission," *Electronics Lett.*, Vol. 38, No. 24, 1555–15556, Nov. 21, 2002.
3. Okamoto, K., *Fundamentals of Optical Waveguides*, 1st Edition, Academic Press, USA, 2000.
4. Stokes, L. F., M. Chodorow, and H. J. Shaw, "All-single-mode fiber resonator," *Optics Letters*, Vol. 7, No. 6, 288–290, Jun. 1982.
5. Zhang, X.-Y., T. Zhang, X.-J. Xue, J.-L. Zhang, J. Hong, P.-Q. Wu, and Q.-Y. Chen, "Tunable optical ring resonator integrated with asymmetric mach-zehnder interferometer," *IEEE Journal of Light Wave Tech.*, Vol. 28, No. 17, 2512–2520, Sept. 2010.

Micro Air-bubble in Hollow-core Optical Fiber for Ultracompact Sagnac Loop Interferometer

Yu-Hsin Hsieh[1], **Jheng-Jyun Wang**[1], **and Nan-Kuang Chen**[1, 2]

[1]Department of Electro-optical Engineering
National United University, Miaoli, Taiwan 360, Taiwan R.O.C.
[2]Optoelectronics Research Center
National United University, Miaoli, Taiwan 360, Taiwan R.O.C.

Abstract— In this work, we demonstrate the novel, ultracompact, robust, and cost-effective all-fiber Sagnac loop interferometer based a micro air-bubble in hollow-core optical fiber (HOF) which is spliced against the end of a singlemode fiber, as shown in Fig. 1(a). The total device length is less than 700 µm. The end of the HOF is intentionally collapsed and sphered by an arc discharging. A CO_2 laser beam was then focused onto the desired region around the sphered end to heat the HOF when the compressed air is injected into the hollow-core from the other end simultaneously. By precisely controlling the injected compressed air pressure as well as the heating laser power, an air-bubble located at around the end of HOF can be created to serve as a loop mirror for coupling the forward propagating light beams into backward direction. In order to equally split the core mode into counter-clockwise (*ccw*) and clockwise (*cw*) directions, the hollow-core close to the HOF-SMF interface is intentionally tapered through an asymmetric arc discharging. Therefore, the split lights will propagate along the cladding of HOF and then turn back in a roundabout way at air-bubble. Since the optical path for *cw* and *ccw* lights can not exactly overlap due to the birefringence, the induced optical path length difference (OPLD) gives rise to interferences, as shown in Fig. 1(b). A longer length of the HOF can lead to a smaller free spectral range (FSR). A smaller angle of the tapered hollow-core near the splicing point is helpful to avoid the excitations of higher-order. This is crucial for converting the core mode into cladding modes smoothly. This micro Sagnac loop interferometer is highly promising for micro Sagnac gyroscope or micro sensors.

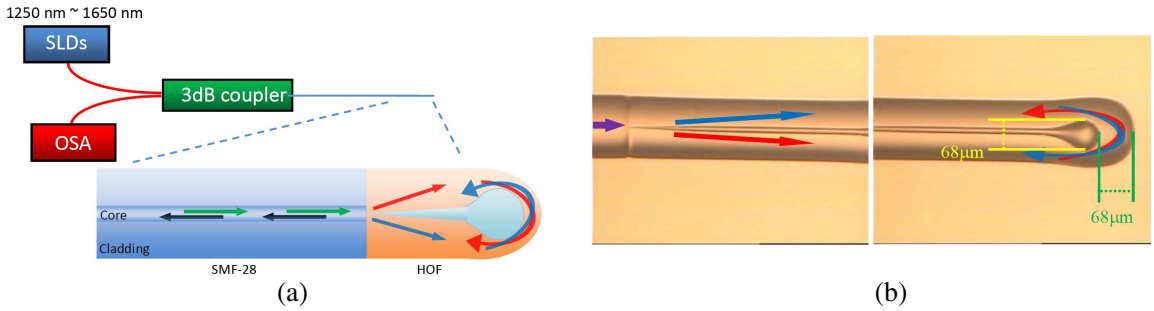

Figure 1: (a) Experimental set-up of Ultracompact Sagnac loop interferometer. (b) Collapse splicing point for excite the core mode to separate into cladding smoothly. (b) Microbubble-structure-end HOF as a loop path for interferometer.

All-optical Gain-dependent Phase Modulation in Micro Abrupt-tapered Mach-Zehnder Interferometers for High Efficiency Wavelength Conversion

Zhao-Ying Chen[1], **Nan-Kuang Chen**[1, 2], **Zhi-Zheng Feng**[1], **and Shien-Kuei Liaw**[3]

[1]Department of Electro-Optical Engineering, National United University
Miaoli 360, Taiwan, R.O.C.
[2]Optoelectronics Research Center, National United University
Miaoli 360, Taiwan, R.O.C.
[3]Graduate Institute of Electro-Optical Engineering
National Taiwan University of Science and Technology, Taipei 106, Taiwan, R.O.C.

Abstract— In this work, an intensity-modulated 980 nm laser is launched into a 32.5-mm-long micro abrupt-tapered Mach-Zehnder interferometer (AT-MZI) [1]. It is made of Er/Yb co-doped fiber (EYDF) to introduce gain-dependent phase shift to modulate another CW external cavity diode laser (ECDL) at 1530.4 nm for wavelength conversion. Fig. 1 shows the experimental set-up of the all-optical gain-dependent phase modulation in AT-MZI for wavelength conversion. The 980 nm diode laser is intensity-modulated by an optical switch which is operated based on an electrical-signal-driven mechanical relay. The modulated pump light is then launched into the AT-MZI to move the resonant dip wavelengths around. The active core of EYDF has peak absorption of about 1000 dB/m at 980 nm. Therefore, a 980 nm pump light can be employed to effectively change the refractive index of this short EYDF to achieve gain-dependent phase shift for all-optical wavelength tuning purposes [2]. Two samples A and B with a EYDF length of 32.5 mm and 12 mm were prepared. The diameters (D_1 and D_2) of the two abrupt tapers and the span length L between them for sample A and B are (35 µm, 40.8 µm, 22 mm) and (51.7 µm, 61.8 µm, 4.17 mm), respectively. The spectral responses are shown in Figs. 2(a)–2(c). It is obvious that a long span length of the phase shifter [2] can cause a smaller free spectral range (FSR) and steeper roll-off curves for resonant dips [3]. Thus, this is better to choose sample A to obtain a high efficiency modulation depth and speed for wavelength conversion. The AT-MZI is subsequently pumped under a pump power of 39.1 mW at 980 nm to move around the resonant dip so that the ECDL is not attenuated. Consequently, the ECDL is modulated with a laser on-off ratio of 8 dB and the modulated signals for input pump light and output laser are shown in Figs. 2(e)–2(f) at a modulation speed of 20 Hz and 25 Hz, respectively. Therefore, we demonstrated an optimized AT-MZI for wavelength conversion and which is also highly promising for Q-switched fiber lasers and high speed phase/intensity modulators.

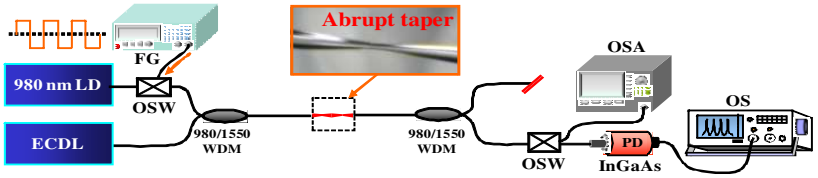

Figure 1: Experimental set-up of the Q-switched fiber laser based on the all-optical gain-dependent phase modulation. LD: laser diode, ECDL: external cavity diode laser, FG: function generator, OSW: optical switch, WDM: wavelength division multiplexer, OSA: optical spectrum analyzer, PD: photodiode, OS: oscilloscope.

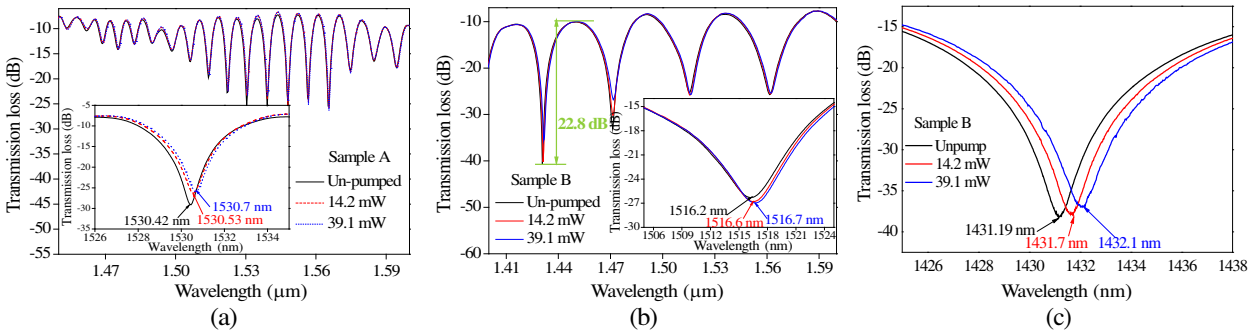

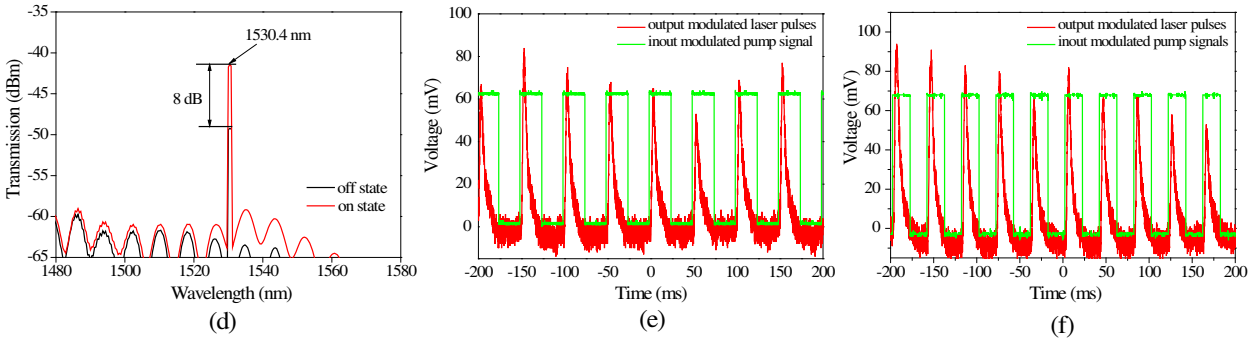

Figure 2: Spectral responses of (a) sample A, (b) sample B, (c) sample B at around 1432 nm and (d) laser output. Input modulated pump signals and output modulated laser signals at modulated speed of (e) 20 Hz and (f) 25 Hz.

REFERENCES

1. Agrawal, G. P., *Fiber-Optic Communication Systems*, 3rd Edition, Chap. 7, John Wiley and Sons, 2002.
2. Chen, N. K. and Z. Z. Feng, "Effect of gain-dependent phase shift for tunable abrupt-tapered Mach-Zehnder interferometers," *Opt. Lett.*, Vol. 35, 2109–2111, 2010.
3. Feng, Z. Z., Y. H. Hsieh, and N. K. Chen, "Successive asymmetric abrupt tapers for tunable narrowband fiber comb filters," *IEEE Photon. Technol. Lett.*, Vol. 23, 438–440, 2011.

Multistage Intra-cavity Short-pass Edge Filters for High Efficiency Femtosecond Pulsewidth Stretching in Mode-locked Erbium Fiber Lasers

Feng-Chou Liu[1], **Yi-Kun Lee**[1], **Nan-Kuang Chen**[1, 2], **and Shien-Kuei Liaw**[3]

[1]Department of Electro-optical Engineering
National United University, Miaoli, Taiwan 360, Taiwan, R.O.C.
[2]Optoelectronics Research Center, National United University
Miaoli, Taiwan 360, Taiwan, R.O.C.
[3]Graduate Institute of Electro-Optical Engineering
National Taiwan University of Science and Technology, Taipei, Taiwan 106, Taiwan, R.O.C.

Abstract— It is known that the mode-locked pulses can be stretched or compressed by adjusting the cavity length or by introducing chirped gratings and filters [1, 2] in fiber ring laser, we, in this work, report a new method of high efficient pulsewidth stretching in Er^3+-doped femtosecond mode-locked fiber lasers (FMLLs) by tailoring cavity dispersion using intracavity multistage short-pass edge filters (SPEF). In our previous work, a single SPEF in laser cavity can achieve the pulsewidth tuning from 176.8 fs to 623.8 fs (total pulsewidth stretching of 447 fs) under a temperature variation of 4°C (from 36°C to 32°C) in the SPEF. This is ascribing to that a steep roll-off spectral curve can come along with a large negative dispersion [3]. Fig. 1 shows the experimental setup of FMLLs. The FMLL is working based on the nonlinear polarization rotation method which is also known as polarization additive pulse mode-locking. A 3.5-m-long EDF (OFS: R37005) has a positive group velocity dispersion (GVD) parameter β_2 is used as the gain medium. In the beginning, the cavity dispersion is fine tuned by using a section of single-mode fiber (SMF-28) with a proper length to make the net cavity dispersion in the anomalous dispersion regime but close to the zero dispersion for acquiring a best compressed pulsewidth of about 150 fs. The SPEFs were prepared by heating and stretching several SMF-28 fibers simultaneously until a tapered diameter of about 30 µm is achieved. The tapered fibers are then immersed in optical liquids with an index of $n_D = 1.456$ to achieve the steep short-pass cutoff edge because the dispersion characteristics of the liquid are much less dispersive when compared with silica fiber. A material and waveguide dispersion must be carefully and properly treated to achieve a dispersion slope higher than −1.5 dB/nm for the spectral roll-off curves. Three SPEFs are discretely incorporated into the fiber ring cavity to move the net cavity dispersion from the anomalous dispersion regime to normal dispersion regime rapidly when the cutoff wavelengths of the three SPEFs are moved by thermo-optic effects. Accordingly, the femtosecond pulsewidth can be significantly and efficiently stretched for more than 800 fs within a temperature variation of less than 6°C in the room temperature range. This approach enables the all-fiber femtosecond laser to be efficiently pulsewidth stretchable without changing the physical length of laser cavity. It is also simple, cost-effective, and wide-range tuning by using multistage intracavity SPEFs in the FMLL.

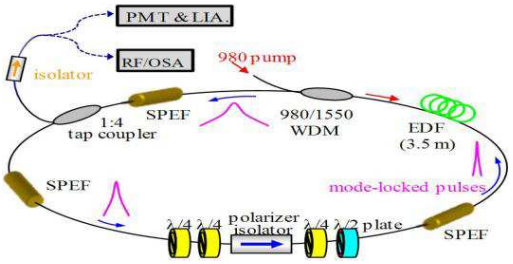

Figure 1: Experimental set-up of pulse-stretchable Er^3+-doped mode-locked fiber laser. WDM: wavelength division multiplexer, OSA: optical spectrum analyzer, RF: RF spectrum analyzer, SPEF: short-pass edge filter, EDF: erbium-doped fiber, PS: pulse shaper, PMT: photomultiplier tube, LIA: lock-in amplifier..

REFERENCES

1. Fermann, M. E., K. Sugden, and I. Bennion, "High-power soliton fiber laser based on pulse width control with chirped fiber Bragg gratings," *Opt. Lett.*, Vol. 20, 172–174, 1995.

2. Kalosha, V. P., L. Chen, and X. Bao, "Ultra-short pulse operation of all-optical fiber passively mode-locked ytterbium laser," *Opt. Express*, Vol. 14, 4935–4945, 2006.
3. Chen, N. K., F. Z. Liu, H. P. Chuang, Y. Lai, S. D. Yang, J. W. Lin, S. K. Liaw, Y. C. Chang, C. B. Huang, and S. Chi, "Highly efficient femtosecond pulse stretching by tailoring cavity dispersion in erbium fiber lasers with an intracavity short-pass edge filter," *Optics Express*, Vol. 19, 15879–15884, 2011.

Influence of Index Profile Dispersion on Cutoff Slope for Short-pass Edge Filters

Yi-Kun Lee[1] **and Nan-Kuang Chen**[1, 2]

[1]Department of Electro-Optical Engineering, National United University
Miaoli, Taiwan 360, Taiwan, R.O.C.
[2]Optoelectronics Research Center, National United University
Miaoli, Taiwan 360, Taiwan R.O.C.

Abstract— In-line tunable fiber short-pass filters have been employed for novel fiber filters, S-band fiber amplifiers, S-band fiber lasers, femtosecond pulsewidth stretching, and so on [1–5]. The short-pass fundamental mode cutoff phenomena were generated ascribing tot the material dispersion discrepancy between core and cladding. A composite waveguide structure with a higher dispersive core and a less dispersive cladding can separate the passband and stopband more distinctly. Since the refractive index dispersion (RID) curves of higher dispersive core and less dispersive cladding will cross at a cutoff point, only the wavelengths at the left-hand side of the cutoff point can satisfy the total internal reflection criteria to produce short-pass spectral curves. However, the cutoff slope for the short-pass spectral curves must be improved to alleviate the deadband between the passband and stopband with the help of waveguide dispersion [1]. The waveguide dispersion becomes effective when the evanescent fields of guided modes significantly interact with the core and cladding boundary. It is known that a long and uniform tapered diameter of around 30 µm can achieve a good cutoff slope of around −1.2 dB/nm. However, a higher cutoff slope is definitely useful when a precisely wavelength separation [4] or a strongly negative dispersion [5] is required. In this work, we investigate the influence of index profile dispersion on cutoff slope for short-pass edge filters. Expect for the material and waveguide dispersion, the index profile dispersion can be used to enhance the cutoff slope. The tapered fibers A and B were made using hydrogen flame at a temperature of 750°C and 950°C, respectively. During fabrication, the Ge dopants in fiber core is easier to diffuse outward and the core and cladding boundary is blurred. In contrast, the step index profile can be remained for sample A. The sample A and B both have a tapered diameter of 30 µm and an optical liquid ($n_D = 1.456$) is used surrounding the tapered region. A temperature controlling device is used to adjust the ambient temperature. The corresponding spectra responses for sample A and B are shown in Fig. 1(a) and Fig. 1(b), respectively. Obviously, the cutoff slopes (slope of the line passing through the two points at −10 dB loss and −30 dB loss) are improved when a step-index profile is kept in the tapered fiber. The cutoff slope for each line is listed in Table 1. The index profile dispersion can improve the cutoff slope from around −1 dB/nm to −2 dB/nm.

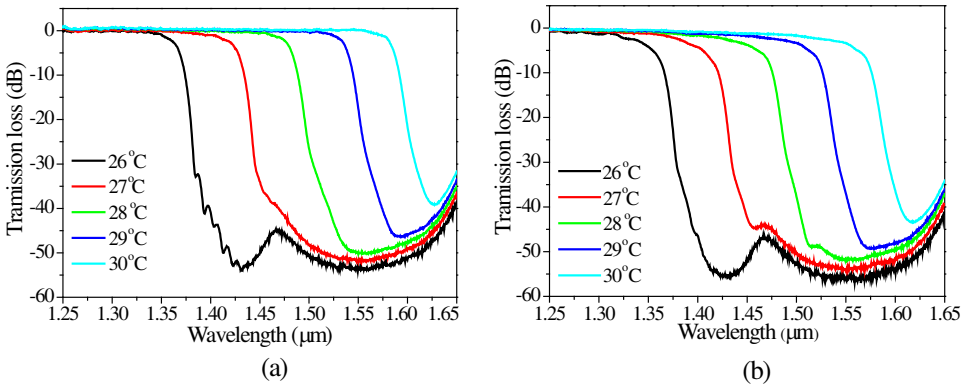

Figure 1. Spectral responses of (a) sample A and (b) sample B when the tapered fiber has a step-index profile and a graded-index profile, respectively.

Table 1.

	26°C	27°C	28°C	29°C	30°C
Sample A	−2.17	−1.82	−1.3	−1.28	−1.25
Sample B	−1.67	−1.47	−1.28	−1.28	−1.19

REFERENCES

1. Chen, N. K., K. C. Hsu, S. K. Liaw, Y. Lai, and S. Chi, "Influence of depressed-index outer ring on evanescent tunneling loss in tapered double-cladding fibers," *Opt. Lett.*, Vol. 33, 1666–1668, 2008.
2. Hsu, K. C., N. K. Chen, S. Y. Chou, S. K. Liaw, Y. Lai, and S. Chi, "Wideband tunable Gaussian-shaped spectral filters based on dispersion-engineering," *Opt. Fiber Technol.*, Vol. 15, 373–376, 2009.
3. Chen, N. K., K. C. Hsu, S. Chi, and Y. Lai, "Tunable Er^{3+}-doped fiber amplifiers covering S and C + L bands over 1490–1610 nm based on discrete fundamental-mode cutoff filters," *Opt. Lett.*, Vol. 31, 2842–2844, 2006.
4. Chen, N. K., C. M. Hung, S. Chi, and Y. Lai, "Towards the short-wavelength limit lasing at 1450 nm over $^4I_{13/2} \rightarrow {}^4I_{15/2}$ transition in silica-based erbium-doped fiber," *Opt. Express*, Vol. 15, 16448–16456, 2007.
5. Chen, N. K., F. Z. Liu, H. P. Chuang, Y. Lai, S. D. Yang, J. W. Lin, S. K. Liaw, Y. C. Chang, C. B. Huang, and S. Chi, "Highly efficient femtosecond pulse stretching by tailoring cavity dispersion in erbium fiber lasers with an intracavity short-pass edge filter," *Opt. Express*, Vol. 19, 15879–15884, 2011.

Session 3A2
Microwave and Millimeter Wave Circuits and Measurements

Optimization of Phase Noise in a 2.3 ∼ 3.5 GHz Voltage-controlled Oscillator Using the Impedance Locus

Kang-Chun Peng[1] and Tzyy-Sheng Horng[2]

[1]Department of Computer and Communication Engineering
National Kaohsiung First University of Science and Technology, Taiwan, R.O.C.
[2]Department of Electrical Engineering
National Sun Yat-Sen University, Taiwan, R.O.C.

Abstract— This work develops a 2.3 ∼ 3.5 GHz wideband voltage-controlled oscillator (VCO) using the impedance locus for both 802.11g and LTE-A applications. The key design considerations of the main VCO is balancing the performance between operation bandwidth and phase noise. According to the spectrum distribution of 802.11g and LTE-A, the wideband VCO requires a 42% fractional bandwidth to cover 2.3 ∼ 3.5 GHz. Besides, the phase noise of the wideband VCO should also be minimized since the 802.11g and LTE-A system applies orthogonal frequency-division multiplexing (OFDM) technique for high spectrum efficiency. In this work, the operation bandwidth is expanded by using capacitor array. The phase noise performance is optimized by applying impedance locus design methodology. The impedance loci of the VCO's active network and the VCO's resonating network are depicted on a Smith Chart. The two loci cross each other at a particular frequency, yielding an included angle. If the included angle at the intersection is between 0° and 180°, then the VCO oscillates at the frequency of the intersection. In contrast, if is between 180° ∼ 360°, then no oscillation occurs. The analysis indicates that as the included angle approaches 90°, the VCO exhibits a better phase noise performance. An impedance locus can also be adopted to predict the VCO output power. To confirm the performance, a 2.3 ∼ 3.5 GHz wideband VCO is designed and implemented with TSMC 0.18 µm CMOS technology. Measurements demonstrate that the wideband VCO design with phase noise optimization has a favorable phase noise and operation bandwidth performance. The phase noise is lower than −114 dBc/Hz at the 1 MHz offset frequencies over the 2.3 ∼ 3.5 GHz operation range. The figure of merit (FoM) and the figure of merit with tuning range (FoMT) are lower than −166 dBc/Hz and −178 dBc/Hz at the 1 MHz offset frequencies.

Solenoid Magnet for Gun-collector Module of 42 GHz 200 kW Gyrotron

Sudeep Sharan[1,*], **Deepak Srivastav**[2], **Anil Kumar**[2], **Udaybir Singh**[2], **Hasina Khatun**[2], **Gernot Zimmer**[1,3], **and A. K. Sinha**[1]

[1]Fachhochschule Frankfurt Am Main, University of Applied Sciences, Germany
[2]Gyrotron Laboratory, MWT Area
CSIR-Central Electronics Engineering Research Institute, Pilani, India
[3]Vietnamese-German University, Vietnam

Abstract— At CEERI Pilani, India, a 42 GHz 200 kW gyrotron is under development for fusion application [1–3]. Figure 1 shows the schematic view of the gyrotron with magnet system at different region to maintain the magnetic field profile for the desire electron beam properties, operating mode, operating frequency and output power. The major specifications are given in the Table 1. The gyrotron produces coherent electromagnetic radiation due to the interaction of gyrating electron beam and transverse electric (TE) wave in the cavity resonator [4, 5]. Thus, the operation of gyrotron requires magnetic system at different regions namely (1) gun magnet system, (2) cavity magnet system and (3) collector magnet system. The gun magnet system near the cathode helps to achieve the desire beam parameters like velocity ratio, larmour radius, velocity spread, beam radius, etc. [3]. The paper discusses the design and testing of solenoid magnet for gun collector module of 42 GHz 200 kW gyrotron. In the gun region, the magnetic field is required to gyrate the electron beam as well as transmits the beam from cathode to dummy collector.

Using EGUN software, the MIG-collector module is designed and the magnetic field profile is optimized as shown in Figure 2. Further, the magnet system is designed using TRAK code. The

*Corresponding author: Sudeep Sharan (sss.ceeri@gmail.com).

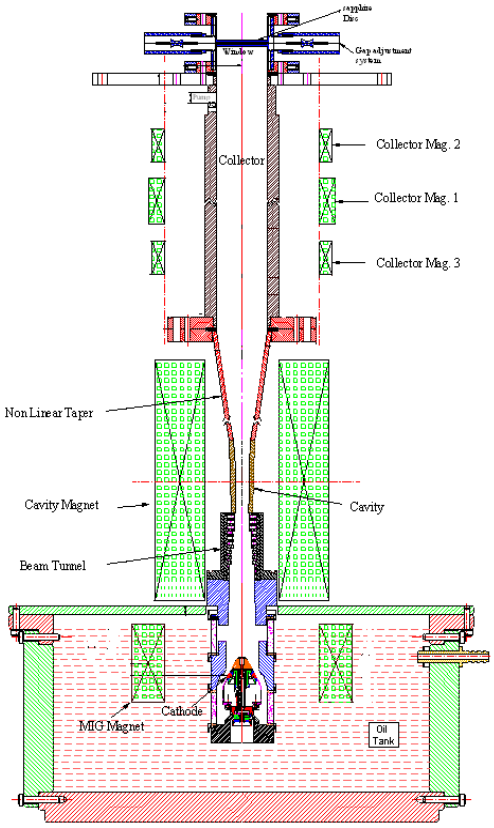

Figure 1: Schematic view of 42 GHz 200 kW gyrotron with magnet system.

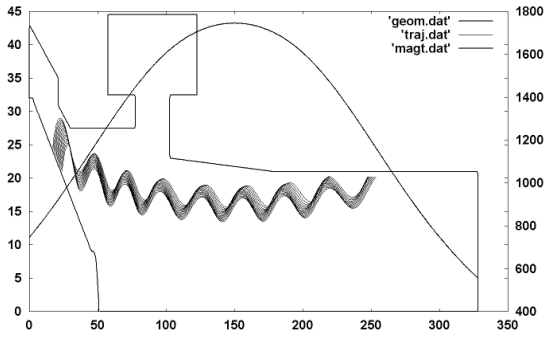

Figure 2: Electron beam trajectory with magnetic field profile for MIG-collector module.

Table 1: Specifications of 42 GHz 200 kW gyrotron.

Frequency	42 GHz
Output power	200 kW
Beam voltage	65 kV
Beam current	10 A
Operating mode	TE_{03}
Velocity ratio	1.4
Cavity Magnetic field	1.61 T
Cathode Magnetic field	0.1080 T
Collector Magnetic field	0.0276 T
Efficiency	$> 30\%$

Table 2: Parameters of the MIG collector module magnet system.

Dimensions	
Inner bore diameter	135 mm
Outer bore diameter	200 mm
Height	150 mm
Max. magnetic field strength	2000 Gauss
Current	7 A

design constraints of the magnet system are (1) the inner bore diameter should be greater than 100 mm and (2) air cool for continuous operation. The required magnetic field along the z-axis is achieved by varying coil thickness, number of layers, coil radius, coil length, current density of the coil. Table 2 shows the optimized design data of the magnet system. The maximum magnetic field strength, 0.2 T is obtained at 7 A. The design magnet system is fabricated by industry. A 19 gauge copper wire with current capability of 20 A is used. The gaussmeter (Model 9200, F W Bell) is used to measure the magnetic field strength. At the centre of the solenoid magnet the measured magnetic field is 2000 Gauss. The tested solenoid magnet will be used during hot testing of the MIG-collector module. The axial profile of the magnetic field value can be varied by changing the operating parameters of the magnet system and shifting the magnet position.

REFERENCES

1. Singh, U., A. Bera, N. Kumar, L. P. Purohit, and A. K. Sinha, "Numerical simulation of MIG for 42 GHz 200 kW gyrotron," *Int. J. Infrared Millim. Terahertz Waves*, Vol. 31, No. 6, 708–713, 2010.
2. Khatun, H., R. R. Rao, A. K. Sinha, and S. N. Joshi, "Optimization of magnetic field for maximum output power of a 42 GHz cw/long pulse gyrotron," *Proceeding of IVEC*, 2009.
3. Kumar, A., U. K Goswami, S. Poonia, U. Singh, N. Kumar, M. K. Alaria, A. Bera, H. Khatun, and A. K. Sinha, "Integrated design of undepressed collector for low power Gyrotron," *Int. J. of Millimetre and Infrared*, Vol. 32, 2011.
4. Nusinovich, G. S., *Introduction to the Physics of Gyrotron*, The Johns Hopkins University Press, Maryland, USA, 2004.
5. Gold, S. H. and G. S. Nusinovich, "Review of high-power microwave source research," *Rev. Sci. Instrum.*, Vol. 68, 1997.

New Measuring Instrument for the Characteristics of the Two-phase Flow of the Particulate Material Based on the Microwaves and Digital Processing of the Signals. Constructional Design Issues

V. F. Novikov
Novosibirsk State Technical University, Russia

Abstract— A scheme of the new measuring instrument for the characteristics of the two-phase flow of the particulate material moving inside the metal pipe line is described. The quantity of material in the flow, the range of velocities of the separate flow components, the discharge rate of the flow during any period are simultaneously measured on-line. The instrument and the measuring method are protected by patent of the Russian Federation.

In the previous author's published works, the problems connected with the development of the measuring instrument theory were solved. The discussion of the questions appearing for the first time during the design of such measuring instrument was started. The discussion is connected with the transportation of the milled coal — the pulverized coal in metallurgy and power engineering. This problem in the sphere of pneumatic conveying of the particulate materials is considered to be the most complex and actual (connected with the opportunity of the coal saving in combined heat and power plants and decreasing the amount of pollutant emissions in the air) and complex (the conveying material is mordant).

A lot of attention is paid underneath to the special design features of the input/output devices on the connected wave guides — bridges for the microwaves energy in/out of the pipe line. A rectangular waveguide is used for a pipe line as primary launching wave guide. The narrow plate in the connection area is taken out ("complete connection"). A peculiar feature is that here it is reasonable to design bridges based on connected wave guides with different sections, opposite to usually applied wave guides with identical sections.

Another characteristic property of considered devices is that it is necessary to introduce in their configuration the so-called "dielectric window" for the acoustical uncoupling of two wave guides. The isolator (dielectric) in "dielectric window" should be durable and must not contribute to friction electrification .Such properties are possessed by isolators from metal oxides. They are marked by the high magnitude of the dielectric constant and while using they destroy the primary bridge setting-up.

The solutions of the given problem are considered. The results of the electrodynamic modeling and experimental research of the bridge on connected wave guides with different sections are presented; in "dielectric window" very hard ceramics is used. The pipe line caliber is 65 mm, the section of the primary launching rectangular wave guide is 61×10 mm. Operating frequency is 3000 MHz.

A SiGe Voltage-controlled Oscillator for 4G LTE Applications

J.-M. Wu[1], **S. Chou**[2], **and Z.-C. Hong**[1]

[1]Department of Electronic Engineering, National Kaohsiung Normal University, Taiwan
[2]T&C Technologies Inc., Taiwan

Abstract— A voltage-controlled oscillator (VCO) for fourth generation (4G) long term evolution (LTE) applications is designed and implemented using a standard 0.35-μm SiGe BiCMOS foundry process in this paper. A crucial goal for the design is to achieve low phase noise required in 4G LTE systems under a low supply voltage. The presented VCO design is based on a NMOS-only cross-coupled pair with an integrated LC tank. An on-chip inductance is used in place of a tail current transistor in a conventional NMOS-only cross-coupled oscillator, which can reduce the supply voltage of the VCO. A phase noise is inversely proportional to the ratio of Q factor to inductance in a tank. Therefore, the tank with high ratio of Q factor to inductance is adopted for low phase noise. A supply voltage of 1 V is used with a power consumption of 5 mW. Measurements of the VCO are made, revealing that the frequency tuning range is 5.4%; the output power is −0.9 dBm; the second harmonic suppression is −29 dBc, and the phase noise is −116 dBc/Hz at a 1 MHz offset.

Planar Heterojunction Diode for Millimeter Waves Detection

A. Sužiedėlis[1], **S. Ašmontas**[1], **A. J. Kundrotas**[1], **J. Gradauskas**[1], **A. Čerškus**[1], **V. Nargelienė**[1], **and T. Anbinderis**[2]

[1]Center for Physical Sciences and Technology, Savanorių Ave. 231, Vilnius LT-02300, Lithuania
[2]Elmika Ltd., Naugarduko St. 41, Vilnius LT-03227, Lithuania

Abstract— Millimeter wave (MMW) receiving systems have been extensively developed in recent years since the waves have better propagation properties in dielectrics and atmosphere, and lower noise characteristics are inherent to the systems in comparison with infrared systems. Deeper insight in a MMW system properties including device fabrication peculiarities provide a shift towards terahertz (THz) region thus giving new possibilities of application in medicine, material research, telecommunication and military sphere.

We have proposed to use a GaAs/AlGaAs point contact heterojunction diode as a detector of electromagnetic radiation both in centimeter [1] and millimeter [2] wavelength ranges. It is an alternative for the present-day very sensitive, however, insufficiently robust detector in millimeter and submillimeter range based on metal/semiconductor Schottky junction [3, 4]. Use of the point contact diodes at higher frequencies becomes inconvenienced due to reduced dimensions of a waveguide. Therefore, to overcome these shortcomings planar GaAs/AlGaAs heterojunction diodes detecting radiation from microwaves up to the infrared were designed [5]. However, strong dependence of the detected voltage on frequency leading to reduced sensitivity at higher frequencies was observed. The heterojunction having potential barrier height $\sim 0.3\,\mathrm{eV}$ was formed between n-GaAs and n-$Al_{0.3}Ga_{0.7}As$ semiconductors. The barrier height was low enough for direct detection of the microwave radiation without external bias voltage, however, its value could determine strong frequency dependence of the detected voltage. Therefore, it is desirable that the heterojunction energetic barrier should be lower leading to weaker dependence of the detected voltage on frequency and thus higher sensitivity at higher frequencies.

Theoretical and experimental investigations of millimeter wave detection using planar microwave diodes on the base of small area GaAs/$Al_xGa_{1-x}As$ heterojunctions with various AlAs mole fraction x values are presented in this report. The microwave detectors with $x = 0.1$; 0.2; and 0.25 were investigated in K_a, W and D frequency ranges. Voltage sensitivity of the heterojunction diodes was achieved to reach thousands of volts per watt at the low-frequency end of the K_a range, while at 170 GHz the sensitivity dropped down to $(30 \div 80)\,\mathrm{V/W}$. However, the dependence of the voltage sensitivity on frequency did not follow the law determined by the intervalley scattering mechanism in a multi-valley semiconductor [2]. Possible reasons of the frequency dependence are discussed in this report.

REFERENCES

1. Sužiedėlis, A., S. Ašmontas, V. Kazlauskaitė, and J. Gradauskas, "Sensitivity increase of a point contact hot carrier microwave detector," *Electronics Letters*, Vol. 45, No. 25, 1328–1329, 2009.
2. Sužiedėlis, A, S. Ašmontas, J. Kundrotas, V. Nargelienė, and J. Gradauskas, "Voltage sensitivity of point-contact GaAs/AlGaAs heterojunction microwave detector," *Phys. Scr.*, Vol. 85, 035702 (5pp), 2012.
3. Crowe, T. W., R. J. Mattauch, H. P. Roser, et al., "GaAs Schottky diodes for THz mixing applications," *Proc. IEEE*, Vol. 80, No. 11, 1827–1841, 1992.
4. Shashkin, V. I., V. L. Vaks, V. M. Danil'tsev, et al., "Microwave detectors based on low barrier planar Schottky diodes and their characteristics," *Radiophysics and Quantum Electronics*, Vol. 48, No. 6, 485–490, 2005.
5. Gradauskas, J., A. Suziedelis, S. Asmontas, et al., "Sensitive planar semiconductor detector from microwave to infrared applications," *IEEE Sensors Journal*, Vol. 10, No. 3, 662–667, 2010.

Temperature Compensated Bulk Acoustic Wave Resonator Using Doped Silicon Dioxide

Hosoo Park, **Insang Song**, **Sang Uk Son**, **Jea-Shik Shin**, **Moon-Chul Lee**, **Chul-Soo Kim**, **Duck-Hwan Kim**, **Jing Cui**, **Keum-Su Song**, **and Ki Young Kim**
Future IT Research Center, Samsung Advanced Institute of Technology, Yongin 446-712, Korea

Abstract— There have been great needs for RF filters and duplexers meeting a narrow band gap in order to obey the cellular standards in wireless communication devices. The band gap is affected by several factors like environment temperatures, fabrication tolerances and circuit designs. Typically, temperature is an uncontrollable variable because of the operation environment of wireless devices. A bulk acoustic wave (BAW) resonator is a fundamental component of a RF filter and has advantages of high quality factor (Q), high effective coupling constant (kt^2), low noise as well as CMOS compatible silicon processes. The BAW resonator consists of a piezoelectric layer sandwiched between bottom and top electrodes. Its resonance frequency shifts as an environment temperature changes, normally ranging $-25 \sim -30\,\mathrm{ppm/^\circ C}$, of which phenomenon is referred to temperature coefficient of frequency (TCF). When a resonator has a large TCF value, the gap between adjacent bands is reduced and interference occurs. To overcome this problem, the BAW resonator should have a low TCF value. So far, the use of silicon dioxide on the top electrode and under the bottom electrode has been a prevailing method for temperature compensation of the BAW resonator because of a positive TCF trend of silicon dioxide. Thicker silicon dioxide can provide more temperature compensation effect however drawbacks such as frequency shift and low Q are also accompanied. In this work, a temperature compensated BAW resonator with doped silicon dioxide is proposed. The doping is intended to harden silicon dioxide at a microstructure level and thereby make it have small stiffness change over temperature, which is known to determine TCF of the BAW resonator. With this approach, a significant improvement of TCF was achieved as $-4.5 \sim -1.2\,\mathrm{ppm/^\circ C}$ with boron doping of $5 \times 10^{15}/\mathrm{cm}^3$ and $-4.3 \sim +1.1\,\mathrm{ppm/^\circ C}$ with phosphorus doping of $1 \times 10^{16}/\mathrm{cm}^3$, respectively. This temperature compensated BAW resonator can be used for low TCF RF filters and duplexers.

Plasma Relativistic Microwave Amplifier

P. S. Strelkov, **E. I. Ivanov**, **and D. V. Shumeiko**
Prohorov General Physics Institute, Vavilova 38, Moscow, Russia

Abstract— The mechanism of amplifying of the microwave signal in the plasma relativistic microwave amplifier is similar to the mechanism of amplifying of the electromagnetic wave in the ordinary traveling-wave tube. The amplifying comes when the electrons beam velocity is nearly equal to the phase velocity of the electromagnetic wave. In order to slow down the wave, in vacuum microwave electronics they put a spiral in cylindrical waveguide or use metal ripple waveguide. The dispersion of this slowing structure determines the frequency band in which the effective amplifying is possible. To amplify the entering signal in some other frequency band, one should work out another amplifier with a new slowing structure. The dispersion of waves in plasma waveguide is determined by the diameters of smooth metal waveguide, electron beam, plasma and plasma density [1]. During the experiment, the plasma density may change very fast in usual time of 100 mks. That's why plasma relativistic microwave amplifier affords to change one frequency band of the amplified signal to another without changing the construction of the device.

The main difficulty of creating a powerful microwave amplifier (with an amplifying coefficient of 30 dB) is the drop-out of the self-excitation. The vacuum relativistic microwave electronics uses here the several sections managed to excite in them different modes with the frequency fixed. That's why these amplifiers have very narrow amplifying frequency band. To extract the self excitation, the plasma relativistic microwave amplifier uses microwave absorbent similarly to the non-relativistic microwave amplifiers, because the frequency band of absorption of such absorbents is high. Still, this method is not sufficient. To reduce the positive feedback we use the mechanism of the resonance of the fast cyclotron wave of the electron beam and plasma wave reflected from the outcome radiating device. The experiments brought another way of reducing of generation. It turned out that, having the high incoming signal, which makes the outcoming signal near to nonlinear regime the level of the generation near the main frequency reduces dramatically.

As a result, we created the plasma relativistic microwave amplifier with the band of changing frequency from 2.4 to 3.2 GHz, with outcoming power of 60–100 MW, effective microwave pulse duration of the 300 ns, efficiency 6–10%, with amplifying coefficient of 30 dB, with signal-noise ratio at 25–32 dB.

REFERENCES

1. Bogdankevich, I. L., I. E. Ivanov, and P. S. Strelkov, "Experimental study and numerical simulations of a plasma relativistic microwave amplifier," *Plasma Physics Reports*, Vol. 36, No. 9, 762–771, 2010.

SOI CMOS Miniaturized Tunable Bandpass Filter with Two Transmission Zeros for High Power Applications

Do-Kyung Im, Donggu Im, and Kwyro Lee
Department of EE, Korea Advanced Institute of Science and Technology, Daejeon, Korea

Abstract— This paper presents a capacitor loaded tunable band-pass chip filter using planar multiple split ring resonators (MSRRs) with two transmission zeros. To obtain high selectivity and minimize the chip size, asymmetric feed lines are adopted to make a pair of transmission zeros located on each side of pass-band. Compared with conventional filters using cross-coupling or source-load coupling techniques, the proposed filter uses only two resonators to achieve high selectivity through a pair of transmission zeros. This saves chip area by removing an additional resonator for transmission zeros. In order to optimize selectivity and sensitivity (insertion loss) of the filter, the effect of the position of asymmetric feed line on transmission zeros and insertion loss is analyzed. The digitally programmable 1 bit capacitor composed of metal-insulator-metal (MIM) capacitor and stacked-FETs is loaded at outer rings of MSRRs to tune passband frequency and handle high power signal up to +30 dBm. By turning on or off the gate of the transistors, the passband frequency can be shifted from 4 GHz to 5 GHz. The proposed on-chip filter is implemented in 0.18-μm SOI CMOS technology that makes it possible to integrate high-Q passive devices and stacked-FETs. The designed filter shows miniaturized size of only 4 mm × 2 mm (i.e., $0.177\lambda g \times 0.088\lambda g$) is implemented, where λg denotes the guided wave length of the 50 Ω microstrip line at center frequency. The insertion loss and return loss at the center frequency are −1.5 dB and −15 dB for the 5 GHz band, and −3 dB and −10 dB for the 4 GHz band, respectively.

A Continues 360° CMOS Phase Shifter for 60 GHz Phased Array Applications

H. Aliakbari[1], **A. Abdipour**[1], **A. Mohammadi**[1], **and R. Mirzavand**[2]

[1]Microwave/mm-wave & Wireless Communication Research Lab
Radio Communications Center of Excellence, Electrical Engineering Department
Amirkabir University of Technology, Iran
[2]Institute of Communications Technology and Applied Electromagnetics
Amirkabir University of Technology, Iran

Abstract— The overall designing of one 90 nm CMOS passive reflective-type phase shifter for the first three channels in 60 GHz band is described. The performance investigation is based on full wave electromagnetic (Momentum) analysis and optimization. This procedure resulted in 360° continues phase shifting with an average insertion loss of 5.5 dB over all phase states, which is desirable for the 60 GHz phased array front ends.

Introduction: The 60 GHz band is of much interest since the wide 7 GHz allocated unlicensed bandwidth enable multi-Gb/s wireless transmission over typical indoor distances. Phased array is one solution for directing the electromagnetic energy to the intended target and is very useful for high path loss in MMW wireless transmitter systems [1]. Furthermore, RF phase shifter is of interest due to the smaller number of physical circuit elements [1]. Nowadays the main efforts in RF phased array configuration is on designing low-loss phase shifters with an analog 360° phase shifting, especially in a low cost CMOS technology. This paper presents a 360° continues CMOS phase shifter, which is desirable for the 60 GHz phased array front ends.

Structure and Simulation Results: A 3-dB CMOS quadrature coupler which use broadside coupling between lines is utilized in RTPS configuration (Figure 1(a)). The current lines are isolated from silicon which has an advantage in lower propagation loss. The analog 360° phase shift in addition to the low loss variation capability of the RTPS can be achieved by optimizing the impedance of the reflective load in EM Simulator [2]. Simulation results in Figure 1(b) shows that more than 360° phase shift can be achieved by varying the applied bias voltage of CMOS varactors which have been used in the Reflective loads.

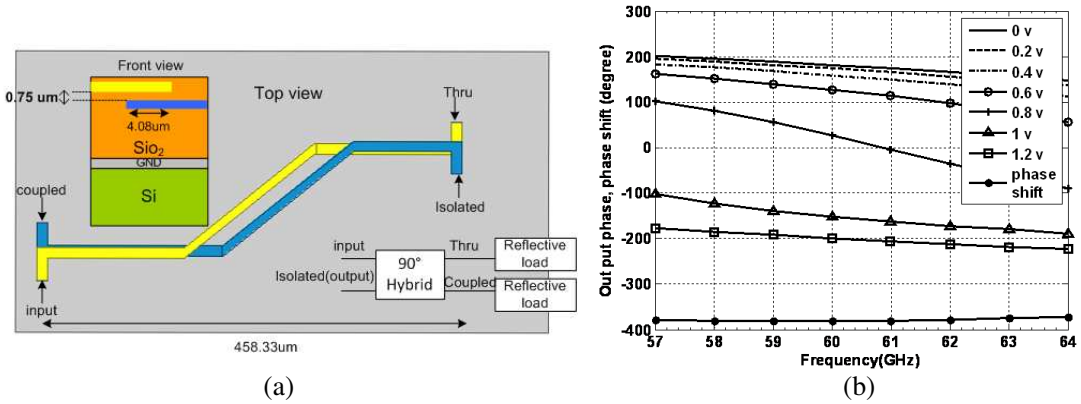

Figure 1: (a) RTPS structure and the layout of the broad side CMOS coupler. (b) Full-wave simulated output phase versus frequency for various varactor control voltages.

REFERENCES

1. Kwang-Jin, K., J. W. May, and G. M. Rebeiz, "A millimeter-wave 16-element phased-array transmitter in 0.18-µm SiGe BiCMOS technology," *IEEE J. Solid-State Circuits*, Vol. 44, No. 5, 1498–1509, 2009.
2. Ellinger, F., R. Vogt, and W. Bächtold, "Compact reflective type phase shifter MMIC for C-band using a lumped element coupler," *IEEE Trans. Microw. Theory Tech.*, Vol. 49, 913–917, 2001.

Session 3A3
Remote Sensing, Imaging and Detection

Online Geomagnetic Field Monitoring System Using Mobile Devices

J. A. Cortés, **F. A. Medina**, **A. M. Knott**, **and I. Arellano**
Universidad Tecnológica de Pereira, Colombia

Abstract— The Earth's magnetic field has been used for centuries as an aid to navigation. Over the last two hundred years, it has been studied in ever-increasing detail, leading to current mathematical models of its overall behavior. More recently, there has been interest in its effect on living beings, especially in the possible effects of man-made electromagnetic fields on human health. Another area of interest is in seismology, where it is thought that changes in the magnetic field could serve as indicators of impending events such as earthquakes or volcanic activity. Both of these areas are more concerned with local variations in the magnetic field, which are less well documented. Such variations, known as anomalies, would require a large number of instruments collecting data, which would also need to be organized in terms of geographic location and time.

This study initially proposed the creation of an online internet database for geomagnetic field vector measurements, and the design and manufacture of a mobile magnetometer to acquire readings for the database. As a further development in view of advancing technology, and to allow a more widespread distribution of magnetic field readings, a mobile telephone application is being developed to take advantage of ubiquitous existing hardware to perform geo-referenced magnetic field measurements. This application, which is compatible with the popular Android operating system, will be available for anyone with a mobile device to download. Given the enormous mobile device user base, this should allow a large amount of data to be obtained. As the database grows, it is hoped that statistical analyses of data will permit correlation of geomagnetic field behavior and other studies.

Variability of GPS-derived Zenith Tropospheric Delay and Some Result of Its Assimilation into Numeric Atmosphere Model

O. G. Khutorova, G. M. Teptin, V. E. Khutorov, V. V. Kalinnikov, and T. R. Kurbangaliev
Kazan Federal University, Russia

Abstract— Numerical weather prediction is an initial and boundary value problem; the more accurate initial conditions could result in the improvement of forecast skill. Over the past decades, considerable progress has been made in satellite navigation systems monitoring technology, which is significantly increasing the atmospheric information. The total zenith tropospheric delay (ZTD) is an important parameter of the atmosphere and directly or indirectly reflects the weather processes and variations. This paper presents a hardware and software complex for continuous measurements and prediction of atmospheric thermodynamics. The main part is a network of ground-based spatially separated GPS-GLONASS receivers, which allows the remote sensing zenith tropospheric delay. Comparing the results with remote sensing data of weather stations, radiosonde and reanalysis showed good agreement. GPS-Derived Zenith Tropospheric Delay shows the day to day variation and mesoscale spatial and temporal variability. Variations of atmospheric integral water vapor were found. Comparison with the numerical weather reanalysis fields and solar photometer measurements showed agreement with the relative deviation of less than 10%. It is noted that when comparing the integral water vapor of satellite navigation system with numerical weather fields, differences arise relating to model overestimations for hydrostatic delay, which leads to integral water vapor underestimation of the moisture content of 0.42 to $0.50\,\mathrm{kg/m^2}$. Also, the differences are due to the additional liquid water contribution in clouds, which causes overestimation of integral water vapor up to $1.18\,\mathrm{kg/m^2}$. Hardware-software complex includes the numerical model of the atmosphere on a computational cluster. A variational assimilation system was used to examine the comparative impact of including satellite derived total zenith tropospheric delay from GPS and GLONASS ground observations. Preliminary results show that the initial field of wind and temperature was improved by assimilating the satellite derived ZTD.

Horizontal Structural Functions in Troposphere for Radio Waves Refractivity Index by Use of Ground Set of GPS-GLONASS Receivers

V. E. Khutorov, A. A. Jurravlev, and G. M. Teptin
Kazan Federal University, Russia

Abstract— In this paper, we show results of troposphere fluctuation analysis and its influence on radiowaves refractive index variations. For comparison of inhomogeneous impurities structure we used electromagnetic waves refraction index data which don't depend on impurity but depend on atmospheric parameters only. Our main object of investigation is a mesoscale process in troposphere. These processes have size from 1 km to 1000 km and time frames around few hours. This task requires system with good temporal and spatial resolution. We can estimate space structure of atmospheric parameters, using the data from network based on Global Navigation System receivers.

For analysis two independent networks of stations were used. The first network of automated stations measure main meteorological parameters. They are located in various sites within urban territory and spaced on distance from 0.9 up to 5.3 km from each other. The second network of GPS-GLONASS collects the data about spatial structure of electromagnetic waves refraction index. They are also located in various sites of city and spaced on distance from 0.83 up to 35 km from each other. Using data from each network we calculated spatial structure of refractivity index.

We used structure function to estimate characteristics of impurities and refraction index fluctuation. Structure function is a basic characteristic of process with random increments. Physically, structure function is a square of fluctuation of investigated parameter. Function shows the contribution of the processes of the defined scale in the total variance of the fluctuations.

The received structure functions demonstrate increasing with distance between stations. The results show a significant effect on electromagnetic wave refraction index caused by the mesoscale troposphere process.

Remote Sensing for Estimating Cultivated and Arable Land Areas on Slopes

Y. Fernandez-Ordoñez[1], **J. Soria-Ruiz**[2], **and M. Mauricio Vázquez-Rivera**[2]

[1]Colegio de Postgraduados, Mexico
[2]Geomatics Lab., National Institute of Research for Forestry Agriculture and Livestock (INIFAP)
Toluca, Mexico

Abstract— Planning and strategies of government subsidized programs for agriculture require accurate information about extents and classification of arable land for crop production. In Mexico 20% of arable land is on slopes and ravines, and cultivated extents vary from one agricultural cycle to the next one due to local practices and other factors. There is a problem posed for government decision makers to obtain accurate estimations of cultivated extents and arable land on a yearly basis. Surface values provided by photographic interpretations or by the producers themselves are inaccurate estimations. To increase accuracy a topographical survey of each parcel and current field data would be required for each agricultural cycle, a practical impossibility. Remote sensing (RS) technologies offer an alternative to timely estimate surfaces for decision making at different scales — local, regional or higher — to support planning and management of government programs. In some places RS based methodologies already provide information about seeded crops, advance estimated yields and accurate arable surfaces. These methodologies are well adapted to relatively flat and large areas. Sloped surface estimation directly from an optical satellite image introduces inaccuracies since the calculated values correspond to a planar view of the terrain. An adjustment method to control slope effects based on regression estimates and adjustment factors according to a slope classification is proposed. This work reports on a pilot study realized on an area located in Central Mexico which covers approximately 25 km^2. Plots with slope intervals of 0–9%; 9.1–19%; 19.1–29%; 29.1–39% and $> 39\%$, which were classified as simple or complex were considered. The plot areas were calculated by triangulation from polar coordinates using one or several points within each polygon on the images. The accuracy of the measurements was verified with topographical instruments on the field. Comparisons were made between remote sensing results and from field surveying data. The study concludes on the advantages and applicability of the method using images from SPOT and Ikonos sensors.

Extraction of Laver Cultivation Area Using SAR Dual Polarization Data

Mitsunobu Sugimoto and Kazuo Ouchi
Department of Computer Science, School of Electrical and Computer Engineering
National Defense Academy, 1-10-20 Hashirimizu, Yokosuka, Kanagawa 239-8686, Japan

Abstract— In this study, we show that laver cultivation area can be extracted more effectively with dual polarization data than with single polarization data. Synthetic aperture radar (SAR) has been proven to be one of the most useful sensors and therefore used in a variety of areas because of its all-weather and day-and-night observation capabilities with high resolution. While most traditional SAR systems operate on single polarization mode, recent technological advancements allowed us to develop and operate SAR systems with multi-polarization observation capability. Multi-polarization data have shown the potential to increase further the ability of extracting physical quantities of the scattering targets. While full polarization data have several advantages, they are relatively few compared with single or dual polarization data because of the operational costs and system constraints of full polarization SAR systems. Although there are many platforms that can be operated on full polarization mode, they are more often to be operated on single or dual polarization mode instead, because of those reasons. Therefore, dual polarization data (HH, VV) is a good compromise between single and full polarization data. Eigenvalue analysis [1] and coherence analysis [2, 3] are one of the methods that can effectively utilize dual polarization data. We used TerraSAR-X dual polarization data to perform experiments. Entropy/alpha decomposition and HH-VV coherence of dual polarization data were chosen as means to extract laver cultivation area and the methods utilizing dual polarization data showed better performance than the amplitudes of each individual polarization channel. These methods could be comparable to previously suggested polarimetric entropy based methods which require full polarization data [4, 5].

REFERENCES

1. Shan, Z., C. Wang, H. Zhang, and J. Chen, "H-α decomposition and alternative parameters for dual polarization SAR data," *PIERS Proceedings*, 1386–1390, Suzhou, China, Sep. 12–16, 2011.
2. Wang, H., M. Iwakiri, and K. Ouchi, "Some potential information in airborne single-pass Pol-InSAR data over land and sea," *Progress In Electromagnetics Research Symposium Abstracts*, Hangzhou, China, Mar. 24–28, 2008.
3. Velotto, D., M. Migliaccio, F. Nunziata, and S. Lehner, "Dual-polarized TerraSAR-X data for oil-spill observation," *IEEE Trans. Geosci. Remote Sens.*, Vol. 49, No. 12, 4751–4762, Dec. 2011.
4. Won, E. S. and K. Ouchi, "A novel method to estimate underwater marine cultivation area by using SAR polarimetric entropy," *Proc. IGARSS*, 2097–2100, Vancouver, Canada, Jul. 2011.
5. Yang, C. S. and K. Ouchi, "Monitoring of marine laver cultivation using two ALOS-PALSAR PLR acquisition mode data," *Proc. APSAR*, Seoul, South Korea, Sep. 2011.

Estimation of Parameters for a Combined Active-passive Surface Soil Moisture Retrieval Algorithm Based on Satellite and Airborne L-band Radar and Radiometer Measurements

María Piles[1], **Kaighin McColl**[2], **Dara Entekhabi**[2], **Narendra Das**[3], **Rajat Bindlish**[4], **Iliana Mladenova**[4], **and Thomas Jackson**[4]

[1]SMOS Barcelona Expert Centre, Universitat Politècnica de Catalunya
Passeig Marítim de la Barceloneta 37-49, Barcelona 08003, Spain
[2]Massachusetts Institute of Technology, 48-216G, Cambridge, MA 02139, USA
[3]Jet Propulsion Laboratory, 4800 Oak Grove Drive, Pasadena, CA 91109, USA
[4]USDA ARS Hydrology and Remote Sensing Laboratory, Beltsville, MD 20705, USA

Abstract— Microwave remote sensing in the L-band (1 to 2 GHz) is considered to be well-suited for the remote sensing of surface soil moisture, the state of the land surface water balance. The atmosphere is nearly transparent at these frequencies and vegetation cover is semi-transparent up to moderate densities. A sub-band of the L-band is reserved for radio-astronomy and hence also suitable for Earth monitoring microwave radiometery. The current ESA (European Space Agency) SMOS (Soil Moisture and Ocean Salinity) and the forthcoming NASA (National Aeronautics and Space Administration) SMAP (Soil Moisture Active Passive) mission include radiometer instruments for this purpose. Given the practical constraints on antenna size and altitude of low Earth orbits, the SMOS and SMAP radiometer data provide coarse-resolution (~ 40 km) mapping with global extent. The SMAP mission additionally includes an L-band radar instrument that will provide high-resolution measurements with a median resolution of about 3 km. The radar measurements are less sensitive to surface soil moisture due to scattering and attenuation by the rough soil surface and vegetation. The SMAP mission plans to take advantage of the higher sensitivity but coarse resolution L-band radiometry and the high-resolution but lower sensitivity radar measurements in order to produce ~ 10 km intermediate scale and intermediate accuracy surface soil moisture estimates. There are a number of key issues associated with the combined radar-radiometer soil moisture estimation approach. First the co-variability of the SMAP radiometer radiobrightness and radar backscatter to soil moisture, vegetation density and surface roughness need to be established. Second the issue of scale differences between the radar and radiometer measurements needs to be addressed given the high degree of heterogeneity over land surface. The SMAP radar-radiometer algorithm that is under consideration now encapsulates these two issues (co-variability of radiobrightness and backscatter, multiscale measurements and surface heterogeneity) into two parameters that should be nearly constant seasonally at each site. The two parameters depend on seasonal plant phenology and surface roughness but independent of soil moisture contributions. The parameters are defined such that they can be estimated based on existing airborne and satellite measurements. In this paper we present observational analysis of these two parameters based on NASA's Aquarius satellite-based L-band radiometer and scatterometer data as well as the NASA UAVSAR airborne synthetic aperture radar (L-band) measurements. The dependence of the two parameters on vegetation characteristics and their heterogeneity across major global biomes will be included in the presentation.

A Novel Proximity Measurement System Using Microwave Antennas

Yongjae Lee, Boris L. Sheikman, and Steven Y. Go
General Electric Corporation, USA

Abstract— In this paper, a novel approach for making proximity measurements using a microwave antenna system in an industrial setting is presented. The proposed technique is demonstrated by designing and building two differently sized antennas. Each antenna was placed inside its own mechanical housing in order to match the form and fit of a standard industrial eddy current sensor head. Matching the form and fit of currently accepted industrial dimensions will reduce the amount of redesign of the sensor mounts to accommodate the new system. Both of the differently sized antennas were designed to electrically resonate at a specific frequency. The first antenna was designed to resonate at $\sim 3\,\mathrm{GHz}$ and the second antenna was designed to resonate at $\sim 5.8\,\mathrm{GHz}$. A vector network analyzer (VNA) is used to create the excitation signals and to monitor return loss changes as the observed target's displacement to the antennas is varied. Additionally, a linear stage from Thor Labs was used to carefully and repeatedly step a flat metal target away from the sensor head with the embedded antenna. This new system showed an extended measurement range compared to the conventional proximity measurement technologies. The microwave antenna system was able to measure a distance equal to at least $1\times$ the diameter of the probe tip. Also, good sensitivity, i.e., significant return loss change ($> 1\,\mathrm{dB/mm}$), was obtained as the observed the target displacement is varied. Furthermore, it showed great immunity to variations in permeability across a selection of meatal targets. For example, at a fixed target displacement, the *Sll* variation between the different target material was $< 5\%$. A commercial software package, Ansys' HFSS, was utilized for the design, modeling, and analysis of the overall microwave antenna system. The modeling results matched the performance of the prototypes to within 3%. Future work in the areas of temperature stability, materials, and signal processing methodologies is also presented.

Modelling the GNSS Reflectometry Signal over Bare and Vegetated Land

Nazzareno Pierdicca[1], **Leila Guerriero**[2], **Marco Brogioni**[3], **and Alejandro Egido**[4]

[1]Department of Information Engineering, Electronics and Telecommunications
Sapienza University of Rome, via Eudossiana 18, Rome 00184, Italy
[2]Department of Computer Science, Systems and Production
Tor Vergata University of Rome, Via del Politecnico, 1, Rome 00133, Italy
[3]CNR-IFAc, Sesto Fiorentino, FI, Italy
[4]STARLAB, C/Teodor Roviralta, 45, Barcelona 08022, Spain

Abstract— The GNSS Reflectometry (GNSS-R) signal (i.e., the one transmitted by the navigation satellites and scattered from the earth surface) is the output of a signal correlation operation, and it is a function of the time delay and of the Doppler shift, i.e., the so called delay-Doppler map. It has been mathematically described in a fundamental work by Zavorotny and Voronovich (2000). When the observed surface is characterized by small scale roughness with respect to wavelength, like in the case of bare soil or vegetated fields, the bistatic signal consists of both a coherent and an incoherent component and, according to recent studies, the coherent scattering in the specular direction can largely overpass incoherent scattering. In the present work, the Advanced Integral Equation Model in the bistatic configuration will be considered to represent the incoherent scattering component from land surfaces, and a formulation for the coherent component of the bistatically scattered field from bare soil will also be introduced. The latter has been derived by generalizing the theory in Fung and Eom (1983), which was limited to the specular and the backscattering directions only. Vegetation (crop and forest) scattering contribution has been also considered through a discrete bistatic approach. It will be pointed out that the knowledge of the relative magnitude of the coherent and incoherent components is an important issue, since they own a different sensitivity to Soil Moisture Content and to the soil coverage biomass, which are the parameter that can be monitored over land by a GNSS-R receiver.

The results that will be presented in this work have been obtained through a GNSS-R signal simulator which has been developed in the framework of the LEiMON project and supported by ESA. Examples of the LEiMON simulator results will be shown to point out the relative contribution of the coherent and incoherent component in the receives signal. The simulator output has been also compared to experimental data collected during the project by a GNSS-R receiver developed by STARLAB. The aim was the assessment of the sensitivity to soil moisture and vegetation biomass as predicted by the model and observed during the experimental campaign.

Session 3A4
Antenna Technologies for Broadband and High-speed Wireless Systems

Metrics of Compactness and Bandwidth for Multiport Communications Antennas

Rodney G. Vaughan[1] **and Jane Xing Yun**[2]

[1]School of Engineering Science, Simon Fraser University, BC, Canada
[2]Norsat International, BC, Canada

Abstract— Multiport antennas are for beamforming, and this is used in MIMO communications. In many propagation environments MIMO offers higher throughput for a given spectral resource. New multiport antenna designs are continually appearing in the literature, but few are analyzed for their fundamental antenna performance parameters of compactness and bandwidth. Although single port antennas have standards for their measured characterization, multiport antennas do not yet have parameters fully developed for their evaluating their performance. For MIMO, the multiport antenna structure and the element terminations impact the performance. Characterization of the antenna effectiveness needs to include this impact. A single metric that compares expected communications performance via compactness and bandwidth would be helpful to systems designers. It would also be useful for antenna designers, who seek to understand and deploy trade-offs between performance and compactness. But this is complicated because the system performance depends on more than just the antenna structure. Here, approaches are discussed for developing a spatial efficiency metric for multiport antennas. These include Chu theory (bandwidth-compactness for a single element) adapted for multiport antennas, the diversity/MIMO signal combining algorithm, mutual coupling, finite correlation, and propagation environment modeling. The combined result is a single figure-of-merit which allows direct comparison between different antenna concepts, designs and configurations operating in different statistically modelled propagation environment. Results for this spatial efficiency will be presented for canonical benchmarks such as idealized (lossless, perfectly uncoupled, perfectly matched) linear and planar arrays, a realized 12-port cube antenna, and a 48-port spherical antenna.

Half Loop Antenna with Ultra-wide Bandwidth

Tae-Hwan Jeong and Jong-Myung Woo
Department of Radio Science and Enginnering, Chungnam National University
99 Daehak-ro, Yuseong-gu, Daejoen 306-764, Korea

Abstract— This paper proposes an ultra-wideband half loop antenna for aircraft. The basic structure of the proposed antenna is a loop antenna applied self-complementary structure to obtain ultra-wide band. The ultra-wide band loop antenna is changed into a half loop structure on the ground plane by using image effect This change reduces the size of the loop antenna in half and the half loop antenna can be installed on metallic surface of aircraft. To minimize wind load for the half loop antenna on aircraft, the height of the antenna is reduced from 0.155λ to 0.11λ where λ is free space wavelength at 0.3 GHz. The overall size of the designed antenna is $315 \times 295 \times 110\,\mathrm{mm}^3$ ($0.315\lambda \times 0.295\lambda \times 0.11\lambda$). The measured -10 dB bandwidth is 100 : 1 ($0.3 \sim 30$ GHz). It shows extremely ultra-wide bandwidth. The radiation pattern in xy-plane shows monopole like radiation pattern and the gain is higher than 0 dBi in the measured frequency $0.3 \sim 18$ GHz. The proposed half loop antenna was simulated with an unmanned aerial vehicle (UAV) to verify the radiation pattern. The antenna was installed on the fuselage of UAV. As a result of the simulation, the radiation pattern on UAV was similar to that of the half loop antenna.

Wideband Linear Antenna with H-shaped Parasitic Element

R. Suzuki[1], **H. Morishita**[1], **and F. Sakuma**[2]

[1]Department of Electrical and Electronic Engineering, National Defense Academy, Japan
[2]Sakuma Antenna Co., Ltd., Japan

Abstract— Many type of linear antennas are widely used in the mobile communication, because they have a simple and light structures. Sleeve antennas, which are one of linear antennas, have a possibility of wider bandwidth. In this paper, a new type of there antennas is prepared and it's characteristics are analyzed. The antenna mainly consists of a semi-rigid coaxial cable and is basically a monopole antenna with no ground plane and X-wire element. X-shaped wire element is loaded with the outer surface of a coaxial cable near the feed point. The antenna length is about a half wavelength and the monopole length is a quarter wavelength. The center frequency is 2.5 GHz in the analysis. The bandwidth is from 1.9 GHz to 6.9 GHz where the VSWR is less than 4 except that from 2 GHz to 2.6 GHz. The bandwidth is from 2.7 GHz to 2.8 GHz, from 3.6 GHz to 5.0 GHz and from 5.7 GHz to 6.3 GHz where the VSWR is less than two. The radiation patterns are almost the same as those of a dipole antenna. Next study of new type of the antenna, where X-shaped wire element is changed to H-shaped palte element, is also investigated.

Reduction of Cross Polarization in Circularly Polarized Broadband Waveguide Antenna Using an L-shaped Probe

S. Yamaura and T. Fukusako
Computer Science & Electrical Engineering
Graduate School of Science & Technology, Kumamoto University, Japan

Abstract— This paper presents a circularly polarized broadband waveguide antenna with low cross polarization. The antenna which consists of a square waveguide aperture, and an L-shaped probe has wideband circular polarization (CP) characteristics. CP is generated by the L-shaped probe which gives a perturbation to the degenerating mode of TE_{10} and TE_{01} mode for the orthogonal electric fields in the waveguide. The center frequency is chosen to be close to the middle value of the cutoff frequency between that of the dominant mode (TE_{10}/TE_{01}) and the second higher-order mode (TE_{20}/TE_{02}). The cross polarization gets worse at a higher frequency which is close to the cutoff frequency of the TE_{20}/TE_{02} This is due to the effect of higher-order mode of TM_{11} For avoiding this effect, four thin metal poles ($2\,\text{mm} \times 2\,\text{mm} \times 52\,\text{mm}$) are installed at the inside corners of the waveguide to reduce cross polarization. The cross polarization becomes lower in the wide azimuth range because the slender poles reduce the electric field concentrating at the corners. As a result, circular polarization with low cross polarization over a wide azimuth range is also achieved even in the higher frequency. The obtained AR bandwidth of the proposed antenna is 54.4% (6.68–11.67 GHz).

The proposed circularly polarized broadband antenna could be available as primary radiator of a parabolic antenna and Pulse radar, Ultra Wide Band technology.

A Compact Tapered Slot Antenna for UWB Applications with Improved Characteristics

Abdelelah M. Alzahed[1], **Dalia M. Nashaat**[2], **Hazem H. Ali**[1], **and Esmat. A. Abdallah**[2]

[1]Arab Academy for Science & Technology and Maritime Transport, Egypt
[2]Electronics Research Institute, Egypt

Abstract— Planar antennas have the advantages of small size, low profile, and easy to mount hosts and are very promising candidates for satisfying this design consideration. The tapered slot-line antenna as one type of the planar antennas is a travelling-wave end-fire antenna [1] with advantages of uni-directive beam, and thin sheet structure. They are used widely in many applications such as the elements of phased arrays, the feed of reflector or reflect array, the UWB radiator for time-domain systems, etc. However, its gain is less than a broadside antenna with similar size. Also, the bandwidth depends on the ratio of the maximum/minimum of the slot-width and the length of taper. The TSA has the disadvantages of complex matching and high back lobe level. The feeding structure usually consists of a microstrip feeding line coupled to the slot line of the tapered antenna. Tapered antennas are classified according to the shape of the taper. The most important types are linear tapered slot antenna, exponential tapered slot antenna, Vivaldi antenna, elliptical tapered slot antenna, etc. Many techniques are used to improve the radiation pattern and bandwidth such as cavity behind the slot, using aperture coupling, using the proper shapes for the slot, using a combination of the shape of feed and slot, etc.

In this paper our objective is to enhance the bandwidth and antenna matching through adding a metallic strips (gratings) in front of the taper aperture that enhanced the S_{11} parameter of the antenna and gain. Then slits in the taper edges also enhance the antenna return loss and the frequency response for UWB range. The antenna was simulated by using CST Microwave Studio Software. The whole antenna was fabricated on a copper coated low loss dielectric substrate with relative permittivity of $\varepsilon_r = 2.2$, dielectric thickness $h = 0.5\,\text{mm}$, and loss tangent $\tan\delta = 0.0004$, using photolithographic technique. The fabricated antenna was tested using ES 8719s Agilant vector network analyzer. The experimental measurements agree well with electromagnetic simulations.

REFERENCES

1. Xu, H. Y., H. Zhang, and J. Wang, "Study on an UWB planar tapered slot antenna with gratings," *Progress In Electromagnetics Research C*, Vol. 1, 87–93, 2008.

Design of Ultra-wideband MIMO Antenna for Mobile Handset Applications

Hong-Kyun Ryu and Jong-Myung Woo
Department of Radio Science and Engineering, Chungnam National University
99 Daehak-ro, Yuseong-gu, Daejoen 306-764, Korea

Abstract— Recently, multiple-input multiple-output (MIMO) antenna technology is becoming very popular in wireless communication systems because this technology can significantly improve data transmission speed and channel capacity. The technology has been adopted in several wireless communication systems and a compact wideband MIMO antenna is needed for mobile handset applications.

This paper presents an ultra-wideband MIMO antenna covering WCDMA, WLAN, WiMax and UWB bands for mobile handset applications. The designed ultra-wideband antenna is consisted of a folded monopole antenna coupled with inverted-L element and meander lines. An open stub is inserted in the folded monopole to block 5 GHz WLAN band which interferes to UWB band. The proposed antennas are symmetrically placed on top part of the mobile handset ground for MIMO antenna technology. Meander lines are positioned between two antennas for improving the isolation in operation bands. The size of the designed MIMO antenna is 55 mm × 13.5 mm. The −10 dB bandwidth was measured as 1.85 ∼ 11.9 GHz without the rejected band (5.15 ∼ 5.85 GHz). The isolation between two antennas is higher than 17.2 dB. Average gain and total efficiency are 4.96 dBi and 91.4% respectively. Due to the compact size and ultra-wide bandwidth, the proposed antenna is a good candidate for a mobile handset antenna that has a limited space available.

Circularly Polarized Leaky Wave Antenna Using Composite Right/left-handed Transmission Line

M. Ishii and T. Fukusako
Computer Science & Electrical Engineering
Graduate School of Science and Technology, Kumamoto University, Japan

Abstract— In recent years, various kinds of leaky wave antennas using composite right/left-handed transmission line have been reported. Such antennas are able to change the radiation direction by changing the operating frequency, and can be applied for radars and sensors. Considering the advantages, this talk presents a circularly polarized leaky wave antenna with the composite right/left-handed transmission structure consisting of an inter-digit and an inductive parallel stub in a unit cell.

For generating circular polarization (CP) in this research, the authors tried to generate CP by using the effect of the radiation from the edge of the ground plane and by adjusting the position of antenna elements in-between the both edges. Especially, the position of the antenna element strongly contributed to improve axial ratio characteristics since the intensity of electric field on the edge of ground plane is controlled. After some optimizations, a bandwidth of 21.8% at 2.7 GHz in axial ratio (< 3 dB) was obtained in both simulation and measurement in the frequency around 2.3 GHz to 3.2 GHz, where the group velocity changes from negative to positive. This results in a beam-steerable circularly polarized antenna with variable frequency. However, a structure which doesn't depend on the antenna position in the ground plane may be required for some applications. Hence, a thin metal wall was embedded in the substrate to control the electric field above the ground plane. This method was found to be effective to obtain good axial ratio. In this talk, this effect will be also presented.

Beam Steering Microstrip Array Antenna Using Orthogonal Excitation

Yu Ushijima, Takeshi Kondo, Eisuke Nishiyama, and Ichihiko Toyoda
Graduate School of Science and Engineering, Saga University, Japan

Abstract— A novel beam steering microstrip array antenna is proposed and the basic antenna characteristics are investigated in this paper. This proposed beam steering microstrip array antenna consists of square patch array, two feed line circuits and a Magic-T. The array antenna is fed by two RF signals with 90 degree phase difference. By changing a ratio of the two RF input powers, it is possible to tile the beam direction of the array antenna. The array elements divide into two array segments. One of the array segments is excited by addition of the two orthogonal RF signals and the other is excited by subtraction of them. As the two input signals are 90 degree phase different, the phase θ of the additional signal is given by an arc-tangent of the RF signals, and the phase of the subtracted signal is an opposite phase of the additional signal. Therefore, the phase difference of the two array segments is 2θ according to an arc-tangent of the amplitude ratio of the orthogonal input RF signals.

In order to realize the additive and subtractive feeding to the segments, a Magic-T circuit is effectively used in the antenna feed circuit. The Magic-T circuit is a kind of directional couplers. It is constructed by the use of the Both-Sided MIC technology in this paper. When two RF signals with 90 degree phase difference are input to the two input ports of the Magic-T, the additive and substantive signals are output from two output ports each other. These transformed signals excite antenna elements of two array segments each other through the feed circuit. Consequently, the antenna beam can be tilt according to the amplitude ratio of the two orthogonal input RF signals. The basic behavior of the proposed antenna is confirmed experimentally. The maximum of the beam tilt of approximately 15 degree is obtained.

Therefore, the proposed antenna will be practically attractive for beam steering RF sensor in many wireless applications with very simple and compact configuration.

Dielectric Rod Antenna Array with SIW Feed Network for Radar Imaging System

Robab Kazemi and Ramezan Ali Sadeghzadeh
K. N. Toosi University of Technology, Tehran 1431714191, Iran

Abstract— Typical array design requirements to achieve high radiation efficiency include low return loss, high gain and minimum feed network insertion loss. The array gain and radiation patterns are functions of the elements' spacing and differential phase between its elements. Using element spacing beyond one wavelength would generate grating lobes in addition to increasing the antenna size, while an inter-element spacing of $\sim 0.9\lambda$ would lead to a maximum directivity. This limits the dimensions of the individual antenna elements and makes using bulky feeds like horns difficult. Dielectric Rod Antennas (DRAs), however, could be designed with even relatively close spacing for a compact overall size due to their high decoupling efficiency without significant gain drop.

One problem, however, in implementing DRA arrays is the difficulty of designing an efficient feed network with a high packing density. We utilize a low loss eight-way splitter that was thoroughly optimized using CST Microwave Studio. This splitter was designed using SIW guides that has 0.4λ (12.1 mm) width for single mode operation at X-band, and provided over 4 GHz operating band with less than 1.1 dB insertion loss when a 1.524 mm thick substrate with a loss tangent of 0.0027 is used.

The structure of the feed network and its measured characteristics are presented in Fig. 1. As can be seen, this feed network covers over 40% bandwidth, and has better than 10 dB return loss and a good power division at the desired frequency range, with less than $\pm 4^\circ$ and ± 0.9 dB phase and amplitude imbalance, respectively.

A prototype eight-element DRA was built by inserting a concentric two-layer rod at the end of each Vivaldi antenna element as shown in Fig. 2(a). By adding the rods, the mutual coupling effects are significantly reduced, especially around the lower end of the frequency band. In our implementation, the separation between the rod center points has been selected to be 0.4λ (12.1 mm) and the overall size of the structure, including the rods, is 10 cm × 9 cm.

As shown in Fig. 2(b), the input return loss is better than 10 dB within the X-band and measured result agrees well with the simulation result. Measured E-plane radiation patterns at different frequencies are shown in Fig. 2(c). Well-formed beams are generally obtained, and the patterns are very similar across the band. The half power beamwidth in the E-plane is 13° with a gain of 14.5 ± 2 dB over the frequency band, side lobe level less than -14 dB and front-to-back ratio is better than 27 dB. Meanwhile, the antenna provides a symmetric radiation pattern with relatively low cross polarization of better than -19 dB.

Since the ultimate purpose of this antenna is for imaging, its performance as a subarray in a full array has been evaluated as a receiving antenna in an imaging system. A UWB standard horn with 1–18 GHz range is used as a transmitting antenna and the developed array is for receiving. The eight subarrays are spaced at 3 cm and the reflected signals from a target located at 1.5 m were collected one at a time using the SAR algorithms. Fig. 2(d) shows the image of a target. The obtained image demonstrated a much higher resolution without side images (i.e., ghost signals). DRAs generally have high x-pol levels that could be problematic in imaging purity. Multi-layer rod antennas fortunately have shown relatively lower x-pol levels.

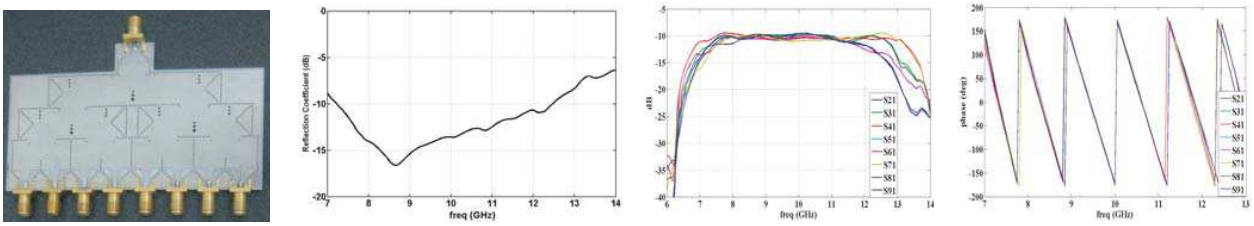

(a) (b) (c) (d)

Figure 1: (a) Manufactured wideband SIW 1×8 power divider, (b) measured input reflection coefficient, (c) amplitude and (d) phase of output signals at X-band.

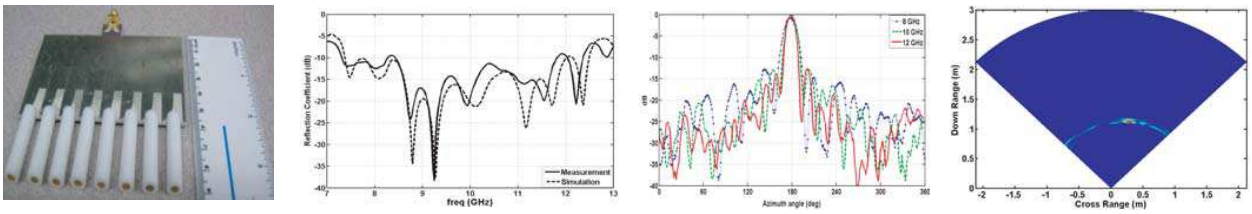

(a) (b) (c) (d)

Figure 2: (a) Manufactured array antenna and (b) its reflection coefficient, (c) E-plane radiation pattern, (d) developed antenna's image.

This array has a good input match, almost constant radiation pattern with a gain of 14.5 ± 2 dB over the frequency band, low dispersion, and low squint performance and only occupies 10 cm $\times$ 9 cm.

Session 3A5
Computational Techniques

Designing Transformation-based Metamaterials for Numerical Modeling of Low Frequency Electromagnetic Scattering

Ozlem Ozgun[1] and Mustafa Kuzuoglu[2]

[1]Department of Electrical and Electronics Engineering
TED University, Ankara, Turkey
[2]Department of Electrical and Electronics Engineering
Middle East Technical University, Ankara, Turkey

Abstract— Electromagnetic wave scattering from electrically-small (i.e., dimensions are small compared to the wavelength) objects or features has always been of interest in various fields of science and engineering for more than a century. However, in such problems, numerical solution techniques suffer from some difficulties due to the necessity to capture the small scale effects on the large scale with adequate numerical precision. For instance, if an electrically-small object is located in a medium together with other large scale objects, the mesh must be refined over the object, leading in turn to a large number of unknowns. Practical applications may include the modeling of a small antenna mounted on a large platform, or simulating thin interconnect structures in integrated circuits. Such problems also complicate the process of mesh generation because of the mesh refinement, and often introduce ill-conditioned matrix systems because of poor mesh quality. This, in turn, makes it difficult to extract an accurate solution of such problems in a numerically efficient manner. In this paper, efficient numerical modeling of electromagnetic low-frequency problems is achieved by means of specially designed transformation-based metamaterials in the context of finite element or finite difference methods. The transformation-based metamaterials, in general, depend on the duality relationship between the coordinate transformation and the material parameters, in conjunction with the form invariance property of Maxwell's equations under coordinate transformations. That is, Maxwell's equations keep their form the same in the modified coordinate system, but the original material parameters are replaced by anisotropic parameters to mimic the field behavior resulting from the coordinate transformation. The principal idea in the proposed techniques is to modify the computational domain and to suitably place transformation-based metamaterial structures within the modified domain, and hence, to devise efficient simulation tools employing uniform and easy-to-generate meshes and less number of unknowns. The proposed techniques are illustrated via several finite element simulations.

Study on Spectral-domain Analysis of Imperfectly Periodic Structures

Koki Watanabe and Yoshimasa Nakatake
Fukuoka Institute of Technology, Japan

Abstract— The electromagnetic scattering problem of periodic structures has been extensively studied for a long time as wavelength and polarization selective components in microwave, millimeter-wave, and optical wave regions. When a plane-wave illuminates a perfectly periodic structure, the Floquet theorem asserts that the scattered fields have a pseudo-periodic property and the scattered fields have discrete spectra in the wavenumber space. The field components can be therefore expressed in the generalized Fourier series expansions, and the analysis region can be reduced to only one periodicity cell. Then many numerical approaches to periodic structures are based on the Floquet theorem. Recently, structures in which the periodicity is locally broken have also received much interest because they induce distinct properties; for example, the field localization induced by defects in the electromagnetic bandgap structures. In such structures, the Floquet theorem is no longer applicable, and the numerical analysis are usually performed with the finite differences time-domain method, the finite element method, the time-domain beam propagation method, the method of fictitious sources, etc.. These approaches are limited to apply to the problems of scatterers with finite extent, and the analysis region has to cover whole scatterers under consideration. In this work, we consider the scattering problems of imperfectly periodic structures and show a spectral-domain approach based on the pseudo-periodic Fourier transform (PPFT). Since the transformed fields have a pseudo-periodic property the conventional grating theory based on the Floquet theorem becomes possible to be applied for the scattering problem of imperfectly periodic structures. Also, the PPFT makes it possible to consider the wavenumber sampling scheme only inside the Brillouin zone.

An Inverse Scattering Approach for Cylindrical Objects without Using the Knowledge of Incident Fields

Takashi Takenaka and Toshifumi Moriyama
Graduate School of Engineering, Nagasaki University
1-14 Bunkyo-machi, Nagasaki 852-8521, Japan

Abstract— Microwave imaging techniques have been attracting much attention of many researchers because of its potentiality in various fields of applied science, such as biomedical imaging, nondestructive testing, and detection of buried objects. Radar-based imaging techniques only give the locations of targets of interest, while inverse-scattering-based imaging techniques estimate electric properties of the targets as well as their locations, shapes and sizes. The most approaches based on inverse scattering analysis apply optimization techniques for minimizing a cost function consisting of the misfit between measured field data and the corresponding calculated ones. Those inverse scattering approaches use not only measured field data but also incident field information. Since inverse scattering problems are ill-posed and nonlinear, it is preferable to exploit the information of the incident field as accurate as possible in those methods. To our knowledge, there is no paper which deal with reconstruction of electrical parameters of inhomogeneous objects only from the measured total field data, not using explicitly the knowledge of the incident field.

In this paper, we propose a novel inverse scattering method for reconstructing of electrical parameters of inhomogeneous objects only from the measured total field data without explicit use of the information of incident field. The basic idea of the proposed method is based on the field equivalence principle. Let an object of interest be illuminated by an incident field and the total field is measured on an observation curve $\partial\Omega$ enclosing the object. We consider an equivalent problem within a region Ω enclosed by the curve $\partial\Omega$: the original fields $(\mathbf{E}, \mathbf{H})$ exist inside $\partial\Omega$ and a null field outside $\partial\Omega$. Suppose the primary source $\mathbf{j}$ generating the incident fields is outside $\partial\Omega$. In the equivalent problem, the original source $\mathbf{j}$ is removed and equivalent sources are placed on the boundary $\partial\Omega$. To support the field $(\mathbf{E}^{eq}, \mathbf{H}^{eq})$ in the equivalent problem, surface electric and magnetic currents $\mathbf{J} = \hat{n} \times \mathbf{H}$, $\mathbf{M} = \mathbf{E} \times \hat{n}$ on the boundary $\partial\Omega$ are required where $\hat{n}$ is a unit inward normal to $\partial\Omega$. Note that the fields $(\mathbf{E}^{eq}, \mathbf{H}^{eq})$ outside $\partial\Omega$ is null only when an object located in the region Ω is the original one. If the original object is replaced by a different one in the equivalent problem, the field outside $\partial\Omega$ is no longer null. Based on this observation, the inverse problem estimating medium parameters is cast as an optimization problem finding the minimizer of a functional given by a surface integral over the region outside $\partial\Omega$ of the field $(\mathbf{E}^{eq}, \mathbf{H}^{eq})$. Numerical results based on the proposed approach will be shown in the presentation.

A Genetic Algorithm Enhanced by SVM and DPE

Zhi Zheng and Xing Chen
College of Electronics and Information Engineering, Sichuan University, Chengdu 610064, China

Abstract— The Genetic Algorithm (GA) is a popular global optimizer. But in many applications, an optimization process of the GA is very computational cost due to the lager quantity of the fitness function evaluations. This paper explores reducing the GA's computation burden by using approximate function with the Support Vector Machine (SVM) to replace some exact fitness function evaluations and the Dynamic Parameter Encoding (DPE) to compress the solution space adaptively. Numerical results are presented on a series of benchmark functions, and show that in comparison with the traditional GA, the proposed GA enhanced by SVM and DPE is able to reduce the quantity of exact fitness function evaluations more than 55%, or even more than 80% while retains the basic robust search capability.

Propagation Characteristics of Dielectric Waveguides with Arbitrary Inhomogeneous Media Along the Middle Layer (Part III)

Ryosuke Ozaki and Tsuneki Yamasaki
Department of Electrical Engineering, College of Science and Technology
Nihon University, Japan

Abstract— Light propagation in periodic structure waveguide such as photonic crystal waveguide is both theoretical and practical interest in many areas of physics and engineering. Applications include integrated optics circuit, optical waveguide filter, and other optical devices. In periodic structures such as photonic crystal structures, it is known that a frequency stop band occurs. Consequently, in the design of photonic crystal structures with periodic constants same as optical wavelength, it is important to investigate the stop band region or photonic band gaps. On the one hand, it can be controlled optical constants by the development of manufacturing technology of semiconductor and optical devices. Thus, many analytical and numerical techniques have been proposed that are applicable to dielectric gratings having arbitrary structures. To deal with multilayered dielectric circular cylinder arrays such as photonic crystal structure, it is necessary to analyze the multilayered periodic arrays.

In previous paper, we analyzed the propagation characteristics of dielectric waveguide composed of dielectric circular cylinders array loaded with dielectric circular cylinders, dielectric triangular cylinders, and rhombic dielectric structure along a middle layer, and investigated the distribution of energy flow by using the propagation constants at the guided area for dominant mode.

In the multilayer method, as the inhomogeneous region is divided into an assembly of stratified thin layers with step index profile, the matrix size depends on the number of layers. In our method, the order of characteristic matrix equation depends on the modal truncation number, but it does not depend on the number of layers. Therefore the range of applicability for the periodic structures is much wider than that of the other method. In particular, our approach is effective method for the guiding problems such as multilayered periodic array. In guiding problem, it is necessary to analyze with high accuracy the complex propagation constants for both stop band region and leaky wave region. However the guiding problem is reported by various numerical techniques, the propagation characteristic is not investigated in detailed in the Bragg region.

In this paper, we have analyzed the propagation characteristics of dielectric waveguide composed of dielectric circular cylinders and the deformed rhombic dielectric structure in the middle layer as shown in Fig. 1(a), and investigated the influence of deformed rhombic dielectric structure loaded with middle layer for TE_0 and TM_0 modes.

Numerical results are given for the complex propagation constants and the distribution of energy flow for the case of loaded with the deformed rhombic dielectric structure as the inhomogeneous media in the middle layer for both TE_0 and TM_0 modes.

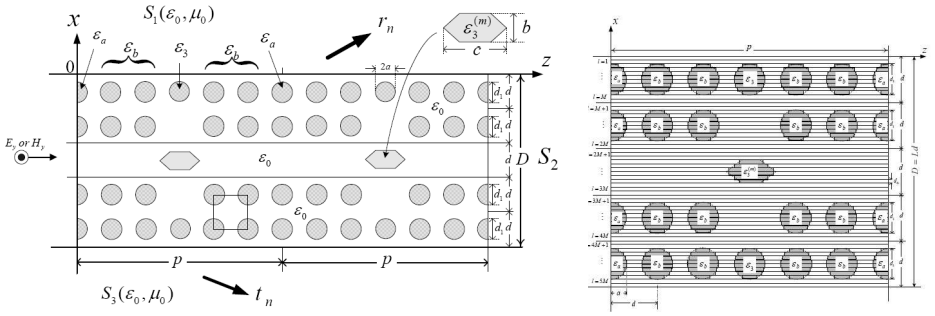

(a) Coordinate system (b) Approximated multilayer method

Figure 1: Structure of dielectric waveguides with arbitrary inhomogeneous media along the middle layer.

Non-uniform FFTs in Near-field/Far-field Transformations

A. Capozzoli, C. Curcio, and A. Liseno
Dipartimento di Ingegneria Biomedica, Elettronica e delle Telecomunicazioni
Università di Napoli Federico II, via Claudio 21, I 80125 Napoli, Italy

Abstract— Near-field antenna characterization consists of measuring, on proper scanning surfaces, the near-field radiated by an Antenna Under Test (AUT) and of determining, from those measurements, the far-field pattern (Near-Field/Far-Field-NFFF-transformation) [1].

Whenever possible, both the amplitude and the phase of the near-field are acquired on a sole scanning surface, so that the NFFF transformation involves only linear operations on the data [1]. When, on the contrary, measuring the phase becomes expensive or difficult, the only amplitude of the near-field is usually collected on two measurement surfaces and the NFFF transformation involves non-linear operations on the data, typically consisting of the iterative optimization of a cost functional [2].

In recent years, significant advancements have been achieved in the framework of the near-field antenna characterization which have concerned new scanning geometries (plane-polar [3], spiral and helicoidal [4]), advanced non-uniform sampling techniques [5] capable to significantly reducing the acquisition time and the ill-conditioning as compared to uniform samplings, and new processing schemes [2, 6].

Whenever an estimate or a measurement of the "complex" (i.e., amplitude and phase) near-field is available, transforming a near-field into the far-field conceptually requires a simple Fourier transform operation. However, when non-uniform grids are involved, such Fourier transformation cannot be performed by a standard Fast Fourier Transform (FFT) algorithm, having a convenient asymptotic computational complexity growing as NlogN. Then, in the case of complex measurements, following the acquisition of non-uniform samples, the most simple way to transform the data to the far-field is to perform an interpolation stage prior to the FFT. This establishes a trade-off between accuracy and computational complexity [7]. Such a trade-off becomes even more relevant in the case of algorithms relying on phaseless data which, at each iteration step, require evaluating the spectrum from estimates of the near-field on non-uniform lattices or calculating the near-field on non-uniform grids from estimates of the spectrum.

In the last years, Non-Uniform FFT (NUFFT) algorithms [8] have been developed enabling to evaluate Fourier transforms from non-uniform grids to uniform ones (Non-Equispaced Data-NED-NUFFT), from uniform grids to non-uniform ones (Non-Equispaced Results-NER-NUFFT) and from non-uniform grids to non-uniform ones ("type-3" NUFFT). Such algorithms enable to accurately performing the interpolation stage in a computationally convenient way, so that their computational burden is proportional to that of a standard FFT. Furthermore, NUFFTs can be made available as library routines to strongly simplify their usage and, accordingly, their exploitation in NFFF transformations.

Purpose of this paper is to show how NUFFT algorithms can be conveniently employed in near-field characterization algorithms, operating both with complex or phaseless data.

REFERENCES

1. Yaghjian, A., "An overview of near-field antenna measurements," *IEEE Trans. Antennas Prop.*, Vol. 34, No. 1, 30–45, Jan. 1986.
2. Capozzoli, A., C. Curcio, G. D'Elia, and A. Liseno, "Phaseless antenna characterization by effective aperture field and data representations," *IEEE Trans. Antennas Prop.*, Vol. 57, No. 1, 215–230, Jan. 2009.
3. Rahmat-Samii, Y., V. Galindo-Israel, and R. Mittra, "A plane-polar approach for far-field construction from near-field measurements," *IEEE Trans. Antennas Prop.*, Vol. 28, No. 2, 216–230, Mar. 1980.
4. D'Agostino, F., C. Gennarelli, G. Riccio, and C. Savarese, "Theoretical foundations of near-field-far-field transformations with spiral scannings," *Progress In Electromagnetics Research*, Vol. 61, 193–214, 2006.
5. Capozzoli, A., C. Curcio, A. Liseno, and P. Vinetti, "Field sampling and field reconstruction: a new perspective," *Radio Sci.*, Vol. 45, RS6004, 31, 2010, doi:10.1029/2009RS004298.

6. Capozzoli, A., C. Curcio, and A. Liseno, "Multi-frequency planar near-field scanning by means of Singular-Value Decomposition (SVD) optimization," *IEEE Antennas Prop. Mag.*, Vol. 53, No. 6, 212–221, Dec. 2011.
7. Capozzoli, A., C. Curcio, A. Liseno, and P. Vinetti, "Fast interpolation accelerated on GPU for SAR backprojection," *Proc. of the 27th Annual Rev. of Progr. in Appl. Comput. Electromagn.*, 1–6, Columbus, OH, Apr. 10–14, 2012.
8. Fourmont, K., "Non-equispaced fast Fourier transforms with applications to tomography," *J. Fourier Anal. Appl.*, Vol. 9, No. 5, 431–450, Sep. 2003.

Image Restoration of the Objects with Superresolution on the Basis of Spline — Interpolation

B. A. Lagovsky
Moscow State Institute of Radio Engineering and Automation (Technical University), Russia

Abstract— The problem is to restore an angular intensity distribution of the reflected signal on the basis of the analysis of locked-on signal and the known directional pattern of antenna arrays.

Angular resolution can be increased due to secondary digital processing the locked-on signals. Necessary algorithms are created on the basis of solutions of inverse ill-posed problems.

The new method of processing of signals is theoretically proved and checked up by smart antenna system during numerical experiments on mathematical model.

Offered methods of signal processing allow to raise the effective resolution without entering any changes in the engineering system.

Let a priori or from the analysis of the given measurements it is known, that the zone of a location of a source of signals is limited by angular area Ω. The approximate solution is under construction by means of a choice of values of intensity of a source of radiation in a number of the discrete points covering all area, and representation of the decision in the form of a spline-interpolation on these points.

The problem thus is reduced to a choice of number of points of restoration, sizing the values of intensity in these points and factors of interpolation function on each segment.

The number of points M sets required angular resolution. At the solution of problem M consistently increases up to achievement of the greatest possible angular resolution.

In a considered problem the values of function are not set and are searched together with values of factors of splines. The problem is reduced to the solution of system of the linear algebraic equations.

The basic spline-interpolation advantage is its stability. Systems of the linear equations which are required to be solved for sizing of factors of splines, are very well conditioned, that allows to receive factors of polynomial with high accuracy.

Using various methods a spline-interpolation, for example, Bessel for more smooth restoration of a signal or Akima for minimization false oscillation, it is possible to restore various types of sources of signals qualitatively and quickly.

Use of offered algorithms at designing new systems allows to simplify technical decisions and to lower their cost.

Superresolution: Simultaneous Orthogonalization of Function Systems Describing the Received Signal and its Source

B. A. Lagovsky
Moscow State Institute of Radio Engineering and Automation (Technical University), Russia

Abstract— The approximate numerical solutions of some inverse problems of electrodynamics allow to increase angular resolution of radar-tracking systems and systems of remote sensing.

The problem consists in an angular intensity distribution restoration on the basis of the analysis of locked-on signal with the greatest possible angular resolution.

The considered problem relates to inverse ill-posed problems. Basic feature of considered inverse problems is poor solution stability. The numerical solutions became unstable when we try to obtain the angular resolution better then it is follows from Rayleigh criterion.

To improve the solution stability the various procedures of regularization are used.

Algebraic methods of reconstruction of an angular intensity distribution on the basis of the locked-on signal analysis and the known directional pattern are investigated.

Shows, that increase of stability of solutions can be reached, if special orthogonal function systems used for signal notation and representation of its source.

The received function systems allow to realize simultaneously the required solution of the integral equation and the investigated signal in the form convenient for the analysis and the numerical solution of inverse problem.

The numerical characteristics of the increase of the angular resolution and its limits were investigated on mathematical model of an antenna array. The improvement of the resolution was estimated in comparison with the beamwidth.

The influence of noise level on the effective resolution was also investigated on mathematical model. Use of the received orthogonal systems has allowed to receive the greater effective angular resolution at high quality of restoration of the image of objects, than other algebraic methods.

Offered algebraic methods and algorithms on their basis favorably differ from known themes that allow, consistently increasing number of used functions, i.e., increasing the angular resolution to come nearer to limiting for each solved problem the effective angular resolution.

As a whole, these algebraic methods allow to increase the effective angular resolution by 4–8 times in comparison with Rayleigh criterion.

Effects of Boundary Conditions on Maxwell Eigenvalue Problem

Ahmad Alkandari[1] **and Fethi Bin Muhammad Belgacem**[2]

[1]Department of Electrical Engineering Technology
College of Technological Studies, (PAAET), Shuwaikh, Kuwait
[2]Department of Mathematics, Faculty of Basic Education, PAAET, Shaamyia, Kuwait

Abstract— In this paper, we study the effects of changing boundary conditions values and designs on the Maxwell Eigenvalue Problem,

$$\begin{cases} (i) \quad \nabla \times \mathbf{E} = -\mu \dfrac{\partial \mathbf{H}}{\partial t} + \lambda m(z,t)\mathbf{H} \\ (ii) \quad \nabla \times \mathbf{H} = \epsilon \dfrac{\partial \mathbf{E}}{\partial t} + \sigma \mathbf{E}. \end{cases} \tag{1}$$

The Magnetically related forcing term, $\lambda m(z,t)H$, has deep effects on the dynamics and solutions of a planar, transverse electromagnetic (TEMP) wave propagating in the direction z in lossy media with constant permittivity ϵ, permeability μ, and conductivity $\sigma > 0$. In this work, we attempt to discover the effects of changing Boundary conditions on the solutions of (1). For null source terms, $m(z,t) = 0$, various forms of solutions for the electric and magnetic fields have been determined by various authors, using various techniques. Setting, $a = 1/\sqrt{\mu\epsilon}$, $b = \sigma/2\epsilon$, a sample of previous results are:

Theorem 1 [Husein-Belgacem]: *For $m(z,t) = 0$, the transient electric field, $E(z,t)$, in the TEMP problem as described in (1), is given by,*

$$E(z,t) = e^{-\frac{b}{a}z} f(t - z/a) - a \int_{z/a}^{\infty} f(t-\tau) e^{-b\lambda} \frac{\partial}{\partial z} J_0\left(\frac{b}{a}\sqrt{z^2 - (a\tau)^2}\right) e^{-t/u} d\tau.$$

Theorem 2 [Rathinavel-Belgacem]: *For $m(z,t) = 0$, the transient magnetic field, $H(z,t)$, in the TEMP problem as described in (1), is given by,*

$$H(z,t) = e^{-\frac{b}{a}z} h(t - z/a) - a \int_{z/a}^{\infty} h(t-\tau) e^{-b\lambda} \frac{\partial}{\partial z} J_0\left(\frac{b}{a}\sqrt{z^2 + (a\tau)^2}\right) e^{-t/u} d\tau.$$

In this work, we distinguish between various cases of boundary conditions (Drichlet, Neumann and Mixed Robin).

The Sumudu transform remains our favorite tool of choice. The Sumudu transform is definded by,

$$G(u) = \mathbb{S}[f(t)] = \int_{-\infty}^{\infty} f(ut)\, e^{-t} dt, \quad u \in (-\tau_1, \tau_2), \tag{2}$$

over the set of functions,

$$A = \left\{ f(t) \,/\, \exists\, M, \tau_1, \tau_2 > 0,\ |f(t)| < M e^{\frac{|t|}{\tau_j}}, \quad \text{if} \ \ t \in (-1)^j \times [0,\infty) \right\}. \tag{3}$$

For instance, we have, $\mathbb{S}[t^\alpha] = \Gamma(\alpha+1)\, u^\alpha$, $\mathbb{S}[t^n] = n! u^n$, and $\mathbb{S}[\exp(at)] = 1/(1-au)$, for $a \in (-1/a, 1/a)$. *The Sumudu of the n'th derivative, $f^{(n)}(t)$, of $f(t)$,* is, $G_n(u) = \frac{G(u)}{u^n} - \sum_{k=0}^{n-1} \frac{f^{(k)}(0)}{u^{n-k}}$. For, $n = 1$, & 2, we have, $G_1(u) = \mathbb{S}(f'(t)) = \frac{G(u) - f(0)}{u}$, &, $G_2(u) = \mathbb{S}(f''(t)) = \frac{G(u)-f(0)}{u^2} - \frac{f'(0)}{u}$.

The Sumudu of the anti-derivative, $(f * 1)$, of the function, $f(t)$, is given by, $uM(u)$. The sumudu Operator exhibits very direct convolution, properties, namely, when $M(u)$, and $N(u)$, are the respective sumudi for the functions, $f(t)$ and $g(t)$, with convolution, $(f*g)(t)$, then, the Sumudu of the convolution of the functions, $f(t)$, and $g(t)$, is given by, $S[(f*g)(t)] = uM(u)N(u)$.

Session 3A6
Applications of EM Field in Medicine

Microwave Multiple Frequency Applicator for SAR Homogeneity Augmentation

T. Vydra, D. Havelka, and J. Vrba
FEE, Department of Electromagnetic Field, CTU in Prague, Czech Republic

Abstract—

introduction: In many industrial and medical applications of electromagnetic field it is essential to ensure that the absorbed energy (represented by the value of SAR — Specific Absorbed Energy) is distributed evenly throughout the processed area. Generally we aim to minimize the hot and cold spot generation and the exposure of unwanted parts of a processed area.

These requirements can be achieved by several approaches. In this paper we propose a solution using two stable frequency sources of electromagnetic energy at frequencies 2.45 GHz and 915 MHz which are both within the ISM band (in USA). The arrangement of our system assures that there are no interferences between sources and we can very well predict the distribution of the electromagnetic field in the quasi-cavity and subsequently the distribution of SAR in an exposed area.

We present results which show how the SAR distribution homogeneity is augmented and in other section we take into consideration changes which can occur especially in industrial applications.

Design Approach:

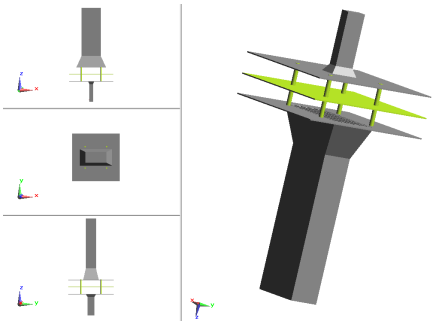

Figure 1: Basic design of the system.

ACKNOWLEDGMENT

This research is supported by the Grant Agency of the Czech Republic by project 102/08/H081: "Non Standard Applications of Physical Fields" and by CTU project SGS12/071/OHK3/1T/13: "Advanced techniques in the processing of industrial materials and biopolymers using electromagnetic field — multi-frequency processing". Further it is supported also by research program MSM6840770012: "Transdisciplinary Research in the Area of Biomedical Engineering II" of the CTU in Prague, sponsored by the Ministry of Education, Youth and Sports of the Czech Republic.

Exposure System with Well Defined Dosimetry

Jan Vrba, Lukas Visek, and Ladislav Oppl
Department of Electromagnetic Field, Faculty of Electrical Engineering
Czech Technical University in Prague, Technicka 2, Prague, Czech Republic

Abstract— The whole-body exposure system for unrestrained mice was designed in order to analyze the influence of electromagnetic field. The setup operating at 900 MHz was designed with respect to induced uniform field, external radiation elimination, absorbed power determination, sufficient space for mice movement together with even mice exposure and costs. The main aim of this paper is to assure that the dosimetry results reached by computer simulations can be used for determination of absorbed power in the unrestrained mouse. The whole-body exposure chamber with anatomical mouse model was simulated by two different numerical methods, e.g., finite-difference-time-domain method (FDTD) and Finite Integration Technique (FIT) and its dosimetry results were compared by computed SAR values.

Introduction: In our modern world various sophisticated devices emitting microwave electromagnetic field are ubiquitous. These devices are used in many branches such as industry, medicine and particularly communication. The advent of a wide penetration of mobile communications has arisen the concern whether the exposure to electromagnetic field could be adverse to the exposed users. The increasing daily exposure has raised the research activities in order to determine the effects of exposure to the electromagnetic radiation of mobile phones. Although a lot of researches have been accomplished, no adverse health effects of cellular phones have been confirmed yet. The main aim of this work was to design exposure chamber for in vivo studies where the impact of electromagnetic field on biological organisms is analyzed.

Methods: The whole-body exposure system for unrestrained mice was designed in order to analyze the influence of electromagnetic field. The setup operating at 900 MHz has been designed with respect to following conditions:

- induced uniform field
- external radiation elimination
- accurate absorbed power determination
- sufficient space for mice
- even mice exposure
- costs

These conditions are grounded on requirements for exposure system from [1]. Such conditions assure an accurate determination of Specific absorption rate (SAR) together with the elimination of stress induced in mice. The major advantage of the system is the capability of direct measurement the whole-body averaged SAR which is performed by analysis of measured scattering parameters.

As the basic structure of the exposure chamber a waveguide was chosen. The advantage of the waveguide structure is a shielding of electromagnetic field generated inside in order to protect the operators and also generated outside the system in order to eliminate outer radiation. Dimensions

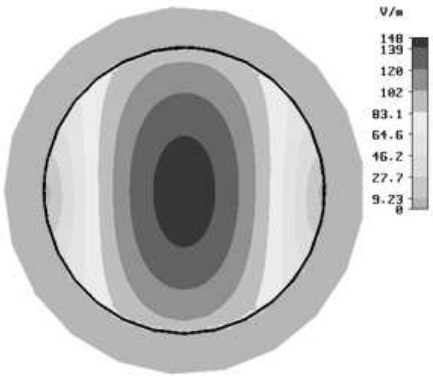

Figure 1: Distribution of electric field strength of TE_{11}.

of the exposure chamber were calculated in order to use desired frequency of operation and the volume needed to exposed mice. The exposure chamber is made of copper plate with dimensions of 1650 mm length and 240 mm diameter. The chamber is terminated by matched loads at both ends. In order to avoid reflection and assure an attenuation of power the loads must be made of lossy dielectric material and must have a suitable shape. The electrical resistance of the shape should grow linearly in a direction of the wave propagation. The designed matched loads are conical, 500 mm long and are made of RF absorber. The reflection loss of the matched load is more than −20 dB at 900 MHz.

The circular polarized wave TE_{11} is excited in the waveguide (Fig. 1).

Environment Protecting Industrial Technologies Based on EM Field

Jan Vrba[1], **Tomas Vydra**[1], **Jan Vrba, Jr.**[2], **and Marika Pourová**[1]

[1]Department of EM Field, Faculty of Electrical Engineering, Czech Technical University
Technická 2, 166 27 Prague 6, Czech Republic
[2]Department of Medical Devices, Faculty of Biomedical Engineering
Czech Technical University, Sitna 2, Kladno, Czech Republic

Abstract—

Introduction: In this contribution, we would like to describe our new results dealing with microwave industrial applicators used for drying of textile materials. We have designed and evaluated two different types of these applicators: open-resonater-type and waveguide-type one. We would like to present theoretical models of the discussed applicators, results of numerical modeling and experimental evaluation as well. Protype of microwave drying machine working at frequency 2.45 GHz will be reported.

Open Resonator Type Applicator: This type of applicator consists of many drying cells (17 in our prototype machine) — each of them is based on the idea of open resonator (i.e., Fabry-Perrot resonator), see Fig. 1. Each of these cells has its own magnetron placed in waveguide holder. Dryed textile material is in the middle plane between parallel conductive plates, distance between these plates is equal to $(3/2)\lambda$. In the right side of Fig. 1 there is a calculated 2D distribution of electric field strength. Plane of the textile material is in this 2D model given by an abscissa in the middle of the resonator — in the same plane there is an expected maximum of electric field strength.

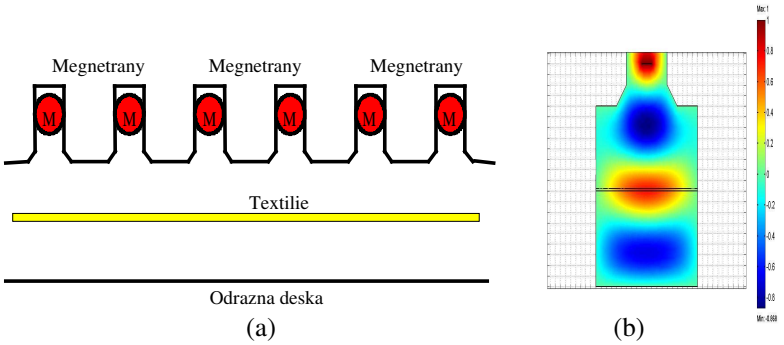

Figure 1: (a) Schematics of 6 cells of open resonator type applicator for drying of textile materials. (b) E field strength 2D distribution in each one of that cells.

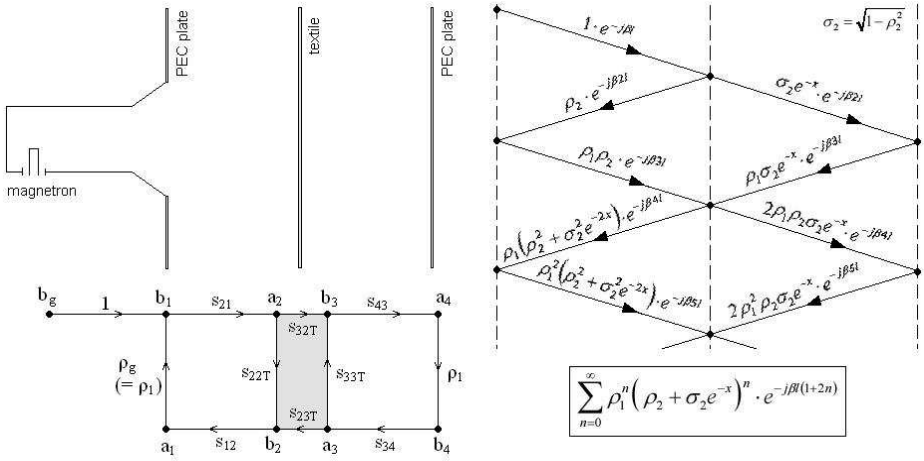

Figure 2: Tools for optimization of microwave dryer in longitudinal direction.

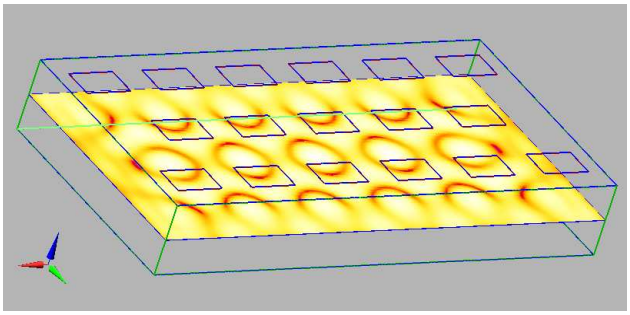

Figure 3: Microwave drying machine 3D schematics and SAR distribution in the plane of the wet textile material (6 cells in first raw, next 5 cells in the second raw and again 6 cells in the last third raw — calculated by SEMCAD).

Optimization of the cells in longitudinal direction of drying machine is given by criteria to create maximum of electric field strength in the plane of dryed textile (E field vector parallel to the textile plane), see diagrams in Fig. 2. We can describe each one of that cells by a simple schematic sketch (left-up) and from it we can create oriented graph of this structure (left-down). Alternatively we can create diagram of EM waves inside this structure (right-up) and we will arrive to the resulting expression (right-down).

For our experiments we have built apparatus with a matrix of 6 cells in first raw, next 5 cells in the second raw and again 6 cells in the third raw — see apertures in the upper conductive plate in Fig. 3. Optimization of overall microwave dryer means to approach to the best possible homogeneity of absorbed microwave energy in the textile material. In the plane of textile material there is shown a calculated distribution of SAR (by aid of software product SEMCAD). Quite a good homogeneity of SAR can be observed and further improvement is obtained thanks to the movement of textile material through microwave drying machine.

New Microwave Technologies for Thermotherapy Applicators

David Vrba, **Barbora Vrbova**, **and Jan Vrba**
Department of EM Field, Czech Technical University in Prague, Prague, Czech Republic

Abstract— In this contribution, we would like to describe our new results dealing with evanescent mode waveguide hyperthermia applicators, typically used for cancer treatment. We have developped theoretical basis of this technology and designed & evaluated different versions of these applicators working below waveguide cut-off frequency.

In our contribution we would like to discuss what happens, when the frequency f of hyperthermia apparatus is either very different (i.e., much higher or lower) from the cut-off frequency f_c or very near (even equal) to the cut-off frequency f_c of the used waveguide applicator. This special case of our interest can happen when either the hyperthermia apparatus is tunable in broader frequency range or the cut-off frequency f_c of the applicator is changed by different dielectric parameters of various types of biological tissues.

There is a substantial difference between the two ways of the waveguide applicator excitation (i.e., above or under the cut-off frequency f_c) and in the propagation and "behaviour" of the EM field inside such applicator also. Basic differences would be explained during the presentation.

For the following discussion we have chosen the case of the rectangular applicator with a flange. But similar results is possible to obtain for other important cases like, e.g., rectangular applicators without flange or for the family of circular applicators.

Waveguide flange is in our approach considered as an electric wall, dashed line going into the biological tissue determines the magnetic wall of our model. The distance between these walls determines the cut-off frequency f_c of the applicator aperture. Of course, f_c is influenced by the tissue permittivity also.

The results we would like to describe in our contribution are interesting from theoretical point of view of the knowledges about the general properties of the waveguide applicators. And are very important also for the treatment — our results demonstrate very substantial changes of SAR distribution in the treated biological tissue. If f is going to f_c then so called hot spots complicating the treatment can arise.

ACKNOWLEDGMENT

This research is supported by the Grant Agency of the Czech Republic and by the Ministery of Education, Youth and Sport of the Czech Republic.

Microwave Thermotherapy: Study of Hot-spots Induced by Electromagnetic Surface Waves

Barbora Vrbova and Jan Vrba
Department of Electromagnetic Field, Faculty of Electrical Engineering
Czech Technical University in Prague, Technicka 2, 166 27 Prague 6, Czech Republic

Abstract—

Background: This paper is a contribution to theory of microwave applicators used in cancer treatment by so called hyperthermia. It deals with a study of excitations of surface waves around of the treated area — one kind of parasitic effects, which can significantly complicate real treatment of patients (they can create superficial hot spots outside treated area). Appropriate treatment planning by aid of numerical simulations of SAR distribution can prevent such cases. In this paper we will demonstrate a possibility to eliminate excitations of surface waves by optimization of water bolus shape and dimensions.

Methods: For our study and discussion we have chosen microwave stripline type applicator with TEM mode, which can be used for treatment of cancer patients at frequency 434 MHz. It was designed at Department of Electromagnetic Field of CTU in Prague for our research purposes.

To understand well the discussed problem we work both on its analytical and on its numerical solutions. We will describe basic approach to analytical solutions of this case. Simulations of several SAR patterns have been done by the FDTD method, in our case it was SEMCAD X EM Field simulator from SPEAG, Schmid & Partner Engineering AG, Switzerland.

Results: Our basic approach to develop analytical solution of the discussed problem comes from idea of resonances in water bolus. If the central circle of the water bolus is approximately equal to any of whole number multiple wavelengths, then under certain conditions surface waves can create hot spots on the surface of the treated area.

Conclusions: This research contains first results of numerical simulations to eliminate excitations of surface waves. In this case we eliminate surface waves by optimization of dimensions of water bolus, which will be demonstrated on pictures in the following full paper. Analytical solutions will be described in the following extended version of this paper.

ACKNOWLEDGMENT

This research is supported by Grant Agency of the Czech Republic by project SGS12/070/OHK4/1T/13 (i.e., student's grant contest of CTU).

Electric Model of Mitotic Spindle

Daniel Havelka[1, 2], **Tomas Vydra**[1], **Michal Cifra**[1, 2], **and Jan Vrba**[1]

[1]Department of Electromagnetic Field, Czech Technical University
Technická 2, Praha 166 27, Czech Republic
[2]Institute of Photonics and Electronics, Academy of Sciences of the Czech Republic, Czech Republic

Abstract— The eukaryotic cell is a basic unit of plants, fungi and animals and it is also a likely source of electromagnetic field whose function we would like to examine in the future. Eukaryotic cells contain various organelles and structures. It is expected that the electromagnetic activity originates mainly in cytoskeleton that is a structure that protects and organizes the cell, enables a motion of the cell and is necessary for cell division. This structure is composed of three types of filaments. Microtubules, which are one of them, fulfil all conditions for generation of cellular electromagnetic field. We approximate electrical properties of basic structure of a microtubule (tubulin heterodimer) as elementary electric dipole. We approximate mechanical oscillations of tubulin heterodimers in one protofilament as mechanical oscillations of the chain of the rigid particles. Movement of particles and corresponding oscillations of dipole moment is described by spatial modulation function: $p_m = p_A? \sin(dam)$, where p_m is modulated dipole moment, p_A is active part of dipole moment of tubulin heterodimer in direction of microtubule axis and dam is distance along microtubule. We used optical brand of oscillations of tubulin heterodimers. We used two different surrounding media around microtubules lossy and lossless and frequency band of oscillations of tubulin heterodimers from kHz to GHz region. The field around oscillating microtubule was calculated as a vector sum of contributions from all elementary electric dipoles. In this paper, we present results from calculations of power and electric intensity around two models of microtubule network. We created symmetric and asymmetric model of microtubule network. The symmetric model is model of non-dividing cell and the asymmetric model represents microtubule network during cell division.

Design of Slot Applicator for Local Thermotherapy

Jaroslav Vorlíček[1], **Jaroslav Kosík**[2], **and Jan Vrba**[1]

[1]Department of Electromagnetic Field, Czech Technical University, Czech Republic
[2]Faculty of Biomedical Engineering, Czech Technical University, Czech Republic

Abstract— Microwave thermotherapy is form of treatment which profits from effect affiliated with higher than common temperatures in biological tissue, such as higher blood flow and thus improved oxygenation and faster cell metabolism. From these effects we profit both in rehabilitation applications and above all in adjuvant cancer treatment. It's well known fact, that hyperthermia used in combination with conventional oncological methods significantly improves results.

The aim of this work was to design and construct a suitable planar slot applicator for microwave thermotherapy. Planar slot applicator is very good solution for superficial treatment, but can also be used for intracavitary treatment, as it can be manufactured from elastic materials. As resonant structure the slot applicator poses very good solution for energy transfer to biological tissue. Crucial for it's function is optimal impedance matching between applicator itself and treated tissue to ensure that all the energy radiated from antenna aperture is delivered to treated area. To allow applicator operate in unshielded room, we set its working frequency to 434 MHZ, which is designated for biomedical and industrial use.

To design and simulate optimal resonant structure we used CST MICROWAVE STUDIO 2011 software suite. The aperture dimensions were set to 45 mm × 45 mm. After the optimal solution was found, applicator was made by the same technique as printed circuit board to evaluate its real behavior on phantom. As biological tissue phantom we chose agar model as one the best models of muscular tissue, or generally tissue with high water content. To simulate dielectric properties of real biological tissue, we added to agar 3g of salt (NaCl). Measurement of scattering parameters was performed on vector analyzer Agilent E5071C.

To analyze how heat is distributed in tissue model was used thermal analyzer FLIR P25. After $t = 300$ s of heating was phantom evaluated with thermal analyzer from above a then immediately cut in pieces to see heat distribution inside.

By analyzing realized applicator was confirmed, that the lowest energy loss is indeed on frequency 434 MHz. So that makes our applicator perfect for furthermore clinical testing. To prevent creating hotspots applicator should be always equipped with water bolus.

Our slot applicator is suitable for use in biomedical applications in human medicine, preferably for cancer treatment, as it is capable delivering high amounts of energy to target tissue.

Complex Permittivity Measurement of Biological Tissue for Hyperthermia Treatment Planning

Jaroslav Vorlíček[1], **Tomáš Jindra**[2], **Ladislav Oppl**[1], **and Jan Vrba**[1]

[1]Department of Electromagnetic Field, Czech Technical University, Czech Republic
[2]Department of Radioelectronics, Czech Technical University, Czech Republic

Abstract— The goal of hyperthermia cancer treatment is to raise the temperature of the targeted tissue area. Thus, temperature can be maintained above 43°C for up to one hour. To evaluate the expositions of microwave radiation from thermo therapeutical microwave applicators, we need to know the dielectric properties of the tissues. This can be performed using measure of the complex permittivity of the tissues in the desired area of the treatment. For this purpose, we constructed a sensor based on the coaxial transmission line for measuring the complex permittivity. Measurement method on an open-ended coaxial line is based on the reality that the reflection coefficient of an open-ended coaxial line depends on dielectric parameters of material which is attached to the coaxial line. For calculation of biological tissue dielectric parameters from the measured reflection coefficient, it is necessary to use an equivalent circuit of an open-ended coaxial line. The values of elements in the equivalent circuit depend on the dielectric properties of the material attached to the end of coaxial line.

To determine the values of elements in an equivalent circuit, we use calibration by means of material with known dielectric properties.Open-ended coaxial probe has a capability of broadband measurements and simple sample preparation. Also, its nondestructive nature and capability for in-vivo measurements provide open-ended coaxial probes with a significant advantage over other techniques for biological applications. There have been many techniques to correlate the measured input admittance to the complex permittivity of the sample material, which resulted in significant improvement in the extraction process. Accurate measurements of the complex permittivity of biological tissues gain great importance in both basic and applied research.

The performance of this system was evaluated by measuring of the deionized water. The measured data were compared with the value calculated by Debye's model. The relative errors between the measurement and the calculation were less than ±4%. The reliability of this method was confirmed by the measurement of deionized water in wide frequency range.

Cellular Communication by Magnetic Scalar Waves

Konstantin Meyl
Faculty of Computer and Electrical Engineering, Furtwangen University, Germany

Abstract— The DNA generates a longitudinal wave which propagates within the magnetic field vector. Computed frequencies from DNA structure agree with bio photon radiation frequencies as predicted. Optimization of efficiency is done by minimizing the conduction losses which leads to the double helix structure of DNA.

The vortex model of the magnetic scalar wave not only covers the many observed structures within the nucleus but also introduces the reader to the hyperboloid channels in the matrix as two cells are then found to communicate with each other.

Physical results were revealed in 1990 which form the theoretical basis of the essential component of a potential vortex scalar wave. An extended field theory approach has been known since 2009 following the discovery of magnetic monopoles. For the first time magnetic scalar wave theory best explains the physical basis of life not only from the biological discipline of science understanding only. And for the first time this interdisciplinary theory and provides a new understanding of cellular functions that are explained such theory depicting the complex relationships of nature.

The characteristics of the potential vortex are decisive. Now using the concentration effect, my theory provides a cellular miniaturization view down to a few nanometers. This theory for the first time allows a better understanding of the outrageously high information density in the nucleus. Magnetic scalar wave theory explains how the dual base pair-stored information of the genetic code is formed. The process of converting electrical modulation into "piggyback" information that transfers or is send from the cell nucleus to another cell is a revolutionary theory. Information transferred at the receiving end during the reverse process takes place involving a change in the physical and chemical cellular structure. The energy required to power the chemical process, is now understood by the extended field theory to come from the magnetic scalar wave itself.

REFERENCES

1. Meyl, K., *DNA and Cell Resonance, Cellular Communication as Explained by Field Physics Including Magnetic Scalar Waves*, INDEL Publ. Villingen, 2011.

Session 3A7
Electromagnetic Theory

The Interaction of Electromagnetic Waves from Sheets of Spherical Nano-elements Meshed on Concentric Spherical Shells

T. Sengor
Yildiz Technical University, Istanbul 34220, Turkey

Abstract— Possibilities creating nano-structures providing unnatural electromagnetic characteristics are given. Co-rings in nano-metric dimensions lying on different azimuth and/or equatorial planes are defined as nano-element providing such possibilities. These nano-elements are meshed on concentric spherical shells. The interaction of electromagnetic wave with both of nano element and meshed spherical surface are studied. For an example, the necessary configurations for both of the electromagnetically effective cloaking and the optically effective cloaking (invisibility) are given for this purpose. The loops are used at meta-material applications, frequently. The using of circular loop combinations on spherical substrates is offered in this paper to consider in both of artificial material studies and cloaking applications. The array combinations of the couples of semi-cross ring balls on dispersive chiralic substrates generate chirality values higher than the chiralities of natural chiral materials besides providing almost zero permittivity and almost zero permeability and negative chirality.

REFERENCES

1. Sengor, T., "The interaction of electromagnetic waves from single sheet of spherical nano-elements meshed on spherical shell," *Proceedings of 6th Nanoscience and Nanotechnology Conference*, NanoTR6, Çeşmir, İzmir, Haziran, Jun. 15–18, 2010.
2. Sengor, T., "Properties of a non-planar metamaterial elements: Ring resonators on a spherical substrate," *Proceedings of the First International Congress on Advanced Electromagnetic Materials in Microwaves and Optics, Metamaterials 2007 Congress*, Italy, Rome, Oct. 22–26, 2007.
3. Sengor, T., "Analytical theory of effective global cloaking processes: Designing the spherical EM cloaking nano-element," *Proceedings of NATO Advanced Research Workshop, META'10, International Conference on Metamaterials, Photonic Crystals and Plasmonics*, Cairo, Egypt, Feb. 21–25, 2009.
4. Sengor, T., "A chiralic circuit element and its use in a chiralic circuit," *Complex Computing-Networks, Brain-like and Wave-oriented Electrodynamic Algorithms*, Series: Springer Proceedings in Physics, L. Sevgi, Eds., Vol. 104, Göknar, I.C., 2006, ISBN: 3-540-30635-8.
5. Sengor, T., "State approach in artificial materials development in electromagnetics," *PIERS Proceedings*, 568, Italy, Pisa, Mar. 28–31, 2004.
6. Sengor, T., "The state space approach and modified state equations solution in dispersive chiral media," *Proceedings of XXVIIIth General Assembly of the International Union of Radio Science*, Poster Presentations Abstracts Book, Conference CD, Paper No. COM2-01430-2005, 86, New Delhi, India, Oct. 23–29, 2005.

Quantum Electrodynamical Interaction Mechanisms in Simple Atoms

T. Sengor
Yildiz Technical University, Istanbul 34220, Turkey

Abstract— This is an abstract of a study suggesting semi-analytical considerations for quantum electrodynamical interaction mechanisms in simple atoms displaying computational processes to perform the task with sufficient accuracy and sensibility. The analytical frame is, basically, an extension of the Frequency Depended Finite Difference Method in Time Domain, E(FD)^{2}TD. The E(FD)^{2}TD scheme is transferred on a state space algorithm (see [1] for the interpretation of the method) to provide the possibility of the application of the method on atomic and/or molecular structures. The interaction of an electron and an electromagnetic field considered applying some modification to the total Hamiltonian, first for this purpose in an E(FD)^{2}TD scheme. Second, the interaction of a proton and an electromagnetic field is considered in a similar way. Later, the $He^{+(-)}$ and $H^{+(-)}$ ions interacting with an external electromagnetic wave is studied by doing some modifications on the process. These modifications are obtained by re-manipulating the equation of total Hamiltonian including the electromagnetic field to get the state equations and suitable variables with appropriate matrix presentations. This approach is used first in [1–6], systematically.

REFERENCES

1. Sengor, T., "Inversion algorithm for chiralic materials," *Proceedings of Progress in Electromagnetics Research Symposium*, The Electromagnetics Academy, Cosmosquare International Education and Training Center, Osaka, Japan, Jul. 18–24, 2001.
2. Sengor, T., "The interaction of electromagnetic waves from single sheet of spherical nano-elements meshed on spherical shell," *Proceedings of 6th Nanoscience and Nanotechnology Conference*, NanoTR6, Çeşme, İzmir, Haziran, Jun. 15–18, 2010.
3. Sengor, N. S. and T. Sengor, "Chiralic circuits," *Proceedings of Progress in Electromagnetics Research Symposium*, The Electromagnetics Academy, Cosmosquare International Education and Training Center, Osaka, Japan, Jul. 18–24, 2001.
4. Sengor, T., "State approach in artificial materials development in electromagnetics," *Proceedings of Progress in Electromagnetics Research Symposium*, 568, The Electromagnetics Academy (USA), University of Pisa, Pisa, Italy, Mar. 28–31, 2004.
5. Sengor, T., "The state space approach and modified state equations solution in dispersive chiral media," *Proceedings of XXVIIIth General Assembly of the International Union of Radio Science*, URSI GA 2005, Abstracts Book, COM2-01430-2005; Conference CD, URSI, New Delhi 2005, Paper No. COM2-01430-2005, New Delhi, India, Oct. 23–29, 2005.
6. Sengor, T., "A chiralic circuit element and its use in a chiralic circuit," *Complex Computing-networks, Brain-like and Wave-oriented Electrodynamic Algorithms*, Series: Springer Proceedings in Physics, Vol. 104, 2006.

Analytical Formulation for the Magnetic Shielding Effectiveness of Enclosures with Apertures

I. Bahadir Basyigit, Sukru Ozen, and Selcuk Helhel
Department of Electrical and Electronics Engineering, Akdeniz University, Turkey

Abstract— The effect of magnetic shielding effectiveness has been investigated for apertures on metallic enclosure. Magnetic shielding effectiveness has been calculated as a function of enclosure dimensions, aperture dimensions position within the enclosure. The calculation magnetic shielding depends upon the frequency and polarization of the applied field, the dimensions of the enclosure and the apertures, the number of apertures, and the position within the enclosure. The analytical formulation presented here provides a fast means of investigating the effect of design parameters on the shielding effectiveness of an enclosure. It confirms that long thin apertures are worse than round or square apertures of the same area. For a typical sized enclosure, the theory predicts that doubling the length of a slot reduces magnetic shielding effectiveness and by about 12 dB, while doubling the width only reduces magnetic shielding effectiveness and by about 2 dB. Calculations using the new formulation show that doubling the number of apertures reduces magnetic shielding effectiveness and by about 6 dB. However, dividing a long slot into two shorter ones increases magnetic shielding effectiveness and by about 6 dB.

The Theoretical Rationale of the Existence of Electric and Magnetic Fields Spreading Instantaneously

A. Chubykalo, A. Espinoza, and R. Ivanov
Unidad Académica de Física, Universidad Autónoma de Zacatecas, A. P. C-580, Zacatecas, México

Abstract— In this report, we show that the use of the Helmholtz vector decomposition theorem leads to the theoretical rationale of the existence of solenoidal electric and magnetic fields which can spread instantaneously. The fact is that in the comparatively recent experimental work [1], it was shown that the standard retardation condition does not take into account the complex structure of the whole electromagnetic field in the near zone. In the experiment described in the above-mentioned work such unusual conclusion was obtained: the bound magnetic field in the near zone spreads with the velocity $v \gg c$, i.e., practically instantaneously. Is it possible to explain this surprising result within the framework of classical electrodynamics? In the modern literature, many publications dedicated to the problem of instantaneous action at a distance (IAAD) just in classical electrodynamics do not exist. In the present report we try to explain the result obtained in this experiment taking advantage of the results of our recent paper [2].

REFERENCES

1. Kholmetzkii, A., O. Missevitch, R. Smirnov-Rueda, R. Ivanov, and A. Chubykalo, "Experimental test on the applicability of the standard retardation condition to bound magnetic fields," *Journal of Applied Physics*, Vol. 101, 023532-1–11, 2007, doi:10.1063/1.2409771.
2. Chubykalo, A., A. Espinoza, and A. Alvarado-Flores, "Electromagnetic potentials without gauge transformation," *Physica Scripta*, Vol. 84, 015009-1–6, 2011, doi:10.1088/0031-8949/84/01/015009.

A Local Ether Lens Path Integral Model of Electromagnetic Wave Reception by Wires

M. J. Underhill
Underhill Research Ltd., UK

Abstract— At present there is no *direct* theory of reception of radiation by a thin wire antenna such as a simple half-wave dipole. The generally accepted *indirect* theory is based on the 'theory of reciprocity'. This states that the radiation patterns of any antenna are the same for transmission and reception. The transmit pattern can be computed *directly* on the classical assumption that the conductor currents are the source of radiation from a wire antenna. A small current element is found to have the classical toroidal 'doughnut' shaped radiation pattern. The pattern of a half-wave dipole is computed by applying array theory to combine the current elements of the dipole antenna. As a consequence the doughnut pattern of a half wave dipole is slightly flattened as compared with the patterns of a small dipole or a single current element. From antenna array aperture theory we find that the maximum receive 'capture' aperture area of a of a dipole is an ellipse with major axis of about $\lambda/2$ at right angles to the dipole wire and a minor axis of about $\lambda/4$ along the wire. Note that the dipole capture area is many times the physical area of the dipole wire. The inescapable conclusion is that the presence of the dipole has modified the properties (ε μ, impedance, and refractive index η) of the local space surrounding the dipole at least out to a distance comparable with the half-major axis. This modification of space is the 'local ether' [1]. It then follows that the local ether effectively is a lens that focuses incoming radiation from an area equal to the antenna aperture onto the wire of the dipole. The problem then is to find the local refractive index profile and hence the power flow lines of the incoming energy captured by the antenna. Figure 1 shows a set of paths on a central cross-section of space heuristically derived from the assumption that the uniform incoming energy density finally approaches the wire with uniform angular intensity. The local refractive index profile can be derived approximately from this within bounds. But it can be found more directly from the assumption of the existence of 'EM coupling' [1]. The EM coupling between two points in space is actually a Feynman 'path integral' as used in Quantum Theory, but it is also defined for wire elements by the evanescent wave profile solutions given in [1]. The EM coupling has been shown to be inversely proportional to the square root of frequency and we show how this impacts on the path profile solutions. At high frequencies (THz) we find that energy is scattered or reflected from the local ether out to a distance of several wavelengths. We find a transcendental differential equation for partially refracted radiation trajectories starting just outside the edge of the capture area with the assumption of a defined radial refractive index profile. This equation appears not to be analytically soluble. But stepped 'projectile trajectory' solutions are found numerically.

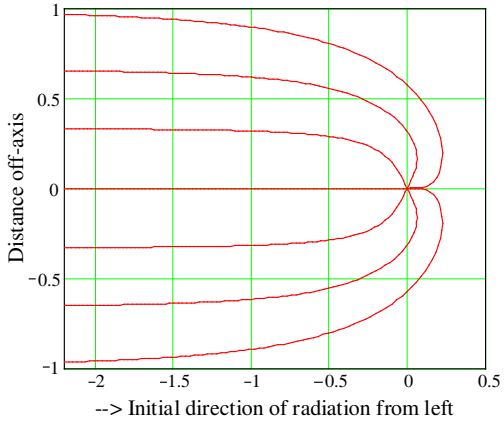

Figure 1: Radiation power flow trajectories on a central crosssection of a thin half-wave dipole at the intersection (0, 0).

REFERENCES

1. Underhill, M. J., "A physical model of electro-magnetism for a theory of everything," *PIERS Online*, Vol. 7, No. 2, 196–200, 2011.

Antenna Pattern Formation in the Near Field Local Ether

Michael J. Underhill
Underhill Research Ltd., Lingfield, UK

Abstract— A trajectory method is proposed for finding the transmission *and* reception power flow lines of multi-element antennas such as the Yagi or phased array. For transmission the trajectories represent the progressive formation of the antenna pattern in the near-field region. For reception the trajectories represent focussing by the near-field ether of incoming plane waves on to the elements of the antenna [1]. Reception and transmission can conveniently be regarded as separate processes occurring in the same region. The region is where the antenna elements are found to modify the 'local ether refractive index'. The power flow line trajectories for transmission and reception are very different but 'reciprocity' always applies.

This 'trajectory method' provides a 'direct' theory of reception (not invoking reciprocity) as well as a complementary theory of transmission of radiation from the antenna.

Refraction, partial reflection and scattering of power flow by the local ether characterise and form the power flow trajectories. Scattering causes progressive decrease of power density in the power flow direction, while still retaining strict power and energy conservation. Power flow trajectories can always be defined in terms of these processes.

The power flow can also be considered to arise from a displacement current component flowing outward in an in-phase potential [2, 3]. Stored energy can be considered as the energy in a standing wave structure surrounding the antenna. The potential is in positive quadrature with the displacement current or magnetic (inductive) energy, and in negative quadrature for electric (capacitative) energy. The two types of energy density are lightly coupled at any point in space and can be power added arithmetically to give the overall power density. In this way the Poynting Vector (PV) may be extended to be the Extended Poynting Vector (EPV) which also encompasses stored energy and local spatial Q.

The power is steered along the power flow lines not only by the local variations of refractive index in the local ether, but also by the combined potential of the excitations of the antenna elements. The far-field antenna pattern is always formed from the combined element potentials. This classical way of finding the far-field antenna pattern is thus retained. Such far field patterns can be suitably modelled by 'Analytic Region Modelling', ARM [4].

Four related problems remain: (a) How is the radiating energy from omnidirectional array elements diverted from the null directions and focussed into the lobe directions? (b) At what distance is the antenna pattern of an array actually formed? (c) For a directional antenna the sum of the momentum from each radiating element is not the same as the overall momentum of the radiation as seen in the far-field. There is a backward force on the antenna, but what are the lines of force for this? Is the antenna actually pushing against the ether or is it purely back pressure from the radiation? (d) Is there any variation in the velocity of power flow in the near field local ether? It may also deviate slightly from the velocity c_{EM} in free space? Is this is of secondary concern? These issues will be addressed in the full paper and the presentation.

REFERENCES

1. Underhill, M. J., "A local ether lens path integral model of electromagnetic wave reception by wires," to be presented at PIERS 2012 Moscow.
2. Underhill, M. J., "A physical model of electro-magnetism for a theory of everything," *PIERS Online*, Vol. 7, No. 2, 196–200, 2011.
3. Underhill, M. J., "Maxwell's transfer functions," *PIERS Proceedings*, 1755–1759, Kuala Lumpur, Malaysia, March 27–30, 2012.
4. Underhill, M. J., "Novel analytic EM modelling of antennas and fields," *PIERS Proceedings*, 1760–1764, Kuala Lumpur, Malaysia, March 27–30, 2012.

Calculation of an Equivalent Electrical Conductivity Tensor for Multidirectional Carbon Fiber Reinforced Materials

N. Athanasopoulos and V. Kostopoulos
Department of Mechanical Engineering and Aeronautics
University of Patras, Greece

Abstract— The ability of carbon fibers to conduct electric current can be used in a plethora of applications. Carbon fibre reinforced plastic materials (CFRPs) can be divided into unidirectional and multidirectional laminates. The electric conductivity of the unidirectional laminates presents strong electric anisotropy and can be expressed by a symmetric, second order tensor. There is no point to study the electrical conductivity of CFRPs ignoring the microstructure of the material. In order to consider a multi-layered material as homogenous, it is of paramount importance that we examine the intralaminar and interlaminar areas.

Using the continuity equation, it can be proved that the electric conductivity of the multidirectional laminates can also be expressed by a second order tensor (equivalent tensor). Hence, the electrical conductivity tensor of the CF preform can be calculated for any stacking sequence assuming that the material is homogenous and the plies' thickness negligible in comparison to the other dimensions. The equivalent tensor can be imported into the elliptic partial differential equation which is the governing equation for steady current in anisotropic media. Therefore, the electric field and the current density can be calculated by solving the aforementioned elliptic PDE.

The validity of the equivalent tensor was confirmed by measuring the electrical resistivity of the multidirectional laminates media for various multidirectional laminates (stacking sequences). For a second confirmation the coupled thermo — electric problem was solved numerically using as input material the calculated equivalent tensor. The calculated temperature field for each multidirectional laminate was confirmed experimentally via a thermal camera.

Spherical Wave Representation of the Dyadic Green's Function for a Spherical Impedance Boss at the Edge of a Perfectly Conducting Wedge

B. Ghassemiparvin and A. Altintas
Electrical and Electronics Engineering Department, Bilkent University, Turkey

Abstract— The electromagnetic scattering by a perfectly conducting wedge has been treated extensively in the literature where both asymptotic and eigenfunction solutions have been presented. In this work, canonical problem of a scatterer at the edge of a wedge is considered and eigenfunction solution is utilized. Initially a dyadic Green's function for a spherical impedance boss at the edge of a perfectly conducting wedge is obtained. Since scattering from objects at the edge is of interest, a three-dimensional Green's function is formulated in terms of spherical vector wave functions. First an incomplete dyadic Green's function is expanded in terms of solenoidal vector wave functions with unknown coefficients, which is not valid in the source region. Unknown coefficients are calculated by utilizing the Green's second identity and orthogonality of the vector wave functions. Then, the solution is completed by adding general source correction term. Resulting Green's function is decomposed into two parts. First part is the dyadic Green's function of the wedge in the absence of the sphere and the second part represents the effects of the spherical boss and the interaction between the wedge and the scatterer. In contrast to cylindrical vector wave function expansions and asymptotic solutions which fail to converge in the paraxial region, proposed solution exhibits good convergence everywhere in space except near the imaginary spherical surface which contains the source point. Scattered field patterns are given for several impedance values and results are compared with those of a perfectly conducting spherical boss. Effects of the incident angle and surface impedance of the boss on the scattering pattern are also examined.

Electromagnetic Sources and Observers in Motion VII — Medium Support for a New Relativity Theory

S. E. Wright
Moor Lane Laboratory, ECASS Technologies Ltd, Kirkburton, Huddersfield, HD8 0QS, UK

Abstract— This is the first of two papers to be presented at the Moscow Symposium, and the seventh paper in the series of electromagnetic (EM) sources and observers in motion. Two given in Xian China, two in Cambridge USA and two in Marrakesh Morocco, over the last two years. This Moscow paper deals with the existence of the propagation medium (ether) and its support for a new relativity theory. The new theory, derived directly from Lorentz's medium based motional transform, simplifies our understanding of the universe. It challenges Einstein's SR as a more logical and comprehensive theory. This theory is not inferring that Einstein's Special Relativity (SR) is in catastrophic error. It simply describes an improved theory based on a medium that agrees with the measured SR predictions, predicts additional measured observations that SR cannot predict, and identifies ether-less aspects of SR that are in error and cannot be measured. Historically, Lorentz was the first to predict the measured effects of EM systems in motion, based on the medium. Einstein solved the EM wave equation (partially), based on Lorentz's transform, predicting the same medium based motional properties as Lorentz. However, Einstein believed there was no medium in support of his ether-less predictions, although he used a medium in his field equations to predict the actual observations. Therefore, Einstein's SR has an ether-less, non causal aspect, which cannot be measured, and a medium based causal aspect that predicts many of today's measured observations. The new relativity theory (NR) is an extension of Lorentz's medium based motional transform. It distinguishes between measured source and observer motional differences and between motional reference frames. These cannot be accounted for without a medium, and are therefore not predicted by Einstein's ether-less SR. Restoring the medium removes the discontinuity between classical and modern physics. The medium's existence provides a common link between EM waves gravitational fields, accelerating frames and perhaps to the unification theory of the universe. The mathematics and physics developed in this new relativity theory perfectly predict and agree with the current perspective and understanding of the universe.

*Corresponding author: Selwyn E. Wright (selwyn.wright@ntlworld.com).

Electromagnetic Sources and Observers in Motion VIII — New Relativity Theory Establishes Einstein's Ether-less Aspect of Relativity as Irrational

S. E. Wright
Moor Lane Laboratory, ECASS Technologies Ltd, Kirkburton, Huddersfield, HD8 0QS, UK

Abstract— This is the second paper to be presented to the symposium in Moscow, and the eighth paper in the series of EM sources and observers in motion. The first paper at this symposium considers the existence of the propagation medium (ether) and its support for a new relativity theory. This paper establishes Einstein's ether-less aspect of relativity as non causal (cannot be measured). The Lorentz Transform (LT), predicts the complete motional transform, including both classical wave propagation time asymmetry (PTA) ahead and behind a moving source, which is fundamental to all wave propagation. And the additional Lorentzian relativistic time rate and system contraction (LC) through high speed motion, (notionally LT = PTA + LC). PTA can exist without LC, but LC cannot exist without PTA. The classical PTA is therefore a vital part of any wave theory. It explains both the classical asymmetrical effects in the frequency domain (Doppler) and time domain (Sagnac). However, Einstein's ether-less Special Relativity (SR) cannot support PTA. Whereas, Lorentz's theory is fundamental, it is causal (the cause must always occur before the effect (event)), it is a solution of the wave equation, predicting measured events. It is the result of motion relative to the medium, as Lorentz predicted, not on relative motion between systems, as Einstein claimed. Einstein's ether-less concept, a belief in his relative motion and his omission of measured PTA, is therefore not supported by the medium based LT. Einstein's ether-less aspect is therefore irrational, it predicts his ether-less properties, such as time travel and no absolute time and space, neither of which can be measured. These ether-less non measureable predictions are based on Einstein's invariant inertial frame, which without the medium cannot anticipate PTA. The measured predictions, are based on Lorentz's moving optical frame, which describes waves and systems moving with respect to the medium. The measured predictions of SR are therefore medium based, in conflict with and discrediting Einstein's own ether-less predictions. SR is therefore inconsistent, incomplete and its ether-less interpretation invalid. To complete the radiation process, distinction should be made between source and observer motion time and spaces scales, allowing their flight paths to be plotted on the same medium space-time diagram.

*Corresponding author: Selwyn E. Wright (selwyn.wright@ntlworld.com).

Session 3A8
Magnetism, Magnetic and Multiferroic Materials, Structures and Devices

Integrated Ferroelectrics: New Trends of Modern Information Technologies

A. S. Sigov
Moscow State Technical University of Radio-engineering, Electronics and Automation
78 Vernadskogo Av., Moscow, Russian Federation

Abstract— The main direction of the development of micro- and nano-electronics is the increase of the treatment speed and amount of information based upon further increase of the IC integration rate. Hence there appear the requirements of new approaches to the principles of information treatment and search for new functional materials.

Up to now dielectric materials in microelectronic devices played a passive role of isolators, while the main active media were: semiconductors in the processes of information treatment, and semiconductors or magnetic materials in memory devices. The implementation of smart (active) dielectric materials into design of information receiving, processing, and storage devices provides one with ample opportunities for a sufficient increase of the amount of information under processing. Among active dielectrics, the most promising for microelectronics are ferroelectrics, pyro-, piezoelectrics, and electrets.

The unique properties of ferroelectrics and related materials cited above make it possible to use them as a base for a new class of integrated ferroelectric devices for information receiving, treatment, and storage with a thin layer of ferroelectric serving as an active element. Thus the spontaneous polarization switching by external electric field is used for creating nonvolatile memory devices; high dielectric constant helps one to develop capacity elements, microwave ICs, etc.; pyroelectric activity allows one to create non-cooled IR array receivers; electromechanical properties are the basis of ferroelectric MEMS. The nonlinear optical properties are of interest for creating devices of optical treatment and recording of information.

The presentation touches upon the subjects of functional ferroelectric materials and their physical properties, thin films and heterostructures preparation, as well as the most interesting cases of their practical applications, for example in telecommunications, memory cells, and so on.

Design of Stripline Structure for Electromagnetic Characterization at Microwave Frequency

Ellen Yoshie Sudo Lutif[1, 2], **Anderson Kenji Hirata**[2],
Alberto José de Faro Orlando[1], **and Antonio Carlos da Cunha Migliano**[1, 2]

[1]Aerospace Technological Institute (ITA), CTA, Brazil
[2]Institute of Advanced Studies (IEAv), CTA, Brazil

Abstract— A comprehensive approach to the design of a stripline for EMC testing is given is this paper. The authors attention has been focused on the design items that are most crucial by the achievement of satisfactory value of the VSWR and impedance. The characteristic impedance of the stripline test section should be smoothly matched with the feed and terminations points in order to minimize the standing waves. Thereby, the most critical parameters that directly determine the physical design of the stripline are impedance matching at the feed port (S_{11} parameter) and transmission between two ports (S_{21} parameter). An analysis can be performed for the stripline configuration using a vector network analyzer. A measurement of the reflection from transmission through a material along with knowledge of its physical dimensions provides the information to characterize electromagnetic waves at microwave frequencies range.

Nonlinear Dynamical Electromagnetic Relaxation in Lanthanum Manganite Toroid

A. P. Nosov and A. B. Rinkevich
Institute of Metal Physics Ural Branch of Russian Academy of Sciences, Ekaterinburg, Russia

Abstract— Magnetic aftereffect or magnetic viscosity is the time-dependent magnetic phenomenon consisting in retardation of response of magnetic system upon variation of magnetic field. Hysteresis loss, temporal decrease of permeability, frequency dependence of permeability are closely related to magnetic viscosity. The goal of this work is to observe and describe the magnetic aftereffects in the toroidal sample of lanthanum manganite and clarify the conditions under which such aftereffects can be observed most pronouncedly. During our experiments the directions of the AC $\mathbf{H}\sim$ and DC $\mathbf{H}$ magnetic fields have been chosen perpendicular each other, $\mathbf{H} \sim\perp \mathbf{H}$. This orientation is hand-picked in order to guarantee easy variations of the AC magnetization vector even in strong DC magnetic field close to saturation. Special experimental method have been developed to observe dynamical nonlinear magnetic aftereffects. Relaxation of second harmonic of signal have been recorded. Lead doped lanthanum manganite $La_{0.6}Pb_{0.4}MnO_3$ have been chosen as a material for investigations because it has the value of the Curie temperature slightly above the room temperature and its linear radiofrequency properties have been investigated in details earlier. The analysis of the results obtained permitted us to classify the aftereffect as a dynamical one since it was observed at radio frequencies. Nonlinear nature of the effect was confirmed by its threshold character and the possibility of its observation via the second harmonic. Experimental results show that the dynamical nonlinear aftereffect is observed in a limited interval of external magnetic fields. We show that magnetic prehistory defines the sign of aftereffect. Coexistence of ferromagnetic and antiferromagnetic phases in doped manganites suggests that there should be glassy behavior associated with the frustration of the different interactions.

ACKNOWLEDGMENT

This work was supported by the Program No. 24 of the Presidium of the Russian Academy of Sciences, and the initiative grant 12-y-2-1010 of the Ural Branch of the Russian Academy of Sciences.

Experimental Evidence for the Magneto-kinematic Effect

Vladimir Leus[1] **and Stephen Taylor**[2]

[1]Sobolev Institute of Mathematics, Novosibirsk 630090, Russia
[2]Department of Electrical Engineering and Electronics
University of Liverpool, Liverpool L69 3GJ, UK

Abstract— The movement of a magnetic field together with its source (a moving permanent magnet) has been a controversial topic in the scientific literature for decades. In essence the debate is hinges upon whether a permanent magnetic field moves like a wave or it moves like a body. The question arises: is the induced EMF measured purely a consequence of electrodynamics or is the EMF kinematically induced? Such a magneto-kinematic effect has been previously observed by two Russian researchers N. Zajev and A. Dokuchajev as early as in 1958 (published in 1964) for the case of a rotating coil energised by a direct current. In this article we present further evidence confirming this effect for a different experimental arrangement: that of a rotating magnetic circuit. The magnetic circuit used comprised a permanent ring magnet and a soft iron yoke rotating together. Two types of magnetic ring were considered: dipole and quadrupole. In each case the resulting induced EMF was quantifiably explicable in terms of the Zajev-Dokuchajev (Z-D) effect: the moving of the magnetic field with the rotating magnet. We also present a novel method for measurement of the induced EMF in a stationary conducting loop in the case of rectilinear motion of a permanent magnetic dipole through the loop. In each case the motion of the magnetic field are detected by measuring the EMF induced in a stationary conductor. A new method of calculation is presented which is applicable to a range of generic problems dealing with moving sources of magnetic flux.

Investigation of Resonance Interactions of Microwaves with 3D Magnetic Nanocomposites Using the Probabilistic Model

G. S. Makeeva[1], **O. A. Golovanov**[1], **and A. B. Rinkevich**[2]

[1]Penza State University, Russia
[2]Institute of Metal Physics, Ural Division of Russian Academy of Science, Russia

Abstract— The opal matrix package with embedded magnetic nanoparticles is a promising material for application in the magnetically tunable microwave devices: attenuators, phase shifters, filters. Typically, the real ferrite filling the octahedral voids between the opal sub-micron spheres in the opal matrix has a random distribution of the shape and the size of nanoparticles. From the TEM microscopy data, the size of particles varies from 5 to 60 nm and the particles can form the aggregates [1].

In contrast to [2] a probabilistic approach to model the resonance interactions of electromagnetic waves (EMWs) with 3D magnetic opal nanocomposites has been developed. We consider the value of the ferromagnetic resonance (FMR) magnetic field H_r of magnetic nanoparticles as a random quantity because the FMR fields are determined by the internal magnetic field depending on the shape of particles. The deterministic model based on the solution of the Maxwell's equations with electrodynamic boundary conditions, complemented by the Landau-Lifshitz equation was developed by us in [2] to simulate a propagation of EMWs in magnetic nanostructured media.

The probabilistic model was created in the following way. We propose that the random quantity H_r has a normal distribution and use the random-number generator for the simulation. The numerical approach is based on the decomposition of domain of the 3D magnetic nanocomposite into autonomous blocks with Floquet channels (FAB) [3], described by its FAB conductivity matrix $\mathbf{Y}$, taking into account electrodynamical boundary conditions, the shape and the number N of magnetic nanoparticles inside.

The propagation constants of clockwise and counterclockwise polarized EMWs, the ordinary and extraordinary modes (for both transverse and longitudinal orientations of DC magnetic field H_0), propagating in the nanostructured medium, were calculated from the characteristic equation [2].

At first stage the effective permeability tensor and the effective permittivity of 3D magnetic opal nanocomposite were determined using the deterministic electrodynamic model. At second stage we find the expectation values of the components of the effective permeability tensor as a function of DC magnetic field H_0 by using the simulation probabilistic model.

In our model the radius of the SiO_2 sub-micron spheres was set $r = 100$ nm and for magnetic nanoparticles $Ni_{0.7}Zn_{0.3}Fe_2O_4$ with saturation magnetization $4\pi M_s = 5$ kG, the exchange constant $A = 2.2 * 10^{-9}$ Oe cm^2 and the number $N = 4$. The influence of the damping parameter of magnetic nanoparticles and the standard deviation of the random quantity H_r are analyzed at a frequency 26 GHz. The agreement of numerical results with the measured values FMR results [1] shows the robustness of the developed probabilistic algorithm.

REFERENCES

1. Ustinov, V. V., A. B. Rinkevich, D. V. Perov, M. I. Samoilovich, and S. M. Klescheva, *Journal of Magnetism and Magnetic Materials*, Vol. 24, 78–82, 2012.
2. Makeeva, G. S. and O. A. Golovanov, *Journal of Communications Technology and Electronics*, Vol. 54, 1379–1383, 2009.
3. Golovanov, O. A. and G. S. Makeeva, *Journal of Communications Technology and Electronics*, Vol. 54, 1345–1352, 2009.

Measured Permeability of Saturated Ferromagnetic Films: Deviations from Kittel's Equations

A. V. Osipov, **I. T. Iakubov**, **A. N. Lagarkov**, **S. A. Maklakov**, **K. N. Rozanov**, **and I. A. Ryzhikov**
Institute for Theoretical and Applied Electromagnetics, Moscow, Russia

Abstract— The presentation reports on experimental studies of microwave permeability of thin ferromagnetic films measured under permanent magnetic bias. The microwave permeability of Fe-N films measured with coaxial technique [1] is shown in Fig. 1. It is well known that the frequency dependence of microwave permeability of a saturated thin thin ferromagnetic film agrees with the Lorentzian dispersion law [2]. The parameters of the Lorentzian law, the static permeability, $\mu_{\rm s}$, and the resonance frequency, $f_{\rm r}$, of the film are related to the magnetostatic parameters by well known Kittel's equations:

$$\mu_{\rm s} = 1 + 4\pi M_0/H_{\rm eff}, \quad f_{\rm r} = \gamma\sqrt{H_{\rm eff}\,(H_{\rm eff} + 4\pi M_0)},$$

where $4\pi M_0$ is the saturation magnetization of the film, γ is the gyromagnetic ratio, and $H_{\rm eff}$ is the effective anisotropy field. This field is constituted by crystallographic anisotropy field, $H_{\rm a}$, external static magnetic field, H_0, and magnetoelastic field, H_λ.

The measured dependence of parameters of ferromagnetic resonance on magnetic bias provides a good qualitative agreement with Kittel's equations as is seen in Fig. 2. However, some deviations from Kittel's equations are also detected. It is shown in the presentation that these deviations may be attributed to the angle distribution of effective anisotropy fields. Therefore, the peremability measurements under external magnetic bias may be employed for obtaining information on the magnetic and crystallographic structure of thin ferromagnetic films.

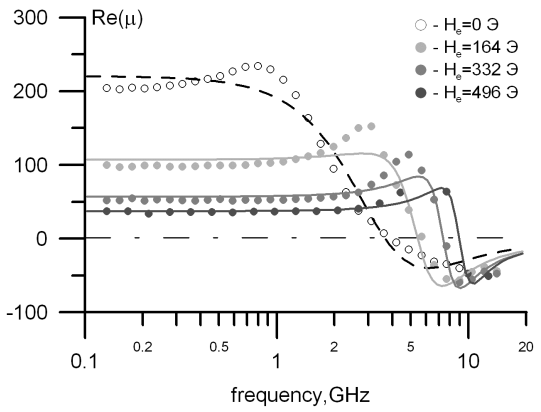

Figure 1: The measured real parts of intrinsic permeability of 100 nm thick Fe film under different values of external static magnetic field. Dots are the measured data, lines are fitting with Lorentzian dispersion law.

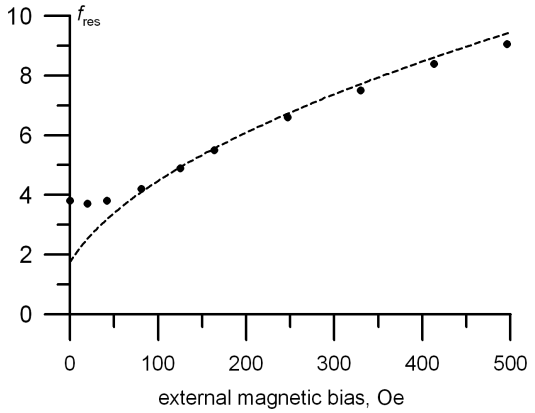

Figure 2: The ferromagnetic resonance frequency retrieved from the measured permeability and plotted against the external static magnetic bias. Dots are the retrieved data, line is fitting with Kittel's equation.

REFERENCES

1. Rozanov, K. N., et al., *J. Communic. Technol. Electron.*, Vol. 47, 210, 2002.
2. Iakubov, I. T., et al., *J. Magn. Magn. Mater.*, 272–276, 2208, 2004.

Spin and Electric Polarization Waves in Dielectric Systems of Different Dimensions

P. A. Andreev[1] and L. S. Kuzmenkov[2]

[1]Department of General Physics, Physics Faculty, Moscow State University, Russian Federation
[2]Department of Theoretical Physics, Physics Faculty, Moscow State University, Russian Federation

Abstract— We study quantum dispersion properties of spin waves and waves of electrical polarization in systems of neutral particles. We pay attention for one-, two-, and three-dimensional dielectric systems. We consider spinning particles in the presence of an external uniform constant magnetic field, and electrically polarized particles are regarded in the presence of an external uniform constant electrical field.

Electric dipole moment and magnetic dipole moment has different nature. It leads to the difference in the dispersion properties of collective excitations. We can watch properties of dipole moments in systems of neutral particles there the Coulomb interaction does not overshadow the dynamical picture.

For collective excitation studying we use the method of many-particle quantum hydrodynamic. Quantum hydrodynamic equations are derived from many-particle Schrodinger equation, so, quantum hydrodynamic equations are deduced from first principles of quantum mechanics. For electrically polarized dielectrics a quantum hydrodynamic equations consist of four tensor equations, these are continuity equation, Euler equation, equation of polarization evolution and equation of polarization current evolution. For magnetized dielectrics a quantum hydrodynamic equations consist of three tensor equations, these are continuity equation, Euler equation and magnetic moment evolution equation (a generalization of Bloch equation).

We brief discuss the evident form of Hamiltonians for spin-spin interaction and electric dipole-dipole interaction. We present Hamiltonians corresponding to the Maxwell equation.

As the result we present the dispersion dependencies for dipole waves in one-, two-, and three-dimensional dielectric systems *and* compare dispersion dependencies for the spin waves and the waves of electric dipole moment.

Evidence of Strain-induced Ferroelectric Phase Transitions in Thin Films by Microwave Dielectric Resonator Technique

V. Bovtun[1], **V. Pashkov**[2], **M. Kempa**[1], **S. Kamba**[1], **and J. Petzelt**[1]

[1]Institute of Physics ASCR, Na Slovance 2, Prague 18221, Czech Republic
[2]NTUU "Kyiv Polytechnic Institute", Prospect Peremogy 37, Kyiv 03056, Ukraine

Abstract— Parameters of the $TE_{01\delta}$ dielectric resonator (DR) composed of the film, substrate and base component are sensitive to the film dielectric properties [1]. Recently we have proposed a thin DR consisting only of the dielectric substrate and deposited film for the electrode-free microwave characterization of thin films [2, 3]. Absence of the base component essentially increases the method sensitivity and allows its application to study the ultra-thin films. In-plane averaged dielectric parameters of the films are determined by comparison of the resonance frequency and quality factor of $TE_{01\delta}$ resonances of identical substrates with and without the film. Here we demonstrate efficiency of the composite and thin DR methods by characterization of high-permittivity films with a strain-induced ferroelectric phase transition.

Ferroelectric phase can be induced in incipient ferroelelectrics, like $SrTiO_3$, $EuTiO_3$ or $KTaO_3$, by strains originated from the crystal lattice parameters mismatch of film and substrate or other interfacial phenomena [4–6]. Usually, the films should be extremely thin to avoid relaxation of the mechanical strain. The following films were studied:

a) epitaxial −0.9% compressively strained $EuTiO_3$ film (22 nm) on (100) LSAT substrate;
b) epitaxial +1% tensile strained $EuTiO_3$ film (100 nm) on (110) $DyScO_3$ substrate;
c) epitaxial +1% tensile strained $SrTiO_3$ films (30 and 100 nm) on (110) $DyScO_3$ substrates;
d) polycrystalline $KTaO_3$ films (50 and 200 nm) on (0001) sapphire and alumina substrates;
e) polycrystalline $KTaO_3$ films (50 and 200 nm) on (100) MgO substrates.

Temperature dependences of their dielectric permittivity and losses were measured between 10 K and 380 K at the DR resonance frequency appearing in the range from 5 to 18 GHz. They are analyzed and discussed together with results of the infrared and THz spectroscopy.

Pronounced permittivity and loss maxima were observed in (b) and (c) films at $\sim$ 250 K and $\sim$ 270 K giving evidence of the strain induced ferroelectric phase transition with a polarization in the film plane [4, 5]. Diffused dielectric anomalies bring evidence for the induced ferroelectric phase transition at $\sim$ 60 K in (d) films [6], while no permittivity maximum was observed in (e) films, whose permittivity saturates on cooling similar to that of $KTaO_3$ ceramics and single crystals. Dielectric anomaly was observed near the antiferrodistortive phase transition at 120 K in (a) films [7].

The DR method potentiality in microwave characterization of multiferroic materials is discussed.

REFERENCES

1. Bovtun, V., S. Veljko, A. Axelsson, et al., *Integrated Ferroelectrics*, Vol. 98, 53, 2008.
2. Bovtun, V., V. Pashkov, M. Kempa, and S. Kamba, *J. Appl. Phys.*, Vol. 109, 024106, 2011.
3. Bovtun, V., V. Pashkov, M. Kempa, et al., *Proc. 21st Int. Crimean Conf. "Microwave & Telecommunication Technology"*, 620, Sevastopol, Sep. 2011.
4. Nuzhnyy, D., J. Petzelt, S. Kamba, et al., *Appl. Phys. Lett.*, Vol. 95, 232902, 2009.
5. Lee, J. H., L. Fang, E. Vlahos, X. Ke, Y. W. Jung, et al., *Nature*, Vol. 466, 954, 2010.
6. Skoromets, V., S. Glinšek, V. Bovtun, et al., *Appl. Phys. Lett.*, Vol. 99, 052908, 2011.
7. Kamba, S., V. Goian, M. Orlita, D. Nuzhnyy, J. H. Lee, et al., Submit to *Phys. Rev. B.*

Shear Vibrations of Magnetostrictive-piezoelectric Film Structure

K. V. Lavrentjeva, **V. M. Petrov**, **and R. V. Petrov**
Institute of Electronic and Information Systems, Novgorod State University
Veliky Novgorod 173003, Russia

Abstract— Because the magnetoelectric (ME) effect in composites is caused by mechanically coupled magnetostrictive and piezoelectric subsystems, it sharply increases in the vicinity of the electromechanical resonance (EMR) frequencies. The present paper focuses on the enhancement of ME coupling at shear modes in magnetostrictive-piezoelectric film structure.

We consider a bilayer of magnetostrictive and piezoelectric films on a substrate that is subject to a bias magnetic field along its axis. Theoretical modeling of ME effect is based on equations of media shear motion for magnetostrictive and piezoelectric phases and substrate. To solve these equations for displacement component, one should use the appropriate boundary conditions for stress and strain components on interfaces. Substituting the found solutions into the open circuit condition enables one to obtain the expression for ME voltage coefficient that is equal to the ratio of induced electric field to applied magnetic field.

It is well known that the lattice mismatch between the substrate and components and piezoelectric and piezomagnetic phases results in variation of piezoelectric coefficients and permittivity that determine the ME voltage coefficient. The variation of considered parameters due to lattice mismatch can be found using the Landau-Ginsburg-Devonshire phenomenological thermodynamic theory.

As an example, we apply the theory to the specific bilayer of lead zirconate titanate (PZT) and nickel ferrite (NFO). One notices an increase in the ME coupling strength by approximately 100 times at the fundamental thickness mode of EMR compared to low-frequency value. Signal attenuation is taken into account in these calculations by introducing a complex frequency and for an imaginary component equal to 10^{-2} of real component.

For the bilayer on $SrTiO_3$ substrate, the peak ME voltage coefficient decreases with increasing the substrate thickness. EMR line spectrum of ME voltage coefficient consists of a family of equal-spaced peaks. The distance between every two peaks is substantially determined by the substrate thickness. The maximum of envelope of resonance lines occurs at the EMR frequency of PZT-NFO bilayer. It should be noted that increasing the substrate thickness results in considerably weaker decrease in ME coupling at shear mode compared to longitudinal mode.

Estimates for PZT-NFO predict ME voltage coefficients on the order of 30 V/cmOe at 1 GHz. The phenomenon is of importance for the realization of multifunctional ME nanosensors/transducers operating at microwave frequencies.

Winter Magnons in Circular and Triangular Vortex State Permalloy Dots

A. Lara[1], **A. Awad**[1], **F. G. Aliev**[1], **K. Y. Guslienko**[2, 3], **and V. Metlushko**[4]

[1]Departamento de Física de la Materia Condensada, C03
Universidad Autónoma de Madrid, Cantoblanco, Madrid 28949, Spain
[2]Departamento de Fisica de Materiales
Universidad del País Vasco, San Sebastian 20018, Spain
[3]Ikerbasque, The Basque Foundation for Science, Bilbao 48011, Spain
[4]Department of Electrical & Computer Engineering
University of Illinois at Chicago, Chicago, IL, USA

Abstract— We present an investigation of the magnetization dynamics in circular Permalloy (Py) dots in the single vortex (SV) or double magnetic vortex (DV) states and in triangular Py dots in SV state by means of broadband ferromagnetic resonance and micromagnetic simulations. The oscillating magnetic field is applied in the dot plane. In the metastable DV configuration we have observed a new type of quasi 1D spin waves excited along the domain walls connecting the vortices and edge half-antivortices [1]. We have also detected several spin excitation modes of the same kind in 25 nm thick Py triangles (Figure). In this case, the domain walls naturally appear in the SV ground state, connecting the vortex core and the vertices of the triangle. These spin waves are analogous to the displacement waves of elastic strings and could be excited in a wide class of magnetic nanostructures possessing domain walls.

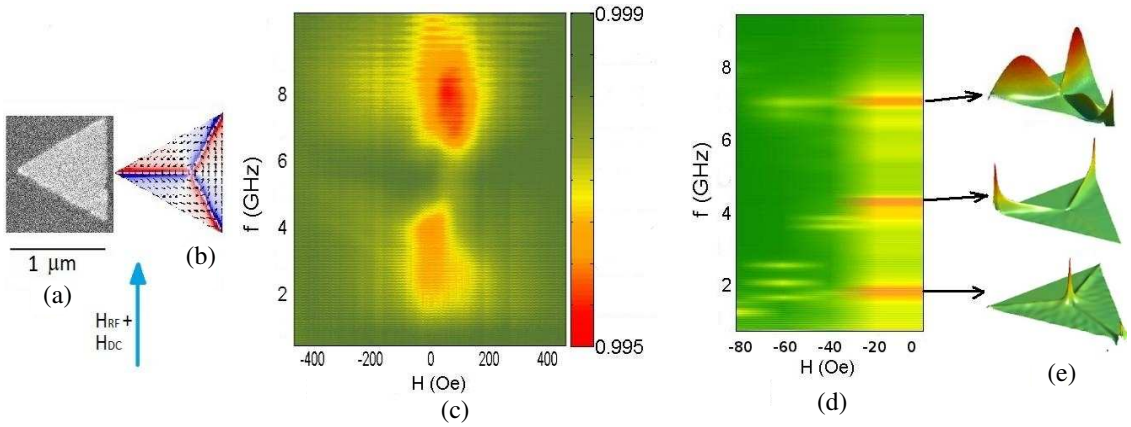

Figure 1: (a) SEM image of a triangular dot. (b) Simulated ground state (vortex state) of a triangular dot. (c) Measured magnetic response of dots array as a function of bias field and frequency of the microwave signal. (d) Dynamic simulation of intensity of eigenmodes as a function of bias field. (e) Simulated amplitude profiles of eigenmodes ($\Delta M_X/M_S$).

REFERENCES

1. Aliev, F. G., A. A. Awad, D. Dielman, A. Lara, V. Metlushko, and K. Y. Guslienko, *Physical Review B*, Vol. 84, 144406, 2011.

A Calibration Technique for Single-port Permeability Measurements at Microwaves

S. N. Starostenko and K. N. Rozanov
Institute for Theoretical and Applied Electromagnetics RAS
Russian Federation, Moscow, Izhorskaya, 13, Russia

Abstract— Microwave measurements of thin film are usually performed in all-in-one shorted stripline cells [1]. The cell length usually is less than 2 cm as the highest operating frequency of a cell is associated with its resonance frequency. But the smaller is the length, the higher is the zone of non-uniform filed in the vicinity of coaxial to stripe coupling and the smaller is the zone of uniform filed that limits the measured sample size. Besides, the smaller is the coupling, the poorer is its matching and the lower is its transparency and the field strength inside the cell. The sample cross-section and the coupling matching define the threshold permeability measured with an available network analyser. The procedures that account for field non-uniformity [2, 3] are numerical and too cumbersome for practice, therefore the measurement of samples with low magnetisation is still a challenging problem. The same considerations are true for other designs of single-port all-in-one transmission lines.

The difficulty arises from unknown S-parameters of a connector or coupling as the standard calibration procedure with zero, infinite and matched loads is inapplicable to a cell with an internal inhomogeneity. It is possible to neglect its contribution to the measured reflectivity response only at frequencies below the resonance of the measurement cell. Therefore this neglection artificially limits the highest operating frequency [1–3]. There are known several calibration procedures appropriate for single-port all-in-one cells. The conventional one is similar to a sliding short method, and is based on measurement of reflectivity response as a function of sample position relative to a short at the each frequency. A drawback is that the wider is the frequency band, the higher should be the sample-slide length and the more measurements are needed. The technique is laborious and is limited by cell design. An alternative procedure is based upon a partial calibration with a reference sample of well-known constitutive parameters. The prototype procedure [4] takes into account sample sizes and shape, but neglects one S-parameter of internal inhomogeneity.

The proposed technique is based on measurement of two complimentary reference samples. The first one is a permeable composite similar to one in the paper [4]. The second sample may be either a dielectric with high permittivity or a stripe of impermeable metal. The dimensions of both reference samples are selected to obtain approximately opposite reflectivity phases within the operating frequency band. The calibration procedure includes the reflectivity measurement of an empty cell and of the cell loaded with each of reference samples.

The measurements are performed in 30 cm-long stripline cell, where the coupling is well matched and low-susceptible samples may be large enough for reliable permeability measurement. Another advantage of the long cell is that the calibration errors reveal themselves as permeability oscillations as the cell resonance is well below the highest operating frequency.

The proposed technique has been tested by measurements of samples with known permeability spectra; the measurement accuracy is almost tenfold higher than in [4]. The accuracy increase makes it possible to measure microwave permeability spectra of bulk permeable metals (thick foils).

ACKNOWLEDGMENT

The partial support by RFBR Grants Nos. 12-08-00954 and 12-02-91667 is acknowledged.

REFERENCES

1. Bekker, V., K. Seemann, and H. Leiste, *J. Magn. Magn. Mater.*, Vol. 270, 327, 2004.
2. Wu, Y. Q., Z. X. Tang, Y. H. Xu, B. G. Zhang, and X. He, *IEEE Trans. Magn.*, Vol. 46, 886, 2010.
3. Liu, Y., L. Chen, C. Y. Tan, H. J. Liu, and C. K. Ong, *Rev. Sci. Insr.*, Vol. 76, 063911, 2005.
4. Starostenko, S. N., K. N. Rozanov, and A. V. Osipov, *J. Appl. Phys.*, Vol. 103, 07E914, 2008.

Session 3A9
Poster Session 4

Impact of Temperature on the Electromagnetic Susceptibility of Operational Amplifiers

R. Fernández-García and I. Gil
Department of Electronic Engineering
Universitat Politècnica de Catalunya, Colom 1, Terrassa 08222, Spain

Abstract— Over recent years, due to the increasing demand for wireless operation electronic devices, a severe and complex electromagnetic pollution environment has been created. Therefore, the susceptibility to Radiofrequency Interferences (RFI) has become a more important constraint for integrated circuit designers, particularly for analogue IC, which are the most sensitive circuits to RFI [1]. In order to characterize the IC susceptibility different standards have been proposed and the IEC 62132-4 Direct RF Power Injection is one of the most extensively used [2]. In this work, the IEC 62132-4 standard has been used in order to characterize the most widely used analog device, the Operational Amplifier (OpAmp). In this case, unlike others works, where the Operational amplifier susceptibility is evaluated [3], the temperature has been taking into account. The impact of the temperature can be critical in a lot of safety application, i.e., automotive, where the electronic equipment's near to the engine should resist, under normal operation conditions, temperatures about 100°C. Fig. 1 shows the experimental setup. It consists of a RF signal generator (providing the RFI disturbance) directly connected to a directional coupler in order to measure the actual level of power injected into the DUT and oscilloscope to measure the OpAmps offset voltage due to RFI. Notice that the PCB is located in an oven in order to control the temperature. In Fig. 2, the offset voltage of a LM741 OpAmp is shown for −20 dBm, −10 dBm and 0 dBm interference at 100 MHz when the temperature is swept from 25°C to 75°C. In all cases the voltage offset is reduced about 10% with the temperature.

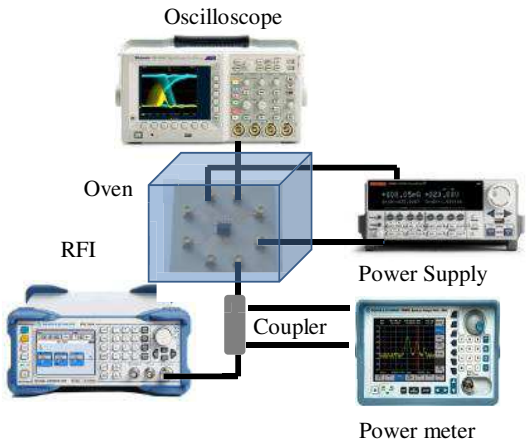

Figure 1: Experimental setup.

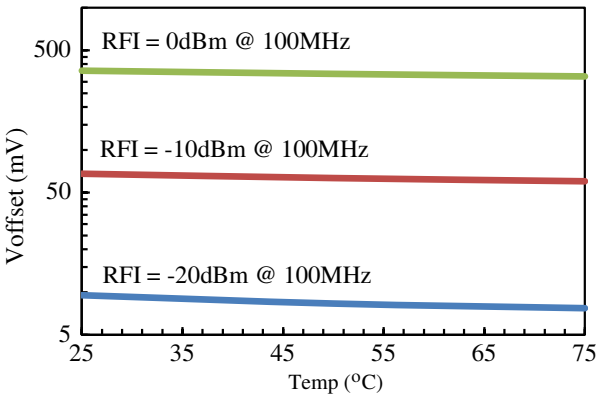

Figure 2: LM741 OpAmp offset.

ACKNOWLEDGMENT

This work has been supported by the Spain-MICINN under Project TEC2010-18550 and AGAUR 2009 SGR 1425.

REFERENCES

1. Ramdani, M., E. Sicard, A. Boyer, S. Ben Dhia, J. J. Whalen, T. H. Hubing, M. Coenen, and O. Wada, "The electromagnetic compatibility of integrated circuits-past, present and future," *IEEE Transactions on Electromagnetic Compatibility*, Vol. 51, 78–100, February 2009.
2. EN IEC 62134-4, "Integrated circuits — Measurement of electromagnetic immunity, 150 kHz to 1 GHz — Part 4: Direct RF Power injection method,".
3. Richelli, A., "Measurements of EMI susceptibility in ultra-low-voltage OpAmps," *Proc. of the EMC Compo.*, Dubrovnik, Croatia, Nov. 13–17, 2011.

A Theoretical Analysis of the Optical Feedback Noise Based on Multimode Model of Semiconductor Lasers

Sazzad M. S. Imran, Minoru Yamada, and Yuji Kuwamura
Division of Electrical and Computer Engineering
Graduate School of Natural Science and Technology
Kanazawa University, Kakuma-machi, Kanazawa, Ishikawa 920-1192, Japan

Abstract— Semiconductor lasers are used as light sources in the fiber optic communication system and the optical disc system, and are required to reveal the lower noise for the higher performance. It is well known that optical feedback creates excess noise in semiconductor lasers. However, the interplay of optical feedback noise and multimode emission was not fully covered yet. Therefore, this manuscript elaborates on detailed variations of the noise characteristics with the optical feedback ratio in the presence of multimode dynamics.

The theoretical analyses of noise in semiconductor lasers are classified into three groups. First one is the small signal analysis on frequency domain where the Langevin noise sources are taken into account. The second group is the single mode model, where the time delay of the feed-backed light is taken into account with or without introduction of the Langevin noise sources. The third group is the multimode model which counts the mode competition phenomena among the lasing modes, but is not counting the Langevin noise sources yet.

In this model, the optical feedback noise in semiconductor lasers is analyzed based on a new multimode model considering mode competition phenomena among lasing modes and Langevin noise sources for intensity and phase fluctuation; hence can be considered as an extension of the third group. Two types of RIN, namely low frequency type and flat type, are well simulated by this model with good correspondence to experimentally obtained data.

Mode dynamics of semiconductor lasers operating under external OFB are governed by the following rate equations of the modal photon number $S_p(t)$, modal phase $\theta_p(t)$ and number of injected electrons $N(t)$.

$$\begin{aligned}
\frac{dS_p}{dt} &= (G_p - G_{tho} + (c/n_r L)\ln|U_p|)\,S_p + (a\xi N/V)/\left[\{2(\lambda_p-\lambda_0)/\delta\lambda\}^2+1\right] + F_{Sp}(t) \\
\frac{d\theta_p}{dt} &= \frac{1}{2}\left[(\alpha a\xi/V)(N-\bar{N}) - (c/n_r L)\varphi\right] + F_{\theta P}(t) \\
\frac{dN}{dt} &= -\sum_p A_p S_p - N/\tau_S + I/e
\end{aligned}$$

The proposed model is applied to investigate the effect of external optical feedback on the characteristics of intensity noise in 850-nm GaAs lasers. Typical noise spectra are shown in Fig. 1, where feedback noise is classified as low frequency type noise and flat type noise. We can find good correspondence between the simulated results and the experimental data shown in Fig. 2. Variations of the RIN with feedback strength are shown in Fig. 3 for $f = 500\,\text{kHz}$ and $f = 10\,\text{MHz}$

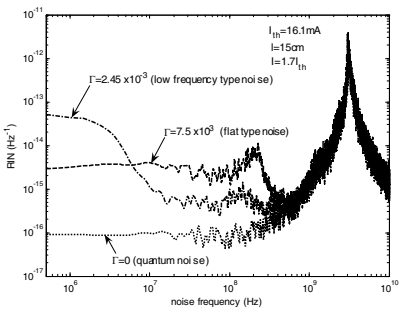

Figure 1: The simulated spectra of RIN profiles for different OFB strengths.

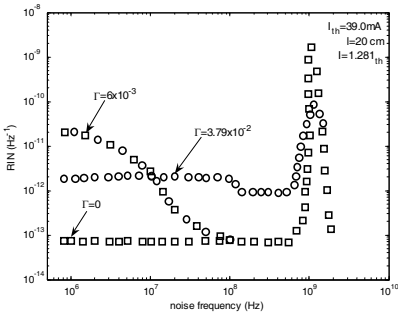

Figure 2: Experimentally observed frequency spectra of the noise, cited from [2].

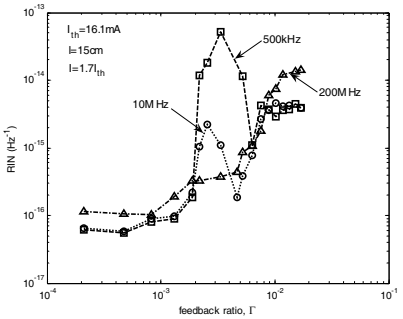

Figure 3: Variation of RIN with feedback strength for low frequency and flat type noise.

representing the low frequency type noise and for $f = 200\,\mathrm{MHz}$ representing the flat type noise, respectively. It was evident from the modal behavior that the low frequency type noise must be caused by unstable mode hopping between bi-stable states, and generating mechanism of the flat type noise must be independent from the mode competition among the lasing modes.

REFERENCES

1. Serrat, C., S. Prins, and R. Vilasec, *Physics Review A*, Vol. 68, 053804, 2003.
2. Yamada, M., A. Kanamori, and S. Takayama, *IEICE Trans. Electron.*, Vol. E79-C, No. 12, 1766–1768, 1996.

Vacuum Ultraviolet Emission from Cubic Boron Nitride Single Crystals in Extremely Non-uniform Electric Field

Gang Jia[1,*], **Shuang Wang**[1], **Xiuhuan Liu**[2], **Feng Yang**[1], **Yanjun Gao**[1], **and Zhanguo Chen**[1]

[1]State Key Laboratory on Integrated Optoelectronics, College of Electronic Science and Engineering Jilin University, 2699 Qianjin Street, Changchun 130012, China

[2]College of Communication Engineering, Jilin University, 5372 Nanhu Road, Changchun 130012, China

Abstract— Vacuum ultraviolet (VUV) has broad applications in industries, militaries, scientific researches and daily lives. The electric field between needle-plate electrodes is extremely non-uniform, and the electric field at the needlepoint is the strongest. Theoretically, if the needlepoint tends to be infinite small, then the electric field at the needlepoint will approach to infinity. The cBN crystal is a kind of synthesized wide bandgap semiconductor, whose bandgap (6.2 ± 0.2 eV) is the widest in all III-V compounds. It has the second highest hardness and thermal conductivity just next to diamond, and possesses greater thermal stability and less reactivity than diamond does. In a vacuum chamber, an unintentionally doped amber cubic boron nitride (cBN) single crystal whose sizes are about $0.3 \times 0.3 \times 0.1$ mm^3 was fixed between needle-plate electrodes, and the two opposite {111} planes of the cBN crystal contacted with the electrodes tightly. The diameter of the point of the tungsten needle electrode is about 10 μm, and the plate electrode is brass. When the dc voltage applied on the cBN crystal reached a critical value between $600 \sim 1550$ V, whatever the polarity of the voltage was, the VUV emission from the cBN crystal took place. When the vacuum degree of the chamber was about 3×10^{-3} Pa, the VUV radiation spectrum of the cBN crystal was measured by a VUV spectrometer, the peak wavelength is about 149 nm. When the vacuum degree of the chamber was about 7×10^{-4} Pa, the green emitting phosphor ($BaAl_{12}O_{19}$:Mn^{2+}) for plasma display panel (PDP) was spread around the junction between the needlepoint and the cBN crystal, and the green fluorescence excited by the VUV from cBN could be observed by naked eyes. The VUV emission from the cBN crystal in the extremely non-uniform electric field can be interpreted by the interband and intraband transitions and the electron-hole direct recombination. First, under the strong electric field, electrons near the top of the valence band at the Γ point are able to jump into the bottom of the X-valley of the conduction band, then electrons in the X-valley will transfer into the Γ-valley with higher energy under the strong electric field, at last, electrons in the Γ-valley of the conduction band recombine with the holes near the top of the valence band, and the VUV emission takes place.

ACKNOWLEDGMENT

Supported by the National Natural Science Foundation of China (Nos. 60976037 and 61077026), the Collaborative Project of NSFC-RFBR (No. 61111120097), and the Natural Science Foundation of Jilin Province, China (No. 201215019).

*Corresponding author: Gang Jia (jiagang@jlu.edu.cn).

Design of Failure-rate Test Method for Chip-type EMI Filter

Soon-Mi Hwang and Kwan-Hun Lee
Korea Electronics Technology Institute (KETI), Korea

Abstract— EMI is the electromagnetic interference that is disturbances in the external device. And EMI Filter is the device that is to block or to eliminate these EMI signals [1]. High-frequency EMI filter is important device used in the mobile (Mobile phone, PMP, Tablet PC) and home appliances (LED TV, PDP TV). For that reason, a lifetime warranty for a period of time is important. This thesis studies the main failure modes and the failure mechanisms of Chip-type EMI filter and suggests test method for calculating the life-time.

Chip-type high-frequency EMI filter has the structure of the laminated ceramic material. That is configured to internal RC circuit blocking high-frequency. Chip-type EMI filter has a simpler production process than a diode-type EMI filter. So the price is cheaper than a diode-type EMI filter. Chip-type EMI filters has the advantage of a well-soldered by coating the electrode with thick laminated process. But it's failure is frequent caused by sudden temperature changes or a physical vibrations.

If a device made of ceramic like chip-type EMI filter has long-term exposure to sudden temperature changes, it can result in cracks in ceramic. This crack is caused the circuit open and changes the characteristic of the device [2]. If the over-stress like surge, electrostatic enter within the filter, it will occur the high heat flow (Joule Heat) in the inner conductor. This heat is destroying the internal circuit isolation and is caused accidental disconnection [3]. When chip-type EMI filter exposed to high humidity environments, the delamination in internal ceramic electrode can occur. This is usually occur when there is a problem in the plastic process (the temperature difference between two materials or too low plastic temperature). Chip-type EMI filters should be minimal damage due to mechanical vibrations, but sometimes mechanical vibrations generate deformation of the PCB attached to the device. This generates cracks between the device and PCB.

Among the various cause, ceramic cracks by rapid temperature changes was set to the main failure modes and failure mechanisms. Because ceramic cracks by rapid temperature changes is an accident failures due to excessive use rather than wear-out failure and deterioration failure, failure rate was selected. The life distribution of the chip-type EMI filter is failure time caused by accidental failures, so that the exponential distribution was assumed. Warranty lifetime, the failure rate levels follows KS C6032. The failure rate is set based on KS C6032, the failure rate levels is separated by M and N, so people can choose that level. The level of confidence is set to 90%. Test time, sample size is determined with reference to the KS C 6032. if the time to failure of the device follow an exponential distribution, the sample size 'n' and the test time to failure 'T', failure rate 'r' follows Poisson distribution. The larger number of acceptance increases test time and cost. Thus to reduce production costs, number of acceptance is used as $c = 0$. The test items for performance verification are cutoff Frequency, impedance, leakage current and capacitance. After testing, all the samples must meet the product specifications.

REFERENCES

1. Hiura, S., T. Kitahara, and Y. Oohashi, "RF design of on-chip EMI filters in CMOS logic IC," *European Microwave Conference*, 187–190, Oct. 27–31, 2008.
2. Pietrikova, A., J. Bansky, M. Bujalobokova, and J. Urbancik, "Thermal shock reliability test of multilayer LTCC modules with thick film conductors," *International Spring Seminar on Electronics Technology*, 485–488, May 8–11, 2003.
3. Vinson, J. E. and J. J. Liou, "Electrostatic discharge in semiconductor devices," *Proceedings of the IEEE*, Vol. 86, No. 2, 399–420, Feb. 1998.

Control of Coherence and Polarization of an Electromagnetic Beam by Means of Liquid Crystal Spatial Light Modulators

C. Rickenstorff, E. Flores-Cruz, and A. S. Ostrovsky
Facultad de Ciencias Físico Matemáticas
Benemérita Universidad Autónoma de Puebla, Puebla 72000, México

Abstract— Since the mid-1980's the nematic liquid crystal spatial light modulators (NLC-SLMs) have gained increasing importance in many optical applications such as optical data processing, beam shaping, optical communication, adaptive optics, real-time holography, etc.. These devices are popular due to their capability to modify both the amplitude and phase of light and being easily controlled by computer. Recently, in connection with the heightened interest in the vector coherence theory of electromagnetic fields, a new possible application of NLC-SLMs has been found. It has been shown that NLC-SLM of certain configuration can realize the controlled changes of statistical properties of an electromagnetic beam, namely the degree of coherence and the degree of polarization. This fact can be successfully used for generating a secondary partially coherent and partially polarized optical source with desired statistical characteristics. Several techniques using NLC-SLMs have been proposed; nevertheless all of them presuppose the use of 0°-twist NLC-SLMs which have a low commercial availability and heightened cost, so that up to now the corresponding experimental results have not been reported. Here we propose an experimental technique for coherence and polarization modulation of the electromagnetic field using the widely available and relatively law-cost 90°-twist NLC-SLMs. The controlled change of coherence and polarization is achieved through computer generated random signals displayed on two 90°-twist NLC-SLMs placed at the opposite arms of a Mach Zehnder interferometer. The validity of the proposed technique is demonstrated by experimental results obtained with the use of commercial specimen of Holoeye 90°-twist NLC-SLM LC2002.

Simple Technique for Generating a Secondary Electromagnetic Source with Desired Degrees of Coherence and Polarization

M. A. Olvera and A. S. Ostrovsky
Facultad de Ciencias Físico Matemáticas
Benemérita Universidad Autónoma de Puebla, Puebla 72000, México

Abstract— During the last decade great attention has been given to the development of the unified theory of coherence and polarization of electromagnetic fields. One of the central problems of this theory is the control of statistical properties of an electromagnetic field. Several techniques have been proposed to modify the degrees of coherence and polarization of an electromagnetic field. Here we propose and analyze a new rather simple technique for generating a secondary electromagnetic source with desired degrees of coherence and polarization. Starting from a completely coherent and completely polarized electromagnetic source (gas laser), two coupled Mach-Zehnder interferometers are used for the experimental synthesis and characterization of the secondary partially coherent and partially polarized electromagnetic source. In order to separate the orthogonal components of the field, a polarizing beam splitter is placed at the input of the first interferometer while the rotating ground glass plates are used at the opposite arms to modify the coherence properties of each component. The corresponding optical beams are superposed at the output by means of a non polarizing beam splitter. An original technique, realized by means of the second Mach-Zehnder interferometer coupled with the first one, is used to measure the cross-spectral density matrix of the generated source. The idea of the matrix elements determination is well known and is realized by means of four two-pinhole Young's interference experiments in which the spectral densities are measured with suitable oriented polarizers and appropriate wave plates. Due to the wide-scale availability of the required optical components we have succeeded in the physical realization of the proposed technique and have demonstrated its efficiency in experiments. The experimental results are in good agreement with theoretical predictions.

Fast Algorithm for Computer Simulation of Optical Systems with Partially Coherent and Partially Polarized Illumination

Andrey S. Ostrovsky, Paulo C. Romero-Soría, and Esteban Vélez-Juárez
Facultad de Ciencias Físico Matemáticas
Benemérita Universidad Autónoma de Puebla, Puebla 72000, México

Abstract— The computer simulation is a very powerful tool in analysis and design of optical systems. As well known an optical system with partially coherent illumination exhibits an essential nonlinear nature. Under certain conditions the output of such a system can be described either exactly or approximately by the third term of the Volterra series which represents the four-dimensional integral transform, so-called bilinear transform, of an object with the kernel depending on the structure of system and the statistical properties of illumination. The direct calculation of such an integral transform represents a very complicated computational problem. So, if an object is given by $K \times K$ pixels, the number of complex multiplications, needed to calculate this transform, reaches the value of K^6 that can easily result in an unacceptably long computation time. Not so long ago we proposed the fast algorithm for bilinear transforms in optics which is based on the coherent-mode representation of scalar illumination and allows reducing the needed computation time by a factor of several orders depending on the degree of coherence of illumination. Here we propose the generalized version of this algorithm for the case of electromagnetic (vector) illumination. It should be noted that the application of this algorithm requires knowledge of the coherent-mode structure of illumination that sometimes represents not an easier computational task than the proper calculation of the optical system output. To resolve this problem, we use an original technique of an alternative coherent-mode representation based on the results of physical measurements of the radiant intensity of illumination. We illustrate the efficiency of the proposed algorithm by the numerical simulation of a simple imaging system with Gaussian Schell model illumination.

Self-assembled Monolayer with Hemispherical Structure for Terahertz (THz) Antireflection Technique

D. S. Kim[1], **D. H. Kim**[1], **S. Hwang**[3], **J. M. Woo**[1], **and Jae-Hyung Jang**[1, 2, 3]

[1]School of Information and Communications, Gwangju Institute of Science and Technology
1 Oryongdong, Buk-gu, Gwangju 500-712, Korea
[2]WCU Department of Nanobio Materials and Electronics, Gwangju Institute of Science and Technology
1 Oryongdong, Buk-gu, Gwangju 500-712, Korea
[3]Research Institute of Solar and Sustainable Energies, Gwangju Institute of Science and Technology
1 Oryongdong, Buk-gu, Gwangju 500-712, Korea

Abstract— The monolayer with hemispherical structure for antireflection technique at terahertz (THz) frequency range was realized by using self-assembly and spin coating process. The monolayer glass spheres was deposited on sapphire substrate via self-assembly process, and then the space between glass spheres and sapphire substrate was filled with B-staged bisbenzocyclobutene (BCB) via spin-coating process. The composition of self-assembled monolayer glass spheres and cured BCB achieved graded effective refractive index on sapphire substrate. The fabricated monolayer has different surface conditions by changing BCB thickness. The effect of surface condition which can lead to different aspect ratios was investigated according to the measured reflectance values. The reflectance of monolayer with hemispherical structure was measured at frequency range from 0.1 to 1.9 THz using a THz time domain spectroscopy system (TPS spectra 3000, Tera View). The average reflectance of the bare sapphire substrate was 29%. On the other hand, the reflectance of the monolayer with hemispherical structure exhibited 6.9% throughout the frequency range investigated in this study. The monolayer with hemispherical structure using the self-assembly and spin-coating process can be excellent candidate for THz antireflection technique with much simpler and less expensive process.

Investigation of Electricity Quality in Ship Integrated Power System

N. F. Djagarov, **S. Z. Zlatev**, **M. B. Bonev**, **and Z. G. Grozdev**
Technical University of Varna, Bulgaria

Abstract— Recently are built more complex and more powerful ship electrical power stations. On modern passenger and cargo ships (floating cranes, dredgers, floating platforms and etc.) majority of electrical consumers are with adjustable electric power drives. Ship's power systems are characterized by commensurability of the power of generators and electric drives. Moreover, the generation and consumption of electricity (excluding additional ships needs) is performed without transformation. All this leads to a strong deterioration of electricity quality which, disturbing work such as electrical drives and other appliances.

In the article is developed full mathematical model of ship electrical power system, which is shown on Fig. 1, with according suggested method [1, 2]. The studied combined power system is consisting from three diesel generators, electrical ship propulsion system (Azipod), controlled frequency converter, permanent magnet synchronous motor which drives ship propeller. Furthermore ships power supply station has step-down transformer supplies additional ships loads (simulated by two equivalent induction drives and static active-inductive load).

Due to used method for creation of mathematical model is obtained noniterative calculation of system processes and saves computational resources. In the MATLAB space is realized this model through which can simulate various operating modes of the studied system and simulation different disturbances.

With so created a mathematical model were examined various operating and emergency operating modes of the ship's electrical power system. Using the FFT was investigated absorbed electric current of ships propulsion system and the presence of harmonics in voltage at various points in the distribution network. Conclusions are made about the appropriateness of using the funds for suppression of harmonics.

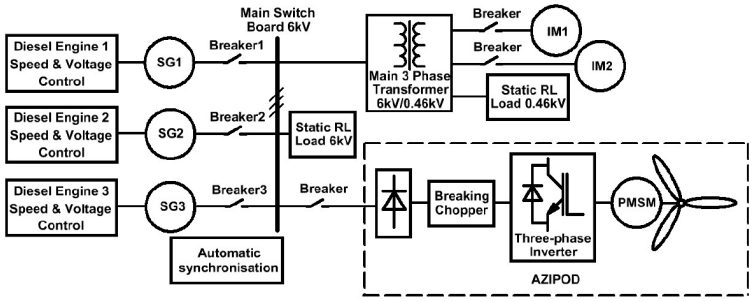

REFERENCES

1.
2. Djagarov, N. F., "A method of transient electromechanical processes modeling in power systems," *IEEE Bucharest Power Tech Conference*, Bucharest, Romania, June 28–July 2, 2009, E-ISBN: 978-1-4244-2235-7.

The All-optical Logic Gates Based on Mach-Zehnder Interferometer Photonic Crystal Waveguides

Yaw-Dong Wu, Teng-Huei Zou, Jian-Jang Lee, and Tien-Tsorng Shih
Department of Electronic Engineering
National Kaohsiung University of Applied Sciences, Kaohsiung 807, Taiwan, R.O.C.

Abstract— Photonic crystal (PC) structures are very suitable for a large number of optical applications. PC is a periodic dielectric structure that has an important characteristic of the PC is photonic bandgap (PBG). Due to the property of PBG that wavelength within the bandgap cannot propagate through the crystal. By introducing defects into PC, it is possible to build waveguide that can channel light along certain paths.

We use the Mach-Zehnder interferometer (MZI) photonic crystal waveguide to design all-optical logic gates. We consider a PC with a triangular lattice of dielectric rods in the air. First, we compute the bandgap by the plan wave expansion method (PWE) in the frequency domain, and then we computer optimum coupling length with the finite difference time domain method (FDTD). Then we propose two logic gate structures with two input ports. The state of input port determines the electric field at the output port. Changing one coupling length to $13a$ can cause the destructive interference, so we can use this property to design XOR gate. Changing two coupling length to $17a$ can cause the constructive interference, so we can use this property to design AND gate.

Because nanotechnology has been making great progress, it surely can be use to demonstrate a practical breakthrough in which the devices based on the PC integrated circuits are realized. The proposed PC device will be useful in the applications of high-speed and high-capacity optical communications and optical data processing systems.

Proposal for Large Mode Area Photonic Crystal Fibers

Yaw-Dong Wu, Jian-Jang Lee, and Tien-Tsorng Shih
Department of Electronic Engineering
National Kaohsiung University of Applied Sciences
415 Chien Kung Road, Kaohsiung 807, Taiwan, R.O.C.

Abstract— Conventional single-mode fibers suffer from small core, leading to limited output power due to generally a single-mode fiber diameter about $8\,\mu m \sim 10\,\mu m$. In order to allow higher output power and improve the influence of external force, currently photonic crystal fibers (PCFs) have overcame the mentioned shortcomings, such as endlessly single-mode operation, large mode area (LMA), and high birefringence et al.. These properties provide scaling potential for fiber laser and amplifier systems.

We present the results of numerical analysis showing that large period can be obtained in LMA PCFs. One of analysis methods corresponds to finite-element method (FEM) with perfectly matched layer boundary conditions. This method respects the sufficient reliability, efficiency, and accuracy for the PCFs. In this paper, we proposed an improvement of PCF to increase the effective mode area as $950\,\mu m^2$. The confinement loss of x-axis is obviously higher than y-axis due to large size difference between x- and y-direction. The confinement loss is less than 1.96×10^{-7} dB/km for the improved PCF.

Broadband Terahertz Surface Relief Structure on Flexible Substrate

D. H. Kim, **D. S. Kim**, **S. Hwang**, **D. M. Geum**, **and J. H. Jang**
School of Information and Communications, WCU Department of Nanobio Materials and Electronics
Research Institute of Solar and Sustainable Energies (RISE)
Gwangju Institute of Science and Technology (GIST)
261 Cheomdan-gwagiro, Buk-gu, Gwangju 500-712, Republic of Korea

Abstract— In recent years, the terahertz (THz) devices with metamaterial structure have been investigated on the flexible substrate due to the merit of the flexible substrate. The flexible THz devices can be easily attached to the non-planar surfaces and applied to the three-dimensional (3D) THz structure. In this study, the THz antireflection structure was employed on the highly flexible substrate by using polydimethylsiloxane(PDMS) substrate. Instead of the conventional pattern transfer to the PDMS substrate with dry etching process, the stamping method with silicon mold was used to get the high reproducibility of the devices.

Terahertz (THz) surface relief structure (SRS) with various periods of 60 μm, 120 μm and 240 μm was fabricated on the flexible PDMS substrate by using silicon master. The silicon mold was made by using the crystallographic wet etching method with 45% KOH solution. At 1 THz region, flexible THz SRS with 240 μm period exhibits the 99.95% reflectance reduction compared to that of bare PDMS substrate with 4.1 mm thick. The reflectance values of fabricated THz SRS shows well matched result compared with the simulation result by applying RCWA calculation method with commercial software (DiffractMod, RSoft Design). From the reflectance measurement along the azimuth angle, the fabricated SRS was demonstrated low reflectance over a wide range for both transverse electric (TE) and transverse magnetic (TM) polarizations. The proposed THz SRS can be a good candidate for the perfect flexible THz absorber with the multi band operation.

Cantor Dust Zone Plates

W. D. Furlan[1], **V. Ferrando**[1, 2], **A. Calatayud**[2], **F. Giménez**[3], **and J. A. Monsoriu**[2]

[1]Departamento de Óptica, Universitat de València, Burjassot 46100, Spain
[2]Centro de Tecnologías Físicas, Universitat Politècnica de València, Valencia 46022, Spain
[3]I.U. Matemática Pura y Aplicada, Universitat Politècnica de València, Valencia 46022, Spain

Abstract— In this paper, we present a novel family of zone plates based on the Cantor dust fractal. Cantor dust is a two-dimensional version of the Cantor set. It can be formed by taking a finite cartesian product of the Cantor set with itself. The pupil function, $p(x, y)$, that defines the Cantor Dust zone plates (CDZP) of order $S = 2$ is represented in Fig. 1(a). Note that the Cantor set is distributed along the squares of the cartesian coordinates and replicated on the x and y axes. The focusing properties of these fractal diffractive lenses are analytically and experimentally analyzed and the influence of the fractality is investigated. The axial irradiances of CDZPs have been computed for different stages of fractal order S. Fig. 1(b) shows the result obtained for the CDZP of Fig. 1(a). The axial response for the CDZP exhibits its characteristic fractal profile. Moreover, under monochromatic illumination a CDZP gives rise a focal volume containing a delimited sequence of two-arms-cross pattern that are axially distributed according to the self-similarity of the lens. Fig. 1(c) shows the experimental transverse diffraction pattern corresponding to the principal focus obtained using a spatial light modulator. CDZPs can have applications in precision alignment systems, in antennas and combined with spiral phase masks can generate hollow beams.

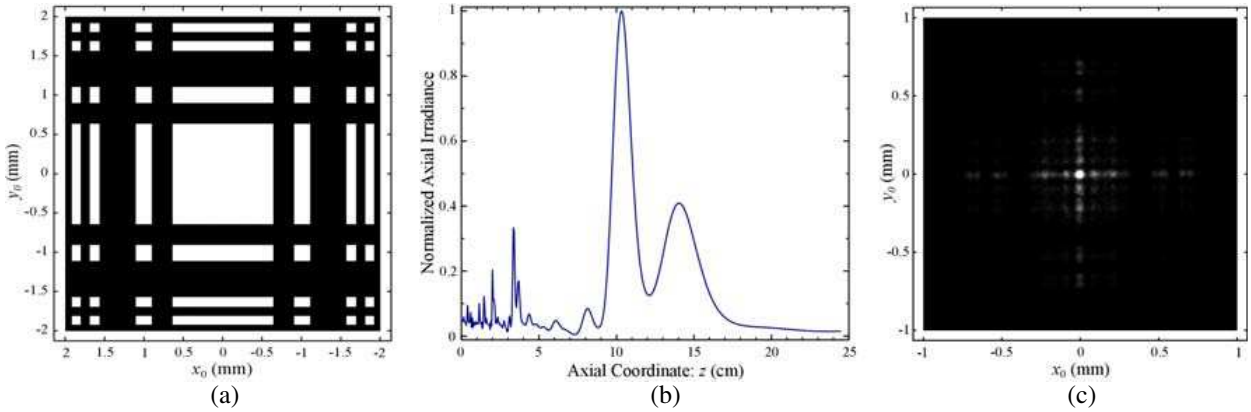

(a) (b) (c)

Figure 1: (a) CDZP for $S = 2$. (b) Normalized axial irradiance provided by it with a wavelength $\lambda = 633\,\text{nm}$. (c) Experimental transverse diffraction pattern at the main focus.

Analysis and Design of a UHF-band Harmonic Meter

A. Naserialiabadi[1], **Gh. Moradi**[1], **A. Kheirdoost**[1], **J. Rashed-Mohassel**[2], **and R. Sarraf Shirazi**[1]

[1]Wave Propagation & Microwave Measurement Research Lab., Department of Electrical Engineering
Amirkabir University of Technology, 424 Hafez Avenue, Tehran 15914, Iran
[2]Center of Excellence on Applied Electromagnetic Systems
School of Electrical and Computer Engineering, University of Tehran, P. O. 14395-515, Iran

Abstract— In this paper, the design and analysis of a system to measure the amplitude of harmonics of a signal in UHF_band is presented. First we propose ananalytical method, and then the results are used to validate the method. Benefits and drawbacks of the system are analyzed. The proposed structure is so simple such that the system includes a single diode mixer. In mixer, harmonics of the desired signal to measure are fed into RF-port and we synthesize a comb to feed in LO-port. The bottle neck determines the amplitude and phase of each harmonic in comb signal. These parameters are found by mathematical calculations and the proposed Design is validated and optimized by using a full-wave electromagnetic simulator. At first a system to measure two harmonics have been designed and investigated. After optimization, a better performance of the system with increased bandwidth will be achieved. The next step is to measure three harmonics. Finally the system to measure two and three harmonics isproposed. Simulations are carried out using ADS, a commercial electromagnetic simulator.

Design and Fabrication of RAS Using CNT Added Glass Fiber Composite Prepreg

J. H. Shin[1], **H. K. Jang**[1], **C. G. Kim**[1], **W. Y. Lee**[2], **and Y. J. Shin**[3]

[1]KAIST, Republic of Korea
[2]Agency of Defense Development, Republic of Korea
[3]Shinsung Basic Materials, Republic of Korea

Abstract— In 1930s, radar system began to use recognize or detect objects. As time has gone on technologies related with radar system were dramatically developed. However, anti-radar system absorbing or cancelling radar signal was also rapidly grown. In these days, anti-radar system is widely used to increase survivability or performance of weapon systems. Anti-radar system which is called stealth can be realized in several ways; stealth shaping, radar absorbing material (RAM), radar absorbing structure (RAS). Among these, RAS was studied in this paper. RAS can be load bearing structure and absorbing electromagnetic wave in same time. Stealth shaping could be affect aerodynamic performance and RAM is required to maintain to show radar absorbing ability. RAS can keep original design shape and less need maintenance time.

In this study, carbon nano tube (CNT) added glass fiber reinforced composite material was used to make RAS. Composite materials compose of reinforce fiber and matrix. Epoxy resin was used for matrix. CNT was added to epoxy resin using three-roll-mill machine.

Complex permittivity of composite materials was measured by rectangular waveguide and network analyzer depending on CNT content. Then, RAS was designed using measured complex permittivity. Thickness and CNT content were design parameters. They could be decided by an equation of non-reflection condition. Electromagnetic wave absorption of RAS was simulated by CST MWS commercial computer program.

Finally, CNT 1.7 wt% added glass fiber prepreg was manufactured and RAS was also realized using the prepreg. Prepreg was cured by autoclave process. It had 16 GHz center frequency and showed over −10 dB (90%) absorption at the center frequency.

Nano Technology in Space and Spacedevices

Diyar Bajalan
Ret., Austria

Abstract— Direct evidence for the occurrence of diamond or diamondlike material in interstellar clouds is less certain, but there have been suggestions that absorption by such material may contribute to ultraviolet extinction in the diffuse interstellar medium. In many nano- and micro-satellite missions, magnetometers are indispensable for attitude control systems and assembled to most of these satellites. In many cases, these are small Magnetic Sensors as well as the application of nanomaterials and nanolayers for space technology (e.g., the development of nanostructured layers for heat-insulating in rocket engines). The most persuasive evidence for the presence of nanodiamonds in the interstellar medium arises from the observation in circumstellar shells around certain young stars.

The same emission features are also found in the spectrum of the postasymptotic giant branch star HR 4049, implying that the conditions for the formation of nanodiamonds are not limited to the environment surrounding young stars.

Nanotechnology and Health Future

Diyar Bajalan
St. Pölten, Austria

Abstract— The multidisciplinary field of nanotechnology is bringing the science of the almost incomprehensibly small device closer and closer to reality. Over the next couple of years it is widely anticipated that nanotechnology will continue to evolve and expand in many areas of life and science, and the achievements of nanotechnology will be applied in medical sciences, including diagnostics, drug delivery systems, and patient treatment. The very properties that make nanomaterials so exciting, such as increased reactivity and the potential to cross cell membranes, may also have negative environment, health and safety (EHS) impacts.

Nano Materials and Devices and Physical Property

Diyar Bajalan
Ret., Austria

Abstract— Carbon nanotubes are cylindrical molecules with a typical diameter of order 1 nm for single-wall nanotubes (SWNT) or a few tens nm for multi-wall nanotubes (MWNT) and a length of many microns. Nanotechnology research and development is directed toward the understanding and control of matter at dimensions of roughly 1 to 100 nanometers. At this size, the physical, chemical, and biological properties of materials can differ in fundamental and potentially useful ways from the properties of individual atoms and molecules, on the one hand, or bulk matter, on the other hand. There has been large interest recently to possibility of channeling in the materials produced by nanotechnology. Magnetic field based micro/nanoelectromechanical systems (MEMS/NEMS) devices are proposed that use 10 nm diameter magnetic particles, with and without a carrier fluid, for a new class of nanoduct flows, nanomotors, nanogenerators, nanopumps, nanoactuators, and other similar nanoscale devices.

A Fiber Optic Sensor Integrated with Fuzzy Similarity Analysis to Evaluate Hydrocarbon Pollutant in Water

I. Palamara, D. Pellicanó, and M. Versaci
Department of Mechanics and Materials, NDT-Lab, University "Mediterranea" of Reggio Calabria, Italy

Abstract— One of the main environmental problem is related to amount and quality of water at our disposal. Water is a natural resource, not industrially reproducible, and the quality issue is a theme absolutely important especially for foodstuffs production and for resulting environmental impacts [1]. Many developed countries have adopted law that call for constant monitoring of water quality. These procedures impose controls both in terms of quality — the possible presence of contaminants — and quantitative — how much they are present (percentage). Monitoring is an essential step in order to implement procedure for purification from contaminants. A possible tool of detection is constituted by employment of optical fibers. Their building features — do not contain electronic part and are geometrically versatile versatility so fiber sensor can be configured in arbitrary shapes — allow an optimal use in liquid environments [2]. By means of a sensor, principally formed of a transmitter and a receiver both in optical fiber, a sample containing water with micro particles of pollutant is put through a light source; the receiver is used to evaluate the absorption of light at different frequencies. This research proposes a new methodology designed to detect and classify micro particles of hydrocarbons, type C14 C40, in water. In particular, the obtained signals are subjected to a fuzzy similarity analysis [3] in order to detect the presence of micro pollution and classify the percentage. A sensor integrated with fuzzy similarity analysis represent an useful tool: easy to use and without implementation of complex procedure. Any technological production would also allow an "in situ" analysis.

REFERENCES

1. Schwarzenbach, R., et al., "Global water pollution and human health," *Annual Review of Environment and Resources*, Vol. 35, 109–136, 2010
2. Udd, E., B. William, and Jr. Spillman, *Fiber Optic Sensors: An Introduction for Engineers and Scientists*, 2nd Edition, Wiley, July 18, 2011.
3. Joniyak, Z. C., "Distance based similarity measures on fuzzy sets," *Proceedings of the Third Slovakian-Hungarian Joint Symposium on Applied Machine Intelligence, SAMI 2005*, Herl'any, Slovakia, 2005.

High Performance Computation of Electrostatic and Magnetostatic fields in the KATRIN Experiment

Thomas J. Corona[1], **Joseph Formaggio**[2], **Ferenc Glueck**[3], **and John F. Wilkerson**[1]

[1]University of North Carolina at Chapel Hill, USA
[2]Massachusetts Institute of Technology, USA
[3]Karlsruhe Institute of Technology, Germany

Abstract— The Karlsruhe Tritium Neutrino (KATRIN) experiment is a tritium beta decay experiment designed to make a direct, model independent measurement of the electron neutrino mass with a sensitivity of $m(\beta) = 0.2\,\mathrm{eV}$ (90% C.L.), an order of magnitude lower than the current established limit. The experiment is located at Karlsruhe Institute of Technology (KIT) in Karlsruhe, Germany, and is being conducted by a multinational collaboration consisting of physicists from both European and US institutions. A potential background in our experiment is from electric breakdown due to Penning discharge, where a charged particle confined within a Penning trap (a potential well along a magnetic field line) ionizes residual gas molecules. Penning traps arise from the interplay between electrostatic and magnetostatic fields, and can therefore be characterized and minimized using electromagnetic field simulation tools.

We have developed a software package designed to compute electrostatic and magnetostatic fields with high precision, and to map out regions in which the geometric configuration used would result in the creation of a Penning trap. These codes apply the boundary element method (BEM) to simulate the resultant electrostatic fields due to arbitrary Dirichlet and Neumann boundaries on high performance computing systems (large-scale clusters and GPU compute machines). Our software has been validated against several analytically soluble and experimentally measured geometry configurations, and has been used to successfully identify known traps in KATRIN's pre-spectrometer.

Simulations of KATRIN's detector region comprising $\sim 500,000$ discretized elements are currently underway, and have thus far further demonstrated the success of our approach. Additionally, we are in the process of simulating a model of KATRIN's mass spectrometer consisting of $\sim 5,000,000$ discretized elements to perform precision electrostatic calculations within this region of the experiment. Application of the BEM on this geometry is expected to take $\sim 300,000$ hours, performed on an MPI-enabled cluster. Subsequent determination of the fields in this region is expected to take $\sim 500,000$ hours, and can be performed on a GPU-enabled cluster.

The Effect of over Voltages Generated by GIS on Nearby Transformers

Ibrahim Rida and Mohamad Rahal
Faculty of Engineering University of Hail, Hail, Saudi Arabia

Abstract— It is well known that over voltages (OV) generated due to the different activities in a Gas Insulated Substation (GIS), whether normal operation of Circuit Breakers (CBs) and disconnectors, closing of a grounding switch, load rejection or clearing faults, propagate to equipment connected in the proximity of the GIS. Arriving at transformer terminals, OV may cause deterioration of the insulation of bushings or windings. These over voltages can be of slow, fast, or very vast wave fronts, spanning over a wide frequency spectrum, ranging from few hertz to tens of MHz. An investigation has been conducted utilizing the Alternative Transient Program (ATP) to analyze these voltage stresses, whereby different models have been used to represent the components of the investigated system to account for the influence of frequency on the system parameters. One of the elements that highly influence the propagating surges is the cable link between the GIS and the transformer. It has been observed that the cable link between the GIS and transformer terminals affects the profile of the voltages arriving at the transformer terminals in different ways depending on frequency. It has been observed that for fast wave front voltages, like the case when transformer is energized, the cable link tends to raise the incident voltages arriving at transformer terminals, whereas for very fast wave front voltages, as in the case of disconnector operation, the cable tends to reduce the voltage at the transformer terminals. This paper presents and discusses the outcomes of the investigation.

Uncertainty Calculation for Phase Noise Optoelectronic Metrology Systems

P. Salzenstein and E. Pavlyuchenko
Franche Comté Electronique Thermique Optique Sciences et Technologies (FEMTO-ST)
Centre National de la Recherche Scientifique (CNRS), Besançon, France

Abstract— In this work we focus on the determination of the uncertainty of phase noise measurements of signals delivered by optoelectronic oscillators [1, 2]. The developed system works for any Device under test (DUT) that delivers a frequency between 8.2 and 12.4 GHz [3, 4]. It works with optical fiber based delay lines for a laser wavelength at 1.55 µm. The measured phase noise includes the DUT noise and the instrument background. It is interesting to notice that the use of a cross correlation decrease the cross spectrum terms of uncommon phase noise as $\sqrt{(1/m)}$, where m is the average number. When we use cross correlation on 500 samples that lead to the noise floor of the instrument typically in the order of $\pounds(f)$ is −170 dBc/Hz at 10^4 Hz from the 10 GHz microwave modulation signal with a 2 km delay lines. Two main categories of uncertainties terms are taken into consideration. "type A", statistic contribution such as repeatability and experimental standard deviation; "type B" due to various components and temperature control, but also to the asymmetry of the instrument. Uncertainty on $\pounds(f)$ strongly depends on propagation of uncertainties through the transfer function when the optical fiber are inserted into the system for operation. Elementary term of uncertainty for repeatability is found to be the main contribution and is up to 0.7 dB at some Fourier frequency. Other elementary terms still have lower contributions. For instance, temperature effects, resolution of instruments are lower. Its leads to a global uncertainty better than 2 dB at 2 sigma.

REFERENCES

1. Volyanskiy, K., P. Salzenstein, H. Tavernier, M. Pogurmirskiy, Y. K. Chembo, and L. Larger, "Compact optoelectronic microwave oscillators using ultra-high Q whispering gallery mode disk-resonators and phase modulation," *Optics Express*, Vol. 18, No. 21, 22358–22363, 2010.
2. Tavernier, H., P. Salzenstein, K. Volyanskiy, Y. K. Chembo, and L. Larger, "Magnesium fluoride whispering gallery mode disk-resonators for microwave photonics applications," *IEEE Photonics Technology Letters*, Vol. 22, No. 22, 1629–1631, 2010.
3. Volyanskiy, K., J. Cussey, H. Tavernier, P. Salzenstein, G. Sauvage, L. Larger, and E. Rubiola, "Applications of the optical fiber to the generation and to the measurement of low-phase-noise microwave signals," *Journal of the Optical Society of America B*, Vol. 25, No. 12, 2140–2150, 2008.
4. Salzenstein, P., J. Cussey, X. Jouvenceau, H. Tavernier, L. Larger, E. Rubiola, and G. Sauvage, "Realization of a phase noise measurement bench using cross correlation and double optical delay line," *Acta Physica Polonica A*, Vol. 112, No. 5, 1107–1111, 2007.

Electrophysical Investigation of the Ferroelectric Conductivity in BTO/LCMO Multilayers

A. M. Buryakov[1], **M. S. Ivanov**[1], **E. D. Mishina**[1], **and V. T. Moshnyaga**[2]

[1]Moscow State Technical University of Radioengineering, Electronics and Automation (MSTU-MIREA)
Prospekt Vernadskogo 78, Moscow 119454, Russia
[2]I-Physikalisches Institut, Friedrich-Hund-Platz 1
Universitaet Goettingen, Goettingen D37077, Germany

Abstract— In this paper, we report the electric current and conductivity dependences of ferroelectric layer thickness were studied in a LaCaMnO3/BaTiO3 (LCMO/BTO) heterostructures. Structures *LCMO/BTO* with respective layer thicknesses of LCMO 12 nm and variable thicknesses of BTO layers were fabricated by aerosol deposition method (MAD) onto MgO (100) substrates. The thickness variations of ferroelectric layers were 2, 4 and 6 nanometers respectively.

For all samples two ranges of applied electric field reveal different behavior of electrical parameters. For high fields, the current-voltage dependence shows ohmic behavior. For low field, the current-voltage dependence shows nonlinear behavior accompanied by conductance dependence with hysteresis. This kind of exponential growth indicates the tunneling current through thin ferroelectric layer, which can be modeled by Sommerfeld-Bethe method. The main questions we addressed were: 1) what is the origin of transport mechanism through BTO junction and LCMO layer? 2) how does the thickness of BTO influence on the tunneling through the ferroelectric barrier? 3) how does the tunneling features manifests itself in the current-voltage characteristics? 4) how the interface BTO/LCMO influence on transport mechanism and tunneling through BTO junction.

For the heterostructures with 2 nanometers thickness of BTO layers the nonlinear behavior of current-voltage dependence more much evidenced compare with the samples 4 nm and 6 nm thickness of BTO layer. We attribute this fact that the tunneling mechanism directly depends on the ferroelectric layer thickness. Below the metal-insulator transition temperature TMI the BTO layer is dielectric, while the LCMO layer becomes metallic. The ratio between the electric field components in the BTO and LCMO layers is determined by the boundary conditions for tangential field components: $E_{\mathrm{BTO}} = E_{\mathrm{LCMO}}$. Then, in the case of an ideal metallic layer, the system may be treated as two ferroelectric capacitors connected in parallel, with the electric field oriented perpendicular to the film plane (z-orientation).

Conductivity as well as current in the multilayer with the smallest BTO layer show increasing with increasing voltage. In other both samples, we also observed the increasing conductance with increase voltage, but rather smaller. Although in the samples with 4 nm and 6 nm thickness of the BTO layers the nonlinearity in electric current and conductivity dependences were not so pronounced, the switching of resistivity was found in that structures. We suppose that the observed effect appears due to the polarization formation in the ferroelectric films and the electric dipoles oriented along the electric field. After changes direction of electric field also observed change the polarization, but slowly up to coercive force. Thus we observed the hysteresis in conductance dependence.

Enhanced Magnetization and Second Harmonic Generation in Multiferroic BST/NBFO Superstructures

K. A. Brekhov[1], **M. S. Ivanov**[1], **N. E. Sherstyuk**[1], **E. D. Mishina**[1], **V. M. Mukhortov**[2], **and V. T. Moshnyaga**[3]

[1]Moscow State Technical University of Radioengineering, Electronics and Automation (MSTU-MIREA) Prospekt Vernadskogo 78, Moscow 119454, Russia
[2]South Center RAS, Rostov-on-Don, Russia
[3]I-Physikalisches Institut, Friedrich-Hund-Platz 1, Universitaet Goettingen, Goettingen D37077, Germany

Abstract— Bulk single phase bismuth ferrite (BFO) exhibits at room temperature both ferroelectric antiferromagnetic order. Since cycloidal spin structure with 62 nm in period cancels net magnetization, various methods are used to rebuild weak ferromagnetism in this material. Non-zero net magnetization may be induced, when this modulated spin structure becomes energetically unfavorable, in thin films by epitaxial strain, or by doping on the perovskite *A*-sites. If the thickness of the films equals half of a cycloid period or smaller, spin cancellation disappears geometrically. In this work we use all possible ways to increase net magnetization in BFO: cut the spin cycloid, introduce interface strain by epitaxial growth and doping by Nd ions. BFO layers alternate with ferroelectric $BaSrTiO_3$ which introduces additional "doping" at interfaces.

Multiferroic $BaSrTiO_3/NdBiFeO_3$ (BST/NBFO) multilayers with 3 nm and 6 nm layer thickness demonstrate superlattice structure in the XRD patterns. The break of the spin cycloide and interface strain results in ferromagnetic behavior and enhancement of magnetization. The total thickness of NBFO is varied in the range of 50–60 nm, and saturation magnetization is varied in the range of 50–60 emu/cm^3, which is an order of magnitude higher than reported for $BaTiO_3/BiFeO_3$ superstructure [1]. Magnetic coercivity does not depend on the layer thickness and equals to 230 Oe.

The structures reveal efficient ferroelectric switchability and very low electric coercivity measured by optical second harmonic generation. For higher number of layers a fraction of un-switchable polarization is 3 times higher and switchability is 4 times lower than for lower number of layers. This fact points to major role of interfaces and, probably, interface stresses for switching efficiency in ferroelectric/magnetic multilayers.

REFERENCES

1. Toupet, H., V. V. Shvartsman, F. LeMarrec, P. Borisov, W. Kleemann, and M. Karkut, *Integrated Ferroelectrics*, Vol. 100, 165, 2008.

Plasmonic Effect on Metallic Nano Particles for the Efficiency Improvement of Amorphous Silicon Solar Cells

Jean Philippe Blondeau
CNRS CEMHTI, 21 rue de Loigny La Bataille, Chartres 28000, France

Abstract— The aim of this study is to evaluate the potentiality of metallic nano particles and plasmon resonance effects for thin solar films improvement efficiency and better absorption of the solar spectrum. According to it's necessary to either evaluate this improvement for little spherical particles with dominant absorption cross section or bigger particles with dominant diffusion cross section. Shape factor can also be a good mean for the tuning of the absorption or the diffusion on the spectral range. Consequently silver and gold metallic nano particles of different size have been synthesised by chemical and physical methods on hydrogenated amorphous silicon substrates in order to evaluate their benefit on the efficiency of the cells. Several structural methods as XRD, SEM and TEM have been used to evaluate the size and the structure of the nano particles. UV visible and photoluminescence lead to the evaluation of the optical properties of the nano particles in comparison with the amorphous silicon and the solar spectrum.

ACKNOWLEDGMENT

Modelling of the nano particles is achieved by Drude and Maxwell Garnet models.

Broadband Emission from Diode-laser-pumped Ti:sapphire Crystal Fibers

K. Y. Hsu[1], **S. C. Wang**[1], **D. Y. Jheng**[1], **T. S. Ho**[1], **C. C. Lai**[1], **S. L. Huang**[1], **and P. S. Yeh**[2]

[1]Institute of Photonics and Optoelectronics, National Taiwan University, Taiwan
[2]Department of Electronic Engineering
National Taiwan University of Science and Technology, Taiwan

Abstract— Ti:sapphire (Ti^{3+}:Al_2O_3) crystals with a broadband fluorescence spectrum pumped by Ar^+ ion laser or frequency-doubled 532-nm laser have been widely used in tunable and mode-locked lasers. The broadband nature of Ti:sapphire crystal makes it also eminently suitable for optical coherence tomography (OCT) capable of acquiring *in vivo* and three-dimensional tomographic images of biological tissues and various kinds of microstructures. Since the axial resolution is inversely proportional to the bandwidth, a continuous wave or pulsed light source with a broad emission bandwidth is preferred. Here we report the fabrication of the Ti:sapphire crystal fibers with glass claddings. The single-crystalline fiber cores with small diameters of a few tens of microns were grown in air by the LHPG method. Both single-clad and double-clad approaches were attempted for high quality cladding formation by the codrawing LHPG method. As a result, up to 2.45 mW of 180-nm emission were generated from a 7.5-cm-long single-clad Ti:sapphire fiber by using a 446-nm laser diode as the pump. As a demonstration for the use on OCT, the achieved axial resolution was 1.5 μm in air. The adjacent and non-adjacent axial pixel cross talks were as low as −23.7 and −42.7 dB due to the near Gaussian spectral shape.

Two Dimensional Nano Photonic Crystals with Metallic Rod and Dielectric Clad in Metallic Background

A. Gharaati and Z. Roozitalab
Department of Physics, Payame Noor University, Tehran, Iran

Abstract— In this paper, dispersion characteristic of two-dimensional dielectric-metal nano photonic crystal with three refractive indices that containing two metallic-dielectric rods in metallic background are studied base on plane wave expansion method (PWEM). Materials of internal, external rods and background are metal (copper), dielectric (Na_3AlF_6) and metal (silver), respectively.

Here, only the TM modes band gap is considered, since there is no band gap or very thin band gap for the TE modes. At first, the eigenvalue equation of TM modes is obtained by using modified PWEM. Then, we draw dispersion curves and gap map for this structure and analysed the influences of radius and dielectric constant on the photonic band gap (PBG), respectively. Our results show PBG become larger in TM modes when we use two concentric rods with metal and dielectric material instead of one metallic rod. It was seen that the PBG shift higher frequency and width of its increases, when the radius of metal rod increases. When the dielectric constant of dielectric rod increases, then the width of PBG decrease. Therefore, by carefully selecting radii of internal and external rod and dielectric constant, moderate band gap structures can be obtained to meet the needs of application. These results may provide theoretical instructions for designing new PC devices using metallic-dielectric structure. All of our calculations have been done by using the Drude model of metal.

REFERENCES

1. Sakoda, K., *Optical Properties of Photonic Crystal*, Springer-Verlag, Berlin, 2001.
2. Ustyantsev, M. A., *Analysis and Design of Metallo-dielectric PC*, University Rovira i Virgili, 2007.
3. Qi, L.-M. and Z. Yang, "Modified plane wave method analysis of dielectric plasma photonic crystal," *Progress In Electromagnetic Research*, Vol. 91, 319–332, 2009.

The Study of Two Dimensional Photonic Crystal Made of Two Concentric Cylindrical Nano-layers of Dielectric with Negative Refraction Index

A. Gharaati and L. M. Ebrahimi
Department of Physics, Payame Noor University, Tehran, Iran

Abstract— In this paper, we study the propagation of electromagnetic wave in 2D photonic crystal (PC) made of two concentric cylinders of dielectric with the negative refraction index for TM mode in two kind structures. Applying the boundary conditions in Maxwell equation in periodic structures, we change this equation to Helmholtz equation. By solving this equation in two dimensions and using plane wave expansion method (PWEM), we can find the band gaps and allowed modes. We consider two structures with two concentric cylindrical rods; the external rode in the first structure consists of negative refraction index material while in the second structure it is made of a dielectric material. It is shown that by increasing the diameter of the cylinder which is composed of negative refraction index material in both structures, we can obtain wider band gaps in compare to the structures which there is positive refraction index materials.

REFERENCES

1. Saleh, B. E. A. and M. C. Teich, *Fundamental of Photonics*, 2nd Edition, Wiley, Ecole Polytechnique de Montreal, Canada University of Vermont, USA, 2007.
2. Sukhovanov, A. and V. Guryev, *Photonic Crystals Physics and Practical Modeling*, Springer Series in Optical Science, New York, 2009.
3. Joannopoulos, J. D., P. R. Villeneuve, and S. Fan, "Photonic crystals: Putting a new twist on light," *Nature*, Vol. 386, 143–149, London, 1997.
4. Marqus, P. and C. M. Soukoulis, *Wave Propagation from Electrons to Photonic Crystals and Left-handed Materials*, Princeton University Press, Canada, 2008.
5. Skorobogatiy, M. and J. Yang, *Fundamentals of Photonic Crystal Guiding*, 1st Edition, Cambridge University Press, 2009.

Investigation of Defect Modes on One-dimensional Ternary Metallic-dielectric Nano Photonic Crystal with Metallic Defect Layer

Abdolrasoul Gharaati and Hadis Azarshab
Department of Physics, Payame Noor University, Tehran, Iran

Abstract— We investigate the characterization of defect mode in one-dimensional ternary metallic-dielectric photonic crystal structures. The defect layer is made of metallic material. We consider defect mode for both symmetric and asymmetric geometries. Additionally, we demonstrate reflectance in terms of wavelength and its dependence on different angles of incidence for both transverse electric (TE) and transverse magnetic (TM) waves. There is just one defect mode when we use metallic defect layer. All of our calculations have done with transfer matrix method (TMM) and the Drude model of metals.

REFERENCES

1. Joannopoulos, J. D., R. D. Meade, and J. N. Winn, *Photonic Crystals: Molding the Flow of Light*, Princeton University Press, Princeton, NJ, 1995.
2. Szipocs, R., K. Ferencz, C. Spielmann, and F. Krausz, *Opt. Lett.*, Vol. 19, No. 3, 201, 1994.
3. Dastmalchi, B., R. Kheradmand, A. Hamidipour, A. Mohtashami, K. Hingerl, and J. Zarbakhsh, "Local dispersion of guiding modes in photonic crystal waveguide interfaces and hetero-structures," *Progress In Electromagnetics Research B*, Vol. 26, 39–52, 2010.
4. Gharaati, A. and H. Azarshab, "Characterization of defect modes in onedimensional ternary metallo-dielectric nanolayered photonic crystal," *Progress In Electromagnetics Research B*, Vol. 37, 125–141, 2012.

Modal Decomposition with Digital Holograms

Igor A. Litvin[1], **Angela Dudley**[1, 2], **Filippus S. Roux**[1], **and Andrew Forbes**[1, 2]

[1]CSIR National Laser Centre, P. O. Box 395, Pretoria 0001, South Africa
[2]School of Physics, University of KwaZulu-Natal
Private Bag X54001, Durban 4000, South Africa

Abstract— In this study, we demonstrate a simple approach, using digital holograms, to perform a complete modal decomposition of an optical field. Importantly, we use a set of basis functions that are not scale dependent so that unlike other methods, no knowledge of the initial field is required for the decomposition. We illustrate the power of the method by successfully decomposing a superposition field comprising of two orbital angular momentum carrying Bessel beams with an arbitrary phase delay between them. From the measured decomposition we show reconstruction of the amplitude, phase and orbital angular momentum density of the field with a high degree of accuracy.

Optimum Parameters for an Undersampled Digitally Heterodyned SFGPR

D. Adirosi[1], **G. Alberti**[2], **and G. Galiero**[2]

[1]Thales Alenia Space Italia, Italy
[2]Consortium for Research on Advanced Remote Sensing Systems — CO.RI.S.T.A., Italy

Abstract— In [1] a new architecture of an Undersampled Digitally Heterodyned SFGPR with variable sampling frequency was presented. The key aspects and the advantages of the new architecture were presented and discussed: signal generation by means of DAC; undersampling of the echoes by means of a large bandwidth ADC with a planned step by step varying sampling frequency; digital quadrature demodulation of the undersampled echoes. In [2] an analysis of the proposed SFGPR's parameters set was performed to indicate a procedure to choose their best values.

The SFGPR architecture presented had the following advantages:

- Absence of a synchronism chain, generally used in SFGPR to get a phase reference of the transmitted signal;
- Simplified RF front end: both Tx and Rx chains are substantially constituted by an amplifier and a filter; this is allowed by the undersampling of the received echoes;
- Simplified Frequency Generation Unit;
- Substantial reduction of the power consumption and weight due to the great simplification brought in the RF front end;

It was also remarked that the achievement of the mentioned goals had been possible by moving SFGPR complexities from the analog domain into the digital one.

Due to the wide bandwidth nature of the described SFGPR an aliased images analysis is needed. The intrisic advantages achievable by moving GPR complexities from the analog domain into the digital one have the side effect to potentially "move" aliased images into the useful intermediate frequency band if a suitable frequency plan is not performed in advance. The mentioned analysis has been performed with the aid of the "normalised acceptable bandpass sampling rates" map [3]: for each frequency step to be generated the first three aliased images are reported on it; in order to filter out them once the digital quadrature downconversion shall be performed they have to fall outside the prohibited band; this is a band centered around the useful intermediate frequency and with a bandwidth related to the transition band desired for the digital LPF to be implemented. Generally these frequencies fall into regions different from the one the useful intermediate frequency falls in (both identified by different values of the parameter m [3]); this can lead to a different choice of the sampling frequency values due to the different slope of the map's lines and it can solve the problem of aliased images falling into the useful intermediate frequency band when it happens.

In [4], this analysis was performed by following a sort of "brute force" approach, that is the results attainable were simulated and checked against the allowed bandwidth. This approach allowed to define a first attempt set of values for the procedures developed in this paper and to verify its validity but there was no way to show if the set chosen was the best one or not and if it was far from being an optimum choice. In this paper, a completely different approach has been followed by using the "normalised acceptable bandpass sampling rates" map [3]. By plotting in this map the different frequencies steps to be generated as well as the aliased images digitally generated, it is possible to determine the best combination and the number of sampling frequencies to be used, where best means the values that allow to relax the requirements on the anti-alias filters in the analog domain as well as the digital low pass filters following the digital quadrature demodulator. The outline of the procedure followed in this paper, and implemented with the aid of ad hoc software tools, is:

- a first attempt set of values is provided by the analysis performed previously [1, 4];
- for each frequency step to be generated a vertical line is plotted on the "normalised acceptable bandpass sampling rates" map [3] and its intersections with the map's lines contained inside a given interval values of sampling frequencies (to be provided as input) are computed;
- once all the computations of the previous step are performed the resulting sampling frequencies values are analysed and only the useful ones are kept for the subsequent aliased images processing.

The mentioned analysis has been performed with the aid of ad hoc software tools.

The main results of the analysis and simulations performed are reported.

REFERENCES

1. Adirosi, D., G. Alberti, and G. Galiero, "Undersampled digitally heterodyned SFGPR with variable sampling frequency," *PIERS Online*, Vol. 7, No. 1, 47–50, 2011.
2. Galiero, G., D. Adirosi, and G. Alberti, "Analysis of a wide bandwidth undersampled digitally heterodyned SFGPR," *Proceedings of "IGARSS 2011"*, Vancouver, Canada, July 2011.
3. Lyons, R. G., *Understanding Digital Signal Processing*, 2nd Edition, Prentice Hall, 2004.
4. Adirosi, D., G. Alberti, and G. Galiero, "'Spurious' analysis of a wide bandwidth undersampled digitally heterodyned SFGPR," *Proc. 6th International Workshop on Advanced Ground Penetrating Radar*, Aachen, Germany, June 2011.

Switch Matrix Logic Implementation for Electrical Impedance Tomography Systems

Mohamad Rahal, **Ibrahim Rida**, **and Muhammad Usman**
Department of Electrical Engineering, University of Hail, P. O. Box 2440, Hail, Saudi Arabia

Abstract— *Electrical Impedance Tomography* (EIT) is non-invasive technique that has the potential to be used in clinical environments for lung ventilation monitoring, cardiac and brain imaging applications. EIT has many advantages in terms of simplicity, cost and the absence of ionising radiations compared to the traditional imaging techniques such as *magnetic resonance imaging* (MRI) and X-rays. EIT systems usually consist of a ring of equally spaced electrodes placed around the part of the body of interest. A sinusoidal current source with a typical frequency of 50 kHz is used to inject current between an adjacent pair of electrodes. Then the imposed voltages on the remaining electrodes are measured sequentially. After that the current source is routed to the next pair and the cycle is repeated until one frame of data is collected. For eight electrodes 8×5 measurements per frame are collected. Mathematical algorithms are used to construct an image of the impedance distribution inside the closed volume. In order to apply the current source and measure the imposed voltages on the electrodes a switch matrix is needed. In this work, a circuit implementation of the switch matrix for eight electrodes is presented. The system consists of logic blocks used to generate eight logic signals (CL_1-CL_8) needed to route the differential current source to the appropriate electrode pair. For example, when the logic signals CL_1 and CL_2 are both high, the differential current is routed to electrode pair 1 and 2. During this time other blocks are used to generate 8 logic signals (VL_1-VL_8) required to measure the imposed voltages on the remaining electrodes in the following sequence, V_3-V_4, V_4-V_5, V_5-V_6, V_6-V_7 and V_7-V_8. The logic blocks used in the implementation consists of mono-stable elements in addition to standard logic gates. Results indicate that the hardware implementation of the designed circuit is feasible in both hardware and software form.

Prediction of a New Superconductivity-like Effect in Galilean Reference Systems (Part II)

Namık Yener
Technology Faculty, Kocaeli University, Izmit, Kocaeli 41380, Turkey

Abstract— Prediction of a hitherto unknown superconductivity-like effect is made which is independent of temperature, but rather requires Galilean reference systems moving at the speed of light in vacuum. As the medium (I) to which the laboratory frame is attached, a Lorentz medium is selected whereas for medium (II) to which the rest frame is attached, a perfectly conducting medium is selected. The interface is an infinite plane perpendicular to the uniform rectilinear motion involved. The fact that the Lorentz medium appears as a metal when observed from the rest frame, is unearthed in a previously reported work by the same author. Next the limit condition which in effect requires attainment of speed of light in vacuum by the uniform rectilinear motions of the Galilean reference systems is considered, and the effective permittivity function of medium (I) observed from the rest frame is found to have a character similar to that of a superconductor. It should be stressed that the fundamental premise of the work is Lorentzian relativistic transformation and not Galilean relativistic transformation under which the permittivity function could have been invariant. This work is presented in a series of two papers. In Part (I) the models for medium (I) observed from the laboratory frame and the rest frame are presented. In Part (II) the prediction of the new superconductivity-like effect is made and equations with the same structure as London equations in a superconductor are presented. Also included in this Part is a discussion proving that the dispersion relation for medium (I) observed from the rest frame can be split as a permittivity function and a permeability that is equal to that observed from the laboratory frame, which is but the permeability of free space.

Allocation of Cognitive Radio Sensing Times Using Distributed Q-learning

Olivier van den Biggelaar, Jean-Michel Dricot, Philippe de Doncker, and François Horlin
OPERA Department, Université Libre de Bruxelles (ULB), Belgium

Abstract— The scarcity of available radio spectrum frequencies, densely allocated by the regulators, represents a major bottleneck in the deployment of new wireless services. Cognitive radios have been proposed as a new technology to overcome this issue [1]. For cognitive radio operation, the assigned frequency bands are opened to secondary users, provided that interference induced on the primary licensees is negligible. Cognitive radios are established in two steps: the radios firstly sense the available frequency bands and secondly communicate using these bands.

To tackle the fading phenomenon — typical in wireless propagation — when sensing the frequency spectrum, cooperative spectrum sensing has been proposed to take advantage of the spatial diversity in wireless channels [2]. In cooperative spectrum sensing, the secondary cognitive nodes send the results of their individual observations of the primary signal to a base station through specific control channels. The base station then combines the received information in order to make a decision about the primary network presence. Each cognitive node observes the primary signal during a certain sensing time, which should be chosen high enough to ensure the correct detection of the primary emitter but low enough so that the node still has enough time to communicate. The sensing times used by the cognitive nodes are generally assumed to be identical and allocated by a central authority [3, 4]. In paper [5], the sensing performance of a network of independent cognitive nodes that individually select their sensing times is analyzed using evolutionary game theory. It is shown that allowing cognitive nodes to selfishly not sense the spectrum during some time slots leads to a higher total throughput than the one obtained when the nodes perform spectrum sensing at every time slot.

In this paper, a decentralized Q-learning algorithm is proposed to share the sensing time among the cognitive radios in a way that maximizes the throughputs of the radios while simultaneously limiting the interference induced on the primary network. The multiple cognitive radios (the agents) self-adapt by directly interacting with the environment in real time and by properly utilizing their past experience. They aim to distributively learn the optimal strategy to maximize their throughputs.

Reinforcement learning algorithms such as Q-learning are particularly efficient in applications where reinforcement information (i.e., cost or reward) is provided after an action is performed in the environment [6]. In the sensing time allocation problem, the throughput achieved by each node can naturally be used as reinforcement information.

The distributed allocation of the sensing times presents several advantages compared to a centralized allocation: 1) robustness of the system towards the variation of the channel parameters; 2) maintainability of the system thanks to the modularity of the multiple agents and 3) scalability of the system as the need for control communication is minimized. There is indeed no need for a central authority to send the result of a centralized allocation to the multiple nodes and conversely there is no need for these nodes to send their specific parameters (sensing signal-to-noise ratios and data rates) to a central authority. Besides, a centralized allocation is not a trivial operation as the sensing time allocation problem is essentially a multi-criteria problem where multiple objective functions to maximize can be defined (e.g., the sum of the individual rewards to aim at a global optimum or the minimum individual reward to guarantee more fairness).

A rigorous proof of the convergence of the proposed Q-learning allocation algorithm is provided. Firstly, we show that the Q-value updating rule is equivalent to Robbins-Monro algorithm [7] which is known to converge to a stationary point which is a limit set of an Ordinary Differential Equation (ODE). Secondly, we apply Lyapunov's method to prove the asymptotic stability of this limit set.

Numerical results show that the throughputs obtained with both the proposed Q-learning allocation algorithm and a reference distributed allocation algorithm based on Evolutionary Game Theory [5] are slightly lower than those obtained with an optimal centralized allocation algorithm based on the maximization of the Equal Gain Combining of the average throughputs. However, both decentralized algorithms minimize the need for exchange of control information between the cognitive nodes and the coordinator node. In addition, numerical results show that the proposed Q-learning allocation algorithm converges faster, with a lower time complexity but with higher

memory requirements than the reference distributed allocation algorithm. Finally it is shown that there is an optimal tradeoff value for the frequency of execution of the proposed Q-learning algorithm.

REFERENCES

1. Weiss, T. A. and F. K. Jondral, "Spectrum pooling: An innovative strategy for the enhancement of spectrum efficiency," *IEEE Radio Communications*, Vol. 42, No. 3, S8–S14, 2004.
2. Bazerque, J. A. and G. B. Giannakis, "Distributed spectrum sensing for cognitive radio networks by exploiting sparsity," *IEEE Transactions on Signal Processing*, Vol. 58, No. 3, 1847–1862, Mar. 2010.
3. Liang, Y.-C., Y. Zeng, E. Peh, and A. T. Hoang, "Sensingthroughput tradeoff for cognitive radio networks," *IEEE International Conference on Communications*, Jun. 2007.
4. Stotas, S. and A. Nallanathan, "Sensing time and power allocation optimization in wideband cognitive radio networks," *GLOBECOM 2010, 2010 IEEE Global Telecommunications Conference*, 1–5, Dec. 2010.
5. Wang, B., K. J. R. Liu, and T. C. Clancy, "Evolutionary cooperative spectrum sensing game: How to collaborate?," *IEEE Transactions on Communications*, Vol. 58, No. 3, 890–900, Mar. 2010.
6. Panait, L. and S. Luke, "Cooperative multi-agent learning: The state of the art," *Auton. Agents Multi-agent Syst.*, Vol. 11, No. 3, 387–434, 2005.
7. Robbins, H. and S. Monro, "A stochastic approximation method," *The Annals of Mathematical Statistics*, Vol. 2, 400–407, 1951.

Dynamics of a Non-autonomous Bright and Dark Soliton in a Generalized Nonlinear Schrödinger Equation

Zhan-Ying Yang[1], **Li-Chen Zhao**[1], **Tao Zhang**[1], **and Rui-Hong Yue**[2]

[1]Department of Physics, Northwest University, Xi'an 710069, China
[2]Faculty of Science, Ningbo University, Ningbo 315211, China

Abstract— For the non-autonomous system, there are three questions to be asked frequently: Do solitons still exist and maintain their identities through nonlinear interaction in time-dependent external potentials? In which condition can a soliton exist? How can the dynamical behaviors of non-autonomous solitons be controlled? In most cases, the dynamics of non-autonomous solitons is governed by the nonlinear Schrodinger equation. We solve analytically a generalized non-autonomous nonlinear Schrodinger equation by performing the Hirota's bi-linearization method. The precise expression of e^2 provides an appropriate way to study the modulation depth. It is shown that dark solitons in nonlinear system exist only when propagation-distance-dependent nonlinearity and inhomogeneous parameter related to phase modulation are suitable chosen. Moreover the precise expressions of a non-autonomous black soliton's intensity, width and the trajectory of its wave center describing the dynamic behavior of soliton's evolution are obtained. We also study the non-autonomous solitons in a planar waveguide with an additional periodical structure, a long-period grating. The explicit functions which describe the evolution of the width, peak, and trajectory of the soliton's wave center are presented exactly. The gain parameter has no effects on the motion of the soliton's wave center or its width; it just affects the evolution of the soliton's peak. The grating term affects the motion of the soliton's wave center without changing its shape. The evolution of the soliton under the propagation-distance-dependent gain term is investigated too. It is reported that an arbitrary additional structure can be added on the graded-index waveguide to control the motion of the soliton without affecting its shape.

Bright Chirp-free and Chirped Nonautonomous Solitons under Dispersion and Nonlinearity Management

Ruihong Yue[1], **Zhanying Yang**[2], **Lichen Zhao**[3], **and Tao Zhang**[1]

[1]Faculty of Science, Ningbo University, Zhejiang 315211, China
[2]Department of Physics, Northwest University, Xi'an 710069, China
[3]Science and Technology Computation Physics Laboratory
Institute of Applied Physics and Computational Mathematics, Beijing 100088, China

Abstract— The concept of soliton management has been proposed with the development of modern technology, which is essential to control the soliton's dynamics by tuning the related parameters. Since then, how to control exactly the soliton's dynamics by dispersion and nonlinearity management with gain term becomes an intensively studied issue. We present a series of chirp-free and chirped analytical non-autonomous soliton solutions to the generalized nonlinear Schrödinger equation with distributed coefficients by Darboux transformation from a trivial seed. For a chirp-free non-autonomous soliton, the dispersion management term changes the motion of a non-autonomous soliton, but does not affect its shape at all. Specifically, the classical optical solitons can be presented with a variable dispersion term and nonlinearity when there is no gain. For a chirped non-autonomous soliton, dispersion management can affect both the shape and motion of non-autonomous solitons. The periodic dispersion term can be used to control its "breathing" shape, and keep the invariance of the trajectory of a non-autonomous soliton center with a certain condition. These expressions can be conveniently and effectively applied to the management of soliton in many fields.

Remote Sensing and Simulation Model for Crop Management

J. Soria-Ruiz[1], **Y. Fernandez-Ordonez**[2], **A. Quijano-Carranza**[1], **J. Macías-Cervantes**[1], **P. Sauceda**[1], **D. Gonzalez**[1], **and J. Quintana**[1]

[1]Geomatics Lab, National Institute of Research for Forestry Agriculture and Livestock (INIFAP) Toluca, Mexico

[2]Colegio de Postgraduados, Montecillo, Mexico

Abstract— When one considers the components involved in studying the worldwide supply and demand for agricultural products, the applications of remote sensing in general are indeed many and varied. The scope of the physical, biological, and technological problems facing modern agriculture is an extremely broad one that is intimately related with worldwide problems of population, energy, environmental quality, climate and weather.

Producers and decision makers in the rural sector require reliable information about the expected production volumes of crops. Maize is a staple crop in Mexico, so it is important to predict yield on a yearly basis. The objective of this research was to determine maize acreage and to predict yield using SPOT images, weather data and field collected data for crop variables. The study area is located in the Corn Belt within the State of Sinaloa in northwestern Mexico. Sinaloa is the main producer of white maize in this country producing around 5 million tons per year.

Yield prediction relies on determining extent acreage of the crop and on monitoring growth and developing using data on vegetation indices (NDVI), on leaf area indices (LAI) and on photosynthetic active radiation (PAR). For determining acreage and NDVI, multispectral and panchromatic scenes of SPOT-5 were processed using supervised classification techniques. NDVI data were obtained from the visible red and infrared bands. LAI and PAR data were gathered with canopy analyzers on 209 maize plots geo-located with GPS. Yield prediction was done with a mathematical model as a function of planting dates considering other relevant data such as crop genotype, crop vigor, phenological data of maize, climate and soil. The prediction yield was produced 40 days before harvest.

Results indicate that, the total cultivated area of maize in State of Sinaloa, the agricultural cycle Fall-Winter 2011, was 383, 693 hectares, it predicted an average yield of 6.84 ton.ha^{-1}, with a confidence interval of 95 percent, a range of 6.58 to 7.9 ton.ha^{-1} and an average output of 2.6 million tons of maize grain. In addition, we obtained an R^2 of 0.68 for the NDVI and LAI variables. The prediction yield model showed an effectiveness of 95%. This prediction of maize yields is already supporting decision makers from the Ministry of Agriculture and farmers as well.

Session 3P1
Advanced Photonics-based Devices and Equipment

A Microwave Optoelectronic Oscillator: Mach-Zehnder Modulator or VCSEL Based Layout Comparison

M. E. Belkin and A. V. Loparev
Joint Research Laboratory "Microwave and Optoelectronic Devices"
Moscow State Technical University of Radio-Engineering, Electronics and Automation (MSTU MIREA)
Vernadskogo Av., 78, Moscow, Russian Federation

Abstract— This contribution is focused a microwave optoelectronic oscillator (OEO) that is one of the most attractive functional examples of microwave photonics devices aspiring to become a new class of highly stable RF oscillators in a frequency range from hundreds of MHz to hundreds of GHz. The key advantage of an OEO in comparison with traditional RF and microwave oscillators is the remarkably high spectral purity achievable [1]. Nowadays such OEOs have a wide area of potential applications in the fields of measurement equipment, telecommunications, and precise sensors.

In most of updating publications referred to OEO the same device configuration with optoelectronic feedback on Mach-Zehnder optical external modulator is examined. In the result, the state of the art for these OEOs is currently considered to be a single-frequency (within the X-band) OEO product from OEwaves Inc. with a phase noise level of −163 dBc/Hz at a 10 kHz offset from the carrier [2]. But, to our mind, this circuitry has at last two serious drawbacks in comparison to typical monolithic microwave oscillators: cost-ineffectiveness and integration inability due to presence of lithium niobate modulator.

In the paper, we studied two versions of microwave OEO's realization: a traditional one based on Mach-Zehnder optical external modulator, and a novel one with feedback through the direct modulation of a potential cost-effective vertical cavity surface emitting laser (VCSEL) that has researched experimentally in [3]. First a large-signal mode simulation of the both versions is fulfilled using optoelectronic CAD tool VPItransmission MakerTM. Then the simulation results of the spectral and phase noise characteristics are verified by experimental data in S-band. Finally, the results of our research are compared with each other and with typical data for modern microwave sources.

REFERENCES

1. Yao, X. S., "Opto-electronic oscillators," *RF Photonic Technology in Optical Fiber Links*, W. S. C. Chang., Ed., 255–292, Cambridge University Press, 2002.
2. Http://www.oewaves.com/downloads/Adv%20OEO%20PB_042610.pdf.
3. Hasegawa, H., Y. Oikawa, and M. Nakazawa, "A 10-GHz optoelectronic oscillator at 850 nm using a single-mode vcsel and a photonic crystal fiber," *IEEE Photonics Technology Letters*, Vol. 19, No 19, 1451–1453, Oct. 2007.

Passive Components Based on Two-dimensional Photonic Crystals

T. N. Bakhvalova and I. V. Khmelnitsky
Joint Research Laboratory "Microwave and Optoelectronic Devices"
Moscow State Institute of Radio-Engineering, Electronics and Automation, MSTU MIREA
Moscow 119454, Russian Federation

Abstract— A photonic crystal (PhC) with photonic band gap is a promising candidate as a platform to construct devices with dimensions of several wavelengths for future photonic integrated circuits. PhCs are particularly interesting, in all-optical systems to transmission and processing information due to the effect of localization of the light in the defect region of the periodic structure [1]. Wavelength filters of optical range based of two dimensional PBG structure can be created by the correct selection of geometrical and physical parameters.

The possibilities of the use and results of modeling of two-dimensional PhC spectral demultiplexer and polarizer were proposed and investigated. Three spectral demultiplexer/multiplexers (DEMUX/MUX) are designed: to separate the channels with wavelengths of 1490 and 1550 nm (Passive optical network PON); 1270 and 1310 nm (IEEE 802.3 40GBASE-LR4 standard); 1270 and 1290 nm (IEEE 802.3 40GBASE-LR4 standard); 1510, 1530, 1550 and 1570 nm (ITU-T G.695). These DEMUX/MUXs consist of circular silicon pillars in rectangular lattice surrounded by air with radius of circular is 0.2a. These devices are based on splitting the wavelength channel using different filters. One filter with three defect pillars inside it and another filter with tapered region are placed at the T-junction. Proposed two-channel DEMUX/MUXs based on PhC are designed to separate the channels with wavelengths which widely used in telecommunications.

For design polarizer it is necessary to use photonic crystal with full photonic bandgap (simultaneously for TE- and TM-polarization). In simple model of lattice (like rectangular or hexagonal lattices) it is impossible to do so in this case we use the honeycomb lattice. Polarizers were investigated for the same wavelength range.

Selection of models geometric parameters is based on the analysis of photonic bandgap maps. The computations were carried out using the OptiFDTD 8 program of Optiwave Software.

REFERENCES

1. *Frontiers in Guided Wave Optics and Optoelectronics*, Bishnu Pal., Ed., 621–645, InTech, 2010.

Photonic-crystal Light Emitters with Quantum-wire Active Medium

K. A. Atlasov, **P. Gallo**, **M. Calic**, **M. Felici**, **K. F. Karlsson**, **A. Rudra**, **B. Dwir**, **and E. Kapon**
Laboratory of Physics of Nanostructures, Ecole Polytechnique Fédérale de Lausanne (EPFL), CH-1015 Lausanne, Switzerland

Abstract— Bandgap effects at particular photon frequencies in photonic crystals (PhC) allow for creating rather tight confinement of light into spatial volumes of the order of a cubic wavelength. Such possibility allows for creating optical microcavities of relatively high Q-factors having at the same time extremely small modal volumes. This enables to exert control on light-matter interaction, and in particular, to control the fundamental process of spontaneous emission, which may be employed in such applications as microlasers [1, 2], single-photon sources [3, 4], experiments in quantum physics and quantum computation [5, 6]. The use of fully embedded quantum nanostructures such as quantum wells (QWs), quantum dots (QDs) or quantum wires (QWRs) is then essential, since the matter active-medium volume has to be small in order to fully exploit the microcavity effects [1, 2] and since the quantum confinement effects — resulting in the discretization of the density of states for charge carriers and excitonic effects — in the nanostructures allow for creating efficient light source. In this paper we present studies of semiconductor GaAs PhC microcavities with integrated quantum-wire active light source [7] based on the fabrication technology that allow for precise and reproducible site and spectral control of the QWR and QD nanostructures as well as PhC microcavities on a chip. The technological approach employs metal-organic vapor-phase epitaxy (MOVPE) on nonplanar substrates — e.g., V-grooved for QWRs — and is combined with a high-precision alignment provided in e-beam lithography. With the QWR-PhC system, effects of microcavity laser [8], optical cavity coupling [9, 10] and photon localization [11] are demonstrated experimentally and the main findings are discussed in this paper.

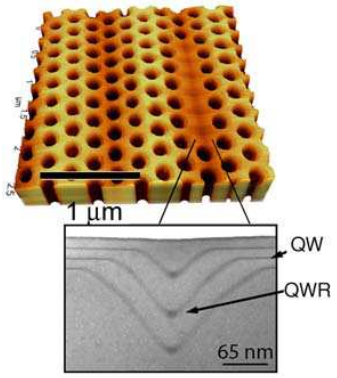

Figure 1: AFM image and TEM cross-section of the active region of the GaAs/InGaAs PhCQWR laser (L6 cavity).

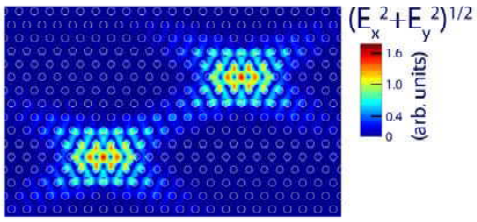

Figure 2: Coupling of two L3 PhC cavities with an optimal arrangement using the pecularities of the optical-field distribution (FDTD simulation).

REFERENCES

1. Björk, G. and Y. Yamamoto, *IEEE J. Quantum Electron.*, Vol. 27, 2386, 1991.
2. Noda, S., *Science*, Vol. 314, 260, 2006.
3. Changm, W.-H., et al., *Phys. Rev. Lett.*, Vol. 96, 117401, 2006.
4. Manga Rao, V. S. C. and S. Hughes, *Phys. Rev. Lett.*, Vol. 99, 193901, 2007.
5. Hartmann, M. J., et al., *Nature Phys.*, Vol. 2, 849, 2006.
6. Raussendorf, R. and H. J. Briegel, *Phys. Rev. Lett.*, Vol. 86, 5188, 2001.
7. Atlasov, K. A., et al., *Appl. Phys. Lett.*, Vol. 90, 153107, 2007.
8. Atlasov, K. A., et al., *Opt. Express*, Vol. 17, 18178, 2009.
9. Atlasov, K. A., et al., *Opt. Express*, Vol. 16, 16255, 2008.
10. Atlasov, K. A., et al., *Opt. Express*, Vol. 19, 2619, 2011.
11. Atlasov, K. A., et al., *Opt. Express*, Vol. 18, 117, 2010.

Deterministic Quantum Nano-photonics with Ordered Systems of Quantum Dots

Eli Kapon
Laboratory of Physics of Nanostructures
Ecole Polytechnique Fédérale de Lausanne (EPFL), Lausanne 1015, Switzerland

Abstract— Systems of semiconductor quantum dots (QDs) with well-defined positions and optical emission or absorption spectra are a pre-requisite for constructing nano-photonic systems for studying fundamental light-matter interaction in the solid state and for future applications in low-power consumption optical interconnects, quantum information technology and novel sensors. However, most progress in this area has been based on self-assembled ensembles of QDs, which lack site and spectral control.

Here we describe the structure and optical properties of III-V compound QD systems grown on patterned substrates. The site-controlled (In)GaAs/(Al)GaAs QDs are fabricated using organometallic vapor phase epitaxy (OMVPE) on (111)B GaAs substrates patterned using electron beam lithography [1]. The unique self-ordering process of these pyramidal QDs results in perfect site control, exceptional uniformity ($\sim$ 1 meV inhomogeneous broadening) [2], and offers the possibility of controlling their heterostructure potential in great detail. Their high C_{3v} symmetry facilitates the generation of polarization-entangled photons with high yield [3, 4]. Integration of pyramidal QDs with photonic crystal (PhC) membrane cavities has been demonstrated, exploiting their inherent site control [5]. Single pyramidal QDs integrated into photonic crystal (PhC) membrane cavities exhibit uniquely near-resonance, phonon mediated coupling [6]. More recently, PhC cavities loaded with a measurable number of QDs (from 2 to $\sim$ 50) have also been studied, being candidates for laser structures incorporating dots that all interact with the same optical cavity mode [7]. The optical properties of these integrated QD systems and their potential applications will be described and discussed.

REFERENCES

1. Biasiol, G. and E. Kapon, *Phys. Rev. Lett.*, Vol. 81, 2962, 1998.
2. Mohan, A., et al., *Small*, Vol. 6, 1268, 2010.
3. Mohan, A., et al., Nature Photonics, Vol. 4, 302, 2010.
4. Dupertuis, M.-A., et al., *Phy. Rev. Lett.*, Vol. 107, 7403, 2011.
5. Gallo, P., et al., *Appl. Phys. Lett.*, Vol. 92, 63101, 2008.
6. Calli, M., et al., *Phys. Rev. Lett.*, Vol. 106, 227402, 2011.
7. Surrente, A., et al., *Nanotehnology*, Vol. 22, 5203, 2011.

Characteristics of a Sub-terahertz Continuous Wave Generated by Photonics

Sungil Kim
Terahertz Research Team, Convergence Components & Materials Research Laboratory
Electronics and Telecommunications Research Institute, Korea

Abstract— We have proposed a sub-terahertz (THz) continuous wave (CW) generation scheme based on a double sideband-suppressed carrier (DSB-SC) scheme using the pump laser of an erbium-doped fiber amplifier (EDFA) as a lightwave source to reduce an implementation cost of photonic-based sub-THz generation technique. The usual DSB-SC scheme has been well-known photonic-based sub-THz generation technique and it consists of a lightwave source, a lightwave modulator, a local oscillator (LO), a Fiber Bragg Grating (FBG) notch filter, and an EDFA. In the proposed scheme, the lightwave source is eliminated and the pump laser output of the EDFA is used as the lightwave source using a feedback loop, which is composed of a circulator and 9 : 1 coupler. Output of the EDFA is firstly inserted to the FBG notch filter and the reflected lightwave signal of the FBG notch filter is feedbacked to the input of the lightwave modulator through the feedback loop. A DSB-SC lightwave has been made by the lightwave modulator with the local oscillator. The DSB-SC lightwave then goes to a photomixer and the sub-THz CW is generated by photomixing. In order to verify our proposed scheme, we have generated and characterized a 120 GHz CW. The measurement results are also compared to that of the usual DSB-SC scheme. A photomixed output power and a phase noise of the proposed scheme is 2 dB higher and 3 dB lower than those of the usual DSB-SC scheme. Based on our measurement results, characteristics of the 120 GHz CW generated by the proposed scheme close to those generated by the usual DSB-SC scheme. Consequently, our proposed scheme can be helpful to make cost-effective sub-THz generator based on photonics.

Low-phase Noise Photonic Millimeter Wave Generation Using a Nonlinear MZM and Four-wave Mixing in Ultra Long SOAs

André Garcia, Vitaly Rymanov, and Andreas Stöhr
Zentrum für Halbleitertechnik und Optoelektronik (ZHO)
Universität Duisburg-Essen, Germany

Abstract— We demonstrate an experimental study the influence of the Semiconductor Optical Amplifier (SOA) interaction length on the four-wave mixing (FWM) efficiency. We furthermore propose and demonstrate a simple set-up for a frequency-tunable (up to 50 GHz) photonic microwave generator using nonlinearities in a Mach-Zehnder modulator (MZM) and the four-wave mixing (FWM) effect in an ultralong semiconductor optical amplifier (UL-SOA). The operation principle of the photonic microwave generator is based on an external modulation scheme using a low phase noise local oscillator (LO) source to multiply the LO frequency in the optical domain. We experimentally characterized the influence of the SOA interaction length on the FWM efficiency using three types of SOAs, as well as, the overall Radio Frequency (RF) conversion efficiency at the different achieved multiplication levels to identify the optimal operation conditions for the SOA. Using a low frequency reference LO source fixed at 4 GHz, the generation of a tunable and low phase noise millimeterwave (mm-wave) signal up to 50 GHz was demonstrated.

A maximum achievable multiplication factor (N) of twelve-times the LO frequency, 48 GHz, has been achieved resulting from the nonlinear behavior of the MZM and the UL-SOA. Additional phase noise measurements were performed for the fundamental LO frequency as well as of the generated mm-wave signal with a multiplication factor of $N = 8$. Those measurements revealed a phase noise level of -96 dBc/Hz and -78 dBc/Hz at 10 kHz offset from the carrier, respectively. By using novel high-output power double-mushroom PDs, output power levels up to about 0 dBm have been achieved.

Extended Cavity Diode Lasers. Development and State-of-the-art

V. V. Vassiliev[1, 2], **S. A. Zibrov**[1, 2], **and V. D. Kurnosov**[3]

[1]Lebedev Physical Institute, RAS, Moscow 117924, Russia
[2]Advanced Energy Technologies LTD, Moscow 107045, Russia
[3]POLYUS Research & Development Institute, Moscow 117342, Russia

Abstract— Optical feedback is a powerful mean to increase coherence of laser diodes. To date extended cavity diode lasers (ECDLs), in which selective optical feedback imposes single frequency and narrow linewidth operation, often replace other types of tunable lasers. Being initially just a laboratory tool, the ECDLs over the past decade began to be produced commercially by many companies in the world including USA, Germany, and Russia.

The most obvious application of ECDLs is high-resolution spectroscopy, laser-cooling, and optical pumping in microwave atomic frequency standards, especially in their on-board versions requiring low weight and dimensions. The insensitive to vibrations chip-size laser diodes such as distributed feedback (DFB) or distributed Bragg reflector (DBR) lasers severely compete with the ECDLs in this field, but due to inherent low-Q cavity have excessive phase noise, which restricts output parameters of the microwave atomic frequency standard.

The overview of different optical schemes for extended cavity diode lasers is presented. Some most popular types of extended cavity diode laser are described and compared. Much of the report is devoted to ECDLs produced in Russia and particular in P. N. Lebedev Physical Institute: fiber-grating diode lasers, diode lasers coupled to "whispering-gallery" microresonator, widely tunable grating-stabilized diode lasers. The commercially available ECDL of Littrow scheme developed in Physical Institute with the continuous tuning range of about 1Å is described in detail. The beat note of two such lasers was 700 kHz at 0.1 second, while instantaneous linewidth of the laser did not exceed 60 kHz. The laser demonstrates tidy passive frequency stability of about 100 MHz per hour.

Physical Package for Miniature Microwave Atomic Clock

A. V. Sivak[1, 2], **V. L. Vassiliev**[2, 3], **S. A. Zibrov**[2, 3], **V. I. Yudin**[2, 4, 5, 6], **and A. V. Taichenachev**[2, 4, 5]

[1]National Research Nuclear University "MEPhI", Moscow 115409, Russia
[2]Advanced Energy Technologies LTD, Moscow 107045, Russia
[3]Lebedev Physical Institute, RAS, Moscow 117924, Russia
[4]Institute of Laser Physics, Siberian Branch of RAS, Novosibirsk 630090, Russia
[5]Novosibirsk State University, Novosibirsk 630090, Russia
[6]Novosibirsk State Technical University, Novosibirsk 630092, Russia

Abstract— An atomic frequency and time reference (atomic clock) is a precision reference oscillator in radio- and microwave-frequency region that ensures the operation of almost all types of high-end and prospective electronics. Many laboratories and companies around the world work on miniature atomic clocks (MAC) which are expected to have an order of magnitude better metrological characteristics, smaller size and diminished power consumption than the best high-precision crystal oscillators [1–3].

The MAC operation is based on coherent population trapping (CPT) phenomenon in alkali metal atoms (usually ^{87}Rb or Cs). This quantum phenomenon is observed in the dependence of absorption of resonant bichromatic laser field on the frequency difference of the two components. For small clocks such field is formed by microwave modulation of the pumping current of a single-mode diode laser.

The report describes a small-scale physical package for the MAC and its characteristics. It includes an atomic cell with ^{87}Rb isotope and mixture of buffer gases Ar and Ne, heaters, vertical cavity surface-emitting laser, photodiode, quarterwave plate, magnetic shield, and solenoid for producing a longitudinal magnetic field. A contrast of the reference CPT resonance formed between ground state sublevels with quantum numbers ($F_g = 1$, $m = 0$)–($F_g = 2$, $m = 0$) in atoms ^{87}Rb is about 4% and its dark width is about 800 Hz. The different factors that influence characteristics of the CPT resonances and overall stability of the MAC are discussed. Our purpose is a development of the MAC with a stability (Allan parameter) no worse than $5 \cdot 10^{-12}$ @ 1 hour.

REFERENCES

1. Knappe, S., P. D. D. Schwindt, V. Shah, L. Hollberg, and J. Kitching, "A chip-scale atomic clock based on ^{87}Rb with improved frequency stability," *Optics Express*, Vol. 13, No. 4, 1249–1253, 2005.
2. Deng, J., P. Vlitas, D. Taylor, L. Perletz, and R. Lutwak, "A commercial CPT rubidium clock," *EFTF08*, 2008.
3. Shah, V. and J. Kitching, "Advances in coherent population trapping for atomic clocks," *Advances in Atomic, Molecular, and Optical Physics*, Vol. 59, Chapter 2, Elsevier Inc., 2010.

Contrast and Quality Factor Enhancement of Dark Resonances for Miniature Microwave Atomic Clocks

A. V. Taichenachev[1, 2, 8], **V. I. Yudin**[1, 2, 3, 8], **D. I. Sevostianov**[4, 8], **A. A. Zibrov**[6], **A. S. Zibrov**[2, 6, 7], **and S. A. Zibrov**[5, 8]

[1]Institute of Laser Physics, Siberian Branch of RAS, Novosibirsk 630090, Russia
[2]Novosibirsk State University, Novosibirsk 630090, Russia
[3]Novosibirsk State Technical University, Novosibirsk 630092, Russia
[4]National Research Nuclear University "MEPhI", Moscow 115409, Russia
[5]Lebedev Physical Institute, RAS, Moscow 117924, Russia
[6]Center for Astrophysics, Harvard University, Cambridge, MA 02138, USA
[7]Physics Department, Harvard University, Cambridge, MA 02138, USA
[8]Advanced Energy Technologies LTD, Moscow 107045, Russia

Abstract— There is a great interest in the development of miniature (chip scale) frequency standards based on the microwave transition between hyperfine ground states of alkali metal atoms. One of the efficient ways to probe the hyperfine transition without using bulky microwave cavity is based on the phenomenon of the coherent population trapping (CPT). By coherent interaction with two resonant optical fields in a Λ-configuration, atoms can be pumped into a noninteracting quantum superposition of the two hyperfine ground states. This "dark" state is very sensitive to detuning of the frequency difference of the two optical fields from the hyperfine splitting of the atomic states. The microwave resonance is detected by the change in transmission of optical fields.

In recent years, atomic frequency standards based on CPT resonances with fractional frequency stability of about 10^{-12} were have been demonstrated [1, 2]. Further improvements in stability require realization of CPT resonances with improved parameters, such as larger amplitude and contrast and smaller linewidth. This becomes possible with the use of new effective schemes of resonance excitation.

In this report, different excitation schemes of high contrast CPT resonances are discussed [3, 4]. A new alternative method of spectroscopy that is based on the locking of the intensity of a spontaneous emission is presented. The method explores the CPT spectra at a fixed level of its spontaneous emission regardless of the microwave frequency, which is achieved by the feedback loop to the laser intensity. It results in the increase of the contrast and quality factor of resonance by several orders of magnitude (two orders in our proof-of-principal experiments) in combination with additional narrowing of the resonance.

REFERENCES

1. Vanier, J., "Atomic clocks based on coherent population trapping: A review," *Appl. Phys. B*, Vol. 81, 421–442, 2005.
2. Knappe, S., "MEMS atomic clocks," *Comprehensive Microsystems*, Vol. 3, 3.18, 571–612, 2008.
3. Taichenachev, A. V., V. I. Yudin, V. L. Velichansky, S. V. Kargapoltsev, R. Wynands, J. Kitching, and L. Hollberg, *JETP Letters*, Vol. 80, 236, 2004.
4. Zibrov, A., I. B. Novikova, D. F. Phillips, R. L. Walsworth, A. S. Zibrov, V. L. Velichansky, A. V. Taichenachev, V. I. Yudin, *Phys. Rev. A*, Vol. 81, 013833, 2010.

Laser-pumped Cs Quantum Magnetometer

A. N. Kozlov[1,3], **V. V. Shutov**[2,3], **V. L. Velichansky**[3,4], **V. Yudin**[2,5,6,7], **A. Taichenachev**[2,5,6], **and E. V. Zhivun**[8]

[1]Pushkov Institute of Terrestrial Magnetism, Ionosphere and Radio Waves Propagation, RAS, Troitsk 142190, Russia
[2]National Research Nuclear University "MEPhI", Moscow 115409, Russia
[3]Advanced Energy Technologies LTD, Moscow 107045, Russia
[4]Lebedev Physical Institute, RAS, Moscow 117924, Russia
[5]Institute of Laser Physics, Siberian Branch of RAS, Novosibirsk 630090, Russia
[6]Novosibirsk State University, Novosibirsk 630090, Russia
[7]Novosibirsk State Technical University, Novosibirsk 630092, Russia
[8]Department of Physics, University of California, Berkeley, CA 94720, USA

Abstract— Optically pumped Cs magnetometers operating in M_x configuration are widely used in geological exploration, archeology, searching for unexploded ammunition. Their advantage is a high sensitivity which allows for detection of small relative variations (of about 10^{-5}) of terrestrial magnetic field. Such a magnetometer (to be carried by an explorer) has typically weight of about 10 kg. Large part of the weight comes from the battery which provides power to a resonance lamp. Power consumption can be decreased at least by an order of value by replacing discharge Cs lamp with a diode laser (DL).

Working Cs cell of investigated magnetometer was a glass cylinder with a length of 20 mm, and anti-relaxation coating of the walls. The DL frequency can be tuned to the four components of the D_1 line of Cs (895 nm) corresponding to transitions $F_g = 3, 4 \rightarrow F_e = 3, 4$ or to the two components of the D_2 line (852,1 nm) in which the hyperfine structure of the excited state is not resolved. The experiments with tunable extended cavity diode lasers (ECDL) have shown that the best choice is the $F_g = 4 \rightarrow F_e$=3 transition of the D_1 line or the $F_g = 4 \rightarrow F_e = 3, 4, 5$ component of the D_2 line. In the last case the laser frequency should be off-tuned to the red wing of the line. For the experiments carried in the lab the ECDL is convenient but for the field operation a more reliable vertical-cavity surface-emitting laser (VCSEL) is needed. Thus most of experiment was made with a VCSEL tuned to the long wavelength component of the D_2 line. We studied the dependencies of the signal to noise ratio, magnetic resonance linewidth, and sensitivity of magnetometer on the laser intensity and frequency. To measure metrological characteristics of the magnetometer we used commercial Cs magnetometer optically pumped with a gas-discharge lamp. We confirmed that by using laser pumping the weight and the power consumption of the magnetometer can be dramatically decreased without decreasing the sensitivity.

Transients of Absorption Spectra of Alkali Atoms in Coated Cells for Microwave Standards and Quantum Magnetometers

D. I. Sevostianov[1, 2], **A. N. Kozlov**[2, 3], **V. L. Velichansky**[1, 2, 4], **and V. P. Yakovlev**[1]

[1]National Research Nuclear University "MEPhI", Moscow 115409, Russia
[2]Advanced Energy Technologies LTD, Moscow 107045, Russia
[3]Pushkov Institute of Terrestrial Magnetism, Ionosphere and Radio Waves Propagation RAS, Troitsk 142190, Russia
[4]Lebedev Physical Institute, RAS, Moscow 117924, Russia

Abstract— The dynamics of nonlinear absorption spectra of monochromatic laser radiation on the $D_{1,2}$ lines of Cs atoms in coated cells is investigated. Antirelaxation coating reduces the probability of atomic depolarization in collisions with walls and leads to the narrowing of microwave and rf resonances used in frequency standards and magnetometers. The internal state of atoms does not change during many wall collisions while their velocities change stochastically. Thus, the optical pumping to nonabsorbing states which provides the nonlinearity of absorption spreads over the Maxwell distribution.

The laser frequency is often changed by fluctuations or deliberately in order to display the line or to produce the error signal needed for frequency stabilization. Atoms, optically pumped at a given time, can return to the resonance with laser field later after wandering in the phase space. As a result the absorption depends on the prehistory. The optical pumping effect integrated over previous time reveals itself most strongly when the time of the tuning through the atomic line is of the same order as the relaxation of atomic distribution in the ground state. It has been confirmed by observation of Doppler-free resonance position. It gives the absolute frequency scale, so the displacement of the line maximum can be easily detected. Directly measured relaxation time agrees with theoretical estimation.

The distortion and the amplitude of the absorption line in the case of D_1 line depends only on time while for the D_2 line it depends also on the sign of frequency change. It is explained by taking into account the sequence of passing of laser frequency through the open and closed optical transitions between the ground and upper sublevels. The zero of the error signal is found to be at different frequencies for coated and uncoated cells which is particularly important for quantum magnetometers and microwave frequency standards utilizing coated cells.

Noise in Radiation of Single Mode Diode Laser in the Range from Audio to Microwave Frequencies. Transformation in Resonance Media

D. I. Sevostianov[1, 2], **V. L. Velichansky**[1, 2, 3], **A. N. Kozlov**[2, 4], **and V. P. Yakovlev**[1]

[1]National Research Nuclear University "MEPhI", Moscow 115409, Russia
[2]Advanced Energy Technologies LTD, Moscow 107045, Russia
[3]Lebedev Physical Institute, RAS, Moscow 117924, Russia
[4]Pushkov Institute of Terrestrial Magnetism, Ionosphere and Radio Waves Propagation RAS, Troitsk 142190, Russia

Abstract— There are many applications of single mode diode lasers (DL) in high resolution spectroscopy, quantum magnetometry and time-frequency metrology. The optimum performance of many devices that combine pumping and/or probing of atomic ensembles absorption depends critically on the intrinsic noise level of DL and its transformation in resonance medium. The report briefly covers the problem of single mode operation of DLs, compares intrinsic noise for different single mode DLs and describes the noise transformation in atomic cells.

Most of the specific spectral and noise properties of DLs stem from the two properties: low value of the Q factor of the cavity and correlation of amplitude and phase noises. The dynamics of diode lasers is very rich, so this report covers (partially) only noise in CW single-mode operation. Typical amplitude, and frequency noise spectra and their correlations from audio to microwave region are described for different single mode diode lasers such as edge emitting stripe lasers, DFB and DBR lasers, extended cavity diode lasers, VCSELs. Particular attention is paid to noise that appears due to relaxation oscillations and noise generated via beating of dominant mode with amplified spontaneous emission of other nonoscillating modes. Although the report mainly deals with the range of single mode operation the danger of coming close to the boundaries of this range which can result in a dramatic change of noise level (such as coherence collapse) is also considered. The report is concluded with some examples of undesired noise transformations in atomic resonant systems.

Analytic Solution in Refractive Index Optimization Problem for Multichannel Fiber Bragg Grating

A. V. Nemykin and D. A. Shapiro
Institute of Automation and Electrometry, Siberian Branch
Russian Academy of Sciences, 1 Koptjug Ave, Novosibirsk 630090, Russia

Abstract— The multichannel optical Bragg filters are of a great importance for lasers and lightwave communication systems. As there is a tendency of precision increase and size minimization of new devices in the worldwide industry, the parallel scheme of fiber Bragg grating (FBG) design is preferable. It means that several FBGs with different central frequency are written in one fiber strip. On a way to the parallel design a restriction appears. The maximum refractive index deviation could be much larger than manufacture process can provide as its theoretical peak value is proportional to N, number of gratings. However, the peak value can be reduced down to its theoretical limit $\sqrt{N}$ by so called phase sampling method when the separate profiles are summed up with matched phases. Some efforts are introduced in [1, 2] but these algorithms take much computation time and do not guarantee good result for an large number of channels.

A new approach of phase sampling allows profile optimization for an arbitrary number of channels. The main idea is the starting point of optimization algorithm when phases are distributed by the second order polynom. The refractive index deviation in multichannel Bragg filter is proportional to an absolute value of function

$$S = \sum_{k=1}^{N} e^{ikx+i\phi_k}, \tag{1}$$

where k is the channel index, N is the number of channels and ϕ_k is a constant phase which should be defined by the formula

$$\phi_k = \frac{\pi}{N} k(k-1). \tag{2}$$

Here the same as above designations are used. After the substitution (2) in (1) the function $|S|/\sqrt{N}$ does not exceed 1.4 regardless N as shown in Fig. 1.

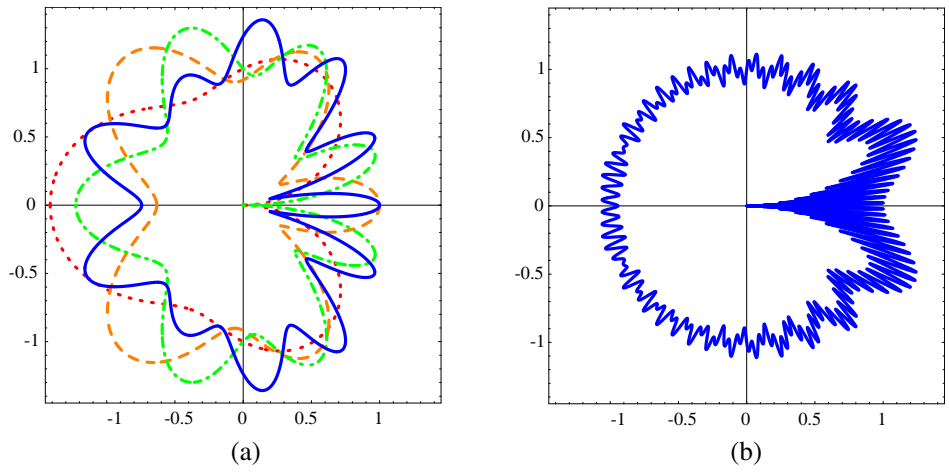

Figure 1: Polar diagram of the function $|S(x)|/\sqrt{N}$ (a) for $N = 4$ channels (dotted line), $N = 7$ (dashed line), $N = 10$ (dot-dashed line), $N = 15$ (solid line) and (b) for $N = 150$ channels.

REFERENCES

1. Kolossovski, K. Y., R. A. Sammut, A. V. Buryak, and D. Y. Stepanov, "Three-step design optimization for multi-channel fiber Bragg gratings," *Opt. Express*, Vol. 11, No. 9, 1029–1038, 2003.
2. Shapiro, D. A. and A. I. Latkin, "Sixth moment optimization of multi-channel Bragg filters," *Opt. Comm.*, Vol. 284, 1565–1568, 2011.

Session 3P2
Optics and Nanoplasmonics, Nano Scale Electromagnetics

Nanoplasmonics Turns on Inherent Linear Birefringence

Srinivasan Iyer[1], **Sergei Popov**[1], **and Ari T. Friberg**[1, 2, 3]

[1]Department of Microelectronics and Applied Physics
Royal Institute of Technology (KTH), Electrum 229, SE-164 40 Kista, Sweden
[2]Department of Applied Physics, Aalto University, P. O. Box 13500, FI-00076 Aalto, Finland
[3]Department of Physics and Mathematics, University of Eastern Finland
P. O. Box 111, FI-80101 Joensuu, Finland

Abstract— One in the class of nanoplasmonic objects, metal split-ring resonator (SRR) can be viewed as a subwavelength LC resonator whose resonance frequency tuned by altering the geometrical parameters and dielectric environment. The transmission of light through a planar square array of single-slit SRRs (SSRR) yields interesting optical properties at normal (pure electrical response) and oblique incidence (electric and magnetic response) [1]. Recently, inter-SSRR coupling effect in a closely packed low-symmetry planar array demonstrated a functionality similar to an effective optical wave plate of low efficiency ($\sim 1.5\%$) [2]. The wave-plate efficiency is defined as the far-field transmittance $T_\perp$ (in percentage) of light polarized in the direction ***orthogonal*** to that of the incident light. In [2], adjacent SSRRs were oriented at 90° to each other, and the small distance between them facilitated an in-plane magneto-inductive coupling among the SSRRs. On the other hand, SSRRs arranged in the bi-layer planar structure reveal the novel optical properties of metamaterial because of inter-SSRR coupling. In this work, we report enhanced wave-plate properties which can be achieved even without these inter-SSRR coupling effects. The SSRR by itself exhibits an *intrinsic linear birefringence* at certain polarizations of the incident light. We also propose that a two-layer array (Fig. 1) of twisted pairs of SSRRs [3], if designed properly, can serve as an effective optical wave plate due to coupling ***along*** the direction of wave propagation. Our entire work is a theoretical investigation based on finite element (FEM) and finite difference time domain (FDTD) methods.

At a normal incidence (wave vector k is in the z direction), only the x and y polarizations are usually considered. Irrespective of the value of unit cell periodicity, linear polarizations of

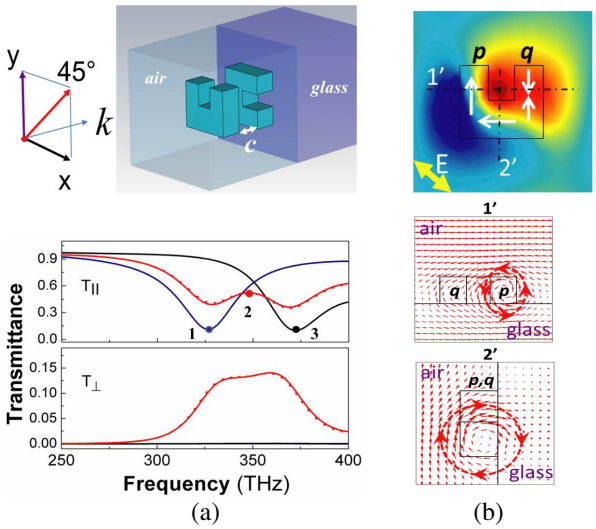

Figure 1: (a) Unit cells of inter-SSRR coupled system with coupling distance c, and corresponding transmission spectra ($T_\parallel$ and $T_\perp$). On the transmission spectra, the color code represents polarizations of incident light along x (black), y (blue), 45 (red solid), and $-45°$ (red dots), respectively. Points 1, 2, and 3 are resonance positions for the y, $\pm 45°$ and x polarizations. One array cell size is 240 nm, the space between two SSRRs is 60 nm. (b) H_z plots (in color scale) for polarizations of incident light along 45 at the LC resonance frequency (338 THz) of the SSRR. The white arrows represent the direction of current flow estimated from the projection of vector magnetic fields H_x, H_y, and H_z (circular arrow plots with emphasized direction) on the cross-sectional planes (1' and 2') of the SSRR arms.

incident light along the x and y axes are strictly preserved upon normal transmission, i.e., no orthogonal polarization emerges out ($T_{\perp} \approx 0$). However, it is found that the same SSRR array exhibits birefringence ($T_{\perp} \neq 0$) at other orientations of linear polarizations, the maximum being at the 45° polarization plane. At 45° polarization, the transmission spectrum for the parallel polarization component ($T_{\parallel}$) looks very similar to that of the x polarization in terms of resonance positions, but a fair amount of polarization conversion is observed, especially at the LC-resonance wavelength of the SSRR (Fig. 1(a)). One can get light of an orthogonal polarization (i.e., at $-45°$ polarization) emerging at normal transmission with an efficiency of $\sim 13\%$ that is almost one order of magnitude higher than the value reported [2]. The power in the orthogonal polarization increases proportionally with decreasing the array periodicity. The linear birefringence in this particular case is an intrinsic property of the SSRR structure and it can be explained by near-field and current distributions (Fig. 1(b)). These findings point out to a complex near-field interaction between the SSRRs in the twisted pair, which is a function of the coupling distance, the geometrical parameters of the SSRRs, and the unit cell periodicity. Also, such system provides comparable birefringence efficiency as the intrinsic effect but double the device bandwidth. This study advances the idea of having SSRR-based wave plates to operate in any specific wavelength regime of choice by a simple scaling of the SSRR size.

REFERENCES

1. Enkrich, C., M. Wegener, S. Linden, S. Burger, L. Zschiedrich, F. Schmidt, J. Zhou, T. Koschny, and C. M. Soukoulis, "Magnetic metamaterials at telecommunication and visible frequencies," *Phys. Rev. Lett.*, Vol. 95, 203901, 2005.
2. Decker, M., S. Linden, and M. Wegener, "Coupling effects in low-symmetry planar split-ring resonator arrays," *Opt. Lett.*, Vol. 34, 1579–1581, 2009.
3. Liu, N., H. Liu, S. Zhu, and H. Giessen, "Stereometamaterials," *Nat. Photonics*, Vol. 3, 157–162, 2009.

Single Atom Trapping of Light

Raphael Tsu[1] and **Michael A. Fiddy**[2]

[1]ECE Department, UNC Charlotte, USA
[2]Center for Optoelectronics, UNC Charlotte, USA

Abstract— Recently it came to our attention that some questions remain when discussing the size of photons when dealing with the absorption and emission of photons by atomic transitions. Generally, one considers sizes such as the Bohr radius, the classical radius of an electron, and the Compton wavelength. We must recognize that size rarely is of any significance in the physics of interactions. Trapping of light in the form of evanescent waves is routinely used to augment interactions via resonances. Obviously it is important to recognize the distinction between waves and particles. Strictly speaking particles all have potentials, including Yukawa potentials, having a r^{-1} singularity, but waves do not. In treating an interface between two piece-wise analytic regions, we must resort to matching wave functions and their derivatives at the interface, creating reflections and leading to confinement, which in turn providing trapping with high Q, as is the case for small antennas in negative permittvity structures [1]. Whenever particles such as atoms appear in the space of a medium supporting waves, we must recognize that: (1) there are r^{-1} singularities to be dealt with involving the interaction of Schrodinger waves for the electrons and protons with light and E & M fields in general; (2) the interaction of two electrons separated by Δd and emitting a photon can be estimated using the uncertainty relationship, $\Delta d\Delta k = 1$. Consequently the ratio of the interaction energy to the photon energy $(e^2/\Delta d)/\hbar\Delta\omega = e^2/\hbar(\Delta\omega/\Delta k) = e^2/\hbar c = \alpha$, the fine structure constant, describing the Coulomb interaction of a particle with photon. Initially there is no way to detect a single photon, until reaching a build-up time, QT, with T being the period of the light and Q, the quality factor. Since we know how to get these figures very accurately with the H-atom, we shall deal with a H-atom interacting with light. Taking the 1S-2P transition of the H-atom, $\hbar\omega = 10.2\,\text{eV}$, with $\lambda = 1.215 \times 10^{-7}\,\text{m}$, the relaxation time (due to spontaneous emission) $\tau = 1.6 \times 10^{-9}\,\text{s}$ and the period $T = 4.05 \times 10^{-16}\,\text{s}$, $Q = \tau/T = 4 \times 10^6$. Only a superconducting cavity can reach such a high Q value at low frequency. Here we are dealing with the light trapped for more than 1 M cycles of the optical field which results in a very high degree of interaction between a single H-atom and light. The Rabi frequency corresponding to spontaneous emission has a value for the electric field of the photon $E_0 \sim 105\,\text{V/cm}$. That should remind us how large is the level of zero-point fluctuation due to all the atoms-photons interactions at thermal equilibrium in space-time. During trapping, one has a trapped oscillating electrostatic field similar to evanescent modes, trapping with Chu's high $Q \sim (kd)^{-3}$ factor in negative permittivity antennas. Furthermore, setting the effective $\epsilon = [1 - \omega_{\text{es}}^2/\omega^2]$, where $\omega_{\text{es}} = (4\pi ne^2/m)^{1/2}$ is the equivalent electrostatic oscillation similar to the plasma frequency, which separates oscillating from propagating modes. Therefore one may replace the density n by the dipole per unit volume occupied by the oscillating electron in the H-atom. Using a volume consistent with the dipole density in a sphere of $4\pi r_{\text{SP}}^3/3 = n$, we arrive at $r_{\text{SP}} = 0.56\text{Å}$, which is smaller than the 2P orbital, but slightly larger than the Bohr radius. The mechanism of long trapping is quite similar to small antenna with a negative permittivity resonance, and is similar to trapping by a black hole except our Coulomb singularity is a pole rather than an extended singularity like a black hole.

REFERENCES

1. Stuart, H. R. and A. Pidwebetsky, *IEEE Trans. Antenna & Propagation*, Vol. 54, 1644, 2006.

Shaping the Fluorescent Emission by Localised and Propagating Plasmons in Hybrid Plasmonic-Photonic Crystals

Boyang Ding, **Nikita Arnold**, **Klaus Piglmayer**, **Calin Hrelescu**, **and Thomas A. Klar**
Institute of Applied Physics, Johannes Kepler University Linz, Altenberger Straße 69, Linz 4040, Austria

Abstract— Plasmonic structures in the proximity of fluorescent light emitters were developed in order to study the nature of light-matter coupling. In particular, we deposited a thin noble metal film on a close-packed monolayer self-assembled from dye-loaded polystyrene nanospheres. Such samples contain hexagonal arrays of metal caps with triangular holes in between. They possess novel optical properties dominated by the synergy of localised surface plasmons, surface plasmon polaritons and the accompanying absorption within the metal. It is observed that the fluorescence emitted from dye molecules embedded in such a hybrid structure has been reshaped spectrally as well as directionally. Comparison with the angle-resolved transmission and reflection measurement reveals that the modified fluorescence is the net result of light-matter coupling between the emission of dyes and several kinds of plasmonic resonances. The numerical calculations indicate that both the localised void plasmons in the metal caps and the propagating plasmons in the periodic array of caps contribute to the interaction with fluorescent emission. The strength of the coupling can be tuned by depositing a dielectric spacer between the silver caps and the dyes contained in the PS nanospheres. As it is prepared by self-assembly method, this hybrid structure can be fabricated over large area and scaled easily, permitting further investigation of the light-matter coupling in sub-wavelength plasmonic structures.

Nanostructuring under Ultrashort Pulse Laser Irradiation

Yasuhiko Shimotsuma, **Miki Nakabayashi**, **Taiga Asai**,
Yuya Yamada, **Masaaki Sakakura**, **and Kiyotaka Miura**
Department of Material Chemistry, Graduate School of Engineering
Kyoto University, Kyoto 615-8510, Japan

Abstract— Self-assembled periodic nanostructure and nanoparticle of intermetallic $Nd_2Fe_{14}B$ with a diameter below the diffraction limit of laser light were successfully prepared under femtosecond laser irradiation. Self-assembled nanostructure in isotropic material, i.e., fused silica, which exhibits form-birefringence, has initially evolved from residual birefringence originated from internal stress distribution. Evolution of such optical anisotropy can be controlled as a function of interpulse time due to thermal accumulation. Another interesting phenomenon is that the self-assembled nanostructure is non-reciprocally induced according to the orientation of writing direction. This intriguing result is also interpreted in terms of the light pressure on electron plasma produced by a tilted front of the ultrashort laser pulse resulting in an anisotropic heat current. Furthermore, intermetallic $Nd_2Fe_{14}B$ nanoparticles with an average diameter of 30 nm, which are smaller than a theoretical single magnetic domain size of 220 nm, were successfully prepared by the femtosecond laser fragmentation in liquid. The self-passivating amorphous carbon layer resulting from the decomposition of the surrounding solvent prevents the $Nd_2Fe_{14}B$ nanoparticle from aggregation and oxidation. The coercivity of $Nd_2Fe_{14}B$ nanoparticle increases with increase of the laser irradiation time, despite the reduction of crystallinity.

Fabrication of Metal Waveguides with High Aspect Ratios Using Highly Ordered Anodic Porous Alumina

Hideki Masuda[1, 2], **Kazuyuki Nishio**[1, 2], **and Toshiaki Kondo**[2]

[1]Department of Applied Chemistry, Tokyo Metropolitan University
1-1 Minamiosawa, Hachioji, Tokyo 192-0397, Japan
[2]Kanagawa Academy of Science and Technology
5-4-30 Nishihashimoto Midori-ku, Sagamihara, Kanagawa 252-0131, Japan

Abstract— Fabrication of ordered nanostructures of metals has attracted increasing interest due to applicability to the several kinds of functional optical devices. For example, metal hole arrays with subwavelength dimensions act as a waveguide for incident electromagnetic waves corresponding to their hole size. Although considerable numbers of studies have been reported on the optical properties of metal hole arrays [1], the aspect ratios of the samples were low due to the limitation in the fabrication technique. In the present report, we describe the fabrication of metal waveguides (metal hole arrays and metal coaxial arrays) with high aspect ratios using highly ordered anodic porous alumina as a starting structure. Anodic porous alumina, which is formed by anodization of Al in acidic electrolyte, is a typical self-ordered material [2, 3] and is promising candidate for the starting structure of waveguides. Advantage of the use of anodic porous alumina as a starting template is easiness in the preparation of nanostructures with high aspect features besides its highly ordered hole arrangement. Metal (Au) hole arrays with ideally ordered hole configuration were prepared with a two-step replication process using anodic porous alumina as a starting template [4]. In this process, the preparation of negative-type and the subsequent formation of positive-type yield the metal hole arrays with geometrical structure identical to that of the anodic porous alumina. The metal hole arrays shows the cutoff wavelength for the incident light of wavelengths corresponding to their hole sizes. Coaxial array structures were also prepared based on the similar process for the preparation of metal hole arrays. This structure was composed of a central metal (Au) wire and a surrounding metal (Au) wall with dielectric medium between metals. The obtained coaxial array structures could pass the incident light of wavelength longer than the cutoff wavelength in the hole array structures. The optical properties of the hole and coaxial array structures were in good accordance with the results by FDTD (finite-difference time-domain) calculations.

REFERENCES

1. Grupp, D. E., H. J. Lezec, T. Thio, and T. W. Ebbesen, *Adv. Mater.*, Vol. 11, 860, 1999.
2. Masuda, H. and K. Fukuda, *Science*, Vol. 268, 1466, 1995.
3. Masuda, H. and M. Satoh, *Jpn. J. Appl. Phys.*, Vol. 35, L126, 1996.
4. Nishio, K., M. Nakao, A. Yokoo, and H. Masuda, *Jpn. J. Appl. Phys.*, Vol. 42, L83, 2003.

Deeper to Nanoscale Via Fs Laser-matter Interaction and SPP Excitation

V. S. Makin and R. S. Makin
Research Institute for Complex Testing of Opto-electron Devices and Systems, Russia

Abstract— The distinct peculiarity of femtosecond laser-matter interaction near the threshold fluence regimes is the formation of structures of nanoscale dimensions. The universal polariton model in conjunction with theoretical model of multiple periods formation was used as the base for consideration. In addition, the role of channel surface plasmon polariton in the interference processes on the vacuum-matter boundary and at inner arising interfaces is elucidated.

According to polariton model the regular structuring of condensed matter is the result of incident radiation and excited surface plasmon polariton (SPP) interference and also mutual SPP interference at the sample-vacuum boundary or inside the matter with periods λ/η, $\lambda/2\eta$; here η is the real part of refractive index for SPP of surface active media — dielectric boundary. The nonlinear model of multiple periods nanostructures formation is based on one-dimensional unimodal logistic map and describes the direct and reversed Feigenbaum universality in periods formation controlled by bifurcation parameter and depending on particular material properties. The Feigenbaum universality is the part of A. N. Sharkovski order and also describes the periods behavior. The role of the period three is outlined as possible route to ordered chaos under surface structuring [1]. A set of the experimental examples of nanostructures formation under the fs linear polarized laser radiation interaction with condensed mater illustrate the theory [2].

Deeper penetration into the small scale dimensions was realized via production of elongated nano sized material peculiarities, excitation of channel surface plasmon polaritons and their participation in interference processes. In this way the theoretical expectations were illustrated by the examples of nanostructures formation with periods down to (40–60) nm on the tungsten surface [3].

REFERENCES

1. Makin, V. S., R. S. Makin, A. Y. Vorobyev, and C. Guo, "Feigenbaum universality and Sharkovski order in laser-induced periodic structures at interface and inside condensed matter," *Nonlinearity in Modern Nature*, 303–322, LKI Publisher, Moscow, 2009.
2. Makin, V. S. and R. S. Makin, "Nonlinear interaction of linear polarized laser radiation with condensed media and overcoming the diffraction limit," *Optics and Spectroscopy*, Vol. 112, No. 2, 162–167, 2012.
3. Makin, V. S., Y. I. Pestov, R. S. Makin, and A. Y. Vorobyev, "Surface plasmon polariton modes and semiconductors nanostructuring by femtosecond laser pulses," *Optical Journal*, Vol. 76, No. 9, 38–44, 2009.

Micro- and Nanostructures Via TEA CO_2 Laser Radiation Interaction with Semiconductors

V. S. Makin, Yu. I. Pestov, and V. E. Privalov
Research Institute for Complex Testing of Opto-electron Devices and Systems, Russia

Abstract— The peculiarities of laser-matter interaction are considered with the particular example of semiconductor in the range of transparency. The group of semiconductors having melting phase transition of semiconductor-metal type and positive temperature derivative of refractive index was chosen. The regime of semiconductor surface partial melting was used. Obtained experimental results were interpreted based on universal polariton model of laser-induced condensed matter damage [1]. In experiments linear polarized TEA CO_2 laser radiation was used. The periodic microstructures having periods $\sim \frac{\lambda}{n}$, $\frac{\lambda}{2n}$ and grating vector orientation $\vec{g} \perp \vec{E}$ were obtained inside the irradiated surface zone. For the progressive laser pulses N the formation of microstructures with typical spatial scale $s \sim (2-4)\frac{\lambda}{n}$ and $\vec{g} \,||\, \vec{E}$ orientation were produced. Here n is the refractive index of semiconductor for laser wavelength (λ). The cause of the $\vec{g} \perp \vec{E}$ structures formation is the interference with excited TE type waveguide (WG) modes. Incident laser radiation heated semiconductor's surface layer and cause the near surface asymmetric spatially limited waveguide due to $\frac{dn}{dT} > 0$ and excites waveguide modes. An interference with progressive number of laser pulses of the pair of TE WG modes with slightly differed wave vectors directions gives the structures with spatial scale $s \sim (2-4)\frac{\lambda}{n}$ and $\vec{g} \,||\, \vec{E}$ orientation. The area of the melted zone is increased from pulse to pulse. And the conditions arise for surface plasmon polariton (SPP) excitation by this grating and their mutual interference of opposite directions. So the orthogonal crossing gratings are formed with periods $d_1 \approx \frac{\lambda}{n}$ and $d_2 = \frac{\lambda}{2\eta}$, $\eta \geq 1$. This bigrating is a template for subsequent tips of conical type formation at the crossings and the density of the tips $D \sim \frac{2n\eta}{\lambda^2}$ and for silicon and $\lambda = 10\,\mu\text{m}$, $D \sim 10^7\,\text{cm}^{-2}$. For $\lambda = 1.06\,\mu\text{m}$ we have $D \sim 10^9\,\text{cm}^{-2}$.

For germanium the modulation of the hills of main period of waveguide structures was discovered and has period equaled to $0.34\,\mu\text{m}$ for $\lambda = 10\,\mu\text{m}$ and grating orientation $\vec{g} \perp \vec{E}$. Their formation is due to channel SPP excitation and involved in the interference process.

ACKNOWLEDGMENT

The work was done under partial financial support of FAP "Scientific and scientific-pedagogic stuff of innovative Russia" (2009–2013), contract No. 16.740.11.063.

REFERENCES

1. Makin, V. S., Y. I. Pestov, and V. E. Privalov, "Thermal waveguide and fine-scale periodic relief on the semiconductor's surface induced by TEA CO_2 laser radiation," *Optical Memory and Neural Network Modelling*, No. 1, 52–61, 2012.

Gold Nanoparticles Chain Waveguide with Enhanced Transmission Method and Spectral Coding

C. Cinar and T. Sengor
Electrical & Electronics Engineering, Yıldız Technical University, Turkey

Abstract— In this study, a known waveguide consisting of fifteen gold cubic nanoparticles is examined using 3D FDTD method with Drude model and auxiliary differential method. The magnitude of transmission rate to the end point of the waveguide is managed to be increased by using total fourteen particles without changing the length of the chain by just removing the 4th particle, where all the other parameters are unchanged. By not deploying 4th particle there became two separate chain which enlightened by single gauss laser beam at the same time and this effect makes surface plasmon polarizations boosted twice like a cascade amplifier. In addition to one removal, two and three removal of particles at a time is studied and their spectral transmission rate characteristics are given as a communication coding or data storage information placement location.

Introduction: In recent years, plasmonics has attracted a great deal of attention due to its important potential toward applications in sensing, medical imaging, and information processing. This branch of photonics develops new concepts to confine light beyond the diffraction limit and enhance the electromagnetic field at the nanoscale. The synthesis and fabrication of disperse noble metal nanoparticles with a variety of shapes, from cubes to spheres and branched multipods. Energy transport in ordered arrays of closely spaced noble metal nanoparticles plasmon waveguides relies on near-field coupling between surface plasmon-polariton modes of neighboring particles. This type of guiding due to near-field coupling was demonstrated experimentally in macroscopic structures operating in the microwave regime. At the submicron scale, a theoretical analysis of plasmon waveguides was done using a point-dipole model in. The chain consists of fifteen gold dots with a square base ($l \times l = 100 \times 100\,\mathrm{nm}^2$) and 40 nm high is modeled in and spectral transmission rates are given for the 600 nm–800 nm wavelength range for three different spacing distance between nanodots. Moreover the behavior of the transmittance spectrum of a chain against its length has been demonstrated in a previously published work [1], where the length of the chain was changed by controlling the number of metallic dots and letting the others parameters unchanged. So that it is shown that the position and the shape of the narrow band in the transmission rate spectrum do not depend on the length of the chain and only the mean value of the transmittance is modified with the varying of the chain's length.

In this work, the chain of metallic nanoparticles studied in is obtained and developed by using 3D FDTD technique with drude model and auxiliary differential method. For the dispersive properties of the gold, Drude parameters are chosen like $\varepsilon_b = 10.48$, $w_p = 1.3755\mathrm{e}16$ ve $\gamma = 1.177\mathrm{e}14$. Waveguide is enlightened with Gaussian laser beam.

REFERENCES

1. Girard, C. and R. Quidant, *Opt. Express*, Vol. 12, 6141–6146, 2004.

Inflective Nano-antenna

T. Sengor
Yildiz Technical University, Istanbul 34220, Turkey

Abstract— In this paper, a new meta-element, overcoming the difficulties of including capacitive elements in integrated electronic circuits and devices is developed. The element is based on the wave phenomena around the inflection points on discontinuities of the field. Inflective coordinates are used to overcome the difficulties coming from the inflection points. The simplest case of such discontinuities is created by joining one end point of a convex semi-circular thin wire with one end point of a convex semi-circular thin wire where all the end points of both wires trace the same line. We call inflector the new element. The inflector is a thin and short wire with an inflection point and has a time varying potential distribution. The deviations of potential of inflective element depend to spatial coordinates on inflective wire. Developing some useful metamaterial structures is studied.

The inflection points still rise some critical problems in electromagnetic phenomena. There are some results related to these problems, to name some: diffraction from S-shaped discontinuities [1], diffraction from the edged concave-convex boundaries [2], and smooth targets with inflection points [3, 4]. These works use some approximations and focus on the uniformization of physical optics. The first paper requires a radius of curvature that is relatively large at every point on the surface but gives more compact solution than the solution given in the second paper. The second paper describes an asymptotic, high frequency solution for the scattering from a concave-convex shaped boundary with an edge. This second paper requires that the associated reflected ray caustic with transition regions of two points of inflection do not come close together. The authors' PO based uniform analysis fails near grazing angles of incidence on the reflecting boundaries with points of inflection. The third and fourth papers have used PO approximations. Therefore, it is clear that the influence of inflection points on electromagnetic field still has some open questions. A recent paper aimed to open the analytical insights behind the inflection points when the solutions of the basic field equations are asked [5]. This last paper describes inflective circular cylindrical coordinates and derives the essential analytical expressions for the solution of problems with inflection points. The evaluation is due to the new defined inflective series obtained by applying the extracted separation method, which is defined here. The extracted separation method comes with some modifications on extended separation method in [5, 6]. In view of the above comments, this paper aims to extend the analytical perspectives of [5–8] for the wave phenomena around inflection points in nano-scale and studying to design useful metamaterial structures.

The separation of wave equation in inflective circular cylindrical coordinates is given. The wave phenomenon is studied near inflection points. The analytical essentials are derived for the solution of Helmholtz's equation when inflective boundaries are included. The evaluation is obtained by the extracted separation method. The results are given by inflective wave series. Nano-scale manipulations for metamaterial structures with designing purposes are studied.

REFERENCES

1. Kempel, L. C., J. L. Volakis, T. B. A. Senior, S. S. Locus, and K. M. Mitzner, "Scattering by S-shaped surfaces," *IEEE Transactions on Antennas and Propagation*, Vol. 41, No. 6, 701–708, 1993.
2. Pathak, P. H. and M. C. Liang, "On a uniform asymptotic solution valid across smooth caustics of rays reflected by smoothly indented boundaries," *IEEE Transactions on Antennas and Propagation*, Vol. 38, No. 8, 1192–1203, 1990.
3. Ikuno, H. and L. B. Felsen, "Complex ray interpretation of reflection from concave-convex surfaces," *IEEE Transactions on Antennas and Propagation*, Vol. 36, No. 9, 1260–1271, 1988.
4. Ikuno, H. and L. B. Felsen, "Complex rays in transient scattering from smooth targets with inflection points," *IEEE Transactions on Antennas and Propagation*, Vol. 36, No. 9, 1272–1280, 1988.
5. Sengor, T., "Contribution of inflection points to field," *Electronics Letters*, Vol. 34, No. 16, 1571–1573, Aug. 6, 1988.
6. Sengor, T., "Static field near inflection points," Helsinki University Technology Electromagnetics Laboratory Report, 350, Jan. 2001.

7. Sengor, T., "Contribution of inflection points to waves," *Electronics Letters*, Vol. 35, No. 19, 1593–1594, Sep. 16, 1999.
8. Sengor, T., "Waves near inflection points," Helsinki University Technology Electromagnetics Laboratory Report, 351, Jan. 2001.

Session 3P3
Electromagnetic Probing of Atmosphere and Ionosphere

Using GNSS-signals and Radio-interpherometry Technique for Study Wave Disturbances in the Ionosphere

V. I. Zakharov, **V. E. Kunitsyn**, **and M. A. Titova**
Faculty of Physics, Lomonosov Moscow State University
GSP-1, 1-2 Leninskiye Gory, Moscow 119991, Russia

Abstract— It is well known, that the modulations of plasma density can be registered by precise radiophysical methods. So, the Earth ionosphere can serve as the indicator of the various processes in system of geospheres.

In our work various aspects of the wave structures allocation by GPS-interhperometry are considered and discussed.

We present and discuss the results of regional GPS-observations of the ionospheric response on the global synoptic and seismic processes — the largest tropical cyclones 2004–2009 and earthquakes 2009–2011. It was pointed out, that wave structures in some cases are geographically connected with places of orographical indignations. Generation of acousto-gravity waves can be connected with the coastal line or mountains. Excitation of such wave structures in the atmosphere most effectively occurs at the high speed of development or recession of a typhoon, and the spectrum of the wave-structures sharply varies.

The obtained data allows to point out: seismically active areas generate acoustic waves not only during, but before and after an active phase of earthquake. A source of wave structures is not only the future epicentre, but first of all the whole area of the earthquake preparation, including borders of tectonic plates and the active breaks located in region. In some cases interpretation of data obtained is too complicated — it is not possible to separate natural wave activity from connected with lithosphere influence.

As the results, the wave transfer of energy from various sources must be take into account for modernization of existing representations about interactions in system of geospheres.

Spatial Processing of Phase Measurements in Diffraction Tomography

S. I. Knizhin[1], **Yu. A. Kravtsov**[2], **and M. V. Tinin**[1]

[1]Irkutsk State University, Gagarin Blvd. 20, Irkutsk 664003, Russia
[2]Institute of Physics, Maritime University of Szczecin, Waly Chrobrego 1/2, Szczecin 70-500, Poland

Abstract— Transparent inhomogeneous media are often studied by tomography methods based on measurements of phase of a wave passing from a transmitter to a receiver. Physical characteristics of the inhomogeneous media may be determined by ray and diffraction tomography in several stages. At the first stage, a receiver registers a field or phase of a wave scattered by inhomogeneity. Then, we choose a computer tomography method optimum for the measurements. At the final stage, a required physical parameter of the inhomogeneous medium is determined. However, it is not always possible to reconstruct inhomogeneity parameters correctly in the diagnostics of inhomogeneous plasma by standard ray and diffraction tomography methods. More exact results of the plasma diagnostics may be obtained through additional processing of phase measurements. Tinin and Kravtsov have proposed using processing based on the method of double weighted Fourier transform (DWFT). This method permits diagnostics of multi-scale inhomogeneous plasma during strong and weak phase fluctuations. Under real conditions, the spatial processing in accordance with DWFT is impossible because of limited sizes of receiving and transmitting antennas. To take the limitations in the DWFT processing into account requires using additional factors standing for amplitude profiles of the antennas. In this work, we have examined the influence of amplitude profiles of antennas on results of the spatial processing of the phase measurements.

Turbulent Parameters Estimation through the Phase Decomposition into the Zernike Polynomials

V. A. Kulikov[1], **M. S. Andreeva**[2], **and V. I. Shmalhausen**[2]

[1]A. M. Obukhov Institute of Atmospheric Physics, Russian Academy of Sciences, Russia
[2]Department of Physics, M. V. Lomonosov Moscow State University, Russia

Abstract— Turbulence is a practically significant physical effect causing the impediment of the signal transfer through the atmosphere or water as well as problems in aeronautics. A great number of methods exist to estimate the turbulent parameters. The problem is that these methods lead to different results, and the search of the method enabling more exact turbulent estimations is still actual.

The wavefront phase of a laser beam is analyzed after it has propagated through the random media. For this purpose two apertures are picked out in the field of phase wavefront on input aperture of Shack-Hartmann sensor. In each of these apertures the field is decomposed into the Zernike polynomials. Having the sufficient statistics of the phase fluctuations the correlation functions of the corresponding Zernike coefficients can be calculated. The result of the analysis enables us to estimate the turbulent parameters.

It becomes possible to sort out the correlation functions depending on the inner scale only, and those depending on both the inner and the outer turbulent scale. First of all, the inner scale should be estimated according to the correlation functions of the high frequency spatial spectrum. Secondly, the outer turbulent scale should be estimated with the use of the correlation functions depending on both scales, considering the inner one known. As a result, the indeterminacy in the estimation of scale usually appearing in the solvation of the two-parametric problem is eliminated.

The proposed methodic was tested during the experiment of the estimation of turbulent parameters in a water cell. The turbulence was created in the water cell by the means of the temperature gradient between the heater and the cooler. The turbulent parameters from 1 to 2 cm for inner scale and from 3 to 30 cm for outer scale were obtained. In addition to the described methodic, the isotropy of the created turbulence was controlled by comparing the correlation functions of some Zernike coefficients on two separated apertures. In the isotropic turbulence the results for the correlation functions of the first two modes along the perpendicular directions must coincide with each other (crisscross, opposite). For example, the correlation functions of the first two Zernike coefficients are equal to each other in the theory of isotropic turbulence.

Some of the correlation functions of high order coefficients should also coincide. If they do not, it not only means the anisotropy but also indicates its characteristics. This can be defined by determining the modes which do not coincide. In the carried out experiment the anisotropy is characteristic mostly for the low-frequency spectrum part, for the lowest Zernike modes correlations responding to the large-scale turbulence. Meanwhile, the small-scale fluctuations remain isotropic.

Possibility of O^+/H^+ Transition Level Determination from Irkutsk Incoherent Scatter Data and GPS Total Electron Content

B. G. Shpynev and D. S. Khabituev
Institute of Solar-Terrestrial Physics, Irkutsk, Russia

Abstract— Experimental data of Faraday rotation at 158 MHz obtained on Irkutsk Incoherent Scatter Radar (ISR) and GPS Total Electron Content (TEC) were used for estimation of the O^+/H^+ transition level and electron density distribution in the upper topside ionosphere and in the plasmasphere. Faraday rotation measurements on Irkutsk ISR give information about integrated electron density from the ground to fixed altitude of topside ionosphere. Joint analyzes of these data with GPS TEC data allows us to make estimation of topside ionosphere/plasmasphere parameters. As model we use modified Chapman function where O^+/H^+ transition level is used as parameters. On the base of this model we considered the typical dynamics of O^+/H^+ transition level in different seasons and different geophysical conditions. This level is very sensitive to parameters of neutral wind and to conditions in geomagnetic field tube. The plasmasphere can contribute as much as 50% to GPS TEC, and the input from plasmasphere can produce the major influence on GPS TEC variations.

ACKNOWLEDGMENT

The work was supported by Russian Found of Basic Research (Grant RFBR 11-05-00622) and RF Ministry of Education and Science, Project 16.518.11.7097.

Radiosounding of Ionospheric Disturbances Generated by Exhaust Streams of the Transport Spacecraft "Progress" Engines

V. V. Khakhinov, **B. G. Shpynev**, **V. P. Lebedev**, **D. S. Kushnarev**, **S. S. Alsatkin**, **and D. S. Khabituev**
Institute of Solar-Terrestrial Physics, SB, RAS
Lermontov st. 126a, P. O. Box 291, Irkutsk 664033, Russia

Abstract— A sequence of active space experiments was carried out in 2007–2011. The goal of the experiment is to study spatial-temporal characteristics of the plasma disturbances caused by the engine burns of orbital maneuvering subsystem engines of automatic transport cargo spacecraft Progress. The Progress orbit altitude was about 340 km. Amount of the engine exhaust products was relatively small — not more 10 kg.

The main research tool is the Irkutsk incoherent scattering radar of Institute of Solar-Terrestrial Physics. Each burn took place exactly over the radar. Exhaust directions and amount of injected products changed for each flight. The data analysis showed that relatively small exhaust products caused considerable changes in the electron concentration profile and Progress radar cross-section value.

Results of the experimental data processing allow us to conclude that artificial ionospheric disturbances, associated with the Progress engine burn, produce significant changes in ionospheric and radar signatures even for a relatively small amount of exhaust product. Changes in ionospheric and radar characteristics strongly depend on geometry of the experiment. The most significant changes are observed when the engine burn is directed towards the radar. Electron density depression ("hole") reaches up to $\sim$ 20%–30%. The hole life-time is about 10–15 minutes. Angular characteristics and RCS are the most sensitive radar parameters.

Spatial Structure of Wave-like Disturbances in Midlatitude Ionosphere Induced by HF-heating

V. E. Kunitsyn[1], **E. S. Andreeva**[1], **M. O. Nazarenko**[1], **A. M. Padokhin**[1], **M. A. Annenkov**[1], **V. L. Frolov**[2], **G. P. Komrakov**[2], **and I. A. Bolotin**[2]

[1]M. V. Lomonosov Moscow State University, Leninskie Gory, Moscow 119991, Russia
[2]Radiophysical Research Institute, Bolshaja Pecherskaja 25/12a, N. Novgorod 603950, Russia

Abstract— Numerous theoretical studies of the possibility of generation of artificial wave-like disturbances in ionosphere modified by powerful HF-heating, for example [Grigor'ev, 1975; Grigor'ev and Trakhtengerts, 1999; Karashtin et al., 1977], raised the problem of their experimental observations. Recently [Burmaka et al., 2009 and Chernogor et al., 2011] reported on the detection of AGW-like disturbances caused by the Sura heating facility (Radiophysical Research Institute, N. Novgorod, Russia) at the distances of about 1000 km by Kharkiv incoherent scatter radar and by Doppler HF vertical sounding.

In the present work, for the first time, the spatial structure of the wave disturbances generated in the ionosphere by high-power HF radio waves radiated by the Sura heating facility with a square wave modulation of the effective radiated power at a frequency lower than or of the order of the Brunt-Vaisala frequency of the neutral atmosphere is imaged using the method of low-orbital radio tomography and GPS/GLONASS data. The obsereved pattern of the disturbances contains a characteristic narrow trough in electron density with a width of ~ 60 km and the depth of the depletion about 15–20%, corresponding to the radiation diagram of the Sura heater and wave-like disturbances propagating off the heated area to the distances up to thousand kilometers, which might me artificial AGWs [Kunitsyn et al., 2012].

We also discuss the influence of the ionospheric disturbances induced by various schemes of Sura heater operation on the signals of low-orbital and high-orbital satellite navigation systems [Frolov et al., 2010; Kunitsyn et al., 2011].

ACKNOWLEDGMENT

The authors are grateful to all the staff of the Sura heating facility for their help in conducting the experiments. The work was supported by the Russian Foundation for Basic Research (grants Nos. 10-05-01126, 11-02-00374, 11-05-01157, 12-05-01000), the Ministry for Education and Science of the Russian Federation (project No. 14.740.11.0203) and grant of the President of Russian Federation (project No. MK-2544.2012.5).

Model Considerations of E-region Critical Frequency Data (foE) over Cyprus

Haris Haralambous
Frederick University, 7 Y. Frederickou St., Palouriotisa, Nicosia 1036, Cyprus

Abstract— The critical frequency (foE) is the most important ionospheric characteristic of the E region (90–150 km) which can provide stable modes of HF propagation but also constitutes an important part of the ionospheric electron density profile. Therefore its accurate specification in terms of adequate prediction of foE is considered as a significant task. An ionospheric station was established in Nicosia (Cyprus) three years ago in order to initiate ionospheric research on the island. The deployment of a DPS-4D (digisonde) developed at the University of Massachusetts Lowell's Center for Atmospheric Research (UMLCAR), is considered very beneficial to the ionospheric scientific community, taking into account the lack of adequate scientific infrastructure, especially at low latitudes of the European sector, for continuous monitoring. Its operation will contribute to international networks for ionospheric nowcasting and forecasting and to the enhancement and validation of ionospheric models in the eastern Mediterranean region. The station is capable of performing fast ionograms and improved layer height variation measurements by taking advantage of the Precision Group Height Measurement technique. In this study manually scaled digital ionosonde ionograms obtained in Cyprus (coordinates: 35°N, 33°E geographic) have been analysed to study the diurnal and seasonal behaviour of foE during a low to medium solar activity period (January 2009 to December 2011). Processing of ionograms and scaling of foE parameters was carried out using SAO explorer developed by UMLCAR. Subsequently comparisons of foE observations with values of the International Reference Ionosphere (IRI-2007) model are carried out and diurnal and seasonal patterns in the deviation of observed and modeled foE values are also identified. Moreover an effort to adjust existing empirical foE model formulations to match Cyprus data is presented.

Investigation of Ionospheric Slab Thickness and Plasmaspheric TEC Using Satellite Measurements

Photos Vryonides, **Christos Tomouzos**, **Giannis Pelopida**, **and Haris Haralambous**
Frederick University, 7 Y. Frederickou St., Palouriotisa, Nicosia 1036, Cyprus

Abstract— The ionospheric slab thickness (τ) is a parameter which provides information about the nature of the distribution of ionization at a specific location and is defined as the ratio of the vertical Total Electron Content (TEC) measured in TEC units (1 TECu = 10^{16} electrons m^{-3}) to the maximum ionospheric electron density in the F-region (NmF2). Slab thickness provides substantial information on the shape of the electron density profile as well as the neutral and ionospheric temperatures/gradients,composition and dynamics. On the other hand the contribution of the plasmasphere to ground-based GPS TEC (PEC) measurements has received increasing interest in the last few years due to its significance in measuring and modeling the ionosphere to altitudes lower than GPS, in the context of transionospheric signal propagation.

Critical Frequencies Comparison of Ionosondes Data and High-orbital Radio Tomography Data in North America and Europe Regions

V. E. Kunitsyn[1], **I. A. Nesterov**[1], **Yu. S. Tumanova**[1], **and Yu. N. Fedyunin**[2]

[1]Faculty of Physics, Moscow State University, Moscow 119991, Russia
[2]Academy of Merchant Marine, New York 11021, USA

Abstract— Nowadays there are a few thousand high-orbital satellite receivers of GNSS (Global Navigational Satellite System), so methods of high-orbital radio tomography (HORT) are being developed rapidly. They allow obtaining 4D (spatio-temporal) distribution of the electron density in the ionosphere. In this work, the results of F_2-layer critical frequency comparison of high-orbital radio tomographic reconstruction with ionosondes data (as a primary control device of other methods of investigation of the ionosphere) are presented. This comparison was carried out for the region of North America and the region of Europe, as in these regions sufficient number of GPS receivers, required for obtaining electron density distribution, are located. Two temporal periods were investigated: the period of weak ionospheric disturbances (29–31 October 2011, $Kp = 1$–3, North America region) and the period of strong geomagnetic storm (October 2003, $Kp = 8$–9, North America and Europe regions). Correlation coefficients between the ionospheric stations measurements and the results of high-orbital radio tomography were calculated as well as root mean square deviations of F_2-layer critical frequencies measured by the ionosondes and the values obtained from the HORT reconstructions. Generally, the results of high-orbital radio tomography correspond with ionosondes data rather well in areas with sufficient dense network of GNSS receivers. It should be noted though, that during the strongest geomagnetic storm of October 2003 measurements of many ionosondes were fragmentary or were absent at all, while the methods of high-orbital radio tomography allow to retrieve distribution of the electron density in the ionosphere and thus to determine various characteristics of the ionosphere such as, for example, critical frequency of F_2-layer.

ACKNOWLEDGMENT

The work was supported by Russian Foundation For Basic Research (RFBR grant No. 1-05-01157).

Plasmas Excited by Extremely Non-uniform Electric Field Using Cubic Boron Nitride Single Crystals in the Atmosphere

Gang Jia[1], **Shuang Wang**[1], **Zhanguo Chen**[1], **Feng Yang**[1], **Yanjun Gao**[1], **and Xiuhuan Liu**[2,*]

[1]State Key Laboratory on Integrated Optoelectronics, College of Electronic Science and Engineering Jilin University, 2699 Qianjin Street, Changchun 130012, China

[2]College of Communication Engineering, Jilin University, 5372 Nanhu Road, Changchun 130012, China

Abstract— The artificial low temperature plasma is mainly induced by gas discharge. The low temperature plasma generated by gas discharge in the atmosphere has been widely investigated for it is the most suitable for applications in industry. The induced electric field between needle-plate electrodes is extremely non-uniform, and it is the strongest at the needlepoint. In theory, the infinitesimal curvature radius of the needlepoint will lead to infinite electric field strength. So high dc voltages applied to the needle-plate electrodes can result in gas ionization from the air gap between the electrodes, then the corona discharge will arise and the low temperature plasmas will be brought out. In the atmosphere, an unintentionally doped amber cubic boron nitride (cBN) single crystal flake whose sizes are $0.3 \times 0.3 \times 0.1\,\mathrm{mm}^3$ was fixed between the tungsten needle with a diameter of 10 μm at the needlepoint and the brass plate electrodes, the two opposite {111} planes of the cBN flake were tightly contacted to the electrodes, that is to say, the cBN flake was substituted for the air gap. When the dc voltages, with a range of 700–1200 V, lower than those in the case of air gap, were applied to the needle-plate electrodes, gas discharge different from the common corona discharge appeared. It seemed to be glow discharge in the first stage, but transited into arc discharge with the increase of the applied voltage, and the low temperature plasmas were then induced. When the tungsten needle was chosen to be the negative electrode, it was surrounded by the bright blue-violet light, and the light was expanding from the needlepoint to the end within a distance. While the needle was the positive electrode, the bright blue-violet light was extending along the upper plane of the cBN flake off the needlepoint. The current-controlled differential negative resistance was synchronously observed. However, no aforementioned phenomena were observed when the cBN flake was substituted by a quartz or mica flake. In the atmosphere, the plasmas excited by extremely non-uniform electric field using cBN single crystals are not only caused by the air ionization due to the electric field. The initial gas discharge may be the air ionization induced by the vacuum ultraviolet with a wavelength of 149 nm emitted from the cBN crystal which is excited by the extremely non-uniform electric field, then the extremely non-uniform electric field keeps the air discharging, and the low temperature plasmas are consequently induced. The vacuum ultraviolet emission from cBN single crystals in extremely non-uniform electric field will be elaborated elsewhere.

ACKNOWLEDGMENT

Supported by the National Natural Science Foundation of China (Nos. 60976037 and 61077026), the Collaborative Project of NSFC-RFBR (No. 61111120097), and the Natural Science Foundation of Jilin Province, China (No. 201215019).

*Corresponding author: Xiuhuan Liu (xhliu@jlu.edu.cn).

The Doppler Effect at the Propagation of the Signal through the Multipath Radio Channel in HF Wave Band

N. V. Ilyin and M. S. Penzin
Institute of Solar-Terrestrial Physics of the Siberian Branch of the RAS, Russia

Abstract— The Doppler frequency shift is usually equal to a part of hertz or several hertz at pulse vertical or oblique ionospheric sounding at carrier frequency of several megahertz. Usually the duration of the probe pulse is hundreds of microseconds and the propagation time is milliseconds. Thus the spectral width of a single pulse is about 10 kHz. It is impossible to measure the frequency shift of a part of hertz. One of the approaches for detecting Doppler frequency shift is that a coherent sequence of pulses is emitted. In this case the spectrum of the pulse sequence is line one. If the sequence length is large enough so that the width of the line was comparable to the frequency shift then the normal spectral analysis of the entire sequence allow us to measure this shift if it does not change during the analysis.

Another approach also uses the coherent pulse sequence but instead the spectrum of the entire sequence we record the shift of the average phase of each pulse in relation to the previous one. This requires a coherent processing, for example, with synchronous phase detector. If the analog outputs of the phase detector are inputted to an oscilloscope then the single pulse reflected from the ionosphere will be represented by the oval whose width is about 10% of its length (the phase distortion due to dispersion of the absorption). The position of such oval will change due to changes in the phase of the propagation function. The oval rotates and at the same time practically the speed of the rotation is not constant. It is the average speed of the rotation that is interpreted as a Doppler frequency shift.

It is shown, using results of modeling with the normal wave method, that the most sensitive characteristic of the signal in relation to the parameters of the radio channel is the phase at propagating the signal in the multipath radio channel in comparison with the amplitude, the angle of coming, the time delay.

The results of modeling the propagation of the quasi-stationary signal through a quasi-stationary multipath radio channel are presented. The behavior of the phase of each beam individually and the quadrature-components behavior of the total signal is shown.

The Real-time Forecast of HF Radio Channel on the Base of Ionoshere Sounding Data

S. N. Ponomarchuk, **V. P. Grozov**, **M. S. Penzin**, **and G. V. Kotovich**
Institute of Solar-Terrestrial Physics SB RAS, Irkutsk, Russia

Abstract— We propose a technique for ionograms interpretation by means of significant signal amplitude relief points, the identification of propagation modes, the operative definition of of modes composition, maximal usable frequencies for each propagation mode and forecast of radio channel working frequencies ranges on the base of techniques and algorithms for radio physical information secondary processing with a help of chirp sounder data in vertical and oblique sounding regimes. The reliability of results depends on ionogram registration accuracy, the presence diagnostically complex binding to uniform time system and accuracy characteristics of forecast techniques. We show that it is necessary to choose the working frequencies for decameter radio communication due to signals propagation conditions along radio path and noise situation in receiving point. This procedure needs the noise measurements problem solving for given frequency range, the determination of signal/noise ratio in accordance with receiving band width, the determination of time and frequency scattering intervals, the choice of calculation criteria for optimal working frequencies ranges due to signal propagation ranges and noise situation. Under service of regional radio communication systems with leap limit for radio paths not exceeding ~ 3000 km the calculation of optimal working frequencies in real time is possible with a help vertical sounding data. We develop an algorithms for direct recalculation of height-frequency characteristic (HFC) in radio path middle point into distance-height characteristic for oblique sounding and for calculation of propagation characteristics by means of electron concentration profile restored from HFC. This assumption corresponds to spherically symmetric ionosphere model and valid for quiet medium conditions in absence of gradients and strong disturbances. We have a set of tracks obtained by secondary processing of oblique sounding current data which characterized the different modes for different reflection regions. Maximal observed frequency obtained by selected ionogram tracks for each selected track is coincides with maximal frequency for this track. Each selected track is corresponds to particular signal propagation mode. Accordingly, a track start point is minimal observed frequency. We develop the technique for OWF range choice on the base of minimal multi-rayed areas determination which satisfied the condition of signal coherency due to signal/noise ratio.

ACKNOWLEDGMENT

This work is supported by the Ministry of Education and Science of the Russian Federation (government contract 14.740.11.0078) and the Russian fund of basic research (grant No. 11-05-00892).

Session 3P4
Antenna Theory and Radiation

A Novel Microstrip-fed Dielectric ROD Antenna Array with High Gain

Y. Liu and X. Chen
College of Electronics and Information Engineering, Sichuan University, Chengdu 610064, China

Abstract— A novel dielectric rod antenna array with printed feed network is presented. The dielectric rods have a simple structure and the material used for them is Teflon with low dielectric constant 2.08. The circular waveguide located on the bottom of the dielectric rod is designed to guide and propagate electromagnetic energy. The corporate feed network is printed on a dielectric substrate as the launcher to excite the rod. On the bottom side of substrate, a metal board acts as a ground plane. After optimization by a parallel genetic algorithm (GA) on a cluster system, a prototype 4×4 array is fabricated and tested. The measured results agree well with the simulated data and show that that this antenna possesses a high gain of 20.3 dBi at the working frequency 8.0 GHz and achieves an impedance bandwidth of 8.3% (from 7.72 GHz to 8.39 GHz) for $S_{11} < 10$ dB.

On the Velocities of Motion of the Electromagnetic Field in the Near Zone of Elementary Radiators

O. V. Missevich[1], **A. L. Kholmetskii**[2], **V. A. Permyakov**[3], **and D. V. Sorokovik**[4]

[1]Institute of Nuclear Problems, Minsk 220030, Belarus
[2]Department of Physics, Belarus State University, Minsk 220030, Belarus
[3]National Research University "Moscow Power Engineering Institute"
Krasnokazarmennaya Str. 14, Moscow 111250, Russia
[4]OAO "RusHydro", Architektor Vlasov Str., Moscow 117393, Russia

Abstract— In a number of experimental works [1–8] the phenoment of an anomalously small delay of the electromagnetic field in the near and intermediate zones of antennas has been discovered and analyzed. Studies performed by O. V. Missevitch, A. L. Cholmetskii, and R. Smirnov-Rueda, are of special interest because, in these works, small (as compared to the mean length of the electromagnetic wave) antennas excited by ultrashort pulses were analyzed. The effect of an anomalously small delay of the electromagnetic field can be most pronounced exactly in the case of small antennas, because the near zone can be treated as a section of an irregular evanescent waveguide.

In order to interpret this effect, in this report, the space-time evolution of the fields in the near zone of elementary dipoles is studied analytically. The study is performed with the use of the methods of the qualitative theory of ordinary differential equations [9].

In the case of ultrashort pulses, the concept of the group velocity loses its meaning and the concept of the phase velocity becomes limited and applicable to only the motion of the field zeros. We studied the instantaneous velocities of motion of the extrema and zeros of the electric and magnetic fields as well as the Poynting vector in the near and intermediate zones of an electric dipole. This approach was applied to the quasi-harmonic and pulse excitation modes of of the electric dipole. It has been shown that, in the near zone, the extrema and zeros of the field components in the signal zone adjoining the signal front motion with velocities exceeding the velocity of the electromagnetic wave in vacuum. This statement is also valid for the instantaneous energy propagation velocities. However, this statement does not mean that the causality principle is violated. During their motion, the extrema and zeros of the field components and the energy do not overtake the signal front traveling with the velocity of light in vacuum (see also [10]). As the fields leave the intermediate zone, the velocities of motion of the extrema and zeros of the field components and the energy approach the velocity of light in vacuum.

Using the principle of permutational dualty, one can transfer the obtained results to the case of a magnetic dipole, which allows us to apply them for the interpretation of the experiments performed by O. V. Missevitch a.o.

REFERENCES

1. Ranfagni, A., D. Murnai, et al., *Phys. Rev. E*, 1998,
2. Ranfagni, A., D. Murnai, et al., *Phys. Rev. E*, 2004,
3. Ranfagni, A., D. Murnai, et al., *Phys. Letters A*, Vol. 247, 1998,
4. Ranfagni, A., D. Murnai, et al., *Phys. Letters A*, Vol. 352, 2006.
5. Ranfagni, A., D. Murnai, et al., *Phys. Letters A*, Vol. 372, 2008,
6. Missevitch, O. V., A. L. Cholmetskii, and R. Smirnov-Rueda, *J. Appl. Phys.*, Vol. 101, 023532, 2007.
7. Missevitch, O. V., A. L. Cholmetskii, and R. Smirnov-Rueda, *J. Appl. Phys.*, Vol. 102, 013529, 2007.
8. Missevitch, O. V., A. L. Cholmetskii, and R. Smirnov-Rueda, *EPL*, Vol. 93, 64004, 2011.
9. Permyakov, V. A., D. V. Sorokovik, and A. N. Korykin, "Qualitative analysis of dipole antennas impulse radiation," *Progress In Electromagnetics Research Symposium Abstracts*, Moscow, Russia, Aug. 18–21, 2009.
10. Wainshtein, L. A., *Sov. Phys. Usp.*, Vol. 19, No. 2, 1976.

Design of Array Synthesis Horn Antenna for High Power Microwave Applications

Jae-Min Lee and Jong-Myung Woo
Department of Radio Science and Enginnering, Chungnam National University
99 Daehak-ro, Yuseong-gu, Daejoen 306-764, Korea

Abstract— In this paper, an array synthesis horn antenna was designed for high power microwave applications. For the high power microwave applications, an antenna should have high gain and small back lobe to focus the beam. Four horn antennas with TE_{10} mode and 10 dBi of gain were arrayed to 2×2. The horn of 2×2 arrayed horn antenna was extended to increase the gain. A higher order mode (TE_{20}) in the arrayed horn antenna with extended horn occurred because of the array distance. This higher order mode reduced the gain and broadened the beamwidth. Therefore, the vertical junction between arrayed horns was controlled to eliminate higher order mode. For small back lobe, two stepped-corrugated structures were attached on the aperture in the 2×2 arrayed synthesis horn antenna. The size of the array synthesis horn antenna is $500 \times 500 \times 836\,\text{mm}^3$ ($4.08 \times 4.08 \times 6.83\lambda^3$, where λ is free space wavelength at 2.45 GHz). The gain and front to back ratio was measured as 21.1 dBi and 38 dB respectively. The beamwidth of E- and H-plane are 14° and 13.6°. The designed antenna would be appropriate for high power microwave applications.

A Symmetrical Theory of Electromagnetism

P. E. Munhoz-Rojas
LACTEC — Instituto de Tecnologia Para o Desenvolvimento, Brasil

Abstract— An axiomatic reformulation of Maxwell's theory of electromagnetism is presented that permits to deduce Maxwell's theory and, also, most of the well known theories of classical electromagnetism. As a result it is shown that these theories are not fully equivalent.

It is shown that electric charges produce two fields of magnetic nature and that magnetic charges produce two fields of electric nature. In each case, one of the fields is of a solenoidal nature and this solenoidal field is related to the other field by a Faraday's law. This result is independent on the existence or inexistence of free magnetic charges.

It is shown that the fields $\mathbf{D_e}$ and $\mathbf{H_e}$ are produced by the free electric charges and by the bounded magnetic charges and, this fact has the interesting result that, independently of the existence or inexistence of free magnetic poles, Maxwell-Hertz's equations are valid microscopically. It is also shown that all interaction processes involve an "electric quantity" and a "magnetic quantity".

Using these concepts, a theory of the interaction between fields and macroscopic matter is presented, which use, as Maxwell did, the fields De and He as excitation fields $\mathbf{D_e}$ and $\mathbf{H_e}$ extends the well known Maxwell-Lorentz's theory. As a result of the fact that the fields $\mathbf{D_e}$ and $\mathbf{H_e}$ are produced by the free electric charges and by the bounded magnetic charges, different phenomena are produced due to the excitation by the free electric charges or by the bounded magnetic charges. As a result, it is shown that Maxwell's theory of light concerns the interaction between bounded magnetic charges and bounded electric charges, which is a phenomenon totally different from the electromagnetic perturbations that are attached to metallic conductors, where the excitation is due to free electric charges moving inside the conductor.

It is believed that these results, besides its academic interest, could be useful for the design and interpretation of the functioning principle of antennas and sensors.

A Method of PCI Planning in LTE Based on Genetic Algorithm

Hao Sun, Nan Li, Yanlei Chen, Jiangbo Dong, Na Liu, Yunbo Han, and Wei Liu
China Mobile Design Institute, Beijing, China

Abstract— Physical Cell ID (PCI) planning is one of the most important steps in whole Long Term Evolution (LTE) network planning and construction. It is difficult to improve the QoS of Network by some traditional methods, such as antenna adjustment in LTE system. Assigning PCI reasonably is able to decrease interference and increase operation rate and performance of the network. A PCI planning system is presented in this paper. This system would analyze the interference of LTE system and build up an interference matrix. Then this system would use genetic algorithm to adjust the distribution of PIC to minimize the interference. Finally a PCI plan scheme would be given by this system.

Investigation of Adaptive Multi-antenna Switching Strategy in TD-LTE Systems

Wei Liu, **Kaikai Liu**, **Nan Li**, **Jiangbo Dong**, **Na Liu**, **Yanlei Chen**, **Hao Sun**, **and Yunbo Han**

China Mobile Design Institute, Beijing, China

Abstract— In TD-LTE system, Multi-antenna technology (MIMO) can be used in several transmission modes to enhance the system performance. This paper introduces principle of two Multi-antenna technology, Spatial Diversity (SD) and Spatial Multiplexing (SM), researchs the application scenarios for Adaptive Multi-antenna technology which based on these two technology. It compares capacity and application scenarios of SD and SM through the data from the test network. Then, it studies on the different performance of capacity on the Adaptive Multi-Antenna Technology under a variety of channel conditions and gives the reason why it can enhance the capacity performance. Factors and notes are proposed when adaptive multi-antenna switching strategy applied to the actual.

A Circularly Polarized Printed Antenna with Modified Slots for RFID Reader

E. M. Ghanem[1], **E. A. Abdallah**[2], **and M. A. Aboul-Dahab**[1]

[1]Arab Academy for Science and Technology and Maritime Transport, Egypt
[2]Electronic Research Institute, Egypt

Abstract— The paper Discusses a new design of RFID antenna. RFID is short for Radio Frequency Identification, which uses wireless radio frequency signal modulated with some information to distinguish different people or items. The system mainly consists of a tag or transponder that carry the required information or Id. One other part of the system is the reader that reads the information on the tag and forwards it to a computer system that identify the reader and classify it as the application require. The proposed design for a reader antenna is working in UHF Band (902–928 MHz) and multiple techniques were used for enhancing the antenna parameters. The matching between the antenna and the integrated circuit (IC) used was performed using a co-axial fed probe with correct point of feeding. Increasing the axial ratio bandwidth to maintain circular polarization transmission and reception is done by using different slots types and shapes. Increasing the −10 dB impedance bandwidth to cover the whole bandwidth required is done using different slot positions. FR4 was used as a dielectric substrate to decrease the cost for mass production. The suggested design is optimized and simulated using the full wave simulation software package Zeland IE3D based on the method of moments (MOM). The design is fabricated using photo-lithographic technique and experimental results are obtained and compared with the simulated ones. Good agreement is found between simulated and measured results.

A Novel Way for Designing Bifocal Reflector Antennas

A. N. Plastikov and B. L. Kogan
National Research University "Moscow Power Engineering Institute"
Krasnokazarmennaya Str. 14, Moscow 111250, Russia

Abstract— Today, the development of multi-beam reflector antennas (MRA), capable to operate (i.e., receive or transmit the information) simultaneously with several rays (plane wave directions), seems quite an important area of antenna technology, relevant for both terrestrial and airborne systems. The obvious advantage of MRA over a single beam reflector antennas is the usage of a single aperture (i.e., one primary mirror) to form multiple beams, which allows a single MRA to "replace" a certain number of "ordinary" reflector antennas.

Bifocal two-reflector antennas have two exact foci and allow aberration-free focusing of the field comes from two different directions. For the first time questions of the theory of designing three-dimensional bifocal reflector antennas (BRA) were examined in the 80 s of XX century in the works of C. M. Rappaport, B. E. Kinber and others. A characteristic feature of the appropriate solutions of the synthesis problem is the fact that it is possible to define a discrete sequence of reference points of reflectors surfaces. To form a continuous smooth surface it was necessary to fulfill the conditions of coupling between adjacent points. It appears that these MRA are not widespread, which may be due to the difficulty of obtaining mirror smooth profiles by solving the synthesis problem.

We have proposed a new approach to the problem of calculating the reflectors surfaces of offset bifocal antennas by raytracing procedure. The use of this approach allows to obtain the analytical expressions for profiles of the two reflectors in the form of two parametric variables functions. In the case of antennas with the size of the aperture 100 wavelengths in the scanning plane a few different variants of the mirror system are identified and compared with each other. The optimization of reflector profiles in order to obtain the minimum root-mean-square optical path length error for the central beam is carried out. Calculations of the secondary radiation field for a specific version of the bifocal antenna for different angles of deflection from the axis of the MRA are performed and achievable scan performance is defined in such a way. Cross-polarization characteristics are also investigated.

The results can be used to construct a multi-beam or scanning reflector antennas.

The Effects of the Tube Characteristics on the Performance of a Plasma Monopole Antenna

F. Sadeghikia[1], **F. Hodjat-Kashani**[1], **J. Rashed-Mohassel**[2], **and S. J. Ghayoomeh-Bozorgi**[1]

[1]Department of Electrical Engineering, Iran University of Science and Technology
P. O. Box 16846-13114, Farjam, Narmak, Tehran, Iran
[2]Center of Excellence on Applied Electromagnetic Systems, ECE Department
University of Tehran, P. O. Box 14395-515, Tehran, Iran

Abstract— This theoretical study examines the effects of the radius of the plasma tube and its thickness on the input impedance, radiation pattern, gain and radar cross section of a surface wave driven plasma monopole antenna using finite difference time domain (FDTD) simulation. Using direct integration method on the combination of Maxwell curl equations for electric and magnetic fields ($\vec{E}$ and $\vec{H}$) and also an auxiliary ordinary differential equation modeling the response of the current density, $\vec{J}$, to the electric field for accounting the effect of plasma simulation of the isotropic cold plasma is done. By performing backward differencing approximation to the mentioned equations a second order approximation for numerical simulation can be derived for Yee's FDTD formulation.

After presenting a case study with constant plasma and collision frequencies in the tube, numerical results are achieved. It will be demonstrated that more broadband characteristics can be obtained by increasing the diameter of the plasma tube. Moreover, the imaginary part of the input impedance of plasma antenna can be eliminated by making the total length of the antenna approximately less than $\lambda/5$, where λ is the wavelength of a wave, and this value decreases while the ratio L/r decreases. The results show that there is an optimum value for L/r ratio to achieve the maximum gain and decreasing the radius of the plasma tube decreases RCS of the antenna. Furthermore, as the radius of the plasma tube increases, the minor lobes diminish in intensity and the nulls are replaced by low level radiation.

Theoretical modeling of the plasma antenna with different thicknesses shows that the least thickness can cause more efficient antenna while minimizing its bandwidth. Therefore, using a higher thickness of the tube is not a very efficient technique to broadband the plasma antenna.

Characteristics of Plasma Antennas under Radial and Axial Density Variations

F. Sadeghikia[1], **F. Hodjat-Kashani**[1], **J. Rashed-Mohassel**[2], **and S. J. Ghayoomeh-Bozorgi**[1]

[1]Department of Electrical Engineering, Iran University of Science and Technology
P. O. Box 16846-13114, Farjam, Narmak, Tehran, Iran
[2]Center of Excellence on Applied Electromagnetic Systems, ECE Department
University of Tehran, P. O. Box 14395-515, Tehran, Iran

Abstract— The knowledge of plasma density distribution as a function of radial and axial variations in the plasma tube is one of the most important aspects of the plasma antennas. To this end, a numerical model of the pre ionized plasma tube is investigated under different radial distribution functions as well as a linear axial one. The model completely characterizes the radiation characteristics of a monopole plasma antenna considering its input impedance, efficiency and radiation pattern using finite difference time domain (FDTD) simulation. Direct integration method is used on the combination of Maxwell curl equations for electric and magnetic fields ($\vec{E}$ and $\vec{H}$) and also an auxiliary ordinary differential equation. This auxiliary equation models the response of the current density, $\vec{J}$, to the electric field for accounting the effect of plasma.

Examinations of scientists reveal that the field intensity concentrates radially at the plasma-dielectric interface as the $\beta \cdot a$ becomes larger (β is the phase coefficient and a is the radius of the tube). So the electron density value at or close to the tube wall is lower than the cross sectional average density. Ferreira's modeling shows thatthe radial distribution is flatter than the Bessel function. However, Trivelpiece approximated that by a parabolic profile. We considered the profile of radial density of plasma as Bessel, parabolic and cosine functions. The axial density variations was assumed linear in the argon at the pressure of 0.4 mb and the excitation power of 120 W. We will show that plasma radial density distribution can change the antenna input impedance and radiation characteristics.Estimation of radial distribution in plasma antenna with the Bessel function leads us to the least minor lobe.

New Bandwidth Limits for Dipoles

Rodney G. Vaughan and Maryam Dehghani Estarki
School of Engineering Science, Simon Fraser University, BC, Canada

Abstract— The dipole is the most fundamental antenna concept and has endured as the simplest, practical element. The half-wavelength wire dipole's resonant resistance can match standard impedances, and its measured bandwidth is about 10%. There are several variations on the Chu limit which indicate the trade-off for lossless antennas between bandwidth and an enclosing spherical volume. Gustafsson et al formulated a limit for arbitrary volume shapes, and this turns out to be looser than the Chu limits for a dipole. The two rigorous theories for the wire dipole are the induced emf method and the wave structure method. There are several numerical solvers but their answers vary and also depend on the rendition (sampling) of the dipole form and the feed model. For the antenna theoretic impedance, the finite gap feed is of particular interest. Feedpoint modeling has known pitfalls, and these are reflected in numerical solutions, but the induced emf method allows a rigorously defined impedance. This means that an exact theoretic bandwidth for a finite gap dipole can be calculated. Here, the impedance bandwidth is calculated from theoretical and numerical approaches. Such calculations are from the match across a bandwidth as well as from the local behaviour at the nominal centre frequency. The 3 dB theoretical bandwidth can reach about 80% for a thin wire dipole with a gap feed of about 20% of the dipole length. In order to realize this kind of bandwidth, a practical feed is still required. This Chu limit-achieving bandwidth motivates researching such a feed.

Circular Array of Inverted F Antennas

F. Sadeghikia[1], **H. H. Mehne**[2], **and M. Ebrahimi**[2]

[1]Department of Electrical Engineering, Iran University of Science and Technology, Farjam, Narmak P. O. Box 16846-13114, Tehran, Iran
[2]Aerospace Research Institute, P. O. Box 14665-834, Tehran, Iran

Abstract— Over the past few years, inverted F antennas (IFA) have been used extensively in aeronautical applications. An IFA is similar to a freestanding quarter-wave monopole above a ground plane, rather than the usual half-wave wire antenna. The two key qualities of an IFA are less complexity in impedance matching and the least air drag in the avionic equipments. Since the increased diameter and rotation are inevitable in some cylindrical vehicular spacecraft, using a circular array of IFAs on the surface of the cylinder is recommended for better coverage. However, increasing the array elements causes deeper nulls in the radiation pattern and increased unwanted interference into nearby receivers. In this contribution, the radiation characteristics and mutual impedance of a circular array of IFAs using full wave simulator are presented and the results are compared with the experimental results of a case study. The results show that the number of elements in such an array is a compromise between the coverage, link budget and the radius of the cylinder.

Session 3P5a
Asymptotic and Hybrid Methods in Electromagnetics

Some Recent Extensions of the Exact Line Integral Representation of the Physical Optics Scattered Field

Frédéric Molinet
MOTHESIM, France

Abstract— This paper presents an extension of the line integral representation of the Physical Optics electromagnetic field to the more general case of multiple Physical Optics interactions.

The Physical Optics (PO) approximation remains an important computational tool for the analysis of large reflector antennas or for the evaluation of the scattering from electrically large objects. Combined with the Physical Theory of Diffraction (PTD) it provides a uniformly accurate evaluation of the co- and cross-polarized radiation patterns and of the Radar Cross Sections (RCS). But for large reflectors and wide angle patterns of multibeam multifrequency systems or for systems of reflectors or electrically large complex objects, the straightforward evaluation of the pertinent integrals for a wide range of observation directions becomes time consuming and inefficient due to its high computational complexity.

A way to reduce the complexity of evaluating the PO integrals consists in making use of the possibilities related in the literature, to reduce radiation integrals which are essentially surface integrals, to line integrals. Following the work of Maggi, Miyamoto, Rubinowicz and Asvestas, an exact line integral representation of the PO scattered field from a perfectly conducting flat plate, illuminated by an electric Hertzian dipole, has been obtained by Johansen and Breinbjerg in 1995. Later on, this result has been extended to a magnetic Hertzian dipole, to a Gaussian beam modeled as a complex point source and in an approximate version to more general configurations.

In this paper, we show that in the case of double interactions of the PO field generated by a dipole in front of two non coplanar plates, the double surface integral can be transformed exactly in a double line integral along the contours of the two plates. However, the line integral corresponding to the second plate contains a dyadic function given by an integral along a generatrix of a cone having the observation point as the tip and the contour of the second plate as the basis. This dyadic function is an extension to the electromagnetic case of the Miyamoto-Wolf vector potential for the scalar case. We have shown that the integral of the dyadic potential function corresponding to the PO integral of the second interaction, is not exactly integrable. However, it can be decomposed into a set of elementary integrals which have no stationary point in the domain of integration and which can be evaluated asymptotically, by integration by parts (end point contributions) in a large domain of the integration variable.

Numerical results for double interactions on two perfectly conducting plates, obtained by the direct computation of the multiple integral of order four, are compared to those obtained by the double line integral representation and the efficiency of the method in computer time saving is shown. The formulas for triple interactions are also presented and the possibilities of extension of the method to non planar surfaces, especially to large reflector antennas, are discussed.

Diffraction by a Sharp Edge for an Electromagnetic Field Described by Summation of Gaussian Beams: The Ufimtsev Way

Jean-Marc Darras[1], **Thierry George**[1], **and Philippe Pouligen**[2]

[1]CELUM, 6 rue des états généraux, Versailles 78000, France
[2]DGA/DS/MRIS, 7 rue de Mathurins, Bagneux 92221, France

Abstract— A wave reflected on a surface or transmitted through an aperture is influenced by the edge of the surface or aperture. The reflected or transmitted field can be classically written as the sum of the geometrical field and the diffracted field by the edge (see Ufimtsev, Mitzner, Pathak, Michaeli, Tiberio, ...).

Our Gaussian Beam Summation (GBS) describes the 3D field by a double integral on the ray parameters:

$$\underline{u}^{GBS} = \iint \underline{\psi}(\underline{\gamma}, s) \exp\left\{-j\omega\left[\tau(\underline{\gamma}, s) + \frac{\delta q^t \cdot \underline{\underline{M}}(\underline{\gamma}, s) \cdot \delta q}{2}\right]\right\} \cdot d\underline{\gamma}$$

As Popov did in 2D, we use the saddle point method to match a 3D formal decomposition in Gaussian Beams to the optic geometrical solution at the receiver, in asymptotic geometrical regular domain. Furthermore, GBS must be valid near the focal points. We obtain a uniform normalization of the integral (George PIERS 2009).

Many authors (see Katsav and Heyman, Chou and Pathak, Takenata, Anokhov, Suedan, Jull, etc.) have studied the diffraction of an incident Gaussian beam on a sharp edge. Their work concerns a single beam and can be used for a discrete set of beams to represent an electromagnetic field. Nevertheless It is difficult to apply these results to our continuous summation method GBS.

As well as Physical Optic (PO), in presence of finite boundaries, GBS contains a part of diffraction (GBSD) but this part is localized near the vicinities of shadow boundaries. GBSD is negligible in deep shadow regions.

We want to model the asymptotic diffracted field in all the regions. For this purpose, we assume that there exists a complementary term (GBSC) to add with the GBS field:

$$\underline{u}^T = \underline{u}^{GBS} + \underline{u}^{GBSC}$$

To solve this problem, we follow the Umfitsev's principle: we subtract the asymptotic contribution of GBS diffraction, named GBSD, and we add the uniform UTD diffraction coefficient for a sharp edge.

$$\underline{u}^{GBSC} = \underline{u}^{UTD} - \underline{u}^{GBSD}$$

GBDS is obtained by studying the asymptotic contributions due to edge in GBS integral. The steps are the following:

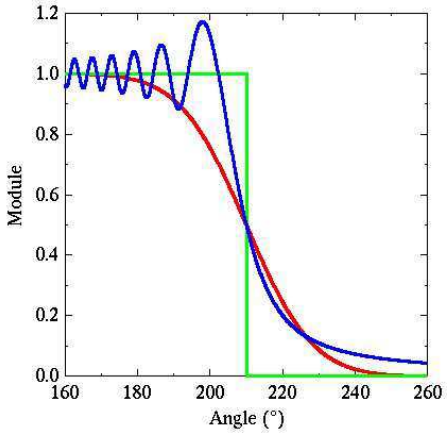

Field for an incident plane wave in function of the angle around a shadow boundary

frequency = 10 GHz
distance = 0.5 m

In green : geometrical optics

In blue : uniform theory of diffraction

In red : Gaussian beam summation

- Ray parameters transformation into surface coordinates, using paraxial relations, in a plan perpendicular to reflected or transmitted ray at a given diffraction point,
- Local approximation of the edge by its osculating circle at the diffraction point,
- Usage of polar coordinates to formalize the influence of the vicinity of the edge on the saddle point approximation in a suitable way for asymptotic resolution (Felsen and Marcuvitz).

The result is expressed in terms of geometric field and error function. It can be written as the sum of two terms. The first is the geometric field and the second is the GBSD field. We found:

$$\underline{u}^{GBSD} \approx \frac{\underline{u}^{*OG}}{2}[\pm 1 - \mathrm{erf}(\sqrt{\omega}\cdot d)] \quad (+ : \text{ shadow area}, \quad - : \text{ illuminated area})$$

d is a complex parameter which represents the distance to the shadow boundary. $\underline{u}^{*OG}$ is the geometric field which would exist without edge.

Using paraxial approximations and adopting the Kouyoumjian and Pathak notations for UTD formulation, a convenient formulation is obtained in the form of a Dyadic Edge Diffraction Coefficient. The paraxial assumption is justified by the fact that GBSD is concentrated around the geometric shadow.

$$\begin{pmatrix} E^d_\beta \\ E^d_\phi \end{pmatrix} = \begin{pmatrix} -D^{GBSD}_s & 0 \\ 0 & -D^{GBSD}_h \end{pmatrix} \begin{pmatrix} E^i_{\beta'} \\ E^i_{\phi'} \end{pmatrix} \sqrt{\frac{\rho}{s(\rho+s)}} \cdot \exp\left\{-j\omega\frac{s}{c}\right\}$$

$$D^{GBSD}_{s,h} = \pm\frac{1}{2}\sqrt{\frac{\rho^{i,r}_1\rho^{i,r}_2 s(\rho+s)}{\rho(\rho^{i,r}_1+s_p)(\rho^{i,r}_2+s_p)}}\left[-\mathrm{sgn}(\hat{s}\cdot\hat{\phi}^{i,r}) + \mathrm{erf}(\sqrt{\omega}\cdot d)\right]\exp\left\{-j\omega\left(\tau_0 - \frac{s}{c}\right)\right\}$$

$(+ :$ reflected field and soft component, $-$: reflected field and hard component or incident field)

The complementary diffraction coefficient ($D^{GBSC}_{s,h} = D^{UTD}_{s,h} - D^{GBSD}_{s,h}$) takes the value zero on the geometric shadow boundaries and is continuous at the crossing of these boundaries which ensures good numerical stability of the total field evaluation.

We shall show numerical applications and illustrations in the oral presentation.

The Kirchhoff-type Formulas for the Time-dependent Electromagnetic Field in a Conducting Medium

A. S. Il'inskii and I. G. Efimova
Moscow State University, GSP-1, Leninskie Gory, Moscow 119991, Russia

Abstract— In the time domain, the electromagnetic field existing in a nonconducting medium can be expressed in an integral form through the intensities of the electric and magnetic fields on a closed surface. In this case, the field intensities entering the integrands are functions of a retarded time argument. Such representations are successfully applied for deriving integral equations used in simulations of scattering of a nonstationary electromagnetic field by perfectly conducting and lossless dielectric bodies located in nonconducting media.

However, the method of time-domain integral equations has not been developed for the case of a conducting medium, because an integral representation for a nonstationary electromagnetic field in such a medium has not been found. In this study, we obtain a time-domain integral representation of a nonstationary electromagnetic field in a homogeneous isotropic medium having conductivity.

A homogeneous isotropic medium with constitutive parameters that do not depend on either time or spatial coordinates is considered. It is assumed that permittivity ε, permeability μ, and electric and magnetic conductances σ^e and σ^m are constants and that electric and magnetic field intensities $\mathbf{E}$ and $\mathbf{H}$ are finite functions continuous along with all of their derivatives at all ordinary spatial points (where the medium does not abruptly change its physical properties). We assume in addition that all functions of time that are considered in this study—the electric-and magnetic-field intensities and volume densities of external currents $\mathbf{j}^{eext}$ and $\mathbf{j}^{mext}$ — are zero along with their derivatives till the instant $t = 0$ inclusively.

In order to derive an integral representation of the intensity of the nonstationary electric field satisfying the inhomogeneous wave equation, we apply the technique from monograph [1] and use the vector analog of the Green's theorem for closed spatial region V bounded by surface S that satisfies the Lyapunov conditions. The wave equation is simplified through eliminating the first-order time derivative of the field with the help of the appropriate replacement. The detailed derivation of the final formula

$$
\begin{aligned}
4\pi\tilde{\vec{E}}\Big|_{\tau=t} = \int\limits_V \Bigg[& -\frac{1}{r}\,\mu\left(\frac{\partial\tilde{\vec{j}}^{eext}}{\partial t}\Big|_{\tau=t-r/c} - \frac{ac^2}{2}\tilde{\vec{j}}^{eext}\Big|_{\tau=t-r/c}\right) - \frac{1}{r}\left(b-\frac{a^2c^2}{4}\right)\tilde{\vec{E}}\Big|_{\tau=t-r/c} \\
& - \left[\tilde{\vec{j}}^{mext}\Big|_{\tau=t-r/c}\frac{1}{r^2} + \frac{1}{rc}\frac{\partial\tilde{\vec{j}}^{mext}}{\partial t}\Big|_{\tau=t-r/c}\right]\times\vec{r}_0 - \frac{1}{r}\sigma^m\tilde{\vec{j}}^{eext}\Big|_{\tau=t-r/c} \\
& + \frac{1}{r}\left(\frac{1}{r}div\tilde{\vec{E}}\Big|_{\tau=t-r/c} + \frac{1}{c}\frac{\partial div\tilde{\vec{E}}}{\partial t}\Big|_{\tau=t-r/c}\right)\vec{r}_0\Bigg] dvdt \\
& - \int\limits_{S_2}\Big(\Big(\frac{1}{r^2}\left(\vec{n}\cdot\tilde{\vec{E}}\Big|_{\tau=t-r/c}\right) + \frac{1}{cr}\Big(\vec{n}\cdot\frac{\partial\tilde{\vec{E}}}{\partial t}\Big|_{\tau=t-r/c}\Big)\Big)\vec{r}_0 + \Big[\vec{r}_0\times\Big(\frac{1}{r^2}\Big[\tilde{\vec{E}}\Big|_{\tau=t-r/c}\times\vec{n}\Big]\Big]\Big] \\
& + \frac{1}{cr}\Big[\frac{\partial\tilde{\vec{E}}}{\partial t}\Big|_{\tau=t-r/c}\times\vec{n}\Big]\Big) - \frac{1}{r}\sigma^m\Big[\vec{n}\times\tilde{\vec{H}}|_{\tau=t-r/c}\Big] \\
& - \frac{1}{r}\mu\Big[\vec{n}\times\Big(\frac{\partial\tilde{\vec{H}}}{\partial t}\Big|_{\tau=t-r/c} - \frac{ac^2}{2}\tilde{\vec{H}}\Big|_{\tau=t-r/c}\Big)\Big]\Big) ds
\end{aligned}
$$

is presented in [2]. Here, $a = \mu\sigma^e + \varepsilon\sigma^m$, $b = \sigma^m\sigma^e$, $c = \frac{1}{\sqrt{\varepsilon\mu}}$ is the velocity of light, and the tilde denotes the product of the corresponding function and the factor $\exp(ac^2t/2)$.

The formula for the magnetic field can readily be found with the help of the duality principle. According to the relationships obtained, the field at any instant at an arbitrary point in a certain volume is expressed through an integral over the surface bounding this volume and an integral over the volume. The integrand functions contain the values of the field intensities and

external currents and the time derivatives of these quantities at instants preceding the observation moment.

The obtained time-domain integral representations for nonstationary electric and magnetic fields can be used for deriving integral equations that make it possible to extend the method of time-domain integral equations to problems of electrodynamic analysis of structures with conducting media.

REFERENCES

1. Stratton, J. A., *Electromagnetic Theory*, McGraw-Hill, New York, 1941.
2. Il'inskii, A. S. and I. G. Efimova, "The equivalence theorem for the vectors of nonstationary electromagnetic field intensities in a conducting medium," *J. Commun. Techn. Electron.*, Vol. 56, No. 2, 125–133, 2011.

High Frequency Diffraction by an Impedance Rectangle for Grazing Incidence

A. D. Rawlins
Brunel University, Uxbridge, UK

Abstract— We shall consider the the problem of determining the scattered far wave field produced when a high frequency plane E-polarized wave is at grazing incident on an imperfectly conducting rectangular cylinder. By using geometrical theory of diffraction, multiple diffraction methods, and the canonical solution for the problem of the diffraction of a plane wave by a right-angled impedance wedge, in conjunction with a new method we derive the a high frequency far field solution to the problem is given.

Introduction: In dealing with propagation in cities the effect of building corners and their surface cladding is of importance for the signal strength. A building of rectangular cross-section can be modelled by four of these corners. With appropriate polarization this building can be effectively modelled for high frequency diffraction by a rectangular impedance cylinder in two dimensions. To obtain quantitative and qualitative results for the signal strength far from the building when there are multiple diffraction from such corners an effective approach is to use the Keller's method of the geometrical theory of diffraction (GTD), and information about the "diffraction coefficient" which are obtained from the solution of canonical impedance wedge problems. In a previous work, by using the uniform asymptotics developed from the canonical wedge solution, useful asymptotic results were obtained for the oblique incidence case. However the the methods used there break down when the incident wave is at grazing incidence, that is when the incident ray is parallel to a side of the rectangular cylinder. In this work, we shall use a new method to address this problem. The determination of the far field when a high-frequency E-polarized electromagnetic plane-wave is at grazing incident on an imperfectly conducting rectangular cylinder is obtained by applying an alternative approach than Keller's method of geometrical diffraction. At grazing incidence the far field varies rapidly for small angular variation and Keller's method seems to be no longer applicable. We shall use an alternative approach, by using Green's theorem and analytic asymptotics of the canonical solution of the impedance wedge diffraction problem. To achieve this the complex integral representation of the canonical problem, for the diffraction field for a right-angled impedance wedge is used; in conjunction with the multiple diffraction that arises from waves travelling from corner to corner of the rectangle. In this work, we shall obtain an expression for the forward scattered field and the total scattering cross-section for grazing incidence.

Session 3P5b
The Modern Hybrid Methods in the Problems of Computational Electromagnetics

The Self-consistent Problem of Scattering and Generation of Oscillations by a Nonlinear Layer Taking into Account the Influence of Weak Fields at Multiple Frequencies

L. Angermann[1], **V. V. Yatsyk**[2], **and M. V. Yatsyk**[3]

[1]Institute of Mathematics, TU Clausthal, Clausthal-Zellerfeld, Germany
[2]Usikov Institute of Radiophysics and Electronics NASU, Kharkov, Ukraine
[3]Kharkov National University of Radio Electronics, Kharkov, Ukraine

Abstract— We investigate the scattering and generation of waves on an isotropic, nonmagnetic, linearly polarised nonlinear layered cubically polarisable dielectric structure (a layer in free space filled with nonlinear medium) excited by a packet of plane waves. The analysis is performed in the domain of resonance frequencies. We show that the propagation of electromagnetic waves in a nonlinear layer with cubic polarisability of the medium can be described by an infinite system of nonlinear boundary-value problems. When considering particular nonlinear effects one can reduce this system to a finite number of problems and leave certain terms in the representation of the polarisation coefficients which characterize the physical problem under investigation [1–3].

We present some results of calculations that describe properties of the nonlinear permittivities of the layers as well as their scattering and generation characteristics. In the numerical experiments we have reached intensities of the excitation field such that the relative portion of total energy generated in the third harmonic is up to 36% which exceeds the known data by a factor about 3.6. The results indicate a possibility of designing a frequency multiplier and nonlinear dielectrics with controllable permittivity.

ACKNOWLEDGMENT

This work was partially supported by the Visby Program of the Swedish Institute.

REFERENCES

1. Shestopalov, Y. V. and V. V. Yatsyk, "Diffraction of electromagnetic waves by a layer filled with a Kerr-type nonlinear medium," *J. of Nonlinear Mathem. Physics*, Vol. 17, No. 3, 311–335, 2010.
2. Angermann, L. and V. V. Yatsyk, "Generation and resonance scattering of waves on cubically polarisable layered structures," *Numerical Simulations Applications, Examples and Theory*, L. Angermann, Ed., 175–212, InTech, Rijeka/Vienna, Croatia/Austria, 2011.
3. Angermann, L. and V. V. Yatsyk, "Resonance properties of scattering and generation of waves on cubically polarisable dielectric layers," *Electromagnetic Waves*, V. Zhurbenko, Ed., 299–340, InTech, Rijeka/Vienna, Croatia/Austria, 2011.

Mathematical Modeling of Plane Chiral Waveguide Using Mixed Finite Elements

A. N. Bogolyubov, **Yu. V. Mukhartova**, **J. Gao**, **and N. A. Bogolyubov**
Faculty of Physics, Moscow State University, Russia

Abstract— This work presents the investigation of a plane waveguide with perfectly conducting walls and nonuniform filling in a form of a chiral insertion that occupies a finite domain inside the waveguide. Chiral media are a subclass of bi-isotropic media. The main difference between ordinary dielectrics or magnetics and bi-isotropic media is that the electric or magnetic field applied to them produces both electric and magnetic polarization.

A numerical algorithm for calculating electrical field inside the chiral insertion, excited by an incident normal wave or a combination of normal waves, is proposed. This algorithm is based on reduction of Maxwell's equations with perfectly conducting boundary conditions to the boundary problem for electric field vector in the finite area, using partial radiation conditions. The finite-element method is a powerful method of analysis of waveguide boundary problems, but it has one drawback. For a full-vector statement of a problem this method can give nonphysical, spurious solutions that satisfy the finite-element equations, but not the original boundary problem. The method of mixed finite elements, that prevents spurious modes appearance, is used for numerical solution of the problem.

The algorithm proposed was tested on empty waveguide and used for modeling electric field inside the chiral insertion for different values of chirality parameter and for incident waves of TM and TE types. Computations made illustrate that the field inside the chiral insertion present a result of interference of different mode types. So we can conclude that this system with appropriate parameters may be used for transformation of one type of normal waves to another.

The method proposed can be generalized for anisotropic filling of a waveguide and for a three dimensional case. It is also suitable for solving inverse synthesis problem of a waveguide with desirable features.

Avoiding Diffraction Order Singularity in Scattering Matrix Approach Used for Grating Modelling

A. A. Petukhov[1], **M. K. Trubetskov**[2], **and A. N. Bogolyubov**[1]

[1]Faculty of Physics, Moscow State University, Russia
[2]Research Computing Center, Moscow State University, Russia

Abstract— Diffraction grating problems, particularly those for multilayer diffraction gratings, require rigorous stable methods, which can provide fast and efficient computations of the grating properties. One of the most efficient numerical techniques is based on a combination of the incomplete Galerkin method and matrix formalism such as transfer matrix method, scattering matrix method etc. Within this approach a grating is approximated by a set of inhomogeneous layers irrespective of the grating groove shape. The structure can also include a stack of homogeneous layers. The diffracted wave field is decomposed into discrete set of plane waves, each of them corresponding to a certain diffraction order. The set of Maxwell equations is reduced to one second-order or a system of two first-order matrix differential equations. The layered structure of the grating makes it reasonable to apply matrix methods. Being rather convenient in implementation, transfer matrix method is numerically unstable due to possible overflows during computations. The existence of evanescent diffraction orders requires taking vary large exponents for thick gratings or for metallic structures, and the calculations are therefore impossible. Scattering matrix approach was suggested as a stable alternative method instead of transfer matrix technique. By implementing the scattering matrix formalism numerical overflows are avoided. However, scattering matrix method has serious problems connected with singularity of a scattering matrix in the case when a new diffraction order appears in one of the grating layers, in an incident medium or in a substrate. The wave vector for this diffraction order is exactly parallel to the layer interface and has zero component in the direction perpendicular to the interface. Treated directly this requires inversion of the propagation matrix, which has a zero eigenvalue. We suggest a rigorous and physically consistent approach to avoid the singularities of this type. We show that additionally in such a case the dimensionality of the matrix equations can be reduced and thus the calculations are simplified.

Projective Methods in Problems of Waveguide with Singularity

A. N. Bogolubov, A. I. Erokhin, and I. E. Mogilevsky
Faculty of Physics, M. V. Lomonosov Moscow State University, Russia

Abstract— Waveguides with reentrant edges in their surfaces are considered. These systems are generally used in microwave devices as filters or their tuning elements. Reentrant edges appear in cases where several waveguides are connected. Reentrant edges can also serve as a model of different scratches in waveguide's surface and a model of electromagnetic probe.

A vectorial mathematical model of electromagnetic waveguides with singularities is proposed. Numerical research is provided using different projective methods. Structure of the electromagnetic field passed through irregular part of the waveguide is obtained using proposed model.

The incomplete Galerkin method as one of projective methods is used to construct approximate solution of the problem. Laplacian Eigen functions of a cross-section of the waveguide irregular part are taken as a basis. This Eigen value problem can be solved by numerical methods only. It is known that the presence of such geometrical singularities as reentrant corners can lead to singularities of solutions of boundary value problems and make the use of numerical methods for the Eigen value problem more complicated.

The asymptotic representation of the solution of Eigen value problem in the vicinity of irregularity of the boundary is obtained by analytical methods. Obtained singularities can be used as testing functions for another projective method, namely finite elements method (FEM). The convergence of numerical solution is proved. Rate of convergence is estimated. As asymptotics by smoothness of singularity is found with arbitrary order of smoothness, the remainder can be obtained with required order of smoothness. An approximation of the smooth part of the solution is a problem that can be solved using standard test functions.

One of the results of mathematical modeling of such structures is a presentation of selective mode propagation through irregular part of the waveguide. It can be explained by the absence of energetical interaction between different modes of the waveguide. Such effect has been already demonstrated using scalar model for description of such systems. The result of the investigation can be used for the development mode filters.

Wavelet Approximation of Discontinuous Solutions in EHD Model of Charged Jet Flow

Oleg Kravchenko[1, 2] **and Dmitriy Churikov**[2]

[1]Bauman Moscow State Technical University, Moscow, Russia
[2]Kotel'nikov Institute of Radio Engineering and Electronics
Russian Academy of Sciences, Moscow, Russia

Abstract— In present work a mathematical two-fluid EHD (Electro-hydrodynamics) model of charged jet flow is investigated numerically. System of nonlinear partial differential equations (PDE) is transformed into Burgers equation with constant source. Afterwards a static case is considered and discontinuous solutions are presented. These discontinuous solutions are approximated numerically by means of wavelet methods and atomic functions theory.

Problems of stability of charged jet flow occupy the central place in EHD. But, the fluid equations are difficult to handle because of their nonlinearity and mathematical complexity as a result. One of the approaches consists to study the influence of an electric field on a velocity field. This approach has been introduced by E. Moreau and O. Vallee [1]. It also has been introduced in [2] by V. I. Pustovoit independently. Such approach allows to reduce a system of nonlinear PDEs into one nonlinear Burgers type equation with constant source.

Wavelet methods are successfully applied to numerical investigation of Burgers type equation [4–6]. Atomic functions have well approximation properties and have found wide application at the decision of applied problems of physics and technics [6, 7].

We consider a static case of Burgers type equation and present a discontinuous solutions governed by conservation low according to [3]. In this paper we employ wavelet numerical method and atomic function theory to construct numerical wavelet approximation of discontinuous solution in EHD problem of charged flow.

ACKNOWLEDGMENT

The author would like to thank Professor Victor Filippovich Kravchenko for his useful comments.

REFERENCES

1. Moreau, E. and O. Vallee, "Connection between the Burgers equation with an elastic forcing term and a stochastic process," *Phys. Rev. E*, Vol. 73, 016112, 2006.
2. Pustovoit, V. I., "Mechanism of lightning discharge," *Journal of Communications Technology and Electronics*, Vol. 51, No. 8, 937–943, 2006.
3. Sapogin, V. G., "On compensation of coulomb interaction of charges by beams self-consistent field (model of isotermal equilibrium with homogeneous temperature)," *Proceedings 1st IEEE International Conference on Circuits and Systems for Communications*, 408–411, St. Petersburg, Russia, 2002.
4. Vasiyev, O. V., "A dynamically adaptive multilevel wavelet collocation method for solving partial differential equations in a finite domain," *Journal of Computational Physics*, Vol. 125, No. 2, 498–512, 1996.
5. Rathish Kumar, B. V. and M. Mehra, "A three-step wavelet Galerkin method for parabolic and hyperbolic partial differential equations," *International Journal of Computer Mathematics*, Vol. 83, No. 1, 143–157, 2006.
6. Kravchenko, V. F., V. I. Pustovoit, and D. V. Churikov, "Application of complex WA-systems of Kravchenko functions to time series processing," *Doklady Physics*, Vol. 56, No. 2, 92–100, 2011.
7. Kravchenko, V. F., *Lectures on the Theory of Atomic Functions and Their Some Applications*, Radiotechnika, Moscow, 2003.

The Scanning Reflective Antenna with an Impedance Conformal Reflector in the Form of Laminated Structure the Semiconductor-dielectric-metal with Photonic Control

A. A. Prilutskiy
JSC Distant Radio Communication Scientific Research Institute
d.12/11, 1-ya Str. Buhvostova, Moscow 107258, Russia

Abstract— Recently the big attention to research of characteristics of reflective arrays with electronic scanning of a beam is paid. The most traditional way of maintenance of phase shift in elements reflective arrays, are phase shifting the short-circuited pieces of transmission lines commutated by pin-diodes (reflective phase shifters). Commutators on the basis of microelectromechanical and nanoelectromechanical systems (MEMS and NEMS), built in radiating structure are even more often used for this purpose. As, the phase shifters using semiconductor devices with variable capacity, operated voltage are applied, ferrite phase shifting sections etc.. For a microwave and millimeter wave the specified approaches lead to the big resistance losses, high currents of consumption and, hence, low radiation efficiency as a whole. In a design of antennas it is required to provide power supplies and management input to the concentrated control elements of the antenna. These elements are in the field of the antenna and often create parasitic effects for which compensation it is necessary to complicate a design essentially.

In this paper, possibility of creation of the conformal scanning reflective antenna with photonic control is investigated. The antenna reflector is executed in the form of the multilayered medium consisting of alternating dielectric layers and semi-conductor films on the metal emulsion carrier which conductivity changes under the influence of optical illumination. Depending on a condition of semi-conductor films on a surface of a reflector of the reflective antenna the cylindrical front of an incident wave is converted to flat front of the reflected. The mathematical model of the reflective antenna in the Kirchhoff approximation is gained. Radiation patterns are resulted at scanning in wide sector of angles. The variants of an antenna design are considered. In the capacity of one of applied application of a layer structure of semiconductor film and dielectric layers on a metal emulsion carrier creation of an antenna reflector is. Such antenna can be not only low profile, but also can possess conformal properties, that are having geometrical matching to a surface, for example flying or a space vehicle.

Mathematical Models of Wave Diffraction Problems and the Numerical Method of Discrete Singularities

Y. V. Gandel[1] and L. Angermann[2]

[1]Karazin Kharkov National University, Kharkov, Ukraine
[2]Institute of Mathematics TU Clausthal, Clausthal-Zellerfeld, Germany

Abstract— We consider boundary-value problems of mathematical diffraction theory and discuss the possibility of reducing them to boundary hypersingular integral equations [1, 2] and solving them numerically. The analytic technique of parametric representations of pseudodifferential and integral operators [3] and the numerical method of discrete singularities [4, 5] are essentially used. We discuss the reasoning in applying this approach to constructing mathematical models of wave diffraction problems and solving them numerically. Diffraction problem is investigated: the problem of electromagnetic wave diffraction on a 3D [2, 6] perfectly conducting plane screen that is situated on a homogeneous media, the problem of electromagnetic wave diffraction on a perfectly conducting plane screen that is situated on a boundary between two media with different permittivity.

REFERENCES

1. Gandel, Y. V., "Boundary-value problems for the Helmholtz equation and their discrete mathematical models," *J. of Mathematical Sciences*, Vol. 171, No. 1, 74–88, 2010.
2. Gandel, Y. V. and V. S. Bulygin, "Boundary integral equations of diffraction problems on flat screens and their discrete mathematical models," *International Journal Electromagnetic Waves and Electronic Systems*, Vol. 15, No. 2, 9–21, 2010.
3. Gandel, Y. V., "Parametric representations of integral and pseudodifferential operators in diffraction problems," *Pros. Tenth Int. Conf. Math. Methods in Electromagnetic Theory*, 57–62, Dnipropetrovsk, 2004.
4. Gandel, Y. V., "The method of discrete singularities in problems of electrodynamics," *Problems of Cybernetic*, No. 124, 166–183, Mosk, 1986.
5. Gandel, Y. V. and A. S. Kononenko, "Justification of the numerical solution of a hypersingular integral equation," *Differ. Equ.*, Vol. 42, No. 9, 1326–1333, 2006.
6. Bulygin, V. S. and Y. V. Gandel, "Boundary-value problems for 3D Helmholts equations, boundary pseudodifferential equations and numerical experiment," *Boundary-Value Problems for Differential Equations*, No. 17, 210–234, 2008.

Session 3P6
Microwave and Millimeter Wave Circuits and Devices, CAD

A New Type of Wilkinson Power Divider with Triple-band Response Based on Dual Transmission Line

Pu-Hua Deng, **Wen-Chian Lai**, **Li-Chi Dai**, **Yu-Ta Chen**, **and Sung-Yen Juang**
Department of Electrical Engineering, National University of Kaohsiung, Taiwan

Abstract— The conventional single uniform transmission line can be equivalent to the dual transmission line, which has been proposed in the previous literature. Because this equivalence is usually not a narrow bandwidth, each transmission line section of conventional tri-band Wilkinson power divider using three-section transmission-line transformers may be replaced by the dual transmission line. Based on this equivalence, a new type of triple-band Wilkinson power divider composed of six dual transmission lines and three resistors between the two transmission paths is presented in this paper. To reduce the total circuit size, the proposed triple-band Wilkinson power divider is implemented by using meander dual transmission lines. Furthermore, the simulated results are good agreement with the circuit models of the proposed divider and conventional tri-band Wilkinson power divider using three-section transmission-line transformers, and the simulated comparison also provides in this study to support our design concept. To verify the proposed design, a new triple-band Wilkinson power divider is carefully examined and fabricated on a substrate with a thickness of 3.2 mm, a relative dielectric constant of 3.55, and a loss tangent of 0.0065.

Nonlinear Phenomena in the Left-handed Ferrite Waveguides

Makoto Tsutsumi[1] **and Kensuke Okubo**[2]

[1]Faculty of Engineering, Fukui University of Technology, Fukui, Japan
[2]Faculty of Computer Science and System Engineering
Okayama Prefecture University, Okayama, Japan

Abstract— Recently we have reported left-handed ferrite waveguide which is based on the composite forms of negative permeability of ferrite and negative permittivity of cutoff TE waveguide, and proposed application to magnetically tunable microwave filter. This paper treats nonlinear phenomena on the left-handed ferrite waveguide both theory and experiments. Perturbation theory on multiple scale was used to solve nonlinear differential equation of electromagnetic field under nonlinear form of ferrite tensor. Dispersion and group delay characteristics were estimated numerically as a function of microwave power. It was found that effect on nonlinearity for left-handed operation is very sensitive compared to the right-handed operation showing change of sign of group delay with microwave power through zero-order resonance. Experiments were undertaken using yttrium iron garnet film and single crystal periodically loaded with several millimeters separation into TE metal waveguide of 10×5 mm cross section under cutoff. Amplitude and phase dependencies on microwave power until 30 dBm were measured. Effect of saturation phenomena on left-handed characteristic was observed at 10 dBm input power along with frequency dispersion. Their results were compared with theory. Application on nonlinear left-handed waveguide was briefly discussed with 20 dBm limiter at S band.

Equivalent Network Extraction of a Coplanar Waveguide

Rizwan Masood[1] **and S. A. Mohsin**[2]

[1]National Engineering and Scientific Commission, Islamabad, Pakistan
[2]The University of Faisalabad, Faisalabad, Pakistan

Abstract— A coplanar waveguide (CPW) is the preferred choice for high frequency structure-design and MMIC applications. The CPW supports a quasi-TEM mode of operation and there is no low frequency cutoff. A CPW can be conventional or conductor-backed (CBCPW). The former has no bottom ground plane whereas the latter has a bottom ground plane in addition to the top semi-infinite ground planes. The lower ground plane not only provides mechanical support to the substrate but also acts as heat sink for CPW based active devices. Furthermore, a CPW can be on a single substrate or on a multilayer dielectric substrate with or without a ground plane. And finally the propagation characteristics (Zo, ε_{eff}, etc.) would also vary based on finite or infinite ground planes.

For Microwave Integrated Circuits (MICs) and Monolithic Microwave Integrated Circuits (MMICs), circuit design is facilitated if a CPW can be replaced by an equivalent network, i.e., the CPW sections are replaced by lumped element network models. This is especially useful for circuit design and CAD applications. Furthermore, CPW based discontinuities can also be replaced by well formulated equivalent networks following the same approach. The CPW open end, short end, series gap, step change in the width of center conductor and the bend are some of such discontinuities.

This work proposes lumped element equivalent networks for a supported CPW, i.e., a CPW on a dielectric substrate with another supporting substrate at the bottom. There is no bottom ground plane and semi-infinite ground planes are assumed. The top substrate considered was Rogers RT 6010 ($\varepsilon_r = 10.2$, $h = 0.635\,\text{mm}$) and the bottom dielectric substrate was RT 5880 ($\varepsilon_r = 2.2$, $h = 1.575\,\text{mm}$).

The scattering parameters of the CPW were obtained by the Method of Moments (MOM) using a commercially available simulator. First, an N-section ladder network equivalent for the CPW is proposed by curve-fitting the already obtained scattering parameters. Then a cascaded lumped Pi network model is proposed by the finite-difference time-domain (FDTD) method using a commercially available CAD program. Finally, a more accurate equivalent network model is proposed by the Model Order Reduction Technique of the FDTD program. This is done by doing a CAD export from the MOM tool to FDTD and generating a SPICE compatible touchtone.

Grounded CPW-WR12 Transition Design for 1.55 μm Photodiode Based E-band Transmitter

Merih Palandöken[1], **Sascha Lutzmann**[1], **Vitaly Rymanov**[2], **Andreas Stöhr**[2], **and Tolga Tekin**[1]

[1]Technische Universität Berlin, Gustav-Meyer-Allee 25, Berlin 13355, Germany
[2]Universität Duisburg-Essen, Lotharstr. 55, Duisburg 47057, Germany

Abstract— As wireless communications have a continuous growth with ever rising demand for higher data-speeds, new technologies and design strategies have to be developed. The most promising method to multi-Gb/s wireless communication is the use of mm-wave frequencies where very large bands of frequency spectrum are available. However, there are important challenges to be overcome such as significantly higher air-link loss (e.g., about 30 dB higher at 60 GHz than at 2.4 GHz), and reduced device performance and lower power efficiency. In addition, the wide channel bandwidth means higher noise power and reduced SNR. Therefore, RF transmission has to be accomplished through high bandwidth and gain antennas with low loss. In order for these antennas to be operated in an optimum manner, the feeding network from mm-wave circuit to the antenna has to be carefully designed. The transitions are therefore important microwave components to obtain optimum coupling from microwave circuits to waveguide feeding networks of high gain transmitting antennas.

In this paper, a grounded coplanar waveguide (GCPW) to rectangular waveguide is proposed as a millimeter wave component in wireless E-band applications. One side of GCPW is terminated with a broadband circular short-circuited slot line. The other side is tapered linearly to be matched to the wave impedance of fundamental mode of rectangular waveguide. The transition design provides easy fabrication of GCPW circuit. Due to the ground plane of GCPW, the transition can be quite precisely positioned inside the waveguide with any dielectric/metallic material under the ground plane. The transition has smaller than 0.5 dB insertion loss in the frequency band of 62–80 GHz. The effects of geometrical parameters on the transmission are additionally investigated in order to verify the design approach and determine the critical design parameters.

Integrating Equal-split Wilkinson Power Dividers and Coupled-line Bandpass Filters

P. H. Deng, L. C. Dai, and Y. D. Chen
Department of Electrical Engineering, National University of Kaohsiung
No. 700, Kaohsiung University Road, Nan-Tzu District, Kaohsiung 81148, Taiwan, R.O.C.

Abstract— Conventional equal-split Wilkinson power dividers usually demonstrate poor selectivity. By cascading an additional bandpass filter before the input or after each output port of the conventional equal-split Wilkinson power divider, the band selection of each transmission path can be enhanced substantially. However, the selectivity has been increased at the cost of a large circuit area by connecting an additional filter. Therefore, integrating bandpass filters and conventional equal-split Wilkinson power dividers may provide a solution for reducing the total circuit size. This paper presents a novel type of divider with favorable selectivity using two coupled-line bandpass filters to replace two quarter-wavelength ($\lambda/4$) transformers of a conventional Wilkinson power divider. Specifically, two crucial design conditions should be met for each coupled-line bandpass filter. The first condition requires fitting a system impedance of $70.7\,\Omega$ for each filter when the termination impedances at all ports of the divider are set at $50\,\Omega$. The second condition requires selecting an even-order coupled-line bandpass filter, because the filter order may significantly affect the performance of the divider. Notably, the selectivity of the proposed divider is similar to that of the conventional equal-split Wilkinson power divider with an additional filter placed before the input port or after each output port. Nevertheless, the proposed type of divider can avoid two $\lambda/4$ transformers, which are usually used in the conventional Wilkinson power divider. For demonstration, two equal-split Wilkinson power dividers with high-quality band selection are proposed in this study, achieving favorable agreement with simulated and measured responses.

Wideband Microstrip Line Diplexer by Bandpass Filters Using Resonators Based on Coupled Line and Transmission Line with Ground

Kosei Tanii and Koji Wada
The Department of Electronic Engineering
The University of Electro-Communications, Chofu-shi, Tokyo, Japan

Abstract— Recently, wireless communication system is getting complex since it is necessary to apply various applications in one radio equipment. To give mobile phone as an example, 3G (WCDMA, CDMA-2000), 4G (LTE, LTE advance), bluetooth and others are available in one. Hence, the components such as antenna, filters and others applying to multi band technology as well as the improvement of their performances are required. On the other hand, the bandwidth of communication system is getting wider in order to increase the bit rate. The bandwidth between 200 MHz and 500 MHz is used for WiMAX and a few GHz is used for ultra-wideband (UWB) although the bandwidth differs according to the country, standard and regulation. From these points of view, wideband frequency multiplexer is being required in near future and it is being researched [1, 2].

In this work, at first, a new BPF is proposed by focusing on wide passband, attenuation poles and steep skirt characteristics. The resonator used in the proposed BPF is composed of a transmission line with ground and a coupled line. As for its characteristics, attenuation pole whose realization condition is obtained by the admittance of each section is realized near lower edge of passband. Furthermore, the BPF using two series of this and open (or short)-circuited stub is realized. Owing to the stub, attenuation pole is realized at higher edge of the passband. With this structure, three types of BPFs are composed and their bandwidths are all 2 GHz and they are 3.1–5.1 GHz, 5.85–7.85 GHz and 8.6–10.6 GHz, respectively. These are decided by UWB spectrum mask in USA as an example of wideband wireless communication system. The attenuation less than −30 dB is obtained at stop band and the edge of pass band is steep by realized attenuation poles. Then, the diplexers are composed by using these filters. Good attenuation level at stop band helps them to be composed easily. Figure 1 shows the layout pattern of the diplexer using of one mentioned BPFs. The proposal diplexer produces two passbands (3.1–5.1 GHz (Filter A) and 5.85–7.85 GHz (Filter B)). The attenuation level at another passband in diplexer characteristics is under −40 dB. Therefore the isolation level at each pass band is also under −40 dB although the return loss should be improved.

All the resonators and BPFs are realized by microstrip line structure. The dielectric substrate is H220A (The relative dielectric constant is 2.2, the dielectric substance thickness is 0.5 mm and the metal thickness is 18 µm, NIPPON PILLAR PACKING CO., LTD.). The electromagnetic simulator of SONNET and the circuit simulator of ADS are used for technical examination.

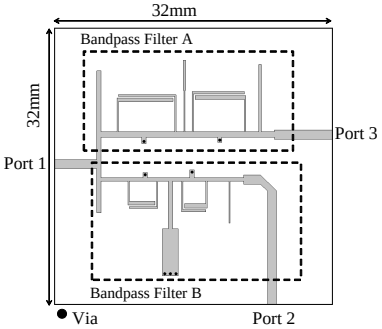

Figure 1: Layout pattern of the diplexer (3.1–5.1 GHz, 5.85–7.85 GHz).

REFERENCES

1. Shinpei, O., et al., "A study on a multilayer diplexer using LTCC technology for ultra-wideband wireless modules," *IEICE Electrocs Express*, Vol. 8, No. 11, 848–853, 2011.
2. Magnus, K., et al., "A frequency triplexer for ultra-wideband systems utilizing combined broadside- and edge-coupled filters," *IEEE Transactions on Advances Pckaging*, Vol. 31, No. 4, 794–801, 2008.

Analyse, Design and Development of 1–26.5 GHz TRL Microstrip Calibration Kit

Ebrahim Feizi Barnaji, Gholamreza Moradi, and Abdolali Abdipour
Amirkabir University of Technology, Iran

Abstract— Known devices called "calibration standards" provide the measurement reference for network analyzer error-correction. Microstrip devices in the form of chips, MMIC's, packaged transistors, or beam-lead diodes cannot be connected directly to the coaxial ports of a network analyzer. The device under test (DUT) must be physically connected to the network analyzer by some kind of transition network or fixture. Calibration for a fixtured measurement in microstrip presents additional difficulties. A calibration at the coaxial ports of the network analyzer removes the effects of the network analyzer and any cables or adapters before the fixture; however, the effects of the fixture itself are not accounted for. An in-fixture calibration is preferable, but high-quality Short-Open-Load-Thru (SOLT) standards are not readily available to allow a conventional Full 2-port calibration of the system at the desired measurement plane of the device. In microstrip, a short circuit is inductive, an open circuit radiates energy, and a high-quality purely resistive load is difficult to produce over a broad frequency range. For removing effect of this fixture, in-fixture calibration named TRL has been introduced. In this work, we have designed TRL microstrip calibration standard kit for frequency band 1–26.5 GHz. This calibration kit contains 3 standards: Thru, Line and a high reflective standard, normally a short. Each of this standards must satisfy some requirements for doing error correction to a reasonable amount of accuracy. After designing, we evaluate this requirements using High Frequency Structure Simulator (HFSS) and FDTD numerical method. After development of the kit we need to evaluate it's performance. So we use some devices to check it's performance. Comparing measurement results and simulation show that the calibration kit has a very good performance.

Functional Digital Materials for Electromagnetic Structures and Circuits

Nadya Peek, **Rehmi Post**, **and Neil Gershenfeld**
MIT Center for Bits and Atoms, 20 Ames st. E15-401, Cambridge, MA 02139, USA

Abstract— We demonstrate a digital manufacturing paradigm applied to the assembly of electromagnetic systems. These *digital materials* are constructed from a small set of discrete parts that fit together in a coded manner with discrete orientations. Additively assembled digital materials offer a new mode of electronic device fabrication with affordances for new device geometries as well as device disassembly and reuse.

Subtractive and additive manufacturing processes have long been the norm for electronics production, using methods like lithography or micromachining to pattern elements onto bulk materials [6]. Additive processes have started replacing subtractive ones for high-throughput production, but it is still difficult to print high-Q structures. Furthermore, as devices grow in complexity and size they impose ever-greater requirements on process control, increasing cost and decreasing yield. Finally, traditionally-fabricated electronic devices cannot easily be reused, resulting in millions of tons of e-waste each year [1].

Instead of shifting from subtractive to additive manufacturing, we propose moving from the analog world to the digital. Just as the digital paradigm revolutionised communications and computation, digital materials will change how we assemble the built world. Codes can dictate how devices are constructed from elemental parts, much like the genome dictates how organisms are constructed from proteins. The parts can be error-correcting, with the materials dictating precision instead of the assembler. Furthermore, devices can be disassembled and their parts reused to make new devices.

To explore new circuit geometries and fabrication methods that allow for disassembly and reuse, we propose to use functional digital materials for electronic device manufacturing. Digital materials have already been proposed for certain types of manufacturing [3–5, 7, 8], and preliminary designs for assemblers that place or recycle digital materials have also been proposed [2, 9–11]. However, there has not yet been a study of digitally fabricated electromagnetic devices.

This paper describes the characteristics and geometries of several different digital material bricks: conductive, resistive, insulative, dielectric, and ferromagnetic. Different part geometries, manufacturing techniques, and electronic properties of each brick are outlined, using both simulated and experimental data. The bricks are designed to be placed by a high-speed assembler for automated construction and disassembly.

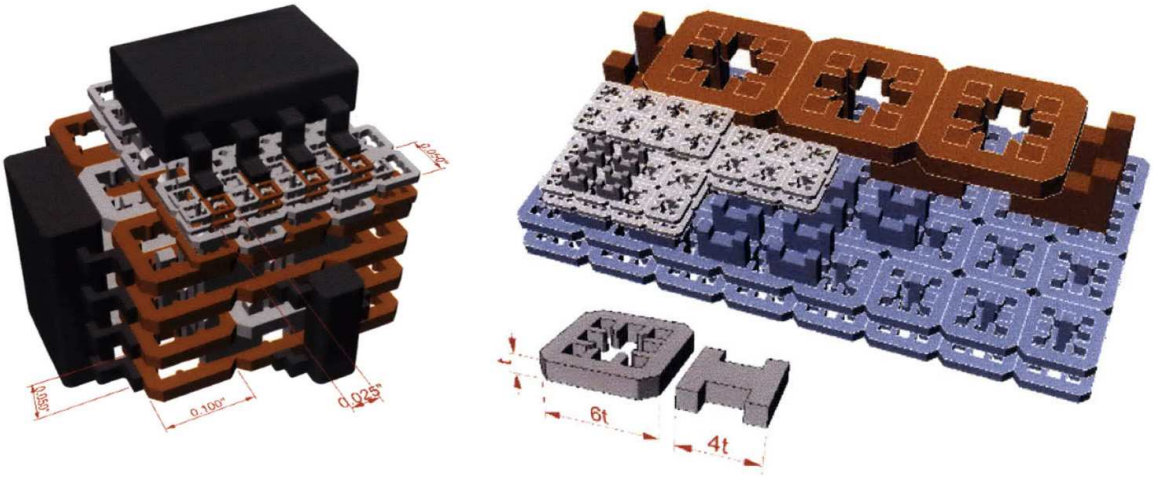

Figure 1: An example of a digital material geometry which can be used as an alternative to printed circuit boards for components with SOIC-pitch [10]. We propose integrating passive components into the 3D structure itself.

Using these bricks as material building blocks we demonstrate how to make circuits with 3D structure and integrated passive components as well as 2-port electromagnetic networks such as microstrip transmission lines and matching networks. We characterise the performance of these devices under various amounts of mechanical loading. Finally we demonstrate a fully functioning data radio circuit including integrated matching network and antenna, fabricated using only digital materials and standard semiconductor devices.

REFERENCES

1. Environmental Protection Agency Office of Research and Development, E-Cycling, US Executive Branch, 2011, http://www.epa.gov/osw/conserve/materials/ecycling/.
2. Griffith, S., D. Goldwater, and J. M. Jacobson, "Self-replication from random parts," *Nature*, Vol. 437, No. 29, 2005.
3. Hiller, J. and H. Lipson, "Design and analysis of digital materials for physical 3D voxel printing," *Rapid Prototyping Journal*, Vol. 15, No. 2, 2009.
4. Hiller, J. and H. Lipson, "Tunable digital material properties for 3D voxel printers," *Rapid Prototyping Journal*, Vol. 16, No. 4, 2010.
5. Hiller, J. D. and H. Lipson, "Fully recyclable multi-material printing," *Proceedings of the Solid Freeform Fabrication Symposium*, 2009.
6. Kaeslin, H., *Digital Integrated Circuit Design: From VLSI Architectures to CMOS Fabrication*, 2008.
7. Popescu, G., "Digital materials for digital fabrication," Master's thesis, Massachusetts Institute of Technology, Cambridge, MA, 2007.
8. Popescu, G., N. Gershenfeld, and T. Mahale, "Digital materials for digital printing," *DF 2006 International Conference on Digital Fabrication Technologies*, Denver, CO, 2006.
9. Popescu, G., P. Kunzler, and N. Gershenfeld, "Digital printing of digital materials," *DF 2006 International Conference on Digital Fabrication Technologies*, Denver, CO, 2006.
10. Ward, J., "Additive assembly of digital materials," Master's thesis, Massachusetts Institute of Technology, 2010.
11. Whitesides, G. M. and B. Grzybowski, "Self-assembly at all scales," *Science*, Vol. 295, No. 5564, 2418–2421, 2002.

Full-wave Modeling of Open Subwavelength Resonator with Metamaterial

A. P. Smirnov, **A. N. Semenov**, **D. O. Ignatyeva**, **and A. P. Sukhorukov**
Lomonosov Moscow State University, Moscow, Russia

Abstract— The properties of an open Fabry-Perot nano resonator containing a layer of metamaterial with a negative refractive index are investigated. Numerical simulation of this cavity is performed using an EMWSolver3D solver based on the FDTD scheme, with Drude model for the frequency dependent media and the UPML absorbing boundary conditions for open region simulations. It demonstrate's that waveguide eigenmodes with arbitrary profiles exist in such a cavity and the metamaterial layer considerably lowers diffraction losses. It was shown that even though diffraction theory is not formally applicable on nano scales, waveguide modes with an arbitrary distribution of amplitude can be excited if the effective diffraction length is zero.

A K-band Low Noise and High Gain Down-conversion Mixer

Chia-Yang Huang and Yen-Chung Chiang
National Chung Hsing University, Taiwan

Abstract— A down-converting mixer implemented in the TSMC 0.18-µm RF-CMOS process technology for applications in the K band is presented in this paper. Based on the conventional Gilbert cell topology, a dynamic current bleeding technique is adopted to suppress the flicker noise generated by the switch stage and thus to improve the noise figure (NF) of the mixer. Besides, an inductor for resonating the parasitic capacitances at the output of the transconductance (Gm) stage is utilized to increase the conversion gain and the linearity of the mixer. The chip size of the proposed mixer is $1.06 \times 0.98\,\mathrm{mm}^2$. The measured peak power conversion gain for the proposed K-band mixer is 9.05 dB and the measured noise figure is 10.64 dB, respectively, at 22 GHz. And the measured 1 dB compression point (P1 dB) and IIP3 are −7.4 dBm and 0.5 dBm, respectively, at 24 GHz. The core circuit of the proposed mixer draws a 3.14 mA dc current from the 1.8 V voltage supply.

Multidimensional *S*-parameters: Modeling, Measurement, Identification and Computer-aided Design of Nonlinear Microwave Circuits

S. M. Nikulin, A. A. Terentyev, and I. P. Shishkina
Alekseev's Nizhny Novgorod State Technical University, Russia

Abstract— In recent years, practically useful results have been achieved in the theory and practice of measuring parameters, as well as in modeling and computer-aided design of nonlinear RF and microwave devices. Here we should first mention an extended version of linear S-parameters-X-parameters and Agilent Technologies' nonlinear vector network analyzer (NVNA). However, X-parameters are characterized by structural imperfection and excessive redundancy of information, and their measurements don't meet the optimal price/quality ratio and therefore encourage seeking and developing alternative solutions.

This paper presents a different mathematical tool for modeling and computer-aided design of nonlinear circuits which has a natural ease for the practice of engineering, a high speed, and doesn't require excessively high costs for the implementation of measurements. A mathematical model of nonlinear microwave circuits is proposed in the form of multidimensional S-parameters as analytical functions of frequency and absorbed power. The key element in solving the problem of measurement and computer-aided design of nonlinear devices is the S-parameters of a cascade consisting of the input circuit A, the output circuit B and the nonlinear circuit.

In this paper, simplified relations for the reflection and transmission coefficients of the cascade at the fundamental and second harmonic are obtained. It is shown that the six significant parameters are involved in the transformation of the fundamental tone of the second harmonic and the second harmonic of the fundamental tone.

Also a new method for the measurement and identification of nonlinear circuit model parameters using a two-port vector network analyzer E5072A is presented. The prospects of computer-aided design of nonlinear circuits with multidimensional analytical models of S-parameters are discussed.

Phase Locking and Phase Control in Oscillators Using a Short External Signal

Mikhail Fuks[1], **Edl Schamiloglu**[1], **and Mikhail Petelin**[2]

[1]Department of Electrical and Computer Engineering, University of New Mexico
MSC01 1100, Albuquerque, NM, 87131-0001, USA
[2]Institute of Applied Physics, Russian Academy of Sciences
46 Ul'yanov Street, Nizhny Novgorod 603950, Russia

Abstract— It is well known [1, 2] that an external signal with sufficiently strong amplitude and with radian frequency ω_{in} introduced into an oscillator whose frequency ω_0 of free oscillations is close to ω_{in} leads to phase locking when the frequency of oscillations becomes the frequency of the external signal and phases of oscillations are uniquely determined by the phases of the external signal. Outside this locking region the beating of the oscillations with these close but isolated frequencies takes place without correlation between their phases. Phase locking is used in many applications [3], such as frequency stabilization, phase and amplitude modulation, coherent generation of pulses, and others. Recently there has been increased interest in the parallel operation of high power oscillators for coherent summation of their radiation (phase coherence) [4], although attempts to use the locking regime for this have a long history [5].

In this present work, we demonstrate that a short pulse duration external signal also leads to phase locking when the amplitude of this signal is sufficiently high; however, outside the region of phase locking when the oscillator operates at the frequency of free oscillations their phases correlate with the initial phase φ_{in} of the external signal $F_{\text{in}} = F_{0,\text{in}} \sin(\omega_{\text{in}} t + \varphi_{\text{in}})$; i.e., phase control takes place in spite of the difference in frequencies of the external signal and the free oscillations. This occurs because in the Fourier integral of the short external signal a spectral component exists whose frequency is that of the free oscillations. The same reason leads to the prevailing of the regular part over noise in the initial seed for start oscillations when the applied voltage has a short leading edge, as in [4].

We illustrate scenarios of phase locking and also phase control outside the region of phase locking using computer simulations for a relativistic magnetron with diffraction output (MDO) [6] controlled by a short external signal when the duration of the leading edge τ_U of the applied voltage pulse is shorter than the characteristic filling time τ_E of the electrodynamic system with electromagnetic energy, $\tau_U < \tau_E = \omega/Q$ (here ω is the radian frequency of generation and Q is the loaded quality factor). For the MDO we found boundaries of the value of the applied axial magnetic field between regions of synchronous interaction of electrons with neighboring modes in which the bifurcation of the frequency of free oscillations takes place. The scenarios of phase locking using an external signal are explained using the properties of dynamical systems with two stable states separated by an unstable saddle point. In particular, it is found that near the boundaries the generation of a switched mode persists in spite of the elimination of the short external signal. We also found that the phenomenon of mode switching is not only attributed to the closeness of frequencies of the free oscillations ω_0 and external signal ω_{in}, and not only to a sufficient amplitude $F_{0,\text{in}}$ of the external signal, but also to the initial phase φ_{in} of the external signal that can be explained by the vector sum of the regular and irregular parts in the initial seed.

Finally, we found that in the regime of phase locking, the phase φ in generated oscillations $F = F_0 \sin(\omega t + \varphi)$ is changed in any time t as the initial phase φ_{in}, whereas outside the locking region the change of the initial phase from 0 to 2π leads to a change in the phase of generated oscillations from 0 to $\omega_{\text{in}} T$, where $T \approx 2\pi \left|\omega_0 - \omega_{\text{in}}\right|^{-1}$, and this dependence is unique. Thus, using an applied short external signal phase control can takes place whether or not oscillators are in the phase locking regime.

ACKNOWLEDGMENT

Research at the University of New Mexico was supported by AFOSR Grant FA9550-11-1-0200.

REFERENCES

1. Van der Pol, B., *The London Edinburgh and Dublin Philosophical Magazine and Journal of Science*, Ser. 7, No. 3, 65–80, 1927.

2. Adler, R., *Proc. IRE*, Vol. 34, 351–357, 1946.
3. David, E. E., *Crossed-field Microwave Devices*, E. Okress, Ed., 375–399, Academic Press, London, NY, 1961.
4. El'chaninov, A. A., A. I. Klimov, O. B. Koval'chuk, G. A. Mesyats, I. V. Pegel', I. V. Romanchenko, V. V. Rostov, K. A. Sharypov, and M. I. Yalandin, *Technical Physics*, Vol. 56, No. 1, 121–126, 2011.
5. Bostick, W. H., E. Everhart, and. M. Labitt, *Tech. Rep.*, No. 14, Research Laboratory of Electronics at MIT, 1946.
6. Fuks, M. and E. Schamiloglu, *IEEE Trans. Plasma Sci.*, Vol. 38, No. 6, 1302–1313, 2010.

Characteristics of Nano-oscillators Loaded by Metamaterials

Ansar Safin[1], **Fedor Kovalev**[1], **and Alexey Basharin**[2]

[1]National Research University "Moscow Power Engineering Institute", Russia
[2]Institute of Electronic Structure and Laser (IESL)
Foundation for Research and Technology Hellas (FORTH), Heraklion, Crete, Greece

Abstract— Recently the problem of signal transmission in the nanoscale has attracted for applications in micro-and nano-processor technology. The most promising radiators of electromagnetic waves at the nanoscale are the spin transfer nano-oscillators (STNO), based on the effects of spin transfer torque and giant magnetoresistance. The maximum of signal power for the standard design STNO less than ??? 10^{-12} W, which is significantly below of the standard method using STNO as a voltage controlled oscillator (less than units of microwatts). In this connection important task is to increase the power of the unit STNO by improving its radiation characteristics. For this task, in this paper we propose a method that proved itself in the optical domain and based on the use of nano-self-Similar chain structures based on metamaterials (structures with negative permittivity and (or) permeability).

Analysis of Embedded-silicon-substrate Impact on CiSP Design

Jang-Hoon Lee, **Jinho Song**, **Jae-Kyung Wee**, **and In-Chae Song**
School of Electronics, Soongsil University, Korea

Abstract— In this paper, we evaluated the embedded-silicon-substrate effects on line characteristics and proposed routing design guides that consider loss by the effect of an embedded IC in a chip-in-substrate package (CiSP). In order to achieve this purpose, the coplanar waveguides (CPWs) over an embedded IC and over a ground plane were devised and analyzed using HFSS. In addition, characteristics of via holes by the silicon substrate were simulated with real via topologies. In the designed CiSP, design guides of line routing are suggested for an optimized signal and power paths which are considered with geometry factors like location, length of CPWs over a silicon substrate, and positions of via holes from a silicon substrate. Of course, the operating frequencies should be considered as a key design factor in order to minimize the dielectric loss by an embedded IC. In the results, we showed four factors for CiSP design, clearly. Firstly, the signal loss of a CPW over an embedded IC is larger than its loss over a ground plane but the effect of IC substrate on signal loss are confined just over around embedded IC. Secondly, the optimal design has the trade-off between the short line over the lossy substrate and the long line over ground plane, e.g., its design needed to consider the view of total losses of transmission lines. The verification for optimized signal and power paths are performed with using *ABCD* matrix chain method. Generally, the length of a line is dominant in low frequencies for the total loss of a transmission line, while the effect of dielectric loss by an embedded IC is dominant in high frequencies. Thirdly, the signal degradation on via holes is strongly dependant on the ratio of the via height and the distance between a via and an embedded IC. Especially, the dependency is severer on the signal degradation at higher frequencies. Finally, a ground guard between a via and an embedded IC reduces the power loss or signal degradation happened by an embedded IC. Therefore, the obtained results can be useful for design of signal and power paths having low loss in small area of CiSP.

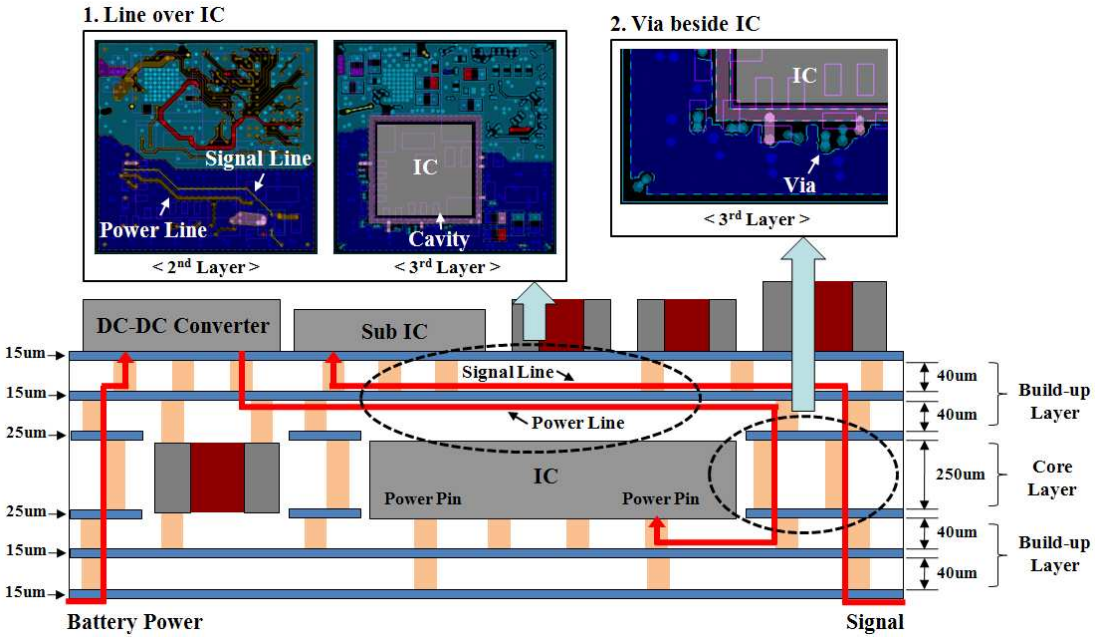

Figure 1: Two design issues of signal and power paths in CiSP.

Session 3P7a
Smart Functional Materials for Non-destructive Control and Stress Monitoring

A MEG Measurement Using Pico-Tesla Sensitivity Amorphous Wire Magneto-impedace Sensor for Brain Activity Evaluation

Tsuyoshi Uchiyama[1], **Kaneo Mohri**[2], **and Shinsuke Nakayama**[3]

[1]1Graduate School of Electrical Engineering and Computer Science
Nagoya University, Nagoya 464-8603, Japan
[2]Nagoya Industrial Science Research Institute (NISRI), Nagoya 464-0819, Japan
[3]Graduate School of Cell Physiology, Nagoya University, Nagoya 466-8550, Japan

Abstract— The highly sensitive micro-sized magnetic sensor due to magneto-impedance (MI) effect has been established avoiding the inner core magnetization accompanied with the demagnetization disturbance and spike domain fluctuation noises [1]. The micro sized linear magnetic sensor using MI element in the pickup coil has been used for electronic compasses in the mobile phone [1]. The magnetic field detection resolution of the liner type MI sensor is estimated to be $1\,\mathrm{pT/Hz^{1/2}}$, which would be useful to measure various bio-magnetic fields. We have proposed the feasibility of the medical application of the very high sensitive linear MI sensor as a noninvasive and non-electrode tool for diagnosis [2, 3].

We have tried to measure magneto-encephalogram (MEG) using the pico-tesla resolution (pT) MI sensor under the no shield environment. Fig. 1 illustrates measurement results of time sires of magnetic field for a seated 50 aged man in comparison with back ground noise. The eyes were opened during first 8 seconds and then closed following 8 seconds. It is shown that magnetic signal intensity from back of the head is more than ten times larger than that of background noise. According to the time series of magnetic an alpha wave component (8–13 Hz) seems to be enhanced after eyes closed. We have been successful to evaluate arousal effect due to physiological magnetic stimulation using MEG signals [4].

Event-related potentials have been widely used to examine brain activity and cognitive functions in a wide variety of stimulus-response paradigms. The P300 is evoked by rare and task-relevant stimuli. That occurs at a latency from 240 to 700 ms, depending on subject and task variables. We also studied magnetic fields related by P300 using pT MI sensor.

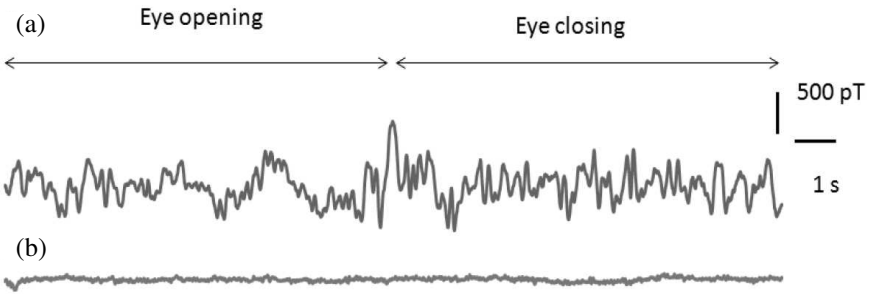

Figure 1: Magnetic field from the back left side of the head in (a) and back ground noise in (b).

REFERENCES

1. Mohri, K. and Y. Honkura, "Amorphous wire and CMOS IC-based magneto-impedance sensors — Origin, topics, and future," *Sensor Letter*, Vol. 5, 267–270, 2007.
2. Uchiyama, T., S. Nakayama, K. Mohri, and K. Bushida, "Biomagnetic field detection using very high sensitivity magnetoimpedance sensors for medical applications," *Physica Status Solidi A*, Vols. 1–5, 639–643, 2009.
3. Uchiyama, T., K. Mohri, and S. Nakayama, "Measurement of spontaneous oscillatory magnetic field of guinea-pig smooth muscle preparation using Pico-Tesla resolution amorphous wire magneto-impedance sensor," *IEEE Trans. Magn.*, Vol. 47, No. 10, 3070–3073, 2011.
4. Mohri, K., T. Uchiyama, M. Yamada, T. Watanabe, Y. Inden, T. Kato, and S. Iwata, "Arousal effect of physiological magnetic stimulation on elder person's spine for prevention of drowsiness during car driving," *IEEE Trans. Magn.*, Vol. 47, No. 10, 3066–3069, 2011.

Ferromagnetic Microwire Usage for Magnetic Tags

S. Gudoshnikov[1, 2], **N. Usov**[1, 2], **A. Ignatov**[3], **V. Tarasov**[3], **A. Zhukov**[2, 4, 5], **and V. Zhukova**[2, 4]

[1]Pushkov Institute of Terrestrial Magnetism, Ionosphere and Radio Wave Propagation (IZMIRAN), Troitsk, Moscow Region, Russia
[2]Ltd. "Magnetic and Cryoelectronic Systems", Troitsk, Moscow Region, Russia
[3]National University of Science and Technology "MISiS", Moscow, Russia
[4]Dpto. de Fisica de Materiales, Fac. Químicas, Universidad del Pais Vasco, San Sebastián, Spain
[5]IKERBASQUE, Basque Foundation for Science, Bilbao, Spain

Abstract— Amorphous and nanocrystalline ferromagnetic microwires exhibit a number of unusual magnetic properties suitable for various technical applications, such as magnetic bistability, excellent magnetic softness or giant magneto-impedance (GMI) effect [1–3]. Due to their small sizes and high magnetic response these microwires have been considered as new Tags for Electronic article surveillance (EAS) applications [3–5]. The available Tags are usually made of an amorphous material with a moderate coercivity (magnetic "hardness"). Detection is achieved by summing or subtracting the non-linear magnetic response signals generated by the amorphous material under the influence of applied magnetic field. The Fe-rich microwires with positive magnetostriction showing magnetically bistable behaviour under the influence of uniform external magnetic field look quite attractive for EAS applications. The bistable behaviour of these microwires has been interpreted as a magnetization reversal of a large magnetic domain in a single Barkhausen jump.

It has been shown that the bistable behaviour exists even in short pieces of Fe-rich microwires of several mm length [6, 7]. Consequently it has been suggested to use small pieces of Fe-rich microwires as passive magnetic Tags to generate electromagnetic response under the influence of alternating external magnetic field of low frequency. However, up to now the registration of the electromagnetic harmonics of magnetic Tags made of Fe-rich microwires was demonstrated only at maximal distances of the order of 10–20 cm [5] The aim of the present paper is a first experimental confirmation of the registration of electromagnetic harmonics of Fe-rich bistable microwires at distances up to 40–45 cm from the receiving coil, i.e., the typical distances for commercially available EAS that uses soft magnetic ribbons with high level of magnetic susceptibility, but showing no bistable behavior.

In the present paper the amplitudes of electromagnetic harmonics generated during the microwire magnetization reversal were measured as a function of a distance of the Fe-rich microwire Tag from a pick-up coil. Several Fe-rich microwire Tags having various lengths l up to 5 cm and metallic nuclear diameters $d = 90$–$100\,\mu$m were investigated. The magnetic Tag is excited by an alternating magnetic field with a maximal amplitude $H_m \sim 8$ Oe at a basic frequency $f = 332$ Hz. The receiving square pick-up coil with $N = 20$ turns has a side $a = 20$ cm. As a registration facility a low frequency spectrum analyser CF 5210 and a digital oscilloscope were used. It has been demonstrated that the amplitudes of the electromagnetic signals of Fe-rich bistable Tags can be detected at the distances ~ 40 cm from the receiving pick-up coil at the signal to noise ratio greater then 2.0. The results obtained show that the Fe-rich bistable magnetic Tags can be considered as good candidates to develop a new generation of passive magnetic Tags for EAS.

REFERENCES

1. Zhukov, A., J. González, J. M. Blanco, M. Vázquez, and V. Larin, *J. Mat. Res.*, Vol. 15, 2107, 2000.
2. Zhukova, V., M. Ipatov, and A. Zhukov, *Sensors*, Vol. 9, 9216, 2009.
3. Vazquez, M., H. Chiriac, A. Zhukov, L. Panina, and T. Uchiyama, *Phys. Status Solidi A*, Vol. 208, 493, 2011.
4. Rodionova, V., M. Ipatov, M. Ilyn, V. Zhukova, N. Perov, J. Gonzalez, and A. Zhukov, *J. Supercond. Nov. Magn.*, Vol. 24, 541, 2011.
5. Gudoshnikov, S., N. Usov, A. Zhukov, V. Zhukova, P. Palvanov, B. Ljubimov, O. Serebryakova, and S. Gorbunov, *Phys. Status Solidi A*, Vol. 208, 526, 2011.
6. Vazquez, M. and A. Zhukov, *J. Magn. Magn. Mater.*, Vol. 160, 223, 1996.
7. Gudoshnikov, S. A., Y. B. Grebenshchikov, B. Y. Ljubimov, P. S. Palvanov, N. A. Usov, M. Ipatov, A. Zhukov, and J. Gonzalez, *Phys. Stat. Solidi A*, Vol. 206, 613, 2009.

GMI Effect in Co-based Amorphous Ribbons Obtained under the Action of a Magnetic Field

L. González[1], **T. Sánchez**[1], **J. D. Santos**[1], **M. L. Sánchez**[1], **B. Hernando**[1], **A. Chizhik**[2], **L. Domínguez**[3], **J. M. Blanco**[3], **V. Zhukova**[2], **M. Ipatov**[2], **A. Zhukov**[2], **and J. González**[2]

[1]Departamento de Física, Universidad de Oviedo, Calvo Sotelo s/n, Oviedo-33007, Spain
[2]Departamento de Física de Materiales, Facultad de Química
Universidad del País Vasco, San Sebastián 20018, Spain
[3]Departamento de Física Aplicada I, EUPD, Universidad del País Vasco, San Sebastián 20018, Spain

Abstract— The magnetoimpedance response of the soft amorphous magnetic CoFeNiSiB alloy can be improved by the application of a small magnetic field during the fabrication process. This route of fabrication would induce a small transverse anisotropy without losing the amorphisation and good mechanical behaviour of the samples with the benefits that such route avoiding the post-processing after the fabrication process following the conventional induction methods. In addition, this transverse anisotropy has associated non-axial components of the magnetic permeability necessary to observe the GMI effect. In this work, we analyse the effect of the induction of a small anisotropy during the quenching procedure by means of magneto-optical Kerr effect and by the magnetic response of the voltage induced in a secondary pick-coil when an ac electrical current is flowing along the ribbon and simultaneously an axial magnetic field is applied. Results show promising behaviour in this type of easily induced magnetic anisotropy, with higher sensitivity to applied magnetic fields, in the field of sensitive magnetic devices for sensor application.

Surface and bulk magnetic (hysteresis loop) behaviour as well as magnetoimpedance response of melt-spun Co-based amorphous ribbons obtained by two different ways of production processes are analysed in this work. One of them was quenched in the usual way (as quenched, aq) and another one was obtained with the simultaneous application of a magnetic field of 700 Oe applied in the transverse direction of the ribbon, perpendicularly to the wheel during the quenching process (field-quenched sample). The ribbons are 10 cm long. High sensitivities to the applied magnetic field up to 320%/Oe are observed when a small transverse anisotropy is induced in the ribbon sample during the fabrication process under the action of a magnetic field.

A different magnetic behaviour has been observed: a small magnetic anisotropy develops in the transverse direction in the fq sample that giving rise to a roughly linear inclination of the hysteresis loop of the fq sample at low applied magnetic field.

Large induced voltage responses are obtained for the field-quenched sample, demonstrating the application of this simple technique for inducing anisotropies strongly affecting to the MI response. The drive current frequency and the anisotropy distribution in the outer shell of the samples play an important role in the response to magnetic fields. TA two-peak structure can be observed in both cases, for the shown drive current frequencies. The sharpest peaks take place at 0.6 MHz. At the higher 1.3 MHz frequency, there is also a smaller peak at $H = 0$ Oe. Sensitivities to the applied field of 320%/Oe and 92%/Oe were obtained for the fq and aq samples respectively at 0.6 MHz. The peaks at 1.3 MHz have lower sensitivities, of 14%/Oe and 13%/Oe for the fq and aq samples respectively. The peak at $H = 0$ Oe has still a high value for the fq sample (67%/Oe) as compared to the aq sample (1%/Oe). The large sensitivities are due to the narrowness of the peaks.

Tailoring of Frequency and Magnetic Field Dependence of Giant Magnetoimpedance Effect in Thin Wires

A. Zhukov[1, 2], **M. Ipatov**[1], **and V. Zhukova**[1]

[1]Dpto. de Fisica de Materiales, Fac. Químicas, UPV/EHU, San Sebastián 20018, Spain
[2]IKERBASQUE, Basque Foundation for Science, Bilbao, Spain

Abstract— Studies of giant magneto-impedance (GMI) effect in different magnetically soft materials attracted considerable interest mainly owing to great sensitivity to applied magnetic field allowing use of materials with high GMI effect for sensitive magnetic field microsensors [1, 2]. Up to now magnetically soft wires exhibiting high circumferential magnetic permeability and excellent soft magnetic properties are considered the best candidates for development of such magnetic microsensors. Therefore, tailoring of magnetic field and frequency dependences of GMI effect are important from point of view of technological applications of these materials.

We present the results on studies of GMI effect in thin microwires at extended frequencies range paying special attention to tailoring the GMI effect and achievement of high GMI effect with low hysteretic behavior. We measured magnetic field, H, dependence of real part, Z_1 of the longitudinal wire impedance Z ($Z = Z_1 + iZ_2$) in frequencies range, f, from 1 MHz to 4 GHz in Co-rich microwires with different geometries and different magnetostriction constant. We studied Co-rich microwires with different diameters of metallic nucleus, d, total diameters, D, and consequently different ρ-ratios ($\rho = d/D$) fabricated by the Taylor-Ulitovsky method.

The strength of internal stresses, σ_i, arising during simultaneous rapid quenching of metallic nucleus surrounding by the glass coating can be controlled by the ρ-ratio: strength of internal stresses increases decreasing ρ-ratio (i.e., increases with increasing of the glass volume). The estimated values of the internal stresses in these glass coated microwires are of the order of 100–1000 MPa, depending strongly on the ratio between the glass coating thickness and metallic core diameter [3, 4], increasing with decreasing ρ-ratio.

On the other hand, the magnetostriction constant is mostly determined by the chemical composition and achieves almost nearly-zero values in amorphous alloys based on Fe-Co with Co/Fe $\approx 70/5\lambda_s \approx 0$ [5]. Therefore, magnetoelastic anisotropy and GMI effect of glass-coated microwires can be controlled by the geometrical ratio ρ through the strength of internal stresses, since the magnetic field and frequency dependences of GMI effect are determined by the magnetic anisotropy. Additionally, heat treatments of microwires affect both magnetoelastic anisotropy and GMI effect.

REFERENCES

1. Jiles, D. C., Vol. 51, 5907–5939, 2003.
2. Zhukova, V., M. Ipatov, and A Zhukov, *Sensors*, Vol. 9, 9216–9240, 2009.
3. Antonov, A. S., V. T. Borisov, O. V. Borisov, A. F. Prokoshin, and N. A. Usov, *J. Phys. D: Appl. Phys.*, Vol. 33, 1161–1168, 2000.
4. Chiriac, H., T.-A., Ovari, and A. Zhukov, *J. Magn. Magn. Mater.*, 254–255, 469–471, 2003.
5. Konno, Y. and K. Mohri, *IEEE Trans. Magn.*, Vol. 25, No. 5, 3623–3625, 1989.

Recent Interest in Magnetoelectric/Multiferroic Hexagonal Ferrites

Robert C. Pullar[1], **Marco Pinheiro de Oliveira**[1], **and João Amaral**[2]

[1]Department of Engenharia Cerâmica e do Vidro/CICECO
Campus Universitário de Santiago, Universidade de Aveiro, Aveiro 3810-193, Portugal
[2]Department of de Fisica, Campus Universitário de Santiago
Universidade de Aveiro, Aveiro 3810-193, Portugal

Abstract— Since their discovery in the 1950's, there has been an increasing degree of interest in the hexagonal ferrites, also know as hexaferrites, which is still growing exponentially today. These have become massively important materials commercially and technologically, accounting for the bulk of the total magnetic materials manufactured globally, and they have a multitude of uses and applications. As well as their use as permanent magnets, common applications are as magnetic recording and data storage materials, and as components in electrical devices, particularly those operating at microwave/GHz frequencies, and as GHz electromagnetic wave absorbers for EMC, RAM and stealth technologies. The hexagonal ferrites are all ferrimagnetic materials, and their magnetic properties are intrinsically linked to their crystalline structures. They all have a magnetocrystalline anisotropy; that is the induced magnetisation has a preferred orientation within the crystal structure. They can be divided into two main groups: those with an easy axis of magnetisation, the uniaxial hexaferrites, and those with an easy plane (or cone) of magnetisation, known as the ferroxplana or hexaplana ferrites.

There has been a great deal of interest in the potential of multiferroic (MF)/magnetoelectric (ME) hexaferrites recently, initially as composites with dielectric materials. This would enable tuning of magnetic/electrical/resonance/optical properties via the remote application of magnetic or electrical fields, or the direct application of a voltage or stress. One of the most exciting recent developments has been the discovery of single phase ME/MF hexaferrites, firstly $Ba_{2-x}Sr_xZn_2Fe_{12}O_{22}$ and $Ba_2Mg_2Fe_{12}O_{22}$ Y ferrites, and recently $BaFe_{10.35}Sc_{1.6}Mg_{0.05}O_{19}$ M ferrite, at cryogenic temperatures. In November 2010, $Sr_3Co_2Fe_{24}O_{41}$ Z ferrite was reported to be MF at room temperature, and in 2011 so was $Sr_4Co_2Fe_{36}O_{60}$ U ferrite. This ME has been attributed to long range helical spin ordering in the hexaferrites, resulting in non-collinear spin structures, which can also induce a ferroelectric-like polarisation — sometimes called *"spin-driven ferroelectrics"*.

This presentation will discuss the global recent progress in ME/MF hexaferrite materials and composites, and the authors will also present some of their own work in this field.

Session 3P7b
Various Models for Electrodynamics and Applications to Moving Media

EM Wave Scattering by Objects Moving on Bowditch-Lissajous Trajectories

Dan Censor
Department of Electrical and Computer Engineering
Ben-Gurion University of the Negev, Beer-Sheva 84105, Israel

Abstract— Scattering of electromagnetic waves by objects performing complicated non-uniform motion is of interest both theoretically and for applied scientific and engineering purposes. Monitoring motion by means of wave scattering facilitates remote sensing of objects and media properties.

In order to analyze such problems, a physical kinematical model must be adopted, that will relate the spatiotemporal coordinates in different frames of reference. Evidently the choice of varying velocity conflicts with the premises of Special Relativity theory whose fundamental tenet is constant relative velocity and the equivalence of all inertial systems. The choice of a kinematical model is not unique, and eventually its adequacy for describing scattering by objects non-uniformly moving at moderate velocities $v \ll c$ will have to be tested experimentally. Moreover, it must be assumed that forces associated with the varying velocity, i.e., acceleration, are negligible, otherwise the model ceases to be purely kinematical, and the Maxwell equations in their traditional form will have to be modified.

Some models have been proposed [1]. Presently a quasi Lorentz transformation is used, which in the limiting case of constant velocity reduces to the Special Relativity theory.

The class of problems considered presently involves quasi-periodic motion along Bowditch-Lissajous trajectories [2]. Salient examples are provided by the motion of spinning devices abounding in machinery and aviation. To obviate encumbering mathematical detail, the general scope is reduced to periodic motion along the principal Cartesian coordinates.

As specific examples, scattering by thin cylinders moving on elliptical trajectories is analyzed. The resultant spectrum is shown to be discrete, with sidebands separated by the mechanical frequency of motion. It is shown that discrete Bessel-Fourier like spectra are involved, with sidebands separated by the mechanical frequencies of motion.

REFERENCES

1. Van Bladel, J., *Relativity and Engineering*, 309, Springer, 1984.
2. http://en.wikipedia.org/wiki/Lissajous_curve.

Relativistic Longitudinal Green's Function in the Presence of a Moving Planar Dielectric-Magnetic Discontinuity

Tatiana Danov and Timor Melamed
Department of Electrical and Computer Engineering
Ben-Gurion University of the Negev, Beer Sheva 84105, Israel

Abstract— Recently plane-wave spectral representations of the relativistic electric and magnetic dyadic Green's functions of a uniformly moving dielectric-magnetic medium were obtained in [1]. By applying a simple coordinate transformation, scalarization of the EM vectorial problem was obtained in which the EM dyads are evaluated from Helmholtz's free-space (isotropic) scalar Green's function. The spectral plane-wave representations of the dyadic Green's functions were obtained by applying the spatial 2D Fourier transform to the scalar Green's function in both under and over phase-speed medium velocity regimes.

The present contribution is concerned with obtaining the relativistic 2D (3D in relativity jargon) Green's function of a time-harmonic line current that is embedded in a moving dielectric-magnetic medium with a planar discontinuity under Einstein's Special Relativity. By applying the plane-wave spectral representation in [1], the exact reflected and transmitted (refracted) fields are obtained in the form of a spectral integral over plane-waves in the socalled laboratory and comoving frames. We investigate these spectral representations as well as their asymptotic evaluations and discuss the associated relativistic wave phenomena of direct reflected/transmitted rays and relativistic head-waves (lateral waves).

REFERENCES

1. Danov, T. and T. Melamed, "Spectral analysis of relativistic dyadic Green's function of a moving dielectric-magnetic medium," *IEEE Trans. Antennas Propagat.*, Vol. 59, 2973–2979, 2011.

Scattering of Gaussian-beams and Pulsed-beams from a Fast Moving Planar Dielectric Magnetic Half-space

Coby Maron and Timor Melamed
Department of Electrical and Computer Engineering
Ben-Gurion University of the Negev, Beer Sheva 84105, Israel

Abstract— This contribution is concerned with deriving the canonical scattering of a single time harmonic Gaussian beam and time-dependent pulsed beam from a fast moving planar nondispersive dielectric-magnetic half space under Einstein's Special Relativity. The incident Electromagnetic wave objects serve as the basis wave propagators of the Phase-Space Beam Summation Method, which is a framework for analyzing radiation from extended sources. In this formulation a generic aperture EM field is expanded into a discrete (phase-space) set of beam Propagators that emanate from of points on the aperture plane, in a discrete set of directions and, for time-dependent fields, in a discrete set of temporal delays.

Both the TE and TM polarized Gaussian and pulsed beams are considered by applying plane wave spectral representation of the incident field in the laboratory frame. By utilizing the Lorentz Transformation and applying Maxwell's boundary conditions in the co-moving frame we obtain an exact solution for reflected and transmitted fields in the laboratory frame in the form of spectral integrals. Finally asymptotic evaluations of the reflected and transmitted vectorial electromagnetic fields are carried out in the laboratory frame and relativistic wave phenomena are discussed.

The Model of Wave Propagation in Classical Physics

Siwei Luo
Southern Illinois University, USA

Abstract— The model of wave propagation is a way to help understand and predict the behavior of wave and the principle of wave propagation. Even though there are a lot of different models and theories aiming to explain wave propagation phenomena, still there is some room for making progress in classical physics under a specific condition, especially, in the field of the electromagnetic waves. In classical physics theory, it is assumed that a wave with a specific frequency has always the same velocity in the same medium, regardless of the velocity of wave source. And the wave has different velocities in different reference systems. Four different circumstances that the source is moving, the medium is moving, both the source and the medium are moving and the wave is in different references systems are analyzed. These results of calculation on the subjects that moving source and moving medium are consistent with conclusions of Doppler effects. In particular, the paper expresses these assumptions in the technique of simple mathematical methods and partial differential equations to make it more straightforward comprehensible and systematic method in explaining these phenomena. Based on these two assumptions, from a different perspective, the paper tries to present an explanation of Michelson-Morley experiment and Fizeau experiment by classical physics theory. Additionally, according to the result of new experiment of neutrino, the main differences between classical physics and modern physics in the field of electrodynamics theory are briefly discussed. Hopefully, it would lead to a more profound calculation and modeling about this subject.

Prediction of a New Superconductivity-like Effect in Galilean Reference Systems (Part I)

Namık Yener
Technology Faculty, Kocaeli University, Izmit, Kocaeli 41380, Turkey

Abstract— Prediction of a hitherto unknown superconductivity-like effect is made which is independent of temperature, but rather requires Galilean reference systems moving at the speed of light in vacuum. As the medium (I) to which the laboratory frame is attached, a Lorentz medium is selected whereas for medium (II) to which the rest frame is attached, a perfectly conducting medium is selected. The interface is an infinite plane perpendicular to the uniform rectilinear motion involved. The fact that the Lorentz medium appears as a metal when observed from the rest frame, is unearthed in a previously reported work by the same author. Next the limit condition which in effect requires attainment of speed of light in vacuum by the uniform rectilinear motions of the Galilean reference systems is considered, and the effective permittivity function of medium (I) observed from the rest frame is found to have a character similar to that of a superconductor. It should be stressed that the fundamental premise of the work is Lorentzian relativistic transformation and not Galilean relativistic transformation under which the permittivity function could have been invariant. This work is presented in a series of two papers. In Part (I) the models for medium (I) observed from the laboratory frame and the rest frame are presented. In Part (II) the prediction of the new superconductivity-like effect is made and equations with the same structure as London equations in a superconductor are presented. The second part also contains a discussion section on the verification of the ideas developed from the point of view of Lorentz transforms.

Hertzian Electrodynamics. Historical Aspects, New Theoretical Developments and Applications to Canonical Bodies in Euclidean Motion

B. Polat
Electrical and Electronics Engineering Department
Trakya University, Edirne, TR-22030, Turkey

Abstract— In the present talk, we review and extend certain aspects of the mathematical foundation, axiomatic structure, principles and applications of the classical electrodynamic theory of moving bodies, which is actually the Heaviside version of frame indifferent Hertz equations and established in literature as Hertzian Electrodynamics (HE). We start with a short review of the basic analytical tools from kinematics of deformable bodies, which can be met in many textbooks on the topic and their incorporation in certain purely mathematical conservation relations. A detailed exposition of the comoving time derivative operator and its various differential and commutative properties are carried out. Hertz equations are derived in a straightforward manner by identifying the purely mathematic fields and conservation relations with electromagnetic field quantities and laws in virtue of Material Frame Indifference Principle. Hertzian wave equations and Lorentz potentials in simple media are demonstrated for the special cases of translational and rotational motions utilizing the commutative properties of the comoving time derivative operator. At this point the specific contribution of the present investigation to literature can be considered as the introduction of commutative properties of the comoving time derivative operator in case of rotational motion, which are employed in the derivation of the corresponding Hertzian wave equations. We also remark on the invariance of wavenumber and reduced field equations for monochromatic waves.

For a demonstration of the predictions of HE in scattering problems, a general formulation is provided which is followed by various applications of the presented methodology to 2-D canonical problems involving a Perfect Electrical Conductor (PEC) plane, a dielectric half-space and PEC/dielectric cylinders under plane wave incidence in a systematic manner for various modes (uniform, harmonic, rotational) of motion.

REFERENCES

1. Polat, B., "On the axiomatic structure of Hertzian electrodynamics," *TWMS Journal of Applied and Engineering Mathematics*, Vol. 2, No. 1, 17–41, 2012.
2. Polat, B., "Scattering by a moving circular cylinder in hertzian electrodynamics," *Selçuk Journal of Applied Mathematics*, Vol. 13, No. 1, 2012.

Session 3P9
Poster Session 5

Satellite Monitoring for Energy Transfer Process of Tsunamigenic Earthquake

Shigehisa Nakamura
Kyoto University, Japan

Abstract— This is a note to crustal plate creeping process for a trigger of great destructive earthquake accompanied by tsunamis in relation to a possible application of satellite monitoring of positioning on the earth surface. At one of the seismic events, a vector pattern of displacements on the earth crust surface monitored by satellite was quite similar to an outflow pattern of a uniform viscous fluid through a conduit to focusing to give a shot to an epicenter of the earth quake. This pattern must be understood as a problem for a visco-plastic process. In order to realize this pattern, a model is introduced. Special reference is the daa of a satellite monitoring at the seismic event on March 11, 2011 obtained by the Geographic Survey lnstitute. In this case, it is necessary to consider on the possible energy transfer process in relation to the fault formation and tsunami generation. This process could help us to see a process found in the plate conveyed by a sporadic shot of the magma in a global scale.

Monitoring for Geomagntic Reversal of the Planet Earth

Shigehisa Nakamura
Kyoto University, Japan

Abstract— It is unfortunate for the author to write on the earth at a certain time in order to discuss the Earth at present. A geophysical research on the magnetic polar wandering was ever seen to reveal that the earth's magnetic pole was in the tropical or equatorial zone after a certain monotonous movement on a track. The movement of the magnetic pole was evaluated for about 10^9 years on the track for a quarter of the earth's circle. Its history is estimated from the age of Cambrian to present in a scope of the geological time scale. This might suggest that a possibility of the earth's magnetic pole movement could be in circulation on a meridional track for the earth's pole reversal when some specific assumptions were taken to be acceptable. Then, the cycle of the north magnetic pole wondering could be a time scale of 4×10^9 years. This could be reliable when some data of geological stratification and of paleo-biography concerning to the Manmoth trace in the subsurface layer covering on the earth. This fact could be understood in a scientific scope when it is taken to be possible to apply a solution as a reduced result of magneto-hysrodynamics for the earth's geomagnetic main field.

Monitoring for Inclination Stability of the Planet Magnetic Axis Normal to the Solar Equatorial Plane

Shigehisa Nakamura
Kyoto University, Japan

Abstract— This is an introduction of a monitoring for inclination stability of the planet magnetic axis normal to the solar equatorial plane. First, the author notes a brief review in his scope to see what problem is left to be solved though various kinds of the data should be analyzed and referred. Then, it is noted what is possible to demonstrate about specific pattern of inclination of the planet axis in the solar system on the basis of the available data. This data could be a reference to introduce a concept model for inclination stability of the planet rotation axis in the solar system. It has been taken to consider that the planet rotation axis is same to the interested planet magnetic polar axis of an equivalent dipole as a model under some conditions with an assumption. The author would raise his concept model for a logical structure illustrating the inclination on order to have a reasonable understanding of the planet rotation axis inclination in the solar system. On the basis of the author's understanding of dynamical mechanics and of electromagnetics, it should be possible to accept a model of the interested inclination if it is introduced to be a result of a dynamical solution that the neutral stability for the inclination axis of the planet parallel to the radial line on the solar equatorial plane and that the final stability for the inclination axis of the planet normal to the solar equatorial plane. This model is consistent at considering the planet polarity reversal as a linear equation for a spherical planet, though the polar wondering of the earth is known and the planet precession and nutation are taken to be care of the dynamical problems. Now, it should be considered to have a project for monitoring of the planet rotation axis for finding a key to a more advanced research in order to have our dynamic understanding of the planet rotation axis as a specific process.

Electromagnetic Nondestructive Testing in Cracked Defects of Oil-gas Casing Based on Ant Colony Neural Network

Wei Zhang, **Yibing Shi**, **Yanjun Li**, **and Zhigang Wang**
School of Automation Engineering, University of Electronic Science and Technology of China
No. 2006, Xiyuan Road, High Technology District, Chengdu, Sichuan 611731, China

Abstract— In this paper, a new method on quantitative analysis of magnetic flux leakage signal by neural network based on ant colony is proposed. Firstly, the parameters of the magnetic flux leakage signal which can reflect the various characteristics of cracked defects are determined by finite element method (FEM) simulation. Secondly, based on the study on principle of ant colony algorithm, the neural network model is established for magnetic flux leakage signals processing. Finally, through the simulated working environment, the performance of the new neural network is tested with the different signal feature as input. Experimental results obviously proved the feasibility of ant colony neural network, verified the increases on the convergence rate and the accuracy of the neural network, also improved the magnetic flux leakage signals in order to identify the efficiency and quality.

Superresolution: Data Mining

B. A. Lagovsky
Moscow State Institute of Radio Engineering and Automation (Technical University), Russia

Abstract— It is well known that to improve the quality of the target image identification we need to improve the angular resolution. Similar problems are especially important in problems of remote sensing. In particular it is required to work out the intensity distribution of the echo signal over a surface or volume of the target.

The considered problem relates to inverse ill-posed problems. The numerical solutions became unstable when we try to obtain the angular resolution better then Rayleigh criterion allows.

To improve the solution stability the various procedures of regularization are used. Such algorithms use a priori the known information on a source of signals. From the mathematical point of view it is impossible to improve the angular resolution without any additional a priori given conditions. For a stable solution with the significant superresolution crucial to have as much as possible the preliminary information on the solution, i.e., on a source of signals. The additional information allows to enter new conditions in the form of the equations and inequalities.

Carried out researches have shown, that such information can be not only a priory information. Algebraic methods of image restoration of radar targets with improved angular resolution are developed. New data about a source of signals during consecutive search of the approached solution with the increasing angular resolution allow to obtain algebraic methods of decisions. Researches of intermediate solutions reveal before unknown, "latent" characteristics of sources of signals. Found thus new information is used as a priory information at a following step of the solution with the increasing superresolution.

It enables to use greater number of functions in a base part of the algebraic solution that increases accuracy of restoration of the image of a source and raises the angular resolution.

The influence of noise level on the effective resolution was investigated on mathematical model.

As a whole, these algebraic methods allow to increase the effective angular resolution by 5–10 times in comparison with Rayleigh criterion.

Focusing GPR Images Collected from Archaeological Investigations along the "Basilian Monks' Path of Faith" (Aspromonte National Park — Southern Calabria, Italy): Analysis of the Performances of Different Strategies

G. Angiulli[1], **V. Barrile**[2], **D. De Carlo**[1], **T. Isernia**[1], **and A. Sgró**[1]

[1]DIMET, University of Mediterranea
via Graziella, Loc. Feo di Vito, Reggio Calabria 89100, Italy
[2]MECMAT, University of Mediterranea
via Graziella, Loc. Feo di Vito, Reggio Calabria 89100, Italy

Abstract— The "Basilian monks' Path of Faith" is a religious route in the Aspromonte National Park (situated in the southern section of the Apennines mountain ranges) that starting from the town of Bova Superiore, a symbol of monasticism and seat of the ancient Diocesi Grecanica, reaches up the Polsi's Sanctuary, touching along the way some ancient buildings and monasteries including the famous San Bruno's Charterhouse in Serre. In the framework of the project TECNE (at the roots of TErritorial identity: innovative interdisCipliNary methods for the idEntification, development, dissemination of artistic and cultural heritage) financed by Region Calabria and held jointly by the Reggio Calabria's Academy of Fine Arts and the University Mediterranea, some archaeological investigations along this route have been carried out with the aid of the Ground Penetrating Radar, expecially in the ancient town of Africo Vecchio [1]. It is well known as this tool has increased in the years its role in the archaeological prospecting applications, mainly because of its ability to provide a non invasive analysis of historical monument and ancient buildings [2]. However, to obtain highly accurate information from raw B-scan images, useful for archaeological purposes, it is often necessary to improve their quality. This is usually achieved by means of a suitable focusing treatment. In the technical literature many algorithms to focus raw B-scan GPR images have been developed [3]. In this study, we have tested the performances of different approaches to the focusing problem and results will be showed at the conference.

REFERENCES

1. Minuto, D., *Catalogo dei Monasteri e dei Luoghi di Culto Tra Reggio e Locri*, Edizioni di Storia e Letteratura, Roma, 1977.
2. Daniels, J. D., *Ground Penetrating Radar*, 2nd Edition, The Institution of Electrical Engineers, London, 2004.
3. Turk, A. S., K. A. Hocaoglu, and A. A. Vertiy, *Subsurface Sensing, Wiley Series in Microwave and Optical Engineering*, Wiley-Blackwell, 2011.

Nested BiCGSTAB to Solve Complex Linear Systems Arising from Discretization of EFIE

G. Angiulli[1], **S. Calcagno**[2], **D. De Carlo**[1], **and A. Sgró**[1]

[1]DIMET, University Mediterranea, via Graziella n.1, Reggio Calabria 89100, Italy
[2]MECMAT, University Mediterranea via Graziella n.1, Reggio Calabria 89100, Italy

Abstract— In Computational Electromagnetics a number of alternative integral formulations are available to model the electromagnetic scattering from metallic objects in the frequency domain. Among these, the standard form of the electric field integral equation (EFIE) still remains extensively exploited, even in spite of some well-known limitations [1, 2]. The large, dense and non-Hermitian linear system of equations provided by its discretization, can be solved in an efficient way only using a Krylov subspace method (KSM) in conjunction with a suitable preconditioning technique (PT) [3]. Nowadays, a good compromise seems reached by the use of the Generalized Minimal Residual method (GMRES), in combination with ILU preconditioning. Nonetheless the GMRES demand in memory space grows linearly with the number of iterations and that could become rapidly prohibitive in term of memory requirements [4]. So, when a very large non Hermitian linear matrix system has to be solved, a technique involving a fixed amount of memory per iteration (i.e., more cheaper in term of memory demand) should be employed, if out-of-memory errors have to be avoided, especially when large EM scattering problems are tackled on small workstations. This is the case of the Bi-Conjugate Stabilized (BiCGStab) method developed by Van der Vost [4]. In spite of being less popular than the GMRES, BiCGStab has been already exploited with success in Computational Electromagnetic literature to treat large electromagnetics problems. As underlined in [5], the performances of the BiCGStab can be improved providing that the preconditioning step is carried out by another Krylov subspace technique so realizing the Nested BiCGStab (N-BiCGStab) or Flexible BiCGStab method. However, little attention has been devoted to N-BiCGStab in CEM, although it has been extensively employed in many others engineering fields. On the basis of these preliminary considerations, in this work a numerical study on N-BiCGStab performances has been carried out considering the plane wave scattering by perfect conducting canonical bodies. Results demonstrate that F-BiCGStab is, at least in the examined cases, is more faster and robust than the standard BiCGStab coupled with an incomplete LU preconditioning.

REFERENCES

1. Angiulli, G. and S. Tringali, "Stabilizing the E-field integral equation at the internal resonances through the computation of its numerical null space," *International Journal of Applied Electromagnetics and Mechanics*, Vol. 32, 63–72, 2010.
2. Chew, W. C., M. S. Tong, and B. Hu, *Integral Equation Methods for Electromagnetic and Elastic Waves, Syntesis Lectures on Computational Electromagnetics*, No. 12, Morgan & Claypool Publisher, 2009.
3. Angiulli, G., P. Quattrone, and S. Tringali, "An algebraic preconditioner based on properties of the skew-hermitian part of the linear systems arising from the discretization of the E-field integral equation," *Proceeding of International Conference on Electromagnetics in Advanced Applications*, 632–635, 2009.
4. Hogben, L., editor, *Handbook of Linear Algebra*, Chapman & Hall, CRC, 2007.
5. Vogel, A. J., "Flexible BiCg and flexible Bi-CGSTAB for nonsymmetric linear systems," *Applied Mathematics and Computation*, Vol. 188, 226–233, 2007.

Comparison of Different Metaheuristic Optimization Methods' Capability in Two Dimensional Inverse Scattering

Maysam Haghparast, S. A. Mirtaheri, and M. S. Abrishamian
Department of Electrical and Computer Engineering
K. N. Toosi University of Technology, Tehran, Iran

Abstract— In this research, the ability of different metaheuristic optimization methods to solve a two dimensional inverse scattering problem is evaluated. Using an optimization method is a common way to solve an inverse scattering problem. From this point of view, selecting an efficient optimization method is a critical step among problem solving procedure. Analytical and traditional optimization methods, such as gradient based methods, are not usually proper choices, because they could be trapped in the local minimums. Metaheuristic optimization methods show their effectiveness in such kind of problems. Although all of introduced metaheuristic optimization methods proved their effectiveness and ability, there are differences between their characteristics and choosing an optimum candidate between them is a matter of discussion. Based on the nature of problem, one of these methods can overcome the others. In order to evaluate these optimization methods in electromagnetic, in this paper a two dimensional reconstruction problem is considered. The defined problem is reconstruction of a two dimensional dielectrics profile. FDTD simulation is used to solve electromagnetic direct problem. For solving inverse problem, we considered 4 optimization methods: Particle swarm optimization (PSO), differential evolution (DE), Ant colony optimization (ACO) and harmony search (HS). Equal initial condition is considered for four methods and the results of reconstruction are compared. After a fixed number of iterations these parameters are compared: total time of optimization, saturation cycle (the cycle in which the convergence stops and the result reaches to its final value) and the final reconstruction error. In addition we reveal the complexity of implementation of each method for inverse scattering problems. Finally, based on these variables, a comprehensive comparison between these methods in inverse scattering problem is presented.

Localization and Electrical Parameters Estimation of a 2D Mass Using a 2 Step Method Using FDTD

Maysam Haghparast, S. A. Mirtaheri, and M. S. Abrishamian
Department of Electrical and Computer Engineering
K. N. Toosi University of Technology, Tehran, Iran

Abstract— In this paper, a 2 step method for localization and electromagnetic profile parameters estimation of unknown 2D mass based on inverse scattering method is presented. Our aim is to localize and estimate permittivity and conductivity of an unknown mass inside of a known media. Usually in this kind of inverse scattering problems, several receivers with one transmitter are considered. The transmitter emits a predefined electromagnetic wave and the receivers gather the reflected waves from the under investigation mass. It is normal to use fixed locations for transmitter and receivers. When the investigated mass for inverse problem is inside of another body, the location of under investigation mass is unknown. So if we consider its location random, based on its position the result of final reconstruction error could be different. Although we consider a symmetrical arrangement for receivers, because only one transmitter is used, it will have an asymmetric position related to overall under investigation area. Here we proposed a 2 step solution. Based on our proposal, in the first step, we consider 4 symmetric positions for transmitter and solve the problem for 4 positions for a limited number of iterations. After that, based on comparison of first step results, our algorithm chooses the optimum position for transmitter and in the second step it solves the problem completely for the optimum transmitter. FDTD is used as EM solver and particle swarm optimization is the employed optimization method. The simulations results show that this 2 step method has the ability to improve the final reconstruction error in comparison with the conventional 1 step method. Numerical results reveal that our proposed method can improve both localization and electrical parameters estimation reconstruction error.

Reconstruction of 1-D Dielectric Scatterer with Cosine and Spline Expansions Using Differential Evolution and Particle Swarm Optimization

M. Haghparast, S. A. Mirtaheri, and M. S. Abrishamian
Department of Electrical and Computer Engineering
K. N. Toosi University of Technology, Tehran, Iran

Abstract— In this paper, a reconstruction method for 1-D dielectric Scatterer's permittivity based on cosine and spline expansions using Differential Evolution and Particle Swarm Optimization is presented. Two methods for expansion, Cubic spline and cosine expansion are explained and then the results of each method's reconstruction are presented. Two optimization methods, differential evolution (DE) and particle swarm optimization (PSO) in solving 1-D inverse scattering problems are used. In this comparison, the efficiency and time duration of both mentioned optimization methods are examined for permittivity profile reconstruction problems. 2 profiles are investigated and complete results of reconstruction are presented and compared. We reconstructed each profile with 2 methods of expansions and for each method of expansions used 2 optimization methods. In the other word, for each profile, 4 simulations are performed and the results are presented in a table. The comparison is carried out under the same conditions of initial population of candidate solutions and number of iterations. Our simulations show that both optimization methods are reliable tools for inverse scattering applications with both methods of expansions. Numerical results prove that both methods of expansion result in accurate reconstruction even when profile has rapid changes. However by comparing the simulation's results, it can be said that spline expansion can estimate the scatterer's profile more accurate than cosine expansion. In addition, the reconstruction error in both expansion methods are nearly identical while the cost functions have considerable differences and it can be considered an advantage for spline method, while having worse cost function value, result in a same reconstruction error. In the term of reconstruction error, DE and PSO result in same values. In the particular case of our investigations, PSO outperforms the DE in terms of reconstruction time.

GOSAT Data Processing for Space-based Carbon Dioxide Retrievals with PPDF-based Method to Account for Atmospheric Light Scattering

Sergey Oshchepkov[1], **Andrey Bril**[1], **Tatsuya Yokota**[1], **Yukio Yoshida**[1], **Isamu Morino**[1], **T. Matsunaga**[1], **D. Wunch**[2], **G. Toon**[2], **C. O'Dell**[3], **A. Butz**[4], **H. Boesch**[5], **N. Eguchi**[6], **Vladimir Budak**[7], **Alexander Lukyanov**[8], **A. Ganshin**[8], **Ruslan Zhuravlev**[8], **and The TCCON Team**

[1]National Institute for Environmental Studies, Japan
[2]California Institute of Technology, Pasadena, CA, USA
[3]Colorado State University, Fort Collins, CO, USA
[4]Karlsruhe Institute of Technology, IMK-ASF, Karlsruhe, Germany
[5]Earth Observation Science, Space Research Centre, University of Leicester, UK
[6]Research Institute for Applied Mechanics, Kyushu University, Japan
[7]Moscow Power-Engineering Institute (MPEI), Moscow, Russia
[8]Central Aerological Observatory, Dolgoprudny, Russia

Abstract— We present a method to detect optical path modification due to atmospheric light scattering in space-based greenhouse gas spectroscopic sounding. This method, which was applied to the analysis of radiance spectra measured by the Greenhouse Gases Observing Satellite (GOSAT), is based on the path length probability density function (PPDF) and on retrieval of PPDF parameters from radiance spectra in the oxygen A-band of absorption at 0.76 μm. We show that these parameters characterize the impact of atmospheric light scattering on carbon dioxide retrieval in the CO_2 absorption bands. The threshold for PPDF parameters is set so that the optical-path modification is negligible, and these settings are recommended as a basic guideline for selecting the clearest atmospheric scenarios. Data processing for 22 months of GOSAT observations shows that PPDF-based selection efficiently removes CO_2 retrieval biases associated with subvisible cirrus and sand storm activities. The retrievals are compared with those derived from FTS measurements for Total Carbon Column Observing Network (TCCON — http://www.tccon.caltech.edu/) validation sites. We also compare PPDF-based data processing with those derived by other algorithms including the official GOSAT data products from the National Institute for Environmental Studies (NIES, Japan) and NASA's Atmospheric CO_2 Observations from Space (ACOS).

Airship Radar System Modeling and Simulation

Li Zhang and Jingwen Li
School of Electronics and Information Engineering, Beihang University, Beijing, China

Abstract— A complete signal simulation system is established according to the characteristics of the airship radar. Based on the classification of different terrain and sea condition, various clutter models are simulated. The simulation results indicate this simulation system is essential and qualified for subsequent data processing.

A complete signal simulation system is established in this paper. It includes five parts: platform design, radar design, antenna design, target design and scene design. Motion errors are considered in the platform design due to the wind and atmospheric flow effects. In the radar design, PD radar system is selected to reduce the load of airship because of its simple structure, and LFM, Baker codes and P4 codes are chosento improve the capability of detection and anti-interference [1–3]. Transceiver and bistatic antennas are adopted to enhance the anti-interceptive capability in the antenna design [1–3]. Low-altitude moving point target is opted as the target model in the target design.

As the characteristics of the clutter the airship radar received in the mode of nadir looking have some important effects on subsequent data processing, it is significant to providedifferent ground scene and accurate clutter model in the scene design to implement radar echo signal simulation [4]. Landform model is grouped into desert, farmland, forest, mountain, city and different sea conditions (level 1–5). Average radar cross-section (RCS) and fluctuant RCS are appliedto the simulation of the landform model clutter. In the fluctuant RCS method, Rayleigh distribution, Log-normal distribution, Weibull distribution and K distribution are chosen as the RCS Probability distribution while Gaussian spectrum and cubic spectrum are selected as RCS related characteristics model [4]. Furthermore, composite landform is also taken into considerationaccording to the weight proportion of RCS Probability distribution [5].

The scatterer units in the irradiated areaare divided with the grid-mapping format method [6], and then the echo signals simulation in different clutter scenes is implemented through the coherent video signal accumulation [4]. All results output are performed via MATLAB GUI, and the agreement between the simulation results and the theory indicates that the airship radar signal simulation system is correct and effective.

REFERENCES

1. Hochstetler, R., "Airships ahoy," *IEEE Spectrum*, Vol. 47, No. 10, 42–47, 2010.
2. Cheng, C. and P. Zhao, "Analysis of tethered aerostat borne radar system," *Radar Science and Technology*, Vol. 5, No. 6, 410–414, 2007.
3. Zhang, M. and X. Wang, *Radar System*, Publishing House of Electronics Industry, Beijing, 2008.
4. Zhang, C., "Modeling and simulation of radar clutter for radar signal simulator," Electronic Science and Engineering National University of Defense Technology, Changsha, China, 2004.
5. Li, Q. and Q. Zhang, "A clutter modeling method in the composite sea-plus-land environment," *Journal of Microwaves*, Vol. 26, No. 1, 22–25, 2010.
6. Cheng, A., "Radar echo signal modeling and simulation," Nanjing University of Science and Technology, Nanjing, China, 2004.

Absorption Dependencies of Dipolar Glass Cylindrical Waveguide Coated by SiC on Temperatures and Coated Layer Thicknesses

L. Nickelson[1, 2], **A. Bubnelis**[1, 2], **and S. Asmontas**[1]

[1]Department of Electronics, Center for Physical Sciences and Technology, Vilnius, Lithuania
[2]Department of Electronic System, Vilnius Gediminas Technical University, Lithuania

Abstract— Dipolar glass-silicon carbide (SiC) waveguides can possess a very large broadbandwidth and superior electrophysical properties in the microwave frequency range. These waveguides can be controllable by temperatures. As it is known SiC waveguides are presently used at high-temperatures, high-voltages, high-powers, high critical breakdown fields and high-radiation conditions. Ceramic SiC does not feel the impact of any acids or molten salts up to 800°C, i.e., this material is resistant to aggressive environments. SiC material has superior properties for high-power electronic devices.

In present work the permittivities of dipolar glass and SiC materials are dependent on the temperature. These permittivities are taken from the measured data [1, 2]. Our electrodynamical modeling was fulfilled by the partial area method with using of the Müller's method for the searching of complex propagation constants of waveguides [3, 4]. We have used our created computer software in the MATLAB language.

We are going to present the phase and attenuation constants of the main and the first higher modes of two layered waveguide with external radius equal to 1 mm at different radii of dipolar glass core and at different temperatures. Here will be also given the waveguide broadbandwidth at different temperatures and different thicknesses of coated SiC layer.

REFERENCES

1. Banys, J., A. Kajokas, S. Lapinskas, A. Brilingas, J. Grigas, J. Petzelt, and S. Kamba, "Microwave and millimeter-wave dielectric response of $Rb_{1-x}(ND_4)D_2PO_4$ diploar glass," *J. of Physics: Condensed. Matter*, No. 14, 3725–3733, 2002.
2. Baeraky, T. A., "Microwave measurements of the dielectric properties of silicon carbide at high temperature," *Egyptian Journal of Solids*, Vol. 25, No. 5, 263–273, 2002, ISSN 1012-5566.
3. Asmontas, S., L. Nickelson, A. Bubnelis, R. Martavicius, and J. Skudutis, "Hybrid mode dispersion characteristic dependences of cylindrical dipolar glass waveguides on temperatures," *Electronics and Electrical Engineering*, Vol. 106, No. 10, 2010, ISSN 1392-1215.
4. Nickelson, L., S. Asmontas, and T. Gric, "Electrodynamical modeling of open cylindrical and rectangular silicon carbide waveguides," *Properties and Applications of Silicon Carbide*, Rosario Gerhardt, Ed., Chapter 6, InTech, 2011, ISBN 978-953-307-201-2.

Dispersion Characteristics of Circular Layered Zero-index Anisotropic Metamaterial — Semiconductor Waveguides

S. Asmontas[1], **A. Bubnelis**[1, 2], **and L. Nickelson**[1, 2]

[1]Department of Electronics, Center for Physical Sciences and Technology, Vilnius, Lithuania
[2]Department of Electronic System, Vilnius Gediminas Technical University, Lithuania

Abstract— In the last decade many specialist focused on the experimental and theoretical investigations of the zero-refractive index (or zero-index) metamaterials. The metamaterials attractive to researches due to their unconventional constitutive parameters and different anomalous effects too [1–3].

Here we are going to present the dispersion characteristic dependencies of propagating eigenmodes of open cylindrical anisotropic metamaterial-semiconductor waveguides when the metamaterial permittivity and permeability tensor components may accept values close or equal to zero. The values of tensor components become equal to zero at the operating frequency f equal to the metamaterial electric or (and) magnetic plasma frequencies. This metamaterial is a plasmonic one. Zero-index metamaterials are dispersive media. A waveguide that has a boundary of anisotropic metamaterial and semiconductor material or dielectric (air) medium can be assigned to plasmonic waveguides. In this work we are going to analyze some plasmonic waveguides when anisotropic metamaterial constitutive parameters were taken of [4, 5].

The solution of Maxwell's equations for the layered anisotropic metamaterial-semiconductor waveguide was carried out by the partial area method. The computer program for the dispersion characteristic calculations has created in MATLAB language. Our computer program allows take into account a very large material attenuation as well as the values of non-diagonal tensor components [6, 7].

Dispersion characteristics of layered waveguides with the external radius equal to 1 mm at the left handed polarization of microwave will be shown here. There are unusual shape of eigenmode dispersion characteristics and anomalous sectors of the characteristics at certain frequencies. The first eigenmode of cylindrical waveguide with the lowest cutoff frequency is a particularly important mode because it is a single one in some frequency range and small variations on the frequency produce large changes in the phase constant. We are going to present here the dependencies of dispersion characteristics on the semiconductor layer thicknesses, the specific resistivity of semiconductor material. It will be shown how the radius value of plasmonic core affects on the propagating eigenmode quantity and mode cutoff frequencies.

REFERENCES

1. Zhou, H., Z. Pei, S. Qu, S. Zhang, and J. Wang, "A planar zero-index metamaterial for directive emission," *Journal of Electromagnetic Waves and Applications*, Vol. 23, No. 7, 953–962, 2009.
2. Oraizi, H., A. Abdolali, and N. Vaseghi, "Application of double zero metamaterials as radar absorbing materials for the reduction of radar cross section," *Progress In Electromagnetics Research*, Vol. 101, 323–337, 2010.
3. Silveirinha, M. and N. Engheta, "Design of matched zero-index metamaterials using nonmagnetic inclusions in epsilon-near-zero media," *Physical Review B*, Vol. 75, 075119-(1–10), 2007.
4. Liu, S.-H., C.-H. Liang, W. Ding, L. Chen, and W.-T. Pan, "Electromagnetic wave propagation through a slab waveguide of uniaxially anisotropic dispersive metamaterial," *Progress In Electromagnetics Research*, Vol. 76, 467–475, 2007.
5. Smith, D. R., P. Rue, D. C. Vier, A. F. Starr, J. J. Mock, and T. Perram, "Design and measurement of anisotropic metamaterials that exhibit negative refraction," *IEICE Trans. Electron.*, Vol. E87-C, No. 3, 359–370, 2004.
6. Nickelson, L., A. Bubnelis, A. Baskys, and R. Navickas, "The magnetoactive p-Ge rod waveguide loss analysis on the concentration of two component hole charge carriers," *Electronics and Electrical Engineering*, Vol. 110, No. 4, 53–56, 2011, ISSN 1392-1215.
7. Nickelson, L., S. Asmontas, T. Gric, J. Bucinskas, and A. Bubnelis, "Electrodynamical analysis of open lossy metamaterial waveguide and scattering structures," *Metamaterial*, Book edited by: Dr. Xun-Ya Jiang, InTech, 2012, ISBN 979-953-307-563-0.

Image Formation and Coregistration via Non-uniform FFTs in SAR Interferometry

A. Capozzoli, C. Curcio, and A. Liseno
Dipartimento di Ingegneria Biomedica, Elettronica e delle Telecomunicazioni
Università di Napoli Federico II, via Claudio 21, Napoli I-80125, Italy

Abstract— In Synthetic Aperture Radar (SAR) Interferometry, accuracy and computational complexity issues arise in all the processing chain leading to the evaluation of the interferograms, namely, both in the formation of the individual images of the pair and in their possible coregistration [1]. In particular and concerning coregistration, resampling one complex SAR image involves interpolation kernels whose kind and length must be chosen according to a trade-off between accuracy and computational efficiency. In some interferometric SAR (InSAR) applications, as the estimation of ground-surface deformations [2], high order and long interpolation kernels are generally required. As a consequence, during the recent years, some interest has been addressed to the selection of convenient interpolation kernels for SAR image coregistration [3, 4], the main interest being to determining the kernel producing the best interpolation accuracy for a given kernel length. At the same time, efficient implementations of the coregistration step in terms of memory requirements and flop-counts have been also proposed [5].

Recently, a backprojection algorithm for the fast and accurate focusing of SAR images has been developed [6]. Differently from other approaches [7], it is based on the use of a Non-Uniform FFT (NUFFT) routine [8] and on a CUDA implementation on a Graphics Processing Unit (GPU) in CUDA language [9]. The NUFFT-based backprojection has proven drastically more accurate than other approaches based on the use of FFTs and interpolators typically used in SAR without a significant increase in the computational cost.

A serious advantage of the backprojection algorithm is the possibility of achieving SAR focused images on arbitrary lattices. In this way, the images forming the interferometric pair can be directly calculated on a common computational grid, without the need of an explicit coregistration step. Alternatively, the coregistration can be achieved, following the use of standard SAR focusing algorithm, by NUFFTs.

In this paper, we show how, by the algorithm developed in [6], it is possible to quickly achieving interferometric pairs with high degrees of coherence, the typical parameter used to evaluate the interferometric phase quality. Results on airborne data provided by the Air Force Research Laboratory are shown.

REFERENCES

1. Li, Z. and J. Bethel, "Image coregistration in SAR interferometry," *Proc. of the Int. Soc. Photogramm. Remote Sens.*, 433–438, Beijing, China, Jul. 3–11, 2008.
2. Ferretti, A., C. Prati, and F. Rocca, "Nonlinear subsidence rate estimation using permanent scatterers in differential SAR interferometry," *IEEE Trans. Geosci. Remote Sens.*, Vol. 38, No. 5, 2202–2212, Sep. 2000.
3. Hannsen, R. and R. Bamler, "Evaluation of interpolation kernels for SAR interferometry," *IEEE Trans. Geosci. Remote Sens.*, Vol. 37, No. 1, 318–321, Jan. 1999.
4. Migliaccio, M. and F. Bruno, "A new interpolation kernel for SAR interferometric registration," *IEEE Trans. Geosci. Remote Sens.*, Vol. 41, No. 5, 1105–1110, May 2003.
5. Selva, J. and J. M. Lopez-Sanchez, "Efficient interpolation of SAR images for coregistration in SAR Interferometry," *IEEE Trans. Geosci. Remote Sens.*, Vol. 4, No. 3, 411–415, Jul. 2007.
6. Capozzoli, A., C. Curcio, A. Liseno, and P. Vinetti, "Fast interpolation accelerated on GPU for SAR backprojection," *Proc. of the 28th Annual Rev. of Progr. in Appl. Comput. Electromagn.*, 305–310, Columbus, OH, Apr. 10–14, 2012.
7. Frölind, P.-O. and L. M. H. Ulander, "Evaluation of angular interpolation kernels in fast back-projection SAR processing," *IET Proc. — Radar Sonar Navig.*, Vol. 153, No. 3, 243–249, Jun. 2006.
8. Fourmont, K., "Non-equispaced fast Fourier transforms with applications to tomography," *J. Fourier Anal. Appl.*, Vol. 9, No. 5, 431–450, Sep. 2003.
9. Capozzoli, A., C. Curcio, and A. Liseno, "GPU-based ω-k tomographic processing by 1D non-uniform FFTs," *Progress In Electromagnetics Research M*, Vol. 23, 279–298, 2012.

Hybrid Method for Analysis of Conformal Ferrite Guides

A. Kusiek, W. Marynowski, and J. Mazur
Gdansk University of Technology, Poland

Abstract— Non-reciprocal devices are key elements of currently developed wireless communication systems [1–3]. Among the non-reciprocal structures a special group constitutes arrangements that are using longitudinally or transversely magnetized ferrite strip/slot conformal guides [2]. Using such guides it is possible to realize phase shifters, as well as longitudinally magnetized circuits based on Faraday rotation effect such as isolators and circulators. In the case of the latter, the conducted research [2] has shown that these devices have much smaller dimensions and transmission losses than the similar planar configurations [1, 3].

The analysis of transversely or longitudinally magnetized conformal line sections is complicated. In the case of longitudinally magnetized cylindrical ferrite coupled slot/strip lines the solution can be found utilizing analytical techniques [4]. Taking into account ferrite rods with arbitrary cross-section and magnetized with arbitrary directed magnetic field (e.g., four-pole magnetization) there is no analytical solution to the problem. The more powerful in this case are based on the discrete methods commercial simulators which allows to take into consideration the different shapes of ferrite elements. However, this software has a number of limitations such as inability to define arbitrary directed magnetization field distribution and the direct determination of the wave properties of conformal ferrite guides (e.g., dispersion characteristics and field distributions of ferrite modes). Moreover, the time of analysis using discrete techniques is long, which disqualifies the use of this software in rapid design and optimization procedures of non-reciprocal devices.

In this paper, we propose a new fast and efficient hybrid approach for the analysis of longitudinally or transversely magnetized cylindrical strip/slot guides made on the ferrite core of arbitrary cross-section. The proposed approach is based on a combination of discrete finite-difference frequency-domain method with method of moments (FDFD/MoM). In the proposed approach, the circular region containing the investigated ferrite core is isolated in the cross-section of the guide. Using FDFD technique within this region the impedance relation between the components of tangential electric and magnetic fields is determined on the region boundary. Next, satisfying the field continuity conditions on this boundary the obtained discrete solution is combined with an analytical solution MoM. As a result of analysis the wave parameters, e.g., dispersion characteristics and transverse field distributions of modes in ferrite strip/slot conformal line are obtained.

The proposed method was applied to the analysis of different types of transversally and longitudinally magnetized ferrite strip/slot conformal guides. The results were compared with the ones published in the literature and experimental results and a good agreement was observed.

ACKNOWLEDGMENT

This work was supported in part by Polish Ministry of Science and Higher Education from sources for science in the years 2012-2013 under Contract No. 0282/IP3/2011/71 and under COST Action IC0803, decision No. 618/N-COST/09/2010/0.

REFERENCES

1. Cao, M. and R. Pietig, "Ferrite coupled-line circulator with reduced length," *IEEE Transactions on Microwave Theory and Techniques*, Vol. 53, No. 8, 2572–2579, Aug. 2005.
2. Kusiek, A., W. Marynowski, and J. Mazur, "Investigations of cylindrical ferrite coupled line junction using hybrid technique," *Progress In Electromagnetics Research*, Vol. 120, 143–164, 2011.
3. Marynowski, W. and J. Mazur, "Study of nonreciprocal devices using three-strip ferrite coupled line," *Progress In Electromagnetics Research*, Vol. 118, 487–504, 2011.
4. Baden Fuller, A. J., *Ferrites at Microwave Frequencies*, Peter Peregrinus Ltd., London, UK, 1986.

Optimized Geometry Wedge Absorbers

S. Kent[1] **and I. Catalkaya**[2]

[1]Electronics and Communication Engineering Department, Electrical and Electronic Engineering Faculty
Istanbul Technical University, Turkey
[2]Satellite Communication & Remote Sensing Department, Informatics Institute
Istanbul Technical University, Turkey

Abstract— To obtain better absorption performance than a wedge type electromagnetic wave absorber, a new absorber shape proposed based on wedge geometry. A wedge absorber which has a certain base width, height and material is divided layers. Each layer has an equal dielectric permittivity and magnetic permeability. Height of the layers is also equal. Layer widths are selected as variable to find an optimum absorber geometry which provides an optimum gradual change of impedance from tip point to the base point of geometry and optimized to find the best width values which provide the best absorption characteristic. Base point of the structure is bonded to a conductive screen layer to prevent and reflect back EM waves which penetrate inside of absorber structure. Obtained absorber geometry has same base width, height and electrical parameters with a similar wedge absorber except its shape.

There are some studies based on modeling a wedge absorber as a combination of a large number of layers with the same width and determining electrical parameters of material to provide better absorption performance by using optimization methods. Genetic algorithm is one of the popular optimization methods to solve electromagnetic problems by using optimization. We also used to find optimum widths of each layer instead of optimum electrical parameters. Absorber structures are illuminated by a TE polarized plane wave. A new absorber shape is obtained for a center value of a certain incidence angle range of incoming EM wave. This approach provides better absorption performance for a specific incidence angle with reasonable normal incidence performance. Results are obtained by using well known simulation software for normal and oblique incidence case. Wedge type absorber and new absorber's reflection performances are compared. Results show that new absorber structures provide more reflection loss than wedge type absorber.

GMI Effect in Glass-coated Microwires with Nanocrystalline Structure

V. Zhukova[1], **A. Talaat**[1], **L. González**[2], **S. Kaloshkin**[3], **M. Churyukanova**[3], **B. Hernando**[2], **and A. Zhukov**[1, 4]

[1]Dept. Phys. Mater., Chem. Faculty, UPV/EHU, P. Manuel de Lardizabal 3, San Sebastian 20018, Spain
[2]Departamento de Física, Universidad de Oviedo, Calvo Sotelo s/n, Oviedo 33007, Spain
[3]National University of Science and Technology "MISIS", Leninsky Prosp., 4, Moscow 119049, Russia
[4]IKERBASQUE Foundation, Bilbao, Spain

Abstract— Recently, studies of amorphous magnetically soft thin wires attracted considerable attention owing to their technological applicability in magnetic sensors and tuneable metamaterials [1]. On the other hand, nanocrystalline materials are currently considered as perspective materials because of their good magnetic softness, high GMI effect and absence of Co in alloy composition. Their microstructure consists basically of small crystallites (mean grain size of 10 nm) embedded in an amorphous residual matrix, exhibit enhanced magnetic softness and GMI effect. Such crystallites facilitate the final soft magnetic behaviour. These materials are obtained by annealing the precursor amorphous alloy and most results have been reported on ribbon shaped materials [2].

We studied the effect of annealing (300–700°C, 1 hour) on GMI effect and magnetic properties of Finemet-type $Fe_{73.4-x}Cu_1Nb_{3.1}Si_{13.4+x}B_{9.1}$ ($x = 1.1$ and 1.6), $Fe_{73.4}Cu_1Nb_{3.1}Si_xB_{22.5-x}$ ($x =$ 11.5; 13.5 and 16.5) glass coated microwires with aim to find the optimal annealing conditions for the achievement of the best magnetic softness and GMI effect. Microstructural character of the samples was analysed by X-Ray Diffraction (XRD) technique.

The evolution of the coercivity with the annealing temperature exhibits some peculiarities comparing with the classical FINEMET ribbon, especially in the temperature range of 400–500°C (first stage of crystallization), showing also a remarkable dependence on the geometry. We observed considerable GMI effect even in samples annealed well below usual temperature of nanocrystallization.

REFERENCES

1. Zhukova, V., M. Ipatov, and A. Zhukov, *Sensors*, Vol. 9, 9216, 2009.
2. Olivera, J., R. Varga, V. M. Prida, M. L. Sanchez, B. Hernando, and A. Zhukov, *Phys. Rev. B*, Vol. 82, 094414, 2010.

Two-dimensional Sensor Design for Vehicular Navigation Applications

George Dekoulis and Haris Haralambous
Frederick University, 7 Y. Frederickou St., Palouriotisa, Nicosia 1036, Cyprus

Abstract— This paper describes the design of a miniature dual-axis magnetic sensor for vehicular navigation applications. The primary feature of the sensing element is the simultaneous measurement of two orthogonal components of the external magnetic field. The measured performance is accurately predicted by means of a quantitative mathematical model based on linear relationships. The dependence of the output voltage on the various technical characteristics is obtained by implementing a Fourier analysis of the captured data. The current implementation has been accomplished mainly by using a new cobaltbased material not previously used in vehicular sensing applications. The material has been used for performing the initial electromagnetic simulations of different sensor's new configurations, which verified that the advanced specifications set at the beginning of the project can be realized for accurate navigation measurements.

The design is based on a new technology 8-layer race-track sensor, which is currently being produced based on the specifications set by a suitable project on vehicular navigation. The sensor is saturated by an excitation current of 220 mA, close to the initial target specifications of 250 mA. This leads to a reduction in power consumption by a factor of 16 compared to existing sensors for navigation applications. The sensor has a guaranteed sensitivity of 100 μV/nT and an output V_{pp} of 24.6 mV. The sensor has a maximum sensitivity of 196 μV/nT. The results of this study are directly applicable to the development of tri-axial sensors, for three-dimensional navigation. Similarly, a tri-axial sensor can be built by making a robust assembly of three single-axis sensors or by designing a compact structure accommodating all axial dimensions. Implementations of both solutions are currently under development.

Defects Characterization in CFRP Materials Industrial e Civil Applications

D. Pellican, **I. Palamara**, **and M. Versaci**
MECMAT Department, University Mediterranea of Reggio Calabria, Italy

Abstract— The process of production of carbon fiber reinforced polymers, is very elaborate and un-free from faults and problems. Problems during the manufacturing, such as inclusion of other materials, can cause flaws in the resulting material, this way compromising its integrity. Reliable performance of a component or structure depends on its pre-service quality and in-service degradation under operating conditions. The importance of Non-Destructive Testing and Evaluation is ever increasing, above all in ensuring pre-service quality and monitoring in-service degradation, in order to avoid premature failure of the components/structures in carbon fiber reinforced polymers for industrial and civil applications. Within this framework, this work aims to propose a design of a new eddy current probe for non destructive evaluation, based on a ferrite core probe, in order to investigate the presence of defects in carbon fiber epoxy composite materials such as delaminations or inclusions [1]. Particularly, in this work we propose a Finite Element Method based approach for modelling a fast and accurate evaluation of defects in composite materials able to easily detect defects, aside from the orientation. The effect of the ferrite core is analyzed in order to focus magnetic flux density on the investigated specimen. Eddy currents generated by high speed ferrite core probe movement were investigated by using numerical simulation. Particularly, Finite Element Approach has been exploited in order to emphasize the presence of defects in a multi-layer carbon fiber epoxy structure. Proposing an high speed inspection system, that involves probe optimization, the extraction of features from FEA signals and defect characterization using signal processing techniques and Soft Compunting techniques for inverse problem solution [2].

REFERENCES

1. Theodoulidis, T. P., "Model of ferrite-cored probes for eddy-current nondestructive evaluation" *J. Appl. Phys.*, Vol. 93, 3071–3078, 2003.
2. Cacciola, M., S. Calcagno, G. Megali, F. C. Morabito, D. Pellicano, and M. Versaci, "FEA design and misdit minimization for in-depth flaw characterization in metallic plates with eddy current nondestructive testing," *IEEE Trans. Magn.*, Vol. 45, No. 3, 1506–1509, 2009.

Ferroelectric Polarization Switching in BST/NBFO Planar Structures Studied by Scanning Near-field Optical Microscopy

K. A. Brekhov[1], S. D. Lavrov[1], N. E. Sherstyuk[1], and E. D. Mishina[2]

[1]Moscow State Technical University MIREA, 119454, Vernadskogo prosp., 78, Moscow, Russia
[2]South Scientific Center of Russian Academy of Science, Rostov-on-Don, Russia

Abstract— Dynamics of polarization switching is the central problem of ferroelectric-based electro-optical modulators, high-speed nonvolatile ferroelectric random access memories and electro-optical switchers. Investigation of the dynamics of polarization reversal is highly important for optimization of the films parameters with respect to their switching characteristics. Resently it was shown [1] that nonlinear-optical microscopy based on second harmonic generation (SHG) allows to investigate both domain structure and polarization switching effecs in ferroelectric and multiferroic materials. Combination of the SHG and scanning near-field optical microscopy (SNOM) techniques provides complex investigations of local ferroelectric properties for nanosized thin films and planar structures with high spatial resolution up to 100 nm.

In the present paper we report the results of polarization switching in $Ba_{0,8}Sr_{0,2}TiO_3/Bi_{0.97}FeN$ $d_{0.03}O_3$ (BST/NBFO) planar structures studied by combination of the SHG and SNOM techniques.

Heteroepitaxial multilayer BST/NBFO structures with various thickness of the single layer ($d_1 =$ 3 nm, $d_2 = 6$ nm) were fabricated by high-frequency sputtering on MgO(100) substrate. Chemiclal compositions of the BST and NBFO layers allows to perform all measurements at the room temperature. Epitaxial structure of the films was confirmed by X-ray diffraction. For electric field application aluminum planar electrode system with the gap of 20 μm was deposited on the film surface by vacuum deposition, which provides in-plane switching of the ferroelectric polarization during voltage application up to ±50 V.

Voltage dependencies of the SHG intensity were investigated for different thickness of the layer as well as spatial distribution of ferroelectric properties in the gap between two planar electrodes during DC voltage application by pattern 0-Umax-0-(-Umax)-0.

ACKNOWLEDGMENT

This work is supported partly by Russian Founadion of Basic Research and Russian Ministry of Science and Education.

REFERENCES

1. Mishina, E. D., S. V. Semin, K. V. Shvyrkov, A. V. Kudryavtsev, N. A. Ilyin, N. E. Sherstyuk, and V. M. Muhortov, *Physics of the Solid State*, Vol. 54, i. 5, 836, 2012.

Coupling Matrix Synthesis by Optimization with Cost Function Based on Daubechies D4 Wavelet Transform

J. J. Michalski, J. Gulgowski, T. Kacmajor, and Mike Piatek
TeleMobile Electronics Ltd., Poland

Abstract— This paper proposes and investigates a new cost function used in coupling matrix synthesis. In this method filter scattering characteristics are transformed with the use of Daubechies D4 transform, and then compressed. The cost function is defined as Euclidean distance between compressed D4 template reflection and transmission characteristics and the compressed D4 characteristics resulting from the optimized coupling matrix. The important feature of this method is that there is no need to represent filter characteristics in an analytical form (e.g., with the use of total least squares method). The optimization experiments show the performance of the proposed cost function in comparison to the ones already known.

Analysis of Electromagnetic Wave Scattering from the Surface of Double Periodic Arrangements of Metalo-dielectric Cylinders

R. Lech, A. Kusiek, and J. Mazur
Gdansk University of Technology, Poland

Abstract— The analysis of electromagnetic wave scattering from double periodic frequency selective surfaces (FSS) is presented. The structure under investigation is composed of an array of uniformly spaced identical cylindrical sections situated in a free space and illuminated by a harmonic wave with arbitrary direction (see Fig. 1). Each section is composed of metalo-dielectric cylinders of finite height arranged periodically (see Fig. 2).

FSSs when multilayered can be utilized as a electromagnetic band structure (EBG) in microwave wavelength range or photonic band structure (PBG) in optical range. Recently, EBGs and PBGs are of great interest due to their extraordinary properties and potential applications, e.g., filters, substrates for radiating elements, or optical switches. FSSs can also find application in polarizers and polarization rotators to change the polarization state of an electromagnetic wave. Through the utilization of these devices the antennas adopted to receive a single linear polarization (vertical or horizontal) are able to work with both polarizations at the same time.

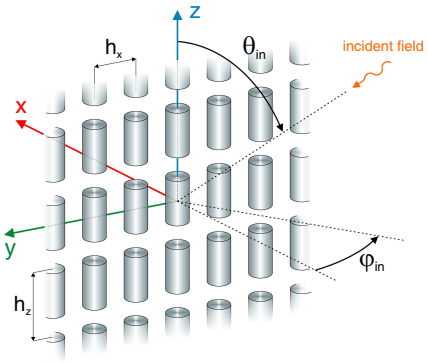

Figure 1: Investigated structure of periodically spaced cylinders.

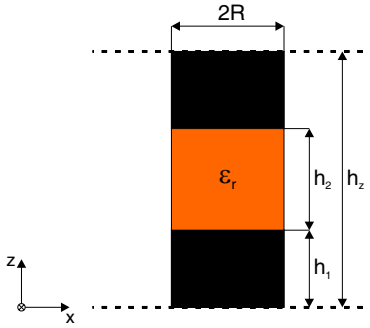

Figure 2: Single section of iso- lated cylinder.

The aim of the analysis is to find scattering parameters of the investigated structure assuming arbitrary incidence angle of the harmonic wave illuminating FSS. The multimodal scattering matrix of such structure is derived. For the analysis we utilize an efficient numerical technique described in [1], which is based on the **T**-matrix approach and uses the lattice sums technique [2]. The technique was previously used to investigate periodic structures employing infinitely long circular cylinders. We developed this approach to analyze the structures which are periodic in two directions. In our method, the scattering matrix which relates the incident space-harmonics to the scattered, both reflected and transmitted ones, is defined for a double periodic array. The scattering matrix is expressed in terms of lattice sums characterizing a periodic arrangement of scatterers and the **T**-matrix for periodic cylindrical unit cell of the structure. The validity and accuracy of the approach are verified by comparing the results with those obtained from alternative methods.

ACKNOWLEDGMENT

This work was supported under Polish Ministry of Science and Higher Education (National Science Center) from sources for science in the years 2010–2012: partially under Contract N515 501740 (decision No. 5017/B/T02/2011/40) and under funding for Statutory Activities for ETI Gdansk University of Technology.

REFERENCES

1. Kushta, T. and K. Yasumoto, "Electromagnetic scattering from periodic arrays of two circular cylinders per unit cell," *Progress In Electromagnetics Research*, Vol. 29, 69–85, 2000.
2. Yasumoto, K. and K. Yoshitomi, "Efficient calculation of lattice sums for freespace periodic Greens function," *IEEE Trans. Antennas and Propag.*, Vol. 47, No. 6, 1050–1055, Jun. 1999.

Analysis of Periodically Loaded Rectangular Waveguide

R. Lech, **A. Kusiek**, **and J. Mazur**
Gdansk University of Technology, Poland

Abstract— Periodic systems are applied when it is desired to reduce the phase velocity of a transmission line waves. Slow waves are required for linear accelerators, delay lines, beam-interaction devices, radars, antenna feed systems and other microwave devices. These systems commonly consist of a set of uniformly spaced identical obstacles such as irises, metallic or dielectric cylinders or other arbitrary shaped posts. All the periodic structures are distinguished by existence of separated passbands and stopbands, which can be illustrated in dispersion $k_0 - \beta$ diagrams. The selectivity of the periodic structures can also be exploited in microwave resonators and filters.

In this paper the analysis of propagation in periodically loaded waveguide structures is conducted. The propagation constants of the Floquet modes are determined using derived eigenvalue equation. The procedure used here allows to determine the propagation constants of the Floquet modes from the classical eigenvalues of a characteristic matrix determined from scattering matrix of the guide section [1, 2]. The method is more time-effective than solving the nonlinear determinant equation by an iterative process. Only the modal scattering matrix of a single section and the period value are needed for the calculations.

In order to calculate the modal scattering matrix of a single section the hybrid approach based on mode-matching technique for post with regular cross-section, combination of mode matching technique with method of moments for metallized cylindrical posts and combination of discrete finite-difference frequency-domain method with method of moments for arbitrary cross-section posts is utilized.

The verification of the obtained results is performed by calculating and measuring semi-periodic structures composed of periodically arranged sections of circular posts of arbitrary cross-section in rectangular waveguide junction. The existence of passbands and stopbands, which are characteristic for periodic structures, is shown.

ACKNOWLEDGMENT

This work was supported under Polish Ministry of Science and Higher Education from sources for science in the years 2010-2012: partially under COST Action IC0803 (decision No. 618/N-COST/09/2010/0) and under funding for Statutory Activities for ETI Gdansk University of Technology.

REFERENCES

1. Amari, S., R. Vahledieck, and J. Bornemann, "Analysis of propagation in periodically loaded circular waveguides," *IEE Proc. Microwaves, Antennas and Propagation/*, Vol. 146, No. 1, 50–54, February 1999.
2. Lech, R. and J. Mazur, "Propagation in rectangular waveguides periodically loaded with cylindrical posts," *IEEE Microwave and Wireless Components Letters/*, Vol. 14, No. 4, 177–179, April 2004.

A Quaternion Widely Linear One-stage Prediction Algorithm

R. M. Fernández-Alcalá[1], **J. Navarro-Moreno**[1], **J. C. Ruiz-Molina**[1], **C. Jahanchahi**[2], **and D. H. Dini**[2]

[1]Department of Statistics and Operations Research, University of Jaén, Spain
[2]Department of Electrical and Electronic Engineering
Imperial College London, London, United Kingdom

Abstract— Recent advances in communication and signal processing have awoken the interest in multidimensional signals. Although these signals could be treated from a real or complex vectorial approach, the lastest studies have shown the enhancement of using quaternions instead of vectorial signals [1].

Basically, quaternions can be considered as a noncommutative expansion of complex numbers which are given by a scalar real part and a vectorial part formed by three imaginary variables. Hence, they are suitable for modeling three and four-dimensional signals, collecting in a natural way the correlation between their components.

Analogously to the complex case, a widely linear processing is the appropriate approach to take advantage of all the available second-order statistical information [2]. Quaternion widely linear processing is characterized by considering a four-dimensional vector whose elements are chosen among the signal, its conjugate, and the three potential involutions, taking into account a possible improperty in the quaternion signals involved.

In this paper, a quaternion widely linear processing is employed in the designing of a one-stage prediction algorithm for a special class of quaternion random signals characterized because the autocorrelation function of the augmented quaternion vector only depends on the difference of time instants. This type of signal will be called wide-sense stationary (WSS). In our methodology, the multivariate Durbin-Levinson algorithm [3], proper of stationary time series analysis, is adapted for the one-stage prediction of a WSS quaternion signal which will be the first step for the one-stage prediction of a function of the quaternion signal.

The achievement of the proposed solution is analyzed by means of a simulation example where the three-dimensional velocity of an aircraft is predicted from the information supplied by its three-dimensional position.

REFERENCES

1. Mandic, D. P. and V. S. L. Goh, *Complex Valued Nonlinear Adaptative Filters. Noncircularity, Widely Linear and Neural Models*, Wiley, 2009.
2. Cheong Took, C. and D. P. Mandic, "Augmented second-order statistics of quaternion random signals," *Signal Processing*, Vol. 91, No. 2, 214–224, 2011.
3. Brockwell, P. J. and R. A. Davis, *Time Series: Theory and Methods*, 2nd Edition, Springer-Verlag, New York, 1991.
4. Navarro-Moreno, J., "ARMA prediction of widely linear systems by using the innovations algorithm," *IEEE Trans. Signal Processing*, Vol. 7, 3061–3068, 2008.
5. Navarro-Moreno, J., J. Moreno-Kayser, R. M. Fernández-Alcalá, and J. C. Ruiz-Molina, "Widely linear estimation algorithms for second-order stationary signals," *IEEE Trans. Signal Processing*, Vol. 51, No. 1, 306–312, 2009.
6. Picinbono, J. and P. Bondon, "Second-order statistics of complex signals," *IEEE Trans. Signal Processing*, Vol. 45, No. 2, 411–420, 1997.

Efficient Root Tracing Method Employing Simplex Chain Vertices Searching Procedure

P. Kowalczyk
Gdansk University of Technology, Poland

Abstract— One of the most common problems of computational electrodynamics is solving of a nonlinear equation. Most frequently the equation is a transformed form of the eigenvalue problem, which is obtained from analysis of resonant frequencies or propagation coefficient. Especially, for some structures, such as ferrite lines, periodic structures, nonuniform waveguides, and any open lines, the problem is defined in complex domain (complex or leaky modes).

Generally, all nonlinear equations can be expressed in a form involving a real or complex function of many variables $F(z_1, z_2, z_3, \ldots) = 0$. Moreover, in numerous cases, the function is defined as a determinant of a high-order matrix and its evaluation can be very time consuming. Thus, it is very important to minimize the number of the function evaluations.

There is a large number of standard numerical procedures that can be successfully applied to find the roots of such function: the Newton iteration method [1], Muller interpolation method [2], and secant method [1]. Despite a large number of known root-finding techniques, new algorithms are still arising. In recent years, a few new methods for finding the roots of real and complex functions were published [3, 4]. However, most of them are based on iterative procedure and concern improving the accuracy of finding a singular root, which are inefficient in electromagnetic analysis. For example, in microwave transmission line theory, the dispersion characteristic is defined as a propagation coefficient in a function of frequency $\gamma(f)$. To determine such relation the roots of the equation $F(\gamma, f) = 0$ must be found. A calculation using a root-finding algorithm for each frequency point is very time consuming. To avoid these disadvantages, a root-tracing algorithm should be utilized.

In this paper a novel efficient method of solving multidimensional equations is presented. The concept is realized as root tracing process of a real or complex function of N variables in the constrained space. We assume that the roots of the continuous function of N variables lie on the continuous $(N-1)$-dimensional hyperplane. The method uses regular N and $(N-1)$-Simplexes, at which vertices the considered function changes its sign. Based on $(N-1)$-Simplex, the function is evaluated at two new points that are vertices of new regular N-Simplexes for which $(N-1)$-Simplex is one of its $(N-1)$-faces. The algorithm, with the usage of stack, runs in an iterative mode tracing the roots inside the volume of the considered simplexes. As a result, the algorithm creates a chain of simplexes in the constrained region.

The proposed algorithm is optimal in the sense of the number of function evaluations. In each iteration, a new generated evaluation point determines a new region where the function has the roots. The accuracy of the procedure depends on the edge length of the initial simplex, and can be defined at the beginning. The numerical results have proven the versatility and efficiency of the proposed algorithm.

REFERENCES

1. Hamming, R. W., *Numerical Methods for Scientists and Engineers*, McGraw-Hill, Inc., New York, 1962.
2. Muller, D. E., "A method for solving algebraic equations using an automatic computer," *Math. Tables and Other Aids to Computat.*, Vol. 10, 208–215, 1956.
3. Zhang, X., X. Chen, and Z. Huang, "Parallel genetic algorithm for finding roots of complex functional equation," *2nd International Conference on Pervasive Computing and Applications, ICPCA 2007*, 542–545, Birmingham, England, July 2007.
4. Alolyan, I., "An algorithm for finding all zeros of vector functions," *Bull. Australian Math. Soc.*, Vol. 77, 353–363, 2008.

Raindrop Size Model Using Method of Moment and Its Applications in Radio Systems

P. A. Owolawi
Department of Electrical Engineering
Mangosuthu University of Technology, KwaZulu-Natal, South Africa

Abstract— Radio communication systems operating at microwave and millimeter wave bands are usually impaired by rain attenuation. This attenuation is caused by raindrop effects by processes of absorption and scattering of the radio wave signal emanation from these frequency bands. Thus, the adequate knowledge of raindrop size distribution is important component in estimate the specific rain attenuation, then total rain attenuation which consequently affect the quality and performance of channel conditions.

In this paper, the raindrop size modeling and analysis are presented. Drop size is classified into different rain types such as drizzle, thunderstorm, widespread and shower. Two major distributions, gamma and lognormal are employed with second, fourth and six method of moment estimators. Both distributions seem appropriate with least percentage of error in lognormal using root-mean-square error.

The details of gamma, lognormal and method of moment estimator employed are presented in the paper. The results are compared with the existing raindrop size models such as lognormal by Ajayi et al., and gamma model as presented by Lakshami et al. This is then followed by the application of rain drop size on terrestrial radio link at 19.5 GHz.

In conclusion, suitable raindrop size models are recommended for the region and parameters derived are very useful for the radio design and satellite communication systems.

Application of the Extended Bi-characteristic System Method at Radio-wave Propagation Modeling in the Ionosphere of the Earth

Kseniya S. Kiryanova, Andrew S. Kryukovsky, Dmitry S. Lukin, and Dmitry V. Rastyagaev
Moscow Physico-Technical Institute, Russia

Abstract— The propagation of decameter radio-waves in ionospheric plasma is considered. At modeling the extended the bi-characteristic system of the equations received by D. S. Lukin which allows to find ray trajectories with the large accuracy, to reveal caustic structures and to calculate amplitude and phase characteristics of electromagnetic fields was used. The modeling of propagation of radio-waves in non-uniform ionosphere is executed in view of influence of a magnetic field of the Earth. At calculations the ionosphere models with horizontal gradients were used. It was taken into account of local heterogeneity, such as the lowered electronic concentration in a maximum of a layer and the raised electronic concentration lower than a maximum of a layer at a various positions of a radiation source. The features of short-wave propagation, such as hit of waves in the ionospheric channel, propagation and exit from it, and also reflection of waves from different ionospheric layers are investigated. It is shown, that the rays can be pushed out from area of propagation and twist at hit in ionospheric heterogeneity. In work caustic surface formation and their dynamics also are investigated. The propagation of radio-waves and in the ionosphere of the Earth is investigated, which structures are restored by scientific group under the direction of the professors V. Eu. Kunitzin by a radio-tomography method on the basis of real supervision. The ray structures in the "equatorial anomaly" vicinity and at presence quasi-periodic wave disturbances of the main maximum of an ionospheric layer are constructed. Ray and amplitude-phase structures of electromagnetic fields at various working frequencies are investigated. The dynamic model of radio-wave ray propagation is developed.

Magnetoelectric Magnetic Field Sensors

I. N. Soloviev, **M. I. Bichurin**, **and R. V. Petrov**
Novgorod State University, Russia

Abstract— The working principle of magnetic sensing in magnetoelectric (ME) laminates is simple: when a magnetic field is applied to the magnetostrictive layer, it strains producing a proportional charge in the piezoelectric layer. Highly sensitive magnetic field sensors can be obtained using large magnetostrictive and high strain-sensitive piezoelectric ME composite materials in long or ring type configurations.

In this work, the ME magnetic field sensors based on ME composites are studied. The ME three-layer laminate consisting of two Metglas (FeBSiC) layer with the middle PZT layer for sensor application was researched.

PZT layer was poled in an electric field and the ME coefficient was measured by subjecting the sample to a dc magnetic bias H and an ac magnetic field δH while measuring the ac induced electrical field. A typical measurement system for the ME effect consists of a dc electromagnet with the Helmholtz coils. The structures to be measured are then placed between the Helmoltz coils. The electromagnet should be driven by a constant-current source, and the Helmholtz coils are typically driven by a low-frequency oscillator with a frequency bandwidth of $1 < f < 10^3$ Hz. To measure the induced voltage, the electrodes of a sample are then electrically connected to an operational amplifier, which subsequently feeds into either an oscilloscope or a lock-in amplifier. The ME voltage coefficient is the ratio of the electric field induced across the piezoelectric component to the magnetic field applied to magnetostrictive one: i.e., $\alpha_E =^p E/^m H$.

The manufactured sensor showed a sensitivity of $\alpha_{\mathrm{ME}} = 25\,\mathrm{mV/Oe}$ at frequency range from 50 Hz to 500 Hz.

Wide applications of the ME sensors are biomagnetic measurements like magnetoencephalography and magnetocardiography, motion detection, engine control, control of linear and angular accelerations and others. For increasing the sensor sensitivity one needs to use large magnetostrictive and high strain-sensitive piezoelectric ME composite materials.

Satellite Remote Sensing of Carbon Monoxide

Jane J. Liu[1, 2], **Aijun Ding**[1], **Ke Ding**[1], **Yong Han**[1], **Jian-Cheng Shi**[3], **Liangfu Chen**[3], **and Tianliang Zhao**[4]

[1]Nanjing University, 22 Hankou Road, Nanjing 210093, China
[2]University of Toronto, 100 St. George Street, Toronto
Ontario M5S 3G3, Canada
[3]Institute of Remote Sensing Applications, Chinese Academy of Sciences
3 Datun Road, Chaoyang District, Beijing 100101, China
[4]Nanjing University of Information Science & Technology
219 Ningliu Road, Nanjing 210044, China

Abstract— Measurements Of Pollution In The Troposphere (MOPITT) on board NASA Terra satellite is a sensor developed for measuring carbon monoxide (CO) from space. The CO measurements made by MOPITT have greatly enhanced our understanding of temporal and spatial distributions of CO in the atmosphere and the mechanisms governing the distributions. In this presentation, the temporal and spatial variations of CO revealed by MOPITT will be overviewed to provide a comprehensive picture of global CO distributions. The information is useful not only to atmospheric science community but also to other disciplines and public, owing to the importance of CO as a major pollutant, a precursor of ozone, and its effects on many atmospheric chemical processes. The CO distributions have illustrated the combined natural and anthropogenic influences. Furthermore, MOPITT's capability in detecting highly polluted regions in China will be discussed. Some results on CO source and sink distributions inversed with MOPITT data will be presented.

The Theory of Wave Propagation Problems in Propagation, Focusing and Diffraction of Radio Waves in Inhomogeneous Media

Andrew S. Kryukovsky, Dmitry S. Lukin, and Dmitry V. Rastyagaev
Moscow Physico-Technical Institute, Russia

Abstract— In the paper, it is presented the results of mathematical and numerical modeling of diffraction, propagation and focusing of electromagnetic waves in inhomogeneous and dispersive media based on the application of the theory of wave catastrophes. The principles of design information and analytical software system modeling of wave processes in inhomogeneous and nonstationary media based on the methods of wave catastrophes. Specific areas (such as the wave catastrophe), corresponding to areas of focal radiation diffraction region, the transitional zone, there are various problems in radio physics, acoustics and quantum mechanics. Such structures are not described by either the traditional asymptotic methods, or a description thereof is extremely difficult or impossible due to the formation of complex focal areas. The paper presents the main provisions of the wave theory of catastrophes: the classification of catastrophe types, and types of indexes focusing, as well as methods for constructing uniform asymptotic applied to describe the structure of wave fields in such areas, the analysis of amplitude and phase structure of the field. Modeling radiation characteristics of families of caustics, wave fronts of bifurcations in the propagation, focusing, scattering and diffraction of waves makes it possible to study the structure of the fields in the focal complex formations and diffraction. The software package, based on infological domain model (classification and hierarchy of types of singularities), allows modeling of the processes of formation, the dynamic development and the "disintegration" of the focal complex formation and diffraction. The individual program modules include a set of numerical calculations of the radiation and caustic structures, the most important from the point of view of applications of singularities (core, edge, and angle accidents), as well as calculations of special functions of wave catastrophes, and their first derivatives required for the construction of uniform asymptotic solutions of wave problems in mathematical physics.

Anomalous Light Scattering by Plasmonic Nanoclusters

M. I. Tribelsky[1, 2] and B. S. Luk'yanchuk[3]

[1]Faculty of Physics, M. V. Lomonosov Moscow State University, Moscow 119991, Russia
[2]Moscow State Institute of Radioengineering, Electronics and Automation (Technical University) Moscow 119454, Russia
[3]Agency for Science, Technology and Research, Data Storage Institute, Singapore 117608, Singapore

Abstract— It is shown that light scattering by a non-magnetic nanocluster with low dissipation rate close to plasmon (polariton) resonance frequencies differs from the one described by the Rayleigh approximation dramatically. Thus, a more accurate approach should be employed. In the present contribution the problem is studied within the framework of the exact Mie solution. It is shown that if imaginary part of the dielectric permittivity of the cluster is small enough, the dissipative damping is replaced by the radiative one. In such a case the problem exhibits sharp giant resonances with very unusual properties. In particular, despite smallness of the cluster relative to the incident light wavelength the extinction cross section for these resonances increases with an increase in the order of the resonance, i.e., the cross section at the dipole resonance is *smaller* than that at the quadrupole resonance, etc. (*inverted hierarchy of the resonances*); the characteristic values of the electric and magnetic fields inside the cluster and in its immediate vicinity are singular in the cluster size, while the energy circulation in the near-field is rather complicated. The corresponding field of the Poynting vector includes singular points, whose number, types and positions are very sensitive to fine changes in the incident light frequency. As an example a bifurcation diagram, describing the behavior of the singular points in the vicinity of the dipole resonance for a cluster with a certain fixed size is obtained. Practical examples of this scattering for different pairs "nanocluster–host medium" with actual (experimentally measured) dispersion relations for dielectric permittivity [1] are presented. The results may provide new opportunities for giant, controlled, highly frequency-sensitive enhancement and variation of electromagnetic field at nano-scales. Our main publications devoted to the subject are as follows [2–6].

ACKNOWLEDGMENT

The work is partly supported by the Russian Foundation for Basic Research, Grant 12-02-00391-a.

REFERENCES

1. Palik, E. D., *Handbook of Optical Constants of Solids*, Academic, New York, 1985.
2. Tribelskiĭ, M. I., "Resonant scattering of light by small particles," *Sov. Phys. JETP*, Vol. 59, 534–536, 1984.
3. Luk'yanchuk, B. S., M. I. Tribelskiĭ, and V. V. Ternovskiĭ, "Light scattering at nanoparticles close to plasmon resonance frequencies," *J. Opt. Technol.*, Vol. 73, 371–377, 2006.
4. Tribelsky, M. I. and B. S. Luk'yanchuk, "Anomalous light scattering by small particles," *Phys. Rev. Lett.*, Vol. 97, 263902, 2006.
5. Tribelsky, M. I. and B. S. Luk'yanchuk, "Anomalous light scattering by small particles," *Virtual Journal of Nanoscale Science & Technology*, Vol. 15, No. 2, 2007
6. Luk'yanchuk, B. S., M. I. Tribelsky, V. Ternovsky, Z. B. Wang, M. H. Hong, and L. P. Shi, and T. C. Chong, "Peculiarities of light scattering by nanoparticles and nanowires near plasmon resonance frequencies in weakly dissipating materials," *J. Opt. A: Pure and Appl. Opt.*, Vol. 9, S294–S300, 2007.

Peculiarities of the Fano Resonances in Light Scattering by Obstacles

M. I. Tribelsky[1, 2], **S. Flach**[3], **A. E. Miroshnichenko**[4], **and Y. S. Kivshar**[4]

[1]Faculty of Physics, M. V. Lomonosov Moscow State University, Moscow 119991, Russia
[2]Moscow State Institute of Radioengineering, Electronics and Automation (Technical University) Moscow 119454, Russia
[3]Max-Planck-Insitut für Physik Komplexer Systeme, Dresden 101187, Germany
[4]Nonlinear Physics Centre, Research School of Physics and Engineering Australian National University, Canberra ACT 0200, Auatralia

Abstract— The problem of the Fano resonances in light scattering by an obstacle is discussed. It is shown that despite a certain similarity between the Fano resonances in quantum scattering of particles by a potential with a quasi-discrete level [1] and the ones at elastic light scattering by a finite-size obstacle, there is a dramatic difference between these two cases. In both the cases the phenomenon is based upon interference of the so-called resonant and background partitions of the incident wave, which results in a typical asymmetric Fano profile with a pronounced peak at the point of the constructive interference and compete (or almost complete) suppression of the scattering at the point of the destructive one (for more details see, e.g., the recent reviews [2, 3]). However, in the case of the quantum scattering the resonant and background partitions both are related to one and the same partial wave, while in optics they are related to *different* electromagnetic modes. This difference in the nature of the resonances gives rise to differences in their manifestations. The general arguments are illustrated by inspection of the Fano resonances in the case of light scattering by a sphere, when the scattering is described by the exact Mie solution. It is shown that if the roles of the resonant and background partitions are played by modes with *different* multipole moments, a new phenomenon, namely *the directional Fano resonances* may be observed. In this case the the asymmetric Fano profile may be obtained at the scattering along *any given direction*, while along other directions the profile is symmetric Lorenzian (Breit-Wigner). The profile of the extinction (scattering) cross section is also Lorenzian. If the resonant and background partitions are presented by different modes with *the same* multipole moment the entire extinction (scattering) cross section profile may be asymmetric Fano. It results in almost complete suppression of the net scattering at the frequencies of the destructive interference (*invisibility of the obstacle*). The case is characterized by multiple Fano's resonances at different frequencies. Two examples of such a kind, namely for a sphere with a large value of dielectric permittivity and the one with spatial dispersion are discussed in detail. The results obtained shed new light on this important and interesting phenomenon and may be employed in various applications. Our main publications devoted to the subject are as follows [4–7].

ACKNOWLEDGMENT

The work is partly supported by the Russian Foundation for Basic Research, Grant 12-02-00391-a.

REFERENCES

1. Fano, U., "Effects of configuration interaction on intensities and phase shifts," *Phys. Rev.*, Vol. 124, 1866–1878, 1961.
2. Miroshnichenko, A. E., S. Flach, and Y. S. Kivshar, "Fano resonances in nanoscale structures," *Rev. Mod. Phys.*, Vol. 82, 2257–2298, 2010.
3. Luk'yanchuk, B., N. I. Zheludev, S. A. Maier, N. J. Halas, P. Nordlander, H. Giessen, and C. T. Chong, "The Fano resonance in plasmonic nanostructures and metamaterials," *Nature Materials*, Vol. 9, 707–715, 2010.
4. Luk'yanchuk, B. S., M. I. Tribelsky, Z. B. Wang, Z. Yi, M. H. Hong, L. P. Shi, and T. C. Chong, "Extraordinary scattering diagram for nanoparticles near plasmon resonance frequencies," *Appl. Phys. A*, Vol. 89, 259–264, 2007.
5. Tribelsky, M. I., S. Flach, A. E. Miroshnichenko, A. Gorbach, and Y. S. Kivshar, "Light scattering by a finite obstacle and Fano resonances," *Phys. Rev. Lett.*, Vol. 100, 043903, 2008.
6. Miroshnichenko, A. E., S. Flach, A. V. Gorbach, B. S. Luk'yanchuk, Y. S. Kivshar, and M. I. Tribelsky, "Fano resonances: A discovery that was not made 100 years ago," *Optics and Photonics News" (A Special Issue Highlighting the Most Exciting Research in Optics to Emerge in 2008)*, No. 12, 48, 2008.

7. Tribelsky, M. I., A. E. Miroshnichenko, and Y. S. Kivshar, "Unconventional Fano resonances in light scattering by small particles," *Europhys. Lett.*, Vol. 97, 44005, 2012.

The Field Finite-difference Approach and Applications in Computational Electrostatics

Dusan Z. Djurdjevic
Faculty of Technical Sciences, University of Pristina
Kneza Milosa 7, Kosovska Mitrovica 38220, Serbia

Abstract— The field finite-difference (FFD) approach is introduced and applied for the solution of two-dimensional (2D) problems described by the Laplace equation in electrostatics [1]. Instead of calculating the electric scalar potential, in the FFD approach the electric field components are calculated first, enabling superior solution accuracy in comparison to standard scalar potential FD approaches. Novel multiple point 2D FFD formulas are derived via a simple collocation procedure for both uniform and non-uniform FD discretization. For the uniform FD-mesh case, the FFD formulas with the 16th order of accuracy are achieved.

The FFD approach is implemented and tested in the high order accurate FD electric field computation of 2D electrostatic systems with cross-sections consisted by linear, oblique, curved and circular dielectric boundaries. The influence of the so-called staircasing effect due to the FD discretizing of the electric field at the points sampled close to the dielectric interfaces is substantially removed by using the improved FFD approach. The improved FFD formulation is designed according to the well-established improved FD approaches proposed in the field of photonics [2] during the last decade. The high level of accuracy, numerical stability and efficiency of the FFD approach is illustrated in the field analysis of the various electrostatic problems with different geometries. The FFD approach can be easily extended in other areas of electromagnetic field analysis, e.g., in solving 3D electrostatic problems, in solving transmission line problems etc.. Furthermore, the FFD idea can be utilized to solve other physical problems and processes where scalar fields fulfil 2D (or 3D) Laplace's or Poisson's equations.

ACKNOWLEDGMENT

This work is based on research conducted within the Project (Project code: TR32052) funded by the Ministry of Science and Technological Development of the Republic of Serbia.

REFERENCES

1. Kantorovich, L. V. and V. I. Krylov, *Approximate Methods of Higher Analysis*, Noordhoff, Groningen, The Netherlands, 1958.
2. Chiang, Y. C., Y. P. Chiou, and H. C. Chang, "Improved full-vectorial finite difference mode solver for optical waveguides with step-index profiles," *J. Lightw. Technol.*, Vol. 20, 1609–1618, 2002.

Electromagnetic Sensing of Partial Discharge in Air-insulated Medium Voltage Switchgear

B. Zheng and A. Bojovschi
School of Electrical and Computer Engineering, RMIT University, Melbourne, VIC 3001, Australia

Abstract— The importance of detecting accurately the partial discharge in high voltage power industry becomes obvious as the infrastructure ages. In this work electromagnetic sensing for detecting the electromagnetic radiation, associated with partial discharge, in an air-insulated medium voltage switchgear (Type D24-121114 of Driescher) is used. The study relies on Finite Element Method as implemented in High Frequency Structure Simulator. The partial discharges are approximated by Gaussian sources. Coaxial patch antenna is employed for electromagnetic sensing. This transducer is optimized to have highest efficiency in the frequency band of interest, for partial discharge detection, of 800 MHz to 900 MHz. The antenna is placed in the switchgear system and its ability to sense partial discharge in the air-insulated switchgear is addressed. The optimized location, in the switchgear system, of the antennas for an efficient sensing is presented. The current density induced in the electromagnetic sensors by the radiation emitted from the partial discharges is used as an indicator of efficient radiative coupling. As repetitive partial discharge leads to the failure of the air-insulated switchgear, this method provides a sensitive method for pre-fault detection.

Anderson Localization of Light and Disorder-enhanced Transport

Mordechai Segev, Liad Levi, and Mikael Rechtsman
Physics Department and Solid State Institute
Technion — Israel Institute of Technology, Israel

Abstract— We will review the recent progress on Anderson localization of light, and describe experiments and theory demonstrating disordered-enhanced transport in photonic quasicrystals, as well as hyper-transport of light in photonic media with evolving disorder: a new regime of transport in which transport is faster than ballistic.

Summary: Anderson Localization is one of the most basic concepts in solid-state physics. However, experiments with electronic systems have eluded scientists for many decades. The concept has been extended to optics, and in 2007, our group made the first demonstration of Anderson localization in its original context, where random fluctuations superimposed upon a periodic structure bring transport to a halt [1]. Many experimental works have followed, in optics and matter-waves. But can disorder work to increase transport beyond diffusion, and perhaps even beyond ballistic transport? The talk will review the recent progress on Anderson localization of light, and will describe experiments and theory demonstrating disorder-enhanced transport in two distinct cases. First, we will show that introducing disorder to photonic quasicrystals can enhance wave transport [2], which stands in contrast to the characteristic suppression of transport by disorder. Second, we will present theory and experiments on hyper-transport of light in photonic media with evolving disorder: a new regime of transport in which transport is faster than ballistic [3].

REFERENCES

1. Schwartz, T., G. Bartal, S. Fishman, and M. Segev, "Transport and anderson localization in disordered two-dimensional photonic lattices," *Nature*, Vol. 446, No. 52, 2007.
2. Levi, L., M. Rechtsman, B. Freedman, T. Schwartz, O. Manela, and M. Segev, "Disorder-enhanced transport in photonic quasicrystals," *Science*, Vol. 332, 1541, 2011.
3. Levi, L., Y. Krivolapov, S. Fishman, and M. Segev, "Hyper-transport by virtue of disorder," submitted, 2012.

Optimal Amplification of Nonautonomous Solitons

R. Peña[1] and C. Hernandez-Tenorio[2]

[1]Benemerita Universidad Autónoma de Puebla, 502, Puebla C. P. 72001, México
[2]Instituto Tecnológico de Toluca, Metepec, Edo. México C. P. 52140, México

Abstract— We show that the methodology based on the generalized inverse scattering transform (IST) concept provides a systematic way to discover the novel exactly integrable nonlinear Schrödinger equation models with varying dispersion, nonlinearity and gain or absorption. This algorithm is a useful tool to design novel dispersion and nonlinear managed fiber optics compression systems.

Concepts of soliton control and of soliton dispersion management in the nonlinear dynamical systems described by the nonlinear Schrödinger equation (NLSE) model with varying dispersion, nonlinearity, and gain or loss, are the new and important developments in the application of solitons for optical transmissions. Soliton control is based on the robustness of solitons. Since a soliton can be described by the four parameters: the amplitude (or width), the frequency (or velocity), the phase and the time position, the soliton dynamics can be investigated by traditional perturbation methods of conserved quantities of the NLSE, such as energy and momentum, or/and perturbed inverse scattering transform, or/and the Lagrangian method. For practical cases, all of these perturbation methods give the same result. Since the Lagrangian method is also applicable to the nonintegrable NLSE models, it is widely using in the concept of dispersion-managed optical solitons.

In this report, we present exact analytic solutions for the nonlinear Schrödinger equation model with varying dispersion and nonlinearity. First, we will present a generalized mathematical algorithm to construct the Lax pairs and to discover the novel exactly integrable NLSE models. We will also turn our attention to finding exact analytical solutions for specified soliton management conditions. Fundamental soliton compression regimes are predicted. Second, we will investigate the main soliton features of the solution presented by the direct computer simulations. The dynamics of nonlinear solitary waves is studied in the framework of the nonautonomous nonlinear Schrödinger equation (NLSE) model with varying nonlinearity, dispersion, gain or absorption and varying in time harmonic oscillator potential. The model allows one to analyze on the general basis a variety of nonlinear phenomena appearing both in Bose-Einstein condensate (BEC), condensed matter physics and in nonlinear optics and biophysics.

Transformations of Field Equations in Octonion Spaces

Zi-Hua Weng
School of Physics and Mechanical & Electrical Engineering
Xiamen University, Xiamen 361005, China

Abstract— J. C. Maxwell was the first to mix two methods, the vector and the quaternion, to describe the feature of electromagnetic fields. The quaternion was invented by W. R. Hamilton. Meanwhile the octonion, as the ordered pair of quaternions, was created by J. T. Graves and A. Cayley independently. Subsequently the quaternion was divided into the scalar part and vectorial part. The latter was evolved into the conventional 3-dimensional vector.

The electromagnetic theory described by the vector is quite brilliant, while it is not successful to adopt the quaternion to depict the electromagnetic features. By contrast, the electromagnetic theory described by the octonion achieves some developments to a certain extent. One octonion can be separated into two components, the quaternion and the S-quaternion. It is found that the quaternion is suitable for describing the gravitational features, while the S-quaternion is fit for depicting the property of electromagnetic field. Nowadays there are abundant in identical inferences between the electromagnetic features described by the S-quaternion and that by the vector. While there are similar conclusions between the gravitational properties depicted with the quaternion and that with the vector.

In order to deduce the above conclusions, it is necessary to transfer equivalently the electromagnetic equations in the S-quaternion space into that in the quaternion space. Further it is requisite to transfer the latter into that in the 3-dimensional vector space, to achieve the contrasting to the Maxwell equations in the classical electromagnetic theory. Similarly the gravitational equations will be transformed into that in the vector space.

In order to deduce the above conclusions, it is necessary to transfer equivalently the electromagnetic equations in the S-quaternion space into that in the quaternion space. Further it is requisite to transfer the latter into that in the 3-dimensional vector space, to achieve the contrasting to the Maxwell equations in the classical electromagnetic theory. Similarly the gravitational equations will be transformed into that in the vector space.

ACKNOWLEDGMENT

The authors are grateful for the financial support from the National Natural Science Foundation of China under grant number 60677039.

Electromagnetic and Gravitational Fields in the Curved Octonion Spaces

Zi-Hua Weng
School of Physics and Mechanical & Electrical Engineering
Xiamen University, Xiamen 361005, China

Abstract— J. C. Maxwell was the first to describe the electromagnetic theory with the quaternion and the vector. This method inspirits the scholars to study the electromagnetic theory and the gravitational theory with the quaternion and the octonion. And then the relevant researches can be extended from the flat octonion space into the curved octonion space.

The octonion can be decompounded into the quaternion and the S-quaternion. Similarly the curved octonion space can be decomposed to the two subspaces, the curved quaternion space and the curved S-quaternion space. The curved quaternion space can be used to depict the gravitational field, while the curved S-quaternion space can be used to describe the electromagnetic field.

The paper discusses the influences of curved octonion spaces on the electromagnetic field and the gravitational field. The field source and the curved octonion space both will impact the object's motion in the fields. In case the octonion field is strong enough, it will curve the octonion space to result in the extra motion of objects in the fields.

In the curved octonion space, by means of the coefficient and the curvature, the field source determinates the field potential. Similarly the field strength decides the integral of the field potential, as well as the force affirms the torque. The related inferences improve some results of the electromagnetic and gravitational theories in the curved Four Space-time.

On-body Textile Monopole Antenna Characterisation for Body-centric Wireless Communications

H. A. Rahim[1], **F. Malek**[1], **I. Adam**[1], **S. Ahmad**[1], **N. B. Hashim**[1], **and P. S. Hall**[2]

[1]Embedded Computing Research Cluster (ECRC)
School of Computer and Communication Engineering
Universiti Malaysia Perlis, Perlis, Malaysia
[2]School of Electronics, Electrical and Computer Engineering
The University of Birmingham, Edgbaston, Birmingham B 15 2TT, United Kingdom

Abstract— In this paper, the on-body performance of a light-weight and simple structure textile monopole antenna was investigated by determining reflection coefficient and bandwidth characteristics using Hugo Body model with CST Microwave Studio software at 2.45 GHz. ShieldIt Super with conductivity of 1.96×10^5 S/m, is used as a conductive textile. Meanwhile, substrate material for monopole antenna is felt fabric, with a relative dielectric permittivity, $\varepsilon_r = 1.22$.

The aim of Body-Centric Wireless Communications (BCWC) is to provide with constant availability, reconfigurability and unobtrusiveness that suits with the need of the future wearable system. Hence, a small, lightweight, robust, unobtrusive to the user and conformal to the body surface is needed for the applications of BCWC. The investigation of textile monopole antenna is carried out in the vicinity of human body, simulated by using HUGO model, defined at a $8 \times 8 \times 8$ mm^3 voxel resolution. The monopole was positioned on the shoulder, as this position is the suitable site to integrate the textile antenna into clothing. The distance of the antenna placed on human body was varying between 0 and 15 mm. The investigation was aimed to study the changes in textile antenna's characteristics in terms of reflection coefficient and impedance bandwidth when the antenna was placed on human's shoulder.

The result showed that the reflection coefficient values were improved by 40.8% with a slight downward frequency shift as the textile monopole was varying between 2 mm and 15 mm. The reflection coefficient for 0 mm (on body) from human's shoulder was obtained less than -10 dB. The result also demonstrated that an improvement of 29.3% in impedance bandwidth was obtained when the textile monopole was positioned in the range of 10 and 15 mm. As the textile antenna was positioned away from human's shoulder, the reflection coefficient and impedance bandwidth improved significantly.

Design and Simulation of a Wearable Textile Monopole Antenna for Body Centric Wireless Communications

H. A. Rahim[1], **F. Malek**[1], **I. Adam**[1], **S. Ahmad**[1], **N. B. Hashim**[1], **and P. S. Hall**[2]

[1]Embedded Computing Research Cluster (ECRC)
School of Computer and Communication Engineering
Universiti Malaysia Perlis, Perlis, Malaysia
[2]School of Electronics, Electrical and Computer Engineering
University of Birmingham, Edgbaston, Birmingham B 15 2TT, United Kingdom

Abstract— This paper presents a light-weight and simple structure of monopole antenna using conductive textile. Pure Copper Polyster Tafetta Fabric (PCPTF) is used as a conductive textile, in comparison with conventional microstrip monopole antenna. The prototype is designed with 40 mm × 60 mm total dimension and spaced by a 2 mm thick felt fabric for Wireless Body Area Network (WBAN) operating in the 2.45 GHz Industrial, Scientific and Medical (ISM) band.

On-body antenna is very important element to be used for various future IEEE 802.15 wireless standard applications. Textile antenna is suitable for on-body radio communication as it is flexible and comfortable to be integrated into clothing. Textile monopole antenna is chosen because this antenna polarizes normally to the body surface and therefore it preserves a strong ray diffracted around the body. This present work describes design and analysis of a textile monopole antenna basic characteristic. The performance of the textile monopole antenna is compared to a conventional microstrip monopole antenna that operates in the 2.45 GHz ISM band. The conducting ground plane and radiating element of the textile monopole antenna comprise of PCPTF, a light-weight and flexible conductive fabric. As for a substrate, felt fabric is utilized.

The result showed that a slight downward frequency shift was observed. The textile antenna is seen to produce about 4 dB higher in reflection coefficient than conventional monopole antenna. This concludes that the textile antenna works like a conventional monopole. The on-body performance of textile monopole antenna was also investigated in this paper.

An Interpretation of a Classical Diffraction Problem of Electromagnetism with a Fractional Derivative

P. Vaudon
Xlim, Mixt Research Unit CNRS, University No. 6172
123 rue Albert Thomas, Limoges 87000, France

Abstract— We propose to show that the formalism using fractional derivatives is adequate to derive some calculations of diffracted fields. First, we analyze the derivative of the e^{jx} function to the fractional order $(-1/2)$, then we show that the FRESNEL integral may be expressed in terms of this fractional derivative: this allows to give an original formulation of the edge diffracted field upon a plane wave incidence. We conclude with a non-integer equation, from which the diffracted field is solution.

The Derivative of Order $(-1/2)$ of the Function e^{jx}: A very important set of propagation phenomena is described with the help of sinusoidal functions, or, in the associated formalism, with complex exponential functions as $\exp(jx)$.

We propose to show that the derivative of order $(-1/2)$ of this function may be expressed with a complex FRESNEL function. This last one plays a fundamental role in many optical problems, and also in many microwave problems of diffraction. This will lead us to express, in the next section, the edge diffracted field as a function of a non integer derivative.

An Expression of the Total Field Surrounding the Edge with a Fractional Derivative: We propose to show in this part, that the total field surrounding a perfectly conducting illuminated by a plane wave, which is a function of the complex Fresnel integral, may be expressed by using the notion of fractional derivative.

Introduction of a Non Integer Differential Equation: The total field surrounding the edge will be expressed as a function of $y(x)$:

$$y(x) = \frac{1}{2}\left\{e^{jx} \pm D_{jx}^{-\frac{1}{2}}\left(e^{jx}\right)\right\}$$

We shall show that this function is a solution of the fractional differential equation:

$$D_{jx}^{-\frac{1}{2}}(y(x)) = \pm y(x) \mp \frac{1}{2}$$

And that the total field is also a solution of this fractional differential equation.

Session 4A1
Electromagnetic Theory and Design on the Optical Dispersive Materials, Invisible Cloak and Photonic Crystals

Gradient Index Metamaterial with Arbitrary Loss Factors in RHM and LHM Media: The Case of Constant Impedance throughout the Structure

M. Dalarsson[1], M. Norgren[1], T. Asenov[2], and N. Dončov[2]

[1]Division of Electromagnetic Engineering, School of Electrical Engineering
Royal Institute of Technology, Stockholm SE-100 44, Sweden
[2]Faculty of Electronic Engineering, University of Niš, Niš 18000, Serbia

Abstract— The transmission and reflection properties of lossy structures involving left-handed materials with graded permittivity and permeability have been investigated. We present an exact analytical solution to Helmholtz' equation for a lossy case with the graded both real and imaginary parts of permittivity and permeability profile changing according to a hyperbolic tangent function along the direction of propagation. This allows for different loss factors in the two media. The expressions and graphical results for the field intensity along the graded structure are presented. The analytical solution is validated by a dispersive numerical model of lossy metamaterials that uses a transmission line matrix method based on Z-transforms, where a close agreement between the analytic and numerical results is obtained.

Electromagnetic metamaterials (MM) in electromagnetics and (nano)plasmonics are defined as artificial composites with electromagnetic properties not readily found in nature. A partcularly important class of MMs are the negative refractive index metamaterials (NRM or NIM), also known as the left-handed materials (LHM). The novel and often counter-intuitive properties of the LHM, which include negative index of refraction, inverse Doppler effect, radiation tension instead of pressure, etc. resulted in numerous proposed applications. They include superlenses and hyperlenses that enable imaging far below the diffraction limit, resonant cavities and waveguides with geometrical dimensions orders of magnitude smaller than the operating wavelength, as well as invisibility cloaks.

A majority of cases consider structures with constant refractive index within the MM structure and abrupt interfaces with the surrounding positive index material ("right-handed" media, RHM). There is however a practical interest for metamaterials with spatially varying refractive index and with gradual transition from the RHM to LHM and vice versa, since many real-world applications would benefit from such structures. Various proposed applications of graded index metamaterials include hyperlenses, invisibility cloaks, beam shaping and directing, enhancement of nonlinear effects, superlenses etc.

The first paper dedicated to gradient index LHM was published in 2005. Analytical approaches to graded MM structures are of special interest, since they ensure fast, simple and direct routes to the analysis of wave propagation within such materials. Here we present an exact analytical analysis of electromagnetic waves propagation through a lossy graded metamaterial structure, where both the permittivity and the permeability vary according to a hyperbolic tangent function. We offer the most general case of lossy wave propagation with constant impedance throughout the entire structure, which provides the opportunity to model the higher losses in LHM materials compared to those in the RHM materials.

At the recent PIERS 2012 Conference in Kuala Lumpur a paper on exact analytical solutions for periodic graded index RHM-LHM structures was presented by two of the present authors, based on the assumption of uniform losses in both RHM and LHM media. After the presentation a question was raised whether the presented model could allow for the possibility of different loss factors in RHM and LHM, as it is empirically well known that that the losses in realistic LHM media are generally significantly higher than in the RHM media.

In response to that question, the present paper demonstrates an exact analytical solution to lossy Helmholtz' equations with graded profile, changing according to a hyperbolic tangent function along the direction of propagation, which allows for different and arbitrary loss factors in RHM and LHM. In addition to that, the enhanced Z-transform based TLM method which enables the direct time-domain modelling of lossy metamaterials has been presented. A comparison of analytical and numerical results, obtained by means of the enhanced Z-transform based TLM method, show an excellent agreement and high accuracy of the results.

Finite Element Method Can Not be Used for Full Wave Simulation in GL Cloak

Ganquan Xie[1, 2], **Jianhua Li**[1, 2], **and Qing Xie**[1]

[1]Hunan Super Computational Center, China
[2]GL Geophysical Laboratory, USA

Abstract— In this paper, we claim that Finite Element Method can not be used for full wave simulation in GL cloak. As well know as the conventional Finite Element Method can not be used for Helmholtz wave equation in the high frequency. In our simulation for the full electromagnetic wave propagation in the GL cloak, the very high frequency is used that is first reason. Second, in the GL cloak, the refractive index $N(r)$ is going to infinite, when the radius r is going to the inner sphere $r = R_1$. The right hand of the *Eikonal* equation is going to infinite. That is serious singularity for conventional Finite Element Method. Our GL electromagnetic modeling method overcomes the above two serious difficulties in FEM. We used GL EM inversion and modeling for our GL cloak and get excellent simulation for electromagnetic wave propagation in GL cloak.

A Dual Band Planar Metamaterial Based on Hybrid Structures in Terahertz Regime

S. Hussain[1, 2], **J. Y. Lee**[1, 2], **and J. H. Jang**[1, 2]

[1]School of Information and Communications
Gwangju Institute of Science and Technology, Gwangju 500-712, South Korea
[2]WCU Department of Nano-Bio Materials and Electronics
Gwangju Institute of Science and Technology, Gwangju 500-712, South Korea

Abstract— The design of a planar metamaterial, based on the magnetically resonant ring and electrically resonant plus shaped strip structures, in terahertz frequencies is presented. The vantages of the metamaterial are (a) dual band behavior that comes from the individual resonance of each structure (b) structural symmetry of the ring shape brings about polarization independency for the first resonance and plus shaped structure, responsible for the second resonance, is insensitive to x-y polarization. We have also shown that by using an ultra-thin substrate, a wide band response may be obtained. The design of the meta-material was analyzed using finite difference time domain method (FDTD) based commercial simulator and was optimized for attaining the superior spectral response. Our planar metamaterial is easy to fabricate, insensitive to the minute fabrication misalignments and furnishes a simple way to realize a metamaterial that may be used in terahertz filter applications.

Effect of Random Variations of Both the Composition and Thickness on Photonic Band Gap of One-dimensional Plasma Photonic Crystal

V. V. Rumyantsev and S. A. Fedorov
Donetsk Institute for Physics and Engineering, National Academy of Sciences, Ukraine

Abstract— Propagation of electromagnetic waves in layered crystalline ambiences is currently drawing a close attention . The interest towards these objects is on one hand due to their significance for electronics, and on the other hand due to the advance of technology allowing growth of periodic structures with controlled characteristics. Investigation of disorder effects in an imperfect superlattice allowing modeling the properties of crystal containing the plasma layers is still of a great interest [1, 2]. Development of the theory of photonic structures requires consideration of model systems such as plasma photonic superlattice with layers of variable composition and thickness. We study a model of 1D-superlattice as a macroscopically homogeneous layered system (which is one-dimensional Si/plasma crystal with two elements-layers in the cell) with randomly included admixture (SiO_2-layers). The virtual crystal approach [3] which is the method to describe quasi-particle excitations in disorder media is used. Peculiarities of the dependence of photonic band gap width on admixture layers concentration have been studied. The results are the evidence of substantial polariton spectrum reconstruction caused by the presence of defect elements.

REFERENCES

1. Prasad, S., V. Singh, and A. K. Singh, "Effect of inhomogeneous plasma density on the reflectivity in one dimensional plasma photonic crystal," *Progress In Electromagnetics Research M*, Vol. 21, 211–222, 2011.
2. Kong, X.-K., S.-B. Liu, H.-F. Zhang, and H.-L. Guan, *Optics Communications*, Vol. 284, 2915, 2011.
3. Parmenter, R. H., *Phys. Rev.*, Vol. 97, 587, 1955.

Resonant-cascoded Micro-strip Lines Analog to Electromagnetic Induced Transparency

Teh-Chau, Liau[1], **Yao-Huang Kao**[2], **and Tzong-Jer Yang**[1]

[1]Ph. D. Program in Engineering Science, College of Engineering
Chung Hua University, Hsinchu 30012, Taiwan, R.O.C.
[2]Department of Communication Engineering
Chung Hua University, Hsinchu 30012, Taiwan, R.O.C.

Abstract— Electromagnetically induced transparency (EIT) observed in three-level atomic media, is a coherent quantum process whose optical response to a laser beam is modified by a second beam with a well-determined detuning. This phenomena performed as absorptive/transmission parameter has been studied by many researchers while its experimental handling of these setups is rather hard due to EIT's extremely sensitivity to the inhomogeneous broadening. Instead, a lot of analog simulation have been presented to other easy-implement non-optical metamaterial, classical RLC circuit, ... etc.. In this paper, we propose a micro-strip transmission line to analogue a 3 level bulk lambda type EIT-material whose atomic spontaneous decay rate is Γ_3. The governing equation for the density matrix is given by $i\frac{\partial}{\partial t}\begin{bmatrix}\rho_{31}\\ \zeta_{21}\end{bmatrix} = \begin{bmatrix}\omega_{31}-i\Gamma_3 & \Omega_c\\ \Omega_c^* & \omega_{31}\end{bmatrix}\begin{bmatrix}\rho_{31}\\ \zeta_{21}\end{bmatrix} + \begin{bmatrix}1\\ 0\end{bmatrix}\Omega_p e^{-i\omega t}$, where ω, Ω_c denote the carrier frequency of the probe field and Rabi frequency between $|2>$ and $|3>$ states respectively. Hence, we can apply a double tuned cascoded micro-strip line to analogue the EIT transparency via transmission merit, i.e., s_{21}. Three-level ($N = 3$) system is made up by inserting one fan-shape capacitive line (coupled to $|2>$ and $|3>$ behave as a coupling field) between ground state (i.e., $|1>$) and excited states (i.e., $|3>$). This coupling capacitor is equivalent to the pumping field with inverse proportionality. In order to observe the highly transparency, two matching circuits are added to the both end of the micro-strip line. This research will be helpful to real atomic experiment.

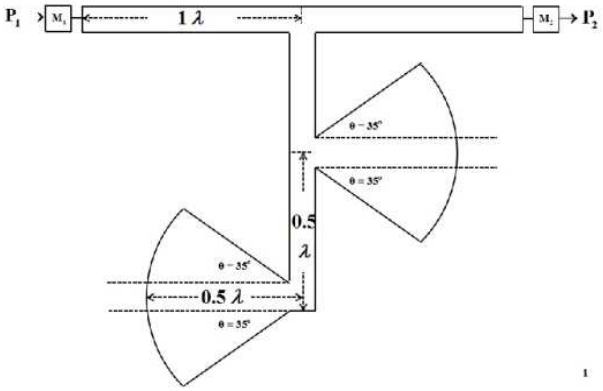

Figure 1: Scheme of EIT-like double tuned micro-strip line.

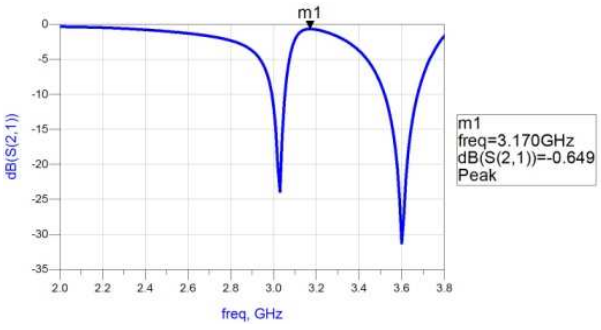

Figure 2: The merit to transparency is $-0.649\,\mathrm{dB}$ after both port are impedance matched.

A Kind of Band Pass Filter Based on Low Frequency Spoof Surface Plasmon Polaritons

Y. H. Kao[1], **I. J. Hsieh**[2], **D. J. Hou**[2], **T. J. Yang**[3], **and J. J. Wu**[2]

[1]Department of Communication Engineering, Chung Hua University, Hsinchu 30012, Taiwan, R.O.C.
[2]Department of Electrical Engineering, Chung Hua University, Hsinchu 30012, Taiwan, R.O.C.
[3]College of Engineering, Chung Hua University, Hsinchu 30012, Taiwan, R.O.C.

Abstract— Based on the mechanism of spoof surface plasmon polaritions (spoof SPPs), we present a kind of microwave band pass filter in both theory and experiment, which is realized by periodic subwavelength metallic Domino array. The transmission bandwidth of spoof SPPs is controllable by designing the geometric parameters of the periodic structure. Simulation and experimental results of the spoof SPPs agree well with each other and verify the feasibility in band pass filter application.

Chinese Poet Shi Su Had Earlist Relativist Idea in the History and in the World

Ganquan Xie[1, 2], **Jianhua Li**[1, 2], **Feng Xie**[2], **and Lee Xie**[2]

[1]Hunan Super Computational Sciences Center, Hunan University, China
[2]GL Geophysical Laboratory, USA

Abstract— In Song Dynasty 1076 Mid-Autumn, Great Poet Su Shi (1037 $\sim$ 1101) wrote a famous and a well-known words "Missing you". That is: "When will the moon be clear and bright? Holding a cup of wine in my hand to ask sky. I do not know in the sky palace, tonight is what year? I want to go back to sky by riding the wind, I also was fearing Qionglouyuyu, standing above the crowd. Dance clarify the shadow, Where and when like in the real world?" In the famous and a well-known words, Famous Poet Shi Su with Super literature and scientific imagination proposed the earliest relativist idea in the history and in the world. First, Professor Shi Su was porting a cup of wine to ask question to sky, the Moon began to appear from what time. Let the position of the Shi Su default as x, he asked that I do not know in the sky palace (x'), tonight (t) is what year (t')? In the Song Dynasty 1076 Mid-Autumn, Professor Shi Su asked and implicit proposed the transform function mapping between his place and time (x, t) in the real world and sky palace and what year (x', t'), $x' = f(x, t)$, $t' = g(x, t)$. Professor Shi Su said that "I want to go back to sky by riding the wind". Let the wind speed is v. In the further, Professor Shi Su said that "I also was fearing Qionglouyuyu, standing above the crowd". That means that the basic physical quantity temperature is also different. Also Professor Su Shi said that "Dance clarify the shadow, Where and when like in the real world?" that means in the different space and time system the movement (Dance) principle is also different and is relativity. After 839 years, in 1915, great physicist Einstein proposed relativist in the physics. Professor Einstein reply Professor Su Shi's "Sky Asking" and proposed "Sky Replying" relativist theory, and wrote Professor Su Shi's implicit proposed space time transform as Lorenz transform: $x' = \frac{x-vt}{\sqrt{1-\frac{v^2}{c^2}}}$, $t' = \frac{t-vx/c^2}{\sqrt{1-\frac{v^2}{c^2}}}$. However, Einstein said the Earlist Relativist Idea was from Ernst Mach (1838 $\sim$ 1916), The wrong statement is because Einstein did not know poet Su Shi and his poem "Missing you" with Super literature and scientific imagination. By the GL EM inversion, the undisputed historic fact "missing you" proved that Shi Su Had Earlist Relativist Idea In The History And In The World. The Copyright and Patent are belong authors in GLGEO.

GL EM Inversion Method For MRI Imaging

Jianhua Li[1, 2], **Ganquan Xie**[1, 2], **Feng Xie**[1], **and Lee Xie**[1]

[1]GL Geophysical Laboratory, USA
[2]Hunan Super Computational Sciences Research Center, China

Abstract— In this paper, we propose a new GL EM inversion method for MRI imaging. In the MRI imaging process, the system noise and non resonance noise and environmental noise are main noises to contaminate the real MRI imaging. Our GL EM inversion contains the random and deterministic inverse filters in it to filter the above noises. Several controlled magnetic sources with approximate magnetic resonances are used to compromise imaging inversion. The random and deterministic weak regularizing is used for compromise resolution and smooth stable. The GL EM modeling and inversion are parallel and alternative for MRI and quasi MRI. By data simulation, the GL EM MRI imaging is reasonable high resolution.

The GL Electromagnetic Modeling and Electromagnetic Education

Ganquan Xie[1, 2], **Jianhua Li**[1, 2], **Qing Xie**[1], **Lee Xie**[2], **Feng Xie**[2], **and Hong Jun Li**[3]

[1]Huann Super Computational Center, China
[2]GL Geophysical Laboratory, USA
[3]Wang Cheng Second High School, Wang Cheng, Chang Sha, China

Abstract— In this paper, we propose a Global and Local GL electromagnetic modeling for education. The Finite Element Method needs artificial boundary and absorption boundary condition. The artificial boundary needs to located in the far way to avoid non accurate boundary reflection to contaminate the wave propagation in the working area. Second, the Finite Element and conventional Finite Difference scheme can not be used to calculate the EM wave and Helmholtz equation in high frequency. Third, the Finite Element Method and the convention Finite Difference Method Needs to solve big or massive matrix equation for the EM wave equation. The long time computational time cost limits the real time simulation of 3D or 2D EM and acoustic wave. Our GL EM modeling has overcome the above difficulties. The GL EM modeling consistently Combine the analytical and numerical methods together for all frequency full EM wave Propagation, The GL EM wave propagation is best and powerful software tool for the Electromagnetic Wave and cloaking education in the high school, and for university, The copyright and patent of the GL EM wave education software are belong to authors in GLGEO.

Session 4A2a
Present and Future of TeraHertz Science & Technology including Application in Remote Sensing, Imaging, and Communications

Plasma Effects in Graphene-based Electro-optical Modulators

M. Ryzhii[1], **T. Otsuji**[2], **S. Yurchenko**[3], **N. Ryabova**[3], **V. Ryzhii**[2, 3], **and M. S. Shur**[4]

[1]Computational Nanoelectronics Laboratory, University of Aizu, Aizu-Wakamatsu, Japan
[2]Research Institute for Electrical Communication, Tohoku University, Sendai, Japan
[3]Center of Photonics and Infrared Engineering, Bauman Moscow State Technical University Moscow, Russia
[4]Department of EECS Engineering, Rensselaer Polytechnic Institute, Troy, USA

Abstract— The gapless energy spectrum of graphene layers (GLs), results in the interband absorption of electromagnetic radiation from the terahertz (THz) to ultraviolet range. This opens up prospects to use GLs in active and passive terahertz and infrared devices. Novel optoelectronic terahertz and infrared devices (lasers, photodetectors, and so on) were proposed and studied. In particular, gated GL structures can be used for electrical modulation of radiation. This is because varying the gate voltage one can effectively change the electron (hole) Fermi energy, affect the Pauli blocking and, hence, the GL interband absorption. Success in fabricating multiple-GL structures with long momentum relaxation time of electrons and holes promises a significant enhancement of the performance of futures GL-based optoelectronic devices due to much stronger absorption an emission in such structures in comparison with single-GL structures. We developed device models for electro-optical modulators based on gated single- and multiple-GL structures as well as in gateless double-GL structures exploiting the electrically-controlled Pauli blocking effect and operating in different ranges of radiation spectrum.

We consider the modulators of the mirror type (with the transverse input of optical radiation, its reflection from highly conducting gate, and the transverse output) and waveguide type (with lateral input and output of radiation).

The device models are based on the hydrodynamic equations for the electron-hole plasma in GLs coupled with the Poisson equation. These equations describe the dynamics of the electron-hole plasma and the variations of the output radiation in a wide range of modulation frequencies. It is shown that in sufficiently perfect GLs, the resonant excitation of standing plasma waves is possible. The latter leads to resonant increase in the modulation depth when the modulation frequency approaches to the plasma frequency. The modulation characteristics of the devices with different structural parameters and modulation frequency were studied. It is shown that the effect of resonant excitation of plasma waves in GL structures can provide the possibility of effective modulation of infrared radiation by terahertz radiation and mixing of terahertz signals.

Terahertz Spectral Analysis and Detection Based on High-T_c Josephson Junctions

V. N. Gubankov[1], **M. Lyatti**[1, 2], **Y. Y. Divin**[1, 2], **and K. Urban**[2]

[1]Kotel'nikov Institute of Radio Engineering and Electronics of Russian Academy of Sciences
Moscow 125009, Russian Federation
[2]Peter Gruenberg Institute, Research Centre Juelich, Juelich 52425, Germany

Abstract— Closing the THz gap in electromagnetic spectrum between microwave and infrared ranges is associated with the development of new approaches in high-speed logic elements, oscillators, detectors, spectrum analyzers and imagers [1]. Superconductive electronics is superior to conventional techniques for these applications, which require very high speed, low-power consumption, extreme sensitivity or extremely high precision [2]. The majority of approaches, which now are involved in superconducting electronics, are associated with low-T_c superconductor technology with operational temperatures of 4.2 K, the boiling temperature of liquid-helium [2]. However, due to much larger values of the energy gap of high-T_c superconductors, the high-T_c Josephson junctions will possess even broader spectral range, higher speed of operation and higher sensitivity to external fields. Moreover, operational temperatures of high-T_c devices will be increased to temperatures of 60–80 K, where space-qualified, compact and reliable, essentially service-free cryocoolers are operating. This development is in the process of changing the market with respect to the application of superconducting devices in many fields. A very broad frequency range from a few GHz to a few THz, sensitivities of 10^{-14} W/Hz$^{1/2}$ and power dynamic range of 5 to 6 orders have been already demonstrated for high-T_c detectors and spectrometers operating in Stirling cryocoolers [3, 4]. This unique combination of parameters has already given us a chance to solve a number of complicated problems of spectral characterization of THz sources, frequency-resolved electron bunch measurements and quick spectroscopic identification of liquids for security applications [4]. Further development of high-T_c technology will result in development of a new generation of THz oscillators and detectors, which will allow realizing a full set of sensors and of instrumentation.

ACKNOWLEDGMENT

This work is supported in part by the joint project HRJRG-207 of Helmholtz Association of German Research Centers and Russian Fund for Basic Research (2011–2014).

REFERENCES

1. Tonouchi, M., "Cutting-edge terahertz technology," *Nature Photonics*, Vol. 1, 97–105, 2007.
2. Anders, S., et al., "European roadmap on superconducting electronics — Status and perspective," *Physica C*, Vol. 470, 2079–2126, 2010.
3. Divin, Y. Y., et al., "Terahertz Hilbert spectroscopy by high-T_c Josephson junctions," *Advances in Solid State Physics*, Vol. 41, 301–313, ed. B. Kramer, Springer, Berlin, 2001.
4. Divin, Y. Y., U. Poppe, V. N. Gubankov, and K. Urban, "High-T_c Josephson square-law detectors and Hilbert spectroscopy for security applications," *IEEE Sensors J.*, Vol. 8, 750–757, 2008.

Novel Terahertz Applications: From Imaging to Waveguiding

R. Morandotti[1], **M. Clerici**[1], **M. Shalaby**[1], **M. Peccianti**[2], **G. Sharma**[1], **I. Al-Naib**[1], **P. Tannouri**[1], **P.-L. Lavertu**[1], **F. Vidal**[1], **and T. Ozaki**[1]

[1]INRS-EMT, 1650 Blvd. Lionel-Boulet, Varennes, Quebec J3X 1S2, Canada
[2]Institute for Complex Systems-CNR, Via dei Taurini 19, Roma 00185, Italy

Abstract— Over the last few years, Terahertz waves (which lie between infrared and microwaves in the electromagnetic spectrum, i.e., roughly in the range $0.1 - 10 \times 10^{12}$ Hz or 3 mm to 30 μm wavelengths), have become a highly promising tool for real-time spectroscopy analysis of a wide variety of materials. In particular, unique and detailed broadband spectral THz fingerprints of many materials of interest, including explosives, illicit drugs, pollutants, biological samples and medicines have already been identified in the transmission mode, in the backscattering mode, as well as in the *waveguide mode*, in which the samples to be analyzed are inserted in a THz waveguide. Not surprisingly, the interest towards Terahertz science and its applications has recently grown dramatically. In this paper, I am going to give an overview of our activities in this exciting field of research, including some of the work lately carried out at the INRS, spanning some of the compelling open problems in THz science.

For example, we have recently investigated numerically the tradeoff between the dispersion properties, the coupling efficiency and the geometrical constrains in dual wire (twin-lead) THz waveguides. Furthermore, we have started to tackle one of the challenges in THz imaging, i.e., the fact that it is strongly limited by its low spatial resolution imposed by the long wavelength. Therefore, THz imaging usually requires near field techniques to overcome the diffraction limit, in which either sub-wavelength apertures or sharp tips are generally used. We have recently explored an apertureless-based alternative, which involves the THz generation in a sub-wavelength area by tightly focusing an optical pump on the generation nonlinear crystal. In this approach the imaging is realized by placing the sample in the near-field region of the THz source and then scanning the optical driving field in order to reconstruct the image. Finally, if time allows, we will discuss how it is possible to carry out polarization-sensitive broadband THz amplitude modulation by applying a low magnetic fields in a liquid medium.

PCB Inspection Using Terahertz Scanning Probe Microscopy

Harun Cetinkaya, **Mustafa Tekbas**, **and Alexey Vertiy**
International Laboratory for High Technologies
TUBİTAK-Marmara Research Center, Gebze/Kocaeli, Turkey

Abstract— Scanning probe microscopy has been employed in various areas such as nano-electronics, biochemical applications, etc. A developing area of microscopy is near field scanning probe microscopy in which the near field scanning optical microscopy and near field scanning microwave microscopy are great of interest. There are, however, few reports related to near field scanning microscopy in sub-Terahertz and Terahertz frequency range [1, 2].

For this purpose, the Terahertz scanning probe microscopy is studied. Printed-circuit board (PCB) inspection is carried out. The measurement is performed at Terahertz (THz) frequency range (between 301 GHz–304 GHz). A tomography algorithm based on finding equivalent currents induced on target is used to reconstruct the PCB image [3]. The obtained image indicates the efficient detection and identification of PCB.

Figure 1: (a) Measurement setup. (b) Dielectric probe mounted into horn antenna. (c) Investigated PCB.

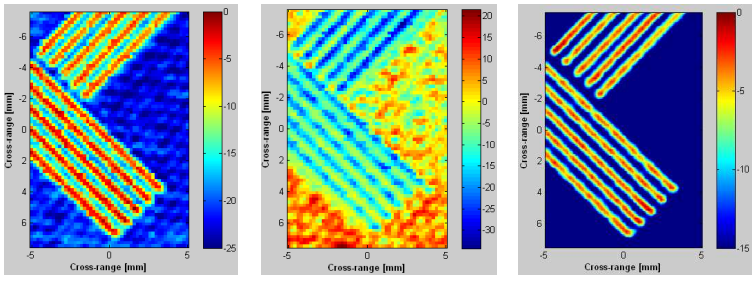

Figure 2: (a) Amplitude distribution. (b) Phase distribution. (c) Reconstructed image.

REFERENCES

1. Kume, E. and S. Sakai, *Journal of Applied Physics*, 99, March 2006.
2. Vertiy, A. A., H. Cetinkaya, and M. Tekbas, "Subsurface sub-terahertz and terahertz tomography" *PIERS Online*, Vol. 6, No. 5, 485–489, 2010.
3. Pichot, C., L. Jofre, G. Perronnet, and J. C. Bolomey, *IEEE Transactions on Antenna and Propagation*, Vol. 33, No. 4, 416–423, April 1985.

Detected Low Contrast Objects with Passive Radiometric Imaging System

A. Vertiy and A. Pavlyuchenko
International Laboratory for High Technology
TUBITAK-MRC, MI, Dr. Zeki Acar Street, Gebze, Kocaeli 41470, Turkey

Abstract— In the work, a prototype of a passive scanning radiometric system operating in frequency range of 97–104 GHz and employing high sensitive ($\Delta' = 0.0031K$) receiver created on super-heterodyne scheme is presented. Polyethylene lens antenna with the aperture size 500 mm was used for carrying out radiometric experiments for distances to objects from 10 m to 2.5 km. Investigations of reflection factors of different construction materials are carried out for through-wall detection of different objects as well as for detection of weapons concealed under person's clothing. The receiver sensitivity achieved allowed us to conduct radiometric scanning of low contrast objects such as ships at different elevation angles for distances from 1 km to 2.5 km. The aim of the work was investigation of potential possibilities of the system and areas of applications of this high sensitive radiometric system.

(a) (b)

Figure 1: (a) Prototype of passive scanning radiometric system. (b) Photo and radiometric image when scanning weapon concealed under clothing at distance of 10 m, building at distance of 150 m and clouds at the background. The outline of the gun is marked by the dotted line.

(a) (b)

Figure 2: Radiometric measurements at sea: (a) photo and (b) ship image at distance of 1000 m.

Session 4A2b
Earth Electromagnetic Environment and Radiowave Propagation & Scattering: Modelling, Observation and Measurements

Review of Man-made Waves Observed in the Ionosphere

M. Parrot[1] **and R. Talhi**[1, 2]

[1]LPC2E/CNRS, 3A Avenue de la Recherche Scientifique, 45071 Orléans Cedex 2, France
[2]Department of EECS, University of Tours, Avenue Monge, Tours 37200, France

Abstract— This paper is a review of ionospheric observations related to man-made waves recorded by the low orbiting satellite DEMETER.

First, the ionospheric perturbations from VLF ground-based transmitters will be presented. Electrostatic waves from HF to ELF ranges are generated and strong turbulence appears. Fluctuations of electrons and ions densities are observed as well as increase of temperature. This phenomenon is due to the electron and ion heating of the ionosphere induced by the powerful transmitters VLF wave. A much smaller effect is also observed in the conjugated location.

Second, in the MF frequency range, the data of an electric field antenna are recorded up to 3 MHz and global maps of the Earth reveal a persistent wave activity at MF frequencies above the location of ground-based VLF transmitters. It is shown that it is due to the perturbation of the ionosphere by these transmitters which produce ionospheric irregularities. Whistler waves generated by lightning strokes can therefore penetrate through the ionosphere at MF frequencies at the location of these VLF transmitters.

Third, the paper will display various man-made waves due to power line harmonic radiation at harmonics of 50 or 60 Hz. It is shown that observations concern harmonics at high orders. ELF/VLF bursty noises are also observed when DEMETER is above very industrial areas.

Procedure of Near Ground Propagation Model Development for Pine Tree Forest Environment

O. Kurnaz[1], **M. Bitigan**[2], **and S. Helhel**[1]

[1]Department of Electrical and Electronics Engineering, Akdeniz University, Turkey
[2]Department of RF Planning, Turkcell Communication Coop., Turkey

Abstract— In this study, the procedure of new model development steps has been presented starting with plane earth measurements. A propagation model experimentally derived from both free space and near ground plane earth path loss models for pine tree forest with foliage depth lower than 400 m has been proposed. It is a piecewise model taking foliage depth of 200 m as a boundary. The ratio of received power P_r from a radiated transmit antenna to base station transmit power P_t is given by the formula $P_r/P_t = (G_t G_r \lambda^2)/([4\pi d]^2 L)$ where G_t is isotropic transmit antenna gain, G_r is receive antenna gain, λ is signal wavelength in meters (m), d is distance between transmit and receive antennas in meters (m) and L is system loss factor not related to propagation ($L \geq 1$). Different from Weissberger, ITU-R and COST235 models, the proposed one takes trunk height gain k into account. Observed average error is about 6 dB for proposed model whereas it is about 25 dB, 17 dB and 18 dB for Cost235, Weissberger and ITU-R models, respectively.

Normalized Differenzial Spectral Attenuation among Co-rotating LEO Satellites: Performance Analysis for Estimating the Tropospheric Water Vapor

F. Cuccoli[1], **L. Facheris**[2], **and F. Argenti**[2]

[1]U.O. CNIT RaSS, c/o Dipartimento di Elettronica e Telecomunicazioni, Università di Firenz
Via di Santa Marta, 3, Firenze 50139, Italy
[2]Dipartimento di Elettronica e Telecomunicazioni, Università di Firenze
via di Santa Marta, 3, Firenze 50139, Italy

Abstract— The Normalized Differential Spectral Attenuation (NDSA) approach is based on the conversion of a spectral parameter called "Spectral Sensitivity" (SS) into the total content of water vapor along the propagation path between the two LEO satellites. In [1] the potential of spectral sensitivity in providing direct estimates of Integrated Water Vapor (IWV) along LEO-LEO tropospheric propagation paths in the 15–25 GHz range is shown while in [2] the accuracy with which the spectral sensitivity parameter can be measured has been analyzed.

A basic result was that the spectral sensitivity measurement accuracy can be estimated through the theoretical approximation as long as the averaged SNR keeps above 20 dB, while below such SNR level measurements become not reliable. Moreover, this holds as long as the integration time used for measurements keeps smaller than the decorrelation time of the scintillation phenomenon.

A complete simulation tool has been presented in [3] for the study of the NDSA measurement performance in counter rotating LEO-LEO configuration (see Fig. 1(a)) at global scale for single and multiple global atmospheric profiles, assuming spherical symmetry for the atmospheric structure, realistic LEO satellites' orbit configuration, link budget, and disturbances sources. The main results of this performance analysis is that NDSA at 17.25 GHz can be measured in case of medium scintillation up to 6 km tangent altitude with NSED (the standard deviation of the absolute error) smaller than 50% and at 20.20 GHz can be estimated both in medium scintillation conditions between 3 and 7 km with NSED smaller than 20% and also in strong scintillation conditions with NSED smaller than 60%.

Some other studies about the NDSA in counter rotating LEO-LEO configuration in K/Ku bands have been completed under the independent ESA (European Space Agency) study called AlMetLEO [4] that provided a significant insight into the SS-IWV relationships up to 12 km altitude in the limb geometry based on an extended radiosonde data analysis, into the modelization of signal fluctuations due to tropospheric turbulence and into the SS accuracy achievable under given SNR and scintillation levels.

In [5] for the first time the use of M band for NDSA measurements, always in counter rotating LEO-LEO configuration, has been introduced. Specifically, 179 and 182 GHz have been proposed as good candidates for water vapor estimates at tangent altitudes higher than 11 km, since M band measurements are very robust to receiver noise and practically insensitive to scintillation effects.

While the counter-rotating configuration provides valid SS measurements data only during the relative set/rise occultation events the co-rotating one provide them in a time continuous manner. For this reason the authors decided to investigate the NDSA capabilities also in LEO-LEO co-rotating configuration (see Fig. 1(b)).

In this paper, we present the main NDSA measurement characteristics of the CO-rotating configuration (see Fig. 1(b)) with one transmitting satellite and many receiving ones. We discuss the result of a performance analysis of the sensitivity measurements assuming the multi-band (K, Ku and M) approach on each radio link and plausible propagation conditions.

Moreover since the NDSA radio links cross the same slice of troposphere at different frequencies, at different altitudes but in a continuous time, it should be possible to process the NDSA measurements also with a tomographic approach. Such approach will be analyzed and some results will be presented about the possibility to estimate the two-dimesional filed of water vapor on the tropospheric ring up to 15 km altitude.

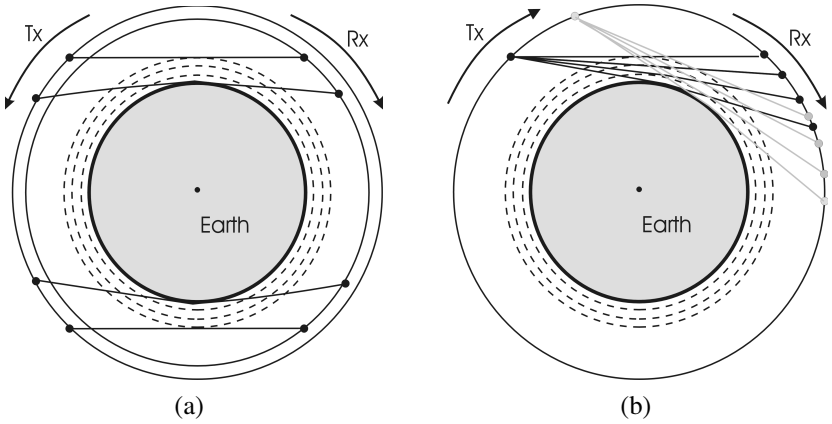

Figure 1: Counter (a) rotating and (b) co-rotating LEO-LEO configuration.

REFERENCES

1. Cuccoli, F. and L. Facheris, "Normalized differential spectral attenuation (NDSA): A novel approach to estimate atmospheric water vapor along a LEO — LEO satellite link in the Ku/K bands," *IEEE Transactions on Geoscience and Remote Sensing*, Vol. 44, No. 6, 1493–1503, 2006.
2. Cuccoli, F., L. Facheris, and F. Argenti, "Normalized differential spectral attenuation (NDSA) measurements between two LEO satellites: Performance analysis in the Ku/K bands," *IEEE Transactions on Geoscience and Remote Sensing*, Vol. 46, 2345–2356, 2008.
3. Cuccoli, F. and L. Facheris, "NDSA measurements between two LEO satellites in KU and K bands for the tropospheric water vapor estimate: Performance evaluation at global scale," *IEEE International, IGARSS*, Vol. 5, V-296–V-299, 2009.
4. Facheris, L., et al., "Alternative measurements techniques for LEO-LEO radio occultation (AlMeTLEO)," ESA-ESTEC Contract No. 17831/03/NL/FF Final Report, July 2004.
5. "ACTLIMB: Study of the performance envelope of active limb sounding of planetary atmospheres," Final Report of ESA Study 21507/08/NL/HE.

The Earthquake-related Disturbances in Ionosphere and the First Seismo-electromagnetism Satellite in China

Xuhui Shen[1], **Xuemin Zhang**[1], **Lanwei Wang**[2], **Huaran Chen**[3], **Yun Wu**[4], **Shigeng Yuan**[5], **Junfeng Shen**[6], **Shufan Zhao**[1], **Jiadong Qian**[1], **and Jianhai Ding**[1]

[1]Institute of Earthquake Science, China Earthquake Administration, Beijing 100036, China
[2]Institute of Earth Crust and Dynamics, China Earthquake Administration, Beijing 100085, China
[3]Institute of Geophysics, China Earthquake Administration, Beijing 100081, China
[4]Earthquake Administration of Hubei Province, Wuhan 430071, China
[5]DFH Satellite Co. Ltd., Beijing 100094, China
[6]State Key Laboratory of Geological Processes and Mineral Resources
Chinese University of Geosciences, Beijing 100029, China

Abstract— Based on the case studies and statistical analysis of earthquake-related ionospheric disturbances mainly from DEMETER satellite, ground-based GPS and ionosounding data, this paper summarizes the statistical characteristics of earthquake-related ionospheric disturbances, including electromagnetic emissions, plasma perturbations and the variation of energetic particle flux. According to the main results done by Chinese scientists, fusing with the existed study from global researches, seismo-ionospheric disturbances usually occur at a few days or hours before earthquake occurrence. Paralleling to these cases study, lithosphere-atmosphere-ionosphere (LAI) coupling mechanisms are checked and optimized. A thermo-electric model was proposed to explain the seismo-electromagnetic effects before earthquakes. A propagation model was put forward to explain the electromagnetic waves into the ionosphere. According to the requirement of earthquake prediction research, China Seismo-Electromagnetism Satellite, the first space-based platform of Chinese earthquake stereoscopic observation system, is proposed and planned to launch at the end of 2014. It focuses on the LAI model checking and earthquake-related ionospheric disturbance distinguishing. The preliminary design for the satellite will adopt CAST-2000 platform, with eight payloads onboard. It is believed that the satellite will work together with the ground monitoring network to improve the capability to capture seismo-electromagnetic information, which is benefited for the earthquake monitoring and prediction researches.

ACKNOWLEDGMENT

This work was done by the working group of earthquake-related satellite mission in China, and is funded by National Key Technology R & D Program in the 11th Five Year Plan of China (2008BAC35B00).

Session 4A3
Modern Aspects of Wave Multiple Scattering in Dense Random and Ordered Media

Dyson Equation Technique for Homogenized Electromagnetic Crystals with Unit Cell formed by not Small Coupled Nonmagnetic Scatterers

Yu. N. Barabanenkov[1], **M. Yu. Barabanenkov**[2], **and Ivan Lisenkov**[1]

[1]V. A. Kotel'nikov Institute of Radio-Engineering and Electronics
Russian Academy of Sciences, Moscow, Russia
[2]Institute of Microelectronics Technology, Russian Academy of Sciences
Chernogolovka, Moscow Region, Russia

Abstract— We start in this report with Maxwell equations for electromagnetic field inside unbounded periodic 3D structure. The unit cell of the structure consists of nonmagnetic particles with given dielectric permittivity and specific conductivity, particle or unit cell size being possible comparable to free space wavelength. The electromagnetic field under consideration is created by electric current density source, which is imposed to have the Floquet property. The electric field averaged according to [1, 2] over unit cell satisfies, as we show, a Dyson equation with tensor mass operator relating to homogenized structure effective dielectric tensor permittivity by usual way, see, e.g., [3]. Our principal result is that the mass operator can be written as Fourier transform over unit cell from the unit cell electric field quantum mechanical tensor T-scattering operator [4]. This lattice unit cell T-scattering operator satisfies the Lippmann-Schwinger (LS) integral equation [4], with including the unit cell scattering potential and a lattice tensor Green function. We show, namely the quantum mechanical T-scattering operator, but not the Waterman transition-matrix (T-matrix) [5], defines the excited current inside a particle and is responsible for effective dielectric tensor permittivity spatial dispersion and hence for effective magnetic tensor permeability appearance according to Lindhard theory [1, 2, 6]. Side by side with the lattice unit cell T-scattering operator, we introduce similar T-scattering operator for the unit cell in free space and rewrite efficiently the LS equation for the lattice unit cell T-scattering operator in terms of free space unit cell T-scattering operator. The transformed such a way LS equation for the lattice unit cell T-scattering operator, as shown in the report, plays role of most general and rigorous Lorentz-Lorenz type formula, which is compared with versions [1, 2, 7] of generalized Lorentz-Lorenz and Clausius-Mossotti formulas written via semi-intuitive approaches. We construct exact analytic solution to the transformed LS equation for the lattice unit cell T-scattering operator, provided the free space unit cell T-scattering operator is sum of separable T-scattering operators. The obtained analytic solution is applied to study the space group resonance [8] effects on peculiarities of homogenized periodic structure effective tensor dielectric permittivity or magnetic permeability, with structure unit cell consisting of coupled parallel thin wire vibrator-dipoles tuned to half wavelength or small coupled resonant dielectric spheres separated on distant possible comparable to wavelength, respectively.

REFERENCES

1. Silveirinha, M. G., *Phys. Rev. B*, Vol. 75, 115104, 2007.
2. Silveirinha, M. G., *Phys. Rev. B*, Vol. 76, 245117, 2007.
3. Barabanenkov, Yu. N., M. Yu. Barabanenkov, and S. A. Nikitov, arXiv:1009.4770v1 [cond-mat.dis-nn], Sep. 24, 2010.
4. Newton, *Scattering Theory of Waves and Particles*, McGraw-Hill, New York, 1966.
5. Waterman, P. C., *Phys. Rev. D*, Vol. 3, 825–839, 1971.
6. Lindhard, J., *Dan. Mat. Fys. Medd.*, Vol. 28. No. 8, 3–57, 1954.
7. Wheeler, M. S., J. S. Aitchison, and M. Mojahedi, *J. Opt. Soc. Am. B*, Vol. 27, 1083–1091, 2010.
8. Barabanenkov, Yu. N. and V. V. Shlyapin, *Phys. Lett. A*, Vol. 170, 239–244, 1992.

Dyson Self-consistent Exact Equations for Averaged Wave Electric Field and Its Local Version inside Dense Random Medium of Dielectric Nonmagnetic Particles

Yuru Nicolaevich Barabanenkov[1] and Mikhail Yurievitch Barabanenkov[2]

[1]V. A. Kotelnikov Institute of Radioengineering and Electronics
Russian Academy of Sciences, Moscow, Russia
[2]Institute of Microelectronics Technology, Russian Academy of Sciences
Chernogolovka, Moscow region, Russia

Abstract— We consider in this report coherent component of electromagnetic wave field inside spatially disordered media composed of dielectric conducting nonmagnetic particles. In paper [1] it was derived via generalized Furutsu-Donsker formalism [2] a Dyson self-consistent exact equation for ensemble averaged wave electric field inside dense discrete random media, with a random mass operator having been put under averaging sign. The random mass operator was written in terms of particle correlation functions of all orders and particle cluster random group T-scattering operators. A group T-scattering operator was constructed via special group operation from T-scattering operators of cluster particles, with T-scattering operator of a particle set having been satisfied a self-consistent Lippmann-Swinger (SCLS) integral equation. This SCLS equation included scattering potential of particle set and the random medium tensor Green function (self-consistency effect). Approximation of the random Green function in SCLS by averaged one made the random mass operator, according [1], equal to nonlinear single- group approximation (NSGA) for mass operator. We show in this report that paper [1] technique leads also to a Dyson self-consistent exact equation for ensemble averaged version of local wave electric field, with a transformed random mass operator being under averaging sign. The version of local wave electric field is defined according [3] by decomposition of host homogeneous medium electric field strong singular tensor Green function inside integral term of integral equation for random wave electric field into delta Dirac function term and the principal part. The transformed random mass operator is obtained from the above random mass operator by replacing in SCLS equation for T-scattering operator of a particle set the random medium tensor Green function to its special principal part. Approximating the random medium tensor Green function principal part by averaged one turns the transformed mass operator into a transformed NSGA mass operator. Next we compare following [3] the initial averaged integral equations for the electric wave field and the version of local wave electric wave field and obtain a generalized Lorentz- Lorenz formula with the transformed NSGA mass operator in the formula right hand side that was actually got in [4] on the way of simple qualitative consideration. The obtained generalized Lorentz- Lorenz formula is applied to study the space group resonance [5] effects in part of electric dipole scattering contribution into effective magnetic permeability and also in part of particle correlation caused decrease of effective magnetic permeability imaginary part.

REFERENCES

1. Barabanenkov, Y. N. and M. I. Kalinin, *Phys. Lett. A*, Vol. 163, 241, 1992.
2. Rytov, S. M., Y. A. Kravtsov, and V. I. Tatarskii, *Principles of Statistical Radiophysics*, Vol. 2, *Random Fields*, Springer, Berlin, 1988.
3. Finkelberg, V. M., *JETP*, Vol. 26, 26, 1968.
4. Barabanenkov, Y. N., M. Y. Barabanenkov, and S. A. Nikitov, arXiv:1009.4770v1 [cond-mat.dis-nn], Sep. 24, 2010.
5. Barabanenkov, Y. N. and V. V. Shlyapin, *Phys. Lett. A*, Vol. 170, 239–244, 1992.

Magnetic Response of Random Ensemble of Small Non-magnetic Particles in Theory of Electromagnetic Wave Multiple Scattering

M. Yu. Barabanenkov
Institute of Microelectronics Technology, Russian Academy of Sciences
Chernogolovka, Moscow Region 142432, Russia

Abstract— Initially artificial metamaterials have been developed as periodic arrays of complex-shaped resonant elements. A homogenization (introduction of effective dielectric permittivity and magnetic permeability) of such periodic structures has included Maxwell's equations averaging over structure unit cell followed by applying some intuitively appropriate Clausius-Mossotti relations [1, 2].

In this report, we consider frequency spectra of effective magnetic permeability and dielectric permittivity of the so-called Mie resonance-based random (not periodic) composites [3], calculated on the basis of general theory of wave multiple scattering in random discrete media [4], with Maxwell's equations averaging over statistical ensemble of particles. The basic equations of the abovementioned theory [5] are the generalized Lorentz-Lorenz formula for transversal and longitudinal components of effective dielectric permittivity tensor with respect to a wave vector in the random media and the Lindhard rule [6] for effective magnetic permeability in the long wavelength limit.

In the approximation of independent particles our calculations predict zero (perfect diamagnetism) and negative values of effective magnetic permeability real part in the visible and terahertz frequency ranges for small silicon and gold particles, respectively. Physically, small size of silicon particles means that only the lowest magnetic Mie mode is excited in each particle during wave scattering (in the calculations radius of silicon spheres was smaller than 0.1 μm with the filling factor of about 0.2). A contribution of high-order Mie modes into magnetic response of random media under consideration is required further investigation.

REFERENCES

1. Silveirinha, M. G., *Phys. Rev. B*, Vol. 75, 115104, 2007.
2. Silveirinha, M. G., *Phys. Rev. B*, Vol. 76, 245117, 2007.
3. Zhao, Q., J. Zhou, F. Zhang, and D. Lippens, *Materials Today*, Vol. 12, 60–69, 2009.
4. Barabanenkov, Y. N., *Physics-Uspekhi*, Vol. 52, 502–506, 2009.
5. Barabanenkov, Y. N., M. Y. Barabanenkov, and S. A. Nikitov, arXiv:1009.4770v1 [cond-mat.dis-nn], Sep. 24, 2010.
6. Lindhard, J., *Dan. Mat. Fys. Medd.*, Vol. 28. No. 8, 3–57, 1954.

On a Solution of Spread Boundary Problem of Bulk Artificial Optical Materials by Riccati Equation Method

M. Yu. Barabanenkov
Institute of Microelectronics Technology, Russian Academy of Sciences
Chernogolovka, Moscow Region, Russia

Abstract— A problem of spread boundary of bulk artificial optical structures is now considering [1] as one of the main shortcoming of adequate theoretical description of metamaterial electromagnetic properties. The aim of this report is to underline that the matrix Riccati equation method [2], being a consequence of the invariant imbedding formalism [3], is able to treat abovementioned spread boundary problem rigorously. Really, according to the principles of the transfer matrix approach [4] one can split virtually any dielectric structure into a stack of slices with splits between them. Let the slices are perpendicular to the z axis. to According to [2], the composition rule of T-matrices leads to a system of exact matrix equations, i.e., transfer relations [2] for the matrix wave reflection and transmission coefficients of a set of slices and the matrix amplitudes of waves in splits between slices. Note, in a derivation of the transfer relations it was supposed the wave field and field's normal derivatives on any interface to be continuous on this interface. The transfer relations give, in particular, a differential basic Riccati equation for the matrix wave reflection coefficient from a slab of the structure, the embedding parameter of these differential equations with given "initial" condition is taken along the z axis. The wave field scattered by the first slice is the initial condition for the next slice. This procedure may be interrupted at any slice forming the scattered wave field from truncated structure with spread boundary. We demonstrate such a possibility of the Riccati equation method with a few examples of arbitrary (but perpendicular to the z axis) truncated diffraction gratings and photonic crystals.

REFERENCES

1. See Challenges Sectin in http://econam.metamorphose-vi.org/.
2. Barabanenkov, Y. N., V. L. Kouznetsov, and M. Y. Barabanenkov, "Transfer relations for electromagnetic wave scattering from periodic dielectric one-dimensional interface: TE polarization lines," *Progress In Electromagnetic Research*, Vol. 24, 39–75, 1999.
3. Klyatskin, V. I., *The Imbedding Method in the Theory of Wave Propagation*, Nauka, Moscow, 1986.
4. Barnes, C. and J. B. Pendry, *Proc. R. Soc. London, Ser. A*, Vol. 435, 185–196, 1991.

Magnetostatic Waves Multiple Scattering Band Structure Calculation for Locally Resonant Magnonic Crystals

Ivan Lisenkov[1, 2] **and Sergey Nikitov**[1, 2, 3]

[1]Kotel'nikov Institute of Radio Engineering and Electronics of RAS, Russia
[2]Moscow institute for Physics and Technology, Russia
[3]N.G. Chernyshevsky Saratov State University, Russia

Abstract— Composite materials attract attention in general radio-physics due to unique exhibited properties. Artificial periodic structures for electromagnetic and acoustic/elastic waves such as photonic and phononic crystals, respectively, were considered theoretically and implemented experimentally in past decades [1, 2]. Special attractive case of artificial materials is quasi-isotropic composites with embedded resonators [3]. Propagation of magnetostatic spin waves in composite media is less covered to date [4]. Our work takes an attempt provide method for calculation of band structure in magnonic crystals with local resonances.

The two-dimensional magnonic crystal [4] is considered as thin ferromagnetic film with nano-sized cylindrical inclusions embedded in matrix and arranged in periodic and non-periodic manner. External magnetic field is applied perpendicular to the film and in parallel to saturation magnetization.

Two types of resonances could occur in such structure: Bragg-type from periodicity of inclusions and Mie-like local resonances inside inclusions. Varying saturation magnetization of composite fractions lead to possibility of forward volume magnetostatic wave (FVMSW) Mie-like resonance scattering regime. The resonance regime and destructive interference open a band gap in FVMSW spectrum. Dependence of band gaps location on external magnetic filed is investigated. It is shown that is is possible to obtain low-frequency local resonance band gaps in ordered and disordered Yittrium-Iron-Garnet (YIG) films. Comparison with other methods like Coherent potential approximation and Plane-wave expansion [5] and numerical stability tests were made.

To sum up, in this work we are presenting multiple scattering calculation method for ferromagnetic films with ordered and random distribution of impurities. Using the method we have shown that such media exhibit local resonance behavior and frequency band gaps for FVSW can be obtained.

ACKNOWLEDGMENT

Work is supported by RFBR Grant #11-07-12052-ofi-m-2011 and Ministry of Science and Education of Russia (agreement #P556).

REFERENCES

1. Joannopoulos, J. D., S. G. Johnson, J. N. Winn, and R. D. Meade, *Photonic Crystals: Molding the Flow of Light*, 2nd Edition, Princeton University Press, Princeton, NJ, 2008.
2. Croenne, C., E. J. S. Lee, H. Hu, and J. H. Page, *AIP Advances*, Vol. 1, 041401, 2011.
3. Lisenkov, I., R. Popov, and S. Nikitov, *Appl. Phys. A.*, Vol. 103, No. 3, 921–925, 2011.
4. Nikitov, S. A., P. Tailhadesa, and C. S. Tsaib, *JMMM*, Vol. 236, 320–330, 2001.
5. Krawczyk, M., et al., *J. Appl. Phys.*, Vol. 108, 093909, 2010.

Analytic Model for Near-Field Interference 3D Radiothermography of Biological Tissue Local Temperature Variation at Radiation Receiving on Coupled Linear Wire Antennas

Y. N. Barabanenkov[1], **M. Yu. Barabanenkov**[2], **and V. A. Chrepenin**[1]

[1]V. A. Kotelnikov Institute of Radioengineering and Electronics
Russian Academy of Sciences, Moscow, Russia
[2]Institute of Microelectronics Technology, Russian Academy of Sciences
Chernogolovka, Moscow region, Russia

Abstract— Measuring method of the temperature spatial distribution inside of a biological tissue object by recording its own thermal radiation in the microwave range is well known at the present time [1]. During the last twenty years, there has been realized that a contact with object antenna [2] or system of contact antennas [3] are situated in the area of a heated object thermal near fields that have basically the form of evanescent electromagnetic waves exponentially decaying in perpendicular to the object boundary surface direction according to Rytov prediction [4]. The known approaches in radiothermography suffer from that they are not aimed directly to reconstruct the 3D localization of a biological tissue local temperature variation. Bearing in mind importance of such 3D localization for exploration, e.g., human head brain cortex, recently [5] there were obtained new results in near-field radiothermography, which enables one to originate a near-field radiothermograph on base of interference-extreme properties of its antenna receiving system, with taking into account wave coupling between single antennas at multichannel receiving. In this report we present an analytical model for above 3D reconstruction. The biological object thermal radiation caused by 3D temperature local variation inside object absorption skin slab area is modeled by radiation of three mutually perpendicular and statistically independent random electric dipoles-sources. For simplicity we choose one electric dipole-source and two parallel to electric-dipole source coupled receiving linear wire antennas placed at object boundary surface and tuned to half wavelength in the object. In the case of single receiving vibrator dipole-antenna it is shown that the fluctuations' spectral density of exciting current distribution along the receiving vibrator amplitude has maximum at random electric dipole-source position near receiving vibrator-antenna equatorial plane, going through vibrator centre perpendicular the vibrator axis. Substantially that experimentally measured the maximum half width at half maximum is expressed by random electric dipole-source "seeming" depth. Measuring seeming depths of random electric dipole-source for two positions of receiving vibrator-antenna on the object surface enables one to evaluate 3D position of random electric dipole-source inside the biological object. In the case of two coupled receiving vibrator dipole-antennas the fluctuations' spectral densities of exciting currents' distributions along the receiving vibrators' amplitudes have a complicate dependence on antennas coupling factor. Nevertheless, in the special case of dipole-source symmetrical position relatively antennas the scanning problem of random electric dipole-source via two coupled antennas is reduced, as we show, to such problem via a single antenna.

REFERENCES

1. Godik, E. E. and Y. V. Gulyev, "Functional imaging of the human body," *IEEE Engineering in Medicine and Biology*, Vol. 10, 21, 1991.
2. Reznik, A. N., *Izv. Vyssh. Uchebn. Zaved., Radiofiz*, Vol. 34, 512, 1991.
3. Anzimirov, V. L., N. A. Arkhipova, V. I. Pasechnik, and A. V. Yanovich, *Biomed. Radioelektron.*, Vol. 8, 22, 2000.
4. Rytov, S. M., *Theory of Electrical Fluctuations and Heat Emission*, Akademii Nauk SSSR, Moscow, 1953.
5. YBarabanenkov, Y. N., M. Y. Barabanenov, and V. A. Cherepenin, *Journal of Radio Electronics*, No. 12, 2011, http://jre.cplire.ru/jre/ dec11./3 / text.html.

Boundary Problem Formulation for Field in Non-uniform Periodical Media

Sergey Bankov, Sergey Nikitov, and Ivan Lisenkov
Institute of Radio Engineering and Electronics of Russian Academy of Science, Russia

Abstract— Novel formulation of boundary problem for electromagnetic field inside non-uniform periodical media is proposed. Regular periodical media is a plurality of 2D or 3D identical elementary particles periodically located in free space. Non-uniform media also contains particles with electromagnetic properties differing from properties of particles in a regular media.

New description of field in periodical media is proposed. Total field in the media is presented as a superposition of fields scattered by all its particles. Solution of a problem about plane wave scattering by a single particle is supposed to be known. Scattered field is presented in form of a sum of space harmonics with coefficients (amplitudes) depending on the incident field. The amplitudes form an amplitude vector U. Each particle in media may be characterized by its vector U. Thus field inside periodical media is described with help of a plurality of vectors U. This plurality replaces vector functions E and H in the conventional approach.

Next conventional electric and magnetic currents are replaced by compensated sources which produce field in form of a sum of space harmonics with fixed amplitudes. These amplitudes form source vector V.

Fundamental for proposed approach problem is a problem of a regular periodical media excitation by a compensating source. This problem is solved for 2D and 3D medias in form of Green's function G that connects plurality of vectors U with source vector V. Obtained Green's function is an analog of free space function in case of uniform periodical media.

Formulation of boundary problem for non-uniform periodical media requires boundary conditions for amplitude vectors U. These conditions should be formulated for vectors corresponding to defects of a regular media. Defect is a particle with properties differing from properties of a regular particle. The simplest defect is a particle removed from media. Boundary condition for such a particle in terms of vector U has a simple form $U = 0$. Boundary conditions for more complicated defects are also discussed.

The last step of boundary problem formulation is a formulation of system of linear algebraic equation which describes non-uniform media. For it we suppose that non-uniform media is still uniform but inside defects we insert compensating sources with unknown source vectors V. Plurality of amplitude vectors U may be found with help of Green's function G. Substituting these vectors in boundary conditions we obtain required system of linear algebraic equations relatively vectors V.

Order of this system is proportional to $N \times M$, where N is a number of defects in non-uniform media and M is a dimension of vectors U and V. We should note that parameter M is typically equal to 3–5 because electrical size of a particle usually is enough small and scattered by it field may be precisely described with help of a limited number of space harmonics. Thus we may conclude that order of the system of equations is much smaller than in other approaches in which it is proportional to a total number of particles (regular particles plus defects). Because of it numerical algorithm built on the base of the proposed approach has very high efficiency.

Several numerical examples are discussed. The proposed approach is applied to electromagnetic bandgap structures with defects. These defects form waveguide elements: waveguide junctions, coupled waveguides, resonators etc..

Additional advantage of the proposed boundary problem formulation is an opportunity to analyze idealized infinite structures in the first turn infinite waveguides in periodical media. Knowledge of eigen modes of such waveguides is critically important for correct formulation of scattering parameters of waveguide devices that may be built up with help of defects in uniform periodical media.

Acoustothermometrical Control of Laser Hyperthermia of Biological Tissues

A. A. Anosov[1], **Yu. N. Barabanenkov**[1], **A. S. Kazanskij**[1], **and A. D. Mansfel'd**[2]

[1]Institute of Radioengineering and Electronics of RAS, Russia
[2]Institute of Applied Physics of RAS, Russia

Abstract— One of the important problems of a laser hyperthermia of human body tissues is a control of their inner temperature. Usage of the noninvasive painless methods is more preferable for this problem solution. In certain cases one can use an acoustothermometry [1]. The acoustothermometry is the measurement of the thermal acoustic radiation in megahertz frequency band. This radiation emitted from an object results from the thermal movement of atoms and molecules in it. The intensity of the thermal acoustic radiation is determined by the absolute temperature and absorption coefficient in the object. The spatial resolution of the acoustothermography is enough for the temperature distribution reconstruction because of the small wave length (about 1 mm).

We carried out a model experiment with a beef liver and controlled the real laser hyperthermia of the thyroid gland. In the model experiment we heated and cooled the liver and measured the its acoustobrightness temperarure with acoustothermometers and the its surface temperature with IR thermometry. The acoustothermometers developed by the Institute of Applied Physics of RAS (Russia, N. Novgorod) had the band equal to 1.7 ± 0.4 MHz. Their sensitivity was equal to 0.3 K for 10 s. The portable computer thermograph IRTIS-2000 developed by "IRTIS" Ltd. (Russia, Moscow) had the sensitivity equal to 0.05 K. The measurement results were connected to each other and correlated with the heating/cooling script.

One carried out the acoustothermometrical control of laser hyperthermia of the thyroid gland. The IR laser (1060 nm) was used. The laser radiation was introduced through optical fiber in the thyroid gland. The time of the procedure was about 10 minutes. The laser radiation was absorbed in the gland and it was heated. The measurements were conducted with two acoustothermometers. The measured acoustobrightness temperarure increased after the heating was switched on and decreased after the heating was switched off. The obtained results showed that the usage of the acoustothermometry of the laser hyperthermia allowed to estimate the heating parameters.

ACKNOWLEDGMENT

This work was partially supported by Russian Foundation for Basic Research.

REFERENCES

1. Bowen, T., *Automedica*, Vol. 8, No. 4, 247–267, UK, 1987.

Radiometric Methods of Measurement of the Total Reflectivity, the Total Transmissivity and the Coherent Transmissivity of a Weakly Absorbing Random Discrete Medium Layer in the Millimeter Wavelengths Range

V. A. Golunov and Yu. N. Barabanenkov
V. A. Kotelnikov Institute of Radioengineering and Electronics of RAS, Fryazino Branch, Russia

Abstract— Set of characteristics such as the total reflectivity, the total transmissivity and the coherent transmissivity provides sufficient information on the effects of volume scattering electromagnetic waves from random discrete medium layer. Radiometric methods of measurement of the characteristics have been devised and are presented. The methods of measurements of the total reflectivity and the total transmissivity are based on changes of front and back radiation background brightness within solid angle 2π.

The method of measurement of the coherent transmissivity is based on the experimental dependence of the transmissivity on angle size of thermal source irradiating the under consideration medium sample. It has been observed that in the case of the test specimen of a weakly absorbing random discrete media particularly the dependence of the transmissivity on the angle size of the thermal source with round form is linear. So using extrapolation of this dependence the coherent, transmissivity is determined provided that the thermal source is point one. In contrast to the classic method based on using an oscillator or a noise generator the devised method permits to measure the coherent transmissivity with the exception of necessity to average out an ensemble of under consideration random discrete medium realizations.

The experimental setup by means of which the characteristics listed above are measured consists of some of radiometers, the metallic chamber with the lens and the black body cooled down by means of liquid nitrogen. Teflon lens with diameter 0.2 m and focus length 0.4 m is placed on the front wall of the chamber. There is a hole for the radiometer guide and irradiator on the opposite wall. The irradiator is located in the lens focus. The sample being investigated are placed into a metallic cylindrical container with diameter 0.2 m and is put closely to the lens during the measurement. The second black body cooled down by means of liquid nitrogen is used to measure the coherent transmissivity. In this case the black body is moved from the sample being investigated along optical axis of lens.

The devised methods and experimental setup have been used for investigation of regularities of volume scattering from dry snow and man-made like-snow media in the frequency range from 15 to 94 GHz.

Session 4A4
Antennas, Shielding and EMC Measurement

Analysis of the Radiated Emissions of IT Equipment

R. Przesmycki, M. Wnuk, L. Nowosielski, K. Piwowarczyk, and M. Bugaj
Faculty of Electronics, Military University of Technology
Gen. S. Kaliskiego 2 Str., Warsaw 00-908, Poland

Abstract— Telecommunications and data communications devices are integral part of complex systems, which determine the correct functioning of economy. Efficiency and reliability of the functioning of electric and electronic devices decide about the functioning and development of national economy. To a large extent it depends on hazards and the level of disturbances occurring in the environment surrounding us. Thus it is necessary not only to study sensitivity of electric and electronic devices to electromagnetic fields but also to control the level of electromagnetic disturbances emitted to the surrounding environment through different ways. The level of disturbance in the environment depends not only on the level of disturbances emitted into the environment by equipment and systems working in the environment surrounding the facility, but also on the level of electromagnetic fields radiated by the object itself.

This problem is important not only because of electromagnetic compatibility but also due to necessity of providing security of sent or processed information. Currently there are available devices which allow reconstructing processed or sent information by using dispersed electromagnetic fields (unintentionally radiated). Therefore issues connected with the control of disturbance emissions become particularly significant. Therefore, issues related to emission and immunity testing IT equipment, in the developed countries, special attention is attached. Requirements for both emission and immunity to electromagnetic exposure, especially computer equipment are today to the category of basic requirements. Each device is characterized by parameter ε determining emission ability. It is the function of emission direction φ, pulsation ω and time t: $\varepsilon = f(\varphi, \omega, t)$.

In the article special attention is undesirable emissions. These emissions are by-products generated unintentionally during realization of basic function of the device. They are formed in electric circuits containing inductances and capacities in which there occur sudden changes of current or voltage, relatively fluctuating changes of density of electric charge carriers or in which there occurs positive back coupling.

In the article presented the disturbances of generated emissions by IT equipments, the methodology of measuring radiated emissions generated by IT devices in accordance with the EN 55022 : 2006 standard is presented and the results of measurements carried out on particular number of samples consisting of central processing units produced in the years 2007–2010 are demonstrated. The measurements of radiated emissions generated by IT equipments have been performed in the Electromagnetic Compatibility Laboratory at the Faculty of Electronics of the Military University of Technology in Poland.

Antenna Gain Measurement by Comparative Method Using an Anechoic Chamber

R. Przesmycki, M. Wnuk, L. Nowosielski, K. Piwowarczyk, and M. Bugaj
Faculty of Electronics, Military University of Technology
Gen. S. Kaliskiego 2 Str., Warsaw 00-908, Poland

Abstract— To define the concept of the antenna in simple words is not easy. Most antenna is defined by the function it fulfills in the radio communication path. So we say that the antenna is a device which allows the conversion of electromagnetic energy pursued in closed line to the electromagnetic wave propagating in free space for the transmitting antennas, and vice versa for receiving antennas. Antenna is characterized by many parameters, which determine the properties of the antenna. Antenna Directivity (D) is a parameter which determines the ability of the directional radiation of electromagnetic energy by a test antenna in comparison to the antenna which is used as a reference model. It is the ratio of active power radiated per unit solid angle by a test antenna and the reference antenna in the direction of maximum radiation of the two antennas, provided that the radiation powers are the same.

Antenna Gain (G) can be defined as the ratio of the value of radiation power in a one of direction to the value of radiation power, which would have been obtained the same power by the antenna radiating isotropic directions. This parameter does not include losses resulting from impedance mismatch and a polarizing (only takes into account losses in the antenna). Directivity and Gain antenna connects the following relationship: $G = D * \eta$, where η — the energy efficiency of the antenna. In practice, usually measured parameters of antennas are the characteristics of radiation, voltage standing wave ratio, directionality and gain of the antenna.

The article focuses on the implementation of the antenna gain measurements in the anechoic chamber. In the article showed a detailed description of the developed procedure of measuring gain by the comparative method. In the article also described the methodology and principles of the laboratory stand for measuring gain of antennas in the anechoic chamber. The developed method of measuring the gain of antennas provides an easy way to determine the value of this parameter and is often used in antenna measurements. It is a method that is not time consuming. However, preparing the measurement requires more attention and time. From preparing the laboratory stand by the right way depends the measurement results. The summary of this article presented the results of measurement and interpretation of results for the sample antenna in anechoic chamber.

Multilayer Microstrip Antennas Array Operating in Dual Bands

Marek Bugaj, **Rafal Przesmycki**, **Leszek Nowosielski**,
Kazimierz Piwowarczyk, **and Marian Wnuk**
Faculty of Electronics, Military University of Technology
Gen. S. Kaliskiego 2 Str., Warsaw 00-908, Poland

Abstract— The paper describes problems related to antenna technology. The paper shows the construction of multilayer microstrip antenna array on a dielectric substrate operating in dual band (2.4 GHz and 5.8 GHz). Microstrip antennas in antenna technology appeared relatively late, but in recent years has been a very large development of the design of these antennas and the huge interest in their capabilities. Microstrip antennas are often used in all areas of radio communications. This is due to the simplicity of their design, ease of implementation and relatively low production costs. An important advantage of these antennas is their shape, small size, low weight and aesthetic appearance. Microstrip antennas also provide high repeatability parameters and high resistance to weather conditions.

The article presents two arrays (2×1 and 4×1) of microstrip antennas operating at frequencies of 2.4 GHz and 5.8 GHz. To the feed microstrip arrays we used parallel feed configuration. The distance from the input port to each radiating element are identical. For a uniform aperture distribution, the power is equally split at each junction. Coplanar microstrip feeds is easy to fabricate. In this antenna two operating frequencies have the same polarization planes. The antenna consists of three layering and has two rectangular radiating elements on different layers. For so performed antenna models was made measurements in the anechoic chamber of typical electrical parameters, such as standing wave ratio, input impedance, radiation pattern, gain. The article also analyzes the results of computer simulations and measurements.

Dual Band Microstrip Antenna Working in the Frequency Bands 2.4 GHz and 5.8 GHz

Marek Bugaj, Rafal Przesmycki, Leszek Nowosielski, Kazimierz Piwowarczyk, and Marian Wnuk
Faculty of Electronics, Military University of Technology
Gen. S. Kaliskiego 2 Str., Warsaw 00-908, Poland

Abstract— The fast development technology of wireless internet access and the requirements to comply of the standards applied to the WLAN (Wireless Local Area Network) as well as the possibility of using the ISM (Industrial, Scientific, Medical) frequency bands in the ranges 2400–2500 MHz and 5725–5875 MHz has forced demand for dual-band antennas, which can be implemented in stationary and mobile devices. The paper describes problems related to antenna technology.

The paper shows the construction of multilayer microstrip antenna on a dielectric substrate operating in 2.4 GHz and 5.8 GHz. Microstrip antennas in antenna technology appeared relatively late, but in recent years has been a very large development of the design of these antennas and the huge interest in their capabilities. Microstrip antennas are often used in all areas of radio communications. This is due to the simplicity of their design, ease of implementation and relatively low production costs. An important advantage of these antennas is their shape, small size, low weight and aesthetic appearance. Microstrip antennas also provide high repeatability parameters and high resistance to weather conditions.

The article presents a multilayer structure of microstrip antennas operating at frequencies of 2.4 GHz and 5.8 GHz. The microstrip patches is feed by coupled microsrip line. Coplanar microstrip feeds is easy to fabricate. In this antenna two operating frequencies have the same polarization planes. The antenna consists of three layering and has two rectangular radiating elements on different layers. For so performed antenna model was made measurements in the anechoic chamber of 2/2 typical electrical parameters, such as standing wave ratio, input impedance, radiation pattern, gain. The article also analyzes the results of computer simulations and measurements.

Methods of Measuring Shielding Effectiveness of Small Shielded Chambers

L. Nowosielski, **M. Wnuk**, **R. Przesmycki**, **K. Piwowarczyk**, **and M. Bugaj**
Faculty of Electronics, Military University of Technology
Gen. S. Kaliskiego 2 Str., Warsaw 00-908, Poland

Abstract— The article concerns problems connected with electromagnetic compatibility (EMC). Its aim is to present sample applications of measuring positions and methodologies of measuring shielding efficiency of small chambers in the frequency range from 80 MHz to 2500 MHz. In the article a description of the positions for measuring shielding efficiency of small chambers has been presented. In the article sample results from measurements of shielding efficiency of one small chamber in the frequency range from 80 MHz to 2500 MHz have been shown too. The measurement results were obtained using two presented in article measurement methodologies. The described in article methodologies are used for conducting research in the Laboratory of Electromagnetic Compatibility, Military University of Technology.

Ambient Electromagnetic Noise Environment Measurement

L. Nowosielski[1], **B. Bogdan**[2], **M. Wnuk**[1], **R. Przesmycki**[1], **K. Piwowarczyk**[1], **and M. Bugaj**[1]

[1]Faculty of Electronics, Military University of Technology
Gen. S. Kaliskiego 2 Str., Warsaw 00-908, Poland
[2]KenBIT Sp.j., Żytnia 15/22 Str., Warsaw 01-014, Poland

Abstract— The external Radio Frequency (RF) ambient establishes the minimum usable signal strength for satisfactory radio communication service. Sources of the RF ambient may be naturally occurring or due to manmade sources. In order to evaluate the level of the local RF electromagnetic environment the level of the electromagnetic field strength for selected frequencies has to be measured. In article is presented the automated measurement system for electromagnetic field strength measurement. In the system the precautions were taken to ensure that the measuring and controlling equipment does not affect the measured electromagnetic fields. The measurement system consists of the measurement receiver, antenna and personal computer. On the deck of the personal computer the dedicated software for remote control of the measurement system is running. In the article is presented the software graphical user interface description and the algorithm for the measurement process, data collection and analysis. The algorithm is based on the IEEE Std 473-1985 standard "IEEE recommended practice for an electromagnetic site survey". The measurement results of the electromagnetic field strength in HF band at selected rural area are presented too.

The Shielding Effectiveness Measurement Using High Voltage Pulse Generator

Kazimierz Piwowarczyk, Marian Wnuk, Leszek Nowosielski, Rafal Przesmycki, and Marek Bugaj
Faculty of Electronics, Military University of Technology
Gen. S. Kaliskiego 2 Str., Warsaw 00-908, Poland

Abstract— The article describes creation of the concept as well as the construction of laboratory stand using high-voltage pulse generator. By using the high-voltage pulse generator it was possible to perform measurements of shielding effectiveness of small chamber shielding. After preparing and creation of the laboratory stand there were series of control tests made to define the level of usability and correctness of the made researches. Tests were made based on the methodology described in the article.

Due to the limited dimensions of the inner shielding of small chamber (less than $1.5\,[\mathrm{m}] \times 1.5\,[\mathrm{m}] \times 1.5\,[\mathrm{m}]$), it was impossible to use the methods described in the available documents of standardization. This is due to the fact that the available measurement antennas, enabling the effective working, have dimensions that unable placing them inside the small chamber shielding and consequently unable the measuring the effectiveness of shielding of these chambers.

Measurement of shielding effectiveness of shielding contributed by the chamber is reduced to perform two measurements of electric field for a given sounding frequency. The first test is the standardization measurement for which we measure the intensity of the electric field in the distance of 1 m from the high voltage pulse generator. During the measurements there are recorded field strength values for each frequency. High voltage pulse generator and the measuring sensor are placed in the opposite of each other without the tested case. The measurements can be performed at discrete frequencies or at the specified frequency range with a specific step.

After the standardization measurement we continue with the principal measurement, where the high voltage pulse generator is placed in front of the measuring sensor, which is located inside the test chamber. The source of the measuring signal and receiver are placed assay facing each other at a distance of 1 m. The measurements should be made in the same way as during the standardization measuring on the discrete frequencies or at a specified frequency range with a specific step.

The Algorithm of Design Multi-layer Microstrip Antenna

Kazimierz Piwowarczyk, Marian Wnuk, Leszek Nowosielski, Rafal Przesmycki, and Marek Bugaj
Faculty of Electronics, Military University of Technology
Gen. S. Kaliskiego 2 Str., Warsaw 00-908, Poland

Abstract— The article describes the construction of multilayer microstrip antennas and algorithm of their designing using CST STUDIO software.

The idea of building microstrip antennas began in the fifties of last century. This was the first time when one observed the undesired effects of electromagnetic radiation from asymmetric stripline, also known as the microstrip line. Initially, the idea of using this phenomenon for building antennas did not arise much interest. The dynamic development of the researches of this type of structures was recorded only since the early seventies, when the microstrip antennas found many military and civilian applications.

At the present time, the role of microstrip antennas in modern telecommunications and radioelectronic systems has become huge. Many advantages of these structures resulted in their very wide application.

Considering the production of antennas and their possibilities of integration with the active systems, placing the transmitter and the power line on the same side of the substrate is an advantage. However, this solution has also many disadvantages, It is impossible to compatible the optimal substrate both for the transmitter and the microstrip line. Considering the efficiency of the antenna, it is desirable that the permittivity of the ground is as small as possible Then, in order to reduce the stray field of microstrip lines and reduce its geometrical dimensions, one should use the material with maximum electrical permeability. These limitations have led to creation of a new type of structure — multi-layer microstrip antenna.

Tuning Fork UWB Antenna with Unsymmetrical Feed Line

A. H. M. Zahirul Alam, **Md. Rafiqul Islam**, **and Sheroz Khan**
Faculty of Engineering, International Islamic University Malaysia
P. O. Box 10, Kuala Lumpur 50728, Malaysia

Abstract— A simple rectangular UWB is designed by optimizing the back plane conducting plane and the frequency band is further enhanced by changing the fed position. It is observed that the back conducting plane length is slightly shorter than the fed line length to obtain ultra wideband range. It is also observed that the shift of fed line from the center position will further enhance the bandwidth of the antenna. Therefore, it may be conclude that the unsymmetrical feed line plays an important role for increasing the antenna bandwidth. It is also observe that the rectangular antenna is further modified to tuning fork shaped with enhanced bandwidth. The tuning fork antenna geometry is shown in Fig. 1. By removing portion of conductive plane from the rectangular patch to makes tuning fork shaped antenna creates additional resonance, thus enhance the bandwidth of the antenna. The open space of the antenna can be utilized for placing other components. The fabricated antenna satisfies the 10-dB return loss requirement from 3.8 GHz to more than 15 GHz. The overall dimension of the antenna is $40 \times 40 \times 1.6\,\text{mm}^3$. The proposed antenna has a simple configuration and is easy to fabricate. Experimental results show that the proposed antenna could be a good candidate for UWB application.

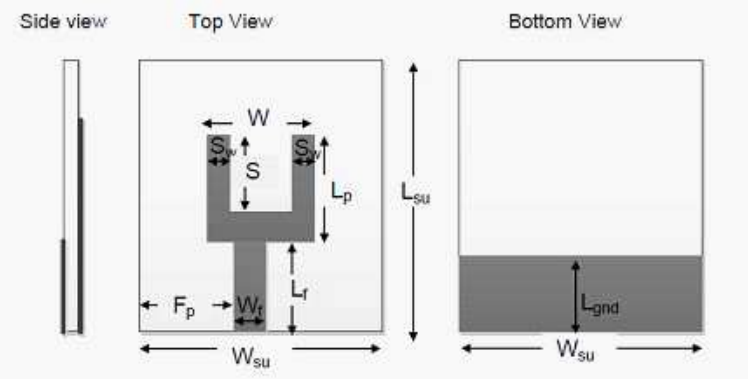

Figure 1: Geometry of proposed antenna with u-shaped slot and conductor-backed plane.

High Power Radiators for Ultra-wideband Electromagnetic Impulses

Vladimir M. Fedorov, Eugene F. Lebedev, Vasily Ye. Ostashev, Vladimir P. Tarakanov, and Aleksander V. Ul'yanov
Institute for High Energy Densities of JIHT of RAS, 13/2, Izhorskaya Str., Moscow 127412, Russia

Abstract— Results of creation and diagnostics of the high power radiators for electromagnetic waves of sub-nanosecond pulses with ultra-wideband (UWB) frequency spectrum are presented in this article. The spectrum of the electromagnetic high power radiation occupies a frequency range out of 100 MHz up to 10 GHz. This electromagnetic high power radiation can be successfully used to examine on electromagnetic compatibility (EMC) of various electronic devices. One module of the multi-unit radiator was made of the UWB radiation antenna of a TEM-horn type and the high power semiconductor generator ("FID Technology"). At our laboratory were made models of compact radiators in which used generators with pulsed voltage of 10–100 kV and repetition pulses of 1–100 kHz. The synchronized radiator array can produce electromagnetic impulse waves with far-zone radiated voltage of the $V_{ER} = E(R) \cdot R = 400$ kV level. We have used experimental and computer modeling methods to investigate the non-stationary processes in a generation of the UWB radiation by the TEM-horn antennas and at propagation and receiving of the electromagnetic video-pulses.

Session 4A5
Optial Linear and Non-linear Near-field and Confocal Microscopy

Two-photon Confocal and Near-field Optics of Bio-inspired Peptide Nanostructures

A. Kudryavtsev[1], **E. Mishina**[1], **S. Lavrov**[1], **A. Handelman**[2], **and G. Rosenman**[2]

[1]Moscow State Institute of Radioengineering, Electronics and Automation
Prospect Vernadskogo 78, Moscow 119454, Russia
[2]Department of Electrical Engineering-Physical Electronics
School of Engineering, Tel Aviv University, Tel Aviv 69978, Israel

Abstract— Small di- and tri-peptides can self-assemble into supramolecular bioinspired nanostructures: nanotubes, nanobelts and nanospheres. Nanoscale dimensions of their nanocrystalline building blocks and their space symmetry is the origin for exceptional physical properties of these nanotubular structures, such as quantum confinement and ferroelectric-related phenomena (piezoelectricity, second harmonic generation and spontaneous polarization). In this work, we study basic intrinsic physical properties in diphenylalanine-based peptide nanostructures, and follow their variation during the phase transition process using high resolution microscopy: confocal and near-field.

Local Nonlinearities of ZnO Nanostructures

K. Shvirkov[1], **A. Kedryavtsev**[1], **S. Lavrov**[1], **N. E. Sherstyuk**[1], **E. D. Mishina**[1], **E. Rusu**[2], **and L. Kulyuk**[2]

[1]Moscow State Technical University MIREA
Vernadskogo 78, Moscow 119454, Russia
[2]Institute of Applied Physics, Academy of Sciences of Moldova
Str. Academiei 5, Chisinau MD-2028, Republic of Moldova

Abstract— Zinc oxide (ZnO) films and nanostructures attract enhanced interest of researchers due to the unique optical properties of ZnO. It has excitonic luminescence in the ultraviolet range that makes it very perspective cheap material for applications in optoelectronic devices. Besides, not only bulk ZnO crystals and films, but also micro and nanostructures demonstrate high optical harmonics conversion efficiency, which is an extremely attractive property for integrated optics. It has been revealed that thin films of ZnO provide even more efficient harmonic generation than crystals due to size effects. Even ZnO nanolaser has been reported with single-photon and two-photon excitation [1, 2]. Apart from application in thin-film based devices, this circumstance makes it possible to use the second harmonic generation (SHG) as a convenient and sensitive method for testing the textures of ZnO films fabricated by different techniques and conditions of growth.

In this work, we report the results of microscopic studies of ZnO nanostructures. We use two-photon far-field as well as near-field microscopy in order to find conditions and geometry for more efficient second harmonic generation, superluminescence and lasing with femtosecond excitation in the range of 700–1000 nm. Efficiency of nonlinear optical processes is calibrated using ZnO single crystal and epitaxial film. To extract the components of the nonlinear susceptibility tensor for both samples as well as characteristics of the film's texture we have developed a theoretical model that allows us numerically to simulate all measured dependencies.

REFERENCES

1. Yan, R., D. Gargas, and P. Yang, *Nature Photonics*, Vol. 3, 569, 2009.
2. Zhang, C., F. Zhang, T. Xia, N. Kumar, J.-I. Hahm, J. Liu, Z. L. Wang, and J. Xu, *Optics Express*, Vol. 17, 7893, 2009.

Human In-vivo Blood Flow Image Velocimetry Using the High Speed Confocal Laser Scanning Microscope

S. H. Choi and H. Lee
School of Mechanical Engineering, Kyungpook National University, Daegu, Korea

Abstract— We demonstrated the feasibility of "the blood cell assisted in vivo Particle Image Velocimetry of human skin capillary." We used the high speed Confocal Microscopy to observe the motion of the blood cells in the capillary of the human lips. The home-built confocal laser scanning microscopy allowed us to take image at the acquisition rate of high speed. The individual blood cells could be distinguished from other cells and the trajectory of the each cell could be followed in the sequential images. The acquired confocal images were used to get the velocity profile of the in vivo blood flow in conjunction with the Particle Image Velocimetry (PIV). Without injecting the exogenous nano/micro particles into the human, the intrinsic blood cells were used as the tracing particles for PIV. We were able to measure the blood velocity up to a few hundred μm/sec for various vessels in a live human. Because there is no need for the injection of the "toxic" exogenous tracing particles, it is expected that we could apply the current technology for the study of human skin capillary blood stream.

ACKNOWLEDGMENT

This research was supported by Basic Science Research Program through the National Research Foundation of Korea (NRF) funded by the Ministry of Education, Science and Technology (No. 2012-0003524).

Nonlinear-optical and SNOM Investigations of Ferroelectric Polarization Switching in BST/NBFO Multilayer Structures

K. A. Brekhov[1], **S. D. Lavrov**[1], **N. E. Sherstyuk**[1], **V. M. Muhortov**[2], **and E. D. Mishina**[1]

[1]Moscow State Technical University MIREA
Prospekt Vernadskogo 78, Moscow 119454, Russia
[2]South Scientific Center of Russian Academy of Science, Rostov-on-Don, Russia

Abstract— Dynamics of polarization switching is the central problem of ferroelectric-based electro-optical modulators, high-speed nonvolatile ferroelectric random access memories and electro-optical switchers. Investigation of the dynamics of polarization reversal is highly important for optimization of the films parameters with respect to their switching characteristics. Resently it was shown [1] that nonlinear-optical microscopy based on second harmonic generation (SHG) allows to investigate both domain structure and polarization switching effecs in ferroelectric and multiferroic materials. Combination of the SHG and scanning near-field optical microscopy (SNOM) techniques provides complex investigations of local ferroelectric properties for nanosized thin films and planar structures with high spatial resolution up to 100 nm.

In the present paper, we report the results of polarization switching in $Ba_{0,8}Sr_{0,2}TiO_3/Bi_{0.97}FeNd_{0.03}O_3$ (BST/NBFO) planar structures studied by combination of the SHG and SNOM techniques.

Heteroepitaxial multilayer BST/NBFO structures with various thickness of the single layer ($d_1 = 3$ nm, $d_2 = 6$ nm) were fabricated by high-frequency sputtering on MgO (100) substrate. Chemiclal compositions of the BST and NBFO layers allows to perform all measurements at the room temperature. Epitaxial structure of the films was confirmed by X-ray diffraction. For electric field application aluminum planar electrode system with the gap of 20 μm was deposited on the film surface by vacuum deposition, which provides in-plane switching of the ferroelectric polarization during voltage application up to ±50 V.

Voltage dependencies of the SHG intensity were investigated for different thickness of the layer as well as spatial distribution of ferroelectric properties in the gap between two planar electrodes during DC voltage application by pattern 0-Umax-0-(-Umax)-0.

ACKNOWLEDGMENT

This work is supported partly by Russian Founadion of Basic Research and Russian Ministry of Science and Education.

REFERENCES

1. Mishina, E. D., S. V. Semin, K. V. Shvyrkov, A. V. Kudryavtsev, N. A. Ilyin, N. E. Sherstyuk, and V. M. Muhortov, *Physics of the Solid State*, Vol. 54, No. 5, 836, 2012.

Femtosecond Infrared Laser Annealing of Ferroelectric PZT Films on a Metal Substrate: Confocal and Near-field Optical Studies

N. Yu. Firsova[1], **E. D. Mishina**[1], **S. V. Senkevich**[2], **and I. P. Pronin**[2]

[1]Moscow State Technical University of Radioengineering, Electronics and Automation (MSTU-MIREA)
Prospekt Vernadskogo 78, Moscow 119454, Russia
[2]Ioffe Physical-Technical Institute of the Russian Academy of Sciences
Polytekhnicheskaya 26, St-Peterburg 194021, Russia

Abstract— The application of ultrashort pulse lasers for precision material processing has been an active area of fundamental and applied research due to their unique properties. When an ultrashort laser pulse interacts with a solid target, the electrons are heated to a high temperature by the absorption of laser energy. By the electron-phonon interactions, the hot electrons transfer energy to the lattice. For the femtosecond laser pulse, energy is transferred to the electrons on a time scale much faster than the transfer time of this energy to the lattice of the material and then the time of further propagation of heat along the sample surface. The latter results in a much smaller lateral thermal damage or heat-affected zone if compared with longer pulses impact.

In this paper, we present the results of femtosecond laser annealing of PZT film studied by second harmonig generation and scanning microscopy methods.

Since the laser beam is Gaussian, the temperature at the laser spot varies within the illuminated area, which results in an annealed area much smaller than the beam diameter. In this way, a diffraction limit can be overcome, and nanosize perovskite structures can be formed.

Several techniques were used to confirm formation of perovskite ferroelectric structure: in-situ during annealing second harmonic generation, confocal and near-field non-linear optical microscopy and piezo-force microscopy.

SHG technique of detection the annealing process is based on the changing of symmetry of the film from centrosymmetric (amorphous) to non-centrosymmetric (perovskite). Since the leading electro-dipole order SHG is allowed only in non-centrosymmetric media, the SHG intensity behavior during annealing let us detect the transition the PZT film to perovskite phase. Except observing time dependence of SHG intensity during annealing, after annealing we performed so called SHG scanning of the film area including annealed region. The observed SHG peak allowed us not only to confirm formation of perovskite ferroelectric structure, but also to estimate the diameter of the annealed area. Combination of the SHG and scanning near-field optical microscopy allows to arise spatial resolution of registration technique up to 100 nm.

Novel nanoscale tools are indeed needed to characterize ferroelectric switching and other electrical properties in the annealed microregions which is very difficult to do by conventional methods as the size of the focused beam is small. Piezo-force microscopy technique allows us to investigate local electromechanical properties of annealed area, including domain switching dynamics.

ACKNOWLEDGMENT

The work is supported by the Ministry of Science and Education of Russia.

Optical Properties of Fotonnokristallicheskih Structures Based on Single-crystal GaAs

A. U. Dobritsky, **N. A. Ilyin**, **T. V. Nikonorova**, **N. E. Sherstyuk**, **and E. D. Mishina**
Moscow State Institute of Radio-Engineering, Electronics and Automation
Prospect Vernadskogo 78, Moscow 119454, Russia

Abstract— Photonic crystals (PhC) offer wide opportunities for creation of small-type components, which allow to downsize the existing integrated circuits. The operation of these devises is based on the presence of photonic bandgap. Size and period of photonic crystal determine effective range of wavelength for the concrete functional element. The creation of PhC structures on the basis of functional materials with the characteristics being switched by external electric/magnetic field allow to manage the propagation parameters of electromagnetic field inside them.

The majority of research in the sphere of PhC waveguides is based on the modeling of their characteristics. Herewith 2 models are used: model of dielectric channels in air and model of ordered group of holes in functional material. The advantage of the first model waveguides lies in the fact that they are single-mode. The literature also offers variants of calculation of deflecting and bisected waveguides. But such a configuration of the waveguide does not provide the acceptable level of losses for the creation of actually functioning prototypes, working in the optical range. PhC structures, based on the second model are much more diverse and allow to create vaweguides of more complicated construction, for example, optical T- and Y-couplers, interferometers and so on.

This work presents the result of the systematical research using the method of numerical simulation of transmission spectra for PhC waveguides with different type of ordering and their characterization by scanning near-field optical microscopy (SNOM).

The modeling of the characteristics of 2D PhC structures was carried out with the help of software package CST StudioSuite. The following parameters were used for modeling: wavelength of 900–2000 nm, ratio of period of the structure to wavelength $0.24 \leq a/\lambda \leq 0.42$; ratio of hole diameter to period $0.5 \leq d/a \leq 0.9$. Photonic crystals based on silicon and gallium arsenide with quadratic and hexagonal ordering were investigated.

ACKNOWLEDGMENT

This work is partly supported by Russian Foundation of Basic Research and Russian Ministry of Science and Education.

Session 4A6
Wireless Network and Applications

Novel Bow-tie Bandpass Filter Design Using Multiple Radial Stubs

Z. Y. Fu, K. M. Lum, and W. T. Koh
School of Science and Technology, SIM University, Singapore

Abstract— A novel bow-tie bandpass filter (BPF) design using multiple radial stubs is presented in this paper. The proposed topology consists of seven radial stubs arranged in periodic angular orientation, a L-shape microstrip line and a pair of U-shape coupling arms. The center frequency of the proposed BPF is 2.8 GHz. A pair of radial stubs with arc size of 20° and 35° respectively is introduced. Three identical pairs of radials stub are positioned at 45 degrees interval, diagonally on the exterior vicinity of the right-angle bend of the L-shape microstrip line. A single radial stub is integrated within the interior vicinity right-angle bend. It should be noted that the seven radial stubs are open-ended. 50 Ω input and output ports are placed at the center of the U-shape coupling arm, namely coupling arm 1 and 2 respectively. The radial stub gives low impedance and it is physically shorter compare with the equivalent transmission line. In addition, the radial stub will have a wider bandwidth in comparison with the corresponding quarter-wave transmission line. Hence, by implementing the proposed BPF using multiple pairs of radial stubs, it allows wider bandwidth to be achieved. The proposed BPF is fabricated on a single layer FR4 substrate with relative permittivity of 4.7, loss tangent of 0.027 and a thickness of 1.6 mm. Overall dimension of the prototyped BPF is 37 mm by 37 mm. The best matched measured return loss S_{11} is obtained at 2.78 GHz with value less than −30 dB. The passband insertion loss S_{21} is approximately −1 dB and the stopband lower and upper attenuation rate are greater than 40 dB/GHz and 20 dB/GHz respectively. The simulation and measurement results are presented and discussed.

Ultra-wideband Bandpass Filter Using Symmetrical Step-impedance Resonators

C. G. Tan and K. M. Lum
School of Science and Technology, SIM University, Singapore

Abstract— This paper presents a compact ultra-wideband (UWB) bandpass filter (BPF) using symmetrical step-impedance resonators (SSIR). The operating frequency range is chosen to fall within the lower UWB spectrum of 3 GHz to 5 GHz. The passband has a centre frequency is 4 GHz. The proposed BPF generates a single passband located at the desired frequency through a single filter circuitry. The highly selective passband effect is obtained by the step-impedance resonators configuration in a similar topology as the classical comb filter. The proposed step-impedance topology consists of several microstrip sections: a main 50 Ω T-shape transmission line and a fork-shape SSIR cascaded with a shunt stub. A ring resonator with an inner circular aperture is further integrated at the end terminate of the two shunt stubs. Within the step-impedance configuration, the topology and position of the fork-shape SSIR is critically important in achieving the desired passband response. The proposed compact ultra-wideband bandpass filter is prototyped using FR4 substrate with a dielectric constant of 4.7, thickness of 1.6 mm, lost tangent of 0.027. The fabricated structure has a miniature dimensional size of 35 mm by 39 mm. The best matched return loss S_{11} is observed at 4.2 GHz with value less than −20 dB. The passband insertion loss S_{21} is greater than −2 dB. Rejection rate is approximately 30 dB/GHz and 18 dB/GHz for the stopband lower and upper transitions respectively. The passband bandwidth is around 0.7 GHz at −3 dB level. The performance measurements showed good agreement with the simulations. Both simulation results and measurement data are presented and discussed.

Dual-band Bandpass Filter Design Using Stub-loaded Resonators

W. T. Koh and K. M. Lum
School of Science and Technology, SIM University, Singapore

Abstract— A novel dual-band bandpass filter (BPF) using stub-loaded resonators (SLR) is presented. The proposed filter consists of a pair of independent open-ended square loops arranged in an adjacent manner with each other. Thus, allowing electromagnetic coupling configuration to be established. In addition, an open-ended microstrip stub is integrated into each respective square loop to achieve the dual-band characteristics at 2 GHz and 4 GHz. The resonant frequencies of the even-mode can be flexibly controlled by tuning the length of the open-ended stub whilst the odd-mode resonant frequencies stay constant. Two microstrip transmission lines with 50 Ω characteristic impedance are fed to the proposed dual-band BPF to act as the input and output feedlines respectively. The proposed dual-band BPF is implemented on a FR4 substrate with dielectric constant of 4.6, loss tangent of 0.027 and thickness of 1.6 mm. It has an overall dimensional size of 53.5 mm by 32.1 mm. The best measured matching return loss S_{11} for the first passband is observed at 2.21 GHz with a value less than −10 dB. The corresponding passband response S_{21} is approximately −1.76 dB with an upper and lower stopband attenuation of more than 20 dB/GHz. Additionally, the best measured matching return loss S_{11} for the second passband is observed at 3.81 GHz with a value less than −10 dB. The corresponding passband response S_{21} is approximately −2.88 dB with a lower and upper stopband rejection rate of more than 10 dB/GHz and 30 dB/GHz respectively. It is also observed that three transmission zeros with more than 30 dB attenuation are realized. Both simulation and measurement results are presented and discussed.

Microwave Bandpass Filter Using Cascaded Bow-tie Resonators

S. B. Sng, K. M. Lum, and L. F. Lim
School of Science and Technology, SIM University, Singapore

Abstract— A microwave bandpass filter (BPF) using cascaded bow-tie resonators is presented. The centre frequency of the proposed BPF is 3 GHz. Two open-ended bow-tie resonators are positioned near the input and output feedlines respectively. Four short-ended bow-tie resonators are cascaded in series along the main transmission line which comprises eleven sub-section using microstrip. A VIA hole with radius of 600 µm is integrated in the four short-ended bow-tie topology to facilitate the shorting effect. The bow-tie configuration is a simple assembly between the imaginary images of two triangular patches. It provides the flexibility in controlling the resonating frequency and passband bandwidth via its bow-shape microstrip topology. In addition, it is well known that bow-tie structures are able to provide wider bandwidth response. A 50 Ω microstrip line is being used for the input and output port respectively. FR4 substrate with relative permittivity of 4.6, thickness of 1600 µm and a loss tangent of 0.027 is being used to fabricate the proposed BPF design. The dimensional size of the prototyped BPF is 15.7 cm by 4.4 cm. The best matched return loss S_{11} is observed at 3.1 GHz with a value less than −10 dB and the corresponding passband insertion loss S_{21} is greater than −3 dB. Rejection rate at the lower and upper stopband response is more than 20 dB/GHz. The passband bandwidth is approximately 2.5 GHz at −3 dB level. Simulation results and measurement data of the proposed microwave BPF using cascaded bow-tie resonators are presented and discussed.

Bandstop Filter Design Using Cascaded Step-impedance Resonators with Defected Ground Structure

L. F. Lim and K. M. Lum
School of Science and Technology, SIM University, Singapore

Abstract— This paper presents a bandstop filter (BSF) design with a center frequency of 8 GHz using cascaded step-impedance resonator (CSIR) with defected ground structure (DGS). The proposed design consists of two single-plane conductor layers. The top conductor layer comprises six square-patch microstrips periodically cascaded in series with microstrip transmission lines, thus forming the cascaded step-impedance resonator structure. The input and output ports are terminated with 50 Ω characteristic impedance. The DGS is laid in the bottom conductor layer beneath the cascaded microstrip resonator. Integration of the DGS into the BSF topology has allowed the flexibility in varying the characteristics response of the cascaded step-impedance resonator structure in the top conductor layer. Furthermore, it also helps to eliminate unwanted harmonic frequencies and increases the effective permittivity which, eventually lead to the enhancement of the desire stopband filter response. It is to be noted that the accurate alignment of the CSIR and DGS structures laid in the top and bottom conductor layers are critically important in achieving the desired stopband response. The proposed BSF is prototyped using FR4 substrate with a relative permittivity of 4.6 and a thickness of 1600 µm. The overall dimension is 68 mm by 14.85 mm. The best measured return loss S_{11} is observed at 7.78 GHz with a value greater than −3 dB and the corresponding stopband insertion loss S_{21} is approximately −15 dB. The lower and upper attenuation rate of the stopband response is greater than 10 dB/GHz. Both simulation data and measurement results are evaluated and discussed for the proposed BSF.

Extraction of Distance-dependent Rain Rate Distributions for Satellite Links Calculation

S. C. Leong
Defence Science & Technology Agency, Singapore

Abstract— Typical satellite communication link budgets use single uplink or downlink fades to determine link margins and radio frequency satellite transponder bandwidth requirements [1]. This methodology results in under-provisioning of transponder bandwidth for small regions such as Singapore where both uplink and downlink may suffer simultaneous fades from a localized rain cell [2]. On the other hand, having a dual rain fade link budget calculation with equivalent uplink and downlink fades at frequencies such as Ku band for separated sites results in unrealistic link requirements.

Joint statistics such as correlation coefficient of rainfall [3], extracted from 13 years of weather radar data [4], has been evaluated for pairs of sites as a function of distance apart in Singapore. Statistical results demonstrate a monotonically decrease in correlation coefficient for increasing distances to 40 km for Singapore. This suggests that co-located transmit and receive sites should utilise dual-rain fade link budget calculations while transmit and receive sites a distance apart should use a modified rainfall distribution curve.

A modification of the single point rainfall distribution curve is proposed to predict the distance dependent average rainfall distribution and subsequently link budget calculation for a pair of transmit and receive sites. Since rain is non-uniform in the two horizontal spatial dimensions, the distance averaged rain rate is taken based on averaging the rain rate located along the 360 degrees circle circumference at a distance from the single point origin.

With the modified rainfall distribution curve, the one-way link budget calculation using ITU-R P. 618-10 [5] is compared with an accurate link budget calculation methodology for sites with a distance apart. Results show that the link budgets using the new distance dependent average rainfall distribution is accurate and there is approximately 20% savings in transponder bandwidth as compared to a dual rain fade Ku band link for 2 sites separately by 40 km in Singapore.

REFERENCES

1. Vuong, X. T. and S. T. Vuong, "Satellite link margin and availability issues, " *IEEE Trans. on Broadcasting*, Vol. 43, No. 2, Jun. 1997.
2. Khamis, N. H., J. Din, and T. A. Rahman, "Determination of rain cell size distribution for microwave link design in Malaysia," *RF and Microwave Conference*, 2004.
3. Fukuchi, H., "Correlation properties of rainfall rates in the United Kingdom," *IEE Proceedings*, Vol. 35, No. 2, 49–51, Apr. 1998.
4. http://www.weather.gov.sg/wip/c/portal/layout?p_l_id=PUB.1023.5, Meteorological Service Singapore, 2011.
5. ITU-R, "Propagation data and prediction methods required for the design of Earth-space telecommunication systems," Recommendation ITU-R P.618-10, Geneva, 2009.

IDMA System Based on Permutation Polynomial Interleaver over Integer Rings

Mohamed Fathey Abo Sree, Esam A. A. A. Hagras,
Mohamed S. El-Mahallawy, and Mohamed Aboul El-Dahab
Electronics and Communications Department, College of Engineering and Technology
Arab Academy for Science & Technology and Maritime Transport, Cairo, Egypt

Abstract— In this paper, an algorithm for implementing Interleave Division Multiple Access (IDMA) is introduced and also a permutation polynomial interleaver (PPI) is suggested as a user specific interleaver in IDMA. The proposed technique can solve the memory cost problem for chip level interleavers and reduce the amount of information exchange between mobile stations and base stations to specify the interleaver used as there identifications. We compare the proposed PPI with recent interleaver designs such as Random, Tree and Prime Interleaver. Performance analysis of IDMA with Binary phase shift keying (BPSK) modulation employing the proposed PPI in Additive White Gaussian Noise (AWGN) channel is carried out. In addition to that, we compare between interleavers from point of view complexity & bandwidth against number of user.

Performance Evaluation of Clipped ML IDMA Communication System

Mohamed F. Abo Sree, Esam A. A. A. Hagras
Mohamed S. El-Mahallawy, and Mohamed Aboul El-Dahab
Electronics and Communications Department, Faculty of Engineering
Arab Academy for Science & Technology and Maritime Transport, Cairo, Egypt

Abstract— In this paper, the performance analysis of Clipped Multi-Layer Interleaver Division Multiple Access (C-ML IDMA) has been simulated in Additive White Gaussian Noise (AWGN) channel to reduce Peak to Average Power Ratio (PAPR) of transmitted signal. High Peak Average to Power Ratio (PAPR) is one of the main drawbacks of the ML IDMA systems currently used in high rate communication standards. It is shown that with proposed technique, the effect of clipping can be efficiently compensated and better performance between PAPR & Bit Error Rate (BER) can be achieved. We compare between original signal without clipping & some values of Clipping Ratio (CR) in ML IDMA systems between Signal to Noise Ratio (SNR) & BER. Not only, we compare between PAPR with BER without CR and with some values of CRs to achieve more better performance in MATLAB simulations.

Concept of Image Based Non-line-of-sight (NLOS) Localization in Multipath Environments

Si Wen Chen, Chee Kiat Seow, and Kai Wen
School of Electrical and Electronic Engineering, Nanyang Technological University, Singapore

Abstract— Current bidirectional localization schemes are able to locate a mobile device using Line-of-Sight (LOS) or Non-Line-of-Sight (NLOS) Time-of-Arrival (TOA) and Angle-of-Arrival (AOA) information measured at both the mobile device and reference device. This information is used to derive line of possible mobile device position (LPMD). The intersection points of LPMDs are used to estimate mobile position. However these algorithms do not work well in a dense multipath environment with high levels of TOA and AOA measurement noise. In addition, these techniques require at least two single bounce reflection paths to locate the mobile position. This paper explores the feasibility of using multiple image theory to obtain the image point of the NLOS single bounce multipath to perform NLOS localization and overcome the abovementioned limitations. Simulation results have shown that there are few variance shape of image point with various combinations of TOA and AOA variance noises. With the discovery of these variance shapes in the image point, it opened up new method and possibility to perform NLOS localization in a more effective and accurate way.

Study of Channel Measurement Parameter Estimation for Precise Mobile Localization Applications

Chee Kiat Seow, **Soon Yim Tan**, **and Kai Wen**
Nanyang Technological University of Singapore, Singapore

Abstract— Recent year has seen the need for precise localization for both commercial and government applications. The underlying first building block that affects the performance of the localization algorithm is the performance of the estimation of position related parameters such as Time of Arrival (TOA) and Angle of Arrival (AOA). These parametric estimation methodologies are generally classified as deterministic or subspace methods. The accuracy and resolution of these parametric estimation algorithms are also usually a function of the channel parameters such as coherence bandwidth, which can either manifest as flat fading or frequency selective fading. In this paper, we will investigate the effect of channel parameters such as bandwidth on the performance of the parametric estimation algorithms in different Non-line-of-Sight (NLOS) multipath environment coupled with experimental channel measurement campaign. The purposes are two fold. In existing NLOS localization schemes, only the dominant NLOS paths are necessary to deduce the position related parameters and hence the estimated position of Mobile Device (MD). As such, we will investigate the accuracy of detecting the dominant multipaths position related parameters. Secondly, the finding of required signal bandwidth needed for precise localization is another motivator for the study especially with the advent of 802.11n implementation.

Session 4A7
Eigenfunction Expansion Based Analysis of Electromagnetic Structures

An Eigenvalue Hybrid FEM Formulation for Three Dimensional Open Cavities

C. L. Zekios[1], **P. C. Allilomes**[1], **A. V. Kudrin**[2], **and G. A. Kyriacou**[1]

[1]Microwaves Lab., Department of Electrical and Computer Engineering
Democritus University of Thrace, Xanthi, Greece
[2]Department of Radiophysics, University of Nizhny Novrogod, Russia

Abstract— The analysis and design of open-radiating cavities is one of the most active research fields in electromagnetics. Broad applications of both typical and non-typical open cavities span from antennas design to optical laser cavities. Numerous attempts towards this direction have been published but most of them employ the deterministic approach, namely the electromagnetic simulati- on in the presence of a specific excitation-source. Moreover, most of the computerized techniques able to solve cavity problems in a unified manner are based on numerical techniques such as the finite element (FE) and the finite difference (FD) methods, which are restricted to handle any but only radiating closed structures. The eigenfrequency of open radiating cavities exploiting all the advantages of the source free problems analysis, namely the stability and physical insight of the structure, constitutes a challenge in this research field. Thus, a numerical analysis tool capable of computing the eigenfrequencies of arbitrary open cavities will significantly contribute to the design and study of many electromagnetic devices. The idea is to bind together the efficiency and the robustness of the numerical technique (in our work the FE) for the physically bounded area with an appropriate method for the description of the semi infinite domain.

Several techniques have been developed for the implementation of FEM in the analysis of such cases, where they are hybridized rendering the open/unbounded solution domain to an equivalent closed one, using an artificial-mathematical separation surface. The hybridization of FEM with Moment Method (FEM-MoM) e.g., [1] and FEM with Boundary Elements (FEM-BEM) e.g., [2], where in both techniques an integral equation is formulated for the unknown equivalent current densities defined over the artificial separation surface. One quite different procedure is that of Unimoment introduced by Mei [3] and Bymoment technique introduced by Cangellaris [4]. In the present work a hybrid FEM formulation capable of handling the eigenvalue analysis of open, arbitrary shaped cavities is described. The 3-D solution domain in the generalized case is enclosed within a fictitious spherical surface S_f. For the field solution inside the surface-S_f the formulation is applied based on a tetrahedral edge elements discretization. Thus, being able to model arbitrary shaped radiating 3D structures. The field solution in the semi-infinite space outside-S_f is expressed by an in principle expansion of an infinite series of spherical harmonics. The final formulation is obtained by imposing the field continuity conditions across the fictitious surface and exploiting the orthogonality properties of the spherical harmonics, which in turn obey the Sommerfeld radiation condition. The final eigenvalue problem is solved using the Arnoldi subspace iterative technique.

ACKNOWLEDGMENT

This work was financially supported by the Greek Ministry of Education, Lifelong Learning and Religious Affairs through the research project THALIS Design Techniques for Digitally Controlled RF-Microwave Structures Appropriate for Software Defined — Cognitive Radio (RF-EIGEN-SDR).

REFERENCES

1. Yuan, X., "Three dimensional electromagnetic scattering from inhomogeneous objects by the hybrid moment and finite element method," *IEEE Trans. MTT*, Vol. 38, 1053–1058, Aug. 1990.
2. Lynch, D. R., K. D. Paulsen, and J. W. Strohbehn, "Hybrid element method for unbounded electromagnetic problems in hyperthermia," *Int. Journal for Num. Meth. in Eng.*, Vol. 23, 1915–1937, Jun. 1986.
3. Mei, K., "Unimoment method of solving antenna and scattering problems," *IEEE Trans. on Ant. and Propagat.*, Vol. 22, 760–766, Nov. 1974.
4. Cangellaris, A. and R. Lee, "The bymoment method for two-dimensional electromagnetic scattering," *IEEE Trans. on Ant. and Propagat.*, Vol. 38, 1429–1437, Sep. 1990.

Controlling Nanoparticle Plasmon Resonances by Faceting

M. V. Gorkunov[1], **B. I. Sturman**[2], **and E. V. Podivilov**[2]

[1]A. V. Shubnikov Institute of Crystallography, Russian Academy of Sciences, Moscow 119333, Russia
[2]Institute of Automation and Electrometry, Russian Academy of Sciences, Novosibirsk 630090, Russia

Abstract— Subwavelength (nano-size) metallic particles (including their regular arrays, e.g., gratings, metamaterials, etc.) offer unique possibilities of adjusting and tailoring the effective optical properties by varying shape, size and arrangement. Potential applications range from nano-lasers to optical sensors of single molecules. As long as a particle is much smaller than the light wavelength, its optical response can be well described in quasistatic terms — discrete electrostatic plasmon resonances. The resonant values of metal permittivity and the corresponding eigenmode structure are fully determined by the particle shape, and it becomes highly valuable to understand if/how one can control the plasmonic resonances by moderate variation of the shape.

Generally, strong enhancement of electromagnetic fields and formation of field singularities at sharp metal corners and tips is well known in electrodynamics. However, the impact of faceting on plasmonic resonances and, especially, the role of the inherent corner rounding have not been analyzed so far. We present the first step towards understanding of this complex phenomenon and study plasmonic resonances in metal nanowires of the rounded-square cross-section, mathematically expressed as $x^n+y^n=1$, which is a cylinder for $n=2$ and tends to ideally sharp square for $n\to\infty$ (see left subfigure). Solving the corresponding surface integral eigenvalue problem, we reveal the impact of faceting on the eigenmode structure and show the formation of characteristic localized charges at sufficiently sharp corners (see e.g., middle subfigure). The eigenmodes can be naturally classified by their symmetry as dipolar, quadrupolar and octupolar. The spectrum of the permittivity eigenvalues appears to saturate rather slowly for large rounding indices n, and in the limit $n\to\infty$ covers densely the interval $\varepsilon\in[-3,-1/3]$ (see right subfigure).

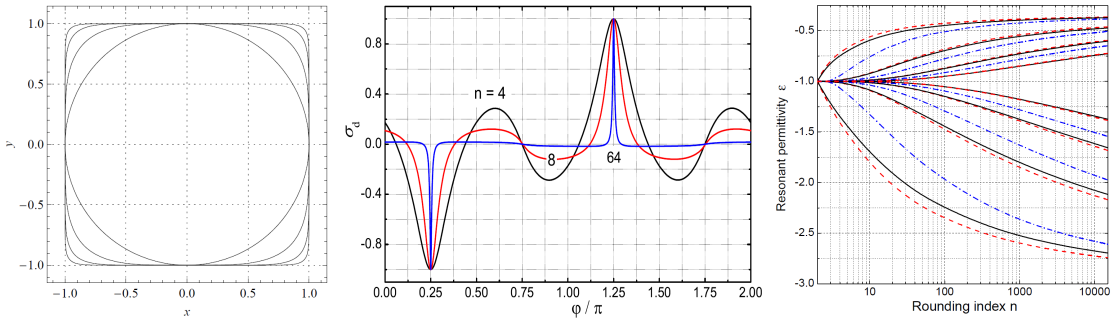

(a) (b) (c)

Figure 1: Plasmon resonances of rounded-square wire. (a) Wire cross-section for rounding indices $n=2$, 4, 8 and 16. (b) Surface charge distribution as function of the azimuthal angle in the lowest-order dipolar mode for $n=4$, 8 and 64. (c) Resonant values of the permittivity for the first 20 modes with dipolar (solid), quadrupolar (dash) and octupolar (dash-dot) symmetry.

ACKNOWLEDGMENT

The work has been supported by the Programs of the Russian Academy of Sciences: Presidium Program No. 24 and BPS Program “Physics of new materials and structures”.

A Mode Matching Methodology for the Analysis of Circular Waveguides Loaded with Infinite and Finite Periodic Structures

Dimitris G. Makris, Spyros J. Lavdas, Christos S. Lavranos, and George A. Kyriacou
Microwaves Lab., Department of Electrical and Computer Engineering
Democritus University of Thrace, Xanthi 67100, Greece

Abstract— Periodic structures have been examined and investigated widely, due to their importance in design and implementation of slow-wave structures, backward oscillators, corrugated antennas, polarizers and mainly microwave filters. The early analysis was based on approximate-analytical techniques and the resultant deviations were regulated with mechanical moving elements. The usage of complex geometries and anisotropic material loadings, offers excellent potential. Additionally electromagnetic band gap (EBG) applications, where the periodic structure is designed to prevent the wave propagation either at certain frequencies (frequency band gap) or in certain directions (space gap or space selective propagation), have been acquired a special attention, particularly in recent years.

In this paper we will examine a circular waveguide loaded with infinite or finite periodic structures. These are mainly comprised of irises etched on diaphragms or corrugations and we will try to investigate their propagation characteristics. Particular effort is devoted to periodic structure loaded with periodically repeated split ring resonators (SRR), printed on dielectric diaphragms, which presents negative refraction phenomena and constitutes a popular physical realization of left handed medium. Explicitly, LH behavior is expected when circular waveguide is operated below cutoff and this phenomenon will be examined herein in order to be verified for both infinite and infinite periodic SRRs sections. Besides that the behavior of periodic complementary split ring resonators (CSRRs) will be studied with the ambition to reveal its characteristics. Recall that a CSRR is implemented by etching a sectorial slot on a metallic diaphragm. Usually such structures are analyzed and designed by usage of advanced numerical methods. However, the increasing demand for accurate prediction of wave propagation behavior and the electrically large dimensions of such structures, render the numerical simulation, time consuming or almost impossible.

Floquet theorem has been used to tackle this problem, but this is possible if only the periodic structure extends infinitely. Then the analysis is restricted to the determination of only one spatial period-cell. The electromagnetic field in one cell is related with electromagnetic field of the next or the previous cell by an exponential function. Hence, periodic boundary conditions are enforced on the unit cell's periodic surfaces in order to introduce the periodicity into the formulation. Initially the infinitely extended circular waveguide is divided into unit cells. The unit cell internal structure, is composed of discontinuities and canonical circular waveguide sections. Each discontinuity is analyzed with the aid of a Mode Matching Technique(MMT) in order to derive its scattering matrix, which describes the electromagnetic properties of this discontinuity. Each canonical circular waveguide or circular sector (full or truncated with a gap), is also described with a scattering matrix. All these matrices are combined and the Generalized scattering matrix (GSM) of the unit cell is derived, which includes the information from the whole geometry boundary conditions. The Floquet theorem, by mean of periodic boundary conditions, is then enforced at the ports of the unit cell in order to include the periodicity information. This framework leads us to a classical eigenvalue problem where the eigenvalues are the Floquet propagation constants. Our ultimate task is to analyze finite periodic structures. For this purpose the electromagnetic field within the periodic section will be expanded into an infinite sum of Floquet eigenfunctions. In turn the MMT will be enforced again at the input and output ports of the periodic section. Results from the infinite periodicity will be presented at the conference along with the finite geometry formulation.

REFERENCES

1. Economou Filandras, P. A., A. P. Orphanides, C. Lavranos, and G. A. Kyriacou, "Mode matching analysis of split ring irises inserted in a circular waveguide," *Mediterranean Microwave Symposium (MMS-08)*, Damascus, Syria, October 14–16, 2008.
2. Esteban, J. and J. M. Rebollar, "Characterization of corrugated waveguides by modal analysis," *IEEE Transactions on Microwave Theory and Techniques*, Vol. 39, No. 6, 1991.

Using the Eigenfunction Expansion Technique for Analysis of the Electrodynamic Characteristics of a Loop Antenna Located on the Surface of a Magnetized Plasma Column

A. V. Kudrin[1], **T. M. Zaboronkova**[2], **and A. S. Zaitseva**[1]

[1]University of Nizhny Novgorod, Russia
[2]Technical University of Nizhny Novgorod, Russia

Abstract— Much previous work on the current distribution and input impedance of a loop antenna in a magnetoplasma applies to the case where the plasma parameters are independent of the spatial coordinates (see, e.g., [1, 2] and references therein). In recent years, a substantial degree of interest has been shown in the characteristics of antennas in the presence of an axially magnetized plasma column [3]. It is the purpose of the present paper to apply the eigenfunction expansion technique for analysis of the current distribution and input impedance of a strip loop antenna located on the surface of such a plasma column.

We consider an antenna having the form of an infinitesimally thin, perfectly conducting, narrow strip coiled into a circular loop. The antenna is located coaxially on the surface of a uniform circular plasma column placed in free space and aligned with an external dc magnetic field, which is parallel to the z axis of a cylindrical coordinate system (ρ, ϕ, z). The medium inside the column is described by a general plasma dielectric tensor. The current on the antenna surface is excited by a time-harmonic voltage which creates an external electric field with the only nonzero azimuthal component E_ϕ^{ext} on the surface of the strip in a narrow angular interval. Using the boundary conditions for the field on the surface of the column as well as the conditions $E_\phi = -E_\phi^{\text{ext}}$ and $E_z = 0$ on the antenna surface, where E_ϕ and E_z are the azimuthal and longitudinal components of the antenna-excited field, respectively, we derive integral equations for the azimuthal harmonics of the surface current density. We represent the kernels of the integral equations in the form of eigenfuntion expansions comprising the contributions related to discrete- and continuous-spectrum waves of the plasma column. It is shown that integration over the continuous-spectrum waves always gives a singular contribution to the kernels, while contribution of the eigenmodes, i.e., discrete spectrum waves, contains a singular part only in the case of a resonant plasma where the diagonal elements of the plasma dielectric tensor have opposite signs. Using the studied properties of the kernels, we solve the integral equations for the current harmonics by methods developed for singular integral equations. Then we calculate the current distribution and input impedance of the antenna and reveal conditions under which these characteristics can be affected most significantly by the presence of a magnetized plasma column compared with the cases where the same antenna is located in either free space or a homogeneous plasma whose parameters coincide with those inside the column.

ACKNOWLEDGMENT

This work was supported by the RFBR (project No. 12-02-00904-a), the Government of the Russian Federation (contract No. 11.G34.31.0048), the Russian Federal Program "Scientific and Educational Personnel of the Innovative Russia" (contract No. P313), and the Greek Ministry of Education through the project THALIS (RF-EIGEN-SDR).

REFERENCES

1. Ohnuki, S., K. Sawaya, and S. Adachi, "Impedance of a large circular loop antenna in a magnetoplasma," *IEEE Trans. Antennas Propagat.*, Vol. 34, No. 8, 1024–1029, 1986.
2. Kudrin, A. V., E. Y. Petrov, and T. M. Zaboronkova, "Current distribution and input impedance of a loop antenna in a cold magnatoplasma," *Journal of Electromagnetic Waves and Applications*, Vol. 15, No. 3, 345–378, 2001.
3. Kudrin, A. V., V. A. Es'kin, C. Krafft, and T. M. Zaboronkova, "Whistler wave excitation by a loop antenna in a bounded collisional magnetoplasma," *Phys. Scr.*, Vol. 77, No. 5, 055501-1–055501-11, 2008.

A Characteristic Mode Eigenanalysis Exploiting FEM Features

R. Maximidis[1], **C. L. Zekios**[1], **P. C. Allilomes**[1], **A. V. Kudrin**[2], **and G. A. Kyriacou**[1]

[1]Microwaves Lab., Department of Electrical and Computer Engineering
Democritus University of Thrace, Xanthi, Greece
[2]Department of Radiophysics, University of Nizhny Novrogod, Russia

Abstract— The current work aims at the development of a tool for the electromagnetic simulation and design of digitally controlled and multifunctional multiple input multiple output (MIMO) antennas integrated on the devices chassis and/or package utilizing Characteristic Mode theory. Several researchers already exploit characteristic modes for the antenna design, but their work is limited to geometries described by the Method of Moments (MoM), namely depending on the availability of the corresponding Green's functions. Usually, only simple metallic surfaces of canonical shapes in free space are efficiently considered.

Characteristic mode eigenanalysis concerns the actual electric current densities owing on the outer surface of possibly radiating objects as well as equivalent electric or magnetic current densities resulting from the adoption of a field (Loves) equivalence principle. According to [1], characteristic modes are real current modes that correspond to the eigenvectors of a particular weighted eigenvalue equation, which involves the complex impedance matrix of the body. Thus, characteristic modes can be numerically computed for conducting bodies of arbitrary shape and since they form a set of orthogonal functions, they can be used to expand the total current on the surface of the body. One main drawback to the wide utilization of characteristic modes until now was the almost exclusive need of the Moment Method (MoM) for their extraction. The main MoM limitation factor lies in its dependence in the availability of the Greens functions corresponding to the device. On the other hand the numerical calculation of Greens functions is as complex as the simulation of the entire structure and has to be repeated for every possible position and orientation of an elementary dipole source. To stress the complexity of the above procedure it is worth mentioning that usually its more preferable to calculate the Greens functions using eigenfunctions. It is obvious that this leads us to a closed loop, since it is not possible to define the eigenfunctions through Greens functions, which are by nature more complex and assume the eigenfunctions knowledge.

The novelty of the proposed research is a new technique of complex impedance calculation based on Finite Element (FEM) method with similarities to FETI (e.g., Kezhong) [2], in contrast to the established use of MoM. The basic idea is: If the structure is simulated solving electric field vector equation, then at the boundary of the solution domain (or on all the metallic surfaces) current densities are defined through the tangential magnetic field. The final system is divided and solved in such a way that the internal field distribution is obliterated ending up to a system with sole unknown the surface current distribution. This system indeed defines the impedance matrix $[Z]$ and is of the same form as defined as an eigenvalue problem $[Z][I] = 0$. This, eventually, will be formulated and solved as a characteristic mode eigenproblem. Namely separating the complex impedance matrix into a real $[R]$ and imaginary $[X]$ parts, a real eigenproblem of the form $[X][I] = \lambda[R]$ is formulated and solved. The use of FEM allows the eigenanalysis of complex structures loaded with inhomogeneous and/or anisotropic media, such as the chassis, or the frame package of mobile devices which can even be curved for conformal integration to the devices.

ACKNOWLEDGMENT

This work was financially supported by the Greek Ministry of Education, Lifelong Learning and Religious Affairs through the research project THALIS Design Techniques for Digitally Controlled RF-Microwave Structures Appropriate for Software Defined — Cognitive Radio (RF-EIGEN-SDR).

REFERENCES

1. Harrington, R. F. and J. R. Mautz, "Theory of characteristic modes for conducting bodies," *IEEE Trans. on Antennas and Propagation*, Vol. 19, 622–628, 1971.
2. Zhao, K., "A domain decomposition method for solving electrically large electromagnetic problems," Doctoral Thesis, Ohio State University, 2007.

Computational Efficient Solution of Maxwell's Equations for Lamellar Gratings

I. Semenikhin[1], **M. Zanuccoli**[2], **V. Vyurkov**[1], **E. Sangiorgi**[2], **and C. Fiegna**[2]

[1]Institute of Physics and Technology RAS, Moscow 117218, Russia
[2]ARCES-DEIS University of Bologna and IUNET, Cesena (FC) 47521, Italy

Abstract— Over the past three decades, a large number of algorithms has been developed to solve Maxwell's equations for the analysis of diffraction gratings and other periodic structures. Among them, algorithms based on eigenmode expansion are widely used. According to these methods, the simulation domain is divided into layers featuring parallel interfaces within which the permittivity varies only in the plane of the layer and is constant along the perpendicular direction allowing the separation of variables. Within each layer the eigenmodes of the electromagnetic field are calculated and the general solution is then expressed by means of an eigenmode expansion. The expansion coefficients can be calculated by applying proper boundary conditions. Several implementations of this general approach have been proposed for two-dimensional (2-D) case, for which the dielectric constant in each parallel layer depends only on one spatial coordinate and, in order to obtain the eigenmodes, the one-dimensional Helmholtz equation has to be solved.

Most proposed implementations differ only by a set of basis functions, through which the eigenfunctions are expressed. Therefore, disregarding the accuracy level attained by all those methods, such approaches merely approximate the eigenfunctions of Helmholtz equation. At the same time, the form of the exact eigenfunctions for piecewise constant permittivity can be explicitly written. Then the only problem remained is to find the corresponding eigenvalues. In [1, 2] the analytic modal method (AMM) has been proposed and the solution for a simple rectangular grating has been derived through the roots of the transcendental equation by using the theory of analytic functions. Subsequently in [3], another method which involves the solution of differential equations in order to calculate the roots has been presented; in such approach the initial condition corresponds to that of the counterpart grating featuring real dielectric constant, for which the solution can be straightforwardly determined. This method has been already ex-tended to multi-groove gratings [4]. In this work we present a new implementation of AMM, exhibiting an improved and computationally efficient approach to calculate the eigenvalues. An initial guess solution is obtained by applying conventional methods such as Rigorous Coupled-Wave Analysis (RCWA) or pseudospectral methods, then the solution is refined by means of modified Newton method. In the case of TE polarization the computational time is remarkably reduced by adopting the perturbation approach. The proposed improved AMM allows to calculate the electromagnetic field in presence of 2-D periodic structures patterning arbitrary geometry.

REFERENCES

1. Botten, L. C., M. S. Craig, R. C. McPhedran, J. L. Adams, and J. R. Andrewartha, "The finitely conducting lamellar diffraction grating," *Opt. Acta*, Vol. 28, 1087–1102, 1981.
2. Botten, L. C., M. S. Craig, R. C. McPhedran, and J. L. Adams, "Highly conducting lamellar diffraction gratings," *Opt. Acta*, Vol. 28, 1103–1106 1981.
3. Tayeb, G. and R. Petit, "On the numerical study of deep conducting lamellar diffraction gratings," *Opt. Acta*, Vol. 31, 1361–1365, 1984.
4. Miller, J. M., J. Turunen, E. Noponen, A. Vasara, and M. R.Taghizadeh, "Rigorous modal theory for multiply grooved lamellar gratings," *Opt. Commun.*, Vol. 111, 526–535, 1994.

Analytical Study of Surface and Leaky Waves on a Grounded Magnetized Plasma Slab

Xenofon M. Mitsalas[1], **Alexander V. Kudrin**[2], **and George A. Kyriacou**[1]

[1]Microwaves Laboratory, Department of Electrical and Computer Engineering
Democritus University of Thrace, Xanthi, Greece
[2]Department of Radiophysics, University of Nizhny Novrogod, Russia

Abstract— The electromagnetic eigenmodes excited on a grounded magnetized plasma are considered. The structure of interest refers to magnetized semiconductors at cryogenic temperatures. A homogeneous magnetization is assumed with the DC-biasing magnetic field parallel to the substrate, but normal to the direction of propagation. While the characteristics of surface waves are extensively studied in the past and especially by Seshadri et al. [3], the possibility of leaky waves is not well examined and constitutes the original contribution of the present effort. The characteristic equation is first obtained analytically and in turn investigated numerically. The important non-reciprocal and unidirectional phenomena due to the non-even expression of the characteristic equation are verified regarding the surface waves while these are then sought herein in the leaky modes regime. The conditions enabling backward waves and particularly unidirectional modes are indeed challenging since they enable numerous novel applications.

The propagation of electromagnetic waves within and around a dielectic slab including the radiation characteristics when leaky waves are excited has been extensively studied as it is involved in important practical applications. The majority of these investigations pertain to the case of a slab of isotropic dielectric. A complete survey of the relevant literature may be found in the work of Oliner and Tamir [1], who have given a comprehensive treatment of the electromagnetic field for a source-excited, isotropic plasma slab. Wait [2] has treated the case of a thin plasma sheet in free space as well as in the vicinity of a ground screen.

Our previous effort directed toward the solution of a canonical problem of a parallel plane waveguide with a truncated (semi-infinite) upper conductor filled with anisotropic plasma [4]. A lot of interesting phenomena regarding the excitation of surface and leaky waves in the grounded plasma region and the radiating space wave are involved in the scattered field expressions. The dependence of the modes turn-on/off conditions from the plasma parameters and especially the magnetizing dc field are of particular importance. A lot of these surface wave phenomena on grounded plasma slabs have been studied by Seshadri [3]. Besides this, higher order modes of this grounded structure are expected to become leaky waves. These waves offer non-reciprocal features and their radiation mechanisms are inevitable in the effort toward completing our previous work [4], by means of studying the radiation from structures printed on magnetized plasma (patch antennas). Explicitly, all these type of modes are indeed involved in the mathematical formulation [4] and are required for the evaluation of the field and especially the radiation of the structure. Herein the study all of those modes and particularly leaky waves dispersion curves for both surface and leaky modes are first studied, in turn their field distribution is calculated and illustrated. The aim of these presentations is to reveal.

REFERENCES

1. Oliner, A. and T. Tamir, "Backward waves on isotropic slab," *J. Appl. Phys.*, Vol. 33, 231–233, January 1962.
2. Tamir, T. and A. A. Oliner, "The spectrum of electromagnetic waves guided by a plasma layer," *Proc. IEEE*, Vol. 51, 317–332, February 1963.
3. Seshadri, S. R. and W. F. Pickard, "Surface waves on an anisotropic plasma sheath," *IEEE Trans. on Microwave Theory and Techniques*, 529–541, 1964.
4. Kyriacou, G. A., "Wiener-Hopf analysis of planar canonical structures loaded with longitudinally magnetized plasma biased normally to the extraordinary wave propagation," *Progress In Electromagnetics Research B*, Vol. 5, 1–34, 2008.

Radiation Efficiency of a Circular Loop Antenna with Pulsed Excitation in a Magnetoplasma Containing a Cylindrical Density Nonuniformity

A. V. Kudrin[1], **N. M. Shmeleva**[1], **N. V. Yurasova**[1], **and T. M. Zaboronkova**[2]

[1]University of Nizhny Novgorod, Russia
[2]Technical University of Nizhny Novgorod, Russia

Abstract— Over the past decade, there has been shown a substantial degree of interest in the excitation of electromagnetic radiation in a magnetoplasma containing magnetic-field-aligned density nonuniformities commonly known as density ducts (see, e.g., [1] and references therein). Such plasma structures consisting of density enhancements or depletions, or combinations thereof can arise near electromagnetic sources in a magnetoplasma due to various nonlinear effects [2, 3] and are capable of guiding electromagnetic waves in some frequency ranges. Much previous theoretical work on the subject is focused on studying the radiation characteristics of monochromatic sources immersed in density ducts [1]. However, there exists a very little theory of the radiation from nonmonochromatic sources operated in the presence of field-aligned plasma density nonuniformities.

In this work, we study the energy radiation characteristics of a pulsed loop antenna placed coaxially in a cylindrical density duct that is surrounded by a uniform cold magnetoplasma. At first, we determine the total field excited by such a source. To describe the temporal behavior of the field, the Laplace transform technique is employed. The spatial structure of the source-excited field is represented in the form of an eigenfunction expansion over the discrete- and continuous-spectrum waves of a density duct [1]. The expansion coefficients are calculated with the help of the approach based on Lorentz's reciprocity theorem. Using the field representation obtained, we derive an expression for the total radiated energy and analyze its distribution over the spatial and frequency spectra of the excited waves as a function of the source and duct parameters. Detailed numerical calculations of these radiation characteristics have been performed in the case where the frequency spectrum of the current pulse is concentrated in the resonant part of the whistler range [1], which is of great importance for many promising applications. It is shown that the presence of a duct with enhanced plasma density can lead to a significant increase in the energy radiated from a pulse-excited loop antenna compared with the case where the same source is immersed in the surrounding uniform magnetoplasma. We demonstrate that the predominant contribution to the increased radiated energy is ensured by slightly leaky modes that can be separated from the continuous part of the spatial spectrum of the excited waves. The results obtained can be useful in interpreting the data of space and laboratory experiments on electromagnetic wave excitation by pulsed sources in a magnetoplasma containing magnetic-field-aligned density nonuniformities of natural or artificial origin.

ACKNOWLEDGMENT

This work was supported by the RFBR (project No. 12-02-00904-a), the Government of the Russian Federation (contract No. 11.G34.31.0048), the Russian Federal Program "Scientific and Educational Personnel of the Innovative Russia" (contract No. P313), the Dynasty Foundation, and the Greek Ministry of Education through the project THALIS (RF-EIGEN-SDR).

REFERENCES

1. Kondrat'ev, I. G., A. V. Kudrin, and T. M. Zaboronkova, *Electrodynamics of Density Ducts in Magnetized Plasmas*, Gordon and Breach, Amsterdam, 1999.
2. Kostrov, A. V., A. V. Kudrin, L. E. Kurina, G. A. Luchinin, A. A. Shaykin, and T. M. Zaboronkova, "Whistlers in thermally generated ducts with enhanced plasma density: Excitation and propagation," *Phys. Scr.*, Vol. 62, No. 1, 51–65, 2000.
3. Kudrin, A. V., L. E. Kurina, and E. Y. Petrov, "Ionization formation of plasma inhomogeneity by the near-zone field of a magnetic-type source in a magnetized plasma," *JETP*, Vol. 92, No. 6, 969–978, 2001.

Eigenanalysis for Lossy or Open Periodic Structures Incorporating the Floquet Field Expansion

Spyros J. Lavdas, Panagiotis Tsompanis, Christos S. Lavranos, and George A. Kyriacou
Microwaves Lab., Department of Electrical and Computer Engineering
Democritus University of Thrace, Xanthi 67100, Greece

Abstract— The unique electromagnetic features of periodic structures attracted a huge research interest during the last decades. These features enabled the development of novel metamaterials and were exploited in frequency selective surfaces and phased arrays. The analysis and design of such structures have received particular attention which is almost exclusively directed toward the deterministic approach. Namely, an electromagnetic simulation of periodic structure excited by a specific source. Even though this analysis served as a very useful tool, it does not offer the required physical insight, while it does not provide any means to devise novel structures. On the other hand, an eigenanalysis reveal the physical behavior of the structure. In particular, the resulting eigenfunctions can be exploited to devise novel features and enable multifunctionality of periodic structures. Besides, a variety of microwave applications and in particular conformal antennas with their beamforming networks, require a simulation tool capable of handling periodic structures loaded with inhomogeneous and anisotropic media.

An appropriate eigenanalysis for the three-dimensional waveguiding periodic structures was developed in our previous work [1], which was able to handle anisotropic media. For this analysis a Finite Difference Frequency Domain (FDFD) method was employed in orthogonal Curvilinear Coordinates Yee type mesh, [2]. At this first attempt the eigenvalue problem was formulated and solved for the eigenfrequencies (ω-formulation) or the wavenumber. Namely, the range of a real valued (ignoring losses or radiation) Floquet wavenumber was defined and scanned in an iterative solution procedure. This procedure yields the Bloch diagrams. However this kind of formulation (ω-formulation) is restricted to closed periodic structures, since we assume the propagation constant to be real.

The present work aims at an eigenanalysis methodology for lossy or open periodic structures incorporating the Floquet field expansion within the FDFD formulation. The ω-formulation of such geometries requires the knowledge of phase and especially attenuation constants which are the unknowns to be sought. For that case, a beta-eigenvalue problem is formulated and solved with the Arnoldi iterative Algorithm. The periodicity of the structure is accounted through the incorporation of Floquet Field Expansion. The boundary conditions are in turn imposed on the remaining surfaces of the unit cell and especially at the interface with free space, where an artificial-separation absorbing boundary is introduced. For that case, the Absorbing Boundary Conditions (ABCs) or the Perfect Matching Layers (PML) are usually assumed, [3] but this approach results to unwanted spurious eigenvalues, the so-called Berenger modes. One of the future tasks of this research aims at overcoming this drawback through exact — global truncation techniques. The main difficulty encountered in the β-formulation is that the eigenproblem becomes no linear and this constitutes the main drawback of the presented approach. However, due to the important applications that can be supported, it worths to deal with this complexity. In order to handle this difficulty the corresponding lossless or closed structure will be solved as a linear eigenproblem and the resulting eigenvalues will be exploited in the iterative solution of the non linear eigenproblem. Numerous investigations are carried out, involving certain periodic structures loaded with anisotropic media in order to reveal the so-called Frozen Mode. The most interesting structures will be discussed during the presentation.

ACKNOWLEDGMENT

This work was financially supported by the Greek Ministry of Education, Lifelong Learning and Religious Affairs through the research project THALIS Design Techniques for Digitally Controlled RF-Microwave Structures Appropriate for Software Defined-Cognitive Radio (RF-EIGEN-SDR).

REFERENCES

1. Lavdas, S., C. S. Lavranos, and G. A. Kyriacou, "Periodic structures eigenanalysis incorporating the floquet field expansion," *Proc. of the ICEAA IEEE ARWC Conference*, Turin, Italy, September 2011.
2. Przybyszewski, P., "Fast finite difference numerical techniques for the time and frequency domain solution of electromagnetic problems," PhD Dissertation, Gdansk, Poland, 2001.

3. Engquist, B. and A. Majda, "Absorbing boundary conditions for numerical simulation of waves," *Applied Mathematical Sciences*, Vol. 74, No. 5, 1765–1766, May 1977.

Author Index